



In this volume are collected the proceedings of the Annual General Meeting of CORILA, held 4th – 6th June 2007 at Palazzo Franchetti, Venice



**SCIENTIFIC RESEARCH
AND SAFEGUARDING OF VENICE
2007**

CORILA
Research Programme 2004 - 2006
2006 Results

Edit by
PIERPAOLO CAMPOSTRINI

© Copyright CORILA. Consorzio per la Gestione del Centro di Coordinamento
delle Ricerche Inerenti il Sistema Lagunare di Venezia

30124 Venezia – Palazzo Franchetti, S. Marco 2847

Tel. +39-041-2402511 – Telefax +39-041-2402512

venezia@corila.it

www.corila.it

Stampa "Multigraf" Spinea, Venezia 2008

INDEX

INTRODUCTION

Introduzione – P. Campostrini XI

SCIENTIFIC BOARD

L'ampliamento delle Gallerie dell'Accademia: aspetti strutturali – R. Codello XVII

Can economic science help protect Venice and its lagoon? – A. Markandya XXIII

The fate of Venice lagoon in the century of global warming: settled and unsettled issues – G. Seminara and N. Tambroni XXVII

Global climate change and impact on Mediterranean – M. Colacino LIX

Indicators of trophic status and sensitivity to eutrophication and organic pollution in transitional waters – P. Viaroli LXIII

AREA 1. Economics

RESEARCH LINE 1.2. Cost-benefits analysis of land reclamation of brownfields in the Venice lagoon

ELGIRA. A support system for knowledge building and evaluation in brownfield redevelopment – D. Patassini, P. Cossettini, A. De Mitri, E. De Polignol, S. De Zorzi, M. Hedorfer, E. Rinaldi 5

Economic valuation for policy making: using conjoint choice experiments to investigate stakeholder preferences for contaminated land cleanup and redevelopment programmes– M. Turvani, A. Alberini, S. Tonin 29

RESEARCH LINE 1.3. Characteristics and conditions for a model of post-industrial sustainable development for Venice

A multicriteria approach for the evaluation of sustainability of the economic re-use of historic buildings in Venice – P. Rosato, S. Giove, M. Dalla valle, M. Breil 55

Redeveloping derelict and underused historical city areas: evidence from a survey of real estate developers – P. Rosato, A. Alberini, V. Zanatta, M. Breil	83
AREA 2. Architecture and cultural heritage	
RESEARCH LINE 2.3. Methodologies and technologies for conservation and restoration of historical Venetian building	
The prototype of the information system for diagnostic of Venetian building (SIDEV) – L. Marescotti, S. Maffulli, M. Mascione	115
MDDS – Venice: try out and improvements of the expert system – R. P.J. van Hees, S. Naldini, I. A.E. de Vent, F. Trovò	123
A structural damage atlas for Venice – F. Doglioni, G. Mirabella Roberti, F. Trovò, M. Bondanelli, A. Squassina	133
From artificial stone to reinforced concrete III: analytical methodologies for the intervention – P. Faccio, G. Bruschi, P. Scaramuzza	147
AREA 3. Environmental processes	
RESEARCH LINE 3.8. Speciation and flow of pollutants	
Suspended Particulate Matter: temporal variations, origin and depositional dynamics – L. G. Bellucci, S. Giuliani, S. Romano, M. Frignani, S. Albertazzi	161
Evaluation of polychaetes, Perinereis cultrifera (grube, 1840), as indicators of sediment micro-organic contamination – N. Nesto, D. Cassin, L. Da Ros	169
Evaluation of polychaetes, Perinereis Cultrifera (Grube, 1840), as indicators of heavy metal variability in sediment – S. Romano, M. Marcheselli, M. Mauri	179
RESEARCH LINE 3.9. Pollutant flows in the lagoon carried by aerosols and atmospheric fall-out	
Aerosol fine fraction characterisation in the venice lagoon – F. Prodi, F. Belosi, D. Contini, G. Santachiara, A. Donateo, L. Di Matteo, D. Cesari	193

Trace elements and organic micropollutants in atmospheric deposition in Venice lagoon – A. Gambaro, L. Zagolin, C. Turetta, S. De Pieri, R. Zangrando, M. Radaelli, A. Stortini, W. Cairns 207

RESEARCH LINE 3.10. Groundwater flows in the Venice lagoon system

Saltwater intrusion at the southern Venice lagoon boundary detected by time-lapse ERT – R. de Franco, G. Biella, A. Corsi, A. Morrone, G. Boniolo, A. Lozej, C. Claude, A. Mayer, G. Saracco, B. Chiozzotto, M. Giada, V. Bassan, V. Bisaglia, T. Abba, A. Mazzuccato, E. Conchetto, M. Barbetta, G. Gasparetto-Stori, F. Rizzetto, L. Tosi, P. Teatini 221

RESEARCH LINE 3.11. Ecological quality indices, biodiversity and environmental management for lagoon areas

A new bioindex, based on macrofouling biocoenosis of hard substrata, for the estimation of the environmental quality: application in the lagoon of Venice – F. Cima, P. Burighel, L. Ballarin 231

In situ monitoring of mussel populations in the Venice lagoon by means of molecular biomarkers – M. Martinuzzi, M. Zanella, L. Pivotti, L. Tallandini 235

A toxicity index for the Venice lagoon – A. Volpi Ghirardini, C. Losso, A. Arizzi Novelli, P. F. Ghetti 249

Biodiversity at genetic level in the Mediterranean shore crab *Carcinus Aestuarii* from the lagoon of Venice – I. Marino, M. Gennari, F. Barbisan, P. M. Bisol, L. Zane 257

Environmental quality indexes for the lagoon of Venice – C. Micheletti, A. Critto, R. Pastres, D. Tagliapietra, A. Volpi Ghirardini, S. Gottardo, S. Chiarato, V. Zanon, C. Losso, S. Ciavatta, P. M. Bisol, A. Marcomini 263

DNA microarray analysis in *Mytilus galloprovincialis* from the Venice lagoon – L. Varotto, S. Domeneghetti, U. Rosani, A. Pallavicini, P. Bisol, G. Lanfranchi, P. Venier 269

RESEARCH LINE 3.12. Trophic chain and primary production in the lagoon metabolism

<i>Growth and net production of the seagrass <i>Nanozostera noltii</i> (Hornemman) Tomlinson et Posluzny in Venice lagoon</i> – A. Sfriso, C. Facca, S. Ceoldo	281
<i>Comparing the diatom occurrence in areas colonised by natural and transplanted <i>Nanozostera noltii</i> (hornemman) tomlinson et posluzny populations in Venice lagoon</i> – C. Facca, A. Sfriso, S. Ceoldo	293
<i>Carbon fluxes through the plankton community in the lagoon of Venice</i> – A. Pugnetti, P. Del Negro, M. Giani, F. Acri, F. Bernardi Aubry, D. Berto, E. Camatti, J. Coppola, A. Valeri	299
<i>Dimensional structure of phytoplankton community in the Venice lagoon</i> – J. Coppola, F. Bernardi Aubry, F. Acri, F. Bianchi, A. Pugnetti	313
RESEARCH LINE 3.13. Meteo-oceanographic conditions and coastal zone water quality	
<i>Post-processing of numerical model output through a neural network</i> – M. Bajo, G. Umgiesser, A. Borghesan, A. Zuliani	325
<i>Current state, scales of variability and decadal trends of biogeochemical properties in the northern Adriatic Sea</i> – C. Solidoro, M. Bastianini, V. Bandelj, R. Codermatz, G. Cossarini, D. Melaku Canu, E. Ravagnan, S. Trevisani	333
<i>Evolution of biomass, abundance and structure of plankton community in the caostal area of the north western Adriatic Sea</i> – V. Bandelj, M. Bastianini, C. Solidoro	347
<i>Classification and drivers of spatial pattern of thermohaline features of the northern Adriatic Sea</i> – G. Cossarini, S. Trevisani, V. Bandelj, S. Salon, C. Solidoro	359
<i>Biogeochemical properties in the coastal area of the north-western Adriatic Sea</i> – C. Solidoro, V. Bandelj, G. Cossarini, D. Melaku Canu, S. Trevisani, M. Bastianini	371
RESEARCH LINE 3.14. Erosion and sedimentation processes in the Venice lagoon	
<i>Preliminary experiments on tidal network growth and development</i> – L. D’Alpaos, L. Carniello, A. Defina, S. Lanzoni, F. M. Susin	385

<i>Long term morphodynamics and hydrodynamics of meandering tidal channels and ebb deltas</i> – V. Garotta, A. C. Rummel and G. Seminara	397
<i>Long-term evolution of tidal channels flanked by tidal flats</i> – A. Canestrelli, A. Defina, S. Lanzoni, L. D’Alpaos	409
RESEARCH LINE 3.15. Solid transport and circulation of the upper layers in the inlets and the coastal zone	
<i>Water and solid transport estimates through the Venetian lagoon inlets using Acoustic Doppler Current Profilers</i> – V. Kovačević, V. Defendi, F. Arena, M. Gačić, I. Mancero Mosquera, L. Zaggia, S. Donà, F. Costa, F. Simionato, A. Mazzoldi	423
<i>Surface current patterns in front of the Venetian lagoon and their variability at different wind regimes</i> – I. Mancero Mosquera, M. Gačić, V. Kovačević, A. Mazzoldi, S. Cosoli, J. D. Paduan, S. Yari	441
<i>Tidal prism variation and associated channel stability in N. Venice lagoon</i> – R. Helsby, C. L. Amos, G. Umgiesser	453
<i>The origin and transport of sand in Venice lagoon, the latest developments</i> – C.L. Amos, R. Helsby, A. Lefebvre, C.E.L. Thompson, M. Villatoro, V. Venturini, G. Umgiesser, L. Zaggia, A. Mazzoldi, L. Tosi, F. Rizzetto, G. Brancolini	467
<i>3D numerical modeling of coastal and sea-lagoon processes</i> – D. Bellafiore, G. Umgiesser	497
<i>Sediment transport simulation compared with adcp data in lido inlet</i> – F. De Pascalis, C. Ferrarin, V. Defendi, G. Umgiesser, L. Zaggia	505
RESEARCH LINE 3.16. Characteristics of the lagoon underground layer	
<i>The subsoil architecture of the Lagoon and Gulf of Venice (Italy) by very high resolution seismic surveys in shallows</i> – G. Brancolini, L. Tosi, L. Baradello, F. Donda, M. Zecchin	517
RESEARCH LINE 3.17. Transport phenomena in the hydrological cycle: model of substances release in lagoon	
<i>Flow resistance in wetlands: experimental investigations</i> – A. C. Bixio	565

RESEARCH LINE 3.18. Residence times and hydrodynamical dispersion in the Venice lagoon

A long-term model for the generation and evolution of a tidal network lagoon – G. Fasolato, C. Dall'Angelo, G. Di Silvio 579

Effects of tidal flats on tide propagation and sediment transport in tidal channels – N. Tambroni, G. Seminara 595

The dynamic simulation of the Venice lagoon and of the north part of the Adriatic Sea – M. Morandi Cecchi, M. Venturin 609

Time scales and the trapping index – G. Umgiesser, A. Cucco 621

AREA 4. Data management

RESEARCH LINE 4.2. Modeling, analysis and environmental data visualization

Improving the access to Geographic Information Systems: an integrated visual approach based on Google Earth and the Web3D – F. Pittarello 637

“La conquista della conoscenza è opera non del singolo uomo, ma della comunità degli scienziati, i quali costituiscono una società aperta di spiriti liberi, insofferente a ogni controllo esterno” - L. Geymonat (Torino 11/5/1908- Rho 29/11/1991), nel centenario della nascita

INTRODUZIONE

Pierpaolo Campostrini

Direttore di CORILA

Il sesto volume di questa serie, che proviene dalla Riunione annuale dei ricercatori CORILA tenutasi nel 2007, rappresenta un traguardo non solo di numerazione, ma riveste una caratteristica speciale, nel sostanziale completamento del secondo Programma di Ricerca intrapreso da CORILA, finanziato con i fondi per la Salvaguardia di Venezia, messi a disposizione dallo Stato italiano.

Si parla qui pertanto di Venezia e della sua laguna e delle nuove conoscenze che possono aiutare la loro salvaguardia. Peraltro, le conoscenze sviluppate nelle ricerche e qui presentate, hanno un'ampia capacità di applicazione anche in luoghi diversamente collocati dal punto di vista geografico e in temi diversi. Per quanto riguarda le discipline “ambientali”, esse contribuiscono in particolare al dominio “lagunare”, sottoinsieme dei cosiddetti ambienti di transizione e senz'altro parte dei sistemi costieri, anche se si confrontano in alcuni casi con temi e luoghi assai più generali. I risultati prodotti dalle discipline economiche sviluppate nel Programma appartengono senza dubbio all'economia dell'ambiente e considerano in particolare il campo della valutazione, che costituisce un tema emergente in tutto il mondo. Per l'Architettura era già chiaro il contributo fondamentale che lo studio delle “cose di Venezia” fornisce alla Storia dell'Arte ed alle tecniche di conservazione dei manufatti: tale riconosciuta capacità viene qui confermata e approfondita fornendo nuovi ed originali strumenti, che possono valere per molte città antiche.

Questo volume, come i precedenti, raccoglie i “riassunti estesi” di articoli che singolarmente potranno apparire nelle riviste scientifiche specializzate di settore, destinati quindi alla lettura di un pubblico molto caratterizzato per ciascuna disciplina. Senza questo volume sarebbe difficile anche per gli stessi scienziati che hanno lavorato al programma avere una visione d'insieme su quanto prodotto dai colleghi di differenti discipline, per la parte che risulta leggibile appunto da chi è in possesso di una cultura scientifica “di base” e condivisa.

E' convinzione di chi scrive, basata sull'esperienza di otto anni come direttore di CORILA e dimostrabile attraverso la lettura di queste pagine, che tale cultura scientifica condivisa sia più estesa ed approfondita di quanto normalmente ritenuto, stante la corsa alla specializzazione che tutte le scienze (quelle “dure” in particolare) hanno intrapreso con velocità crescente almeno da vent'anni a questa parte.

Nell'esperienza di tutti i Gruppi che hanno lavorato al Programma di ricerca CORILA ci sono stati diversi momenti in cui è risultato necessario al singolo ricercatore colloquiare con una disciplina diversa da quella del proprio background, per porre delle domande o fornire delle risposte ai colleghi. Credo di poter dire che non si è trattato di rapporti occasionali ed effimeri, ma di un percorso interdisciplinare che si è fatto negli anni sempre più consapevole e convinto.

Il Secondo programma di ricerca CORILA fornisce ai decisori politici ed alle Amministrazioni risposte concrete sulle domande che erano state presentate per indirizzare la ricerca: in alcuni casi vengono forniti gli elementi utili a considerare sufficientemente completo il quadro conoscitivo, in altri si fanno dei passi avanti sostanziali e si individuano con maggior precisione gli eventuali approfondimenti ulteriormente necessari, ed infine in altri ancora si delineano le prospettive delle applicazioni di nuove conoscenze.

A tali risposte la comunità scientifica si augura corrispondano altrettanto chiari interventi legislativi ed amministrativi che possano da un lato regolare più efficacemente le pressioni antropiche sull'ambiente (per esempio dalla pesca al turismo, alle emissioni industriali), dall'altro recuperare gli errori del passato (per esempio le bonifiche di Marghera), dall'altro ancora un proseguimento convinto e focalizzato dei monitoraggi ambientali, secondo un loro continuo adattamento alle nuove conoscenze e necessità. Per la città storica, il cui utilizzo ci ostiniamo a credere non sia solo quello turistico, possiamo augurarci che gli strumenti elaborati e messi a disposizione per la conservazione ed il restauro degli edifici possano essere di sostegno anche alle necessarie politiche di sostegno alla residenza dei veneziani.

Devo infine sottolineare la collaborazione di tutte le Amministrazioni pubbliche nel fornire informazioni e dati alle ricerche, anche quelli di più difficile reperibilità, segno che il nostro sforzo è compreso, ma anche che è possibile superare diffidenze e pregiudizi, laddove essi ancora permangono.

Il ruolo di coordinamento di CORILA è stato possibile grazie alla costante dedizione dei giovani che ne costituiscono lo staff, dieci persone in tutto, ed al competente indirizzo offerto dagli eccellenti componenti del Comitato Tecnico Scientifico, che qui voglio ringraziare nominandoli uno per uno in ordine alfabetico: Renata Codello, Michele Colacino, Anil Markandya, Giovanni Seminara, Pierluigi Viaroli. Parimenti fruttuosa e vieppiù necessaria è stata la vigile collaborazione del Consiglio di Amministrazione tutto ed in particolare del suo Presidente Paolo Cescon.

Devo sottolineare infine che il finanziamento di CORILA alle ricerche, nella larga maggioranza dei casi è andato al sostegno delle posizioni di giovani ricercatori, ai quali è stata offerta un'opportunità in un momento particolarmente difficile per la ricerca italiana. Anche questo è per noi un motivo di soddisfazione e un segno di speranza per il futuro di questa delicata città che deve essere capace di rinascere continuamente.

Riteniamo, in sintesi, di avere adempiuto nella sostanza al mandato ricevuto

nella Riunione del Comitato di Indirizzo e Controllo ex lege 794/84 che nella seduta del 6 dicembre 2001 che ci ha affidato i fondi per lo svolgimento delle ricerche. Esse sono qui presentate dai singoli Gruppi e dagli scienziati che le hanno eseguite, con innegabile competenza, ma soprattutto con passione ed entusiasmo.

L'attività di preparazione editoriale del presente volume è stata seguita con dedizione dalla dott.ssa Caterina Dabalà di CORILA, che merita un sentito ringraziamento.

"The conquest of knowledge it is not performed by the single person, but by the community of scientists, who constitute an open society of free minds, intolerant of any external control" - *L. Geymonat (Torino 11/5/1908- Rho 29/11/1991), in the centenary of his birth*

INTRODUCTION

Pierpaolo Campostrini

Director of CORILA

The sixth volume of this series, corresponding to the Proceedings of the Annual Meeting of CORILA's researchers, held in 2007, has a particular characteristic, as it appears at the completion of the Second Research Program, performed by CORILA with the funds given by the Italian State for the Safeguarding of Venice.

Therefore here we speak about Venice and its lagoon and how the new findings can help their safeguarding. However, the knowledge developed in the researches and presented here, can be applied even in other geographical areas and in different themes. With regard to the contributions to the "environmental" disciplines, they are addressed in particular to the "lagoons" domain, which can be seen as a subset of the "transitional environments" and is certainly part of the coastal systems, even if in some cases the results of the researches can be also compared with much more general issues and places. The findings of the economic disciplines involved in our Program belong without doubt to the "environmental economy" sector and they particularly regard the field of evaluation, which is an emerging issue all over the world. In the Architecture field, it was already clear the key contribution that the study of the "things of Venice" provides to the History of Art and to the techniques of conservation of the artefacts: this recognized capacity is here confirmed and deepened by providing new and original instruments that can be applied to many old cities.

This volume, like the previous ones, collects the "extended abstracts" of articles that individually may appear in specialised scientific journals, then intended to be read by a very specific public for each discipline. Without this volume, it would be difficult, even for the scientists who worked on the programme, to have an overall view on what produced by colleagues of different disciplines, even for the part that is legible by those in possession of a "basic" and shared scientific knowledge.

I have the firm conviction, based on the experience of eight years as director of CORILA and proved reading these pages, that this shared scientific knowledge is more spread and detailed than what generally considered, due to the race for specialization that all sciences (those "hard" in particular) have undertaken with increasing speed in the last twenty years at least. .

According to the experience of all the Groups who worked in the CORILA research programme, there have been several times when it was necessary to

the individual researcher to approach a different discipline from that of his background, to ask questions or provide answers to colleagues. I believe that these were not occasional and temporary relationships, but parts of an interdisciplinary path that has been covered with increased and convinced awareness over the years.

The Second Research Programme of CORILA provides policy makers and Administrations with concrete answers to the questions that were submitted to address the research: in some cases the useful elements to sufficiently consider the present understanding complete, are provided, in other ones substantial progress is achieved, also in order to more clearly identify the thorough analysis further needed (if any), and finally in further ones the emerging prospects of applications of new knowledge are envisaged.

The scientific community hopes that to these answers, equally clear legislative and administrative actions could correspond, on one hand able to mitigate more effectively the anthropic pressures on the environment (e.g. fisheries, tourism, industrial emissions), on the other hand able to recover the mistakes of the past (e.g. Marghera reclamation) as well as allow a continuous focus on environmental monitoring, which needs a continuous adaptation to new knowledge and techniques. For the historic city, whose destiny we obstinately continue to believe is not only in tourism, we hope that the tools developed and made available for the conservation and restoration of buildings can be also useful to the required policies for supporting the residence of Venetians.

Finally, I must emphasize the cooperation of all the Public Administrations in providing information and data useful to the researches, even those more difficult to find. This is a sign that our effort is understood, but also that it is possible to overcome mistrusts and prejudices, if they still remain.

The coordinating role of CORILA was possible thanks to the constant dedication of CORILA's staff, ten people in all, and the competent guide offered by the excellent components of Technical and Scientific Committee, that here I want to thank naming them explicitly (in alphabetical order): Renata Codello, Michael Colacino, Anil Markandya, Giovanni Seminara, Pierluigi Viaroli. Similarly fruitful and even more fundamental was the vigilant collaboration of the entire Board of Directors and in particular of its President Paolo Cescon.

Finally, I must stress that the financing of CORILA research, in the large majority of cases, has been used for supporting the positions of young researchers, who were offered an opportunity in a particularly difficult period for the Italian research. Again, this is for us a reason for satisfaction and a sign of hope for the future of this delicate city that often in the history proved to be able to continuously revive.

We believe, in short, to have fulfilled in substance the mandate received by the Committee of Address and Control (Law 794/84) which, during the meeting of December 6, 2001 has entrusted to us the funds to conduct such researches. They are presented here by individual groups and by the scientists who worked not only with undeniable skill, but above all with great passion and enthusiasm.

The activity of editorial preparation of this volume was followed with dedication by Dr Caterina Dabalà of CORILA, who deserves sincere thanks.

L'AMPLIAMENTO DELLE GALLERIE DELL'ACCADEMIA: ASPETTI STRUTTURALI

Renata Codello

Soprintendente ai Beni Ambientali e Architettonici di Venezia

Il progetto strutturale affronta due distinti temi: i nuovi interventi e il risanamento statico degli edifici antichi del complesso della Carità.

I nuovi interventi sono costituiti dalla realizzazione dei vani tecnici in cui trovano spazio il depuratore, le centrali di alimentazione degli impianti e i nuovi servizi igienici per il pubblico necessari per l'adeguamento sanitario e per l'aumento del numero di utenti. Tutte queste funzioni sono localizzate in un vano interrato sotto il cortile fra l'edificio del Palladio e quello del Lazzari. L'accesso a questi locali, soprattutto quelli di servizio per il pubblico si trova invece all'interno dell'edificio dove il progetto prevede l'inserimento di un nuovo vano scale e ascensori che giunge fino alla quota del locale interrato.

Le tecniche esecutive sono diverse a seconda che si operi all'interno delle strutture murarie antiche per realizzare i collegamenti, oppure a cielo libero. In entrambi i casi si opera, realizzando prima le paratie in calcestruzzo e dopo eseguendo lo scavo all'interno, con l'utilizzo di puntoni provvisori. Particolare attenzione sarà posta nell'esecuzione delle berlinesi di protezione all'interno delle vecchie murature. Nella prima fase si dovranno eseguire le perforazioni, i micropali ed i consolidamenti murari che dovranno permettere successivamente l'esecuzione dei diaframmi a palificata necessari per l'inserimento delle scale e degli ascensori.

Nel cortile palladiano l'esecuzione dei diaframmi ad elementi è stata progettata in modo da non creare eccessivi problemi esecutivi, salvo il delicatissimo aggettamento delle acque necessario per lo scavo e la realizzazione dei locali interrati. In questa fase si dovranno predisporre dei piezometri che possano indicare l'eventuale abbassamento della falda al di sotto degli edifici circostanti.

Il risanamento statico degli edifici riguarda tutti gli interventi necessari per ripristinare, integrare e mantenere l'efficienza statica delle strutture murarie e degli elementi in legno. Il progetto esecutivo redatto contiene un'ampia serie di schede operative redatte sull'approfondita campagna di indagini preliminari al progetto. Si è ritenuto, però, di fare un ulteriore sforzo nel definire una serie di soluzioni cosiddette "equivalenti". Si tratta di un abaco di procedure d'intervento che, a parità di costo, possono essere realizzate dall'impresa in cantiere. Vale a dire che in ragione del particolare stato di conservazione di un elemento strutturale la direzione dei lavori può decidere *ad hoc* la soluzione migliore da realizzare in opera senza che la specificità della decisione determini conseguenze organizzative e contabili nello svolgimento dei lavori. Non solo, il progetto così redatto espone dei costi calcolati sulla qualità e quantità verificata e prevedibile degli interventi, codificati in una serie di "schede", permettendo anche di ridefinire alcuni aspetti tecnici in fase esecutiva. Questo vero

patrimonio progettuale, che integra gli elaborati di cantiere, dovrebbe contribuire alla qualità di realizzazione dei lavori, alla durata degli interventi e alla loro buona manutenzione.

In sintesi, il progetto di mantenimento dei solai estende le verifiche e la definizione degli interventi al 95% della loro consistenza, così come i calcoli statici interessano tutte le travi e solai in legno.

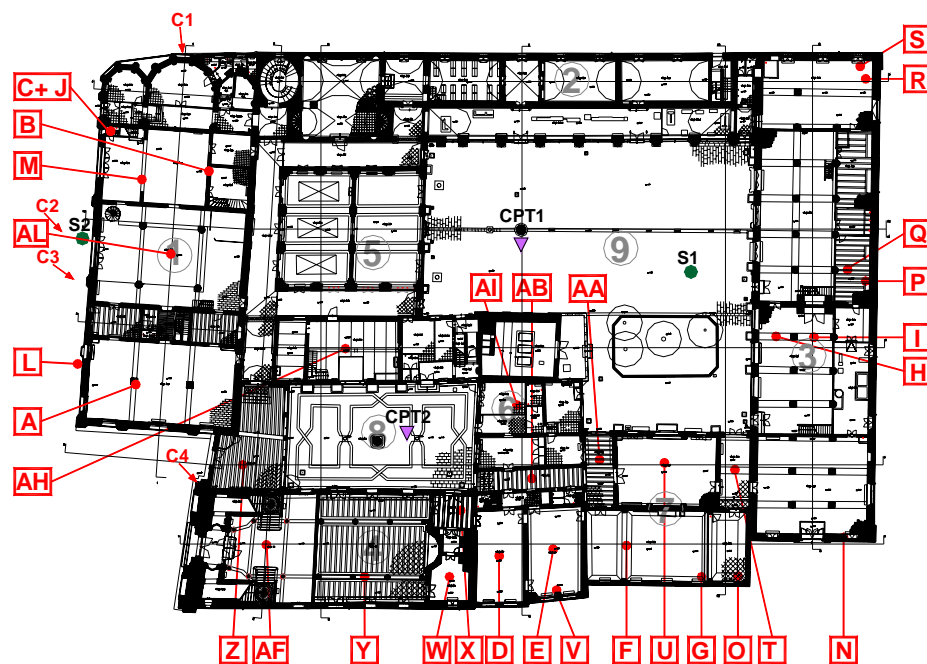


Fig 1 – La planimetria rappresenta “in lettere” le zone a cui si fa riferimento.

Di particolare interesse è il criterio di consolidamento di alcune travi a vista di antica fattura. Si tratta di dare portanza statica sufficiente con l'accoppiamento di due lame d'acciaio sagomate e brunite. Infatti, accertato che non era praticabile la soluzione con barre da sottoporre a tensione, è stata definita questa procedura d'intervento dopo aver eseguito numerosi test e verificato che il coefficiente di sicurezza raggiunge valori positivi.

La qualità delle fondazioni, pur risultando buona in tutti i saggi eseguiti, ha un grado di sicurezza piuttosto basso rispetto ai parametri teorici. Evidentemente, il costipamento naturale ha creato nel tempo, a scapito di qualche deformazione delle murature, un incremento di portanza nelle fondazioni senza tuttavia creare dissesti rilevanti.

La capacità portante delle fondazioni dirette fa riferimento ai parametri di resistenza al taglio del terreno naturale. In realtà, i tempi di costruzione molto lenti hanno fatto sì che, al disotto delle fondazioni, il terreno si potesse consolidare migliorando così le sue caratteristiche di resistenza. Un confronto qualitativo può essere fatto paragonando le resistenze a compressione monoassiali sui campioni prelevati nel sondaggio 1 (terreno indisturbato) e nel sondaggio 2 (terreno consolidato sotto il peso della fondazione). La capacità portante del terreno, al disotto delle fondazioni dirette, si può attualmente ipotizzare con riferimento ad una resistenza al taglio $C_u = 30 \div 35$ kPa; la capacità portante unitaria ammissibile diviene pertanto pari a $75 \div 85$ kPa.

Il confronto tra tensioni trasmesse e capacità portante deve quindi fare riferimento ai suddetti valori.

Si riportano alcuni dati sulle *tensioni teoriche di esercizio* calcolate sul parametro di riferimento delle *tensioni teoriche a rottura* del terreno e sul coefficiente di sicurezza conseguente.

Descrizione	Tensioni teoriche di esercizio (daN/cm ²)	Tensioni teoriche a rottura (daN/cm ²)	Coefficiente di sicurezza Δ
Basilica			
Fond. Perimetrali	1.3÷1.5 daN/cm ²	2.25÷2.55 daN/cm ²	$\Delta=1.5\div1.96$
Fond. interne a plinto	1.94÷2.32 daN/cm ²	2.25÷2.55 daN/cm ²	$\Delta= 1.16\div1.3$
Abside			
Fondazioni su pali di costipamento	2.6÷3.2 daN/cm ²	2.85÷3.3 daN/cm ²	$\cong 1$
Ed. Palladio			
Fondazioni dirette	$\cong 1$ daN/cm ²	2.25÷2.55 daN/cm ²	2.2÷2.5
Ed del Lazzari			
Fondazioni perimetrali su pali	1.65 daN/cm ²	3.3 daN/cm ²	2
Fondazioni interne a plinto	1.82 daN/cm ²	2.25÷2.55 daN/cm ²	1.23÷1.4

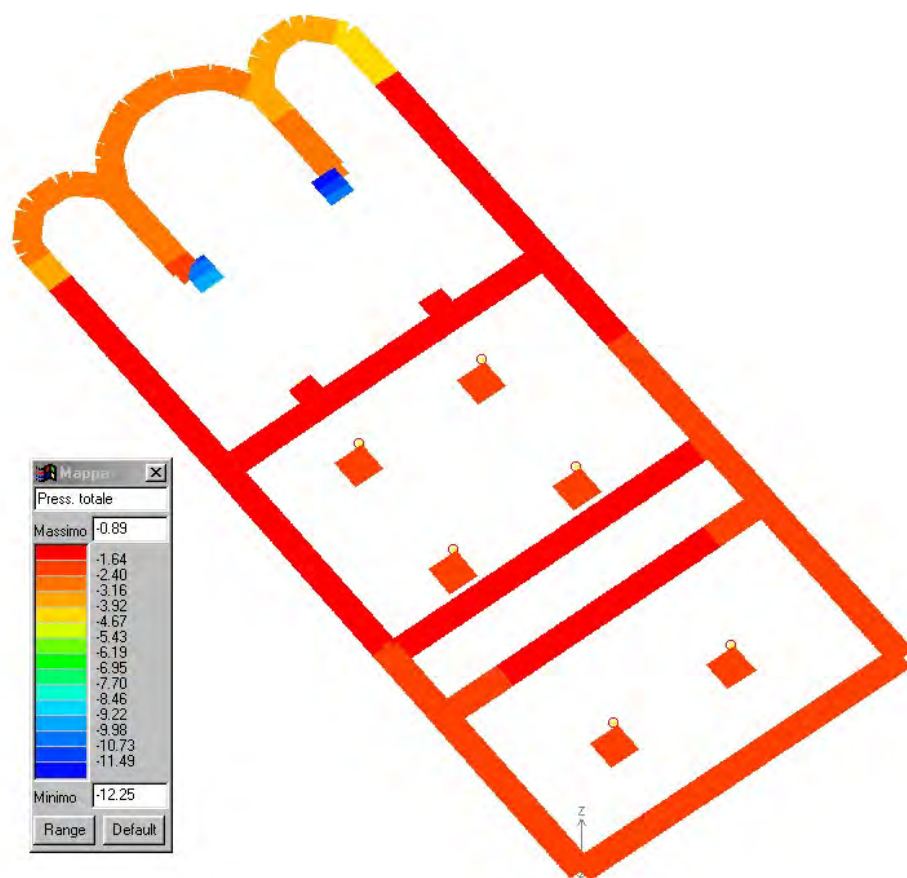


Fig 2 – Basilica: tensione sul terreno.

Il progetto prevede anche la protezione dalla alte maree per eventi di risalita dell'acqua fino a quota = +2.00 m sul livello medio mare (zero assoluto = + 0.235 m sul valore assoluto di punta della Salute).

Si è prevista una protezione impermeabile zavorrata su tutta l'area, con risvolti di vario tipo a seconda della quota del pavimento. Per capire ed individuare il tipo di intervento adottato si sono predisposte delle schede specifiche per ogni situazione allegate agli esecutivi di progetto. Infatti, in alcuni edifici quali l'antica Scuola Grande (ex aula magna della scuola d'Arte), i vani ad essa collegati e la fabbrica del Lazzari, che risultano parzialmente esposti agli eventi di alta marea da quote superiori a 1.40 m (edificio 4), 1.50 m (edificio 7), 1.70 m (edificio Lazzari), sono state predisposte protezioni speciali per il tratto interessato in altezza, non essendo possibile impiegare delle guaine a totale tenuta per la presenza di marmi o di mattoni a vista.

Appendice fotografica: il cantiere





CAN ECONOMIC SCIENCE HELP PROTECT VENICE AND ITS LAGOON?

Anil Markandya

University of Bath, UK and FEEM, Italy

Introduction

In environmental policy economics has, perhaps surprisingly, an important role to play. It allows the monetary valuation of goods and services that do not have a market value and, by combining these with other measures of value, it defines the category of **social value** or **total economic value**, which can form the basis of regulatory and investment decisions involving the environment. The difference between market values and social values is referred to as the 'externality'.

The concept of total economic value is the basis of a branch of economics known as welfare economics. The total economic value of a natural resource such as the lagoon of Venice can also be defined as made up of 'use' values and 'non-use' values. Use values in turn are made up of direct use values – e.g. the exploitation of fisheries in a water body – and indirect use values – e.g. the use of the same water body for recreational purposes. Non-use values in turn are subdivided into bequest values and existence values – i.e. values attached to a resource by people simply from the knowledge that the resource is cared for and protected.

Although this taxonomy is clear, the empirical valuation of the different categories raises some challenges for economists working on the environment. These relate to estimating the impacts of economic activities of the quality of a natural resource and in placing accurate and credible monetary values on that resource.

Notwithstanding these difficulties we have had a number of studies of the Lagoon that have produced useful valuations of the different services provided by that resources. These include values of:

- The regeneration and redevelopment of contaminated sites around the lagoon.
- Sustainable reuse of degraded lands around the lagoon
- Environmental impacts of anthropogenic activities within the lagoon
- Adaptation to climate change of sea level rise in the lagoon¹

¹ This refers to the project VECTOR, which is just starting.

Case studies

1. Regeneration and redevelopment of contaminated sites

This study has developed an instrument that values the potential from the cleanup of the sites, taking into account the economic and environmental dimensions. Especially important are estimates of the risks associated with different uses of that land. The aim is to estimate the value attached to the risk of mortality associated with a contaminated site and the changes in these values arising from improvements to the site from the cleanup. So far the first stage of this valuation has been carried out.

The surveys conducted around Venice and other cities reveal that the public is well informed on the status of contaminated sites. Furthermore it supports programs of remediation even when the costs are high and the benefits will be derived in the distant future. Their willingness to pay for the remediation programmes, however, is yet to be determined.

2. Sustainable reuse of degraded lands around the lagoon

This study has identified the following:

- The expectations of investors in these areas in terms of property rights to use the land for commercial or residential purposes and transparency in the negotiations in the property markets.
- The factors that are of concern to investors, namely the fact that rights for a particular use are often for short periods only, and on the types of industrial use that are permitted.
- The factors that are not of importance to investors. Notably they do not seem so concerned by the many constraints that may be imposed on the restoration of properties in these areas.

These findings can help the formulation of land development policy in the area, for which it is important to know what incentives are needed by investors to undertake sustainable reuse programs in the area.

3. Environmental impacts of anthropogenic activities within the lagoon

One study of interest has investigated the impact of the introduction of the Philippine clam to the lagoon, an exotic species that has had significant negative environmental impacts, especially as a result of the fishing practices employed to catch these clams. The study has estimated the damages caused by these fishing methods and the reductions in damages resulting from the adoption of more environmentally friendly methods. An important conclusion is that the benefits of reverting to traditional methods depend on the 'rate of discount' i.e. on how much we discount the future benefits from the adoption of these methods. There is also of course the question of how to compensate fishers who will lose income now if traditional methods are adopted (although they will benefit in the future). This has yet to be studied.

These examples illustrate what can be done, but much more research is needed. As far as regeneration and redevelopment of contaminated sites is concerned we need to value the residual risks associated with different uses and to understand better why public perceptions of these risks are so different (so much higher) than expert assessments. We also need to analyse the advantages and disadvantages of different methods of financing the remediation of the sites.

On the sustainable reuse of brown field sites we must bear in mind that the market values of these sites and of their development is not the same as the social value. Based on market values almost all developments would be related to tourism – hotels, restaurants souvenir shops etc. Researchers must develop models where the incentives given to developers reflect social values, based on the concepts described earlier.

The study of the clam fishery is only a beginning of the economic study of the environmental problems of the lagoon. It is necessary to extend this to other areas – naval traffic, especially the presence of cruise ships in the lagoon, non-point pollution in the lagoon etc., and to identify the tolerance thresholds of the lagoon's ecosystems to different environmental pressures. Based on these and on estimates of damages from exceeding these thresholds regulations can be designed to protect the lagoon.

Now we are facing another challenge – that of climate change in the face of which Venice must formulate a policy of adaptation. Scientists have already prepared a probabilistic assessment of local impacts based on 'Business As Usual'. The economists now need to value these impacts, taking account of the uncertainties that are present in the scenarios. Together the scientists and economists must value the impacts under different scenarios and under different adaptation measures. This will provide a benefit cost assessment of the measures that can inform policy.

Conclusions

What then is the answer to the question, can economic science help protect Venice and its lagoon? I would respond strongly to say yes, it can. Its major role is to:

- Quantify the social values associated with the changes of the lagoon's ecosystem
- Quantify the social values associated with different sustainable and non-sustainable uses of the territory.
- Develop incentives that direct stakeholders to act in a way that maximises these social values.

Some of the results obtained from work so far has been very useful but more remains to be done. The research to date has focussed on the use of land around the lagoon and less on the values of the lagoon's ecosystem itself. Within any such studies the estimation of the risks involved and the values

attached to those risks has a central role.

THE FATE OF VENICE LAGOON IN THE CENTURY OF GLOBAL WARMING: SETTLED AND UNSETTLED ISSUES

Giovanni Seminara and Nicoletta Tambroni

Dipartimento di Ingegneria delle Costruzioni, dell'Ambiente e del Territorio Università di Genova, Via Montallegro 1, 16145 Genova, Italy

Riassunto

Un'allarmante conseguenza del globale aumento di temperatura sarebbe un'accelerazione della crescita del livello medio dei mari [IPCC, Intergovernmental Panel on Climate Change, 2007]. La valutazione dell'impatto di quest'ultimo effetto sul degrado morfologico della Laguna richiede innanzitutto una profonda conoscenza dei meccanismi che controllano lo scambio dei sedimenti fra le diverse parti della Laguna e fra la Laguna ed il mare. A conclusione del Programma di Ricerca triennale del CORILA ci pare opportuno fare il punto sugli sviluppi delle conoscenze cui la Ricerca ha dato luogo e sulle questioni che restano aperte.

Abstract

Scientists seem to agree that a most alarming consequence of the ongoing process of global warming might be an accelerated sea-level rise [United Nations Intergovernmental Panel on Climate Change, IPCC, 2007]. Evaluating the impact that this effect might have on the progressive loss of wetlands experienced in the last century by Venice lagoon, is not an easy job, which calls for a deep understanding of the exact nature of the mechanisms controlling the exchange of sediments among the different parts of the lagoon as well as the long term loss of sediments experienced by the lagoon. At the conclusion of the Research Project funded by CORILA, it appears useful to attempt assessing the development of knowledge in the field, as well as further research needs.

1. Introduction

Scientists seem to agree that global warming is a process of increasing significance. One of the most alarming consequences of such a process would be an accelerated sea-level rise. According to the United Nation's Intergovernmental Panel on Climate Change [IPCC, 2007] the increase in sea-level rise in the next century may be so large as to threaten many of the world's coasts, lagoons, estuaries and river deltas, where the increasing vulnerability to inundation is accompanied by a progressive deterioration of the natural defences against flooding, i.e. barrier islands and wetlands. This is also the case of Venice Lagoon, where, after years of controversies, a vast complex of structures aimed to protect Venice from high waters is now under construction.

2. Impact of sea level rise on the defence of the city of Venice from high waters

Formulation

It is well known that the defence system under construction in Venice consists of a series of gate barriers that will normally lie on the bottom of each of the three inlets and will be lifted up during high water events. Management of the MoSE (MOdulo Sperimentale Elettromeccanico) system is flexible enough to cope with the problem of high waters in various ways. As the gates are all independent, the defence strategies may in principle be designed adopting various options, depending on the characteristics and scale of the tidal event: the simultaneous closure of all the inlets, the closure of one or two inlets only, or the partial closure of each inlet. It is then of some interest to ascertain whether the adoption of an appropriate strategy would allow to cope with the effects of global warming with the foreseen scenarios of climate change: bearing in mind that the aim is to guarantee a satisfactory defence of Venice and of the neighbour lagoon islands from high waters as well as to minimize the impacts of gate closure on the port activities and on the quality of the lagoon environment.

Let us then define our envisaged scenarios. The data recently published by IPCC [2007] show that the *mean sea level rose* at an average rate of 1.8 (1.3 to 2.3) mm per year from 1961 to 2003. The rate was faster between 1993 and 2003, about 3.1 (2.4 to 3.8) mm per year. Whether the faster rate from 1993 to 2003 reflects decadal variability or an increase in the longer-term trend is unclear. However, the increase in the rate of the observed sea level rise from the 19th to the 20th century can be taken as an established fact.

IPCC-2007 also provides estimates of the projected globally-averaged surface warming and sea level rise at the end of the 21st century [2090–2099] relative to the period 1980–1999 for different emission scenarios. Each IPCC scenario refers to a different but equally possible development of the driving forces of climate change, including population growth, socio-economic development, land use and energy sources. However, as stated in the report, “no scenarios assume implementation of the United Nations Framework Convention on Climate Change or the emissions targets of the Kyoto Protocol”. Hence, in this sense, all the IPCC predictions may be intended as quite conservative.

The Report concludes that the best estimate of sea level rise for the more favourable scenario is 0.28 m (with an uncertainty range likely assessed between 0.18 and 0.38 m), while the best estimate for the worst scenario is 0.43 m (with an uncertainty range between 0.26 and 0.59 m).

Along with sea level rise, *subsidence* will contribute to variation of the relative land elevation. It is well known [Gatto and Carbognin, 1981] that, during the last century, the relative elevation of Venice has decreased by 0.23 m, including 0.11 m of sea-level rise and about 0.12 m of land subsidence, both natural (0.03 m) and anthropogenic (0.09 m). Anthropogenic subsidence was mainly the result of the progressive and intensive depletion of artesian aquifers. Once the impact of this activity has come to be properly understood, drastic measures to

strongly reduce [groundwater](#) pumping were taken. Since 1970 a very rapid recovery of the pressure in the aquifer system has been obtained, and the ensuing subsidence has quickly slowed down. Currently, only a residual subsidence of about 0.4 mm per year is left [Leatherman and Kershaw, 2001].

Hence, if we account for both the effects of sea level rise (averaging roughly 0.43 m according to the worst IPCC scenario) and of ground sinking due to subsidence, we can reasonably assume that, in one of the most unfavourable scenarios, Venice relative elevation could decrease roughly by 0.5 m before the end of the 21st century. Though aware of the uncertainty of these estimates, in the following we investigate the major consequences of such a relative sea level rise on the frequency of flooding of the city of Venice.

To gain some insight on this problem, it is sufficient to employ the simplest model of inlet hydrodynamics recently formulated by Tambroni and Seminara [2006]: the three Venice inlets are modelled as straight rectangular channels of length L , constant width B , flat and fixed bottom, connecting a closed basin (the portion of the lagoon drained by the inlet) with an open sea subject to the imposed tidal free surface oscillation h_1 .

Geometrical parameters and sediment size typical of the Venice inlets are reported in Table 1.

Since the length scale characteristic of each basin as well as the lengths of inlet channels are small compared with the tidal wavelength, the hydrodynamic formulation is based on the assumption that the free surface in the basin is effectively horizontal. Employing a 1D approach to investigate the tide propagation in the inlet channels, Tambroni and Seminara [2006] show that the temporal development of the free surface oscillation h_2 in the basin and the instantaneous cross-sectionally averaged velocity U at the inlet can be easily derived from the solution of the following differential equations:

$$h'_1 - h'_2 = \delta_1 \frac{d^2 h'_2}{dt'^2} + \delta_2 \frac{dh'_2}{dt'} \left| \frac{dh'_2}{dt'} \right|; \quad U' = \frac{dh'_2}{dt'}. \quad (1)$$

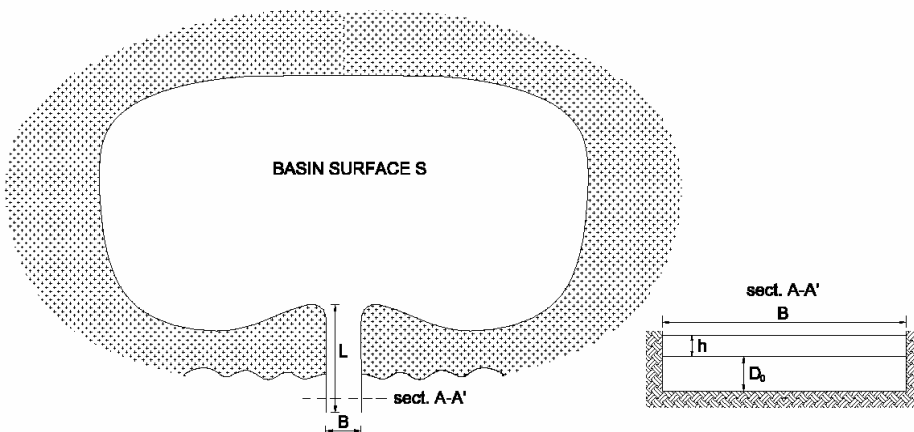


Fig 1 – Sketch of the model of the system sea-channel-lagoon and notations.

Tab 1 – Geometrical parameters and sediment size for Venice inlets.

INLET	Lido	Malamocco	Chioggia
L[m]	4500	3000	2000
S[10 ⁸ m ²]	1.55	1.30	0.82
D ₀ [m]	8.99	14.4	8.5
B[m]	900	500	570
d _s [mm]	0.08-0.20	0.25-0.30	0.10-0.20

In (1) the variables have been made dimensionless as follows:

$$t' = \omega t \quad , \quad (h'_1; h'_2) = \frac{(h_1; h_2)}{a_0} \quad , \quad U' = \frac{U}{U_0} \quad (2)$$

and the parameters δ_1 and δ_2 read

$$\delta_1 = \frac{U_0 L \omega}{g a_0} \quad , \quad \delta_2 = \frac{U_0^2 L}{g a_0 C_0^2 D_0} \quad , \quad (3)$$

with

$$U_0 = \frac{S a_0 \omega}{B D_0} \quad , \quad (4)$$

having denoted by C_0 a characteristic scale for the flow conductance, by U_0 the characteristic scale of the average channel velocity and by D_0 the mean inlet depth. Finally, ω is the angular frequency of the tidal wave and a_0 its characteristic amplitude, while S is the surface area of the basin drained by each inlet and g is gravity.

Frequency of high waters

As a first exercise let us consider the sequence of tidal oscillations recorded in the years 1994-1998 by the CNR gauge station located in the sea region adjacent to Venice Lagoon. Simulations have been carried out assuming the present mean sea level and the 2100 scenario, characterised by 50 cm sea level rise.

At present, it has been established that gate closure at the inlets will be activated for tides higher than 110 cm as this is the level up to which Venice will be protected at completion of the so called 'Insula Project', consisting of construction works aimed at raising quaysides and paving. These works enable to reduce the number of gate closures to a minimum (roughly 3 times per year, see Fig. 2). If we assume that no other complementary work to further raise up the banks and pavements is undertaken in the next century, the 2100 scenario is obviously characterised by a greater number of alerting events (corresponding to roughly 10% of the total time).

Let us then estimate to what extent the already discussed main characteristic of the MOSE system, namely its high flexibility, may help reduce the actual time in a year the lagoon has to be kept isolated from the Adriatic Sea. Mobile barriers consist of 8 independent floodgates at Chioggia inlet, 19 gates at Malamocco

and 41 at Lido.

Many different defence strategies, involving closure of one inlet at a time rather than partial or alternate closure of each inlet, may be envisaged depending on the characteristics of the tidal event. However, the analysis of all the possible management strategies of the mobile barriers is outside our goals and is left to those who will be in charge of managing the gate system. Here we are simply interested in showing that the time duration of complete temporary isolation of the lagoon from the sea can be drastically reduced by choosing different strategies of gate closure.

As shown in Figure 3, in the 2100 scenario, the number of hours in a year when the water level exceeds the safeguarding threshold of 110 cm, decreases from roughly 860 employing an “all the inlets closure” strategy, to 400 (L) , 570 (M), 250 (C) employing one of the three possible “two inlet closure” strategies. If the safeguarding threshold is increased to 120 cm, then the closure durations become 390 (all inlets closed), 300 (L) , 225 (M), 190 (C) hours respectively. Finally, if the threshold elevation for closure activation were increased to 125 cm (thus allowing for a short period of inundation of the city), then the closure durations would become 250 (all inlets closed), 90 (L), 140 (M), 50 (C) hours respectively. In the latter case Venice would be inundated for a total time amounting to 210 (L), .85 (M), 140 (C) hours respectively.

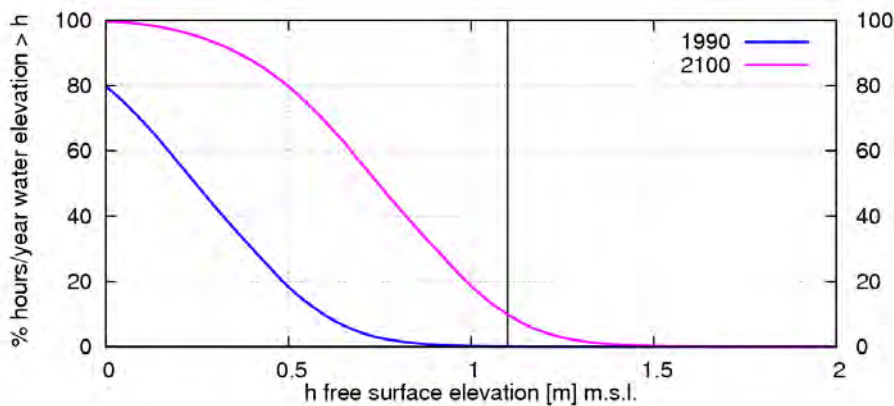


Fig 2 – Percentage of time the water elevation in Venice has exceeded a given value in 1990 and corresponding value which would be experienced in 2001 under the assumption of 50 cm relative sea level rise.

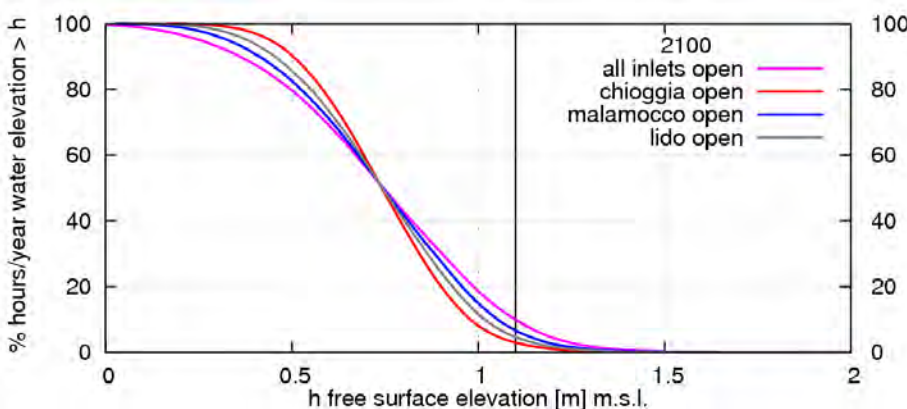


Fig 3 – Percentage of time the water elevation in Venice would exceed a given value in 2001 under the assumption of 50 cm relative sea level rise and for different closure strategies.

In other words, it is not necessary to keep the lagoon completely isolated from the sea during all the alarming events: one out of the three inlets may be safely

kept open for roughly 60% of the emergency hours in a year (30% by increasing the safeguarding threshold) without diminishing the degree of safety achieved. The choice of the most appropriate strategy will obviously depend on a variety of factors, mostly navigation, which will have to be carefully analyzed. The implications in terms of the impact of such measures on water quality, morphological degradation and biodiversity will also have to be fully investigated.

3 Lagoon Morphology and sea level rise

In many low-lying coastal areas, the increasing vulnerability to inundation associated with sea level rise and subsidence is accompanied by a progressive deterioration of natural defences against flooding, i.e. barrier islands and wetlands. The coast of Louisiana is a major example, as the lesson of Katrina has clearly shown. A second important example is Venice. Here, the lagoon environment is threatened by a morphological degradation displayed by the loss of a consistent portion of the salt marsh area throughout the last century. Why has this happened?

Note that salt marshes are characterized by the presence of halophytic vegetation and of microphytobenthos, which play a major role in controlling the dynamics of intertidal flats and marshes [e.g. Allen, 2000]. In fact, on one hand vegetation affects the hydrodynamics, increasing friction and opposing resuspension: marshes function essentially as sinks for suspended sediments. Vegetation is also a producer of organic material known to contribute significantly to marsh building. A quick glance at the recent history of Venice lagoon then suggests that part of the degradation process is likely to be of *anthropogenic* origin: major rivers discharging into the lagoon were diverted by Venice Republic in the Renaissance to prevent siltation; jetties have been constructed at the lagoon inlets starting from the mid XIX century in order to deepen the inlet channels and allow for steam navigation. The amount of mineral sediments supplied to the lagoon has obviously decreased as a result of these actions. This is very well known. However, examples are known [Redfield 1965, 1972] of salt marshes which have been able to adjust their elevation to sea level rise for as long as 4,000 yr through deposition of mineral sediments and production of organic matter, such to maintain an elevation of the marsh platform within the intertidal zone close to the mean high tide (MHT) [Krone, 1985]. Why has Venice lagoon been unable to adjust to a relative sea level rise which has not been dramatically high in the last century? And is the degradation process bound to continue to the extent that Venice lagoon will transform into Venice bay? In order to clarify these points, two major steps are required. A deep understanding of the exact nature of the mechanisms controlling the **long term net sediment balance** in the whole lagoon is preliminarily needed. Next, a clear understanding of the processes controlling **the redistribution of sediments among the various components of the lagoon** (namely channels, tidal flats and salt marshes) is required.

Below, we attempt to provide a brief state of the art review of some recent and relevant contributions concerning the subtle interplay among hydrodynamics,

geomorphology and ecology which control the above mechanisms. It turns out that considerable progress has been obtained in the last decade, thanks to the efforts of various research groups, many of them funded by CORILA. However, a number of major unresolved issues are still left and call for further research if the consequences of the predicted sea level rise are to be seriously assessed.

3.1 Assessing the long term net sediment balance in Venice lagoon

Various mechanisms control the long term net sediment balance in estuaries and lagoons. Let us review some of them

3.1.1 Sediment availability

A first mechanism is obviously associated with *sediment availability*. In the absence of fluvial supply, the availability of *mineralogenic* sediments depends crucially on the amount of sand and silt exchanged between the lagoon and the Adriatic sea, with minor contributions supplied from the drainage basin.

Some insight on the mechanics of the sediment exchange through tidal inlets has been recently provided by the work of Tambroni and Seminara [2006]. In order to be able to estimate with a non prohibitive numerical effort the net exchange of sand associated with a sequence of tidal events recorded in the Adriatic Sea for periods of the order of decades, the latter Authors, employed the simple hydrodynamic model outlined above. Once the hydrodynamics was known, an estimate of sediment exchange was readily achieved assuming that the sediment supply equals the transport capacity of tidal currents during both the flood and the ebb phases. The total sediment load was evaluated at each instant of time throughout the tidal cycle using Engelund and Hansen's [1967] predictor. Despite its simplicity, this model provides interesting suggestions concerning the physical processes governing sediment loss in Venice lagoon.

The major observation arising from results (Fig. 4) is that the yearly loss of sand from Venice Lagoon, ranges approximately about 50,000 m³, hence about an order of magnitude smaller than the overall loss of sediments usually claimed [MAV-CVN, 2002]: hence, the major contribution to the yearly sediment loss from Venice Lagoon cannot be simply associated with the exchange of the sand available in the bed close to the inlets, amenable to transport either as bed load or as suspended load. Also, the net sand exchange displays a repetitive seasonal dependence, being invariably positive (entering the lagoon) roughly in winter and summer. This estimate was also shown to be only slightly affected by the sand supplied to tidal currents through wave resuspension in the far field, whose **short term effect** is to store sediments in the near-inlet region.

The following scenario was then envisaged in order to explain the total loss of sediments experienced by the lagoon. Loss is likely associated with the very fine material resuspended by wind storms in the shallow regions of the lagoon. A part of these sediments is fine enough to be transported by tidal and wind currents as 'wash load': in other words, it may be unable to settle within the lagoon but rather carried by ebb currents to the inlets where the ebb jets advect

it far enough from the inlets to be deposited or further transported along shore by littoral currents. The feasibility of the above interpretation has been qualitatively substantiated by Tambroni and Seminara [2006] on the basis of field measurements of the typical grain size distribution and depth averaged concentrations of sediments resuspended by wind in the shoals, along with evaluations of the ebb water volume yearly exchanged with the sea. The water volume exchanged annually with the sea is of the order of $2 \cdot 10^{11} \text{ m}^3/\text{yr}$: sediment volumetric concentrations of the order of 5 p.p.m. would then be sufficient to drive a yearly loss of very fine sediments of the order of 10^6 m^3 .

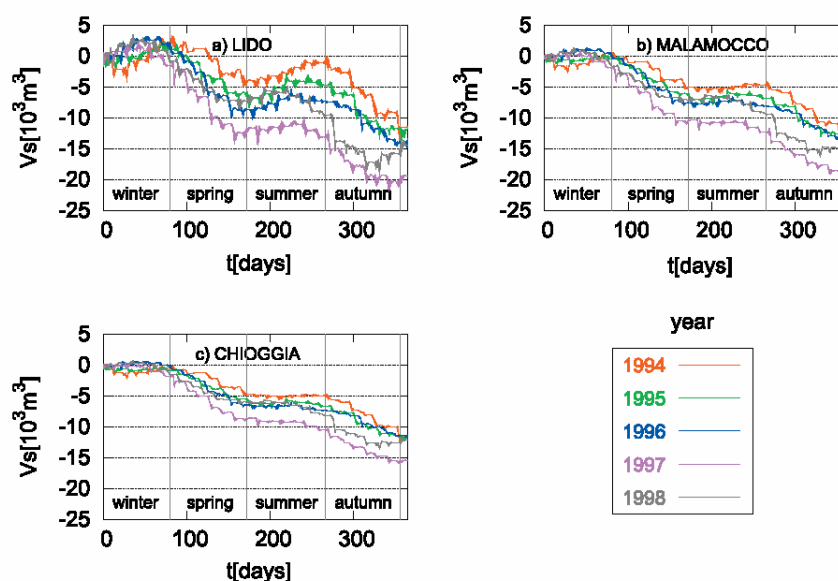


Fig 4 – Temporal evolution of the net volume of sand exchanged through (a) Lido, (b) Malamocco, and (c) Chioggia inlets in the years 1994–1998.

Various developments of this idea have followed since. Before we discuss some of them, it is of interest to ascertain how the above picture would change as a result of *sea level rise and land subsidence*. Let us then perform the same exercise presented above, assuming a relatively sea level rise of 50 cm. It emerges that the yearly loss of sand from Venice lagoon would be reduced by an amount ranging about 15% with respect to the value calculated assuming the present sea level (Fig. 5). This result is not surprising as the first effect of sea level rise is an increase of inlet depth which, as shown in Figure 6, implies a decrease of the inlet velocities, hence a decrease in the sediment transport capacity.

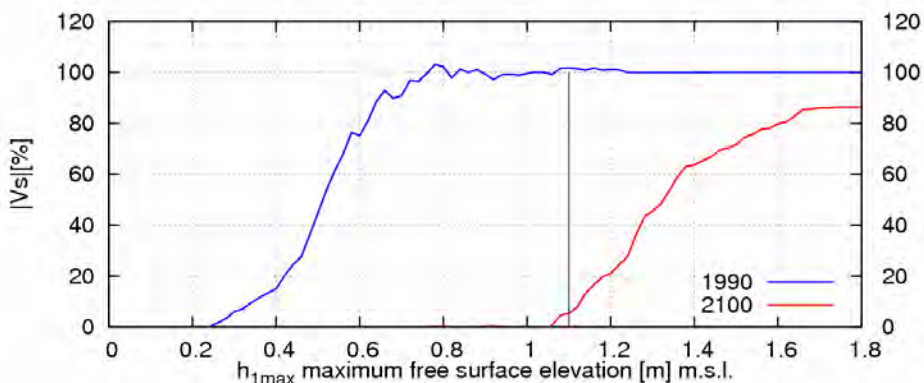


Fig 5 – The average percentage volume of sand yearly lost to the sea in the period 1994–1998 is plotted as a function of the maximum free surface elevation experienced by the corresponding events (blue line). The same calculation has also been performed assuming 50 cm of sea level rise (red line).

On the other hand the ebb volume of water exchanged with the sea increases only slightly in the 2100 scenario. This notwithstanding, significant impact on the loss of very fine sediments could result from:

- variations induced on wind resuspension of fine sediments in the shoals;
- variations induced on the ability of tidal currents as well as of wind currents to advect sediments.

Detailed measurements as well as theoretical understanding of wind driven sediment resuspension in the inner lagoon is needed. Some progress in this respect has been recently made and is discussed below.

A second source of sediment supply is associated with *organic sediments*. Their availability depends on sewage disposal, industrial wastes and lifecycle of small living organisms (e.g. mollusc shells), fairly minor contributions which do not depend on sea level rise. Different and more delicate is the issue of *production* of *organic sediments* in salt marshes. This is discussed below.

3.1.2 Sediment production

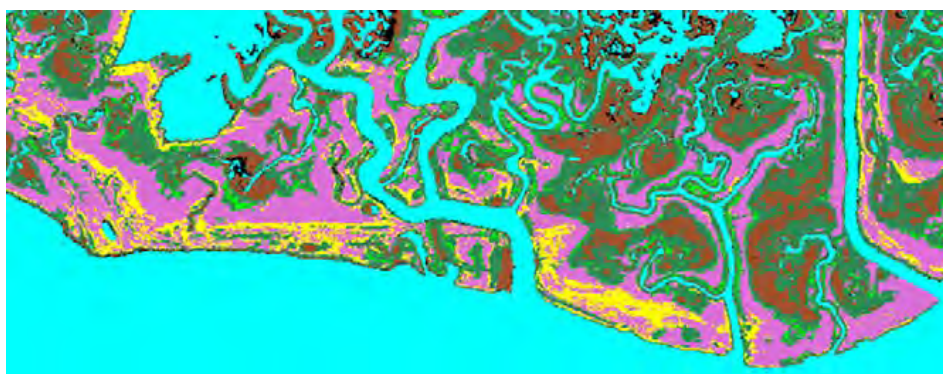
Halophytic Vegetation

As pointed out above, it has long been recognized that halophytic vegetation exerts fundamental controls on marsh dynamics. Besides opposing resuspension, vegetation is also a producer of organic material known to contribute significantly to marsh building. Below, we denote by B the annually-averaged spatial density of biomass associated with above-ground halophytic vegetation, a quantity which will be measured in kg m^{-2} . In order to discuss the mechanisms whereby vegetation ‘produces organic sediments’, the first ingredient preliminarily needed is the ability to characterize the spatial distribution of different vegetation species in the intertidal area. This is a subject which has received enormous impetus from the recent development of remote sensing techniques, as demonstrated by the interesting developments pursued by the CORILA group led by Prof. Marani. In particular, the important observation that species organize themselves into zones [Pignatti, 1966] strictly linked with distance from the channel network and marsh elevation has been confirmed [Silvestri, 2000, Silvestri et al., 2000]. Moreover, the latter Authors

observe that some species, like *Puccinellia palustris*, *Inula crithmoides* and *Suaeda maritima*, are found mostly along the edges of creeks and channels, while *S. maritima*, *Limonium narbonense* and *Juncus maritimus* do not exhibit any preferential sites. Moreover, the frequency of occurrence of different species exhibits a clear dependence on soil elevation: only *Juncus maritimus* does not seem to be clearly correlated with any elevation range. The Figure 6 shows a map of vegetation in San Felice salt marsh drawn by Marani et al. [2003] using the so called SAM [Spectral Angle Mapper, Kruse et al., 1993] classification.

Silvestri et al. [2000] also show that an identical sequence of vegetation species is encountered, as soil elevation increases, in different salt marshes of the Venice lagoon, but a given species is found at preferential elevations which are not identical in distinct marshes. Hence, no unique correlation appears to exist between the presence of halophytic vegetation species and submersion periods, a result which modifies a quite consolidated traditional view.

Fig 6 – SAM [Spectral Angle Mapper, Kruse et al., 1993] classification of San Felice salt marsh [after Marani et al., 2003]. The classes are: *Spartina maritima* (dark green), *Limonium narbonense* (purple), *Sarcocornia fruticosa* (yellow), *Juncus* spp. (light green), soil (brown) and water (blue).



Growth and decay of halophytic vegetation

Since the production of organic sediments is naturally and strictly connected with the amount of biomass available in the marsh, it is then preliminarily necessary to be able to predict the growth and decay of vegetation.

The above ground production of vegetation depends on several factors, most notably the elevation of marsh platform relative to MSL (which controls flood frequency and soil salinity, Morris 1995) and evapotranspiration (which also affects soil salinity). Within the intertidal range, Pomeroy et al. [1981] observe that primary production of *Spartina alterniflora* is characteristically greatest at the lowest elevations of the salt marsh range (depth between 40 and 60 cm below MHT in the salt marsh investigated by Morris et al. [2002] (Fig. 8). At larger hypoxic depths, growth of *Spartina alterniflora* decreases and macrophytes are progressively replaced by unvegetated, tidal mudflats. Morris et al. [2002] point out an important feature of their observations, namely that “.. there is an optimum marsh elevation for coastal wetland productivity...”. The latter varies regionally as well as with tidal range.



Fig 7 – Sketch and notations for marsh dynamics (MHT= mean high tide elevation, MSL= mean sea level).

The existence of both upper and lower limits of elevation for the productivity \dot{B} of *Spartina alterniflora* as well as the dependence of \dot{B} on the depth D of the marsh platform below MHT (see Fig. 7) was approximated by Morris et al. [2002] through the relationship:

$$\dot{B} = a D + b D^2 + c \quad (5)$$

with a , b , and c site specific coefficients.

The Authors note that the equation (5) “..... satisfies the ecological principle that a plant’s distribution will span a range of tolerance to an abiotic variable, like flooding depth, with an optimum somewhere in the middle of the range.....”

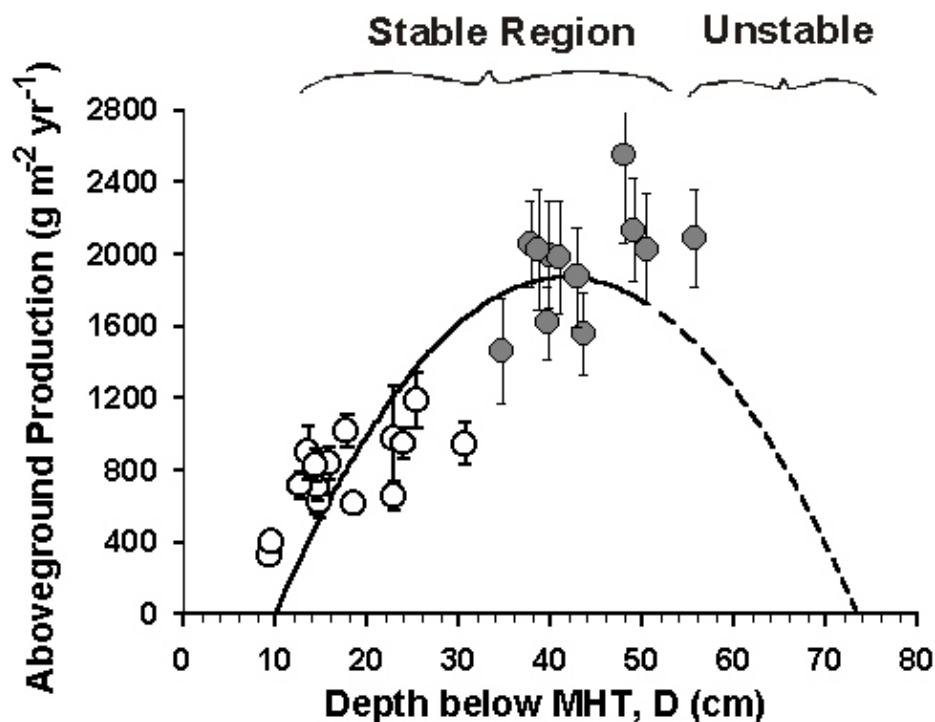


Fig 8 – Correlation between the observed productivity of the salt marsh macrophyte *Spartina alterniflora*, measured annually since 1984 [Morris 2000] and depth below mean high tide (MHT) of sites in the high (○) and low marsh (●). The line shows the equilibrium correlation predicted by Morris et al. [2002] in the stable (—) and unstable (----) regimes (corresponding to the values $a = 155$, $b = -1855$ and $c = -1364$ in the equation (5)).

Recently, Marani et al. [2007] have employed a logistic model [Levins, 1969] to describe the dynamic of vegetation. Having denoted by p the vegetation fractional cover and by d the maximum biomass density (such that $B=p d$), the latter Authors write:

$$d p/dt = r(z) p (1-p) - m(z) p \quad (6)$$

with z elevation relative to MSL, and $r(z)$, $m(z)$ elevation-dependent reproduction and mortality rates, respectively. Moreover, in the *Spartina Alterniflora* dominated case, both the reproduction rate and the mortality rate

are assumed to vary linearly with elevation, the former decreasing from 1 year⁻¹ to 0.5 year⁻¹, the latter increasing from 0 to 0.5 year⁻¹. We are not aware of the substantiation that the latter model might have received in the plant physiology literature. However, we note that the equation (6) has some non obvious implications. Firstly, it does not allow for the possibility that vegetation can grow from no previous existing vegetation through the dissemination of propagules. Secondly, it assumes that vegetation has a maximum production rate at MHT ($z=H$ in the notations of the Authors), contrary to observations which suggest that production vanishes at MHT, while it does not consider the lower range where productivity decreases progressively (Fig. 10). Thirdly, it assumes that vegetation has a maximum mortality rate at MHT, where vegetation is not present, while it does not consider the lower range where it is likely that mortality increases progressively due to the increasing effects of hypoxia.

Production of organic matter

An attempt to quantify the various contributions to the production of organic matter based on field observations performed on various marshes of Venice lagoon has been performed by Day et al. [1999]. These Authors considered both the aboveground biomass (*leaf*, B) and the belowground biomass (*root*, B_{bel}). The productivity of each of them was estimated in terms of (a) net primary production; (b) leaf litter production during the growing season, (c) leaf litter production at the end of the growing season/beginning of the dormant season, (d) root litter production and (e) root to shoot ratio. Belowground production was assumed to be a function of aboveground biomass. Litter production was calibrated to reflect field measurements [Scarton and Rismondo, 1996].

Based on unpublished data of F. Scarton the latter Authors were able to perform some estimates of the *densities of production rates of organic matter* (both aboveground q_{ab} and belowground q_{bel}) in various marsh areas where different species prevailed (Tab. 2).

Elev. (cm)	Species	q_{ab} (g m ⁻² yr ⁻¹)	q_{bel} (g m ⁻² yr ⁻¹)	Max B (g m ⁻²)	Max B_{bel} (g m ⁻²)
30–40	<i>Arthrocnemum Fruticosum & Halimione portulacoides</i>	666	1378	766.9±285.3	3496±2171
20–30	<i>Limonium serotinum & Puccinellia palustris</i>	307	1368	512.8±252	3421±1999
10–20	<i>Spartina maritima & Limonium serotinum</i>	311	932	662.4±304.7	2221±1778
0–10	<i>Salicornia sp</i>	307.2±106.9	100	307.2±106.9	100

Tab 2 – Estimates of densities of production rates of organic matter (both aboveground q_{ab} and belowground q_{bel}) in various marsh areas of Venice lagoon where different species prevail [from Day et al., 1999].

The ratio q_{ab} / q_{bel} appears to be quite variable: Allen [2000] defines the latter ratio as 'unpredictable' and quotes reported variations in the range 0.25 – 3.3 , for the widely studied case of Spartina. The Table above shows that a similarly wide range can be estimated for other species in Venice lagoon.

An old proposal [Randerson, 1979] for the marsh accretion rate $(dz/dt)_{org}$ associated with the production of organic matter (both above- and below-ground) is the relationship $(dz/dt)_{org} = \gamma B$. Marani et al. [2007] employ the latter relationship with $\gamma \approx 2.5 \cdot 10^{-3} \text{ m}^3 \text{ kg}^{-1} \text{ year}^{-1}$. For values of B in the range 0-1 kg m^{-2} , it leads to values for $(dz/dt)_{org}$ in the range 0- 2.5 mm/year. Day et al's [1999] estimates fit reasonably Randerson's [1979] relationship for the case of Spartina. Other species appear to be up to four times more productive (in fact the constant $10^3 \gamma$ attains the values 4.5 ; 9.1 ; 3.1 ; 2.2 for the species investigated by Day et al's [1999]). It thus follows that biomass production may, at least in principle, be sufficient to counteract the effect of sea level rise even in the absence of significant supply of mineral sediments.

In order to clarify the respective roles of mineral deposition and organic production, the mechanisms of sediment redistribution among different portions of the lagoon need be investigated in depth. In this respect, it proves instructive to consider a sequence of model problems in which attention is focused on a single element of the lagoon 'puzzle' with the adjacent elements playing the role of boundary conditions to be suitably modeled. This is discussed in the next sections.

3.2 Sediment redistribution in lagoons: inlet equilibrium

The first model problem: inlet stability

Some insight on the problem of inlet stability can be achieved using the approach of Tambroni and Seminara [2006] previously outlined, in which the inlet is the element on which attention is focused, while the lagoon and the sea are modelled through the boundary conditions discussed in sect. 1. Assuming a simple M2 forcing tide characterized by an amplitude a_0 equal to 0.5 m, a value fairly typical of tidal events in the Adriatic Sea close to Venice inlets, Tambroni and Seminara derived the dimensional dependence of the maximum value of the inlet velocity in a tidal cycle on the inlet depth. This is plotted in Figure 4 for values of the relevant parameters appropriate to each of Venice inlets. Each curve displays a peak. For the value of the tidal amplitude chosen to construct Figure 4 the peak value of U_{max} is associated with a value of the inlet depth D_c smaller than the value presently experienced by that inlet. This is an important observation. In fact, as pointed out by Marchi [1990], while the branch of the curve corresponding to values of $D > D_c$ describe *stable conditions*, the branch of the curve corresponding to values of $D < D_c$ describes *unstable conditions* (reduction of the flow depth is then associated with a reduction of the flow speed, hence with a decreased sediment transport capacity which encourages deposition and a further reduction of the inlet depth). Lido inlet appears to operate very close to the peak of the curve (Fig. 9); hence, the present results suggest that the danger of inlet siltation may be brought up by a relatively small

reduction of the inlet depth. Indeed, as shown in Figure 10, a tendency to inlet siltation has already been detected at both Lido and Chioggia.

Fig 9 – The maximum speed at each of Venice inlets is plotted versus the inlet depth for a pure M2 forcing sea oscillation with amplitude $a = 0.5$ m.

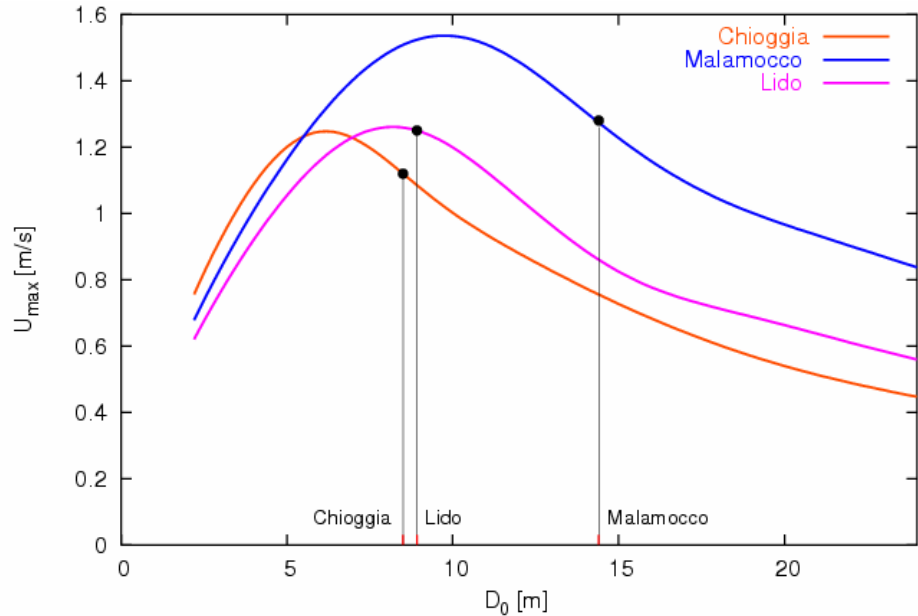
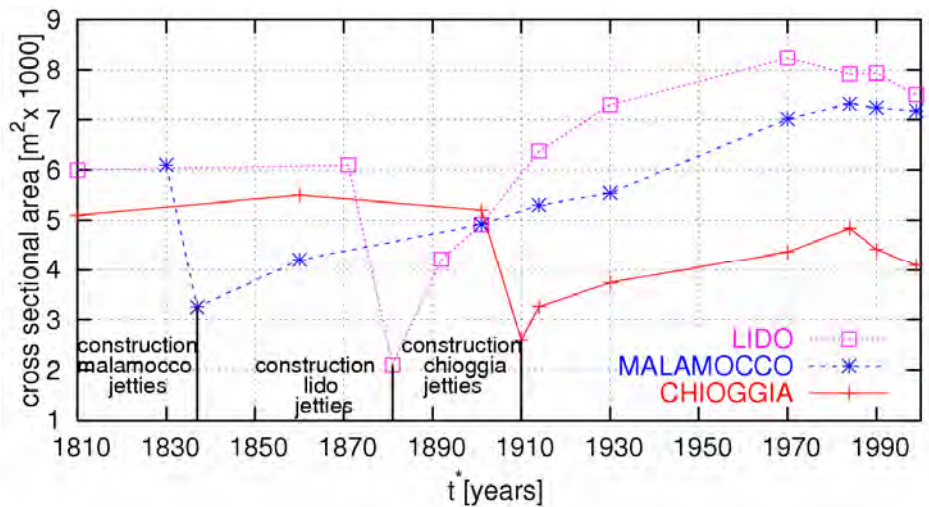


Fig 10 – Temporal evolution of the cross-sectional area of each of Venice inlets (data from MAV-CVN [2002]). Following an erosion process undergone since the construction of the jetties for more than one century, around 1990 the inlets have reached a state of temporary equilibrium. Lido and Chioggia inlets have then overcome this temporary equilibrium state and display a tendency to siltation, probably encouraged by the sand supplied by flood currents overloaded by wave resuspension in the far field.



Tambroni and Seminara [2006] have also estimated to what extent the availability of sand resuspended in the surf zone, i.e. in the far field, may modify the supply of sand to the inlet in the flood phase. To this aim the flood currents were modeled as plane irrotational, an assumption, which simplified the treatment considerably. Laboratory observations on both mobile and fixed bed models of tidal inlets [Blondeaux et al., 1982, Tambroni et al. 2005a] provide some support to the latter approach. The main conclusions reached in the latter work can be summarized as follows. The *role of sediment supply from the sea is to store sediments in the near inlet region*. Lido inlet is obviously more prone to deposition due to the pronounced progradation of the northern coast, compared with Malamocco inlet, which is less exposed to the sediment supply from the sea, being located farther from the shoreline and less exposed to

littoral currents. On the contrary, *the amount of sand exchanged between the lagoon and the sea in the short term is not significantly affected by the sediment supply in the far field*: the stream can only transport through the channel the amount of sand which it is able to entrain as bedload and suspended load with its hydrodynamic characteristics. *Enhancing the sediment supply from the sea by modifying the inlet shape and location would drive inlet siltation and would affect the inner lagoon only in the long term* when aggradation would significantly propagate landward.

In fact, it should be noted that the depth at the inlet is ultimately controlled by the net sediment flux supplied from the sea, which in turn depends on wave climate and on inlet shape. Let us see how.

- i) If supply is in excess of transport capacity at the inlet, then the inlet tends to silt up, flow depth decreases and an aggradation wave propagates inward, eventually aggrading the whole channel until the inlet depth has decreased enough (moving along the stable branch of the curve in Fig. 9) for transport capacity to balance supply. Of course, any inlet is characterized by a maximum transport capacity: if supply exceeds this value the inlet continues to silt up jumping into the unstable branch of the curve of Figure 9: the lagoon continues to silt up and eventually disappears.
- ii) If supply is in defect of transport capacity at the inlet, then the inlet tends to deepen, flow depth increases and an erosion wave propagates inward, eventually degrading the whole channel until the inlet depth has increased (still moving along the stable branch of the curve in Fig. 9) such that the decreased transport capacity is able to balance supply. Of course, if supply vanishes, then erosion continues until the inlet speed has lowered to the point that no sediment transport is allowed any longer.

If the above picture is correct, then the effects of the construction of inlet jetties become obvious. Narrowing the inlets through the construction of the inlet jetties has increased their total transport capacity. This is readily understood noting that the maximum speed at the inlet may be written [Tambroni and Seminara, 2006] as follows:

$$U_{\max} = \psi(\delta_1, \delta_2) \frac{S \omega a_0}{BD_0} \quad (7)$$

where the coefficient ψ is a function of the dimensionless parameters δ_1 and δ_2 , plotted in Figure 11 for a pure M2 forcing tide with amplitude $a_0 = 0.5\text{m}$.

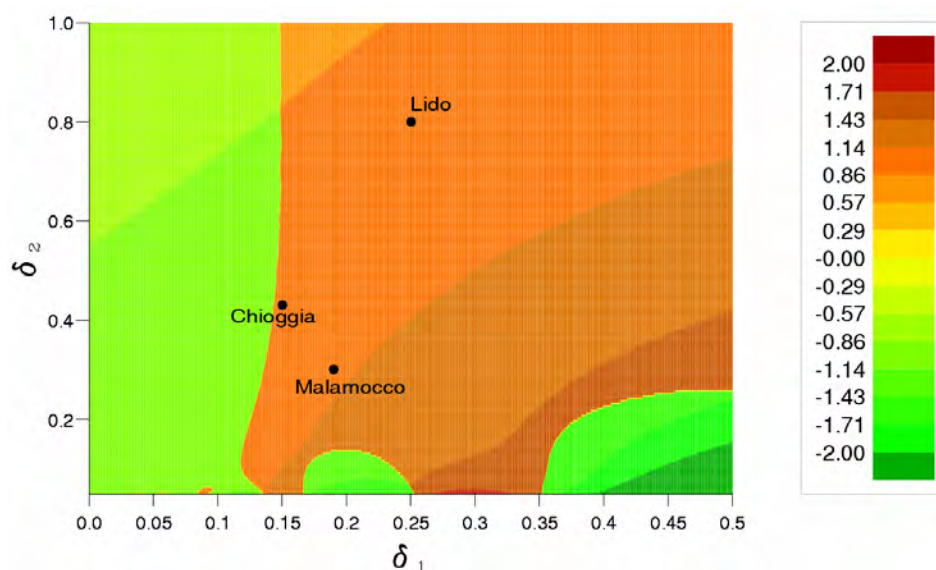


Fig 11 – The coefficient Ψ of the inlet speed relationship (7) is plotted as a function of the dimensionless parameters δ_1 and δ_2 for a pure M2 forcing tide with amplitude $a_0 = 0.5m$.

Hence, a reduction of inlet width, gives rise to an increased value of the inlet speed. Since the transport capacity of the inlet current per unit width is proportional to a power of flow speed with exponent, say n , larger than 1 (ranging roughly between 3 and 5), a reduction of inlet width leads to an increased total transport capacity (proportional to $n-1$). On the other hand, the supply from the sea did definitely decrease, at least initially, as a result of the inlets having been moved from the shoreline farther into the sea. Hence, the inlets have operated in regime ii) (described above) since the construction of the jetties and only recently they have reached a state such that the average supply (increased as a result of beach progradation at Lido) roughly balances the total transport capacity (see Fig. 10).

Impact of different closure strategies on inlet stability

Having suggested the temporary closure of just one or two inlets as a possible closure strategy, it may then be of some interest to get some insight on the implications of the above actions in terms of inlet stability. To examine this issue, we will employ the same approach used before, adding a simple, albeit somewhat severe, mathematical approximation, consisting of distributing the surface area S of the portions of the lagoon drained by the closed inlets among the adjacent open inlets. (the whole S is attributed to the open inlet if two inlets are closed, the area drained by Chioggia (Lido) is attributed to Malamocco if only Chioggia (Lido) inlet is closed, half the area drained by Malamocco is attributed to Lido and half to Chioggia, if only Malamocco is closed).

The maximum flow velocity at Chioggia when all the inlets are open is plotted in Figure 12a as a function of the local depth. The curves obtained for the case of Malamocco closed and both Lido and Malamocco closed are reported in the same Figure to allow comparison. Figures 12b and 12c display analogue plots for Malamocco and Lido inlets, respectively.

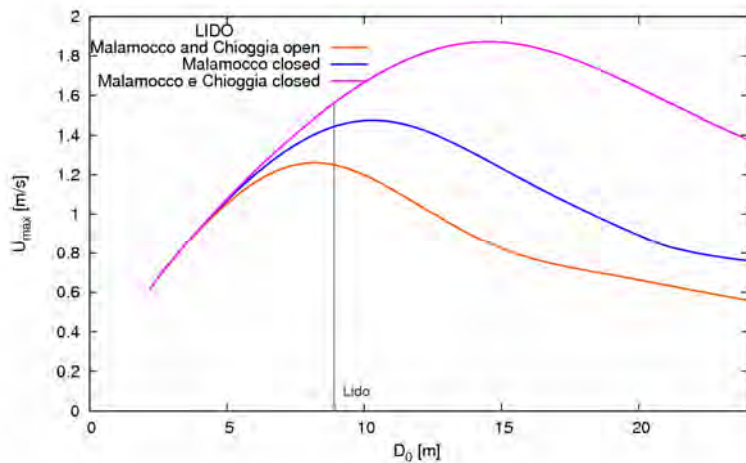
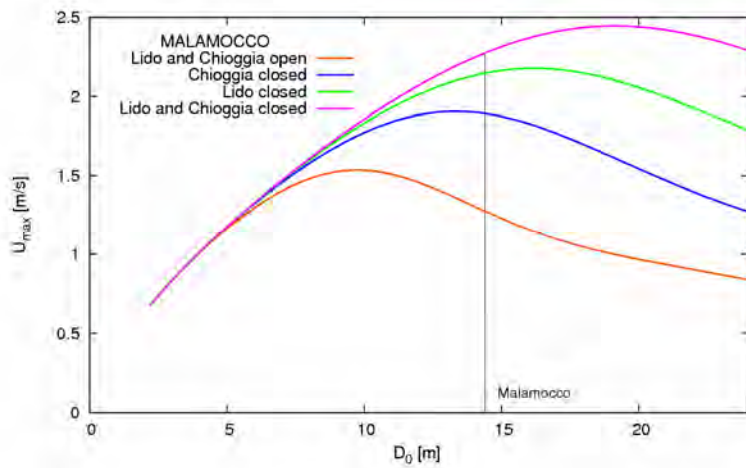
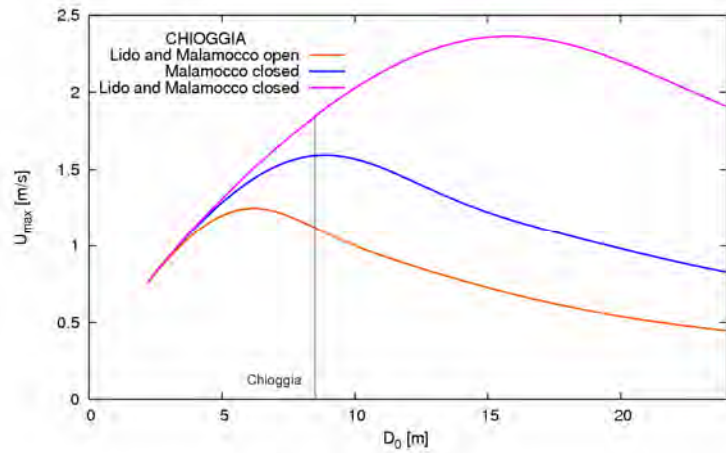


Fig 12 – Maximum velocity at (a) Chioggia, (b) Malamocco, and (c) Lido plotted versus depth. The red line refers to the case of all inlets open. The blue and green lines refer to the closure of only one inlet, while the purple line refers to the closure of two inlets.

Results may be summarized as follows:

- The first obvious consequence of inlet closure will be an increase of the velocity in the inlets kept open.
- Secondly, the closure of two out of three inlets leads to a progressive transition of the operating conditions of the open inlet towards the unstable

branch of the curve.

These results have significant implications. In fact, an increase of inlet velocity induces an increase in the sediment transport capacity, hence a tendency of the stream to erode, i.e. to increase its depth. The inlet regime then changes, moving towards the unstable branch of the curve such that an increase of inlet depth drives a further increase of the flow speed. In other words, a progressive process of inlet deepening is temporarily established in the open inlet when the remaining two inlets are closed. The impact of this increase of inlet speed on inlet navigation as the long term effect of the enhanced erosive capacity of the streams will have to be carefully evaluated. The latter effect may turn out to contribute to counteract the tendency to siltation displayed by Lido and Chioggia inlets thus reducing the need for the dredging operations presently required in order to maintain the inlets deep enough to allow for navigation.

3.3 Sediment redistribution in lagoons: channel equilibrium

The second model problem which proves instructive is the morphodynamic evolution of a tidal channel connected to a tidal sea with no tidal flats and no marshes. Here, *attention is focused on the channel*, while the inlet and the inner lagoon play the role of boundary conditions. This simplest model has been investigated theoretically by Lanzoni and Seminara [2002]. Laboratory experiments have been performed by Tambroni et al. [2005a]. Several lessons have been learnt from these studies.

Essentially, starting from a channel with given width, length and lateral convergence, for given sediment size and tidal forcing, an initially flat bottom profile evolves, through the slow propagation of a sediment wave, into a sloping profile deepening at the inlet and aggrading landward to the extent that the bed emerges and a shore develops. Eventually, the bottom reaches equilibrium conditions characterized by vanishing net sediment flux in a tidal cycle at any cross section and weak sediment transport everywhere. Note that the timescale T_m of the process reproduced in the laboratory is of the order of thousands of tidal cycles, hence years in the prototype: field observations reported in Figure 10 exhibit a time scale of the order of decades.

At equilibrium, a submerged channel develops in the near inlet region and a tidal delta forms as a result of sediment deposition near the inlet. A plot of the laboratory observations as well as of the 2-D numerical simulations performed by Tambroni et al. [2005b], showing the equilibrium pattern of the submerged outer channel and tidal delta, is reported in Figure 14. While 2-D modeling appears to be able to capture the gross features of flow and bed topography, however it also appears to be unable to reproduce the formation of large scale eddies as well as meso-scale bedforms, at least in the context of the present numerical simulations.

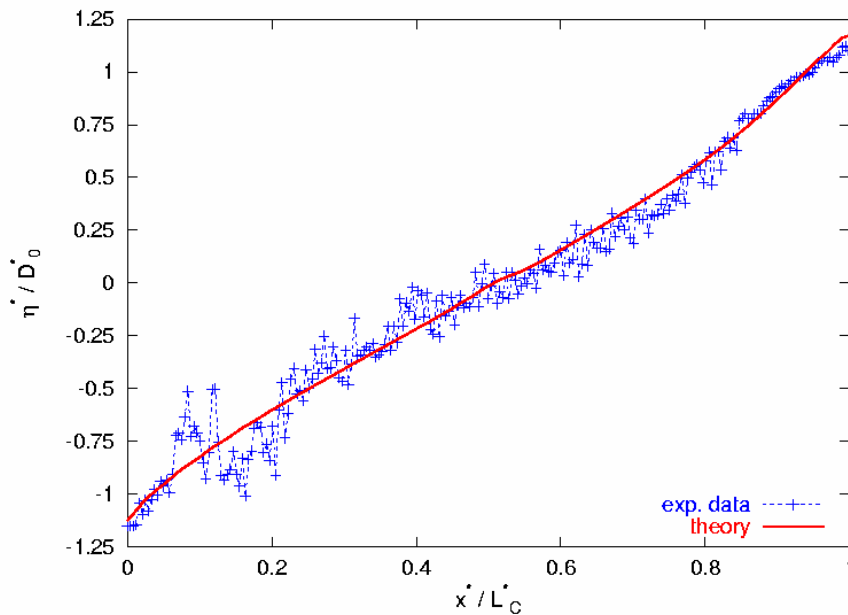


Fig 13 – Equilibrium of the bed profile reached after 2000 tidal cycles in the laboratory experiments of Tambroni et al. [2005a] and comparison with the theoretical results of Lanzoni and Seminara [2002]. Note that the initial bed profile was horizontal with $\eta = 0$. Oscillations around the equilibrium profile are associated with large and small scale bedforms observed to develop throughout the experiment.

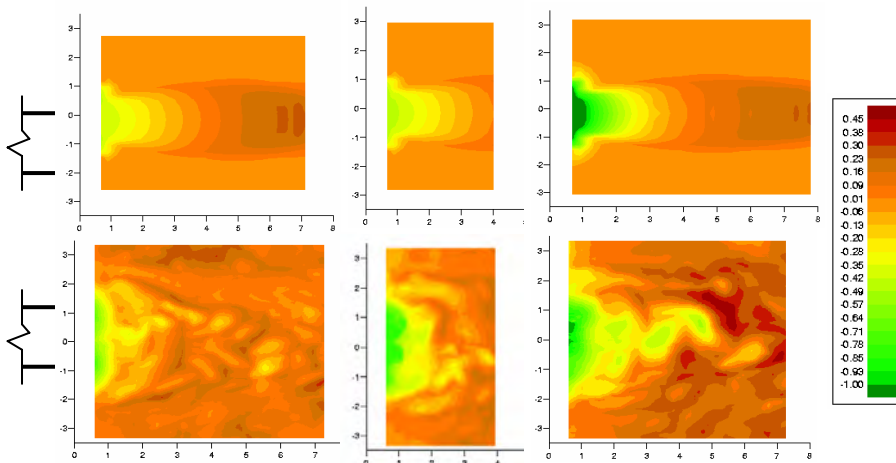


Fig 14 – Morphodynamic evolution of a tidal inlet: laboratory observations [Tambroni et al, 2005a, below] and numerical simulations [Tambroni et al., 2005b, above] a) 20 cycles; b) 80 cycles ; c) 200 cycles. Quotes are scaled by the inlet depth at equilibrium.

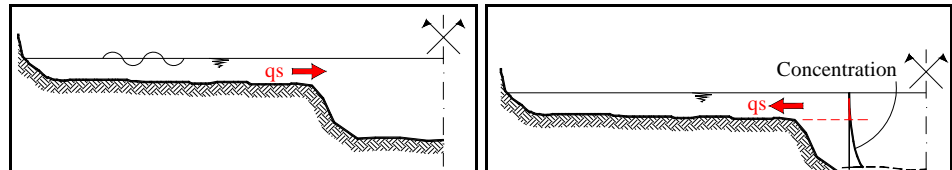
3.4 Sediment redistribution in lagoons: tidal flats

The *third model problem* is the investigation of the morphodynamic equilibrium of a tidal channel with adjacent tidal flats, but still no marshes. The addition of flats exchanging sediments with the channel reveals a number of novel effects. It proves instructive, in this respect, to distinguish between two cases: in the former, no wind acts on the free surface; in the latter wind dominates.

The first case: no wind acts on the shoals

Some insight on the former case (Fig. 15) can be easily achieved, starting from the hydrodynamics [Tambroni and Seminara, 2007]. Firstly, for a given channel length, as a result of the presence of tidal flats, the flow velocity (*hence the transport capacity*) in the channel is typically increased. Secondly, the flow field in the channel, which is typically flood dominated in the absence of tidal flats, becomes *ebb-dominated* for sufficiently wide flats, the more so as the flat width

Fig 15 – Sketch illustrating the exchange of sediments between channels and tidal flats: in the flood phase (a), sediment is exported from the channel, while the opposite occurs during the ebb phase (b): net export occurs in the absence of significant wind action.



During the flood phase, sediment is exported from the channel, while the opposite occurs during the ebb phase. In the absence of wind, the balance between the latter effects depends in a fairly delicate fashion on the geometry of the shoals, most significantly on flow depth and bottom roughness: in fact, the concentration in the upper part of the channel stream is small but non zero, while ebb currents in the shoals are not typically able to resuspend significant amounts of sediments. The exchange of sediments from the channel to the shoals during the flood phase tends to form along the shoal margins natural levees which are also clearly detectable in the field (see Fig. 16).

The case of no wind acting on the shoals is however of relatively little interest for Venice lagoon which, morphologically speaking, is wind-dominated.

The stirring effect of wind acting on the shoals

Let us briefly summarize some of the available knowledge.

Starting from the simplest case of small amplitude Stokes waves in shallow depth. The ability of a Stokes wave to resuspend sediments is naturally related to its ability to produce turbulence. This occurs in the Stokes boundary layer adjacent to the erodible bed. However, the flow regime in the boundary layer may be laminar or turbulent, depending on the values attained by two parameters: the *Reynolds number* $R_E (= a U_{1m} / \nu)$, with a and U_{1m} amplitudes of the displacement and velocity oscillations of the free stream) and the *relative roughness* k_N / a (with k_N equivalent sand roughness of the bed). In the absence of bedforms and vegetation, k_N may be taken as equal to $(2.5 d_{50})$ with d_{50} average grain size. What conditions prevail in the shoals? Consider a typical wind wave with a period T ranging about 2 s and a height H , say of 0.2 m, propagating on a shoal with depth D , say, of 1 m, and erodible silty bed with d_{50} ranging about 50 μm (see Fig. 19). This wave will have wavelength $L \cong T \sqrt{gD} \cong 6.3 \text{ m}$, amplitude of velocity oscillation of the free stream $U_{1m} = \pi H / [T \sinh(kD)] \cong 26 \text{ cm/s}$, amplitude of displacement oscillation of the free stream $a = TU_{1m} / 2\pi \cong 8.5 \text{ cm}$, Reynolds number $R_E \approx 22500$ and relative roughness $a/k_N \approx 678$. Under these conditions the boundary layer would be *laminar!*

Hence, estimating the correct value of the equivalent roughness appears to be crucial. The latter is likely enhanced by the presence of microvegetation, and microphytobenthos: note that the equivalent roughness must be at least an order of magnitude larger than assumed above in order to reach values of (a/k_N) small enough to induce transition to rough turbulent conditions. In the absence of precise information, let us consider an equivalent roughness in the range 1-10 mm such that $a/k_N \approx (8.5 - 85)$. The maximum shear stress induced on the bottom under these conditions can be written in the form: $\tau_{\max} = f_w \rho U_{1m}^2 / 2$ with f_w wave friction coefficient, a function of (a/k_N) which can be expressed in the form appropriate to small values of (a/k_N) [Kamphuis, 1975], namely $f_w = 0.4 (a/k_N)^{-0.75}$ ($a/k_N < 50$). Hence, f_w falls roughly in the range $(1.3 - 8.) 10^{-2}$. With the above estimates, one finds values of τ_{\max} in the range $(0.43 - 2.72)$ Pa. Correspondingly, the thickness δ of the turbulent boundary layer, which can be estimated by the relationship $\delta = 0.09 k_N (a/k_N)^{0.82}$ ranges about 5 - 3 mm assuming for the equivalent roughness k_N the value 1 mm.

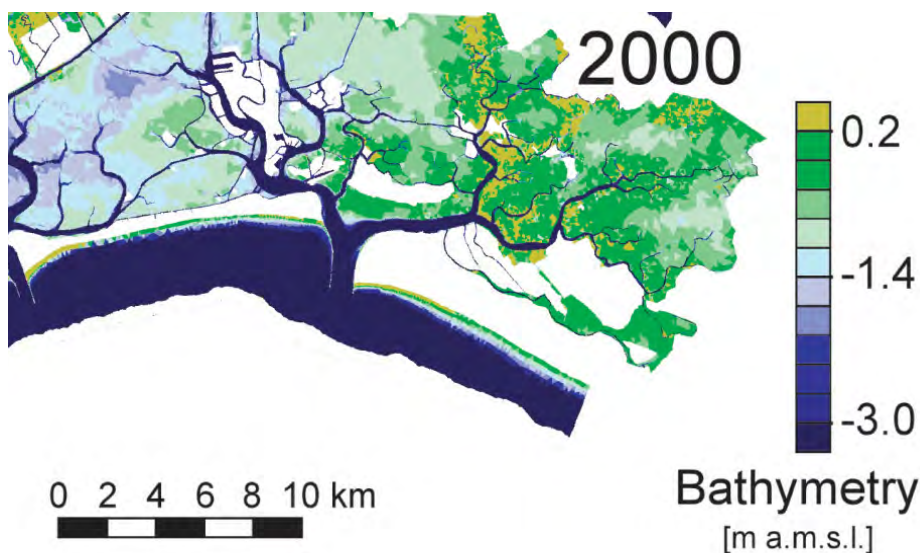


Fig 16 – The pattern of bathymetry from a survey of 2000 performed in the northern lagoon of Venice [from Marani et al., 2007]: note the presence of natural levees bounding the lagoon channels. Also note the asymmetry often displayed by the levees on the two sides of the channel.

Recalling that the critical stress for bottom erosion is strongly dependent on the nature of the bed surface (e.g. the presence of stabilizing polymeric bio-films produced by benthic microbes [Paterson, 1989; Amos et al., 2004]), it emerges clearly that a better understanding of the structure and size of bottom roughness is crucially needed in order to reach definite conclusions about the ability of wind waves to resuspend sediments.

Further need for developments arises when one attempts to estimate the direction (!) and the *intensity of sediment flux*. In fact, several features are yet to be fully understood.

Firstly, it is unclear whether or not small scale bedforms form during the tidal cycle. Ripples are known to form on sandy beds subject to wave propagation, as long as the peak Shields stress does not exceed a value ranging about 0.8. Assuming a value for d_{50} equal to 50 μm , one readily shows that ripples would form for values of the peak bottom stress which do not exceed $\tau_{\max} = 0.66$ Pa.

This is sufficiently small to suggest that small scale bed forms are likely to be the exception rather than the rule. In other words, the bed can be assumed morphologically 'plane' and sediment transport occurs in the form of the so called 'sheet flow'. Extrapolating results of Fredsøe et al. [1985] one readily ascertains that the volumetric concentration of sediments entrained in the boundary layer (where turbulence occurs) peaks near the bed where it assumes maximum values $C_{b\ max}$ in the wave cycle of the order of 0.1 and average in the wave cycle around 35-50 % of the peak. Moreover, the average concentration decays to 10% of the peak at a distance of the order of 10 times the equivalent roughness (i.e. few centimetres). Hence, depth averaged concentrations of the order of 10^{-4} are to be expected. Does this fit the available observations? Indeed, the Figure 17 confirms such expectations in the range of wind speeds 8 – 10 m/s.

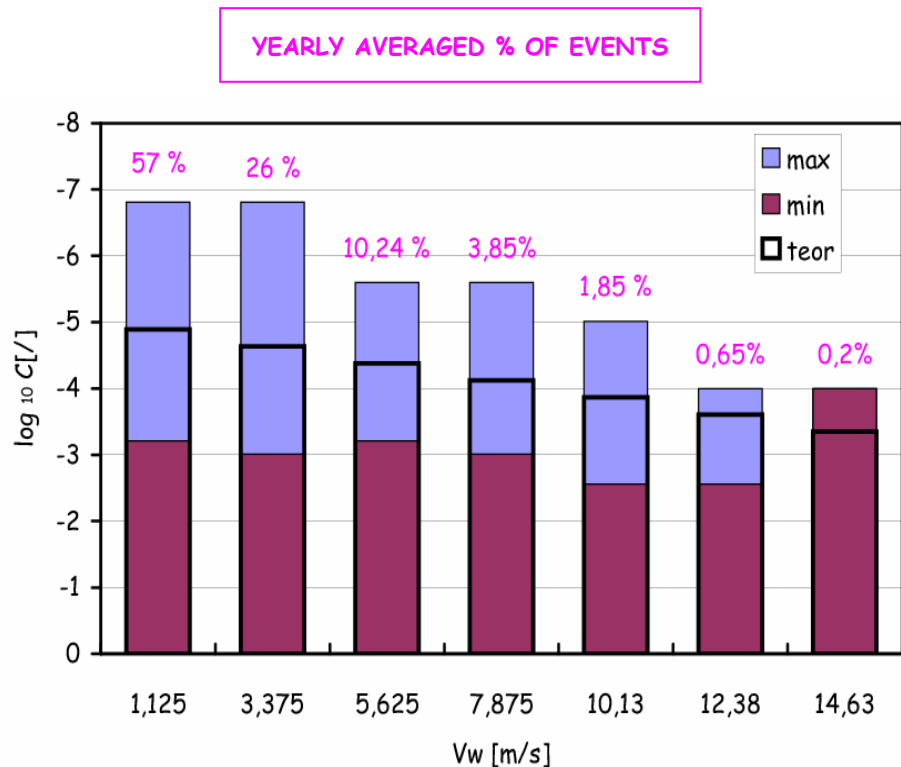


Fig 17 – Correlation between wind intensity and concentration of sediments resuspended in the shoals: field observations performed at various sites of Venice Lagoon [MAV, 1992].

The sediment flux associated with this distribution of concentration has two distinct contributions.

- i) The first contribution is associated with the *effect of tidal currents*: and has the direction of tidal currents. Moreover, since the logarithmic distribution is such that, for the typical configuration described above, the speed at a distance from the bed $z/k_N \approx 10$ ranges about 0.6 times the depth average speed U , a rough estimate of the order of magnitude of the sediment flux per unit width is $(10^{-4} q)$ with $q = U D$: in other words, the flux of sediments resuspended by non breaking wind waves and advected by tidal currents through the shoals is roughly 4 orders of magnitude smaller than the fluid flux!

-
- ii) The second contribution is due to the effect of currents *driven by wind stress and wind setup*. In fact, it is well known that the wind stress acting on the free surface of a basin, besides generating wind waves, gives rise to a surface setup leading to sloping of the free surface in the direction opposite to the wind: as a result, a counter-flow is generated which superimposes on the Couette type flow driven by the wind stress. The resulting flow has the wind direction close to the free surface and the opposite direction close to the bed. Since sediment concentration is highest close to the bed, it follows that the average sediment flux driven by the wind setup is directed against the wind. For values of the wind speed of the order of 10 m/s, the return current has speed of the order of few (2-3) cm/s, hence the return flux (of the order of 2.5 cm³/m-s) is comparable with (though somewhat smaller than) the flux advected by tidal currents: with one major difference, though: that its direction is constant (provided the wind direction does not vary).

The above picture is still somewhat simplified.

In fact, firstly we have ignored the effects of *wave nonlinearity* as well as of *wave breaking*. While the turbulence generated by spilling breakers is not likely to contribute significantly to sediment entrainment, however turbulence spreading by diffusion may contribute to keep particles in suspension longer than settling and advection would allow. Ascertaining the importance of this effect will require special attention.

Secondly, wind wave generation is a highly complex phenomenon investigated mostly in deep seas. The amplitude of wind generated waves in shallow waters is spatially dependent and is mainly controlled by *wind intensity* and *available fetch* (the length of the region where wind has been able to act). Moreover, a number of additional effects play a role in the process: energy transfer from the wind, energy spreading through non linear interactions, frictional dissipation, breaking. The *wind field is also spatially non uniform*, due to the presence of obstacles, such as islands. The picture is seen to be complex enough to discourage superficial attempts to model the process.

In the engineering literature, commercial codes (e.g. SWAN), originally developed to model the spatial development of wave spectra from deep to shallow seas, have been recently employed [Umgiesser et al., 2004; Carniello et al, 2005; Fagherazzi et al, 2007] to estimate the distribution of wind waves generated by severe atmospheric events in Venice Lagoon.

The complexity of the process also suggests the opportunity to take advantage of field observations. A fairly interesting example of field experiment performed in shallow lakes under carefully controlled conditions is due to Young and Verhagen [1996] (but see also Breugem and Holthuijsen [2007]). The main result of the above investigation, of relevance for our problem, is the dependence of the significant wave height H and wave period T on the available fetch x . Further denoting by D the flow depth and by U_w a uniform wind speed the dimensionless form of such a dependence is found to read:

$$\frac{H}{U_w^2/g} = 0.17 \left\{ \tanh A_1 \tanh \left[\frac{B_1}{\tanh A_1} \right] \right\}^{0.87} ; \quad (8 \text{ a, b})$$

$$\frac{T}{U_w/g} = 7.518 \left\{ \tanh A_2 \tanh \left[\frac{B_2}{\tanh A_2} \right] \right\}^{0.37}$$

where

$$A_1 = 0.493 \left(\frac{D}{U_w^2/g} \right)^{0.75} ; B_1 = 3.13 \cdot 10^{-3} \left(\frac{x}{U_w^2/g} \right)^{0.57} \quad (9)$$

and

$$A_2 = 0.331 \left(\frac{D}{U_w^2/g} \right)^{1.01} ; B_2 = 5.215 \cdot 10^{-4} \left(\frac{x}{U_w^2/g} \right)^{0.73} \quad (10)$$

For a representative shoal with depth $D = 1 \text{ m}$, uniform wind speed U_w of 10 m/s , it turns out that the wave height would reach its asymptotic fully developed state ($H = 0.2 \text{ m}$) within a distance of roughly 10 Km and would not exceed half that value if the fetch were decreased from 10 Km to 1 Km . This observation may turn out to play a quite important role when attempting to design suitable measures to counteract the morphological degradation of Venice Lagoon. In fact, recalling the estimate of bottom stress made above, if the wave height is halved (say $0,1 \text{ m}$) and the period is decreased to $1,5 \text{ s}$, one finds that $U_{1m} = 12 \text{ cm/s}$ and $a = 2.82 \text{ cm}$. Using Kamphuis' formula, f_w falls in the range ($0.032 - 0.18$), and one ends up with an estimate for τ_{max} in the range ($0.3 - 1.23$) Pa .

Morphological implications of wind resuspension

Once the processes described above will be appropriately quantified, we will be able to move to investigate the morphological evolution of tidal flats. Let us see what we can envisage on purely physical ground.

Firstly, how frequent are intense atmospheric events? The fraction of them characterized by wind speed higher than, say, 7.5 m/s is typically 6.6% (see Fig. 18) amounting to a time of the order of 1 Ms .

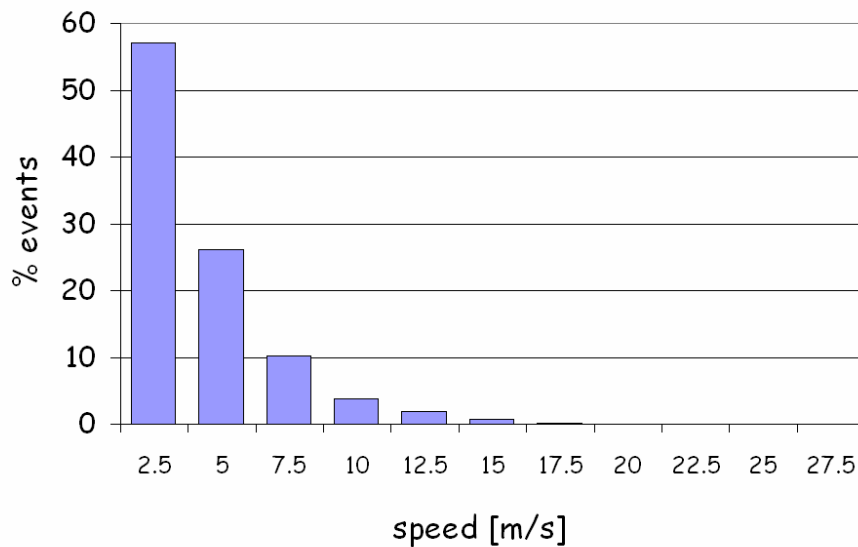
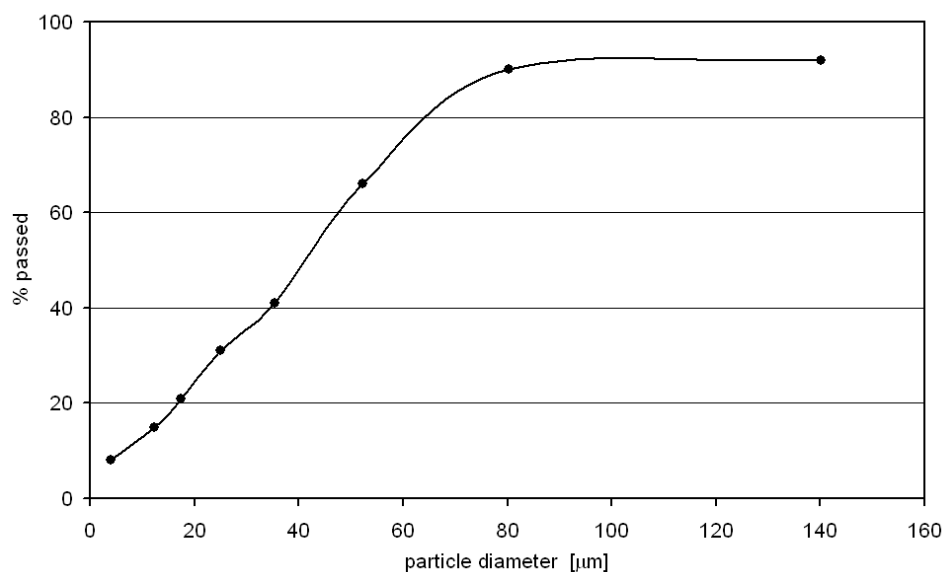


Fig 18 – Frequency distribution of wind events recorded in Venice lagoon [MAV-CVN, 1992].

Secondly, what sediment sizes are typically contained in the resuspended matter? The Figure 19 shows results of field observations. In order to clarify the fate of resuspended matter, it is instructive to recall that sizes ranging about $20 \mu\text{m}$, $50 \mu\text{m}$, $100 \mu\text{m}$ settle with settling speeds 0.4 mm/s , 2.2 mm/s , 10 mm/s respectively. If particles are concentrated in the bottom layer (say few centimetres) then, in a time of the order of half the tidal cycle, tidal currents are able to advect sediments through distances of the order of the shoal width. Thirdly, since marshes are unable to resuspend significant amounts of sediments, during the *ebb* phase the sediment flux exported from marshes to flats is negligible. On the contrary, a significant amount of sediments resuspended by wind in the shoals is exported to the adjacent channels. Less obvious is the balance between sediments leaving the shoals to adjacent marshes and those entering the shoals from the channels during the flood phase. The observations that i) dredging is needed to compensate for the tendency of canals to silt up and ii) flats are progressively deepening, suggests that the former flux typically prevails on the second. Why? And how can we affect such a balance in order to invert the process? This is the major issue of the morphologic plan of Venice lagoon.

Fig 19 – A typical grain size distribution of the sediments suspended in the shoals of Venice lagoon (data kindly made available by Magistrato alle Acque di Venezia and Consorzio Venezia Nuova).



3.4 Sediment redistribution within lagoons: salt marshes

Interesting, specific observations of the accretionary dynamics of wetlands in Venice lagoon were made for three years (1993-1996) by Day et al. [1999]. The latter Authors measured vertical accretion, short term sedimentation, soil vertical elevation change and horizontal shoreline change at various sites. The average short term sedimentation ranged about $3\text{--}7\text{ g m}^{-2}\text{ day}^{-1}$ with peaks reaching $76\text{ g m}^{-2}\text{ day}^{-1}$, recorded during intense atmospheric and/or hydrologic events. Marsh accretion ranged from $2\text{ to }23\text{ mm yr}^{-1}$ and soil elevation change ranged from $-32\text{ to }13.8\text{ mm yr}^{-1}$. An artificial marsh displayed a high rate of elevation loss, suggesting the important role of sediment compaction in marsh dynamics. Shoreline retreat and expansion of tidal channels were also observed at various sites.

Recently Morris et al. [2002] have performed a detailed investigation of BGP in salt marshes of South Carolina, showing that salt marsh equilibrium adjusts upward by increased production of macrophyte *Spartina alterniflora* and downward by an increasing rate of relative sea-level rise. The *rate of accretion* (mineral as well as organic) corrected for subsidence, was found to *increase* with the *depth D of the marsh* surface below mean high tide as well as with the *standing density of plant biomass*. For simplicity, Morris et al. [2002] assume this relationship to be linear and write:

$$dz/dt = (q + kB)D, \quad \text{for } D > 0 \quad (11)$$

where, quoting Morris et al. [2002] "... q and k are parameters that are proportional to the rate of sediment loading (q) and the efficiency of the vegetation (k) as a sediment trap. The k value also accounts for positive contributions to elevation resulting from the accumulation of plant-derived organic matter [e.g. Bricker-Urso et al. 1989, Turner et al. 2000]. The values of q and k are likely to vary locally and regionally as a function of sediment availability and tidal range [e.g. Stevenson et al. 1986]."

The constraint on biomass productivity is an important factor in maintaining elevation because a rise in relative sea level brings about an increase in production and biomass density that will enhance sediment deposition by increasing the efficiency of sediment trapping [Gleason et al. 1979, Leonard and Luther 1995, Yang 1998]. This positive effect of the plant community on sediment trapping was demonstrated experimentally by Morris et al. [2002].

The models of *salt marsh evolution* proposed in the literature (which can be defined as *zero-order models*) are fairly simple and attempt to describe the latter effect by formulating simple continuity statements closed by empirical correlations between the physical quantities involved; flow and sediment dynamics are totally absent in these models.

Essentially, the system considered in a model of this type is an ideal shallow basin, representing schematically a salt marsh, which exchanges water and sediments with a surrounding environment, say a shoal of a lagoon, and is subject to sediment deposition, wind induced erosion, sediment trapping and production of organic sediments by vegetation, sea level rise and subsidence. The exchange of sediments with the surrounding environment can be roughly modelled by assuming that the concentration \tilde{C}_0 of the exchanged water is such that the flux entering the shallow basin during the flood phase carries a depth averaged concentration C_0 (representing in some sense the supply from the surrounding environment), distinct from the concentration C characterizing the water contained in the basin which leaves it during the ebb phase. The latter must satisfy a continuity equation which reads:

$$\frac{d[h(t) - z]C(z, B, t)}{dt} + c_M \frac{dz}{dt} = \tilde{C}_0 \frac{dh}{dt} \quad (12)$$

where:

- $z(t)$ is the average elevation of the marsh bottom;
- $h(t)$ is the free surface elevation in the shallow basin;
- $C(z, B, t)$ is the *depth averaged sediment concentration*;
- c_M is the *packing concentration of the bottom sediment*

The above equation must be coupled with a second continuity statement whereby the evolution of bottom elevation is coupled with the various processes occurring in the water column. This equation reads:

$$c_M \frac{dz}{dt} = q_s(z, B) + q_T(z, B) + q_0(B) - e(z, B) - c_M s \quad (13)$$

where:

- $q_s(z, B)$ is the flux of deposited sediments, which reads:

$$q_s(z, B) = C(z, B, t) W_s \quad (14)$$

- $q_T(z, B)$ is the deposited flux due to sediment trapping by vegetation, which, following Mudd et al. [2004], is proportional to the depth averaged concentration C and to some power of the biomass:

$$q_{\tau}(z,B)= C(z, B, t) \alpha B^{\beta} \quad (15)$$

- $q_o(B)$ is the flux of organic soil produced by vegetation, which has been given the form [Randerson,1979]:

$$q_o(B)=\gamma B \quad (16)$$

with γ a parameter with value ranging about $2.5 \cdot 10^{-3} \text{ m}^3 \text{ kg}^{-1} \text{ year}^{-1}$.

- $e(z, B)$ is the *erosive flux due to wind resuspension*, which may be taken to be a function of the excess bottom shear stress, e.g.

$$e(z, B)= \text{function}[(\tau- \tau_c) / \tau_c] \quad (17)$$

Here, τ is an *effective stress*, a function of wind speed, fetch and vegetation which efficiently dissipates wind waves, τ_c is the *critical stress for erosion*.

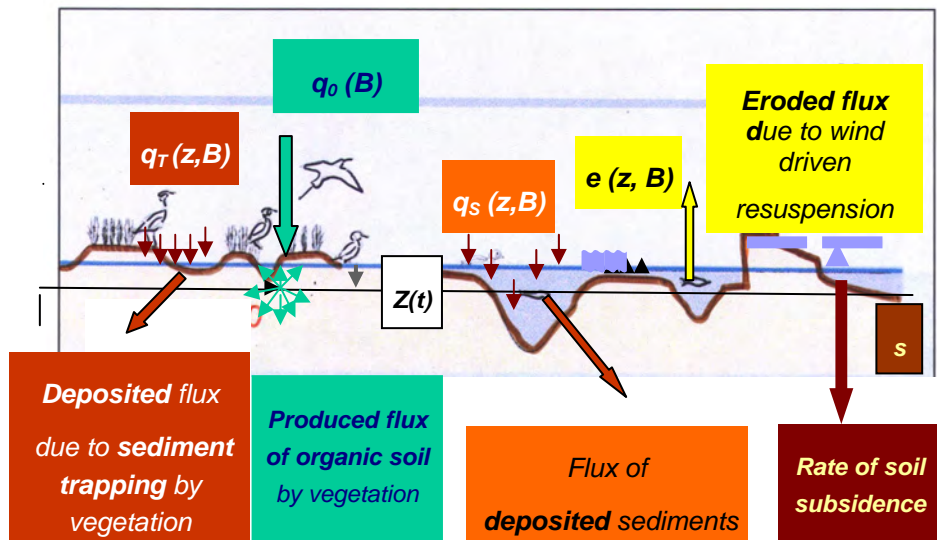


Fig 20 – Sketch illustrating the continuity statement.

The above formulation must be coupled with some quantitative description of biomass production (e.g. equation (5)).

A model of this type has been recently produced by the Corila group led by Prof. Marani at the University of Padua [Marani et al., 2007]. These Authors assume a constant value for the concentration C_o of the fluid entering the basin in the flood phase. Moreover, they write equation (12) in a different form, which might need to be somewhat revisited, while the equation (13) is averaged over a tidal cycle.

The above formulation, due to its zero-order character is bound to have some severe limitations, namely the need to average spatially processes occurring in the basin and the need to make unavoidably rough assumptions about the value attained by the concentration of the fluid entering the basin in the flood phase.

This notwithstanding, some qualitative insight on the general trends in the

morphological evolution of a salt marsh might be obtained from the above model if the zero order model for the salt marsh, correctly formulated, were coupled with some physically sound model of the surrounding environment, able to account for the various mechanisms which determine the actual time dependent value of the concentration C_0 .

4 Towards a morphological model of Venice Lagoon

Constructing a morphological model of a lagoon has been seen to be a quite complex job. Some ingredients needed to fulfill this job are already available; others will require attention in the near future.

Once processes will have been clearly understood, a number of issues will arise.

- i) The first: can we envisage suitable, environmentally friendly, works which might reduce significantly the net amount of sediments leaving the shoals to the channels and requiring periodic and expensive dredging operations?
- ii) The second: how quick would shoals respond to the construction of these works?
- iii) The third: how would marshes be affected by such interventions in the presence of enhanced sea level rise?

Resolving the latter issues will be the major challenges for those who will be in charge to develop a morphological plan for Venice lagoon.

References

Allen, J.R.L., 2000 Morphodynamics of Holocene salt marshes : a review sketch from the Atlantic and Southern North Sea Coasts of Europe. *Quaternary Science Reviews* 19, 1155-1231.

Amos, C. L., A. Bergamasco, G. Umgiesser, S. Cappucci, D. Cloutier, L. DeNat, M. Flindt, M. Bonardi, and S. Cristante, 2004, The stability of tidal flats in Venice lagoon—The results of in-situ measurements using two benthic, annular flumes, *J. Mar. Syst.*, 51, 211– 241.

Blondeaux, P., De Bernardinis, B. and Seminara, G., 1982. Correnti di marea in prossimità di imboccature e loro influenza sul ricambio lagunare, *Atti XVIII Conv. Idraulica e Costruzioni Idrauliche*, Bologna, 21-23 Sett. 1982.

Breugem W. A. and Holthuijsen L. H., 2007. Generalized Shallow Water Wave Growth from Lake George, *Journal of Waterway, Port, Coastal, and Ocean Engineering*, Vol. 133, No. 3,173-182.

Bricker-Urso, S., S. W. Nixon, J. K. Cochran, D. J. Hirshberg, and C. Hunt. 1989. Accretion rates and sediment accumulation in Rhode Island salt marshes. *Estuaries* 12: 300-317.

Carniello, L., A. Defina, S. Fagherazzi, and L. D'Alpaos, 2005, A combined wind wave–tidal model for the Venice lagoon, Italy, *J. Geophys. Res.*, 110, F04007, doi:10.1029/2004JF000232.

Day J. W., J. Rybczyk, F. Scarton, A. Rismondo, D. Are and G. Cecconi, 1999. Site accretionary dynamics, sea-level rise and the survival of wetlands in Venice lagoon: A field and modelling approach, *Estuarine Coastal Shelf Sci.*, 49, 607-628.

Engelund F. and Hansen E., 1967, A monograph on sediment transport in alluvial streams, Danish Tech. Press, Copenhagen.

Fagherazzi, S., C. Palermo, M. C. Rulli, L. Carniello, and A. Defina, 2007, Wind waves in shallow microtidal basins and the dynamic equilibrium of tidal flats, *J. Geophys. Res.*, 112, F02024, doi:10.1029/2006JF000572.

Gatto P. and Carbognin L., 1981. The Lagoon of Venice; natural environmental trend and man-induced modification. *Hydrol. Sci. Bull.* 26 (4), 379-391.

Gleason, M. L., D. A., Elmer, N. C. Pien and J. S. Fisher. 1979. Effects of stem density upon sediment retention by salt marsh cord grass, *Spartina alterniflora* Loisel. *Estuaries* 2(4):271-273.

Intergovernmental Panel on Climate Change , 2001: Climate Change 2001. The Scientific Basis. Contribution of Working Group I to the Third Assessment Report of the Intergovernmental Panel on Climate Change.

Intergovernmental Panel on Climate Change, 2007. Climate Change 2007. The Physical Science Basis. Contribution of Working Group I to the Fourth Assessment Report of the Intergovernmental Panel on Climate Change.

Kamphuis, J.W., 1975. Friction factors under oscillatory waves. *ASCE J. Waterw., Harbors, Coastal Eng. Div.* 10 WW2, pp. 135–144.

Krone R. B., 1985. Simulation of marsh growth under rising sea levels. In: W.R. Waldrop, Editor, *Hydraulics and Hydrology in the Small Computer Age*, Hydraulics Division, ASCE, Washington, DC, pp. 316–323.

Kruse F.A., Lefkoff A.B., Boardman J.W., Heidebrecht K.B., Shapiro A.T, Barloon P.J. and Goetz A.F.H., 1993. The Spectral Image-Processing System (Sips)-interactive visualization and analysis of imaging spectrometer data, *Remote Sensing of Environment* 44, pp. 145–163.

Lanzoni, S. and Seminara, G., 2002. Long term evolution and morphodynamic equilibrium of tidal channels, *Journal of Geophysical Research-Oceans*, 107(C1), art. 3001, 2002.

Leatherman S. P. and Kershaw P. J., 2001, Sea level rise and coastal disasters, summary of a forum, October 25, Washington.

Leonard, L. A. and M. E. Luther. 1995. Flow dynamics in tidal marsh canopies. *Limnol. Oceanogr.* 40: 11474-1484.

Levins, R. 1969, Some demographic and genetic consequences of environmental heterogeneity for biological control, *Bull. Entomol. Soc. Am.*, 15, 237–240.

Magistrato alle Acque di Venezia – Consorzio Venezia Nuova, 1922, Interventi per il recupero morfologico della Laguna. Progetto di Massima, Rep. VE3910-PMRF03, Venice, Italy.

Magistrato alle Acque di Venezia – Consorzio Venezia Nuova, 2002, Valutazione degli effetti delle nuove configurazioni sulla gestione delle opere mobili, VEN340-STUDIOB.5.58, Venice.

Marani, M., E. Belluco, A. D'Alpaos, A. Defina, S. Lanzoni and A. Rinaldo, 2003. The drainage density of tidal networks, *Water Resources Research*, 39 (2), 1040, doi:10.1029/2001WR001051.

Marani, M. A. D'Alpaos, S. Lanzoni, L. Carniello and Andrea Rinaldo, 2007. Biologically-controlled multiple equilibria of tidal landforms and the fate of the Venice lagoon, *Geophys. Res. Lett.*, 34, L11402, doi:10.1029/2007GL030178.

Marchi E., 1990, Sulla stabilità delle bocche lagunari a marea, *Rend. Fis. Acc. Lincei*, 137-150.

Morris, J. T. 1995. The mass balance of salt and water in intertidal sediments: results from North Inlet, South Carolina. *Estuaries*, 18: 556-567.

Morris, J.T., 2000. Effects of sea level anomalies on estuarine processes, p. 107-127. *In* J. Hobbie [ed.], *Estuarine Science: A Synthetic Approach to Research and Practice*. Island Press.

Morris, J. T., P. V. Sundareshwar, C. T. Nietch, B. Kjerfve, and D. R. Cahoon, 2002, Responses of coastal wetlands to rising sea level, *Ecology*, 83, 2869–2877.

Mudd, S. M., Fagherazzi S., Morris J. T. and Furbish D.J., 2004. Flow, sedimentation and biomass production on a vegetated salt marsh in South Carolina: toward a predictive model of marsh morphologic and ecologic evolution, in *The Ecogeomorphology of Salt Marshes, Coastal and Estuarine Stud.*, vol.9, edited by S. Fagherazzi, M. Marani and L.K. Blum, pp.165-188, AGU, Washington, D. C.

Paterson, D. M., 1989. Short-term changes in the erodibility of intertidal cohesive sediments related to the migratory behaviour of epipelagic diatoms, *Limnol. Oceanogr.*, 34, 223– 234.

Pignatti, S., 1966. La vegetazione alofila della laguna veneta, Istituto Veneto di Scienze, Lettere ed Arti, Memorie, Volume 33(1), Venezia, 174 pp.

Pomeroy, L. R., Darley, W. M., Dunn, E. L., Gallagher, J. L., Haines, E. B., and D. M. Whitney. 1981. Primary production, p. 39-67. *In* L. R. Pomeroy, L. R. and R. G. Wiegert [eds.], *The Ecology of a Salt Marsh*. Springer-Verlag, New York.

Randerson, P. F. 1979, A simulation model of salt-marsh development and plant ecology, in *Estuarine and Coastal Land Reclamation and Water Storage*, edited by B. Knights, and A. J. Phillips, pp. 48 – 67, Saxon House, Farnborough, U. K.

- Redfield A. C. 1965. The ontogeny of a salt marsh estuary. *Science*, 147 : 50-55.
- Redfield A. C. 1972 Development of a New England salt marsh. *Ecol. Monogr.* 42(2):201-37.
- Scarton, F and Rismondo, A. 1996, Primary production and decomposition in the Po Delta. Report to E.C. and MEDDELTA. Impact of Climate Change on Northwestern Mediterranean Deltas. Final Report to the European Community, Contract EV5V-CT94-0465. Tecnomare S.p.A., san Marco n. 3584, 30124, Venice, Italy, pp. 6.37-6.53.
- Silvestri, S., La vegetazione alofila quale indicatore morfologico negli ambienti a marea, Ph.D. thesis, Univ. of Padova, Padova, Italy, 2000.
- Silvestri, S., Marani, M., Rinaldo and A., Marani, A., 2000. Vegetazione alofila e morfologia lagunare, *Atti dell'Istituto Veneto di Scienze, Lettere ed Arti*, 68, Classe di scienze fisiche, matematiche e naturali, pp. 333–359.
- Stevenson, J. C., L. G. Ward and M. S. Kearney. 1986. Vertical accretion in marshes with varying rates of sea level rise, p. 241-259. *In* D. A. Wolfe [ed.], *Estuarine Variability*. Academic Press.
- Tambroni N., Bolla Pittaluga M. and Seminara G., 2005a. "Laboratory observations of the morphodynamic evolution of tidal channels and tidal inlets". *J. Geophys. Res.*, 110, F04009, doi:10.1029/2004JF000243, pp. 1-23.
- Tambroni N., Stansby P.K. and Seminara G., 2005b. Modeling the morphodynamics of tidal inlets. *Flooding and environmental challenges for Venice and its lagoon: state of knowledge*, Ed. C.A. Fletcher and T. Spencer, Cambridge University Press, Cambridge, pp. 379-389. ISBN: 0521840465.
- Tambroni, N., and G. Seminara, 2006. Are inlets responsible for the morphological degradation of Venice Lagoon?, *J. Geophys. Res.*, 111, F03013, doi:10.1029/2005JF000334.
- Tambroni N. and Seminara G., 2007. Tide propagation in channels with adjacent tidal flats. *Proceedings of the 32nd Congress of IAHR Harmonizing the Demands for Art and Nature in Hydraulics 1-6 July 2007*, Lido, Venezia, Italia, Abstract vol 2, pp. 731 (paper on cd-rom) (ISBN 88-89405-06-6).
- Turner, R. E., E. M. Swenson and C. S. Milan. 2000. p. 583-595. *In* N. P. Weinstein and D. A. Kreeger [eds.], *Concepts and Controversies in Tidal Marsh Ecology*. Kluwer.
- Umgiesser G., M. Sclavo, S. Carniel and A. Bergamasco, 2004. Exploring the bottom stress variability in the Venice Lagoon *Journal of Marine Systems* 51 161– 178.
- Yang, S. L. 1998. The role of *Scirpus* marsh in attenuation of hydrodynamics and retention of fine sediment in the Yangtze estuary. *Estuarine, Coastal and Shelf Science*, 47: 227-233.

GLOBAL CLIMATE CHANGE AND IMPACT ON MEDITERRANEAN

Michele Colacino

Istituto di Scienze dell'Atmosfera e del Clima, CNR, Roma

Riassunto

Le ricerche sul clima globale sono volte a determinare se e in che misura il clima stia cambiando. Nel presente lavoro, dopo una breve introduzione al problema, vengono presentati i risultati delle analisi dei dati a scala globale e mediterranea, che indicano come a partire dalla seconda metà del XIX secolo si stia verificando una modifica del clima, che investe anche le nostre regioni.

Abstract

Researches on Global Climate are aimed to establish if the Earth climate is changing. In the present work, after a short introduction, the results of the analyses carried out on secular data series are presented concerning both the global and Mediterranean scale. The trends indicate that since the second half of XIX century a climatic variation is occurring.

1. Introduction

The problems of climate change are followed both by scientists and public opinion due to the impact that climate variation could determine on our way of life. Researches are carried-out all over the world aimed to analyse the climate evolution since the second half of XIX century and foresee the future changes.

As it is well known, the climate is defined as mean of weather recorded in a time period of at least 30 years. In order to establish if the climate is changing in a time interval of about 100 ÷ 150 years it is necessary to define a reference mean and to evaluate the deviation from the fixed mean of the yearly values of climatic parameters. From the distribution of above said deviations it is possible to assess by simple regression if and how much the climate is changing.

In the present work, after a short recall about trends recorded at global scale, the trends relative to the Mediterranean climate in the last 150 years are presented. The obtained results indicate that a climate change is occurring whose future evolution is difficult to assess. This is true also for the Mediterranean region where some effects show a greater intensity.

2. The trends recorded at global and Mediterranean scale

The study of the recent evolution of the climate is based on the analysis of secular series of observation data. The research starts with the analysis of air temperature, that is the more significant climatic parameter since other atmospheric trends are tightly connected. The analysis carried out at global

scale on the last 150 years indicate a positive trend of about $0.7^{\circ}\text{C}/100$ years with a greater increase in the last 20 years of past century. Rainfall is the other important climatic parameter because on rainfall depends the availability of water resources for the different uses, but, while the trend of temperature is more or less uniform all over the Planet, the distribution of precipitation is strongly variable. We remember that more than 200.000 stations carry out rainfall measurements: however, only a relative small number gives reliable data and therefore is difficult obtain definitive conclusions. From different works we can say that there is not variation in the global amount of rainfall while some modifications occur in the distribution: in northern hemisphere rainfall is reduced in low latitudes and increases over 50° latitude and in polar region. In southern one the conclusion are more uncertain, because the measurements are effected only on the continents and information about the precipitation over the ocean are lacking.

Other indicators of climate change are the variation in the glacier extension, sea level rise and frequency of the extreme events. As far as the first item the observations indicate a strong regression of mountain glaciers, while seems to be stationary the polar cap over Antarctica. For the second topic the sea level is increased by about 16 cm in the last century. Finally for the extreme events recent studies indicate that in the last 30 years are redoubled the catastrophical hurricanes of category 4 and 5 following the Saffir-Simpson classification (Emanuel, 2005; Webster *et al.*, 2005).

Considering the Mediterranean region and our Country the first interesting effect is the increase of high pressure to which an increase of solar radiation and temperature is connected (Piervitali *et al.*, 1997). Temperature data show a trend similar to the global, but with an higher gradient around $1,0^{\circ}\text{C}/100$ years (Nanni *et al.*, 2007). It must be stressed, however, the increase of thermal waves, that occur during summer with values of temperature higher than the seasonal mean by $8 \div 15^{\circ}\text{C}$. (Colacino *et al.*, 1997; Baldi *et al.*, 2006). This event that can last many days, as in summer 2003, impacts either on health, due to thermal stress, or on forest fire which occur frequently during the warm season.

Concerning the precipitations, trend depends on the length of the record examined: if the analysis starts from 1850 no significant variation is found, if the analysis is effected on the last 50 years a reduction of more than 15% clearly appears on the central-western basin (Piervitali *et al.*, 1998; Brunetti *et al.*, 2001, 2002). This reduction is more marked on the southern region of Italy where is higher than 20%. Another aspect concerns the intensity, that is the ratio between the amount of rainfall and the duration of the event: the data indicate for the period 1951-2000, particularly in Italy, a reduction of the precipitations of low intensity and an increase of those of greatest intensity (Alpert *et al.*, 2002, Brunetti *et al.*, 2004). Therefore, trend of precipitations is twofold negative: firstly because the reduction of amount of rainfall reduces the water resources, and secondly because the intense rainfall can give rise to other consequences as floods and landslides.

Finally, alpine glaciers are strongly reduced starting from eighties of past century while the sea level rise is around 15 cm in the last 100 years. A different value has been recorded in Venice where an increase about 27 cm has been measured. This is a local effect due to the water drainage of ground water over which city is founded.

3. Future perspectives

Future scenarios, based on the hypothesis of global warming due to the anthropogenic enhancement of greenhouse effect, foresee for the end of the century an increase of temperature in the range 2,0-4,5 °C (IPCC-WG1, 2007) and this could have a very serious impact. In particular, in addition to the ablation of glaciers two aspects are very important for our Country: the sea level rise and the reduction of rainfall. The sea level should rise between 0,25 and 1,0 m and this could affect many coastal zones: lagoon, flat planes as Po valley, harbours, coastal railroad and highways are exposed to the risk of frequent flood and could require great works of defence. In addition salt marine water could intrude in the ground water reducing the availability of drinkable water. About the availability of water resources the scenario presents a strong asymmetry between Northern and Southern Europe: in the North an increase of rainfall is foreseen with greater amount of rain-off water; in South a reduction, and the amount of water could be reduced up to 60%. Finally a strong increase of torrential rainfall could occur with an increase of this kind of rainfall around 25% with respect to the present day values.

The change, as above summarised, could have a very strong impact: however the scenario models, even if very complex, do not include all the processes that occur in the climatic system. This one includes air, water, land, ice, biosphere and in order to obtain reliable forecasts all the interaction among them and feedback processes should be parameterised, but we are far from to be able to do this because to reach this goal it is necessary to develop still a lot of research.

Conclusions

From the above it is possible to draw some conclusions:

- the data analysis confirms that climate is changing in a very rapid way;
- the change is present all over the world, but with different intensity in the various regions of the Earth;
- the change is characterised by the speed with which is occurring: changes that in the past occurred in many hundreds years have been recorded in few decades;
- the consequences of change could be serious and the process must be followed with great attention;
- the scenario models require more and more research in order to give more reliable results: therefore the alarm tight to the climate variations is not fully

justified.

References

Alpert P., T. Ben-Gai, A. Baharad, Y. Benjamini, D. Yekutieli, M. Colacino, L. Diodato, C. Ramis, V. Homar, R. Romero, S. Michaelides, A. Manes, 2002. The paradoxical increase of Mediterranean daily rainfall in spite of decrease in total values. *Geophys. Res. Lett.* 29, 11: 31-1 – 31-4.

Baldi M., G. Dalu, G. Maracchi, M. Pasqui, F. Cesarone, 2006. Heat waves in the Mediterranean: a local feature or a larger scale effect? *Int. Journal of Climatology* 26: 1477 - 1487

Brunetti M., M. Colacino, M. Maugeri, T. Nanni, 2001. Trends in the daily intensity of precipitation in Italy from 1951 to 1996. *Int. Journal of Climatology* 21: 299-316.

Brunetti M., M. Maugeri, F. Monti, T. Nanni, 2004. Changes in daily precipitation frequency and distribution in Italy over the last 120 years. *J. Geophys. Res* 109 D05102: 1-16.

Colacino M., M. Conte, E. Piervitali, 1997. Heat waves in the Central Mediterranean basin, in "Proceedings of INM/WMO Int. Symposium on Cyclones and Hazardous Weather in the Mediterranean", Palma de Mallorca, pp. 561-566.

Emanuel K., 2005. Increasing destructiveness of tropical cyclones over the past 30 years. *Nature* 436: 686-688.

IPCC-WG1: *Climate Change 2005 - The Scientific Basis*, Cambridge, 2007

Nanni T., M. Brunetti, M. Maugeri, 2007. Variabilità e cambiamenti climatici in Italia nel corso degli ultimi due secoli, in "Clima e Cambiamenti climatici: le attività di ricerca del CNR", eds. B. Carli, G. Cavarretta, M. Colacino, S. Fuzzi, CNR, Roma, pp. 225-228

Piervitali E., M. Colacino, M. Conte, 1997. Signals of climatic change in the Central-Western Mediterranean basin. *Theor. Appl. Climatology* 58: 211-219.

Piervitali E., M. Colacino, M. Conte, 1998. Rainfall over the central-western Mediterranean basin in the period 1951-1995. Part I: precipitation trends. *Nuovo Cimento* 21C, 3: 331-34.

INDICATORS OF TROPHIC STATUS AND SENSITIVITY TO EUTROPHICATION AND ORGANIC POLLUTION IN TRANSITIONAL WATERS

Pierluigi Viaroli

Department of Environmental Sciences, University of Parma

Coastal lagoons undergo a number of pressures that can primarily be attributed to an excess of organic matter and nutrient inputs from the watershed (Cloern, 2001). Further impacts are related to the human exploitation of the aquatic environment - e.g. as tourism, waterways and ports - and of biological resources - e.g. aquaculture and fish farming (Karakassis et al., 2000).

Due to the shallowness and to the inherent high sediment surface area to water volume ratios, the sediment and its resident benthic communities are the most sensitive components of the ecosystems and act as triggers for processes in the water column. Sedimentary and benthic elements support also organic matter and nutrient recycling and the reactivity of biogeochemical buffers (Golterman, 1995; De Wit et al., 2001).

Lagoons quality and sensitivity to nutrient and OM loadings from watershed have been assessed mainly with water chemistry and phytoplankton indicators, basically referring to the trophic reference system proposed by Vollenweider and Kerekes (1982) and Nixon (1995). Furthermore, Vollenweider et al. (1998) proposed a trophic index (TRIX) which integrates chlorophyll-a, oxygen saturation, total nitrogen and total phosphorus to characterise the trophic state of coastal marine waters, which is nowadays largely applied to coastal lagoons. TRIX is based on the assumption that eutrophication processes depend primarily on phytoplankton community, which is indeed not the case for shallow coastal lagoons where both microphytobenthos (MPB) and benthic vegetation are the main components of the primary producer community.

Most often, the issues to be analysed are complex and cannot be resolved by considering only simple variables and linear relationships. Nevertheless, one can identify a set of basic variables which are indicative of ecosystem properties and functions, can be easily measured and are suited for classification and assessment of sensitivity to external stressors (Viaroli and Christian, 2003; Viaroli et al., 2004). Basic morphometric parameters, hydrological variables, sediment characteristics and biological elements have been extensively applied and validated in deep aquatic ecosystems. Nevertheless, applications to shallow coastal lagoons require ad hoc calibration and further validations using the weight-of-evidence approach. In order to bring together information from multiple indicators, metrics which allow integration or combination of multiple variables will also greatly improve the capacity of representing ecological status or sensitivity to a given stressor (Viaroli et al., 2004). The mean depth is an

indicator of the development of the water-sediment interface with respect to the water volume. The freshwater discharge to recipient volumes ratio could be either a measure of freshwater flushing or a proxy of sensitivity to pressures from watershed. According to Vollenweider and Kerekes (1992) the combination of hydrological variables with loading estimates gives an assessment of the lagoon sensitivity to eutrophication. However, this approach is valid only for deep and mixed aquatic ecosystems dominated by phytoplankton communities. Recently, water budgets and nutrient loadings have been widely used for assessing the net ecosystem metabolism (NEM) of coastal lagoons with a wide array of primary producer communities (Giordani et al., 2005; 2007). Basically, NEM is calculated with the LOICZ biogeochemical model from dissolved inorganic phosphorus loadings; thus NEM gives a measure of the trophic status and its dependency on nutrient delivery from watershed.

The susceptibility to eutrophication is not a simple function of nutrient loadings, but also depends on sedimentary processes which are mainly controlled by a suite of sedimentological and geochemical variables. Granulometry and sedimentary organic matter provide basic information on sediment composition and are important determinants of exchanges of oxygen and nutrients across the water-sediment interface. The C to N ratio of the sediment OM pool is a good indicator of organic matter lability (Enriquez et al., 1993). The sedimentary carbonate content can be used to assess the capacity of the sediment to retain phosphate through the calcium/carbonate/phosphate system (Golterman, 1995; Rozan et al., 2002). Reactive iron provides an indication of the sediment capacity to buffer against sulphides and phosphate (De Wit et al., 2001; Richard and Morse, 2005). Yet, the above biogeochemical variables are also related to benthic vegetation and, to a some extent, the macroalgae to phanerogam ratio could be a proxy of their relative dominance.

Sedimentary variables can be integrated with water quality using simple metrics, namely modified versions of the WQI, in which utility functions and weight criteria are used to transform measured variables into quality scores (Cude, 2001). A transitional water quality index (TWQI) is now implemented, which integrates oxygen saturation, dissolved inorganic phosphorus (DIP) and nitrogen (DIN), phytoplankton chlorophyll-a, macroalgal and seagrass coverage (Giordani et al., in preparation).

Macrophyte-based indicators have been recently developed, namely the Ecological Evaluation Index – EEI (Orfanidis et al. 2001, 2003) and the IFREMER's classification scheme (Souchu et al., 2000). The EEI uses benthic seaweeds as bioindicators of ecosystem changes from pristine status (Ecological Status Group I, ESG I) to deteriorated status (ESG II). ESG I includes species with low growth rates and long life cycles, whereas ESG II includes opportunistic species with high growth rates, short life cycles and high biodegradability rates. The classification scheme developed by IFREMER aims at implementing an operational tool for assessing eutrophication levels in French Mediterranean lagoons. The scheme allows the classification into five quality levels, which correspond to different macrophyte communities spanning climax species, mainly phanerogams, phytoplankton and macroalgae. The

macrophyte index is then integrated with data on zoobenthos, sediment and water quality.

A number of indices has been also developed taking into account the benthic macrofauna (Grall and Chauvaud, 2002; Magni et al., 2005). Among others, AMBI (Borja et al., 2003) and BENTIX (Simboura and Zenetos, 2003) indices are widely used in marine coastal areas. Both are based on the principle of the ecological identity of benthic species according to their response to pollution. Nevertheless they produce similar results, there are discrepancies observed in the scoring of species and further restrictions to their use in certain environments. A better assessment is provided by the taxonomic distinctness, which has the potential to evaluate the integrity of benthic communities in relation to anthropogenic disturbances (Warwhich and Clarke, 2001). Attributes of this measures of biodiversity are sample-size independence, low sensitivity to data noise, not influenced by natural controlling factors (e.g., changes in salinity), and high sensitivity to detection of pollution impacts.

Coastal lagoons have a great internal patchiness and heterogeneity (Tagliapietra and Volpi Ghirardini, 2006) which can either amplify or bias the stressor effects. Examples are given by both taxonomic richness and body size which are chiefly related to the lagoon surface (Sabetta et al., 2007). Nonetheless, the size distribution within the macrozoobenthic community seems a simple and promising tool for assessing the degree of disturbance and the ecological status of coastal lagoons (Reizopoulou and Nicholaidou, 2007).

Further indicators of either state or health of benthic communities have been implemented by the IOC Study Group on Benthic Indicators (<http://www.ioc.unesco.org/benthicindicators>), among which relevant synoptic information on benthic faunal condition (e.g. measures of community composition), controlling natural abiotic factors (e.g. sediment organic matter), and levels of contaminants were tested world-wide (Hyland et al., 2000). This approach has also been applied to coastal lagoons using organic carbon as a tracer of stressors against the benthic community (Magni and Tagliapietra, pers. comm.).

Ecosystem modelling would be greatly beneficial in order to evaluate status and trends in ecological conditions at a regional scale, allowing to distinguish between natural and human-induced stressors. Moreover, in order to reflect the real complexity of ecosystems, indicators have to include structural, functional, and system-level aspects (Zaldivar et al., 2003). Indices as exergy and specific exergy cope with these goals allowing the assessment of ecosystem health and ecological status (Jørgensen et al., 2005). A good agreement between exergy and macrophyte indicators has been recently evidenced (Austoni et al., 2007), although a wealth of problems exist when considering animal species, especially vertebrates.

Studies in the lagoon of Venice have contributed significantly to the development of indicators suited at detecting and monitoring impacts and their evolution in a composite and shallow ecosystem under treats from human pressures, as the lagoon of Venice is. Among others, one can refer to works on the implementation of a multi-metric index of chemical contaminantion, ecotoxicological test, risk assessment evaluation, and environmental monitoring which are reported in this volume.

Austoni M, Giordani G., Viaroli P, Zaldivar J., 2007. Application of specific exergy to macrophytes as an integrated index of environmental quality for coastal lagoons. *Ecological Indicators* 7: 229-238.

Borja A, Franco J, Pèrè V, 2000. A marine biotic index to establish the ecological quality of soft bottom benthos within European estuarine and coastal environments. *Marine Pollution Bulletin* 40: 1100-1114.

Castel J, Caumette P, Herbert RA, 1996. Eutrophication gradients in coastal lagoons as exemplified by the Bassin d'Arcachon and Étang du Prévost. *Hydrobiologia* 329: ix-xxviii.

Cairns, J. Jr, McCormick P.V., Niederlehner B.R., 1993. A proposed framework for developing indicators of ecosystem health. *Hydrobiologia*, 263: 1-44

Cloern, J.E., 2001, Our evolving conceptual model of the coastal eutrophication problem: *Marine Ecology Progress Series* 210: 223-253.

Cude, CG, 2001. Oregon water quality index: a tool for evaluating water quality management effectiveness. *Journal American Water Resource Association* 37: 125-137

de Wit R, Stal LJ, Lomstein BA, Herbert RA, van Gemerden H, Viaroli P, Ceccherelli VU, Rodríguez-Valera F, Bartoli M, Giordani G, Azzoni R, Shaub B, Welsh DT, Donnely A, Cifuentes A, Anton J, Finster K, Nielsen LB, Underlien Pedersen AG, Neubauer AT, Colangelo MA, Heijs SK, 2001. ROBUST: The ROle of BUffering capacities in STabilising coastal lagoon ecosystems. *Continental Shelf Research* 21: 2021-2041.

Enriquez S, Duarte CM, Sand-Jensen K, 1993. Patterns in decomposition rates among photosynthetic organisms: the importance of detritus C:N:P content. *Oecologia* 94: 457-471.

Giordani G, Viaroli P, Swaney DP, Murray CN, Zaldivar JM, Marshall Crossland JI. (eds) 2005. Nutrient fluxes in transitional zones of the Italian coast. *LOICZ Reports & Studies* 28, ii+157 p.

Giordani G., Austoni M., Zaldivar J.M., Swaney D.P., Viaroli P, 2008. Modelling ecosystem functions and properties at different time and spatial scales in shallow coastal lagoons: an application of the LOICZ biogeochemical model. *Estuarine, Coastal and Shelf Science* (in press)

Golterman HL, 1995. The role of the iron hydroxide-phosphate-sulphide system in the phosphate exchange between sediments and water. *Hydrobiologia* 297:

43-54.

Golterman HL, 1995. The labyrinth of nutrient cycles and buffers in wetlands: results based on research in the Camargue (Southern France). *Hydrobiologia* 315: 211-222.

Grall J, Chauvaud L, 2002. Marine eutrophication and benthos: the need for new approaches and concepts. *Global Change Biology* 8: 813-830.

Hyland J, Balthis LW, Karakassis I, Magni P, Petrov A, Shine JR, Vestergaard O, Warwick R, 2005. *Organic carbon content of sediments as an indicator of benthic stress*. *Marine Ecology Progress Series* 295: 91-103.

Karakassis I, Tsapakis M, Hatziyanni E, 1998. Seasonal variability in sediment profiles beneath fish farm cages in the Mediterranean. *Marine Ecology Progress Series*, 162: 243-252.

Kristensen E, Haese RR and Kotska J (eds), 2005. Interactions between macro- and microorganisms in marine sediments. *Coastal estuarine Studies* 60, 390 p.

Jørgensen, S. E., Constanza, R., Xu, F.-L.(Eds.), 2005a, Handbook of ecological indicators for assessment of ecosystem health. CRC Press, Boca Raton (FL).

Magni P, Hyland J, Manzella G, Rumhor H, Viaroli P, Zenetos A (eds), 2005. Indicators of stress in the marine benthos. *Proceedings of the Workshop "Indicators of Stress in the Marine Benthos"*, Torregrande-Oriстано (IT). 8–9 October 2004. *IOC Workshop Reports*, 195, pp. iv-45Nixon

Orfanidis S, Panayotidis P, Stamatis N, 2001. Ecological evaluation of transitional and coastal waters: a marine benthic macrophyte-based model. *Mediterranean Marine Science* 2: 45-65.

Orfanidis S, Panayotidis P, Stamatis N, 2003. An insight to the ecological evaluation index (EEI). *Ecological Indicators* 3: 27-33.

Reizopoulou S., Nicolaidou A, 2007. Index of size distribution (ISD): a method of quality assessment for coastal lagoons. *Hydrobiologia* 577-141-149.

Rickard D, Morse JW, 2005. Acid Volatile Sulphide (AVS). *Marine Chemistry* 97: 141-197.

Rozan TF, Taillefert M, Trouwborst RE, Glazer BT, Ma S, Herszage J, Valdes LM, Price K, Luther III GW, 2002. Iron-sulphur-phosphorus cycling in the sediments of a shallow coastal bay: Implications for sediment nutrient release and benthic macroalgal blooms. *Limnology and Oceanography* 47: 1346-1354.

Sabetta L, Barbone E, Giardino A, Galoppo N, Basset A, 2007. Species-area patterns of benthic macro-invertebrates in Italian lagoons. *Hydrobiologia* 577: 127-139.

Simboura, N, Zenetos, A., 2002. Benthic indicators to use in ecological quality classification of Mediterranean soft bottoms marine ecosystems, including a new biotic index. *Mediterranean Marine Science* 3/2: 77-111.

Souchu, P., M.C. Ximenes, M. Lauret, A. Vaquer, E. Dutriex, 2000. Mise à jour d'indicateurs du niveau d'eutrophisation des milieux lagunaires méditerranéens, Ifremer-Créocéan-Université Montpellier II, 412 pp

Tagliapietra D, Volpi Ghirardini A, 2006. Notes on the coastal lagoon typology in the light of the EU Water Framework Directive: Italy as a case study. *Aquatic Conservation: Marine & Freshwater Ecosystems* 16: 457-467.

Viaroli P, Bartoli M, Giordani G, Magni P, Welsh DT, 2004. Biogeochemical indicators as tools for assessing sediment quality/vulnerability in transitional aquatic ecosystems. *Aquatic Conservation: Marine and Freshwater Ecosystem* 14: S14-S29

Viaroli P, Christian RR, 2003. Description of trophic status of an eutrophic coastal lagoon through potential oxygen production and consumption: defining hyperautotrophy and dystrophy. *Ecological Indicators* 3: 237-250.

Vollenweider R.A., Kerekes, J.J., 1982. *Eutrophication of Waters, Monitoring Assessment and Control-O.E.C.D.-Paris*, pp. 154.

Vollenweider, R.A., Giovanardi F., Montanari, G., Rinaldi, A, 1998. Characterization of the trophic conditions of marine coastal waters, with special reference to the NW Adriatic Sea: proposal for a trophic scale, turbidity and generalized water quality index. *Environmetrics*, 9: 329-357.

Warwick, R.M., Clarke, K.R. 2001. Practical measures of marine biodiversity based on relatedness of species. *Oceanography and Marine Biology: an Annual Review*, 39: 207-231.

Zaldívar JM, Austoni M, Plus M, De Leo G., Giordani G, Viaroli P, 2005. Ecosystem health assessment and bioeconomic analysis in coastal lagoons. In Jørgensen S.E., F.-L. Xu and R. Costanza (eds), *Handbook of Ecological Indicators for Assessment of Ecosystem Health*. CRC Press, Boca Raton: 163-184

AREA 1
Economics

RESEARCH LINE 1.2

Cost-benefits analysis of land reclamation of brownfields in the Venice lagoon

ELGIRA. A SUPPORT SYSTEM FOR KNOWLEDGE BUILDING AND EVALUATION IN BROWNFIELD REDEVELOPMENT

Patassini D.¹, Cossettini P.², De Mitri A.¹, De Polignol E.³, De Zorzi S.⁴, Hedorfer M.¹, Rinaldi E.⁴

1 Regional and Town Planning Department, University IUAV of Venice,

2 VESTA Venice Territorial and Environmental Services

3 Venice Municipality; Environment and Territorial Safety Management

4 CORILA Consorzio Lagoon Research Consortium, Venice

Translation from Italian: Judith McGrath

Riassunto

Egira è un modello di aiuto alla conoscenza e alla decisione nel campo delle bonifiche dei siti contaminati. Messa a punto con test ripetuti nel mega-sito di Porto Marghera, consente di generare opzioni di bonifica a partire da ipotesi di riqualificazione (uso del suolo) e da vincoli di caratterizzazione. Ogni opzione viene valutata in termini di costo e di riduzione del rischio sanitario e ambientale secondo la normativa vigente.

La procedura presenta numerose 'finestre' interattive e può essere utilizzata per scopi diversi. Può accompagnare la valutazione ex-ante di un intervento di bonifica; aiuta a ripercorrere a ritroso un intervento concluso per la calibrazione di parametri, la selezione o l'aggiornamento di tecnologie, la ponderazione di criteri; può essere utilizzata per la certificazione di interventi bonifica e dei dati di caratterizzazione; aiuta a 'catturare' effetti spaziali.

Abstract

Elgira is a support system for knowledge building and decision making in brownfield redevelopment. It was piloted and tested in the Porto Marghera mega-site and proved capable of generating reclaim options starting from redevelopment hypotheses (land use) and characterization limitations. Each option is then evaluated in terms of cost and of the reduction of environmental and health risks in accordance with current legislation.

The procedure uses several interactive 'windows' and can be utilised for various purposes. It can accompany ex-ante evaluation for a reclaim; it can aid post-implementation examination of an intervention aimed at the calibrating of parameters, the selection or updating of technologies, and the consideration of criteria. It can also be used for the certification of reclaim interventions and of characterization data. It aids in 'capturing' spatial effects.

1. Introduction

The reclaim and redevelopment of brownfields are priorities of economic, territorial and environmental importance. Over the last few years strategies have been drawn up to comply with these priorities, and legislation regarding planning and control, as well as new procedure methodologies, has been strengthened. Authorities, political administrations and businesses have supplied precision censuses for sites of both national and local interest. The former are subject to specific legislation.

The recent Italian government decree (D.L. no. 152; 2006) has organised environmental issues organically, in compliance with EU legislation, so that 'brownfield reclaim' is treated under Title V, which deals with the discipline of "... *interventions of reclaim and environmental cleansing of brownfields...*", (...) "*the procedures, the criteria, and the methodologies for the execution of the operations necessary to the elimination of the sources of pollution and in any case to the reduction of polluting substances, ... with special reference to the principle that 'who pollutes, pays'*". Regional legislation necessarily refers to national law: "*Reclaim interventions ... must be disciplined by the regions with specific plans ... according to general criteria...*".

Within this framework, it has become necessary to have both the methodologies and tools for the planning of the reclaim interventions, with an operational approach that is integrated and agreed upon, scientifically sound, and efficient. Not only does a reclaim plan require interdisciplinary and specific skills in the fields of pollutant chemistry, environmental engineering, statistical analysis of data and geographical representations aided by GIS, it also involves skills in economics, town and regional planning, and environmental analysis and evaluation.

ELGIRA is a *Support System for Decision-making* in the planning and execution of reclaim interventions that enables the user to gain knowledge of and thereby assess detailed or macro-area interventions based on general scenarios, agreements and limitations. The system also enables the constructing of redevelopment scenarios based on final usage, residual risk management, control and improvement of environmental quality, and minimization of costs.

The system is addressed to *public administrations* for the construction of evaluation scenarios of support to the territorial redevelopment strategies according to law; for the preparation or verification of executive reclaim plans (including ex-post evaluations or 'hindsight' analyses); for the integrated and efficient management of tools for town and regional planning, building, and investment opportunities for private investors in the area to be redeveloped. Finally, it is also designed for *universities and research centres* for professional and scientific training.

The system was developed within the Research Programme of CORILA 2001-2003 and 2004-2006 on the basis of a convention with the Regional and Town Planning Department, University IUAV of Venice.

2. System performance

2.1 Applications

The system may be applied according to three different operational modalities: *identification of reclaim scenarios* applicable to a site, including comparisons among possible alternatives; *ex-ante or ex-post analyses of reclaim planning* coherent with redevelopment proposals; *verification of the hypothesis of final usage variations* foreseen by the general and operational regional and town plans, including cost-benefit analysis of the redevelopment of the brownfield.

A. Identification of reclaim scenarios applicable to a site with comparison between options. Starting from characterization and other information regarding the context, ELGIRA identifies the reclaim scenarios applicable to a site thus enabling comparison among possible alternatives.

The operational phases include: the construction of the land-pollution model, the selection of the applicable technologies, the construction of the model for zoning of the polluted areas, the determination of costs and of the performance of the adoptable technologies, the identification of reclaim options (all the technologies applicable to the entire site), analysis of health risk (prior to and post- reclaim, evaluation of local effects produced by the reclaim intervention (first- and second-level proximity).

B. Analyses of reclaim projects coherent to redevelopment programmes. The system is able to evaluate and investigate hypotheses of public or private nature by reprocessing, with its own techniques, characterization data, the pollution model, the scenarios of applied technologies and other contextual information.

C. Variations of final usage with cost-benefit analysis. The reclaim of a highly polluted site and its subsequent return to residential and 'green' usage may at times prove non-sustainable from a financial point of view, however desirable this may be for other reasons. In these cases, the final usage of portions of the area, or the entire area itself, must be reviewed with the intent to optimize costs and benefits of the redevelopment. ELGIRA is able to evaluate the new hypotheses of final usage, re-elaborate the operational phases, and establish the costs of a new configuration. Thus it becomes possible to identify the portions of the larger area in question and the polluting elements which are most sensitive to variation, and then propose planning scenarios at sustainable costs.

2.2 From characterization to the evaluation of effects

The organization and evaluation of a project for the reclaim and redevelopment of an area are disposed according to phases.

First of all it is necessary to produce an accurate and efficient *representation model of area pollution*, with the appropriate processing of data regarding the *characterization matrix*. The model generates a representation of the geography of the pollutants. The system offers a specific procedure for the creation of the model and the visualization of the areas which are potentially implicated in the

reclaim project according to current legislation. The system also enables the creation of maps to facilitate the analysis of health and environmental risks.

The *reclaim technologies* coherent with characterization are selected through a process of comparison on the basis of the characteristics of the intervention context, and according to the results of national and international best practice. Reference to these practices means that benchmark parameters can be used (or referred to regarding performance). ELGIRA contains, moreover, a *database of reclaim technologies* rich with information, open, and with a WEB interface. This database allows the user, with the aid of multi-criteria methodologies, to consult, assess, extract and classify the most appropriate technologies for any particular context.

A complete, but at the same time synthetic view of the scenario of the polluted areas to be associated to applicable technologies is obtained by creating a pollution model with the selected technologies. With ELGIRA a *zoning model* can be constructed that places in relation the polluted areas with the technologies. This model has a graphic interface which functions as of the preliminary evaluation of worksite options (timing, phases, management).

An estimate of *health risk* and *environmental risk* (biodiversity) may be ante- and post-reclaim; if it is ante-, it then leads to the identification of the areas that should be subject to reclaim. With the system it is possible to make selections among standard (commercial) procedures or *ad-hoc* procedures designed for risk analysis by organising the necessary information alongside the pollution model. An internal risk analysis procedure is also available.

A *reclaim project* is an intervention option that implies the putting together of applicable technologies resulting in an optimal combination of efficiency, cost effectiveness, and minimal environmental impact. Identification of the optimal options is not immediate, but it is worthwhile to consider various comparable options. ELGIRA can provide the guided construction of the whole range of reclaim possibilities, on the basis of selected technologies and pollution zoning. It is therefore possible to classify them according to general parameters such as performance and costs, and produce a preliminary estimate of the overall costs of the reclaim project.

The best options are then subjected to cost-benefit analysis. It is in this phase that the working plan is laid out, including specifications as to resources, timing and duration, and reclaim operation costs. Information regarding the selected technologies and the zoning model come together in the module that then subjects each option to an evaluation of the *reduction of the risk* that may be produced by the reclaim, of the *environmental benefits*, and of the *overall costs*. These criteria help to identify the option that best represents the optimum definitive reclaim project.

The redevelopment of any area generates effects on the local population: on urban and environmental quality, on the job market and work in general, accessibility, and land and house values. In order to understand the consequences of a redevelopment intervention on the expectations and

The production of the *environmental characterization matrix* consists of the organization and geographical referencing of the data regarding concentration levels of the polluting substances found during site surveying. The data must be certified and available in formats that reveal the level of concentration at each point of the stratigraphic survey.

The construction of the *pollution model* consists of the production of maps revealing the distribution of the polluting substances throughout the entire site. Information on characterization, gained also via interpolation techniques, describes the distribution of the concentrations of each substance. Via the application of threshold values, it is possible to define those maps where there are areas that exceed the legal limit values.

The *technologies* considered appropriate for the site are extracted from a database according to specific criteria: treated pollutants, inhibiting pollutants, costs, performance, terrain, etc. The technologies may be subjected to multi-criteria evaluation in order to create a merit classification.

The definition of the *zoning model* consists of the identification, within the pollution map, of partitions characterized by one or more polluting agents. This model allows for the juxtaposition of single pollutant maps and is put into correlation with reclaim technologies. The reclaim options are then created; and each option, referring to the entire site, is composed of all the technologies applied to the polluted areas. After this the most appropriate technologies are chosen. During this phase it is possible to make the first swift evaluation of the costs of the reclaim option by option.

The *ante-reclaim health risk* is assessed with the aid of the pollution model and major exposure locations. Afterwards, a post-reclaim evaluation is made and the chosen reclaim options are examined, which produce the significant risk indices (e.g. cancerogenous and non- index).

Each of the technologies included in the chosen options is examined according to energy consumption, costs, and other criteria crucial to the reclaim project. Characteristics of the technologies are studied, as well as the areas and the volumes to be treated and the necessary resources. The selected options and data produced by the technologies come together then in the evaluation module of the redevelopment scenarios.

At this point, the *redevelopment scenarios* are evaluated via a specific module which produces a synthesis indices for Residual Risk, Environmental merit, and Costs, plus other information regarding the evaluation of the scenarios themselves. It is possible to create a *multi-criteria classification* among the various scenarios produced (options) by considering as criteria the three synthesis values and their relative importance. This study may be effectuated either in direct form, indirect, or mixed, using procedures such as *Delphi*, *focus group*, *nominal group technique*, compulsory priority scale, cognitive maps, and so on. The evaluation may include analyses of 'sensitivity' and 'robustness' aimed at the stability of results and the management of the uncertainty of the process.

Evaluation of the areal effects of reclaim consists of creating simulations of variations (due to the redevelopment) of the indicators, such as real estate values within the areas or perception of stigma. Variations within values of suburban areas are assessed on the basis of rules governing the distribution of values and distance interaction.

3. Development of the system in the period 2003-2006

During the three-year research period 2003-2006 certain features of ELGIRA were completed and integrated, and further functions were developed. Certain process 'windows' were opened in order to facilitate the interaction and the transmission of information between the modules. Integration involves the database of the reclaim technologies, the zoning model, the analysis of health risk according to new national legislation, the creating of reclaim options, the option modules for REC input, and final multi-criteria evaluation of the options.

3.1 Reclaim technologies database

Available reclaim technologies for the project in progress are held in the ArTe Database, which was designed especially for ELGIRA applications.

In this database, technologies are presented by general (type of reclaim process, etc.) and specific (costs, performance, etc.) descriptors which are used in the selection of the preliminary reclaim plan for the area in consideration.

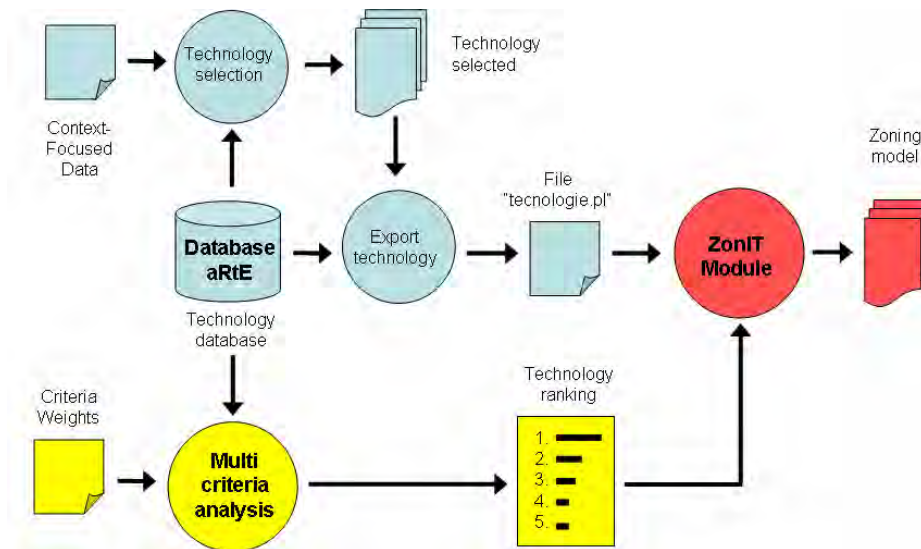


Fig 2 – Selection and evaluation of reclaiming technologies.

The database has an interrogation interface for the selection of the most appropriate technologies according to certain specific selection criteria – *treatment location, type of treatment, type of terrain, state of the terrain, maximum costs, pollutant classification*. The technologies may be subjected to preliminary screening. Those technologies selected by the ArTe database are forwarded to the ZonIT module, which carries out zoning of the polluting agents, the technique – area relation, and creates the options.

The classification of techniques is of great help in the selection of those which will prove optimal when options are being created in the ZonIT module.

The reclaim technologies archive is structured in the form of a *web interface database*. It acts therefore as a provider, with an dual-channelled interface for the *consultation* and *insertion* of information. Consultation permits the user to search the archive in order to choose between one or more technologies on the basis of either single or multiple parameters, while insertion means that new techniques or updated data may be added to those already present.

The techniques (either all those present in the database or only those selected) may be compared and contrasted according to criterion groups and descriptors on the basis of choice-making problems, classification, assignment, or exploration. ELGIRA is able to accommodate several algorithms with a view to aggregation which may be total, partial, iterative, or interactive with MCDA or MCDM.

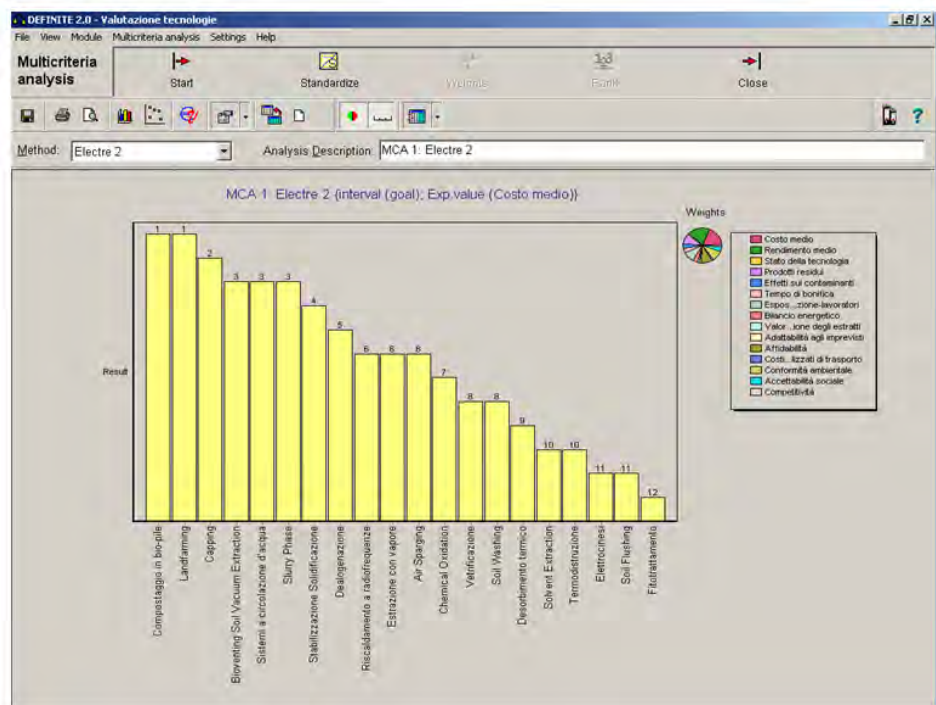


Fig 3 – An example of technologies classification using the Electra II technique. Software printout.

3.2 The zoning model

The ZonIT (ZONizzazione degli Inquinanti e delle Tecnologie di bonifica - Zoning of the polluting agents and reclaim techniques) module prepares the scenario of a reclaim site with indications as to the contaminated areas and the applicable reclaim technologies.

With ZonIT, both the land pollution model (maps created via interpolation) and information derived from the technologies archive may be used. This information then goes on as input to the *technology costs and performance evaluation module*, reclaim options identification, the REC module for the analysis of Risk reduction, of Environmental merit evaluation, and of Costs.

Bi-dimensional maps of substance concentration derived from the land pollution model may be subjected to thresholding in order to produce meaningful subsets and possible combinations. With these it is then possible to define a zoning as

an areal juxtaposition of polluting agents. The technologies are correlated to the pollutants in the zoning results, thus identifying plausible collusions.

The phases of construction of the zoning model are illustrated in the figure below.

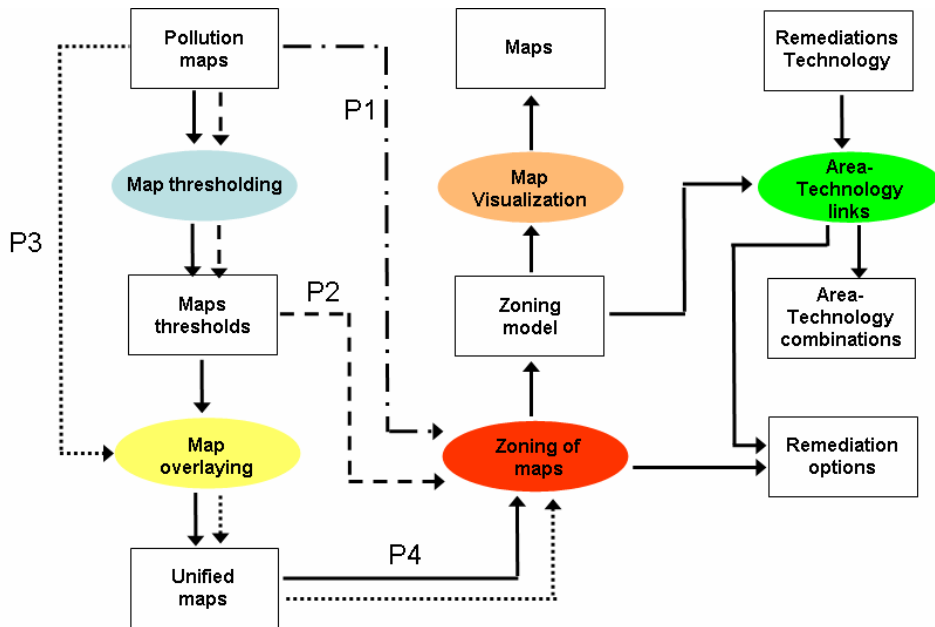


Fig 4 – ZonIT: phases and functions.

Zoning is carried out by using pollutant concentration maps of single or group polluting agents. The complexity of the aggregation depends on the number of layers and on the way in which they are connected and interpreted.

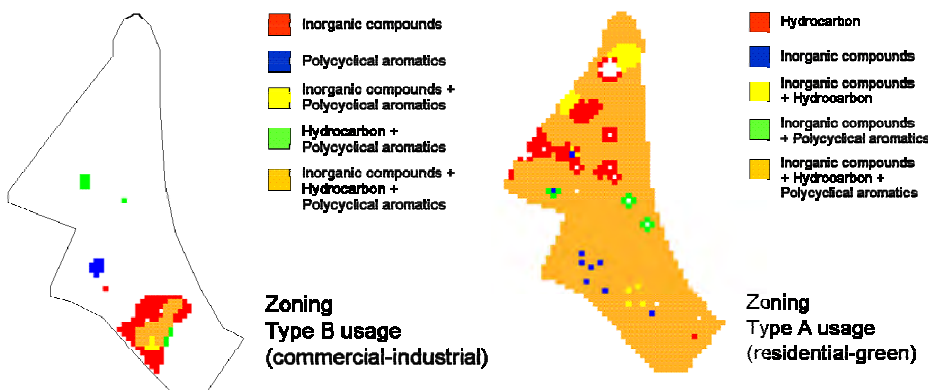


Fig 5 – Zoning maps of polluting agents. The SMP area of Porto Marghera.

3.3 Environment risk analysis

ELGIRA uses specific software for health (human) and environment (ecosystems) risk analysis: Giuditta, ROME, and Risc are all used for the health component, while a module of the REC (Risk, Environment, Cost) procedure is used for environmental analysis.

New Italian legislation (law no. 152, 2006) has shifted the priority of health risk regarding the identification of areas to be subjected to reclaim compared to previous ruling (Ministerial Decree no. 471, 1999).

The previous decree stated that the reference thresholds for an intervention were to be found within the tabular limits of concentration of a polluting substance (in regards to type A and type B sites). Areas with concentrations higher than those limits were to be subject to reclaim. Analysis of health risk was carried out ex-post to verify that the reference indices (for cancerogenous and non substances) had not been breached in the case that it had not been possible to reduce the concentration level to below the maximum legal limit via reclaim.

ELGIRA and the new environmental italian law L. 152/2006

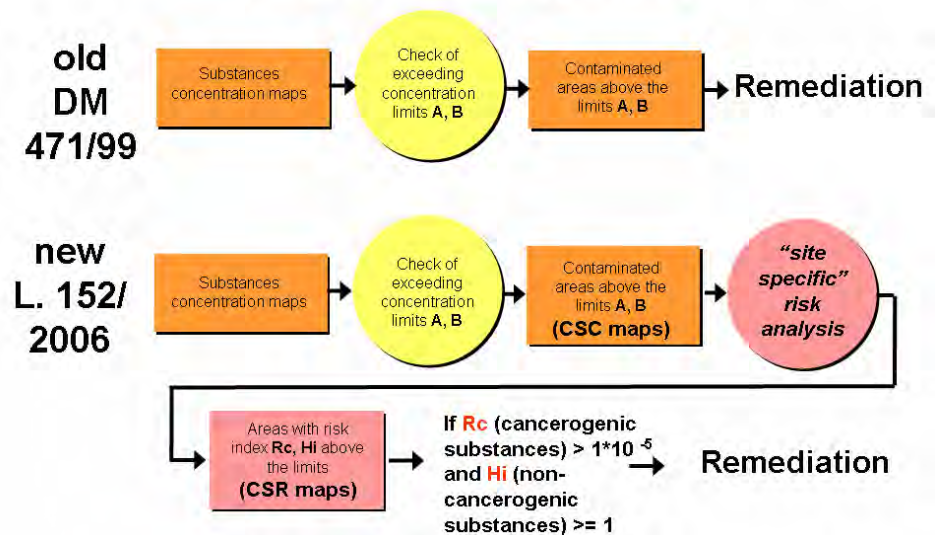


Fig 6 – Risk analysis and reclaim areas: comparison between old and new legislation.

The new ruling calls for a preliminary test of the overshooting of the concentration values of substances in reference to sites of type A and B (similar to the values in the previous decree 471/99). Should the CSC (or “warning”) thresholds be overshoot then it is necessary to carry out a characterization along prescribed lines, thus laying the foundations for a risk analysis which is “site specific” in the survey points.

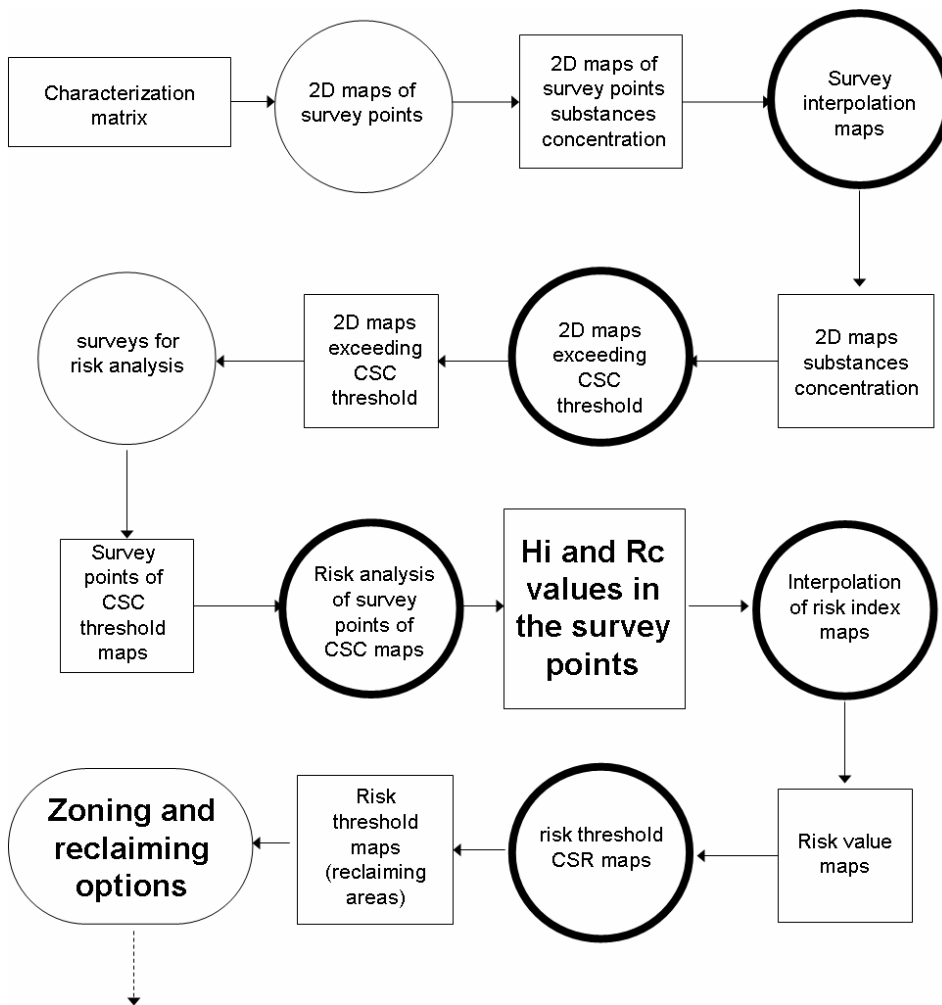


Fig 7 – Zoning of reclaim areas according to Law 152/2006.

Areas in which the risk is superior to the limits imposed by law (CSR thresholds of risk indices for cancerogenous and non substances) will be subjected to reclaim operations with the aim of bringing the risk within the legal limits. Unlike the previous law 471/99, zoning with law 152/2006 depends on the mapping of health hazards.

Health hazards indeed 'lead' the reclaim and are no longer considered 'objective' side-concerns (in fact they were referred to as 'residual risks') as was the case with law 471. Now a strategic component, health hazard analysis can deploy greater degrees of freedom.

The operational phases of ELGIRA in the determining of reclaim areas on the basis of Law 152 are evident in fig. 7.

Phase 1 Substance concentration at 'surface points' and creation of value distribution maps

Values of substance concentration at surface level and bi-dimensional maps for each of the substances in question are estimated by using the data produced from characterization sounding.

Complete maps of substance concentration are produced with the application first of surface sounding points and then bi-dimensional interpolation.

Phase 2. CSC threshold excess maps.

With the use of thresholding algorithms for the complete maps of substance concentration it is possible to identify the areas where the limits of CSC concentration has been exceeded, either for sites of type A or of type B. Should none of the areas within the site prove positive to CSC excess, no further identification of potential reclaim areas is carried out.

Phase 3. Health hazard analysis in the sounding points

The sounding points of the areas produced by thresholding are subjected to site-specific analysis. Alternatively, the totality of the points are taken into consideration. In the case that a preliminary characterization does not satisfy the legal requirements, another characterization will be necessary.

survey	x	y	Hi<1	Hi>=1	Rc<1*10 ⁻⁵	Rc>=1*10 ⁻⁵
1	10	27		1.3	5*10 ⁻⁶	
2	15	31		1.5		5*10 ⁻⁵
3	16	43		1.2		1.2*10 ⁻⁵
4	22	47		1.3		5*10 ⁻⁵
5	31	44		1.1	2*10 ⁻⁶	
6	32	53	0.7		8*10 ⁻⁶	
7	33	60	0.85		2*10 ⁻⁶	
8	42	48		1.1	1*10 ⁻⁶	
9	66	65	0.9		4*10 ⁻⁶	
10	80	46		1.25		3*10 ⁻⁵
11	69	45		1.1		2*10 ⁻⁵
12	64	32	0.5		6*10 ⁻⁶	
13	51	36	0.6		1*10 ⁻⁶	
14	50	28	0.8		7*10 ⁻⁶	
15	37	19		1.2		1.5*10 ⁻⁵
16	32	28		1.1	8*10 ⁻⁶	
17	24	18	0.7		8*10 ⁻⁶	
18	24	11	0.5		1*10 ⁻⁶	

Fig 8 – Risk analysis in the sounding points-of the SMP area of Porto Marghera. Hi indices (non-cancerogenous substances) and Rc (cancerogenous substances) indices. (Legal limits: Hi=1, Rc=1*10⁻⁵).

For the health risk analysis, one of the software systems quoted above is utilized. The procedure determines the index values of risk (cancerogenous and non-cancerogenous) for each of the substances or for groups of substances, for single pathways and receptors or else in a synthetic manner.

Phase 4 Interpolation of the risk index maps.

Bi-dimensional interpolation of risk index generates the hypothetical distribution of index values throughout the whole surface of the site.

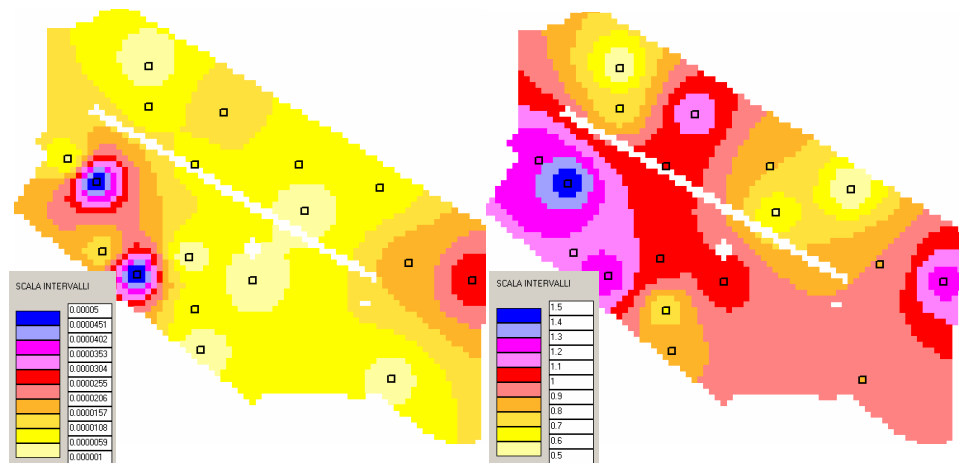


Fig 9 – Estimated distribution of risk indices Hi (right) and Rc (left). The SMP area of Porto Marghera.

Phase 5 Maps of the values in excess of the CSR threshold.

At this point, maps are created of the areas within the site where risk index values have exceeded the CSR thresholds: for each index, pathway, receptor, and substance in consideration.

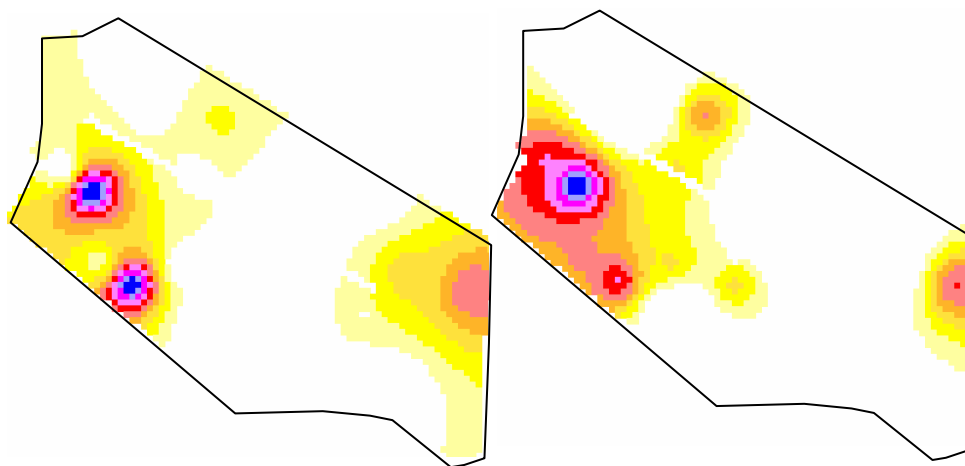


Fig 10 – Areas with values superior to the legal limit: H_i (right) ≥ 1 and R_c (left) $> 1 \cdot 10^{-5}$. The SMP area of Porto Marghera.

The maps produced in Phase 5 can be used for zoning and the identification of reclaim technologies and options.

3.4 Reclaim options

With ELGIRA it is possible to create a preliminary series of reclaim options. Each option is composed of a set of technologies associated to treatable polluting agents. Through the zoning (of areas, pollutants, etc) carried out hitherto and the technologies chosen from the archives, the possible combinations of technology/pollutant are produced. Each of the options has its own descriptors and a maximum of nine are chosen. It is on the basis of these descriptors that the reclaim options are then constructed.

A maximum limit of permissible technologies means that the theoretical combinations and option redundancy can be reduced. It is worth remembering here that a detailed characterization, together with a complete pollution and zoning model represents very effectively the geography of the polluting agents.

The selection of technologies can be carried out with the aid of ranking techniques.

Without a preliminary selection, the choice of technologies is guided by criteria related to the technologies themselves: terrain, type of treatment, costs, performance, etc.

Tabella Sintetica Valutazione Opzioni									
A	B	C	D	E	F	G	H	I	J
Opzioni tecnologie applicabili	Tecnologia su famiglie inquinanti			Rendimento medio opzione (%)	Costo totale opzione	R medio	C medio	C trasf	R trasf
OPZIONE n. 1	Desorbimento termico su Famiglia Aromatici policiclici	Capping su Famiglia Composti inorganici	Elettrocinesi su Famiglia Idrocarburi	90	338436000	88,7274	523772333	-185336333	1,2726
OPZIONE n. 2	Desorbimento termico su Famiglia Aromatici policiclici	Elettrocinesi su Famiglia Composti inorganici	Elettrocinesi su Famiglia Idrocarburi	90	445900000	88,7274	523772333	-77872333	1,2726
OPZIONE n. 3	Desorbimento termico su Famiglia Aromatici policiclici	Soil washing su Famiglia Composti inorganici	Elettrocinesi su Famiglia Idrocarburi	90	660828000	88,7274	523772333	137055667	1,2726
OPZIONE n. 4	Elettrocinesi su Famiglia Aromatici policiclici	Capping su Famiglia Composti inorganici	Elettrocinesi su Famiglia Idrocarburi	90	267768000	88,7274	523772333	-256004333	1,2726
OPZIONE n. 5	Elettrocinesi su Famiglia Aromatici policiclici	Elettrocinesi su Famiglia Composti inorganici	Elettrocinesi su Famiglia Idrocarburi	90	375232000	88,7274	523772333	-148540333	1,2726
OPZIONE n. 6	Elettrocinesi su Famiglia Aromatici policiclici	Soil washing su Famiglia Composti inorganici	Elettrocinesi su Famiglia Idrocarburi	90	590160000	88,7274	523772333	66387667	1,2726
OPZIONE n. 7	Soil washing su Famiglia Aromatici policiclici	Capping su Famiglia Composti inorganici	Elettrocinesi su Famiglia Idrocarburi	90	474336000	88,7274	523772333	-49436333	1,2726
OPZIONE n. 8	Soil washing su Famiglia Aromatici policiclici	Elettrocinesi su Famiglia Composti inorganici	Elettrocinesi su Famiglia Idrocarburi	90	581800000	88,7274	523772333	58027667	1,2726
OPZIONE n. 9	Soil washing su Famiglia Aromatici policiclici	Soil washing su Famiglia Composti inorganici	Elettrocinesi su Famiglia Idrocarburi	90	796728000	88,7274	523772333	272955667	1,2726
OPZIONE n. 10	Soil flushing su Famiglia Aromatici policiclici	Capping su Famiglia Composti inorganici	Elettrocinesi su Famiglia Idrocarburi	88,4064	322128000	88,7274	523772333	-201644333	-0,321
OPZIONE n. 11	Soil flushing su Famiglia Aromatici policiclici	Elettrocinesi su Famiglia Composti inorganici	Elettrocinesi su Famiglia Idrocarburi	88,4064	429592000	88,7274	523772333	-94180333	-0,321
OPZIONE n. 12	Soil flushing su Famiglia Aromatici policiclici	Soil washing su Famiglia Composti inorganici	Elettrocinesi su Famiglia Idrocarburi	88,4064	644520000	88,7274	523772333	120747667	-0,321
OPZIONE n. 13	Desorbimento termico su Famiglia Aromatici policiclici	Capping su Famiglia Composti inorganici	Soil flushing su Famiglia Idrocarburi	88,2516	398076000	88,7274	523772333	-125696333	-0,4758
OPZIONE n. 14	Desorbimento termico su Famiglia Aromatici policiclici	Elettrocinesi su Famiglia Composti inorganici	Soil flushing su Famiglia Idrocarburi	88,2516	505540000	88,7274	523772333	-18232333	-0,4758
OPZIONE n. 15	Desorbimento termico su Famiglia Aromatici policiclici	Soil washing su Famiglia Composti inorganici	Soil flushing su Famiglia Idrocarburi	88,2516	720468000	88,7274	523772333	196695667	-0,4758
OPZIONE n. 16	Elettrocinesi su Famiglia Aromatici policiclici	Capping su Famiglia Composti inorganici	Soil flushing su Famiglia Idrocarburi	88,2516	327408000	88,7274	523772333	-196364333	-0,4758

Fig 11 – Reclaim options. Synthesis table.

There may be a great number of options arising from the elaboration process (even tens of various options may be produced), not all of which applicable, in that some areas are non-treatable (interference between pollutants and technologies).

Fig. 12 shows a classification of the options according to parameters of performance and costs. The selection has been ratified by experts in the field.

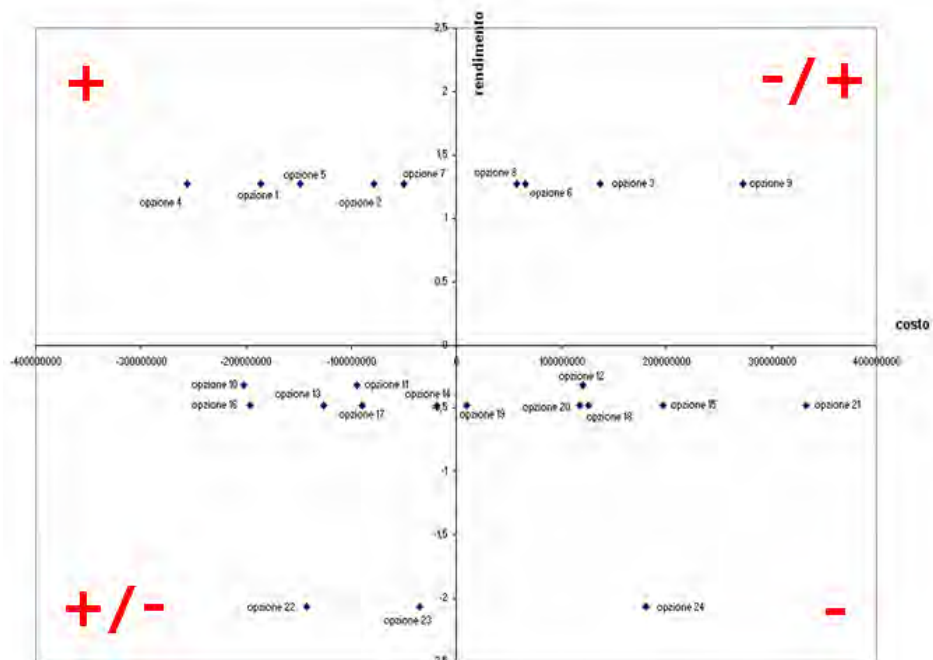


Fig 12 – Reclaim option evaluation. The relation between performance and costs in the ensuing options.

3.5 Input to REC: costs and performance

Via the 'Options Profile' it is possible to view and utilize the information for the REC module in an appropriate input format. Information for the Options Profile come from the database for the ArTE technologies, from the pollution model, and the zoning model.

The Options profile is made up of four sheets of calculations: Variables, Performance, Timing and Costs. One of these profiles is compiled for each of the options.

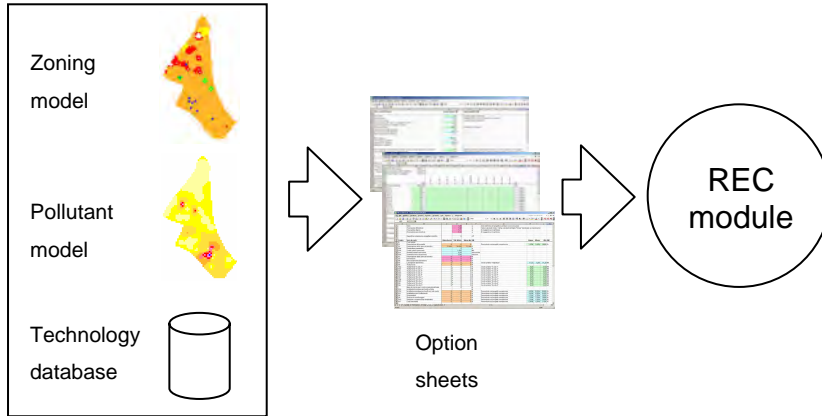


Fig 13 – Options profiles for module REC input.

The Variables sheet contains the values for the modalities used in other parts of the profile.

The Performance sheet contains information regarding the project area (areas, volumes, etc.); the amount of surface area to be reclaimed with the chosen technologies; the consumption of energy and resources during the reclaim operations, and the waste produced and the space occupied.

The Timing sheet refers to the time taken to effect the reclaim, on the basis of the areas treated by each technology, the number of treatment lines, to the capacity, and to the productivity. Treated volumes and weights within each intervention area are calculated.

The Costs sheet comprises sections dedicated to initial costs, current costs, renewal costs and others.

Codice	Voce di costo	Stima base	Val. atteso	Stima alta LIM	Rasca	Attica	Alta LIM
10 A1	Preparazione del progetto	0	0	0	1,35%	1,50%	1,65%
11 A2	Preparazione delle opere di bonifica	22.500	25.000	27.500			
12 A2a	Durata fase preparativa	5	5	5			
13 A2b	Costo unitario personale	1.000	1.000	1.000			
14 A2c	Quantità ventata personale	5,00	5,00	5,00			
15 A2d	Quantità minima di persone	5,00	5,00	5,00			
16 A3	Preparazione delle opere di bonifica	0	0	0			
17 A3	Demolizioni	0	0	0			
18 A4	Risassettamento del terreno	0	0	0			
19 A5	Lavorazione del terreno	0	0	0			
20 A6	Trattamenti	0	0	0	11,70	13,00	14,30
21 A6a	Trattamento "in situ 1"	0	0	0	0,00	0,00	0,00
22 A6b	Trattamento "in situ 2"	0	0	0	0,00	0,00	0,00
23 A6c	Trattamento "in situ 3"	0	0	0	0,00	0,00	0,00
24 A6d	Trattamento "in situ 4"	0	0	0	0,00	0,00	0,00
25 A6e	Trattamento "in situ 5"	0	0	0	0,00	0,00	0,00
26 A6f	Trattamento "Ex situ 1"	0	0	0	0,00	0,00	0,00
27 A6g	Trattamento "Ex situ 2"	0	0	0	0,00	0,00	0,00
28 A6h	Trattamento "Ex situ 3"	0	0	0	0,00	0,00	0,00
29 A6i	Trattamento "Ex situ 4"	0	0	0	0,00	0,00	0,00
30 A6j	Trattamento "Ex situ 5"	0	0	0	0,00	0,00	0,00
31	Base di calcolo per i costi a base percentuale	0	0	0			
32 A7a	Installazioni prelievo per bonifica in situ	0	0	0			
33 A7b	Installazioni prelievo per bonifica in situ studio	0	0	0	4,50%	5,00%	5,50%
34 A7c	Installazioni per il trattamento	0	0	0	4,50%	5,00%	5,50%
35 A8	Schemature	0	0	0	1,35%	1,50%	1,65%
36 A8	Sistema di monitoraggio	0	0	0	1,35%	1,50%	1,65%
37 A10	Gestione e sospensione ambientale	0	0	0	1,35%	1,50%	1,65%
38 A11	Costi secondari	0	0	0	0,90%	1,00%	1,10%

Fig 14 – Options Profile. Resource and costs sheet.

3.6 Multicriteria scenario evaluation

The REC procedure, which is a central component of ELGIRA, supplies certain reclaim scenarios, based on the options referred to above. The performance of such scenarios can be measured using three criteria, Risk reduction, Environmental merit and Cost (R, E, C).

This is a synthetic representation of the scenarios, limited to a trade-off between the three criteria. Each of these has come about through complex construction and has much to contribute to the evaluative process. With its specific response functions, the criteria are able to configure the stability of the scenarios

Three tests

The results from three test areas in the Porto Marghera (Venice) site are illustrated below. The indices for Risk reduction, Environmental merit and Cost, supplied by REC processing, are indicated below.

43 ettari site		Scenery/Reclaim options				
REC index	Thermic desorbition + soil washing	Soil washing (two lines)	Soil washing (one line)	Capping	Dumping	
R. Risk reduction	21,49	21,00	20,49	12,19	28,40	
E. Environmental merit	-4,86	-4,79	-4,82	2,84	-1,32	
C. Cost (Mil. Euro)	20,387	20,558	20,558	5,322	45,590	

Ex Sava site		Scenery/Reclaim options					
REC index	Soil washing + incinerat. + dumping	Thermic desorp. + incinerat. + dumping	Solvent extraction acid/bivitation + incinerat. + dumping	Bioremediation with bacteria + incinerat. + dumping	Incineration	Capping	Dumping
R. Risk reduction	4,53	4,53	5,46	5,46	5,52	2,93	5,52
E. Environmental merit	70,36	76,70	76,06	76,82	65,79	26,71	90,76
C. Cost (kEuro)	66,788	72,889	43,215	84,494	72,889	27,579	49,102

SMP site		Scenery/Reclaim options				
REC index	Thermic desorp + dumping + electrokinesis	Thermic desorp + electrokinesis	electrokinesis + dumping	electrokinesis	Soil washing su Aromatici + dumping + electrokinesis	Dumping
R. Risk reduction	12,43	12,39	12,45	12,38	12,43	13,09
E. Environmental merit	-0,8992	-0,8271	-0,1631	-0,0981	-0,1975	-1,8311
C. Cost (Mil. Euro)	18,881	39,270	10,562	34,319	27,295	12,346

Fig 15 – R, E, C, indices for three test sites.

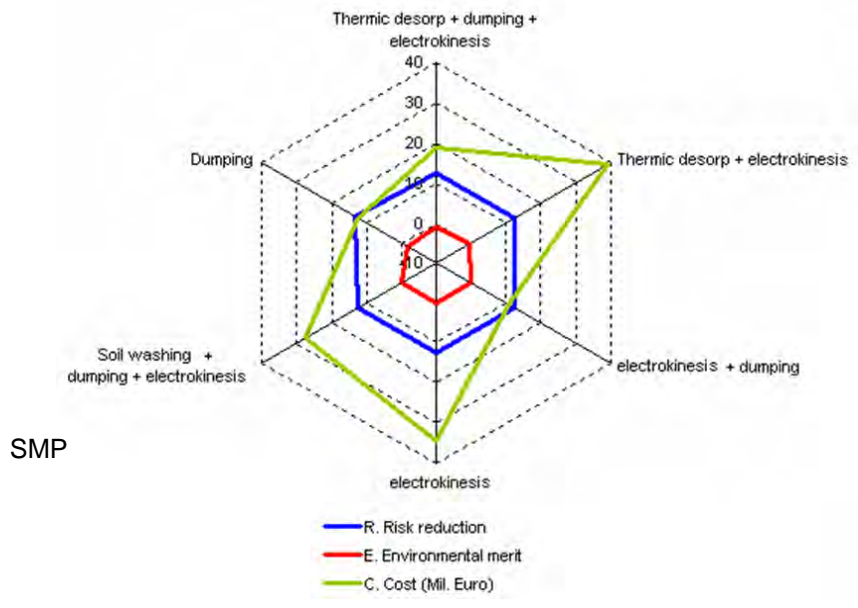
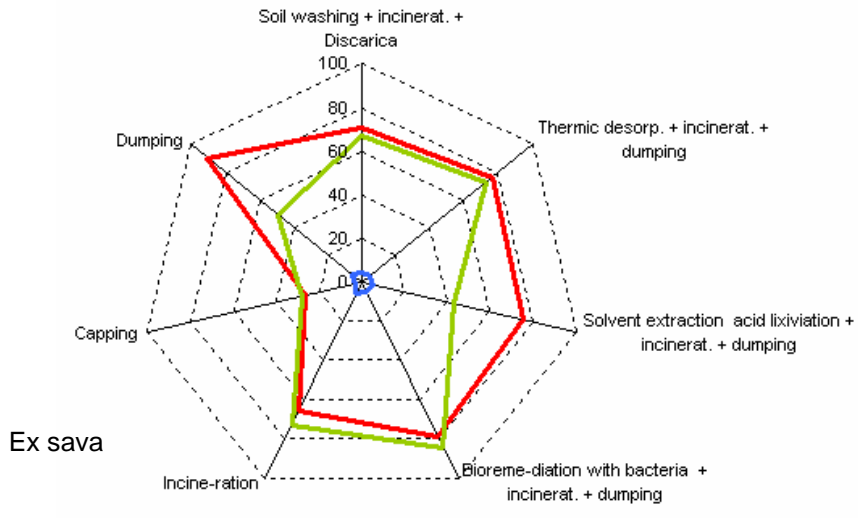
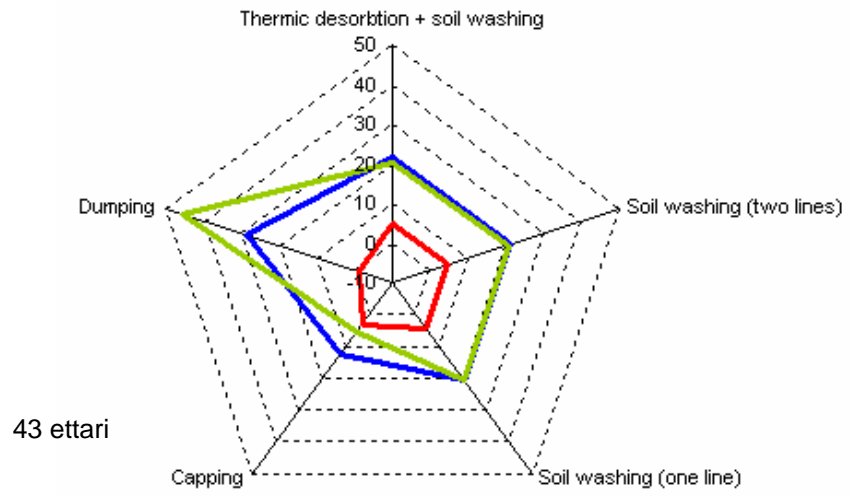


Fig 16 – Standardized index R, E, C for the sample sites.

The weights attributed to criteria via direct procedures (experts), for all three sites are as follows:

R index (Risk reduction): 0.3; E index (Environmental merit): 0.2; C index (Cost): 0.5.

The multi-criteria evaluation is carried out using an ELECTRE II extrapolation algorithm. The data is processed with Definite software (v.2.0).

The following figures illustrate the classification of performance of the scenarios in the three sites, according to evaluation results.

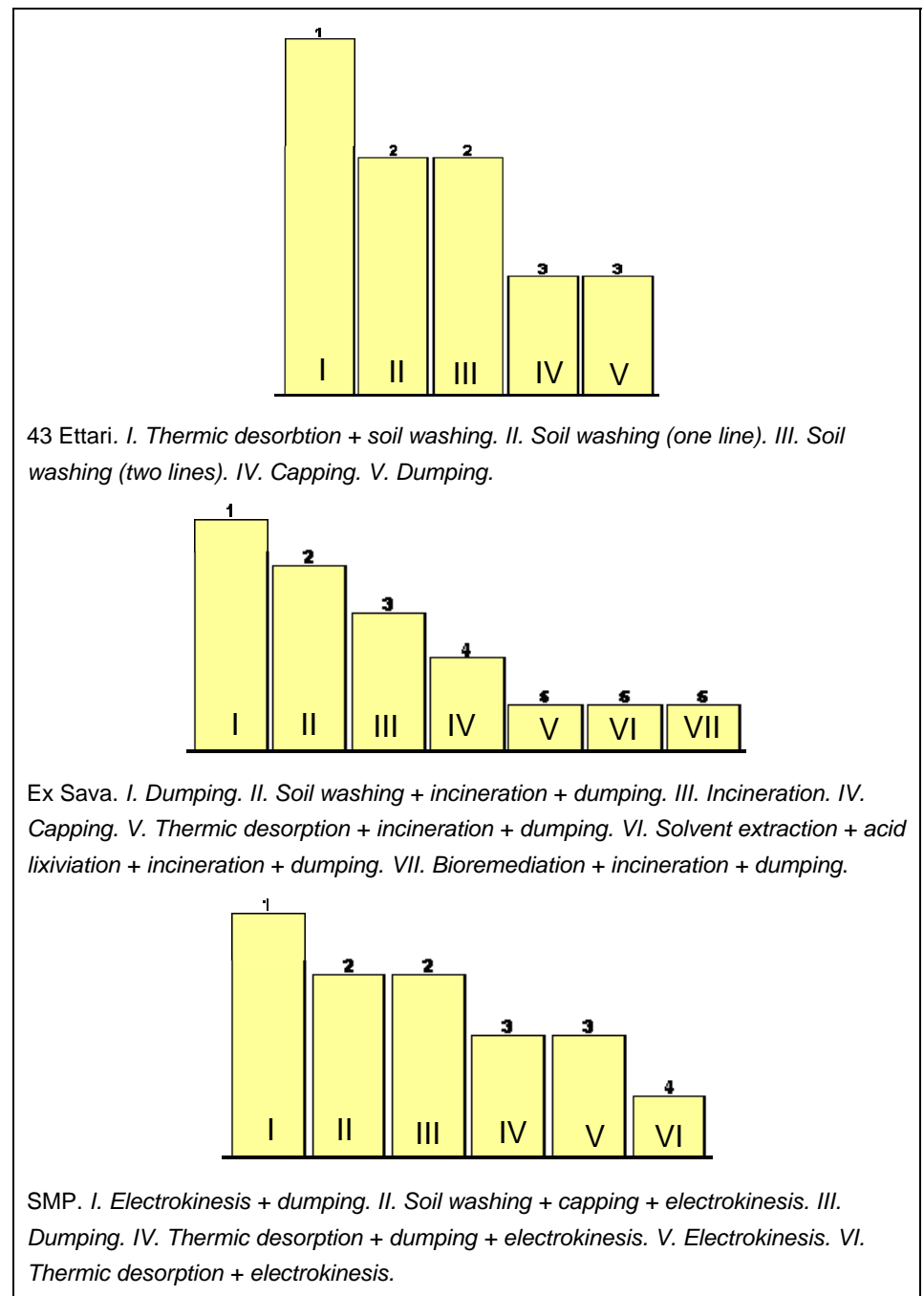


Fig 17 – Classification of the reclaim options for the three test sites.

3.7 Areal effects: AURES module

The redevelopment of a site produces precision and areal affects for both the natural and the urban surroundings. These effects regard the variations within such qualities as urban life, accessibility, eco-systemic continuity, area value. In order to comprehend the effects of a redevelopment intervention it is fundamental to estimate the dynamics that produce these effects. This can be done via simulation procedures that refer to widespread “rules” or “laws” that may in their turn derive from spatial models which have already been ratified in similar contexts and are able to indicate implicit costs in appropriate hedonic functions, or from empirical studies regarding the expectations and behaviour of investors, city users, real estate agents, and other interested subjects.

ELGIRA uses the module AURES to create the areal effect simulation. AURES is a procedure based on cellular automaton methodology in which a spatial scenario is modified in its evolution by both local and global rules which act on the component elements (cells). Two rules are used for the interaction: local and distance. The former enables the simulation of value variation in an area according to the values of adjacent areas; the latter captures the effects on areas located further from the reclaim site. In both cases the effects follow particular ‘regimes’ due to inertia, ‘rugosity’, or roughness, and assimilations within the territory concerned.

With AURES it is possible to impose parameters for the local and distance rules.

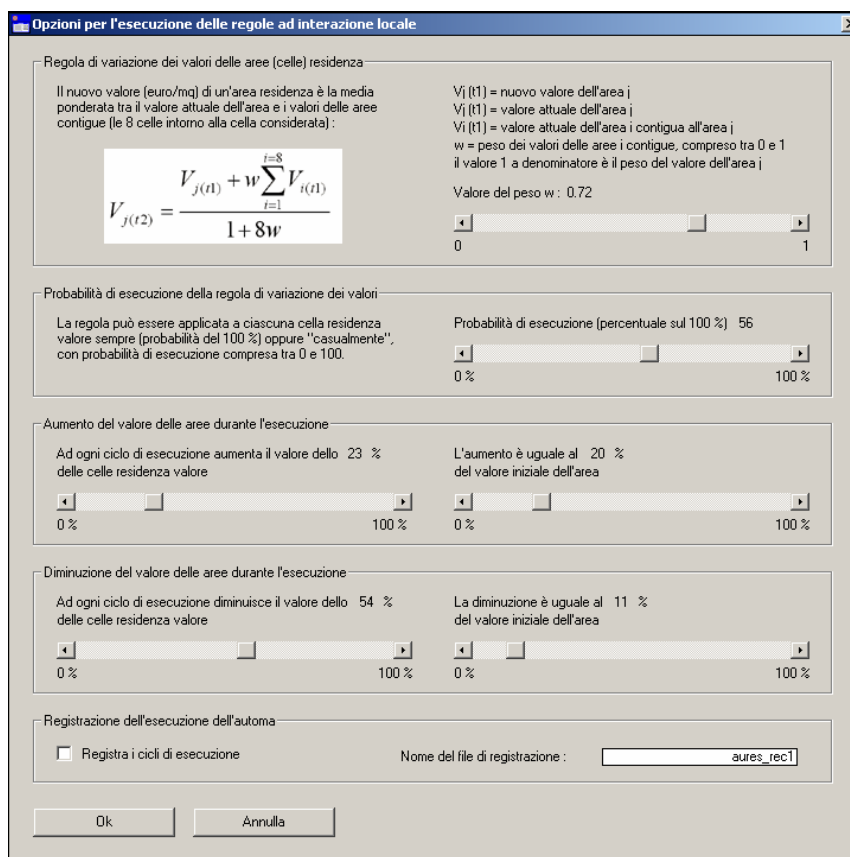


Fig 18 – AURES: simulation model of areal effects and rules of distance interaction.

With the distance interaction rule (fig. 19), it is possible to indicate the scenario for the redeveloped area, choose between two types of value “perception at a distance” functions (exponentially decreasing or increasing-decreasing), as well as other parameters such as quality or prestige of the redevelopment. Dependence of the new values on the original value is mediated by limitations, opportunity, public investment projects and market logic.

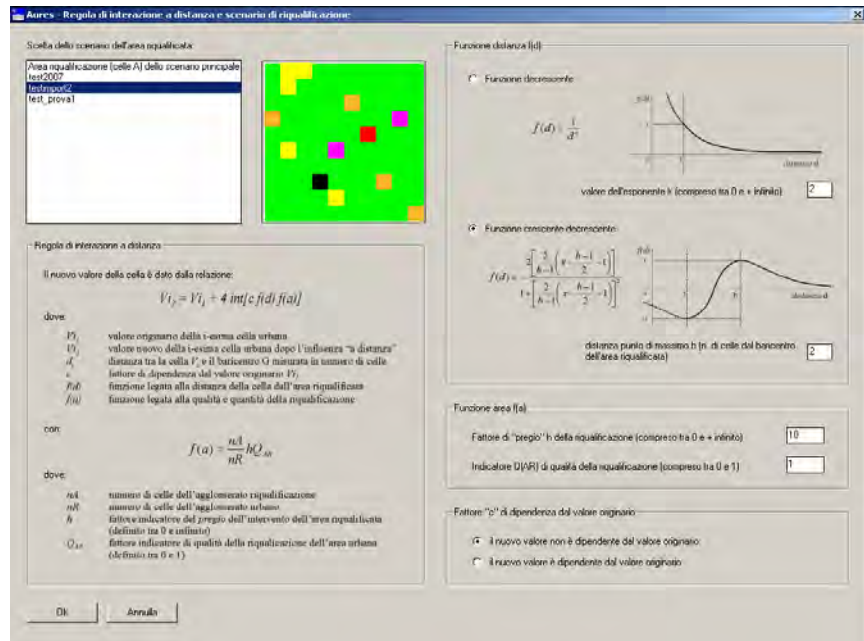


Fig 19 – AURES: simulation model of areal effects and rules of distance interaction.

With the distance interaction rule (fig. 19), it is possible to indicate the scenario for the redeveloped area, choose between two types of value “perception at a distance” functions (exponentially decreasing or increasing-decreasing), as well as other parameters such as quality or prestige of the redevelopment. Dependence of the new values on the original value is mediated by limitations, opportunity, public investment projects and market logic.

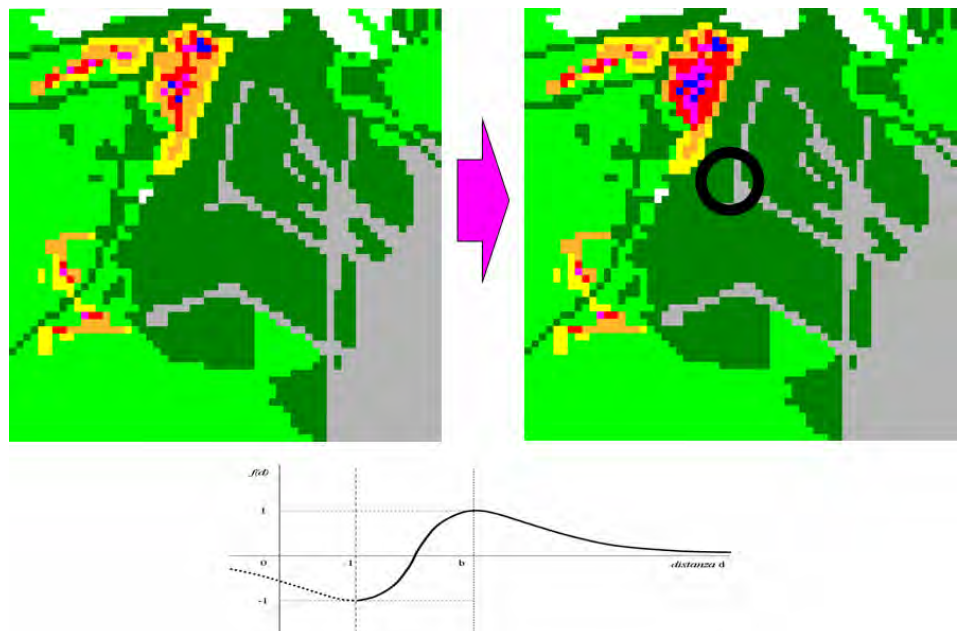


Fig 20 – AURES. Simulation at Marghera (Venice).

Fig. 20 shows the results of a simulation of the effect of reclaim on the property market in a test area (the urban district of Marghera, province of Venice). The property values used in the simulation are land registry estimates which have been updated on the basis of interviews with workers in the sector and information on transactions. These present only a relative 'validity', although sufficient to represent the oscillations within the interested area.

The area subjected to reclaim is highlighted by the circle; the property values (indicated by colours from yellow to blue) before (left) and after (right) the redevelopment operation. The local and distance rules were applied according to the increasing-decreasing function.

Conclusions

The results from this research highlight how in the Porto Marghera mega-site the costs of reclaim of contaminated land are extremely high. If the costs of monitoring, externalities and alternative land uses (opportunity costs) are taken into account, then the costs of safety-ensuring, capping and dumping also all increase well beyond the estimates carried out in the first three tests. Safety-ensuring and capping interventions are non definitive solutions to the geographic-morphological characters of the borders of the lagoon, nor the eustasy phenomena, the permeability level of the land and the hydro-dynamic pressure, the degradation of the structures, or the risks connected to the possible variations in the sea level-health mean due to climate change.

To these direct costs must be added the costs of characterization, updating, and the certification of data gathered via sampling and surveys. All these components exert an influence on the economic profitability of investment in reclaim, thereby laying the burden on the public administration for financing that would be very difficult to charge to private investors.

The results of the tests, therefore, lead to the conclusion that the Master Plan should foresee mixed scenarios that include substantial components of re-naturalization that are coherent with a morphological redesigning of the waterfront.

References

- Fabris E., 2005, 'Area Ex-Sava: analisi del rischio eseguita su diversi scenari di bonifica del suolo e sottosuolo', Rapporto interno CORILA, Venezia.
- Fabris E., 2006. 'Analisi del rischio sanitario in Italia: quadro generale dei software in uso e delle metodologie applicative di riferimento'. Rapporto interno CORILA, Venezia
- Hedorfer M., 2004, Elgira Toolkit 1, 'Algoritmi di interpolazione verticale delle concentrazioni di inquinanti', Rapporto interno CORILA.
- Patassini D., Cossetini P., De Mitri A., De Polignol E., Hedorfer M., Rinaldi, De Zorzi S. 2005. 'The new version of ELGIRA: a support system for knowledge

building and evaluation in brownfield redevelopment'. In *Scientific research and safeguarding of Venice*, CORILA Research Programme 2004-2006, Volume V, 2005 results. CORILA.

Patassini D., Cossettini P., De Polignol E., Fabris E., Hedorfer M., Rinaldi, Verni E. 2005. 'The EL.GI.R.A support system for knowledge building and evaluation in brownfield redevelopment. An application in the 'Ex Sava Alumix' area in Porto Marghera (Venice), in *Scientific research and safeguarding of Venice*, CORILA Research Programme 2004-2006, Volume IV, 2004 results. CORILA.

Patassini D., Cossettini P., De Polignol E., Hedorfer M., Paneghetti C., Rinaldi , 2005. 'ELGIRA – A Knowledge Support Procedure to reclaim Porto Marghera Brownfield. In Environmental Protection of the Lagoon of Venice: An Economic Valuation', Rapporto interno, CORILA.

Patassini D., Hedorfer M., Rinaldi E., De Polignol E., Cossettini P., Paneghetti C., 2005, 'Contextual knowledge generated by a dss for brownfield development- the case of Porto Marghera (Venice)', in D. Miller, D. Patassini 2005, *Beyond benefit cost analysis. Accounting for non-market values in planning evaluation*, Ashgate, Aldershot.

Patassini D., Hedorfer M., Rinaldi E., De Polignol E., Cossettini P., 2004, 'ELGIRA: Support System for Knowledge Building and Evaluation in Brownfield Redevelopment', in *Scientific Research and Safeguarding of Venice*, CORILA Research Programme 2001-03, CORILA.

Patassini D., Hedorfer M., Rinaldi E., De Polignol E., Cossettini P., 2005c, 'ELGIRA - A Knowledge Support Procedure to reclaim Porto Marghera Brownfields, Environmental Protection of the Lagoon of Venice: An Economic Valuation', Rapporto interno, CORILA.

Patassini D., Rinaldi E., 2004. 'Aures Guida Utente. Versione 2.0', Rapporto interno, CORILA.

Patassini D., Rinaldi E., 2007. 'Aures Guida Utente. Versione 3.0', Rapporto interno, CORILA.

Patassini D., Rinaldi E., 2006. 'ELGIRA. Sistema di aiuto alla conoscenza e alla valutazione nella riqualificazione dei siti inquinati. Linee guida per la esecuzione di una sessione di valutazione. Versione 1.5', Rapporto interno, CORILA.

Patassini D., Rinaldi E., 2006. 'ZonIT. Modello di zonizzazione degli inquinanti e delle tecnologie di bonifica. Guida Utente. Versione 1.5', Rapporto interno, CORILA.

Patassini D., Rinaldi E., 2007, 'Prove di riqualificazione dei siti contaminati a Porto Marghera. L'esperienza di ELGIRA', in *DA Speciale Marghera*, XIX, Luglio, pp. 46-53.

Rinaldi E., 2006. 'Valutazione multicriteriale delle tecnologie di bonifica', Rapporto interno, CORILA.

Wimmer S., 2004. 'ELGIRA. Concentration limits and levels of attention in Europe and in the United States. A comparative study about the legal settings in

Italy, the Netherlands, the United Kingdom, Germany, France, the EU, and the USA'. English and Italian version.

Economic Valuation for Policy Making: Using Conjoint Choice Experiments to Investigate Stakeholder Preferences for Contaminated Land Cleanup and Redevelopment Programmes

Margherita Turvani¹, Anna Alberini², Stefania Tonin¹

1 Dipartimento di Pianificazione, Università IUAV di Venezia,

2 AREC, University of Maryland

Riassunto

L'abbandono di aree urbane, la dismissione di siti industriali e il degrado di aree di pregio ambientale costituiscono un significativo problema urbanistico ed economico la cui origine può essere ricondotta all'evoluzione stessa del sistema economico e a fattori normativi ed istituzionali di tipo ambientale ed in materia di sicurezza. L'intervento teso alla riqualificazione di tali aree urbane ha ampio impatto, spesso di difficile quantificazione, e produce effetti positivi sulla qualità della vita, sull'ambiente e sullo sviluppo economico sociale. Se i benefici connessi ai processi di recupero urbano ed ambientale sono molteplici, tali processi sono tuttavia costosi e chiamano in causa nuovi attori, sia nel settore pubblico sia in quello privato. La realtà di Porto Marghera rappresenta un esempio particolarmente significativo ed emblematico di queste problematiche, non solo per la sua collocazione nell'area della laguna di Venezia, ma per la sua importanza in quanto sito industriale soggetto a riconversione con notevoli impatti sul sistema naturale e antropico. Questo articolo riassume 5 anni di ricerca del Dipartimento di Pianificazione nel tentativo di stimare i costi e i benefici della bonifica e della riqualificazione dei siti contaminati in generale e di Porto Marghera in particolare. Attraverso l'applicazione del metodo dell'analisi congiunta sono state realizzate due importanti indagini con due prospettive diverse, la prima quella del developer che deve realizzare gli interventi e la seconda quella della collettività che può beneficiare di simili interventi.

Abstract

Cities are currently faced with the problem of abandoned industrial sites, derelict urban areas, and environmental degradation of large spaces, due to two major concurrent factors: the structural change in the economy and the development of environmental and safety regulations. Urban regeneration and remediation interventions are likely to have large, but hard to quantify, impacts on human health, on the economic and social development, on life quality, and on the environment. While there are many benefits associated with urban and environmental regeneration, these interventions are very expensive, and call for public and private sectors' active participation. Porto Marghera in the Lagoon of

Venice represents an outstanding and challenging example of the aforementioned processes. This article presents the results of a 5 year research program at the Department of Planning of the University IUAV aiming to value cost and benefits of contaminated sites cleanup and redevelopment in the area of Porto Marghera. Using the conjoint choice methodology, two important surveys were implemented adopting two different perspectives. The first assumes the point of view of the developers who have to realize the interventions and the second represents the population who can benefit from these interventions.

1 Introduction

The Lagoon of Venice is a complex ecological system that has been shaped through centuries by human action, offering support for a long lasting and successful social and economic development. The industrial sites of Porto Marghera have contributed a great deal over the last decades to this development, giving way nowadays, after a long period of industrial restructuring, to a contaminated megasite, posing a wide range of ecological and socio-economical problems. Part of this area still hosts ongoing relevant economic activities, while major areas constitute 'brownfields'. These are defined as 'real property, the expansion, redevelopment, or reuse of which may be complicated by the presence or potential presence of a hazardous substance, pollutant, or contaminant'¹.

All industrialised economies are experiencing two concurrent processes: the first is the transformation of the economy, with the downsizing and relocation of manufacturing and the increasingly larger role of the service sector. The second is a profound institutional change, with the introduction of environmental legislation for the protection of public health and the environment, imposing liability for environmental damages.

These two reasons have spurred the creation of large areas of brownfields, especially in urban areas, in Europe and the US, opening up serious ecological and economic problems for public action.

The economic problems posed by the presence of such large contaminated areas, including the potential damages to human health and the ecosystem, are well recognized in literature (Ferguson, 1999; USEPA, 2005). Appropriate legislation has been passed over the past 30 years by all the major industrialized countries to address the issue of liabilities for cleaning up these sites and to possibly stimulate the reuse of these properties with a wide array of economic and social benefits. Experiences in these fields have been developed mainly in USA and Europe and they now constitute examples for the new EU

¹ The Brownfields Site definition is found in Public Law 107-118 (H.R. 2869) - "Small Business Liability Relief and Brownfields Revitalization Act" signed into law Jan. 2002

countries and for the newly rapidly industrialised countries, all facing similar problems.

Experiences of remediation report the high costs of these projects, including the costs to identify not only the contaminants and the appropriate techniques but also the liable parties, plus the actual costs of cleanups and the cost of realization of the projects to eventually reuse these properties. The overall costs are quite significant and they are incurred now or in the near future, while in most cases the benefits of remediation and reuse actions take much longer to realize and to be perceived. This is especially true when the sites have to be cleaned up because of the high risk they impose on human health and the ecosystem, irrespective of the existence of a feasible and at hand solution for reusing the site. Furthermore in many cases liable parties cannot be identified and/or cannot be forced to pay for damages and the financial burden is on public money.

For these reasons it is important to assess both from a social perspective the benefits of cleaning up contaminated sites, and to identify those policies and actions that could be effective in stimulating private parties to take action and invest in this area of economic activity, developing financially viable projects for cleanup and reuse of contaminated properties.

Italy, as most of the industrialized countries, has developed appropriate regulations to deal with the problem of contaminated sites, and it has gained its own experiences in dealing with these problems. Contaminated sites represent a relevant problem in Italy, where it is possible to count around 13,000 potentially contaminated sites (APAT, 2006) and where a National Priorities List of large and dangerous sites has been defined, including 53 major sites, all over the Country.

One of these large areas is located on the northern border of the Lagoon of Venice, just a few kilometres from the historical city of Venice, posing huge ecological and economic problems on the Lagoon and the whole Region. Porto Marghera is one of the 53 contaminated sites of national interest managed directly by the Italian Ministry of Environment under the Law 471/99 and its subsequent modifications. Since the beginning of the 20th century, the industrial area of Porto Marghera (3,000 hectares of land and water) hosted heavy industries, an industrial port, and a huge petrochemical plant with an overall employment of about 33,000 workers. After decades of activity, during the 80's industrial transformations took place, implying dismissal of land and activities, leaving behind wide contaminated areas, and ongoing industrial and tertiary activities employing around 12,000 employees.

Central and local governments are thus facing the problems caused by past polluting industrial activities and the related damage to the environment and possibly to human health. The most common harmful substances contaminating soil and water are heavy metals (e.g. lead and arsenic), oil products, polyaromatic hydrocarbons, polychlorinated biphenyls, chlorophenols, and pesticides. These dangerous substances are present in high concentration and have been linked to the high incidence of specific types of cancer like soft tissue

sarcoma, angiosarcoma and asbestos-related cancers.

It is unquestionable that remediation of contaminated soil and groundwater would yield numerous benefits to the society, the economy, and the ecosystem. The benefits relate to positive health impact, environmental quality, urban environment, stigma elimination and productive reuse of the property. Yet, many difficulties have been experienced through time in successfully cleaning up these sites and redeveloping them for the profit of the whole society.

In the last 5 years, the Department of Planning of the University IUAV of Venice and a local research Institutions, the consortium CORILA, have developed a common research programme to assess the benefits of the cleanup and redevelopment of contaminated sites. The immediate purpose is to promote improved decision making in public action in the area of Porto Marghera, at the same time the research has been designed with the more ambitious goal of addressing the issue at the national level, where sound policy making can take advantage from the local experience and from the findings of this research, and with the willingness to contribute to the international debate which is particularly lively.

The research programme specifically addressed the question of evaluation of the benefits related to health risk reduction for people living close to contaminated areas on the one side, and it investigated real estate developers' perspectives and decision making when developing projects for cleanup and reuse of contaminated sites.

Our research approached the process of economic valuation of policy making of contaminated sites from two relevant interrelated perspectives. On the one side, the real estate developer's point of view, including incentives and obstacles to brownfields redevelopment, such as liability, lack of financial resources and stigma; the aim was to improve public policies supporting private investment and public and private partnerships in this field, with the purpose of increasing the supply of remediated land for redevelopment and accelerating the pace of cleaning up contaminated sites. On the other side, our research addressed the effect of contamination on human health and the ecosystem, and the public demand for risk reduction, the perceived benefits of public policies related to mortality risk, the value of statistical life (VSL), and issues of risk perception and knowledge.

Results from both research areas are rather valuable for local and national decision making and offer relevant contributions to economic and environmental research from a methodological point of view. The common denominator, and the added value, of our research programme is the adoption of the same methodological approach to valuation and to investigate stakeholder preferences and perception. We refer to a family of techniques called *stated preference*, and more specifically we applied conjoint choice analysis.

This paper reports major research activities and findings of the aforementioned research programme, specifically focusing on the two surveys that have been developed to assess stakeholder preferences (citizens and real estate

developers) for contaminated land cleanup and redevelopment programmes, by using conjoint choice techniques. Both surveys implied the development of appropriate questionnaires to investigate general understanding and perspectives on the issues involved and elicit WTP values; both questionnaires implied an in depth analysis of relevant literature (Tonin, 2006), an extensive study of legislation and policies in USA and Europe (Turvani et al, 2006). The development of the surveys was accompanied by several focus groups in Venice and in Italy with the involved stakeholders for preliminary investigation and for testing and refinements of the interview-tool (Tonin et al. 2005).

In section 2, we explain the main market-based instruments and other incentives for promoting and regulating environmental cleanup and redevelopment. In this context we describe the results of a conjoint choice survey to assess the responses of real estate developers to different variations of these incentives. In section 3, we analyse the main benefits of contaminated sites cleanup and redevelopment and we present the results of our survey aiming to valuing a mortality risk reduction for different public programs of contaminated sites remediation. In section 4, we investigate more deeply the public opinion regarding the phenomenon of contaminated sites and the necessity of public programs to address the redevelopment of these sites, whilst section 5 concludes.

2 Regulation, Liability and Economic Incentives for Remediation and Redevelopment of Contaminated Sites: Investigating Developers' Perspective

2.1 The Role of Public Regulation

The large number and extension of contaminated sites is a substantial economic and territorial issue, and a serious environmental problem. Contaminated sites potentially create several types of externalities that include adverse effects of pollution on human health; adverse effects on other determinants of human welfare such as aesthetic values, urban congestion and degradation; damage to ecological systems; and perception of a subjective decrease in welfare of agents or of an increase in risk. These externalities may affect many parties, including residents, workers, tourists, and users of natural resources.

Economic theory distinguishes two types of government intervention aimed to correct environmental externalities, e.g. economic instruments and incentives such as taxes, subsidies, tradable permits, deposit refund systems. Command and control instruments or a regulatory approach, such as emission standards, concentration limits, and mandatory certification are also available.

A major legal and economic tool to address the problem of negative externality is the identification of the liable parties. Liability for the cost of remediation of contaminated sites is a widely adopted approach, but it too can create high costs or risks, to the point that potentially attractive sites are left idle, thus defeating one of the purposes in establishing the liability system. Many western

countries have adopted a liability framework for handling contaminated sites, on the grounds that it is felt that the burden of environmental restoration should be placed on the responsible parties regardless of other economic factors.

Liability forces firms to internalize the external damages of their production activities, and is thus regarded as an economic incentive to reduce pollution. Whilst working as an ex-ante economic tool, but also offering ex-post coverage for damages, individuating the responsible party and generating a source of financing for remediation. It is the approach adopted to deal with hazardous waste sites in the US, Germany, the Netherlands and Italy.

The principle underlying liability is to define what is to be considered as polluted and to spell out the criteria for identifying the parties that are legally held responsible for the pollution and must pay for remediation. Responsible parties can be obliged to clean up and sued if they fail to do so.

National legal traditions differ greatly and deeply influence the choice of the type of liability applied. All liability regimes share the same goal of getting polluters to pay for the damages they have caused, but in practice there may be significant differences in how the liability regimes work. In Italy, legislation addressed contaminated sites starting in 1997—fifteen years later than in other western countries. Article 17 of D. Lgs. 22/1997 and its application, art.9 of DM 471/1999, states that the party who is responsible for the pollution has to bear the cost of the cleanup, even if pollutants are released into the environment by accident.

In Europe, the Directive on Environmental Liability with regard to the prevention and remedying of environmental damage (2004/35/EC) draws from the Superfund Law, the US law for contaminated sites, whilst trying to avoid some of the drawbacks identified in the Superfund program. The EU legislation is not retroactive and will apply only to damages caused after the Directive enters into force in the Member States. Moreover, the most obvious difference between the Superfund Law and the European Directive is that the former is a comprehensive cleanup program that employs liability as one of its funding approaches. The Directive, on the other hand, allows Member States to hold parties liable for the environmental damages they have caused, without however creating a comprehensive cleanup program.

Observers believe that fear of liability can have both direct and indirect effects on brownfield development. The direct effects are that developers may shy away from properties believed to be contaminated for fear of future liability and because immediate cleanup costs may prove too high for the development project to be viable. Regarding the indirect effects, developers may fear that lenders may deny financing for brownfield projects to avoid liability, and/or undervalue the property as a collateral for the loan. In addition, it is sometimes

speculated that “contamination stigma”² may raise the uncertainty about demand for or reduce the revenue from the sale of contaminated sites.

2.2 Market-based mechanisms, incentives, and liability to promote the environmental remediation and reuse: a survey of developers

Command and Control has been the prevailing answer of the Regulator in the past; more recently a new approach has been developed both in USA and Europe, combining the previous command and control approach and tight liabilities system with several innovative forms of incentive measures, and regulatory relief to help more effective voluntary agreements at the local level with the purpose to promote more cleanups and to collect larger financial means.

Regulatory practices in the area of contaminated sites entails creating new knowledge in technology and capacity building, some consensus around controversial environmental issues, appropriate institutional structures and norms to address site specific risks and environmental issues. Finally a monitoring system to evaluate the performance of the selected solutions and the possible undesired consequences should be implemented.

Our research programme assumed a theoretical framework where liabilities, incentives, deterrents and enforcement are conceived as parts of a unified system of governance for the remedial process. The first application of our research has been designed with the specific purpose to examine the role of different market based regulatory mechanisms, and other incentives intended to promote the environmental remediation and reuse of “brownfields”.

We examined the value of interventions and policies targeting brownfields from the perspective of the key actors involved—mainly private real estate developers. We posed three related research questions. First, what economic incentives can be offered to developers to encourage cleanup and reuse of brownfields, and how effective are they? Second, what kind of site characteristics and available infrastructures make a parcel attractive for cleanup and reuse, and to what kind of developers? If sites/developers can be identified that are more likely candidates for development, this may allow more effective targeting of policies based on economic incentives and liability or regulatory relief. Third, are developers truly influenced by contamination stigma, whereby a parcel’s potential or past contamination makes it less desirable?

2.3 The questionnaire and main results

² Stigma is defined as “a market imposed penalty that can affect a property that is known or suspected to be contaminated, property that was once contaminated but is now considered clean, or a never contaminated property located in proximity to a contaminated property” (Dybvig, 1992).

We use conjoint choice experiments to study the responses of real estate developers to different variations of these incentives in different possible investment choices, under different specific circumstances. Our survey instrument written in three languages, namely English, Italian and French, was administered in person to a sample of developers and real estate professionals (out of some 17,000 real estate developers) randomly intercepted at the *Marché International des Professionnels de l'Immobilier (MIPIM)* in Cannes, France, in March 2002.

The interview begins with a series of screening questions intended to determine whether the respondent is a developer, whether he or she works for a private company, a non-profit organization, or a government agency, and whether his/her company's principal business is within the real estate development market.

The questionnaire gathers more specific information on the business of the respondent's company, such as the typical project the company is involved in and the associated revenue. Respondents are also asked whether his/her company has ever purchased, leased or developed sites located in industrial areas, or contaminated sites.

We then provide information on cleanup responsibilities, highlight the advantages and disadvantages of developing contaminated sites, and describe the incentives available in some countries to encourage the re-use of previously used sites. The respondent is then asked whether he is familiar with the cleanup legislation of the countries where his/her company does business, and whether his/her company has ever benefited from financial assistance from the government for redeveloping used sites.

The core of the questionnaire is the section with the four conjoint choice exercises. Conjoint choice is a family of survey-based methodologies for modelling preferences for goods, where goods are described in terms of their attributes and the levels that these take. Respondents are presented with various alternative descriptions of good, differentiated by their attributes and levels, and are asked to choose their most preferred (Hanley et al., 2003).

Each conjoint choice exercise describes two hypothetical development projects (Site A and Site B). Each site is described by seven attributes: (i) presence/absence of contamination; (ii) cleanup standards; (iii) availability of transportation network within 20 km from the site; (iv) presence/absence of a certificate issued by a government agency that relieves the developer from liability for further cleanup; (v) time for approval of development/cleanup plans by the appropriate government agency; (vi) presence/absence of a city within 20 km; and (vii) government financial incentives, expressed as a percentage of the value of the project. In each choice exercise, Site A differs from Site B in the level of two or more attributes. For each pair, the respondent is first asked which project he/she finds more attractive between A and B, and is then asked to repeat the choice between A, B and the option of not participating in either of the two projects. In Fig. 1 it is possible to see an example of our conjoint choice question.

Site choice

Now, we would like to ask you to choose between two hypothetical areas to develop. For each question, you will be described two hypothetical sites and will be asked to choose which one you believe is the more attractive of these two sites, based on the characteristics of the site.

In answering the following questions, please imagine that you are considering development projects of value/size similar to those of your company's typical project. The development project will be in the country or countries where your company generally does its business. Please be assured that your answers will be kept strictly confidential.

Choice 1

Attributes	Site A	Site B
Site contamination	Present	Present
Transportation network available within 20 km	Highway	Highway and railroad
Certificate of no further action	Yes	No
Oversight by government agency	Response to developer's application within 6 months	Response to developer's application within 6 months
Cleanup standards	Flexible	Flexible
City within 20 km	Present	Present
Government financial incentives as % of the value of the project	20%	10%

Which project do you find more attractive between A and B?

A B

If you were to choose between A, B, and the option of not participating in either of the two projects, which would you choose?

A B Neither

Fig 1 – Example of conjoint choice experiment.

Finally, we ask further information about the position of the respondent within his/her company, and ask whether he/she takes part in the final investment decision (or collaborates with the committee that makes the final decision) about undertaking or not undertaking a real estate development project. The respondent is asked to report the number of employees of his/her company and the 2001 level of sales. Other socio-demographic characteristics of the respondents, such as age and education, are also collected.

Our respondents were introduced to the conjoint experiments by being told that real estate developers who buy contaminated land must clean it up at their expense. They may find themselves responsible for cleaning up the parcels they have purchased to build infrastructure, industrial and commercial facilities, or homes, if hazardous waste is found on these parcels. This may occur, for example, when developers buy real estate that was previously used as an industrial or commercial site. Cleanup may be expensive, but abandoned or underused areas may be attractive to developers for a number of reasons.

The survey was successful and we completed about 300 questionnaires, which worked well, in the sense that respondents did not report problems with the conjoint choice questions, and exhibited well-behaved response patterns. Conditional and random-coefficient logit models of the responses to the choice questions indicate that developers find sites with contamination problems less attractive than others, and that they do value liability relief. This confirms our expectation that contaminated sites are less desirable because of the associated cleanup costs, but refutes earlier claims (Urban Institute et al., 1997) that liability does not matter.

These policies may affect different components of the costs and revenues associated with redeveloping the site. Liability relief, for example, reduces or eliminates the risk of future liability for cleanup costs, as long as the developer meets certain requirements. It may, in addition, help raise the revenue from the sale or rental of the site due to avoiding the stigma associated with existing or suspected contamination. For this attribute, we consider two possible levels: (a) no certificate of assurance issued, and (b) certificate of assurance issued.

Faster response time by the Agency encharged to approve the developer's project may reduce its costs, and eliminate some of the uncertainty typically associated with undertaking brownfield projects. Earlier research in this area suggests that reducing uncertainty may be an important component of effective brownfield programs. We use two levels of this attribute, setting response times within 6 months, and 24 months, respectively, of the date of the application.

Direct financial incentives can be taken in the form of low-cost loans, tax credits, and rebates offered to the developer. In our survey, however, we do not specify what form they may take, and simply tell the respondent that they are for 10%, 20% and 30% of the value of the project.

We reason that different policy mixes can have a different appeal to the developer, depending on the attributes of the site where the redevelopment project is to be undertaken. Accordingly, we include three more attributes to describe the project: the presence of contamination at the site, the availability of transportation networks near the site, and the presence of a city within 20 km of the site to capture access to markets and suppliers.

Regarding contamination, each alternative is characterized by one of three possibilities: (a) no contamination, (c) contamination, or (c) the site was previously contaminated by remediation has taken place. The latter level of the attribute allows us to check for developers' fears of a possible contamination stigma. Assuming that all sites would have regular access to highways, the alternatives can also have access to rail, an airport, and a harbour.

We then collected data regarding the experiences of respondents to check whether they significantly influence their choices. For example we tried to understand if familiarity with legislation governing clean-ups or previous experiences with contaminated facilities affect willingness to intervene in brownfield redevelopment. Preliminary processing of data shows that some personal factors may influence the probability of choosing a contaminated site. Complete results in this line of research may be found in Alberini et al. (2005).

Main results of our statistical model indicate that market-based incentives and regulatory relief can influence land use redevelopment. Developers find contaminated sites less attractive, and they value liability relief in the form of a certificate of "no further action needed". Liability relief is worth about 21% of the value of the median development project (€7 million). Moreover, developers with prior contaminated site experience are very responsive to government subsidies, whereas inexperienced developers are more responsive to liability

and regulatory relief. Table 1 displays in more detail the marginal prices of the attributes for the sample as a whole and for specific groups of developers, based on the median value of a project.

	Complete Sample	Experience with contaminated sites	No Experience with contaminated sites	Larger Firms	Smaller Firms
CONTAM_P	€ 2.549 (1.267)*	€ 1.455 (0.702)*	€ 7.119 (4.310)	€ 5.029 (3.306)	€ 2.081 (1.015)*
CERTIFIC	€ 1.464 (0.302)*	€ 0.921 (0.209)*	€ 3.433 (1.743)*	€ 2.521 (1.384)	€ 1.240 (0.271)*
OVERS	€ 0.108 (0.019)*	€ 0.059 (0.010)*	0.277 (0.127)*	€ 0.164 (0.076)*	€ 0.096 (0.016)*
FLEXSTDS	€ 0.738 (0.222)*	€ 0.318 (0.164)	€ 2.066 (1.172)	€ 1.540 (1.029)	€ 0.572 (0.204)*

Tab 1 – Marginal Prices in million of euros, based on median project value (€7 million).

The table shows that the presence of contamination is worth €2.5 million, in the sense that, all else the same, developers would require financial assistance for €2.5 million for a €7 million project involving a contaminated site where remediation has not yet been undertaken. An alternative interpretation is that developers would be willing to sacrifice up to 2.5 million € to obtain a pristine site. This accounts for almost 37% of the revenue from the project. There is, however, much variability in the value of avoiding contamination between different types of developers. Developers with contaminated site experience, for instance, would require only €1.46 million, smaller developers €2 million, and larger developers €5 million.

The certification of completion, which exempts the developer from future liability over contamination at the site, is worth about €1.5 million, implying that developers would sacrifice this amount to secure a letter of completion by the appropriate government agency. This is approximately 21% of the revenue from the project. This time, it appears that developers with no experience at contaminated sites are willing to pay more to obtain one such a letter (€3.4 million v. €0.9 million of developers with experience).

Our model also implies that each month of delay in the approval of cleanup plans is worth €108,000. It is interesting that developers who have previously engaged in projects at contaminated sites and smaller developers attach lower values to a delay of one month in the agency's response time (€59,000 and €96,000, respectively).

Finally, the marginal price of flexible standards is €738,000, implying that respondents would pay this amount to have the opportunity to negotiate the cleanup standards with the government agency. This figure represents roughly ten percent of the value of the project here considered (€7 million).

Developers with prior experience with contaminated sites are more responsive to financial assistance than the others. The likelihood of selecting the contaminated site vis-à-vis with a pristine site increases by roughly 11 percent points for every additional 10-percent subsidies for developers with contaminated site experience, but by only 2 percent points for developers without contaminated site experience.

The developers who are not experienced in contaminated sites are relatively insensitive to subsidies and more responsive to liability relief. Similar considerations hold for larger firms. Those developers who sell their development projects, as opposed to using them themselves however, value liability relief even more highly.

Summarising, our respondents are not deterred by prior contamination, once it has been cleaned up, suggesting that “contamination stigma” is not very important, and appreciate fast-track review of development and remediation plans, direct financial incentives, and flexible (negotiable) cleanup standards. Our survey data suggest that developers are generally responsive to policies that encourage redevelopment and reuse of brownfields through market mechanisms, such as transfers and liability relief, and through regulatory relief. The impact of these policies, however, varies with the type of developer. This information, especially if confirmed by studies based on other techniques or on administering our survey instruments to samples of developers from different universes should be useful in recognizing what types of developers respond to brownfield policies and in designing brownfield policies.

3 The benefits of contaminated sites cleanup and redevelopment: people’s preference and WTP for risk reduction

3.1 Health benefits and risk reduction

A major goal of environmental programs for contaminated sites is to address the protection of human health and reduce the sources of risks for the population involved. Attaining this goal requires making decisions regarding the extent of pollution that must be removed from soil, the subsurface and groundwater in order to protect human health, whether contaminants should be removed, as opposed to implementing remedies that simply prevent human exposure to contaminants and/or off-site migration of the polluting substances in the short term. Clearly, it would be useful to compare the (monetized) value of more permanent reductions in the risks to human health with the costs of treating contaminated soil, groundwater and surface water. Doing so requires finding out how much the beneficiaries of these risk reductions are willing to pay to obtain them.

Since contaminated sites often entail exposure to carcinogens and other toxicants with long-term effects on health, the reductions in risks to human health delivered by remediation must be paid for now but are accrued in the future. Thus it is of interest to find out if the willingness to pay for risk reductions is affected by such a delay (“lag”), and, if so by how much.

With this broad perspective in mind, the research group at the Luav Department of Planning, thanks to the financial support from CoRiLa, set up a second survey, to be developed at the local and national level, focusing on people’s willingness to support public programmes aimed at reducing health risks. Specifically we dealt with the risks of death associated with exposure to contaminants at hazardous waste sites using conjoint choice questions to

answer this matter and to explore people's preferences for permanent remediation, and hence permanent risk reductions. We then illustrate the use of this approach with a sample selected as representative of the residents of four cities in Italy with significant contaminated site problems.

In this part of our research programme it was our aim to answer three main issues. First, how much are people willing to pay for each unit of mortality risk reduction? In other words, what is the public's Value of a Statistical Life (VSL) which should be used for computing the benefits of contaminated site policies that save lives? The VSL is the marginal value of a reduction in the risk of dying, and is therefore defined as the rate at which people are prepared to trade off income for a risk reduction. Second, do people favour permanent cleanup policies, and are they willing to pay more for longer-lasting risk reductions? Third, what is the effect on willingness to pay for delaying the beginning of the mortality risk reductions? Full details of methodology and results are reported in Alberini et al. 2007.

3.2 Questionnaire development and survey administration

The survey was self-administered using computers by respondents recruited from the general population in four Italian cities (Venice, Milan, Bari and Naples in May 2005, for a total of 804 completed questionnaires. The sample was stratified by age, with an equal number of respondents in each of three broad age groups (25-44, 45-54, 55-65), and was comprised of a roughly equal number of men and women.

The questionnaire has been designed to ask people about their awareness of the problems related to contaminated sites—including their perceptions about health risks associated with contaminated site exposures—and to elicit an assessment of the public's WTP for various policies addressing health risk reductions. It begins with asking people whether and how they are acquainted with contaminated sites. Since a respondent's notion of a contaminated site may be different from our own, we then provide the following definition: "A contaminated site is a parcel or an area with hazardous substances that pose risks to human health or the environment, now or in the future. These hazardous substances are the result of human activities. Electromagnetic fields/pollution and air pollution are not considered contaminated sites in this questionnaire." The questionnaire offers a description of the problem of contaminated sites in Italy providing information about the total population living in areas with sites on the National Priorities List—the most egregious contaminated sites—and thus potentially exposed to contaminants, current legislation and government policies.

Health risks as perceived by people and associated with contaminated sites is investigated and we focus on mortality endpoints and provide an estimate of the baseline mortality risks associated with exposure to pollutants found in contaminated sites.

When asking people to value risk reductions for a specific cause, it is important that respondents are told how this risk compares with mortality rates for other

causes and we offered the relevant information. Respondents are subsequently tested for risk comprehension.

Since our conjoint choice questions are concerned with public programs, we subsequently inquire about how important it is for the respondent to reduce the health risks posed by contaminated sites, and how much confidence they place in public policies such as economic incentives for firms, dissemination of information, more stringent inspections, institutional controls, and remediation undertaken directly by the government at orphan sites (see next section for results).

We present the concept of remediation and provide examples of possible remediation technologies, pointing out that they vary in terms of cost and time of completion, and that different type of sites and pollutants require different remedies. For example, pump-and-treat options are appropriate for contaminated groundwater, while bioremediation may be used at petroleum sites.

This is followed by the conjoint choice experiment portion of the questionnaire. Specifically, we showed people pairs of hypothetical public programs described by five attributes—the annual risk reduction afforded by the program, the size of the population living in the area with the contaminated sites that would be addressed by the program, how soon such risk reductions would be observed, the number of years over which the risk reduction would be observed (and hence lives would be saved), and the cost to the taxpayer. We then asked them to indicate (i) which they would prefer out of these two programs, and (ii) which they would prefer, program A, program B, or neither. In Fig. 2 it is possible to see an example of conjoint choice experiment.

Piani di intervento A e B

Nella tabella seguente ti presentiamo due diversi piani di intervento, A e B, che lo Stato può realizzare per bonificare dei siti contaminati. Questi piani di intervento garantiscono l'efficacia della bonifica e salvano vite umane.

Ciascun piano di intervento, come vedi, ha effetti diversi e salva un numero diverso di vite umane. Ti chiediamo di scegliere quello che preferisci.

Caratteristiche	Piano d'intervento A	Piano d'intervento B
Numero di vite salvate ogni anno su 1.000.000 di abitanti	30 su 1.000.000 ($\frac{30}{1.000.000}$)	20 su 1.000.000 ($\frac{20}{1.000.000}$)
Popolazione: il numero di abitanti potenzialmente esposti alla contaminazione	2.000.000	2.000.000
Tempo di attesa: numero di anni che devono trascorrere per cominciare a vedere le vite salvate	2 anni	2 anni
Contributo straordinario non ripetibile: somma di denaro che ciascun nucleo familiare dovrà versare per la realizzazione della bonifica	950 euro	300 euro
Durata: numero di anni durante i quali si continuano a vedere le vite salvate	30 anni	30 anni

16. Quale piano d'intervento sceglieresti tra A e B?
 A B

17. E se potessi scegliere tra A, B e nessuno dei due, quale sceglieresti?
 A B Nessuno

Indietro **Avanti**

Fig 2 – An example of conjoint choice experiment.

We use additional questions to gather further evidence about preferences for saving lives and about the rate of time preference. For example, we ask our respondents which option they would prefer, a program that saves 100 lives now, or one that saves $(100+X)$ in Y years, where the respondents are told to assume equal costs, and both X and Y are varied for the respondents. The discount rate for lives saved implicit in the responses to these questions can be compared to the one implicit in the money v. future risk reductions tradeoffs in the conjoint choice questions. We also ask people to express their agreement or disagreement about possible priorities for cleanup and risk reductions. Finally, we conclude the questionnaire with the usual sociodemographic questions and with questions about the respondent's own health.

3.3 Major findings

The concept of VSL is reasonably well accepted in academic and policy circles, and the VSL has been estimated using a variety of approaches. Yet, there is surprisingly little empirical evidence about the appropriate VSL that should be used in the context of risk reductions from remediation of contaminated sites.

Statistical modelling of the conjoint choices responses allows us to estimate the VSL—the first of our research questions. In addition, it allows us to answer two related questions: In the context of contaminated site policies, is the VSL affected by the individual characteristics of the respondent? Are the responses to the choice questions and the implied WTP figures internally valid, in the sense that they depend in predictable ways on variables suggested by economic theory and confirm opinions expressed by the respondent elsewhere in the questionnaire?

As the time it takes before lives are saved and the number of years over which lives would be saved are varied for the respondents, the responses to the conjoint choice questions can be used to estimate the rate at which people discount future risk reductions. Were such a rate found to be low, we would conclude that people care for permanent risk reductions, and that their WTP for risk reductions is slightly affected by the lag until the risk reductions are incurred. The opposite conclusions would be reached if the discount rate was found to be relatively high.

Earlier research has estimated the rates at which people discount lives saved in the future (Cropper et al., 1991, 1992) and the rates at which people trade off current income for future reductions in their own risk of dying (Horowitz and Carson, 1990; Moore and Viscusi, 1990; Hammitt and Liu, 2004), but to our knowledge none of these studies are specific to or easily adapted to contaminated site cleanup policies. Nor did any of them answer the question of how much more people are prepared to pay for permanent risk reductions.

In this study, we pay special attention to the internal validity of the responses, and so we inquire about people's preferences for permanence through direct attitude questions. We also compare the discount rate estimated from money v. risk tradeoffs with which people discount lives.

Finally, we note that by including, among the attributes of the hypothetical programs, the size of the population living in the areas with the targeted contaminated sites, we explore the question whether people care more for small risk reductions spread over a large population or for larger risk reductions that affected a smaller population.

Summing up, we found that people are willing to pay for permanence, but not at just any price. Using the responses to the conjoint choice questions, we estimate the VSL for an immediate risk reduction over the current year to be about €5.6 million. The VSL does not vary significantly with the size of the population that would be affected by the policy. However, the VSL is lower if the risk reduction occurs in the future. For a risk reduction occurring exactly 20 years from now, for example, we estimate our respondents' VSL to be only €1.27 million. We estimate that people discount future risk reductions at a 7.41% discount rate, which means that each respondent is willing to pay €340 now for a risk reduction of 10 in a million per year that begins in two years and continues over 10 years. For a more permanent risk reduction, i.e. one that continues over 20 years, each respondent would be willing to pay €502. For one that continues over 30 years, the WTP would be €579, and for one that lasts 45 years, €626. Clearly, people are willing to pay for permanence, but not just about any price, and risk reductions that take place in the more distant future are valued less highly than more immediate risk reductions. We find evidence that the VSL is individualized, in that it depends on (i) observable individual characteristics (e.g., age, gender and income), (ii) familiarity with contaminated sites, (iii) concern about the health effects of exposure to contaminants, and (iv) direct experience with cancer, one of the possible outcomes of exposure to toxicants at contaminated sites. The VSL also depends on what the respondent thinks the goals of a remediation program should be, and on which government actions he or she deems appropriate. However, we wish to emphasize that policymakers may not be able to use all of this information in policy analyses, because attitudes, beliefs and confidence in specific government actions are usually not known for the entire population of beneficiaries of the policy. Additional questions indicate that the rate at which people discount future risk reductions in money versus risk tradeoffs is within the ballpark of the rate at which they discount future lives. We interpret this as further evidence of good internal validity of the data, and of the fact that people were paying attention to the attributes of the program we wanted to focus on, including the futurity of risk reductions.

3.4 Applying results to Porto Marghera

The results of this study could be used in benefit-cost analyses of specific programs. Unfortunately, information about current risks associated with contaminated site exposures before and after cleanup of sites on the Italian National Priorities List is not publicly available. Without this data, we perform an illustrative benefit-cost analysis for a 43-hectare operating unit within the broader NPL site at Marghera, near Venice, Italy. In this operating unit—a former industrial waste dump owned by the City of Venice—soil and

groundwater are heavily contaminated with PAHs, heavy metals, and many other toxicants. Following Patassini et al. (2003, 2005), we focus on soil, for which remediation options include soil washing, thermal desorption, capping, and excavation with subsequent shipment of the contaminated soil to an approved hazardous waste disposal facility. We restrict attention to capping—the least permanent of remedies—and to excavation and removal of soil—the most permanent and the most expensive, and assume reuse for residential purposes. Based on their estimate of excess lifetime cancer risks ($4.78E-03$) and a conservative assumption of 70% conditional mortality, the annual mortality risk for residents is $4.54E-05$. Assuming that risk reductions would begin 10 years from now, and an exposed population of 30,000—as estimated in the Master Plan of the City of Venice (Regione Veneto and Comune di Venezia, 2004)—a permanent remedy such as excavation and removal of the contaminated soil would require at least an 87% risk reduction for the mortality benefits to exceed the cost of remediation (€45,589 million). By contrast, the least permanent of remedies, capping, which is estimated to cost about €5 million, results in positive net benefits even for 20% reductions from the baseline risk, and still, if we assume that the lifetime of the cap is only 10 years. Caution should be taken in interpreting our results, however, because they are based on one operating unit, and the Marghera NPL site is comprised of many operating units. In addition, our estimates do not include other benefits of cleanup, such as benefits to the ecological system, other economic benefits from the redevelopment of the area, etc. The results from our study can also be used to cast some light on the issue of re-use of contaminated sites, which is an important goal of current policies and programs (US GAO, 1995, 1997b). For industrial and commercial use, cleanup targets are often allowed to be less stringent than for residential use. This may in turn, imply that cleanup is completed earlier. The discount rate estimated in this study suggests that to achieve the risk reduction sooner, people would be willing to settle for a smaller risk reduction. Suppose cleanup delivers an annual risk reduction of 10 in a million for 10 years beginning 10 years from now. To bring these risk reductions forward to 2 years from now, people would be willing to settle for an annual risk reduction of 5.53 in a million. Likewise, achieving the risk reduction sooner, people would be willing to accept less permanence. Consider for example an annual risk reduction of 10 in a million to begin in 10 years and continue for 30 years. To bring the risk reductions forward to 2 years from now, people would be willing to settle for a remedy that lasts 9.25 years. These are intriguing implications of the preferences elicited through our approach, which we hope to explore more explicitly in future research.

4 Public Policies for Contaminated Sites: the Opinion of the Italian Public

Contamination of soil and water, at the surface and underground level, poses a serious threat to human health and the ecosystem and most countries have passed their own regulation to control this phenomenon and to put in place appropriate cleanup plans and standards. Remediation action at contaminated sites mitigate the risks to human health and the environment by interrupting

exposure pathways and reducing the amount, mobility and toxicity of uncontrolled hazardous wastes in the environment. Little is known, however, about whether the public is in favour of them: is the public supportive of direct public interventions? What are people's opinions about various priorities for public remediation of contaminated sites?

Surveying public opinion regarding the phenomenon of contaminated site and the necessity of public programmes to address remediation is interesting for two reasons. First, they allow us to assess whether policy programs currently being considered in Italy and the European Commission reflect the public's preferences. Second, people's support of these programs should be an important determinant of their willingness to pay for them, which measures their benefits (see the above paragraph).

The survey of residents in four Italian cities—Venice, Milan, Naples and Bari—selected to ensure a varied geographical coverage of the country and as they have serious contaminated site problems, has provided the opportunity to find out how familiar people are with contaminated sites, what human health effects they link with contaminated site exposures, and how much they worry about such health effects.

We focus on three main research questions. First, how well acquainted are people with contaminated sites, and where did they seek information about them? Second, what do people believe should be the goals of public remediation programs? Third, are the priorities people assign to such contaminated site programs systematically related to their individual and socio-economic characteristics, and to their degree of civic and environmental activism? Do they depend on how much people know about contaminated sites in their area, how much they know about remediation, and whether they approve of government cleanup activities in general?

A full report of methodology and findings may be found in Turvani et al., 2007.

The first order of questions we were able to answer with our survey was how well people knew about contaminated sites in general, in relation to direct personal experience, and where and how they found their information. The data shows that 90% of our respondents have previously heard of contaminated sites. This seems reasonable, since our respondents were selected among the residents of cities with a serious contaminated site problem. Further examination of the data reveals that there is variation across cities in the degree of awareness regarding contaminated sites: In Bari, only 81.50% of the respondents have heard of contaminated sites prior to the survey, while in Milan, Venice and Naples the corresponding figures are 96.52%, 91.63% and 90.50%. Respondents in the Bari sub-sample are less educated than the rest of the respondents, and thus we turn to look at the correlation between educational levels and prior knowledge about contaminated sites. Finally, 43% of our respondents are aware of the existence of contaminated sites near their homes or workplaces. These respondents generally are more concerned with health risks associated with contamination and, even before providing them with relevant information about possible health risks, they consider it more likely that

exposure to toxicants at contaminated sites will result in a number of adverse health effects, including allergies, respiratory problems, damage to liver and other organs, and cancer.

In general, having once been informed about the health effects of exposure to contaminated sites, including mortality risks, almost 90% of the respondents subscribe to the statement that it is “very important” to reduce such adverse health effects.

Moving to the second order of questions addressed in the survey, we now turn to people’s opinion and support for public remediation programmes in general and more specifically their priorities for targeting these public programmes to some preferred goals.

Most of our respondents ask for active involvement on the part of the government at contaminated sites: 83.6% believe that government-led remediation at orphan sites is “very useful” (on a scale from 1 to 5), 6.72% find them “useful”, 4.73% “somewhat useful”, and only 2.26% opts for response category 1 (“not useful”) or 2. Respondents’ beliefs about priorities for contaminated sites policies are also important: priorities reveal a general attitude of the respondents toward particular target for different remediation programs and do not necessarily entail technical knowledge about the feasibility of these hypothetical targets.

People do care about permanent remediation and about protecting the health of children who, absent from such public programmes, will suffer from exposure in the future. In detail, over 79% of the respondents fully agree with giving priority to permanent cleanup and effective remediation plans, even if they cost more and 76% of the respondents fully agree with investing more resources for the cleanup of sites where children are the most exposed.

While human health is probably their strongest concern, our respondents also care about the consequences of pollution on the ecological system: 85% of the sample questioned completely agree that remedies should be chosen so as to protect the ecosystem. Respondents, even though worried about health risks due to contamination at sites, show a bimodal distribution when asked to agree with the statement that “remedial actions should be carried out only if contamination is a threat to human health”.

The third order of matters to be dealt with when analysing the priorities of the public in relation to a general and a specific support for public intervention in relation to contaminated sites and their remediation is to investigate if people dispositions are systematically related to individual socio-economic characteristics, to civil and environmental attitudes, and their prior knowledge about contamination and remediation.

People’s preferences for cleanup priorities are generally not significantly associated with the individual characteristics of the respondents. The only exception is that respondents with children (or more children) tend (as expected) to be willing to devote more resources to cleaning up sites where the most highly exposed group is children and to be less in favour of focusing

exclusively on sites where human health is at risk. Older respondents agree that sites where pollutants have entered the food chain should be given higher priority.

Regarding socioeconomic status, which we measure using education and income, more highly educated people tend to disagree with programs that imply a narrow focus on very specific pathways, age group and human health effects of pollution. The responses from people that already knew about contaminated sites or remediation before participating in the survey are not systematically different from those of the other respondents. Being concerned about the health risks due to pollution exposures tend to result in being more favourable to cleanup even where the benefits would be incurred in the distant future (as is typically the case with carcinogens) and when programmes are targeting children as the most highly exposed category. The same applies for respondents approving active government involvement with cleaning up orphan sites. Respondents volunteering their time to social causes show less support for narrowly focused cleanup priorities, and, as expected, people who participate in environmental organizations are more concerned with protecting the ecosystem.

5 Conclusions

Cleaning up contaminated sites is currently considered a priority for environmental policies in many countries. Remediation of contaminated sites is attractive because it reduces risks to human health and ecological systems, and brings a host of potential social and economic benefits, because contaminated areas are often found in urban areas where the majority of Europe's population resides. Yet, cleaning up is a costly and time consuming effort, with the taxpayers shouldering much of the financial burden, while its benefits are incurred primarily in the future.

Contaminated sites are often also abandoned sites and in these cases, government intervention is needed because remediation is costly and the land values are low. It is acknowledged that the clean up and reuse of brownfields brings different kinds of positive impacts for society as a whole (Tonin, 2006). First of all, considering the fact that contamination causes water, soil and air pollution, the reclamation brings direct benefits such as reduction in health risk together with improvements in amenity values and ecosystem services. Secondly, redevelopment could create jobs and revitalise economic activities, either in the reclamation phase or afterwards, when new buildings are built and new economic and social activities settled. Other benefits arising from cleanup and reuse of contaminated sites stem on the different land use patterns.

These benefits have been experienced in US and Europe where appropriate legislation and public interventions have supported cleaning up and reusing many of such sites (De Sousa, 2002, USEPA, 2005, Nijkamp, 2000). In Italy, even though contaminated sites are quite widespread in many urban areas and major national cases, notably Porto Marghera amongst them, are posing urgent problems to human and ecological safety, experiences are quite limited and

their study insufficient. Public action is strongly needed in this field, both to refine the appropriate regulation and promote voluntary initiative and public and private partnership.

For these reasons, in the last 5 years, the Department of Planning of the University IUAV of Venice and a local research Institution, the consortium CORILA, have developed a common research programme to assess the benefits of contaminated sites cleanup and redevelopment. The main objective of our research is to promote improved decision making in public contaminated site remediation and redevelopment policy. Moreover, the research aims to better understand what economic instruments may provide incentives and foster brownfields cleanup and redevelopment and what kind of policies people can sustain and appreciate for addressing and solving contaminated site problems.

In this paper we offer the results of two surveys designed for developing sound economic valuation for policy making addressing contaminated sites. Using conjoint choice experiments we investigated stakeholder preferences for contaminated land cleanup and redevelopment programmes.

A survey of real estate developers and professionals, randomly intercepted at the *Marché International des Professionnels de l'Immobilier (MIPIM)* in Cannes, France, in March 2002, was administered to examine different market-based mechanisms and other incentives intended to promote the environmental remediation and reuse of brownfields. We use conjoint choice experiments—a stated preference approach—to assess the responses of real estate developers to different mixes of certain incentives. For example, we proposed different policy instruments such as, letters of no further action, certificates of completion, or covenants not to sue that reduce or eliminate future liability risks, different cleanup standards (more flexible or not), and direct financial incentives to the developers in the form of loans, grants, rebates and/or tax credits.

Analysis of the responses to the choice questions indicate that developers are generally responsive to policies that encourage redevelopment and reuse of brownfields through market mechanisms, such as transfers and liability relief, and through regulatory relief. The impact of these policies, however, varies with the type of developer. Moreover, developers find sites with contamination problems less attractive than others, and we calculate that for a project worth €7 million in revenue (the median revenue) developers need to be compensated €2,5 million for them to accept a contaminated site (in the absence of other policies), and are willing to give up €1,5 million to secure a certificate of completion that would exempt them from future liability.

A national survey was conducted in 2005 in Italy (800 people), where we question people about their awareness regarding problems related to contaminated sites—including their perceptions about the health risks associated with contaminated site exposures—and to elicit an assessment of public's preferences regarding various policies currently being considered in Italy and the European Union. We found that the majority of people in Italy are informed about the existence of contaminated sites and 84% of our sample deems it “very useful” for the government to conduct cleanups of orphan sites

directly. People are in favour of permanent remediation, even if more expensive and in general even if the benefits will be experienced in the long term and our respondents support for public remediation. In the same survey we use conjoint choice questions to investigate people's preferences for income and reductions in mortality risks delivered by contaminated site remediation policies. We estimate the Value of a Statistical Life to be about €5.6 million for an immediate risk reduction. If the risk reduction takes place 20 years from now, however, the implied VSL is about €1.26 million. We estimate the discount rate implicit in the responses to the conjoint choice questions to be about 7%.

While developing this research, the EU has launched the Soil Strategy (2006) and Italian legislation has been changed (Dlgs 152/2006), giving way to a new approach in dealing with risk assessment and management according to land future uses. European Union is working to a new Directive, and it probably will help a common European approach and a better knowledge of the problem to support actions in this field. During the same period EU passed Directive 35 on environmental Liability, and all European countries will adjust to it.

The EU can look forward and take action both to reduce the stock of existing contaminated sites and to reduce the generation of future contamination problems, in soil and water.

Decisive actions are needed on the public side, to move from cleanups to reuse and get the benefits for the population and the environment, and in these processes communities involvement could work as a trigger.

References

- Alberini, A., Longo, A., Tonin, S., Trombetta, F., Turvani, M. 2006. Developer Preferences for Brownfield Policies, in Alberini, A., Rosato, P., Turvani, M. (ed.). *Valuing Complex Natural Resource Systems: The Case of the Lagoon of Venice*. Cheltenham, Edward Elgar.
- Alberini, A., Rosato, P., Turvani, M. 2006. *Valuing Complex Ecological Systems: The Case of the Lagoon of Venice*. Cheltenham, Edward Elgar.
- Alberini, A., S. Tonin, M. Turvani, e A. Chiabai. 2007. Paying for Permanence: Public Preferences for Contaminated Site Cleanup. *Journal of Risk and Uncertainty*, 35, 155-178.
- Alberini, A., Turvani, M., Tonin, S., Longo, A. Trombetta, F. 2005. The Role of Liability, Regulation and Economic Incentives in Brownfield Remediation and Redevelopment: Evidence from Surveys of Developers. *Regional Science and Urban Economics*, 35, 327-351.
- APAT. 2006. *Annuario dei dati ambientali*. Roma
- Cropper, M. L., Sema K. Aydede and P.R. Portney. 1991. Discounting Human Lives. *American Journal of Agricultural Economics*. 73(5), 1410-1415.
- Cropper, M. L., Sema K. Aydede and P.R. Portney. 1992. Rates of Time Preference for Saving Lives. *American Journal of Agricultural Economics*, 82(2),

469-472.

De Sousa, C.A. 2002. Measuring the public costs and benefits of brownfield versus greenfield development in the Greater Toronto area. *Environment and Planning: Planning and Design*. 29, 251-280.

Dybvig, L.O. 1992. Contaminated Real Estate Implications for Real Estate Appraisers. The Research and Development Fund. Appraisal Institute of Canada.

Ferguson, 1999. Assessing Risks from Contaminated Sites: Policy and Practice in 16 European Countries. *Land Contamination and Reclamation*. 7 (2), 33-54.

Hammitt J.K., J.T. 2004. Effects of Disease Type and Latency on the Value of Mortality Risk. *The Journal of Risk and Uncertainty*, 28(1), 73-95.

Hanley N., S. Mourato L., R.E. Wright, 2003. Choice Modelling Approaches: a Superior Alternative for Environmental Valuation?. *Journal of Economic Surveys*, 15(3), 435-462.

Horowitz, J.K., R.T. Carson. 1990. Discounting Statistical Lives. *Journal of Risk and Uncertainty*. 3, 403-413.

Moore, M.J., W. Kip Viscusi. 1990. Models for Estimating Discount Rates for Long-Term Health Risks Using Labor Market Data. *Journal of Risk and Uncertainty*. 3, 381-401.

Nijkamp, P. 2000. Critical Success Factors for Soil Remediation Policy: A Meta-Analytic Comparison of Dutch Experiences. *Journal for Environmental Policy and Law*. 23, 81-99

Patassini, D., P. Cossetini, E. De Polignol, M. Hedorfer, E. Rinaldi. 2003. El.Gi.R.A. Una procedura di aiuto alla conoscenza nelle aree di bonifica di Porto Marghera (Venezia). Paper presented at a FEEM seminar, http://www.iuav.it/Didattica1/pagine-web/facolt--di2/Domenico-P/ricerca/Bonifiche-/slide_ELGIIRA.pdf (accessed July 31, 2006).

Patassini, D., P. Cossetini, E. De Polignol, M. Hedorfer, E. Rinaldi. 2005. ELGIIRA: Support System for Knowledge Building and Evaluation in Brownfield Redevelopment. In CORILA (ed.), *Scientific Research and Safeguarding of Venice, Research Programme 2001-2003, Volume III, CORILA, Venice*, 5-20.

Patassini, D., M. Turvani, F. Trombetta. 2002. Cost and Benefit Analysis of Brownfield Remediation and Redevelopment, in CORILA Research Report, Istituto Veneto di Scienze, Lettere ed Arti, Venezia, 43-49.

Tonin, S. 2006. Measuring the socio-economic benefits of brownfields remediation projects. PhD thesis.

Tonin, S. 2006. What is the value of brownfields? A review of possible approaches. in Alberini, A., Rosato, P., Turvani, M. (ed.). *Valuing Complex Natural Resource Systems: The Case of the Lagoon of Venice*. Cheltenham, Edward Elgar.

Tonin, S., Turvani, M. 2005. Contamination of the Lagoon of Venice: People's

Risk Perception. CORILA Research Report. Istituto Veneto di Scienze, Lettere ed Arti, Venezia, 43-49.

Turvani M., Tonin S. 2007. Brownfield Remediation and Reuse: an Opportunity for Sustainable Development, in C. Clini, I. Musu, M. L. Gullino, (ed.) Sustainable Development and Environment Management: Experiences and Case Studies, Heidelberg, Springer (also in Chinese)

Turvani, M., A. Alberini, S. Tonin, A. Chiabai. 2006. Politiche di bonifica dei siti contaminati: primi risultati di un'indagine nazionale presso la popolazione, in Indagini epidemiologiche nei siti inquinati: basi scientifiche, procedure metodologiche e gestionali, prospettive di equità. F. Bianchi e P. Comba (ed.), Rapporti ISTISAN 06/19, Istituto Superiore di Sanità, Roma, Italia, Agosto.

Turvani, M., A. Chiabai, A. Alberini, S. Tonin (forthcoming), Public Policies for Contaminated Site Cleanup: Evidence from a Survey of the Italian Public, International Journal of Environmental Technology and Management.

Turvani, M., A. Chiabai, A. Alberini, S. Tonin. 2007. Public Policies for Contaminated Site Cleanup: The Opinions of the Italian Public. FEEM working paper 11.2007. Milano, Italia, Gennaio.

Turvani, M., Trombetta, F. 2006. Governing Environmental Restoration: Institutions and Industrial Site Cleanups, in Alberini, A., Rosato, P., Turvani, M. (ed.), Valuing Complex Natural Resource Systems: The Case of the Lagoon of Venice, Cheltenham, Edward Elgar.

Urban Institute, Northeast-Midwest Institute, University of Louisville and University of Northern Kentucky. 1997. The Effects of Environmental Hazards and Regulation on Urban Redevelopment. Report to the US Department of Urban Development. Washington, DC, August.

US Environmental Protection Agency. 2005. Superfund Benefit Analysis, Partial Draft prepared for US Environmental Protection Agency Office of Superfund Remediation Technology Innovation.

US General Accounting Office. 1995. Community Development: Reuse of Urban Industrial Sites, GAO/RCED 95-172, Washington, DC, June.

US General Accounting Office. 1997. Superfund: State Voluntary Programs Provide Incentives to Encourage Cleanups, GAO/RCED-97-66, Washington, DC, April.

RESEARCH LINE 1.3

Characteristics and conditions for a model of post-industrial sustainable development for Venice

A MULTICRITERIA APPROACH FOR THE EVALUATION OF SUSTAINABILITY OF THE ECONOMIC RE-USE OF HISTORIC BUILDINGS IN VENICE

Paolo Rosato¹, Silvio Giove², Mila Dallavalle¹ and Margaretha Breil³ ¹

¹ Department of Civil and Environmental Engineering, University of Trieste, Trieste, Italy;

² Department of Mathematics, Cà Foscari University of Venice, Venice, Italy;

³ Fondazione Eni Enrico Mattei, Venice, Venice, Italy

Riassunto

Il contributo presenta un modello multicriteriale di tipo gerarchico per la valutazione della sostenibilità di progetti di riuso economico per edifici storici a Venezia. Il modello si basa su indicatori rilevanti per la stima della sostenibilità, che vengono aggregati in tre macro-indicatori: *sostenibilità intrinseca*, *contesto* e *fattibilità economica e finanziaria*. Il modello è stato calibrato da un panel di esperti ed è stato testato su due ipotetici progetti di riuso per l'Arsenale di Venezia.

Abstract

The paper presents a hierarchical multiple criteria model for the evaluation of the sustainability of projects for the economic re-use of historical buildings in Venice. The model utilises the relevant indicators for the appraisal of sustainability, aggregated into three macro-indicators: *intrinsic sustainability*, *context* and *economic-financial feasibility*. The model has been calibrated by a panel of experts and tested on two reuse hypothesis of the Arsenale in Venice.

1 Evaluation of the concept of cultural heritage

Mapping out the guidelines for the sustainable economic re-use of historic buildings cannot avoid the complexity of the objectives and methodologies for the safeguarding of the cultural heritage.

The historic, aesthetic and artistic implications which characterise cultural

¹ The authors wish to express their thanks to Valentina Zanatta, who collaborated in an early phase of the project.

Their further thanks go to the following architects who contributed to compiling the questionnaire: Gianluca Frediani, Roberta Galli, Gabriele Ghiglioni, Alberto Guzzon, Raffaella Lioce, Danila Longo, Silvia Marini, Emilio Natarelli and Marco Storelli.

assets make it difficult to apply a solely qualitative approach. The complexity of the investigation is also due to the public nature of these goods, not necessarily as far as the property right is concerned – many are privately owned – but rather the which relate to historic, artistic and cultural value [Brosio 1993]. The evolution of the concept of cultural heritage in Italian laws and regulations is very interesting. An important law passed in 1939² deals with “moveable and immovable assets which are of artistic, historic, archaeological or ethnographic interest”, as objects which are aesthetically pleasing and, as such, should be safeguarded by appropriate legislation. Article 9 of the Constitutional Charter refers to these concepts and states: “ The Republic [...] safeguards the historic, artistic and land heritage of the nation”, affirming the central Government’s sovereignty over the cultural heritage and the values of national identity.

Italy’s post-war cultural developed new views by proposing innovative laws and Commissions, including the Franceschini³ Commission, which first used the term “cultural heritage” to mean “material evidence of civil value”. The cultural heritage assets are no longer simply aesthetically pleasing but also a palimpsest of the history of a culture.

The cultural heritage and landscape is currently safeguarded by the “Codex of cultural heritage”⁴, and together with the prior law⁵, defines heritage as assets that also encompass the qualities and attributes of objects that have ethnic, anthropological, archivist or literary value covered by law or based on the law, for past, present or future generations.

In recent years, there has been an increasing interest concerning the economic value of the cultural heritage. A value, not only in terms of price, but rather a recognised asset based on objective considerations.

The conservation of these assets also generates economic benefits to the society as a whole [Forte, 1977; Throsby, 2002].

Throsby defines heritage as cultural capital which is “an asset which embodies, stores or provides cultural value in addition to whatever economic value it may possess” [Throsby, 2001 and 2002]. By comparing cultural capital and physical capital, Throsby states that, if economic capital is to maintain its efficiency, restoration must be constant: the latter is comparable with maintenance of artistic and architectural assets. Even when dealing with cultural goods, initial

² Law 1089 of June, 1st 1939.

³ Franceschini Commission operated from 1964 to 1966.

⁴ Legislative Decree bearing the “Codex of cultural heritage”, in accordance with article 10 of the Law no. 137 dated July, 6th 2002.

⁵ In January 2000 the “Consolidated Law on natural and cultural heritage” (TU 490, 1999) came into force; article 4 takes up the idea of cultural heritage as a testimony to civil value.

creative and material intervention is called for, followed by constant maintenance and, in the long term, more substantial interventions, which could lead to the modification of its use.

The difference, however, between physical assets (from a strictly economic viewpoint) and cultural capital is indeed this concept of “culture” which bestows the historic goods with an added dimension of quality. It is this cultural quality which must be maintained and not simply the materials with which the asset is built.

In the scientific literature [Randall, 1991; Stellin and Rosato, 1998], the economic and cultural value of a historic asset are to be distinguished based on two macro-categories which refer to distinct two spatial and temporal dimensions. The difference lies in the use and non-use values:

- use value, linked to the benefits the consumer receives directly from the asset itself, is a contingent prerogative; it is that quality that the historic artefact offers the consumer from the very moment he comes into contact with it. For this reason synchrony must be created between the cultural asset and the user;
- non-use value, instead, does not have the same contingent obligation of the above and, as a result, does not require such close synchrony (but rather a diachrony).

2 The sustainability of the re-use of historic artefacts

The issue of the sustainability of the economic re-use of historical heritage is pertinent to this discussion and helps to tailor, safeguard and protection policies.

Starting with the well-known declination of the concept of economic, social and environmental sustainability, literature on the matter refers to a common premise according to which the ultimate objective of any type of intervention should develop local resources and, as a consequence, should contribute to enhancing the quality of life of the public at large. This is a multi-dimensional concept in so far as “the quality of life” touches on a lot of economic and social aspects [Fusco Girard, 1987; Howarth 1997].

The objective of our research has been to construct a model which is capable of summarising, as far as the use of historic artefacts are concerned, the most important aspects which determine the intervention to be carried out. This was brought about by supporting the evaluation of sustainability indicators of interventions, from a physical point of view, with economic and social indicators. When the interventions concern goods which are deemed to be “cultural heritage”, evaluation becomes more problematic, given that the objective of sustainability requires an equilibrium between the economic re-use of the asset and its conservation [Nijkamp and Voogd, 1989].

The concept of sustainability was initially presented by the World Commission on Environment and Development [1987] with reference to the effects of development on environmental assets. Sustainable development is

“development that meets the needs of the present without compromising the ability of future generations to meet their own needs”.

As far as the cultural heritage is concerned, architectural assets in particular, the concept of sustainability is influenced by the environment and involves two main aspects: the sustainability of the material and formal application of the building and the sustainability of the new function that is to be installed therein. On both counts, the impact on current and future generations must be evaluated.

Current debate on the theories of restoration, which is particularly active in Italy today, follows two lines of thought.

- The first is defined as *critical restoration*, and stems from the conviction that each intervention is a case unto its own. It must also transmit the asset to the future by guaranteeing and facilitating its interpretation without losing sight of the fact that it is a “non-verbal criticism expressed in concrete non verbal ways” [Carbonara, 1987, Marconi, 1993].

On the other hand we have the pure *conservationists* who support the conservation of each strata of material or matter which the building has accumulated over time. This becomes a sort of palimpsest where it becomes impossible to identify what exactly has to be conserved or removed: “The aim of restoration is to conserve both the matter and substance which represents a documentary record of what the building is actually made of” [Dezzi Bardeschi, 1977].

A re-use project attributing a new function to the building often involves transforming, consolidating, adding and removing and may alter the various strata of existing materials.

The decision not to use however, gives the impression that it undermines the intrinsic value of the asset. Furthermore non-use poses the threat of possible abandonment and subsequent loss of the asset itself⁶.

⁶ The European Charter of Architectural Heritage adopted by the Council of Europe (1975) introduces the social and economic issues related to restoration and formalises the concept of “integrated conservation”, or rather the integration of heritage into the “context of public life”, by means of restoration and appropriate employment. In the same year, the Declaration of Amsterdam stated that the attribution of new functions should respect architectural characteristics and guarantee their survival; the conservation effort “must be based on the cultural and utilisation value of the building”.

Carlo Forte, on the other hand, claims that the conservation of the cultural heritage aimed at its integration into modern day life “constitutes a true and proper productive activity” and an essential priority. The limited funding available do not allow conservation to be the sole finality of the intervention, but make it necessary that the building be put to compatible use. By so doing the cultural capital will generate assets and services which

Often, however, historic architectural complexes are employed for purposes which are completely different from those for which they had originally been built and the interventions required (especially in terms of the quantity, standards and building regulations that need to be respected) might not always be compatible with the typology and structure of the architectural asset on which works are being carried out. Over-use or incompatible use can have similar consequences to those of abandonment and can gradually nullify the cultural value and historic evidence of the artefact.

Literature does not deal with the definition of what is, or is not sustainable as far as work carried out on historic buildings are concerned, for the simple reason that it is an interdisciplinary issue. Indicators may be based on a variety of parameters that are both historically and aesthetically sensitive. The resulting operating indicators should be geared to the sole purpose of defining the limit of the building's critical analysis; it must stop at the point where conjecture begins⁷. The project is no longer primarily conditioned by conservation but by the new function of the building.

Moreover this cut off point should also help to distinguish when the new use ceases to enhance the asset, and begins to consume and erode the original value.

3 Multicriteria aggregation

Many methods have been proposed in the literature to approach multicriteria problems. Following [Vincke 1989], a commonly used classification distinguishes

- Approaches derived from Multi Attribute Value Theory (MAVT);
- Outranking approaches, whose most famous methods are belonging to the ELECTRE family and its derivatives;
- Interactive approaches,

The MAVT methods compute a score for each alternative, using Aggregation Operators⁸ (AO). Many of the MAVT methods are based on common sense rules, since they need to be applied by Decision Makers (DM) who frequently are not confident with mathematic algorithms. In this contribution, we propose a mathematically founded MAVT approach, easily to be understood by poorly mathematically skilled DM(s).

First of all, let us remark that the most common aggregation function is the (simple) Weighted Averaging approach (WA), consisting in the computation of

will increase its social function and its availability to the general public.

⁷ *Venice Charter*, 1964.

⁸ See (Klement 2000, Kolesarova 2001).

the weighted average of the score of each criterion for each alternative. It is a simple and intuitive compensative method, but no interaction among the criteria can be implemented, since the Independent Preference axiom is assumed. For this reason, many alternative methods have proposed. We remember among these the Geometric Averaging (GA) which computes the geometrical averaging of the scores, instead of the arithmetic averaging used by the WA. It can be usefully applied in strong conservative cases, since it gives a null global score if only one criterion is null (thus impeding compensation in those cases where one criteria scores zero). An other class of Aggregation Operators consists of the Ordered Weighted Averaging operators (OWA) introduced by Yager [Yager 1988, 1992]. It includes, as particular cases, the weighted averaging, and, as extreme situations, the Max and the Min operators. If the weights are obtained by a non monotonic quantifier [Yager 1993], the OWA operator implements linguistic statements as “at least”, “at most”, “at least the half” and so on⁹. The compensation operator introduced by Zimmermann [Von Altrock 1995], uses a tuning parameter, representing thus more or less conservative situations (even if the identification of these parameters is not easy to be implemented). A different approach is obtained using a Fuzzy Expert System, which, being an *Universal Approximator* can represent every possible mathematical (regular) function, but its usefulness is limited by the difficulty in determining the parameters, and by the choice of the implication operator required by the rule inference [Von Altrock 1995].

More recently, the introduction of methods based on non additive measures (NAM) helped to solve many theoretically cumbersome problems, and at the same time offers a wide range of possibilities of aggregation. Up to now, the multicriteria community considers these methods the most complete and mathematically well founded MAVT approach. Roughly speaking NAM consists in assigning a suitable weight to every possible coalition of state of the criteria¹⁰. So the importance of a coalition of criteria can be greater, equal, or less than the sum of the importance (weights) of each criteria included in the coalition. Both synergic and redundancy interaction among the criteria can be modelled in this way. If the importance of the coalition for each them is equal to the sum of weights of the included criteria, the operator degenerates the WA approach. In the other cases, a simple algorithm¹¹ can compute the score of the alternatives, considering the interactions among the criteria given by the non additive measures. Moreover, some indices can be computed showing the tendency towards pessimism or optimism reflected in the valuation of the set of alternatives. It should be remembered that the NAM can be directly obtained by

⁹ Indeed, the OWA operator is a particular case of the Choquet integral, see later.

¹⁰ And not to a single criteria only, as the WA approach.

¹¹ i.e. the Choquet integral or the *multi-linear* approach used in the following.

experimental data, or implicitly elicited from expert's judgements¹². The price to be paid with respect to WA or to OWA consists in an increase in the number of parameters, which are equal to the number of all possible coalitions of criteria. For example using only two possible states for each criteria, 4 criteria request 16 parameters, with 5 criteria 32 parameters, and with 6 criteria 64 parameters are needed, making the method rather difficult to be used in practical applications. Verifying the absence of interaction between higher order coalitions, we can use a reduced order model (see later) where the number of parameters is strongly reduced.

3.1 Non additive measures

Let $N = \{1, 2, 3, \dots, n\}$. A non additive measure¹³, [Marichal 1998, 1999-a, 1999-b], is a set function $m : S \subseteq N \rightarrow [0, 1]$, so that, $\forall S, T \subseteq N$ the following condition holds:

$$m(\emptyset) = 0, \forall S, T \subseteq N : S \subseteq T \Rightarrow m(S) \leq m(T), m(N) = 1$$

Such a measure is able to represent interaction among the criteria, giving a different weight to every possible coalition of them, and not only to a single one as in the case of the WA operator. The first and the third conditions limit the variability inside the domain $[0, 1]$, while the second condition is a monotonicity constraint, namely, if more criteria are satisfied (all of them are intended as benefit) the global satisfaction cannot decrease¹⁴.

Since the measure of a set can be different from the sum of the measure of the subset of every its partition (from which the attribute non additive), a non additive measure will be named as:

additive if: $m(S \cup T) = m(S) + m(T), S \cap T = \emptyset$

sub-additive if: $m(S \cup T) < m(S) + m(T), S \cap T = \emptyset$

super-additive if: $m(S \cup T) > m(S) + m(T), S \cap T = \emptyset$

For an additive measure, no interaction is possible among the criteria and the linear superposition holds. For a sub-additive measure a redundant effect is modelled, while the contrary holds for a super-additive effect (synergic effect).

3.2 The Choquet integral

Given a non additive measure m , let (x_1, \dots, x_n) be the criteria values for a

¹² In this contribution, we propose an implicit approach.

¹³ Sometimes named also as *fuzzy measures*.

¹⁴ Really the violation of some constraints can be admissible in all the cases where a criterion can be a benefit for one coalition, and a cost for an other one. *Non monotonic* measure can capture this effect, but we do not consider them in the following.

particular alternative, normalized in a common scale. The Choquet integral of the vector (x_1, \dots, x_n) with respect to the measure m is defined as follows:

$$C_M(x_1, \dots, x_n) = \sum_{i=1}^n (x_{(i)} - x_{(i-1)}) \cdot m(A_{(i)})$$

Being (\cdot) an index permutation so that: $x_{(1)} \leq \dots \leq x_{(n)}$, and $A_{(i)} = \{i, \dots, n\}$, $A_{(n+1)} = \emptyset$.

It can also be written as:

$$C_m(x_1, \dots, x_n) = \sum_{i=1}^n x_{(i)} \cdot [m(A_{(i)}) - m(A_{(i+1)})]$$

This operator satisfies the following properties [Marichal 1999-a]:

1) it coincides with the WA operator if the measure is additive with:

$$m(A) = \sum_{i \in A} w_i$$

being w_i the weight of the i -th criterion,

2) every OWA operator is a Choquet integral if every subset of the same cardinality has the same measure:

$$m(A) = \sum_{j=0}^{i-1} w_{n-j}, \quad \forall A : |A| = i$$

For an intuitive explanation of the Choquet integral, see the example in [Murofushi 1989].

3.3 The Möbius transform and the dual values

Given a non additive measure m , its dual values can be (biunivocally) obtained from the following Möbius transform [Grabish 2003, Marichal 1998]:

$$\alpha(S) = \sum_{T \subseteq S} (-1)^{s-t} m(T), \quad \forall S \subseteq N$$

And the inverse transform is given by:

$$m(T) = \sum_{S \subseteq T} \alpha(S), \quad \forall T \subseteq M$$

To be the dual of a non additive measure, the 2^n coefficients $\{\alpha(S) | S \subseteq N\}$

need to satisfy¹⁵:

$$\alpha(\emptyset) = 0, \sum_{T \subseteq N} \alpha(T) = 1, \sum_{T \in P(S)} \alpha(T) \geq 0, \forall S \subseteq N$$

The Choquet integral can be written in the dual space as:

$$C_m(x_1, x_2, \dots, x_n) = \sum_{T \subseteq M} \alpha(T) \cdot \min_{i \in T} \{x_i\}$$

Moreover, if $\alpha(T) > 0$, the coalition T is synergic, if $\alpha(T) < 0$, it is redundant, if $\alpha(T) = 0$, there is no interaction and the Choquet integral collapses into the WA operator [Marichal 1998, 1999-a, 1999-b].

From a computational point of view, given n criteria, a non additive measure requires the assignment of 2^n coefficients, and their number can be very high. In order to avoid this, the k -order models were introduced, which assume interactions between subsets of cardinality less or equal to k , typically the second order models are considered, that is, $k=2$. Even though in many applications it can be reasonably assumed that there are 0 interactions for high cardinality subsets, this hypothesis needs to be tested a priori.

3.4 Andness and orness measures

Given a non additive measure, it is possible to compute an *andness* measure together with its complementary *orness* measure. If the *andness* measure is close to 1, it means that the measure set tends to the MIN operator, that is to the logical conjunction of the criteria value, showing a conservative tendency of the Decision Maker (*pessimistic* behaviour). Conversely, if *orness*=1 we obtain the MAX operator, the logical disjunction, a totally compensative operator, corresponding to an *optimistic* behaviour. The computation of the *orness* index in the dual space is given by:

$$\text{orness}_m = \frac{1}{n-1} \sum_{T \subseteq N} \frac{n-t}{t+1} \alpha(T)$$

Moreover:

$$\text{andness}_m = 1 - \text{orness}_m(i)$$

Both indices can be easily computed given the dual values of the measure.

¹⁵ $P(S)$ is the power set of the set S .

3.5 Non additive measures and the multi-linear operator

In the dual space, the Choquet integral computes, for each coalition, the minimum of the criteria values of the coalition. The MIN operator belongs to a wide class of operators, the *triangular norm* (T-norm), which satisfies a set of rationality properties and are widely used in the field of MCDA analysis, especially in the fuzzy logic applications [Klement 2000]. Since the MIN is not compensative at all, some authors proposed to substitute the MIN operator, in the dual space, with a smoother T-norm, [Kolesarova 2001, Klement 2000, Despic 2000, Fujimoto 1997]. A natural choice can be the product of the values, that is a differentiable and partially compensative operator. We obtain the so called *multi-linear* operator [Grabish 2001]. In the dual space, substituting the MIN operator with the product, we obtain:

$$V(x_1, x_2, \dots, x_n) = \sum_{i=1}^n a_i x_i + \sum_{i_1=1}^n \sum_{i_2=i_1+1}^n a_{i_1 i_2} x_{i_1} x_{i_2} + \sum_{i_1=1}^n \sum_{i_2=i_1+1}^n \sum_{i_3=i_2+1}^n a_{i_1 i_2 i_3} x_{i_1} x_{i_2} x_{i_3} + \dots + \sum_{i_1=1}^n \sum_{i_2=i_1+1}^n \dots \sum_{i_n=i_{n-1}+1}^n a_{i_1 i_2 \dots i_n} x_{i_1} x_{i_2} \dots x_{i_n}$$

In the measure space the multi-linear operator has the following formulation [Marichal 1992-b]:

$$V(x_1, x_2, \dots, x_n) = \sum_{T \subseteq N} a(T) \prod_{i \in T} x_i (1 - x_i)$$

which represents a pseudo-boolean function.

3.6 Identification of the measure

As said above, one of the most critical points in the evaluation consists in the assignment of the numerical values of the non additive measures. Many methods were presented in the literatures, but most of them are based on quite complex optimization algorithms, or on data mining techniques. In this case study, we preferred a user friendly approach, and adopted a method based on a suitable questionnaire [Despic 2000]. Let us suppose that the DM(s) judgements are in the scale [0, 100], with the usual meaning for the numerical values, i.e. 0= WORST, 50= MEDIUM, 100= OPTIMAL, and so on, and every criterion is ordered (as a *benefit* or as a *cost*). For each criterion two particular extreme cases are enhanced, the OPTIMAL and the WORST ones, conventionally indicated with 1 and 0 respectively from now on. An *edge* is a (fictious) scenario formed by a combination of (only) WORST and OPTIMAL evaluation. Each edge is nothing else that a question that is asked to the DM(s), which will assign his/(their) evaluation in the scale [0,100]. The edges are the vertex of an hyper-polyhedron in the criteria space. It is obvious) that it is sufficient to define the values in all those vertex to obtain the values of the measure. The value of the vertex is the minimum information required. This simplification causes a poor statistical robustness, since it corresponds to the minimum number of interpolating points in an n-dimensional space, but given

the unavoidable uncertainty which is implicit in every human decision process, this does not seem to be a serious obstacle, considering the information gain that we should obtain explicitly considering the possible interactions among the criteria. The advantages with respect to WA are evident.

The Figure 1. reports an instance of the questions that need to be formulated in the case of 3 criteria. Referring to the case study, we are considering the node in the Sustainability Tree which evaluates the Sustainability starting from Intrinsic Sustainability, Economic-Financial Sustainability, and Context. The fourth column reports the DM evaluation (only one DM is here simulated). For a better comprehension, the third row implements the question:

“How would you score an hypothetical case where the Economic-Financial Sustainability is OPTIMAL, and the two other criteria, Intrinsic Sustainability and Context are WORST?”

After having fulfilled all the answers, a simple algorithm computes the dual values and passes such parameters to a procedure that implements the computation of the multi-linear aggregator for a real case. Moreover, the *andness* and the *orness* degrees can be computed and the behavioural nature of the DM can be obtained.

Assuming, for the previous Example with 3 criteria represented in Figure 1., the “weight” of the first criterion to be equal to 30, the second to 20, the third to 30, and the “weight” of the coalition formed by the 3 criteria together to be equal to 70, a synergic effect can be observed, since the “weight” of the coalition is greater than the sum of the criteria weights.

SUSTAINABILITY			
Intrinsic sustainability	Context	Economic & financial feasibility	Evaluation
worst	Worst	worst	0
optimal	Worst	worst	
worst	Optimal	worst	
worst	Worst	optimal	
optimal	optimal	worst	
optimal	worst	optimal	
worst	optimal	optimal	
optimal	optimal	optimal	100

Fig 1 – The valuation table.

Evaluation in intermediate points would increase the statistical robustness but the numerical complexity of the algorithm would significantly increase. We feel that the edges evaluation and the multi-linear operator are a good compromise choice between theoretical complexity and operative usefulness. Other solutions, see for instance [Fujimoto 1997], are difficult to be implemented and require a strong computational effort. Moreover, the same approach can be used in the case of multi-person decision scenario, where many Experts or Decision Makers cooperate in the assignment of the “weights” of the criteria

coalitions, and a measure of consensus could be easily defined and computed [Kacprzyk 1987, 1988, 1982].

4 The model for the evaluation of sustainability of re-use projects.

In the previous paragraphs, we saw how integrated conservation is defined as being the best possible compromise in dealing with conflicting objectives. Therefore the operative phase of the study concentrated on the definition of indicators which would allow for the evaluation of sustainability of alternative re-use projects for historic artefacts.

The construction of a hierarchy model for the evaluation of the sustainability of re-use projects for historic architectural assets was based on the definition of criteria synthesizing of the main characteristics, which could influence the evaluation of sustainability. This initial phase was completed by consulting experts in urban re-qualification and the re-use of historic buildings. The resulting, proposed indicators take into consideration the effects of the intervention on the artefact by using three main points of view: the impact on the historic building (defining future re-use – and relative standards – to be housed in the historic building); the social impact; the economic and financial feasibility (Figure 2).

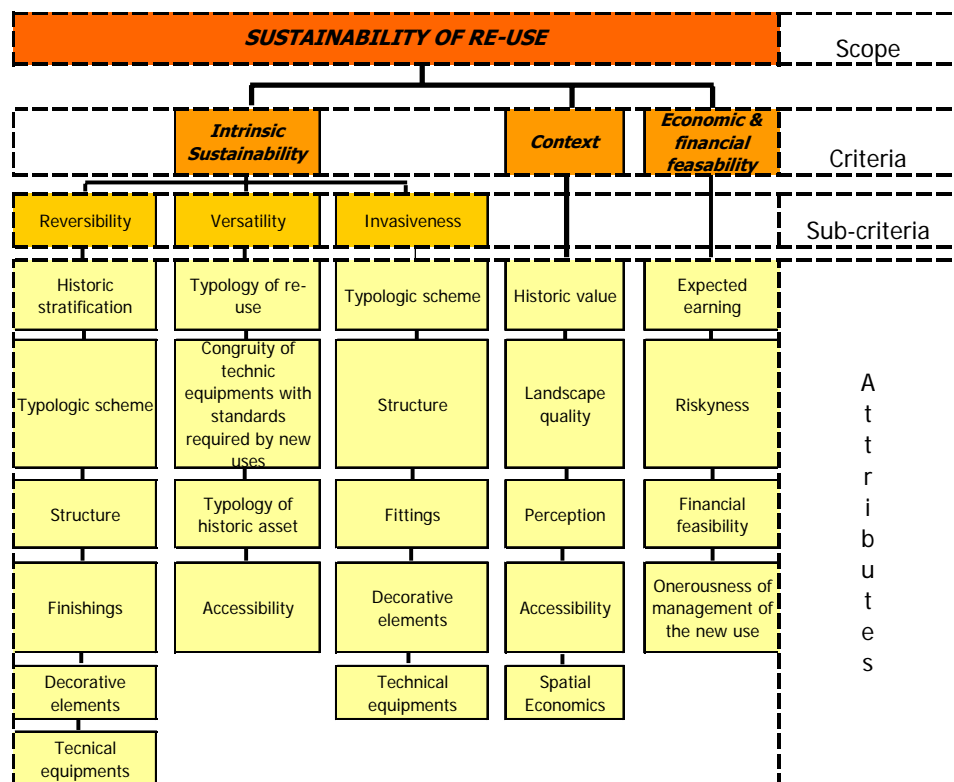


Fig 2 – Hierarchic structure of the evaluation model.

The latter three macro-criteria are followed by sub-criteria, which are specific indicators ordered in accordance with their role defining the sustainability of the intervention in terms of “impact”. This “impact” derives from the historic building’s new function and the “contribution” that its cultural and economic values make towards its conservation.

Figure 2 shows the three criteria identified:

Intrinsic sustainability: an intervention which respects the characteristics of the historic building, its materials and typology. This criterion has been divided into three sub-criteria:

- *Reversibility*: seen as the opportunity to restore the artefact to the state it was in before addition or modification was carried out based on the re-use project.
- *Versatility*: seen as the possibility to eventually modify the function of the building proposed by the re-use project, without having to carry out substantial work.
- *Invasiveness*: the degree to which the project interferes with the materials the historic artefact is composed of.
- *Context*: refers to the project for the economic re-use of the historic, cultural complex and the extent to which it enhances the social, economic and environmental context in which the building is set and its contribution to the local identity. The re-use project must, where possible, rebuild a relationship between the building and its environmental setting. The local community's reaction to the project must be such that it induces the local authorities to view it positively. It is also hoped that the project will bring about positive externalities on circulation and bring economic advantages to the territory.
- *Economic, financial feasibility*: evaluation of the project according to main economic and financial principles. The model implies that the objective of sustainable re-use also depends on the project's foresight in guaranteeing financial independence to the economic activity it hosts and sufficient income to cover maintenance costs.

Moreover, the risk factor concerning the investment must also be taken into account together with the type of activity that is intended to be housed in the building and its financial feasibility.

Each criteria, sub-criteria and attribute was given a weight within the hierarchical tree which defines its contribution towards sustainability. In order to calculate the weight of each single characteristic, an evaluation questionnaire was compiled which applies the edge's method described in the previous paragraph.

The questionnaire had a page for each of the nodes on the hierarchical tree, so that each node would be given a weight. It was completed by 11 experts who gave their evaluations of proposed scenarios.

Figure 3 shows the vectors of the evaluation given by the experts for the spreadsheet relating to the "sustainability" node.

In order to obtain a single evaluation vector for each single node, an aggregation operator must be chosen: in the current study, the average of the expert's evaluation was chosen. .

Figure 3 presents the average vector for the evaluations given for the “sustainability” node obtained by applying the average of the evaluations for the scenarios the experts had previously supplied. We can see that the experts gave quite different evaluation scores for the indicators regarding the “context” criterion and “economic-financial feasibility”. The value of the variation coefficients for the evaluation of scenarios that aggregate more indicators at the excellent level are, however, more contained, which indicates more consensus.

Fig 3 – The weights attributed to the “sustainability” node.

SUSTAINABILITY			Average	Stand.De v.	V.C.
Intrinsic sustainability	Context	Economic & financial feasibility			
worst	worst	worst	0,00	0,00	-
best	worst	worst	29,55	11,72	39,66
worst	best	worst	24,73	19,31	78,09
worst	worst	best	20,00	14,32	71,59
best	best	worst	65,18	9,97	15,29
best	worst	best	57,73	10,34	17,90
worst	best	best	48,18	25,52	52,97
best	best	best	100,00	100,00	0,00

Once the vectors of weights had been inserted in the computerised questionnaire with the application of the “edge” method, it generated a median weight vector for each scenario contained in the nodes inserted in the hierarchical tree. The total weight of each node was obtained by summing all the products lying between the technical evaluation attributed to the indicator and its weight.

The following equation illustrates the value of function of the sustainability objective:

$$I_s = 0,295SI + 0,247C + 0,200FEF + 0,109SI \cdot C + 0,082SI \cdot FEF + 0,035C \cdot FEF + 0,032SI \cdot C \cdot FEF$$

Where:

I_s = Sustainability

SI = Intrinsic sustainability

C = Context

FEF = Economic financial feasibility

In the model the technician responsible for evaluating the sustainability of re-use projects expresses a judgement (0,100) for each sustainability attribute; the score is multiplied by the weight attributed to the indicator and by the weights assigned to the nodes higher up; by repeating the same procedure, and giving a technical evaluation to each attribute associated with the project under examination, the result will be the comprehensive evaluation of the sustainability of the re-use project.

The model is useful when there are several alternative projects to choose from, as it supplies a final sustainability score for the project and also because it gives

intermediate scores which refer to the criteria, sub-criteria and attributes. This favours the analytical examination procedure of the project data.

As previously described, in order to give the criteria, sub-criteria and attributes a weight, the experts consulted filled out a questionnaire and gave scores ranging from 0 to 100 to hypothetical situations described in two scenarios.

The experts shared cultural knowledge in at least two fields: the *conservationists* were architects operating in the restoration of the materials of historic buildings; the *designers* and *planners* were specialists in analysing and identifying the function that the historic artefact should be given and the economic evaluation of re-use.

It was thus useful to establish indices which would indicate the degree of conservationalism shown by each expert's judgement.

Andness and *orness* indices were used, where the index value may vary between 0 and 1 in both cases and takes on the following significance:

- total *andness*: the expert consulted considers that the sustainability of a project is guaranteed only if all the indicators are attributed the maximum score (*andness* index =1; *orness* index = 0);
- total *orness*: the expert consulted considers that the sustainability of a project is guaranteed if one of the indicators is given the highest (*andness* index=0; *orness* index= 1);
- mainly *andness*: the expert consulted considers that the sustainability of a project is guaranteed only if the majority of the indicators are attributed a high score (*andness* index > 0,5; *orness* index < 0,5);
- mainly *orness*: the expert consulted considers that the sustainability of a project is sufficiently guaranteed when one indicator rather than another receives a high score (*andness* index< 0,5; *orness* index > 0,5);

		Average	Std. Dev.	C.V.
Sustainability	<i>orness</i>	0,409	0,087	0,214
	<i>andness</i>	0,591	0,087	0,148
Intrinsic sustainability	<i>orness</i>	0,493	0,079	0,160
	<i>andness</i>	0,507	0,079	0,156
Reversibility	<i>orness</i>	0,482	0,110	0,228
	<i>andness</i>	0,518	0,110	0,212
Versatility	<i>orness</i>	0,474	0,083	0,175
	<i>andness</i>	0,526	0,083	0,158
Invasiveness	<i>orness</i>	0,476	0,059	0,124
	<i>andness</i>	0,524	0,059	0,113
Context	<i>orness</i>	0,501	0,050	0,099
	<i>andness</i>	0,499	0,050	0,100
Economic and financial feasibility	<i>orness</i>	0,480	0,071	0,149
	<i>andness</i>	0,520	0,071	0,137

Fig 4 – Indices of 'Andness' and 'Orness' for the most important criteria.

- *Additive* measure: the expert consulted considers that the sustainability of a project depends on the sum of the scores assigned by the indicators, without there being any synergy between them (*andness* index = 0, 5; *orness* index = 0, 5).

The majority of experts tended towards *andness* in all the nodes examined which means that, according to their evaluations, a project can be considered sustainable if at least two or more criteria are deemed “excellent”; thus it is not enough for the project to respect the historic building, but it must also be economically sustainable, and its reference context must be carefully considered see Figure 4 **Errore. L'origine riferimento non è stata trovata.**

5 Sustainability evaluation for the re-use of the Arsenale-

Out of an analysis of the political debate on alternative options for the re-use of the Arsenale two fundamental directions could be extrapolated. The first one is pointing to installing “poor” functions in the ancient complex without consideration of the historic significance of the area, but well compatible with the historic building structures. The functions to be introduced are generally mostly already working within the historic centre but often under menace of expulsion because of pressings from the real estate market. The second option points to the introduction of “new” uses somehow connected to the Arsenale’s historic function. On the basis of these basic assumptions two hypothetic projects or scenarios have been created in order to evaluate the sustainability of both alternatives for the re-use of the historic Arsenale.

5.1 1st Scenario: Area for artisans

In the first scenario it is assumed to use the buildings of the Arsenale for craftsmen’s activities actually dispersed in the historic centre. The surfaces of water of the main dock and some of the buildings will be used for laying up small boats owned by Venetian residents.

It is presumed that the whole surface and all buildings, except those actually occupied by the Navy, will be used by artisan’s activities. The re-conversion will take place after a restoration programme managed by the municipality, which will adapt the buildings to the requirements of craftsmanship and small manufacturing activities. The industries which are going to settle within the restored buildings will pay rent ruled by a medium-long term contract (around 20 years).

The surface of the big dock (Darsena Grande) will be used for mooring of Venetian boats. A limited number of buildings, including the covered docks, will be used for mooring and laying up of boats on high rise racks.

5.2 2nd Scenario: Marina

The second scenario refers to a proposal made in different occasions, which was to use the historic Arsenale as an attractive Marina for permanent and temporary mooring. The activities to be introduced regard, beyond the berths themselves (approx. 220 places), the facilities will comprise some high quality

shipyards, boats repair and laying up services and shops and services necessary for tourism, like retail stores for nautical equipment.

In this proposal the area's original nautical vocation is taken up, expecting the nautical tourism, to contribute to a revival of the traditions of this place in terms of boatbuilding. The berths of the main dock will be assigned only in part on a permanent basis, a consistent part 25% will be reserved for temporary mooring.

The historic buildings will house the facilities connected to the port such as marine shops, craftsmen activities connected to marine activities and boatbuilding as well as a shipyard for the production of leisure time boats. A supermarket will be located in a position easy to access from the surrounding residential areas as well.

The open spaces, transformed in quays, are used as slipways for the marine activities and shipyards.

Some buildings on the southern front of the main dock will be transformed in reception area with restaurants and bars, a yacht club, and rooms for small events, sailing schools etc. as well as services offering technical assistance for guests.

Introducing productive activities into the historic buildings does not represent a particular problem from the point of view of conservation aims, as long as principles similar to those described in the previous scenario will be followed. Some more problems may be represented by the introduction of commercial facilities and supermarkets, which might ask for divisions of the bigger spaces, with consequently major alterations of the typologies of the historic buildings.

5.3 The assessment of sustainability of re-use projects

The evaluation of these two scenarios described above refers to the sustainability model's indicators. For each group of criteria a comprehensive judgement is added. Furthermore, for the evaluation of intrinsic sustainability which represents the most complex criteria, an additional judgement for sub-criteria is added.

5.4 Intrinsic sustainability

Reversibility

The typological scheme of the Arsenale's historic buildings is easy to be adapted to the insertion of productive activities. The free surface inside the buildings allows, up to a certain extent, for the insertion of internal structures as galleries. These structures have to remain detached from the main structures and allow for the perception of the original shape of the building. The transformation of the shipyard buildings, which were initially open towards the waterfront, into closed buildings with no predominant orientation towards the water, has already taken place during the 19th and 20th century, and will be reconfirmed by the project for the artisan's area. A further problematic aspect of reversibility regards the lack of natural illumination of the original buildings,

requiring thus transformation of parts of the coverage, which may partly alter the visibility of the original buildings.

Within the project for the Marina, the problems raised by the necessary transformation for the introduction of productive activities, are similar to those mentioned above, as the complex was created as a productive structure, and is relatively easy to be adapted to new uses of the same type. Within some limits the same can be said about the insertion of commercial services and restaurants, which might be practiced in a similar way to the productive activities, using detached structures inside the original buildings, emphasizing the technical and productive character of the context-The transformation of structures of support for the marina will be less simple: the serial buildings have no lateral openings, it will thus be necessary to distribute accurately the functions inside each building in order to assure sufficient illumination for all sensible functions. In no case an irreversible transformation of buildings is foreseen. As in the case of Scenario 1, the problems will be raised by the introduction of sanitary services in the case of both scenarios.

Finishings

Due to the original character of the buildings, no particular problems of conservation of finishing are to be expected. In the case of the Marina the lack of finishing can be used as an evocation of the historic character of the area.

Technical installations

The introduction of new technical installations will represent in some problems as partial transformation of roofs and/or openings will be required. In both cases, technical structures will be distributed and designed according to the requirements of the single enterprise, although the concentration of some facilities as of heating and some support services (reception, administration, canteen) in separate structures is planned.

Criteria, subcriteria and attributes	Average of judgments	
	Artisan's area	Marina
Reversibility	89,2	76,6

<i>Typologic scheme/structures</i>	90,8	73,3
Demolitions	90	80
Subdivisions	85	60
Conservation of characterizing elements	90	70
Walls	90	80
Floors	85	60
Roofing	90	70

<i>Finishing</i>	97,5	92,5
Plasters and hangings	100	95
Thresholds, benches	95	90
<i>Technical installations</i>	77,5	65,5
Removable housings	75	70
Compacting	80	60

5.5 Versatility

Typology of re-use

The high grade of reversibility of both projects guarantees for a high grade of versatility, allowing eventually for the insertion of alternative productive uses. This is assured by the design principle of inserting new structures and vertical connection as independent elements respect to the historic building, from the static point of view as well as from the visual point of view. In the case of the Marina project, where the internal divisions to be introduced for restaurants, spaces for reception etc. might require more important transformations, results in a lower grade of versatility respect to future alternative uses. In no case an irreversible transformations of relevant parts of the existing structures are planned.

The re adaptation of the buildings of the Arsenale to the necessities of small enterprises does not present particular problems for what regards the insertion of adequate technical structures (except for eventual transformation of the roofs) as long as the principle of introducing independent structures inside the historic buildings is followed. In analogous way the Marina project allows for the adaptation of the historic buildings by insertion of independent structures detached from the historic elements. Major difficulties might arise in this case of the restaurants and commercial facilities.

With respect to the type of use chosen in the first scenario, the Arsenale would regain its original productive destination, albeit from the symbolic point of view the significance of these new uses is quite different from the original one: whereas the production of ships was a crucial activities for the maintenance of the geopolitical role of the republic as one of the mayor commercial and political forces in the Mediterranean, the craftsmen activities represent a mere support to the every-day maintenance of the city itself, without any strategic role for its economic base.

The symbolic value of the new use in the second scenario is quite high, and is congruent with the historic function of the complex. Similar to the period of the Venetian republic, the use of the Arsenale the new destinations contribute and are complementary to the economic role of the city, based today mainly on tourism.

For both scenarios, accessibility for pedestrians is determined by the original asset of the complex which aimed at a maximum level of control for access to an area conceived and managed as an isolated complex which was neatly separated from the city. Some new accesses have already been created during

the transformations in the past two centuries, and only few further access points can be created if heavy transformations should be avoided. Furthermore the area is situated in a peripheral situation with respect to the recent asset of the city centre – oriented towards the principal accesses to the mainland. The accessibility within the complex is determined by the situation of the single building with respect to the nearest point of access, and can in some cases reach considerable distances.

With respect to the accessibility by boat from outside for the first scenario, there are two accesses from public transport lines on from the north and one from the south, which connect to the pedestrian accesses to the area (Casermette area in the north and Tana Area with the main entrance from the south. The access for private boats can be considered optimal for all areas except for the Corderie which have no direct access to a quay or a canal.

Circulation inside the main dock may be made difficult by the presence of landing stages for the mooring of Venetian boats for both scenarios; access for boats to the port is optimal for the second scenario as the north-eastern opening of the main dock is easy to access from the lagoon from the S. Nicolo Lagoon Outlet or from other canals of the lagoon. The entrance into the main dock is possible also for small ships.

Invasiveness

The concept of detached structures to be introduced into the buildings guarantees for a good visibility of the original typological scheme. Albeit the convergence among traditional and new uses, not in all cases the coherence with traditional functions is assured, which may result in difficulties in re-establishing the original orientation of the buildings towards the water and or quays where part of the activities took place. With the new asset of uses quays and watersides may become frequently the side towards which the activities close themselves.

The same can be said for the second scenario, although a stronger orientation towards the water surface is guaranteed by the specific functions foreseen. In the case of commercial services some important modifications of the distributional schemes will be necessary.

Criteria, subcriteria and attributes	Average of judgments	
	Artisan's area	Marina
<i>Versatility</i>	75,0	74,0
Typology of re-use	87,7	78,3
Rigidity of installations	80	80
Poss. Surface removal	90	85
Prevision of vertical connections	90	70
Congruity of technical installations with the standards required	98,3	93,3
Dedicated rooms	100	100
Comfort	95	95
Number of terminals	100	85

<i>Typology of the historic complex</i>	65,0	75,0
Historic character	70	80
Congruity of technical installations with the standards required	98,3	93,3
Dedicated rooms	100	100
Outdoor spaces	60	70

<i>Accessibility</i>	50,0	50,0
Public transport	40	40
Parking spaces	100	100
Access for disabled	10	10

<i>Invasiveness</i>	81,7	79,6
Typological scheme	80,0	81,7
Visibility of the asset	90	85
Functional coherence	70	90
Changes in distribution	80	70

<i>Structures</i>	91,7	86,7
Substitutions can be recognized	90	85
Similarity of materials	85	60
Removal of decay	90	70
Finishing and decorative elements	Not relevant	Not relevant
Reconstructions can be recognized	100	100
Conservation	100	100
Removal of decay	100	100

<i>Technical installations</i>	55,0	50,0
Visual impact	50	50
Compacting	60	50

No substitution of structures is planned, but new structures may be necessary under both projects where the original buildings are lost (for instance in the area of the Galeazze). Technical structures will be realised for the both projects in a detached manner which results in an elevated visual impact. For the artisan's project a medium rate of compacting is expected, for the Marina project this rate will be medium – high.

5.6 Context

Quality of urban landscape

In the both scenarios, the scarce level of invasiveness of the measures on the buildings will determine a substantial conservation of the urban shape of the Arsenale. This is true for the buildings, but not for the outside areas and the water surface, which will be fragmented by the floating structures used for the mooring of small Venetian boats and for leisure time boats in the second case. The impact of the re use on the surrounding area is limited, as no new uses will be introduced, and the area is substantially closed towards the surrounding.

The decision to open the Arsenale to urban productive functions and – also passing for the access to the moorings – to the citizens; will create a good level of consensus to the artisan's project.

Also under the marina project the Arsenale will be made accessible and a somehow “noble” function will be introduced, reconnecting to the area’s original function. These facts will be able to move a positive perception of the project, whereas critical voices will note that by this way the predominant function of the tourism sector in the urban economy will be further fortified, and interest urban areas which used to be interested by tourism in a less intense manner up to now.

Judgements on the impacts on traffic foresee only scarce impacts for both scenarios.

The impact on the urban economy to be expected from the project described in the first scenario, will be rather scarce as the occasion of introducing a more qualified function has not been used. New uses in the Arsenale might be able to develop the urban economy and, as described in the second scenario, might be used to qualify the predominant sector of urban economy, tourism.

In the second scenario some positive effects may be expected in terms of re-qualification of the tourism sector and in terms of economical impacts on the surrounding areas.

Criteria, subcriteria and attributes	Average of judgments	
	Artisan’s area	Marina
Context	80,6	82,9
Quality of urban landscape	80,0	96,7
Maintenance of landscape quality	100	90
Maintenance of aesthetic quality	90	100
Positive externalities on the built env.	50	100
Perception	85,0	52,5
Sharing of functions with the community	100	30
Public use	100	40
Maintenance perception in the community	70	70
Increase in perception of cultural value	70	70
Impacts on traffic	97,5	92,5
Pedestrian	100	100
Private transport	100	90
Public transport	100	100
Natural and cultural paths	90	80
Spatial economics	60,9	90,9
Benefits for the community	100	100
New economic activities induced by re-use	100	90
Diversification of economic activities	100	100
Natural and cultural paths	90	80

5.7 Economy

Expected earnings

The expected earning performance of the project described in scenario a will be rather low, as a high level of public aid is needed for the activity of restoration, these initial investments to be made by the municipality will only in part be covered by the concessions. Also the moorings for residents will have a low return. On the contrary the attended earnings from the Marina project will be high as a high number of moorings for transit and of big boats allows for pointing to high market segments.

Under the Artisan's project predominantly already existing functions will be transferred from other urban areas to the Arsenale. Consequently the level of risk is low, but also the insertion of new activities is accompanied by a relatively low level of risk as activities in the tourist sector in the Venetian context generally prove to be quite sure.

The initiative for Artisans activities requires a high level of external financing (subventions) for the restoration works and has low return rates to be expected albeit low management costs, whereas the marina initiative will guarantee for financial feasibility also without initial subventions, although management activities required will be more onerous in this case.

As this confrontation shows, the evaluation of sustainability of the hypothetical projects for the Marina is slightly more favourable than the results for the artisan's area. The project for the Marina would ask for mayor transformations of the original buildings, resulting in judgement on intrinsic sustainability which is slightly less favourable than for the artisan's area. The judgement for the sustainability with respect to the context is slightly more favourable for the Marina project, as positive impacts on the local economy outweigh the negative impacts expected in terms of social consensus and in terms of traffic.

The judgement on the economic sustainability is favourable for the tourist marina project, as it can be expected to produce a sufficient return to cover expenses for restoring and maintenance of the structures.

Criteria, subcriteria and attributes	Average of judgments	
	Artisan's area	Marina
Economics	67,5	82,5
Expected earning	40	100
Riskyness	90	80
Financial feasibility	50	90
Onerousness of management of the new use	90	60

As this comparison shows, the evaluation of sustainability of the hypothetical projects for the Marina is slightly more favourable than the results for the artisan's area. The project for the Marina would ask for mayor transformations of the original buildings, resulting in judgement on intrinsic sustainability which is slightly less favourable than for the artisan's area. The judgement for the

sustainability with respect to the context is slightly more favourable for the Marina project, as positive impacts on the local economy outweigh the negative impacts expected in terms of social consensus and in terms of traffic.

The judgement on the economic sustainability is favourable for the tourist marina project, as it can be expected to produce a sufficient return to cover expenses for restoring and maintenance of the structures.

	Artisan's area	Marina
Intrinsic sustainability	0.640515	0.58867
Sustainability with respect to the context	0.832227	0.85029
Economic Sustainability	0.6581	0.80422
Comprehensive evaluation	0.649371576	0.674792177

Conclusions

The aim of the paper has been to face the evaluation of the sustainability of projects for the economic re-use of historical buildings in Venice. A multiple criteria model able to analyse alternative projects for re-use and to support the choice was set up. The model adopts a hierarchical approach that identifies the relevant indicators for the appraisal of sustainability, and groups them into three macro-indicators: *intrinsic sustainability*, *context* and *economic-financial feasibility*. A panel of experts filled a questionnaire on hypothetical scenarios, which allowed the calibration of the value functions with which to analyse the sustainability.

Starting from the opinions expressed, indicators were then drawn up to estimate the level of conservativeness of the expert evaluations.

Operationally, the evaluation model was tested on two reuse hypothesis of the Arsenale in Venice. The evaluation model seems able to provide interesting results on the sustainability of re-use projects, correctly considering the environmental, social and economic components of the works and highlighting the strengths and weaknesses.

Such analysis can be used in various ways. Primarily, it can provide a useful support to the identification of the critical point, at the preliminary stage, of projects aiming at combining conservation and economic improvement. Secondly, it can be a support for the selection of projects to be financed in that it allows the trade-off between economic use and conservation to be appraised and thus, implicitly, the cost of the conservation. Finally, it can be a means of reading the re-use projects, providing a check list of variables to be considered in the evaluation of the proposals.

References

- Ackerman J. 1992, *La villa: forma e ideologia*, Turin, Einaudi.
- Brosio G. 1993, *Economia e finanza pubblica*, Rome, NIS.
- Carbonara G. 2001, *Trattato di restauro architettonico*, Turin, UTET.
- Despic O., Simonovic S.P., 2000; Aggregation operators for soft decision making in water resources, *Fuzzy Sets and Systems*, 115, 11-33.
- Dezzi Bardeschi 1991, *Restauro: punto e da capo. Frammenti per una (impossibile) teoria*, Milan, Franco Angeli.
- Forte C. 1977, 'Il valore di scambio e valore d'uso sociale dei beni culturali immobiliari, in *Restauro*, 35: 99-105.
- Fujimoto K., Murofushi T., 1997; Some characterizations of the systems represented by Choquet and multi-linear functional through the use of Möbius inversion, *Int. Journal of Uncertainty, Fuzziness and Knowledge-based Systems*, 5, n. 5, 547-561, 1997.
- Fusco Girard L. 1987, *Risorse architettoniche e culturali: valutazione e strategie di conservazione. Una analisi introduttiva*, Milan, Franco Angeli.
- Giannini, M.S. 1976, 'I beni culturali', *Rivista Trimestrale di Diritto Pubblico*, cit. in Alibrandi T., Ferri P. 1995, *I beni culturali e ambientali*, Milano, Giuffrè, p. 17.
- Grabish M., 1997 K-order additive discrete fuzzy measures and their representation, *Fuzzy Sets and Systems*, 92, 167-189, 1997.
- Grabish M., Labreuche C. and Vansnick J.-C., 2001, Construction of a decision model in the presence of interacting criteria, *Proceedings of AGOP 2001, Asturias (Spain)*, 28-33, 2001.
- Grabish M., Labreuche C. and J.C. Vasnick 2003, On the extension of pseudo-boolean functions for the aggregation of interacting criteria, *European Journal of Operational Research*, 148(1): 28-47.
- Grabish M., Labreuche C. and Vasnick J.C., 2003; On the extension of pseudo-boolean functions for the aggregation of interacting criteria, *European Journal of Operational Research*, 148, 1, 28-47, 2003.
- Howarth, R.B. 1997, 'Defining Sustainability', *Land Economics*, 73(4): 445-621.
- Kacprzyk J., 1987, Towards "human consistent" decision support system through commonsense-knowledge based decision making and control models: a fuzzy logic approach, *Comput. Artificial Intelligence*, 6, 97-122, 1987.
- Kacprzyk J., Fedrizzi M., 1988; A "soft" measure of consensus in the setting of partial (fuzzy) preferences, *European Journal of Oper. Res.*, 34, 315-325, 1988.
- Kacprzyk J., Fedrizzi M. and Nurmi H., 1992; Group decision making and consensus under fuzzy preferences and fuzzy majority, *Fuzzy Sets and Systems*, 49, 21-31, 1992.
- Keeney R., Raiffa H., 1976; *Decision with multiple objectives: preferences and*

value trade-off, Wiley, New York, 1976.

Klement E.P., Mesiar R. and Pap E., 2000; *Triangular norms*, Kluwer Academic Publishers, Netherlands, 2000.

Kolesàrovà A., Mordelovà J., 2001; 1-Lipschitz and kernel aggregation operators, *Proceedings of AGOP'2001*, 2001.

Marconi P. 1993, *Il restauro e l'architetto. Teoria e pratica in due secoli di dibattito*, Venice, Marsilio.

Marichal J. L., 1998; Dependence between criteria and multiple criteria decision aid, *Proceedings of 2nd International Workshop on Preference and Decisions TRENTO'98*, Trento, 1998 (invited lecture).

Marichal J. L., 1999-a; *On Choquet and Sugeno integrals as aggregation functions*, working paper n. 9910, G.E.M.M.E., Faculté d'Economie de Gestion et de Sciences Sociales, 1999.

Marichal J. L., 1999-b; *Aggregation of interacting criteria by means of the discrete Choquet integral*, working paper n. 9814, G.E.M.M.E., Faculté d'Economie de Gestion et de Sciences Sociales, 1999.

Marichal J.L. and M. Roubens 2000, Determination of weight of interacting criteria from a reference set, *European Journal of Operational Research*, 124: 641-650.

Marichal J.L., Roubens M., 2000 Determination of weight of interacting criteria from a reference set, *European Journal of Operational Research*, 124, 641-650, 2000.

Murofushi T., Sugeno M., 1989; An interpretation of fuzzy measures and the Choquet integral as an integral with respect to a fuzzy measures, 1989, *Fuzzy Sets and Systems*, 29 201-227, 1989.

Nijkamp P. e H. Voogd 1989, *Conservazione e sviluppo: la valutazione nella pianificazione fisica*, Milan, Franco Angeli.

Randall, A. 1991, 'Total and Non Use Values', in J.B. Braden and C.D. Kolstad (ed.), *Measuring the Demand for Environmental Quality*, North Holland, Amsterdam.

Scheubrein R., Zionts S., 2006; Problem structuring front end for a multiple criteria decision support system, *Computers&Operation Research*, 33, 18-31, 2006.

Settis S. 2002, *Italia S.p.A. L'assalto al patrimonio culturale*, Turin, Einaudi.

Stellin G. e P. Rosato 1998, *La valutazione economica dei beni ambientali: metodologia e casi di studio*, Turin, Città Studi.

Stellin G., Faggiani A., Zanatta V. and C. D'Alpaos 1997, 'Oltre il vincolo: un nuovo approccio alla gestione dei beni storico culturali nelle aree rurali', *Diritto agrario e ambiente*, Cristiani E. and Massart A. (ed.), atti del Convegno di Studi, Pisa, 30-31 October 1997, Pacini Editore.

Throsby D. 2002, 'Cultural capital and sustainability concepts in the economics of cultural heritage', *Assesing the values of cultural heritage*, Los Angeles, The Getty Conservation Institute.

Throsby, D. 2001, *Economia e cultura*, Bologna, Il Mulino.

Vincke P., Gassner M. and B. Roy 1989, *Multicriteria Decision Aid*, New York, John Wiley&Sons.

Von Altrock Constantin, 1995; *Fuzzy logic and neurofuzzy applications explained*, Prentice Hall PTR, Upper Saddle River, NJ, 1995.

World Commission on the Environment and Development (Brundtland) 1987 *Our Common Future*, Oxford University Press, Oxford.

Yager R. R., 1988; On ordered weighted averaging aggregation operators in multicriteria decision making, *IBEE Trans. Systems Man Cybernet.*, 18, 183-190, 1988.

Yager R. R., 1992; Applications and extensions of OWA aggregation, *Internat. Journal Man Machine Studies*, 37, 103-132, 1992.

Yager R. R., 1993; Families of OWA operators, *Fuzzy Sets and Systems*, 59, 1 25-148, 1993.

REDEVELOPING DERELICT AND UNDERUSED HISTORICAL CITY AREAS: EVIDENCE FROM A SURVEY OF REAL ESTATE DEVELOPERS

Paolo Rosato^{1,2}, Anna Alberini^{2,3}, Valentina Zanatta², Margaretha Breil²

1 Dipartimento di Ingegneria Civile, Università degli studi di Trieste,

2 Fondazione Eni Enrico Mattei,

3 Dept. of Agricultural and Resource Economics, University of Maryland

Riassunto

Gli incentivi economici e gli aiuti legislativi sono spesso ritenuti metodi utili per incoraggiare il riuso di siti urbani dismessi. Ma questi approcci sono efficaci anche quando i siti in stato di abbandono sono edifici storici o aree con un valore architettonico? Questo aspetto è sicuramente un elemento chiave per Venezia e ha importanti implicazioni sulla sua sostenibilità.

In questo studio sono stati usati esperimenti di scelta congiunta (conjoint choice) per esplorare l'importanza di incentivi economici, aiuti legislativi, diritti di concessione e proprietà relativi ad aree dismesse presenti nel centro storico di Venezia. In particolare sono stati intervistati investitori e operatori immobiliari a due fiere immobiliari internazionali, a cui è stato chiesto di esprimere una preferenza tra due tipi di progetti di investimento in aree di Venezia attualmente dismesse, e in un secondo momento è stata testata la preferenza di investimenti a Venezia rispetto ad altre aree in terraferma. I dati raccolti sono stati analizzati usando un modello logit, che ha evidenziato da una parte l'importanza per gli investitori dei diritti di uso e proprietà delle aree oggetto dell'investimento e dall'altra la poca rilevanza dei limiti associati al restauro dei siti e di eventuali miglioramenti al sistema di trasporto dell'area. Dei tre siti oggetto dell'indagine la zona di S. Marta è risultata la più interessante per gli investitori.

Lo studio si è inoltre focalizzato su un'analisi approfondita dei fattori che influenzano maggiormente le decisioni degli operatori immobiliari nella proprie scelte di investimento e sulla loro disponibilità ad investire a Venezia. Dalla ricerca emerge che 2/3 degli intervistati sarebbero interessati a considerare Venezia come una possibile area per i propri investimenti.

Abstract

Economic incentives and regulatory relief are sometimes advocated as useful approaches for encouraging regeneration of derelict urban sites. Would these approaches be effective when the underutilized urban sites are historical buildings or areas that are also prized for their architectural value? This is, of course, a key policy and research question in Venice, and one that has

important implications for sustainability.

We use conjoint choice experiments to explore the relative importance of economic incentives, regulatory relief, land use and property regime offerings at underutilized historical sites in Venice. We survey developers and real estate investors at two international trade fairs, asked them to choose which project they prefer out of two projects at underutilized historical sites in Venice. This question is followed by another where we ask whether they would prefer the investment project in Venice they have just selected, or another project at another locale. We model the responses to these questions using logit models. We find that our respondents care about the allowed land use and property regime, but that –surprisingly– they are not sensitive to conservation restrictions and improved transportation links. Of the three Venice locales we query them about, the most appealing is S. Marta, which is also the most easily accessible.

In addition to the conjoint choice questions, we query our respondents extensively about the factors that matter the most in their decisions to undertake development projects, and query them about their interest in Venice as a possible location for a project. We find that over two-thirds of our interviewees would be willing to consider Venice as a possible investment venue.

1 Introduction and Motivation

Local authorities and highly regarded observers have recently expressed concerns that sustainability goals for the city of Venice might be seriously hindered by its current dependence on tourism as the main driver of its economy. Moreover, current trends suggest that such dependency will worsen in the future because of the increasing demand from emerging countries (China, India, Eastern Europe) and of the competitive disadvantages of localizing economic activities in the center of Venice (poor accessibility, high real estate prices, etc.).

The problem is compounded by the need to strike a balance between city regeneration, a more diversified economy, and conservation of Venice's stock of buildings, which often have great historical, cultural and architectural value, and at the same time are vulnerable to massive tourist use. The local administration and other policymakers concur that it is necessary to find new ways for the City of Venice to achieve sustainable development from both the economic and the social/environmental points of view.

A number of sites in the city center of Venice are currently abandoned or underused and in poor condition. Searching a new identity for these urban areas and buildings and analyzing public policies designed to favor the redevelopment of these areas (and hopefully the establishment of sustainable activities housed or headquartered in them) may help devise and promote new opportunities for sustainable urban development in Venice. The purpose of our research and of this paper is, therefore, to analyze the potential demand for obsolete or abandoned buildings in Venice by potential real estate developers or businesses.

In this paper we focus on real estate developers and investors and their potential role in the sustainable reuse of certain areas of Venice. For this purpose, we created a questionnaire and administered it to real estate developers and investors. We use the questionnaire to examine the factors that real estate developers find attractive (or unattractive) in a place like Venice, and the policy offerings that could be devised to attract real estate development projects and investments in the city. We ask a series of direct questions to investigate the former issue, and deploy a stated-preference approach to answer the latter. Specifically, we ask respondents to focus attention on three underused or abandoned areas in the city of Venice, namely, the Santa Marta Waterfront, and two portions of the Arsenale, the ancient shipbuilding yard. Respondents are to consider hypothetical redevelopment projects at these locations and to choose between pairs of them (or one hypothetical project at one of these locations and a generic project elsewhere).

In our study, the hypothetical development projects are described by a total of 7 attributes: (i) location (at S. Marta, Arsenale Darsena Grande [Marina] and Arsenale Bacini [Shipbuilding Yard]), (ii) allowable use (commercial or light industrial with an emphasis on artisanal production activities); (iii) access (current or improved by rapid transit systems); (iv) presence or absence of conservation restrictions; (v) property regime (lease or full property), and (vi) cost per square meter, which includes the cost of the purchase or lease and development costs, and ranges from €400 to 4000. We arrived at this list of attributes after consulting with local public officials and a small number of real estate developers and real estate agents specializing in the commercial sector.

We use conjoint choice experiments –a stated-preference method based on asking people what they would do under well-specified hypothetical circumstances– for four main reasons. Earlier literature has assessed the attractiveness of economic inducements to developers by observing the occurrence of actual redevelopment projects and land use changes as economic incentives and/or regulation are established (or repealed) over time or by exploiting their variation over a relatively broad geographical area or jurisdiction (Bartik, 2004). These studies have used regression analysis and controlled for other characteristics of properties or policies thought to influence redevelopment.

Unfortunately, these analyses are not possible for buildings with historical and cultural value in Venice due to (1) the lack of transactions (these buildings or complexes sit idle), (2) the lack of policy variation over space and time, and (3) the very small study area. Moreover, if even transactions did occur, (4) the records documenting such transactions are not publicly accessible. Conjoint choice questions make it possible to circumvent all of these problems.

By using conjoint choice experiments, we continue our use of this technique to study the preferences, and hence the response to incentives and regulation which can be altered by policy, of real estate developers. Our earlier studies based on the same method –but focusing on contaminated sites and brownfields– are reported in Alberini et al. (2005), and Wernstedt et al. (2006).

We use stated preferences to investigate the preferences of residents for alternative land uses at an underused site –the Arsenale– in Alberini et al. (2006).

The remainder of the paper is organized as follows. Section 2 reviews the urban and regional economics literature about the role incentives in stimulating economic development at “generic” locales. Section 3 describes the conjoint choice technique and its application to the three underutilized areas of Venice studied here. Section 4 describes the questionnaire and the survey administration. Section 5 presents the theoretical framework and the econometric model. Section 6 describes the data and section 7 the results of the econometric model of the responses to the choice questions. We offer concluding remarks in section 8.

2 Previous Literature

We are not aware of previous empirical work that has assessed the effectiveness of economic incentives and policies aimed at stimulating the reuse of abandoned/underutilized sites of historical and artistic significance. There is, however, an extensive and rather controversial empirical literature about the effectiveness of economic development incentives with “generic” properties. Such incentives typically include industrial development bonds, tax credits for job creation or business location, property tax abatement, tax increment financing, and downtown development authorities.

Recent studies suggest a statistically significant, positive relationship between tax incentives and regional and local growth and property values (Bartik, 1991; Greenstone and Moretti, 2003; Newman and Sullivan, 1988; Wasylenko, 1997), but researchers dispute the magnitude of the impacts of incentives on overall economic gains in targeted areas (Fisher and Peters, 1998; Fox and Murray, 2004; Peters and Fisher, 2002).

Research in this area is afflicted by the problem that concurrent incentives make it very difficult to disentangle the effects of each, a problem that can be remedied only by deploying very careful quasi-experimental approaches with control and treatment groups (Bartik, 2004; Greenstone and Moretti, 2003). It remains difficult, however, to ascertain whether incentives were effective or business locations and/or area redevelopment would have taken place even in their absence (Peters and Fisher, 2004).

Much attention has been devoted as of late to abandoned sites without any particular historical or cultural value but with suspected or confirmed contamination problems –the so-called “brownfields.” Economic inducements have indeed been advocated as potentially effective for stimulating cleanup and redevelopment of brownfields (Bartsch et al., 1996; DeSousa, 2004; Howland, 2000, 2004; Yount and Meyer, 1999). For these sites, the economic incentive toolbox also includes regulatory relief, liability relief, and expedited or simplified cleanup standards.

We are aware of only few studies about the effects of liability relief granted to

the developer or property owner. Using data from the State of Ohio for 1989-1992, Sementelli and Simons (1997) find that receiving a letter of “no further action” from the State does not improve transaction rates for sites with leaking underground storage tanks (LUST), which remain much lower than those for non-tank commercial properties. Alberini (2007) recently examines Colorado’s Voluntary Cleanup Program, finding that very little cleanup activity was associated with participation, and concluding that the owners of participating properties were simply seeking a clean bill of health from the state in preparation for possible sale of the properties in areas with high redevelopment potential.

Lange and McNeil (2004a, 2004b) survey over 100 EPA brownfield grant recipients and other stakeholders. They find that community support, consistency with local plans, cost minimization, financial incentives, and minimizing the time it takes to put the site back into productive use are the most often cited variables that influence brownfield development success.

Based on interviews with real estate agents, Howland (2004) refutes the notion that contamination is the most serious hindrance to redevelopment of previously used properties. She suggests that incompatible land uses, inadequate infrastructure and obsolete buildings are more important barriers than contamination to the revitalization of brownfields in Baltimore. These findings would suggest that subsidizing infrastructure and removing obsolete zoning restrictions might be useful policy options for encouraging redevelopment—a matter than we also explore in our conjoint choice experiments.

On their part, real estate developers claim that they are responsive to a broad range of inducements. In surveys in Europe (Alberini et al., 2005) and in the US (Wernstedt et al., 2006) choice experiments reveal that developers can be attracted to contaminated sites by offering them subsidies, liability relief, and less stringent regulation. Prior experience with projects at contaminated sites matters, in the sense that these incentives do not appeal to the same extent to all developers. Meyer and Lyons (2000) suggest that low property prices have played a larger role than subsidies in stimulating entrepreneurial redevelopment activity on contaminated sites, and that obtaining subsidies may entail significant transaction costs that offset their value. It remains to be seen, of course, if similar considerations apply with underutilized sites with historical and architectural significance, and these are precisely the issues we explore using conjoint choice questions.

3 Conjoint Choice Experiments: Theory and Practice

In this section, we first describe conjoint choice experiments and then provide details on the design and structure of the conjoint choice experiment questions used in our study.

3.1 Conjoint Choice Experiments

Conjoint choice experiments are a survey-based technique used to investigate the tradeoffs that people are prepared to make between different goods or

policies. In general, this technique can be used to find the monetary value that people ascribe to goods or to the benefits of a policy. It is a stated-preference technique, in that it relies on individuals saying what they would do under hypothetical circumstances, rather than observing actual behaviors in marketplaces.

In a typical conjoint choice experiment survey, respondent are shown alternative variants of a good described by a set of attributes, and are asked to choose their most preferred (Hanley et al., 2001). The alternatives differ from one another in the levels taken by two or more of the attributes. Statistical analyses of the responses to the choice questions can be used to obtain the marginal values of these attributes and the willingness to pay for any alternative of interest. Marginal prices of the attributes can be calculated if one of the attributes is cost; the full value (willingness to pay or WTP) of any specified alternative can be estimated if the "do nothing" or status quo option is included in the choice set.

One advantage of conjoint choice experiments, which is in common with other stated-preference methods, is that they allow the analyst to study people's responsiveness to goods, levels of environmental quality, or policy offering that do not currently exist. The technique is also very flexible, in that it can be adapted to a variety of policies and situations.

To motivate the statistical analysis of the responses to conjoint choice questions, it is assumed that the choice between the alternatives is driven by the respondent's underlying utility. The respondent's indirect utility is broken down into two components. The first component is deterministic, and is a function of the attributes of alternatives, characteristics of the individuals, and a set of unknown parameters, while the second component is an error term. Formally,

$$V_{ij} = \bar{V}(\mathbf{x}_{ij}, \boldsymbol{\beta}) + \varepsilon_{ij} \quad (1)$$

where the subscript i denotes the respondent, the subscript j denotes the alternative, \mathbf{x} is the vector of attributes that vary across alternatives (or across alternatives and individuals), and is an error term that captures individual- and alternative-specific factors that influence utility, but are not observable to the researcher. Equation (1) describes the random utility model (RUM).

In many applications, it is further assumed that , the deterministic component of utility, is a linear function of the attributes and of the respondent's residual income, $(y - C)$:

$$V_{ij} = \beta_0 + \mathbf{x}_{ij}\boldsymbol{\beta}_1 + (y_i - C_{ij})\beta_2 + \varepsilon_{ij}, \quad (2)$$

where y is income and C is the cost of the alternative program to the respondent. Clearly, the coefficient is the marginal utility of income.

Respondents are assumed to choose the alternative in the choice set that results in the highest utility. Because the observed outcome of each choice task is the selection of one out of K alternatives, the appropriate econometric model

is a discrete choice model expressing the probability that alternative k is chosen. Formally,

$$\pi_{ik} = \Pr(V_{ik} > V_{i1}, V_{ik} > V_{i2}, \dots, V_{ik} > V_{iK}) = \Pr(V_{ik} > V_{ij}) \quad \forall j \neq k, \quad (3)$$

where signifies the probability that option k is chosen by individual i .

This means that

$$\pi_{ik} = \Pr(\beta_0 + \mathbf{x}_{ik}\beta_1 + (y_i - C_{ik})\beta_2 + \varepsilon_{ik} > \beta_0 + \mathbf{x}_{ij}\beta_1 + (y_i - C_{ij})\beta_2 + \varepsilon_{ij}) \quad \forall j \neq k \quad (4)$$

and hence that

$$\pi_{ik} = \Pr[(\varepsilon_{ij} - \varepsilon_{ik}) < (\mathbf{x}_{ik} - \mathbf{x}_{ij})\beta_1 - (C_{ik} - C_{ij})\beta_2] \quad \forall j \neq k. \quad (5)$$

Equation (5) shows that the probability of selecting an alternative no longer contains terms in (2) that are constant across alternatives, such as the intercept and income. It also shows that the probability of selecting k depends on the differences in the levels of the attributes across alternatives, and that the negative of the marginal utility of income is the coefficient on the difference in cost or price across alternatives.

If the error terms are independent and identically distributed and follow a standard type I extreme value distribution, one can derive a closed-form expression for the probability that respondent i picks alternative k out of K alternatives.

Since the cdf of the standard type I extreme value distribution is $F(\varepsilon) = \exp(-e^{-\varepsilon})$, and its pdf is $f(\varepsilon_i) = \exp(-\varepsilon_i - e^{-\varepsilon_i})$, choosing alternative k means that $\varepsilon_k + V_k > \varepsilon_j + V_j$ for all $j \neq k$, which can be written as $\varepsilon_j < \varepsilon_k + V_k - V_j$. The probability of choosing k is, therefore,

$$\begin{aligned} \pi_{ik} &= \Pr(\varepsilon_{ij} < \varepsilon_{ik} + V_{ik} - V_{ij}) \quad \text{for all } j \neq k \\ &= \int_{-\infty}^{+\infty} \prod_{j \neq k} F(\varepsilon_{ik} + V_{ik} - V_{ij}) \cdot f(\varepsilon_{ik}) d\varepsilon_{ik}. \end{aligned} \quad (6)$$

Expression (6) follows from the assumption of independence, and the fact that is an error term and not observed, so that it is must be integrated out of $F(\varepsilon_{ik} + V_{ik} - V_{ij})$. The product within expression (6) can be re-written as

$$\begin{aligned} \prod_{j \neq k} F(\varepsilon_{ik} + V_{ik} - V_{ij}) \cdot f(\varepsilon_{ik}) &= \prod_{j \neq k} \exp(-e^{-\varepsilon_{ik} - V_{ik} + V_{ij}}) \exp(-\varepsilon_{ik} - e^{-\varepsilon_{ik}}) \\ &= \exp\left[-\varepsilon_{ik} - e^{-\varepsilon_{ik}} \left(1 + \sum_{j \neq k} \frac{e^{V_{ij}}}{e^{V_{ik}}}\right)\right]. \end{aligned} \quad (7)$$

Now write

$$\lambda_{ik} = \ln\left(1 + \sum_{j \neq k} \frac{e^{V_{ij}}}{e^{V_{ik}}}\right) = \ln\left(\sum_{j=1}^K \frac{e^{V_{ij}}}{e^{V_{ik}}}\right), \quad (8)$$

which allows us to rewrite (6) as

$$\int_{-\infty}^{+\infty} \exp(-\varepsilon_{ik} - e^{-(\varepsilon_{ik} - \lambda_{ik})}) d\varepsilon_{ik} = \exp(-\lambda_{ik}) \int_{-\infty}^{+\infty} \exp(-\varepsilon_{ik}^* - e^{-\varepsilon_{ik}^*}) d\varepsilon_{ik}^*, \quad (9)$$

where $\varepsilon_{ik}^* = \varepsilon_{ik} - \lambda_{ik}$. The integrand in expression (9) is the pdf of the extreme value distribution and is, clearly, equal to 1. Equation (9) thus simplifies to $\exp(-\lambda_{ik})$, which by (8) is in turn equal to $\exp(V_{ik}) / \sum_{j=1}^K \exp(V_{ij})$.

Recalling (2), the probability that respondent i picks alternative k out of K alternatives is

$$\pi_{ik} = \frac{\exp(\mathbf{w}_{ik} \boldsymbol{\beta})}{\sum_{j=1}^K \exp(\mathbf{w}_{ij} \boldsymbol{\beta})} \quad (10)$$

where $\mathbf{w}_{ij} = \begin{bmatrix} \mathbf{x}_{ij} \\ C_{ij} \end{bmatrix}$ is the vector of all attributes of alternative j , including cost, and is equal to $\begin{bmatrix} \boldsymbol{\beta}_1 \\ -\boldsymbol{\beta}_2 \end{bmatrix}$.

Equation (10) is the contribution to the likelihood in a conditional logit model. The full log likelihood function of the conditional logit model is

$$\ln L = \sum_{i=1}^n \sum_{k=1}^K y_{ik} \cdot \log \pi_{ik}, \quad (11)$$

where y_{ik} is a binary indicator that takes on a value of 1 if the respondent selects alternative k , and 0 otherwise. The coefficients are estimated using the method of Maximum Likelihood.

For large samples and assuming that the model is correctly specified, the maximum likelihood estimates $\hat{\boldsymbol{\beta}}$ are normally distributed around the true vector of parameters $\boldsymbol{\beta}$, and the asymptotic variance-covariance matrix, $\boldsymbol{\Omega}$, is the inverse of the Fisher information matrix. The information matrix is defined as

$$I(\boldsymbol{\beta}) = \sum_{i=1}^n \sum_{k=1}^K \pi_{ik} (\mathbf{w}_{ik} - \bar{\mathbf{w}}_i)(\mathbf{w}_{ik} - \bar{\mathbf{w}}_i)', \quad (12)$$

where $\bar{\mathbf{w}}_i = \sum_{k=1}^K \pi_{ik} \mathbf{w}_{ik}$.

Once model (11) is estimated, the rate of tradeoff between any two attributes is the ratio of their respective $\boldsymbol{\beta}$ coefficients. The marginal value of attribute 1 is computed as the negative of the coefficient on that attribute, divided by the coefficient on the price or cost variable:

$$MP_1 = -\frac{\hat{\boldsymbol{\beta}}_1}{\hat{\boldsymbol{\beta}}_2}. \quad (13)$$

The willingness to pay for a commodity is computed as:

$$WTP_i = -\frac{\mathbf{x}_i \hat{\beta}_1}{\hat{\beta}_2}, \quad (14)$$

where x_i is the vector of attributes describing the commodity assigned to individual i . It should be kept in mind that a proper WTP can only be computed if the choice set for at least some of the choice sets faced by the individuals contains the “status quo” (in which no commodity is acquired, and the cost is zero). Expression (14) is obtained by equating the indirect utility associated with commodity and residual income with the indirect utility associated with the status quo (no commodity) and the original level of income y , and solving for C .

When reporting the estimates of the marginal prices of the attributes and the WTP, it is important to report the standard errors around these estimates. As shown in (13) and (14), marginal prices and WTP are the ratios of variables that in large samples are jointly normally distributed. This means that standard errors around them must be computed using the delta method (Greene, 2003, p. 193), or, alternatively, simulation-based procedures (see Alberini et al., 2007).

The conditional logit model described by equations (10)-(11) is easily amended to allow for heterogeneity among the respondents. Specifically, one can form interaction terms between individual characteristics, such as age, gender, education, etc., and all or some of the attributes, and enter these interactions in the indirect utility function.

Whether or not interaction terms are included, implicit in the conditional logit model is the assumption of Independence of Irrelevant Alternatives (IIA), which states that the ratio of the odds of choosing any two alternatives depends only on the attributes of the alternatives being compared, and is not affected by the attributes of other alternatives. An implication of the IIA is that adding another alternative, or changing the characteristics of a third alternative, does not affect the relative odds between alternative k and h . IIA generally imposes restrictive substitution patterns among the alternatives. To illustrate, when we change the level of the l th attribute of alternative k , the marginal change in the probability of choosing k is:

$$\Pr(k) \cdot [1 - \Pr(k)] \cdot \beta_l, \quad (15)$$

whereas changing the level of the l th attribute of another alternative—alternative j —, implies that the marginal change in the likelihood of choosing k is:

$$-\Pr(k) \cdot \Pr(j) \cdot \beta_l. \quad (16)$$

A change in the attributes of one alternative, therefore, changes the probabilities of the other alternatives proportionately to satisfy the conditional logit’s requirement that the ratio of these probabilities remains the same (Train, 1999). This implies that the conditional logit is not well suited for alternatives that individuals perceive as close substitutes of one another.

3.2 Application of Conjoint Choice to Underutilized Historical Sites in Venice

In our conjoint choice experiments, the alternatives were real estate development projects to be completed at one of four possible locations: (i) the former gasometers in the S. Marta area of Venice (Figure A.3), (ii) the central part of the Arsenale, the historical shipbuilding in Venice (Figure A.4), (iii) the northeastern part of the Arsenale, which is currently used as a shipbuilding yard (Figure A5), and (iv) a generic real estate investment project elsewhere.

The alternative programs were described by four more attributes, in addition to the location: (i) access (at the current level or improved), (ii) allowed use (commercial or light industrial with an emphasis on artisanal/handicraft activities), (iii) conservation restoration (required or not required), (iv) property regime (full private property or lease), and (v) price per square meter.

Attributes and levels of the attributes are summarized in table 1. It should be emphasized that attributes (ii), (iii) and (iv) could be altered through changes in the City's policy or through negotiations with developers on an individual basis (see Stellin and Zoboli, 2006). The City could also offer tax credits or other subsidies to developers in order to encourage reuse of the three abandoned or underused areas studied here, in which case such offerings would be captured into attribute (v)—price per square meter.

A series of sample conjoint choice questions is reproduced in the Appendix. As shown in Figure A.1, we first asked respondents to choose between hypothetical projects A and B, each entailing a transformation of one of the three areas in Venice. We followed up this question with another binary question that asked respondents which they would prefer—the project they had just chosen in the previous exercise, or the typical project they usually undertake elsewhere. This choice task is shown in Figure A.2.

Each respondent was shown a total of 4 project A-project B pairs, plus 4 project (A/B)-project elsewhere questions, for a total of 8 conjoint choice questions.

Attribute	Levels of the attribute
Location	S. Marta Arsenale Darsena Grande (Marina) Arsenale Bacini (Shipbuilding Yard)
Land use	Commercial Light Industrial
Access	Current Improved
Building Conservation as per Regulations	Required Not required
Property rights	Full property Lease
Cost per square meter (in euro)	150, 300, 500, 700, 1000, 1500

Tab 1 – Attributes and attribute levels in the conjoint choice experiments.

4 Structure of the Questionnaire and Survey Administration

Our survey questionnaire is self-administered by the respondents using stand-alone computers or on-line, and is divided into 4 sections.

In **section 1**, we asked the respondent to describe the nature of his or her company's business. Is it a real estate development company, a real estate investment firm or bank, a lender, or a consulting outfit that works primarily for developers? If the respondent's company has done development projects in the last five years, we ask him or her to describe three of them to us: Where did each take place? Was it a residential, industrial, or commercial project? Was it an office building? Did the company sell it, lease it to tenants, or does it manage it directly? And what was the volume built?

Next, we ask the respondent to tell us if his company does residential, commercial, or industrial projects, or office buildings, and what percent of all projects are accounted for each of these types. We recognize that pinpointing exact percentages might be difficult, so we provide ranges (0-20%, 21-40%, 41-60%, 61-80%, or 81-100%) to facilitate the respondent's task. We also inquire which markets the respondent's company usually does these projects in—is it the Veneto? Northern Italy? The rest of Italy? Abroad?

This section ends with questions that inquire about development projects and decisions. We show respondents a list of factors surrounding real estate deals and investments, and ask them to tell us if each of these factors is "always," "almost always," "often," "sometimes" or "never" crucial in their investment decisions. In the last screen of section 1, we ask respondents what they usually look for when making investment decisions. Is it new buildings in turn-key conditions? Existing buildings that need some restructuring? Buildable parcels? Derelict sites that must be regenerated?

Section 2 of the questionnaire is about Venice. We first wish to find out whether the respondent's company has ever done any real estate development in Venice proper or the Venice hinterland, and, if so, what type of projects. Then, we wish to find out whether the respondent would ever consider Venice and the Venice hinterland for development projects. If the answer is "yes," respondents are to pinpoint the reasons why they find Venice attractive for business out of a list of possibilities. If the answer is "no," we show them a list of possible disadvantages of Venice as a location for business, and ask them to indicate which ones apply to them.

The purpose of asking these questions is two-fold. First, it is of independent interest to find out what makes Venice attractive or unattractive to developers. Second, by making respondents focus on the pros and the cons of doing business in Venice, these questions serve as a useful "bridge" towards section 3 of the questionnaire—the conjoint choice questions.

The conjoint choice questions (described in section 3 of this paper) are preceded by a brief introduction of the S. Marta and Arsenale developable areas. Respondents wishing to obtain fuller descriptions of these areas (see Figure A.3 in the Appendix) can do so by double-clicking hyperlinks on the

screen.

The fourth and last section of the questionnaire asks general questions about the annual revenue of the company, its headquarters, whether the company is partly owned or controlled by a government entity, and the position held by the respondent within the company.

Ideally, we would have liked to administer the questionnaire to a sample drawn from the universe of developers based in Italy and in other European countries. We had a list of developers that do business in the Milan area and in the Veneto, and we contacted these firms by e-mail and over the telephone, asking them to participate in the survey, which they would complete on-line. This approach resulted in a total of 38 completed questionnaires. Three “recalcitrant” developers agreed to meet with one of our interviewers in their offices and to fill out the questionnaire using a laptop computer.

Since our list cannot be considered exhaustive, and at any rate we had only been able to gather a total 41 completed questionnaires in this way, we expanded our sample by going to professional real estate developer meetings and trade fairs, where we asked attendees to participate in the survey on the spot. We were able to obtain 60 completed questionnaires at the MIPIM trade fair in March 2006 and 45 more questionnaires at the REAG in Milan in May 2006. (The UrbanPromo conference in November 2005 in Venice served to administer a pre-test questionnaire to a total of 10 attendees.)

5 The Model

We assume that the responses to the conjoint choice questions are motivated by a random profit model.¹ Formally, we posit that project j 's profit is

$$\pi_{ijm} = [L_{ijm} \alpha + ACC_{ijm} \cdot \beta_1 + USE_{ijm} \cdot \beta_2 + CONS_{ijm} \cdot \beta_3 + PROPR_{ijm} \cdot \beta_4 + P_{ijm} \cdot \gamma + (L_{ijm} \times P_{ijm}) \cdot \delta] + \varepsilon_{ijm}, \quad (17)$$

where i denotes the respondent, j denotes the alternative, m denotes the choice question ($m=1, 2, \dots, 8$), L is a vector of location dummies, ACC is a dummy denoting current or improved access, USE is a dummy for the allowed use of the property (commercial or light industrial), $CONS$ is a dummy capturing whether any construction on the premises must satisfy building conservation restrictions, $PROPR$ describe the property regime, and P stands for the price in square meters. Equation (17) also contains unknown coefficients α , β and δ , and an error term ε that is assumed to be an i.i.d. draw from the standard type I extreme value distribution.²

¹ This implies only a slight change in the interpretation and minor notational abuse of the material presented in section 3.A.

² This assumption implies that the error terms and hence the choice responses are

The term in brackets in equation (17) can be thought of as the deterministic components of profits. If we denote this term as $\bar{\pi}_{ijm}$, equation (17) can be re-written as

$$\pi_{ijm} = \bar{\pi}_{ijm} + \varepsilon_{ijm}, \quad (18)$$

and it is easily shown (see section 3.A and Alberini et al., 2007) that the probability that the respondent selects alternative k out of the choice set for question m is

$$\Pr(i \text{ chooses } k \text{ in choice question } m) = \frac{\exp(\bar{\pi}_{ikm})}{\sum_{j=1}^{J_m} \exp(\bar{\pi}_{ijm})}. \quad (19)$$

In this study, J_m , the size of the choice set for question m , is 2 for all m , since the respondent always makes two binary choices (first between projects A and B in Venice, and then between the preferred Venice project and a project elsewhere). Equation (19) is the contribution to the likelihood in a conditional logit model, which we estimate by the method of maximum likelihood. In our case, since $J_m=2 \forall m$, the model is simplified to a binary logit. Formally, the log likelihood function is:

$$\ln L = \sum_{i=1}^n \sum_{m=1}^8 \sum_{k=1}^2 y_{ikm} \ln \left[\frac{\exp(\bar{\pi}_{ikm})}{\sum_{j=1}^2 \exp(\bar{\pi}_{ijm})} \right], \quad (20)$$

where y_{ikm} is an indicator that takes on a value of one if respondent i select alternative k in choice question m .

All binary attributes are coded as 0/1 binary variables,³ while the price per square meter is entered in the model as a continuous variable. We represent the “investment elsewhere” project as follows: all locations dummies=0, access=1, use=1, property regime=0 (full property), conservation restrictions=0 (not required), and price=500 if the average volume built by this company is greater than 30,000 cubic meters, and price=700 if if the average volume built by this company is less than or equal to 30,000 cubic meters.⁴

independent across and within respondents. Because the distribution of the error terms is a standard type I extreme value, and the scale parameter cannot be estimated separately, the profits in equation (1) should not be thought of as expressed in euro. They should be thought of as a scaleless index of profitability.

³ Other analyses of conjoint choice responses have sometimes preferred factor coding, i.e., -1 and 1.

⁴ We consider 30,000 m³ the cutoff for classifying a project as medium-sized to large.

6 The Data

6.1 Characteristics of the Respondents and of their Investment Projects

Our first order of business is to examine the characteristics of the respondents, the companies they represent, and the development projects that their companies undertake. As shown in table 1, developers account for over one-half of our sample (51.77%), and the second most heavily represented category is consultants or advisors to real estate developers or investors (22%). Lenders, construction companies, and real estate investment firms account each for 7% of the sample.

TIPOIMP	PERCENT OF THE SAMPLE
Developer	51.77
Construction company	7.09
Lender providing financing to firms	7.80
Real estate investment	7.80
Loans and savings	1.42
Consultant/advisor	21.99
Other	2.13

Tab 2 – Type of firm or company (N=141).

Regarding the headquarters of the company, 87.23% are based in Italy and 12.77% in other countries. Only 5.84% of the respondents reported that their firm was partially owned or controlled by a government entity. Figure 1 displays information about the distribution of companies by the size of their business, showing that companies with annual revenue greater than €10 million account for over two-thirds of the sample.

What type of projects do our respondents' companies do? About 85.5% of the companies do office buildings, 89.9% do shopping malls and commercial projects, 41% do projects entailing industrial land uses, and 69% do residential projects. A vast majority of these projects (85-90%, depending on the type) take place in Italy. Table 2 shows the degree of diversification of operations of each firm: only for less than 10% of the sample does a specific type of projects account for the lion's share (81-100%) of all projects.

Finally, we asked respondents to describe three recent projects for us. The characteristics of these three recent projects are described in table 3. They were, for the most part, residential or commercial projects, or office buildings. Projects slated for industrial use were much less frequent. Over three-quarters of these projects were sold. About 14% of the projects were leased to tenants, and in about 10% of the projects the company managed the project directly.

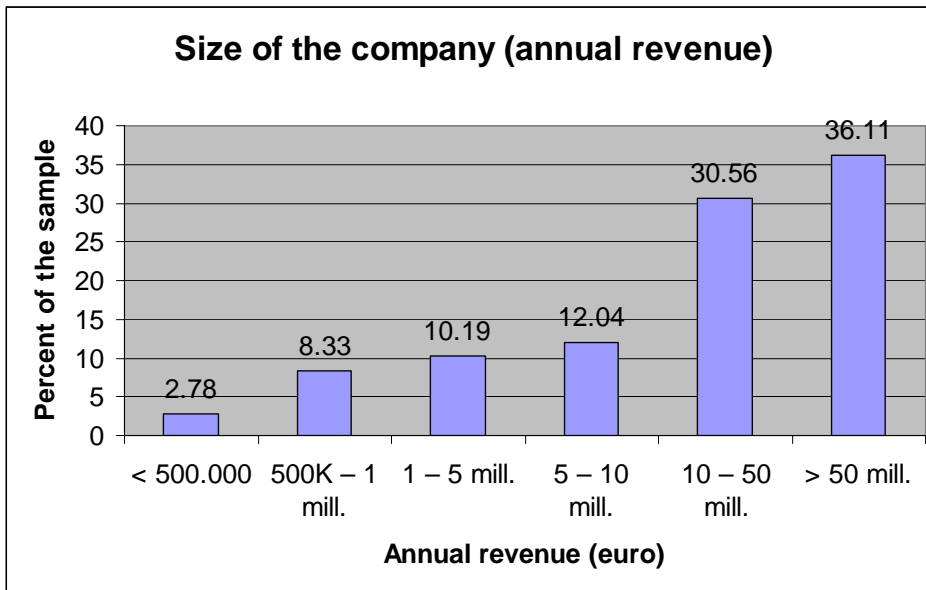


Fig 1 – Size of the company.

percent of all projects	percent of the sample			
	office buildings	commercial	industrial	residential
0-20	25.64	36.89	40.35	22.92
21-40	38.46	42.62	31.58	28.13
41-60	18.8	9.84	10.53	22.92
61-80	11.97	3.28	10.53	16.67
81-100	5.13	7.38	7.02	9.38
	N=117	N=122	N=57	N=96

Tab 3 – Type of projects as share of total projects.

	first project	second project	third project
A. Land use			
Office buildings	29.46	22.02	23.47
Commercial	28.68	34.86	36.73
Industrial	9.3	16.51	6.12
Residential	32.56	26.61	33.67
	N=129	N=109	N=98
B. What did the company do with the project?			
Sold it	72.87	78.38	75.51
Leased it to tenants	13.95	9.91	17.35
Directly managed it itself	13.18	11.71	7.14
	N=129	N=111	N=98
C. Volume built (m³)			
< 10000	7.87	7.34	6.12
10001-30000	21.26	15.6	16.33
30001-60000	15.75	20.18	27.55
60001-100000	23.62	26.61	25.51
> 100000	31.5	30.28	24.49
	N=127	N=109	N=98

Tab 4 – Description of three recent projects. Percentage of the sample that reports.

6.2 Attractiveness of Investments and Projects in Venice

One of the goals of this research projects is to find out what makes Venice an attractive (or unattractive) destination for business, and what can be done to improve its appeal to real estate investors. Before we inquire about this, it is important to find out which factors developers consider crucial in making or breaking a deal.

Table 4 summarizes the responses to exactly this latter question. Opportunities for agreements (item 1) with local public administration agencies is “always” or “almost always” crucial for over two-thirds of the sample, as are warranties and reassurances on the time needed to get permits (line 3). The possibility of purchasing the property (item 4) –as opposed to leasing it– is also important, as are the prestige of the locale (item 11), and, of course, the cost of the land (item 12) and construction costs (13).

Of less importance are the duration of the lease (item 5), the possibility to subdivide the development or the building (item 6), the presence of land use and historical-architectural conservation restrictions (item 7), environmental impact assessment requirements (item 8), and proximity to transportation nodes and network (items 9-10), where respondents were more evenly distributed among the various response categories.

	Always	Almost always	Often	Sometimes	Never
Agreement with local authority	44.37	23.24	14.79	12.68	4.93
Fiscal exemptions	11.27	12.68	16.9	35.92	23.24
Guarantees on the terms necessary for the authorization	35.92	30.28	20.42	8.45	4.93
Full property	52.82	20.42	15.49	7.04	4.23
Years of leasing (if leased)	32.39	16.9	11.97	16.2	22.54
Possibility to fraction the property	22.54	23.94	27.46	22.54	3.52
Urban and restoration constraints	35.92	21.83	17.61	19.72	4.93
Compulsory Environmental Impact Assessment procedure	19.72	17.61	17.61	26.06	19.01
Closeness to highway	17.61	16.9	26.06	32.39	7.04
Closeness to airport	11.97	12.68	21.83	36.62	16.9
Prestigious location	48.59	27.46	16.9	6.34	0.7
Construction cost	69.72	17.61	5.63	5.63	1.41
Price	66.2	18.31	9.86	4.93	0.7

Tab 5 – When making investment decisions, which of the factors listed below is crucial? (N=142).

As shown in table 5, 26 respondents (18.31% of the sample) have previously done real estate development in Venice and 26 have done projects in the Venice hinterland. Specifically, 15 respondents has done projects in Venice proper but not in the hinterland, 15 reports having done projects in the Venice mainland but not in Venice proper, and 11 have done projects at both locations.

When asked whether they would consider Venice as a possible location for business, 74% and 63% of the respondents indicated that they would, for Venice proper and for its mainland, respectively. What's even more astounding is that only 22 respondents (15% of the sample) said that they would not consider either location.

As shown in table 6, the main reasons for considering Venice a potentially attractive location for business are prestige, profitability and the fact that it attracts many tourists. Another popular response category is the appreciation in the value of the buildings or the land. One respondent also volunteered that Venice grants access to domestic markets and users, and another that it offers prestigious deals for investors. Reasons for finding Venice *unattractive* for business include the lack of developable areas, high construction costs, problems specific to the City and the excessive reliance of the city on tourism (see table 7). Individual respondents volunteered other reasons why they do not

consider Venice attractive for business. To one, the city is too “local;” four said that the Venice area is a poor fit for their company’s specialization;⁵ another yet considers it a poor market for the service sector, and, finally, one mentioned that it is problematic to negotiate and come to agreements with the public administration.

Those who would consider the Venice hinterland for business mentioned its proximity to international routes, the supply of developable land, high profitability, and closeness to a major tourist destination (the city of Venice) (table 8). Table 9 shows that those who would not consider the Venice hinterland for business believe that its image is incompatible with their company’s business, profitability would be low, and real estate values would not appreciate enough.

Tab 6 – Actual and potential interest in Venice as project/investment locale. N=142.

	Have you ever done a project/investment in...?		Would you consider...for your projects/investments?	
	Venice	the Venice hinterland	Venice	the Venice hinterland
no	81.69	81.69	26.06	37.32
yes	18.31	18.31	73.94	62.68

Tab 7 – Reasons for considering Venice a potentially attractive location for business. N=116.

Reason	Number of respondents	Percentage of the total*
Prestige	70	60.34
Profitability	62	53.45
Increase in value	33	28.45
Proximity to international routes	11	9.48
Liveliness of the real estate market	16	13.79
Funding available as per the Special Law for Venice	17	14.66
Touristic nature of the city	73	62.93

*: Multiple responses were possible, so percentages do not sum to 100.

⁵ One of these respondents specifically mentioned that his company focuses on derelict sites in Milan, and another in sites for industrial use.

REASON	NUMBER OF RESPONDENTS	PERCENTAGE OF THE TOTAL*
Image of Venice is not compatible with the company's business	1	3.85
Profitability	3	11.54
Increase in value	1	3.85
Distance from international routes	3	11.54
Lack of undeveloped areas	10	38.46
Lack of transparency in the real estate market	5	19.23
Construction is too expensive	14	53.84
Problems specific to Venice	16	61,53
Touristic nature of the city	9	34.61

Tab 8 – Reasons for considering Venice a potentially unattractive location for business. N=26.

*: Multiple responses were possible, so percentages do not sum to 100.

REASON	NUMBER OF RESPONDENTS	PERCENTAGE OF THE TOTAL*
Have a "Venice" address	5	5.61
Profitability	38	42.70
Increase in value	27	30.33
Proximity to international routes	42	47.19
Availability of undeveloped land	41	46.07
Easy access to the real estate market	13	14.61
Proximity to a major tourist destination (Venice)	45	50.56

Tab 9 – Reasons for considering the Venice hinterland a potentially attractive location for business. N=89.

REASON	NUMBER OF RESPONDENTS	PERCENTAGE OF THE TOTAL*
Image of Venice is not compatible with the company's business	17	32.07
Profitability	10	18.87
Increase in value	6	11.32
Access is difficult	0	0
Lack of undeveloped areas	2	3.77
Lack of transparency in the real estate market	2	3.77
The proximity to a major tourist destination (Venice) is a minus	2	3.77

Tab 10 – Reasons for considering the Venice hinterland a potentially unattractive location for business. N=53.

6.3 Responses to the Conjoint Choice Questions

Table 10 reports the relative frequency of the various response categories for

the conjoint choice questions. In choice questions 2, 3, and 4, the percentage of “project A” and “project B” responses is generally well-balanced, suggesting that there were no obviously superior alternatives. In choice question 1, almost two-thirds of the respondents selected project A. Comparison between the responses to questions 1-4 and those to questions 1a-4a suggests that when pressed to indicate which they would prefer—the previously selected project in Venice or a project elsewhere—about 50% of the respondents announced that they would still choose the Venice project and the other 50% would take the project at another location.

CHOICE QUESTION	PERCENT CHOOSE A	PERCENT CHOOSE B	PERCENT CHOOSE “A PROJECT ELSEWHERE”*
1	64.08	35.92	
1-a	30.99	15.49	53.52
2	50.70	49.30	
2-a	26.06	22.54	51.41
3	53.52	46.48	
3-a	26.06	17.61	56.34
4	51.41	48.59	
4-a	18.31	22.54	59.15

Tab 11 – Frequency of the responses to the conjoint choice questions.

* Choose “another project elsewhere” or confirm the project selected in the immediately preceding choice question.

7 Econometric Estimation Results

The results for two specifications of the conditional logit model are reported in table 11. We remind the reader that because $J_m = 2 \nabla m$, the conditional logit is simplified to a binary logit, and that in this paper we assume that all responses are independent across and within respondents. Specification (A) in table 11 corresponds to a parsimonious version of equation (1) which omits the interactions between the price and the location dummies. Specification (B) is the full model, i.e., the underlying random utility is equation (1).

Based on the results of specification (A), we would conclude that, all the same, S. Marta is the most preferred location, followed by Arsenale Grande, which is turn more preferred than Arsenale Bacini. All of these locations are, all else the same, chosen more frequently than the “project elsewhere” option. We do not find that improving access makes a project more attractive. This is probably because the most attractive location, S. Marta, already has good access (it is the only location that can be reached by cars and trucks). Improving access to the Arsenale locations will not, all else the same, make them more attractive to investors and developers.

We coded the allowed land use attribute as 0 to mean light industrial use, and 1 to mean commercial use. It is clear that light industrial use at these locations is of little interest to developers. Allowing commercial use raises dramatically the probability of selecting a project in Venice. Notably, the presence or absence of conservative restoration requirements do not affect the respondent’s profit

calculus, whereas full property in lieu of a lease makes a project much more attractive. (We coded this attribute as zero for full property and 1 for lease, so the negative sign of the coefficient on this attribute implies that, all else the same, a project is judged less appealing under lease conditions.)

Finally, the coefficient on the price per square meter is negative and significant, implying that, as expected, the higher the price, the less attractive the project is. The absolute value of this coefficient, however, is very small, suggesting a perplexing lack of responsiveness to price on the part of our developers. For example, S. Marta at conditions similar to the current ones (and slated for industrial use) would be judged worth €6500 per square meters, a value that is outside of the range of prices assigned to the respondents in our survey, and is much higher than current prices in that part of town. (Indeed, this value is closer to and more representative of prices in the exclusive S. Marco area.)

We suspect that these implausible results might be an econometric artifact due to the considerable amount of heterogeneity in the way our respondents reacted to the price per square meter seen in the questionnaire. Random utility model (1) –our broadest model– accommodates for this possibility. The results, reported in panel (B) of table 11, confirm our suspicions.

Variable	Specification A		Specification B	
	coefficient	T statistic	coefficient	T statistic
Smarta	1.5719	6.42	1.3992	1.68
Arsgrande	1.0424	5.14	0.5516	0.68
Arsbacini	0.6074	3.07	0.4491	0.55
Accesso	0.1598	1.19	0.1609	1.18
Uso	0.7595	6.63	0.7751	6.73
Restauro	-0.0236	-0.19	0.000609	0.00
Proprieta	-0.4839	-4.00	-0.4787	-3.94
Costo	-0.000192	-4.20	-0.00063	-0.48
Costosmarta			0.000396	0.3
Costobacini			0.000377	0.29
Costogrande			0.000548	0.42
Log likelihood	513.90		-512.48	

Tab 12 – Conditional logit model. Nobs=823.

As before, projects at S. Marta are chosen more frequently than projects at the other locales, although this effect is statistically significant only at the 10% level. The coefficients of the two Arsenale locations are positive but insignificant, suggesting that these locales are only weakly preferred to or regarded just as desirable as an investment at another location. It should be noted that the coefficients on all location dummies are now smaller in magnitude and statistically weaker than before.

As before, improving access does not appreciably change the attractiveness of an alternative and neither does relaxing conservation restoration restrictions, while the coefficients on allowable land use and property v. lease regime retain their magnitudes and statistical significance levels.

Variable COSTO now captures the cost for the “elsewhere” alternative. Clearly,

its coefficient is much larger than in specification (A). The coefficient on the price per square at S. Marta is $(-0.00063+0.000396)=-0.00023$, that on the price per square at the Arsenale Grande is $(-0.00063+0.000377)=-0.00025$, and that on the price per square at the Arsenale Bacini is $(-0.00063+0.000548)=-0.000079$. While not statistically significant, these coefficients suggest an interesting story: That our respondents are quite responsive to price in general, but much less so at S. Marta and the Arsenale Darsena Grande, and completely insensitive to price per square meter at the Arsenale Bacini, which is the least attractive location.

For a typical parcel for commercial use not in Venice (and so easily accessible and subject to the usual property regime), our developers are willing to pay €1493 per square meter, which seems reasonable. Even under the least attractive clauses (lease, light industrial use), for S. Marta our developers would be willing to pay €4691 per square meter—again a figure that exceeds those shown to the respondents in the conjoint choice exercises. These figures, however, should be interpreted with caution, because in specification B the coefficients on price are not individually statistically significant at the conventional levels.

Conclusions

We have used conjoint choice questions to explore the preferences of real estate developers and investors for projects in Venice involving the reuse of abandoned or underused areas. We found that, when forced to choose among locations in Venice, our respondents were relatively insensitive to price, especially at the most remote location (the Venice Bacini, which is difficult to access and is partially used for shipbuilding purposes). We also found that the presence of conservation restrictions is not important.

This raises doubts about the concerns sometimes expressed by city officials and observers, who fear that conservation restrictions may have a deterrent effect on non-local investors. By contrast, respondents tended to avoid alternatives slated for light industrial use, and cared about having full property, rather than mere leases. These results are consistent with the opinions about the importance of certain aspects of an investment project reported by the respondent in another section of the questionnaire.

The questionnaire inquired extensively about the reasons that make Venice (the city and its hinterland, examined separately) an attractive or unattractive location for business, finding that, as one would expect, its feature as a tourist destination is attractive to some developers and unattractive for others.

Potential for appreciation, access to and transparency of the real estate market, and fit of local conditions with the company business specialization and practice were often-cited measures for considering Venice an attractive or an unattractive location.

Presumably, the possibility to consider Venice more or less attractive as investment location depends on the familiarity of the developer with the tourist

infrastructure. This confirms the tendency to the specialization of the investments in this field and, therefore, also of the consequent economic activities.

Finally, the results of the survey are useful to inform policymakers about policy options that would attract private investors and developers to the Arsenale, the most problematic of the three locations studied here due to its historical and architectural value, difficult access, and the fact that it is owned by the Italian government. Clearly, there is divergence between what public officials would like and what developers find interesting and attractive. The survey results clearly show that developers and investors are not interested in artisanal activities at the Arsenale—the use suggested in the current plans of the Administration—and that neither favorable financial circumstances nor improved access are sufficient to arouse interest under that allowed land use. Likewise, leases are judged to be very unattractive. In sum, leases combined with light-industrial/artisanal activities use are not sufficiently profitable for the size of the investment required.

Commercial and residential use is more attractive, although we only explore the former in our conjoint choice experiments. If these uses are not allowed, investors and developers are unlikely to undertake redevelopment projects at the Arsenale. We would therefore recommend flexibility about land use and willingness to negotiate on it with individual developers. The specific characteristics of the Arsenale and the fact that there are few potential developers interested in it suggest that excessively restrictive land use ordinances are likely to discourage its redevelopment.

The opportunity to negotiate with developers the details of the restoration project and allowed land use also influences the choice of the institutional framework for the realization of this bargaining. The need for both flexibility and certainty in the permitting schedule suggests that the best policy tools are what Stellin and Zoboli (2006) term “strumenti operative,” such as Program Agreements (It. Law 142/1990), Public-Private Partnerships (It. Law 127/1997) and Project Financing (Laws 415/1998 and 144/1999) (see Stellin and Zoboli, 2006 for details).

Only the latter lend themselves to precise agreements between the public administration and developers by offering developers some guarantee about the time required to process applications and receive permits, which many of the developers in our survey judged to be one of the most important factors in their investment decisions. We wish to remind the reader, however, that these are initial suggestions stemming from the results of our survey, which is based on a relatively small sample, and that more research is needed for more definitive findings and recommendations.

References

Alberini, Anna (2007), “Determinants and Effects on Property Values of Participation in Voluntary Cleanup Programs: The Case of Colorado,”

Contemporary Economic Policy.

Alberini, Anna, Alberto Longo and Patrizia Riganti (2006), "Using Surveys to Compare the Public's and Decisionmakers' Preferences for Urban Regeneration: The Venice Arsenale," FEEM working paper 137.07, Milan, Italy, November.

Alberini, Anna, Alberto Longo and Marcella Veronesi (2007), "Basic Statistical Models for Conjoint Choice Experiments," in *Valuing Environmental Amenities using Choice Experiments: A Common Sense Guide to Theory and Practice*, Barbara Kanninen (ed.), Darmstadt, Germany: Springer.

Anna Alberini, Alberto Longo, Stefania Tonin, Francesco Trombetta and Margherita Turvani, (2005), "The Role of Liability, Regulation and Economic Incentives in Brownfield Remediation and Redevelopment: Evidence from Surveys of Developers," *Regional Science and Urban Economics*, 35, 327-351.

Bartsch, Charles, E. Collaton, and E. Pepper (1996), *Coming clean for economic development: A resource book on environmental cleanup and economic development opportunities*, Washington, DC: Northeast-Midwest Institute.

Bartik, T. J. (1991). *Who benefits from state and local economic development policies?* Kalamazoo, MI: W. E. Upjohn Institute for Employment.

Bartik, T. J. (2004). *Evaluating the impacts of local economic development policies on local economic outcomes: What has been done and what is doable?* In *Evaluating local economic and employment development: How to assess what works among programmes and policies* (pp. 113-141). Paris: OECD.

DeShazo, J.R. (2002), "Designing Transactions without Framing Effects in Iterative Question Formats," *Journal of Environmental Economics and Management*, 43, 360-85.

DeSousa, C. (2004), "The Greening of Brownfields in American Cities," *Journal of Environmental Planning and Management*, 47(4), 579-600.

Fisher, P., and A. Peters (1998), *Industrial Incentives: Competition among American States and Cities*, Kalamazoo, MI: W.E. Upjohn Institute for Employment Research Press.

Fox, W. F., and M. N. Murray (2004), "Do Economic Effects Justify the Use of Fiscal Incentives?" *Southern Economic Journal*, 71(1), 78-92.

Greene, W.H. (2003), *Econometric Analysis*, 4th edition, Upper Saddle River, NY: Prentice Hall.

Greenstone, Michael and Enrico Moretti (2003), "Bidding for Industrial Plants: Does Winning a 'Million Dollar Plant' Increase Welfare?" NBER Working Paper No. 9844, Cambridge, MA.

Hanemann, W.M. (1984), "Welfare Evaluations in Contingent Valuation Experiments with Discrete Responses," *American Journal of Agricultural Economics*, 66(3), 332-41.

- Hanley, N., S. Mourato and R.E. Wright (2001), "Choice Modelling Approaches: A Superior Alternative for Environmental Valuation?" *Journal of Economic Surveys*, 15(3), 435-62.
- Howland, Marie (2000), "The Impact of Contamination on the Canton/Southeast Baltimore Land Market," *Journal of the American Planning Association*, 66(4), 411-420.
- Howland, Marie (2004), "The Role of Contamination in Central City Industrial Decline," *Economic Development Quarterly*, 18(3), 207-219.
- Krinsky, I. and A. Robb (1986), "Approximating the Statistical Properties of Elasticities," *Review of Economics and Statistics*, 68, 715-19.
- Lange, D., and S. McNeil (2004a), "Brownfield Development: Tools for Stewardship," *Journal of Urban Planning and Development*, 130(2), 109-116.
- Lange, D., and S. McNeil (2004b), "Clean It and They Will Come? Defining Successful Brownfield Development," *Journal of Urban Planning and Development*, 130(2), 101-108.
- Magat, W.A. and W.K. Viscusi (1992), *Informational Approaches to Regulation*, Cambridge: MIT Press.
- McFadden, D.L. (1974), "Conditional Logit Analysis of Qualitative Choice Analysis," in *Frontiers in Econometrics*, ed. P. Zarembka. New York: Academic Press, 105-42.
- Meyer, Bruce D. (1996), "Natural and Quasi-Experiments in Econometrics," *Journal of Business and Economic Statistics*, 13(2), 151-161.
- Meyer, P. B., and T.S. Lyons (2000), "Lessons from Private Sector Brownfield Redevelopers: Planning Public Support for Urban Regeneration," *Journal of the American Planning Association*, 66(1), 46-57.
- Mitchell, R.C. and R.T. Carson (1989), *Using Surveys to Value Public Goods: The Contingent Valuation Method* (Washington, DC: Resources for the Future).
- Newman, R. J., and D. Sullivan (1988), "Econometric Analysis of Business Tax Impacts on Industrial Location: What Do We Know and How Do We Know It?" *Journal of Urban Economics*, 23(2), 215-234.
- Peters, A., and P. Fisher (2002), *State Enterprise Zone Programs: Have They Worked?* Kalamazoo, MI: W.E. Upjohn Institute for Employment Research Press.
- Peters, A., and P. Fisher (2004), "The Failure of Economic Development Incentives," *Journal of the American Planning Association*, 70(1), 27-37.
- Sementelli, A. J. and R. A. Simons (1997), "Regulation of Leaking Underground Storage Tanks: Policy Enforcement and Unintended Consequences," *Economic Development Quarterly*, 11(3), 236-48.
- Stellin, Giuseppe and Giorgia Zoboli (2006), "Le Politiche di Sostegno in Interventi di Riuso di Aree Dismess: Il Caso dell'Arsenale di Venezia,"

unpublished paper, Fondazione Eni Enrico Mattei, Venice, December.

Train, K.E. (1999), "Mixed Logit Models for Recreation Demand," Chapter 4 in Joseph A. Herriges and Catherine L. Kling (eds.), Valuing Recreation and the Environment. Revealed Preference Methods in Theory and Practice, Cheltenham, UK: Edward Elgar Publishing.

Train, K.E. (2003), Discrete Choice Models with Simulations, Cambridge: Cambridge University Press.

Wasylenko, M. (1997). "Taxation and Economic Development: The State of the Economic Literature," New England Economic Review, March/April, 37-52.

Wernstedt, Kris, Peter Meyer, and Anna Alberini (2006), "Attracting Private Investment to Contaminated Properties: The Value of Public Interventions," Journal of Policy Analysis and Management, 25(2), 347-369.

Wooldridge, J. (2002), Econometrics Analysis of Cross Section and Panel Data, Cambridge, MA: MIT Press.

Appendix

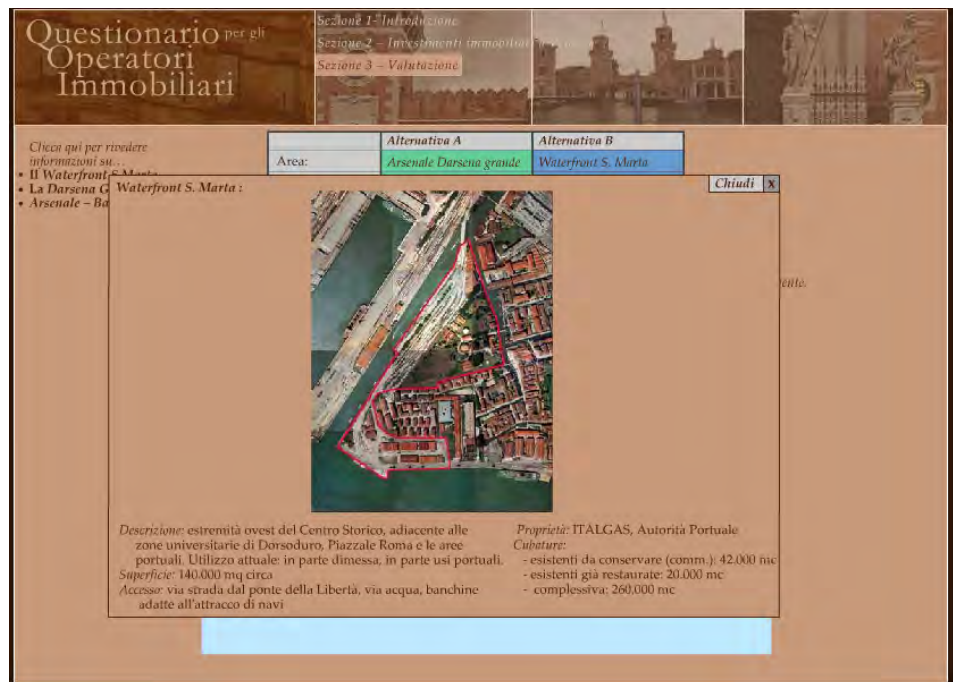


Fig A.1 – Example of Choice between two Venice alternatives.



Fig A.2 – Example of Choice between a Venice and a non-Venice alternative.

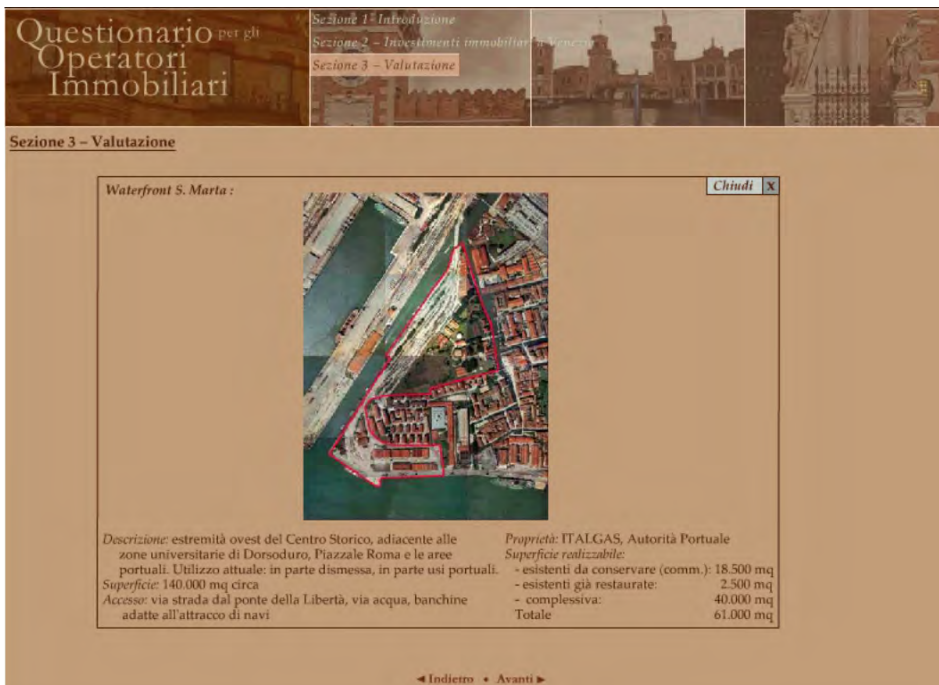


Fig A.3 – Description of Venice investment sites: S. Marta.

Questionario per gli Operatori Immobiliari

Sezione 1 - Introduzione
Sezione 2 - Investimenti immobiliari
Sezione 3 - Valutazione

Clicca qui per rivedere informazioni su:
 • Il Waterfront S. Maria
 • La Darsena Grande
 • Arsenale - Bacini

	Alternativa A	Alternativa B
Area:	Arsenale Darsena grande	Waterfront S. Maria

Chiudi X

Arsenale Darsena Grande:

Descrizione: Lati nord e sud del bacino grande nell'Arsenale storico
 Superficie: 81.000 mq
 Accesso: accesso pedonale diretto dal quartiere di Castello, accesso via acqua, banchine adatte all'attracco di navi.

Proprietà: Comune di Venezia/Agenzia del Demanio
 Cubature:
 - esistenti da conservare: 335.000 mc
 - non è concessa nuova costruzione

Fig A.4 – Description of Venice investment sites: Arsenale Darsena Grande.

Questionario per gli Operatori Immobiliari

Sezione 1 - Introduzione
Sezione 2 - Investimenti immobiliari
Sezione 3 - Valutazione

Clicca qui per rivedere informazioni su:
 • Il Waterfront S. Maria
 • La Darsena Grande
 • Arsenale - Bacini

	Alternativa A	Alternativa B
Area:	Arsenale Darsena grande	Waterfront S. Maria

Chiudi X

Arsenale Area bacini:

Descrizione: nord-est Arsenale. Uso attuale: manutenzione di navi, dispone di tre bacini di carenaggio.
 Superficie: 164.000 mq
 Accesso: accesso pedonale dal quartiere di Castello, accesso via acqua, banchina adatta all'attracco di navi.

Proprietà: Comune di Venezia/Agenzia del Demanio
 Cubature:
 - esistenti da conservare: 262.000 mc
 - nuova costruzione: 255.000 mc
 - complessivo: 517.000 mc

Fig A.5 – Description of Venice investment sites: Arsenale Bacini.

AREA 2

Architecture and Cultural Heritage

RESEARCH LINE 2.3

Methodologies and technologies for conservation and restoration of historical Venetian building

THE PROTOTYPE OF THE INFORMATION SYSTEM FOR DIAGNOSTIC OF VENETIAN BUILDING (SIDEV)

Luca Marescotti¹, Stefano Maffulli², Maria Mascione¹

1. Dipartimento BEST, Politecnico di Milano. 2. Libero professionista

Riassunto

Il prototipo del Sistema Informativo per la Diagnostica dell'Edilizia Veneziana è un'applicazione webmap che permette ai gruppi di ricerca l'inserimento dei dati delle proprie attività secondo un'architettura distribuita client-server. Le funzionalità del sistema derivano dall'analisi dei requisiti e delle interazioni tra utenti e sistema: interessano principalmente l'inserimento dati, la consultazione e la ricerca. Il SIDEV utilizza basi cartografiche provenienti da CORILA, che invece di essere duplicate, corrette, o modificate, sono state arricchite di tematismi derivanti dalle attività di ricerca.

L'esperienza del SIDEV ha evidenziato l'importanza del progetto concettuale e dell'analisi dei requisiti come fasi strategiche nella progettazione e nello sviluppo del sistema. Fasi che devono essere condivise tra tutti i gruppi di lavoro, produttori di dati e progettisti del sistema. Le potenzialità del sistema come supporto alle analisi pre-intervento sull'edilizia veneziana riguardano principalmente: il riconoscimento di SIDEV come base comune dei gruppi di lavoro, la crescita di SIDEV attraverso l'incremento del database e la definizione di nuovi criteri di ricerca, il potenziamento di SIDEV attraverso la verifica della sua efficacia nelle analisi pre-intervento e di diagnostica.

Abstract

The SIDEV (Sistema Informativo per la Diagnostica dell'Edilizia Veneziana) prototype is a diagnostic information system for Venetian buildings. It is a webmap application that allows research groups to contribute data from their studies using client-server architecture. Information system functionalities derive both from extensive analysis of the requirements of end users together with system analysts. Main functions are data entry, data retrieval search and presentation. The SIDEV uses CORILA's cartography, that instead of being duplicated, corrected, or modified, are served via standard OGC services to elaborate thematic maps, derived from research activities.

SIDEV's experience has underlined the importance of the conceptual project and of requirements analysis as strategic phases in system planning and implementation. These phases must be shared between: research groups, surveyors and data providers and system designers. The SIDEV information system is a support system for pre-intervention analysis Venetian buildings. Its potentialities can be fully expressed once it becomes a common base for all

research groups. Only then the size of the data collected will allow the definition of new tools for extensive analysis and retrieval and SIDEV will express its effectiveness for evaluation and diagnostic in the pre-intervention analyses.

1 Introduction

The working group WP5 has been responsible for developing information system SIDEV prototype application (Information System for Diagnostic Of Venetian Buildings), designing and implementing a support tool for the research project to help research groups sharing knowledge. The application domain is architecture and territory preservation.

2 System design

SIDEV's prototype application is made of a tool for data entry and retrieval of data gathered from on-field inspections of buildings, including photographs, quantitative and qualitative data. SIDEV's webmap application presents this data geographically, importing information from other sources. The prototype implementation is the result of the analysis of requirements, raw data and interactions between the system and its users. The products of this phases has been the UML model of the information system, formalized in use cases and classes diagram.

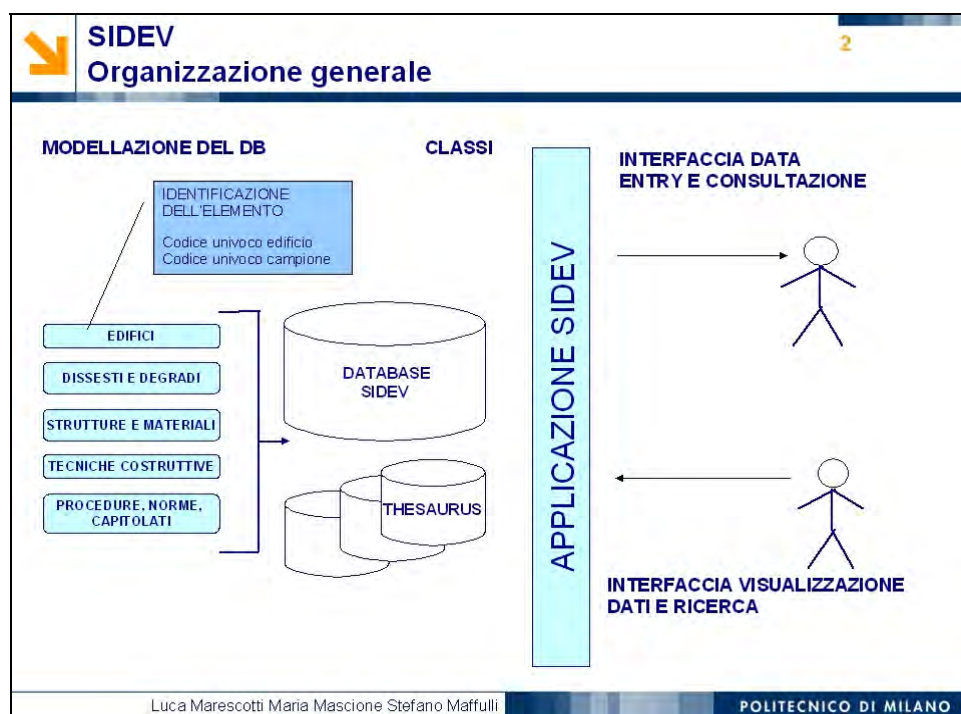


Fig 1 – SIDEV, general scheme.

2.1 Data sets

The database stores in entity/relations schema data about buildings; constructive techniques; structures and materials; damage and mechanisms of damage, phenomena of deterioration; geometric and photogrammetric survey; rules of procedures, norms and specifications. The database allows for the necessary generalizations for rational analysis of data. To improve

interoperability of information, all the elements that describe the buildings, like constructions techniques or styles, are stored in separate multidisciplinary thesaurus shared between all work groups. This approach allows for multidisciplinary exchange of information and increases the usefulness of the system (Fig. 1).

2.2 Requirements

Functional requirements concern two areas: data entry and retrieval. The interactions have been identified working together with research groups on the field, looking at the recording material used. Mainly these are based on paper, photos and on sets of classification terms. A lot of work has been done to simplify and homogenize such classifications between workgroups. Most of the differences existed in the terms used by groups dealing with modern architecture and those studying historical buildings. The guideline has always been not to duplicate any information already available and use open standard based solution to increase systems interoperability. The requirements have been prioritized and translated into functionalities of the prototype in agreement with the working groups.

2.3 System architecture

The system's architecture is distributed, client-server architecture, based on open standards. The overall design takes into account that working groups were distributed in different cities (Fig. 2). Its open architecture allows also for incremental addition of information from results of later investigations, making it possible for the information to grow over time.

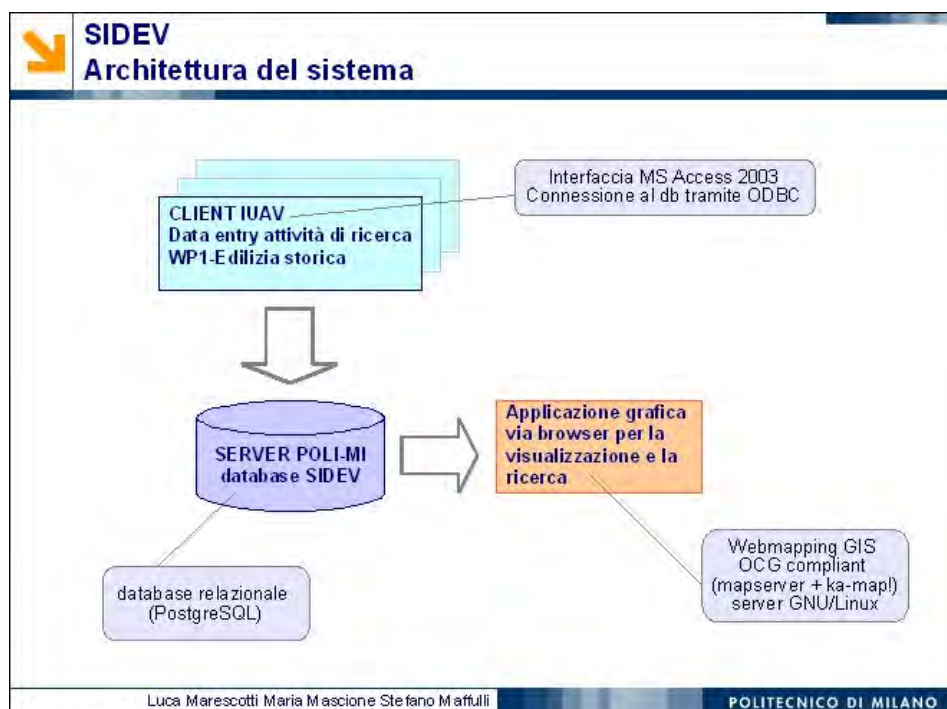


Fig 2 – System architecture.

3 Functionalities

3.1 Data entry interface

Custom user interfaces have been developed using MS Access to allow researchers of the work groups (Fig. 3). The classes diagram has been implemented on top of the open source object-relational database PostgreSQL with spatial extension PostGIS. The choice to use MS Access was due to the rapid interfaces prototyping and its convenience while the open source client/server architecture allows the development of the solid base necessary to build on top for future research. Data stored on PostgreSQL can be easily moved to the Oracle backend used by CORILA, should the need arise.

Fig 3 – Data-entry form.

The close collaboration with work group 1-Historic building has allowed to validate the graphic interfaces, both that concern data entry and online retrieval.

3.2 Data display interface

Geographical display interface has developed based on use cases written in collaboration with all other working groups. The solution is based on the open source webmapping framework ka-map, which sits on top of well known open source mapserver. The data system are displayed according to specified themes that the user can activate autonomously:

Context and relationship

- Presence of canal
- Context relationship
- Location

- Number of floors

Constructional parameters

- Presence of deflection toward inside
- Corner's morphology
- Resistent elements
- Presence of alтинelle
- Characteristic of the base portion
- Type of wall-plug

Structural instabilities

- Mechanisms that's operate out of plan
- Mechanisms that's operate into within the plan
- Combined mechanisms
- Specific mechanisms

Legend description is taken from thesaurus.

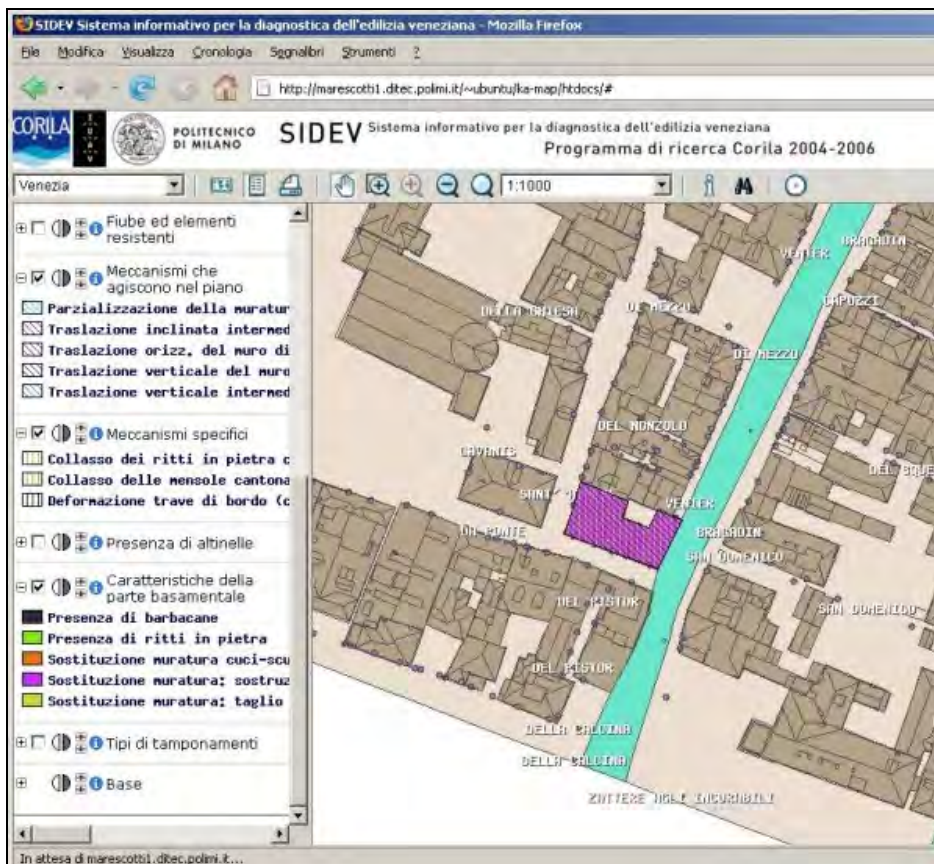


Fig 4 – Screen shot from webmap application.

3.3 Search rules

The system, allows to identify zones or specified buildings through alphanumeric

and graphical research criteria:

- 1 using an Ajax based form entering sestiere/district and civic number, or rio and island;
- 2 visually through "point and click" on the map zoom and pan.

3.4 Enclosed documentation

All binary data about the building, like photographs or laboratory tests, are stored in the database as binary blobs.

4 Hardware e software characteristics

The spatial database is the PostgreSQL server with the spatial extension PostGIS, running on MS Windows operating system.

The geometries of venitian buildings could not be loaded from an OGC compliant map server, so mapinfo files had to be loaded into the spatial database SIDEV.MIF: *civici.mif*, *edifici.mif*, *tetti.mif*, *isole.mif*, *toponimi.mif*, *toponimicanali.mif*. The spatial corresponding tables are *sp_civici*, *sp_edifici*, *sp_tetti*, *sp_isole*, *sp_toponimi*, *sp_toponimicanali*.

The interface for data entry and buildings case study retrieval is a MS Access 2003 application. A control panel allows the thesaurus update, the retrieval and data entry. The connection with it is realized through an ODBC driver. The security and the accesses control is managed on the ODBC connection: only qualified users can access the server database through MS Access application.

Webmap application has been realized through the Open Source mapserver, on GNU/Linux server.

Graphic application through browser has been developed on the Open Source framework ka-map!.

5 Interoperability and standard

While developing SIDEV it was necessary to reach interoperability on two levels: on one side there was the technical transport level, to move information from different CORILA systems and to the wider public. On the other side there was the need to develop semantic agreements between different research groups of the Architecture and cultural asset group.

Interoperability for transport of information allows access to data from CORILA research to different applications using existing standards developed by international groups like the Open Geospatial Consortium (OGC), World Wide Web Consortium (W3C) or International Organization of Standardization (ISO).

SIDEV is based on the concept of reuse of available information, avoiding duplications. Cartographic layers can be imported from sources like feature servers and map server using OGC web services.

Since RIVELA database is not yet capable of serving web maps, it was necessary to load geographic layers in the PostgreSQL database from Mapinfo

files. This doesn't preclude the possibility to add to the SIDEV prototype layers from other OGC sources.

It wasn't as simple to define an internal standard for the working groups for the semantic of information. Thesaurus were necessary and a long work of coordination was activated to allow multidisciplinary approach to work. Without the agreement on semantics and simplification of thesaurus it would be impossible to extrapolate meaningful information from the data entered by the research groups.

Conclusions

The SIDEV's experience has to pointed out the importance of conceptual project and requirement analysis as strategic phases in design and development of the system. Phases, that must be certainly shared between data providers and future users of the system, that depend from specific skills dedicated at design system. The achieved result allows to identify clearly the development prospects, which can develop in three directions:

- The first concerns the growth of the system through the database enriching and the definition of new criterias that allow analysis much more in-depth, as well as extension of the system in integration with CORILA systems.
- The second concerns the system use that depends from SIDEV recognition as common base of the work groups and accessibility informations.
- The third direction concerns the strengthening of SIDEV effectiveness reachable through the comparative review of the information, the verification of its usefulness for analysis before execution and diagnostic analysis, and the archival of the restoration work done to evaluate their effectiveness.

The cultural presuppositions of these development directions are researchs integration, the coherence of work groups, the interdisciplinary knowledge, and building an "operative and control room" for the built ecosystem, of wich CORILA can become a focal coordinator. The results concern the possibility of transfer of experience to other fields, where various work groups are involved with different heterogeneous background, but whose works must integrate themselves to provide a common development of knowledges.

References

Marescotti L., Mascione M., Maffulli S., 2007. SIDEV: towards a service based architecture, in *Scientific Research and Safeguarding of Venice-CORILA Research Programme 2004-2006*, Venezia, CORILA, 147-152.

Maffulli S., Mascione M., 2006. Il sistema informativo per la diagnostica dell'edilizia veneziana, in M. Salvemini, P. Di Donato (a cura di), *Conferenza*

Tematica AMFM2006 Informazione Geografica: Data Harmonisation, Interoperabilità e Standard, Reti e Facilities Management, Ubiquitous GIS, (atti della conferenza, Roma 21-22 settembre 2006), Roma, 207-212.

Marescotti L., Mascione M., Maffulli S., 2006. Venetian building diagnostic system, in *Scientific Research and Safeguarding of Venice-CORILA Research Programme 2004-2006*, Venezia, CORILA, 135-145.

Documentation about SIDEV's design and development

Marescotti L., Maffulli S., Mascione M., 2007. SIDEV – Sistema informativo per la diagnostica dell'edilizia veneziana: rapporto finale.

Maffulli S., Mascione M., 2006. Modello UML del Sistema Informativo per la Diagnostica dell'Edilizia Veneziana: specifiche dei requisiti.

Marescotti L., Maffulli S., Mascione M., 2005. Modello UML del Sistema Informativo per la Diagnostica dell'Edilizia Veneziana.

Mascione M., 2005. WP2.2 Degradi e dissesti edifici moderni/sezione B-componente: analisi scheda.

Mascione M., Maffulli S., 2005. WP2.2 Degradi e dissesti edifici moderni/sezione A-edificio:analisi dei dati usati per la schedatura.

Mascione M., 2005. WP1.2 -Edilizia storica: analisi dei dati usati per la schedatura.

Marescotti L., Maffulli S., Mascione M., 2004. WP 5 Sistema informativo per la diagnostica dell'edilizia veneziana. Analisi dei materiali e individuazione utenti e gruppi dati. Analisi dei requisiti del sistema informativo.

SIDEV: design and development credits

Data cataloguing: IUAV, DSA.

Design and development: Politecnico di Milano, BEST.

Webmap development: Ominiverdi.org.

Development software: Linux/Windows xp; ka-Map!; Mapserver; PostgreSQL; Postgis; Apache Php.

The prototype SIDEV is available on

<http://marescotti1.ditec.polimi.it/~ubuntu/ka-map/htdocs/>

MDDS – VENICE: TRY OUT AND IMPROVEMENTS OF THE EXPERT SYSTEM

Rob P.J. van Hees^{1,3}, Silvia Naldini^{2,3}, Ilse A.E. de Vent³, Francesco Trovò⁴

¹ TNO Built Environment and Geosciences, Delft, The Netherlands ² Silvia Naldini
Advice, Zoetermeer, The Netherlands ³ Delft University of Technology, The Netherlands
⁴ DSA – IUAV, S. Polo 2468 Venezia

Riassunto

MDDS (Masonry Damage Diagnostic System), il sistema esperto del TNO, è stato utilizzato con profitto, durante in progetto CORILA, per la diagnosi di forme di degrado non strutturale presenti in monumenti veneziani. Per poter ottenere una diagnosi del danno di origine strutturale è stato creato un 'Atlante del Danno Strutturale a Venezia', facendo riferimento ai risultati di casi – studio. I più rilevanti tipi di degrado sono stati definiti e illustrati al fine di creare uno strumento valido per fare una diagnosi basata su un'indagine visiva. Un nuovo progetto sul danno strutturale consentirebbe un ulteriore sviluppo dell'Atlante e del sistema.

Abstract

TNO's expert system MDDS (Monument Damage Diagnostic System) was successfully employed during the CORILA project to diagnose non structural damage types found in Venetian buildings. To reach a diagnosis in case of structural damage a 'Venice Structural Damage Atlas' was created, taking into account the results of case studies. The most relevant types were defined and illustrated aiming at creating a valid instrument to make a diagnosis on the basis of a visual inspection. It would be profitable to start a new project focused on structural damage and aiming at further developing the Atlas and the system.

1 Introduction

TNO's task in the CORILA project [Scientific Research and Safeguarding of Venice – CORILA Research programme 2004-2006, Venice] was to verify whether TNO's expert system MDDS (Monument Damage Diagnostic System) [Balén, et al., 1999] could be used to identify and diagnose the damage found in Venetian buildings. The system was tried out and proved to meet the needs of the users and to be suitable for the diagnosis of most forms of recurrent damage, like salt damage. For what concerns structural damage, more work needed to be done to the system to enhance its performance and make it a valid instrument to be used in the conservation of monuments in Venice. A 'Venice Structural Damage Atlas' containing significant examples of structural damage and based on case studies locally carried out was developed and inserted in MDDS. Therefore, the Atlas does not contain a complete overview of structural damage types: its aim is to meet the needs of the users in Venice. A

more comprehensive Atlas has been worked out in the meantime for MDDS.

The newest version of MDDS will be officially handed over to the representatives of CORILA and, on that occasion, a workshop on MDDS will be given.

MDDS, the Monument Damage Diagnostic System, is meant to guide the user in the process leading to the identification and the diagnosis of the damage to monumental buildings. Only on the basis of a sound and well supported diagnosis, in fact, the necessary interventions can be planned.

MDDS is both an expert system and a 'decision supporting tool'.

An expert system for diagnosing cases of damage, will ask the user questions, and achieve its goal on the basis of the provided information, by means of deductions and inference procedures. The damage will be associated to one or more damaging processes within a certain context.

A 'decision support tool' is not only meant to lead the user to the diagnosis, step by step, by means of questions and answers, but also to provide the user with the necessary, practical information to formulate himself a sound diagnosis.

In order to make a diagnosis, the user needs to obtain specific data, e.g. by visual inspection or by means of laboratory tests or measurements, and to insert them into the system.

MDDS is a very flexible system, meant to meet the needs of different users (from restoration architects to university students or Monument Watch). In the course of time it has been constantly updated with the knowledge derived from research, experts, and EU projects. Information is structured to be practice-oriented and easily retrievable.

2 The try out of MDDS in Venice

The information of cases of damage to Venetian buildings deriving from studies carried out within the CORILA project was elaborated at TNO (Delft, Netherlands) and inserted in the system. Five case studies concerning salt crystallisation problems were successfully carried out (see report on Ex Scuola dei Calegheri building, fig. 1). Notwithstanding the absence of important data on salt and moisture, the diagnosis was reached, on the basis on known facts, like the presence of rising damp and salt (sources: ground, flooding etc.). Still, it should be stressed that data on salt and moisture type and distribution should be gained in order to complete the investigation and provide it with a scientific basis.

<p>Report on: Scuola dei Calegheri</p> <p>General information</p> <p>Building address : San polo 2857 Building owner : Municipality Inspector : Silvia, Francesco Inspection date: 6 Jul 2006</p>	
<p>Description (inspector)</p> <p>Building dating half XV cent.. Brick masonry, Gothic bricks, called "cobotoni" (29x7x15 ca.). Important to underline the fact that the building is homogenous and all materials (brick and mortars) date back to time of construction. Corners furnished by Istria stone. Same portals, frames and Madonna. Facade in very good condition. Damage present on SW wall.</p> 	<p>Observations on damage (inspector)</p> <p>Analyses should be carried out to objectively find out more about the salt and moisture content and distribution. Re-pointing is necessary to avoid ingress of rain water, further stimulating damage. Rising damp is most probably present and should be handled.</p> <p>Advice (inspector)</p> <p>The materials being original should be preserved at all costs, the pointing and (part of) the bedding mortar should be substituted with compatible ones (salts present in the masonry and type of brick). The difficulty is the thickness of the joints and the depth of the material loss. To be avoided is the succeeding material spreading on the brick (damaged) surface. The pointing should rather be recessed. Mechanically hindering rising damp could generate further severe problems and its possibility of success should be carefully evaluated.</p>
<p>Inspected wall : SW wall</p> <p>Properties: width : 800 cm height : 300 cm thickness: 40 cm</p> <p>Description (inspector)</p> <p>The decay is due to salt damaging processes. Rising damp occurs in the lower part and carries salts. Salts will probably reach the wall also in the form of air spray.</p> 	<p>Parts:</p> <p>brick: Gothic bricks</p>  <p>bedding mortar: mortar pointing: pointing</p> <p>Description (inspector)</p> <p>Sanding of the pointing is sure, whereas we do not know whether also push out occurs. This should be checked on the spot.</p> <p>Damage areas:</p> <p>lower part: left 0 cm, bottom 0 cm, right 800 cm, top 200 cm</p> <p>Description</p> <p>this part of the wall shows the most severe efflorescence and powdering. The damage is spreading all over the wall (5) though.</p> <p>Observed damage: Gothic bricks: Efflorescence (moderate), powdering (moderate-to-severe) pointing: "Push out" (severe), Sanding (moderate-to-severe)</p> <p>Diagnosis:</p> <p>Diagnosis (system) Gothic bricks: salt crystallization (effloresc) pointing : frost (excluded), salt crystallization (effloresc), salt swelling (excessive)</p> <p>The described damage(s) may be due to:</p> <ul style="list-style-type: none"> • RH changes through the equilibrium RH of the salt present. • rising damp • seafooding in the past

Fig 1 – Report of MDDS on Ex Scuola dei Calegheri building.

All types of damage found in the cases could be defined referring to the Atlas contained in MDDS, including description and illustration of all types of damage to buildings, which can be distinguished in practice.

The background information section can be consulted by the CORILA members to carry out measurements and obtain some data, necessary and sufficient for a sound scientific evaluation of all made hypotheses. Such measurements are very little destructive and do not disturb the perception of the building.

Advice is also given by the system in terms of a reminder: methods to hinder rising damp, the most recurrent source of moisture, for instance, should be carefully evaluated and both the consequences and the expected effectiveness of a treatment very well thought of.

3 Data on moisture and salt types (L.A.M.A.- IUAV)

The assessment of several types of damage to buildings achieved with the support of MDDS (WP6) showed that salt damage - mostly involving rising damp - is the cause of very severe and dangerous damaging processes in Venice.

MDDS makes it possible to show - in the form of a graph - the presence and distribution of salt and moisture in walls, thus furnishing important evidence on the state of the masonry. On this basis, the parts of the building most prone to decay can be pointed out.

A try out of the method to obtain salt and moisture distribution profiles was done at Palazzo Pisani near to campo Santa Marina, in Cannaregio.

The building is dated to the XV cent. (1460) and was transformed in the XVII cent. It has two important facades on canals. In the brick masonry there are

replaced areas, in particular on the basement part of two walls on canal, in the chimney areas and near the portal. The bedding mortar is not homogeneous, due to replacements. The facade was furnished with an old plaster named "rigalzier" on small areas and a more recent (XIX cen.) plaster consisting of lime and sand.

A newly applied lime plaster is now present.



Fig 2 – Palazzo Pisani near campo Santa Marina, in Cannaregio.

In co-operation with L.A.M.A. – IUAV (Stefano Cancelliere) two profiles have been obtained by drilling powder at various heights (cm 20, cm 50, cm 100 e cm 180) and depths of the wall (cm 0 - 2, cm 2 - 5, cm 5 - 10, cm 10 - 15, cm 15 - 20 and 20 - 30). At some heights the masonry was hollow, and the drilling was performed again, near the location. The drilling itself shows much of the continuity of the masonry.

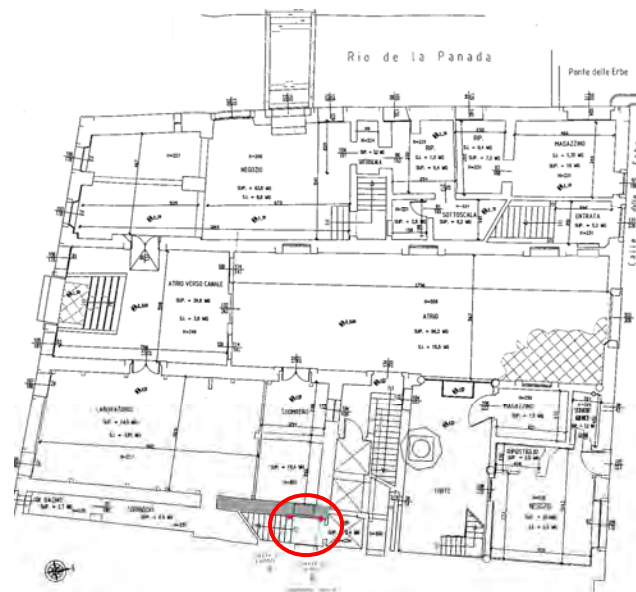


Fig 3 – Palazzo Pisani, plan of ground floor. The masonry where the drilling was done is highlighted. It was originally an external wall, ca. 60 cm thick. The wall became internal due to transformation of the palace when an adjacent building was made higher.



Fig 4 – Detail of masonry in which drilling was performed.

The samples are transported, hermetically closed in containers to the laboratory, where they are weighted, dried, and weighted again, to assess their actual moisture content.

The presence of salt is also gravimetrically assessed, deriving it from the hygroscopic moisture uptake of the sample due to the contained salt.

The analysis of the salts was carried out by means of ion chromatography, which is different from the method proposed in TNO's MDDS. In this way the type and amount of ions were determined.

Results

There is a very high moisture content with peaks which are difficult to explain (see tables). The pattern of the distribution of the moisture points at the presence of rising damp, but no final conclusion can be drawn because the upper fringe of the rising damp was not measured (being higher than 200 cm). At the surface, where evaporation occurs, there is a still very high moisture content, sometimes even higher than inside the wall.

This may be due to:

1. the presence of a newly applied plaster and also
2. differences in material properties (porosity and pore size distribution).

There is a lot of salt. The main types of salt present are chlorides, which is to explain as:

1. the building lies near the water
2. there are frequent floodings
3. the wall used to be external, and therefore directly exposed.

Further the context favours the presence of chlorides in the wall (sea-salt spray, ground water rich in salt and rising damp). Like in the case of the moisture

distribution, the pattern of salt distribution due to rising damp is not very clear. Chlorides, the most soluble salts, accumulate not only at the surface and in the upper part of the wall (evaporation area, rising damp pattern), but they are rather spread. The amount of salt present in the plaster is not as high as expected: this is due to the fact that this plaster has been very recently applied.

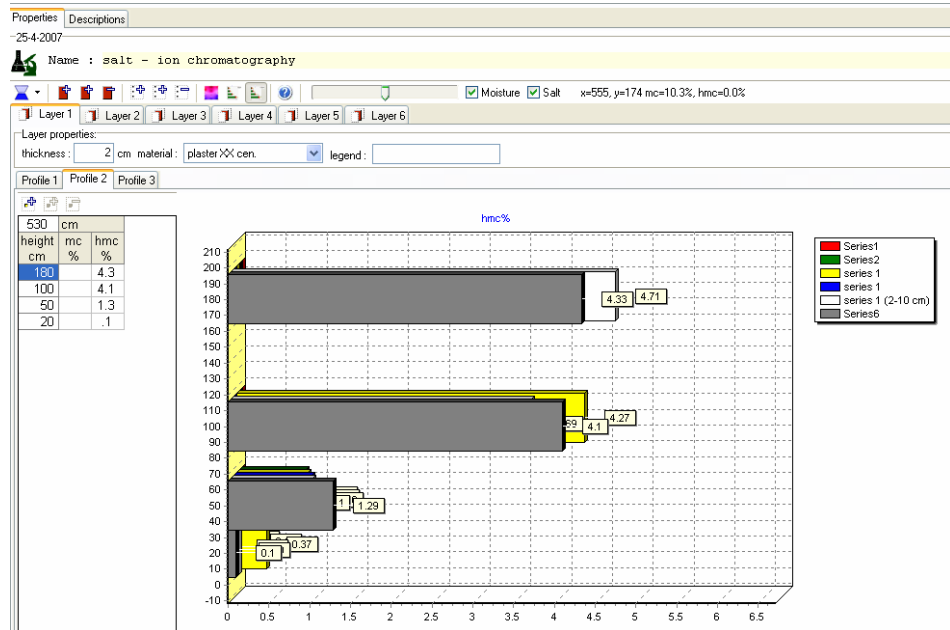


Fig 5 – Profile: 530 (salt).

4 The Venice Structural Damage Atlas

Originally created for brick masonry, MDDS has been further developed including stone and mortar problems, and has been constantly improved with updated scientific information. A sound information section on structural damage was worked upon when the Venice project begun. At that time structural problems were only tackled within an Atlas on Cracks. This Atlas included annotated examples of cracks, from micro cracks in single materials to long cracks running along the wall height. The cracks were described and illustrated using a method already employed for creating other atlases contained in MDDS. Damage Atlases on different problems had also been produced within various EU projects, as they had proven to furnish a good basis for focussing problems and to provide the partners with a common terminology [Naldini et al., 2003 and 2006, Van Hees et al., 2005].

Within the CORILA project a new Atlas on structural damage has been created, based on case studies carried out in Venice. Its aim is to identify and define cracks and deformation patterns [Doglioni, 2000], and to help the user recognise them *in situ*. The most recurrent types of structural damage have been defined and organized in categories and the possible causes leading to them have been pointed out. It should be underlined that most damage types result from a synergistic action of various forces and may easily include cracking and deformation patterns. Besides, some types of damage looking similar may have different causes, even non structural.

The Venice Structural Damage Atlas represents a practical way of facing the problems daily met in the conservation of local buildings. It allows to identify the damage and to lay a basis for planning an intervention, when needed.

The Atlas is now part of the 'Background information section' of the expert system MDDS (fig. 6).

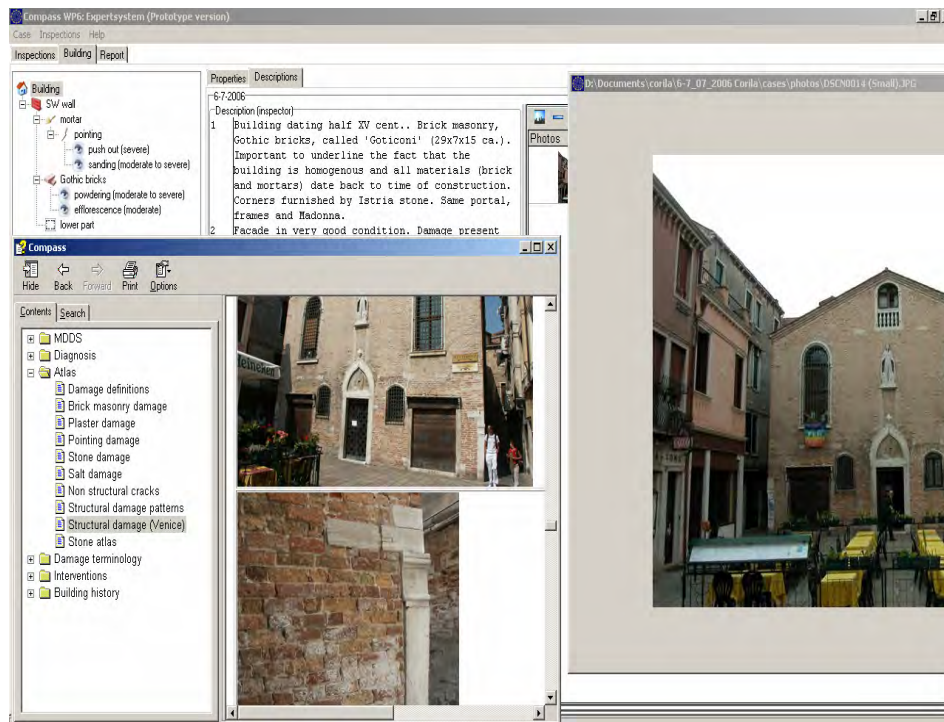


Fig 6 – Consultation of MDDS: the damage to a column in the monument is investigated referring to the Damage Atlas.

In the Atlas the damage types are organised in relation to the most relevant mechanism(s) causing them. All defined types are in fact *visually recognizable* patterns, because the first analysis and diagnosis on the cause of damage should be the result of a visual inspection. When needed, measurements and testing will be planned.

Some types of damage are the consequence of wrong restorations, whereas others are strictly related to the building techniques used in Venice.

It is advisable to carefully read the definitions of all damage types, in order to be aware of all differences and similarities (Tab. 1).

Tab. 1 – Types of damage and damaging mechanisms

VENICE STRUCTURAL DAMAGE ATLAS	
<p>Settlement</p> <p>Process: vertical displacement of a building due to changes (settlement) in the ground or in the foundations.</p>	<p>Overloading</p> <p>Process: the structure is more loaded than it can bear, due to its own weight or an external load.</p> <p>Creep</p> <p>Process: long term overloading, depending on the materials. The process concerns especially slender, high structures, like towers, columns and pillars.</p> <p>Cracks may develop very slowly, over decades or even centuries, but can eventually lead to sudden collapse, if the process is not stopped.</p>
Damage patterns	
<p>Arch-like pattern</p> <p>Parallel vertical cracks in the lowest zone of the façade</p> <p>Cracks running along one vertical line over the whole height</p> <p>Subsidence of a corner</p> <p>Leaning (e.g. of tower)</p>	<p>Cracking and detachment of a corner, starting from the base</p> <p>Displacement of part on columns/pillars</p> <p>Deformation of façade out of plane, e.g. at floor level</p> <p><i>Cracking Barbacane</i></p> <p>Top corner of façade cracks and detaches and /or deforms</p> <p>Vertical, parallel cracks in old area between new areas</p> <p>Creep</p> <p>Vertical, parallel cracks in a certain area of the construction</p>

Tab 1 – Types of damage and damaging mechanisms.

In the Atlas there are very clear patterns of damage, like the ‘arch-like pattern’ (fig. 7), well illustrated by a couple of examples and to be related to a settlement process. There are other types, still, like the ‘cracks running along one vertical line over the whole height’ (fig. 8), which characteristics can be less easily pointed out and translated into a pattern, especially if the origin of the damage should also be included.



Fig 7 – Arch type crack pattern: after appearance of damage, collapse of portion of wall underneath occurred. Building, rio di S. Barnaba, Dorsoduro.

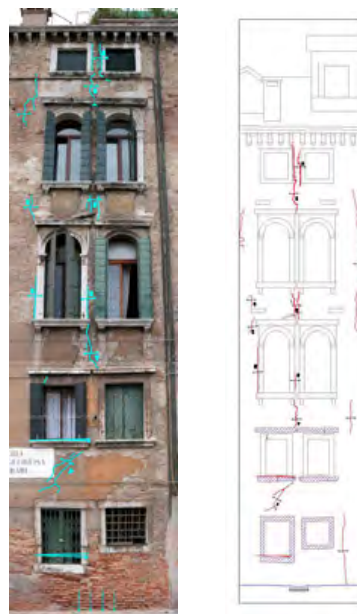


Fig 8 – Cracks running along one vertical line over the whole height. Building, Castelforte San Rocco, sestiere S. Polo 3105.

Conclusions

MDDS can be used for assessing the damage found in Venetian buildings and for planning interventions. The tried out method to obtain salt and moisture content and distribution in walls proved to be very useful.

The Structural Damage Atlas created for Venice aims at providing support in the identification of the most recurrent visible types of structural damage. It is also part of the expert system MDDS, which will be given to the representatives of the CORILA project. The use of MDDS for carrying out investigations will show whether the Atlas is developed enough or needs to be further broadened. It would be profitable to organize a new phase of the project centered on

structural damage.

References

Balen K. Van, Mateus J., Binda, L., Baronio, Hees R.P.J. van, Naldini S., Klugt L.van der, Franke L., 1999. *Expert System for the evaluation of the deterioration of ancient brick structures*, EU Environment Program, EV5V-CT92-0108, Research report No. 8. The system was completed re-structured during the EU project: 'Compatibility of plasters and renders with salt loaded substrates in historic buildings' (EVK-CT 2001-00047).

Doglionni F., 2000. Codice di pratica della Regione Marche, Ancona, Regione Marche.

Hees R.P.J. van, Naldini S. & Sanders M., *An expert system for analysis of damage to plasters due to salt and moisture*, in Proceedings Seminar 'Soluble salts in the walls of old buildings. Damages, processes and solutions', pp. 16.1-16.11, Lisbon, LNEC, 14-15 February 2005

Naldini S., Hees R.P.J. van, Lubelli B., Zezza F., Auger F., *Implementing an expert system in the study of sea salt damage*, 6th Int. Symp. On the Conservation of Monuments in the Mediterranean Basin, Sept. 2003.

Naldini S., Hees R.P.J. van, Nijland T. G., *Definitie van schade aan metselwerk*, PIM, II,4, aug. 2006, pp. 2-19.

A STRUCTURAL DAMAGE ATLAS FOR VENICE

Francesco Doglioni, Giulio Mirabella Roberti, Francesco Trovò, Michele Bondanelli,
Angela Squassina

DSA – IUAV, S. Polo 2468 Venezia

Riassunto

Le osservazioni sui fenomeni di dissesto degli edifici veneziani riconducibili alle caratteristiche costruttive loro proprie hanno consentito di mettere a punto una proposta di abaco di forme di dissesto, in cui vengono evidenziati i legami fra quadro fessurativo/deformativo e carattere/peculiarità costruttiva. Tale atlante costituisce un primo elemento di riferimento per la lettura e l'interpretazione delle diverse forme del dissesto.

In questo modo è emersa la possibilità di un collegamento fra carattere costruttivo e comportamento atteso, che pone nelle condizioni di poter ipotizzare, con una buona approssimazione, l'evoluzione futura del danneggiamento nei singoli casi. Una possibilità di sicuro interesse diagnostico ma che diviene particolarmente preziosa in ambito operativo, in considerazione della opportunità di calibrare le scelte di progetto alle effettive carenze strutturali dell'edificio di volta in volta esaminato.

Abstract

The structural damages observations in venetian buildings and their relationship to some peculiar construction features allowed to set up an atlas of the main forms of structural damage, in which the attention is focused on the link between the deformation or cracking pattern and the constructional characteristics of the buildings.

This atlas contains a synthesis of the whole DSA-IUAV activity and aims to act as a first reference for the comprehension of the different forms of structural damage.

1 Introduction

IUAV-DSA task in the CORILA project [Scientific Research and Safeguarding of Venice – CORILA Research programme 2004-2006, Venice] was to recognize the main links between civil building characters and their damage phenomena.

From the structural point of view, one of the main peculiarity of historical buildings in Venice is related to some particular constructive forms and to their specific ways of damaging. Therefore the first aim of the research has been to

understand the Venetian building conception and its behavior in the long run, by recognizing and describing the structural behaviour and more generally the building features, as well as the related forms of damage and material decay.¹

A systematic recognition campaign has been lead, first by means of a general survey, followed by a selection of samples, characterized by peculiar building arrangements or damage mechanisms that are meaningful in order to explain a particular structural behavior.

Although mainly based on single samples, the analysis was detailed enough to outline some of the most peculiar features of a “Venice way-of-building”, which main aspects were studied:

- constructional features and building components,
- the building structural conception,
- long run behavior: the ways and forms of damage.

2 Selected observations for the damage atlas

The study of Venice buildings structural damage phenomena² in the CORILA research was lead in order to identify the main damage appearances (cracking and deformations) on the different constructive components of the buildings, pointing out the connection, where existing, between type of damage and morphological appearance.

Several damage cases were observed and classified according to the main types of structural damage detected; then the data were entered in an Information System³, designed and set up in collaboration with the Department BEST of the Politecnico di Milano.

During the research some cases were selected for the interest they arouse as particular forms of damage patterns, described (causes, mechanisms, damage features) and arranged in an Atlas, that is briefly outlined in the followings.

The same cases were used as benchmark for testing the effectiveness of the TNO Expert System, MDDS (Monument Damage Diagnostic System)⁴, in

¹Dogliani F., Mirabella Roberti G., Bondanelli M., Trovò F., Detecting constructive patterns for structural damage interpretation of historic buildings in Venice, in *Scientific Research and Safeguarding of Venice – CORILA Research programme 2004-2006*, Volume IV – 2005 results, Venezia 2006, pp 115-133.

² The study of Venice bell towers is not a part of this work, although these buildings show some significant damage phenomena.

³ See the article in this book: Marescotti L., Maffulli S., Mascione M., “The prototype of the information system for diagnostic of venetian building (SIDEV)”.

⁴ The present version of the system was developed during the EU project: ‘Compatibility

detecting and making diagnosis of Venetian buildings damage⁵.

The definitions of the structural damage are based upon the MDDS – Venice Structural Damage Atlas.

The phenomena recorded in the Atlas are described on the intensity of the damage appearance (1) and arranged according to the main damage mechanisms which is responsible of the observed phenomena (2). The damage pattern and its location within the building should provide the user with a clue to make some hypotheses on its cause.

(1) The visual characteristics used to identify the damage pattern are:

- the form (shape) of the cracks and / or deformation or displacements distribution,
- the length and width of the cracks,
- the location of the damage in the building.

Beside the visual aspect of the damage, other elements should be taken into account:

- the evolution of the damage during time (e.g. whether crack are increasing in width or length, if collapses are to be expected),
- the construction techniques and the materials used in the construction process,
- repairs or conservation measures taken in the past.

The damage found must be investigated in order to observe if other types of damage are present, e.g. a crack and deformation. All visual information collected may be of help to make a sound hypothesis on the damage cause.

(2) These phenomena fall in the following topics:

Settlement: vertical displacement of a building due to changes (settlement) in the ground or in the foundations. Appearance:

of plasters and renders with salt loaded substrates in historic buildings' (EVK-CT 2001-00047). R.P.J. van Hees, S. Naldini & M. Sanders, *An expert system for analysis of damage to plasters due to salt and moisture*, in Proceedings Seminar 'Soluble salts in the walls of old buildings. Damages, processes and solutions', pp. 16.1-16.11, Lisbon, LNEC, 14-15 February 2005.

⁵ See the article in this book: Hees R.P.J. van, Naldini, S., de Vent, I., Trovò F., *MDDS – Venice: try-out and improvements of the expert system* and the "Venice Structural Damage Atlas" in the 'Background information section' of the expert system MDDS.

- a. arch-like pattern: cracks appear forming an arch and collapse of portion of wall underneath may follow;
- b. cracks running along one vertical or diagonal line over the whole height: settlement, lateral part of wall/façade (middle-to corner), cracks sloping towards the base of the building, through the weakest parts of the façade/wall;
- c. Parallel vertical cracks in the lowest zone of the façade;
- d. Subsidence of a corner.

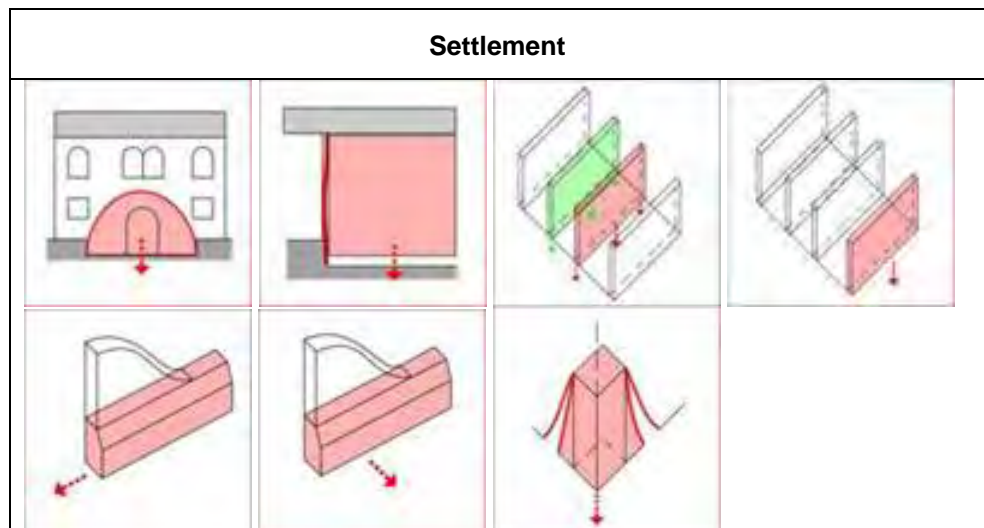
Overloading: the structure stand more load than it can bear, due to its own weight or to an external load. Appearance:

- a. Cracking and deformation of a corner;
- b. Displacement part on columns/pillars;
- c. Deformation of façade out of plane, e.g. at floor level;
- d. Top corner of façade cracks and detaches and /or deforms;
- e. Cracking Barbacane.

Creep: long term overloading, depending on the materials. The process concerns especially slender, high structures, like towers, columns and pillars, and also buildings with restored masonry panels (consequence of wrong restorations). Appearance:

- a. Vertical, parallel cracks in a certain area of the construction.

3 Types of damage and damaging mechanisms



Arch-like pattern

Cracks appear forming an arch and collapse of portion of wall underneath may follow.



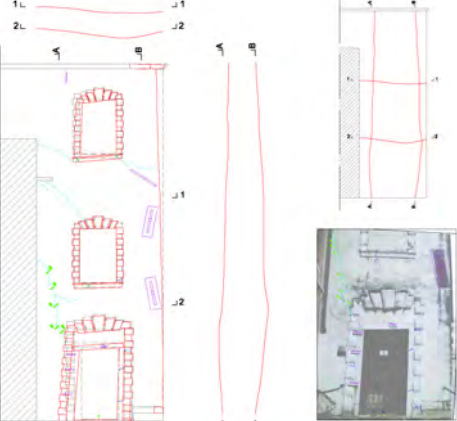
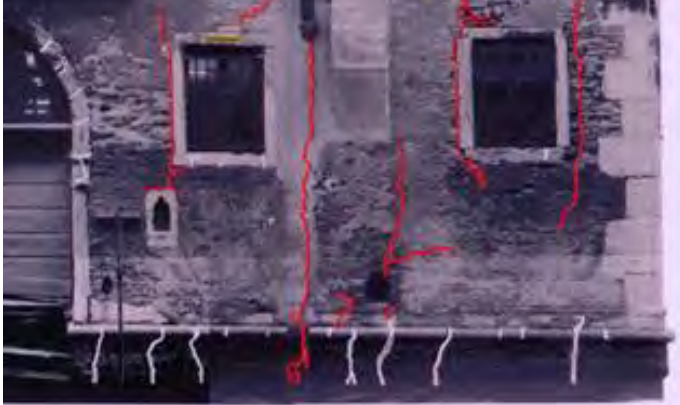
Crack appeared forming an arch and collapse of portion of wall underneath followed (see following picture). Picture taken while repair work was done. Detail of previous picture. Building, rio di S. Barnaba, Dorsoduro.



Crack in the form of an arch appearing in the middle of a wall. The lateral cracks tend to form a second arch, probably due to settlement process concerning a larger part of the wall then the first one. Building, rio S. Aponal, San Polo.



Example of unfinished site-building. The external wall should have been an internal one is showing a portion of arch shaped cracks Palazzo Flangini Cannaregio

		<p>Lateral wall showing crack and deformation that suggest the arch type pattern. Casa Correr, Santa Croce 1728</p>
		<p>Internal wall showing arch-shaped cracks (when not connected with the external walls, the damage is limited). Ca Mocenigo, Santa Croce 1992.</p>
<p>Parallel vertical cracks in the lowest zone of the façade</p>		
	<p>Parallel cracks in the lowest zone of the façade due to lack of load bearing capacity of foundations (lateral sliding). Ca Bernardi, rio S. Aponal, S. Polo 1321.</p>	



Parallel cracks in the lowest zone of the façade (due to lateral sliding of foundation). Palazzo Grimani, S. Boldo, S. Polo 2271.



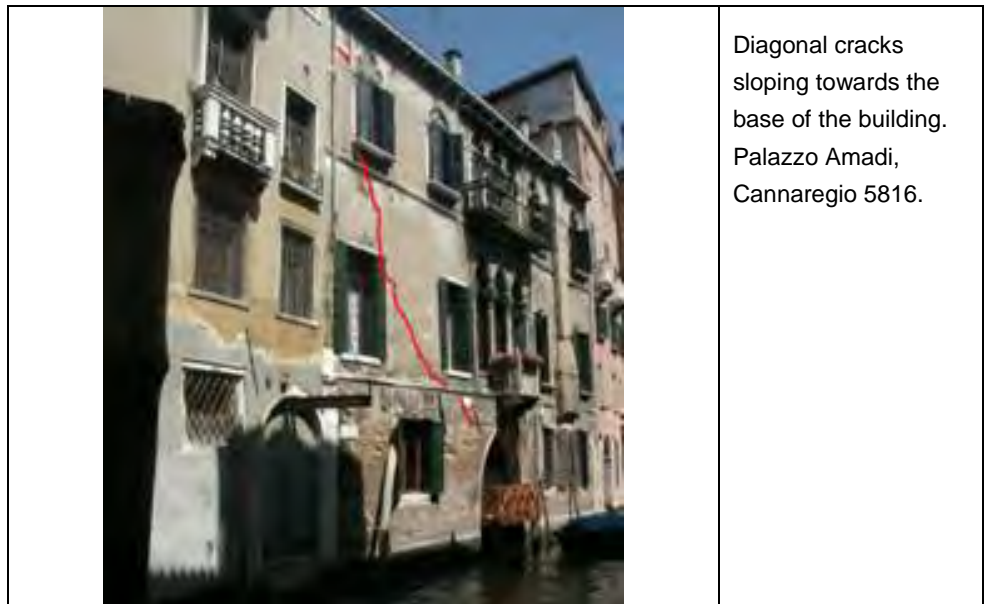
Beside the cracks in the lowest zone of the façade, more cracks appear in the form of an arch. In this case the arch-like cracks are a consequence of the lateral sliding of the façade. Building in Rio S.Fosca, Cannaregio 2324.

Cracks running along one vertical or diagonal line over the whole height

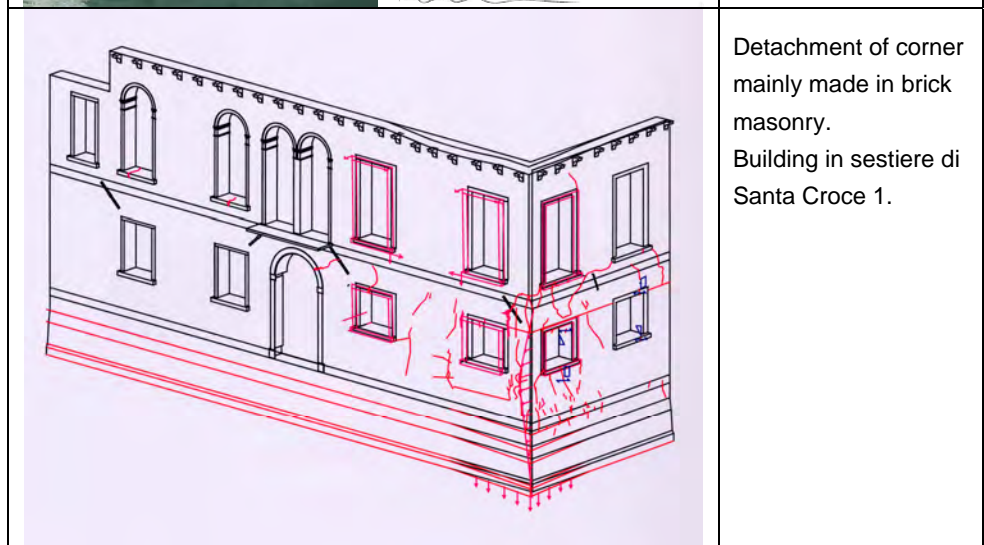
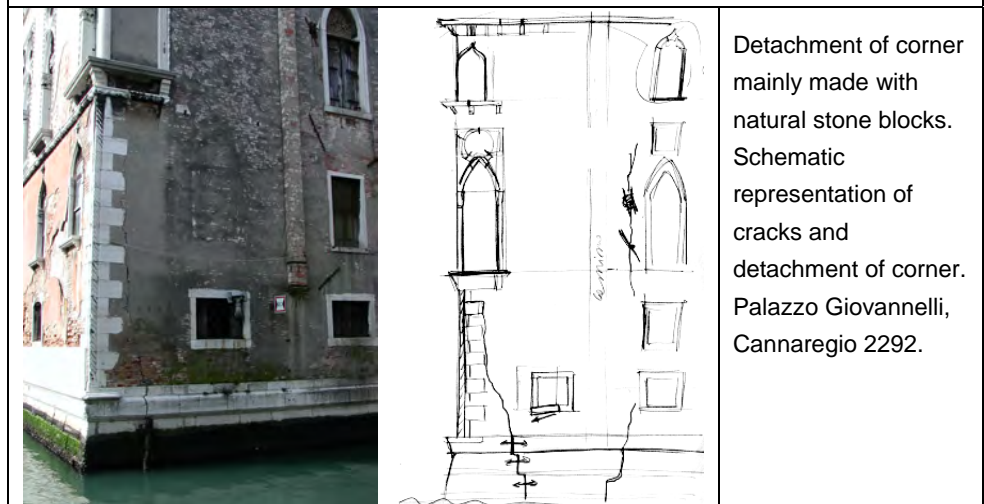
Settlement, lateral part of wall/façade (middle-to corner), cracks sloping towards the base of the building, through the weakest parts of the façade/wall.



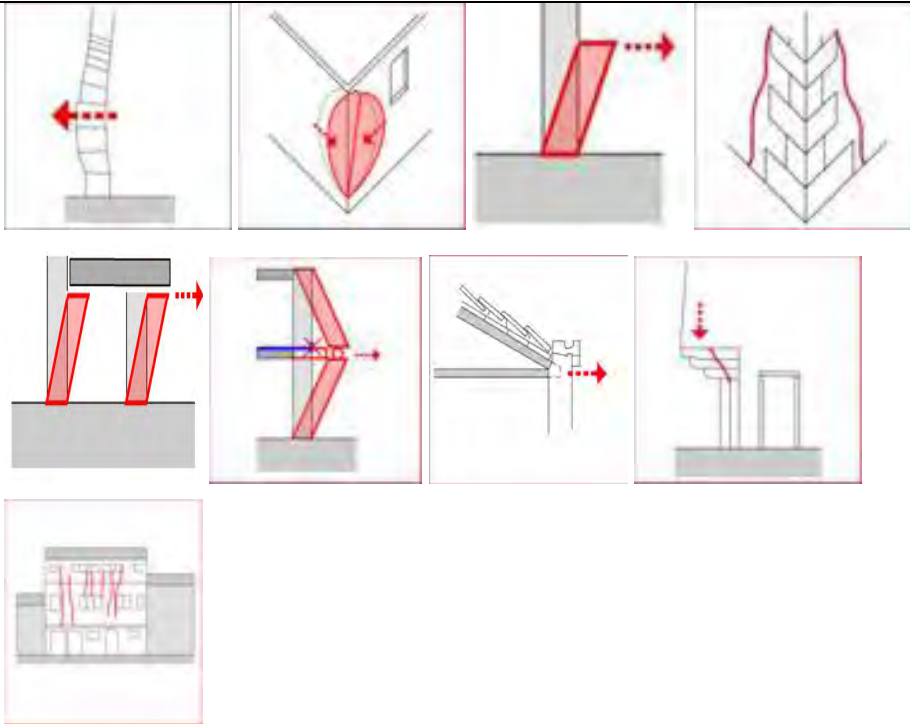
Cracks sloping towards the base of the building, through the weakest parts of the façade/wall. Castelforte San Rocco, San Polo 3105.



Subsidence of a corner



Overloading

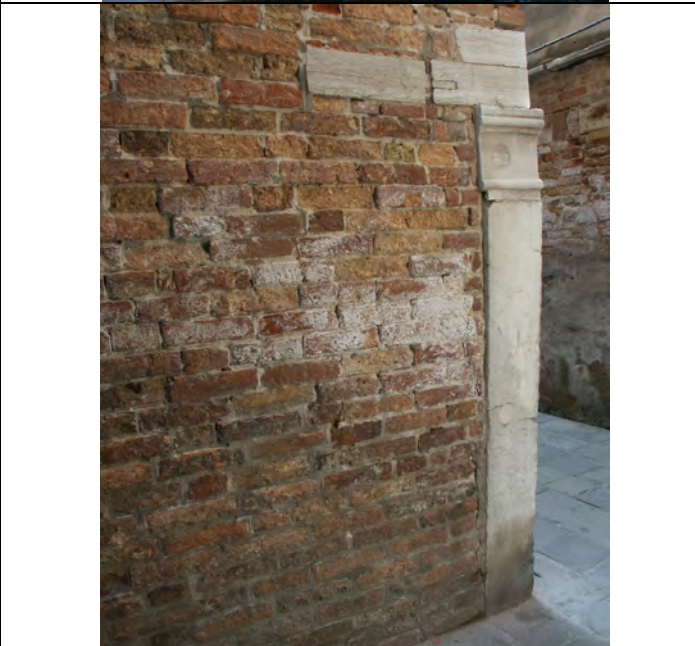


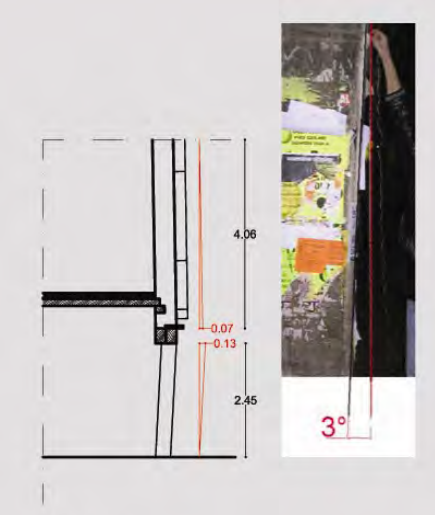
Cracking and deformation of a corner



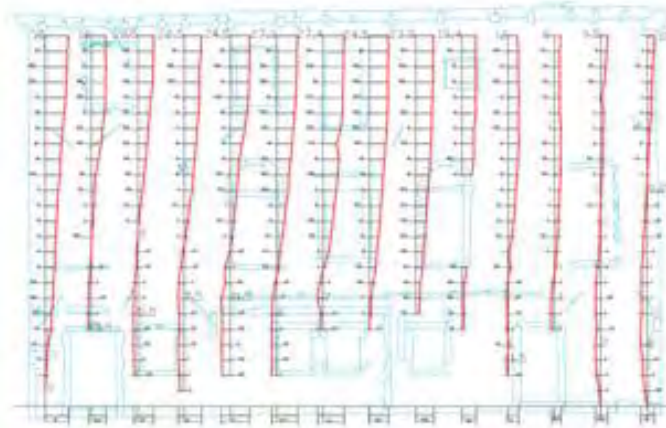
Bulging of corner including natural stone blocks. This type of damage may be related to lateral force exerted by the floor.

Building, Palazzo Nani, Dorsoduro 960.

	<p>Detachment of corner mainly made with natural stone blocks. Palazzo Centani, S. Polo 2793.</p>
	<p>Detachment of corner mainly made with natural stone blocks. Palazzo Corner della Frescada, Dorsoduro 3911.</p>
	<p>Detachment of pillar or a column in corner which fulfils the support function. Ex "Scuola dei Calegheri", S. Polo 2857.</p>

	<p>Detachment of corner. Palazzo Bernardi San Polo.</p>
<p>Displacement part on columns/pillars</p>	
 <p>sez. A-A</p>	<p>Displacement of part of building on columns/pillars, due to slenderness of supports and implying horizontal sliding of architrave above columns/pillars. These eventually break. Building in campo degli Squellini, Dorsoduro 3224.</p>
	<p>Displacement of façade on slender supports. Displacement of part of building on columns/pillars, due to slenderness of supports and implying horizontal sliding of architrave above columns/pillars. These eventually break. Building in campo Spezier, S. Croce 204.</p>

Deformation of façade out of plane, e.g. at floor level



Outward displacement.
Ca Zusto, Santa Croce.



Top corner of façade cracks and detaches and /or deforms



Roof thrust on the top of bearing walls.
Frequently roof inclined beams push walls at corner outwards.
Building, Ca Zusto, S. Croce.

Cracking *Barbacane*



Stone barbancane showing cracks.
left: building in calle lunga S. Barnaba, Dorsoduro 2614
right: building in campo San Marziale, Cannaregio.

Vertical, parallel cracks in a certain area of the construction



Vertical parallel cracks running all along original/old masonry panels between two restored masonry panels
Palazzo Pisani, S. Marina.

Conclusions

Some interpretative proposals of the venetian structural device were given (the structural conception comes from the cognition of an expected behavior) and urge for further investigation upon the dependencies between knowledge of behavior and of decay and choice restoring interventions. The question is posed whether the intervention is to be conceived as a repair or as a full changing of the device. A deeper study of different and alternative solutions could help in defining some guide-lines for the damage diagnosis and a consequent conservative strengthening intervention.

Acknowledgements

The authors want to thanks the students of Architecture of IUAV University of Venice (Restauration Courses – prof. Doglioni, prof. Mirabella 2003-2007) for their contributions.

References

Doglioni F. e Mazzotti P. (a cura di), 2007, Codice di pratica per gli interventi di miglioramento sismico nel restauro del patrimonio architettonico, Regione Marche, Ascoli Piceno.

Doglioni F., Mirabella Roberti G., Bondanelli M., Trovò F., Detecting constructive patterns for structural damage interpretation of historic buildings in Venice, in Scientific Research and Safeguarding of Venice – CORILA Research Program 2004-2006, Volume IV – 2005 results, Venezia, pp. 115-133.

Doglioni F., Mirabella Roberti G., Squassina A. , Trovò F., Meccanismi e fattori di crisi del sistema strutturale ad entro-piombo ed aspetti concettuali degli interventi di consolidamento, in Atti del workshop Sicurezza e consolidamento degli edifici storici in funzione delle tipologia edilizia, della concezione

costruttiva e dei materiali (PRIN 2004-2006, coordinatore prof. L. Binda), 18-19 dicembre 2006, Dipartimento di Ingegneria Strutturale – Politecnico di Milano, testo e cd-rom, Edizioni del Politecnico di Milano – DIS, Milano 2007.

Dogliani F., Squassina A., Trovò F., Detective constructive dispositions of inward out-of-plumb on venetians dwelling houses external masonries, in *Scientific Research and Safeguarding of Venice – CORILA Research Program 2004-2006, Volume V – 2006 results*, Venezia, pp. 89-100.

Dogliani F., Squassina A., Trovò F., Assetto ad entro-piombo dei fronti esterni e concezione strutturale dell'edilizia civile di Venezia, in *Atti del workshop "Sicurezza e consolidamento degli edifici storici in funzione delle tipologia edilizia, della concezione costruttiva e dei materiali"* (PRIN 2004-2006, coordinatore prof. L. Binda), 18-19 dicembre 2006, Dipartimento di Ingegneria Strutturale – Politecnico di Milano, testo e cd-rom, Edizioni del Politecnico di Milano – DIS, Milano 2007.

Mirabella Roberti G., Trovò F., Bondanelli M., Lettura dei modi costruttivi per l'interpretazione dei dissesti dell'edilizia storica veneziana, atti del Seminario internazionale di Studi "Teoria e pratica del costruire: saperi, strumenti, modelli – Esperienze didattiche e di ricerca a confronto", Ravenna, 27-29 ottobre 2005, pp.1375-1384.

Squassina A., A Venezia si perde il senso della verticale.- Some meaningful episodes of the historical debate about the nature of the geometrical organization of venetian buildings in *Scientific Research and Safeguarding of Venice – CORILA Research Program 2004-2006, Volume V – 2006 results*, Venezia, pp. 131-145.

Van Balen K., Mateus J., Binda L., Baronio G., van Hees R.P.J., Naldini S., van der Klugt L., Franke L., 1999. Expert System for the evaluation of the deterioration of ancient brick structures, EU Environment Program, EV5V-CT92-0108, Research report No. 8. The system was completely re-structured during the EU project: 'Compatibility of plasters and renders with salt loaded substrates in historic buildings' (EVK-CT 2001-00047).

FROM ARTIFICIAL STONE TO REINFORCED CONCRETE III: ANALYTICAL METHODOLOGIES FOR THE INTERVENTION

Paolo Faccio, Greta Bruschi, Paola Scaramuzza

Dipartimento di Costruzione dell'Architettura, Università IUAV di Venezia

Riassunto

Per la definizione di adeguate metodologie di indagine necessarie ad identificare l'insorgere di fenomeni di degrado nei manufatti cementizi, i risultati ottenuti attraverso la sperimentazione permettono di trarre alcune indicazioni utili alla comprensione dei meccanismi di alterazione e all'individuazione di markers del degrado e dei rispettivi livelli soglia, elementi fondamentali per lo sviluppo e la sperimentazione di prodotti e metodologie da impiegare per migliorare lo stato di conservazione del calcestruzzo.

In questa fase del progetto-intervento di restauro vale il principio del minimo intervento, evitando quindi l'estensione indiscriminata della campagna diagnostica, la cui esecuzione viene definita e codificata, enfatizzando in tal modo il momento operativo, ma al contempo quello programmatico, basato sulle analisi dirette svolte e sulle valutazioni che ne sono derivate.

Questo processo mette in evidenza la necessità che la diagnostica venga accuratamente progettata, sia attraverso la conoscenza puntuale dei problemi da affrontare sia tramite le capacità di controllo delle possibilità offerte dalle diverse tecniche a disposizione.

Abstract

To define suitable investigation methodologies necessary to identify the singling out of pathologies of degeneration of concrete elements, the results obtained through the experimental data control section allow to get useful information to comprehend the characterization of decay pathologies and to identify deterioration markers, fundamental elements for development and testing of products to use to improve concrete conservation.

This stage of project-intervention of restoration is defined by minimum intervention principle, avoiding indiscriminate extension of diagnostic survey, whose execution is defined and codified, emphasizing in such a way the operating moment, but at the same time the programmatic one, based on the carried out direct analyses and on the appraisals derived.

This process puts in evidence the necessity that diagnostic have to be accurately planned, either through the punctual acquaintance of the problems to face or through the abilities to control possibilities offered from the various techniques available.

1 Instrumental surveys and laboratory analysis

Inspection and diagnosis in the case of reinforced concrete works are necessary to set up an effective intervention of restoration.

During the controls it is needed to use different technics, as for example visual inspections, samples, chemical analysis, application of more or less sophisticated technics that supply useful parameters for the diagnosis.

Inspection and macroscopic survey constitute the minimal level of diagnosis for the appraisal of conservation of a reinforced concrete work in order to collect the necessary informations characterizing the causes of degradation and the damage entity.

Indirect surveyings, that is the collection of relative data about history of the building, data plan, information about construction, location and exposure data (file A), concur to formulate the first hypotheses characterizing possible causes of degradation and excluding others.

The real inspection begins from one macroscopic visual observation to assess the type and the extension of the damages let alone "errors" of planning (file B).

In this phase of reading particular attention is necessary to be given to the characteristics of the material as it is possible to define defects of the concrete characteristics which could be infact an architect casting design decision.

Therefore "nidi di ghiaia" and macroporosity generally signaled like executive errors, are pointed out, as elements that characterize the material for will of the craftsman and not as a form of decay.

The reading of the surface qualities of concrete and artificial stone, at this first step is limited to the macroscopic phenomena; the survey, in the prompt phase, documents the technological quality of the surface (porosity, un-homogeneity), the environmental variables (position of the element, exposure, contact with water or land, presence of polluting agents), the techniques of working (surfaces, textures), pathologies of decay.

It follows an analytical second phase, with the aim to determine the relations between the variable ones over described (concrete quality, ambiental context, feasible techniques, decay pathologies), through a further deepening and collection of direct and indirect information let alone through the aid of aimed chemical-physical surveyings.

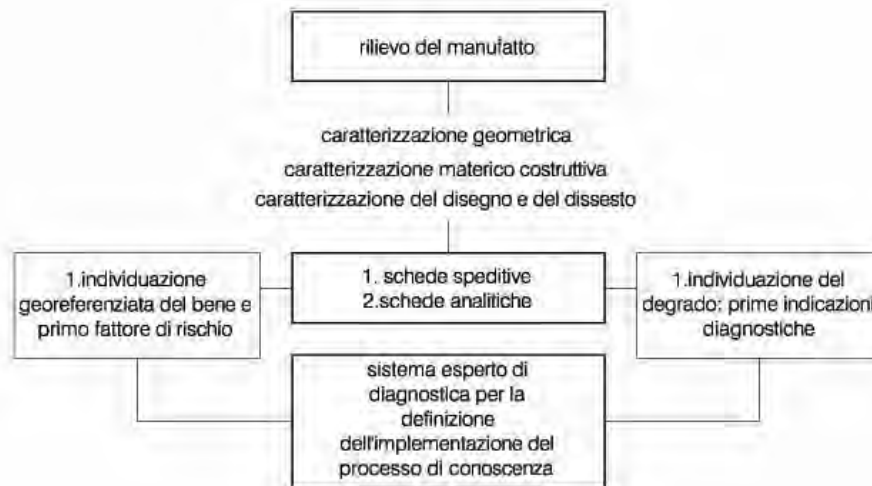
Briefly the necessary information for an exhaustive reading of concrete elements will have to include:

- plan information that is the collection of document and iconographical sources concerning plan and realization
- environment information concerning the geographical position of the cast, the role or structural engagement in the element, the exposure and the presence of risk factor
- information on the consistency of casting that is the analysis of the quality of

inert - mix design and measuring of the components

- information on the constructive techniques, casting treatments, formwork techniques

-information about the conservation of the element coming from in situ and/or of laboratory surveyings.



The direct knowledge presents limits that today, thanks to the aid of the diagnostic analyses in situ and laboratory is possible to exceed.

The achieved development from the so-called "analytics" allow nowadays to gain qualitative and quantitative information fundamental to formulate diagnosis and consequently to measure the intervention and limiting it at the minimum, with advantages for the architecture on which we are called to work on.

The analyses on concrete and the laboratory tests are often expensive therefore demanded when absolutely necessary. The correct way to proceed is to formulate reasonable hypothesis and to verify the consequent scenario in relation to the observed conditions.

Some hypotheses could be further investigated and others rejected. There are many possible analyses on concrete and can supply various useful information, as the concrete structural content, the water/concrete relation, the presence of reactive inert and so on.

2 Experimentation results

In the choice of the techniques to be employed it comes sure given the preference to those not destructive (or minimally destructive), in relation to the problem to face, to their cost and the possible results.

Also in this phase of the plan-participation of restoration it is worth the principle of the minimal participation, avoiding therefore the indiscriminate extension of the diagnostic survey, whose execution comes defined and codified,

emphasizing in such a way the operating moment, as well as the programmatic side, based on direct analyses and resulting evaluation.

This process underlines the necessity that the diagnostic needs to be accurately planned, both through the punctual acquaintance of the problems to face and the abilities to control the possibilities offered from the various techniques available.

To achieve this purpose laboratory surveyings on concrete materials have been limited to samples on the surface. Being the less invasive survey capable to give an evaluation of the conservation conditions in historical buildings.

Through diffractometric analyses on surface samples has been possible to identify the constitutive materials at the time zero and their transformations during the artificial ageing like disappearing of portlandite and identification of: rustomite in the samples threated with salty solutions, ettringite for samples aged with ground salts, thenardite and chalk dangerous products in relation to their ability to hydrate itself with a consisting increase of volume)⁶.

The analyses with the scansion electron microscope and the mapping on cross-sectional fragment give the possibility of studying the cracking condition in order to obtain more information about the possible chemical and physical transformations induced from the presence of salts and termic excursions, let alone these analyses give informations related to the alteration of the hydroxide passivated layer of bars iron.

Finally always carrying out analysis in proximity of the surface of the tests through ionic chromatography the characterization of Ionian soluble the chloride, sulfate and nitrate, responsables of the most serious alteration of armor irons (primes of the phenomena of corrosion for vaiolatura and pitting) and therefore of the concrete. This last surveying allows therefore to find the nature and the amount of dangerous salts.

⁶ The experiment results are in: doc. Monica Favaro, *L'edilizia storica veneziana in pietra artificiale e calcestruzzo: sperimentazione di laboratorio per l'identificazione dei processi di degrado e definizione di opportune metodologie analitiche per la valutazione dello stato di conservazione. Relazione finale*, CNR, I.c.i.s. di Padova.

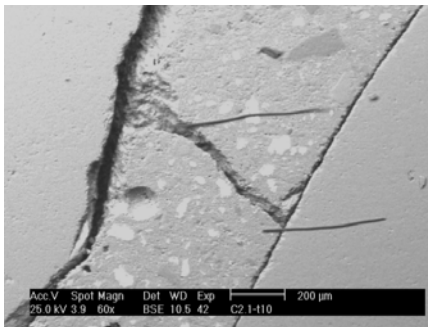


Fig 1 – Morphologic observations to the SEM of the sections of C2.1 after 10 cycles of salt ageing put in evidence fractures both inside the concrete matrix and in correspondence of the interface surface of the inert-concrete.

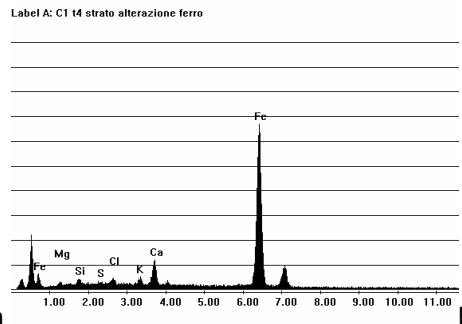
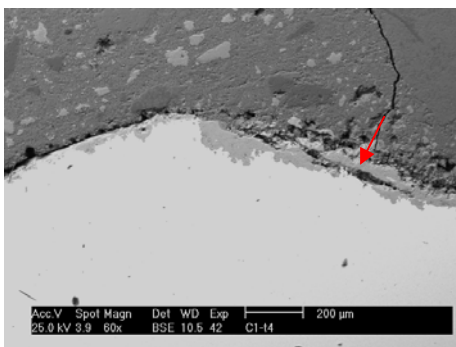


Fig 2 – C1 concrete test after 4 cycles of salt ageing. a) SEM observation of the section in the zone of interface between the iron bars and the concrete (evidenced from the arrow); b) microanalysis EDS in correspondence of the corrosion zone.

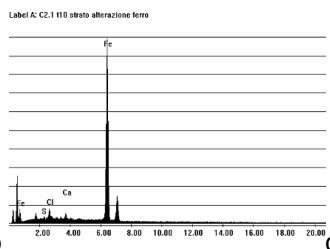
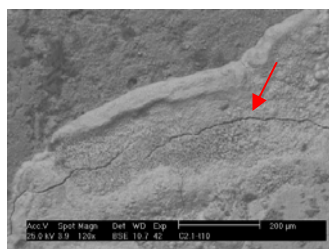


Fig 3 – C2.1 concrete test after 10 cycles of salt ageing. a) spread on the surface of the test of alteration compound of the iron bar; b) SEM Observation of the section in the interface area between the iron bars and the concrete (evidenced from the arrow); c) microanalysis EDS in correspondence of the corrosion zone.

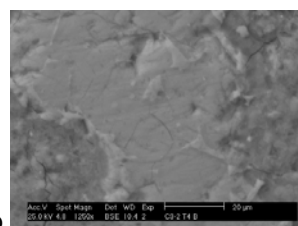
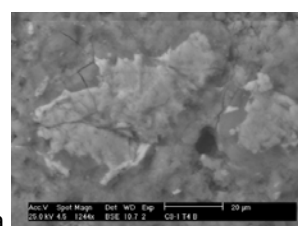


Fig 4 – C3 concrete test: SEM Observation of a concrete grain before the ageing (a) and after 4 cycles of salt ageing (b, c). After the ageing, the presence of sulfur and chloride in the edges of reaction and the fessurazione of the grain is found.

Fig 5 – Percentage Concentration of ione chloride depending on the ageing cycles of with solutions of marine salts in the tests of armed concrete C.

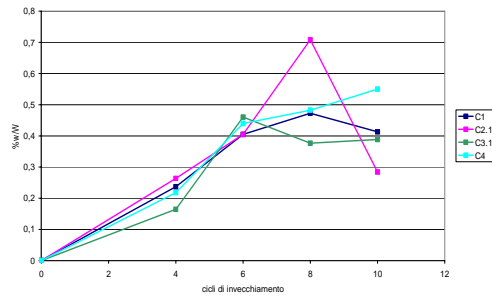


Fig 6 – Concentration percentage of ione sulfate depending on the cycles of ageing with solutions of marine salts in the test of armed concrete C.

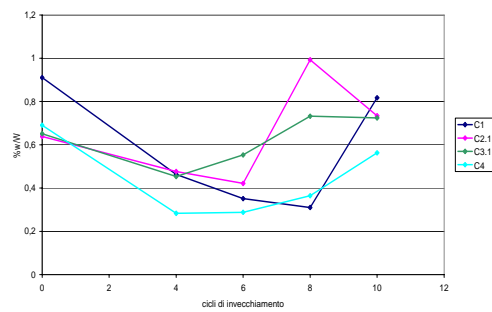
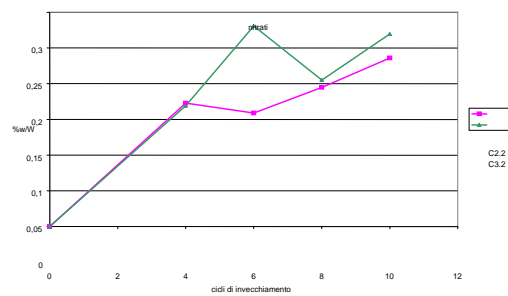
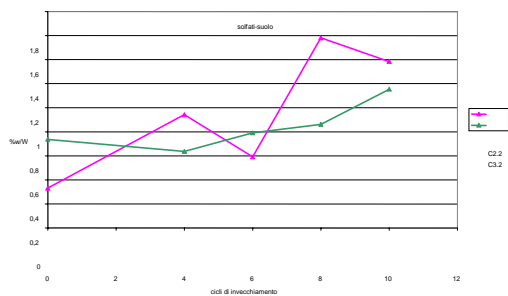


Fig 7 – Concentration percentage of Ionian sulfate (a) and nitrate (b) depending on the cycles of ageing with solutions of ground salts in the tests of armed concrete C.



a

b

For the definition of adequate surveying methodologies and to identify the appearance of degradation phenomena, the results obtained through the experimentation allow to draw some indications:

- the experimental data of ultrasonic speed are not directly linked to those of the bounce index. This last one, although it is often used the measures of the ultrasonic speed in order to define the hardness of concrete materials, in order to supply reliable data must rather be connected with measures of prepared compression tests. In fact beyond the hardness of the material, various factors influence the measures of bounce index, among which are the roughness of the surface and its texture, the water content, the inert type of and its particle-size and finally the carbonation;
- the degradation of the iron protection induced from the carbonation happens to distances from the surface greater of that effectively evidenced from the colorimetric tests. This pushes to think that the test with fenolftaleina submits the effective thickness of the carbonation layer; further surveyings with more sensitive methodologies (i.e analysis with infrared spectrophotometry) must however be carried out in order to confirm such hypothesis;
- the diffraction to X rays and the observation of surface sample with the electron microscope allow an effective definition of the present species of degradation;
- the rustomite mineralogical phase, seems to form itself before the ettringite mineralogical phase, usually used like a marker of degradation of concretes. For one more effective appraisal of the state of conservation of concretes, is supposed that the rustomite could be used as a pointer of the first symptoms of degradation



Fig 8 – Location of possible strategies of intervention.

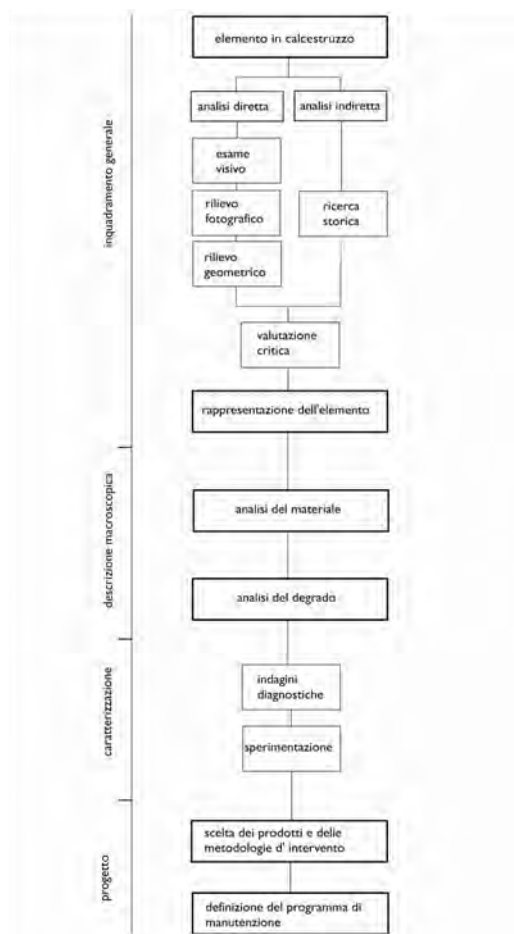


Fig 9 – Realization of a flow diagram of a possible expert system for the analysis and the determination of a plan of direct experimentation of hadcraft and a program of monitoring, also intended for the realization of a project of programmed maintenance.

Conclusions

The assumed position in relation to the topic of the intervention is based on the idea that the aim has to be the maximization the conservative requests.

The conservative attitude constitutes a limit to maintain all the expressions that characterize the considered architecture, this doesn't mean to assume a renouncing attitude, but operating, in this case, adding rather than taking off matter, and therefore signs, mean and values to the considered work.

All the other conditions in which the project takes place has to be considered following these aspects. These conditions might be as relevant as the time passing qualities, and as relevant as partial integrations, which are signs and patina that, more than record the conditions of ageing, could also be a decaying indicator. These considerations can not allow beforehand to define the intervention limits, but needs to lead to a strong metrological attitude.

Design choices as such therefore involve the necessity pursue the experimentation of different techniques for a direct intervention on concretes through products capable to consider the conservation problem of surfaces and not only the mechanical resistance of the material.

At the same time are expected, where possible, a series of indirect interventions as, for example the protection from rain water and from water coming from the ground, intended to slow down the degradation, which, through a constant monitoring, will concur to verify the effectiveness.

References

Pucinotti R., 2006, *Patologia e diagnostica del cemento armato. Indagini non distruttive e carotaggi nelle opere da consolidare*, Flaccovio Dario.

Pedefferri P., Bertolini L., 2000, *La durabilità del calcestruzzo armato*, Mc Graw Hill

Siviero E., Cantoni R., Forin M., 1996, *Durabilità delle opere in calcestruzzo*, Franco Angeli

AREA 3

Environmental processes

RESEARCH LINE 3.8

Speciation and flow of pollutants

Suspended Particulate Matter: temporal variations, origin and depositional dynamics

Luca Giorgio Bellucci, Silvia Giuliani, Stefania Romano, Mauro Frignani, Sonia Albertazzi

CNR-ISMAR – Via Gobetti 101, 40129 Bologna

Riassunto

Nel corso delle quattro campagne stagionali (SPRING, SUMMER, FALL e WINTER) previste dal protocollo di progetto 2005-2006 linea 3.8 (Speciazione e flussi di inquinanti), sono state promosse delle attività di campionamento finalizzate allo studio dei processi che interessano il particolato in sospensione ed il materiale sedimentato risospeso. I siti di studio sono stati scelti nelle aree di Campalto e Sacca Sessola.

Le concentrazioni di materiale sospeso (SPM) mostrano valori più elevati durante le stagioni estive/autunnali e a Campalto, come conseguenza diretta del maggiore traffico di natanti in quest'area ed in tali periodi. D'altra parte le attività di rastrellamento del fondale per la raccolta dei mitili hanno contribuito ad innalzare notevolmente i valori di SPM nella zona di Sacca Sessola.

I risultati delle analisi sulla composizione della materia organica (POC e N) nel particolato sospeso definiscono uno scenario marino per entrambi i siti, con apporti continentali progressivamente più importanti al passaggio dall'estate all'autunno.

I tempi di residenza di SPM nella colonna d'acqua, calcolati tramite il disequilibrio $^{234}\text{Th}/^{238}\text{U}$, sono molto bassi (qualche ora) con flussi verso il sedimento comparabili tra le due stazioni sia in estate che in autunno.

Abstract

During four seasonal campaigns (SPRING, SUMMER, FALL and WINTER) several sampling activities were promoted for the study of suspended and resuspended particulate matter processes, as required by line 3.8 (Speciation and contaminant fluxes) project sampling protocol 2005-2006. Selected sampling sites belong to the areas of Campalto and Sacca Sessola.

Suspended Particulate Matter (SPM) concentrations in the water column showed higher values during summer/fall and at Campalto, as a direct consequence of more enhanced boat traffic in this area and period. On the other hand the massive sediment dredging for mussel fishing greatly increased SPM concentrations at Sacca Sessola.

Organic matter composition (POC and N) in suspended particles defined a marine footprint for both sites, with continental inputs progressively increasing from summer to fall.

SPM residence times, measured through the $^{234}\text{Th}/^{238}\text{U}$ disequilibrium, were always extremely low (few hours), with comparable fluxes between the two sites in summer and fall.

1 Introduction

The research project “Speciation, distribution, fluxes, bioaccumulation and toxicity of principal contaminants in the Lagoon of Venice: experimental and modeling approach”, Line 3.8 “Speciation and contaminant fluxes”, will have as major output the development of mass balance coupled speciation/complexation and fugacity/aquivalence models applicable to a wide range of chemicals in the Venice Lagoon environment. These models will be very important to understand the mechanisms of some key processes that are still poorly defined and refer to: i) transport of contaminants within the system, ii) mobility of contaminants as a function of speciation, iii) prediction of the effects of environmental and anthropogenic factors on the availability of contaminants, iv) bioaccumulation in selected lagoon species, v) effects of contaminants on both fauna and human population, vi) assessment of scientifically sound threshold values. Among the many requirements for the model development, one is relative to the study of specific environmental exchange processes such as those linking sediment and water. In this paper we present the results of the experiments, carried out in the framework of the project, regarding time series data (concentration and fluxes) for suspended particle dynamics at two test site.

2 Materials and methods

Fig. 1 shows the location of Campalto (Ca) and Sacca Sessola (SS) study sites and Tab. 1 lists sampling dates for all four seasonal campaigns with the correspondent experimental activities.

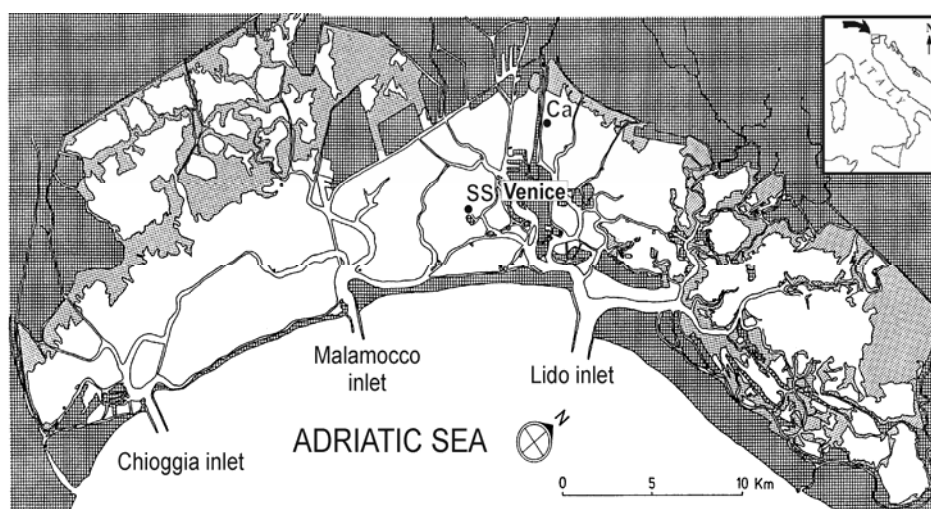


Fig 1 – Sampling locations in the Venice Lagoon. Ca and SS refer to Campalto and Sacca Sessola, respectively.

campaign	date	location	activity
SPRING	05/04/05	SS	<ul style="list-style-type: none"> • LVF for ^{234}Th experiment; • Water sampling for SPM, OC and N
	06/04/05	Ca	<ul style="list-style-type: none"> • LVF for ^{234}Th experiment; • Water sampling for SPM, OC and N
	14/04/05	Ca & SS	<ul style="list-style-type: none"> • Sediment traps positioning
	29/04/05	Ca & SS	<ul style="list-style-type: none"> • Sediment traps recovery
SUMMER	07/07/05	Ca & SS	<ul style="list-style-type: none"> • Sediment traps positioning
	08/07/05	Ca & SS	<ul style="list-style-type: none"> • LVF for ^{234}Th experiment; • Water sampling for SPM, OC and N
	21/07/05	Ca & SS	<ul style="list-style-type: none"> • Sediment traps recovery
FALL	19/10/05	Ca & SS	<ul style="list-style-type: none"> • Sediment traps positioning
	25/10/05	Ca & SS	<ul style="list-style-type: none"> • LVF for ^{234}Th experiment; • Water sampling for SPM, OC and N
	08/11/05	Ca & SS	<ul style="list-style-type: none"> • Sediment traps recovery
WINTER	25/01/06	Ca & SS	<ul style="list-style-type: none"> • LVF for ^{234}Th experiment; • Water sampling for SPM, OC and N
	30/01/06	Ca & SS	<ul style="list-style-type: none"> • Sediment traps positioning
	21/02/06	Ca & SS	<ul style="list-style-type: none"> • Sediment traps recovery

Tab 1 – Sampling dates and activities for each seasonal campaign. LVF means Large Volume Filtration.

Water samples for SPM measurements were collected with plastic bottles (500 ml), repeating the collection three times over two hours at each location. Water was then filtered over Millipore polycarbonate filters (ϕ 0.40 μm) and the filters were then air dried and weighed to measure SPM concentration in the water column. Glass fiber filters (GFF, 0.70 μm) were used for the determination of POC and N in suspended organic matter. After acidification, the analyses were performed with a Carlo Erba Elemental Analyser coupled with a mass spectrometer.

Samples for dissolved and particulate ^{234}Th were collected using a submerged pump powered by an electric generator. Pumping times were generally 1-2 hours and volumes ranged from 200 to 1000 litres of lagoon water. The particulate fraction was collected on a 0.5 μm polypropylene pre-filter followed by two manganese-coated cartridges (MnA and MnB) for the dissolved fraction [Buessler et al., 1992; Frignani et al., 2002]. Once in the laboratory, all cartridges were ashed at 500°C for 5 hours. The ashes were sealed into plastic boxes and gamma counted on high purity germanium detectors. ^{238}U activity was determined from salinity measurement through Chen et al. (1986).

Sediment traps were positioned by a scuba diver and left in place for two-three

weeks. Two sizes (37 and 61 μm^2) were selected to evaluate possible differential collections. The material collected by the traps was then oven dried at 60°C and weighed.

3 Results and discussion

Suspended Particulate Matter (SPM) average concentrations in the water column varied from 4.23 mg L^{-1} (SS-WINTER1) to 32.97 mg L^{-1} (CA-FALL2), showing higher values during warm-temperate seasons (SPRING and SUMMER) and in the Campalto area (Fig. 2). In this latter case, the proximity of the San Giuliano canal can justify the measured higher values, as a result of extensive resuspension determined by boats. On the contrary, the massive sediment dredging, caused by seasonal mussel fishing activities in the Sacca Sessola area, can strongly modify the actual scenario with a temporarily increase of SPM concentrations (87.88 mg L^{-1} in SS-WINTER3 not shown in Fig. 2).

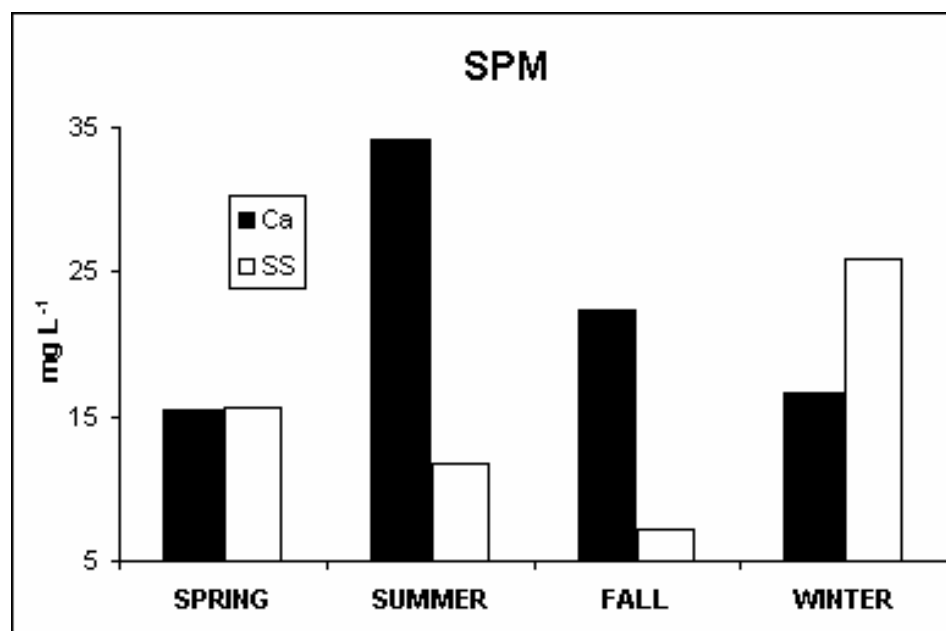


Fig 2 – Suspended Particulate Matter (SPM) average concentrations for all seasonal campaigns and sites.

Data of organic matter composition in suspended matter are available only for the campaigns carried out in SPRING, SUMMER and FALL (Fig. 3). Nevertheless, results until now contribute to define a mixed scenario for both sites, with continental inputs progressively increasing from SUMMER to FALL but always superimposed to a marine footprint ($\text{C/N} < 10$ and $\delta^{13}\text{C} \sim -21.26$, Faganeli et al., 1994). In fact, C/N ratios and $\delta^{13}\text{C}$ values varied from 6.31 and -21.68, respectively, in summer (CA-SUMMER) to 10.39 and -25.53 in fall (SS-FALL). It is interesting to notice how, from these results, the continental influence at Sacca Sessola seems to be higher than that measured at Campalto, in spite of their relative closeness to land. Also Particulate Organic Carbon and Nitrogen (POC and N) percent contents were mostly higher at Sacca Sessola than at Campalto, both sites following a similar trend (SUMMER~SPRING>FALL) with higher seasonal differences at Sacca Sessola.

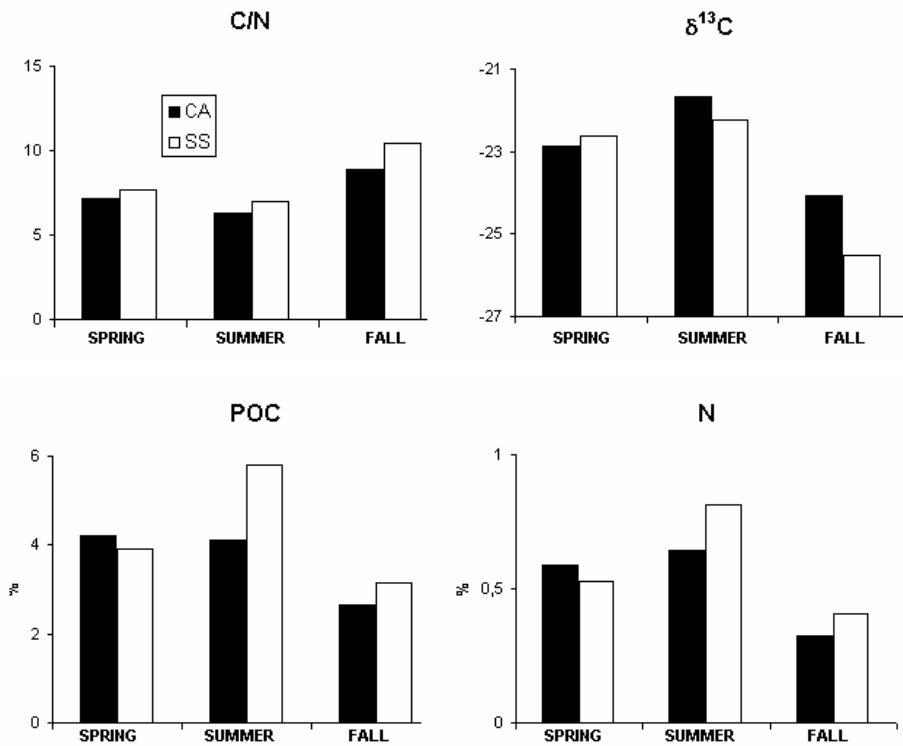


Fig 3 – Particulate Organic Matter composition (C/N, $\delta^{13}\text{C}$, POC and N) in the water column for all seasonal campaigns and sites.

$^{234}\text{Th}/^{238}\text{U}$ disequilibrium data were used to estimate SPM fluxes to the sediment (P_{Th}) and residence times in the water column (τ), by virtue of ^{234}Th strong affinity to suspended particles. Thorium fluxes (P_{Th}) to the sediment were calculated with the following relation [Cochran et al., 1995]:

$$P_{\text{Th}} = \lambda_{\text{Th}} [A_{\text{U}} - (A_{\text{Th}}^{\text{d}} + A_{\text{Th}}^{\text{p}})] \quad (1)$$

where λ_{Th} is the decay constant of ^{234}Th (0.0288 day^{-1}), A_{U} and A_{Th} are ^{238}U and ^{234}Th inventories (this latter as dissolved and particulate forms), respectively. SPM fluxes (P_{SPM}) to the sediment were then calculated from P_{Th} values in the following way [Savoie et al., 2006]:

$$P_{\text{SPM}} = P_{\text{Th}} \frac{[\text{SPM}]}{A_{\text{Th}}^{\text{p}}} \quad (2)$$

where [SPM] defines SPM concentrations. Fig. 4 (left) reports thorium derived SPM fluxes in Sacca Sessola and Campalto for all campaigns. The very high value observed at Sacca Sessola in WINTER are a consequence of the strong impact of mussel fishing activities during this period that determined a very strong increase of suspended particle concentration. For the other periods, P_{SPM} at Sacca Sessola are lower than at Campalto only in SPRING, whereas they are quite similar in the following periods. This seems in contrast with SPM concentration measurements that are always higher at Campalto during SUMMER and FALL and should determine higher fluxes than at Sacca Sessola. This apparent contradiction can be explained by more enhanced sediment resuspension events taking place in Campalto that could prolong residence times in the water column with the continuous input of deposited sediments.

This hypothesis was confirmed by direct measurements with sediment traps (Fig. 4, right): resuspension fluxes at Campalto are always higher than those at Sacca Sessola (from 3 to 8 times), with the exception of the WINTER campaign.

Conclusions

The development of mass balance coupled speciation/complexation and fugacity/aquivalence models, aimed to study contaminant fate and sediment toxicity in the Venice Lagoon, required the direct definition of specific exchange processes rates in the environment, linking sediment and overlying waters. For this reason, a series of sampling activities were promoted to define temporal variations, origin and depositional dynamics of suspended particulate matter in two areas of the Venice Lagoon: Sacca Sessola and Campalto.

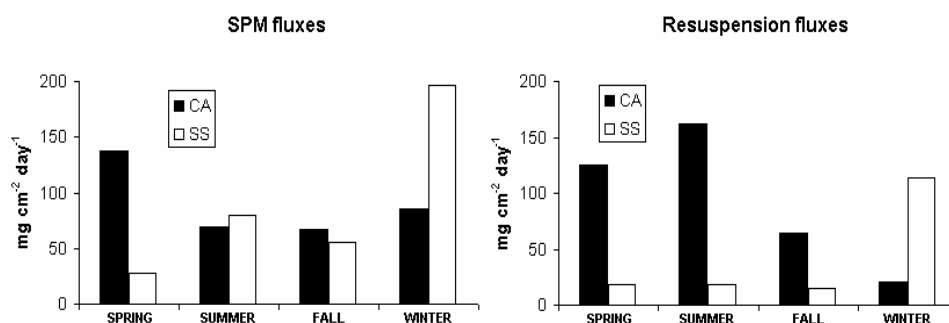


Fig 4 – Thorium derived SPM fluxes to the sediment and resuspension fluxes for all seasonal campaigns and sites.

The results underline once again the strong impact of anthropogenic activities on depositional dynamics in the lagoon environment, as a consequence of local boat traffic and mussel fishing. The high fluxes strongly suggest that particle sediment resuspension and displacement are the major transfer mechanisms in the lagoon, also driving the transport and fate of contaminants.

References

- Buesseler, K.O., Cochran, J.K., Bacon, M.P., Livingston, H.D., Casso, S.A., Hirschberg, D.J., Hartman, M.C., Fleer, A.P., 1992. Determination of thorium isotopes in seawater by non-destructive and radiochemical procedures. *Deep-Sea Research II*, 39, 1103-1114.
- Chen, J.H., Lawrence, E.R., Wasserburg, G. J., 1986. ²³⁸U, ²³⁴Th and ²³²Th in seawater. *Earth Planetary and Science Letters*, 80, 241-251.
- Faganeli, J., Pezdič, J., Ogorelec, B., Misic, M., Hajdek, M., 1994. The origin of sedimentary organic matter in the Adriatic. *Continental Shelf Research*, 14, 365-384.
- Frignani, M., Courp, T., Cochran, J.K., Hirschberg D., Vitoria Codina, L., 2002. Scavenging rates and particle characteristics in and near the Lacaze-Duthiers submarine canyon, *Continental Shelf Research*, 22, 2175-2190.
- Savoie, N., Benitez-Nelson, C., Burd, A.B., Cochran, J.K., Charette, M.,

Buesseler, K.O., Jackson, G.A., Roy-Barman, M., Schmidt, S., Elskens, M., 2006. ^{234}Th sorption and export models in the water column: a review. *Marine Chemistry*, 100, 234-249.

EVALUATION OF POLYCHAETES, *PERINEREIS CULTRIFERA* (GRUBE, 1840), AS INDICATORS OF SEDIMENT MICRO-ORGANIC CONTAMINATION

Nicoletta Nesto, Daniele Cassin, Luisa Da Ros

Istituto di Scienze Marine, CNR, Venezia

Riassunto

Dati preliminari sul possibile utilizzo del polichete *Perinereis cultrifera*, specie diffusa in laguna di Venezia, come indicatore della contaminazione da inquinanti organici nei sedimenti, sono stati ottenuti da esperimenti di laboratorio. A tal fine, esemplari adulti di policheti provenienti da un sito di riferimento, sono stati sperimentalmente esposti per 14 e 25 giorni a due sedimenti naturali diversamente contaminati da PCB ed IPA. La risposta biologica è stata valutata in termini di variazioni percentuali della concentrazione corporea di ciascun inquinante e di malondialdeide, un metabolita cellulare che segnala stress ossidativo.

I risultati hanno indicato in generale un significativo bioaccumulo di tutti i congeneri di PCB nei policheti esposti per 25 giorni al sedimento più contaminato, diversamente da quelli esposti al sedimento di controllo, in cui è stato evidenziato un trend alla diminuzione. Dopo 14 giorni di esposizione ad entrambi i sedimenti gli organismi hanno invece mostrato trend discordanti. Le variazioni percentuali del contenuto di IPA sono risultate molto differenti, in relazione ai singoli composti esaminati, ma in generale è stata evidenziata una chiara tendenza alla diminuzione, spiegabile parzialmente con la elevata capacità detossificante degli organismi per questi composti.

La percentuale di variazione del contenuto di Malondialdeide è risultata maggiore nei campioni esposti per 25 giorni ad entrambi i sedimenti, non essendo stata evidenziata alcuna differenza tra i campioni esposti ai due tipi di sedimenti. Questo risultato indica che tale parametro può essere influenzato da molteplici fattori ambientali, e va quindi considerato un indicatore di stress generico.

Questi risultati, pur preliminari, indicano che il polichete *P. cultrifera* può essere considerato un potenziale indicatore della presenza di PCB nei sedimenti lagunari.

Abstract

This study aims to evaluate the possible use of the polychaetes, *Perinereis cultrifera*, as indicators of organic contamination in the sediments of the Lagoon of Venice. Organisms from a reference site were exposed in laboratory to

natural sediments differently contaminated by PCBs and PAHs for 14 and 25 days. The biological responses were evaluated as percentage variations relating to controls of the body burden of each contaminant and of malondialdehyde (MDA), a metabolite indicating oxidative stress within the organisms.

The results showed a significant bioaccumulation of each PCB congener in worms exposed for 25 days to the most contaminated sediment, whereas a slight depletion was evidenced in worms exposed to the reference sediment. On the contrary, the samples exposed for 14 days to both sediments evidenced more erratic trends. The PAH concentrations resulted highly variable according to each different compound; however, their reduction was more repeatedly observed, following the induction of the efficient enzymatic systems able to metabolised them. The results of MDA content demonstrated that also in this species this metabolite should be considered as a generic stress index, influenced by various environmental and endogenous disturbing factors.

Although preliminary, these data indicate that the polychaete *P. cultrifera* may be a promising indicator of the sediment PCB contamination in the Venice Lagoon.

1 Introduction

The sediments of the Lagoon of Venice may be considered a sink, source and cycling centre for micro-organic pollutants, therefore the assessment of their contamination level holds an important role in the management of the Lagoon ecosystem, although it does not necessarily reflect the bioavailable fraction of these compounds. For this reason, the evaluation of the pollutant content in the biota, which reflects different types of exposure route, physiological status and age of the organism, is an integrated parameter and therefore may be a more useful tool in defining the quality status of an environmental compartment. Among a great variety of biomonitor organisms which have been proposed and used in the last decades in biomonitoring surveys in the framework of both national and international research programmes, the polychaetes represent a large group of bottom dwelling organisms able to accumulate in their tissues organic xenobiotics from water and sediment (Magnusson et al., 2006; Cornellissen et al., 2006; Ruus et al., 2005; Maruya et al., 1997; Meador et al., 1997; Means & McElroy, 1997; Driskoll & McElroy, 1996). Moreover, these organisms are important preys of several bottom dwelling fish species, and therefore may contribute to the transfer of contaminants to higher levels in the food chain (Ruus et al., 2002; 2005). The polychaetes belonging to Neredidae family, for their wide spatial distribution, food web position, and a relatively long life cycle, generally characterized by a singular reproduction event, were included as bioaccumulation indicators in US-EPA official procedures (US-EPA, 1995). Due to the lack of organic pollutant bioaccumulation data in the polychaetes of the Venice Lagoon, the aim of this study was to verify the possible use as organic pollutant biomonitor, to date relatively unexplored, of the Neredidae polychaetes *Perinereis cultrifera*. This species is widely

distributed within the lagoon, and therefore it might be a more suitable sentinel organism than the most studied *Hediste diversicolor*, which is found predominantly along the inner borders of the lagoon. *P. cultrifera* is a gonochoric species characterized by semelparous reproductive strategy which is preceded by epitokous metamorphosis, and it lives in sandy silt sediments at a maximum depth of 15 cm. In Lagoon of Venice these worms can reach 11 cm length and reproduce in March (Prevedelli & Simonini, 2003).

In the framework of the Corila Research Program 2004-2006 - Research Line 3.8. Speciation, distribution, fluxes, bioaccumulation and toxicity of the main contaminants in the Lagoon of Venice, a laboratory experiment was performed to assess the bioaccumulation ability of *P. cultrifera* for organic pollutants. Moreover, to evaluate the well-being of the organisms, the malondialdehyde content (MDA), was determined as a generic biomarker of oxidative stress (Gérard-Monnier et al., 1998).

2 Materials and Methods

2.1 Sediment collection and preparation

A long-term sediment laboratory assay was performed in May 2006 using sediments collected from two differently impacted areas of the Lagoon: Tresse (T) as a polluted site and Palude della Rosa (PR) as a reference. Composite subtidal surface sediment samples (5-10 cm) were collected from each site using a Van Vleet grab, transferred to the laboratory and then sieved (1.5 mm mesh size) to remove indigenous animals and large debris. The sediments were stored at 4°C in darkness for two weeks before the initiation of the assay. Four plastic aquaria (30x20x13 cm) were prepared for testing each sediment type. A 3 cm layer of sieved sediment was placed at the bottom of each aquarium and afterwards 3 litres of filtered seawater (36 PSU) were carefully added. After a conditioning period of 2 hours, aeration was provided using plastic tips suspended 2 cm above the sediment surface. Subsamples of the two field sediments were stored at -20°C until chemical analyses.

2.2 Polychaetes collection and preparation

About 300 organisms (5±1 cm length) were collected at low tide at a pristine site in the Lagoon. Once in laboratory, they were rinsed in sea water and put in aerated aquaria containing quartz sand and sea water at 20°C, 34±1 PSU for a two-weeks acclimatization period, during which the organisms were deprived of food and subjected to a photoperiod of 12h light and 12 h dark.

2.3 Sediment exposure design

Thirty acclimated individuals were carefully added to each test aquarium. They were kept to a constant temperature of 20°C, with a photoperiod 12 h light:12 h dark, and no food was supplied during the assay. For each sediment trial, a subsample of 50-60 individuals were randomly recovered at different time: T0 (reference sample after the acclimatization period), T14 (after 14 days

exposure) and T25 (after 25 days exposure) and differently processed according to the various chemical and biological analyses.

2.4 Chemical and biological analyses

Polyaromatic hydrocarbons (PAH) and chlorinated hydrocarbons (PCBs) were Soxhlet-extracted from both organisms (after a 3 days depuration period in aquaria containing quartz sand and sea water) and sediments for eight hours with n-hexane. The extract was evaporated at 50°C to constant weight for the determination of Extractable Organic Matter (EOM) and, after dissolution in 1 cm³ n-hexane, fractionated by chromatography on an alumina/silica gel column. PCBs from the first fractions of column eluates were analysed by ECD gas chromatography (C. Erba 4160 GC) using a 30 m x 0.32 mm i.d. SE-54 fused silica column with hydrogen as a carrier gas. The concentration of 14 USEPA priority pollutant PAHs were analyzed with high performance liquid chromatograph (HP 1090, USA) on a reverse-phase column (Supelcosil LC-PAH 250 mm x 2.1 mm 5 µm) with a programmed fluorescence detector.

The content of MDA was determined spectrophotometrically in 3 pools of 0.5 g of minced frozen worms according to the method described by Gérard-Monnier et al. (1998). The evaluation of MDA is widely used as indicative of lipid peroxidation and it is based on the rapid reaction between the 1-Methyl-2-phenylindole with MDA yielding a stable carbocyanine dye with maximal absorption wavelength of 586 nm. MDA content was estimated using the tetramethoxypropane as reference standard.

The results of both chemical and biological analyses were expressed, for each group of exposed organisms, as percentage variations with regard to the control (at time 0)

3 Results

The test sediments used in the exposure experiment resulted differently contaminated by PCBs and PAHs (Tab.1). The PCBs content in the sediment from Tresse (T) was approximately 10-fold higher than the sediment from Palude della Rosa (PR). PCB 153, PCB 138 resulted the most abundant congeners at both sites representing roughly the 30% and 20 % of the total PCBs. The PAHs contamination in sediment from Tresse was 35-fold higher than the reference one (Palude della Rosa), showing that pyrene and fluoranthene were the most abundant compounds at both sites. In T sediment they represented the 25% and 19% respectively, of total PAHs and in PR sediment the 19% and 14%.

The percentage variations of PCBs (individual PCB congeners, Sum and Arochlor 1254+1260) in exposed polychaetes are presented in Fig. 1. In general, the most remarkable results were recorded after 25 days, when a marked bioaccumulation for all the examined PCB congeners (except PCB 52) and Arochlor 1254+1260 was identified in polychaetes exposed to T sediment, whereas a small reduction was evidenced in the sample exposed to PR

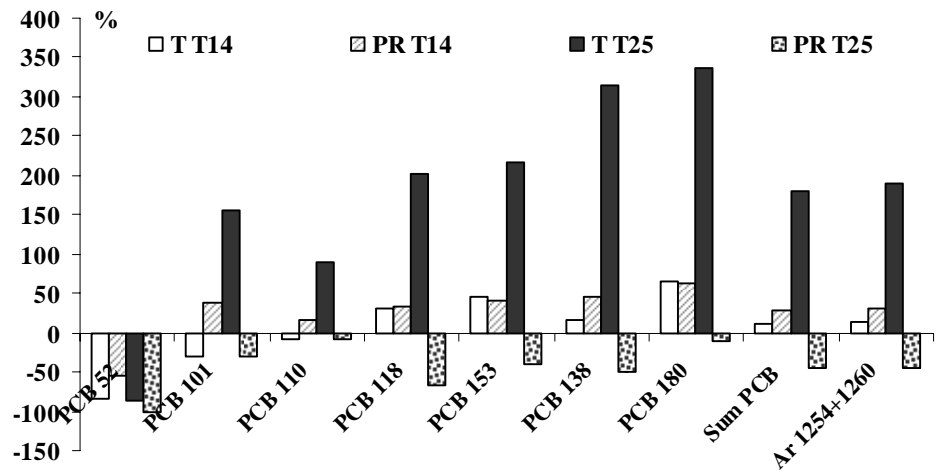
sediment. After 14 day exposure results showed less and erratic variations. The PAH percentage variations resulted different in relation to each individual PAH, although a general reduction was observed in samples exposed to both sediments (Fig. 2). In particular, phenanthrene and benzo(a)anthracene resulted slightly bioaccumulated only in sample exposed to PR sediment for 14 days, fluoranthene only in sample exposed to PR sediment for 25 days, and benzo(b)fluoranthene only in sample exposed to T sediment for 14 days. Anthracene was marked bioaccumulated in samples exposed to both sediments only for 14 days, whereas pyrene resulted differently bioaccumulated in the samples exposed to T sediment, showing higher bioaccumulation level in organisms exposed for 14 days. All the other PAHs were lower than in the reference organisms for both sediments.

The percentage variation of MDA resulted higher in samples exposed to both sediments for 25 days, accounting for an increase of 29% and 23% in Tresse and Palude della Rosa sediments, respectively (Fig. 3). After 14 day exposure the variations in MDA content were lower and exhibited opposite trends in the two sediments.

Microorganic pollutants	T	PR
PCB 52	2.48 ± 1.22	0
PCB 101	3.15 ± 1.38	0.30 ± 0.03
PCB 110	1.95 ± 0.17	0.46 ± 0.01
PCB 118	3.08 ± 0.47	0.29 ± 0.03
PCB 153	10.30 ± 2.04	0.96 ± 0.27
PCB 138	6.38 ± 2.11	0.50 ± 0.09
PCB 180	5.02 ± 3.09	0.29 ± 0.14
Sum PCB	32.37 ± 3.96	2.81 ± 0.28
Ar 1254+1260	67.16 ± 3.90	6.30 ± 1.05
Naphthalene	0.00	0.00
Acenaphthylene	0.00	0.00
Acenaphthene	5.57 ± 0.23	0.00
Fluorine	30.88 ± 4.33	0.00
Phenanthrene	338.85 ± 44.27	5.85 ± 1.41
Anthracene	18.68 ± 5.04	2.20 ± 0.02
Fluoranthene	673.41 ± 40.25	14.93 ± 2.75
Pyrene	889.69 ± 377.95	18.47 ± 10.67
Benz[a]anthracene	202.21 ± 16.59	9.25 ± 1.18
Chrysene	223.97 ± 41.46	9.96 ± 1.84
Benzo[b]fluoranthene	283.24 ± 38.36	13.16 ± 3.45
Benzo[k]-fluoranthene	203.52 ± 11.95	8.71 ± 1.00
Benzo[a]pyrene	314.82 ± 33.83	9.24 ± 2.88
diBenzo[a,h]anthracene	28.20 ± 4.14	0.64 ± 0.08
Benzo-[g,h,i]perylene	357.60 ± 82.62	6.68 ± 2.12
Indeno[1,2,3-cd]pyrene	0.00	0
Sum PAHs	3570.64 ± 620.24	99.08 ± 25.71

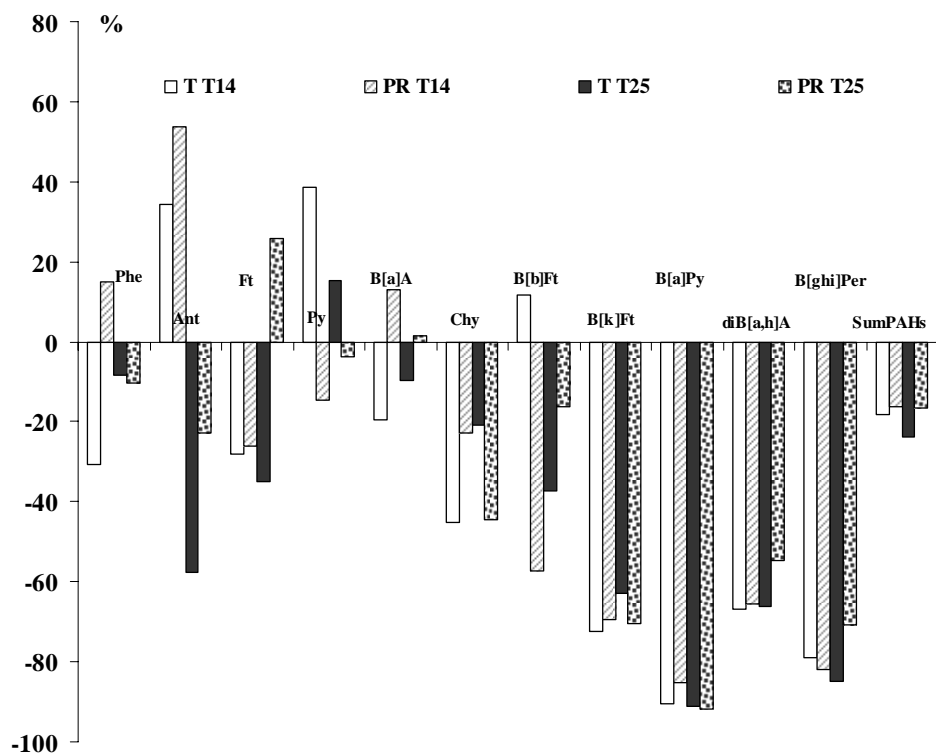
Tab 1 – Organic micropollutants content ($ng\ g^{-1}\ dw$) in sediments from Tresse (T) and Palude della Rosa (PR), used in the exposure experiment.

Fig 1 – PCB content in samples of *P. cultrifera* exposed for 14 and 25 days to different contaminated sediments (T= Tresse, PR= Palude della Rosa). Values are expressed as percentage variations with regard to the time 0 control.



Legend: T T14= sample exposed to Tresse sediment for 14 days; PR T14= sample exposed to Palude della Rosa sediment for 14 days; T T25= sample exposed to Tresse sediment for 25 days; PR T25= sample exposed to Palude della Rosa sediment for 25 days.

Fig 2 – PAH content in samples of *P. cultrifera* exposed for 14 and 25 days to different contaminated sediments (T= Tresse, PR= Palude della Rosa). Values are expressed as percentage variations with regard to the time 0 control.



Legend: T T14= sample exposed to Tresse sediment for 14 days; PR T14= sample exposed to Palude della Rosa sediment for 14 days; T T25= sample exposed to Tresse sediment for 25 days; PR T25= sample exposed to Palude della Rosa sediment for 25 days.

PAHs abbreviation: Phe= phenanthrene; Ant= anthracene; Ft= fluoranthene; Py =pyrene; B[a]A= benz[a]anthracene; Chy= chrysene; B[b]Ft= benzo[b]fluoranthene; B[k]Ft=

benzo[k]-fluoranthene; B[a]Py= benzo[a]pyrene; diB[a,h]A= dibenz[a,h]anthracene; B[g,h,i]Per= benzo-[g,h,i]perylene.

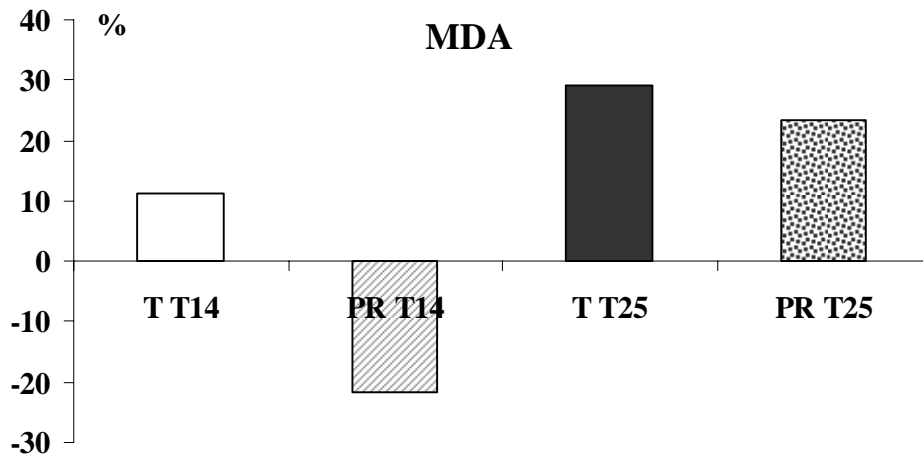


Fig 3 – MDA content in samples of *P. cultrifera* exposed for 14 and 25 days to different contaminated sediments (T= Tresse, PR= Palude della Rosa). Values are expressed as percentage variations with regard to the time 0 control.

Legend: T T14= sample exposed to Tresse sediment for 14 days; PR T14= sample exposed to Palude della Rosa sediment for 14 days; T T25= sample exposed to Tresse sediment for 25 days; PR T25= sample exposed to Palude della Rosa sediment for 25 days.

4 Discussion

The long-term exposure to different contaminated sediments highlighted that *P. cultrifera* is able both to bioaccumulate PCBs and to metabolize the PAHs. In particular, all the examined PCB congeners resulted actively bioaccumulated after 25 day in the most contaminated sediment, apart from the less chlorinated compound, PCB 52, possibly because more dissolved in water than associated with particles, due to its low octanol/water partition coefficient ($\text{Log } K_{ow} = 5.84$) (Ruus et al., 2002). On the contrary, the organisms exposed to the reference sediment for 25 days exhibited a marked reduction of all PCB congeners. The hexa- and hepta-chlorinated biphenyls, i.e. PCB 153, PCB138 and PCB 180, which are characterized by a moderate hydrophobicity, resulted the most bioaccumulated, and were in agreement with previous studies dealing with infaunal organisms (Goerke & Weber, 1990; Meador et al., 1997; Pruell et al., 2000; Ruus et al., 2005). As these type of congeners are the most abundant in both test sediments, it may be suggested that the accumulation is mainly related to the ingested sediments, although the direct absorption through the cuticle could not been excluded (Fowler et al., 1978). The low and erratic variations of the PCB congeners after 14 day exposure to both sediments suggests that the steady-state for the tissue residues may be reached after a longer exposure time, as already observed for *Hediste diversicolor*, for which the EPA procedures recommend a 28 days test (US-EPA, 1995).

The variations of PAHs contents in *P. cultrifera* resulted quite different for each considered compound, but a clear reduction was generally evidenced in both sediments, due to their low environmental persistence and the rapid induction of

specific detoxifying enzymatic system (Christensen et al., 2002; Driscoll & McElroy, 1996; Forbes et al., 1996; McElroy, 1990).

The PAH compounds, accumulated indifferently after 14 or 25 days from both sediments, were phenanthrene, anthracene, fluoranthene, pyrene and benz(a)anthracene. Previous studies indicated that they are highly bioaccumulated in different polychaetes species as *Arenicola marina*, *Abarenicola pacifica*, *Nereis diversicolor* and highlighted a wide variability of bioaccumulation factors among various species, in relation to different feeding and behavioural strategies and/or routes of exposure (Cornelissen et al., 2006; Christensen et al., 2002; Weston, 1990; Augenfeld & Anderson, 1982). It has also been suggested that compounds with log K_{ow} around 5 have the highest bioaccumulation factors in comparison with contaminants with lower or higher log K_{ow} as the former are quickly eliminated and the last are not bioavailable due to extensive sorption to particulate matter in the sediments (Christensen et al., 2002).

The higher MDA content recorded in samples exposed for 25 days to both sediments, indicated that also in polychaetes, like in other invertebrate taxa, this metabolite may be considered as a generic stress biomarker, influenced by numerous confounding factors. A very marked intraspecific agonistic behaviour, reported for this species by Scaps (1995) might have been an important stressing factor for the individuals maintained in each aquarium.

Conclusions

The long term exposure experiment showed a significant bioaccumulation of all PCB congeners in worms exposed for 25 days to the most contaminated sediment, whereas a slight depletion was evidenced in worms exposed to the reference sediment. According to these preliminary results, *P. cultrifera* might be a promising suitable bioindicator of the PCBs in the lagoon sediments. The PAH concentrations resulted highly variable in relation to the different compounds, although in general a depletion was observed in worms exposed to both sediments, possibly because they are metabolized by efficient enzymatic systems.

References

- Augenfeld J.M., Anderson J.W., 1982. The fate of polyaromatic hydrocarbons in an intertidal sediment exposure system: bioavailability to *Macoma inquinata* (Mollusca: Pelecypoda) and *Abarenicola pacifica* (Anellida: Polychaeta). *Marine Environmental Research*, 7, 31-50.
- Cornelissen G., Breedveld G.D., Næs K., Oen A.M.P., Ruus A., 2006. Bioaccumulation of native polycyclic aromatic hydrocarbons from sediment by a polychaete and gastropod: freely dissolved concentrations and activated carbon amendment. *Environmental Toxicology and Chemistry*, 25 (9), 2349-2355.

- Christensen M., Andersen O., Banta G.T., 2002. Metabolism of pyrene by the polychaetes *Nereis diversicolor* and *Arenicola marina*. *Aquatic Toxicology*, 58, 15-25.
- Driscoll S.K., McElroy A.E., 1996. Bioaccumulation and metabolism of benzo(a)pyrene in three species of polychaetes worms. *Environmental Toxicology and Chemistry*, 15 (8), 1401-1410.
- Forbes V.E., Forbes T.L., Holmer M., 1996. Inducible metabolism of fluoranthene by the opportunistic polychaete *Capitella* sp. I. *Marine Ecology Progress Series*, 132, 63-70.
- Fowler S.W., Polikarpow G.G., Elder D.L., Parsi P., Villeneuve J.P., 1978. Polychlorinated biphenyls: accumulation from contaminated sediments and water by the polychaete *Nereis diversicolor*. *Marine Biology*, 48 (4), 303-309.
- Gérard-Monnier D, Erdelmeier I., Régnard K., Moze-Henry N, Yadan J.C., Chaudière J., 1998. Reactions of 1-methyl-2-phenylindole with malondialdehyde and 4-Hydroxyalkenals. Analytical applications to a colorimetric assay of lipid peroxidation. *Chem. Res. Toxicol*, 11, 1176-1183.
- Goerke H, Weber K., 1990. Population dependent elimination of various polychlorinated biphenyls in *Nereis diversicolor* (Polychaeta). *Marine Environmental Research*, 29, 205-226.
- Magnusson K., Ekelund R., Grabic R., Bergqvist P.A., 2006. Bioaccumulation of PCB congeners in marine benthic infauna. *Marine Environmental Research*, 61, 379-395.
- Maruya K.A., Risebrough R.W., Horne A.J., 1997. The bioaccumulation of polynuclear aromatic hydrocarbons by benthic invertebrates in an intertidal marsh. *Environmental Toxicology and Chemistry*, 16 (6), 1087-1097.
- McElroy A.E., 1990. Polycyclic aromatic hydrocarbon metabolism in the polychaete *Nereis virens*. *Aquatic Toxicology*, 18, 35-50.
- Meador J.P., Adams N.G., Casillas E., Bolton J.L., 1997. Comparative bioaccumulation of chlorinated hydrocarbons from sediment by two infaunal invertebrates. *Archives of Environmental Contamination and Toxicology*, 33, 388-400.
- Means J.C., McElroy A.E., 1997. Bioaccumulation of tetrachlorobiphenyl and hexachlorobiphenyl congeners by *Yoldia limatula* and *Nephtys incisa* from bedded sediments: effects of sediment- and animal-related parameters. *Environmental Toxicology and Chemistry*, 16 (6), 1277-1286.
- Prevedelli D., Simonini R., 2003. Life cycles in brackish habitats: adaptive strategies of some polychaetes from the Venice Lagoon. *Oceanologica Acta*, 26, 77-84.
- Pruell R.J., Taplin B.K., McGovern D.G., McKinney R., Norton S.B., 2000. Organic contaminant distribution in sediments, polychaetes (*Nereis virens*) and American lobster (*Homarus americanus*) from a laboratory food chain

experiment. *Marine Environmental Research*, 49, 19-36.

Ruus A., Ungland K.I., Skaare J.U., 2002. Influence of trophic position on organochlorine concentrations and compositional patterns in a marine food web. *Environmental Toxicology and Chemistry*, 21 (11), 2356-2364.

Ruus A., Schaanning M., Øxnevad S., Hylland K., 2005. Experimental results on bioaccumulation of metals and organic contaminants from marine sediments. *Aquatic Toxicology*, 72, 273-292.

Scaps P., 1995. Intraspecific agonistic behaviour in the polychaete *Perinereis cultrifera* (Grübe). *Vie Milieu*, 45 (2), 123-128.

US-EPA, 1995. Standard Guide for determination of bioaccumulation of sediment-associated contaminants by benthic invertebrates. Designation: E 1688-1995.

Weston D.P., 1990. Hydrocarbon bioaccumulation from contaminated sediment by the deposit-feeding polychaete *Abarenicola pacifica*. *Marine Biology*, 107, 159-169.

EVALUATION OF POLYCHAETES, *PERINEREIS CULTRIFERA* (GRUBE, 1840), as INDICATORS OF HEAVY METAL VARIABILITY IN SEDIMENT

Stefania Romano^{1,2}, Marco Marcheselli¹, Marina Mauri¹

¹ Dipartimento di Biologia Animale, Università degli Studi di Modena e Reggio Emilia

² Istituto di Scienze Marine, CNR Bologna

Riassunto

La capacità del polichete *Perinereis cultrifera* (Grube, 1840) di segnalare variazioni della disponibilità di metalli nel sedimento è stata valutata con un approccio di laboratorio a breve termine. A tal scopo esemplari di un sito di riferimento sono stati sperimentalmente esposti fino a un massimo di 14 giorni a fango naturale con contaminazione da Cd, Cu e Zn maggiore rispetto a quella del sedimento originario (esperimento di bioaccumulo) e a una matrice simulante il sedimento originario ma priva di contaminanti (sedimento-controllo) (esperimento di depurazione). La risposta biologica è stata valutata in termini di metallo corporeo e biomarkers di stress generico quali hsp60 e hsp70.

I risultati hanno indicato che, in sedimenti che presentano una concentrazione di Cd e Zn dieci volte più alta e valori di Cu circa doppi rispetto al sedimento nativo, *P. cultrifera* mostra per Cd una netta fase di bioaccumulo, al contrario di Cu e Zn che non variano significativamente rispetto alle concentrazioni iniziali. Gli organismi mantenuti nel sedimento-controllo mostrano un diverso andamento per Cd e Cu, che non sembrano variare nel tempo, rispetto a Zn che risulta invece in diminuzione. Questi comportamenti potrebbero essere legati al diverso significato metabolico, alle diverse modalità di immagazzinamento e alle diverse vie di detossificazione di questi tre metalli nei policheti nereidi.

Gli organismi esposti al sedimento naturale mostrano inoltre un incremento dell'espressione di hsp60 e hsp70 già a 3 giorni di esposizione, mentre gli esemplari mantenuti nel sedimento privo di contaminanti mantengono livelli di hsp60 e hsp70 costanti.

Questi risultati preliminari indicano che *P. cultrifera* è in grado di modificare il contenuto corporeo di metalli in risposta a variazioni della loro disponibilità nei sedimenti. Ciò avviene in relazione alla capacità di regolazione specifica per ogni metallo e può comportare l'attivazione di meccanismi di riparo con conseguenti segnali di stress.

Abstract

The ability of the polychaete *Perinereis cultrifera* (Grube, 1840) to highlight

variations in the sediment metals availability was assessed by a short-term laboratory experiment. Specimens from a reference site were experimentally exposed for a period of 14 days to a natural mud characterized by a heavier contamination in Cd, Cu and Zn in comparison to the native sediment (bioaccumulation experiment) and to an artificial exposure-media depicting the native sediment, but devoid of contaminants (deuration experiment). Our results indicated that *P. cultrifera* exposed to sediments with a tenfold higher Cd and Zn concentration and to twofold higher Cu values than the native sediment, shows for Cd a clear bioaccumulation phase, while Cu and Zn do not vary significantly. The individuals reared in the control-sediment show a different trend for Cd and Cu, which remain constant, in respect to Zn whose concentration decreases over the 14 day period. Such behaviour could be due to the different metabolic features, storing ways and detoxification paths of these three metals in nereid polychaetes. Moreover, the specimens exposed to the natural contaminated sediment showed an increased hsp60 and hsp70 expression after only 3 days. On the contrary the hsp60 and hsp70 levels of the specimens maintained in the uncontaminated media remained constant. These preliminary results indicate that *P. cultrifera* is capable of modifying his metal body burden as a response to the variations on metal availability in sediments. This feature is related to their capacity to regulate, which is specific for every metal, and can involve the activation of repair mechanisms and thereby stress signals.

1 Introduction

The relationships between sediment metals availability and infaunal biota responses in aquatic ecosystems are uncertain and contradictory as yet because of the difficulty to assess what is the bioavailable fraction that may interact with the biological compartment (Bernds *et al.*, 1998, Wang *et al.*, 1999, Argese *et al.*, 1999, Frangipane *et al.*, 2005, Amiard *et al.*, 2006). Actually this lack of information contrasts with the need of evaluating the ecological risk of the anthropogenic contamination in coastal and confined habitats. Experimental studies demonstrated that the ingestion of sediments and the uptake from solution may both be important pathways of metal bioaccumulation in deposit/detritus feeding species (Zhou *et al.*, 2003). Nevertheless investigations on time course of bioaccumulation and clearance of metals in organisms, in relation to varying environmental metal exposures, are needed to check the biological fate of the sediment metals and their effects, namely changes on the biological performances or damages (Geracitano *et al.*, 2004).

As a matter of fact many heavy metals are well known to be toxic to cells under certain circumstances (De Moor and Koropatnick, 2000). To minimize oxidative damage and to cope with stressors, eukaryotic cells utilize a variety of protective mechanisms, including the expression of an assortment of proteins which are collectively referred to as "stress proteins". In case of stress, such as metal exposure, a common early cytoprotective function of the heat shock proteins hsp60 and hsp70, which aid in the folding or removal of damaged

proteins, is well documented (Downs *et al.*, 2005, Franco *et al.*, 2006).

The natural populations of sediment dwelling species, i.e. nereid polychaetes, seem to represent an excellent biological tool to study the relationships between metal contamination in sediments and its biological effects. In fact their bioturbation effects on metal speciation (Petersen *et al.*, 1998), their ability to accumulate from both water and sediment particles and their role within the foodweb as fast transformers of bottom organic matter and as food for species of higher level of ecological complexity (Rainbow *et al.*, 2006), have a great importance.

The polychaete *Perinereis cultrifera* (Grube, 1840) (Nereididae) is a key species of the macro-zoobenthos in the soft-bottom mud flat of the Venice Lagoon and is thus an interesting candidate for biomonitoring of this area as an indicator of the sediment contaminants effects, because of their wide presence in sandy silt bottoms within the lagoon (Prevedelli and Simonini, 2003). Field investigations of the bioaccumulation responses to environmental contaminants are informative about the suitability of the polychaetes for biomonitoring only if the paths for metal in these organisms are known.

In the framework of the CORILA Research Program 2004-2006 - Research Line 3.8 Speciation, distribution, fluxes, bioaccumulation and toxicity of the main contaminants in the Lagoon of Venice, a laboratory experiment was performed on *P. cultrifera* to assess the patterns of both metal bioaccumulation and depuration ability, depending on sediment metal variations. Furthermore the study focuses on the relationship between contaminant exposure and biological responses highlighting the well-being status of individuals, namely the hsp expression as a generic biomarker of stress.

2 Materials and methods

2.1 Sampling

Individuals to be used for the toxicokinetic experiments were picked from sediment by hand within one day-sampling campaign in June 2006 on a reference site of Sacca Sessola in the Venice Lagoon, a small island close to the historical centre of Venice. The animals were separated from sediments after sieving and immediately transferred to polystyrene basins coated with wet filter paper (seawater) and kept cool during transportation using ice-packs. In the laboratory animals were kept for 3 days in aquaria containing quartz sand of appropriate granulometry (0.1-0.4 mm) and artificial sea water (33‰, Instant Ocean's Reef Crystals) to purge sediment particles from intestine and to acclimatise to experimental conditions (20°C, 12:12 light-dark cycle).

The native sediments in which the animals were found were collected using a plastic paddle and placed immediately in a plastic box which was filled to the brim to eliminate air. In the same sampling campaign mud were gathered from the lagoon bottoms at a site in the vicinity of the Isola delle Tresse, which is believed to be a contaminated area, closed to the industrial site of Porto

Marghera.

After acclimation, a subsample of 15-18 organisms (3-5 cm in length) was collected from the quartz sand, immediately frozen in liquid nitrogen and stored at -80°C until the biomarker and metal content analyses (this set of animals will be referred to as the control/T0 group).

2.2 Toxicokinetic study

The toxicokinetics experiments were designed for subsequent evaluation of two-compartment models, involving the exposure media as the first, and the organisms as the second compartment. Two different experiments were set up: they comprised a bioaccumulation and a depuration experiment.

Worms were sorted into the two experimental groups: the first group was placed in a tank filled with the mud collected from the Isola delle Tresse site and 33‰ artificial seawater (exposure/bioaccumulation group), the other was transferred to a plastic tank containing a 2-3 cm layer of clean quartz sand and a further 33‰ artificial seawater 2-4 cm layer (depuration experiment group). Tanks were kept in a controlled temperature room (20°C), with a 12:12 light-dark cycle. The specimens were fed with Tetra Min marine fish food every 2 days, 6 hours before the renewal of water. Controlled conditions were maintained for 14 days, replacing the water every 2 days. Mortality was checked daily by gently disturbing the media with a spatula. Dead, damaged or mature (green) worms were removed from the experiment. Worms were considered dead when they no longer responded to mechanical stimulation. Subsamples of 12 animals were collected from all experimental groups after 3 and 14 days, kept for 24 hours in aquaria containing quartz sand and artificial sea water (33‰) to purge particles from intestine and then immediately frozen in liquid nitrogen and stored at -80°C until the biomarker and metal content analyses. At the same time sediments were also sampled to check for metal contents.

2.3 Chemical analysis

Metal concentrations (Cu, Cd, Zn) were determined with flame and furnace AAS (Varian SPECTRAA10, Perkin-Elmer SIMAA 6000) on pools of 3 specimens each after drying at 60 °C for 12 hours and total HNO₃ bomb digestion in microwave and on whole fresh sediments after hot nitric acid extraction under reflux (Bellucci *et al.*, 2002), respectively. This sediment-treatment was applied in order to extract the easily exchangeable and carbonate-associated metal, the metal in the interstitial water and the metal bound to organic matter. All results were referred on matrix-dry weight.

2.4 Hsp expression analysis

Protein western blot: pools of three specimens were created by combining metamers of the same size from individuals that were similar in length and weight. Frozen tissues (300–400mg) were homogenised on ice in 1ml of protease inhibitor cocktail. The homogenates were then centrifuged (13000g,

10min, room temperature). A subset of supernatants was used for protein determination. Total protein content was determined using the procedure described by Bradford (1976) with bovine serum albumin standard using a Jasco V-530 spectrophotometer. The remainder was diluted in sample buffer (12.5% 0.5 M Tris– HCl pH 6.8, 10% glycerol, 2% SDS, 0.5% 2-mercaptoethanol, 0.025% bromophenol blue) to a final protein concentration of 2 mg/ml for each sample and boiled for 5 min before loading. 30 micrograms of protein were loaded in each lane, separated by electrophoresis in a 12% SDS-polyacrylamide gel and electrophoretically transferred to PVDF membranes (0.2 mm pore size). The following primary antibodies were used: anti-HSP27 polyclonal antibody (pAb) (1:1000), anti-HSP60 pAb (1:1000), anti-HSP70 pAb (1:1000) and anti- β -tubulin mAb (1:1000) (Sigma-Aldrich). Immunoreactive bands were visualized using a NBT/BCIP detection system (Roche). Immunoblot images were acquired using a HP Scanjet 2300c digital scanner with default settings and analysed with ImageJ analysis software.

2.5 Statistical analysis

When normality of data (Shapiro-Wilk's test) and homogeneity of variances (Bartlett's test) could be established, the differences in metal content among the experimental groups, as well as the densitometric data, were assessed by one way-ANOVA, followed by the Duncan multiple comparison test. A statistical level of $p < 0.05$ was considered significant.

3 Results

3.1 Exposure media

Salinity (33 ± 0.5 S‰), temperature ($20 \pm 1^\circ\text{C}$) and dissolved oxygen (6.5 ± 0.5 mgO₂/l) were maintained constant throughout the entire experiment period. Cd, Cu and Zn contents of the whole fresh exposure-media (native sediment, Isola delle Tresse exposure-mud, and quartz sand artificial sediment) along the experiment-time are reported in Table 1. Cd and Zn concentrations in the exposure-sediment were tenfold higher than in native one, Cu values approximately twofold.

MEDIA	Cd	Cu	Zn
Native sediment	0.39	30.5	77.1
Quartz sand sediment	0.02	< 0.001	< 0.001
Isola delle Tresse sediment (T0)	4.37	59.8	633
Isola delle Tresse sediment (T14)	5.46	65.2	661

Tab 1 – Metal concentrations ($\mu\text{g/g}$) in the different media used in the experiments.

3.2 Bioaccumulation experiment

Metal concentrations in worms experimentally exposed to the mud from the Isola delle Tresse for 14 days are shown in Table 2. Only for Cd a clear bioaccumulation trend could be observed. A significant increase in concentration of Cd was detected in worms after 3 days and again after 14 days. Despite the considerably higher amounts of the metals levels in the exposure medium, in comparison to the native sediment from which the worms were collected, there was no significant variation in the concentration of accumulated Zn and Cu in the worms over the 14 day period. Clearly *P. cultrifera* shows to regulate Zn and Cu very efficiently, in respect of the concentrations it was exposed to.

Tab 2 – Tissue concentrations (mean value \pm s.d., $\mu\text{g/g d.w.}$) of metals in *Perinereis cultrifera* at different times of the bioaccumulation experiment. Three pools of 3 specimens each for every experimental group were analysed for metal content. * indicates a significantly higher concentration in comparison to the control group (ANOVA + Duncan post hoc multiple comparison test).

BIOACCUMULATION EXPERIMENT	Cd	Cu	Zn
Control (T0)	0,300 \pm 0,058	28,8 \pm 11,2	164 \pm 11
Isola delle Tresse sediment (T3)	0,701 \pm 0,069*	18,4 \pm 6,2	121 \pm 30
Isola delle Tresse sediment (T14)	0,732 \pm 0,004*	16,8 \pm 5,3	127 \pm 31

A significant difference in both hsp60 and hsp70 expression between animals collected from the control group and the animals exposed to the mud from the Isola delle Tresse for 3 and 14 days was detected (Fig.1 and Fig.2).

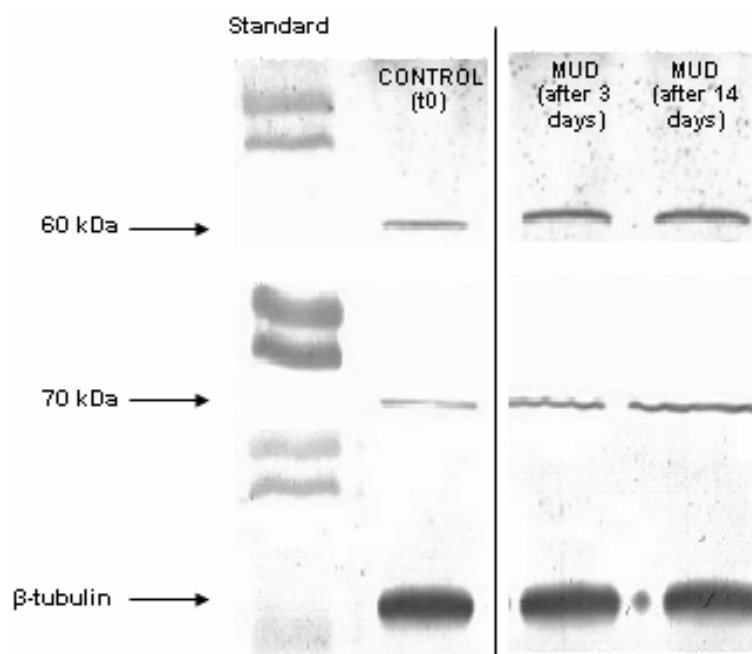


Fig 1 – An immunoblot of hsp60 and hsp70 in specimens of *P.cultrifera* (pools of 3 individuals each) (β -tubulin is shown as loading control) exposed to a highly contaminated sediment (bioaccumulation experiment).

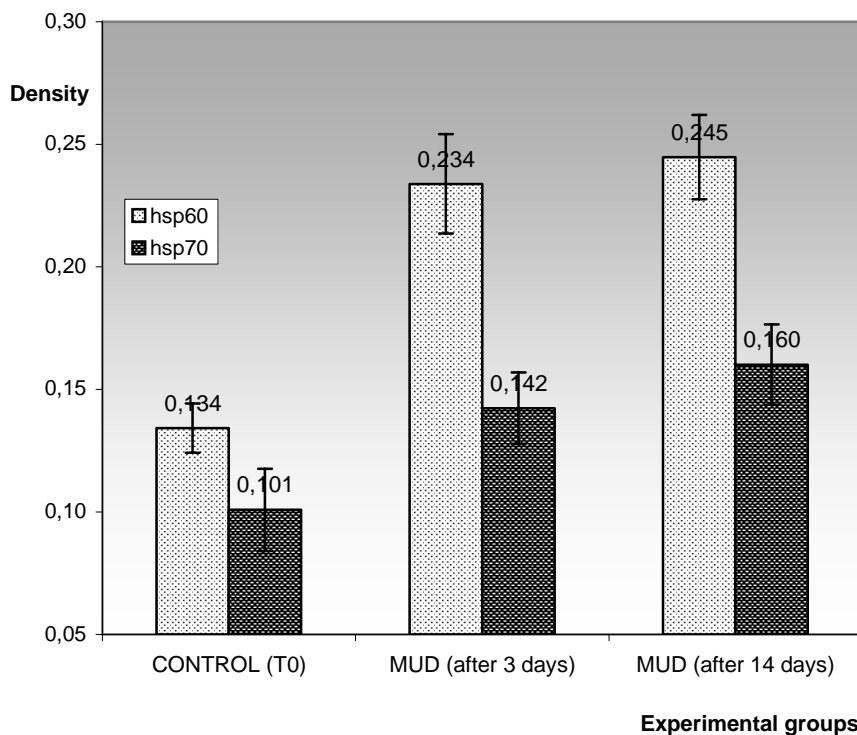


Fig 2 – Densitometric evaluation (mean + S.D. of blot densitometric analysis from four independent experiments) of the immunoblot of hsp60 and hsp70 in specimens of *P.cultrifera* from the 3 different experimental groups of the bioaccumulation experiment.

3.3 Depuration experiment

Metal concentrations in worms experimentally exposed to a metal-free quartz sediment are shown in Table 3. A significant decrease of the Zn levels was detected in worms after 3 days and again after 14 days, while no significant Cd or Cu variation occurred over the 14 day period.

DEPURATION EXPERIMENT	Cd	Cu	Zn
Control (T0)	0,300 ± 0,058	28,8 ± 11,2	164 ± 11
Quartz sand sediment (T3)	0,324 ± 0,113	23,7 ± 1,42	102 ± 13 *
Quartz sand sediment (T14)	0,348 ± 0,026	22,8 ± 0,82	84 ± 3 *

Tab 3 – Tissue concentrations of metals (mean value ± s.d., µg/g d.w.) in *P. cultrifera* at different times of the depuration experiment. Three pools of 3 specimens each for every experimental group were analyzed for metal content. * indicates a significantly lower concentration in comparison to the control group (ANOVA + Duncan post hoc test).

We didn't detect any significant difference in either hsp60 or hsp70 expression among animals collected at different times during the experiment (Fig.3 and Fig.4).

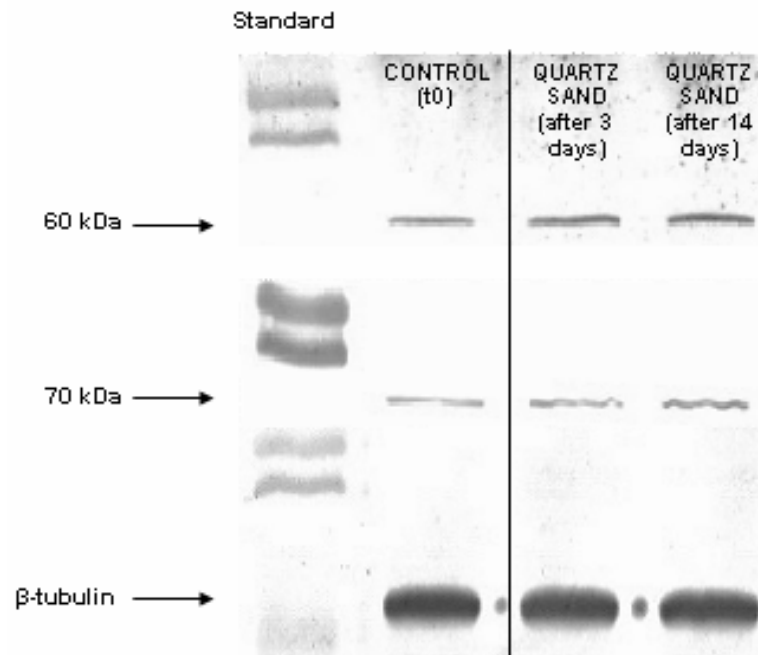


Fig 3 – Hsp60 and hsp70 expression in *P. cultrifera* during the depuration experiment. An immunoblot of hsp60 and hsp70 in specimens of *P. cultrifera* (pools of 3 individuals each) from the 3 different experimental groups of the depuration experiment (an immunoblot of β -tubulin is shown as loading control).

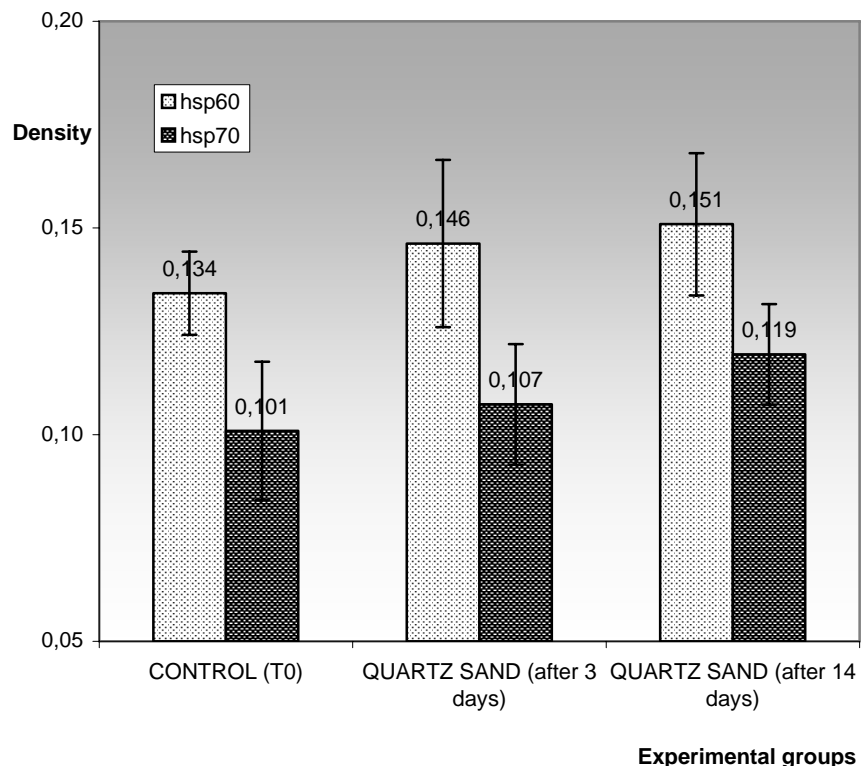


Fig 4 – Densitometric evaluation (mean + S.D. of blot densitometric analysis from four independent experiments) of the immunoblot of hsp60 and hsp70 in specimens of *P. cultrifera* from the 3 different experimental groups of the depuration experiment.

4 Discussion

Despite the considerably higher amounts of metals in the Isola delle Tresse exposure-mud in comparison to the sediment from which the worms were collected, *P. cultrifera* showed a significant bioaccumulation only for Cd, while

there was no significant variation in Zn or Cu levels. On the other hand a clear depuration under no-contamination conditions seemed to occur only for Zn. As suggested by many Authors (Marigomez *et al.*, 1995, Mason & Jenkins, 1995, Gibbs *et al.*, 2000) Cu and Zn can be sequestered by many invertebrates as electron-dense concretions. Cu-containing granules in the epicuticle cells and Zn-containing spherocrystals in cells of the gut wall have been described for the nereid *Hediste diversicolor* as a strategy to prevent metal toxicity, limiting metal bioaccumulation (Mouneyrac *et al.*, 2003). Zn has been found to accumulate also in jaws of nereids (Broomell *et al.*, 2006). Moreover Mouneyrac *et al.* (2003) suggested that the excretion of Zn may occur in *H. diversicolor* by exocytosis, via amoebocytes.

Similar detoxification mechanisms are hypothesisable also in the case of *P.cultrifera*, in which regulation processes were probably activated for these metals in place of bioaccumulation at the contamination levels experimented in the present study. Furthermore, Zn excretion was demonstrated by the depuration experiment.

In contrast, a Cd accumulation and no evidence of Cd excretion at the studied conditions were noticed. Demuyck *et al.* (2004) demonstrated for the nereid *Hediste diversicolor* the existence in the cells of the intestine of a cadmium-binding protein, the MP11, belonging to the group of hemerythrins and myohemerythrins, synthesized as a response to Cd exposures. Furthermore Berthet *et al.* (2003) have shown that *H. diversicolor* is able to bind Cd with metallothionein-like proteins, suggesting a different detoxification strategy in respect to Cu and Zn.

Evidence exists that, in addition to the environmental metal exposure conditions, the accumulation or depuration patterns depend also on the adaptation ability of the population considered and the metal-specific detoxification and regulation processes (Zhou *et al.*, 2003; Luoma and Rainbow, 2006; Geffard *et al.*, 2005; Virgilio *et al.*, 2005; Rainbow, 2007). Time-course of the environmental exposures is also an important variable to be considered, because slight and quick variations, like seasonal variations of the metal bioavailability, probably affect only the free-circulating portion of the internal metals without any induction of detoxification or sequestering processes (Luoma and Rainbow, 2005).

Moreover the short-term exposure experiments highlighted that an increased hsp60 and hsp70 expression occurred after only 3 days in higher contamination conditions than native ones, whereas no stress was caused by maintaining individuals in the metal-free artificial sediment. A rapid induction of stress proteins in invertebrates as a consequence of the exposure to heavy metals is well documented (Tedengren *et al.*, 2006). The effort to cope with stressors such as heavy metals and to keep a physiological fitness by the activation of detoxification systems is shown to cause an enhanced expression of hsp.

Conclusions

The short-term experiment highlighted the ability of the sediment-dwelling polychaete *P. cultrifera* to record quick variations on the metal availability in sediments, activating various physiological mechanisms depending on the contaminant considered. The preliminary results allow to indicate that *P. cultrifera* may be used as bioindicator species for sediment metal contamination taking in account both accumulation processes and the exposure/stress signals such as, in this case, an induced hsp expression.

References

- Amiard J.C., Geffard A., Amiard-Triquet C. and Crouzet C., 2007. Relationship between the lability of sediment-bound metals (Cd, Cu, Zn) and their bioaccumulation in benthic invertebrates. *Estuarine, Coastal and Shelf Science*, 72, 511-521.
- Argese E., Ghetti P.F., Volpi Ghirardini A., Cavallini L., Delaney E., Tagliapietra D. and Bettiol C., 1999. *H. diversicolor*, *N. succinea* and *P. cultrifera* (Polychaeta: Nereididae) as bioaccumulators of cadmium and zinc from sediments: preliminary results in the Venetian lagoon (Italy). *Toxicology and Environmental Chemistry*, 71, 457-474.
- Bellucci LLG, Frignani M., Paolucci D. and Ravanelli M., 2002. Distribution of heavy metals in sediments of the Venice Lagoon: the role of the industrial area. *The Science of the Total Environment*, 295, 35-49.
- Bernds D., Wubben D. and Zauke G.P., 1998. Bioaccumulation of trace metals in polychaetes from the German Wadden Sea: evaluation and verification of toxicokinetic models. *Chemosphere*, 37 (13), 2573-2587.
- Berthet B., Mouneyrac C., Amiard J.C., Amiard-Triquet C., Berthelot Y., Le Hen A., Mastain O., Rainbow P.S. and Smith B.D., 2003. Accumulation and soluble binding of cadmium, copper and zinc in the polychaete *Hediste diversicolor* from coastal sites with different trace metal bioavailabilities. *Archives Environmental Contamination and Toxicology*, 45, 468-478.
- Broomell C.C., Mattoni M.A., Zok, F. W., Waite J.H., 2007. Critical role of zinc in hardening of *Nereis* jaws. *J. Exp. Biol.*, 209, 3219-3225.
- De Moor J.M., Koropatnick D.J., 2000. Metals and cellular signalling in mammalian cells. *Cellular and Molecular Biology*, 46, 367-381.
- Downs C.A., Dillon R.T., Fauth J.E. and Woodley C.M., 2001a. A molecular biomarker system for assessing the health of gastropods (*Ilyanassa obsoleta*) exposed to natural and anthropogenic stressors. *Journal of Experimental Marine Biology and Ecology*, 259, 189-214.
- Downs C.A., Fauth J.E. and Woodley C.M., 2001b. Assessing the health of grass shrimp (*Palaeomonetes pugio*) exposed to natural and anthropogenic stressors: a molecular biomarker system. *Marine Biotechnology*, 3, 380-397.

Downs C.A., Fauth J.E., Halas J.C., Dustan P., Bemiss J. and Woodley C.M., 2002. Oxidative stress and seasonal coral bleaching. *Free Radical Biology and Medicine*, 33, 533–543.

Downs C.A., Fauth J.E., Robinson C.E., Curry R., Lanzendorf B., Halas J.C., Halas J. and Woodley C.M., 2005. Cellular diagnostics and coral health: declining coral health in the Florida keys. *Marine Pollution Bulletin*, 51, 558–569.

Franco J.L., Trivella D. B., Trevisan R., Dinslaken D.F., Marques M.R., Bainy A.C. and Dafre A.L., 2006. Antioxidant status and stress proteins in the gills of the brown mussel *Perna perna* exposed to zinc. *Chem. Biol. Inter.*, 160, 232–240.

Frangipane G., Volpi Ghirardini A., Collavini F., Zaggia L., Pesce A. and Tagliapietra D., 2005. Heavy metals in *Hediste diversicolor* (polychaeta: nereididae) and salt marsh sediments from the lagoon of Venice (Italy). *Chemistry and Ecology*, 21 (6), 441–454.

Geffard A., Smith B.D., Amiard-Triquet C., Jeantet A.Y. and Rainbow P.S., 2005. Kinetics of trace metal accumulation and excretion in the polychaete *Nereis diversicolor*. *Marine Biology*, 147, 1291-1304.

Geracitano L.A., Luquet C., Monserrat J.M. and Bianchini A., 2004. Histological and morphological alterations induced by copper exposure in *Laeonereis acuta* (Polychaeta, Nereididae). *Marine Environmental Research*, 58, 263-267.

Gibbs P.E., Burt G.R., Pascoe P.L., Llewellyn C.A. and Ryan K.P., 2000. Zinc, copper and chlorophyll-derivates in the polychaete *Owenia fusiformis*. *Journal of the Marine Biological Association of the United Kingdom*, 80, 235-248.

Luoma S.N., Rainbow P.S., 2005. Why is metal bioaccumulation so variable? Biodynamics as a unifying concept. *Environmental Science and Technology*, 39 (7), 1921-1931.

Marigomez I., Soto M. and Cajaraville M.P., 1995. Morphofunctional patterns of cell and tissue systems involved in metal handling and metabolism, in “ Cell Biology in Environmental Toxicology” by University of the Basque Country Press, Bilbao, Spain, 89-134.

Mason A.Z., Jenkins K.D., 1995. Metal detoxification in aquatic organisms, in “Metal speciation and bioavailability in aquatic systems” by Tessier A., Turner D.R. Editors, Wiley Publisher, Chirchester, 479-608.

Mouneyrac C., Mastain O., Amiard J.C., Amiard-Triquet C., Beaunier P., Jeantet A.Y., Smith B.D. and Rainbow P.S., 2003. Trace metal detoxification and tolerance of the estuarine worm *Hediste diversicolor* chronically exposed in their environment. *Marine Biology*, 143, 731-744.

Petersen K., Kristensen E. and Bjerregaard P., 1998. Influence of bioturbating animals on flux of cadmium on estuarine sediments. *Marine Environmental Research*, 45 (4/5), 403-415.

Prevedelli D., Simonini R, 2003. Life cycles in brackish habitats: adaptive strategies of some polychaetes from the Venice Lagoon. *Oceanologica Acta*, 26, 77-84.

Rainbow P.S, Poirier I., Smith B.D, Brix K.V. and Luoma S.N., 2006. Trophic transfer of trace metals: subcellular compartmentalization in a polychaete and assimilation by a decapod crustacean. *Marine Ecology Progress series*, 308, 91-100.

Rainbow P.S., 2007. Trace metal bioaccumulation: Models, metabolic availability and toxicity. *Environment International*, 33, 576–582.

Tedengren M., Olsson B., Bradley B. and Zhou L., 2006. Heavy metal uptake, physiological response and survival of the blue mussel (*Mytilus edulis*) from marine and brackish waters in relation to the induction of heat-shock protein 70. *Hydrobiologia*, 393, 261-269.

Virgilio M., Maci S. and Abbiati M., 2005. Comparisons of genotype-tolerance responses in populations of *Hediste diversicolor* (Polychaeta: Nereididae) exposed to copper stress. *Marine Biology*, 147, 1305-1312.

Wang W.X., Stupakoff I. and Fisher N.S., 1999. Bioavailability of dissolved and sediment-bound metals to a marine deposit-feeding polychaete. *Marine Ecology Progress Series*, 178, 281-293.

Zhou Q., Rainbow P.S. and Smith B.D., 2003. Tolerance and accumulation of the trace metals zinc, copper and cadmium in three populations of the polychaete *Nereis diversicolor*. *Journal of the Marine Biological Association of the United Kingdom*, 83, 65-72.

RESEARCH LINE 3.9

Pollutant flows in the lagoon carried by aerosols and atmospheric fall-out

AEROSOL FINE FRACTION CHARACTERISATION IN THE VENICE LAGOON

Franco Prodi¹, Franco Belosi¹, Daniele Contini², Gianni Santachiara¹, Antonio Donateo²,
Lorenza Di Matteo¹, Daniela Cesari²

1 Istituto Scienze dell'Atmosfera e del Clima, CNR, Bologna

2 Istituto Scienze dell'Atmosfera e del Clima, CNR, Lecce

Riassunto

In questo lavoro si riporta un'analisi per caratterizzare la frazione fine dell'aerosol sull'Isola di Mazzorbo nella Laguna di Venezia. I risultati della ricerca hanno permesso di approfondire le caratteristiche chimico-fisiche del particolato presente in Laguna, le possibili sorgenti ed il suo destino.

Ciò che emerge dalla ricerca è la presenza di aerosol costituito da solfati e nitrati di ammonio nella frazione fine (PM_{2.5} e PM₁) in concentrazioni paragonabili con siti urbani nella stagione invernale (la più critica da un punto di vista ambientale essendo caratterizzata da concentrazioni più alte di aerosol atmosferico rispetto a quella estiva) e con siti di fondo urbani nel periodo estivo. Inoltre per i solfati d'ammonio sono emerse indicazioni per un prevalente trasporto atmosferico su media distanza, con particolare riferimento alla Pianura Padana. Per i nitrati d'ammonio invece vi è un significativo contributo della generazione locale, da precursori derivanti da processi industriali e da emissioni dovute al traffico. È stata inoltre evidenziata la modesta presenza di aerosol marino. Per il cloro si rileva prevalentemente un arricchimento rispetto al contributo marino, e quindi sono state ipotizzate diverse sorgenti: emissioni industriali e possibili emissioni dalla laguna, per l'abbondanza di questo elemento nelle acque lagunari a seguito dei processi di potabilizzazione che utilizzano composti clorurati. I solfati sono prevalentemente di origine antropogenica, con un contributo (circa il 10%) della componente biogenica marina. Questa deriva dalla ossidazione in atmosfera di di dimetilsolfuro (DMS) emesso dalla acque del mare, prodotto in processi metabolici che interessano il fitoplankton marino. Questo composto viene ossidato in atmosfera con produzione di acido metansolfonico (MSA) e di solfati.

Le misure in continuo di particolato fine (PM_{2.5}) hanno evidenziato la presenza di un andamento giornaliero nella concentrazione che presenta un minimo nelle ore più calde. Questo andamento è presente sia nel periodo primaverile ed estivo sia in quello invernale pur in presenza di valori assoluti diversi della concentrazione di PM_{2.5}: maggiori in inverno rispetto all'estate. Il ciclo giornaliero della concentrazione è inoltre correlato con l'andamento giornaliero dell'umidità relativa e con il regime di brezza presente in laguna (notturna e di mare). È stata osservata una buona correlazione fra l'andamento giornaliero medio delle concentrazioni e l'altezza dello strato limite (valutata in maniera

indiretta dalle misure al suolo) specialmente nella fase di evoluzione diurna (dalle 0am alle 4pm). È stato osservato anche un pattern stagionale dei flussi verticali turbolenti con i casi di deposizione maggiormente presenti nel periodo primaverile ed estivo mentre nel periodo invernale sono stati invece osservati flussi verticali turbolenti prevalentemente positivi. Le indicazioni dell'aerosol optical thickness (AOT) del fotometro di AERONET sono state correlate con eventi di trasporto a medio raggio.

Abstract

In this work a characterisation of fine aerosol on the Mazzorbo Island in the Venice Lagoon is presented. Results allowed getting information about the physical/chemical characteristics of fine aerosol, the possible sources and its fate. The research results show winter concentration levels of ammonium nitrate and sulphate, in the fine fraction of the aerosol (PM1 and PM2.5) comparable with urban site and summer concentrations comparable with urban background site. Furthermore the ammonium sulphate might be transported from the Po Valley; instead the ammonium nitrate is locally produced through traffic and industrial emissions. The marine aerosol concentration is low. The content of chlorine in the aerosol particle is higher than expected from marine environment (considered on the basis of Cl/Na ratio), therefore specific sources for the element have been suggested: industrial emissions and possibly emissions from the municipality water treatment plant. Sulphate from sea water through oxidation of DMS (originated from marine fitoplankton metabolism processes) are not negligible (about 10% of the anthropogenic sulphate).

Real time measurements of PM2.5 put in evidence a short-term (daily) pattern with a lower average concentration during day-time with respect to night-time. This pattern has been measured in spring, in summer and in winter, although the absolute concentration levels are different: higher in winter respect to the spring and summer. Furthermore the daily pattern is well correlated with the daily relative humidity pattern and with the local breeze regime. The daily average PM2.5 concentration is correlated with the boundary layer altitude (obtained from indirect ground measurements) particularly in the diurnal trend (from 0am to 4pm). The vertical turbulent fluxes of PM2.5 also show a seasonal pattern with higher deposition fluxes (towards ground) in spring and summer with respect to the winter season. The optical aerosol thickness (AOT) from AERONET sun photometer network has been correlated with middle range transport events

1 Introduction

The most important processes responsible of the contamination of the Venice Lagoon are the direct injection of industrial effluents in water, sewage from the city and its hinterland, the atmosphere-water exchanges of pollutants, the inflow of rivers and the water-sediments exchanges and the emission from motorboats. In addition it should be considered the exchange of pollutants between the Lagoon and the Adriatic Sea at any tidal cycle. In this work we

analyze the results from the study on the chemical and physical characterization of the aerosol by considering the fine fraction (PM_{2.5} and PM₁). Three experimental campaigns have been carried out at Mazzorbo (northern part of the Venice Lagoon), aimed at the aerosol characterization: from 30th June to 21st July 2004, from 15th February to 10th March 2005 and from 8th May to 25th May 2006. Measurements have been carried out in order to have a physical and chemical characterization coupled with a real-time analysis of concentrations and vertical turbulent fluxes (with the eddy-correlation method). The experimental set-up allows getting information about the diurnal and seasonal pattern of concentrations and fluxes and physical/chemical properties of fine aerosol and how these patterns are correlated with local meteorological parameters thereby improving the knowledge of sea/air exchange of fine aerosol in the Venice Lagoon.

2 Measurement site and experimental set-up

Measurements have been carried out at an extra-urban site placed on island of Mazzorbo in the Venice lagoon. The site is a field (45° 29' 09.5" N, 12° 24' 12.7" E) located at about 8 km NE of the town of Venice. Instruments for real time measurements of PM_{2.5} concentrations and vertical turbulent fluxes were mounted on a horizontal bar placed at the top of a telescopic mast at 9.6m above the ground. The measuring station is based on a three-dimensional ultrasonic anemometer, Omnidirectional R3 (Gill Instruments), operating at 100 Hz in calibrated mode. A low response thermo-hygrometer Rotronic MP100A (Campbell Scientific) is used to detect relative humidity and air temperature. The optical aerosol sensor used is a pDR-1200 (Personal Data logging Real time Aerosol Monitor) by Thermo Electron - Mie Corp. (Chakrabarti et al., 2004). The pDR-1200 was operating in active sampling at 1 Hz using a pump (TECORA Bravo H-Plus) and a cyclone (2.5 µm cut-off at the 4l/m flow-rate used). The first-order time response of the pDR-1200 (about 1.1s) is enough to obtain detailed information about turbulent phenomena and, in particular, about PM_{2.5} turbulent fluxes (Donateo et al, 2006). Concentration measured by the pDR-1200 have been corrected for the effect of relative humidity by using an apposite procedure (Donateo et al, 2006) that allows to obtain a reasonable correlation (Pearson coefficient 0.93) with reference gravimetric measurements taken in the observation site.

The aerosol has also been sampled by means of a size spectrometer (INSPEC) for PIXE analysis and a low volume sampler for the assessment of the soluble fraction. The INSPEC samples the aerosol on Nuclepore filters (0.1 µm porosity) and separates the particles on the basis of their aerodynamic size. After the sampling the filters were analysed at the electronic microscope (SEM interfaced with EDAX) and with the PIXE - Particle Induced X-ray Emission.

The fine aerosol fraction has been obtained in the second and in the third campaign by means respectively of a cyclone with a cut-off size at 1µm and a low volume sampler (PM_{2.5}). The aerosol, collected on teflon and nylon filters in order to collect the particles and the semivolatile fraction (Kerminen et al. 2000), were analyzed with the ion chromatograph. The aerosol sampled on the

filter packs has been extracted by means of an ultrasonic bath in 10 ml of Milli-Q water, filtered through a 0.45 μm porosity membrane filter, and successively injected into the chromatographic column (Dionex DX 120). The determination of the inorganic cations has been carried out through a CG12A column followed by the Dionex CS12A. The columns allow the simultaneous assessment of the monovalent and the bivalent species. The analysed ion species have been Cl^- , NO_2^- , NO_3^- , SO_4^{2-} , Na^+ , NH_4^+ , K^+ , Mg^{2+} , Ca^{2+} . Among the organic compounds only the MSA was analysed by means of a Dionex DX 500 chromatograph with a Dionex AS11 column preceded by a AG11 column.

3 Aerosol characterization

The results show that sulphate and ammonium nitrates are largely present in the soluble fraction of PM1 and PM2.5 particulate. In PM2.5 the sum of concentration of NH_4^+ , SO_4^{2-} and NO_3^- (anthropogenic ions) is a percentage of aerosol concentration, that varies from 51% to about 100%. From a comparison between the values measured in Venice Lagoon and the ones measured in different European cities, reported in literature, it can be asserted that:

- SO_4^{2-} and NH_4^+ ions concentrations are comparable, both in spring and winter campaigns, with the ones measured in other cities, as Zurich (Hueglin et al., 2005) - PM2.5 average annual value = $19 \mu\text{g m}^{-3}$, Barcelona (Querol et al., 2001) sited on the coast, Birmingham (Turnbull et al., 2000) with high industrial activity (measurements in a park). Sulphates are very lower than those measured in Milan (Giugliano et al., 2005).
- Nitrates concentrations in winter campaign (about $9 \mu\text{g m}^{-3}$, with a range $5\text{-}12 \mu\text{g m}^{-3}$) and in spring campaign (about $3.5 \mu\text{g m}^{-3}$) are comparable with the values measured in Milan (background zone) in the same seasonal period. Higher concentration in winter period depends on the greater concentration of NO_x and on a longer average life time for nitrates (greater stability with lower temperature). Nocturnal samples contain higher nitrate concentrations (average $6.1 \mu\text{g m}^{-3}$) than diurnal ones (average $3.1 \mu\text{g m}^{-3}$). This pattern is in agreement with the results obtained in other European cities, and it is probably due to the high volatility of NH_4NO_3 ; therefore its stability is favoured by low temperatures and high relative humidity (r.h.=62%) frequent during night-time.
- Concerning sulphates there are no differences between diurnal and nocturnal samples, and in particular in all measurements there is a limited variability. Sulphates production should be theoretically greater during day and in general during summer period, because in this period there is a great photochemical production of OH radicals. Mean value in winter period ($3.3 \mu\text{g m}^{-3}$) is comparable to that in spring campaign ($4.4 \mu\text{g m}^{-3}$). There is also a contribution to sulphates deriving from oxidation of dimethylsulfide (DMS) produced in seawater from the activity of various phytoplanktonic species. From measured value of MSA

(methanesulfonic acid) that is the final product, with sulphates, of DMS oxidation process. It has been estimated a contribution of this source to anthropogenic sulphate of about 10%. Greater stability of sulphates respect to nitrates is indicative of a regional transport.

- Marine aerosol contribution, estimated from sodium concentrations, is very low. Ratio Cl^-/Na^+ , generally higher than sea-water value, indicates an anthropogenic source for chlorine (i.e. industrial activities or combustion process). Probably there is an additional chlorine source in atmosphere from the city drainage water, as potable water is treated with chlorine (about 120.000 kg/year of chlorinate compounds).

In Fig.1 correlation between nitrate or sulphate concentrations versus ammonium levels are reported, respectively for winter and spring period. Concentrations are expressed as microequivalent per cubic metre.

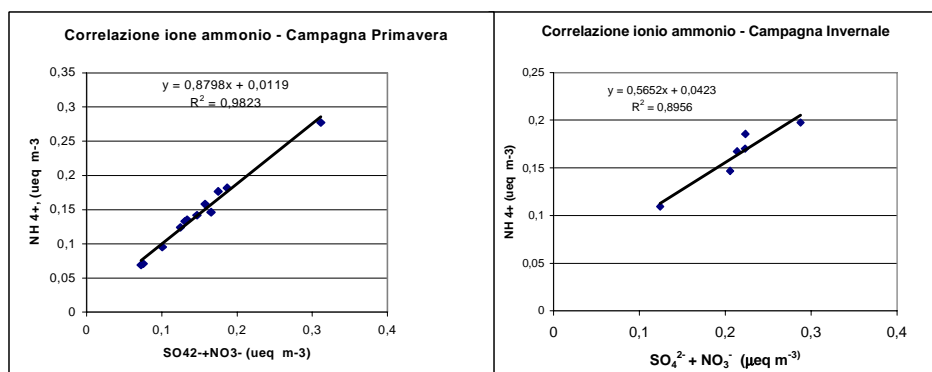


Fig 1 – Correlation between sulphates and nitrates versus ammonium concentration for winter and spring period, respectively.

Elemental analysis performed with PIXE technique on filters sampled with INSPEC (this method can obtain particles dimensional distributions, based on aerodynamic diameter) shows that there is, generally, a variable percentage of elements in different size ranges. For example for sulphur, an element of anthropogenic origin, the minimum ratio between fine and coarse fraction, deduced from PIXE analysis, is about 20%, while maximum ratio is about 60%. In spring campaign mean total sulphur concentration in $\text{PM}_{2.5}$ ($1,6 \mu\text{g m}^{-3}$) is the same that in soluble fraction ($1,5 \mu\text{g m}^{-3}$), so it is possible to deduce that sulphur in this size range is constituted by sulphates from a gas to particle process (reaction of H_2SO_4 with NH_3).

It has been noted that in all examined filters the ratio between fine and coarse fraction for S is similar to that for Fe. This indicates, probably, a similar source for Fe and S in coarse fraction. Si and Ca, typical crustal element, are present especially in coarse fraction. Na, Mg are present especially in fine fraction and in some case in coarse fraction. Marine aerosol can be found mostly in coarse fraction

From a comparison with other measurements in different Italian cities (Firenze, Genova, Milano, Napoli) (D'Alessandro et al., 2003) it can be deduced that Pb, Fe and Mn have lower values, Zn and Ni have similar concentration, while Cr is present with greater concentration respect to the mentioned cities.

Vehicular traffic is the most likely responsible for presence of Pb in air, so

reported concentrations indicate that there is a pollution transport from near area, but not prevalent. Also Mn and Fe can be partially associated with vehicular traffic, while Cr high concentration with respect to urban area is due to industrial activity.

Histogram in Fig. 2 reports metal concentrations (ng/m^3) obtained with PIXE technique in the PM10 fraction.

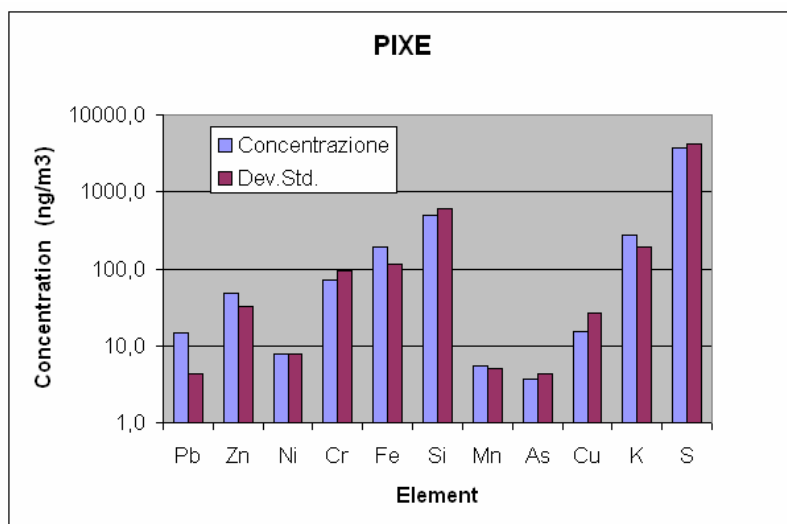


Fig 2 – Elemental concentration in the PM10 fraction.

4 PM2.5 concentrations and turbulent fluxes

Optical PM2.5 measurements have been processed on 30 minutes averages in the “streamlines” reference system. A correction of the effect of relative humidity and a linear detrend (Rannik & Vesala, 1999; Buzorius et al., 1998) was used before the calculation of the vertical turbulent fluxes with the eddy-correlation method. A stationarity test has been performed, in particular the one reported in Mahrt (1998), applied to particulate concentration time series. The percentage of instationary data, characterized in this way, is relatively small: 4.9% in summer campaign, 7.1% in winter campaign and 6.3 in spring campaign.

Results indicate that several concentration peaks, especially in the summer, are associated to a structure of the vertical turbulent fluxes in which a deposition is observed during the build-up of the concentration peaks followed by positive fluxes indicating a mixing with clean air present above the measurement height. In summer period, and to some extent also in spring, the behavior of wind direction put in evidence a general circulation with wind blowing from NE during the night (from Alps mountains) and wind blowing from SE during the day (from Adriatic Sea) similarly to the results of Camuffo (1981). The transition from NE to SE is usually happening between 9am and 11am and the opposite transition from SE to NE is usually happening between 11pm and 1am. In the period in which circulation from NE and SE is present the wind speed is generally lower. In Figure 3 wind roses are reported for three measurement periods. It can be noted an evident similarity between measurement taken in spring and summer, during which dominant wind direction are from SSE-SE and NNE-NE sector, while in winter period wind from SSE-SE sector is less frequent.

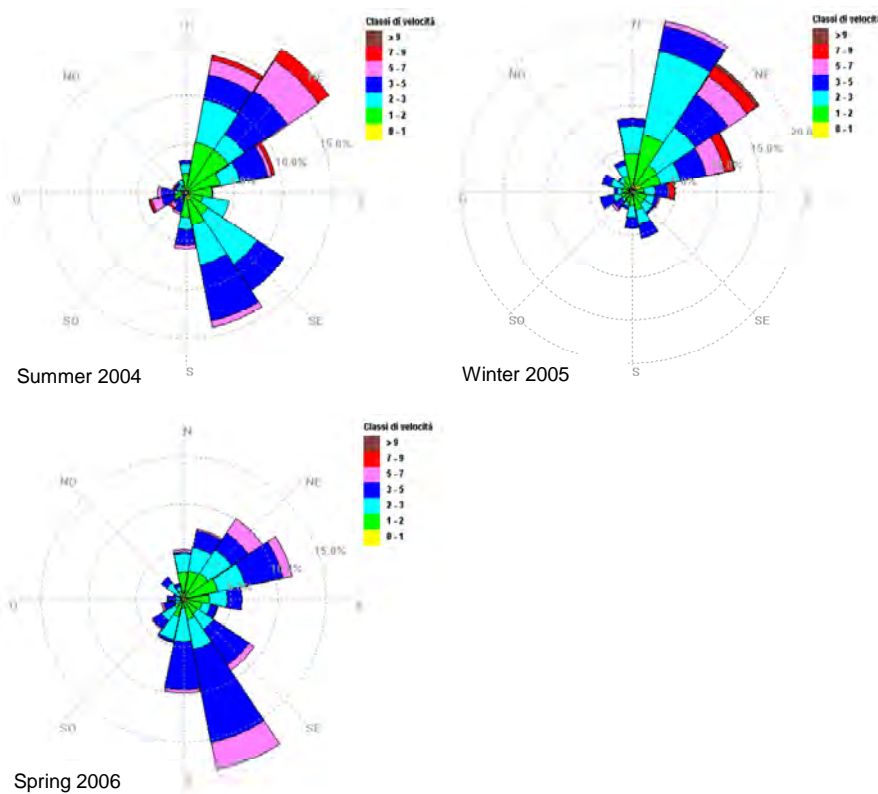


Fig 3 – Wind roses of the three measurements periods.

In Figure 4 time series of PM2.5 concentration and vertical turbulent flux relative to spring period (2006) from 12/05/2006 to 23/05/2006 is reported. In the mentioned period there are several cases of deposition often associated to relatively short concentration peaks.

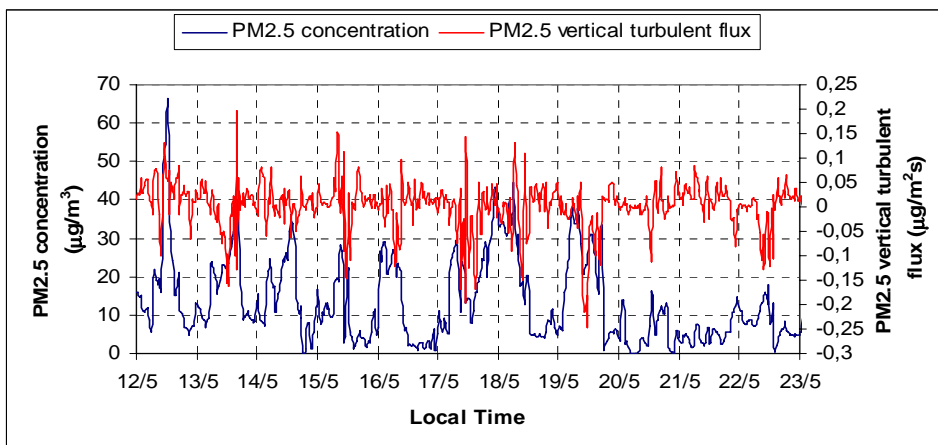


Fig 4 – Example of PM2.5 concentration and vertical turbulent flux measured during the spring campaign in 2006.

A comparison between average PM2.5 concentration has been realized for three measurement periods (summer, spring and winter) and for all data together (Table 1). A mean value for all data is equal to 27.5 $\mu\text{g}/\text{m}^3$ with a average mass level larger in winter period (41.8 $\mu\text{g}/\text{m}^3$) with respect to summer (16.7 $\mu\text{g}/\text{m}^3$) and spring campaign (16.9 $\mu\text{g}/\text{m}^3$). Thus a seasonal pattern is present with PM2.5 concentrations generally higher in winter with respect to summer and spring. This pattern is very typical in the north of Italy and it is observed also in other sites (Marcazzan et al, 2001). Results also indicate that

PM2.5 concentrations are generally higher during night-time with respect to day-time (Table 1).

$(\mu\text{g}/\text{m}^3)$	Mean Conc. All day	Mean Diurnal Conc. (8am-8pm)	Mean Nocturnal Conc. (8pm-8am)
Summer 2004	16.7	14.2	19.2
Winter 2005	41.8	36.3	48.0
Spring 2006	16.9	15.7	18.4
All data	27.5	24.3	31.6

Tab 1 – Average PM2.5 concentration for all the day and separately for night-time (8pm-8am) and day-time (8am-8pm).

The daily patterns of PM2.5 concentration and flux are reported in Fig. 5 for the three measurement periods. The graphs clearly show that the seasonal pattern is not only in concentration levels but also in the turbulent fluxes with positive fluxes prevalent in the winter and negative fluxes prevalent in the spring and summer periods. On average the vertical turbulent fluxes (positive or negative), that indicate an aerosol exchange between surface and atmosphere, are different from zero during day-time hours where the turbulence is more intense and atmosphere is locally unstable.

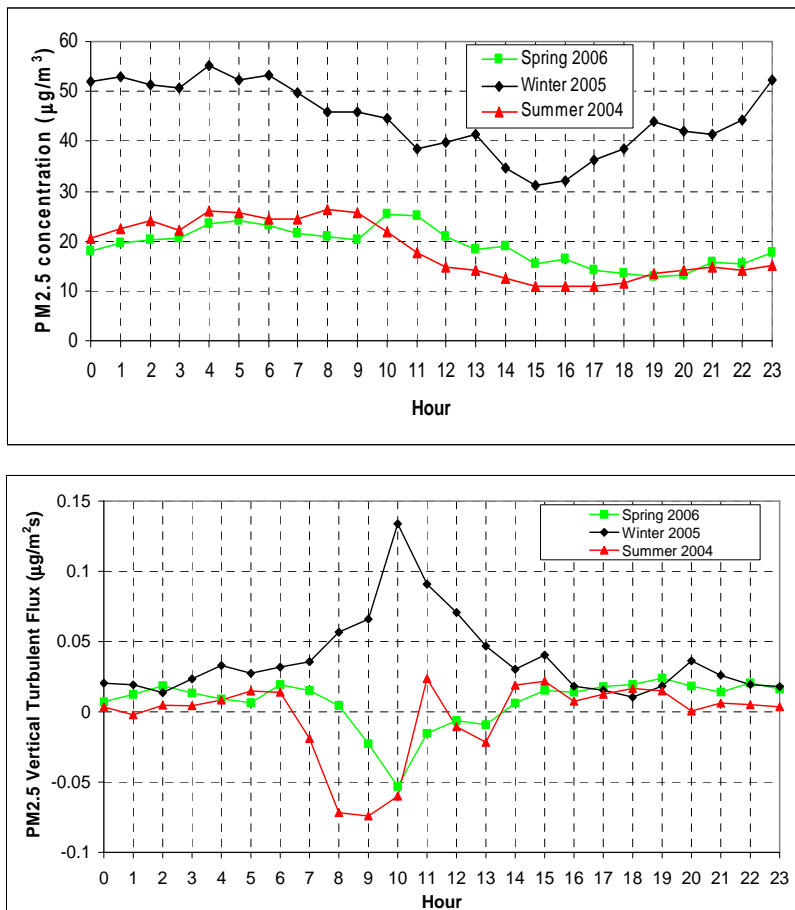


Fig 5 – Daily patterns of PM2.5 concentration (top) and vertical turbulent flux (bottom).

To put in evidence this daily pattern of PM2.5 concentration with respect to the seasonal change the mean daily pattern for hourly concentration fluctuations C_f is obtained with respect to daily average, as:

$$C_f = \frac{C - \langle C \rangle_{daily}}{\langle C \rangle_{daily}},$$

where C is hourly concentration. In Figure 6 the pattern of C_f is reported. It is clearly present a daily pattern, similar for the different measurement periods, although PM2.5 concentration is higher in winter. In general this pattern is characterized by a decrease in mass concentration from 9am until late afternoon, when a minimum concentration is reached.

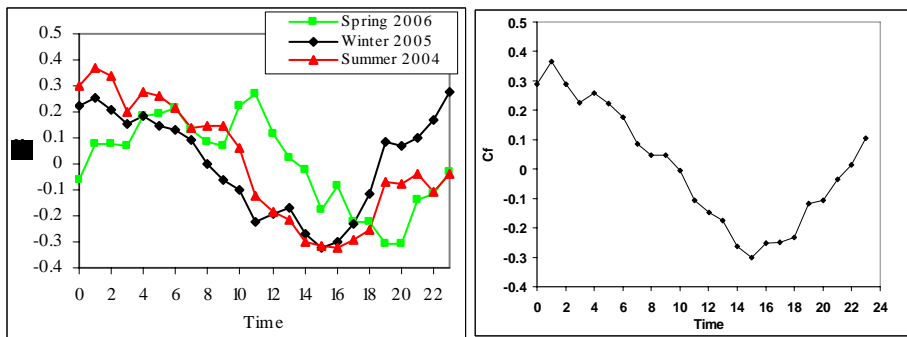


Fig 6 – (left) Daily patterns of PM2.5 concentration fluctuations for the different periods and (right) the cumulative pattern.

In order to obtain more detailed information about aerosol dynamics, and about aerosol sources or sinks, the concentration levels as well as the vertical turbulent fluxes have been correlated with wind speed and direction. Our results show that low wind velocities are generally associated to higher level of PM2.5 mass concentration (above $20 \mu\text{g}/\text{m}^3$), especially in winter and summer season. However the daily pattern of wind velocity is different from the one of concentration and it is therefore not correlated. To have mean pattern of concentration vs wind direction, average value has been calculated of PM2.5 concentration, in correspondence of certain intervals in wind direction. Intervals in wind direction have been determined in 30° steps. Results, reported in Figure 7, show an increase in average concentration for wind direction from SW-NW sector, overall in winter and summer, while an almost uniform pattern is present in spring period.

The daily pattern of prevalent wind direction is affected by local breeze and it is well correlated (Pearson -0.86 on average terms) with the pattern of concentration as shown in Figure 8.

The height of turbulent atmospheric boundary-layer, H, is characterized by a typical diurnal cycle, increasing during day-time because of the heat flux from the surface and strongly decreasing during the night. Boundary-layer height can influence ground level concentration therefore we correlated the observed diurnal pattern with an estimate of H. A one-dimensional model for the calculation of time dependent boundary layer height was used.

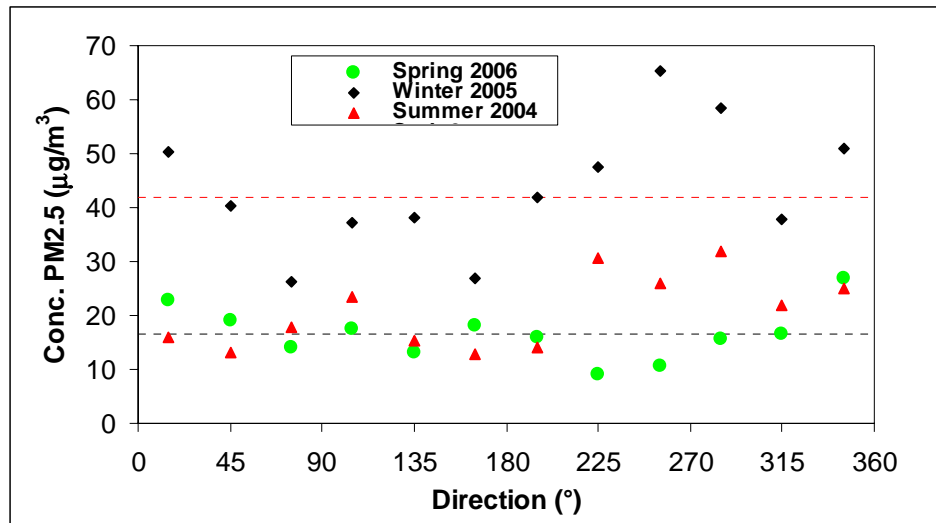


Fig 7 – Average PM2.5 concentrations as function of wind direction.

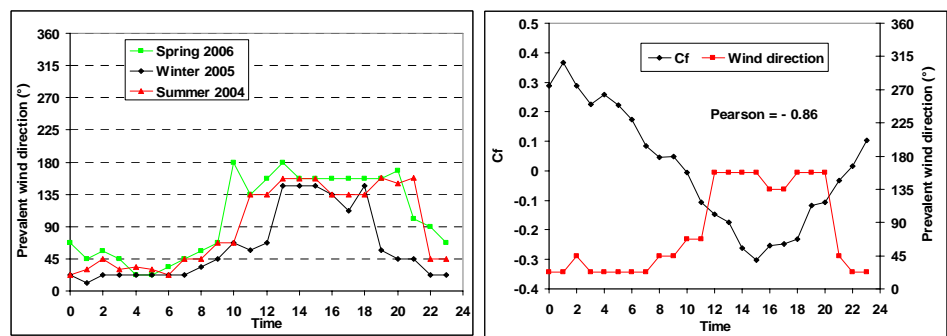


Fig 8 – (left) Daily patterns of prevalent wind direction and (right) comparison with the PM2.5 concentration pattern.

The model is based on point surface data (Martano & Romanelli, 1997) and it attempts to join together already existing models for convective boundary layer growth [Batchvarova & Gryning, 1991 et 1994], stable boundary layer (SBL) decay [Tennekes and Nieuwstadt, 1981] and surface inversion height development [Yamada, 1979]. The algorithm uses a stationary solution that allows the reduction of the problem to a direct integration in time. The model needs wind, temperature, heat flux and momentum flux, hourly averaged, as input data. The algorithm divides the diurnal cycle in two parts: night-time and day-time, according to the sign of the sensible heat flux at the surface (negative or positive respectively). The other parameter needed in the calculation routine is the potential temperature lapse rate $\gamma = \partial\theta/\partial z$ above the temperature inversion at sunrise, which is the only not surface quantity that remains to be given as model input. During the summer and spring campaign Sodar-Rass measurements were available from Ente Zona Industriale di Porto Marghera and the daily lapse rate was calculated from an analysis of the hourly Rass measurements at sunrise time. For the winter campaign Sodar-Rass measurements were unavailable so that the average lapse rate of all the measurement period has been calculated by using the temperature profiles of radio soundings performed at Udine airport. From this radio soundings an average value, for whole period, of $0.003 \text{ }^\circ\text{Km}^{-1}$ has been calculated and used in the model. Calculated values of H indicate that there are several periods in

which H and C are correlated (at hourly level), especially in the summer period, but also other in which this correlation is not present and this means that the growth of the boundary-layer is not the only driving force of concentration changes. This is likely because changes in the sources and in the meteorological conditions are also present and they affect environmental concentrations. To put in evidence the correlation between the daily concentration pattern and the evolution of the boundary layer a calculation of the typical daily pattern of the fluctuations H_f in the hourly boundary layer height has been evaluated as:

$$H_f = \frac{H - \langle H \rangle_{\text{daily}}}{\langle H \rangle_{\text{daily}}}$$

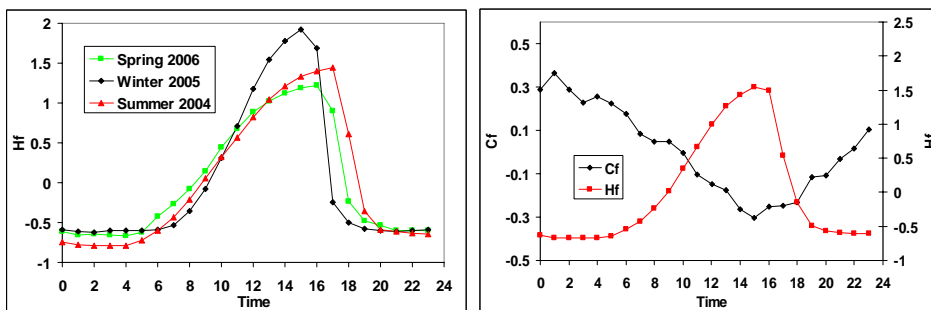


Fig 9 – (left) Daily patterns of calculated boundary-layer height and (right) comparison with PM2.5 concentration pattern.

Results are reported in Figure 9 and they show a good correlation (Pearson coefficient -0.78) between the two patterns. The correlation coefficient increases up to -0.97 if it is calculated only from 0am to 16pm, so mainly during the phase of growth of the boundary-layer at the sunrise. This is expected because early in the morning and during most of the day the boundary-layer is actually growing from the bottom, because of the convective turbulence, and the pollution that was trapped near the ground during the night is mixed in a much larger volume. At sunset there is not a compression of the boundary layer but it takes place the formation of a new stable boundary layer, which again starts near the ground and it is not coupled with the residual layer above in which the turbulence tends to decrease. The newly formed boundary layer will develop during the night, trapping again part of the atmospheric pollution near the ground, and it will start again to grow at the next sunrise. Therefore the correlation is good when the nocturnal boundary layer is established and it will develop during the next day; the correlation is instead poor when the new boundary-layer is created near the ground.

Daily RH pattern is also strongly correlated with PM2.5 concentration pattern (Pearson 0.86) as shown in Figure 10. Thus a consistent interaction exist between water vapour and particulate concentration, essentially in two ways: size growth of aerosol by hygroscopic aerosol and nucleation events with nitrates formation that is favourite by the presence of high relative humidity values.

Fig 10 – (left) Daily patterns of relative humidity and (right) comparison with PM2.5 concentration pattern.

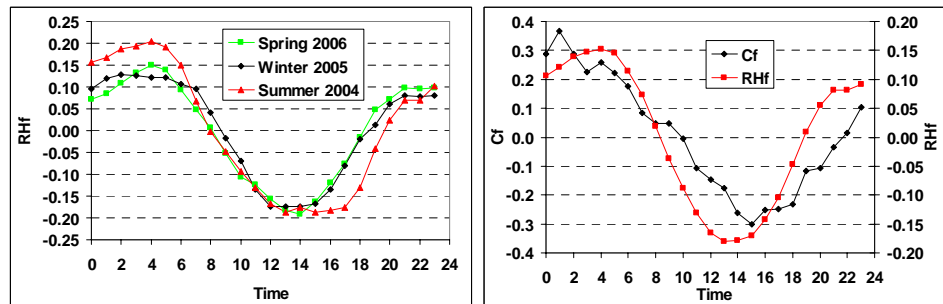


Fig. 11 shows the fine fraction (PM2.5) daily average, obtained during the first campaign, against the Aerosol Optical Thickness (AOT) from AERONET. For comparison also the daily total particle concentration (PTS) from Campagna Lupia station (Ente Porto Industriale Porto Marghera) are shown. It can be seen the correlation between the concentration levels of PM2.5, PTS and the AOT both for high concentration days (July 8th and 23rd) and for low concentration ones (July 11th and 28th).

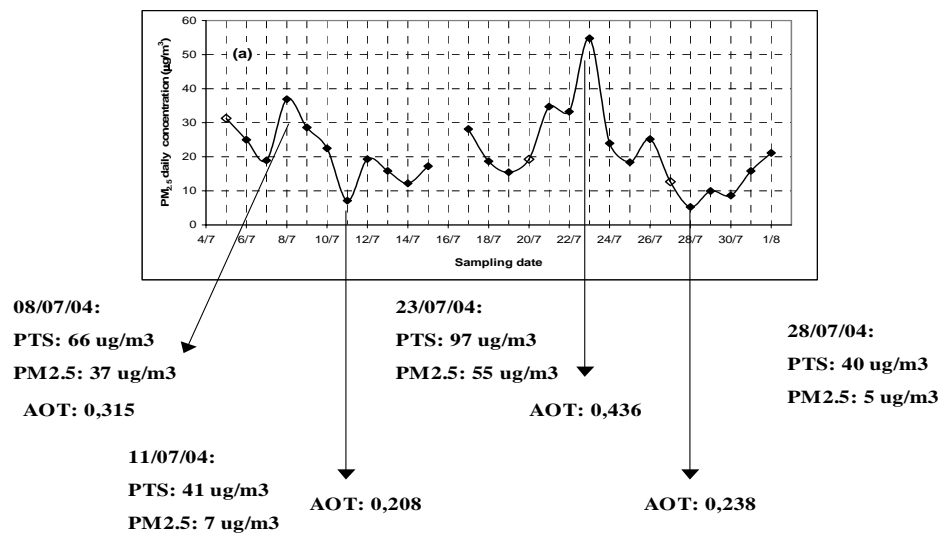


Fig 11 – Daily concentration of particle fine fraction, PTS and AOT during the first experimental campaign.

Conclusions

In this work an analysis of fine aerosol characterisation on the Mazzorbo Island in the Venice Lagoon is presented. Results gave information about the possible sources of fine aerosol and its fate. The analysis shows low levels of marine aerosol and the presence of particles rich in chlorine as a probable consequence of local emissions: industrial processes and water treatment. Sulphate from sea water through oxidation of DMS (originated from marine fitoplankton metabolism processes) are not negligible (about 10% of the anthropogenic sulphate). Ammonium nitrate is likely locally produced through traffic and industrial emissions instead ammonium sulphate might be transported from the Po Valley indicating the presence of middle range transport of aerosol towards the Venice Lagoon.

Real time measurements of PM2.5 put in evidence a seasonal pattern in concentration (with higher level in winter) and in the vertical turbulent fluxes with

a prevalence of positive fluxes during winter and a prevalence of negative fluxes during spring and summer. Results also show a short-term (daily) pattern with a lower average concentration during day-time with respect to night-time. Day-time hours are also the period in which happens most of the aerosol exchange between surface and atmosphere. The normalised concentration pattern is similar in the different measurement periods and it is well related to meteorological parameters: prevalent wind direction, relative humidity and boundary-layer height especially in the phase of growth of the boundary-layer at sunrise. This means that the local micro-meteorology is likely responsible of the presence of this pattern modulating the atmospheric concentration levels.

The optical aerosol thickness (AOT) from AERONET sun photometer network has been correlated with middle range transport events

Acknowledgments

Authors wish to thank the Ente Zona Industriale di Porto Marghera (via delle Industrie, 19 - 30175 Porto Marghera, VE) for providing some meteorological data, Dr. G. Zibordi (JRC, Ispra) for providing Aeronet data, Dr. M. Snells and Mr. M. Morbidini (ISAC-Rome) for their help with the LIDAR measurements, Mr. G. Trivellone, M. Tercon (ISAC-Bologna), Mr. Italo Ongaro (Università Ca' Foscari di Venezia) and Mr. F. Grasso (ISAC-Lecce) for their technical support. Authors also wish to thank Dr. F. Luccarelli (Univ. of Florence) for the PIXE analysis, Dr. R. Udisti (Univ. of Florence) for the Ion Chromatograph investigations and Mr. S Berti (Univ. of Bologna) for the SEM observations.

References

- Batchvarova, E & Gryning, S 1991. Applied Model for the growth of the daytime mixed layer. *Boundary Layer Meteorology*, 56, 261-274.
- Batchvarova, E & Gryning, S 1994. Applied Model for the height of the daytime mixed layer and the entrainment zone. *Boundary Layer Meteorology*, 71, 311-323.
- Buzorius G., Rannik U. Makela J.M., Vesala T., Kulmala M., 1998. Vertical aerosol particle fluxes measured by eddy covariance technique using condensational particle counter. *J. Aerosol Sci.*, 29, 157-171.
- Camuffo D., 1981. Fluctuations in wind direction at Venice, related to the origin of the air masses. *Atmospheric Environment*, 15, pp. 1543-1551.
- Chakrabarti B., Fine M.P., Delfino R., Sioutas C., 2004. Performance evaluation of the active-flow personal DataRAM PM2.5 mass monitor (Thermo Anderson pDR-1200) designed for continuous personal exposure measurements. *Atmospheric Environment*, 38, 3329-3340.
- D'Alessandro A., Lucarelli F., Nava S., Zucchiatti A., 2003. Hourly elemental composition and sources identification of fine and coarse PM10 particulate matter in four italians towns. *J.Aerosol Sci.*, 34, 243-259.

Donateo A., D.Contini, F.Belosi, 2006. Real time measurements of PM_{2.5} concentrations and vertical turbulent fluxes using an optical detector. *Atmospheric Environment*, 40, 2006, pp. 1346-1360.

Giugliano M., Lonati G., Butelli P., Romele L., Tardivo R., Grosso M., 2005. Fine particulate at urban site with different traffic exposure. *Atmospheric Environment*, 39, 2421-2431.

Hueglin C., Gehrig R., Baltensperger U., Gysel M., Monn C., Vonmont H., 2005. Chemical characterisation of PM_{2.5}, PM₁₀ and coarse particles at urban, near-city and rural sites in Switzerland. *Atmospheric Environment*, 39, 637-651.

Kerminen V.M., Tienila K. and Hillamo R., 2000. Chemistry of sea-salt particles in the summer Antarctic atmosphere. *Atmospheric Environment*, 34, 2817-2825.

Mahrt L., 1998. Flux Sampling Errors for Aircraft and Towers. *Journal of Atmospheric and Oceanic Technology*, 15, pp. 416-429.

Marcazzan G.M., Vaccaro S., Valli G., Vecchi R., 2001. Characterisation of PM₁₀ and PM_{2.5} particulate matter in the ambient air of Milan (Italy). *Atmospheric Environment*, 35 (27), 4639-4650

Martano, P. & Romanelli, A. 1997. A routine for the calculation of the time – dependent height of the atmospheric boundary layer from surface-layer parameters. *Boundary Layer Meteorology*, 82, 105-117.

Querol X., Alastuey A., Puig O., 2001. PM₁₀ and PM_{2.5} source apportionment in the Barcelona Metropolitan area, Catalonia, Spain. *Atmospheric Environment*, 35, 6407-6419.

Rannik U. & Vesala T., 1999. Autoregressive filtering versus linear detrending in estimation of fluxes by the eddy covariance method. *Boundary Layer Meteorology*, 91, 259-280.

Tennekes, H & Nieuwstadt, F.T.M. 1981. A rate equation for the nocturnal boundary layer height. *Journal of Atmospheric Science*, 38, 1418-1428.

Turnbull A.B., Harrison R.M., 2000. Major component contribution to PM₁₀ composition in the UK atmosphere. *Atmospheric Environment*, 34, 3129-3137.

Yamada, T. 1979. Prediction of the nocturnal surface inversion height. *Journal of Applied Meteorology*, 17, 526-531.

TRACE ELEMENTS AND ORGANIC MICROPOLLUTANTS IN ATMOSPHERIC DEPOSITION IN VENICE LAGOON

Andrea Gambaro¹, Luca Zagolin¹, Clara Turetta², Silvia De Pieri², Roberta Zangrando¹,
Marta Radaelli², Angela Stortini¹, Warren Cairns¹

1 Dipartimento di Sc. Ambientali, Università Ca' Foscari, Venezia

2 Istituto per la Dinamica dei Processi Ambientali, CNR, Sezione di Venezia

Riassunto

Lo scopo di questo studio è stato quello di valutare il ruolo delle deposizioni, nel trasporto di microinquinanti organici e inorganici nei sistemi acquosi e terrestri valutando le concentrazioni nelle deposizioni secche e umide nella laguna di Venezia. La determinazione di microinquinanti organici ed inorganici è stata effettuata mediante HRGC/HRMS e ICP/MS.

Abstract

Transport via the atmosphere is an important route by which pollutants are transported from continents to both coastal and open seas. The purpose of this study is to evaluate the role of aerosol deposition, in the transport of organic and inorganic micropollutants in water and soil systems evaluating concentrations in wet and dry deposition in the Venice lagoon. The organic and inorganic micropollutants determinations were made by high resolution gas chromatography and high resolution mass spectrometry (HRGC/HRMS) and inductively coupled plasma-mass spectrometry (ICP/MS).

1 Introduction

Atmospheric particles have an important role in the transport of different substances and pollutants through the different compartments of the environment [Gambaro *et al.*, 2005a,b].

The aerosol is commonly defined as suspended solid and wet particles in a gaseous body that represents the atmosphere. The particles dimensions change from some nm up to some mm. The aerosol can be divided into primary aerosol in which the particles enter directly in the atmosphere and second aerosol in which the particles derive from processes in the gaseous phase that take place within the atmosphere [Raes *et al.* 2000].

The aerosol present in the atmosphere is subject to the transport of the air masses, which is derives controlled by meteorological conditions and from the physical and chemical characteristics of the particles themselves.

The city of Venice and its lagoon represent a complex system including the historic, artistic and environmental aspects. Past studies show that the most significant processes in the contamination of the lagoon environment are the

direct emission of industrial waste, the exchange of pollutants at the atmosphere-water [Manodori *et al.*, 2006; Manodori *et al.*, 2007] and water-sediment interfaces and finally the transfer of contaminants to river and lagoon waters.

This work attempts to study the role of aerosol deposition, in the transport of organic and inorganic micropollutants in water and soil systems evaluating the organic micro pollutants and trace elements concentrations in wet and dry depositions in the Venice lagoon.

2 Materials and methods

The organic deposition determinations were made on water samples (wet depositions) and on the particulate collected on the filters utilized for collecting the dry depositions.

The sampling site was situated on the Mazzorbetto island, near Burano in the northern part of the lagoon of Venice. The sampling period was from February 2004 to October 2005.

The organic micropollutants on the water samples were obtained by continuous liquid-liquid extraction using a mixture of hexane-dichloromethane (1:1). The particulate matter was extracted in a closed flask by sonication bath, using a mixture of pentane- dichloromethane (2:1).

The extract solution were dried by anhydrous Na_2SO_4 , and then reduced under a gentle stream of N_2 and a subsequent to clean-up step. The purification of the extracted was done using a POWER PREP and the organic pollutants were analyzed by high resolution gas chromatography and - high resolution mass spectrometry (HRGC/HRMS).

Before the extractions 7 PBDE carbon-13-labelled (PBDE, 28, 47, 99, 100, 118,153, 183) and 7 PCB carbon-13-labelled (PCB 28,52, 101, 138, 153,180,209) and 1 IPA carbon-13-labelled (Phenanthrene) were added to the water and particulate samples for use as internal standards in the quantification of the analytes in the samples.

3 PCB

3.1 Wet and Dry depositions

Tab. 1 shows the variation of the fluxes of PCB dry deposition during the sampling period.

	Minimum Flux [ng m ⁻² d ⁻¹]	Maximum Flux [ng m ⁻² d ⁻¹]	Mean Flux [ng m ⁻² d ⁻¹]
Σ fluxes 1-2-3 CB	1.42	4.82	3.04
Σ fluxes 4 CB	1.59	3.96	2.60
Σ fluxes 5 CB	2.56	5.94	4.34
Σ fluxes 6 CB	3.91	9.24	6.38
Σ fluxes 7-8 CB	2.84	13.17	5.58
Σ fluxes 9-10 CB	0.21	0.93	0.57

Tab 1 – Fluxes of PCB dry deposition during the sampling period.

In a similar way for the dry depositions, Tab. 2 shows the flux variations for wet deposition, during the sampling period.

	Minimum Flux [ng m ⁻² d ⁻¹]	Maximum Flux [ng m ⁻² d ⁻¹]	Mean Flux [ng m ⁻² d ⁻¹]
Σ fluxes 1-2-3 CB	1.33	42.56	14.39
Σ fluxes 4 CB	1.63	23.90	8.21
Σ fluxes 5 CB	2.02	20.06	8.21
Σ fluxes 6 CB	2.37	19.84	8.20
Σ fluxes 7-8 CB	1.51	10.25	5.08
Σ fluxes 9-10 CB	0.22	10.51	3.87

Tab 2 – Wet deposition fluxes variation during the sampling period.

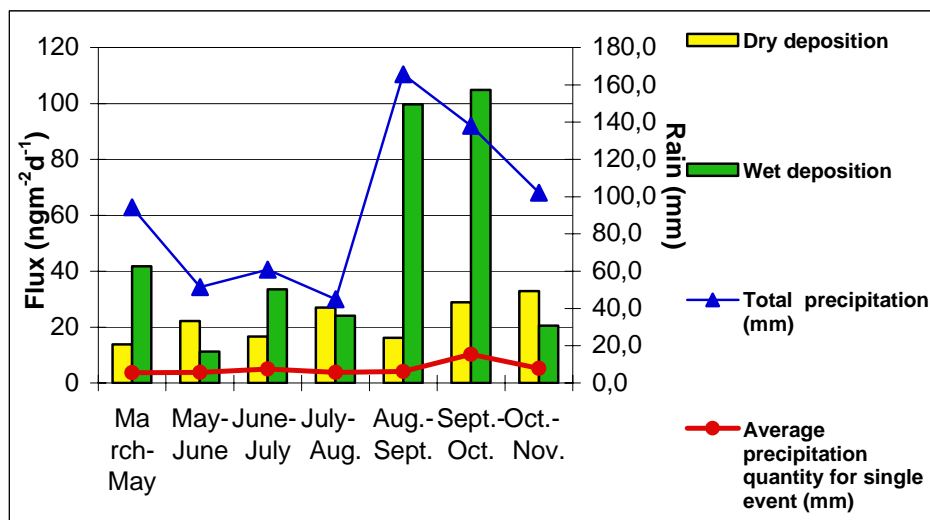
It's interesting to note that the fluctuation of the wet fluxes is more significant when compared with that concerning the dry deposition.

Fig. 1 reports the fluxes of dry and wet deposition, and emphasizes the differences between them. The data referring to the wet deposition differ more in time, if compared with those relative to the dry depositions. Looking closely at Fig.1 it can be observed that the mean flux increases with increasing precipitation, while the corresponding dry deposition flux decrease at the same time.

An exception to this is observed in the data relating to the period between 20th September-17th October, when the wet deposition flux was highest (105 ngm⁻²d⁻¹).

Considering the average quantity of water, relative to a single event, and not the total quantity of precipitation events, it is possible to see that the values increased in the period between 20 September- 17 November. This suggested the presence of storm events, the intensity of which probably promoted the scavenging process, increasing the wet deposition flux of PCB.

Fig 1 – PCB: Fluxes of dry and wet depositions.



When the dry deposition prevailed the hepta-CB, hepta/octa-Cb and penta-CB were mostly deposited, while during wet deposition there was the clear prevalence of PCB with a low chlorination number. Probably the precipitation scavenging effect was more efficient towards the lighter compounds in relation to their major solubility in water.

4 PAH

4.1 Wet and Dry depositions

Tab. 3 -Reports the PAH dry fluxes during the sampling period.

PAH	Minimum flux [ngm ⁻² d ⁻¹]	Maximum flux [ngm ⁻² d ⁻¹]	Mean flux [ngm ⁻² d ⁻¹]
Acenaphthylene	1.2	2.8	1.6
Acenaphthene	0.2	23.2	10.0
Fluorene	3.9	9.5	5.5
Phenanthrene	6.0	14.6	8.9
Anthracene	0.2	1.6	0.6
Fluoranthene	2.5	12.4	7.7
Pyrene	1.7	7.2	4.4
Benzo(a)anthracene	0.5	2.7	1.6
Chrysene	1.6	8.0	4.6
Benzo(b)fluoranthene	3.5	29.3	12.4
Benzo(k)fluoranthene	2.4	9.9	6.4
Benzo(a)pyrene	1.2	15.9	5.7
Indeno(1,2,c-d) pyrene	1.5	24.8	8.3
Dibenzo(a,h)anthracene	1.2	7.9	3.5
Benzo(g,h,i)perylene	1.2	24.1	5.9

Tab 3 – PAH: dry fluxes.

As for dry deposition in the wet depositions (Tab.4) is evident that anthracene ($4 \text{ ngm}^{-2}\text{d}^{-1}$), acenaphthylene (maximum value $11.1 \text{ ngm}^{-2}\text{d}^{-1}$), and benzo(a)anthracene (maximum value $18.2 \text{ ngm}^{-2}\text{d}^{-1}$) are the less abundant compounds. On the other hand the more abundant are phenanthrene with a medium value of $43,2 \text{ ngm}^{-2}\text{d}^{-1}$ and the indeno (1,2,c-,d) pyrene with a medium flux of $36,3 \text{ ngm}^{-2}\text{d}^{-1}$.

PAH	Minimum flux [ngm ⁻² d ⁻¹]	Maximum flux [ngm ⁻² d ⁻¹]	Mean flux [ngm ⁻² d ⁻¹]
Acenaphthylene	0.0	11.1	5.7
Acenaphthene	3.2	35.3	18.5
Fluorene	2.9	35.4	13.9
Phenanthrene	8.2	100.2	43.2
Anthracene	0.5	4.0	2.0
Fluoranthene	5.5	51.9	31.2
Pyrene	1.2	32.3	20.6
Benzo(a)anthracene	2.8	18.2	8.3
Crysene	4.3	52.6	22.3
Benzo(b)fluoranthene	11.6	57.5	28.5
Benzo(k)fluoranthene	3.3	52.8	19.3
benzo(a)pyrene	7.9	50.9	27.5
Indeno(1,2,c-d) pyrene	10.7	99.6	36.3
Dbenzo(a,h)anthracene	5.6	49.5	18.0
Benzo(g,h,i)perylene	3.8	27.0	13.0

Tab 4 – PAH: Wet fluxes.

It is evident that the PAH total wet deposition fluxes can be 5 time more intense if compared with the respective dry depositions, even though, in particular periods of the year, (for instance between 4 may- 1 June and 7 July -2 august) the wet deposition fluxes can be lower than dry depositions.

The comparison between dry and wet PAH deposition fluxes, collected in the aerosol sampling shows that the wet fluxes follow the atmospheric precipitations: in particular in the second and third period, when there are the lowest wet deposition values is the time when the precipitations infrequent or less intense. In this period the dry deposition fluxes are more elevated than those obtained with the wet depositions, in agreement with that observed for PCB. It can be observed that the maximum wet flux, during the first period of sampling, is due principally to Indeno(1,2-cd)pyrene, that represents the 20% of the total. Instead the fluxes registered at the end of the summer show a clear prevalence of phenanthrene (more than 20% in the sample between 2 August-20 September) and fluoranthene. The atmospheric precipitations in April were

characterized by weaker but longer events, while like said before for the PCB, the precipitations at the end of the summer were characterized by storm events. Also in this case it is possible to assume that the efficiency in the wet removal is more elevated, because of the scavenging effect present during the intense rain fall.

The comparison among the data present in this work, with those reported in bibliography (Rossini et al. 2005) is reported in Tab. 5

The fluxes obtained in this study are easily comparable with those reported in Rossini's publications concerning PAH.

Sampling site	Mean deposition fluxes [$\text{ngm}^{-2}\text{d}^{-1}$]
Industrial Porto Marghera	3381
Dogaletto	957
Mestre	624
Venice City	560
Lagoon	385
Lagoon 2	447
Lagoon 3	357
Mazzorbetto	333

Tab 5 – Mean deposition fluxes in the different sites.

In particular the flux relative to the Mazzorbetto zone is lower than those observed in all other stations (EZI, Dogaletto and Mestre) and is similar to the fluxes registered in the other lagoon sites.

5 Trace elements

5.1 Dry depositions

The value of the inorganic species are reported in Tab. 6 which includes also the sampling period, the mean flux for each element expressed as $\mu\text{g m}^{-2} \text{g}^{-1}$, and the total flux relative to the elements present in each exposure range.

Examining the mean fluxes values obtained, it is possible to note that all the elements can be divided in two main groups. The first group includes Ca, Na Mg, Al, K, Fe, and their mean fluxes assume values between $170 \mu\text{g m}^{-2} \text{g}^{-1}$ for Al and $1652 \mu\text{g m}^{-2} \text{g}^{-1}$ in the case of Ca. In the second group, are present V, Cr, Mn, Zn, Cu, Cd, Pb with mean fluxes going from $0.1 \mu\text{g m}^{-2} \text{g}^{-1}$ for Cd to $13,1 \mu\text{g m}^{-2} \text{g}^{-1}$ for Zn. The large difference between the dry fluxes shows that the first group elements contribution represents 99% of the mean total flux in every sampling period. Finally, it is possible to note that the mean total daily flux for the dry deposition has a minimum during the second exposure period that goes from 16 March to 4 May.

Sampling period	Na	Mg	Al	K	Ca	V	Cr	Mn	Fe	Ni	Cu	Zn	Cd	Pb	Σelements
	Flux [$\mu\text{g m}^{-2}\text{d}^{-1}$]	Flux [$\mu\text{g m}^{-2}\text{d}^{-1}$]													
20/02-16/03	567,2	424,4	97,4	108	1542	0,5	0,3	7,1	148,4	0,7	3,4	17,1	0,2	0,9	2915
16/03-04/05	32,9	71,1	30,1	22,1	259,2	0,1	0	1,1	33,2	0,1	0,5	2,4	0	0	453
04/05-01/06	1315,1	669,7	223,8	1503,1	2355,3	1	0,5	10,2	239	1,1	4,7	17,6	0,1	0,4	6341
01/06-06/07	1708,1	716,8	127,8	1662,1	2367,6	0,7	0,4	8,2	145,4	0,6	5,2	22,8	0,1	1,2	7037
07/07-02/08	1150,2	541,6	340,6	263,9	1881,9	1	1	11,4	279,8	0,8	5,4	7,7	0	1,6	4487
02/08-20/09	797,4	380,5	202,3	208,6	1235,6	1,2	0,6	8,5	130,2	1	7,1	11,3	0,1	1,5	2986
Mean flux	928	467	170	628	1652	0,7	0,5	7,7	163	0,7	4,4	13,1	0,1	0,9	

Tab 6 – Dry fluxes during the sampling period.

5.2 Wet depositions

Tab. 7 reports the wet deposition fluxes concerning the trace elements in the same way as was done for the dry depositions. Also in this case, it is possible to divide the elements into two groups. Like before the first group, that also in this case represents the major fluxes, includes Ca, Na Mg, Al, K, Fe, while the second group containing V, Cr, Mn, Zn, Cu, Cd, Pb represents lower fluxes.

Observing the data is possible to see that the mean wet deposition fluxes, during the sampling, for each element are bigger than those obtained for the dry depositions, even though in particular periods (26 February-16 March and 4 May-1June) this trend is reversed.

The comparison between the dry and wet deposition fluxes obtained for the inorganic species, during the present study evidences the different time trends for the two types of fluxes during the studied periods. The maximum dry flux ($7037 \mu\text{g m}^{-2} \text{g}^{-1}$) was observed in period 1 June- 6 July, while the minimum was in the period 16 March- 4 May. But in this period there also appears the maximum wet deposition flux equal to $14443 \mu\text{g m}^{-2} \text{g}^{-1}$, while the minimum value was observed between 26 February and 16 March. As with the case of organic micropollutants the wet deposition fluxes follow the precipitation trends.

Table 8 shows the results deriving from the comparison among the mean fluxes relative to each element, obtained by summarizing the value of the dry and wet depositions with the concentrations deriving from the studies of Rossini et al. (2005) collected in the bulk Venice lagoon sample.

This study shows that "crustal" elements (Na, Mg, Al, K) have larger fluxes in comparison to that obtained in other investigations. Some elements (Cr,V,Ni, Cd) have the fluxes that are comparable with those reported in literature, while in the case of Zn and Pb the fluxes are lower than those relative to the other samples collected in all other stations.

The differences between the fluxes, especially for metals of natural origin, can be explained by the seasonable fluctuations.

Sampling period	Na	Mg	Al	K	Ca	V	Cr	Mn	Fe	Ni	Cu	Zn	Cd	Pb	Σelements
	Flux [$\mu\text{g m}^{-2} \text{d}^{-1}$]														
20/02-16/03	228.8	22.7	2.2	35.3	135.1	0.2	0	0.5	20.7	0.3	1.1	12.9	0	0	406
16/03-04/05	3347.8	1286.7	1362.1	1491.5	5872.7	4.2	0.6	26.2	1016.1	1.9	7.9	22.9	0.3	2.1	14443
04/05-01/06	1549	400.2	490.7	808.6	1558.9	2.2	3.8	21.2	422.8	2.5	4.2	17.6	0.1	0.8	5283
01/06-06/07	5546.6	1027.8	747.8	597.8	2720.2	5.3	3.5	25.1	713.1	4.2	10.1	20.7	1.1	8.1	11431
07/07-02/08	4369.8	579.8	334.8	226.9	825.4	1.2	0.9	9.3	207.2	1	4.6	7.3	0.1	2.6	6571
02/08-20/09	4288.7	1172.7	3205.6	1089.6	1337.6	7.9	5.7	30.4	2001.7	4.2	14.7	17.1	0.2	13.6	13190
Mean flux	3222	748	1024	708	2075	3.5	2.4	18.8	730	2.3	7.1	16.4	0.3	4.5	

Tab 7 – Wet fluxes during the sampling period.

	Na	Mg	Al	K	Ca	V	Cr	Fe	Ni	Cu	Zn	Cd	Pb
Mazzorbo	5408	1517	907	1957	3476	4.7	4.3	891	4.55	13.89	36.12	0.29	3.25
Venice	3894	1337	722	804	3506	5.5	4.6	594	5.7	12.3	76.3	0.4	14.5
Nord Lagoon	3138	1139	450	959	4666	3.5	1.5	286	2.5	6.8	53.7	0.14	5
Sud Lagoon	2800	1011	542	800	3509	4.9	2.9	361	4.1	8.2	53.8	0.22	10.7
Marghera	1488	1021	894	927	6032	7.8	2.4	437	6.9	8.6	79.4	0.2	8.6

Tab 8 – Mean luxes fluxes ($ng\ m^{-2}\ d^{-1}$) relative each element, obtained summarizing the value of the dry and wet depositions and bulk depositions.

References

Gambaro A., Manodori L., Zangrando R., Cincinelli A., Capodoglio G., Cescon P., 2005. Atmospheric PCB concentration at Terra Nova Bay, Antarctica. *Environmental Science & Technology*, 39, 9406-9411.

Manodori L., Gambaro A., Zangrando R., Turetta C., Cescon P., 2006. Polychlorinated Naphthalenes in the gas-phase of the Venice Lagoon atmosphere. *Atmospheric Environment*, 40, 2020-2029.

Manodori L., Gambaro A., Moret I., Capodoglio G., Cescon P., 2007. " Air-sea gaseous exchange of PCB at the Venice Lagoon (Italy), 54, 1634-1644.

Raes F., Van Dingenen R., Vignati E., Wilson J., Putaud J.P., Seinfeld J.H., Adams P., 2000. Formation and cycling of aerosol in the global troposphere. *Atmospheric Environment*, 34, 4215-4240.

Rossini P., Guerzoni S., Molinaroli E., Rampazzo G., De Lazzari A. and Zancanarp A. 2005. Atmospheric bulk deposition to the lagoon of Venice: Part I. Fluxes of metals, nutrients and organic contaminants. *Environment International*, 31, 959-974.

Toscano G., Gambaro A., Moret I., Capodoglio G., Turetta C., Cescon P., 2005. Trace metals in aerosol at Terra Nova Bay, Antarctica. *J. Environ. Mn.*, 7, 1275-1280.

RESEARCH LINE 3.10

**Groundwater flows in the Venice lagoon
system**

SALTWATER INTRUSION AT THE SOUTHERN VENICE LAGOON BOUNDARY DETECTED BY TIME-LAPSE ERT

Roberto de Franco¹, Giancarlo Biella¹, Adelmo Corsi¹, Antonio Morrone¹, Graziano Boniolo¹, Alfredo Lozej², Christelle Claude³, Adriano Mayer³, Ginette Saracco³, Barbara Chiozzotto⁴, Marco Giada⁴, Valentina Bassan⁵, Vittorio Bisaglia⁵, Tiziano Abba⁵, Andrea Mazzuccato⁵, Enrico Conchetto⁵, Massimo Barbetta⁶, Giuseppe Gasparetto-Stori⁶, Federica Rizzetto⁷, Luigi Tosi⁷, Pietro Teatini⁸

1 IDPA–CNR, Milano, 2 Dip. Scienze della Terra, Università degli Studi di Milano, 3 CEREGE, Aix en Provence, France, 4 Morgan Srl, Marghera (VE), 5 Provincia di Venezia-Servizio Geologico, Venezia, 6 Consorzio di Bonifica Adige-Bacchiglione, Padova, 7 ISMAR–CNR, Venezia, 8 DMMMSA, Università di Padova

Riassunto

In questo lavoro vengono presentati i risultati di un esperimento elettrotomografico tempo variante (ERT) volto al monitoraggio della dinamica dell'intrusione salina nella zona a sud della Laguna di Venezia. L'acquisizione dei dati è iniziata nel Novembre 2005 e terminata a Settembre 2006 utilizzando un prototipo sviluppato appositamente. Il sistema ha acquisito 10 pseudo sezioni di resistività apparente al giorno, 5 ad alta risoluzione con una linea di 97.5 m e spaziatura elettroica di 2.5 m e 5 su una linea di 300 m e spaziatura di 5m, per una profondità di investigazione di 50-60 m. Nei pressi della linea sono stati perforati due pozzi a carotaggio continuo, profondi rispettivamente 20 e 50 m, che hanno identificato un acquifero freatico superficiale e due acquiferi confinati. I dati di pozzo hanno permesso di vincolare l'elettrostratigrafia ottenuta dalla prospezione elettrica. L'acquifero superficiale, compreso fra 4 e 13 m sotto il livello medio del mare, è il più contaminato dall'intrusione salina e presenta valori di resistività della formazione di 0.8 ohm.m. I dati mostrano una fluttuazione stagionale dei valori di resistività con minimo di intrusione in Marzo-Aprile e un massimo nella stagione secca estiva. Gli acquiferi più profondi mostrano un aumento di resistività, che corrisponde a una diminuzione del contenuto salino, all'inizio dell'estate, probabilmente a causa di un maggior contributo di acqua dolce a livello sub regionale.

Abstract

The results of a time-lapse electrical resistivity tomography (ERT) experiment conducted for monitoring saltwater intrusion dynamics in the coastland bounding the southern Venice Lagoon, near Chioggia (Italy), are presented. The survey has been carried out from November 2005 to September 2006 using a prototype developed for this specific purpose. The system acquired 10 apparent resistivity pseudo-sections per day, five of which with high resolution by a 97.5 m long ERT line with a 2.5 m electrode spacing and five by a 300 m

long and 5 m electrode spacing ERT line, suitable to monitor the intrusion process down to 50-60 m depth. Two boreholes (20 and 50 m deep) drilled near the test site identified a shallow phreatic aquifer and two confined aquifers within the depth of interest and allow to constrain the electro-stratigraphy obtained by the resistivity tomography. The shallow aquifer, located between 4 and 13 m depth below mean sea level, is the most contaminated by the salt intrusion with a minimum resistivity formation value of 0.8 ohm.m. The experimental data reveal a seasonal resistivity fluctuation corresponding to a minimum salt intrusion in March-April and a maximum in the dry summer season. The deeper aquifers, characterized by a resistivity ranging from 3.0 ohm.m to 10 ohm.m, show a resistivity rise at the beginning of the summer time probably due to an increasing contribution of fresh water from sub-regional aquifers.

1 Introduction

In the framework of the 2004-2006 Research Program of Co.Ri.La. (Consortium for Coordination of Research Activities concerning the Venice Lagoon System) an experimental program has been carried out to evaluate the groundwater exchange between the southern part of the Venice Lagoon and the surrounding farmland by means of natural isotopic tracers and electrical resistivity tomography (ERT). The present paper is focused on a time-lapse ERT experiment implemented in a test area at the southern margin of the Venice Lagoon (Figure 1) to characterize the dynamics of the saltwater contamination.

The electrical resistivity is one of the most efficient and powerful technique to map the fresh/salt water interface. Because of the dynamic behavior of the saltwater intrusion, a time variant observation is needed to assess its evolution, especially in reclamation areas such as the Venice coastland where very complex geomorphological, hydrogeological and drainage systems significantly affect the groundwater flows (Rizzetto et al., 2003). To this aim, the time-lapse electrical resistivity tomography (TL-ERT) has proved to be an efficient and cost-effective tool to monitor the saltwater intrusion dynamics.

Many TL-ERT applications are discussed in literature (White, 1994; Barker and Moore, 1998; Ramirez and Daily, 2001; Slater *et al.*, 2002; Singha and Gorelick, 2005; Cassiani *et al.*, 2006). However all these experiments, mainly devoted to the use of the ERT for tracer tests, are characterized by a short monitoring period due to the complexity and problems of long-time instrument maintenance. In this paper we show that a long period (about 1 year) time-lapse monitoring of salt-water intrusion with the electrical resistivity tomography is feasible and it is capable to capture the process dynamics.



Fig 1 – Map of the experimental site at the Venice Lagoon margin with the trace of the geophysical investigations (VES, integrative ERT profiles, TL-ERT lines) and the location of the shallow and deep piezometers.

2 Objectives

The objectives of the present study were i) to perform an electrical resistivity tomography (ERT) time-lapse experiment aimed at monitoring the dynamics of the saltwater intrusion in the coastland bounding the southern Venice Lagoon by means of ii) the development of a dedicated apparatus which can operated for very long time period (on the order of a year).

A specific TL-ERT apparatus was developed due to the complexity of the experiment from the technical, logistic, and environmental point of views. The equipment is a 2 channels 24 bit digital resistivity meter – electro-tomograph, designed for the high accuracy measure of potential, current, resistance and resistivity. The system allows the acquisition of 2-D or 3-D electrical tomography resistivity and time-lapse measurements. A GSM modem connected to the acquisition system allowed the remote system control and FTP data download.

The experiment consists of a low resolution 300 m long ERT line (TL-ERT LR, Figure 1), which was sampled with a Wenner configuration and a 5 m electrode spacing (61 electrodes), and an overlapping higher resolution ERT line (TL-ERT HR, Figure 1) along the northernmost 97.5 m portion with an electrode spacing equal to 2.5 m (40 electrodes). The acquisition started in November 2005 and ended in September 2006. A total number of 1430 apparent resistivity pseudo-sections, reduced to 1148 after a pre-processing based on the data quality analysis, were obtained over the period of acquisition.

3 Results

The data sets were transformed in a Matlab format for the data pre-processing and a format which was suitable for the apparent resistivity data inversion and modeling procedure. Figure 2 shows an example of the reconstructed resistivity sections (electro-tomograms) for the 5 m electrode configurations.

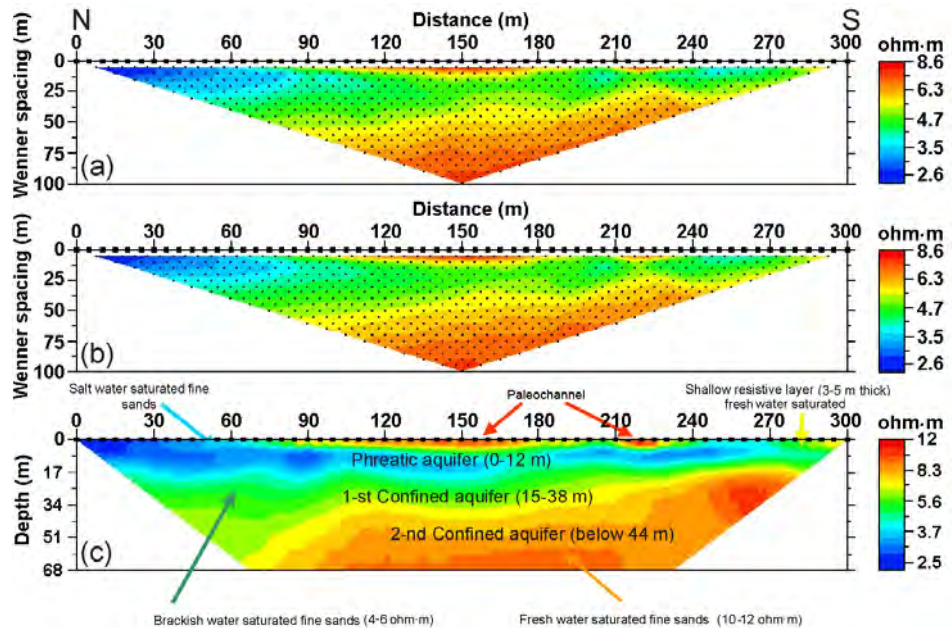


Fig 2 – Example of a TL-ERT HR tomographic section: (a) apparent resistivity data, (b) calculated apparent resistivity, and (c) resistivity model with the hydrogeological interpretation. The trace of the profile is shown in Fig. 1.

Three aquifers are recognizable, the shallower two suffering from the saline intrusion. At about 45 m depth a resistivity greater than 10 ohm-m is interpreted as fine sands saturated with fresh water. This limit constitutes the bottom of the saline intrusion. Due to the low resolution characterizing the longer ERT configuration, the first aquifer seems to start from the surface with an averaging effect that yields a quite uniform resistivity value of about 3 ohm-m in the northern part. The high resolution 2.5 m resistivity tomogram gives a detailed image of the first two units. A shallower 3 m thick layer composed of clayey peat saturated with freshwater overlies a layer of fine sands saturated with fresh/brackish water. The underlying deposits, that extends down to 12 m depth, show the lowest resistivity of the order of 1 ohm-m. This unit constitutes the top of the saline intrusion and is separated from the first confined aquifer by a 3 m thick clay layer.

The collected data allow to outline the time behavior of the resistivity along the monitored alignment and the correlation between the salty water movements. Figures 3 and 4 show the pseudo-sections recorded at different times by the low and high resolution TL-ERT lines, respectively. The general features of the pseudo-sections are similar and three main behaviors of the apparent resistivity can be detected during the monitoring period at different depths.

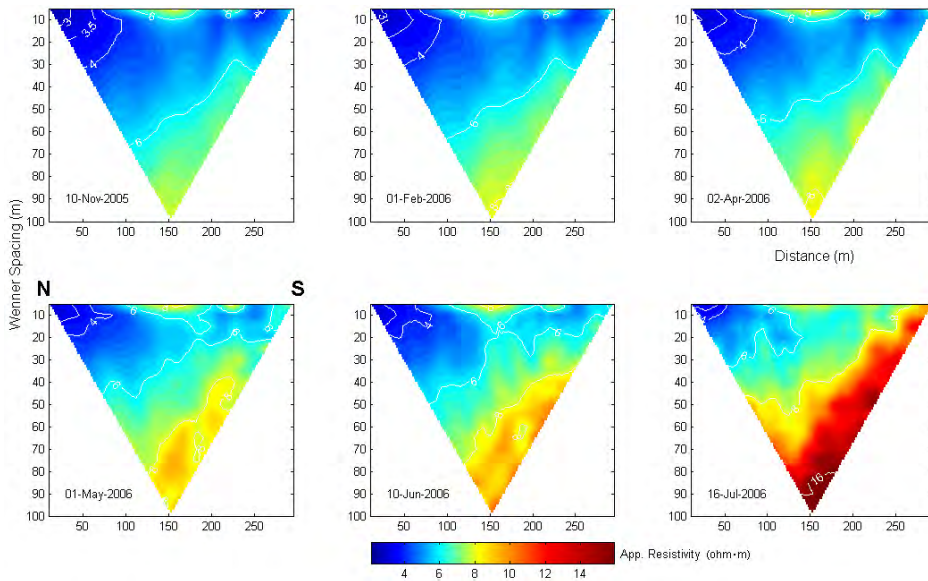


Fig 3 – Apparent resistivity data obtained by the TL-ETR LR in a) November 2005, b) February 2006, c) April 2006, d) May 2006, e) June 2006, f) July 2006.

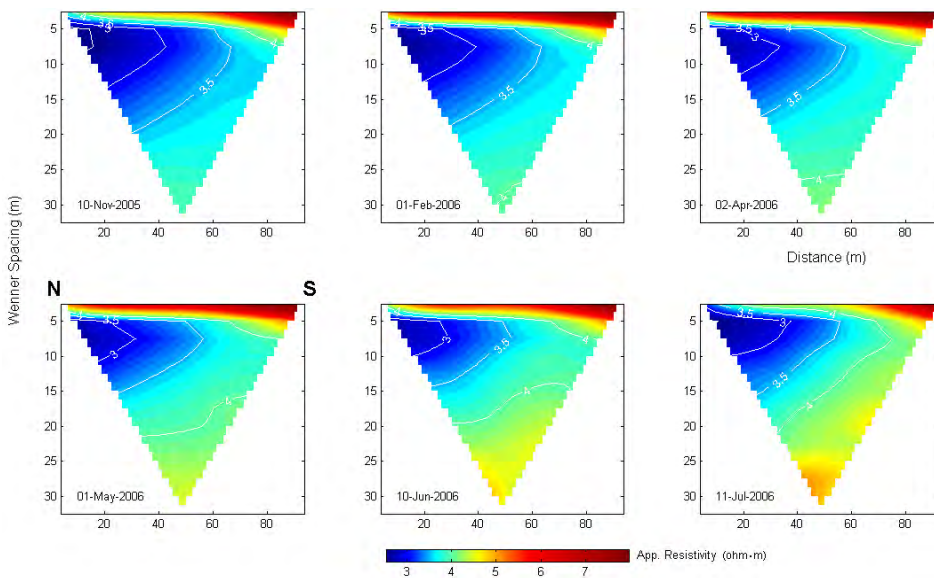


Fig 4 – Apparent resistivity data obtained by the TL-ETR HR in a) November 2005, b) February 2006, c) April 2006, d) May 2006, e) June 2006, f) July 2006.

For Wenner Spacing less than 5-7.5 m (about 3-4 m depth), a progressive increase of the apparent resistivity is observed until March and April in the northern part of the section nearest to the lagoon. At the end of May 2006 the apparent resistivity began to decrease, reaching the minimum values in summer when the lowering of the resistivity value involved also the upper 2.5 m Wenner Spacing (1-2 m depth). Between 7 to 30-40 m Wenner Spacing (from 4 to 20-25 depth), the minimum apparent resistivity occurred in winter when values less than 5 ohm-m affects the whole line. Finally for Wenner Spacing larger than 40 m the apparent resistivity increased mainly in the early summer.

The seasonal fluctuation of the resistivity, mainly observed in the first two aquifers is representative of the saltwater intrusion dynamics occurring at a seasonal time scale along the lagoon boundary. With the exception of the first 2-4 m depth layer, the contamination reached the maximum inshore extent from

the lagoon margin during the wet season contrarily to the general behavior observed in other coastal sites governed by temperate climate (Michael *et al.*, 2005). This occurrence is likely to be due to the superposition of the pumping station activities, which keep the lowest groundwater levels in the winter to reduce the risk of lowland flooding, and seasonal changes in lagoon water levels that usually reach the maximum values from November to March (Figure 4). The resistivity changes in the first confined aquifer (Figure 3) are probably due to an increased fresh water recharge coming from the mainland at regional scale (Provincia di Venezia, 2000).

Conclusions

The farmland bounding the southern Venice Lagoon suffers from the saltwater contamination process which involves soils devoted to agricultural and horticultural activities that are the main economic resources. The contamination process in this part of the Venice coastland is due to complex inter-relationships between ground-, surface-, and lagoon-water levels superposed to a very heterogeneous subsoil. The dynamics of saltwater intrusion along a profile perpendicular to the lagoon margin has been studied by an electrical resistivity tomography time-lapse experiment. The tomographic time-lapse acquisition system provided a continuous monitoring of the electrical resistivity changes that are related only to the variation of the salt concentration in the groundwater. The accurate processing and interpretation of the entire data set allow to point out the evolution of the saltwater contamination process at different time scales. The monitoring results show that a certain salinity degree affects the shallow subsoil all over the year. The recorded resistivity fluctuations are related to the variation of the salt concentration and are mainly observed in the phreatic aquifer down to 15 m depth. The contamination degree regresses toward the lagoon (to the north) from February to early summer and, after a couple of months of substantial stability, it progresses inland (to the south) reaching the maximum extent in winter (from November to January). The modeling study under way will be efficiently supported by the huge dataset collected by the hydrogeophysical investigation.

References

- Barker, R. and Moore, J. (1998): The application of time-lapse electrical tomography in ground water studies, *The leading Edge*, 17: 1454–1458.
- Beinat E., 1997, Case study: expert based value function models for cleaning up a polluted site, in “Value Functions for Environmental Management”, by Beinat Euro, Kluwer Academic Publishers, Netherland.
- Cassiani, G., Bruno, V., Villa, A., Fusi, N. and Binley, A. M (2006): A saline trace test monitored via time-lapse surface electrical resistivity tomography, *J. Appl. Geophys.*, 59: 244–259.
- Fox W.M., Connor L., Copplestone D., Johnson M.S. and Lee R.T., 2001. The

organochlorine contamination history of the Mersey estuary (UK) revealed by analysis of sediment cores from salt marshes. *Marine Environmental Research*, 51, 213-227.

Michael, H. A., Mulligan, A. E. and Harvey, C. F. (2005): Seasonal oscillations in water exchange between aquifers and the coastal ocean, *Nature*, 436: 1145–1148.

Pastres, R., Solidoro, C., 1999. Trattamento ed analisi dei dati anche mediante un modello di qualità dell'acqua (ex art. 55 del Capitolato Speciale) - Rapporto finale. In "Interventi per l'arresto del degrado connesso alla proliferazione delle macroalghe in laguna di Venezia 1997-1998". Consorzio Interuniversitario "I.N.C.A." - Consorzio "Venezia Nuova" - Istituto Nazionale di Oceanografia e Geofisica Sperimentale, Venezia.

Provincia di Venezia (2000), Indagine idrogeologica del territorio provinciale di Venezia.

Ramirez, A. and Daily, W. (2001): Electrical imaging at the large block test - Yucca Mountain, Nevada, *J. Appl. Geophys.*, 46(2): 85–100.

Rizzetto, F., Tosi, L., Carbognin, L., Bonardi, M. and Teatini, P. (2003): Geomorphological setting and related hydrogeological implications of the coastal plain south of the Venice Lagoon (Italy). In: Servat, E. (Ed.) *Hydrology of the Mediterranean and Semiarid Regions*, IAHS Red Book n. 278, IAHS Press, Wallingford, UK, 463-470.

Singha, K. and Gorelick, S. M. (2005): Saline tracer visualized with three dimensional electrical resistivity tomography: Field-scale spatial moment analysis, *Water Resour. Res.*, 41, W05023, doi:10.1029/2004WR003460.

Slater, L., Binley, A., Versteeg, R., Cassiani, G., Birken, R. and Sandberg, S. (2002): A 3D ERT study of solute transport in a large experimental tank, *J. Appl. Geoph.*, 49: 211–229.

White, P.A. (1994): Electrode Arrays for measuring groundwater flow direction and velocity, *Geophysics*, 59: 192–201.

RESEARCH LINE 3.11

Ecological quality indices, biodiversity and environmental management for lagoon areas

A NEW BIOINDEX, BASED ON MACROFOULING BIOCOENOSIS OF HARD SUBSTRATA, FOR THE ESTIMATION OF THE ENVIRONMENTAL QUALITY: APPLICATION IN THE LAGOON OF VENICE

Francesca Cima, Paolo Burighel, Lorian Ballarin

Dipartimento di Biologia, Università di Padova

Riassunto

È stata effettuata la validazione del bioindice sviluppato durante la campagna di raccolta di parametri chimico-fisici e biotici 2004-2005 relativi allo studio della qualità ambientale di due stazioni nel bacino meridionale della Laguna di Venezia. Il bioindice ha permesso di confermare un buono stato di salute delle due stazioni prese in esame. I dati di questa campagna sono comparabili con quelli della campagna precedente, nonostante si siano verificate delle variazioni dovute alle aberrazioni meteorologiche del periodo preso in esame, confermando la bontà del bioindice.

Abstract

We carried out the validation of the bioindex developed during the 2004-2005 campaign of sampling and collection of physico-chemical and biotic parameters related to the study of the environmental quality of two stations of the southern basin of the Venice Lagoon. This bioindex confirmed the good health of the examined stations. In addition, the data collected in this campaign are comparable with those of the preceding one, in spite of the aberrations of the meteorological parameters in the examined period, thus confirming that the bioindex is a good tool for environmental health evaluation.

1 Introduction

Fouling of coastal hard substrata is characterised by higher biodiversity and biomass than that of open sea. The reasons of the higher organism concentration in shallow waters can be various: i) the higher temperature of the superficial layer of the water column which contributes to render it very productive; ii) the concentration of superficial food and biogenic factors supporting the organism growth; iii) a greater amount of hard substrata enabling settlement; iv) the density of benthic communities representing an important biofouling source. Moreover, coastal areas are unstable habitats in which biocoenoses do not reach a fully climax status since their ecological successions are interrupted by various factors, such as storms, breaker abrasion, and high predation. In these cases, biocoenosis successions start again from stages featuring the presence of fast-growing species causing a very

high total growth rate of the communities [Railkin, 2004a,b].

In order to evaluate the ecological status of a lagoon, the use of biological indexes, which summarises data on various environmental parameters, is much easier and prompter than monitoring, which takes much more time and is unstable in recording both normal cycles and the occurrence of persisting environmental crisis.

The use of bioindexes is based on the assumption that benthic communities respond to improvement of habitat quality with i) an increase of organism abundance; ii) the rise in biodiversity when new taxa are able to survive; iii) the shift of dominant species from tolerance to sensitivity to pollution [Chang et al., 1992].

We have recently proposed a new environmental quality index for the macrofouling biocoenosis of hard substrata in the lagoon of Venice [Cima et al., 2007]. This biological index considers the species richness, the area occupied by the species and quality values attributed to chemical-physical parameters such as seawater temperature, pH and salinity. This new index is evaluated in a dynamic matter, as previously reported [Cima et al., 2007].

The environmental quality index, specific for the community of hard substrata, is represented by the following algorithm:

$$\text{Log}_{10} (R \cdot A \cdot I_{\text{pH}} \cdot I_{\text{T}} \cdot I_{\text{S}})$$

where:

R = species richness, i.e., number of species monthly recorded on all panels of the same type

A = area of the surface monthly recorded for each species (cm²)

I_{pH} = pH quality index

I_T = temperature quality index

I_S = salinity quality index.

The development of a quality index in logarithmic scale, from 1 to 10, allows to really evaluate the state of health of the lagoon environment assigning to it a numerical value.

In order to validate this index, we collected new data in the same stations used in the 2004-2005 campaign, located in the southern lagoon (Chioggia): station 1 (Lat. 45° 15' N, Long. 12° 15' E) and station 2 (Lat. 45° 14' N, Long. 12° 17' E), characterised by different bathymetric and hydrodynamic features and anthropic impact as described previously [Cima et al., 2007].

Artificial substrata - constantly immersed wood and stain panels - were used and data were collected in the four more significant months for the ecological succession:

- I. April 2006 (beginning of settlement of pioneer organisms)
- II. June 2006 (beginning of macrofouling expansion)

III. September 2006 (appearance of macrofouling dominant species)

IV. December 2006 (final stage: stable community).

2 Results and Discussion

Physico-chemical parameters played a very important role as autumn and winter 2006 were unusual warm periods with scarce rainfalls and the consequent rise the salinity to high levels with an anomalous peak in December. The value of pH in station 1 reached the minimum value (7.85) in December and the maximum one (8.32) in April; in station 2 the minimum value (7.91) was reached in June and the maximum (8.5) in April. Temperatures were always similar in both the stations, with differences lower than 1°C but, generally, higher than the seasonal mean values: 12.4°-13.2° in April, 18.5°-17.7° in June, 23-22.3° in September, 9°-9.08° in December (the numbers refer to values recorded in station 1 and 2, respectively).

In general, with respect to previous samplings (2004-2005 campaign), we observed a delay in colonisation by pioneer organisms, probably due to lower temperatures and the higher salinity and pH values.

Station 2 showed a species richness always higher than station 1 in almost all the considered months and in all the panels. This is closely related with the disturbance degree: the higher wave motion and depth and the lower nutrient supply of station 1 limited the number of species able to settle on the substrata. In the same station 2, we observed an unusual precocious and massive settlement of tunicates and bryozoans, which caused a progressive and continuous increase in both species richness and the extension of the surface covered by fouling. In June, the community of station 2 resulted more structured than station 1.

Even the substratum quality seems to influence the settlement and covering: in both the stations, wood panels were colonised by a higher number of species than steel ones.

As for the environmental quality index (bioindex; Fig. 1), physico-chemical parameters seem to be the factors which mostly influence the health status of aquatic ecosystems, prevailing on biotic factors.

In particular, salinity represented the most influential factor in the considered period as it underwent wide changes, exceeding 40‰ in both stations during the dry periods. High salinity values were observed as early as April which lowered the bioindex, calculated in both the panel types, to values ranging between 6.4 and 7. In summer months, particularly rainy and fresh, salinity decreased to 34.6-34.5 ‰ in June and 32.6-31.33‰ in September, in station 1 and 2, respectively. As a consequence of the low salinity and a moderate increase of the temperatures, the bioindex was very high (ranging between 8.01 and 9.31), indicating that optimal ecological conditions were reached.

In December, a scanty rainy month, the bioindex decreased as a consequence of the deterioration of environmental conditions, mainly due to the increase in salinity and decrease in temperature.

Similarly to April, even in December station 1, showed the lower values of the bioindex which ranged from 5.3 to 6.44.

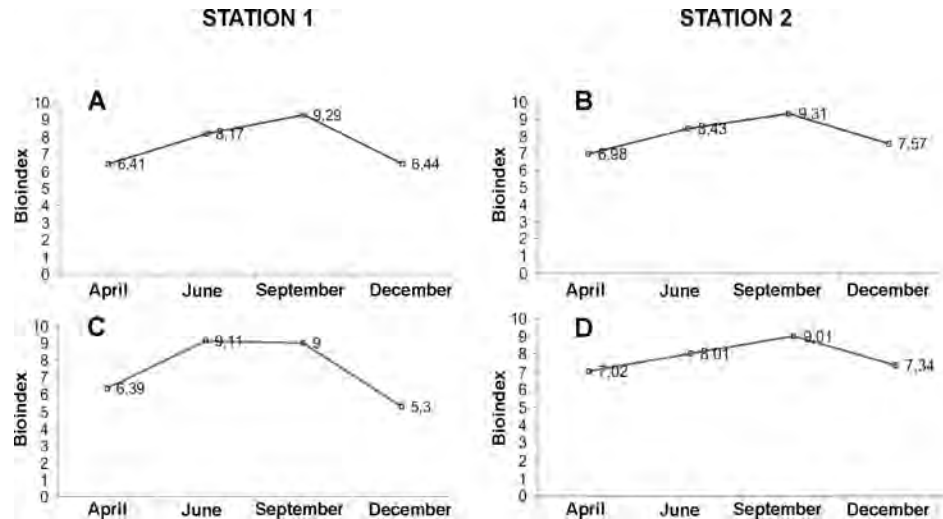


Fig 1 – Trend of the bioindex for macrofouling of hard substrata in the two stations near Chioggia from April to December 2006. A, B: steel panels; C, D: wood panels.

Conclusions

The examined stations reveal a good health status. The bioindex resulted a valid tool, useful and sensitive, to evaluate the health condition of the lagoon of Venice. In particular, data from the 2006-2007 campaign are comparable, although with minimum fluctuations mainly due to the meteorological aberrations during the sampling period, with those from the 2004-2005 campaign.

The bioindex furnishes an immediate value in logarithmic scale and its seasonal variations can give information on environmental changes, also related to anthropic impact; in our opinion it allows a qualitative comparison of various lagoon zones.

References

- Chang S., Steimle F. W., Reid R.N., Fromm S.A., Zdanowicz V.S. and Pikanowski R.A., 1992. Association of benthic macrofauna with habitat types and quality in the New York bight. *Marine Ecology Progress Series*, 89, 237-251.
- Cima F., Burighel P. and Ballarin L., 2007. Proposal of a new environmental quality index for the macrofouling biocoenosis of hard substrata in the lagoon of Venice, in "Scientific Research and Safeguarding of Venice – Vol. V", by P. Campostrini Ed., Istituto Veneto di Scienze, Lettere ed Arti, Venezia, 227-234.
- Railkin A.I., 2004a. Biofouling as a process. Colonization, in "Marine biofouling: colonization processes and defenses". CRC Press LLC, Boca Raton, 25-28.
- Railkin A.I. 2004b. Biofouling as a process. Primary succession, in: "Marine biofouling: colonization processes and defenses". CRC Press LLC, Boca Raton, 28-35

***In situ* monitoring of mussel populations in the Venice Lagoon by means of molecular biomarkers**

Marco Martinuzzi¹, Maura Zanella¹, Luigi Pivotti¹, Laura Tallandini¹

¹Dipartimento di Biologia, Università di Padova, Via U. Bassi 58b, Padova[§]

Riassunto

Utilizzando diversi biomarcatori ecotossicologici, è stato valutato lo stress ambientale di esemplari nativi di *Mytilus sp.* provenienti da cinque specifici siti interni alla laguna di Venezia (ed uno posizionato in mare aperto).

Lo studio riguarda la valutazione degli effetti genotossici e citotossici, come rotture al DNA ed apoptosi, effettuata su cellule della ghiandola digestiva di mitili attraverso l'utilizzo dell'SCGE Test, ossia il Comet Assay.

Con l'intento di valutare l'andamento temporale e spaziale di questi biomarcatori nel contesto lagunare Veneziano, si è ripetuto il medesimo schema di campionamento in due diversi studi, prelevando mensilmente gli organismi durante un periodo di sette mesi, da Dicembre a Giugno del 2000 e successivamente del 2006.

Relativamente all'andamento temporale, c'è da notare il fatto che i valori di danno al DNA risultano più bassi nello studio del 2006 rispetto a quelli del 2000. Tuttavia nel secondo studio si evidenziano livelli di mortalità cellulare quasi doppi rispetto al primo.

Per quanto riguarda l'andamento spaziale, in entrambi gli anni i mitili provenienti dall'interno della Laguna hanno mostrato livelli di danno al DNA più elevati rispetto al controllo prelevato in mare, con un andamento che presenta un significativo incremento dalle zone più esterne verso le più interne.

Abstract

The environmental stress of *Mytilus sp.* specimens collected from five specific sites in the Venice Lagoon (and from one offshore site nearby) has been investigated by means of different ecotoxicological biomarkers.

The study evaluated genotoxic and cytotoxic effects, such as DNA strand breaks and apoptosis, on the digestive gland cells of mussels by using the Single Cell Gel Electrophoresis Test, i.e. Comet Assay.

[§] Please send all correspondence to laura.tallandini@unipd.it

In order to assess the temporal and spatial trends of these biomarkers within the Venice Lagoon, the same sampling scheme was repeated in two field studies: mussels were collected monthly for a period of seven months from December 1999 to June 2000 and then from December 2005 to June 2006.

Regarding the temporal trend, the DNA damage values were lower in the 2006 study than in the 2000 study. However cell mortality values in the second monitoring were almost double those of the first one.

As for the spatial trend, in both studies mussels collected from the Venice Lagoon showed a higher level of DNA damage than offshore mussels, a trend that increased significantly as we moved from the lagoon border towards the lagoon interior.

1 Introduction

The Venice Lagoon is a complex ecosystem covering an area of 548.8 square kilometres. It encompasses the drainage basin of a region of about 200,000 ha with a population of more than 1,300,000 people, including 200,000 people living in the lagoon area, mainly in the towns of Venice, Chioggia and Marghera [Ghetti and Batisse, 1983]. The surrounding urban and industrial community, which comprises a number of chemical industries, intensive agriculture, as well as boating and fishing activities, releases anthropogenic contaminants into the lagoon waters. As a consequence, a number of xenobiotics, among them PAHs, PCBs, heavy metals and organo metallic compounds, have been found in the lagoon [Magistrato alle Acque di Venezia, 2000; Fossato *et al.*, 2000; Gallina *et al.*, 2000, Critto and Marcomini, 2001; Dalla Valle *et al.*, 2005; Frignani *et al.*, 2005]. Xenobiotic exposure can produce multiple consequences on the organisms, affecting organ function, reproductive ability, population size and ultimately biodiversity. However the presence of xenobiotics in a segment of an aquatic ecosystem does not, by itself, indicate injurious effects. Relations have to be established between external levels of exposure, internal levels of tissue contamination and adverse effects in order to assess the environmental risk [Depledge and Fossi, 1994].

Deleterious effects on populations are often difficult to detect in feral organisms since many of them tend to manifest these effects only after longer periods of time. The sequential order of responses to pollutant stress within a biological system always starts from molecular and subcellular damage. Effects at the higher end of the hierarchy are always preceded by these kinds of changes in biological processes, which go unobserved unless molecular and cellular biomarkers (early-warning signals) are evaluated [Bayne *et al.*, 1985]. Biomarkers can demonstrate that a toxicant has entered an organism, has been distributed between tissues, and is eliciting a toxic effect at critical targets [McCarthy and Shugart, 1990] promptly offering a warning as to the relative toxicity of polluting chemicals. Without the study of these signals, a prognostic evaluation of dystrophy cannot not be made and, when the effect finally becomes clear, the destructive process may have gone beyond the point where it can be reversed by remedial actions or risk reduction [van der Oost *et al.*,

2003].

A quantity of evidence shows that exposure to xenobiotics is very often the cause of early DNA damage. Besides direct adduct formation, damage may include double and/or single strand breaks (SSB and DSB) and alkali labile sites (ALS) in the DNA polymer, changes in the DNA's minor base composition or an increase in the level of DNA repair [Nacci *et al.*, 1992; Shugart *et al.*, 1992; Vukmirovic *et al.*, 1994; Venier *et al.*, 1997; Lee and Steinert, 2003; Bolognesi *et al.*, 2004; Kalpaxis *et al.*, 2004; Jaksic *et al.*, 2005; Marigomez *et al.*, 2006; Nigro *et al.*, 2006].

Apoptosis, the programmed cell death that leads to DNA fragmentation of multiples of 180-200 basepairs, also seems to be promptly elicited as a consequence of exposure to xenobiotics. Indeed, an immediate significant increase in apoptotic process frequency has been observed in many tissues of vertebrate and invertebrate aquatic organisms as a consequence of exposure to PCBs, Cd, BKME (Bleached Kraft Mills Effluent), organometals, and oxidative stress [Janz *et al.*, 1997; Cima and Ballarin, 1999; Piechotta *et al.*, 1999; Tallandini *et al.*, 2001, van der Oost *et al.*, 2003, Jiang and Wang, 2004, Sokolova *et al.*, 2004, Kefaloyanni *et al.*, 2005]. While DNA SSB, DSB and ALS are direct genotoxic effects, apoptosis seems to proceed from cytotoxic effects [Henderson *et al.*, 1998]. Due to the above background increases, DNA damage is often used as a biomarker of various genotoxic and cytotoxic endpoints in different monitoring campaigns.

Comet Assay, which was first introduced in the late 1980s on mammalian cells [Östling and Johansen, 1984], is now commonly used to estimate DNA damage, DNA repair and ladder DNA (such as cell death in apoptosis) in different cell types from different vertebrate and invertebrate aquatic organisms. Due to its ease, speed and low cost, Comet Assay is well suited not only to laboratory tests, but also to the routine in situ monitoring of sentinel organisms that are chronically exposed to waterborne pollutants. The feasibility of using this technique, the advantages and disadvantages of which have been extensively described in literature [Mitchelmore and Chipman, 1998, Cotelle and Ferard, 1999, Dixon *et al.*, 2002; Lee and Steinert, 2003] provides the field of ecotoxicology with an innovative tool [Jha, 2004].

This work reports the results from two monitoring studies of indigenous blue mussels, *Mytilus sp.*, collected from different sites around the Venice Lagoon, in which alkaline Comet Assay was employed in order to ascertain the ecotoxicological potential of the water environment. Mussels were chosen as a sentinel organism due to their great filtration capacity, which ensures xenobiotic assumption and bioaccumulation, and to their low mobility, which ensures that any adverse effects detected are most probably due to in situ pollution. The tissue studied was the digestive gland because of the central role in the assumption, bioaccumulation and metabolism of both organic and inorganic xenobiotic compounds [Mitchelmore *et al.*, 1998a,b; Shaw *et al.*, 2004].

The first study was carried out from 1999 – 2000, the second from 2005 – 2006.

The two field studies report and compare the results on DNA damage (SSB, DSB and ALS) that were observed in the same period of seven months, from December to June. Apoptosis incidence in nuclei population was also evaluated in the second study. From 1999 – 2000 five sites were monitored while from 2005 – 2006 only four of the previous five sites could be used to collect and examine mussels again because no living in situ mussels were found in the fifth location.

2 Materials and Methods: Experimental Design

2.1 Mussel collection and sampling site

In order to assess temporal and spatial trends within the Venice Lagoon, the same sampling scheme was repeated in the two field studies.

Mussels (*Mytilus galloprovincialis*, Lam) were collected monthly at 0.4 – 0.6 m depth during a period of seven months from December to June in five sites around the Venice Lagoon. The sites were selected in order to draw a transect from the coast to the lagoon interior. The sites were: 1. *Porto di Chioggia*; 2. *Porto di Malamocco*; 3. *Canale San Domenico*; 4. *Canale Lombardo Esterno*; 5. *Area Industriale di Marghera* (Fig. 1). Sites 1 and 2 were the most external and directly exposed to the tide inflow and outflow; site 3 was the most directly exposed to urban drainage as it was in the centre of Chioggia town; sites 4 and, especially, 5 were the most internal and directly exposed to industrial waste. The distances from the sea were calculated starting from the line of the mussel farms outside the lagoon (Fig.1, dotted line).

Twelve mussels (length: 6 ± 0.6 cm) were collected from each site at each collection time and quickly transferred to the laboratory, where they were stored overnight in individual flasks in filtered aerated seawater to clear gut contents prior to the Comet Assay.

During the second study, which was conducted from December 2005 to June 2006, we were not able to find native mussels in site 5, *Area Industriale di Marghera*.



Fig 1 – Map of the Venice Lagoon showing the mussel collection sites throughout the two campaigns (1999 – 2000 and 2005 – 2006). The dotted line indicates the line of mussel farms.

2.2 Cell isolation from digestive gland

Comet Assay was performed on digestive gland cells. A slightly modified version of the protocols of Lowe and Pipe (1994) and Mitchelmore and Chipman (1998) were used for cell isolation.

The individual digestive glands of five mussels were carefully dissected, washed twice in Ca^{2+} - Mg^{2+} free saline (CMFS) buffered solution (20 mM HEPES-NaOH, 500 mM NaCl, 12.5 mM KCl, 5 mM EDTA pH 7.3), and minced into small pieces.

The tissue pieces were transferred to flasks containing 4 ml CMFS and slowly shaken in a regular manner for 60 minutes at 15°C.

At the end of the incubation time, cell suspensions were filtered through 100 μm and 25 μm strainers to remove cell clumps and oocytes.

The filtrate was centrifuged at 200xg for 10 minutes at 4°C [Birmelin *et al.*, 1998].

The pelleted cells were resuspended in 0.5 ml CMFS and combined to a density of approximately 10,000 cells in 10 μ l. Cell viability was checked using the Trypan blue dye exclusion test.

2.3 Alkaline Single Cell Electrophoresis

For the SCGE procedure the protocols of Singh *et al.* (1988) and Singh (2000) were followed with minor adjustments. In short, 10 μ l of CMFS cell suspension containing 10^4 cells were mixed with 75 μ l of Low Melting Agarose (0.7% in PBS) and layered on a microscope slide precoated with Normal Melting Agarose (0.8% in PBS). The slides were then suspended in the lysis buffer (10 mM Tris-HCl, 2.5 M NaCl, 0.2 M NaOH, 100 mM EDTA, 1% Triton X-100, 10% DMSO pH 10) and after cytoplasmic membrane lysis, DNA was unwound with immersion for 60 min. in freshly prepared electrophoretic buffer (0.3 M NaOH, 1 mM EDTA pH 13.5). After the electrophoretic run (25 V, 300 mA for 10 min.), washing twice with 0.3 mM Tris at pH 7.5 and staining with ethidium bromide, the slides were examined at 400X using a fluorescent microscope (LEICA, excitation filter BP515-560 green light and BA590 barrier filter). Starting from the lysis step, all of the activities were performed exclusively in the dark.

Computer software was used to score individual parameters for each nucleus examined. The software was developed (Co. Casti Imaging 2001) on the basis of the public domain analysis program for SCGE [Helma and Uhl, 2000].

The images observed were described (Fig. 2) as: 1) Nuclei: in the case of a subspheric core; 2) Cometiae: in the case of a tail exceeding the right edge of the subspheric core circle (DNA fluorescence exceeding 10% of the total DNA fluorescence); 3) Apoptotic nuclei: in the case of DNA fluorescence completely migrating and almost detaching from the subspheric core of the nucleus, which appears drastically reduced.

The comet image analysis included the evaluation of the following parameters: total DNA; percentage of DNA in the comet head and tail; Tail Length (TL) and Tail Moment (TM), ($TM=TL \times \% \text{ DNA fluorescence in the Tail}$) [Ashby *et al.*, 1995; Helma and Uhl, 2000] (Fig. 3).

At least 50 cells per animal were examined for each sample. Statistical analysis was performed with the Student's t test and the ANOVA test, and was completed by Tuckey's test with the help of "Statistica" software, version 6.

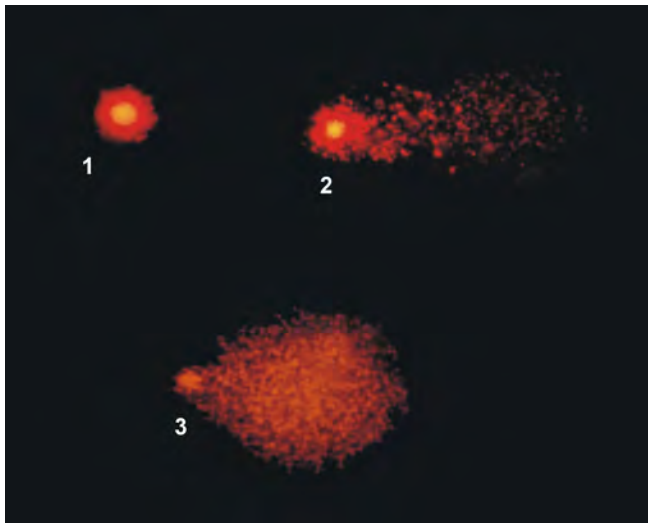


Fig 2 – Images of nuclei after SCGE: 1) intact nucleus, 2) comet, 3) apoptotic nucleus.

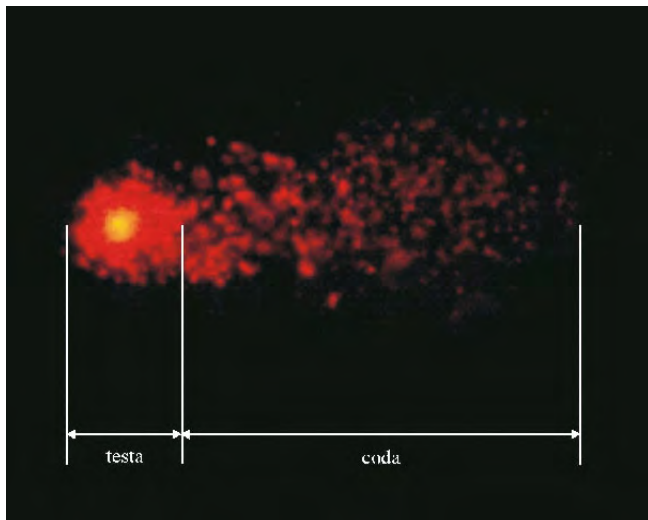
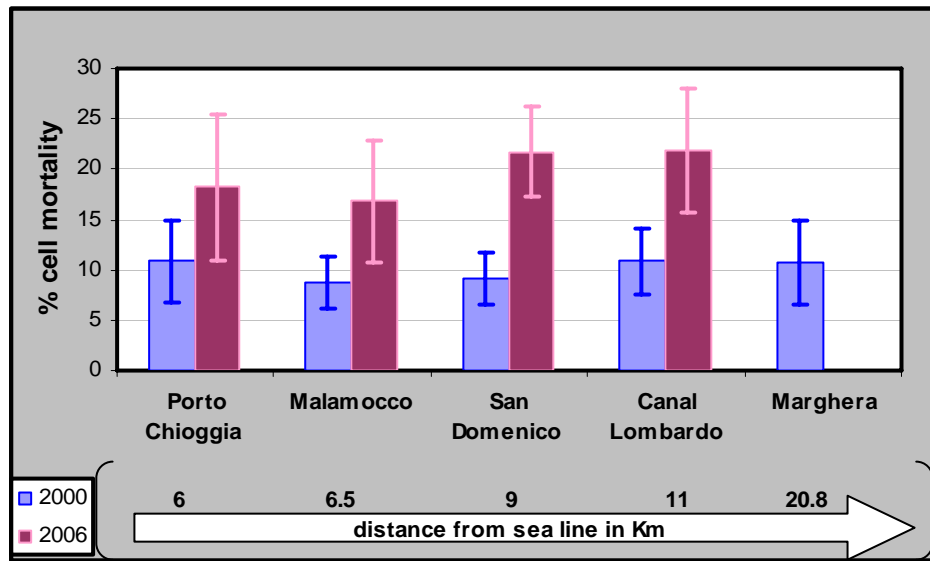


Fig 3 – Schematic representation of comet head and tail parameters according to Helma and Uhl 2000.

3 Results

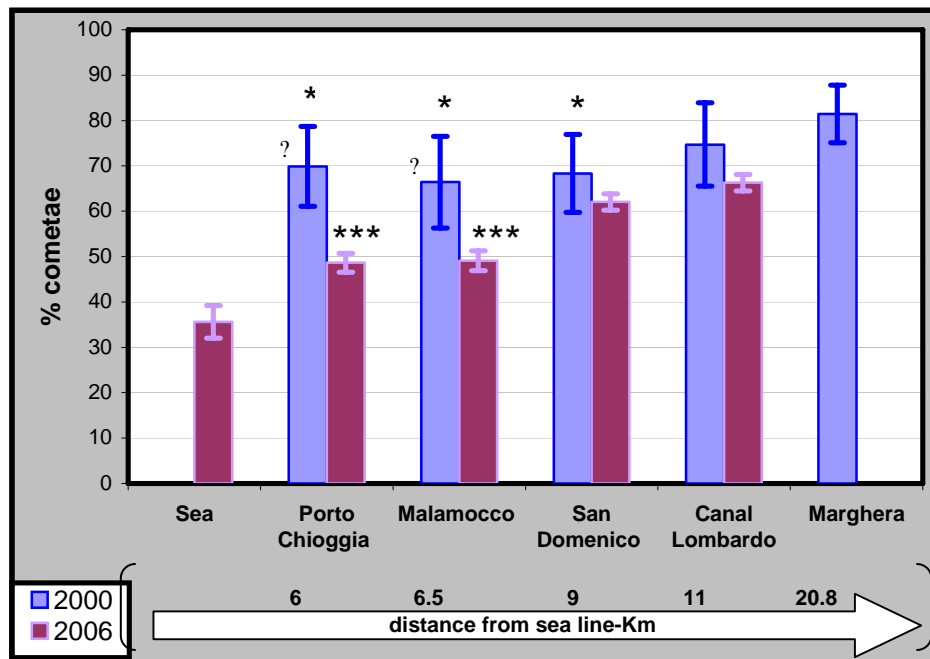
Fig. 4 reports the mean mortality values (%) of digestive gland cells in the two studies from December to June. The only exception is the site *Area Industriale di Marghera* (indicated by Marghera in the graph) in which mussels were not found in the second study. While in 2000 the mean mortality value was $10.8\% \pm 1$ s.d. without significant differences among the different sites, in 2006 the overall mean mortality value was almost double at $19.5\% \pm 4$ s.d. Furthermore, we observed that in 2006 cell mortality increased as we headed away from the outer sites towards the inner sites.

Fig 4 – Mean values of cell mortality (%) in the monitored sites in the 2000 and 2006 field studies. Note that only data from the 2000 study were available at the Marghera site due to the absence of living mussels in 2006.



In Fig. 5 cometae (%), i.e. nuclei whose DNA had migrated out of the original nucleus perimeter by more than 10%, shows that the cometae values (%) in the 2006 study were lower than 2000. However, when the two studies were compared the only major differences were observed in *Porto Chioggia* and *Malamocco*. As already observed with mortality, the percentage of cometae also increased as we headed away from the outer sites towards the inner sites.

Fig 5 – Mean values of cometae (%) in the monitored sites in the 2000 and 2006 field studies. By way of comparison, the graph also illustrates the mean value obtained in May 2006 with control samples taken from a mussel farm in the open sea.



Note that in Marghera only the 2000 campaign data were available.

Asterisk symbol (*) in the 2000 campaign: significant difference with Marghera site; (*) $P \leq 0.05$ (**) $P \leq 0.001$;

Asterisk symbol (*) in the 2006 campaign: significant difference with Canal Lombardo site; (****) $P \leq 0.0001$.

Triangle symbol (▲): significant difference between the two campaigns (▲) $P \leq 0.05$.

Fig. 6 illustrates the DNA values (%). In the 2006 study, values were significantly lower than in 2000 at all four of the sites. Note that while in 2000 the damage values were very similar in three sites (*Porto Chioggia*, *San Domenico* and *Canal Lombardo*), slightly lower in *Malamocco* and significantly higher in *Marghera*, in 2006 cells were found to be increasingly damaged as we headed from the outer to the inner sites in the lagoon. Indeed the % DNA values found in *San Domenico* and *Canal Lombardo* were significantly higher than those observed in *Porto Chioggia* and *Malamocco*.

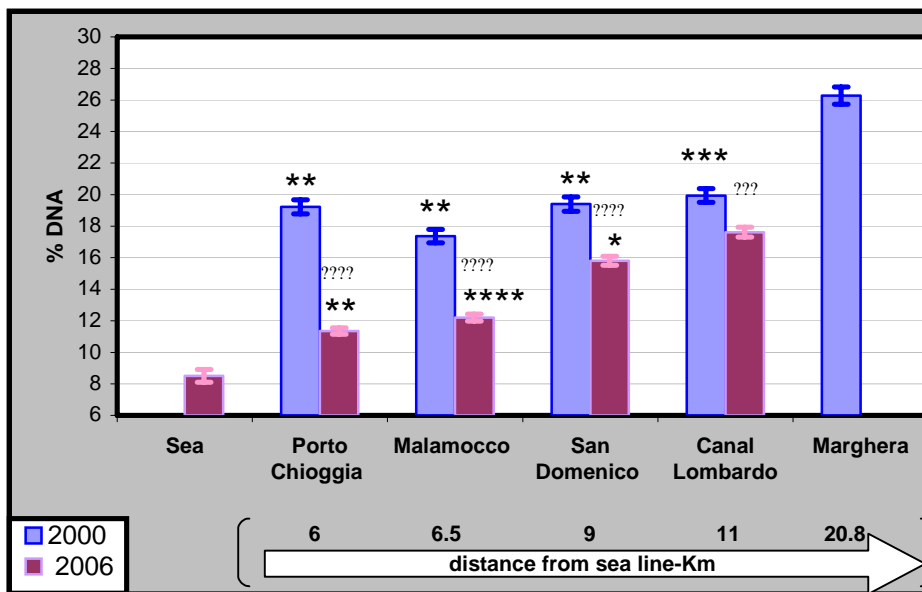


Fig 6 – Mean DNA values (%) observed in the lagoon sites in the 2000 and 2006 studies.

By way of comparison, the graph also illustrates the mean value obtained in May 2006 with control samples taken from a mussel farm in the open sea.

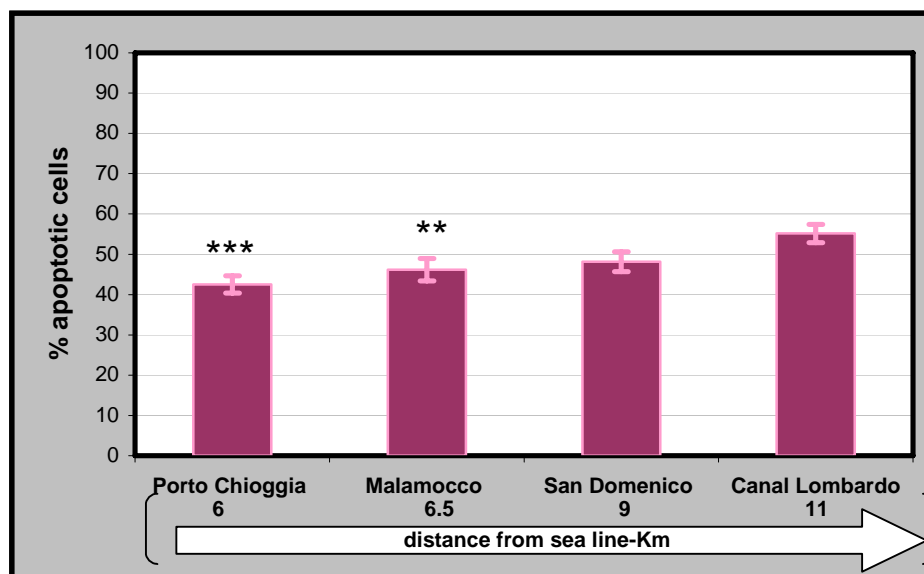
Asterisk symbol (*) in the 2000 study: significant difference with Marghera site; (***) $P \leq 0.001$; (****) $P \leq 0.0001$;

Asterisk symbol (*) in the 2006 study: significant difference with Canal Lombardo site; (***) $P \leq 0.001$; (****) $P \leq 0.0001$.

Triangle symbol (▲): significant difference between the two campaigns (▲▲▲) $P \leq 0.001$; (▲▲▲▲) $P \leq 0.0001$.

Fig. 7 illustrates the percentage of apoptotic nuclei observed in the 2006 study. The values are dramatically high, ranging from 42.5% in the site of Porto Chioggia, the nearest to the sea, to 55% in the Canal Lombardo site, the furthest from the sea; the overall mean value was 48%. As already observed for the other parameters, including apoptosis, values increased as we moved from the outer sites towards the inner sites. Unfortunately we had no apoptosis data for the same period in 2000 to use by way of comparison.

Fig 7 – Mean values of apoptotic nuclei (%) observed in the lagoon sites in 2006.



Asterisk symbol: significant difference with Canal Lombardo site; (**): $P \leq 0.01$; (***): $P \leq 0.001$.

Conclusions

The use of cellular and molecular biomarkers in ecotoxicology has become a major issue in environmental risk assessment. Analysis of early biological alterations caused by contaminants in sentinel species demonstrates that a toxicant is eliciting a toxic effect on critical targets by providing a prompt warning as to the relative toxicity of a dystrophic situation. These signals therefore give a prognostic evaluation of environmental risk before those effects at the higher end of the hierarchy have gone beyond the point where they can be reversed by remedial actions or risk reduction.

A quantity of evidence shows that exposure to xenobiotics is very often the cause of early DNA damage. Comet Assay, which was first introduced in the late 1980s on mammalian cells, is now increasingly used to estimate DNA damage, such as SSB, DSB, ALS and also apoptosis, in vertebrate and invertebrate organisms [Ballarin *et al.*, 2007]. The data obtained from the two field studies in the Venice Lagoon, which were carried out between December and June 1999 – 2000 and between the same months in 2005 – 2006, show dystrophy within the lagoon, which worsened as we headed away from the coast towards the lagoon interior. In the 2006 study, cell mortality and apoptosis levels were very high. As for cell mortality, the values in the second monitoring were almost double those in the first one. As for apoptosis, we have no data for the same period in the first study. The extremely high values of apoptosis and mortality parameters in 2006 seem to suggest that organisms were suffering severer dystrophy during the second monitoring period than during the first one. The data reported could have two possible explanations/interpretations: the first is that the living cells examined for DNA damage were more resistant to polluting agents than the dead cells; the second is that the living cells were

young cells and consequently had been exposed to polluting agents for a shorter time. In both cases we may have been observing the effect of damaging agents on cells in a phase in which damage and repair actions were not totally impaired. This could explain why the second study showed apparently lower genotoxic damage, such as DNA SSB, DSB and ALS, than in the first one. On the other hand, the damage increased significantly as we moved from the sites with a high water exchange towards those furthest from the sea where the studies revealed a higher environmental impact.

Furthermore, remember that mussels collected in a sea farm showed the least damage and that during the second monitoring we were unable to collect mussels from the *Marghera* site, the innermost site, which showed the highest damage values in the first study.

In conclusion, in the light of this paper's results, the monitoring of a sentinel organism by Comet Assay seems to be a major tool for studying/following/ascertaining the presence of dystrophy in aquatic environments. Therefore it would be very interesting to complete this kind of study with data about the chemical pollution in the same sites in order to evaluate whether there is a link between the two.

References

- Ashby J., Tinwell H., Lefevre P.A., Browne M.A., 1995. The single cell gel electrophoresis assay for induced DNA damage (comet assay): measurement of tail length and moment. *Mutagenesis*, 10, 85-90.
- Ballarin L., Menin A., Tallandini L.; Matozzo V.; Burighel P., Basso G., Fortunato E., Cima F., 2007. Haemocytes and blastogenetic cycle in the colonial ascidian *Botryllus schlosseri*: a matter of life and death: *Cell & Tissue Research*, in print.
- Bayne B.L., Brown D.A., Burns K., Dixon D.R., Ivanovici A., Livingstone D.A., Lowe D.M., Moore M.N., Stebbing A.R.D., Widdings J., 1985. The effects of stress and pollution on marine animals. Praeger, New York, USA.
- Birmelin C., Mitchelmore C.L., Goldfarb P.S., Livingstone D.R., 1998. Characterization of biotransformation enzyme activities and DNA integrity in isolated cells of the digestive gland of the common mussel, *Mytilus edulis* L. *Comp. Biochem. Physiol.*, 120 (A), 51-56.
- Bolognesi C., Frenzilli G., Lasagna C., Perrone E., Roggeri P., 2004. Genotoxicity biomarkers in *Mytilus galloprovincialis*: wild versus caged mussels. *Mutat. Res.*, 552, 153-162.
- Cima F. and Ballarin L., 1999. TBT-induced apoptosis in tunicate haemocytes. *Appl. Organometal Chem.*, 13, 697-703.
- Cotelle S. and Ferard J.F., 1999. Comet assay in genetic ecotoxicology: a review. *Environ. Mol. Mutagen.*, 34, 246-255.
- Critto A. and Marcomini A., 2001. *Rischio ecologico ed inquinamento chimico lagunare*. Cà Foscari Ed. Venezia, Italia.

Dalla Valle M., Marcomini A., Jones K.C., Sweetman A.J., 2005. Reconstruction of historical trends of PCDD/Fs and PCBs in the Venice Lagoon, Italy. *Environ. Int.*, 31(7), 1047-1052.

Depledge M.H. and Fossi M.C., 1994. The role of biomarkers in environmental assessment (2). *Ecotoxicology*, 3, 161-172.

Dixon D.R., Pruski A.M., Dixon L.R.J., Jha A.N., 2002. Marine invertebrate ecogenotoxicology: a methodological overview. *Mutagenesis*, 17, 495-507.

Fossato V.U., Campesan G., Craboledda L., Dolci F., Stocco G., 2000. Organic micropollutants and trace metals in water and suspended matter. In: *The Venice Lagoon Ecosystem*, P. Laserre and A. Marzollo ed., Parthenon Publishing: 81-95.

Frignani M., Bellocci L.G., Fagotto M., Albertazzi S., 2005. Pollution historical trends as recorded by sediments at selected sites of the Venice Lagoon. *Environ. Int.*, 31(7), 1011-1022.

Gallina A., Magno F., Tallandini L., Passaler T., Caravello G., Pastore P., 2000. Simple and effective gaschromatographic mass spectrometric procedure for the speciation analysis of organotin compounds in specimens of marine mussels. An evaluation of the organotin pollution of the Lagoon of Venice. *Rapid Commun. Mass Spectrom.*, 14, 373-378.

Ghetti A. and Batisse M., 1983. The overall protection of Venice and its lagoon. *Nature Res.*, 19, 7-19.

Helma C. and Uhl M., 2000. A public domain image-analysis program for the single-cell gel-electrophoresis (comet) assay. *Mutat. Res.*, 466, 9-15.

Henderson L., Wolfreys A., Fedyk J., Clare B., Windebank S., 1998. The ability of Comet assay to discriminate between genotoxins and cytotoxins. *Mutagenesis*, 13 (1), 89-94.

Jakšić Z., Batel R., Bihari N., Mičić M., Zahn R.K., 2005. Adriatic coast as a microcosm for global genotoxic marine contamination: A long-term field study. *Mar. Pollut. Bull.*, 50, 1314-1327.

Janz D.M., McMaster M.E., Munkittrick K.R., Van der Kraak G., 1997. Elevated ovarian follicular apoptosis and heat shock protein-70 expression in white sucker exposed to bleached kraft pulp mill effluent. *Toxicol. Appl. Pharmacol.*, 147, 391-398.

Jha A.N. 2004. Genotoxicological studies in aquatic organisms: an overview. *Mutat. Res.*, 552, 1-17.

Jiang X. & Wang X., 2004. Cytochrome c-mediated apoptosis. *Annu. Rev. Biochem.*, 73, 87-106.

Kalpaxis D.L., Theos C., Xaplateri M.A., Dinos G.P., Catsiki A.V., Leotsinidis M., 2004. Biomonitoring of Gulf of Patras, N. Peloponnesus, Greece. Application of a biomarker suite including evaluation of translation efficiency in *Mytilus galloprovincialis* cells. *Environ. Res.*, 94, 211-220.

- Kefaloyianni E., Gorgou E., Ferle V., Kotsakis E., Gaitanaki C., Beis I., 2005. Acute thermal stress and various heavy metals induce tissue-specific pro- or anti-apoptotic events via the p38-MAPK signal transduction pathway in *Mytilus galloprovincialis* (Lam.). *J. Exp. Biol.*, 208, 4427-4436.
- Lee R.F. and Steinert S., 2003. Use of the single cell gel electrophoresis/comet assay for detecting DNA damage in aquatic (marine and freshwater) animals, *Mutat. Res.*, 544, 43-64.
- Lowe D.M and Pipe R.K., 1994. Contaminant induced lysosomal membrane damage in marine mussel digestive cells: an in vitro study. *Aquatic-Toxicology.*, 30(4), 357-365.
- Magistrato alle Acque di Venezia – Consorzio Venezia Nuova, 2000. Mappatura dei fondali lagunari. Rapporto Finale. Consorzio Venezia Nuova, Venezia, Italia.
- Marigómez I., Soto M., Cancio I., Orbea A., Garmendia L., Cajaraville M.P., 2006. Cell and tissue biomarkers in mussel, and histopathology in hake and anchovy from Bay of Biscay after Prestige oil spill (Monitoring Campaign 2003). *Mar. Pollut. Bull.*, 53, 287-304.
- McCarthy J.F. and Shugart L.R., 1990. Biological markers of environmental contamination. In: McCarthy J.F. and Shugart L.R. (Eds.), *Biomarkers of environmental contamination*. Lewis Publishers, Boca Raton, FL, USA, pp.3-16.
- Mitchelmore C.L. and Chipman J.K., 1998. Detection of DNA strand breakage in aquatic organisms and the potential value of the comet assay in environmental monitoring, *Mutat. Res.*, 399, 135-147.
- Mitchelmore, C.L., Birmelin, C., Chipman, J.K. and Livingstone D.R. (1998a). Evidence for cytochrome P-450 catalysis and free radical involvement in the production of DNA strand breaks by benzo[a]pyrene and nitroaromatics in mussel (*Mytilus edulis* L.) digestive gland cells. *Aquat. Toxicol.*, 41 (3), 193-212.
- Mitchelmore C.L., Birmelin C., Livingstone D.R. and Chipman J.K. (1998b). Detection of DNA strand breaks in isolated mussel (*Mytilus edulis* L.) digestive gland cells using the "comet" assay. *Ecotoxicology Environmental Safety*, 41 (1), 51-58.
- Nacci D., Nelson S., Nelson W., Jackim E., 1992. Application of DNA alkaline unwinding assay to detect DNA strand breaks in marine bivalves. *Mar. Environ. Res.*, 33, 83-100.
- Nigro M., Falleni A., Del Barga I., Scancelli V., Lucchesi P., Regoli F., Frenzilli G., 2006. Cellular biomarkers for monitoring estuarine environments: transplanted versus native mussels. *Aquat. Toxicol.*, 77, 339-347.
- Östling, O. & Johanson K.J. 1984. Bleomycin, in contrast to gamma irradiation, induces extreme variation of DNA strand breakage from cell to cell. *Int. Journal of radiation biology*, 52, 683-691.
- Piechotta G., Lacorn M., Lang T., Kammann U., Simat T., Jenke H.S., Steinhart H. 1999. Apoptosis in dab (*Limanda limanda*) as possible new biomarker for anthropogenic stress. *Ecotoxicol. Environ. Safe*, 42, 50-56.

Shaw J.P., Large A.T., Donkin P., Evans S.V., Staff F.J., Livingstone D.R., Chipman J.K., Peters L.D., 2004. Seasonal variation in cytochrome P450 immunopositive protein levels, lipid peroxidation and genetic toxicity in digestive gland of the mussel *Mytilus edulis*. *Aquat Toxicol.*, 67(4), 325-336.

Shugart L.R., Bickham J., Jackim G., McMahon G., Ridley W., Stein J., Steinert S., 1992. DNA alterations. In: Huggett R.J., Kimerly R.A., Mehrle P.M., Jr, Bergman H.L. (Eds). *Biomarkers: Biochemical, Physiological and Histological Markers of antropogenic stress*. Lewis Publishers, Chelsea, MI, USA, pp. 155-210.

Singh N.P. 2000. Microgel for estimation of DNA strand breaks, DNA protein crosslinks and apoptosis. *Mutat. Res.*, 455, 111-127.

Singh N.P., McCoy M.T., Tice R.R., Schneider E.L., 1988. A simple technique for quantification of low levels of DNA damage in individual cells. *Exp.Cell.Res.*, 175, 184-191

Sokolova I.M., Evans S., Hughes F.M. 2004. Cadmium-induced apoptosis in oyster hemocytes involves disturbance of cellular energy balance but no mitochondrial permeability transition. *J. Exp. Biol.*, 207, 3369-3380.

Tallandini L., Modenato M., Pivotti L., 2001. Tributyl effects at cellular level in mussels: cell survival, apoptotic effects and cell survival. In: *FESTEM International Congress on trace elements and minerals in medicine and biology* 85.

Van der Oost R., Beyer J., Vermeulen N.P.E., 2003. Bioaccumulation and biomarkers in environmental risk assessment: a review. *Environ. Toxicol. Pharmacol.*, 13, 57-149.

Venier P., Maron S., Canova S., 1997. Detection of micronuclei in gill cells and haemocytes of mussels exposed to benzo[a]pyrene. *Mutat. Res.*, 390, 33-44.

Vukmirović M., Bihari N., Zahn R.K., Müller W.E.G., Batel R., 1994. DNA damage in marine mussel *Mytilus galloprovincialis* as a biomarker of environmental contamination. *Mar. Ecol. Prog. Ser.*, 109, 165-171.

A TOXICITY INDEX FOR THE VENICE LAGOON

Annamaria Volpi Ghirardini, Chiara Losso, Alessandra Arizzi Novelli,
Pier Francesco Ghetti

Dipartimento di Scienze Ambientali, Università Ca' Foscari di Venezia

Riassunto

Nell'ambito del programma di ricerca promosso dal Co.ri.La sugli "Indicatori e indici di qualità ambientale per la laguna di Venezia", è stato sviluppato un indice di tossicità in grado di sintetizzare le risposte derivanti da più test di tossicità con diversi organismi acquatici applicati su diverse matrici estratte dal sedimento. L'indice di tossicità è uno strumento utile perché classifica la tossicità dei sedimenti lagunari in 5 classi di tossicità (assente, bassa, media, alta e molto alta), permette una facile visualizzazione delle informazioni e rappresenta un passo fondamentale nell'integrazione delle risposte ecotossicologiche con quelle chimiche ed ecologiche inerenti la comunità bentonica.

Abstract

During the Research Program promoted by Co.ri.La on "Environmental quality indicators and indices for the Venice lagoon", a toxicity index was developed that can synthesise responses from different bioassays with a variety of aquatic organisms on various phases of exposure deriving from sediment. The toxicity index is a useful tool because it classifies sediment toxicity in five classes (absent, low, medium, high and very high), permits easy representation of the information and allows ecotoxicological responses to be integrated with chemical and ecological ones.

1 Introduction

The research project (as part of line 3.11) aims to identify indicators and develop indices of environmental quality of the lagoon of Venice, based on the approach established by the Water Framework Directive (EU, 2000), which focus on the integration of chemical, physical and ecological parameters, in order to define ecological quality classes for the different water bodies. The main reasons for developing quality indices are chemoassessment and bioassessment; toxicity of environmental compartments is one element of bioassessment. We use toxicity bioassays related to sediment contamination at whole-lagoon scale, with the aim of identifying the most representative bio-indicators for the lagoon and developing a multimetric toxicity index.

Many toxicity bioassays for sediment assessment have been developed internationally in recent decades, involving various phases of exposure (pore water, fractionated and unfractionated organic extract and whole sediment),

conducted on a variety of aquatic organisms and considering a lot of endpoints, so that toxicity data are often difficult to interpret.

Toxicity indices are intended to combine bioassay results into a single response, synthesizing toxicity information and translating the results into simple terms for decision-makers. The representation of all results from the different sediment toxicity tests on a common, easily interpreted scale is the main and recognised application of environmental indices [Shin and Lam, 2001].

In this paper we briefly describe our research activities for developing the toxicity index; details on methods and results are reported in Losso et al. [submitted].

2 The conceptual model

We proposed a stepwise procedure to select, according to specific criteria, a minimum number of toxicity bioassays on suitable matrices in order to integrate their responses into a multimetric toxicity index (Fig. 1).

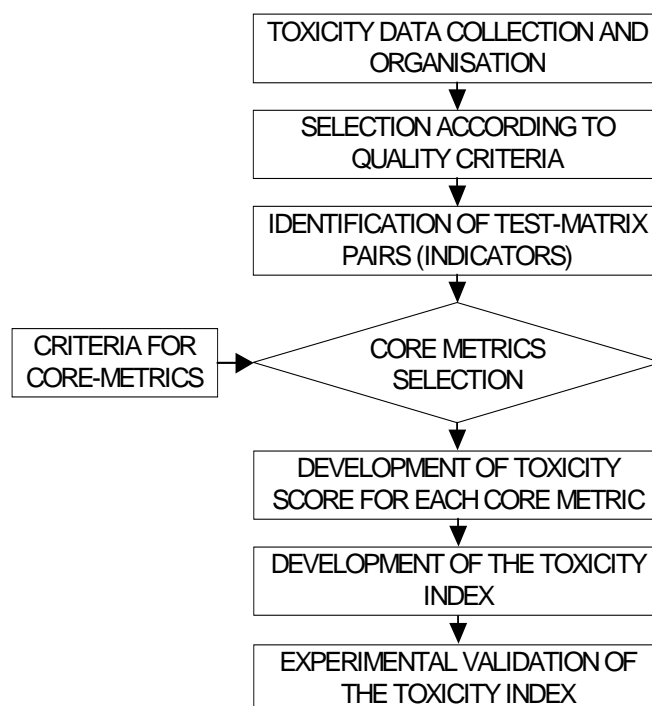


Fig 1 – Stepwise procedure to develop the toxicity index.

2.1 First steps: the toxicological database for the Venice lagoon

We collected and organised all available toxicity data for the Venice lagoon. As first output, a toxicity database was created including the main information regarding the toxicity test (species, endpoint, test protocol), test matrix (matrix typology, protocol used for matrix preparation), study site (site name, site mark, coordinates, sampling year, depth and type), toxicity data (Percentage of Effect with standard deviation or, if calculable, EC50 and TU50 with confidence limits

at 95%), data quality (use of negative control, positive control, sediment control) and the reference for data availability.

Toxicity data were then selected according to quality criteria using the standard protocol and Quality Assurance/Quality Control criteria for sampling and preparing the test matrix and performing the toxicity bioassay.

All available test–matrix pairs for the lagoon were thus identified: they represent the TOXICOLOGICAL INDICATORS and are: sperm cell toxicity test with *Paracentrotus lividus* on pore water; sperm cell toxicity test with *P. lividus* on elutriate; embryotoxicity test with *P. lividus* on pore water; embryotoxicity test with *P. lividus* on elutriate; embryotoxicity test with *Mytilus galloprovincialis* on pore water; embryotoxicity test with *M. galloprovincialis* on elutriate; embryotoxicity test with *Crassostrea gigas* on pore water; embryotoxicity test with *C. gigas* on elutriate; test with *Vibrio fischeri* (Microtox® test) on solid-phase.

2.2 The selection of toxicological core-metrics

Toxicity core-metric (CM-tox) selection identifies the test-matrix pairs considered significant for the elaboration of the toxicity index. The selection was made according to specific criteria, suggested by the literature and expert judgment. We divided the criteria into four categories, based on the suggestion of Viaroli et al. [2004]:

- ECOLOGICAL SIGNIFICANCE (ES), regarding the species used and endpoint in relation to the study environment. This category includes the following criteria: species representativeness for the study environment, test representativeness for the investigated matrix and endpoint.
- UNCERTAINTY (U), concerning the uncertainty of bioassay response and including: test sensitivity, reproducibility, test species availability and influence of confounding factors.
- COST EFFECTIVENESS (CE) referring to the possibility of using the test for monitoring purposes: including execution rapidity, ease of execution and costs.
- DATABASE CHARACTERISTIC (DC), depending on the available information and regarding data abundance and result complementarity.

Comparative weights in the 0-1 range were assigned to each criteria. As a result, the selected CMs-tox for the Venice lagoon were:

- bioluminescence reduction with *V. fischeri* on solid phase;
- embryotoxicity test with *P. lividus* on elutriate;
- embryotoxicity test with *M. galloprovincialis* on elutriate;
- sperm cell test with *P. lividus* on pore water;
- embryotoxicity test with *C. gigas* on pore water.

2.3 The toxicity scores

We recently developed toxicity scores for elutriates [Losso et al., 2007]. These scores are based on five toxicity classes (absent, low, medium, high and very high). The first toxicity threshold, defining when a sample is toxic, is determined by a statistical approach, following the Minimum Significance Difference (MSD) suggested by Phillips et al. [2001]. The other toxicity thresholds, defining how toxic a sample is, are based on data distribution.

The same approach was used for the toxicity tests on pore waters as the tests on elutriate.

For the Microtox® test on solid-phase, such an approach is not applicable as the control response is from a solid matrix. For this reason the toxicity thresholds were defined only on data distribution; the first threshold defining when a sample is toxic was the 10th percentile (TU50=322, n=122).

2.4 Developing the toxicity indices

Two toxicity indices were developed for the Venice lagoon: the Toxicity Effect Index (TEI index) following an approach suggested in the literature and the Weighted Average Index (WATI Index).

The TEI index was calculated starting from the SED-TOX index [Bombardier and Bermingham, 1999], which is not applicable to the Venice lagoon as it is, because other toxicity bioassays are considered and toxicity ranges are different. We therefore introduced substantial modifications to the SED-TOX. Briefly, the TEI index starts from the toxicity values expressed as TU, which are normalised to dry weight. Data are thus normalised to the TU_{lim}, i.e. the minimum toxicity revealed by the test. Normalised data are summarised, taking into account the sensitivity weight of each CM-tox. Finally, the logarithm of the weighted sum is considered. TEI values were classified in five toxicity classes: $0 \leq \text{TEI} \leq 0.3$ for absent toxicity; $0.3 < \text{TEI} \leq 0.7$ for low toxicity; $0.7 < \text{TEI} \leq 1.23$ for medium toxicity; $1.23 < \text{TEI} \leq 1.8$ for high toxicity; $\text{TEI} > 1.8$ very high toxicity.

The WATI index started from the toxicity classes determined by the toxicity scores. A score was assigned from 0 to 4 to each toxicity class, where 0 defines the absence of toxicity and 4 very high toxicity. The scores of each CM-tox were summarised and weighted according to the comparative weights (at 0-1 range) assigned by the criteria for CM-tox selection. The WATI values were classified in five equivalent sub-ranges, determining five toxicity classes: $0 \leq \text{WATI} \leq 0.2$ absent; $0.2 < \text{WATI} \leq 0.4$ low; $0.4 < \text{WATI} \leq 0.6$ medium; $0.6 < \text{WATI} \leq 0.8$ high; $0.8 < \text{WATI} \leq 1$ very high.

3 Application of the toxicity indices to the Venice lagoon

The indices were applied to the available toxicity data, concerning 110 sediment samples collected between 1994 and 2005 from 21 sites (Figure 2) in the lagoon of Venice, most of which were sampled twice at different seasons. Despite the experimental activity (in the field and laboratory) to fill the gaps in the lagoon toxicity dataset, there are only 52 sediment samples with more than one CM-tox. The TEI index showed values from 0 to 2.42: 10 samples were classified as toxicity absent, 14 as low, 13 as medium, 10 as high and 5 as very

high. For the WATI index, 11 samples were classified as toxicity absent, 16 as low, 6 as medium, 7 as high and 12 as very high. Both indices evidenced that samples with very high toxicity are from the industrial area of Porto Marghera, but high or medium toxicity was also attributed to sediment samples from sites far removed from direct contamination. Toxicity indices also highlighted the high temporal variability of sediment toxicity: for example, the Tresse site, in front of the industrial area, showed low toxicity in summer 2000, absence of toxicity in winter 2001, medium toxicity in summer 2001 and high toxicity in winter 2003.

Figure 2 reports an example of data visualization: the central circle in the pie chart shows the integrated toxicity according to the WATI index while the slices represent each CM-tox toxicity.

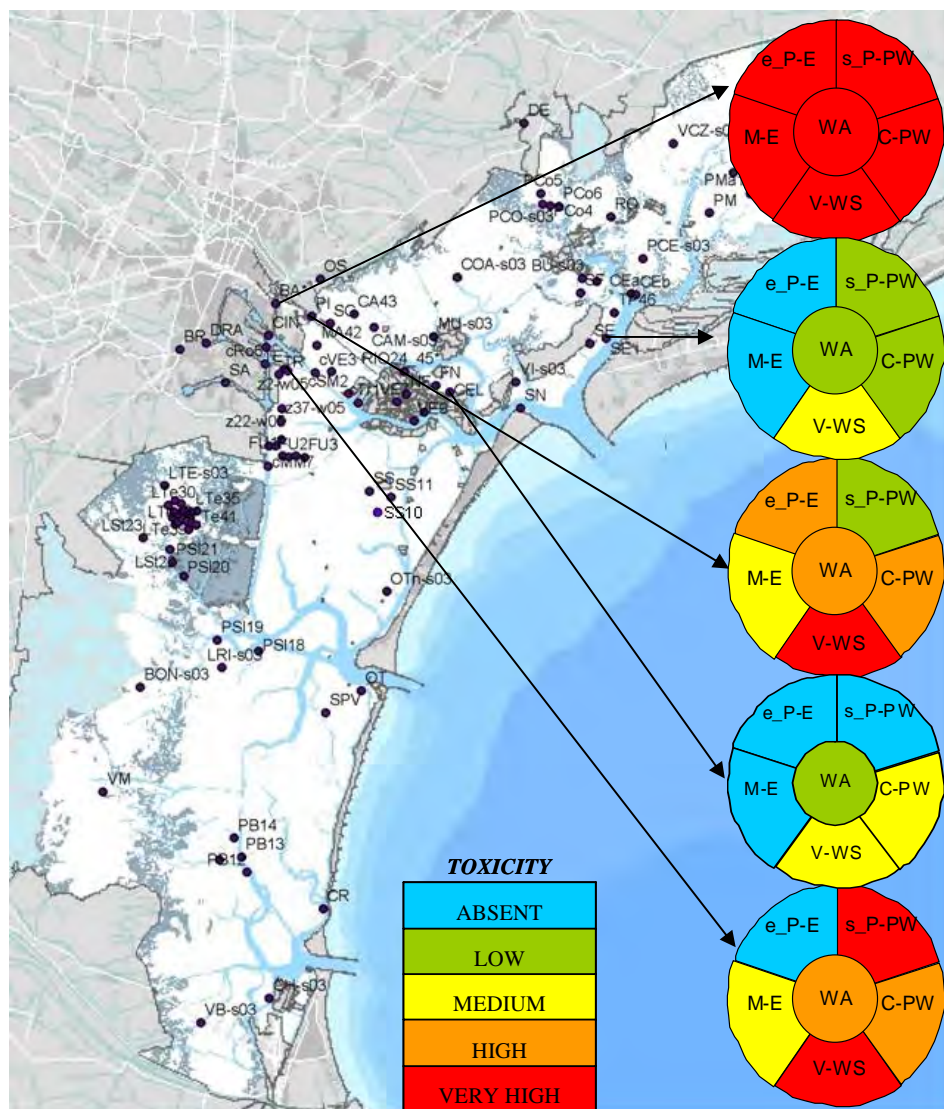


Fig 2 – Location of investigated sites and example of toxicity data visualization (Microtox test on solid-phase= b_Vf_sp ; embryotoxicity test with *P. lividus* on elutriate= e_Pl_e ; embryotoxicity test with *M. galloprovincialis* on elutriate= e_Mg_e ; sperm cell test with *P. lividus* on pore water= s_Pl_pw ; embryotoxicity test with *C. gigas* on pore water= e_Cg_pw).

Lastly, some considerations on the two indices. The TEI index is more complex to calculate than the WATI index; to be applied, it needs a characterisation of the sediment sample, i.e. the water content in fresh and centrifuged sediment. For the TEI index we calculated the error due to the sensitivity variability of biological response that is valuable using the sensitivity of each CM-tox through

the reference toxicant; we demonstrated that this variability is quite low for the CMs-tox used, validating the choice of a 5 toxicity classes ranking. In the WATI index, simpler than the TEI index in conception and calculation, the toxicity data is ranked twice (first for the toxicity scores and then for the index). This guarantees easy treatment of each data processing step, but has the drawback of introducing a higher error in data treatment as the toxicity information is approximated twice, increasing the truncation errors.

The responses of both indices obviously depend on the available toxicity data; in particular, we showed how the absence of one CM-tox influences the indices results and demonstrated that the lack of Microtox test on solid phase causes the greatest error.

Conclusions

We developed a toxicity index for integrating responses from a battery of toxicity bioassays, using a stepwise procedure. Among all available indicators for the Venice lagoon, the 5 most representative core-metrics were selected according to specific criteria. These 5 CMs-tox were integrated using two mathematical approaches, and two toxicity indices (TEI and WATI) were developed. Both indices, applied to the toxicity dataset for the lagoon, were able to discriminate among sites with different quantitative and qualitative chemical contamination, so they can be considered as evidence in sediment quality assessments. A final validation of the two indices requires proper field measurements.

The use of one of the two indices can be a useful tool for decision-making processes as this integrates toxicity responses deriving from toxicity bioassays with different sensitivity applied on a different test matrix. Moreover the classification in five toxicity classes (absent, low, medium, high, very high) can be easily visualised or depicted on a coloured map.

References

- Bombardier M. and Bermingham N., 1999. The SED-TOX index: toxicity-directed management tool to assess and rank sediments based on their hazard-concept and application. *Environ. Toxicol. Chem.*, 18, 685-698.
- Losso C., Picone M., Arizzi Novelli A., Delaney E., Ghetti P.F., Volpi Ghirardini A. 2007. Developing toxicity scores for embryotoxicity tests on elutriates with the sea urchin *Paracentrotus lividus*, the oyster *Crassostrea gigas*, and the mussel *Mytilus galloprovincialis*. *Arch. Env. Cont. Tox.*, 53, 220-226.
- Losso C., Arizzi Novelli A., De Salvador D., Ghetti P.F., Volpi Ghirardini A. Development of a toxicity index to integrate responses from a suite of bioassays for transitional environments. *Environ. Toxicol. Chem.*, *submitted*.
- Phillips B., Hunt J.W., Anderson B.S., Puckett H.M., Fairey R., Wilson C.J., Tjeerdema R., 2001. Statistical significance of sediment toxicity test results: threshold values derived by the detectable significance approach. *Environ.*

Toxicol. Chem., 20, 371-373.

Shin P.K.S. and Lam W.K.C., 2001. Development of a marine sediment pollution index. Environ. Pollut., 113, 281-291.

Viaroli P., Bartoli M., Giordani G., Magni P., Welsh D.T., 2004. Biogeochemical indicators as tools for assessing sediment quality/vulnerability in transitional aquatic ecosystems. Aquatic Conserv: Mar. Freshw. Ecosyst., 14, S19-S29.

BIODIVERSITY AT GENETIC LEVEL IN THE MEDITERRANEAN SHORE CRAB *CARCINUS AESTUARIUS* FROM THE LAGOON OF VENICE

Ilaria Marino, Micol Gennari, Federica Barbisan, Paolo Maria Bisol, Lorenzo Zane

Dipartimento di Biologia, Università degli Studi di Padova

Riassunto

Nell'ambito del programma Corila 2004-2006 è stato condotto uno studio sul crostaceo decapode *Carcinus aestuarii* con un approccio interdisciplinare che integrava metodologie proprie della fisiologia delle proteine respiratorie, dell'analisi morfologica di instabilità dello sviluppo e dell'analisi genetica di microsatellite. Lo scopo era quello di valutare il possibile uso della specie come bioindicatore. In questo contributo vengono riferiti i dati ottenuti con le indagini a livello di popolazione sulla biodiversità genetica valutata attraverso i parametri del polimorfismo di dieci loci microsatellite in sei campioni raccolti sia in Laguna di Venezia. I risultati mostrano un elevato grado di polimorfismo in tutti i campioni, con variazioni delle frequenze geniche sia spaziali che temporali dipendenti dalla dinamica della popolazione.

Abstract

In the framework of the Corila Programme 2004-2006 a study was carried out on the Mediterranean shore crab *Carcinus aestuarii* using an interdisciplinary integrated approach analyzing the same individuals with physiological and genetics techniques and morphological measures. The aim was to evaluate the possible use of the species as a reliable biological indicator. This paper concerns the results of the investigations carried out at the population level on genetic biodiversity. The genetic polymorphism parameters were evaluated on 6 population samples from three different area of the Venetian basin. The results of microsatellite analysis for 10 loci indicate a high level of genetic polymorphism in all samples. The observed variations of gene frequencies, both spatial and temporal, suggest the influence of the population dynamics.

Introduction

The genetic diversity is a primary component of biodiversity. Genetic biodiversity involves nucleotides, genes, chromosomes, individuals and populations and it influences all other aspects of biodiversity at species and community levels. The genetic patterns concern the ecological responses to environmental pressure and the consequential evolutionary processes. Different genetic structures have an effect on reproductive mechanisms, adaptive capability, and interactions of individuals and of populations.

Consequently, an adequate knowledge of genetic biodiversity is a basic requirement in planning measurements aiming at preserving biological equilibriums. This is particularly important in coastal and lagoon zones affected by resource overexploitation, habitat alteration, introduction of exotic species (Cognetti and Maltagliati, 2004).

For this reason, in the framework of the Corila Programme 2004-2006, out of several biological aspects related to pollution and stress (*biomarkers*, morphological asymmetries, effect on gene expression, effect on protein levels and their quality), the genetic diversity was studied on crustacean decapod *Carcinus aestuarii*, using an interdisciplinary integrated approach analyzing the same individuals with morphological measures and physiological and genetics techniques (Giomi et al, 2006 and 2007).

This paper presents the results of genetic investigations carried out on populations samples collected from different areas of the lagoon of Venice in order to evaluate the effect of different environmental conditions.

1 Materials and Methods

A total of 279 of Mediterranean shore crab *Carcinus aestuarii*, representing 6 different samples, were collected in April 2005 and May 2006 from three sites (Fusina, Ca' Roman lagoon side, Ca' Roman sea side) representative of different environmental conditions (Table 1 and Fig. 1).

The sampling sites were classified by environmental risk class reported in Critto and Marcomini (2001).

Station	Basin	N° 2005	N° 2006	TEL	PEL
1 Ca' Roman Sea side	Adriatic Sea	37	69	3	0
2 Ca'Roman Lagoon side	Southern Lagoon	32	44	3	0
3 Fusina	Central Lagoon	50	47	6	1

Tab 1 – Sampling details for *Carcinus aestuarii* samples indicating location, number of specimen collected for year (N°) and class of ecological risk as reported by Critto and Marcomini (2001).

Microsatellite loci were isolated from a partial genomic library enriched for the AC motif, following published protocols (Zane et al., 2002). The details are reported in Marino et al. (2007).

Number of alleles and heterozygosity frequencies were calculated using Genetix 4.05.2 (Belkir et al. 2001); departure from Hardy-Weinberg equilibrium and linkage disequilibrium were calculated using Genepop on the web 3.4 (Raymond & Rousset 1995).

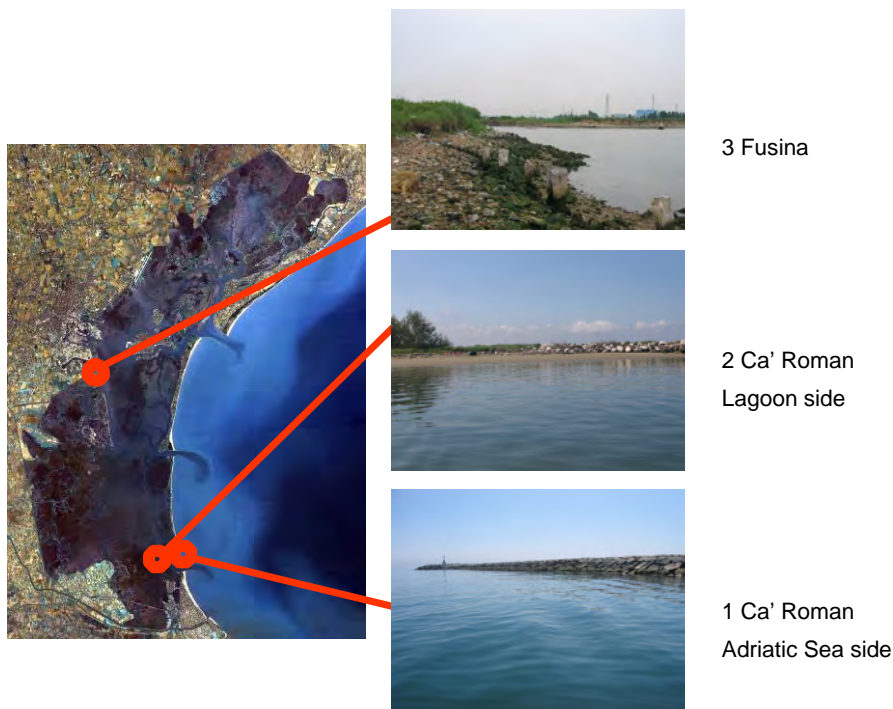


Fig 1 – Sampling locations of *Carcinus aestuarii* in the Venetian basin.

2 Results

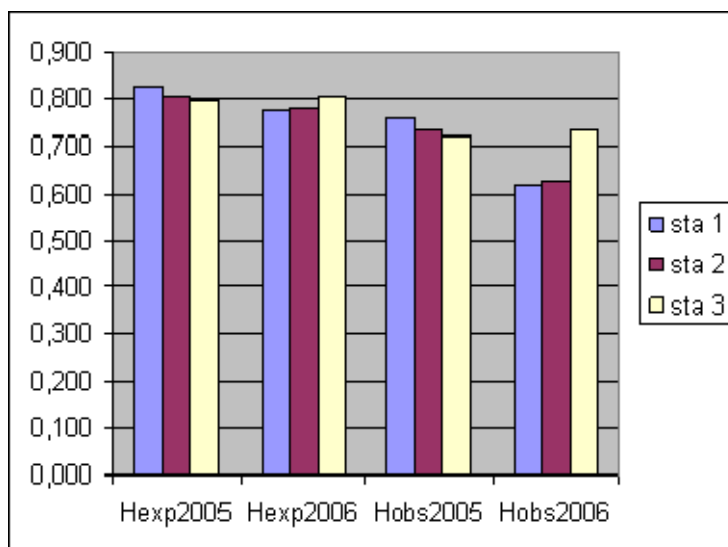
Microsatellite analyses of ten loci revealed a substantial molecular variability (Table 2). The number of allele ranged from three to 42; observed heterozygosity ranged from 0.10 to 1.00, while expected heterozygosity ranged from 0.83 to 0.98. The heterozygous frequencies, both observed and calculated in the 2005 samples from the Lagoon of Venice, showed a cline distribution related to environmental conditions (Fig. 2). The highest values are in the marine sample collected at Ca' Roman while the lowest values are in Fusina sample, from the innermost station affected by the warm water pipes of the near thermoelectric power plant.

Exact test of genetic differentiation allowed to reject the hypothesis of homogeneity between samples (Tab. 2). A significant reduction of genetic variability between 10 km far samples indicated the possibility of investigations by microsatellite marker on little spatial scale. These results suggested that the Venetian samples have an evident genetic structure.

Station	1 Ca' Roman Sea Side	2 Ca' Roman Lagoon Side	3 Fusina
1 Ca' Roman Sea Side		0.579794	0.193070
2 Ca' Roman Lagoon Side	0.075133		0.526088
3 Fusina	0.002789	0.0001546	

Tab 2 – P-values of genetic differentiation tests for each population pair, obtained from 2005 data set (lower diagonal) and 2006 data set (upper diagonal).

Fig 2 – Expected and Observed Heterozygosity in *Carcinus aestuarii* from three stations at different time (Stat. 1 = Ca' Roman Adriatic Sea side; Stat. 2 = Ca' Roman lagoon side; Stat. 3 = Fusina).



The results obtained at 2006 resulted different in reason of the lack of the cline distribution (Fig 2). Exact test of genetic differentiation supported the hypothesis of homogeneity between the samples (Tab. 2). The loss of the spatial differences described for the 2005 samples suggests a role of populations dynamics for the species which can be clarified with longer temporal series of sampling. At the same time, other studies are required to clarify the role of biomarker of microsatellite.

Conclusions

Carcinus aestuarii (order Decapoda, family Portunidae) is a common crab in estuarine and lagoon water of the Mediterranean Sea. In the lagoon of Venice the species play an important role not only from ecological point of view – the specie is an efficient carnivorous predator (Mistri, 2003) - but also from economic point of view (Nunes et al., 2004).

Our researches give a contribute to the knowledge of the species given that a new, specific methodology was displayed for the study of genetic biodiversity and the genetic population structure was evaluated using microsatellite loci.

This method will be useful not only for the population assessment but also for other applications. In particular, it can possible to investigate on fine-scale patterns of differentiation and subdivision among population. This is a relevant aspect of the species because of its recent success as a global invader (Yamada Behrens and Hauk, 2001).

The study, still in progress, of the new material collected in the summer 2007 from selected site of Lagoon of Venice, characterised by different level of pollution and biotic condition, will contribute to definition of biological role of the microsatellite loci polymorphisms and their possible biomarker function.

References

- Cognetti, G., Maltagliati F., 2004, Strategies of genetic biodiversity conservation in the marine environment. *Marine Pollution Bulletin*, 48, 811–812.
- Belkir K., Borsa P., Goudet J., Chikhi L., Bonhomme F., 2001, GENETIX, Logiciel Sous Windows Pour la Génétique Des Populations. Laboratoire Génome et Populations, Montpellier, France.
- Bisol P.M., Gallini A., Prevedello S., Rianna E., Bernardinelli E., Franco A., Zane L., 2007, Low variation at allozyme loci and differences between age classes at microsatellites in grass goby (*Zosterisessor ophiocephalus*) populations. *Hydrobiologia*, 577, 151-157, ISSN: 0018-8158. doi:[10.1007/s10750-006-0424-5](https://doi.org/10.1007/s10750-006-0424-5).
- Critto, A., Marcomini A., 2001, Rischio ecologico e inquinamento chimico lagunare. Libreria Editrice Cafoscarina Milano
- Raymond, M., Rousset F., 1995, Genepop (version 1.2): population genetics software for exact tests and ecumenism. *Journal of Heredity*, 86, 248–249.
- Giomi F., Beltramini M., Fusco G., Maruzzo D., Zane L. and Bisol P.M., 2006, An integrated approach to biological monitoring in the Lagoon of Venice, in “Scientific Research and Safeguarding of Venice. Research Programme 2004-2006” by In: Campostrini Pierpaolo, vol. IV, 2005 results. Co.Ri.La, Venezia, 247-257.
- Giomi F., Beltramini M., Lanfrit C., Maruzzo D., Fusco G., Perilli L., Zane L., Gennari M., Marino I., Barbisan F. and Bisol P.M., 2007, Testing an integrated approach bioindicator for the Venetian Lagoon, in “Scientific Research and Safeguarding of Venice. Research Programme 2004-2006”, by Campostrini Pierpaolo vol. V, 2006 results. Co.Ri.La. 219-225
- Marini I.A.M., Barbisan F., Gennai M., Bisol P.M., Zane L. , 2007, Isolation and characterization of microsatellite loci in the Mediterranean shore crab *Carcinus aestuarii* (Decapoda, Portunidae) *Molecular Ecology Notes* doi: 10.1111/j.1471-8286.2007.01960.x
- Mistri, M., 2003 Foraging behaviour and mutual interference in the Mediterranean shore crab, *Carcinus aestuarii*, preying upon the immigrant mussel *Musculista senhousia*. *Estuarine, Coastal and Shelf Science*, 56, 155-159.
- Nunes P. A. L. D.-Rossetto L.-Blaeij de A., 2004 Measuring the economic value of alternative clam fishing management practices in the Venice Lagoon: results from a conjoint valuation application, *Journal of Marine Systems*, 51, 309-320
- Zane L, Bargelloni L, Patarnello T (2002) Strategies for microsatellite isolation: a review. *Molecular Ecology*, 11, 1–16.
- Yamada Behrens S., Hauk L., 2001, Field identification of the European green crab species: *Carcinus maenas* and *Carcinus aestuarii*. *Journal of Shellfish Research*,. 20, 905-9 12.

ENVIRONMENTAL QUALITY INDEXES FOR THE LAGOON OF VENICE

Micheletti Christian¹, Critto Andrea¹, Pastres Roberto², Tagliapietra Davide³, Volpi Ghirardini Annamaria¹, Gottardo Stefania¹, Chiarato Sara¹, Zanon Veronica⁴, Losso Chiara¹, Ciavatta Stefano², Bisol Maria Paolo⁵, Marcomini Antonio¹

1 Dipartimento di Scienze Ambientali, Università Cà Foscari di Venezia, 2 Dipartimento di Chimica-Fisica, Università Cà Foscari di Venezia, 3 Consiglio Nazionale delle Ricerche, CNR-ISMAR, Venezia, 4 CORILA, Venezia, 5 Dipartimento di Biologia, Università di Padova

Riassunto

La direttiva quadro sulle acque (WFD) richiede la valutazione integrata dello stato ecologico delle acque superficiali, incluse le lagune costiere quali acque di transizione. Nelle lagune costiere caratterizzate da acque poco profonde come la laguna di Venezia, i sedimenti giocano un ruolo fondamentale nel determinare lo stato ecologico, in quanto supportano la biodiversità fornendo un habitat per molte specie animali e vegetali, ma allo stesso tempo costituiscono una sorgente secondaria di contaminanti. In accordo al ruolo determinante dei sedimenti nella valutazione della qualità ambientale delle lagune costiere, e tenendo conto della necessità di implementare la WFD anche in questi ambienti complessi, è stata sviluppata una procedura per la valutazione integrata della qualità dei sedimenti della laguna di Venezia, sulla base degli approcci Weight-of-Evidence (WoE) e TRIAD. Sulla base dell'approccio TRIAD, sono state considerate informazioni riguardanti tre categorie: l'esposizione ai contaminanti, la tossicità dei sedimenti e la biodiversità. Al fine di ottenere una classificazione adeguata dello stato ecologico dei corpi idrici lagunari, le informazioni sono state integrate utilizzando 5 indici: i) contaminazione del sedimento, ii) bioaccumulo di inquinanti organici ed inorganici in organismi bentonici, iii) bioaccumulo di inquinanti organici lungo la rete trofica lagunare, iv) tossicità del sedimento, e v) biodiversità macrobentonica. I punteggi medi degli indici, calcolati in ogni corpo idrico lagunare, sono stati analizzati statisticamente (analisi uni e multivariata) per identificare le correlazioni fra i 5 indici, e riportati su una mappa GIS per identificare la presenza di pattern nella distribuzione spaziale e la coincidenza dei risultati degli indici nei singoli corpi idrici.

Abstract

The Water Framework Directive (WFD) requires the integrated evaluation of the ecological status of surface waters, including coastal lagoons as transitional waters. In the shallow coastal lagoons, sediments play an essential role for the environmental quality, supporting the biodiversity (i.e. providing a habitat for several vegetal and animal species), but also representing a secondary source of contaminants. According to the sediments relevance for coastal lagoon quality, and taking into account the requirement to implement the WFD also in

these complex environments, an integrated environmental quality assessment procedure for the Venice lagoon sediments was developed on the basis of the Weight of Evidence and TRIAD approaches. According to TRIAD approach, three type of information were considered: exposure to chemicals, sediment toxicity, and biodiversity. In order to obtain an effective ecological status assessment of the identified homogeneous lagoon water bodies, information were integrated by using 5 indexes: i) sediment contamination, ii) organic and inorganic pollutants bioaccumulation in benthic organisms, iii) bioaccumulation of organic pollutants through the lagoon food web, iv) sediment toxicity and v) macro-benthic biodiversity. The average index scores calculated in the lagoon water bodies were statistically evaluated (uni- and multivariate techniques) to identify the correlations between the 5 indexes. Finally, in order to identify spatial patterns, and to assess the co-occurrence of the indexes results, the spatial distribution of indexes scores was represented in GIS maps.

1 Introduction

The environmental quality assessment in European countries is regulated by the Water Framework Directive [EC, 2000], which requires from the Member States the integrated evaluation of the ecological status for different water bodies, by taking into account different environmental quality elements. Specifically, the WFD establishes to define the ecological status of surface waters (e.g. rivers, lakes, transitional waters) by integrating hydromorphological, physical-chemical and biological parameters. The final goal is to develop quality indices and classify each water body in order to reach a good ecological status before 2015. The quality evaluation for each parameter has to be expressed as the distance from a reference value to define five quality classes (from 1: high to 5: bad).

Among the transitional and coastal waters, the WFD includes the assessment of the ecological status of coastal lagoons. Coastal lagoons are complex environments, densely populated, providing several ecological and socio-economic functions both to people living in coastal areas and along the tributaries river basin. A relevant environmental compartment, especially for shallow lagoons, is represented by the sediment bed. On one hand, sediments provide a habitat to several organisms with a significant ecological and economic relevance, such as sea-grasses, shellfish, and bivalves. On the other hand, anthropogenic organic and inorganic persistent pollutants can be stored in sediments causing direct and indirect (e.g. through bioaccumulation) toxic effects on biota. Therefore, the assessment and management of sediment quality is essential to assure a high ecological status of the whole lagoon. By integrating the response of different evidences (e.g. biodiversity, sediment contamination, etc.) the sediment quality can be assessed taking into account all relevant environmental quality elements.

2 Methods

The integrated assessment of the sediment quality was accomplished by means of the weight-of-evidence (WoE) approach [Menzie et al., 1996]. The WoE

approach is defined as a procedure to evaluate the potential impacts on the ecosystem on the basis of multiple lines of evidence (LOE: e.g. test results and information such as chemical concentration in sediment, comet bioassay results, etc.). This procedure integrates judgments concerning quantity, quality and congruence of the data extrapolated from different lines of evidence [Chapman, 2002; Burton 2002]. The TRIAD approach is an example of the WoE methodology application. According to the literature (i.e. Sediment Quality Triad) [Chapman, 2000], sediment quality was assessed by integrating measurements concerning three LOE: exposure to chemicals, sediment toxicity, and biodiversity. For the “exposure to chemicals” LOE three indexes were applied: i) the Marine Sediment Pollution Index (MSPI), ii) the Tapes Index (TI), and iii) the Food Web Index (FWI); for the “sediment toxicity” was applied the Weighted Average Toxicity Index (WATI); and finally for the “biodiversity” line of evidence the macro-benthic Biodiversity Index (BI) was developed. The scores of each index were scaled in the 1-5 range, where 1 means high relative quality and 5 bad relative quality. Univariate and multivariate statistical analysis of the indexes scores and their GIS spatial distribution analysis supported the integrated environmental quality assessment of each homogeneous water body identified within the Lagoon. Before to present in detail the integrated quality assessment results, a brief introduction of the selected indexes is reported in the next sub-paragraph.

2.1 Index description

The Marine Sediment Pollution Index (MSPI) was proposed by Shin and Lam (2001) to assess the sediment contamination of coastal ecosystems, and it is based on chemical-physical parameters which are normally collected in monitoring activity. The calculation of this index is based on the Principal Component Analysis. The MSPI score is comprised between 0 and 100, where 0 represent the lower and 100 the higher sediment contamination with respect to the lagoon concentration range. To facilitate the results communication, a qualitative judgment based on a 5 scores (i.e. 1 to 5) qualitative scale was defined. The Tapes Index (TI) aims to evaluate the bioaccumulation of inorganic and organic pollutants in benthic organisms, using clam *Tapes philippinarum* as representative specie. The index score was included in the 1 to 5 range, where 1 means the lower bioaccumulation and 5 the higher bioaccumulation with respect to the tissue concentrations observed in the lagoon experimental dataset. The quality score was assigned on the basis of the cumulative frequency distribution of all the available experimental pollutants concentrations in lagoon clam tissues. The Food Web Index (FWI) estimates the potential bioaccumulation of persistent organic pollutants (i.e. PCBs and PCDD/Fs) through a representative lagoon food web by means of a state-of-the-art bioaccumulation model proposed in the literature [Arnot and Gobas, 2004], calibrated and validated for the lagoon of Venice [Micheletti et al., in press]. The FWI was calculated as the ratio between the pollutant concentration (i.e. sum of PCBs and PCDD/Fs congeners) at the highest food web level (i.e. *Dicentrarchus labrax*) and the bioaccumulation in the benthic organism representing the highest diet contribution for the considered predator (i.e.

omnivorous-filter feeder macrobenthos, which represent 50% of the *Dicentrarchus labrax* diet). The Weighted Average Toxicity Index (WATI) was applied in 164 sampling stations to assess the toxicity of the sediment contamination for biota, integrating the results of 5 Core Metrics (CM-tox): 1. *Vibrio fischeri* test on bulk sediment; 2. *Paracentrotus lividus* spermiotoxicity test on pore water; 3. *Paracentrotus lividus* embriotoxicity test on elutriate; 4. *Mytilus galloprovincialis* embriotoxicity test on elutriate; 5. *Crassostrea gigas* embriotoxicity test on pore water. A score was assigned from 0 to 4 to each toxicity class, where 0 defines the absence of toxicity and 4 very high toxicity. The scores of each CM-tox were summarised and weighted according to the comparative weights (at 0-1 range) assigned by the criteria for CM-tox selection. The WA values were classified in five equivalent sub-ranges, determining five toxicity classes: $0 \leq WA \leq 0.2$ absent; $0.2 < WA \leq 0.4$ low; $0.4 < WA \leq 0.6$ medium; $0.6 < WA \leq 0.8$ high; $0.8 < WA \leq 1$ very high. The WATI application and responses reliability was highly influenced by the availability of the toxicological data (see sub-chapter 2.2), since it was impossible to obtain data for all the 5 selected CM-tox in all sampling stations. The Biodiversity Index (BI) developed and proposed in the 3.11 research line was applied to evaluate the macro-benthic biodiversity of transitional environments. In fact, the BI is a new protocol for the normalisation of diversity indexes (e.g. Shannon diversity index) to the transitional gradient [Tagliapietra et al., submitted], integrating scores from both vegetal and animal compartments, and taking into account the potential habitat biodiversity. The BI index was estimated by using the macro-benthos abundance and biomass data. The biodiversity values were expressed as the distance from the reference conditions (i.e. maximum potential/expected biodiversity), which were defined according to the biodiversity distribution model obtained for the different habitat typologies of the lagoon of Venice by using multivariate statistics.

2.2 Index estimation

The five selected indexes were calculated in sampling stations located over the whole lagoon, on the basis of available experimental data. The data used to estimate the selected indexes were collected mainly from monitoring studies carried out by the Magistrato alle Acque di Venezia [MAV-CVN, 1999; MAV-CVN, 2005] and from the Regione Veneto. Finally, the toxicity dataset applied to estimate the WATI index, which included data collected during a 10-years time span (1994-2005), was completed thanks to an experimental activity carried out by University Ca' Foscari of Venice during the CORILA project. It is important to highlight that all these studies were carried out in different years and with different aims, and the selected sampling stations were generally not the same. The dataset characteristics should be taken into account for the results assessment.

2.3 Integrated quality assessment

The integrated quality assessment was applied on a regional basis, by using the lagoon water bodies as analytical spatial units. Lagoon water bodies were

defined by aggregating contiguous Lagoon Units (UL; individual territorial units recognizable on the basis of their morphology) of the same typology. In order to identify the typology, the gradient from the inlets to the inner lagoon of the physical and physical-chemical parameters (e.g. hydrodynamic, salinity, degradable organic carbon fraction in sediments) affecting the lagoon biodiversity was considered. The spatial-based approach was proposed in order to allow the quality evaluation of the whole lagoon addressing the lack of coincidence of the sampling stations location and sampling time in the available dataset.

In detail, for each water body the average, minimum, and maximum scores of each index were calculated from the indexes scores obtained in the available sampling points. Subsequently, univariate and multivariate statistical analyses were carried out in order: i) to evaluate the scores distribution of each index within each water body (i.e. through the estimation of the standard deviation and of the frequency distribution); and ii) to assess the correlation between indexes (i.e. by means of correlation assessment and Cluster Analysis). Finally, the spatial distribution of water bodies average scores of the five indexes was mapped in GIS by using a pie chart representation, to highlight spatial patterns in the environmental quality of the lagoon and data gaps.

Conclusions

The application of the proposed quality assessment indexes permitted to draw a picture of the relative environmental quality of the lagoon of Venice sediments, allowing the comparison and ranking of the water bodies identified in the lagoon. In addition, the identification of experimental data gaps and indexes validation needs were identified in order to improve the quality indexes application and reliability.

References

- Arnot J.A., Gobas F.A.P.C., 2004. A food web bioaccumulation model for organic chemicals in aquatic ecosystems. *Environmental Toxicology and Chemistry* 23:2343-2355.
- Burton G.A., Chapman P.M., Smith E.P., 2002. Weight-of-Evidence approaches for assessing ecosystem impairment. *Human and Ecological Risk Assessment* 8:1657-1673.
- Chapman P.M., 2000. The Sediment Quality Triad: then, now and tomorrow. *International Journal of Environment and Pollution* 13:351-356.
- Chapman P.M., McDonald B.G., Lawrence G.S., 2002. Weight of evidence frameworks for sediment quality (and other) assessment. *Human and Ecological Risk Assessment* 8:1489-1516.
- European Commission, 2000. Water Framework Directive 2000/60/EC, "Directive 2000/60/EC of the European Parliament and of the Council

establishing a framework for the Community action in the field of water policy".

Magistrato alle Acque di Venezia-Consortio Venezia Nuova, 1999. Mappatura della contaminazione dei sedimenti lagunari. Rapporto finale. Consortio Venezia Nuova, Venice, Italy.

Magistrato alle Acque di Venezia-Consortio Venezia Nuova, 2005. Attività di monitoraggio ambientale della Laguna di Venezia (MELa2). Attività C: Rilievo della distribuzione delle comunità bentoniche di substrato molle (macro e meiozoobenthos e macrofitobenthos) in Laguna di Venezia (2002-2003-2004). Rapporto finale. Consortio Venezia Nuova, Venice, Italy.

Menzie et al., 1996. Special report of the Massachusetts weight-of-evidence workgroup: a weight-of-evidence approach for evaluating ecological risks. *Human and Ecological Risk Assessment* 2:277-304.

Micheletti et al. Spatially distributed Ecological risk for fish of a coastal food web exposed to dioxins. *Environmental Toxicology and Chemistry*, in press (May 2008).

Shin P.K.S., Lam W.K.C., 2001. Development of a marine sediment pollution index. *Environmental Pollution* 113:281-291.

Tagliapietra D., Volpi Ghirardini A. Water Words at Work: comments on the use of the term "transitional waters". Submitted to *ECSS*.

DNA MICROARRAY ANALYSIS IN *MYTILUS GALLOPROVINCIALIS* FROM THE VENICE LAGOON

Laura Varotto¹, Stefania Domeneghetti¹, Umberto Rosani¹, Alberto Pallavicini³, Paolo Biso¹, Gerolamo Lanfranchi², Paola Venier¹

¹ Dipartimento di Biologia e ² CRIBI, Università di Padova, Padova; ³ Dipartimento di Biologia, Università di Trieste, Trieste

Riassunto

Nell'ambito del Secondo Programma di Ricerca Co.Ri.La (linea 3.11, Indicatori ed indici di qualità ambientale per la Laguna di Venezia) abbiamo studiato i profili trascrizionali di mitili provenienti da zone lagunari di riferimento (canali industriali di P. Marghera, P. Lido) e mitili trattati con metalli pesanti. In generale, l'analisi di espressione genica mediante DNA microarray è fra le principali tecnologie innovative oggi applicate allo studio delle complesse interazioni tra geni e ambiente intese come modulazione naturale di processi fisiologici, aggiustamenti indotti da fattori di stress e reazioni di sopravvivenza. I dati di espressione genica finora ottenuti usando un cDNA microarray di *Mytilus galloprovincialis* e l'ulteriore produzione di EST stanno progressivamente ampliando e consolidando il significato di questi nuovi marcatori di stato funzionale dei mitili lagunari.

Abstract

In the frame of the Second Research Programme Co.Ri.La (line 3.11, Indicators and indexes of environmental quality for the Venice Lagoon) we have studied transcriptional profiles of mussels from reference lagoon sites (industrial canals of P. Marghera, P. Lido) and mussels treated with heavy metals. Now-a-days, gene expression analysis based on DNA microarrays is one of the main advanced technologies applied to the study of complex gene-environment interactions, i.e. natural fluctuation of physiological processes, stress-related adjustments and survival reactions. Overall, the gene expression profiles obtained with a cDNA microarray of *Mytilus galloprovincialis*, and further EST production, increase and consolidate the meaning of these novel molecular descriptors of functional status in the lagoon mussels.

1 Introduction

The development of functional genomics in *Mytilus galloprovincialis* started at the University of Padova (CRIBI and Dept. Biology), with more than one research group and institution supporting the costs of experimental work and instrument maintenance. The initial idea was to provide basic knowledge and new tools for eco-toxicological studies and quality assessment of edible mussel stocks.

Since mid 70's, native and transplanted mussels are used for monitoring coastal water pollution [Goldberg, 1975; Viarengo *et al.*, 2007]. Anchored to hard substrates and filtering in the intertidal zone, they accumulate various contaminants from the surrounding water and act as biological integrators of pollution in space and time. The contaminant concentration in soft mussel tissues reflects toxico-kinetic factors as well as induced functional responses, being mainly determined by contaminant partitioning, reactivity and persistence, structural organism traits, species and live-stage competence for activation/detoxification, sequestration, elimination.

Depending on the dose, the exposure to toxic contaminants may result in physiological adjustments and recovery, or depression of vital functions and death. In the latter case, unusual variation of chemico-physical parameters and population dynamics of potential pathogens may play a role [Auffret *et al.*, 2006; Altieri and Witman, 2006; Garnier *et al.*, 2007].

The most common measures of contaminant-induced effects in mussels are exemplified by the balance of the available energy for growth and reproduction, life resistance in air, lysosome and DNA damage, levels of specific messenger RNAs and proteins. Compared to them, the analysis of transcriptome and proteome (all the gene transcripts and proteins in a defined cell type or tissue at a given moment) provides an holistic approach to the understanding of complex biological responses. More advanced in humans and other model organisms, molecular profiling can reveal pathways and single alterations relevant to the emergence of physiological disorders or diseases as well as toxicant signatures [Denslow *et al.*, 2007; Sen *et al.*, 2007; Albermann *et al.* 2008].

One main drawback in the use of 'omics' technologies in aquatic toxicology is the lack of sequence data and genome projects for ecologically relevant species. For instance, genome sequencing has been completed for the green spotted puffer fish (*Tetraodon nigroviridis*), the Japanese puffer fish (*Takifugu rubripes*), the zebrafish (*Danio rerio*) and for the purple sea urchin (*Strongylocentrotus purpuratus*) whereas it is in progress for the Atlantic salmon (*Salmo salar*), the cat fish (*Ictalurus punctatus*), the eastern oyster (*Crassostrea virginica*), the California mussel (*Mytilus californianus*) and the freshwater snail (*Biomphalaria glabrata*), intermediate host of the human parasite *Schistosoma mansoni* (project details at <http://www.ncbi.nlm.nih.gov/sites/entrez> and <http://www.jgi.doe.gov>).

Among the genome-based technologies, the production and sequencing of ESTs (*Expressed Sequence tags*: partial cDNA sequences that are unique to the complementary DNAs from which they were derived) identify the active part of a given genome, i.e. the set of genes transcribed in transient mRNA molecules. Following such more feasible approach, a huge number of ESTs have been made available for various organisms of interest and can be used not only for defining cDNA microarrays but also for population genetic analyses [Schena *et al.*, 1995; Ellis and Burke, 2007; Quilang *et al.*, 2007; Tanguy *et al.*, 2007].

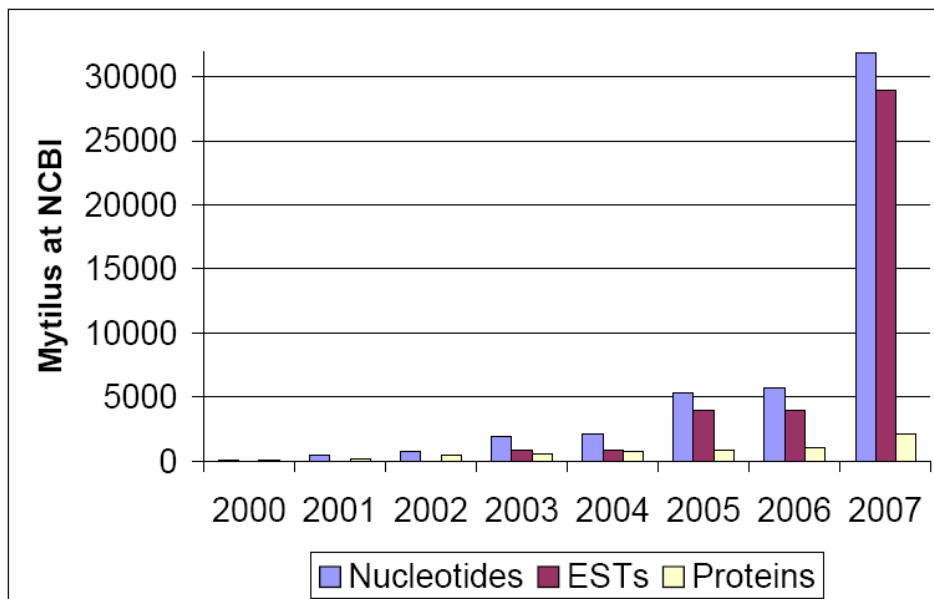


Fig 1 – Publicly available *Mytilus* records at NCBI (2000-2007).

In the last seven years, the sequence data recorded at NCBI for the genus *Mytilus* have increased up to 2433 protein and 37026 nucleotide sequences (91.2% ESTs) (Fig. 1). Most of the 5133 ESTs available for *Mytilus galloprovincialis* (5984, the total nucleotide records) have been submitted by our group and, as a result of the joined effort of the Department of Biology and C.R.I.B.I., many thousands of new ESTs will be recorded, altogether representing ~ 7000 independent sequence clusters.

Using the first set of good quality ESTs, we defined the first genome-scale cDNA microarray of *Mytilus galloprovincialis* [Venier *et al.*, 2003 and 2006]. It includes 1714 mussel cDNA probes plus unrelated controls all printed in duplicate in two independent arrays per slide, and now under validation. The performance of the new molecular tool (MytArray 1.0) was preliminary assessed on mussels exposed in controlled conditions to contaminant mixtures (heavy metals and persistent organic pollutants) and mussels collected from the industrial canals of Porto Marghera and from the Lido lagoon inlet.

The first gene expression profiles resulting from dye-swap hybridization experiments, highlighted the transcriptional specificity of different mussel tissues (digestive gland, gills, gonad and mantle, contractile tissues) and correctly discriminated the different groups of mussels under study. Accordingly, a first list of cDNA probes, potential markers of mussel contamination, was compiled by comparing the differentially expressed genes detected in mussels from the polluted industrial canals with those detected in the laboratory-contaminated mussels.

To better investigate peculiarities and common features of gene expression profiles in mussels, new samplings in the same lagoon sites have been performed in 2005, 2006 (and 2007, beyond the second CoRiLa Research programme) and related DNA microarray analyses have been performed. Transcriptional changes induced by heavy metals in mussels were also studied with new experimental treatments.

2 The mussel EST collection and gene expression profiling

2.1 Protocol optimization, EST maintenance, data availability

Advanced molecular and technological knowledge is essential to launch and develop the DNA microarray approach in a species scarcely studied from the genetic point of view. Protocols commonly used with mammalian cells have to be verified and adapted to the organism of interest, also finding out new solutions. For instance, the purification of cellular RNAs and their storage can be difficult when dealing with complex tissues rich of hydrolytic enzymes, glycogen or fibrous (e.g. digestive gland, muscles, gills, gonadal tissues of bivalves). On the other hand, preservation of cell components is crucial when making a cytological preparation with standard balanced salt solutions from euryhaline marine bivalves adapted to salinity values as high as 35‰ psu.

Since cDNA microarray analyses consume slides with spotted cDNA probes, periodical amplification of the EST collection is necessary. Depending on the total EST number, months of experimental work are needed to set new cultures of all the bacterial clones bearing specific cDNA inserts in recombinant plasmids, to amplify, purify and check the related cDNAs and, finally, to prepare new microarray slides (work done).

The detailed description of MytArray 1.0, part of the sequenced ESTs and gene expression profiles have been deposited and are publicly available at <http://www.ncbi.nlm.nih.gov/> in the GenBank™/EBI Data Bank [AJ516921-AJ516092, AJ623313-AJ626468] e in the Gene Expression Omnibus [GPL1799 (*MytArray platform*) and GSE2176, GSE2183, GSE2184 (*expression data series*)].

Now recorded in GenBank [EH662451–EH663597] is also a new group of 1147 mussel ESTs resulting from Italian-Spanish collaborative work (Pallavicini *et al.*, 2008). In the frame of the European project Imaqunim (FOOD-CT-2005-007103) we have started to identify and study the genes involved in the mussel immune responses. This first set of ESTs refers to genes transcribed in haemocytes of Spanish mussels (*M. galloprovincialis*) in response to *in vivo* immuno-stimulation with bacterial and viral-like antigens. Many of the new ESTs were identified as antimicrobial peptides, potent mediators of innate immunity. Among the most abundant haemocyte transcripts, a new myticin (Myticin C) was discovered as cluster of polymorphic sequences independent from the already known Myticin A and Myticin B.

2.2 Gene expression profiling in mussels from the Venice lagoon

The research activity concerning the indigenous mussels of the Venice lagoon started in the previous Research Programme 2001-2003 and continued in the Programme 2004-2006. In this report, DNA microarray data obtained in three subsequent years are presented in brief (detailed results are being available in more technical publications).

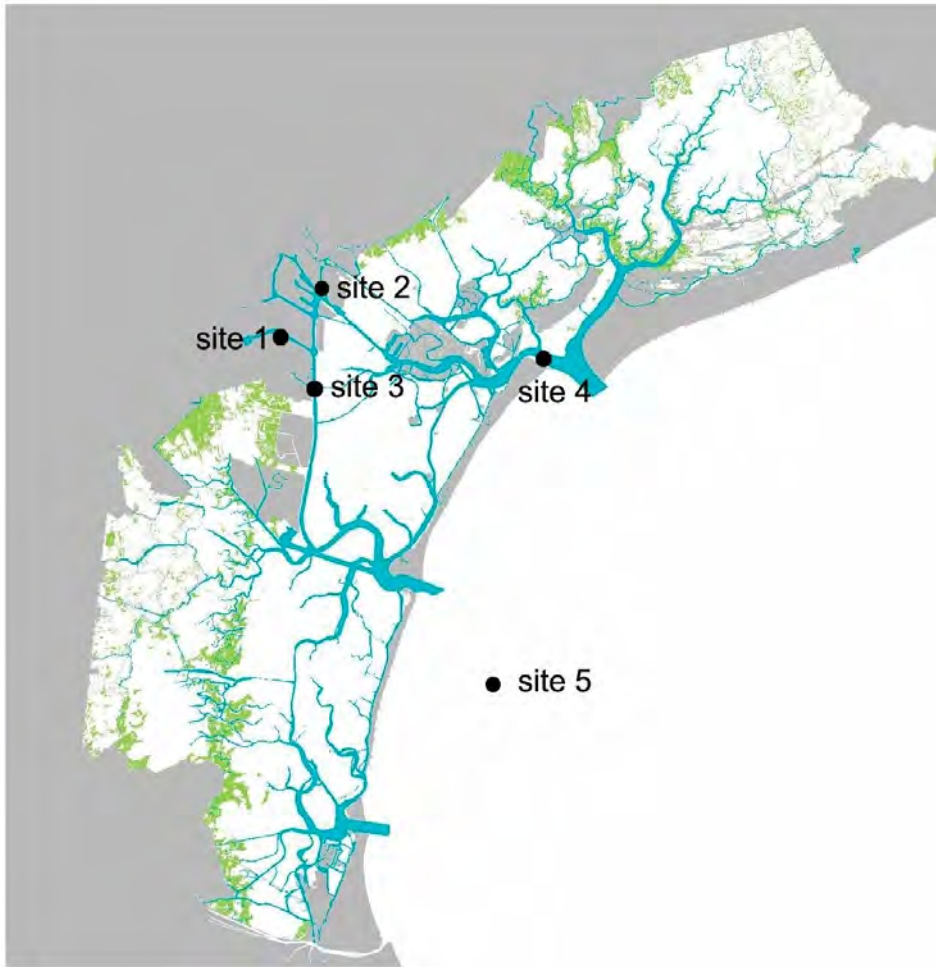
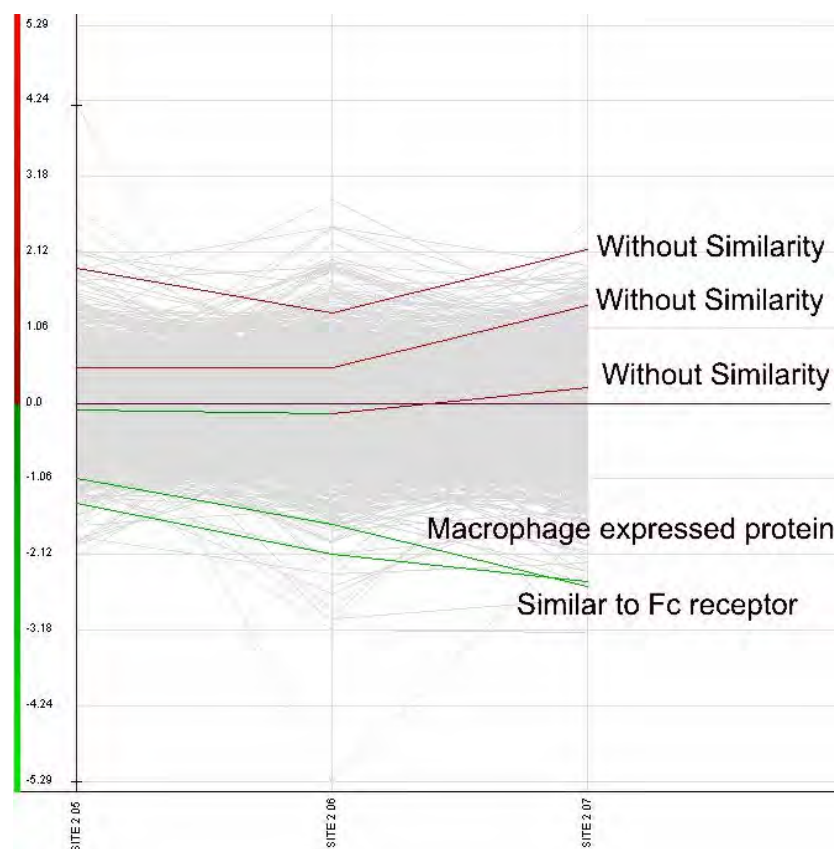


Fig 2 – Mussel sampling sites (2005-2007, early summer).

Fig. 2 shows the sites 1-4 where indigenous mussels were collected, below the tidal level, in 2005, 2006 and 2007 (native mussels of site 1 were not available in 2007). Site 5 was used as source of reference farmed mussels (controls). Total RNA was purified from individual digestive glands (DGs) and carefully checked for quality and quantity. Then, pooled samples (N=5) were composed and processed for the subsequent DNA microarray analysis. Each sample (target cDNAs derived from pooled mRNA samples) was labelled with a suitable fluorochrome (Cy3 or Cy5) and hybridised on MytArray 1.0 (probe collection) in competition with an alternatively labelled pooled sample (Cy5 or Cy3) prepared from the control mussels (site 5). During image scanning, fluorescence signals detected at the emission wavelengths of 570 nm (Cy3) and 670 nm (Cy5) on the whole microarray slide are converted in electric traces (ScanArray Lite, Perkin Elmer). The Cy3 and Cy5 fluorescence of each cDNA probe is then merged, quantified with precise rules and results are expressed as \log_2 values of test sample/control sample (data conversion with ScanArray Express, ScanArray Quantitate and Midas). Hence, the resulting data refer the levels of a given transcript sequence in the tested sample relative to the control sample, for all the probes spotted on the MytArray 1.0.

Fig 3 – Output image of a series of DNA microarray data. Each gray line describes a relative transcript level (whole MytArray). A few red and green lines exemplify increasing and decreasing trends, respectively, for genes over-expressed (positive \log_2 values) or under-expressed (negative \log_2 values) in mussels of the industrial site 2 vs. control mussels of site 5 (pooled DG samples) in 2005, 2006 and 2007.



Many gene expression changes were detected in mussels from the industrial canals of P. Marghera (exemplified for site 2 in Fig. 3). For instance, the unknown mussel transcript Myt01-013A05 varied in \log_2 expression levels from 1.9 in 2005 (3.7 times folds than in control mussels) to 1.3 in 2006 and 2.2 in 2007 (4.5 times folds than in control mussels). Actually, putatively identified and unknown transcripts both significantly contribute to the transcription profile of a given mussel sample. The transcription profiles obtained from lagoon mussels were processed with suitable software (J- Express, Rank Product) and statistically significant changes were identified. In 2005, 2006 and 2007, the greatest number of alterations was found in the mussels living in the industrial canals (up to 104 genes significantly over- or under expressed) whereas minor transcriptional changes observed in mussels from the Lido inlet which functional status appeared more similar to that of control mussels. Hierarchical clustering of gene expression profiles and qualitative detailed inspection of data indicated, once again, that MytArray correctly discriminated mussels from P. Marghera from mussels of the Lido inlet. According to the functional annotation of the available mussel probes, a number of the detected transcriptional changes suggests that mussels from the industrial district are still exposed to toxic contaminants, with significant variations in transcripts involved in protein synthesis and turnover, cell cycle and signaling, metal binding, membrane transporters and immune functions. These results appear consistent with the contaminant levels detected in the soft tissues of the lagoon mussels collected in 2005. Further description and more detailed discussion of these microarray data are being reported elsewhere (Varotto *et al.*, 2008).

Conclusions

Marine mussels appear suitable environmental sensors of water contaminants and other stress factors; nevertheless, improved knowledge on their physiological processes and defense reactions can provide new simple indicators and indexes of functional condition and quality. Following the quick development of molecular biology and bioinformatics, we have started to investigate gene expression in *M. galloprovincialis* through EST production and cDNA microarray analysis. Since the modulation of gene function can occur very rapidly in different cell types of a given organism, correct classification of the transcriptional changes triggered by specific stress factors or by the natural fluctuation of other chemico-physical factors is fundamental. To this purpose, the gene expression profiles of mussels collected in three subsequent years from the lagoon environment constitute a precious dataset to be compared to that resulting from laboratory mussel treatments and to be anchored, whenever possible, to traditional biomarker measures and sampling-site data.

The results obtained until now indicate the feasibility of the DNA microarray approach and the progressive discovery of genes tracing vital processes in mussels. In fact, gene expression profiling goes far beyond single or few biomarker measures, and it has the potential to disentangle complex biological responses. Further validation and enrichment of the MytArray will provide more robust indexes of functional mussel status (global transcription profile, crucial changes of specific gene categories) as well as single instructive signals to complement other measures relevant for the environmental risk assessment. These are our answers to the basic project questions 1.3.2 (how to measure toxic effects in organisms at different levels of biological organization and what the proper bioindicators?) and 1.3.1 (what environmental quality indexes at medium/long term?). Since mussels are important components of the coastal benthic communities, a better understanding of their functional responses could contribute to the evaluation of population changes induced by environmental stressors. Based on sequence knowledge and probe design, the DNA microarray technology can also measure molecular biodiversity (Jaccoud *et al.*, 2001) and can identify pathogenic strains (Apte and Singh, 2007) (question 1.3.3: how to measure the biodiversity of lagoon systems and translate it in an indicator of environmental quality?).

Acknowledgements

The CoRiLa Research programme 2004-2006, the European project FOOD-CT-2005-007103 and the Quicksilver-Biotec Action (DGR 2112/02.08.2005 Veneto Region) granted specific parts of the work described in this report.

References

Albermann, K., Lang, S., Zeidler, R., 2007. Molecular profiling for the identification of new biomarkers in smokers and cancer patients. *Cancer*

Genomics Proteomics 4(5), 349-58.

Altieri, A.H, Witman, J.D., 2006. Local extinction of a foundation species in a hypoxic estuary: integrating individuals to ecosystem. *Ecology* 87(3), 717-30.

Apte, A., Singh, S., 2007. AlleleID: a pathogen detection and identification system. *Methods in Molecular Biology* 402, 329-46.

Auffret, M., Rousseau, S., Boutet, I., Tanguy, A., Baron, J., Moraga, D., Duchemin, M., 2006. A multiparametric approach for monitoring immunotoxic responses in mussels from contaminated sites in Western Mediterranean. *Ecotoxicology and Environmental Safety* 63(3), 393-405.

Denslow ND, Garcia-Reyero N, Barber, DS., 2007. Fish 'n' chips: the use of microarrays for aquatic toxicology. *Mol Biosyst.* 3(3), 172-7.

Ellis, J.R., Burke, J.M., 2007. EST-SSRs as a resource for population genetic analyses. *Heredity.* 99(2), 125-32.

Garnier, M., Labreuche, Y., Garcia, C., Robert, M., Nicolas, J.L., 2007. Evidence for the involvement of pathogenic bacteria in summer mortalities of the Pacific oyster *Crassostrea gigas*. *Microbial Ecology* 53(2), 187-96.

Goldberg, E.D., 1975. The Mussel Watch — a first step in global marine monitoring. *Marine Pollution Bulletin* 6, 111.

Jaccoud, D., Peng, K., Feinstein, D., Kilian, A., 2001. Diversity arrays: a solid state technology for sequence information independent genotyping. *Nucleic Acids Research* 29(4), E25.

Pallavicini, A., Del Mar Costa, M., Gestal, C., Dreos, R., Figueras, A., Venier, P., Novoa, B., 2008. High sequence variability of myticin transcripts in hemocytes of immune-stimulated mussels suggests ancient host-pathogen interactions. *Developmental Comparative Immunology* 32(3), 213-26.

Quilang, J., Wang, S., Li, P., Abernathy, J., Peatman, E., Wang, Y., Wang, L., Shi, Y., Wallace, R., Guo, X., Liu, Z., 2007. Generation and analysis of ESTs from the eastern oyster, *Crassostrea virginica* Gmelin and identification of microsatellite and SNP markers. *BMC Genomics.* 8, 157.

Schena M, Shalon D, Davis RW, Brown PO., 1995. Quantitative monitoring of gene expression patterns with a complementary DNA microarray. *Science* 270(5235), 467-70.

Sen, B., Mahadevan, B., De Marini, D.M., 2007. Transcriptional responses to complex mixtures: a review. *Mutation Research* 636(1-3), 144-77.

Tanguy, A., Bierre, N., Saavedra, C., Pina, B., Bachère, E., Kube, M., Bazin, E., Bonhomme, F., Boudry, P., Boulo, V., Boutet, I., Cancela, L., Dossat, C., Favrel, P., Huvet, A., Jarque, S., Jollivet, D., Klages, S., Lapègue, S., Leite, R., Moal, J., Moraga, D., Reinhardt, R., Samain, J.F., Zouros, E., Canario, A., 2008. Increasing genomic information in bivalves through new EST collections in four species: Development of new genetic markers for environmental studies and genome evolution. *Gene* 408(1-2), 27-36.

Varotto et al., 2008 (manuscript in submission)

Venier, P., Pallavicini, A., De Nardi, B., Lanfranchi, G., 2003. Towards a catalogue of genes transcribed in multiple tissues of *Mytilus galloprovincialis*. *Gene*, 314C, 29-40.

Venier, P., De Pittà, C., Pallavicini, A., Marsano, F., Varotto, L., Romualdi, C., Pondero, F., Viarengo, A., Lanfranchi, G., 2006. Can gene expression trends reveal coastal water pollution? *Mutation Research* 602, 121-134.

Viarengo, A, Lowe, D, Bolognesi, C, Fabbri, E, Koehler, A., 2007. The use of biomarkers in biomonitoring: a 2-tier approach assessing the level of pollutant-induced stress syndrome in sentinel organisms. *Comparative Biochemistry and Physiology, Part C*, 146(3): 281-300.

RESEARCH LINE 3.12

Trophic chain and primary production in the lagoon metabolism

GROWTH AND NET PRODUCTION OF THE SEAGRASS *NANZOOSTERA NOLTII* (HORNEEMAN) TOMLINSON ET POSLUZNY IN VENICE LAGOON

Adriano Sfriso, Chiara Facca, Sonia Ceoldo

Department of Environmental Sciences, University of Venice, Calle Larga, S. Marta
2137, 30123 Venice, Italy. Reference Author: e-mail sfrisoad@unive.it

Riassunto

Le variazioni di biomassa, dei caratteri morfologici e della produzione netta della fanerogama marina *Nanozostera noltii* (Hornemman) Tomlinson et Posluzny, sono state studiate bimensilmente da Gennaio a Dicembre 2005 in due stazioni (Lido partiacque nel bacino centrale, Petta di Bò nel bacino meridionale) della laguna di Venezia. Contemporaneamente sono state misurate le principali variabili ambientali e le concentrazioni di nutrienti. Queste stazioni sono state scelte con lo scopo di studiare la crescita di *N. noltii* in un ambiente naturale (Petta di Bò) ed in un'area dove era stata trapiantata soggetta ad interventi antropici con immissione di sedimenti sabbiosi (Lido partiacque). I risultati ottenuti nelle due stazioni hanno permesso di capire le strategie di crescita di questa specie e di calcolarne la produzione netta in tutta la laguna mediante l'utilizzo del rapporto P/B, ottenuto durante l'anno di campionamenti, e la mappatura della biomassa effettuata in estate 2003. I dati di biomassa, le metriche e i parametri ambientali legati all'accrescimento di questa specie nella stazione di Petta di Bò sono stati comparati con quelli ottenuti nella stessa stazione nel 1994.

Abstract

The biomass, the morphometric variation and the net production of the seagrass *Nanozostera noltii* (Hornemman) Tomlinson et Posluzny, were studied bimonthly, from January to December 2005, in two stations (Lido watershed, in the central basin and Petta di Bò in the southern basin) of the Venice lagoon. Concurrently, the main environmental variables and nutrient concentrations were also recorded. The selected stations allowed to study the growth of that species in a natural environment (Petta di Bò) and in an area affected by anthropic interventions with inputs of sandy sediments (Lido watershed) where it had been transplanted. The results obtained in the two stations allowed to understand the growth strategy of that species and to calculate the total lagoon net production by the P/B ratio, obtained during one year sampling, and its distribution in the lagoon according to a biomass map drawn in summer 2003. The plant biomass, the metrics and the main environmental variables linked to the growth of that species obtained at Petta di Bò were also compared with those obtained in the same station in 1994.

1 Introduction

In Venice lagoon in field studies on the net primary production (NPP) of macroalgae and the seagrasses *Zostera marina* L. and *Cymodocea nodosa* (Ucria) Asherson have started since 1987. The results obtained on an annual basis at different biomass densities and in different stations allowed to determine the P/B ratios for each taxon [Sfriso *et al.*, 1988, 1989, 1992a, 1993, 2004; Sfriso and Ghetti, 1998]. The P/B ratios were employed to calculate the biomass production over the whole lagoon by biomass maps drawn in summer during the highest biomass growth. For macroalgae, maps of the entire lagoon and primary production calculations were performed in 1980 and 2003 [Sfriso and Facca, 2007]. Additional maps and NPP estimation were carried out in the central lagoon in summer 1987, 1993 and 1998 [Sfriso *et al.*, 2003]. Maps of seagrass coverage were drawn in 1992 [Caniglia *et al.*, 1990, 1992] and 2002 [Rismondo *et al.*, 2004] but no biomass determination was done. The first map of biomass distribution per biomass intervals was performed in summer 2003 [Sfriso and Facca, 2007]. By applying the P/B ratios to these data the total NPP of *Z. marina* and *C. nodosa* were also determined. However, no information on the NPP and P/B ratios of *Nanozostera noltii* were available in Venice lagoon and in the past [Sfriso and Facca, 2007] its total production was only estimated by analogy with *Z. marina*. In fact, the in field NPP measurement of *N. noltii* is difficult because of the small size of its leaves and rhizomes which are deeply sunken into the sediment.

Although the sampling difficulties, to fill this gap and to complete the knowledge of the total macrophyte production in the lagoon, it was decided to study the production also of that species. After some preliminary measurements to set up the in field procedure, *N. noltii* sampling started in January 2005 and continued for one year till December with bimonthly campaigns.

2 Materials and Methods

The biomass of *N. noltii* was sampled by using a sampling frame of 20 x 25 cm (0.05 m²) in an area of ca. 15 x 15 m. Six replicates of all the above and below-ground biomass were collected monthly according to the procedure reported in Sfriso and Ghetti [1998] which guarantees a sampling accuracy >95%. Biomass samples were washed by using a 3mm mesh sieve to remove sediment, epiphytes and other organisms and transported to the laboratory for the material examination. There, each plant sample was carefully washed in tap water to remove salts and the remaining epiphytes. Then the material was separated in shoots, rhizomes-roots and dead parts (i. e. rhizome and leaf black parts) and weighed by means of an electronic balance (precision: 0.1 g), after drying with blotting-paper. Shoots length was obtained by measuring (precision 1 mm) ca. 30 plants of each sample.

Shoots, rhizomes-roots and dead parts sample aliquots were frozen, lyophilised and analysed to determine the dry/wet weight ratio and the concentrations of total carbon, total nitrogen and total phosphorus.

In August, 4 additional leaf samples composed only from the 1st, 2nd, 3rd and 4th

leaf were sorted in order to analyse the nutrient contents separately.

Plant growth was obtained by marking bimonthly with a hole the shoot apical leaf bundle and the rhizomes above the leaf and knot meristems [Sfriso and Ghetti, 1998] and measuring their increase in ca. 10 plants on the successive sampling date. This procedure allows to take into account the total plant increase and to consider also the biomass of the most external leaves that after detaching from the plants are spread in the lagoon or transferred in the sea shoreline. However, because of their small size and the impossibility to perforate the plants directly underwater, during each sampling a sediment core (diameter 16 cm, depth 20 cm) colonised by *N. noltii* was collected. About 20-30 shoots were marked with a hole, then the core was placed again in the bottom till the next sampling when plants were collected, washed and stored in nylon bags for laboratory measurements.

At each monthly campaign nutrient concentrations in the water column and in the pore-waters were also determined according to Strickland and Parson [1972] and sediment samples for the analysis of the total nutrient concentrations, grain-size (fraction < 63 μ m) and density were collected. Sedimentation rates were obtained by using sedimentation traps placed on the surface sediment and emptied with a bimonthly or monthly frequency according to Sfriso *et al.* [1992b, 2005].

2.1 Study area

Nanozostera noltii colonises mainly the areas of the Venice lagoon close to the tidal marshes and at the edges of small canals called "ghebbi". However, because of the impact of heavy fishing gears for harvesting the clam *Tapes philippinarum* Adams & Reeve and the works for the reinforcement of tidal lands the spread of *N. noltii* in the last years decreased markedly [Rismondo *et al.*, 2004, Sfriso and Facca, 2007]. For this reason the growth of that species was studied in two areas, one placed in a natural bed at Petta di Bò, in the southern basin, and the other in the Lido watershed, in the central basin, where *N. noltii* had been transplanted. The station at Petta di Bò is characterised by fine sediments and a dense seagrass population already studied in 1994 [Sfriso and Ghetti, 1998]. The station in the Lido watershed exhibits sandy sediments, which had been introduced in that area characterised by low water renewal in order to avoid Ulvaceae blooms, and is characterised by a small transplanted population.

3 Results

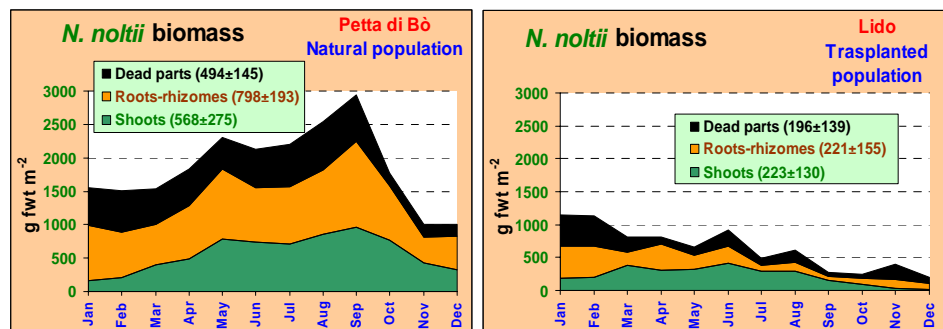
3.1 Biomass, metrics and growth of *N. noltii*

Plants at Petta di Bò were well developed with leaves of ca. 1.75 mm width and a compact below-ground system, whereas at Lido plants were suffering and showed a lower density, a reduced leaf width (ca. 0.85 mm) and a below-ground system very unpacked.

The mean biomass was 1860 ± 478 g fwt m^{-2} at Petta di Bò and 640 ± 330 g fwt

m^{-2} at Lido with peaks up to 2941 e 1150 g fwt m^{-2} , respectively, but the Lido population exhibited a progressive decrease and in September-October the biomass was about one order of magnitude as low as at Petta di Bò (Fig. 1). In fact, in 2005 the weather was not favourable for the growth of that species and frequent meteorological perturbations affected particularly the Lido area where sediments were almost free of biomass and the re-suspension of the fine fraction was very high with the consequence of reducing underwater light transmission.

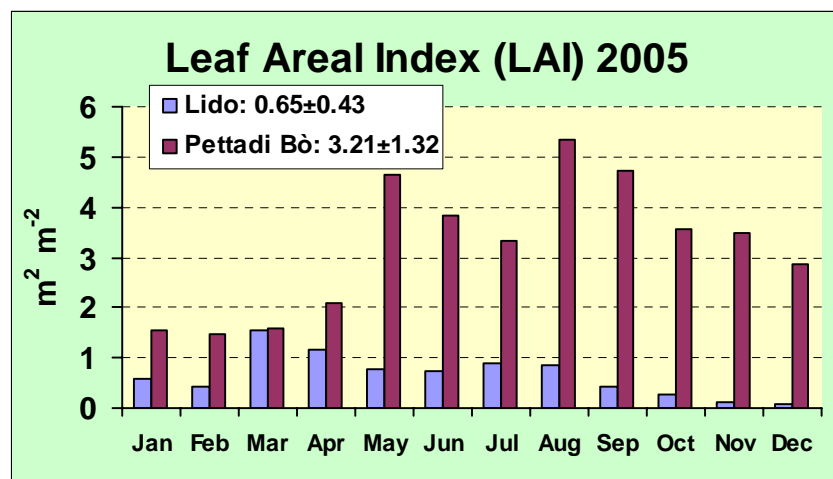
Fig 1 – *Nanozostera noltii* trends at the two sites from January to December 2005.



By considering plant composition, at Lido the mean weight of the underground and below-ground parts was similar, whereas at Petta di Bò the shoot biomass was only 70% of the total rhizome-root system.

The mean shoot length was 20.3 ± 3.9 cm at Petta di Bò and 16.9 ± 4.0 cm at Lido. Similarly, the mean leaf number per shoot was 2.60 ± 0.34 at Petta di Bò and 2.23 ± 0.43 at Lido. However, at Petta di Bò the mean shoot number (ca. 4568; 2443 at Lido) and consequently the mean number of leaves (12186; 6031 at Lido) was twice as large. The highest seasonal values were 7093 shoots m^{-2} and 21917 leaves m^{-2} at Petta di Bò in May and 5800 shoots m^{-2} and 13746 leaves at Lido in March.

Fig 2 – Leaf Areal Index in the two sampling sites.



Taking into consideration leaf width, length and their number for square meter it was estimated that the mean leaf areal index (LAI) was 3.21 ± 1.32 $\text{m}^2 \text{m}^{-2}$ at Petta di Bò and 0.65 ± 0.43 $\text{m}^2 \text{m}^{-2}$ at Lido with monthly peaks up to 5.3 and 1.6 $\text{m}^2 \text{m}^{-2}$, respectively (Fig. 2).

3.2 Net primary production

The determination of *N. noltii* production on an annual basis was only possible at Petta di Bò because of the reduced size of shoots and the progressive decrease of the Lido population that disappeared almost completely in late summer.

By measuring the growth of leaves, the number of leaves per shoot and the number of shoot per square meter, *N. noltii* produced 14600 m² of leaves on a yearly basis (Fig. 3). As the mean leaf width was 1.75 mm and leaf weight was 0.274 g fwt m⁻² that value accounted for a leaf surface of ca. 25.3 m² m⁻² y⁻¹ and a leaf weight of ca. 4.01 kg fwt m⁻² y⁻¹ (Fig. 3). The annual production of rhizomes was 1.68 kg fwt m⁻² y⁻¹. The total annual biomass production was 5.69 kg fwt m⁻² y⁻¹. By considering that the peak biomass was 2.98 kg fwt m⁻², the P/B ratio was 1.91.

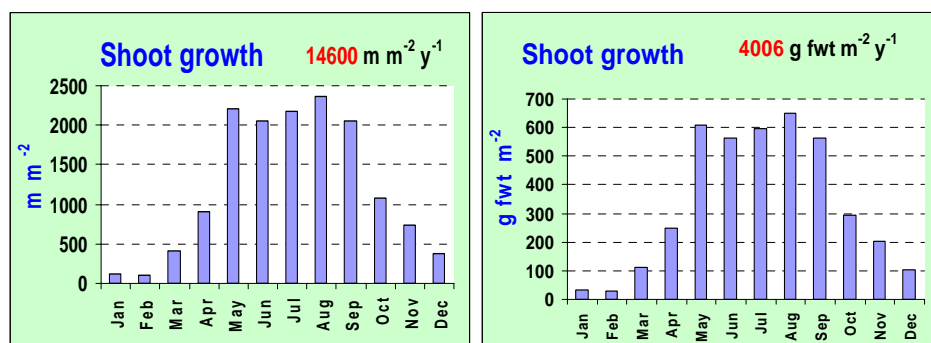


Fig 3 – Growth of shoots at Petta di Bò.

These values are as low as those of *Z. marina* and *C. nodosa* and depended on the small size of that species. In fact, although the leaf production on a length basis was similar to that of the other seagrasses, *N. noltii* leaf surface (LAI), and the leaf weight were as low. Similar results were recorded for rhizomes.

By considering the lagoon surface colonized by *N. noltii*, according to the different biomass densities found in field in summer 2003, it is possible to estimate the total net primary production of that species in the whole lagoon. In fact, in 2003, *N. noltii* colonized ca. 6.2 km² of lagoon surface and the mean and maximum standing crop were ca. 10 and 14 ktonnes, respectively, on a wet weight basis. The annual net production was estimated to be ca. 27 ktonnes.

Taking into account the mean dwt/fwt ratio and the mean carbon concentration in leaves and rhizomes, at Petta di Bò the annual NPP was ca. 245 g C m⁻² y⁻¹, with a mean and maximum daily production of ca. 0.67 and 1.41 g C m⁻² d⁻¹, respectively.

On the whole the total contribution to the lagoon primary production in 2003 was 1133 C tonnes corresponding to a mean production of 182 g C m⁻² y⁻¹.

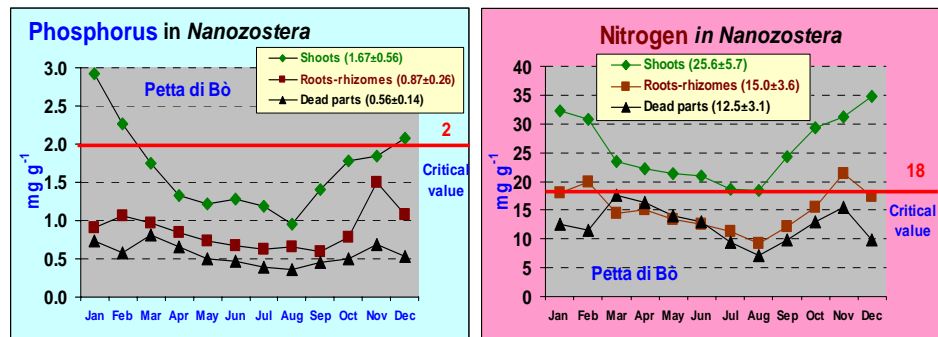
3.3 Nutrient concentrations in leaves, roots-rhizomes and dead parts

The samples of *N. noltii* collected monthly at Petta di Bò and at Lido stations were analysed to determine the internal quota of phosphorous, nitrogen and

carbon.

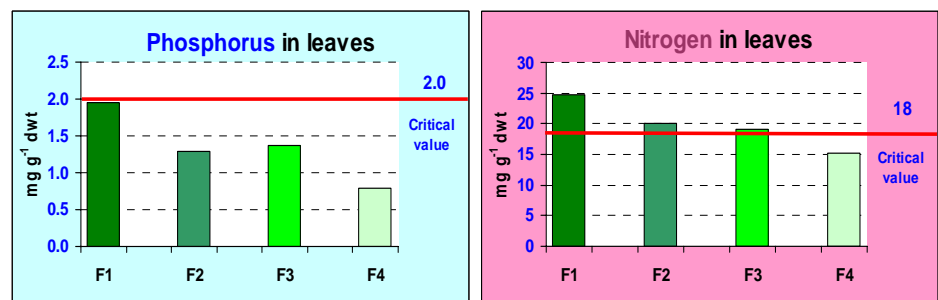
As we can see the phosphorus (P) concentration in shoots during the spring-summer period decreased markedly below the limiting value [2.0 mg g⁻¹, Duarte, 1990] in both the stations. Moreover, P concentration was steadily low both in the rhizomes and the dead parts of the plant because of the nutrient translocation to the growing parts. By analysing the P concentration in the different leaves of the shoots (1st, 2nd, 3rd, 4th) it was found that the concentration of this element not only was below to the limiting value in the external leaves but a critical value was found also in the 1st leaf (Fig. 4). Therefore, phosphorus concentration is, at present, an important limiting factor that controls the growth of *N. noltii* in Venice lagoon.

Fig 2 – Nutrient concentration trends in *Nanozostera* at Petta di Bò.



On the contrary, the concentration of Nitrogen (N) in shoots was always above the limiting value [18 mg g⁻¹, Duarte, 1990], even during the highest growth of the plant whereas that element was found below this value in roots-rhizomes and in the dead parts affected by the translocation processes.

Fig 2 – Nutrient concentrations in *Nanozostera* leaves at Petta di Bò.



High N concentrations were also found in the different leaves, especially in the 1st, 2nd and 3rd leaf which exhibited the highest growth. Nitrogen concentration was the lowest in the 4th and oldest leaf (Fig. 4), where growth had already stopped.

On the contrary, the seasonal carbon concentration changes were not significant because that element was a structural element and not a nutrient. In addition, limiting values are not known.

3.4 Settled particulate matter (SPM) rates

During *N. noltii* measurements, the rates of particulate matter settled (SPM) in the study areas have been also recorded by using sedimentation traps placed

on the bottom (base: 20x20 cm, mouth 15x15 cm, height 10 cm). As expected, at Lido, where bottoms were almost free of vegetation, the SPM amount was twice as high ($644 \text{ kg dwt m}^{-2} \text{ y}^{-1}$ with a mean of $1768 \pm 1323 \text{ g dwt m}^{-2} \text{ d}^{-1}$) as at Petta di Bò ($322 \text{ kg dwt m}^{-2} \text{ y}^{-1}$ with a mean of $885 \pm 478 \text{ g dwt d}^{-1}$) whose area was covered by dense seagrass beds which prevented sediment re-suspension. At Lido, water was turbid and *N. noltii* population was affected by a poor light availability not only because of the reduced water transparency but also because of the high sediment deposition on the plant leaves.

The comparison between the SPM rates at Lido and Petta di Bò in 1994 shows a strong increasing trend, especially at Lido where sediment rate, passing from 39 to $644 \text{ kg dwt m}^{-2} \text{ y}^{-1}$, was 16.5 times as high as in the past (Fig. 6).

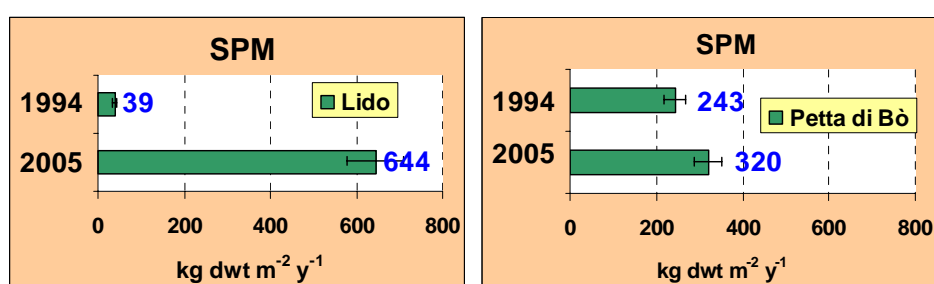


Fig 3 – Comparison between SPM rates in the two sampling sites in 1994 and 2005.

4 Discussion

This research allowed to determine the growth and production of *N. noltii* in single stations on an annual basis and, by applying the P/B ratio to the biomass distribution recorded in 2003, to estimate the production of that species in the whole lagoon. Moreover, it was possible to make also a comparison with data collected in the past and to evaluate the causes of *N. noltii* decrease in the lagoon.

For the first time the net production of that species, whose small size had until now discouraged any tentative, was measured in field. In fact, as for the other seagrasses, the primary production of this species cannot be determined by applying the biomass variation method, as it happens for seaweeds, because of the fall and loss of leaves. Therefore, growth measurements are obtained by making a hole with a needle in the shoot leaf bundle and in the rhizomes of the plants above the meristematic zone in order to measure their prolongation. The results obtained by marking ten plants at any bimonthly sampling were then transformed in biomass increase per square meter and the sum of them accounted for the annual production.

However, that technique was successful only at Petta di Bò where *N. noltii* grew naturally, while at Lido the markedly decreasing population provided only fragmentary data. In contrast, measurement of the *N. noltii* biomass and metrics was successful also at Lido and the results allowed the comparison of the two populations and the study analysis of the causes of the population decline both at Lido and in the lagoon in general. In fact, at Lido, bottoms had been filled up with sand, in order to reduce the Ulvaceae growth and avoid anoxic crises, but sand was not the suitable substratum for the growth of *N. noltii* that naturally

grows in fine sediment bottoms. Transplanted populations of *N. noltii* in that substrata were doomed to decrease or under-develop. Leaves and rhizomes are thinner, longer and more scattered.

Net Primary Production (NPP) and P/B ratios											
Reference	Station	Species	kg fwt m ⁻² y ⁻¹			g C m ⁻² y ⁻¹			g C m ⁻² d ⁻¹		P/B
			shoots	rhizomes- roots	total	shoots	rhizomes- roots	total	max		
Sfriso & Ghetti (1998)	Petta di Bò	<i>Z. marina</i>	15.0	5.9	20.9	835	258	1093	5.6	(May)	3.30
Sfriso (1999)	S. Maria del Mare	<i>C. nodosa</i>	16.0	3.1	19.1	1061	228	1289	11.0	(Aug)	3.93
Sfriso et al. (2004)	S. Nicolò	<i>C. nodosa</i>	13.7	1.6	15.3	1044	103	1147	17.9	(Jul)	2.90
Sfriso (2007)	Petta di Bò	<i>N. noltii</i>	4.0	1.7	5.7	181	64	245	1.41	(Sep)	1.91
Sfriso et al. (1988)	Lido part. (1985-86)	Macroalghe	-	-	20.0	-	-	646	30.5	(Apr)	1.61
Sfriso et al. (1993)	S. Sessola (1989-90)	Macroalghe	-	-	16.1	-	-	350	32.7	(May)	1.55
	S. Sessola (1990-91)	Macroalghe	-	-	15.5	-	-	337	17.2	(May)	1.46

Tab 1 – Primary production and P/B ratios of macroalgae and seagrasses in Venice lagoon.

By a comparison with the past data collected at Petta di Bò in 1994 a general biomass decrease was also recorded. The mean biomass in that station decreased from 2587 ± 1578 g fwt m⁻² y⁻¹ in 1994 to 1860 ± 588 g fwt m⁻² y⁻¹ in 2005, with a marked reduction of shoots that halved their biomass. Concurrently, the number of shoots decreased from 7135 ± 4218 m⁻² in 1994 to 3665 ± 944 in 2005 and LAI decreased by ca. 40%, from 6.4 ± 6.8 m² m⁻² to 2.6 ± 1.1 m² m⁻², respectively. These results are probably due to the sediment re-suspension that increased markedly, 16.5 folds at Lido, and to the reduced phosphorus availability both in the environment (water column, surface sediments and SPM) and in the tissues of *N. noltii* itself.

The determination of the *N. noltii* production allows also to estimate the total macrophyte production in the lagoon and to make a comparison with the production of macroalgae and other seagrasses. As we can see in Table 1 *N. noltii* with 245 g C m⁻² y⁻¹ total production was less productive than the other taxa. To go on with 646 g C m⁻² y⁻¹ maximum production measured in the Lido station in 1985-86 for macroalgae, 1093 g C m⁻² y⁻¹ measured at Petta di Bò in 1994-95 for *Zostera marina* and 1289 g C m⁻² y⁻¹ measured at Santa Maria del Mare near Malamocco inlet in 1998-99 for *Cymodocea nodosa*. However, the highest daily value was 32.7 g C m⁻² d⁻¹ measured at Sacca Sessola in 1999-90 for macroalgae whereas *C. nodosa* reached 17.9 g C m⁻² d⁻¹ in the Lido inlet in 2001-02. The maximum daily production of *N. noltii* was 1.41 g C m⁻² d⁻¹ only.

Lagoon macrophyte production (2003)						
Species	SC		NPP		GPP	
	Tonnes C	%	Tonnes C	%	Tonnes C	%
<i>C. nodosa</i>	6826	49	25431	44	50862	30
<i>Z. marina</i>	3318	24	13180	23	26360	16
<i>N. noltii</i>	416	3	1133	2	2266	1
<i>Macroalgae</i>	3364	24	18031	31	89132	53
Total	13924		57775		168620	

Tab 2 – Macrophyte primary production in the whole lagoon in 2003. SC = standing crop, NPP = net primary production, GPP = gross primary production, C = carbon.

Finally, by considering the total lagoon NPP on the basis of the macrophyte distribution recorded in 2003 (ca. 57775 tonnes C y⁻¹) the contribution of *N. noltii* (1133 tonnes) was negligible (Tab. 2). In fact, the highest NPP belonged to *C. nodosa* (44% of the total). Macroalgae (31%) and *Z. marina* (23%) followed, whereas the contribution of *N. noltii* was only ca. 2%.

Conclusions

This study, carried out in the framework of the CORILA Research Programme 2004-2006 (Line 3.12), fills up a knowledge gap on the primary production of the macrophytes which colonise Venice lagoon and supplies information on the cause of decline of that species. On the whole, *N. noltii* is less productive than both the macroalgae and the other lagoon seagrasses. Its contribution to the total lagoon production in 2003 was <2% of the total. The annual NPP recorded in the natural population at Petta di Bò was ca. 245 g C m⁻² y⁻¹, with daily peaks of 1.17 g C m⁻² y⁻¹, values as low as those of the other macrophytes which showed annual production up to 1289 g C m⁻² (*C. nodosa*) and daily peaks up to 32.7 g C m⁻² (macroalgae).

By comparing the *N. noltii* growth in a natural station with the one in an artificial station we found that this species decreases or disappears when it is transplanted in areas characterised by sandy substrata, as it happened for the populations transplanted in the Lido area or along the tidal marsh-edges filled up with sand after their reinforcement with wood poles or Istrian stones. In fact, the natural substrata for that species are fine sediment.

In addition, a comparison with *N. noltii* biomass and plant metrics recorded in the natural station of Petta do Bò in 1994, puts also in evidence that in that station *N. noltii* was suffering, probably because of the increase of re-suspended sediments in the water column and the reduced availability of orthophosphate both in the water column and the surface sediments.

References

Caniglia G., Borella S., Curiel D., Nascimbeni P., Paloschi F., Rismondo A., Scarton F., Tagliapietra D. and Zanella, L., 1990. Cartografia della distribuzione delle fanerogame marine nella laguna di Venezia. Giorn. Bot. Ital., 124(1), 212.

Caniglia G., Borella S., Curiel D., Nascimbeni P., Paloschi F., Rismondo A., Scarton F., Tagliapietra D., Zanella L., 1992. Distribuzione delle fanerogame marine *Zostera marina* L., *Zostera noltii* Hornem., *Cymodocea nodosa* (Ucria) Asch. in Laguna di Venezia. Lavori della Società Veneziana di Scienze Naturali, 17, 137-150.

Duarte C. M., 1990. Seagrass nutrient content. Marine Ecology Progress Series, 67, 201-207.

Rismondo A., Curiel D., Scarton F., Mion D. and Caniglia, G., 2003. A New Seagrass Map for the Venice Lagoon, in: Proceedings of the Sixth International Conference on the Mediterranean Coastal Environment - MEDCOAST 2003, by E. Özhan, Ravenna, Italy. Vol II. pp. 843-852.

Sfriso A., Marcomini A., Pavoni, B. and Orio A.A., 1988. Macroalgal production and nutrient recycling in the lagoon of Venice. Ingegneria Sanitaria, 5, 255-266.

Sfriso A., Pavoni B. and Marcomini A., 1989. Macroalgae and phytoplankton standing crops in the central Venice lagoon: primary production and nutrient balance. Science of the Total Environment, 80, 139-159.

Sfriso A., Racanelli S., Pavoni B. and Marcomini A., 1991. Sampling strategies for measuring macroalgal biomass in the shallow waters of the Venice lagoon. Environmental Technology, 12, 263-269.

Sfriso A., Pavoni B., Marcomini A. and Orio A. A., 1992a. Macroalgae, nutrient cycles and pollutants in the lagoon of Venice. Estuaries, 15, 517-528.

Sfriso A., Pavoni B., Marcomini A., Racanelli S. and Orio A.A., 1992b. Particulate matter deposition and nutrient fluxes onto the sediments of the Venice lagoon. Environmental Technology, 13, 473-483.

Sfriso A., Marcomini A., Pavoni B. and Orio A.A., 1993. Species composition, biomass and net primary production in coastal shallow waters: the Venice lagoon. Bioresource Technology, 44, 235-250.

Sfriso A. and Ghetti, P.F. 1998., Seasonal variation in the biomass, morphometric parameters and production of rhizophytes in the lagoon of Venice. Aquatic Botany, 61, 207-223.

Sfriso A., Facca C. and Ghetti P. F., 2003. Temporal and spatial changes of macroalgae and phytoplankton in shallow coastal areas: The Venice lagoon as a study case. Marine Environmental Research, 56, 617-636.

Sfriso A., Facca C. and Ceoldo S., 2004. Growth and production of *Cymodocea nodosa* (Ucria) Ascherson in the Venice lagoon, in "Scientific Research and Safeguarding of Venice. CoRiLa. Research Programme 2001-2003. 2002 Results", by P. Campostrini, Multigraf, Spinea, Vol II. pp. 229-236.

Sfriso A., Facca C. and Marcomini A., 2005. Sedimentation rates and erosion processes in the lagoon of Venice. Environment International, 31(7), 983-992.

Sfriso A. and Facca C., 2007. Distribution and production of macrophytes in the lagoon of Venice. Comparison of actual and past abundance. Hydrobiologia,

577, 71-85.

Strickland, J.D.H. and Parsons, T.R., 1972. A practical handbook of seawater analyses. Fish. Res. Board Can. Bull., Ottawa.

COMPARING THE DIATOM OCCURRENCE IN AREAS COLONISED BY NATURAL AND TRANSPLANTED *NANOZOSTERA NOLTII* (HORNEEMAN) TOMLINSON *ET* POSLUZNY POPULATIONS IN VENICE LAGOON

Chiara Facca, Adriano Sfriso, Sonia Ceoldo

Dipartimento di Scienze Ambientali, Università di Venezia,
Calle Larga Santa Marta 2137, 30123 Venezia

Riassunto

Nell'ambito del progetto CORILA 2004-2006, un'area, in cui è stata introdotta la fanerogama marina *Nanozostera noltii* (Hornemann) Tomlinson *et* Posluzny su sedimento sabbioso di riporto, è stata confrontata con un sito in cui questa specie è presente naturalmente. Particolare attenzione è stata posta alla distribuzione delle diatomee planctoniche e bentoniche in entrambi i siti. L'area con sedimento naturale è risultata più ricca di biomassa, probabilmente perché presentava una granulometria più fine e una maggior disponibilità di nutrienti.

Abstract

In the framework of the CORILA Research Programme 2004-2006, one site, where *Nanozostera noltii* (Hornemann) Tomlinson *et* Posluzny had been transplanted on an artificial sandy bank, was compared with another where grew naturally. The main topic of the present work was to study the cell abundance trends and the taxonomic composition of the planktonic and benthic diatoms in the two studied stations. The "natural" site was richer in microalgal biomass than the "artificial" one. Such difference was probably due to the sediment grain-size, which in the natural site had a larger amount of fine particles and to a major nutrient availability.

1 Introduction

The prevention and recovery of erosion processes induce several types of interventions which often involve the use of filling materials. The sediments used to re-built banks are generally characterized by physical properties (density, humidity, grain-size...), which can highly differ from the characteristics of the destination sites. As it is supposed that the sediment refilling can be more successful, in terms of material stabilization, if the area is rapidly colonized by seagrasses, the effort of a biological recovery is often coupled to prevent erosion. To study the evolution of an area (Lido station, central basin) of the Venice lagoon where sandy sediments were imported and *Nanozostera noltii* was transplanted, samplings were carried out monthly during one whole year. Community records were integrated with measurements of physical, chemical

and biological parameters of the water column and of the surface sediments. In particular, the present paper focuses on planktonic and benthic diatom occurrence in the “artificial” site (Lido station, central basin) and compares that area with another (Petta di Bò station, southern basin) naturally colonized by *N. noltii* population.

2 Material and Methods

Samplings were carried out monthly from January to December 2005 in the framework of the CORILA Research Programme 2004-2006 (Line 3.12) at a site located in the Lido watershed, close to Lido island (Lido station) and at a site in southern lagoon called Petta di Bò (Petta di Bò station). The interventions for the banks refilling were carried out at Lido where *N. noltii* was also transplanted. At the Petta di Bò documented presence of a natural *N. noltii* population goes back to 1994 [Sfriso and Ghetti, 1998].

Water sample aliquots were collected by sampling the whole water column by means of a home-made bottle (diameter: 4 cm, length: 150 cm,) repeatedly plunged into the water in order to obtain an average sample. Sub-samples of ca. 200 ml were preserved with 4% formaldehyde and employed for the planktonic diatom cell count and the taxonomic identification at the inverted light microscope (Axiovert 10 ZEISS). Undisturbed sediment samples were collected in submerged areas by means of a box corer (i.d. 10 cm). The core surface layer was sampled by means of a syringe deprived of the point in order to determine the benthic diatom abundance and taxonomic composition of the sediment first cm according to Totti *et al.* [2003]. Planktonic and benthic diatom cell abundance were compared by reporting the results per surface unit (cm⁻²) taking into account the depth of the water column for the phytoplankton determination.

Nutrient concentrations in the water column and in the pore-water of the 5cm-sediment top-layer were determined according to the spectrophotometrical method [Strickland and Parsons, 1972]. Organic and Inorganic Phosphorus (OP and IP) extraction from the surface sediments were obtained according to Aspila *et al.* [1976] and Strickland and Parsons [1972]. Total Nitrogen (TN), Organic and Inorganic Carbon (OC and IC) in the surface sediment were obtained by using a Carlo Erba CNS Autoanalyser (mod. NA 1500) after removing carbonates. The seagrass biomass was estimated according to the procedures reported in Sfriso and Ghetti [1998].

3 Results

By considering the main environmental parameters, sampling sites mostly differed because of the sediment characteristics. In fact, the one-way ANOVA test was significant ($p < 0.05$) for the grain-size, the nutrient and carbon content in the surface sediments and the ammonium concentrations in pore-waters (see parameters in grey in Tab. 1). Excluding IP, all the other significant parameters were higher at Petta di Bò, particularly ammonium concentrations (on average, 3.5 times as high as at Lido, Tab. 1). The other water parameters were quite

similar at both the sites (one-way ANOVA $p > 0.05$).

The biological parameters, i.e. chlorophyll concentration and cell abundance, in the water column were quite similar whereas significant differences were recorded for *N. noltii* biomass (Tab. 1, Fig. 1) and the benthic diatom cell abundance.

		Petta di Bò				Lido			
		Mean	Std. Dev.	Min	Max	Mean	Std. Dev.	Min	Max
Temperature	°C	16.2	7.60	5.20	25.5	16.4	8.60	5.80	29.3
pH water		8.04	0.24	7.63	8.43	8.05	0.20	7.72	8.50
pH sediment		7.45	0.17	7.07	7.75	7.60	0.30	7.28	8.32
E _h water	mV	318	15.8	295	340	320	37.3	244	371
E _h sediment	mV	-36.8	101	-226	110	125	129	105	295
Salinity	g l ⁻¹	33.6	1.47	31.8	36.3	34.5	1.02	33.3	36.3
Dissolved oxygen	mg l ⁻¹	9.61	2.03	5.80	12.1	9.63	1.60	7.45	11.8
Depth	cm	64.2	16.2	40.0	90.0	77.5	25.9	40.0	110
Chl a	µg l ⁻¹	1.77	1.47	0.24	5.61	0.91	0.70	0.20	2.56
Phaeo	µg l ⁻¹	2.05	2.46	0.00	7.11	0.69	0.54	0.04	1.62
Macrophytes	g m ⁻² fwt	2325	735	1256	3676	800	412	244	1437
Sediment density	g cm ⁻³ dwt	1.19	0.04	1.13	1.27	1.37	0.04	1.26	1.40
Grain size <63 µm	%	15.6	3.18	12.4	20.6	5.31	1.76	3.32	8.90
Reactive P	µM	0.43	0.57	0.07	2.14	0.27	0.16	0.05	0.60
Silicate	µM	3.21	4.53	1.10	17.0	2.28	1.49	0.95	4.99
Nitrite	µM	1.00	0.66	0.23	2.14	0.81	0.48	0.19	1.62
Nitrate	µM	8.52	7.43	0.73	23.0	8.33	6.98	1.09	25.5
Ammonium	µM	24.5	25.8	1.37	82.3	6.97	3.26	0.65	11.3
RP pore-water	µM l ⁻¹ sed.	37.4	24.0	10.2	78.7	27.6	12.8	10.5	50.7
NO _x pore-water	µM l ⁻¹ sed.	128	83.7	41.1	298	118	68.8	40.5	256
NH ₄ pore-water	µM l ⁻¹ sed.	2988	2054	882	6564	1344	671	675	3060
OPhosphorus	µg g ⁻¹ sed.	54.3	13.8	35.0	72.0	33.8	20.6	10.5	71.0
IPhosphorus	µg g ⁻¹ sed.	331	9.36	312	344	390	50.2	319	470
Total nitrogen	mg g ⁻¹ sed.	0.70	0.35	0.36	1.49	0.29	0.26	0.09	1.09
Organic carbon	mg g ⁻¹ sed.	9.20	4.60	4.70	19.4	2.69	1.32	1.10	4.90
Inorganic carbon	mg g ⁻¹ sed.	46.1	3.31	40.0	53.6	13.7	1.49	11.5	17.5

Tab 1 – Means, standard deviations, minimum and maximum values of the main environmental and biological parameters at the two stations. Significant parameters (one-way ANOVA $p < 0.05$) are in grey.

At Petta di Bò *N. noltii* biomass was almost 3 times as high as at Lido, but the main difference concerned the seasonal trends: at Petta di Bò the biomass

started to increase in March and peaked in September, at Lido the peak was in January, then the biomass progressively decreased.

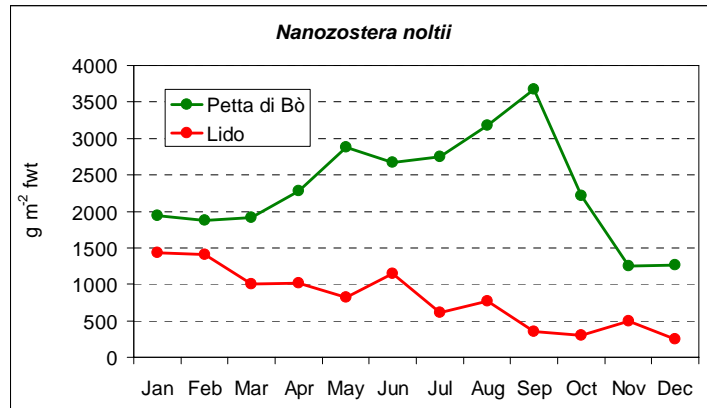


Fig 1 – *Nanozostera noltii* trends at the two sites from January to December 2005.

Although the overall cell abundance of planktonic diatoms was similar at both stations, important differences concerned the community composition. At Petta di Bò, *Skeletonema* was dominant from February to April, and then *Navicula* and *Nitzschia* became the most abundant genera. At Lido, *Skeletonema* was almost negligible and *Chaetoceros* was dominant in March, May and September. During the other months *Nitzschia* was quite abundant and *Thalassiosira* had some importance (Fig. 2).

In the surface sediments five genera (*Amphora*, *Cocconeis*, *Navicula*, *Nitzschia*, *Thalassiosira*) represented most of the community composition during the whole sampling period. The genera occurrence was the same, but their abundance was significantly higher at Petta di Bò than at Lido (Fig. 3). *Nitzschia* always constituted a significant portion of the community while the presence of *Thalassiosira* and *Navicula* was constant, but not so important. *Amphora* and *Cocconeis* displayed some variability which depended on the site and the period of the year.

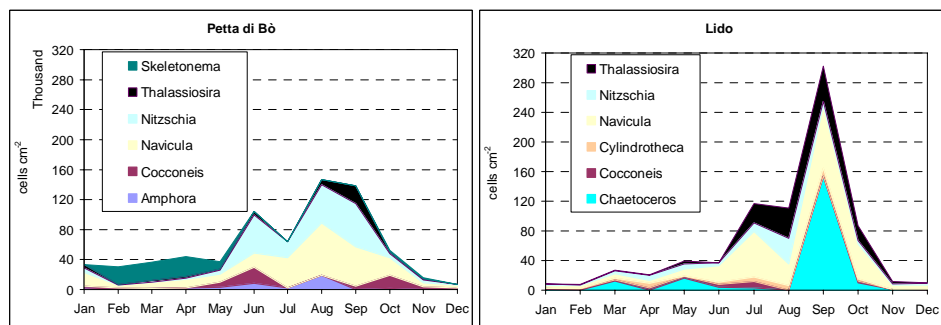


Fig 2 – Planktonic diatom cell abundance from January to December 2005. Both scales are in thousand cells per cm².

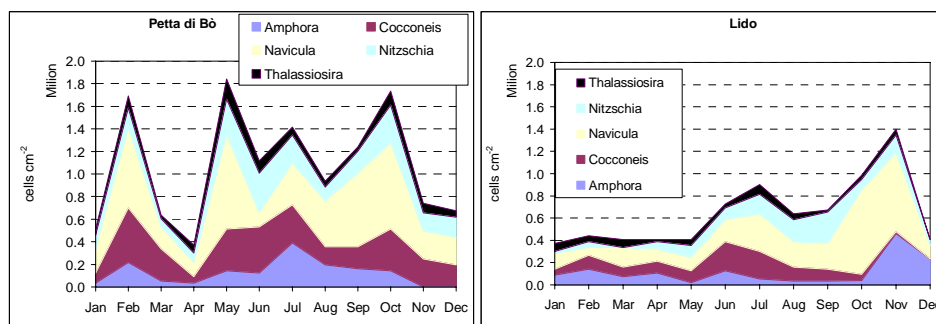


Fig 3 – Benthic diatom cell abundance from January to December 2005. Both scales are in million cells per cm².

By comparing the planktonic and benthic communities, it can be observed that the seasonal trends were more marked for the water community. In fact, in winter and in autumn, benthic diatoms displayed values as high as in spring and summer. Moreover, the cell abundance per unit was 6-30 times higher in the sediment than in the water column. In contrast, excluding *Skeletonema* and *Chaetoceros* (centric and colonial diatoms), the genera occurrence was similar.

At Petta di Bò planktonic and benthic cell abundance was twice as much as at Lido site. In addition to the significant correlations (Pearson correlation $p < 0.05$) of planktonic diatoms with temperature and salinity, both the communities appeared to be mostly correlated to the nitrogen compound availability. Moreover the benthic diatom cell abundance increased with the increasing of the fine sediments percentage.

Nanozostera noltii biomass at Petta di Bò was significantly and positively correlated (Pearson correlation $p < 0.05$) to the total planktonic diatom abundance and to the genera *Navicula* and *Nitzschia* in the water column and to *Amphora* in the surface sediments. At Lido some significant correlations were observed only with the abundance of *Cocconeis* and *Navicula* in the surface sediments.

Conclusions

The water column parameters, both for chemical and biological variables of the considered stations, appeared quite similar. On the contrary, the characteristics of the sediments highlighted significant differences which lead to important changes in the benthic microalgal community. The grain-size played an important role in favouring benthic diatom abundance. The presence of fine sediments ($< 63 \mu\text{m}$) is recognized to be an important factor for both diatom [Facca *et al.*, 2002 and reference therein] and *N. noltii* biomass [Sfriso and Facca, 2007]. Moreover the presence of a thick seagrass bed allowed the settlement of epiphytes which were able to survive also on the surface sediment.

The positive correlation between *N. noltii* biomass and the planktonic diatom at Petta di Bò was probably due to similar seasonal trends rather than to relationships between the two populations. The major abundance of diatoms at Petta di Bò highlighted that there was not competition for resources between the microalgal community and the seagrasses.

On the whole, *N. noltii* population on the artificial bank was disappearing. This can mean that the environmental conditions recorded at Lido are not suitable for the growth of that species and also the benthic diatom colonization was not so important as in the natural station.

References

Aspila, K.I., Agemian, H., Chau, A.S.J., 1976. A semiautomatic method for the determination of inorganic, organic and total phosphate in sediments. *Analyst*, 101, 187-197.

Facca, C., Sfriso, A., Socal, G., 2002. Temporal and spatial distribution of diatoms in the surface sediment of the Venice lagoon. *Botanica Marina*, 45, 170-183.

Sfriso, A., Ghetti, P.F., 1998. Seasonal variation in biomass, morphometric parameters and production of seagrasses in the lagoon of Venice. *Aquatic Botany*, 61, 207-223.

Sfriso, A., Facca, C., 2007. Distribution and production of macrophytes and phytoplankton in the lagoon of Venice: comparison of actual and past situation. *Hydrobiologia*, 577, 71-85.

Strickland, J.D., Parsons, T.R., 1972. A practical handbook of seawater analyses. Fisheries Research Board Canada Bull. No. 167, Ottawa.

Totti, C., De Stefano, M., Facca, C., Ghirardelli, L.A., 2003. Il microfitobenthos. In: Gambi M.C., Dappiano M. (eds) *Manuale di metodologie di prelievo e studio del benthos mediterraneo*. *Biologia Marina Mediterranea*, 10, 263-284.

CARBON FLUXES THROUGH THE PLANKTON COMMUNITY IN THE LAGOON OF VENICE

Alessandra Pugnetti¹, Paola Del Negro², Michele Giani³, Francesco Acri¹, Fabrizio Bernardi Aubry¹, Daniela Berto³, Elisa Camatti¹, Joan Coppola¹, Annalisa Valeri²

¹*Consiglio Nazionale delle Ricerche, Istituto di Scienze Marine (ISMAR), Castello 1364/A, I-30122 Venezia, Italy*

²*Dipartimento di Oceanografia Biologica, Istituto Nazionale di Oceanografia e Geofisica Sperimentale (OGS), Via A. Piccard 54, I-34014 Trieste, Italy*

³*Istituto Centrale per la Ricerca scientifica e tecnologica Applicata al Mare (ICRAM), Brondolo, I-30015 Chioggia, Italy*

Riassunto

In questo lavoro è stata analizzata, per la prima volta in questo ambiente, l'importanza dei processi autotrofi, rispetto a quelli eterotrofi, nel sistema planctonico della Laguna di Venezia. La produzione batterica supera, per la maggior parte dell'anno, la produzione primaria e, pertanto, la base della rete trofica planctonica è spesso eterotrofa. Inoltre, poiché i processi respiratori prevalgono su quelli fotosintetici, il sistema planctonico lagunare è principalmente una fonte, piuttosto che un pozzo, di CO₂. La richiesta di carbonio da parte dei batteri è soddisfatta solo molto parzialmente dalla produzione e dal rilascio di essudati da parte del fitoplancton. Pertanto, gli apporti di carbonio organico, esterni al sistema planctonico, risultano di fondamentale importanza per il sostegno del metabolismo complessivo del comparto eterotrofo. La comunità batterica presenta un metabolismo prevalentemente catabolico, indirizzato, cioè, alla mobilizzazione del carbonio attraverso una intensa attività enzimatica.

Abstract

The autotrophic vs. heterotrophic nature of the plankton system and the role of the organic carbon have been analyzed, for the first time, in the Lagoon of Venice. Bacteria production has a similar or higher importance than phytoplankton production for most of the year and, therefore, the base of the planktonic trophic web may be heterotrophic. Moreover, the plankton system of the lagoon acts prevalently as a source, rather than a sink, for CO₂. The carbon requirements of bacteria are only very partially satisfied by the production and by the release of exudates by phytoplankton. The inputs of organic matter, allochthonous to the planktonic system, contribute substantially to fuel the heterotrophic metabolism in the lagoon. The prevalent catabolic metabolism of the bacterial community mobilizes the organic carbon from the dissolved and particulate pools through bacterial exoenzymatic activity and appears sufficient

to meet bacteria C requirements for maintenance and growth.

1 Introduction

Planktonic and microbial food web processes influence the fate of organic carbon in aquatic ecosystems. When the main source of organic carbon is phytoplankton photosynthesis, net autotrophy generally dominates and bacterial production is broadly related to primary production (Cole et al., 1988). In contrast, in estuaries and coastal lagoons the inputs of external organic carbon may influence strongly the ecosystem metabolism. These ecosystems might show a net heterotrophic metabolism (respiration > gross primary production) or a seasonal shift from net autotrophy to net heterotrophy, in relation with allochthonous inputs of organic carbon and nutrients and with turbidity variations (Jensen et al., 1990; Kemp et al., 1997; Caffrey et al., 1998). The autotrophic or heterotrophic nature of a coastal ecosystem can be influenced by human pressure, mainly through the alteration of light availability and of nutrient and organic matter inputs. In the planktonic system high bacteria biomass and production can occur and the secondary production might be based, at least in some periods, on bacterial mobilization of chemically bound energy, rather than on phytoplankton photosynthesis (Gaedke and Kamjunke, 2006; Berglund et al., 2007).

In the Lagoon of Venice information on the prevalent pattern of carbon fluxes through the planktonic and microbial communities is very scarce. A considerable amount of information is available for phytoplankton and mesozooplankton composition and biomass (Acri et al., 2004), while quite sporadic is the knowledge of phytoplankton photosynthetic rates (Vatova, 1960; Degobbis et al., 1986; Bianchi et al., 2000), bacterial community (Sorokin et al., 1996; 2002) and dissolved organic carbon (Marcomini et al., 2001).

The objective of this work, carried out in the framework of the second CORILA research Program (2004-2006), is to quantify the importance and the significance of the planktonic and microbial-mediated carbon fluxes in the Lagoon of Venice and their seasonal variations. The work focuses on the water column, which is considered in a shallow environment, such as the lagoon, to be the result of the continuous water-sediment interactions and of the dominant benthic-pelagic coupling.

2 Materials and methods

We have considered 3 shallow (2-3 m deep) sites (Fig. 1), located in plankton-dominated areas of the Northern and Central sub-basins of the lagoon, representative of their main habitats (Acri et al., 2004; Sfriso et al., 2005).

Transparency (Secchi disk), Photosynthetically Active Radiation (PAR; LiCor Li-192), temperature, salinity, dissolved oxygen and pH (Itronaut Ocean Seven 316 multiprobe) were measured in the whole water column. Samples for the analysis of dissolved inorganic macronutrients (Grasshof et al., 1983), phytoplankton and bacterial communities, respiration, particulate and dissolved organic carbon, were collected at the surface water layer, that was considered

fairly well representative of the whole water column. Hydrological parameters, nutrients and chlorophyll a were determined monthly. Samplings for the studies of the microbial carbon fluxes were carried out seasonally on January, April, July and October 2005. Monthly and seasonal samplings were always performed at neap tide, in order to minimize the effects of tidal currents.

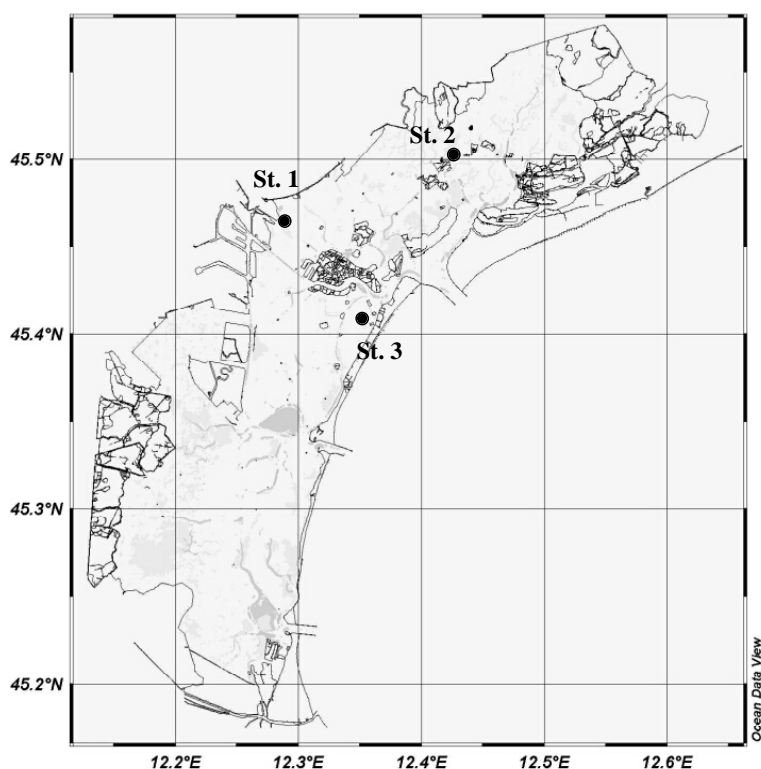


Fig 1 – The Lagoon of Venice: the three sampling stations are indicated.

Phytoplankton chlorophyll a was determined according to Holm Hansen et al. (1965).

Water samples for primary production measurements (^{14}C method; Steeman-Nielsen, 1952) were incubated at simulated in situ conditions, under natural sunlight and maintaining in situ temperature, for two hours around noon. 250 ml sub-samples were inoculated with 148 kBq of $\text{NaH}^{14}\text{CO}_3$. Six light levels (100%, 70 %, 50 %, 25 %, 10 % and 5%) were obtained by means of neutral optical filters, in order to mimic natural light attenuation at different depths in the water column. Total primary Production (PP) was determined on duplicated sub-samples (5 ml) that were acidified and stirred for one hour. Ultima Gold XR was added and the samples were then counted in a Beckman scintillation counter (LS 6000 TA). Specific production (P_b) was calculated as PP normalized to chlorophyll a concentrations. Dissolved Primary Production (DPP) was measured after filtrations of 10 ml of samples on 0.2 μm polycarbonate filters at low (< 10 mm Hg) vacuum pressure. Two sub-samples of the filtrates (5 ml each) were removed and treated in the same way as the PP. From the arithmetical integration of the PP data obtained from the measurements at different light intensities we obtained the total and average PP of the water

column. The daily PP was estimated according to Platt (1971). Community respiration (CR) was estimated as the difference in dissolved oxygen at the beginning and after 24-hour incubation of triplicate 250 ml water samples in the dark, at in situ temperature. Oxygen was assayed with potentiometric Winkler titrations (794 Basic Titrino, Metrohm). The oxygen uptake rates were transformed into inorganic carbon production considering the molar ratio between carbon and oxygen (0.375). In order to calculate the CR for the whole water column and for comparative purposes with PP, the surface CR rate was assumed to be constant throughout the water column.

Samples (10 ml) for estimate heterotrophic bacterial abundances (HBA) were fixed with 2% final concentration borate-buffered formalin and stained for 15 min with 4'6 diamidino-2-phenylindole (DAPI, Sigma) at $1 \mu\text{g ml}^{-1}$ final concentration (Porter and Feig, 1980). Bacterial abundance was converted into carbon equivalents using the conversion factor of 20 fgC cell^{-1} (Lee and Fuhrman, 1987). Bacterial carbon production (BCP) was estimated from the rates of protein and DNA synthesis determined by the incorporation of ^3H -leucine (Leu) and ^3H -thymidine (TdR), respectively, into cold trichloroacetic acid (TCA) (Fuhrman and Azam, 1980; Kirchman et al., 1985). Conversion factor, which relates rates of TdR incorporation to rates of bacterial carbon production, was obtained by Fuhrman and Azam (1982). Incorporation of ^3H -leucine was converted into carbon produced via bacterial protein production according to Simon and Azam (1989), assuming a 2-fold isotope dilution for Leu. Bacterial carbon demand (BCD) is the sum of BCP and bacterial respiration (BR). Because of methodological difficulties, BR is usually not measured directly and is instead computed from BCP and an assumed value of bacterial growth efficiency (BGE). We used a medium BGE of 30 % (e.g. Hoppe et al. 2002) for our computations. Excluding extreme values, BGE is in the range < 10 % to 50 % (del Giorgio et al. 1997). Harris et al. (2001) applied a growth efficiency of 40 % to a large data set in the oligotrophic Western Mediterranean Sea. Recently Becquevort et al. (2002) reported a growth yield of 23 % as estimated from bioassays performed in the Danube–Black Sea mixing zone.

Hydrolytic exoenzyme activities were measured with fluorogenic analogs of natural substrates (Hoppe, 1993) derived from 7-amino-methyl-coumarin (AMC) and 4-methyl-umbelliferone (MUF). Aminopeptidase activity was assayed as the hydrolysis rate of L-leucine-AMC. β -D-glucosidase, α -D-glucosidase β -D-galactosidase, α -D-galactosidase, lipase, N-acetyl glucosaminidase and alkaline phosphatase were assayed using MUF-compounds. The bacterial exoenzymatic activities were converted to carbohydrate and protein mobilized using the conversion factor $72 \mu\text{g C } \mu\text{mol}^{-1}$ (Hoppe, 1993). The organic carbon potentially mobilised by bacteria enzymatic activities was estimated as the sum of the aminopeptidase, β -D-glucosidase, α -D-glucosidase β -D-galactosidase, α -D-galactosidase, lipase, N-acetyl glucosaminidase and alkaline phosphatase expressed as $\mu\text{g C l}^{-1} \text{ h}^{-1}$.

Water samples for dissolved organic carbon (DOC), dissolved carbohydrates (DCHO) and chromophoric dissolved organic material (CDOM), particulate organic carbon (POC) and particulate carbohydrates (PCHO) were analyzed

after filtration through precombusted (4h, 450°C) Whatman GF/F. The DOC concentrations were measured using a Shimadzu TOC 5000 Analyzer with a 1.2 % Pt on silica as catalyst at 680°C (Cauwet, 1994). Samples were acidified (pH 2) with HCl and purged with pure air for 10 min immediately prior to analysis. DOC concentrations were calculated by subtracting the system blanks and dividing by the slope of the calibration curve (Thomas et al., 1995). Potassium hydrogen phthalate was used as standard. 100 µl of sample were injected for each analysis and the concentration was calculated as the average of three to five replicates. The average instrumental blank was $8.7 \pm 0.9 \mu\text{mol l}^{-1}$ and the reproducibility was high (<3 %). POC concentrations were determined with a CHN Elemental Analyzer Carlo Erba Mod. EA1108, after acidification with HCl (8 N) (Nieuwenhuize et al., 1994) to remove the inorganic carbonate fraction, with high reproducibility (<2%). Acetanilide was used as standard. DCHO and PCHO were determined spectrophotometrically by the MBTH (3-methyl-2-benzothiazolinone hydrazone hydrochloride) assay after 1N HCl hydrolysis (Johnson and Sieburth, 1977). The UV-VIS spectra of the filtered lagoon water were performed by UV2 spectrophotometer ATI Unicam from 270 to 800 nm with 5-cm quartz optical cell using Milli-Q water as the blank, as reported by Vodacek et al. (1997). To quantify the chromophoric dissolved organic matter (CDOM) in each sample, we used the absorption coefficient (aCDOM, in m^{-1}) at 355 nm as a proxy, calculated from the sample absorbance (A) in nm^{-1} and pathlength (L) in meters as follows:

$$a\text{CDOM}(355)=2.303A \text{ CDOM} (355)/L$$

3 Results and discussion

At the three stations (Fig. 1) a prevalent unimodal phytoplankton seasonal cycle can be recognized, with chlorophyll *a* maxima occurring mostly in summer. The average seasonal variations of chlorophyll *a* ($1.2 \pm 0.9 - 8.9 \pm 9.7 \mu\text{g l}^{-1}$) appeared mainly related to those of temperature and solar irradiance (temperature: $N = 12$, $r^2 = 0.90$, $p < 0.01$; irradiance $N = 12$, $r^2 = 0.55$, $p < 0.05$), but not with inorganic nutrients. DIN (Dissolved Inorganic Nitrogen) concentrations were characterized by autumn maxima ($107 \pm 48 \mu\text{M}$) and summer minima ($10 \pm 5 \mu\text{M}$), while silicate ($16 \pm 14 - 62 \pm 30 \mu\text{M}$) and phosphate concentrations ($0.3 \pm 0.3 - 0.8 \pm 0.4 \mu\text{M}$) varied much more irregularly throughout the year. The N/P ratio was always much higher than 16, pointing out that inorganic P could be the potential limiting macronutrient. However, P limitation doesn't seem actually to occur and P never appear to be exhausted, even in summer, when the highest plankton activities and biomass were observed.

The photosynthetic activity of the phytoplankton is characterized by a very marked variability ($0.8 \pm 0.7 - 130 \pm 150 \mu\text{g C l}^{-1} \text{ h}^{-1}$): the maximum primary production (PP) values, attained in summer, represent more than three times the sum of the photosynthetic rates in the other seasons. The seasonal variation of PP and of specific production (P_b : $1.2 \pm 1.5 - 12.8 \pm 3.5 \mu\text{g C} (\mu\text{g chl } a)^{-1} \text{ h}^{-1}$) matched quite closely that of chlorophyll *a* and it appeared mainly related with that of temperature rather than with nutrients. The whole water column was

always euphotic, even though PAR was rapidly attenuated and only the 5-20 % of surface irradiance reached the bottom. The PP vertical profiles, estimated from the samples incubated at decreasing light intensity, were very steep: from surface to bottom light intensity, PP decreased from 6 to 20 times.

Bacterial abundance (HBA: $1.9 \pm 1.3 - 7.3 \pm 2.8 \cdot 10^9$ cells l^{-1}), and bacterial carbon production detected as Leucin incorporation (Leu-BCP: $2.8 \pm 0.5 - 6.1 \pm 2.1 \mu\text{g C } l^{-1} \text{ h}^{-1}$) showed a seasonal cycle qualitatively similar to that of phytoplankton biomass and production. Both HBA and BCP, however, were much less variable than PP showing an average value nearly fourfold (HBA) and twofold (BCP) in summer than in winter.

The ratio between daily PP ($1.2 \pm 1.2 - 575 \pm 745 \mu\text{g C } l^{-1} \text{ d}^{-1}$) and BCP ($66 \pm 53 - 147 \pm 50 \mu\text{g C } l^{-1} \text{ d}^{-1}$) was definitely higher than 1 only in summer (Fig. 2). The base of the planktonic trophic web in the Lagoon of Venice resulted to be more often heterotrophic (based on BCP) than autotrophic (based on PP). The shift between heterotrophy to increasing net autotrophy seems to be mainly related to the seasonal variations of temperature and light, affecting the phytoplankton standing crop and production. The bacteria-based food webs have generally more trophic levels than phytoplankton-based food webs (Gaedke and Kamjunke, 2006; Berglund et al., 2007) and, consequently, the energy loss from the base to the top of the food web (i.e. its ecological efficiency) is larger. The occurrence of a phytoplankton based food web in the lagoon appears mostly dependent upon increased PP rates. PP/BCP ratio were, indeed, definitely higher than the unity only in correspondence with the highest PP and biomass peaks, that is for PP values higher than $200 \mu\text{g C } l^{-1} \text{ d}^{-1}$, corresponding to chl *a* values higher than $5 \mu\text{g } l^{-1}$ and to concomitant average daily PAR higher than $800 \mu\text{moles m}^{-2} \text{ s}^{-1}$. Considering the threshold of $5 \mu\text{g chl } a \text{ } l^{-1}$ and the monthly chlorophyll *a* variations throughout the year, the bacteria based food web is expected to prevail in the 75 % of the cases.

The average plankton community respiration rates (CR) encompass quite a wide range ($70 \pm 65 - 860 \pm 640 \mu\text{g O}_2 \text{ } l^{-1} \text{ d}^{-1}$) that fell within the values generally reported for estuarine and coastal waters (Jensen et al.1990; Smith and Kemp, 1995; Iriarte et al., 1996). The spatial and temporal variations of CR match quite closely those of PP and of chlorophyll *a*: indeed, the maximum CR occurred during the maximum phytoplankton production and biomass. This pattern is reported also for other coastal ecosystems (Jensen et al., 1990; Blight et al., 1995; Caffrey et al., 1998; Cloern, 1999). The rates of oxygen consumption were much less variable than those of PP. This may indicate that CR and PP do not respond with the same intensity at the environmental variations and that the community respiration is fuelled by sources that are in addition to phytoplankton production (e.g. organic loads from external sources) and that are supplied also more constantly through time. Daily CR was mostly higher than daily PP (Fig. 3): considering both the surface and the whole water column, PP exceeds CR only in summer, showing a prevalent heterotrophy in the planktonic system. The relative degree of autotrophy vs. heterotrophy indicates that the planktonic system seems to be prevalently supported by stored or imported organic matter. However, the periods in which the system is

heterotrophic do not appear to be related with concomitant increase of BCP or of DOC concentrations. On the contrary, the system appears to be generally heterotrophic, with autotrophy prevailing only when elevated PP are allowed, that is when PP exceeds $500 \mu\text{g C l}^{-1} \text{d}^{-1}$ and chlorophyll *a* attains concentrations definitely higher than $5 \mu\text{g l}^{-1}$. As observed before, the threshold of $5 \mu\text{g chl a l}^{-1}$ is found only in the 25 % of the sampling, considering the monthly values throughout the whole year.

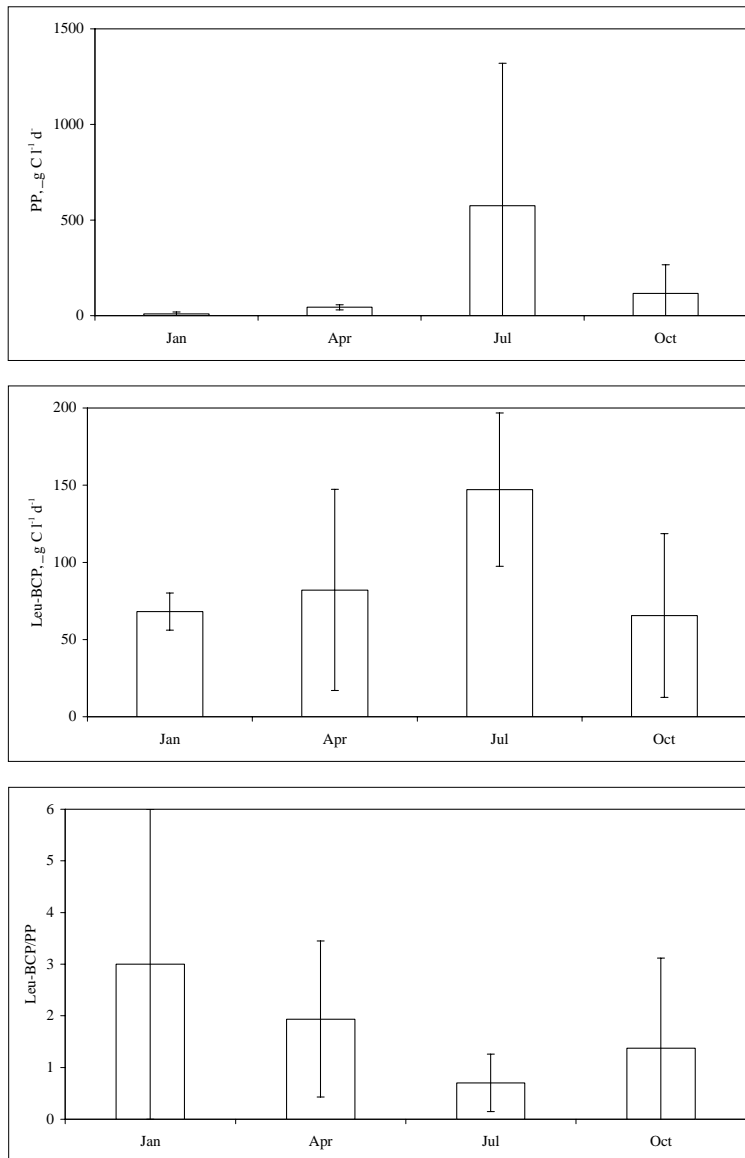
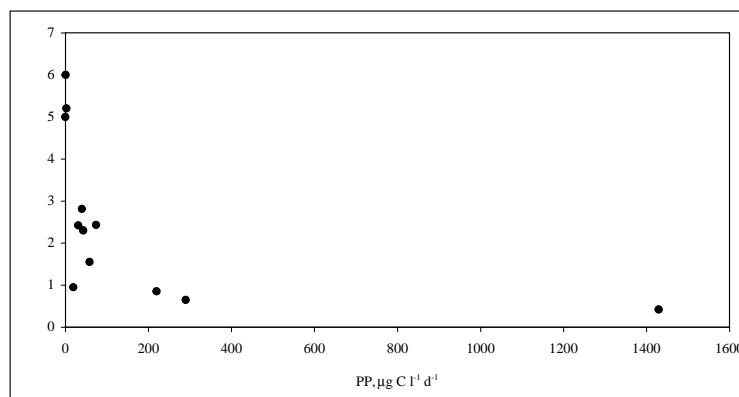


Fig 2 – Daily primary production (PP), bacteria production (BCP) and ratio between BCP and PP. Average values and standard deviations in the water column at the three stations.

Fig 3 – Daily community respiration/primary production ratio (CR/PP) in relation with PP. The dashed line indicate $PP = CR$.



The organic carbon released during photosynthesis by phytoplankton is considered one of the most important sources of labile organic molecules for bacteria growth (e.g.: Cole et al., 1988; Baines and Pace, 1991; Norrman et al., 1995). The short-term carbon exudates release (DPP) during phytoplankton photosynthesis represented a small amount of total primary production: the seasonal average of the percentage extracellular release (PER: 1-8 %) ranged between the lowest range reported in the literature (Baines and Pace, 1991). BCD was always too large to be supported by DPP: the comparison of BCD and DPP, averaged over the whole water column, show that DPP did never appear sufficient to meet bacterial C requirements, ranging between 1 and 18 % of BCD. Moreover, BCD could be sustained completely by total PP only once (in summer, at one station), while in all the other cases BCD largely (> 30 %) exceeded PP. If BCD exceeds DPP, then bacteria must have other sources of organic carbon for their growth. The coupling between bacteria and phytoplankton through DPP, is, indeed, expected to be highly variable in relation with the relative contribution of autochthonous and allochthonous organic carbon inputs. Therefore, sources of C other than phytoplankton PP are clearly necessary to sustain the bacteria carbon requirements, supporting the heterotrophic nature of the system.

The potential bacterial carbon mobilization (C_{mob}), calculated from bacterial exoenzymatic activity, appears to fully satisfy the BCD. C_{mob} , showed the highest average values in summer ($2650 \pm 2610 \mu\text{g C l}^{-1} \text{d}^{-1}$) and the lowest in winter ($720 \pm 260 \mu\text{g C l}^{-1} \text{d}^{-1}$). It was positively correlated both with Leu-BCP ($r^2 = 0.62$, $N = 12$; $p < 0.01$) and with BCD ($r^2 = 0.78$, $N = 2$; $p < 0.01$), suggesting that BCP was mainly addressed towards enzyme synthesis and that the carbon that is potentially mobilized by enzymatic activity generally meets the bacterial carbon requirements. In the Lagoon of Venice Leu-BCP was clearly prevalent over TdR-BCP, from 2 to 9 times, giving clues of a prevalent catabolic metabolism.

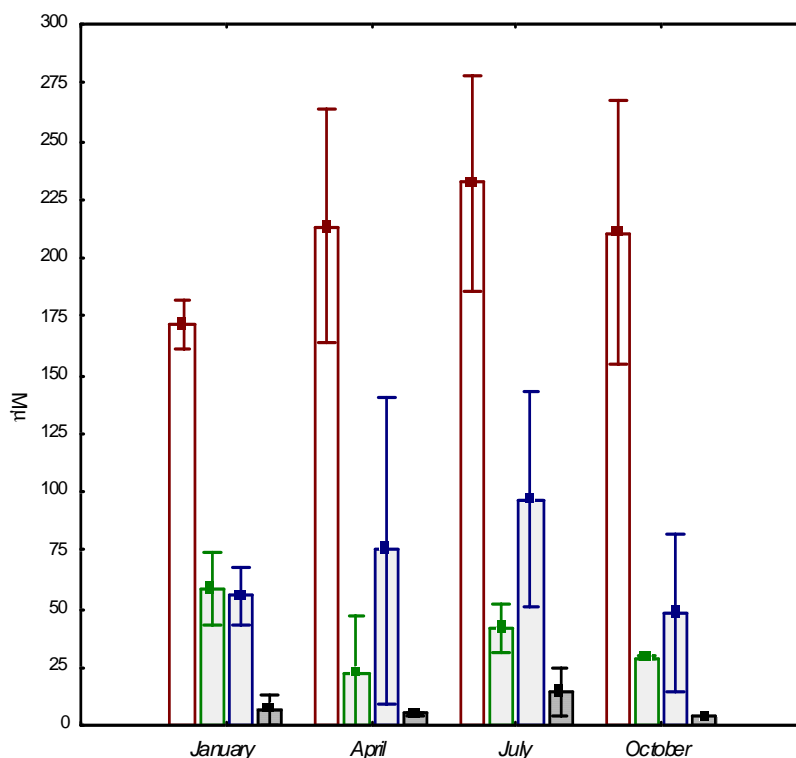
C_{mob} (showed a positive correlation with DOC ($r^2 = 0.68$, $N = 11$, $p < 0.005$). From this regression it was extrapolated the DOC concentration corresponding to a C_{mob} equal to zero: this value, 147 μM , can be considered as the amount of DOC that cannot be mobilized by bacterial exoenzymatic activity and it corresponds, on the average, to the 71 % of the mean DOC concentration. Considering the daily BCD, it is possible to estimate that the remaining 29 % of

DOC can be re-elaborated by the bacterial community, on average, in 3 days. This time scale represents the typical turnover rate for HMW matter.

Non-phytoplanktonic sources of organic carbon may be both autochthonous and allochthonous. The major autochthonous sources of DOM in wetlands are leachates from plants, exudates from phytoplankton, microalgae, or macrophytes, and pore water from sediments and soils (Ziegler and Benner 1999; Bertilsson and Jones 2003; Maie et al., 2006). Rivers and salt-marsh dominated estuaries are considered to be the largest source of CDOM to coastal waters (Blough et al., 1993; Wang et al., 2007 and reference therein). In the shallow areas considered in this study, organic matter from the sediments may give an important contribution to the organic matter in the waters (Sfriso et al., 2005), as a consequence of both natural (e.g. wind, storm, tidal flushing) and anthropogenic (clam harvesting, maritime traffic) sediment resuspension. The main part of the total organic carbon in the waters was in the dissolved form (average: 80 %; range: 63-90 %). DOC concentrations (Fig. 4) ranged between 171 and 232 μM , showing minimum in winter and maximum in summer. DCHO concentrations were higher in winter and summer (Fig. 4). POC concentrations (Fig. 4) ranged between 55 and 97 μM and increased from winter to summer, whereas the PCHO (Fig. 4) showed the highest values in winter and summer, similarly to the variations of DCHO concentrations. DCHO constituted, on average, 20 ± 11 % of DOC and 83 ± 11 % of total carbohydrates. In the suspended particulate matter the carbohydrates made up 11 ± 1 % of POC. The magnitude of chromophoric dissolved organic carbon (aCDOM) varied on average from 0.3 to 3.9 nm^{-1} , with minimum values in winter ($0.6 \pm 0.3 \text{ nm}^{-1}$).

The amount of non-absorbing DOC concentration was extrapolated from the positive correlation ($r^2 = 0.75$, $N = 11$, $p < 0.05$) between aCDOM and DOC. The chromophoric dissolved organic matter, on average, contributed to 81% of the total DOC concentrations in the lagoon water.

Fig 4 – Seasonal variations of the mean concentrations (μM) of dissolved organic carbon, dissolved carbohydrates (DCHO-C), particulate organic carbon (POC) and particulate carbohydrates (PCHO-C). Error bars represent the standard deviation.



Dissolve Organic Nitrogen (DON) was inversely correlated with salinity ($r^2 = 0.704$, $p < 0.001$, $N = 12$). The DOC/DON atomic ratio ranged from values (22.31 ± 27.74) similar to those reported by Bronk (2002) for coastal waters to much lower ones (3.93 - 6.7), close to those found by Kerner and Spitzzy (2001) in the Elbe estuary, especially due to quite high concentrations of DON. The lowest DOC/DON ratio in the spring-autumn period could be due to a higher release/degradation of DON from macrophytes as protein and humic-like materials that could be rapidly released from marsh grasses when they are flooded at high tides (Wang et al., 2007).

Conclusions

The results of this study indicate that, at least in some periods of the year, bacteria production have a similar or higher importance than phytoplankton production and, therefore, that the base of the planktonic trophic web may be heterotrophic. The plankton system of the lagoon acts prevalently as a source, rather than a sink, for CO_2 . Although our study was limited to the planktonic compartment, the prevalence of a positive net metabolism only in summer is confirmed also for the whole lagoon, by estimates carried out in the framework of the LOICZ (Land-Ocean Interactions in the Coastal Zone) activities and based on the nutrient budgets (Giordani et al., 2005).

The bacteria compartment and the heterotrophic processes have been largely neglected in the past in the Lagoon of Venice. However, all the studies carried out on the autotrophic components of the lagoon agree in evidencing, in the last 20 years, the reduction in the frequency and intensity of phytoplankton blooms. These changes could be attributed to an increase in water turbidity, related to

increased sediment resuspension, by clam harvesting and sediment management (Sfriso et al., 2005; Sfriso and Facca, 2007). These conditions might have enhanced the relative importance of the heterotrophic processes. Most aspects concerning the heterotrophic compartment and the qualitative and quantitative characteristics of the organic carbon are, at present, largely neglected in the on-going lagoon monitoring activities and management plans. The currently measured parameters, although of basic importance, leave largely incomplete the information necessary to define the trophic state of the lagoon and its natural and anthropogenic evolution.

References

- Acri F., Bernardi Aubry F., Berton A., Bianchi F., Boldrin A., Camatti E., Comaschi A., Rabitti S., Socal G. 2004. Plankton communities and nutrients in the Venice Lagoon. Comparison between current and old data. *J. Mar. Syst.*, 51: 321-329.
- Baines S.P., Pace M.L. 1991. The production of dissolved organic matter by phytoplankton and its importance to bacteria: patterns across marine and freshwater systems. *Limnol. Oceanogr.*, 36: 1078-1090.
- Becquevort S., Bouvier T., Lancelot C., Cauwet G., Egorov V., Popovichev V. 2002. The seasonal modulation of organic matter utilization by bacteria in the Danube-Black Sea mixing zone. *Estuar. Coast. Shelf. Sci.*, 54(3): 337-354.
- Berglund J., Muren U., Bamstedt U., Andersson A. 2007. Efficiency of a phytoplankton-based and a bacteria-based food web in a pelagic marine system. *Limnol. Oceanogr.*, 52(1): 121-131.
- Bertilsson S., Jones J.B. 2003. Supply of dissolved organic matter to aquatic ecosystems: autochthonous sources. In: Findlay S.E.G, Sinsabaugh R.L., (eds).. *Aquatic Ecosystems. Interactivity of dissolved organic matter*. Elsevier Science , pp3-24.
- Bianchi F., Acri F., Alberighi L., Bastianini M., Boldrin A., Cavalloni B., Cioce F., Comaschi A., Rabitti S., Socal G., Turchetto M. 2000. Biological variability in the Venice lagoon. In : Lasserre, P. and Marzollo, A. (Eds) *The Venice Lagoon Ecosystem. Inputs and interactions between land and sea. Man and the biosphere series volume 25*. UNESCO and Parthenon Publishing Group: 97-125.
- Blight S.P., Bentley T.L., Lefevre D., Robinson C., Rodrigues R., Rowlands J., Williams P.J. leB. 1995. Phasing of autotrophic and heterotrophic plankton metabolism in a temperate coastal ecosystem. *Mar. Ecol. Prog. Ser.*, 128: 61-75.
- Blough N.V., Zafirou O.C., Bonilla J. 1993. Optical absorption spectra of waters from the Orinoco river outflow: terrestrial input of colored organic matter to the Caribbean. *J. Geophys. Res.*, 98: 2271-2278.
- Bronk D.A. 2002. Dynamics of DON. In: (Hansell D.A., Carlson C.A. eds.)

Biogeochemistry of Marine Dissolved Organic Matter. Academic Press, London. pp. 153-247.

Caffrey J.M., Cloern J.E., Grenz C. 1998. Changes in production and respiration during a spring phytoplankton bloom in San Francisco Bay, California, USA: implications for net ecosystem metabolism. *Mar. Ecol. Prog. Ser.*, 172: 1-12.

Cauwet G. HYCO. 1994. Method for dissolved organic carbon analysis in sea water: influence of catalyst on blank estimation. *Mar Chem.*, 47:55-64.

Cloern J.E. 1999. The relative importance of light and nutrient limitation of phytoplankton growth: a simple index of coastal ecosystem sensitivity to nutrient enrichment. *Aquatic Ecology* 33: 3-16.

Cole J., Findlay S., Pace M.L. 1988. Bacterial production in fresh and saltwater ecosystems: a cross-system overview. *Mar. Ecol. Prog. Ser.*, 43: 1-10.

Degobbi D., Gilmartin M., Orio A.A. 1986. The relation of nutrient regeneration in the sediments of the Northern Adriatic to eutrophication, with special reference to the Lagoon of Venice. *Sci. Tot. Environ.*, 56: 201-210.

del Gioglio P., Cole J., Cimblaris A. 1997. Respiration in bacteria exceed plankton production in unproductive aquatic systems. *Nature*, 385: 148-151.

Fuhrman J.A., Azam F. 1982. Thymidine incorporation as a measure of heterotrophic bacterioplankton production in marine surface waters: evaluation and field results. *Mar. Biol.* 66: 109-120.

Gaedke U., Kamjunke N. 2006. Structural and functional properties of low- and high-diversity planktonic food webs. *J. Plankton Res.*, 28 (7): 707-718.

Giordani G., Viaroli P., Swaney D.P., Murray C.N., Zaldivar J.M., Marshall Crossland J.I. 2005. Nutrient fluxes in the transitional zones of the Italian coasts. LOICZ Reports and studies No. 28: ii+157 pp. LOCZ, Texel, The Netherlands.

Grasshoff K., Cremling K., Erhardt M. (eds). 1983. Methods of seawater analysis, Wiley-VCH Verlag.

Harris J., Stutt E., Turley C. 2001. Carbon flux in the Northwest Mediterranean estimated from microbial production. *Deep Sea Res. Part I*, 48: 2631-2644.

Holm-Hansen O., Lorenzen C.J., Holmes R.W., Strickland J.D.H. 1965. Fluorimetric determination of chlorophyll. *J. Cons. perm. int. Explor. Mer*, 30: 3-15.

Hoppe H.G. 1993. Use of fluorogenic model substrates for extracellular enzyme activity (EEA) measurement of bacteria. In: Kemp P.F., Sherr B.F., Sherr E.B., Cole J.J. (eds). *Current methods in aquatic microbial ecology*. CRC Press; Boca Raton, pp 423-431.

Iriarte A., de Madariaga I., Diez-Garagarza F., Revilla M, Orive E. 1996. Primary production, respiration and nitrification in a shallow temperate estuary during summer. *J. Exp. Mar. Biol. Ecol.* 208: 127-151.

- Jensen L.M., San-Jensen K., Marcher S., Hansen M. 1990. Plankton community respiration along a nutrient gradient in a shallow Danish estuary. *Mar. Ecol. Prog. Ser.*, 61: 75-85.
- Johnson K., Sieburth J. MCN. 1977. Dissolved carbohydrates in seawater. A precise spectrophotometric analysis for monosaccharide. *Mar Chem* 197; 5: 1-13.
- Kemp W.M., Smith E.M., Marvin-Di Pasquale M., Boynton W.R. 1997. Organic carbon balance and net ecosystem metabolism in Chesapeake Bay. *Mar. Ecol. Prog. Ser.*, 150: 229-248.
- Kirchman D., K'nees E., Hodson R. 1985. Leucine incorporation and its potential as a measure of protein synthesis by bacteria in natural waters. *Appl. Environ. Microbiol.*, 49: 599-607.
- Lee S., Fuhrman J.A. 1987. Relationship between biovolume and biomass of naturally delivered marine bacterioplankton. *Appl. Environ. Microbiol.* 53: 1298-1303.
- Maie N., Jaffe´ R., Miyoshi T., Childers D. L. 2006. Quantitative and qualitative aspects of dissolved organic carbon leached from senescent plants in an oligotrophic wetland. *Biogeochem.*) 78: 285–314.
- Marcomini A., Pojana G., Giacometti A., Oppo C. ANNO Aerosolization of an anionic surfactant (LAS) and dissolved organic carbon (DOC) under laboratory conditions. *Chemosphere*, 44: 257-262.
- Nieuwenhuize J., Maas E. M. Middelburg J. J. 1994. Rapid analysis of organic carbon and nitrogen in particulate materials. *Mar. Chem.*, 45: 217-224.
- Norrman B., Wweifel U.L., Opkinson Jr C.S., Fry B. 1995. Production and utilization of dissolved organic carbon during an experimental diatom bloom. *Limnol. Oceanogr.*, 40: 898-907.
- Platt T. 1971. The annual production of phytoplankton in St. Margaret's Bay, Nova Scotia. *J. Cons. Explor. Mer.*, 33: 324-333.
- Porter K.G., Feig Y.S. 1980. The use of DAPI for identifying and counting aquatic microflora. *Limnol. Oceanogr.* 25: 943-948.
- Sfriso A., Facca C. 2007. Distribution and production of macrophytes and phytoplankton in the lagoon of Venice: comparison of actual and past situation. *Hydrobiologia* 577: 71-85.
- Sfriso A., Facca C., Ceoldo S., Marcomini A. 2005. Recording the occurrence of trophic level changes in the lagoon of Venice over the '90s. *Environ. Internat.* 31: 993-1001.
- Sorokin Yu. I., Sorokin P.Yu., Giovanardi O., Dalla Venezia L. 1996. Study of the ecosystem of the lagoon of Venice with emphasis on anthropogenic impact. *Mar. Ecol. Prog. Ser.*, 141: 247-261.
- Sorokin P. Yu., Sorokin Yu. I., Zakuskina O. Yu. and Ravagnan G.-P. 2002. On the changing ecology of Venice lagoon. *Hydrobiologia*, 487: 1-18.

Steeman-Nielsen E. 1952. The use of radioactive carbon (^{14}C) for measuring organic production in the sea. *J. Cons. Explor. Mer.*, 18: 117-140.

Thomas C., Cauwet G., Minster J.F. 1995. Dissolved organic carbon in the Equatorial Atlantic Ocean. *Mar Chem.*, 49 : 155-169.

Vatova A., 1960. Primary production in the High Venice Lagoon. *J. Cons.*, 26: 148-155.

Vodacek A., Blough N.V., DeGrandpre M.D., Peltzer E.T., Nelson R.K. 1997. Seasonal variation of CDOM and DOC in the Middle Atlantic Bight: terrestrial inputs and photooxidation. *Limnol. Oceanog.*, 42: 674–686.

Wang X.-C., Litz L. Chen R. F.,Huang W. ,Feng P., Altabet M. A. 2007. Release of dissolved organic matter during oxic and anoxic decomposition of salt marsh cordgrass. *Marine Chemistry* 105: 309-321.

Ziegler S. and Benner R. 1999. Dissolved organic carbon cycling in a subtropical seagrass-dominated lagoon. *Mar. Ecol. Prog. Ser.* 180: 149–160.

DIMENSIONAL STRUCTURE OF PHYTOPLANKTON COMMUNITY IN THE VENICE LAGOON

Joan Coppola, Fabrizio Bernardi Aubry, Francesco Acri, Franco Bianchi,
Alessandra Pugnetti

C.N.R. ISMAR Istituto di Scienze Marine – Sede di Venezia, Castello 1364/A, I-30122

Riassunto

In questo lavoro, svolto nell'ambito del II Programma di Ricerca CORILA 2004-2006 (Linea 3.12), sono state indagate le variazioni spaziali e temporali delle differenti frazioni dimensionali del fitoplancton (pico-, nano- e microfitoplancton), al fine di studiarne il contributo relativo in termini di biomassa e di abbondanza, anche in relazione ai principali parametri idrologici e di stato trofico. I campionamenti sono stati effettuati nel 2005, a cadenza mensile, in quattro stazioni della Laguna di Venezia caratterizzate da un differente grado di trofia e confinamento. La biomassa fitoplanctonica presenta i valori più elevati in primavera ed estate, in tutte le stazioni. Per tutto l'anno domina la frazione nanoplanctonica, seguita da quella microfitoplanctonica, mentre il contributo della frazione picoplanctonica, è consistente solo nel periodo tardo-estivo, soprattutto nella stazione della bocca di porto di Lido.

Abstract

In the framework of the CORILA Research Programme 2004-2006, Line 3.12, the size distribution of the phytoplankton community and the relative contribution of the different size fraction (pico-, nano- and microphytoplankton) to total biomass and abundance has been analyzed in relation with the main hydrologic and trophic parameters. Samples were collected monthly during 2005, at four stations characterized by different trophic conditions. Phytoplankton biomass presents highest values in spring and summer at every station. Nanoplankton and, to a lesser extent, microphytoplankton prevail throughout the year, whereas picophytoplankton becomes important in late summer, mainly at the most marine station (Lido).

1 Introduction

The size distribution within the phytoplankton community plays an essential role in determining the direction and the magnitude of biogenic carbon and energy fluxes in aquatic ecosystems (Bell and Kalff, 2001). In estuarine and coastal ecosystems of the temperate zone, the marked seasonal changes in light, temperature, nutrient inputs may lead to the coexistence and, sometimes, to the seasonal alternation of smaller and larger algae, with important implications for the structure of the prevailing trophic webs (Riegmann *et al.*, 1993).

In the Lagoon of Venice the information on larger fraction of the phytoplankton community ($> 5 \mu\text{m}$) is available since the '60s. The seasonal cycle of the phytoplankton has been described in the southern (Tolomio and Bullo, 2001), central (Socal *et al.*, 1999; Facca *et al.*, 2002) and northern basins (Voltolina, 1973; Bianchi *et al.*, 1999). The community is mainly made up by diatoms and nanoflagellates (chlorophyceae, cryptophyceae, prasinophyceae, crysophyceans, prymnesiophyceans) and it is characterized by the coexistence of pelagic and benthic forms (Socal *et al.*, 1985; 1987, Tolomio *et al.*, 1999; Facca *et al.*, 2002). On the contrary, only very few studies on the size distribution of the planktonic primary producers have been carried out (Sorokin *et al.* 1996; Sorokin *et al.* 2002, Coppola *et al.* 2006, Del Negro *et al.* 2006, Paoli *et al.* 2007).

The main aim of this study, carried out in the framework of the II CORILA Research Programme, 2004-2006, was: - to describe the temporal variations of the different phytoplankton size classes (pico-, nano- and microphytoplankton); - to evaluate the contribution of the different size classes to total phytoplankton biomass; - to correlate the phytoplankton size structure with the main hydrological and trophic state parameters.

2 Methods

The investigation was carried out at four sampling stations, located in the northern and central basins of the Lagoon of Venice (Fig. 1) and representative of the main characteristics of these areas (Bianchi *et al.*, 1996; 1999; Socal *et al.*, 1999).

At every station, measurements and samplings were carried out monthly from January to December 2005. Water and phytoplankton samples were taken at surface, at neap tide.

Transparency was measured by Secchi disk. Temperature, salinity, dissolved oxygen and pH were recorded by an Idronaut Ocean Seven 316 multiprobe and compared with the discrete measurements performed in the laboratory (Guildline Autosol 8400 B salinometer, Dosimat for Winkler titrations and pH meter). Nutrients (N-NH_3 , N-NO_2 , N-NO_3 , Si-SiO_4 , P-PO_4) were analyzed according to Hansen, H.P. e Koroleff, F., 1999

In order to estimate the autotrophic picoplankton ($0.2 - 2 \mu\text{m}$: APP) abundance, water samples were preserved with pre-filtered buffered formaldehyde and kept at 4°C . Duplicate slides were prepared from the samples by filtering 5-10 ml of water from each sample onto $0.2 \mu\text{m}$ pore size Nucleopore black membranes. The cell counts were made using a Zeiss Axiovert 35 microscope, equipped with a HBO 100 W light. A BP 450-490 exciter filter, an FT 510 chromatic beam splitter and an LP 520 barrier filter were used. At least 20 randomly selected fields, for each slide, were counted at a final X 1000 magnification. On average, about 400 cells were counted to determine abundance. Cell sizes of about 50% randomly selected individuals were measured by Image analysis, using Image Pro Express (Media Cybernetics). Most APP cells were coccoid or rod-shaped; therefore, in order to determine their carbon biomass, cell volume was

calculated by approximation to a sphere or to a rotation cylinder. For *Synechococcus*, dominant in this study, there are a number of published factors to convert biomass to carbon, ranging from 85 to 400 fg C μm^{-3} , and the actual values are supposed to be even higher (Li, 1986). We followed the indications by Tamigneaux et al., (1995) for coastal area and for cells of the same size of ours. The coefficients here applied were, therefore: 0.250 fg μm^{-3} , for *Synechococcus*, and 220 fg μm^{-3} , for eukariotes.

For autotrophic nanoplankton (2-20 μm) analyses, water samples were preserved with glutaraldehyde (10% final concentration) and stained with DAPI (Porter and Feig, 1980) at 1 $\mu\text{g ml}^{-1}$ of final concentration, and then duplicate slide were prepared from the samples by filtering 20 ml of water from each sample onto black pre-stained Nuclepore polycarbonate filters of 0.8 μm in pore size and 25 mm in diameter. The cell counts were made using a Zeiss Axiovert 35 microscope, equipped with a HBO 100 W light. A BP 450-490 exciter filter, an FT 510 chromatic beam splitter and an LP 520 barrier filter were used for autotrophic nanoplankton; a BP 365/12 exciter filter, an FT 395 chromatic beam splitter and an LP 397 barrier filter were used for heterotrophic nanoplankton. About 200 cells were observed by selecting a variable number of microscopic fields randomly. Cell size measurement was carried out individually and cell volume was calculated from a two-dimensional cell image by considering appropriate geometric forms. The resulting volumes were transformed into organic carbon values by using Edler (1979) conversion factors: $\text{pg C} = \mu\text{m}^3 \times 0.14$.

The samples of microphytoplankton (>20 μm) community were fixed with exametilentetramine-neutralized formaldehyde to a final concentration of 4% and examined with an inverted microscope Zeiss Axiovert 35, equipped with phase contrast (model Zeiss Axiovert 35), at a final X 400 magnification. Sub-samples from 5 to 50 ml were allowed to settle for 12-48 hours and examined (Utermöhl, 1958). A variable transect number was observed until at least 200 (but often more than 500) cells were counted for each sample (Zingone et al., 1990). Species composition was defined according to Tomas (1997). Cell size and volume of UFP were determined according to Strathmann (1967) and the phytoplankton carbon was obtained by multiplying cell or plasma volume by 0.11 for diatoms and coccolithophorids and by 0.13 for thecate dinoflagellates (Smetacek, 1975).

Statistical analyses (principal component analysis—PCA, one-way ANOVA and linear correlation analysis) were performed using Statistica by Statsoft, after log-transformation of biological data (Cassie, 1962).

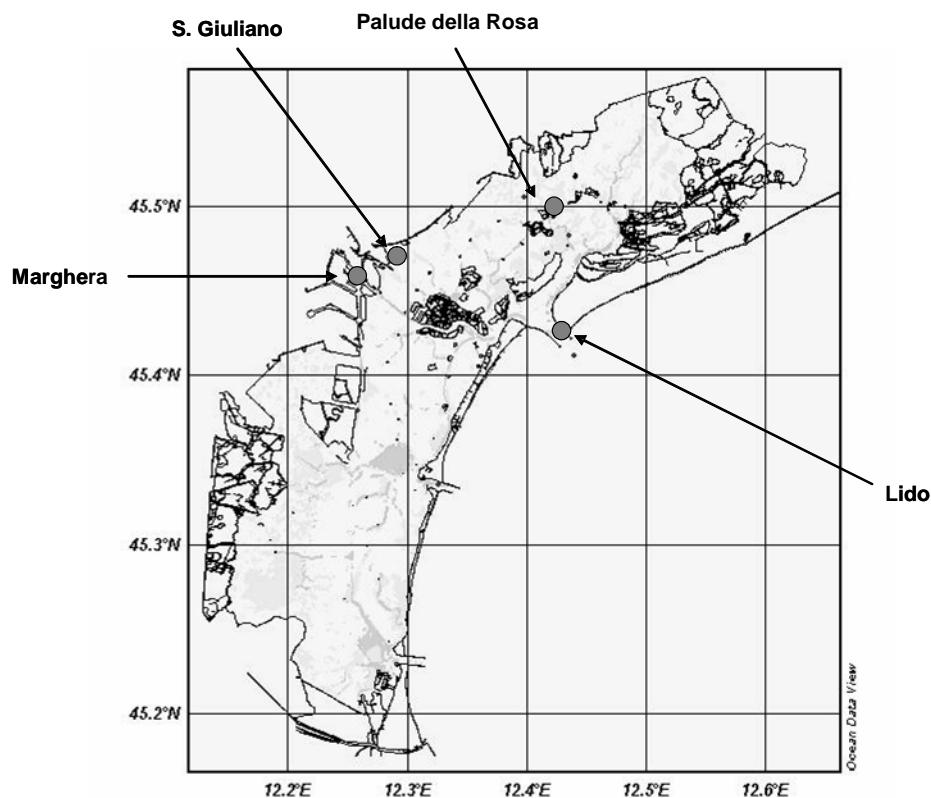


Fig 1 – The lagoon of Venice. Location of the four sampling stations.

3 Results

Considering the whole data set, the phytoplankton biomass, on the average, was dominated by nanoplankton ($69 \pm 19\%$), and followed by microphytoplankton ($27 \pm 19\%$) and picoplankton ($4 \pm 5\%$). The temporal variations of phytoplankton biomass (Fig. 2 and 6) were mainly driven by nano- and microphytoplankton, that showed the lowest values in winter ($14,2 \pm 3,2$ and $4,6 \pm 2,3 \mu\text{g C dm}^{-3}$ in January and November, respectively) and the highest in summer ($183,3 \pm 119,2$ and $52,3 \pm 62,2 \mu\text{g C dm}^{-3}$ in July, respectively); picophytoplankton attained the highest biomass in autumn ($5,9 \pm 7,4 \mu\text{g C dm}^{-3}$, in September).

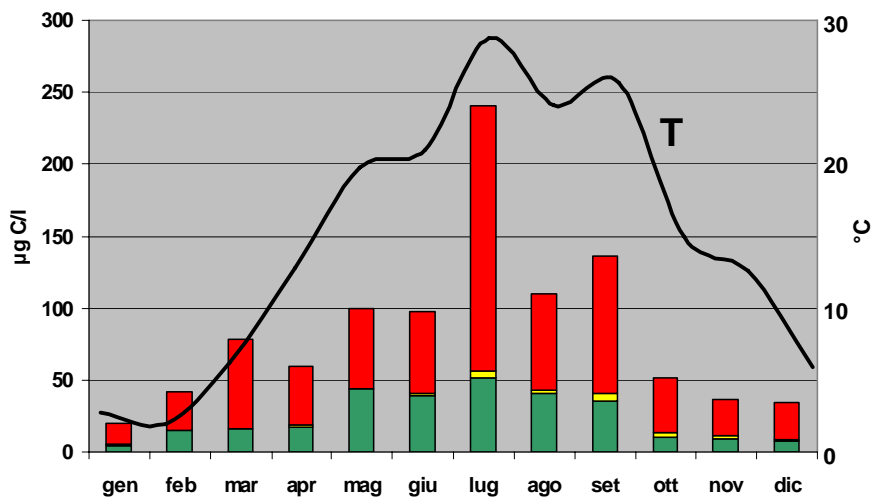


Fig 2 – Temporal variation of micro- (green), nano- (red) and picophytoplankton (yellow) plotted against mean water temperature.

On the average, the nanoplankton community was mainly made up by flagellates (chlorophyceae, cryptophyceae, prasinophyceae, crysophyceans, prymnesiophyceans), benthic diatoms re-suspended from the sediments (e.g. *Amphora*, *Navicula*, *Nitzschia*) and colonial pelagic diatoms (e.g. *Skeletonema*, *Thalassiosira*). Large pelagic (e.g. *Rhizosolenia* spp., *Pseudo-nitzschia* spp.) and benthic diatoms (e.g. *Cylindrotheca closterium*, *Pleurosigma* spp., *Melosira* spp.) were the main components of microphytoplankton. Picophytoplankton was mainly represented by *Synechococcus* spp.

In order to summarize the main environmental variables influencing the temporal and spatial variations of phytoplankton biomass, we applied to our data set the Principal Components Analysis (PCA). From the correlation matrix two components were extracted with eigenvalues greater than 1, explaining 68% of the total variance. The first principal component (40% of variance) is related to hydrological and trophic state variables (salinity, turbidity and inorganic nitrogen concentration); the second component (28% of variance) is related to temperature and nanophytoplankton biomass (Fig. 3).

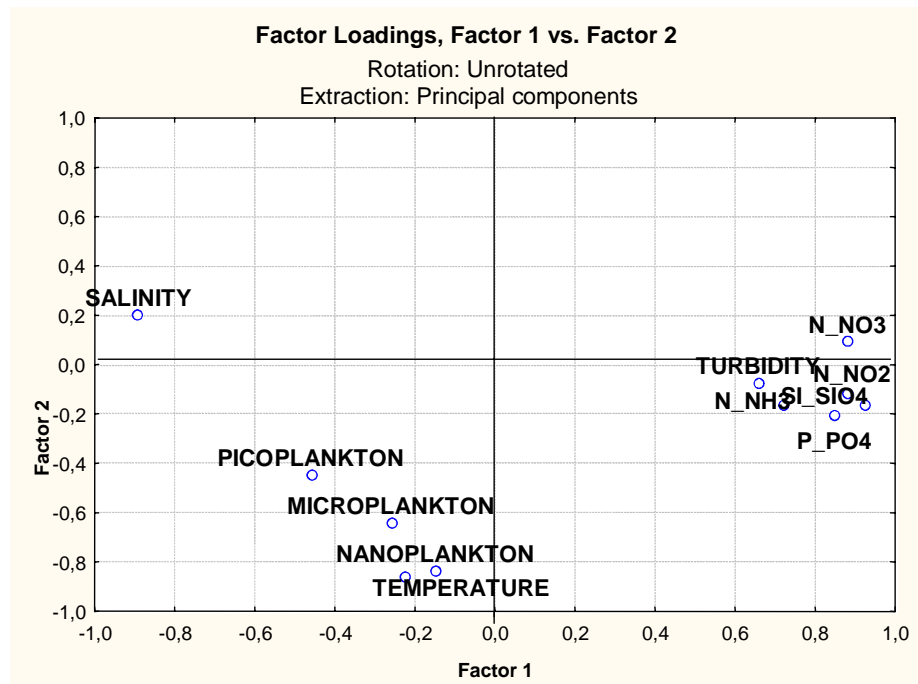


Fig 3 – Loadings of environmental variables on the first two Principal Components extracted (PCA).

Total phytoplankton biomass was significantly correlated with water temperature ($r= 0.61$; $p<0.01$; $N=48$). The inverse correlation with dissolved inorganic nitrogen (DIN) was significant only in summer ($T > 20$ C; $r = -0,42$; $p<0,01N = 29$), in correspondence with the phytoplankton biomass peaks. Only the picophytoplankton size fraction showed a weak, but significant, correlation with salinity ($r=0.27$; $p<0.05$; $N=48$) (Fig. 4). The highest picoplankton biomass was, indeed, observed at the most marine station (Lido, Fig. 5 and 6).

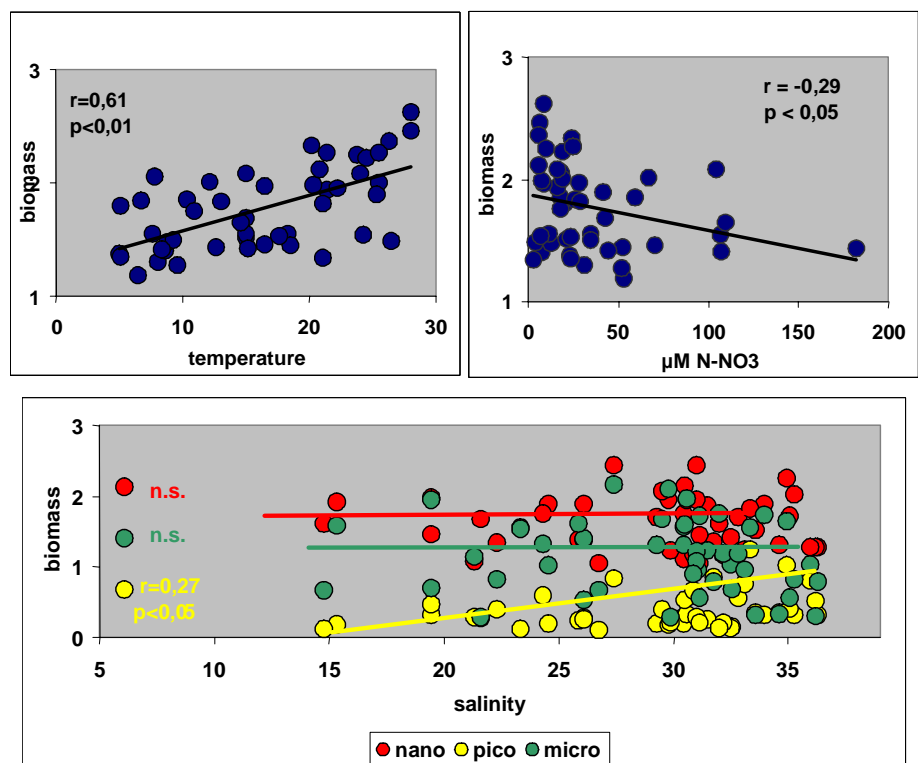


Fig 4 – Linear regression between phytoplankton biomass and temperature (left upper picture), DIN (right upper picture) and salinity (lower picture).

The other two size fractions (nano- and microphytoplankton), which made up the bulk of total biomass, do not appear influenced by salinity. Rather, they were related to the seasonal variation of temperature and photoperiod.

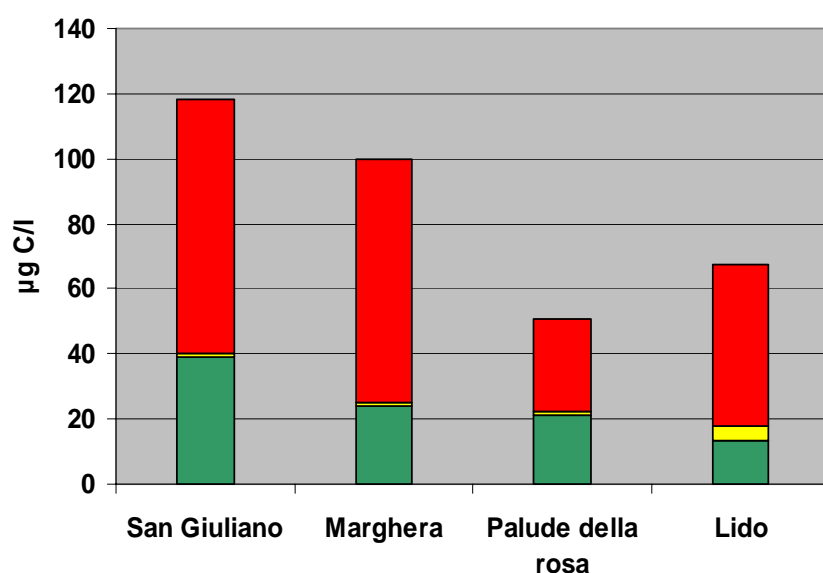


Fig 5 – Yearly average biomass of micro-(green), nano- (red) and pico-phytoplankton (yellow) at the four stations.

The highest mean phytoplankton biomass was recorded at San Giuliano ($119 \pm 110 \mu\text{g C dm}^{-3}$) and Marghera ($100 \pm 87 \mu\text{g C dm}^{-3}$). At both stations, on the average, nanophytoplankton clearly prevailed ($72 \pm 16\%$ and $76 \pm 15\%$, respectively), followed by microphytoplankton ($27 \pm 16\%$ and $22 \pm 15\%$); picoplankton contribution was quite low ($1 \pm 0,6\%$ and $2 \pm 1,5\%$). The lowest mean phytoplankton biomass was recorded at Palude della Rosa ($52 \pm 34 \mu\text{g C dm}^{-3}$) and Lido ($65 \pm 62 \mu\text{g C dm}^{-3}$). At these two stations the highest picophytoplankton contribution to total phytoplankton biomass was recorded ($4 \pm 4\%$ and $8 \pm 6\%$, respectively at Palude della Rosa and Lido). Nanoplankton dominated at Lido ($76 \pm 15\%$), while at Palude della Rosa microphytoplankton and nanophytoplankton showed a quite similar importance ($43 \pm 22\%$ and $54 \pm 21\%$, respectively).

The typical seasonal phytoplankton variations, characterized by two peaks at the end of winter and in summer (Socal *et al.*, 1985; Acri *et al.*, 2004), could not be evidenced in the present study (Fig. 6). Indeed, phytoplankton peaks occurred in July and September at San Giuliano, in March, July and September at Marghera and Lido, in February, June and September at Palude della Rosa.

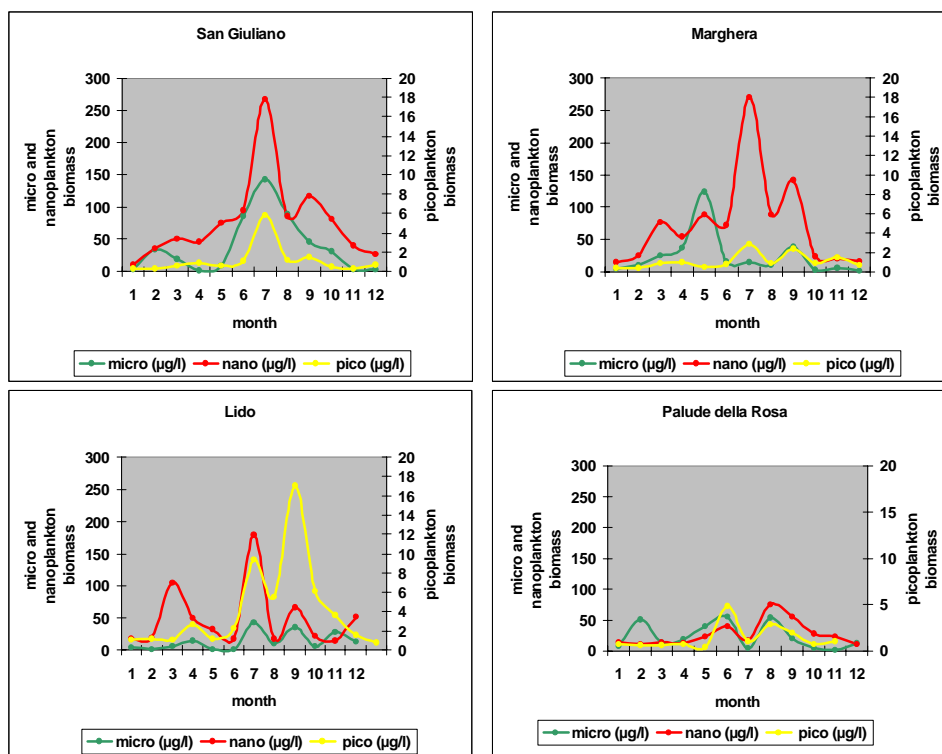


Fig 5 – Temporal variations of micro-, nano- e picophytoplankton at the four stations.

4 Concluding remarks

- The phytoplankton in the Venice Lagoon appear dominated by nanoplankton, in particular by the smallest nanoplankton fraction (nanoflagellates and small diatoms in the range 5-10 µm), followed by microphytoplankton (both large pelagic and benthic diatoms resuspended from the sediments).
- The lowest contribution to total biomass was determined by picophytoplankton; this fraction attains the highest importance (up to 20 % of total phytoplankton biomass) only at Lido, in autumn.
- The temporal pattern of phytoplankton biomass appears mainly driven by the seasonal variations of temperature and photoperiod, rather than by nutrients.
- Inorganic macronutrients generally do not appear to limit phytoplankton growth. Very likely, they allow and modulate the coexistence of the different phytoplankton size classes.

References

- Acri F., Bernardi Aubry F., Berton A., Boldrin A., Camatti E., Comaschi A., Rabitti S., Socal G., 2004. Plankton communities and nutrients in the Venice Lagoon. Comparison between current and old data. *Journal of Marine Systems*, 51: 321-329
- Bell T., Kalff J., 2001. The contribution of picophytoplankton in marine and

freshwater systems of different trophic status and depth. - *Limnol Oceanogr.* 46 (5): 1243-1248.

Bianchi F., Socal G., Alberighi L. and Cioce F. 1996. Cicli nictemerali dell'ossigeno disciolto nel bacino centrale della laguna di Venezia. *Biol. Mar. Medit.*, 3 (1), 628-630.

Bianchi F., Comaschi A. and Socal G. 1999. Ciclo annuale dei nutrienti, del materiale sospeso e del plancton nella laguna di Venezia. In: *Aspetti Ecologici e Naturalistici dei sistemi Lagunari e Costieri*, Arsenale Editrice, Venezia, 231-240.

Cassie R. M., 1962. Frequency distribution model in the ecology of plankton and other organisms. *Journal of Animal Ecology* 31, 65-92

Coppola J., Bernardi Aubry F., Acri F., Puggnetti A., Picophytoplankton contribution to phytoplankton community in the Venice lagoon. In: *Scientific Research and Safeguarding of Venice*, CORILA Research Programme 2001-2003, Volume III, 2003 results

Del Negro P., A. Puggnetti, F. Acri, A. Valeri, C. Larato, A. Beran, F. Bernardi Aubry, E. Camatti, Coppola, J., C. Facca, M. Giani, D. Berto, (2006). Ripartizione del carbonio nel comparto planctonico della laguna di Venezia. 5° Convegno Nazionale per le Scienze del Mare, Viareggio 14-18 Novembre 2006, pag. 31

Edler, L., 1979. Recommendations on Methods for Marine Biological Studies in the Baltic Sea. *Phytoplankton and Chlorophyll*, Vol. 5. BMB Publ., Lund, 38pp.

Facca, C. Sfriso, A. and Socal, G. 2002. Phytoplankton changes and relationships with microphytobenthos and physico-chemical variables in the central part of the Venice lagoon. *Estuarine Coastal Shelf Science* 54,5,773-792

Hansen H.P. e Koroleff F., 1999. Determination of nutrients. In Grasshoff K., Cremling K., Erhardt M. (eds), *Methods of seawater analysis*, Wiley-VCH Verlag: 159-228

Iriarte A., Purdie D. A., 1994. Size distribution of chlorophyll a biomass and primary production in a temperate estuary (Southampton Water): the contribution of photosynthetic phytoplankton. - *Mar. Ecol. Progr. Ser.*, 115: 283-297.

Li- W. K. 1986. Experimental approaches to field measurements: methods and interpretation. In: Platt T., Li W. K. (eds) *Photosynthetic picoplankton*. Can J. Fish. Aquatic Sci., Department of Fisheries and Oceans, Ottawa, p 251-286.

Murrel M.C., Lores E.M., 2004. Phytoplankton and zooplankton seasonal dynamics in a subtropical estuary: importance of cyanobacteria. - *J. Plankton Res.*, 26 (3): 371-382.

Paoli A., Celussi M., Valeri A., Larato C., Bussani A., Fonda Umani S., Vadrucci M. R., Mazziotti C., Del Negro P., 2007. Picocyanobacteria in Adriatic transitional environments. - *Estuarine, Coastal and Shelf Science* 75: 13-20.

Porter K. G. & Feig Y. S., 1980. The use of DAPI for identifying and counting

aquatic microflora. *Limnol. Oceanogr.*, 25(5): 943-948

Riegman R., Kuipers B. R., Noordeloos A.A.M., Witte H.J., 1993. Size-differential control of phytoplankton and the structure of plankton communities. - *Neth. J. Sea Res.*, 31 (3): 255-265.

Smetacek, V., 1975: Die Sukzession sed Phytoplankton der westlichen Kieler Butch. - PhD Thesis, Univ. Kiel.

Socal, G. Ghetti, L. Boldrin, A. and Bianchi. F. 1985. Ciclo annuale e diversità del fitoplancton nel porto canale di Malamocco. Laguna di Venezia. *Atti Ist. veneto Sci. Lett. Arti.* 143, 15-30

Socal, G., Bianchi, F., Comaschi, A. and Cioce, F., 1987. Spatial distribution of plankton communities along a salinity gradient in the Venice lagoon. *Archo Oceanogr. Limnol.* 21, 19-43.

Socal, G., Bianchi, F. and Alberighi, L., 1999. Effect of thermal pollution and nutrient discharges on a spring phytoplankton bloom in the industrial area of the lagoon of Venice. *Vie et milieu* 49, 19-31.

Sorokin Yu. I., Sorokin P.Yu., Giovanardi O. and Dalla Venezia L., 1996. Study of the ecosystem of the lagoon of Venice with emphasis on anthropogenic impact. *Marine Ecology Progress Series*, 141, 247-261.

Sorokin P. Yu., Sorokin Yu. I., Zakuskina O. Yu. and Ravagnan G.-P., 2002. On the changing ecology of Venice lagoon. *Hydrobiologia*, 487, 1-18.

Stratmann, R.R., 1967: Estimating the organic carbon content of phytoplankton from cell volume or plasma volume. - *Limnol. Oceanogr.*, 12: 411-418.

Tamigeaux E., Vasquez E., Mingelbier M., Klein B., Legendre L., 1995. Environmental control of phytoplankton assemblages in nearshore waters, with special emphasis on phototrophic ultraplankton. *J. Plankton Res.* 17: 1421-1447

Tolomio C., Moschin E., Moro I. and Andreoli C., 1999. Phytoplankton de la Lagune de Venise. I. Bassins nord et sud (avril 1988-mars 1889). *Vie et Milieu* 49,33-44.

Tolomio, C., Bullo, L., 2001. Prelievi giornalieri di fitoplancton in una stazione del bacino meridionale della laguna di Venezia; aprile 1993 - marzo 1994. *Boll. Museo Civ. St. nat. Venezia*, 52, 3-23.

Tomas, C. R., 1997. Identifying Marine Phytoplankton. Academic Press, Arcourt Brace & Company.

Utermöhl H., 1958: Zur Vervollkomnung der quantitativen Phytoplankten-Methodik. - *Mitt. Int. Ver. Limnol.*, 9:1-38.

Voltolina D., 1973. A phytoplankton bloom in the lagoon of Venice. *Archo Oceanogr. Limnol.* 18, 19-37.

Zingone A., G. Honsell D. Marino M. Montresor and G. Socal, 1990. Fitoplancton. - In: Innamorati M., Ferrari I., Marino D., Ribera D'Alcalà M., (Eds.) *Metodi nell'ecologia del plancton marino. Nova Thalassia*, 11: 183-198.

RESEARCH LINE 3.13

Meteo-oceanographic conditions and coastal zone water quality

POST-PROCESSING OF NUMERICAL MODEL OUTPUT THROUGH A NEURAL NETWORK

Marco Bajo¹, Georg Umgieser¹, Andrea Borghesan², Aleardo Zuliani¹

1 Istituto di Scienze Marine, CNR, Venezia,

2 Dipartimento di Matematica Applicata, Università di Venezia

Riassunto

Nel presente articolo si descrive una procedura di post-processing per il miglioramento dei risultati forniti dal modello idrodinamico SHYFEM per la previsione della marea a Venezia. La procedura, che utilizza una rete neurale, corregge il livello previsto in piattaforma "Acqua Alta" basandosi sui dati osservati il giorno precedente la previsione.

La rete è stata calibrata utilizzando i risultati degli anni 2003 e parte del 2004, l'ultimo periodo del 2004 è stato utilizzato per testare la previsione. La tecnica è promettente, ulteriori miglioramenti saranno possibili variando e aumentando i dati utilizzati e la struttura stessa della rete.

Abstract

A post-processing method of numerical model output based on neural networks has been developed. The numerical model forecasts the storm surge near Venice. The results of the operational simulations of the years 2003 and 2004 have been collected into a database and a neural network post-process algorithm has been applied. A first version of this procedure will be operational at the Venice municipality within the end of the year 2007.

1 Introduction

Since the end of 2002 a numerical model, named SHYFEM, runs daily at the Centre for sea level forecasting and flood warning (ICPSM) of the Venice municipality. It forecasts the hourly sea level at the "Acqua Alta" Platform near the Venice Lagoon for five days in advance.

The model has been validated and improved during the years. A first post-processing routine based on a MOS system [Kalnay, 2003] was implemented two years ago to correct the sea level forecast in the "Acqua Alta" platform, near Venice [Bajo *et al.*, 2007]. Since the results were promising a more complex post-processing procedure based on a neural network (NN) has been developed.

The network is calibrated with observed data and for the moment accepts 51 input data, but can be adapted to accept other input variables correlated with the forecast surge. The procedure is not yet operative and in this paper it is tested for three different lead times.

2 Methods

2.1 The SHYFEM numerical model

The hydrodynamic model used, named SHYFEM, was developed at CNR-ISMAR in Venice. The code is freely downloadable from the web page: www.ve.ismar.cnr.it/shyfem.

The SHYFEM model solves the following vertically integrated shallow-water equations:

$$\begin{aligned} \frac{\partial U}{\partial t} - fV + gH \frac{\partial}{\partial x} \left(\zeta + \frac{p}{\rho_0 g} \right) - A_H \left(\frac{\partial^2 U}{\partial x^2} + \frac{\partial^2 U}{\partial y^2} \right) - \frac{1}{\rho_0} (\tau_{sx} - \tau_{bx}) &= 0 \\ \frac{\partial V}{\partial t} + fU + gH \frac{\partial}{\partial y} \left(\zeta + \frac{p}{\rho_0 g} \right) - A_H \left(\frac{\partial^2 V}{\partial x^2} + \frac{\partial^2 V}{\partial y^2} \right) - \frac{1}{\rho_0} (\tau_{sy} - \tau_{by}) &= 0 \\ \frac{\partial \zeta}{\partial t} + \frac{\partial U}{\partial x} + \frac{\partial V}{\partial y} &= 0 \end{aligned} \quad (1)$$

where ζ is the water level, U and V the vertically-integrated velocities (total or barotropic transports), t the time, g is the gravitational acceleration, p the atmospheric pressure at the mean sea level, ρ_0 is the water density, $H = h + \zeta$ the total water depth, h the undisturbed water depth, f the variable Coriolis parameter, τ_s is the wind stress, τ_b is the bottom stress, A_H is the horizontal diffusion coefficient.

The model uses finite elements for spatial integration and a semi-implicit algorithm for integration in time. The terms treated semi implicitly are the water level gradients and the Coriolis term in the momentum equations and the divergence term in the continuity equation, the bottom friction term is treated fully implicitly. All other terms are treated explicitly.

The model domain is reproduced by means of a staggered finite element grid made up of 18,626 triangular elements varying in size and shape and covers the whole Mediterranean Sea. The grid elements describing the Adriatic Sea vary in size between 1.5 and 10 km, whereas in the Mediterranean region the spatial resolution is less than 35 km (Fig. 1).

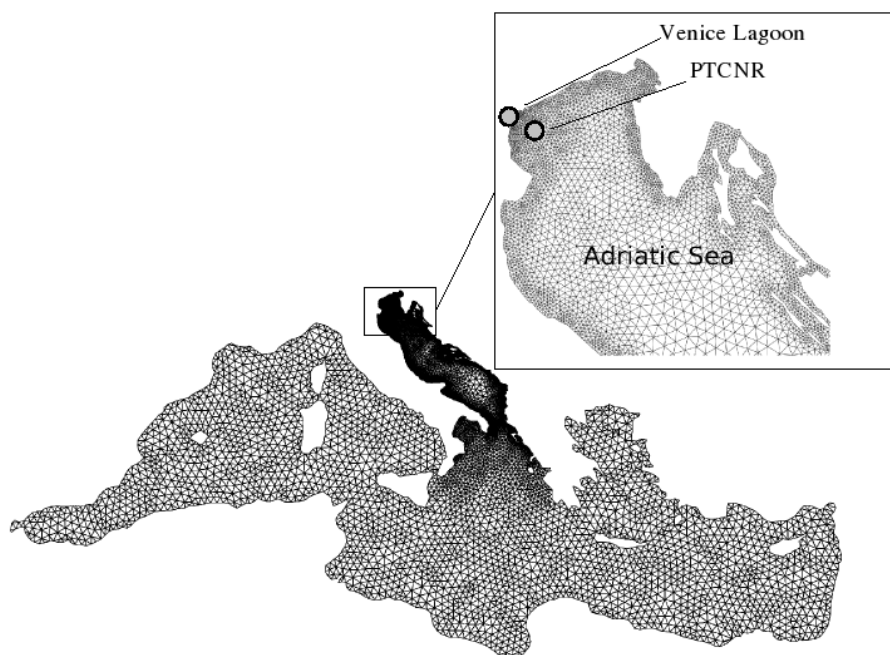


Fig 1 – Grid of the Mediterranean Sea used by the operational model. The grey dots mark the Venice Lagoon and the CNR oceanographic platform, “Acqua Alta” (PTCNR).

At the closed boundaries only the normal velocity is set to zero and the tangential velocity is a free parameter. This corresponds to a full slip condition. At the open boundary in the Gibraltar Straits, a water level equal to zero is imposed, since it is unknown.

Wind and atmospheric pressure data used by the model are provided by the European Centre for Medium-Range Weather Forecasts (ECMWF). The Centre supplies mean sea level pressure and surface wind fields over the Mediterranean area, at synoptic hours 00, 06, 12, 18 UTC, with a resolution of 0.5 degree both in latitude and longitude. Only the storm surge component is computed by the dynamic model, since it is independent by the astronomical component [Lionello *et al.*, 2006]. The total sea level is computed simply by adding the astronomical component, which is computed for the City of Venice by means of harmonic analysis [Defant, 1960; Polli, 1960; Istituto Idrografico della Marina, 2004].

3 The neural network model

The neural network model was created in 2001 [Borghesan and Zuliani, personal communication]. The first goal of the project was the simulation of the spread of a pollutant in the Venice inner canals [Zuliani *et al.*, 2006]. The model is a recursive neural network (Helman’s network) with a back propagation learning algorithm at one hidden layer [Sejnowsky *et al.*, 1988; Takeda *et al.*, 1986].

The code is written in Visual Basic, but has now been ported to Real Basic in order to have full compatibility with the SHYFEM model that runs under Unix or Linux OS [Aho *et al.*, 1974].

4 Set up of the post-processing routine

4.1 Database structure

The SHYFEM model produces a daily time series with the sea level forecast at the CNR platform "Acqua Alta", near Venice.

These time series were collected for two years, 2003 and 2004, into many databases, one for each hour of forecast. The model gives forecasts from 1 to 134 hours in advance.

For each forecast hour yearly databases have been created, therefore 134 databases have been set up. The database of one hour of forecast is composed by about 300 records for each year (some data are missing) with 52 columns. The first column contains the observed surge level, S_i^o , given by the observed sea level minus the astronomic tide at time i . The second column contains the surge predicted by the model, S_i^m , at the same time, and the rest of the columns contain three different groups of data. The first group consists of model errors during the analysis period, DS_j , where j runs from the 1st to 24th hour of the analysis period (the day before the run):

$$DS_j = S_j^m - S_j^o \quad (2)$$

The second group consists of observed surge data during the analysis period, S_i^o , the third group consists of two values of forecast data one hour before and ahead, S_{i-1}^m , S_{i+1}^m , in order to have information about the right and left derivatives of the water level time series.

4.2 Set up of the neural network

Representing the NN algorithm with a functional F , the new forecast surge, S_i^* at time i is given by the following expression:

$$S_i^* = F(S_i^m, DS_1, \dots, DS_{24}, S_1^o, \dots, S_{24}^o, S_{i+1}^m, S_{i-1}^m) \quad (3)$$

The input variables have been previously introduced and are all present in the database from the second to the 52th column. The observed surge, S_i^o that is placed in the first column of the database is used during the training as the desired output to find the best weights for the network.

The last 100 records of the database have been used to test the network. In this case the observed values, S_i^o , are used to compute the differences $S_i^* - S_i^o$ and to compare them with the differences $S_i^m - S_i^o$.

5 Results and discussion

The post-processing procedure has been tested for the 24, 48 and 72 forecast hours. For each forecast hour different databases were used with the structure previously described. As expected, the skill of the network is higher for the first hours of forecast but remains good also for longer forecasts.

In Fig. 2 and 3 the dispersion diagrams for the 24th and 48th hours are reported. The width of the distributions is remarkably reduced by the use of the post-processing procedure. Moreover the maximum errors, very important in an operational model that has to give reliable predictions, are considerably lower.

In Tabs. 1 and 2 a quantitative analysis is made, with the mean values and standard deviations of the distributions of the differences $\Delta S = S^m - S^o$ for both the model forecast and the output of the neural network.

In Tab. 1 the values are related to the training period, with 440 records of the years 2003 and 2004. In Tab. 2 the values are related to the forecast period, with 100 records of the year 2004. The values are expressed in meters; to have an idea of the magnitude of these quantities consider that the surge in Venice is more than one meter only during very strong storm events.

The means and standard deviations get worse in forecast mode by respect to calibration, but they are considerably better than the values without the neural network post-processing. Particularly, the 72 hour forecast corrected with the neural network becomes better than the 24 hour forecast without NN correction. Note that in the forecast period the standard deviation of the 72th hour is smaller than the standard deviation of the 48th hour. This is probably due to a statistical fluctuation caused by the small number of records.

Conclusions

A post-processing procedure based on neural network has been successfully developed. The results obtained allow an improvement of the quality of the forecast. The procedure can be changed, other variables can be added, both in input and output, in order to look for better results. However the next objectives will be a calibration with more records and an operational version of the procedure here described within the end of 2007.

Acknowledgments

We would like to remember and thank Aleardo Zuliani for his great effort in developing the post-processing routine based on neural networks during his grave illness and up until his death. This work has been partially funded under the Corila project 3.13 *Condizioni meteo-oceanografiche e qualità delle acque della zona costiera* and the Vector 5.2 CLIVEN project *Idrodinamica e Climatologia*.

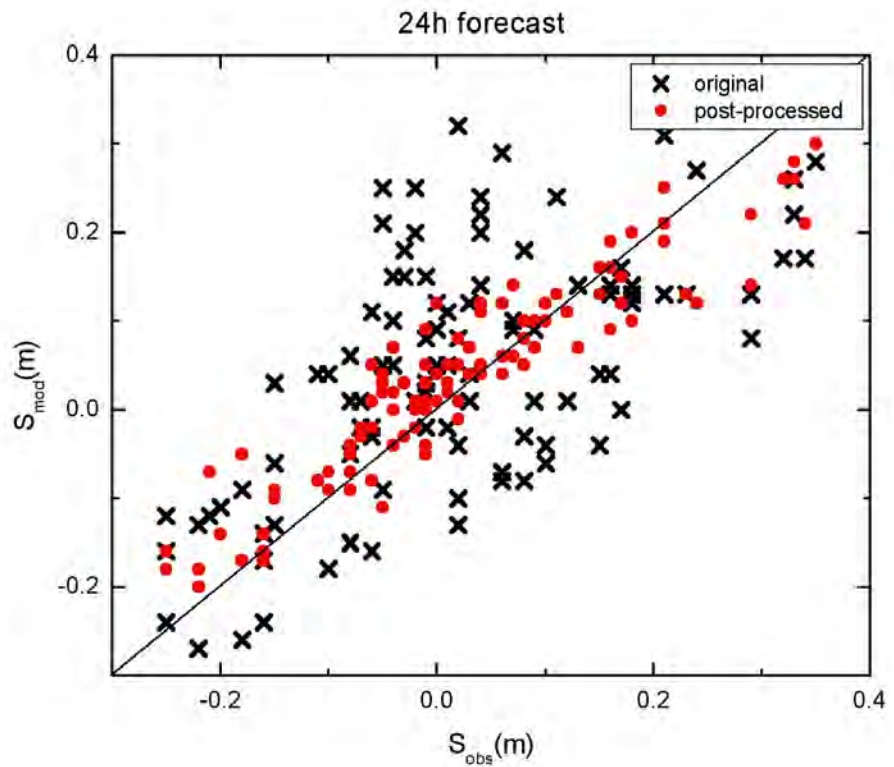


Fig 2 – Dispersion diagram of 24h forecast surge by respect observed surge. Two distributions are plotted: the original model data (cross) and those obtained by the neural network use (dot).

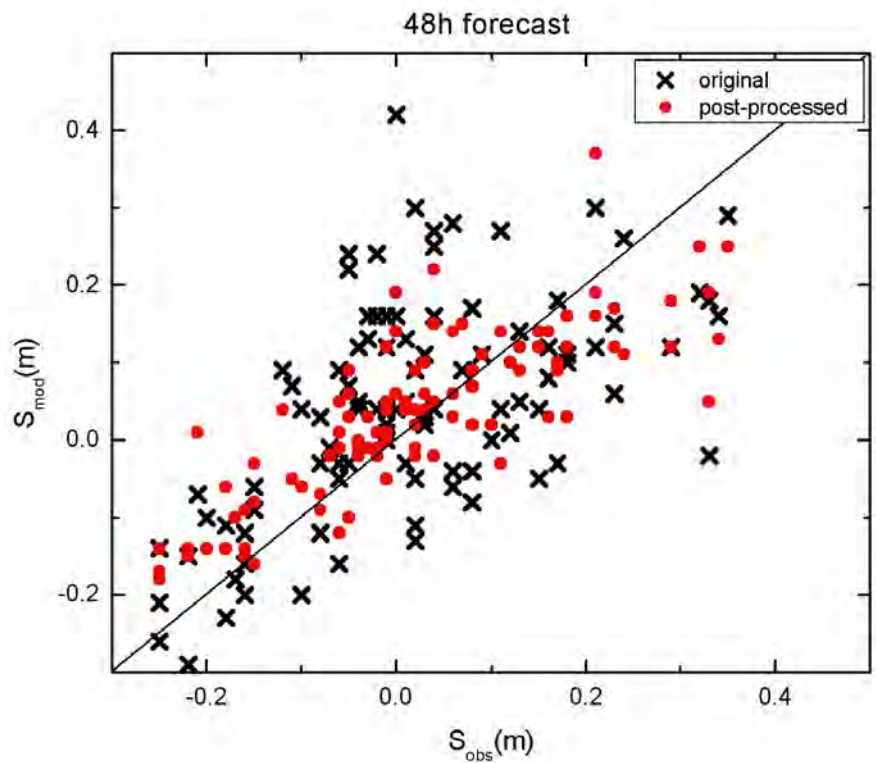


Fig 3 – Dispersion diagram of 48h forecast surge by respect observed surge. Two distributions are plotted: the original model data (cross) and those obtained by the neural network use (dot).

Model Version	Mean (ΔS_{24h})	σ (ΔS_{24h})	Mean (ΔS_{48h})	σ (ΔS_{48h})	Mean (ΔS_{72h})	σ (ΔS_{72h})
Original	-0.0107	0.105	-0.0134	0.109	-0.0165	0.120
NN	0.0002	0.054	0.0001	0.072	0.0001	0.084

Tab 1 – Training period. Means and standard deviations of the distributions of the differences for three different forecast hours: 24, 48 and 72. All Values are expressed in meters.

Model Version	Mean (ΔS_{24h})	σ (ΔS_{24h})	Mean (ΔS_{48h})	σ (ΔS_{48h})	Mean (ΔS_{72h})	σ (ΔS_{72h})
Original	0.0281	0.121	0.0297	0.140	0.0141	0.134
NN	0.0148	0.053	0.0130	0.085	0.0362	0.087

Tab 2 – Forecast period. Means and standard deviations of the distributions of the differences for three different forecast hours: 24, 48 and 72. All Values are expressed in meters.

References

- Aho, A.V., Hopcroft, J.E., and Ullman, J.D., (1974) The Design and Analysis of Computer Algorithms, Addison-Wesley.
- Bajo, M., Zampato, L., Umgiesser, G., Cucco, A. and Canestrelli, P. (2007) A finite element operational model for the storm surge prediction in Venice. Estuarine, Coastal and Shelf Science 75 (1-2), pp. 236-249.
- Defant, A. (1960). Physical Oceanography, volume 2. Pergamon Press, New York.
- Istituto Idrografico della Marina (2004). Tavole di marea e delle correnti di marea. Genova.
- Kalnay, E., 2003. Atmospheric Modeling, Data Assimilation and Predictability, first ed. Cambridge University Press, Cambridge.
- Lionello, P., Sanna, A., Elvini, E., and Mufato, R. (2006). A data assimilation procedure for operational prediction of the storm surge in the northern Adriatic Sea. Continental Shelf Research, 26(4):539-553.
- Mitsuo, T., and Joseph, W.G. (1986) Neural networks for computation: number representations and programming complexity, Applied Optics, Vol. 25, Num. 18, 15, 3033-3046.
- Polli, S. (1960) La propagazione delle maree nell'Adriatico. Technical Report Pubbl. n. 370, Istituto Sperimentale Talassografico, Trieste.
- Sejnowsky, T.J. (1988) Neural Network Learning Algorithms, NATO ASI Series, Vol. F41, Springer-Verlag, Berlino.
- Zuliani, A., Zaggia, L., Baruffi, F., Borghesan, A., Todaro, R., (2006) Metodologia di misura della portata nel tratto terminale del fiume Piave, Technical Report, ISMAR-CNR, Venezia.

CURRENT STATE, SCALES OF VARIABILITY AND DECADAL TRENDS OF BIOGEOCHEMICAL PROPERTIES IN THE NORTHERN ADRIATIC SEA

Cosimo Solidoro¹, Mauro Bastianini², Vinko Bandelj¹, Raffaella Codermatz¹, Gianpiero Cossarini¹, Donata Melaku Canu¹, Stefano Salon¹, Elisa Ravagnan², Sebastiano Trevisani¹

*1 Dipartimento di Oceanografia, Istituto Nazionale di Oceanografia e di Geofisica
Sperimentale OGS,*

2 Istituto di Scienze del Mare, ISMAR- CNR, Venezia

Riassunto

In questo articolo sono presentati i principali risultati delle analisi statistiche e numeriche prodotte su un dataset che comprende dati sperimentali raccolti in molti progetti di ricerca oceanografica nel Nord Adriatico. Le osservazioni coprono la finestra temporale degli ultimi 30 anni e hanno permesso di ottenere una descrizione robusta dello stato presente e delle scale di variabilità spaziale e temporale di temperatura, salinità, concentrazione di nutrienti, ossigeno disciolto e clorofilla. L'analisi ha permesso inoltre di ricavare indicazioni sulle tendenze pluriennali delle variabili investigate. I risultati rappresentano un contributo alla caratterizzazione biogeochimica del Nord Adriatico e alla comprensione delle interazioni tra le zone a largo e le acque costiere (includendo anche la laguna di Venezia). Questo lavoro rappresenta inoltre un aggiornamento della climatologia del bacino, e rappresenta pertanto un importante termine di riferimento per l'identificazione di possibili anomalie e cambiamenti futuri.

Abstract

This paper illustrates selected major results of numerical analysis performed on a data set obtained by integrating experimental observations collected during many oceanographic research projects on the Northern Adriatic Sea. Observations cover last 30 years, and provide a robust base for assessment of present state and scales of variability for temperature, salinity, nutrients, dissolved oxygen and chlorophyll a. Indication on multiyear evolution are derived too. Results represent a contribution to the characterization of the waters of Northern Adriatic Sea, to the comprehension of interactions of these waters with coastal waters, including the Lagoon of Venice, and an updated climatology of the basin, which can be used as an important reference term for assessment of anomalous behavior and future changes.

1 Introduction

During the last decades, the northern Adriatic Sea has been the object of a number of research projects. These projects were typically funded by different agencies and performed by different people, in agreement with different motivations which driven the researches. Results covered different topics and scales, and originates a large body of oceanographic and ecological literature. However, papers devoted to synthesis and integration, in which results of different project are collated and integrated, and in which reanalysis of integrated data set are performed, are not very common. In particular, the last attempt to compile biogeochemical observation and compute a climatological description of this basin dates back to a decade ago, when Zavatarelli and coauthors (1998) derived a climatology for different area of the Adriatic Sea, including the northern part, by considering data from 1911 to 1991.

In the frame of the project "Climatologia e qualità delle acque costiere della regione veneto", funded by CORILA and endorsed by LOICZ as a relevant LOICZ project, we performed a similar tasks, but focusing only on then northern part of the Adriatic Sea, and starting from an update, and quality checked, data base. This choice, enable us to offer a more detailed, and hopefully accurate, description of this basin, which we believe can constitute an important reference term for future studies on this area.

2 The data set

The analysis focused on the area of the Adriatic Sea of latitude between 44°30' and 45°45', and of longitude between 12°13' and 13°56', that is the area north of the Valli of Comacchio and west of the Lagoon of Grado and Marano. We excluded by the data observation referring to the Gulf of Trieste, because there was too many of them, and by considering them we would have introduced a bias in the results. Also, we did not consider data referring to the coastal area, defined as 1 miles off the coast, since they are likely to be affected by a variety of processes which are not relevant for the pelagic environment, and their analysis would require the consideration of different spatial and temporal scale. In fact the analysis of the coastal data is the object of a separate paper.

The phase of data rescue enable us to produce a first data set including experimental observation covering most of the 20th century, back from 1991. However, the analysis of time distribution of data made evident that there are enough data only after 1970, and only after 1985 the density of observation somehow 'stabilizes' to an acceptable level of coverage, with around 200 observation per year (Fig.1). Therefore, we chose to focus on the last 20 years (from July 1986 to July 2006) for the analysis aimed to derive an estimate of current state of the system, and of considering last 30 years (by adding observations from 1976) for estimation of multidecadal trends. In this way we also restricted the analysis to data collected by scientific institutions in the frame of oceanographic projects ATOS, Alto Adriatico, PRISMA, Interreg II and Interreg III, a fact which gives more confidence on quality of the measures and comparability of observations.

The final data set is made of around 200000 records, referring to several hundreds monitoring stations and major biogeochemical parameters (temperature, salinity, nutrients, and dissolved oxygen). As it frequently observed in these cases, the number of experimental observation is higher in summer than in winter, and much higher for physical parameters acquired by probe than for biogeochemical ones (fig.2).

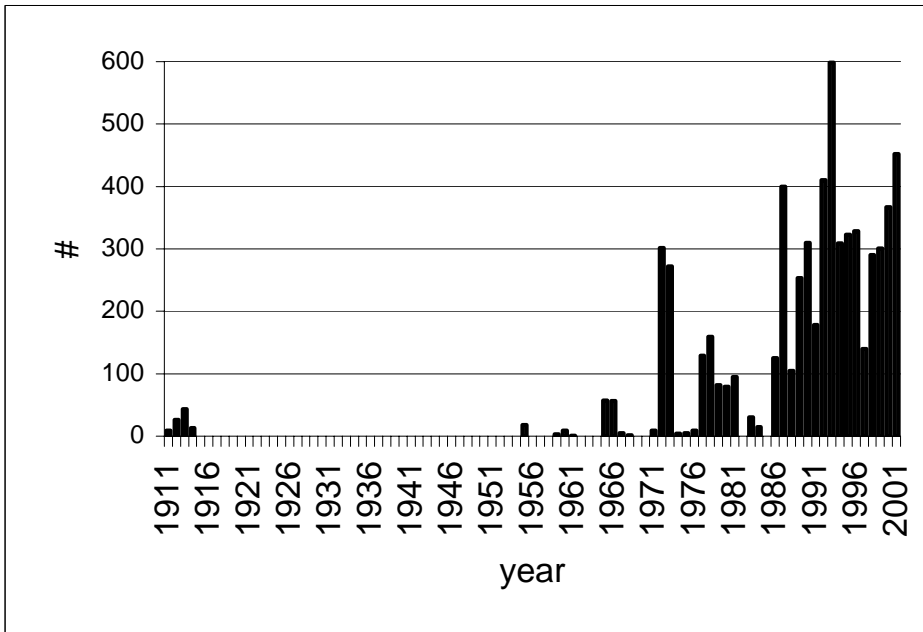


Fig 1 – Time distribution of data gathered in the project.

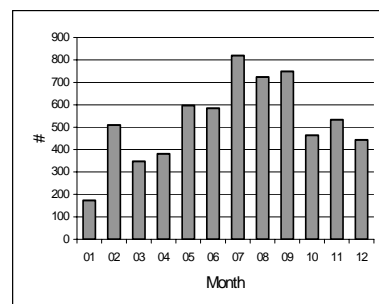
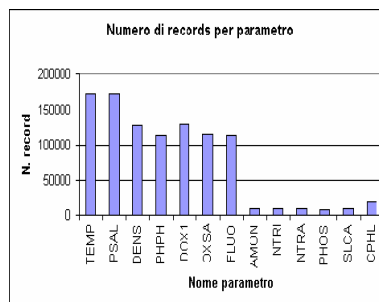
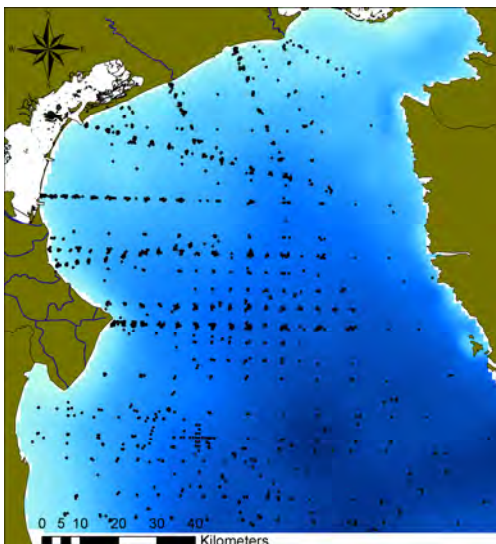


Fig 2 – Localization, time distribution and type of data considered in the analysis.

3 The northern Adriatic Sea

The Adriatic Sea is composed by three regional basins, differing for latitude, bathymetry, physiographic and physical-chemical-biological features. The northern basin presents peculiar characters because of the shallow depths, of the significant influence of major rivers along the Italian coast and of meteorological conditions, which force wind driven circulation and heat fluxes at the air water interface.

Several processes concur in defining physical properties of this sea. The outflow from Po and other major rivers give raise to southern coast current along the Italian coast and fuel and sustain the main cyclonic circulation -typical of all the Adriatic- which favors the ingression of Intermediate Levantine Waters along the Croatian coast. Topographic and bathymetric controlled processes interact with this picture, originating the transversal current along the 50 meter isobathic which somehow 'close' the northern basin. Wind driven circulation and convective motions caused by dense water formation add on the resulting circulation pattern, and define general features of dynamic field. Observed structure usually are more energetic in winter than in summer. Dominant winds are Sirocco (from south east), which pile up waters along the Italian coast, and Bora (from north-east) which might force a close cyclonic gyre in the northern part of the basin able to bring Po water up to the istrain coast and the Gulf of Trieste, and of decoupling the northern and central basin.

4 Present state and scales of variability

The assessment of present day typical values and scales of variability for biogeochemical properties has been made by subdividing the study area in 11 boxes, and computing for each box surface (0-5 meters) and bottom (20 meters) seasonal spatial distributions (maps), monthly evolution of surface and bottom parameter distribution, and seasonal evolution of vertical profiles. Results are resumed in 8 tables, one for each biogeochemical parameter: temperature, salinity, nutrients (nitrate, ammonia, phosphate, silicates), dissolved oxygen and chlorophyll a (figs 3 to 10).

Two alternative dividing of the basin were considered first, one made of a regular 20kmx20km grid, and the other one based on bathymetry and differences along the coast. Eventually, the analysis shows that the second subdivision was the best trade off among simplicity, accuracy, and data density for box (and therefore statistical robustness). More in detail, this subdivision considered the area deeper than 35 meters as a box (box 11), those between 30 and 35 meters as a two box (boxes 9 and 10), whereas area between zero and 20 meters and between 20 and 30 meters were partitioned in 4 sections each, basing on geographical features along the coast, that is the presence of the Po mouth (1 and 5), the presence of rivers Adige, Bacchiglione and Brenta (2 and 6), the presence of the lagoon of Venice (3 and 7), the presence of minor rivers north of the lagoon of Venice (4 and 8).

Spatial localization of boxes is illustrated in each of the tables which resume biogeochemical properties of the basin. the Box are depicted in all plates

describing biogeochemical properties of the area (figs 3 to 10)

Analysis of results confirm the presence of a clearly recognizable area influenced by coastal processes. This area runs along the coast, it is narrower in the northern part and more extended towards off-shore waters in correspondence of the Po river plume, and it is more marked in winter time. Along this area mean values and variability are higher. Others features are recognizable too, including the double gyre structure induced by bora winds in winter time, and the alternation of mixing and stratification processes along the water column depending on the combination of freshwater discharge (moment of the year and position in respect to river mouths), meteorological forcing (season) and dense water formation.

All this feature are described by the figure here proposed, and exactly quantified by tables available in the atlas produced during the project, which contain also the spatial reconstructions of all events, and an analysis of how different events, grouped by similarity in patterns, relate to external forcing.

Results represent a contribution to the characterization of the waters of Northern Adriatic Sea, and an updated climatology of the basin, which can be used as an important reference term form assessment of anomalous behavior and future changes.

5 Decadal trends

The 20 years data set has been enlarged, by including observation from the seventies, in order to test the existence of significant trends of variation in the physical and biogeochemical parameters. For this kind of analysis, in fact, the regularity in time distribution of observation is not crucial, while it is important to consider at least 30 years. Furthermore, since the results of the analysis performed on each of the boxes indicated that the abundance of data were not sufficient to guarantee significant results for each box, an aggregation of several boxes in macroareas has been performed, in order to increase reliability of the results. In this way, boxes 8,10 and 11, the farrest from the coast, define the area 'open water', while boxes 1 and 5, close to Po mouth merged into the 'Po' area. Boxes 2, 3 and 4, which are coastal –but representative of different reality- remained unmerged, and boxes 6,7 and 8, whose characteristic are intermediated were not considered , in order not to dilute the signals.

Then, we extracted surface and bottom data, and subdivided data of each area according with seasons, so to have – in the end- 8 homogenous data set for each area. Finally the existence of significant trend in each of this dataset has been tested by applying the Kendal-Tau-Sien test. This is a nonparametric test, which computes the slopes defined by all possible couples of data, and check if the median of the resulting distribution is significantly different from zero, and – in such a case- what is the value of the typical slope. In this way no assumption on the distribution of data is need, nor is required the assumption of any specific model for the interannual trend, as it is implicitly (and incorrectly) done when using linear regression for estimating interannual evolution.

Analysis of the results (table 1) evinces an increment in salinity, which might be interpreted as a consequence of both reduced outflows from rivers (higher salinity in coastal areas) and a more sustained ingression of Levantine water (higher salinity in 'open water' area). It is also possible to observe a clear reduction in concentrations of phosphate and ammonia in all coastal areas, both in winter and in summer, and at both depths, whereas concentration of silicates decreases only at the bottom. On the contrary no decrement is observed for concentration of nitrate, which actually tends to increase in some situations along the coast. The analysis performed on extreme values (observation higher than 75% of the data, that is on the magnitude of the maxima) confirmed this indication.

Remarkably, very little evidence supports the hypothesis of significant warming of northern Adriatic waters during the last 30 years. In particular, no significant trends are observed for the 'open water' area, neither at surface nor at bottom, but for a very modest and poorly significant ($p < 0.25$) decrement in surface summer water. A clearly significant signal is registered for summer bottom water in the coastal area south of the lagoon of Venice, and in surface winter water too. However, opposite indications –tough less significant- came from other coastal area, so that – globally- it is difficult to maintain that a clear significant signal can be confirmed.

References

Solidoro C., Bastianini, M. Bandelj V., Bellafiore D., Codermatz R., Cossarini G., Melaku Canu D., Ravagnan E., , Umgiesser G. , Vazzoler M.. 'Climatologia e qualità delle acque costiere della Regione Veneto'. Rapporto finale linea 3.13 programma di ricerca CORILA 2004-2006

Zavatarelli M, Raicich F, Bregant D., Russo A., Artegiani A. 1998 Climatological biogeochemical characteristics of the Adriatic Sea *Journal of Marine Systems* 18 1998 227–263

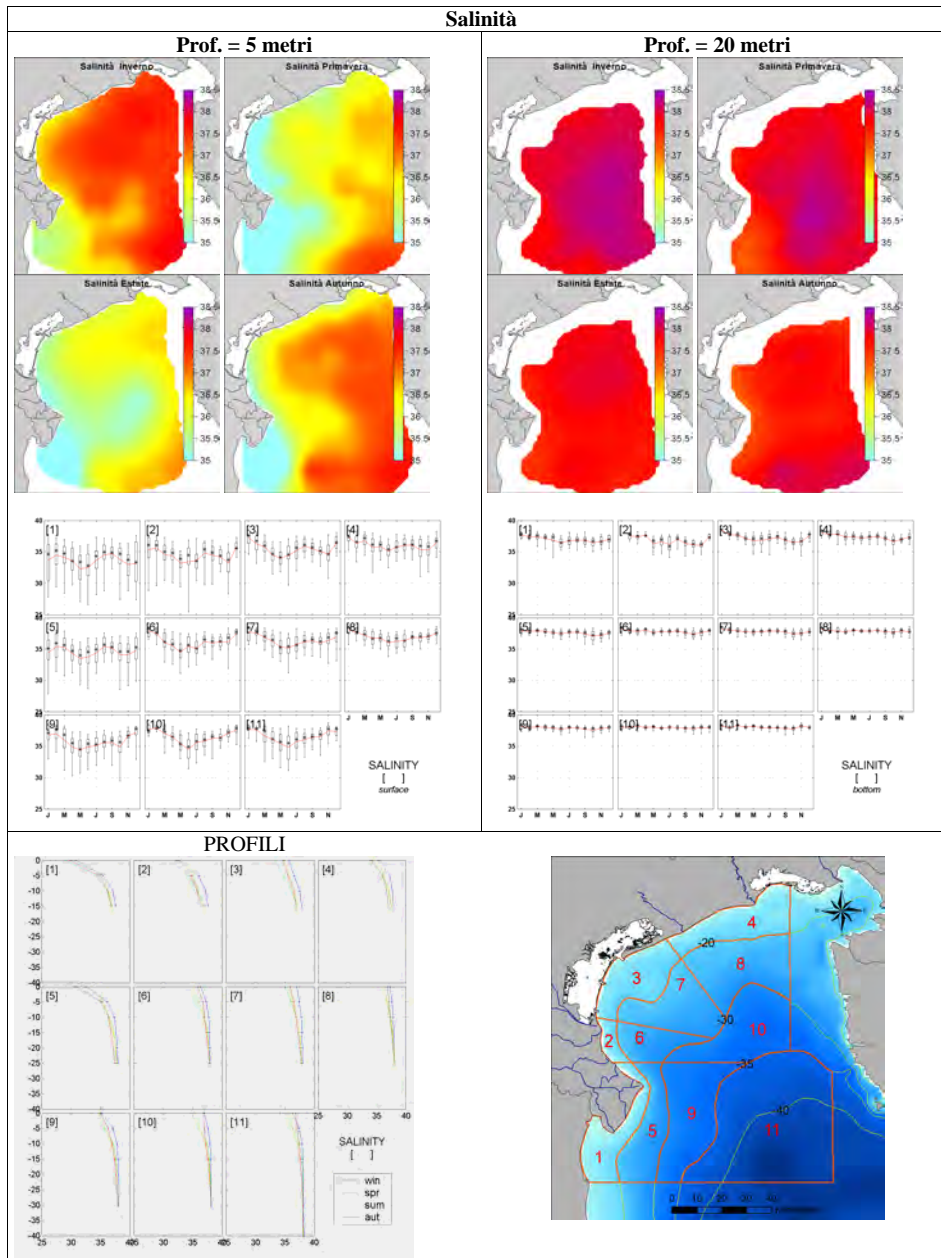


Fig 3 – Seasonal evolution and spatial distribution for biogeochemical properties: Salinity.

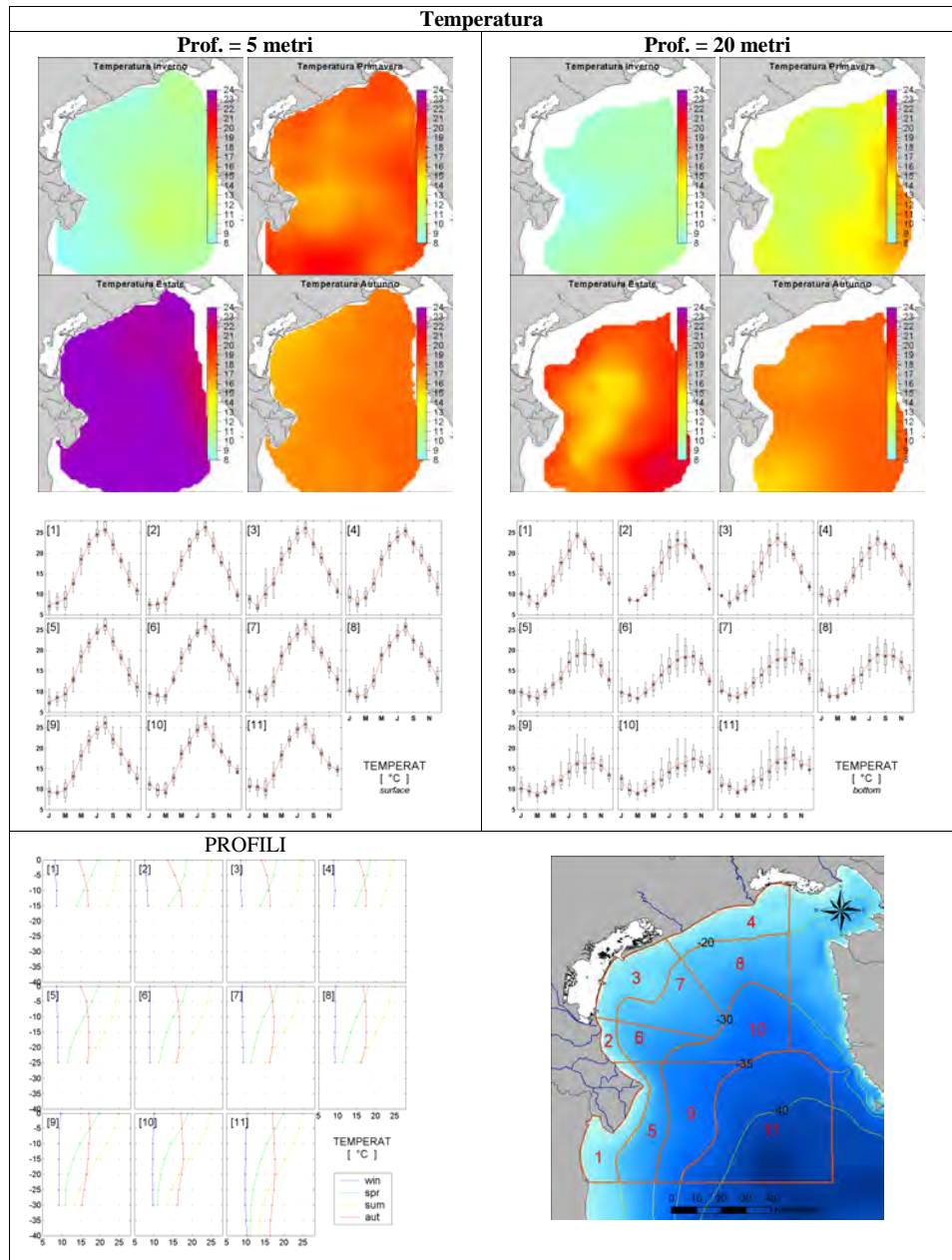


Fig 4 – Seasonal evolution and spatial distribution for biogeochemical properties: Temperature.

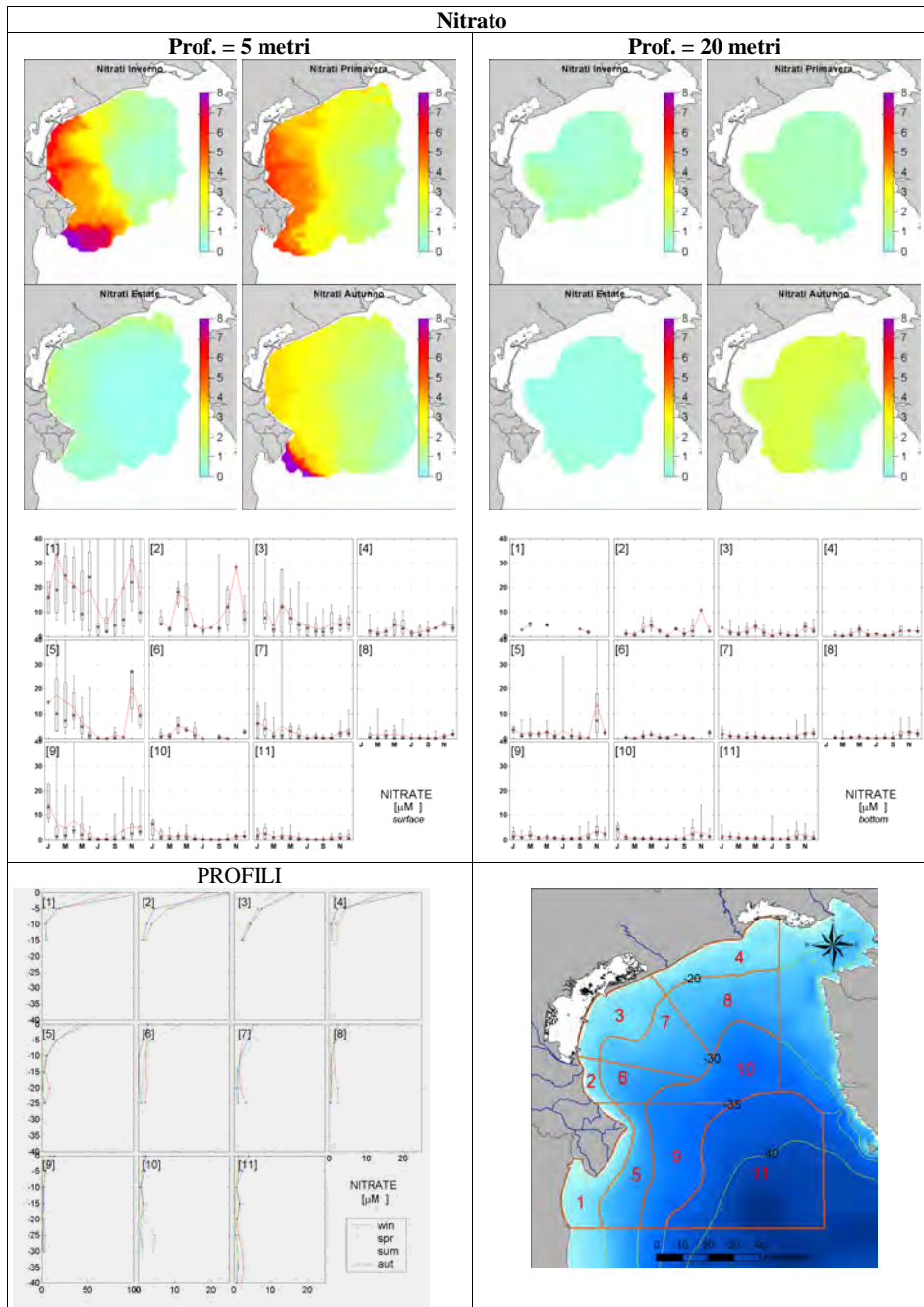


Fig 5 – Seasonal evolution and spatial distribution for biogeochemical properties: Nitrate.

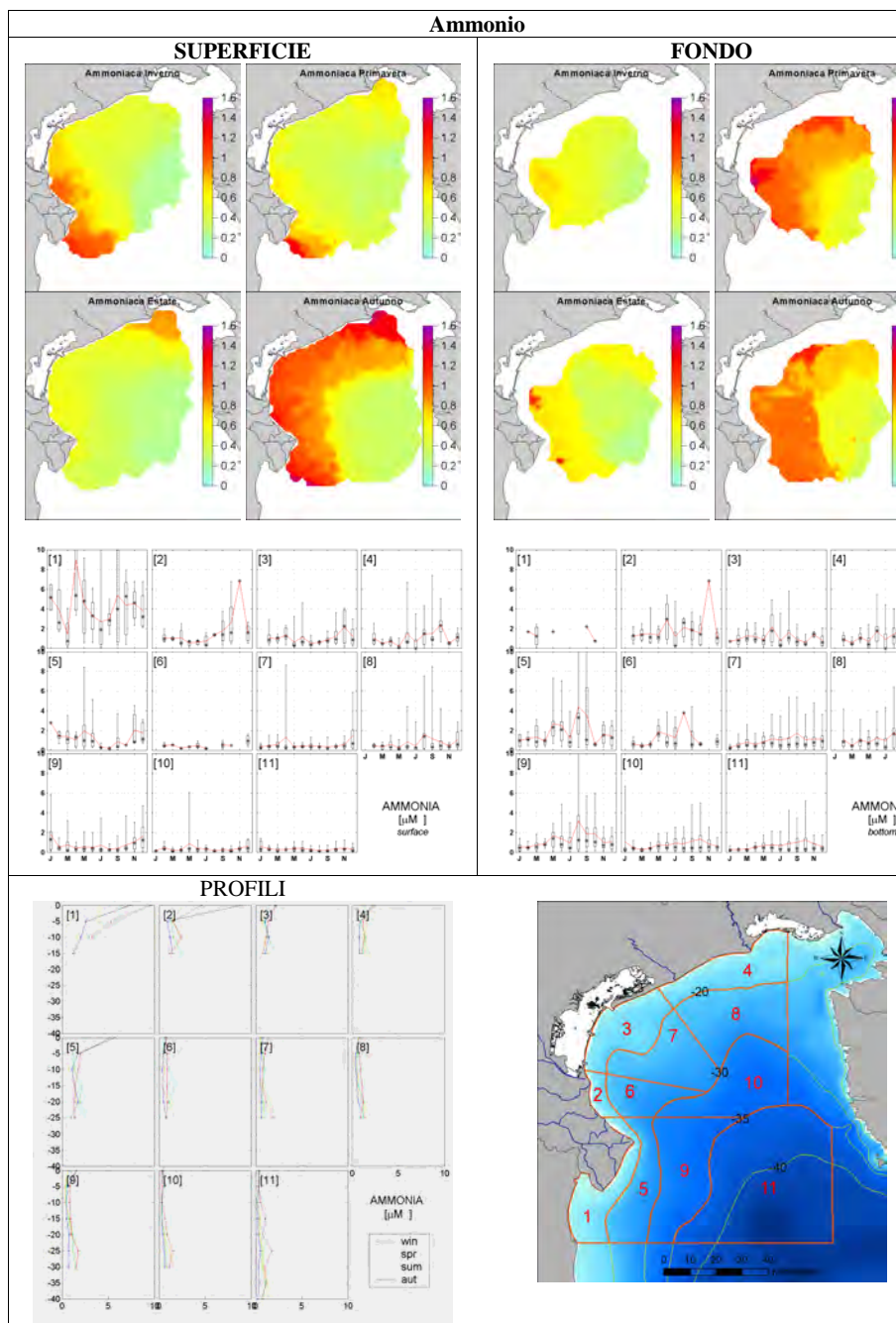


Fig 6 – Seasonal evolution and spatial distribution for biogeochemical properties: Ammonia.

. Fosfato

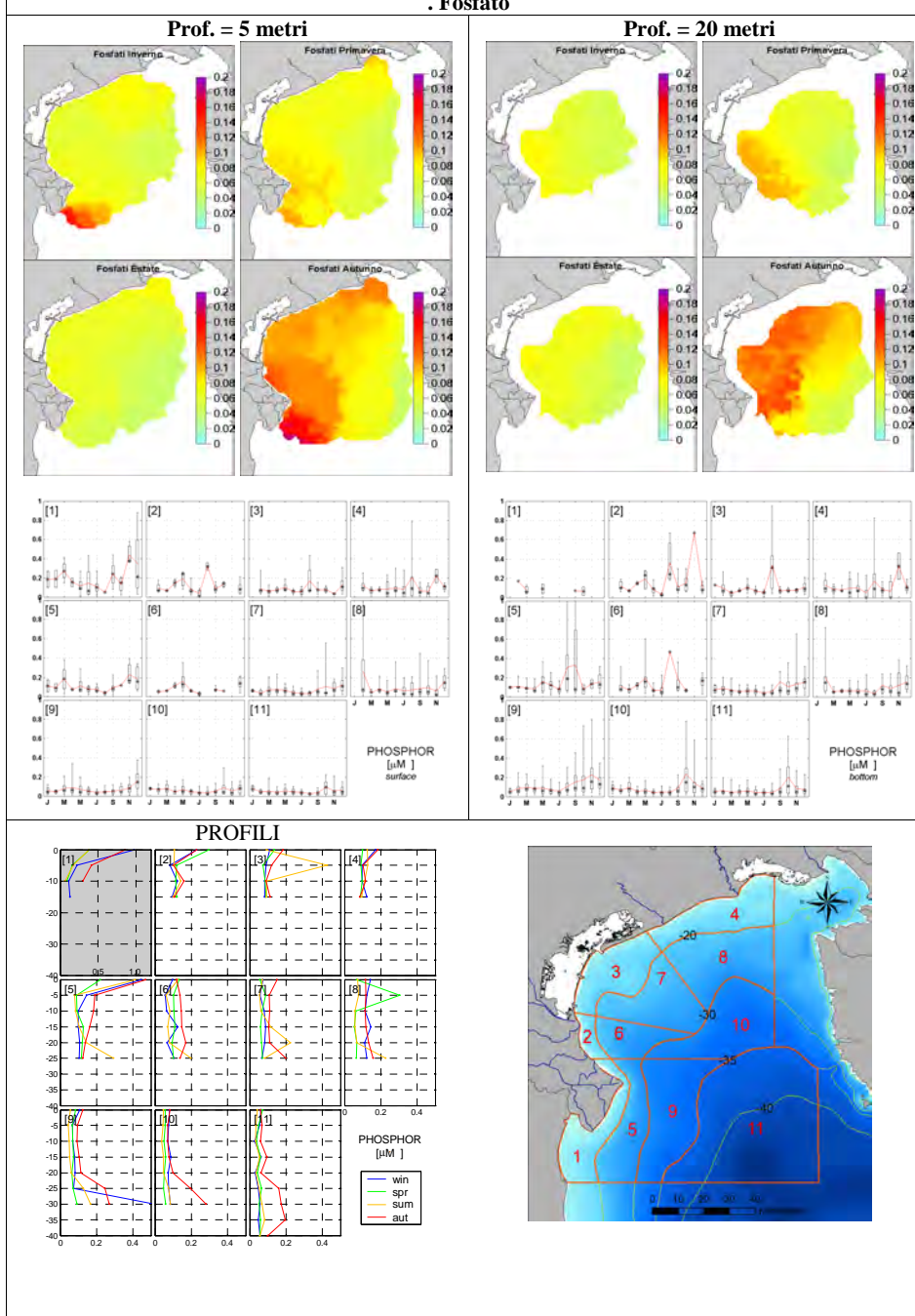


Fig 7 – Seasonal evolution and spatial distribution for biogeochemical properties: Phosphate.

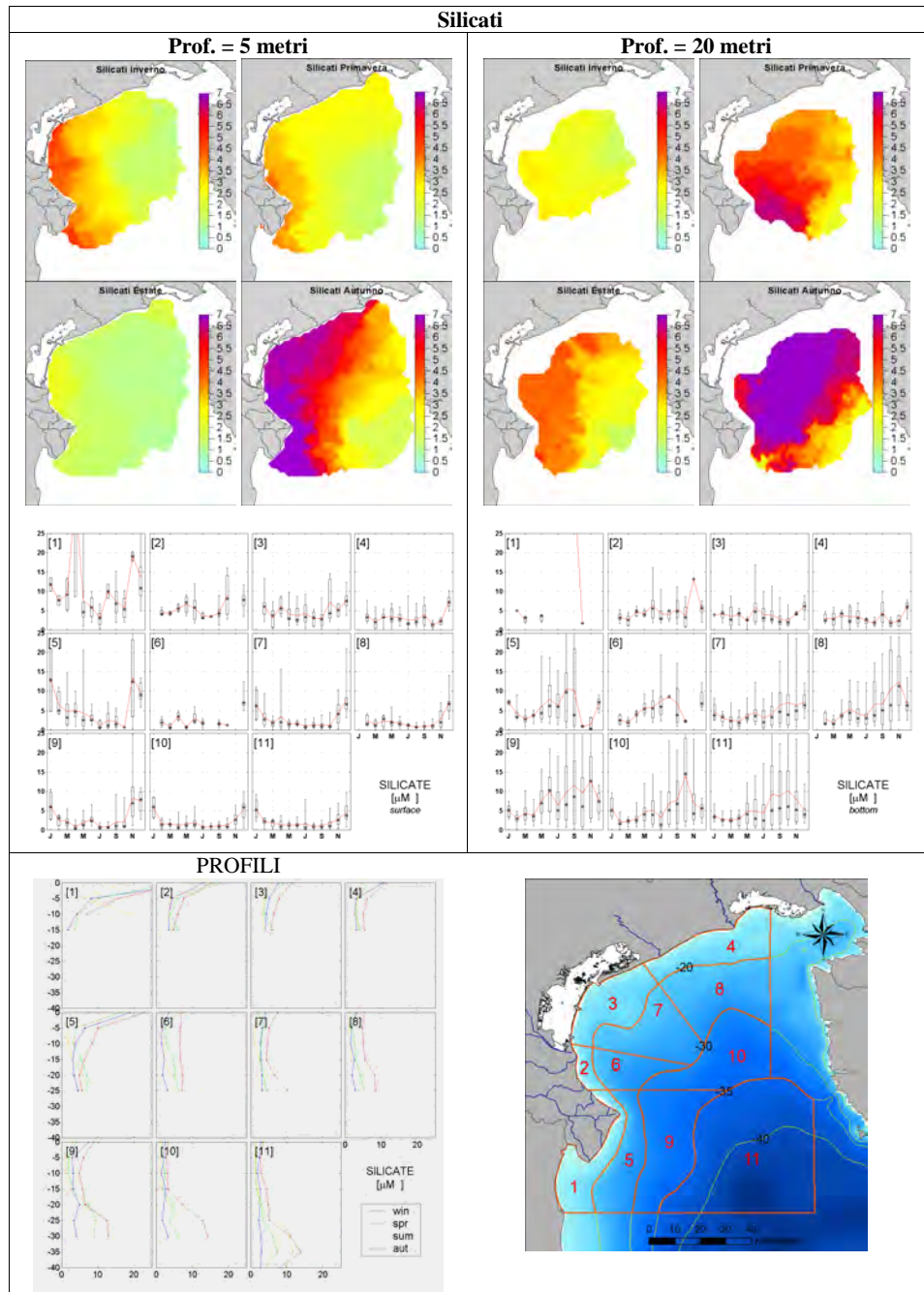


Fig 8 – Seasonal evolution and spatial distribution for biogeochemical properties: Silicates.

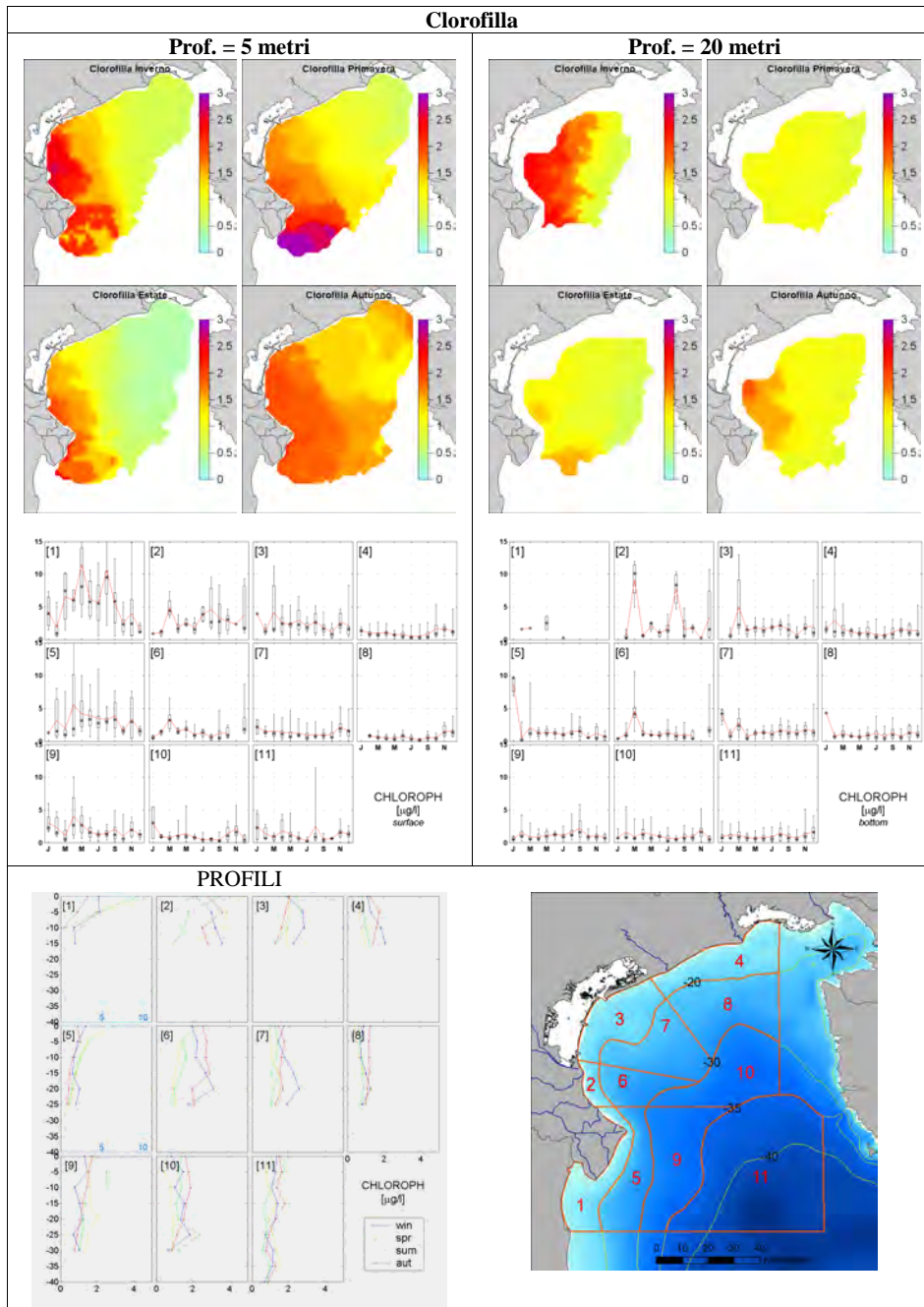


Fig 9 – Seasonal evolution and spatial distribution for biogeochemical properties: Chlorophyll a.

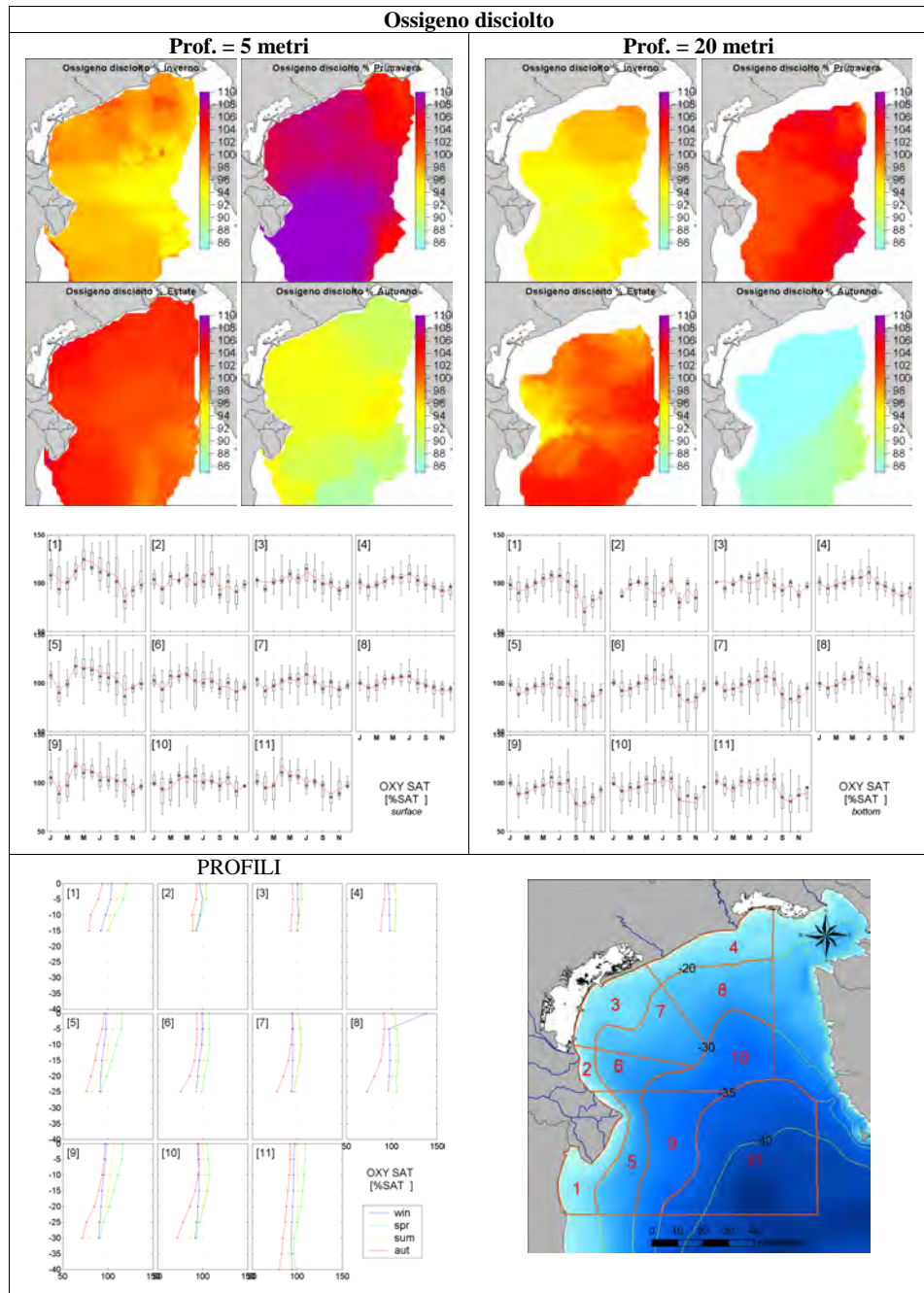


Fig 10 – Seasonal evolution and spatial distribution for biogeochemical properties: Dissolved Oxygen.

EVOLUTION OF BIOMASS, ABUNDANCE AND STRUCTURE OF PLANKTON COMMUNITY IN THE CAOSTAL AREA OF THE NORTH WESTERN ADRIATIC SEA

Vinko Bandelj¹, Mauro Bastianini², Cosimo Solidoro¹

1 Dipartimento di Oceanografia, Istituto Nazionale di Oceanografia e di Geofisica Sperimentale OGS,

2 Istituto di Scienze del Mare, ISMAR- CNR, Venezia

Riassunto

Il presente articolo illustra la variabilità spaziale e l'evoluzione stagionale della comunità planctonica nell'area costiera dell'Adriatico nord-occidentale sulla base di campioni raccolti in 10 anni di monitoraggi. I risultati costituiscono un contributo alla caratterizzazione delle acque del Nord Adriatico, alla comprensione delle interazioni di tali acque con le acque costiere, incluse quelle della Laguna di Venezia, ed inoltre un aggiornamento della climatologia di questa regione, prestandosi quindi ad essere un importante riferimento per comportamenti anomali e futuri cambiamenti.

Abstract

This paper illustrate space variability and seasonal evolution of plankton community in the coastal area of the north-western Adriatic sea, basing on observation collected in a 10-years period. Results represent a contribution to the characterization of the waters of Northern Adriatic Sea, to the comprehension of interactions of these waters with coastal waters, including the Lagoon of Venice, and an updated climatology of this region, which can be used as an important reference term for assessment of anomalous behavior and future changes.

1 Introduction

Information on composition, abundance and biomass of living organisms can offer a significant contribution to the assessment of the quality status of an aquatic ecosystem. Indeed they are nowadays considered in most of modern procedure enforce my new regulation for water protection and conservation, such as the water frame directive. In particular, great attention is devoted to plankton, because it represents the base of the trophic chains, and because of its relatively fast response to alterations of environmental variables, which might not be emphasized by longer living biological elements, such as benthic organisms. The analysis of abundance data however pose a number of challenges, because statistical distribution of data usually are very skewed, and inflated by zero, so that traditional statistical methodology might not be

appropriate. The so-called double zero problem is a typical point in case.

On the other hand, it is important to be able to derive objectively a typical situation to be used as a reference term, for assessment of anomalous behaviour and future changes. In this paper, carried on within the frame of the project "Climatologia e qualità delle acque costiere della Regione Veneto", funded by CORILA and endorsed by LOICZ as a relevant LOICZ project, we tried to derive such a reference term for the phytoplankton community in the coastal area in the north-western area of the Adriatic Sea. In particular we aimed to derive a space time-evolution of phytoplankton community, and therefore have a number of reference points, associated to different area and moment.

2 Material and methods

The analysis focused on the area of the Adriatic Sea of latitude between 44°30' and 45°45', and of longitude between 12°13' and 13°56', that is the area north of the Valli of Comacchio and west of the Lagoon of Grado and Marano, and it is restricted to the coastal area, define as the area within 2.5 nautical miles off the coast. This area has been regularly monitored on behalf of Regional Water Authority, by monthly sampling along a number of regular transects orthogonal to coast. More in detail, our dataset was made by samples collected in transects 8, 24, 40, 56 e 72, in the two external stations of each of them (1 and 2.5 nm from the coast respectively) in surface and bottom layers (FIG: 1). They were collected monthly (biweekly in summer months) from May 1992 to December 1999. Several species were joined at a genus level due to identification problems (e.g. *Pseudonitzschia* spp). Only species or genera with more than 6% of presences were retained for the analysis in order to decrease heterogeneity due to rare and occasional species (Table 1). Seven water quality parameters were used too: temperature, salinity, inorganic nitrogen (NH₄, NO₃, NO₂), silicate (SiO₄) and phosphate (PO₄). Samples with missing values were discarded from the analysis.

The final dataset was made of 2520 samples with abundances of 31 phytoplankton species or genera, 7 water quality parameters and information on station, depth, transect, month and year of sampling.

Partitive clustering method k-means was used to identify a discrete number of plankton populations: centroids were randomly initialized for 100 runs and for a number of clusters from 2 to 15. For each number of clusters the best partitions was selected based on the sum of square errors. The most appropriate number of clusters was then selected inspecting the values of the Davies-Bouldin index (Davies & Bouldin, 1979).

The abundance distribution was highly asymmetric and skewed and inflated by zero values. To prevent the "double zero" problem (Legendre & Legendre, 1998) the phytoplankton abundances were transformed with the Hellinger transformation (Legendre & Gallagher, 2001) prior to analysis.

The IndVal method (Dufrière & Legendre, 1997) was used to identify indicator

taxa for each cluster with IndVal values >25%. As dominant species were defined those, whose total sum represented more than 90% of the total abundance of each cluster.

The spatial and temporal interpretation of the clusters was done on the basis of time, place and depth of sampling of the samples belonging to each cluster. The description of the abiotic environment of each plankton community was made considering the values of the environmental variables. For each variable 5 classes of 20 percentiles were defined and the median value of each cluster was assigned to one of these classes. The classes were labelled with qualitative descriptions.

3 Results

From the inspection of the Davies-Bouldin values we chose the partition in 9 clusters. Indicator taxa and dominant taxa are listed in Table 1 and Table 2 respectively.

Cluster 1 has 136 samples from May and June (Fig. 1), evenly distributed among transects (Fig. 3) and depths, and with slightly more samples from the most external station. Samples were collected mainly in 1994, 1995 and 1997 (Fig. 2). Cluster 1 is characterized by average values for all environmental parameters (Table 3). The genus *Cyclotella* spp (69.14%) had the highest IndVal value and was the main dominant taxon (61.68%). Other dominant taxa were diatoms *Nitzschia* spp, *Thalassiosira* spp, *Cylindrotheca closterium*, *Dactyliosolen fragilissimus* and *Chaetoceros* spp, and dinoflagellates *Protoberidinium* spp and *Prorocentrum micans*.

Cluster 2 was the biggest with 508 samples, especially from May-June and August-September. It was present in all the monitoring years, with peaks in 1996 and 1998 and minimum in 1994 and 1995. It was abundant in all sampling depths, in the external station and mainly in the three northernmost transects. Cluster 2 was characterized by high phosphate concentrations. The highest IndVal was 47.94% for *Thalassiosira* spp, which represented 68.8% of the total abundances. Other dominant taxa were *Cyclotella* spp, *Protoberidinium* spp, *Chaetoceros* spp, *Cylindrotheca closterium* and *Nitzschia* spp.

Cluster 3 has 145 samples, mainly collected in July and in years 1998-1999. The maximum number of samples was collected in transect 8 and the minimum in transect 72. The cluster 2 is characterized by high temperature and low salinity and inorganic nutrients. *Chaetoceros compressus* has an IndVal of 90.03% and represents 58.10% of the total abundance.

Other 4 diatoms, *Chaetoceros* spp, *Thalassiosira* spp, *Leptocylindrus danicus* and *Skeletonema costatum*, and 2 dinoflagellates, *Protoberidinium* spp e *Ceratium* spp, are also dominant in cluster 3.

Cluster 4 has 378 samples, mainly from May-September and November-December. It is present especially in surface waters of the station closest to the coast, and it shows a gradient from minimum frequencies in the northern transects to maximum frequencies in the southern transects.

The cluster is characterized by high temperature and phosphates and average values of other parameters. *Chaetoceros* spp is the genus with highest IndVal (63.98%) and highest abundances (63.64% of the total abundance). Other dominant taxa are dinoflagellates *Protoperidinium* spp e *Ceratium* spp, and diatoms *Thalassiosira* spp, *Skeletonema costatum*, *Chaetoceros compressus* and *Cylindrotheca closterium*

The cluster 5 has 322 samples, mainly from late summer and late autumn months (from August to December). Bottom samples are particularly abundant, as well as samples from northern transects. It was present in all the sampling years, with a peak in 1993 and low frequencies in 1995-1997. The cluster 5 is characterized by high values of salinity and ammonium. The biological description of the cluster is not very clear, since the highest IndVal value is 28.71% for *Nitzschia* spp, which represents only 27.45% of the total abundance. Other dominant taxa are *Leptocylindrus danicus*, *Thalassiosira* spp, *Cylindrotheca closterium*, *Chaetoceros* spp, *Navicula* spp, *Guinardia striata*, *Thalassionema nitzschioides*, *Skeletonema costatum*, *Protoperidinium* spp and *Ceratium* spp.

The cluster 6 has 442 samples, mainly from spring (March-April) and late summer months (July-October). It is present especially in the external station and at greatest depths, with a peak for the transect 56. There are samples from all years in cluster 6, with a peak for 1995 and low frequencies for 1992-1993. Abiotic environment of cluster 6 is characterized by low values of NO₂ and SiO₄. The taxon with highest IndVal (54.01%) is *Protoperidinium* spp, whose abundances amount at 62.66% of the total cluster abundances. Dinoflagellates *Ceratium* spp and diatoms *Chaetoceros* spp, *Skeletonema costatum*, *Leptocylindrus danicus* and *Chaetoceros compressus* are the other dominant species of cluster 6.

In cluster 7 there are 149 samples. The highest frequency is for July samples, followed by August and September samples. The cluster was very abundant in 1996-1997 and shows an evenly distribution over transects, stations and depths. It shows high temperature, average SiO₄, and low salinity and inorganic nutrients. As cluster 6, also cluster 7 is characterized by dinoflagellates: *Ceratium* spp has an IndVal value of 76.5% and represents 53.76% of the total abundance, followed by another dinoflagellate, *Protoperidinium* spp, and diatoms *Thalassiosira* spp, *Chaetoceros* spp, *Chaetoceros compressus*, *Nitzschia* spp, *Cylindrotheca closterium* and *Leptocylindrus danicus*.

Cluster 8 has 247 samples, mainly from late winter and early spring months (January-April). Samples were mainly collected in surface layer of the southern transects. Two peaks of this cluster were registered in years 1993 and 1999, while in 1995 there was a minimum. The cluster is characterized by very low temperature, average salinity and NH₄ values, and high concentrations for all oxidized inorganic nutrients (NO₂, NO₃, PO₄, SiO₄). The phytoplankton community is dominated by diatom *Skeletonema costatum* (71.19% of the total abundance), which shows also the highest IndVal (86%). Other dominant taxa are dinoflagellates *Protoperidinium* spp and diatoms *Chaetoceros* spp and

Thalassiosira spp.

In the cluster 9 there are 193 samples from late autumn-winter months (October-February), mainly from the bottom layer and from the external station of all transects. The cluster was almost absent in 1993 and 1998, and very abundant in 1996-1997. Temperature is very low, and concentrations of inorganic nutrients, with the exception of NH₃, are high or very high. The community is characterized by coccolithophoride *Emiliana huxleyi* (IndVal 68.02%, 53.73% of total abundance). There are other 8 dominant diatoms (*Skeletonema costatum*, *Nitzschia* spp, *Chaetoceros* spp, *Navicula* spp, *Leptocylindrus danicus*, *Cylindrotheca closterium*, *Proboscia alata*) and one taxon of dinoflagellates (*Protoperidinium* spp).

SPECIES	TAXON	KM	IndVal
<i>Cyclotella</i> spp	Diatoms	1	69.14
<i>Thalassiosira</i> spp	Diatoms	2	47.94
<i>Chaetoceros compressus</i>	Diatoms	3	90.03
<i>Chaetoceros</i> spp	Diatoms	4	63.98
<i>Nitzschia</i> spp	Diatoms	5	28.71
<i>Protoperidinium</i> spp	Dinoflagellates	6	54.01
<i>Ceratium</i> spp	Dinoflagellates	7	76.5
<i>Skeletonema costatum</i>	Diatoms	8	86
<i>Emiliana huxleyi</i>	Coccolithophorides	9	68.02

Tab 1 – Indicator taxa (IndVal>25%) for each cluster: all these taxa are also dominant.

SPECIES	TAXON	CLUSTER	MEAN	SUM	CUMUL PERC
<i>Cyclotella</i> spp*	Diatoms	1	322244	43825235	61.68
<i>Nitzschia</i> spp	Diatoms	1	29230	3975223	67.28
<i>Protoperidinium</i> spp	Dinoflagellates	1	28415	3864425	72.71
<i>Thalassiosira</i> spp	Diatoms	1	27516	3742211	77.98
<i>Cylindrotheca closterium</i>	Diatoms	1	22826	3104374	82.35
<i>Proocentrum micans</i>	Dinoflagellates	1	15831	2152992	85.38
<i>Dactyliosolen fragilissimus</i>	Diatoms	1	14066	1912910	88.07
<i>Chaetoceros</i> spp	Diatoms	1	11344	1542775	90.24
<i>Thalassiosira</i> spp*	Diatoms	2	628804	319432453	68.80
<i>Cyclotella</i> spp	Diatoms	2	66538	33801549	76.07
<i>Protoperidinium</i> spp	Dinoflagellates	2	57397	29157589	82.35
<i>Chaetoceros</i> spp	Diatoms	2	35131	17846670	86.20
<i>Cylindrotheca closterium</i>	Diatoms	2	24765	12580597	88.91
<i>Nitzschia</i> spp	Diatoms	2	21733	11040440	91.29
<i>Chaetoceros compressus</i> *	Diatoms	3	1216934	176455398	58.10
<i>Chaetoceros</i> spp	Diatoms	3	231471	33563327	69.16
<i>Protoperidinium</i> spp	Dinoflagellates	3	142875	20716943	75.98
<i>Thalassiosira</i> spp	Diatoms	3	138380	20065062	82.59
<i>Ceratium</i> spp	Dinoflagellates	3	102637	14882307	87.49
<i>Leptocylindrus danicus</i>	Diatoms	3	38271	5549337	89.31
<i>Skeletonema costatum</i>	Diatoms	3	37010	5366460	91.08
<i>Chaetoceros</i> spp*	Diatoms	4	1242634	469715668	63.64
<i>Protoperidinium</i> spp	Dinoflagellates	4	158082	59755166	71.74

Tab 2 – Dominant taxa of each cluster. Table reports mean, sum and cumulative percentages. Abundances are given in cell L⁻¹. The stars mark indicator taxa.

Vare	C11	C12	C13	C14	C15	C16	C17	C18	C19
TEMP	normal	normal	high	high	normal	normal	high	very low	very low
SAL	normal	normal	low	normal	high	normal	low	normal	normal
NH3	normal	normal	low	normal	high	normal	low	normal	normal
NO2	normal	normal	low	normal	normal	low	low	high	very high
NO3	normal	normal	low	normal	normal	normal	low	high	high
SiO4	normal	normal	low	normal	normal	low	normal	high	high
PO4	normal	high	low	high	normal	normal	low	high	high

Tab 3 – Qualitative description of biogeochemical properties of clusters.

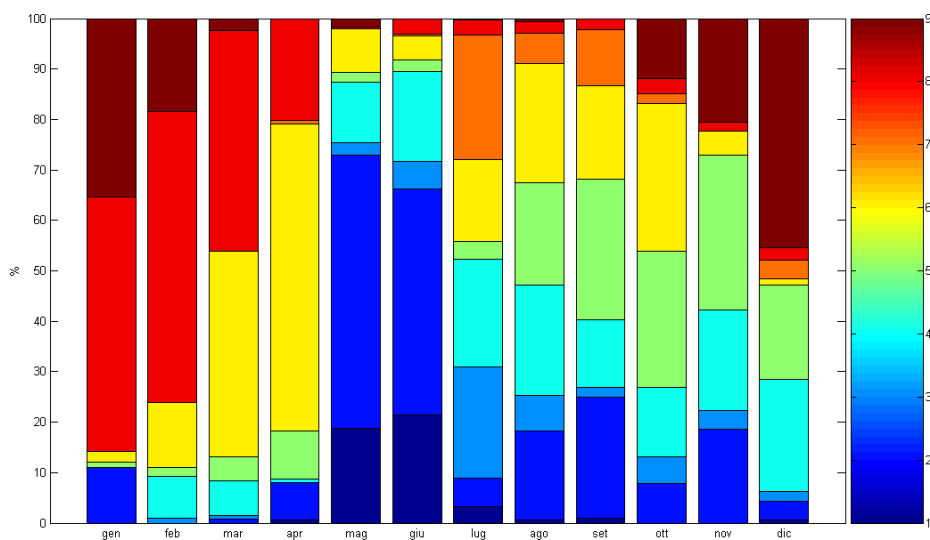


Fig 1 – Subdivision of samples of each month among different clusters. The clusters are marked by colours, as in the column on the right.

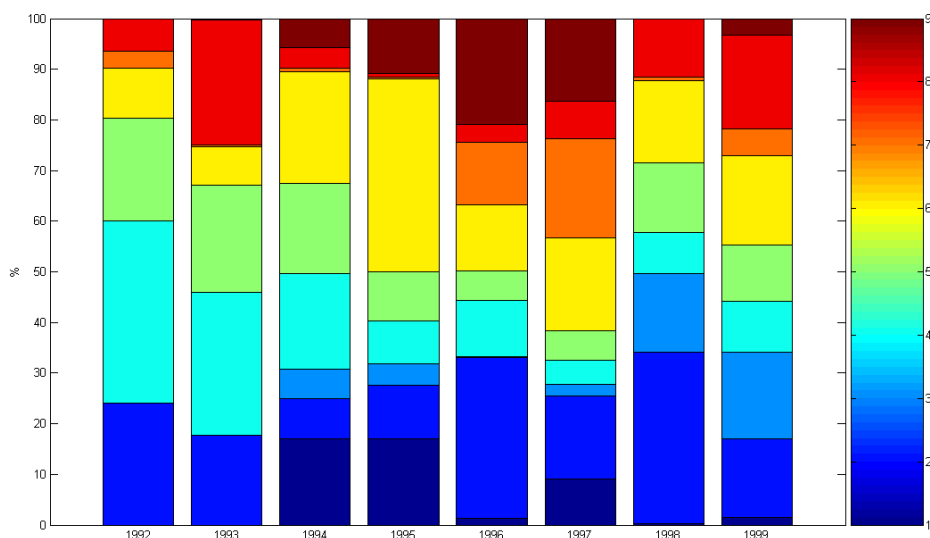
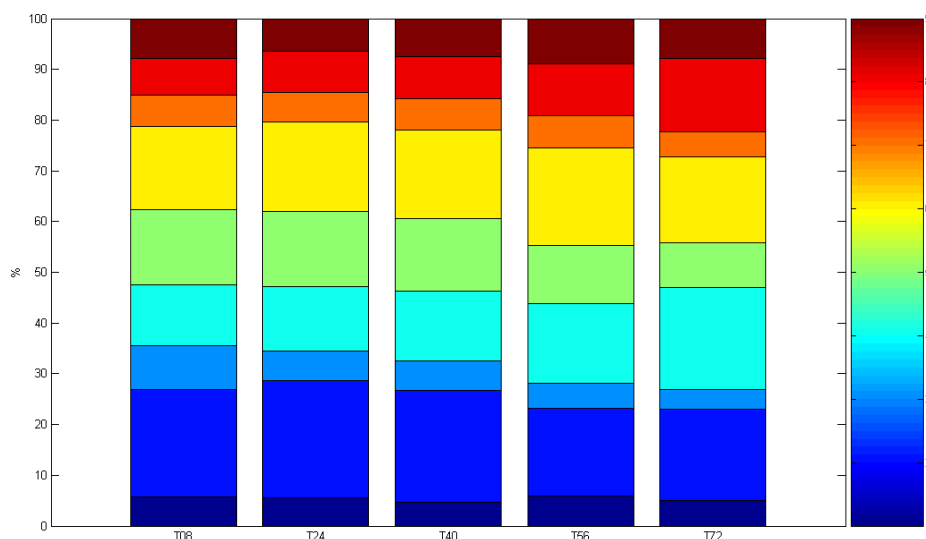


Fig 2 – Subdivision of samples of each year among different clusters. The clusters are marked by colours, as in the column on the right.

Fig 3 – Subdivision of samples of each transect among different clusters. The clusters are marked by colours, as in the column on the right.



4 Discussion

The coastal belt of Veneto region is characterized by high spatial and temporal variability (Bernardi Aubry et al., 2004). The main direction of spatial variability is along the coast from north to south. In the northern part there are some torrential rivers (Tagliamento, Lemene, Livenza, Piave, Sile), with occasional and highly variable freshwater inputs. The central part is located in front of the lagoon of Venice, which acts as phytoplankton or inorganic nutrients exporter, according to the season (Gačić e Solidoro, 2004; Bernardi Aubry e Acri, 2004). Several large rivers (Brenta, Adige, Po) flow in the sea in the southern area with constant inputs of freshwaters and inorganic nutrients: this is the most eutrophic area of the Adriatic Sea (Cushman-Roisin et al., 2001). The spatial and temporal variability observed in water quality parameters is not reflected in phytoplankton communities characteristics (Bernardi Aubry et al., 2004). This is confirmed also by the present study: clusters identified on the basis of phytoplankton abundances do not show great differences in their horizontal or vertical distributions. Clusters 2 and 5 are more frequent in northern transects and clusters 4 and 8 in surface waters of southern transects. Clusters 6 and 9 are abundant in the external stations of each transect, and along with cluster 5 they are more abundant in the bottom layer.

From our study clearly emerged the influence of season and year variability on plankton communities. Each cluster was regarded as a plankton community, strongly dominated and characterized by only one phytoplankton taxon. A total number of 17 phytoplankton taxa represents more than 90% of the abundances of each cluster. We can say that in the coastal belt of Veneto high abundance blooms of a reduced number of species make the seasonal phytoplankton cycle. As a result of our study, the following seasonal cycle can be outlined.

Late winter and early spring months are in surface characterized by communities of *Skeletonema costatum* (cluster 8), which is a small diatom with high surface/volume ratio, thus favoured by high concentrations of nutrients in water (Bernardi Aubry et al., 2006). In our study the community was indeed

related to waters with high nutrients and low temperatures, as consequence of freshwater inputs in preceding months. It was frequent especially in southern areas, where the largest rivers flow. At the beginning of spring, the consumption of fresh nutrients and the increase of temperature build up favourable conditions for a bloom of dinoflagellates of genus *Protoperdinium* (cluster 6). Dinoflagellates are usually more competitive than diatoms in exhausted and oligotrophic environments. Cluster 6 is mainly present in more open sea areas and at greatest depths, which are less influenced by rivers freshwater inputs. A new diatom peak can be observed between May and July, where communities dominated by *Cyclotella* (cluster 1), *Thalassiosira* (cluster 2) and *Chaetoceros* (cluster 3 and 4) may develop. Species of *Thalassiosira* genus are negatively correlated with salinity and positively with inorganic nutrients in the North Adriatic waters (Bernardi Aubry e Acri, 2004). Both, *Thalassiosira* and *Cyclotella*, are small species with high growing rates and high surface/volume ratios, thus they can take advantage of high nutrient concentrations (Bernardi Aubry et al., 2006). Blooms of *Cyclotella* and *Thalassiosira* are limited to late spring months (May-June), while *Chaetoceros* species may dominate all summer months. In particular, *Chaetoceros compressus* (cluster 3) is strongly associated to the July phytoplankton peak and to transect 8, while the community dominated by other *Chaetoceros* species is more abundant in southern area and in the bottom layer. The community dominated by *Thalassiosira* spp is frequently found in the 3 northern transects (8, 24, 40). Again, to this second diatoms peak, other dinoflagellates blooms follow dominated by either *Protoperdinium* spp (cluster 6) or *Ceratium* spp (cluster 7). The succession between spring blooms of small-sized diatoms with high surface/volume ratio, and summer oligotrophic blooms of larger dinoflagellates with low growing rates and surface/volume ratio, is a steady characteristic of Northern Adriatic (Bernardi Aubry et al., 2006). Dinoflagellates communities dominate summer months until the beginning of autumn (from July to September-October), when they are replaced by diatoms dominated communities: cluster 2, dominated by *Thalassiosira* spp, and cluster 5, dominated by *Nitzschia* spp. This latter community is present mainly in the deepest layers of northern transects and probably they are interested by resuspended benthic diatoms such as *Nitzschia longissima* (Bernardi Aubry et al., 2006). High NH₄ and salinity values might be a signal of ongoing remineralization processes, which usually take place in deep waters in late summer and autumn. In late autumn the cluster 4 reappears, even if probably due to blooms of different *Chaetoceros* species as those of summer blooms (compare Bernardi Aubry et al., 2004). Finally, late autumn and winter months are characterized by blooms of the coccolithophoride *Emiliana huxleyi*. Temperatures in this period are low, nutrients concentrations high, because of continental waters inputs and reduced consumption. The community dominated by *Emiliana huxleyi* are associated especially to waters of the bottom layer and of more external sampling stations, as already observed (Bernardi Aubry et al., 2006).

The interannual phytoplankton succession identified in our study starts with

abundant communities of *Thalassiosira* spp, *Chaetoceros* spp and *Nitzschia* spp in 1992 and 1993; when also a huge bloom of *Skeletonema costatum* was observed. In 1994 the *Thalassiosira* dominated community was replaced by the *Cyclotella* dominated community in May-June and by the *Protoperdinium* dominated community in late summer and early autumn. *Chaetoceros* spp and *Nitzschia* spp blooms were still present in 1994. The year 1995 was interested by *Cyclotella* and *Protoperdinium* blooms. In 1996 communities dominated by *Thalassiosira* spp e *Chaetoceros* spp reappeared again at high frequencies, along with *Protoperdinium* spp community. High abundances were detected also for *Ceratium* spp and *Emiliana huxleyi*. The next year *Ceratium* spp dominated community reached its peak, beside high abundances of the communities characterized by *Emiliana huxleyi*, *Protoperdinium* spp, *Cyclotella* spp and *Thalassiosira* spp. The same year was interested also by the presence of large mucilage patches (Bernardi Aubry et al., 2006). In 1998 the blooms of *Ceratium* spp and *Emiliana huxleyi* were not present and were replaced by blooms of *Skeletonema costatum*, *Chaetoceros compressus* and *Nitzschia* spp. Communities dominated by *Thalassiosira* and *Protoperdinium* were also detected in 1998. In the last year of monitorings, the same communities as in 1998 were present and *Chaetoceros* spp blooms appeared again.

5 Conclusions

From our study emerged that phytoplankton communities have a spatial variability, which is related to changes in total abundances, but not to changes in species composition. This is also the reason why it is difficult to find clear relationships between a certain species presence and the environmental characteristics as described by physico-chemical variables. The trophic level of different areas along the Veneto coastal belt influences only the abundance of the species, not their presence/absence.

The study area is much probably too limited to detect variations in the composition of communities made of small, current transported organisms. Furthermore, the phytoplankton species that were analyzed in the present study are much probably highly tolerant to different environmental conditions. The gradients of the physico-chemical parameters in the study area are known to change fast and abruptly, thus much probably the phytoplankton communities do not have time to adapt to such changes.

In our opinion, the occurrence of single phytoplankton species cannot be utilised as an integrated indicator of biogeochemical dynamics of different areas. The absence of clear relationships between plankton communities and biogeochemical variables indicates that the two type of descriptors bring different and possibly complementar information. Thus, it is necessary to find and describe a reference condition for plankton communities present in different ecological situations, as it was made in the present study.

References

- Bernardi Aubry F., Acri F., 2004: Phytoplankton seasonality and exchange at the inlets of the Lagoon of Venice (July 2001 – June 2002). *J. Mar. Syst.* 51: 65-76
- Bernardi Aubry F., Acri F., Bastianini M., Bianchi F., Cassin D., Pugnetti A., Socal G., 2006: Seasonal and interannual variations of phytoplankton in the Gulf of Venice (Northern Adriatic Sea). *Chem. Ecol.* 22: 71-91
- Bernardi Aubry F., Berton A., Bastianini M., Socal G., Acri F., 2004: Phytoplankton succession in a coastal area of the NW Adriatic, over a 10-year sampling period (1990-1999). *Cont. Shelf Res.* 24: 97-115
- Cushman-Roisin B., Gačić M., Poulain P.-M., Artegiani A., 2001: *Physical Oceanography of the Adriatic Sea: Past, Present, Future*. Kluwer Academic Publishers
- Davies D.L., Bouldin D.W., 1979: A cluster separation measure. *IEEE Trans. on Pattern Analysis and Machine Intelligence*, PAMI-1:224-227
- Dufrêne M., Legendre P., 1997: Species assemblages and indicator species: the need for a flexible asymmetrical approach. *Ecol. Monogr.* 67: 345-366
- Gačić M., Solidoro C., 2004: Lagoon of Venice. Circulation, water exchange and ecosystem functioning. *J. Mar. Syst.* 51: 1-3
- Legendre P., Gallagher E.D., 2001: Ecologically meaningful transformations for ordination of species data. *Oecologia* 129: 271-280
- Legendre P., Legendre L., 1998: *Numerical Ecology*, 2nd english edn. Elsevier Science BV, Amsterdam

CLASSIFICATION AND DRIVERS OF SPATIAL PATTERN OF THERMOHALINE FEATURES OF THE NORTHERN ADRIATIC SEA

Gianpiero Cossarini, Sebastiano Trevisani, Vinko Bandelj, Stefano Salon, Cosimo Solidoro

Dipartimento di Oceanografia, Istituto Nazionale di Oceanografia e di Geofisica Sperimentale OGS, Trieste, Italy

Risunto

Questo articolo presenta i risultati di un'analisi di classificazione di circa 200 mappe di distribuzioni spaziali di salinità e temperatura in Nord Adriatico. Le mappe sono state ottenute dall'interpolazione spaziale di dati sperimentali campionanti durante i diversi progetti di ricerca oceanografica che hanno interessato il bacino del Nord Adriatico negli ultimi 20 anni. La classificazione è stata effettuata utilizzando la metodologia delle Growing Hierarchical Self Organizing Map, che ha il vantaggio di combinare assieme le caratteristiche dei metodi di reti neurali senza supervisione e dei metodi di classificazione gerarchica. La classificazione ha prodotto una tipologia di sei diversi pattern spaziali delle caratteristiche termohaline nel bacino. I diversi pattern individuati sono poi stati discussi anche in relazione alle condizioni meteorologiche e di portata del Po esistenti durante i campionamenti appartenenti alle sei classi.

I risultati hanno permesso di ottenere una caratterizzazione delle condizioni termohaline del Nord Adriatico, e di investigare le relazioni tra le condizioni forzanti, le caratteristiche generali della circolazione e le distribuzioni spaziali emergenti nell'area del Nord Adriatico.

Abstract

This paper illustrates the results of a classification analysis of around 200 spatial distributions of temperature and salinity in the Northern Adriatic Sea. Maps are obtained by spatial interpolation of experimental observations collected during many oceanographic research projects performed in this area during the last 20 years. The classification is based on Growing Hierarchical Self Organizing Map, a numerical procedure which combines advantages of competitive unsupervised artificial neural networks and hierarchical clustering procedure. The classification returns a typology of spatial patterns of the thermohaline features of the system. Meteorological conditions associated to each pattern, together with information of the regime of Po river, are used to infer on relationship between these forcing and the emerging structures.

Results represent a contribution to the characterization of the waters of Northern Adriatic Sea, to the comprehension of interactions between major forcing of the Northern Adriatic Sea, its general circulation patterns and spatial

distribution of biogeochemical properties.

1 Introduction

The northern Adriatic Sea has been the object of a number of research projects, however, papers devoted to synthesis and integration, in which results of different project are collated and integrated, and in which reanalysis of integrated data set are performed, are not very common. Within the frame of the project "Climatologia e qualità delle acque costiere della regione veneto", funded by CORILA and endorsed by LOICZ as a relevant LOICZ project, we undertook such an effort, by deriving a climatological description of biogeochemical observations on the Northern Adriatic Sea, based on an update, and quality checked, data base which included results of major oceanographic projects carried on in this area during last 20 years (Solidoro et al. this issue). In that paper an assessment of present state and typical values of scales of variability for biogeochemical properties is made by subdividing the study area in 11 boxes, and analysing averaged conditions of each box. In this way, however, the averaging procedure - by filtering over 20 years- were likely to mask also information and signals potentially interesting, such as the pattern typically associated to some specific scenario of meteorological forcings or freshwater river discharge.

Because of this, in this paper we dealt with actual data, rather than mean values, and reconstruct specific pattern referring to short time intervals, which we terms 'events'. More in detail, we tried to reconstruct the pattern observed in each of the oceanographic cruises, that is relative to a time period of few days, and to associate them to prevailing meteorological conditions and actual discharge from Po rivers.

Then, a classification analysis of the spatial distribution of temperature and salinity of all events provided a typology of the events, and of the external conditions associated to each of the typical discovered patterns.

2 The data set

The analysis focused on the area of the Adriatic Sea of latitude between 44°30' and 45°45', and of longitude between 12°13' and 13°56', that is the area north of the Valli of Comacchio and west of the Lagoon of Grado and Marano, and on the period from July 1986 to July 2006. We excluded by the data observation referring to the Gulf of Trieste, because there are too many of them, and by considering them we would have introduced a bias in the results. Also, we did not consider data referring to the coastal area, defined as 1.5 miles off the coast, since they are likely to be affected by a variety of processes which are not relevant for the pelagic environment, and their analysis would require the consideration of different spatial and temporal scale.

As detailed in the companion paper (Solidoro et al 2008) we chose to consider data collected by scientific institutions in the frame of oceanographic projects ATOS, Alto Adriatico, PRISMA, Interreg II and Interreg III, a fact which gives more confidence on quality of the measures and comparability of observations.

The final data set is made of around 200000 records, referring to several hundreds monitoring stations and major biogeochemical parameters (temperature, salinity, nutrients, and dissolved oxygen). As it frequently observed in these cases, the number of experimental observation is higher in summer than in winter, and much higher for physical parameters acquired by probe than for biogeochemical ones

Further, we considered additional data about Po river discharge and wind for the characterization of the water typology classification. In particular, the Po river discharge data consist of daily measurements at Ponte Lagoscuro for the period 1986-2006. Wind data consist of hourly data from the Piattaforma CNR "Acqua alta", located 12 miles off-shore the Venice Lagoon, for the period 1986-2006.

3 The northern Adriatic Sea

The area under study was the northern basin of the Adriatic Sea. The dynamics in the area of interest are driven by the interaction of several factors: the shallow bathymetry, that gently deepens toward south; the wind stress forcing; the heat budget; and the freshwater input from the rivers along the western Italian coast.

In particular, the outflow from Po and other major rivers give raise to southern coastal current along the Italian coast (Western Adriatic Current, WAC) and fuel and sustain the main cyclonic circulation which favours the ingression of Intermediate Levantine Waters along the Croatian coast (Kuzmić et al. 2006).

The dominant wind is Bora, blowing from north-east in fall and winter. It forces the close cyclonic gyre in the basin, which is able to bring the Po water toward the Istrian coast. Sirocco, a south east wind, blows typically during spring and summer months and pile up waters along the Italian coast.

During winter negative heat budget and intense wind driven evaporation cool the surface layer that drives dense water formation and barotropic circulation. On the other hand, stratification is observed during summer and possible spatial gradients are induced by differences on thermal inertial of the water column over the bathymetric gradient.

Further, dynamics of the Northern Adriatic Sea can be influence by short time scale forcing (of the order of days) that produces complex features of the spatial scale of 10 km (Ursella et al., 2007).

4 Reconstruction of specific events

The basis of the present analysis is the identification and reconstruction of events, defined as specific spatial patterns referring to short time intervals. Therefore we select time interval within which the data are considered synoptic and the interpolation procedure is done. Information about the dates of the cruises of the different project are not fully available, then we manually search for group of at least 10 stations that were sampled within a period of +/- 5 days. Further, the cluster of stations had to be close enough in order to guarantee the

successful outcome of the interpolation procedure.

At the end of the selection procedure, 206 events were identified, containing the 92,5% of the casts of the dataset. Most of the data of the present dataset were gathered during transect sampling cruises from coast to off-shore, (see Fig. 2 in Solidoro et al., this issue), therefore the adopted selecting criterions allow for the identification of the surveying cruises (i.e. clusters of close stations observed in quasi synoptic period of time). Automatic procedures, based on the analysis of the variance of grouping data, did not have produced satisfied results since the time and spatial scattering of the data.

The spatial interpolation procedure was, then, applied to each of the 206 identified events for the salinity and temperature fields at the depth of 5 and 20 meter. The two depths, that describe the surface and the deep layers, allowed for the characterization of the thermohaline condition of the water column in the basin.

The interpolation method consists of the kriging KT3D algorithm of the GSLib software library (Deutsch and Journel, 1998); an horizontal regular grid of 1000 m and a searching radius of 10km are used. A blank point is place in when less than 4 observations are located within the searching radius.

Events are not homogeneous distributed among the year and the spatial coverage varies from one event to another. As an example of the results of the events identification and interpolation, Figure 1 shows the date of the events identified for the year 1996 (lower right panel), and the interpolated maps of salinity at the surface layer of the corresponding events. The reported events show the presence of particular patterns due to the specific condition and forcing acting at the time of the events. In particular, the events of 2/02 and 9/02 showed a uniformed pattern of high values of salinity over the whole basin. A group of 3 events (17/05, 12/10 and 25/11) portrayed a belt of freshwater (salinity <33) among the western coast as a consequence of the discharges from the PO rivers (see the graph in Fig. 1 reporting the Po river discharge timeseries and the date of the events). Further, in the map of 25/11 it is also evident the effect of the discharges from Adige, Brenta and Bacchiglione rivers. The feature of the cyclonic circulation which brings western coastal fresh water toward the center of the basin is portrayed on the 19/04 and 15/07 maps. Finally, maps of 18/06 and 30/09 have a poor spatial coverage and it is not possible to detect or infer any specific pattern.

This sequence of maps exemplifies well the importance of using the event maps as the basis of the analysis and that the observed patterns can be related to specific external forcing acting at the time of the surveys.

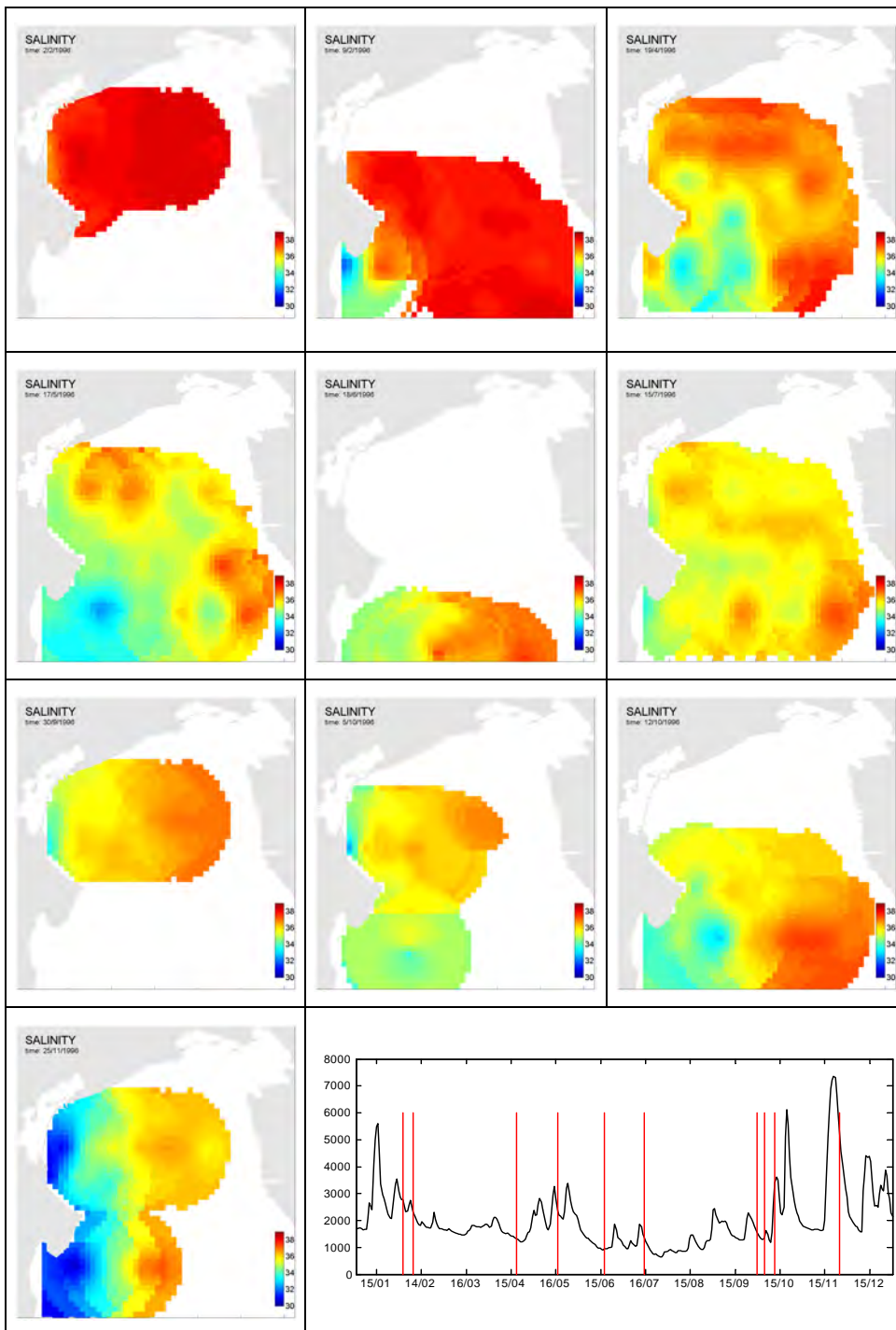


Fig 1 – sequence of the salinity maps at the surface layer for the events of the year 1996. The lower right panel reports the time series of Po river fresh water discharge in 1996 (black line) and the dates of the events (vertical red bars).

5 Classification

The events were then grouped by using a classification method. A single event consists of the combination of 4 maps: salinity and temperature at the two depth of 5 and 20 meter. It represents a specific 3D themohaline pattern at a given time. The classification methods here used is the Growing Hierarchical Self Organizing Map (GHSOM, Liu et al., 2006). This method was preferred to other classical clustering methods (like k-means or hierarchical methods) since it

combines advantages of competitive unsupervised artificial neural networks and hierarchical clustering procedure. Further GHSOM can handle the presence of missing data and the no-homogenous spatial coverage of the different events. Basically, GHSOM consists of independent SOMs (Self Organizing Map, Kohonen et al., 2006) each of which is allowed to grow in size during the training processes (Liu et al., 2006). A quality criterion of the data representation fix the dimension and shape of the resulted GHSOM. We used the free GHSOM matlab toolbox downloadable at www.ofai.at/~elias.pampalk/ghsom/.

Prior the analysis, the maps were vectorized and standardized using T and S mean and standard deviation. Further, 28 out of the 206 events were not used in the analysis because their spatial coverage is less than 50% of the area of interest.

GHSOM analysis resulted in a first-level classification of six units (i.e. typology of thermohaline pattern), that are depicted in the Figure 2-7. The six map-units of the first level can be eventually expanded in a number of sub-map units on the second level, respectively 0, 9, 8, 6, 6, 9 (not shown). This reflects the fact that the typologies of thermohaline pattern of the first level have an intrinsic variability (expect for the first one) and that their variability is explained by the second level sub-maps. However, in this short paper, we limited the discussion to the first 6 maps.

Maps 1 and 4 (Figure 2 and 5, respectively) are characterized by a well thermal mixed column with temperature of around 10°C. These two unit maps differ since the first one shows the presence of freshwater (salinity <35) among the western coastline, while unit map 4 is characterized by salinity up to 37 both in surface and bottom layers. Unit map 2 (Fig. 3) shows a certain degree of thermal stratification (around 17°C and 14°C respectively in the surface and bottom layers) and the presence of fresh water (salinity < 35) in the upper layer that extensively broadens from the western coast toward the center of the basin. A lighter thermal stratification than that of unit 2 characterizes the unit map 5 (Fig. 6) which shows 17-18°C in the surface and 15°C in the bottom layer and a salinity pattern similar to that of unit map 1. Finally, unit maps 3 and 6 (Fig. 4 and 7) show a strong thermal stratification (temperature up to 24°C and down to 16°C respectively in the surface and bottom layers). These two unit maps differ since map 3 displays also a strong saline stratification. In fact map 3 shows the presence of a freshwater (salinity <35) in the surface layer extended to the whole basin.

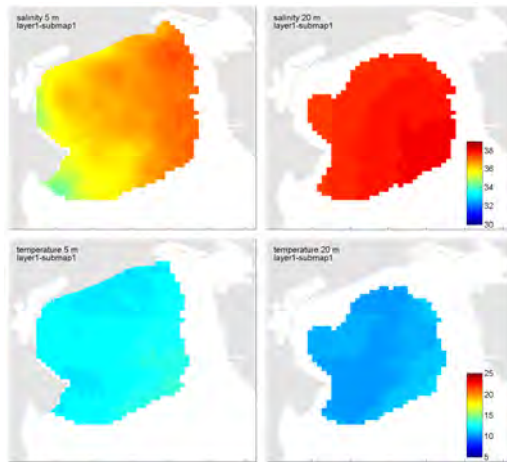


Fig 2 – first unit map of GHSOM: spatial distributions of salinity (first row) and temperature (second row) at 5 (first column) and 20 meter (second column).

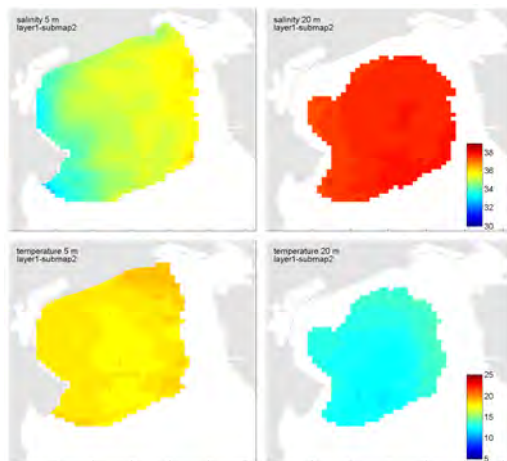


Fig 3 – second unit map of GHSOM: spatial distributions of salinity (first row) and temperature (second row) at 5 (first column) and 20 meter (second column).

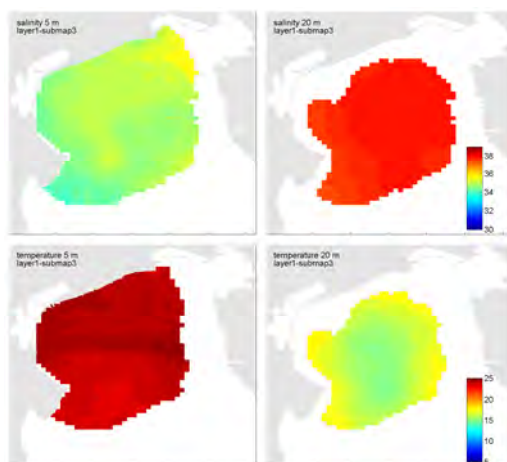


Fig 4 – Na third unit map of GHSOM: spatial distributions of salinity (first row) and temperature (second row) at 5 (first column) and 20 meter (second column).

Fig 5 – fourth unit map of GHSOM: spatial distributions of salinity (first row) and temperature (second row) at 5 (first column) and 20 meter (second column).

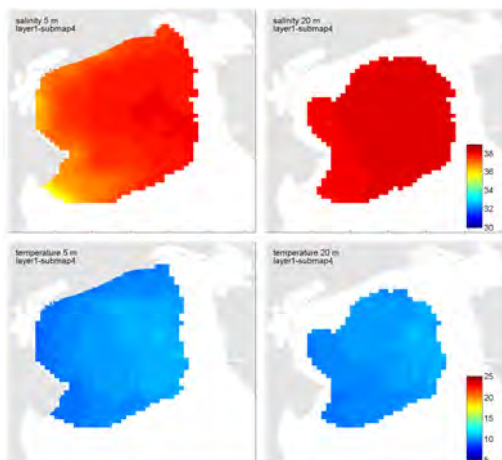


Fig 6 – fifth unit map of GHSOM: spatial distributions of salinity (first row) and temperature (second row) at 5 (first column) and 20 meter (second column).

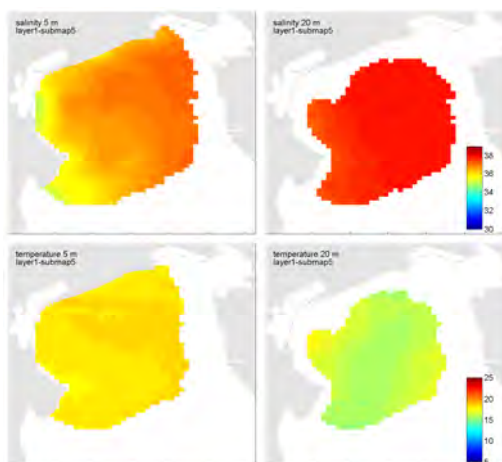
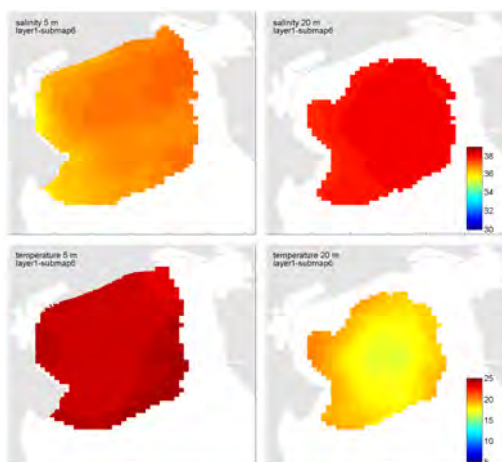


Fig 7 – sixth unit map of GHSOM: spatial distributions of salinity (first row) and temperature (second row) at 5 (first column) and 20 meter (second column).



6 Results and discussion

Each map unit is the combination of a certain number of the original events. Then, knowing the date of the events, it is possible to investigate which forcing contribute in generating the particular typology of thermohaline pattern represented by the unit map.

In particular, we consider the month of the year of the event, that gives an indication of the thermal fluxes condition (Fig. 8); the 5-days Po discharge (Fig. 9) and the 2-days wind distribution previous the event (Fig. 10).

Unit maps 1, 4 and 5 are scenarios characterized by the dominance of Bora wind: the first represents spring wet conditions, the fourth represents winter dry conditions, and the fifth autumn conditions.

More in particular, unit map 1 represents events mainly of April, a few cases are gathered also during January, February, March and May. The Po discharges are slightly higher than the other units (except unit map 2) and the wind condition show the prevalence of the Bora wind although not of the highest intensity wind class. On the other hand, winter conditions, characterized by low Po discharges and strong Bora wind, characterize the events of the unit map 4. Events of the unit map 5 are mainly distributed in autumn months although several are recorded in May, and are characterized by Po discharge around the average, and the prevalence also of northerly wind with the Bora.

Because of the cyclonic circulation driven by Bora wind (Ursella et al., 2007) we expect to observe a circulation of freshwater from the Po coastal area toward the center of the basin on the spatial pattern of salinity maps for these three unit maps. Indeed, this is actually observed in unit 1 and 5. Unit 4 represents a well mixed winter condition when Po discharge are relative low, therefore the cyclonic circulation is masked by barotropic circulation and the absence of a spatial salinity gradient.

The scenario showed by unit map 2 represents the condition of very high outflow from Po river during spring. As a consequence the salinity of the entire northern basin is affected by the fresh water input while a slightly thermal stratification occurs. In fact, events belonging to unit map 2 occur mainly in May (a few cases in June and October). They are characterized by the highest values of Po discharges (mean up to $2500\text{m}^3/\text{s}$) while the wind distribution shows the presence of both Bora and Scirocco, that relieves the transit of spring weather westerly fronts that are usually associated with heavy rain in the Padania plain.

Unit 3 and 6 represent typical summer scenarios characterized by strong thermal stratification. In both scenarios the prevalent wind is from NE however a presence of southerly wind is important too. They differ since the sixth is characterized by the minimum of Po discharge (mean of $903\text{m}^3/\text{s}$), and indeed it shows higher values of salinity in the whole basin.

Fig 8 – Monthly frequency of the event belonging to the six map units.

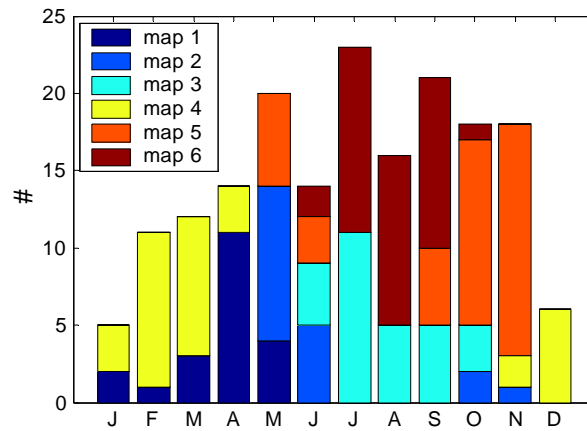


Fig 9 – Distributions of the mean daily discharge of Po river within the 5 day preceding the events of the six unit maps. The boxplots report median (asterisk), IQR (box), min-max range (vertical bar) and mean (blue circle).

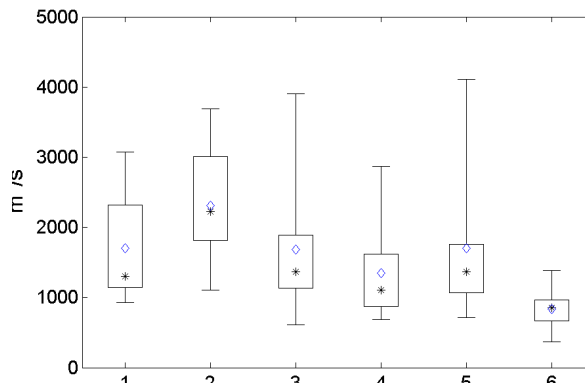
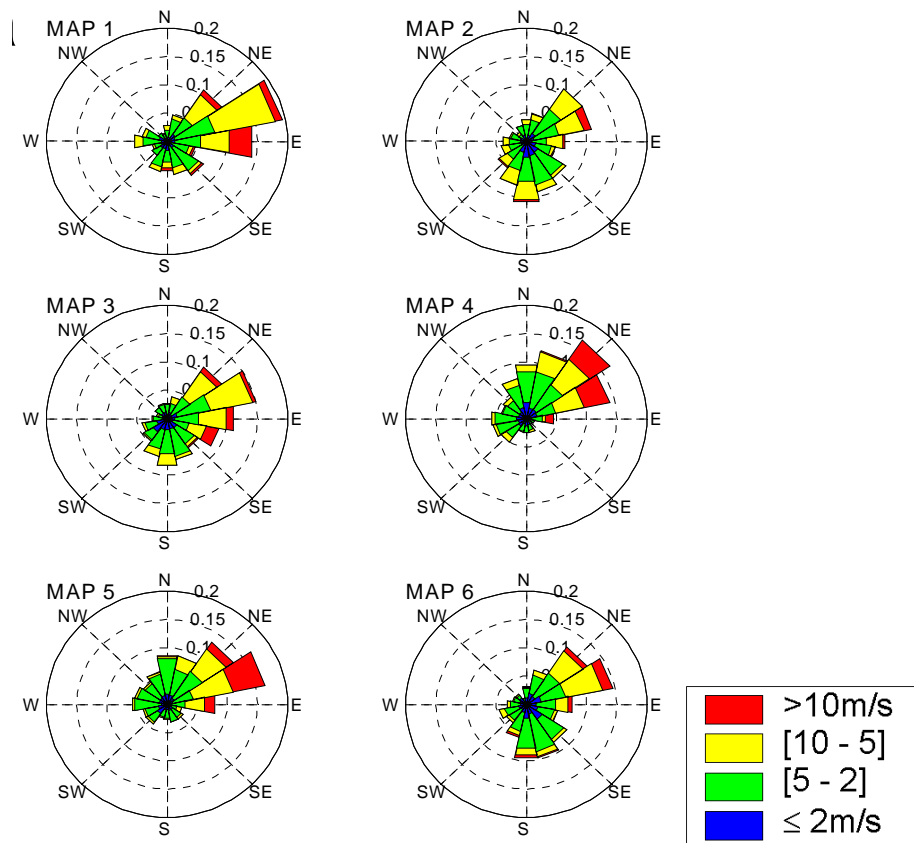


Fig 10 – Distribution of the hourly wind at the CNR marine station “Acqua alta” during the two day preceding the events that constitute the six unit maps.



Acknowledgement

The author thank Alessandro Allodi (Regione Emilia Romagna, ARPA - SIM, Area Idrologia, PARMA) for providing the Po discharge data.

References

Deutsch CV. and Journel AG., 1998 Geostatistical software library and user's guide: Oxford University Press, New York.

Kohonen T., 2001. Self-Organizing Maps. Springer Series in Information Sciences, Vol. 30, Springer, Berlin, Heidelberg, New York, 2001

Kuzmić, M., I. Janeković, J. W. Book, P. J. Martin e J. D. Doyle, 2006. Modeling the northern Adriatic double-gyre response to intense bora wind: A revisit. *J. Geophys. Res.*, 111, C03S13, doi:10.1029/2005JC003377.

Liu Y. e Weisberg R.H., 2006. Sea Surface temperature patterns on the West Florida shelf using Growing Hierarchical Self-Organizing Maps. *Journal of Atmospheric and Oceanic Technology*, 23, pp325-338.

Solidoro C., Bastianini, M. Bandelj V., Bellafiore D., Codermatz R., Cossarini G., Melaku Canu D., Ravagnan E. Trevisani S., Current State, scale of variability and decadal trends of biogeochemical properties in the Northern Adriatic Sea. This Issue.

Ursella L., Poulain PM. e Signell R.P., 2007. Surface drifter derived circulation in the northern and middle Adriatic Sea: Response to wind regime and season. *J. Geophys. Res.*, VOL. 112, C03S04, doi:10.1029/2005JC003177

Zavatarelli M, Raicich F, Bregant D., Russo A., Artegiani A. 1998 Climatological biogeochemical characteristics of the Adriatic Sea *Journal of Marine Systems* 18, pp. 227–263

BIOGEOCHEMICAL PROPERTIES IN THE COASTAL AREA OF THE NORTH-WESTERN ADRIATIC SEA

Cosimo Solidoro¹, Vinko Bandelj¹, Gianpiero Cossarini¹, Donata Melaku Canu¹,
Sebastiano Trevisani¹, Mauro Bastianini²

*1 Dipartimento di Oceanografia, Istituto Nazionale di Oceanografia e di Geofisica
Sperimentale OGS,*

2 Istituto di Scienze del Mare, ISMAR- CNR, Venezia

Riassunto

Il lavoro presenta un'analisi delle caratteristiche, stato e scale di variabilità spazio-temporali, delle proprietà biogeochimiche della fascia costiera nord-occidentale del Mar Adriatico, e delle relazioni fra queste e la presenza di fiumi e lagune costiere lungo la costa medesima. L'analisi è basata su un insieme di dati provenienti dall'integrazione dei risultati dei programmi di monitoraggio costiero promossi dalle autorità regionali e da diversi programmi di ricerca oceanografica condotti in questa area. Sono state identificate le distribuzioni spaziali tipiche per ogni stagione di nutrienti e clorofilla a, ed è stata derivata una prima descrizione delle dinamica nell'area. La decomposizione della variabilità del data base costiero nelle componenti spaziali e temporali, ottenuta per mezzo di un analisi Empirical Orthogonal Functions, unitamente ad i risultati di una analisi di ordinamento vincolato (Redundancy Discriminant Analysis), in cui si è cercato di quantificare l'importanza della posizione spaziale nel determinare i valori delle variabili chimico fisiche, hanno permesso di derivare una partizione dei transetti in gruppi di stazioni 'omogenee' in termini di comportamento trofico. La classificazione che ne emerge ha un razionale geografico, parzialmente quantificato dalla RDA, e può essere interpretata sulla base della prossimità dei diversi gruppi a diversi elementi forzanti, quali fiumi maggiori, fiumi minori, piccole lagune costiere e laguna di Venezia. La classificazione proposta è coerente con quella già proposta in letteratura sulla base di considerazioni soggettive, e ne rappresenta anzi una corroborazione oggettiva oltre che un affinamento in termini di risoluzione spaziale ed una spiegazione in termini di processi fisici soggiacenti. E' quindi possibile caratterizzare ogni gruppo, in termini di valori medi e variabilità stagionale, ed offrire termini di riferimento precisi con cui confrontare eventuali anomalie.

Abstract

In this paper we present an assessment of present state and scales of variability of biogeochemical properties along coastal zone of the North Western Adriatic Sea, and discuss emerging properties in view of the influence of water runoff from many rivers, interaction with the lagoons (Venice and Caorle) and influence of the open sea.

The analysis relies on a data set obtained by integrating experimental observations collected in the frame of monitoring programs enforced by Regional Water Authority and of oceanographic research projects on the Northern Adriatic Sea. Observations cover last 20 years, and provide a robust base for assessment of present state and scales of variability for temperature, salinity, nutrients, dissolved oxygen and chlorophyll a.

Results emphasize the existence of high spatial variability along the coastal area, depending on the influence of exchanges with the coastal lagoon and inputs from rivers. A set of multivariate analysis (PCA, EOF, RDA) indicates that several subarea can be identified, basing on trophic conditions, and that these groups reflect the presence of different sources potentially impacting the water quality status, such as the large rivers in the southern part, the minor rivers in the northern one and the presence of the lagoon of Venice. A comparison of values assumed by the trophic index TRIX indicates that the latter is the most oligotrophic subarea, a fact that underline the role of the lagoon in reducing nutrient loads in this zone.

Results represent a contribution to the characterization of the waters of Northern Adriatic Sea, to the comprehension of interactions of these waters with coastal waters, including the Lagoon of Venice, and an updated climatology of the basin, which can be used as an important reference term form assessment of anomalous behavior and future changes

1 Introduction

Coastal area are characterized by high variability in chemical, physical, and biological parameters, because of the interaction among different coexisting processes and sources of disturbances, including inputs of nutrients from rivers, exchanging with the lagoons, bentic-pelagic coupling, anthropogenic impacts.

On the other hand a proper management of these area, requires a objective definition of the status and scale of variability of main biogeochemical parameters, as well as a comprehension of the underlying main causes-effects relationships among stressors, abiotic factors and living organisms, as a prerequisite for the understanding of the basic mechanisms of ecosystem functioning, and for a realistic implementation of water conservation regulations.

Within the frame of the project "Climatologia e qualità delle acque costiere della regione veneto", funded by CORILA and endorsed by LOICZ as a relevant LOICZ project, we retrieved and collated data from different projects, and performed an integrated analysis with the specific aim of performing this task. In particular, we tried to derive a climatological description of biogeochemical observations on the Northern Adriatic Sea, based on an update, and quality checked, data base which included results monitoring programs enforced by Regional Water Authority and of oceanographic research projects on the Northern Adriatic Sea. Observations cover last 20 years, and provide a robust base for assessment of present state and scales of variability for temperature, salinity, nutrients, dissolved oxygen and chlorophyll a.

Results represent a contribution to the characterization of the coastal waters of Northern Adriatic Sea, to the comprehension of interactions of these waters with the Lagoon of Venice, and an updated climatology of the area, which can be used as an important reference term form assessment of anomalous behaviour and future changes

2 Study area and data set

The analysis focused on the coastal area of the Adriatic Sea in front of the lagoon of Venice, from the mouth of Tagliamento to the Po river Delta. Along this coast several major rivers discharge freshwater and nutrients, drained over an area vastly urbanized and characterized by intensive agriculture land use.

The dataset consists of the integration of two data sets. The first one is the data set compiled in the same project for analyzing the northern Adriatic Sea, and described in Solidoro et al. 2008 (this issue). The second one is made by the observation collected along a number of transects orthogonal to the coast in the frame of the monitoring programs promoted by regional water authority, Each transect consists of 3 points, located at 500m, 926 and 3704m from the coast (Fig. 1). Observation included main physical and water quality parameters, and covered the period from 1986 to 2004, with monthly frequency. The number and location of the transects varied along the years, but a subset of 5 transects exist, which was maintained all over the period.

The northern Adriatic is a shallow sea, influenced by the discharges of important river (Po and Adige) on the western part, and by intrusion of highly saline waters from the southern Adriatic basin along the eastern coast (Aubry et al., 2004). General circulation is cyclonic and due to fresh water input, along the western coast a transition zone between shallow mesotrophic and saline oligotrophic off-shore waters. This frontal area is located at 8-16 km from the coast (Aubry et al., 2004, Solidoro et al. 2008).

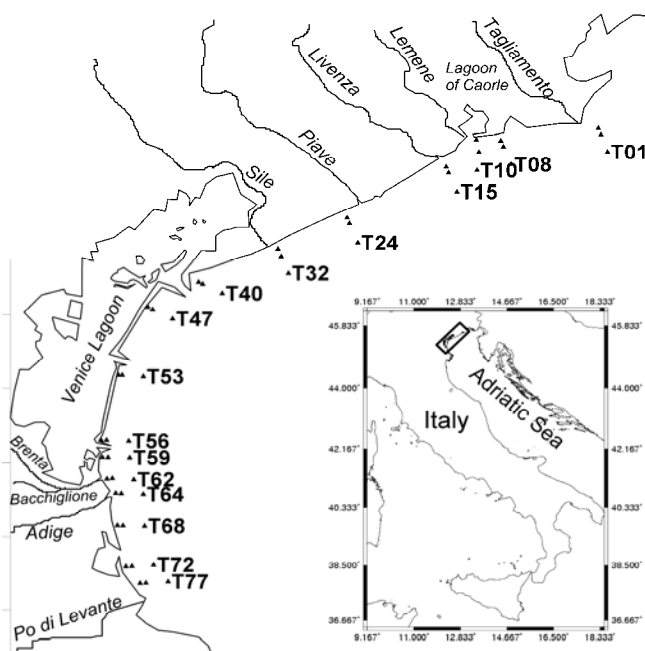


Fig 1 – Location of the stations of the dataset maintained by the regional water authority. Each transect consists of 3 stations coded as 1 (inshore), 2 (intermediate) and 3 (off-shore) in the text.

3 Present state and scales of variability

The assessment of present day typical values and scales of variability for biogeochemical properties has been identified by computing the seasonal spatial distributions (maps), which give for each of the considered variable the value expected for each season in each different area. The spatial distributions has been obtained by spatial interpolation of seasonally averaged values, by using a moving average methods, and considering the medians as the proper measures. The interpolation procedure used a radius of 15 km and a minimum of 10 data. This choice resulted as the trade off between the detail request to model coastal area and the number and coverage of available observation. Results are resumed in fig. 2 and 3 for temperature, salinity, nutrients (nitrate, ammonia, phosphate, silicates), dissolved oxygen and chlorophyll a

Visual inspection of the evolution of typical spatial distribution enable one to identify important feature of the area. In particular it is possible to recognize the high variability exist not only between the coastal area and the off shore region, as observed in Solidoro et al. 2008, but also along the coast itself, with higher concentration of nutrient and chlorophyll in the southern part, close to the Po river, and minima in front of the lagoon of Venice. Also both the plumes of northern and southern rivers can be observed. The emerging interpretation is that river mouths are the main forcing of the system, and that distance from the them is a key factor in determining the characteristic of a site. On this respect, the lagoon physically separates the coastal area from the mouth of rivers discharging within the lagoon, and exports waters to the sea only after that dilution and biological processes taking place within the lagoon abate the nutrient loads.

Furthermore, the analysis of descriptive statistic computed over the observations referred to the coastal dataset collected by the regional water authority (Fig. 1), evidences that variability of biogeochemical properties always is higher than 100% of the median values, while a smaller range is associated to physical parameters. It is worth to mention also the fact that concentration of phosphate was lower than 0.07 $\mu\text{mol/l}$ in half of the samples.

	median	25th percentile	75th percentile	CV%
Temperature (°C)	19.85	12.48	24.1	58.5
Salinity	32.53	29.55	34.38	14.8
Density (kg/m ³)	22.71	20.36	24.58	18.6
Ph	8.21	8.15	8.26	1.3
Oxygen (ml/dm ³)	5.61	5.09	6.22	20.1
OD%	101.5	94.69	109.39	14.5
N-NH ₃ (μmol/l)	0.77	0.34	1.54	155.8
N-NO ₂ (μmol/l)	0.40	0.22	0.67	112.5
N-NO ₃ (μmol/l)	11.40	5.17	21.5	143.2
Si-SiO ₄ (μmol/l)	7.16	3.96	12.98	126.0
P-PO ₄ (μmol/l)	0.070	0.03	0.17	200.0
Chlorophyll a (mg/l)	2.1	1.24	3.73	118.6

Tab 1 – median and percentiles of biogeochemical properties.

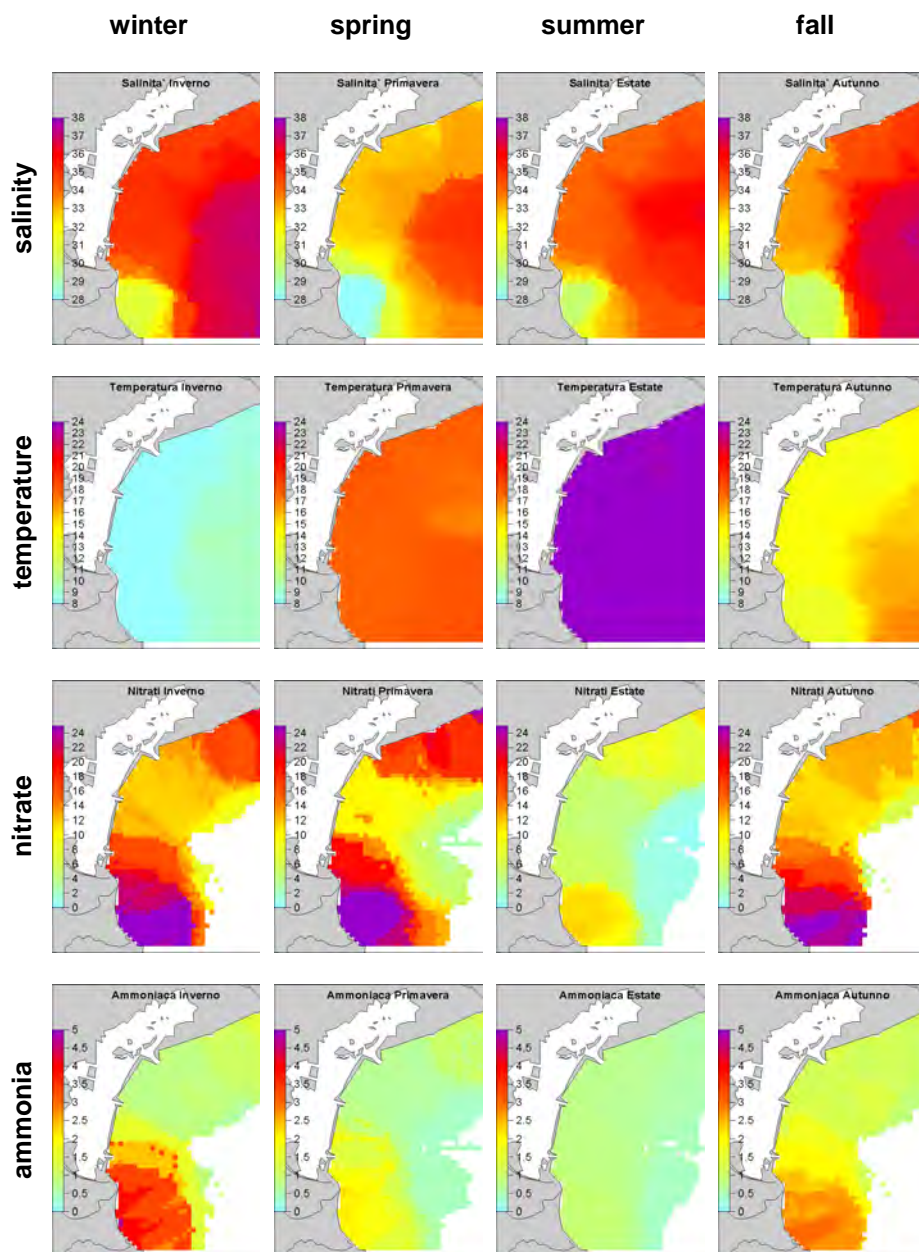


Fig 2 – typical seasonal evolution of spatial distribution for biogeochemical parameters.

The classification of the sampling locations of the coastal dataset was performed comparing the results of Empirical Orthogonal Functions analysis and Redundancy Analysis. The analysis referred to the period 1989-2001, since during this period the dataset was almost regular and contiguous in all of the sampling locations, except for data in winter of 1991, 1994 1995 and January of 1996 and 1999.

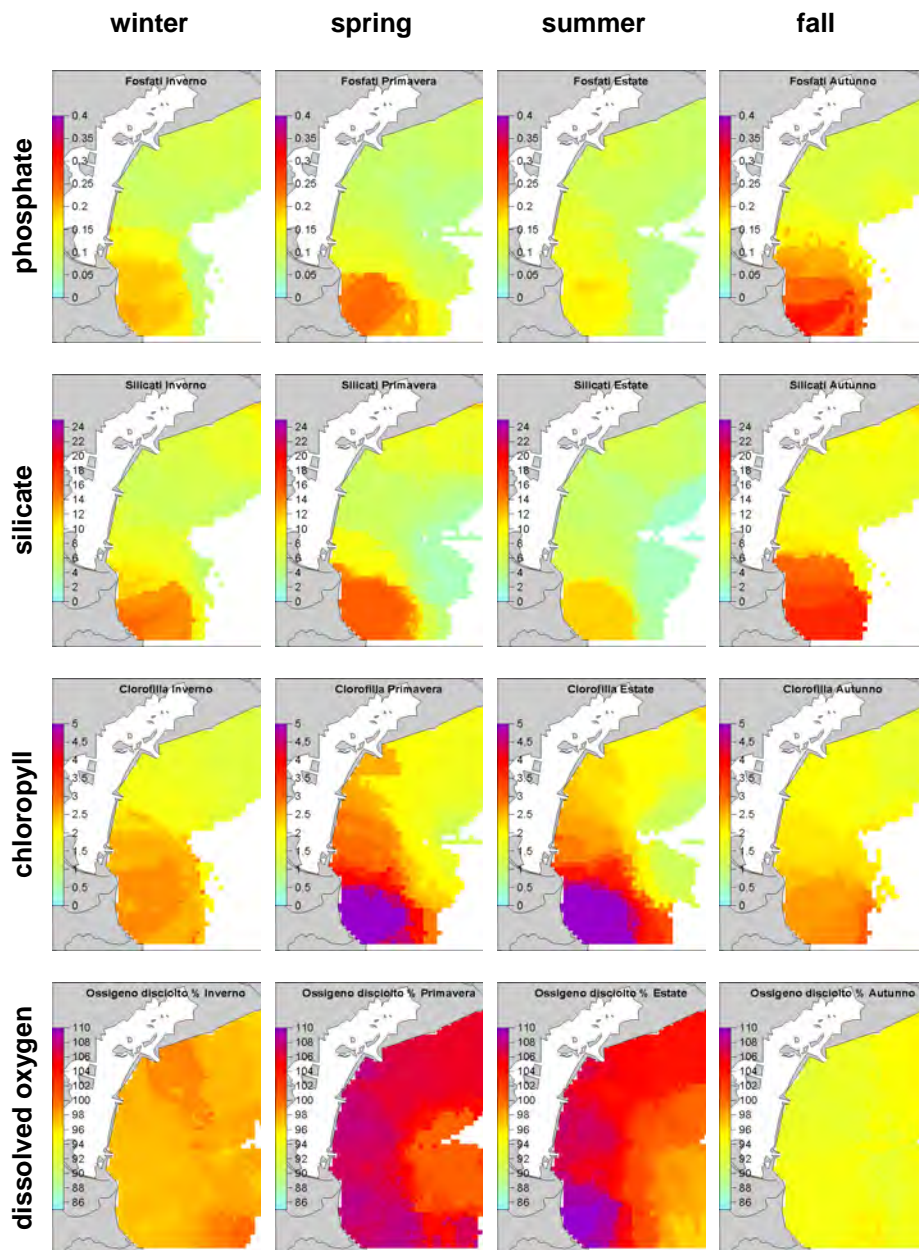


Fig 3 – typical seasonal evolution of spatial distribution for biogeochemical parameters.

Empirical Orthogonal Functions - EOFs - method allows for a separation of data information into spatial functions “spatial factors” and time-varying amplitudes, $D(x, t) = \sum A(x) * b(t)$. The spatial factors $A(x)$ are orthogonal and they are found by maximizing the residual variance, such that the major part of the variance from a time series of spatial data is concentrated in a few new dimensions: the spatial factors. The coefficient $b(t)$ give the importance at time t of each of the factor (Fig. 4).

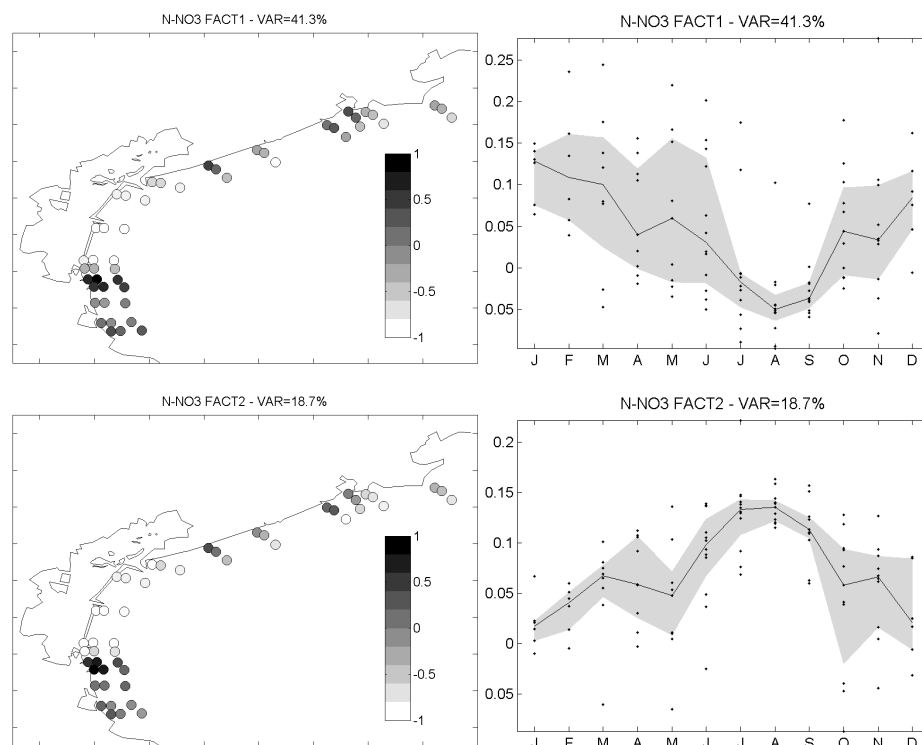


Fig 4 – Spatial factors and monthly mean evolution of temporal mode for first 2 modes of NO₃.

Redundancy Analysis (RDA) is a constrained ordination technique, which give a projection of original data in a reduced space spanned by axes which can be modelled as multiple linear regression of a predefined set of explanatory variables. In this way it is possible to analysis the variability of a set of variables in terms of the variations of a second set of variables.

In our case the variability in biogeochemical properties has been explained in terms of the categorical variable '*position along the coast*', suitably coded through dummy variables.

Results give a clusterization of the sampling sites in 7 groups, and proofed that such a classification is geographically meaningful, and reflect the presence of different sources potentially impacting the water quality status, such as the large rivers in the southern part, the minor rivers in the northern one and the presence of the lagoon of Venice. A comparison of values assumed by the trophic index TRIX indicates that the latter is the most oligotrophic subarea, a fact that underline the role of the lagoon in reducing nutrient loads in this zone.

Basically seven groups can be distinguished:

- Group 1 corresponds to sampling points of the transect T01, T08 and T24 that are located near Tagliamento and Piave rivers. These two rivers have a considerable mean flow rate of 97 and 54 m³/s, but are considered torrent since they come from the alps and are characterized by drought period during winter, high discharge rates during spring and fall and low discharges during summer (Raicich, 1994).
- Group 2 is composed by the sampling locations coded 1 and 2 of the transects T10, T15 and T32. Livenza, Lemene and Sile are the rivers whose

discharges influence this group. These three rivers are more regular streams originating from off-spring in the plan, with a mean discharge rate of 45, 88 and 53 m³/s (Raicich, 1994). This group differs from the previous group because of higher level of nitrate and silicates.

- Group 3 consists of sampling locations coded as 3 of transects T10, T15 and T32. Respect the previous groups these sampling points are less influenced by rivers discharges, since fresh water plum is presumable deviated on the right along coast by the general anticyclonic circulation of the Northern Adriatic Sea
- Group 4 consists of transects T40, T47, T53 and T56. These area is strongly influenced by the exchanges with the lagoon of Venice. Inside the lagoon, discharges from rivers account for less than 40 m³/s (Collavini et al, 2005). And even if there are important nutrient rich point sources, from urban and industrial areas (Collavini et al, 2005), the lagoon acts as a filter (Solidoro et al., 2004) and these coastal area represented the one with the lowest nutrient and chlorophyll contents;
- Group 5 is composed of transect T59 and highlights the sharp transition between the very different condition of the previous and the following group
- Group 6 consists of stations of transects T62 and T64 that are influenced by the discharges of the Adige, Brenta and Bacchiglione rivers. These 3 rivers account for the 47% of the fresh water discharges along the Veneto coastline, excluding Po and the contribution of the rivers inside the lagoon of Venice. They drain a huge and densely populated area and their impact on the coastal area is clearly evident; highest concentration of all the nutrients and of chlorophyll were registered in these sampling points.
- Group 7 contains transects T62, T72 and T77 that are positioned southward respect the sixth group. The conditions of this group are similar to the previous since the costal circulation deviates west-southward the plum of the Adige. Distance from the mouth of the river and the presence of small coastal lagoon contribute to dilute nutrients but concentration of chlorophyll in this group is higher than that of the previous one.

The proposed subdivision in seven groups differs from the one proposed by Aubry et al. (2004) since it was based on differences in chemical and physical conditions between sampling locations and a *posteriori* the subdivision has been explained on the basis of the processes and source of variability, setting a rational geographic criteria.

Finally, it is possible to derive median value and interquartile range for each of the groups. (table 2 and 3 for fall-winter and spring-summer, respectively).

Results represent a contribution to the characterization of the coastal waters of Northern Adriatic Sea, to the comprehension of interactions of these waters with the Lagoon of Venice, and an updated climatology of the area, which can be used as an important reference term form assessment of anomalous behaviour and future changes

Tab 2 – median values and interquartile range for different variables in winter fall. Maxima of each variable are shaded in grey. Minima are underlined.

	Group 1	Group 2	Group 3	Group 4	Group 5	Group 6	Group 7
Temp	10.4 (3.4)	10.3 (3.1)	10.4 (3.3)	10.2 (3.3)	10.0 (3.6)	10.0 (3.4)	<u>9.9</u> (3.2)
Sal	33.3 (1.7)	31.2 (2.1)	32.8 (1.7)	34.2 (1.4)	33.8 (1.5)	31.3 (3.9)	<u>29.9</u> (4.0)
Dens	25.3 (1.7)	23.8 (2.1)	24.8 (1.9)	26.2 (1.7)	25.8 (1.8)	23.7 (3.3)	<u>22.8</u> (3.1)
pH	8.16 (0.06)	<u>8.15</u> (0.05)	8.17 (0.06)	8.18 (0.05)	8.19 (0.04)	8.18 (0.04)	8.19 (0.05)
Oxyl	6.0 (0.5)	6.1 (0.6)	6.0 (0.6)	<u>5.9</u> (0.6)	6.0 (0.6)	6.0 (0.6)	6.3 (0.5)
Oxy sat	95.8 (4.4)	95.1 (4.7)	95.6 (4.6)	95.4 (5.7)	95.7 (5.5)	<u>94.6</u> (5.0)	96.4 (4.8)
Ntot	17.0 (7.4)	26.5 (11.8)	16.8 (8.0)	<u>11.9</u> (3.8)	13.5 (5.4)	35.3 (17.9)	27.0 (12.1)
NH3	0.92 (0.45)	1.42 (0.73)	0.98 (0.56)	<u>0.70</u> (0.41)	1.31 (1.06)	3.83 (2.88)	2.05 (1.27)
NO2	0.48 (0.18)	0.62 (0.22)	0.53 (0.19)	<u>0.46</u> (0.18)	0.56 (0.25)	0.98 (0.35)	0.75 (0.25)
NO3	15.6 (7.3)	24.9 (11.4)	15.6 (7.3)	<u>10.5</u> (3.6)	11.3 (4.6)	29.8 (15.8)	23.9 (11.1)
SiO4	8.6 (3.8)	12.3 (5.0)	9.2 (4.2)	<u>6.1</u> (2.5)	6.7 (3.1)	16.8 (8.5)	16.6 (8.2)
PO4	0.05 (0.04)	0.12 (0.10)	0.08 (0.07)	<u>0.04</u> (0.04)	0.10 (0.08)	0.30 (0.23)	0.18 (0.14)
CHLA	<u>1.4</u> (0.6)	1.5 (0.6)	1.5 (0.5)	1.8 (0.6)	2.1 (1.1)	2.2 (1.2)	2.1 (1.2)

Tab 3 – median values and interquartile range for different variables in spring-summer. Maxima of each variable are shaded in grey. Minima are underlined.

	Group 1	Group 2	Group 3	Group 4	Group 5	Group 6	Group 7
Temp	22.9 (2.5)	22.8 (2.5)	22.9 (2.7)	22.9 (2.7)	22.4 (2.6)	<u>22.2</u> (2.8)	<u>22.2</u> (2.7)
Sal	32.8 (1.9)	30.6 (2.6)	33.4 (1.5)	33.9 (1.3)	32.8 (2.0)	30.3 (3.4)	<u>28.9</u> (3.8)
Dens	22.3 (1.5)	20.8 (2.0)	22.6 (1.3)	23.1 (1.1)	22.5 (1.9)	<u>20.5</u> (2.7)	19.3 (3.0)
pH	8.21 (0.05)	<u>8.20</u> (0.04)	8.21 (0.04)	8.23 (0.05)	8.23 (0.05)	8.24 (0.06)	8.27 (0.07)
Oxyl	5.3 (0.4)	5.4 (0.5)	<u>5.2</u> (0.4)	5.3 (0.5)	5.5 (0.5)	5.6 (0.5)	5.8 (0.6)
Oxy sat	<u>104.3</u> (5.6)	105.7 (6.7)	104.8 (5.7)	106.1 (6.8)	106.0 (8.0)	105.8 (7.8)	108.8 (10.4)
Ntot	10.2 (6.3)	17.9 (10.2)	7.9 (5.4)	<u>5.1</u> (3.7)	6.4 (5.8)	18.1 (11.9)	13.2 (8.6)
NH3	0.59 (0.39)	0.83 (0.55)	0.52 (0.28)	<u>0.49</u> (0.28)	0.61 (0.42)	1.41 (1.22)	0.69 (0.50)
NO2	0.28 (0.14)	0.46 (0.20)	0.23 (0.11)	<u>0.19</u> (0.11)	0.29 (0.21)	0.59 (0.40)	0.42 (0.21)
NO3	9.1 (6.1)	16.6 (9.8)	7.2 (5.1)	<u>4.2</u> (3.7)	5.4 (5.5)	15.8 (10.7)	11.9 (8.4)
SiO4	5.9 (3.2)	9.0 (4.6)	4.6 (2.3)	<u>3.7</u> (2.0)	4.4 (2.7)	11.0 (7.3)	10.7 (7.6)
PO4	0.05 (0.05)	0.07 (0.07)	<u>0.04</u> (0.04)	<u>0.04</u> (0.04)	0.07 (0.04)	0.14 (0.12)	0.08 (0.07)
CHLA	1.6 (0.7)	2.4 (1.1)	<u>1.5</u> (0.6)	2.1 (1.0)	3.8 (1.8)	4.5 (2.3)	5.0 (2.2)

References

- Aubry F. B., Berton A., Bastianini M., Socal G., Aciri F., 2004. Phytoplankton succession in a coastal area of the NW Adriatic, over a 10-year sampling period (1990–1999). *Continental Shelf Research*, 24, pp. 97–115.
- Collavini, F., Bettioli, C., Zaggia, L., Zonta, R., 2005. Pollutant loads from the drainage basin to the Venice Lagoon (Italy). *Environment International*, 31, 939–947.
- Degobbis, D., Precali, R., Ivancic, I., Smolaka, N., Fuks, D., Kveder, S., 2000. Long-term changes in the northern Adriatic ecosystem related to anthropogenic eutrophication. *International Journal of Environmental Pollution* 13, 495–533.
- Raicich F., 1994. Note on the flow rates of the Adriatic rivers. Technical report RF02/94. CNR-Istituto Sperimentale Talassografico, Trieste, Italy.
- Solidoro C., Pastres R., Cossarini G., Ciavatta S., 2004a. Seasonal and spatial variability of water quality parameters in the lagoon of Venice. *Journal Marine System*, vol. 51, pp. 179–189.
- Solidoro C., Bastianini, M., Bandelj V., Bellafiore D., Codermatz R., Cossarini G., Melaku Canu D., Ravagnan E., Umgiesser G., Vazzoler M. 'Climatologia e qualità delle acque costiere della Regione Veneto'. Rapporto finale linea 3.13 programma di ricerca CORILA 2004–2006
- Solidoro C., Bastianini, M., Bandelj V., Bellafiore D., Codermatz R., Cossarini G., Melaku Canu D., Ravagnan E., Trevisani S., 2008. Current State, scale of

variability and decadal trends of biogeochemical properties in the Northern Adriatic Sea. This Issue.

RESEARCH LINE 3.14

**Erosion and sedimentation processes in the
Venice lagoon**

PRELIMINARY EXPERIMENTS ON TIDAL NETWORK GROWTH AND DEVELOPMENT

Luigi D'Alpaos, Luca Carniello, Andrea Defina, Stefano Lanzoni, Francesca M. Susin

Dipartimento IMAGE, Università degli Studi di Padova

Riassunto

Nel presente contributo vengono presentati una serie di esperimenti di laboratorio aventi lo scopo di riprodurre la formazione di un tipico ambiente lagunare per effetto della sola marea. Nel corso degli esperimenti si è potuto analizzare la nascita e lo sviluppo di una rete di canali a marea mettendo in luce il ruolo svolto dalle caratteristiche della forzante mareale nello sviluppo della rete stessa. Le configurazioni sperimentali sono state analizzate anche avvalendosi di modelli numerici che hanno permesso di valutare delle caratteristiche morfometriche delle reti e di studiare i processi idrodinamici e di trasporto solido durante le varie fasi dell'evoluzione morfologica.

Abstract

In this paper we present the first results of a series of laboratory experiments carried out in a large experimental apparatus, aimed at reproducing a typical lagoonal environment subject to tidal forcings. We observed the growth and development of a tidal network and analyzed its most relevant features, taking into account the role played by the characteristics of the tidal forcings in driving the development of channelized patterns. Such experiments were designed in order to improve our understanding of the main processes responsible for channel network ontogeny and evolution. Mathematical and theoretical analyses of network configurations were also carried out through the use of simplified and complete morphodynamic models. In particular, we analyzed the evolution in time of the morphometric characteristics of the developed networks, and studied the hydrodynamics and sediment transport processes related to different channel configurations.

1 Introduction

Tidal channel networks exert a strong control on hydrodynamics, sediment and nutrient dynamics within tidal environments. Improving our understanding of their origins and evolution is of critical importance when addressing issues of conservation of tidal systems.

A wide literature exists, developed especially in the last three decades, describing the hydrodynamics of tidal systems and their morphodynamic evolution [see e.g. Allen, 2000; Friedrichs & Perry, 2001, for thorough reviews]. In spite of their fundamental role in driving the morphological evolution of tidal basins, only in the last few years mathematical and numerical models analyzing the morphogenesis and long-term morphodynamic evolution of tidal channels

have been proposed [Schuttelaars & de Swart; 2000, Lanzoni & Seminara, 2002; Fagherazzi & Furbish, 2001; Fagherazzi & Sun, 2004; D'Alpaos et al., 2005, 2007]. Moreover, even though the development of tidal channel networks has been analyzed both through field observations and conceptual models [Pestrong 1965; French & Stoddart 1992] the description of the processes leading to the initiation and early development of tidal networks still lacks a proper de-lineation. In particular, attempts to investigate such processes on the basis of controlled laboratory experiments have not been pursued, except for those recently carried out by Tambroni et al. [2005], who investigated the morphodynamic evolution of the bottom of a single straight tidal channel closed at one end and connected at the other end to a rectangular basin representing the sea. Towards the goal of gaining fundamental knowledge into the description of the main physical processes responsible for tidal network ontogeny, we carried out a series of laboratory experiments in a large experimental apparatus schematizing a typical lagoonal environment, subject to tidal forcings.

We furthermore used simplified and complete hydrodynamic models to carry out numerical and theoretical analyses of the experimental network configurations and to compare the relevant features of experimental and observed morphologies.

2 Experimental Apparatus

The experimental apparatus, schematically depicted in Fig. 1, consists of two adjoining basins reproducing schematically the sea and the lagoon.

The lagoon basin is 5.3x4.0m wide, while the much deeper adjacent sea basin is 1.6x4.0m wide. The bed of the lagoon was uniformly covered with a 30cm-thick layer of sediments during the experiments. The sea is separated from the lagoon by a barrier of wooden panels; the lagoon inlet (whose shape and width may be varied) is located in the middle of this barrier while in front of the inlet a shelf enables to reproduce the gentle slope of the sea bed (Fig. 1).

The tide is generated at the sea by a vertical steel sharp-edge weir, oscillating vertically. The water continuously flowing over the weir is collected to a separated tank, where a set of pumps re-circulates the flow.

An ad hoc software has been implemented to drive the weir, allowing us to reproduce a sinusoidal tide of fixed amplitude and period, oscillating around a prescribed average level. The software continuously corrects the motion of the weir on the basis of a feedback instantaneously controlled by water-level measurements at the sea, carried out through ultrasonic probes.

A computer-driven pantograph is used to survey bottom elevations within the lagoon. The apparatus consists of a laser system (300 μm resolution) which measures bottom elevation coupled to an ultrasonic probe which simultaneously gauges the associated water level. The latter measurement is used to determine the local flow depth and to correct laser measurements from refraction effects induced by the presence of water. The bathymetric survey of

the lagoonal bottom, in fact, is carried out without stopping the experiment and drying the sediment surface, thus avoiding undesired perturbations of bed topography.

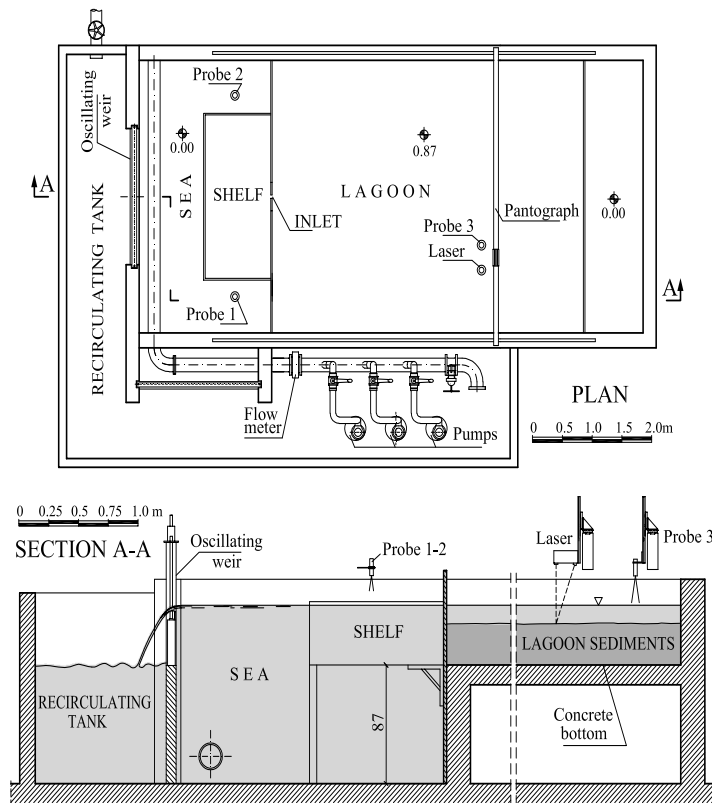


Fig 1 – Sketch of the experimental apparatus.

The sediments used in the experiments are cohesionless plastic grains, with density of 1041 kg/m^3 and median grain size, d_{50} , of 0.8 mm.

3 Experiments

The experiments carried out so far mainly aimed at understanding under which conditions a channel network develops. To this end various tides (i.e., characterized by different amplitude, period and mean level) and different shapes and dimensions of the tidal inlet have been considered.

Each experiment started forcing an initially flat bed topography with a given tidal wave. A tidal network was observed to form only for small enough values of the tidal amplitude (1.0-2.0 cm) and of the flow depth (1.0-2.0 cm) and for a mean water level allowing the drying of the sediment surface during the ebb phase. A tidal period of 8-12 minutes was chosen in order to avoid perturbing vortices and ensure the long-wave character of the tide.

In the presence of a too high tidal amplitude the sediments tended to be transported as suspended load, large dunes formed, and the growth of the channel network was inhibited. In any case, a wide scour, covered by dunes, formed in correspondence of the inlet. The channel network was eventually observed to originate only from the landward border of such a scoured region. It

is worthwhile to observe that bed load sediment transport was active during the whole experiment, while ebb and flood peak velocities promoted suspended load along the channels. Finally, in all the experiments the lagoon experienced a progressive net erosion, with the consequent reduction of its mean bottom level.

In the following we focus our attention on two typical experiments, denoted as Run 1 and Run 2.

3.1 Run 1

The forcing tide with amplitude of 2 cm and period of 8 minutes, was oscillating around a mean level equal to the initial bed elevation. A 0.50 m wide rectangular-shaped inlet was located at the center of the sea-lagoon boundary.



Fig 2 – Lagoon topography observed in Run 1 after: a) 1200 cycles b) 6000 cycles and in Run 2 after: c) 6000 cycles; d) 7710 cycles.

As pointed out before, a wide scour region rapidly formed in front of the inlet. After 220 tidal cycles a few isolated channels started to form at the landward edges of this scour region, beginning to cut the portions of the lagoon subject to draining. These channels progressively experienced a head cut-growth during the ebb phase and, after 500 cycles, some little ramifications began to form. After 1200 cycles, four main, nearly straight channels were present (Fig. 2a). The ramifications of these channels in some cases were unstable: some smaller creeks were observed to abandon a main channel to join another one. In some cases these smaller creeks migrated laterally, forming little bends. After 2300 cycles, the main channels lengthened significantly and at 2800 cycles three pronounced bends were observed to develop along one of these channels. However, the small scale bed forms, initially covering the deep scour facing the inlet, progressively extended throughout the lagoon, tending to destroy the channel network. In order to smooth out these undesired bed forms and enhance the growth of a well de-fined channel network, we slightly decreased the mean sea level (about 0.5 cm). Fig. 2b shows the bed configuration obtained after 6000 cycles, when the experiment was stopped.

3.2 Run 2

This experiment was characterized by a forcing tide with amplitude of 2 cm, period of 10 minutes, oscillating around a mean level 1.5 cm higher than the bed elevation. The width of the trapezoidal-shaped inlet varied from 0.05 m at the lagoon concrete bottom to 0.20 m at the sediment surface.

At the beginning of the experiment the mean sea level submerged the sediments during the whole tidal cycle. A wide scour region, covered by dunes, rapidly formed near the inlet. The scour was deeper than in Run 1 because of the larger values attained by the velocity (and hence by the bed shear stress) as a consequence of the narrower inlet. After 800 cycles, some isolated and unstable channel started to form at the landward boundary of the inlet scour. At 1300 cycles we reduced the mean sea level to allow draining of the sediment surface during the ebb phase and, soon after, a more defined tidal network began to form, characterized by three main channels that lengthened significantly during the following tide cycles. Some bends were also observed to form. The well developed small scale bed forms, previously observed to form in the main channels, tended to reduce sensibly their dimensions. Moreover, pronounced localized scours formed at the main junctions (Fig. 2d). The evolution was anyhow very slow and only in the last 1000 cycles the channels deepened appreciably, forming a more complex network, with some bends forming also along the main channels (Fig. 2c). The run was stopped after 7710 cycles.

4 Analysis of the experiments

Bed elevations acquired through the laser system and suitably corrected to account for refraction effects were used to produce topographic maps of the lagoon bed at various instants. Fig. 3 shows the distribution of bed elevations at four different instants of Run 1 and Run 2: the temporal evolution of channel networks clearly emerges.

In order to classify small scale bed forms, which were observed to form during both the experiments, we used the bottom topographies measured at the end of Run 1 and Run 2 to carry out some fixed bed numerical simulations. The 2D shallow water equations were solved numerically by using a semi-implicit staggered finite element model, based on Galerkin's approach. The equations were modified to deal with wet-drying processes in irregular domains [D'Alpaos & Defina, 1995; Defina, 2000; D'Alpaos & Defina, 2006].

The numerical results, obtained setting to $30 \text{ m}^{1/3}\text{s}^{-1}$ the Gauckler-Strickler friction coefficient, K_s , indicate that in Run 1 the higher values of both flow velocity U ($\sim 3.7 \text{ cm/s}$), and bed shear stress τ ($\sim 0.091 \text{ Pa}$), were attained during the ebb phase, in correspondence of the deep scour which formed in front of the inlet and in the first reaches of the channels departing from it. Secondary channel ramifications exhibited lower values of U ($\sim 2 \text{ cm/s}$) and τ ($\sim 0.0002 \text{ Pa}$).

A similar picture emerges from the simulation of Run 2 but with higher values of

both the velocity (~5.8 cm/s) and the bed shear stress (~0.24 Pa) in the scour facing the inlet and in the reaches of the two main channels developing from it. Conversely, secondary channel ramifications exhibited lower values of U (~ 1.5 cm/s) and τ (~ 0.0015 Pa).

The bed shear stress resulting from numerical calculation was used to determine the dimensionless Shields stress, τ^* :

$$\tau^* = \frac{\tau_0}{g \cdot (\rho_s - \rho) \cdot d} = \frac{u^{*2}}{\Delta \cdot g \cdot d} \quad (1)$$

where: d is the representative sediment grain size, g is the gravity constant, ρ and ρ_s are water and sediment specific weight, respectively, $u^*=(\tau^*/\rho)^{1/2}$ is the friction velocity, ν is the kinematic water viscosity, and $\Delta=(\rho_s-\rho)/\rho$ is the relative density of submerged sediment.

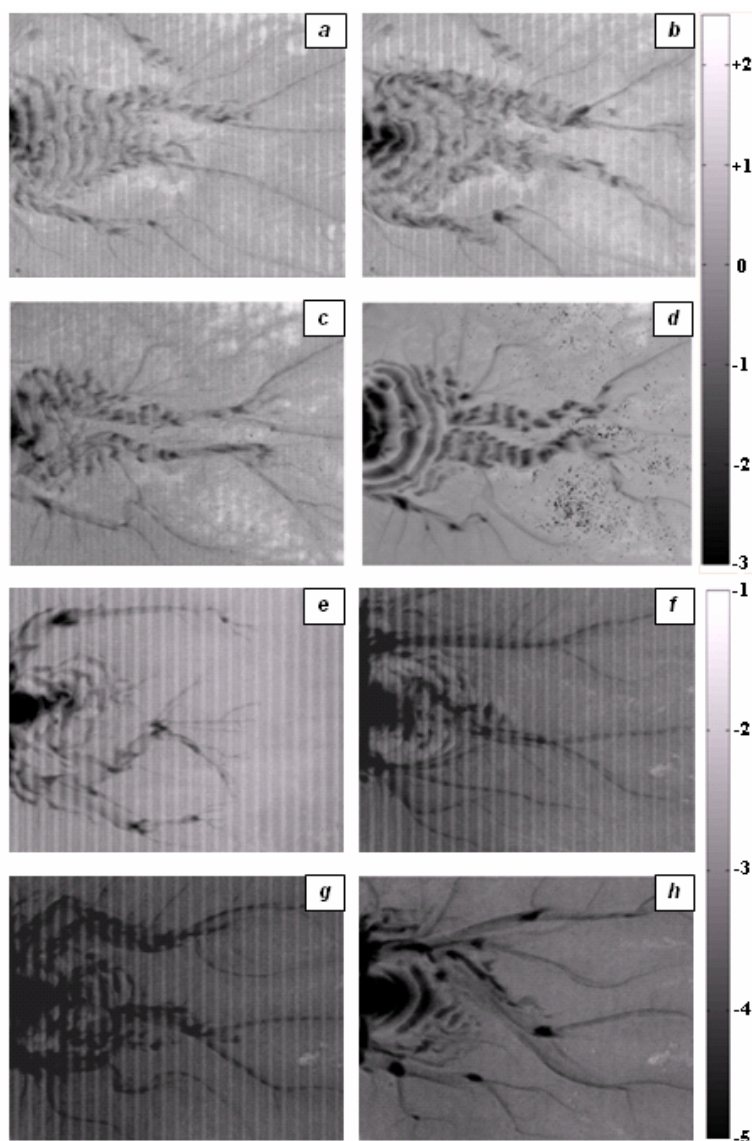


Fig 3 – Distribution of bottom elevations measured within the lagoon in Run 1 after: a) 1650 cycles; b) 2900 cycles; c) 3910 cycles; d) 5950 cycles; in Run 2 after: e) 2200 cycles; f) 6270 cycles; g) 6845 cycles; h) 7700 cycles. Elevations are referred to the initial uniform bottom elevation.

Fig. 4a,b show the spatial distribution of the excess Shield stress, $\tau^* - \tau_c^*$, during the ebb phases of Run 1 and Run 2, i.e., when bottom shear stress attains its maximum. The critical value τ_c^* for incipient sediment motion has been evaluated using the analytical relationship proposed by Brownlie [1981].

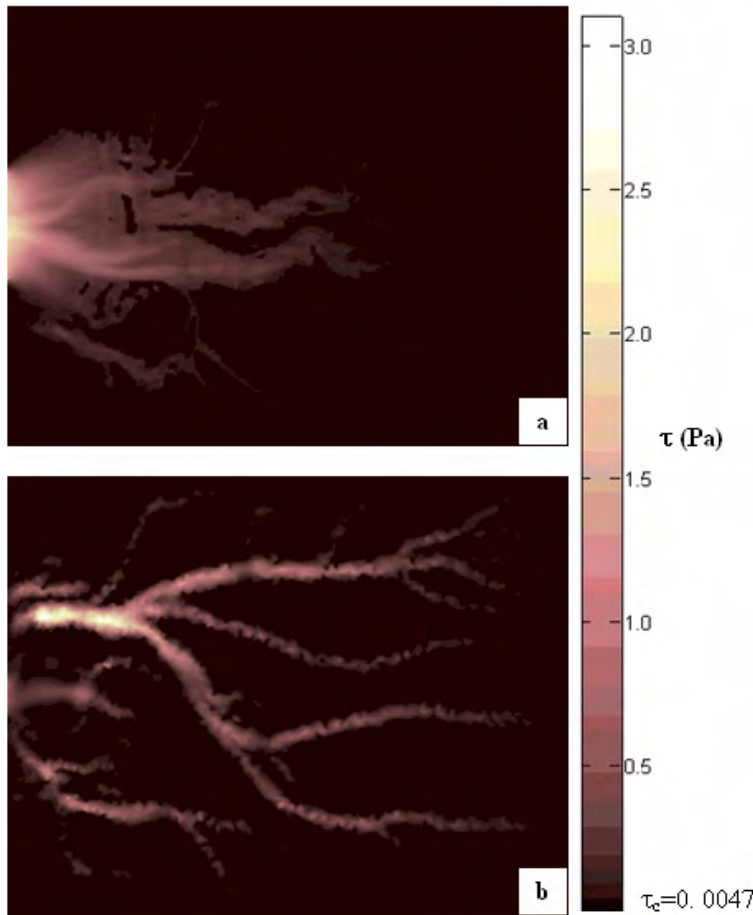


Fig 4 – Spatial distribution of the excess Shield stress, $\tau^* - \tau_c^*$, computed for the final configuration of Run 1 (a) and of Run 2 (b).

It clearly emerges that in both runs a large portion of the lagoon is interested by sediment transport. Additional analyses showed that choosing a different value of the representative grain diameter (e.g., d_{90}) does not significantly modify the percentage of lagoonal surface interested by sediment transport.

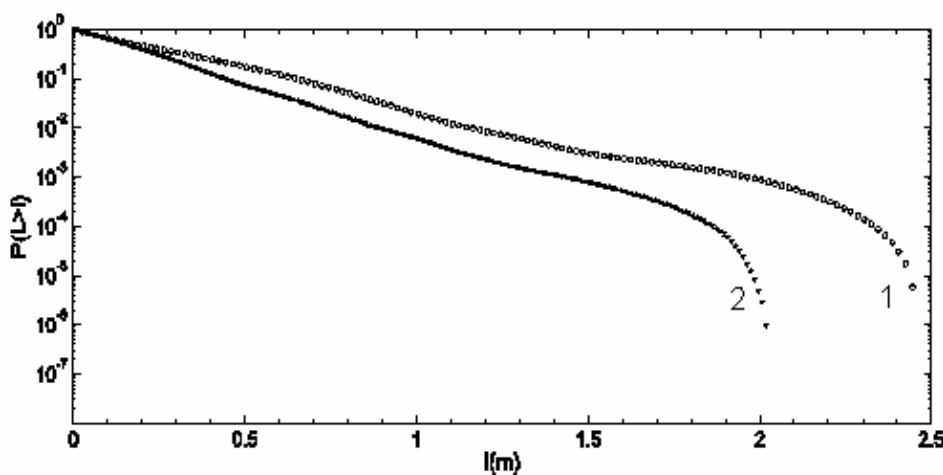


Fig 5 – Probability distribution of unchanneled lengths for the channel network observed at the end of Run 1 and Run 2.

We also carried out morphometric analyses of the experimental networks by using a simplified hydrodynamic model [Rinaldo et al., 1999a, b], successfully applied to the study of various tidal environments [Marani et al., 2003]. The hydrodynamic flow field obtained through this simplified model makes it possible to determine the unchanneled hydrodynamic flow path connecting any unchanneled site to the nearest tidal channel and to compute its length. The probability distributions of unchanneled flow lengths, ℓ , exhibits a linear trend in a semi-log plot (Fig. 5), suggesting the same type of exponential decay determined by Marani et al. [2003] in different areas of the Venice lagoon. Fig. 7 shows the two digitalized final network configurations of Run 1 and Run 2. In both runs, channel width, B , and channel depth, D , attained relatively small values, falling in the range 1-2 cm and 8-10 cm, respectively. The results shown in Fig. 7 suggest that, for a given channel, a nearly linear relationship exists between D and B .

Fig 6 – Border of final network configurations obtained in Run 1 (a) and Run 2 (b). Channels denoted by numbers 1, 2, 9 and 15 are those considered in the plots of Fig. 7 and Fig. 8.

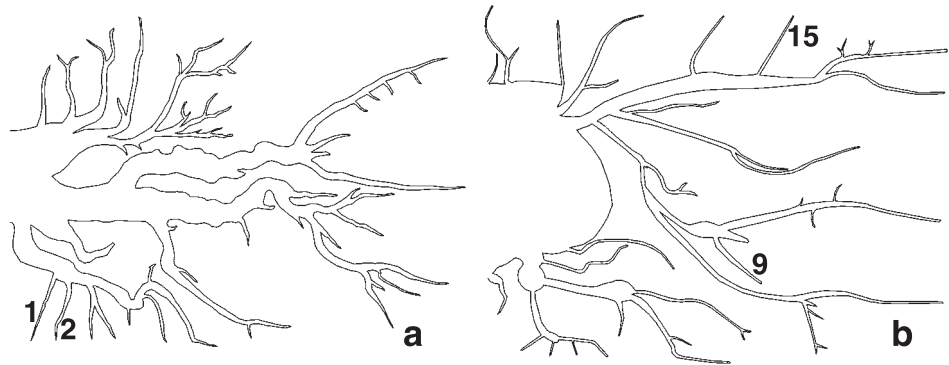
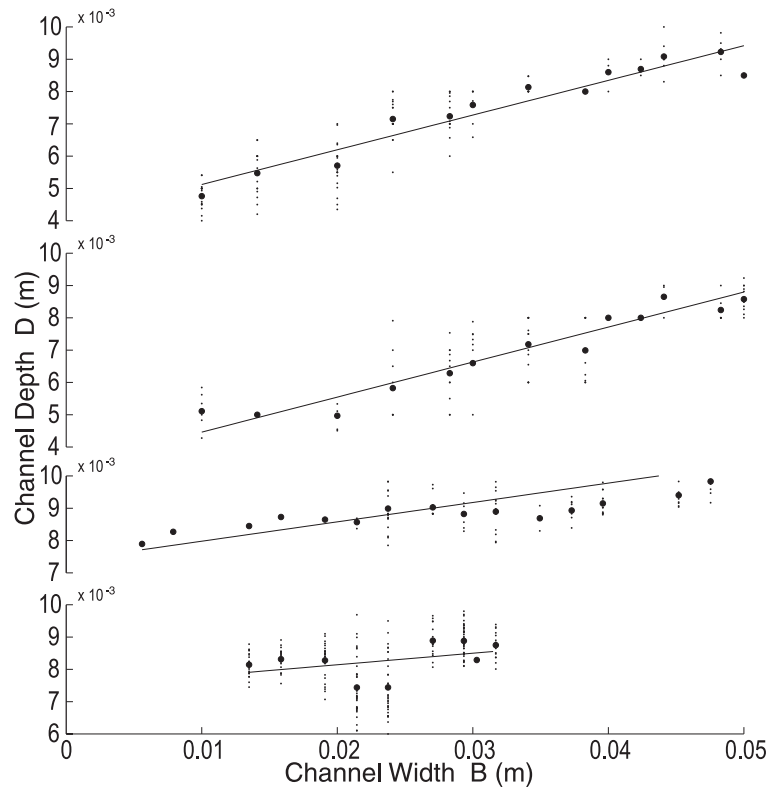


Fig 7 – Channel depth versus width for the cross sections of channels indicated in Fig. 6.



We finally reported in a semi-log plot channel width, B , versus the along channel intrinsic coordinate, s (Fig. 9). The results emphasize the progressive exponential widening experienced seaward by channels, which is typical of tidal environments [Lanzoni & Seminara, 1998; Marani et al., 2002].

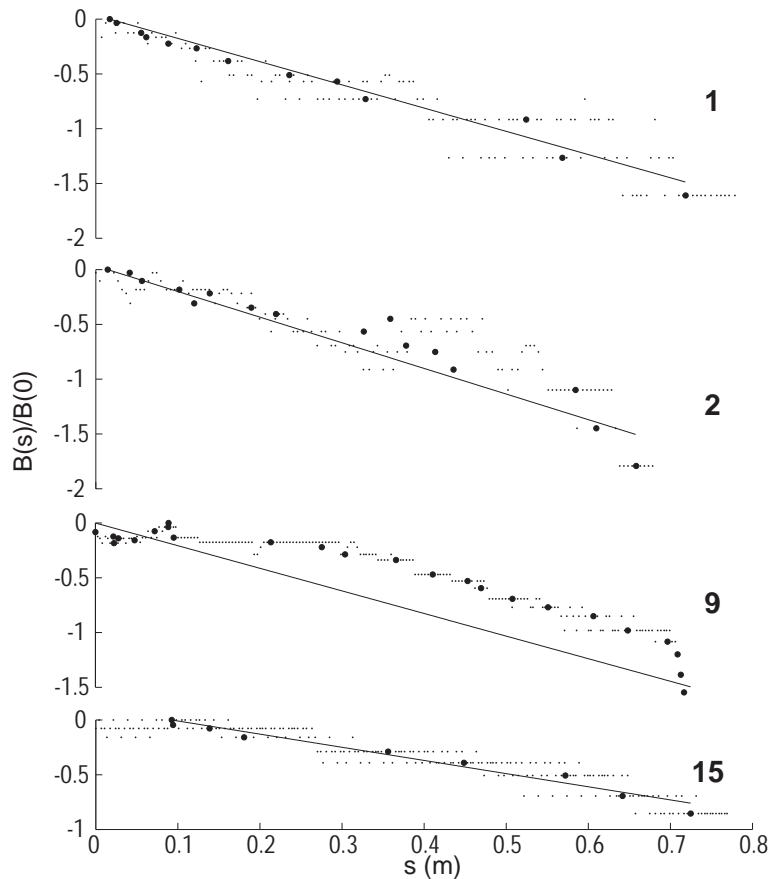


Fig 8 – Logarithm of the ratio $B(s)/B(0)$, with versus the intrinsic coordinate, s , for the channels indicated in Fig. 6. $B(s)$ is channel width at s , $B(0)$ is width at channel inlet.

Conclusions

The morphometric analyses of the laboratory generated tidal channels described in the present contribution suggest a close analogy with real networks. The similarity between field and laboratory probability distributions of unchanneled flow lengths suggests that present experiments can be used to get a better understanding of the morphodynamic processes responsible for the initial growth and subsequent development of channel networks within tidal basins.

Laboratory channel networks were observed to form, starting from an initially flat and horizontal bed, only for: i) low enough values of the flow depth; ii) a mean sea level allowing the drying of the bottom during the ebb phase; iii) a tidal period of about 8-12 minutes. Higher flow depths enhance the formation of bed forms (ripples and dunes) and prevent the formation of well defined channels. Channel networks were observed to form mainly through headward growth. The rate of network growth was very slow at the beginning of the experiment whereas as soon as a well developed network began to form, the

mean rate of channel elongation was approximately of 1.5-2 cm every 150 tidal cycles. After a quite rapid growth phase the tidal network appears to be subject only to small adjustments, thus supporting the usually adopted hypothesis that a time in the life of a tidal network exists during which it quickly cuts down the intertidal areas giving them a permanent imprinting. Such a process is later followed by slower elaborations including meandering and network contractions/expansions.

Clearly, a more systematic series of experiments is needed to further support the above findings.

References

- Allen, J. R. L. 2000. Morphodynamics of Holocene salt mar-shes: a review sketch from the Atlantic and Southern North Sea coasts of Europe. *Quat. Sci. Rev.* 19 (17-18), 1155-1231.
- D'Alpaos, A., S. Lanzoni, M. Marani, S. Fagherazzi & A. Rinaldo 2005. Tidal network ontogeny: channel initiation and early development. *J. Geophys. Res.* 110, F02001, doi:10.1029/2004JF000182.
- D'Alpaos, A., S. Lanzoni, M. Marani, & A. Rinaldo 2007. Landscape evolution in tidal embayments: Modeling the interplay of erosion, sedimentation and vegetation dynam-ics. *J. Geophys. Res.* 110, doi:10.1029/2006JF 000537.
- D'Alpaos, L. & A. Defina 1995. Modellazione matematica del comportamento idrodinamico delle zone di barena solcate da una rete di canali minori. Istituto Veneto di SS.LL.AA., Rapporti e studi, Vol. XII, 353-372.
- D'Alpaos, L. & A. Defina, 2006. Mathematical modeling of tidal hydrodynamics in shallow lagoons: A review of open issues and applications to the Venice lagoon. *Computer & Geoscience.* doi:10.1016/j.cageo.2006.07.009.
- Defina, A. 2000. Two Dimensional Shallow Flow Equations for Partially Dry Areas. *Water Resources Research*, vol.36, 11, 3251-3264.
- Fagherazzi, S. & D. J. Furbish 2001. On the shape and wid-ening of salt-marsh creeks. *J. Geophys. Res.*, 106(C1), 991-1003.
- Fagherazzi, S. & T. Sun 2004. A stochastic model for the formation of channel networks in tidal marshes. *Geophys. Res. Lett.* 31, doi:10.1029/2004GL020965.
- French, J.R. & Stoddart D.R. 1992. Hydrodynamics of saltmarsh creek systems: Implications for marsh morpho-logical development and material exchange. *Earth Surf. Proc. Landforms* 17: 235-252.
- Friedrichs, C. T. & J. E. Perry 2001. Tidal salt marsh mor-phodynamics. *J. Coastal Res.* 11(4), 1062-1074.
- Lanzoni, S. & G. Seminara 1998. On tide propagation in convergent estuaries. *J. Geophys. Res.* 103, 30,793-30,812.
- Lanzoni, S. & G. Seminara 2002. Long-term evolution and morphodynamic equilibrium of tidal channels. *J. Geo-phys. Res.* 107(C1), 3001,

doi:10.1029/2000JC000468.

Marani, M., S. Lanzoni, D. Zandolin, G. Seminara & A. Rinaldo 2002. Tidal Meanders. *Water Resources Research* 38 (11), 1225-1239.

Marani, M., S. Lanzoni, E. Belluco, A. D'Alpaos, A. De-fina & A. Rinaldo 2003. On the drainage density of tidal networks. *Water Resources Research* 39 (2), 105-113.

Pestrong, R. 1965. The development of drainage patterns on tidal marshes. Stanford Univ. Publ. Geol. Sci., Tech. Rep. 10, 87pp.

Rinaldo, A., S. Fagherazzi, S. Lanzoni, M. Marani, & W.E. Dietrich 1999a. Tidal networks 2. Watershed delineation and comparative network morphology. *Water Resources Research* 35(12), 3905-3917.

Rinaldo, A., S. Fagherazzi, S. Lanzoni, M. Marani, & W.E. Dietrich 1999b. Tidal networks 3. Landscape-forming discharges and studies in empirical geomorphic relationships. *Water Resources Research* 35(12), 3919-3929.

Schuttelaars, H. M. & H. E. de Swart 2000. Multiple morphodynamic equilibria in tidal embayments, *J. Geophys. Res.* 105, 24, 10524,118.

Tambroni, N., M. Bolla Pittaluga & G. Seminara 2005. Laboratory observations of the morphodynamic evolution of tidal channels and tidal inlets. *J. Geophys. Res.* 110, F04009, doi:10.1029/2004JF000243.

LONG TERM MORPHODYNAMICS AND HYDRODYNAMICS OF MEANDERING TIDAL CHANNELS AND EBB DELTAS

Valeria Garotta, Andreas Christof Rummel and Giovanni Seminara

Dipartimento di Ingegneria delle Costruzioni, dell'Ambiente e del Territorio, Università degli Studi di Genova

Riassunto

Le osservazioni di campo suggeriscono che i canali a marea in estuari e lagune hanno tipicamente un andamento meandriforme. A differenza del contesto fluviale, i processi morfodinamici che caratterizzano i meandri dei canali a marea non sono stati oggetto di ricerche sistematiche e attendono ancora interpretazioni definitive. Risultati teorici suggeriscono che, in una sequenza di meandri a marea sinusoidali in cui il moto possa ritenersi pienamente sviluppato, le oscillazioni associate alla marea danno luogo ad oscillazioni della posizione delle barre di deposito, simmetriche rispetto all'apice della curva. Inoltre, la topografia del fondo raggiunge asintoticamente una configurazione di equilibrio morfodinamico, mediata su un ciclo di marea.

Al fine di approfondire la comprensione del processo per cui, in un canale meandriforme a marea di dimensioni finite, si forma una successione di barre di scavo e deposito, è stato realizzato un modello fisico costituito da una sequenza di cinque meandri ad andamento sinusoidale della linea d'asse, di larghezza pari a 0.4 m. Il canale era lungo 21.3 m, chiuso ad un estremo e connesso all'altro estremo con un bacino, che simulava il mare, dove veniva generata un'onda di marea. È stato predisposto quindi un primo esperimento caratterizzato da un valore iniziale della profondità media D_0 tale da determinare un valore del parametro di larghezza $\beta = B/D_0$ pari a 2. L'evoluzione del pattern di scavi e depositi indotti dalla presenza della curvatura, è stata monitorata nel corso di un lungo esperimento, durato circa 400 h, corrispondenti a circa 11 anni nel prototipo. Le osservazioni hanno confermato le previsioni teoriche, cioè il raggiungimento di una configurazione di quasi-equilibrio del profilo medio del fondo del canale, caratterizzata da un profondo scavo in corrispondenza della bocca e dalla graduale formazione di un'area emersa all'estremità di terra. Il pattern delle barre forzate era in fase con la curvatura soltanto nel tratto interno del canale. Al contrario, nel tratto verso mare si riscontrava la formazione di depositi lungo la sponda esterna e scavi lungo la sponda interna, una configurazione che in natura sarebbe planimetricamente instabile. Si suggerisce che quest'ultimo risultato possa interpretare l'osservazione secondo cui il tratto a mare dei canali mareali ha spesso andamento quasi rettilineo. Al fine di investigare il possibile ruolo del parametro di larghezza β sul pattern di scavi e depositi indotti dalla curvatura del canale, è stato predisposto un secondo esperimento, caratterizzato da un valore del parametro di larghezza $\beta = B/D_0$ pari a 5. Nelle fasi conclusive dell'esperimento si è osservato come le barre

puntuali fossero sfasate rispetto alla curvatura lungo quasi l'intero canale.

Entrambi gli esperimenti hanno consentito di riprodurre la formazione di un 'ebb-tidal delta': già nella fase iniziale degli esperimenti, i sedimenti erosi in prossimità della bocca sono stati depositati nella regione centrale del bacino. Al fine di studiare la struttura del campo di moto in questa regione, sono state predisposte misure PIV. I risultati mostrano come la fase di riflusso sia caratterizzata da un getto turbolento e da due celle di circolazione ai lati. Durante la fase di flusso il moto risulta invece quasi irrotazionale.

Abstract

Field observations suggest that tidal channels in estuaries and lagoons are typically characterized by a meandering pattern. In order to investigate the long-term dynamics of the bar-pool pattern, we have carried out a laboratory experiment on a tidal meandering channel. The channel was composed by five sine generated meanders with constant width $2B$. Moreover, it was closed at one end and connected at the other end with a basin, representing the sea, where a tidal wave was generated. A first experiment has been carried out, with an initial flow depth D_0 such to determine a value of the aspect ratio $\beta = B/D_0$ ranging about 2. The bar-pool pattern was surveyed throughout the course of a long experiment lasted about 400 h, corresponding to about 11 years in the real world. Observations have confirmed the theoretical expectations, namely the development of a quasi equilibrium state of the longitudinal bed profile, characterized by a deep scour at the inlet and deposition at the inner end, eventually leading to the formation of a shore. Furthermore, the bar-pool pattern was in phase with curvature only in the inner half of the channel. On the contrary, the seaward pattern displayed deposition at the outer bends and scour at the inner bends, a pattern which would clearly be planimetrically unstable if the channel walls were erodible. The peculiar pattern of point-bars in the seaward reach seems to be consistent with field observations, which suggest that tidal creeks are often quasi straight near the inlet. In order to evaluate the possible effect of the channel aspect ratio on the phase-lag between bar-pool pattern and channel curvature, a second experiment has been carried out, with an initial value of the channel aspect ratio β ranging about 5. In the final stage of the experiment, i.e. close to an equilibrium state, point bars were out of phase with respect to curvature along almost the whole channel. The present laboratory study was also able to reproduce the formation of an ebb-tidal delta: from the very beginning of the experiment, sediments eroded close to the inlet, in the channel as well as in the sea basin, deposited in the central region of the latter. In order to study the flow field in the inlet region, we have performed some detailed PIV measurements. Results show the formation of a turbulent jet and a dipole, during the ebb phase, while during the flood phase, the flow was nearly irrotational.

1 Introduction

Tidal channels in estuaries and lagoons often display a meandering pattern.

The problem of the possible existence of an equilibrium configuration of the bed profile of tidal channels has been the subject of theoretical investigations by Schuttelaars and De Swart (1996, 2000) and by Lanzoni and Seminara (2002). Controlled laboratory experiments have been carried out by Tambroni et al. (2005). The latter authors have shown that straight and weakly convergent tidal channels closed at one end, do indeed evolve towards an equilibrium configuration, slightly concave seaward and convex landward, in accordance with the theoretical predictions of Lanzoni and Seminara (2002).

Channel curvature modifies the lateral structure of bed topography significantly. Tidal meanders display some similarities with river meanders (Marani et al., 2002), in particular they exhibit deposition (point bars) at the inner bends and scour (pools) at the outer banks. In the wide literature developed for the fluvial case, it has been clarified that these sequences of bars and pools are almost steady features, which propagate at the very slow time scale associated with the plan form evolution of the meandering pattern, migration rates being typically of the order of meters per year. Essentially, the formation of the bar-pool pattern is due to a secondary flow which affects the trajectory of sediment particles. Laboratory experiments (Colombini et al., 1992) carried out on a meandering flume subject to a stationary flow have shown that the phase lag of the bar pool pattern relative to curvature depends on the meander wavenumber and on the aspect ratio of the channel.

Solari et al. (2001) and Solari and Toffolon (2001) have recently proposed theoretical models for flow and bed topography in infinite sequences of tidal meandering channel. They found that a symmetrical tidal wave gives rise, through a transient process, to an equilibrium bar-pool pattern characterized by relatively small symmetrical spatial oscillations throughout the tidal cycle. The average equilibrium topography is characterized by amplitudes of the point bar comparable with the mean flow depth.

The aim of the present experiments is to study the transient process whereby an equilibrium bed topography is established in a meandering channel, connected with a tidal basin. In particular we focus our attention on the characteristics of the cross-sectionally averaged bed profile and on the structure of the bar-pool pattern: the finite length of the channel will be seen to give rise to spatial variations of the latter displaying interesting features. This study also describes the formation and evolution in the near inlet region of an ebb tidal delta similar to those encountered in nature. A detailed set of measurements of the flow field in the basin at equilibrium shows the formation of a strong shallow unsteady jet during the ebb phase and of a quasi-irrotational flow during the flood phase.

Besides its obvious geomorphic interest, the practical relevance of the problem is related to the goal of predicting bend scour in tidal settings and shedding further light on the mechanisms that lead to the formation of ebb – tidal deltas.

The plan of the paper is as follows. A brief description of the experimental apparatus is presented in section 2. Results concerning the morphodynamic evolution of bed topography in the channel and in the seaward basin are

discussed in sections 3 and 4. Finally, some remarks follow in the last section.

2 Experimental Set-up

Experiments were carried out on a large indoor platform above which a meandering channel was built using zincked plate. The Cartesian length of the channel was 21.3 m. Moreover, the channel was 0.4 m wide, closed at one end and connected at the other end to a rectangular basin (2.23 m wide and 6.5 m long) representing the sea. The flume was composed of a sequence of five meanders with intrinsic wavelength L_s^* of 4 m, connected at each end to a straight reach 1 m long. The shape of the channel axis was chosen such to follow the law $y^*(x^*) = A^* \sin(\lambda_x^* x^*)$, with an amplitude A^* of 0.35 m and a Cartesian meander wavelength ($L_x^* = 2\pi/\lambda_x^*$) taking the value 3.7 m.

The inlet walls were rounded off, in order to avoid the formation of deep scour holes. The Figure 1 shows a sketch of the apparatus.

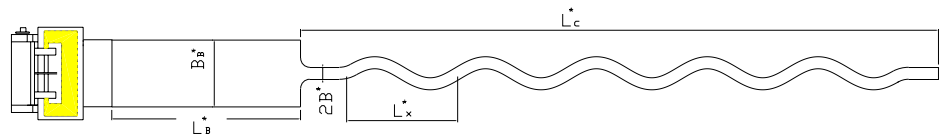


Fig 1 – Sketch of the physical model and notations.

Finally, an oscillating discharge was supplied to the basin from a tank where the apparatus for tide generation was installed. The latter consisted of a cylinder set in motion by a piston held by a steel frame and controlled by an oleodynamic mechanism driven by a control system, which generated the desired law of motion. In particular, a sinusoidal tide was generated:

$$h^*(t^*) = a_0^* \sin(2\pi t^* / T) \quad (1)$$

with $h^*(t^*)$ free surface oscillation in the basin, T tidal period and a_0^* amplitude of the tidal wave.

A uniform layer of cohesionless granular material of sufficient thickness was laid on the bottom of both the flume and the basin. Sediments were chosen light enough to be entrained in suspension throughout most of the tidal cycle with the values of friction velocity typically generated in the present experiments. The final choice was to use polycarbonate grains, characterized by a density of $1.27 \times 10^3 \text{ Kg/m}^3$ and median grain size $d_s^* = 0.15 \text{ mm}$.

Two experiments have been carried out, changing the initial value of the mean flow depth D_0^* . The table 1 shows the values of the relevant parameters for the two experiments.

		EXP. 1	EXP. 2
Tidal period	T [s]	170	170
Mean flow depth at the channel inlet	D_o^* [m]	0.085	0.04
Tidal peak velocity at the channel inlet	U_{max}^* [m/s]	0.3	0.2
Wave amplitude at the channel inlet	a_o^* [m]	0.021	0.009

Tab 1 – Values of the relevant parameters at the initial conditions of the two experiments.

3 Morphodynamic evolution of a tidal meandering channel

3.1 Bed profile

Let us first briefly discuss the morphodynamic evolution of the cross – sectionally averaged bed profile. Due to the flood dominant character of the tidal wave in the initial stage (displayed by peak velocities higher during the flood phase than during the ebb phase, and high-water period shorter than low-water period), a net sediment flux directed landward arises. Sediments are then eroded in the seaward portion of the channel, driven landward, and deposited in the inner reach. In particular, a fairly sharp front of the bed profile develops and migrates landward. This is consistent with the theoretical results obtained by Lanzoni and Seminara (2002) and with laboratory observations on rectilinear and weakly convergent tidal channels (Tambroni et al., 2005). The Figure 2 shows the final configuration of the laterally averaged bed profile for run 1 and 2. Note that D_o^* is the mean flow depth at the channel mouth at the beginning of the experiment, η^* is the local and instantaneous value of the average bed elevation and s^* is the landward oriented intrinsic coordinate measured along the channel axis, with origin located at the channel inlet.

The bed profile evolves starting from an initial configuration which was set horizontal. The scour depth at the channel inlet evolves throughout the experiment, reaching a quasi equilibrium value of the order of the initial mean flow depth. The sediment front develops quite rapidly, grows and migrates landward, reaching the channel end. Proceeding with the experiment, a wet and dry region forms and the depositional area grows until the bed elevation reaches the mean water level.

The small scale oscillations displayed by the bed profile in the laboratory are associated with the presence of small-scale bed forms. Larger scale fluctuations occur on the meander scale. It is interesting to note that during the Experiment n° 1 these oscillations were observed only in the initial stage of the experiment (say after 100 cycles), being damped afterwards. On the contrary, large scale oscillations of the bed profile persisted until the final stage of Experiment n° 2. Furthermore, the fact that they are observed close to the inlet, suggests that they might arise as a bottom instability forced by the inlet boundary condition. Channel curvature may also play some role, leading to a local adaptation of bed topography as explained by Seminara and Solari (1998). However, the lack of a

systematic theory for finite tidal channels, does not allow for a conclusive interpretation of this phenomenon.

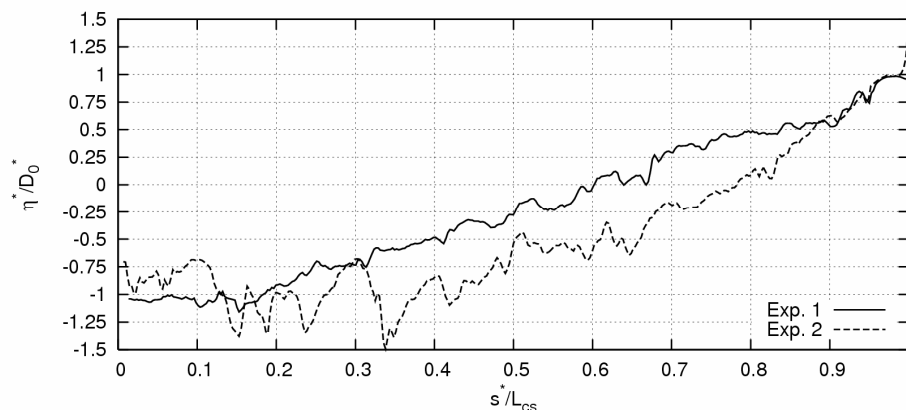


Fig 2 – Final configuration of the laterally averaged bed profile along the channel for Experiment n° 1 and 2.

3.2 Point bar pattern

We now proceed to discuss the evolution of the bar-pool pattern driven by channel curvature. In the initial stage of the first experiment a phase lag between scour and curvature was observed throughout most of the channel. Proceeding with the experiment, the deposits located in the outer region of the bends have been partially eroded. On the other hand, the bar-pool pattern in the landward reach of the channel appears to reach a stable configuration, with scours located at the outer bend and depositions at the inner bend. On the contrary, the seaward half of the channel displays a peculiar bar-pool pattern, with deposition bars out of phase with respect to channel curvature (see the first plot in Figure 3, where bed elevation has been plotted after subtracting the average profile). The observed tendency of bed topography in the seaward portion of the channel is to reach a configuration which would not be stable in nature: indeed, bank erosion would rapidly suppress curvature and the channel would recover a rectilinear pattern. This is suggestive of a strong influence of the inlet condition, which appears to force a spatial transient which delays the development of a fully developed meander pattern. In the first experiment the latter was reached in the landward portion of the channel while, in the second experiment, the whole channel was invariably covered by point bars out of phase relative to curvature (see the second plot in Figure 3). As pointed out above, this configuration would clearly be planimetrically unstable if the channel walls were erodible. We suggest that our observations may provide an explanation for the observation that, in nature, tidal channels are seldom curved close to their inlets (Figure 4).

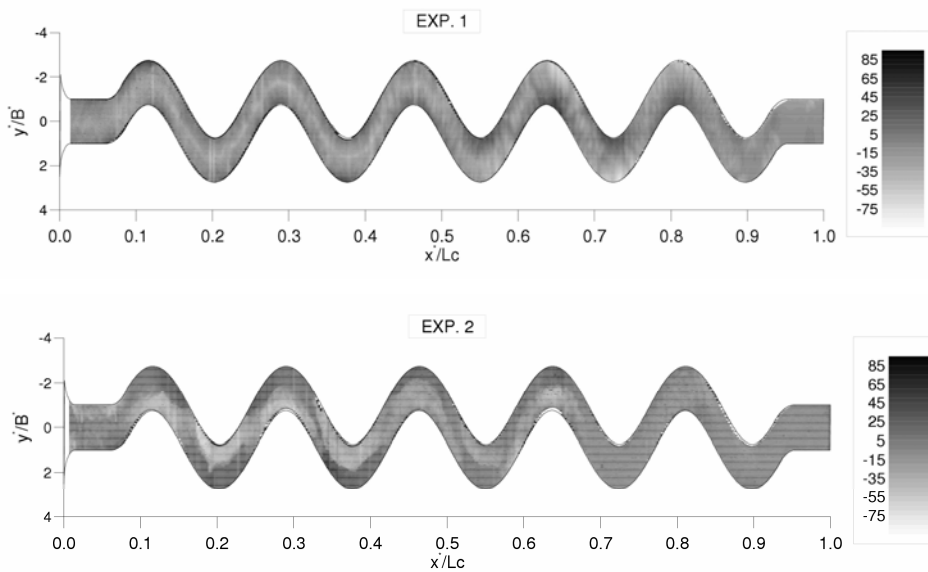


Fig 3 – Map of bed topography showing the bar-pool pattern in the final stage of Experiment n°1 and 2. Note that the laterally averaged bed profile has been subtracted. Bottom elevation is expressed in mm, with positive values corresponding to depositional areas.

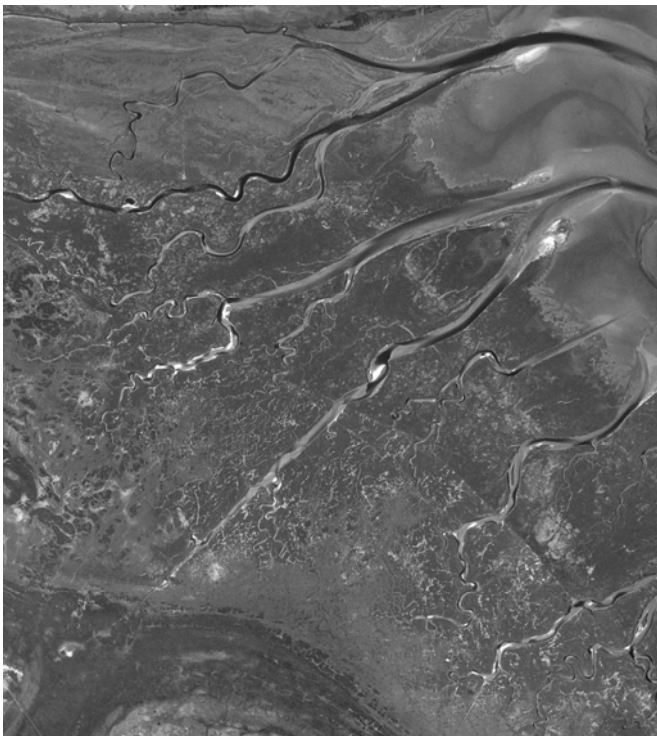


Fig 4 – An aerial image of tidal flats and salt marshes (Skallingen, Denmark). Note that the terminal reach (towards the inlet) of tidal channels is almost rectilinear. Courtesy of Aart Kroon.

4 Ebb tidal delta

Tidal entrances are a crucial dynamic boundary condition with respect to the coastal ocean regime due to their role as interfaces for exchange between seawater and embayed waters. At sandy entrances, the three most important morphologic features are the inlet channel, the ebb delta, and the flood delta (Davis, 1996, Powell et al., 2006).

The present laboratory experiments allowed us to observe the formation of an ebb-tidal delta (Figure 5). From the initial stage, sediments were eroded close to the inlet, both in the channel and in the sea basin. Part of these sediments were

observed to deposit in the central region of the basin. The initial width of the depositional area was approximately coincident with the channel width. Proceeding with the experiment, the extension of the ebb-tidal delta grows, both in the longitudinal and lateral directions. Scour spits are also formed in the central region of the basin: they eventually develop into a submerged channel. Along the seaward side of the barriers, i.e. along the walls of the basin adjacent to the inlet, two swash bars form, a feature typically observed in nature. The field measurements recently carried out by Amos et al. (2005) in the Venice Lagoon have shown the presence of an ebb-tidal delta outside the Lido inlet, inclined towards the direction of the main littoral current.

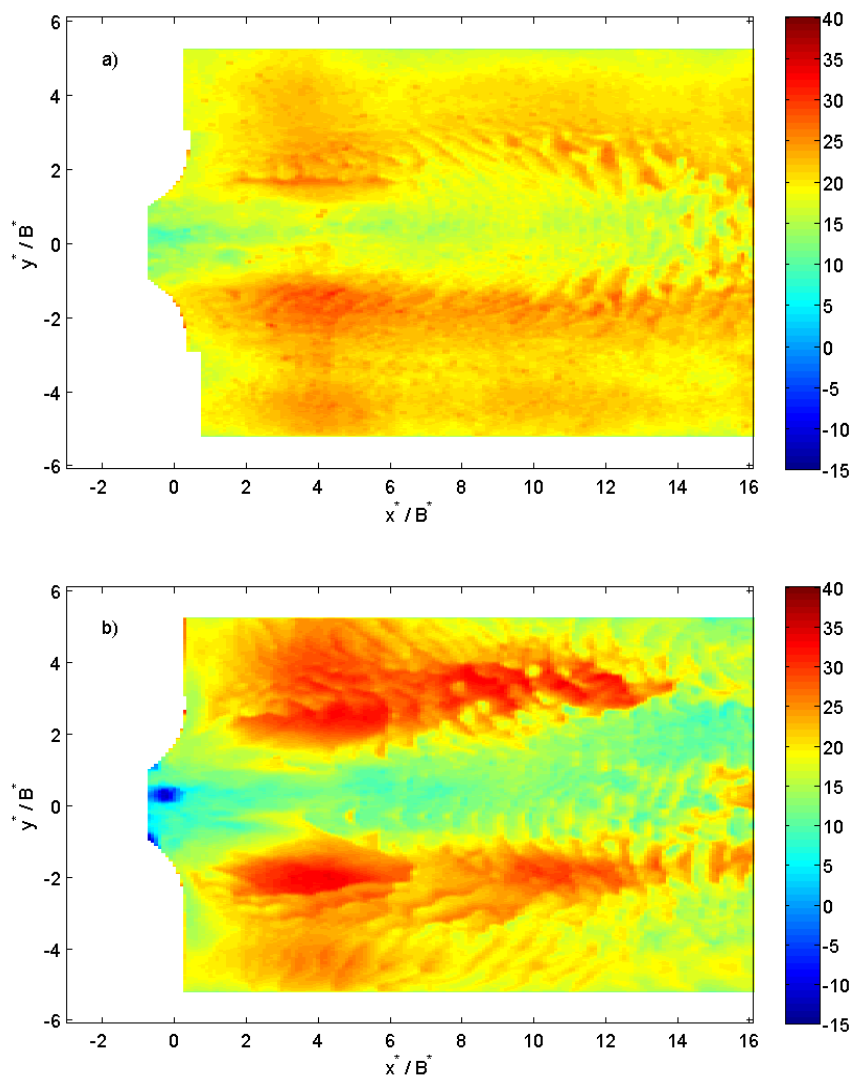


Fig 5 – Pattern of bed topography of the ebb tidal delta: a) after 120 cycles; b) after 2000 cycles. Bottom elevation is reported in mm.

In order to pick up the details of the physical processes that lead to the formation of an ebb-tidal delta, we have performed PIV measurements of the surface velocity in the basin at significant stages of the experiment. A strong turbulent shallow jet was observed during the ebb-phase. The jet leads to an erosion of sediment in the central region of the basin. During the flood-phase the flow has a radial inflow pattern.

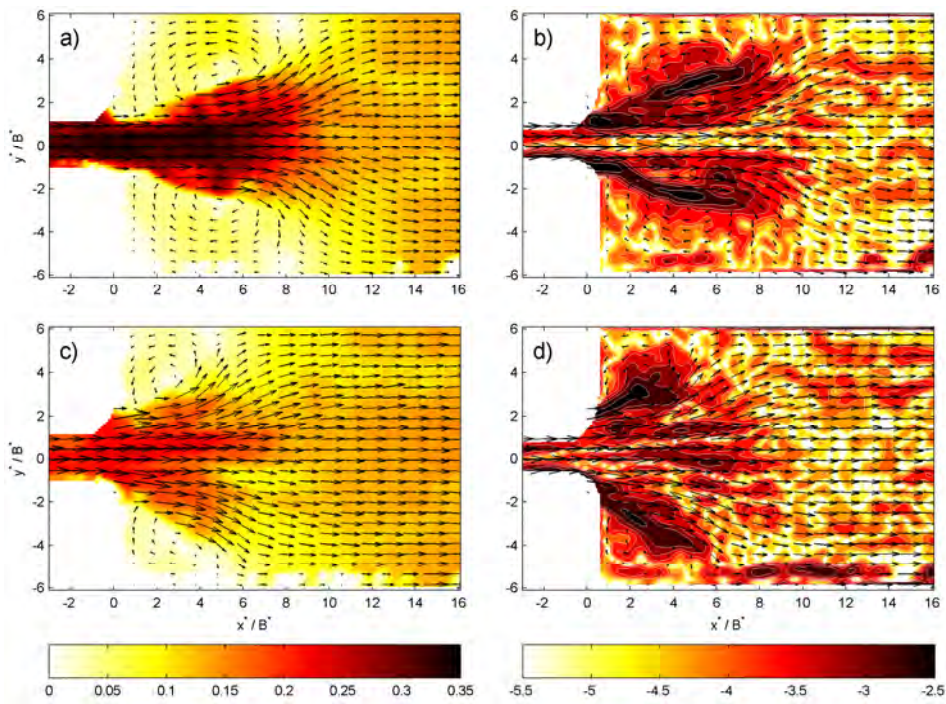


Fig 6 – Flow field at the early stage of the ebb phase. On the left: magnitude (colours) and direction (vectors) of surface velocity after a) 120 cycles and b) 2000 cycles. On the right: $\log_{10}(\text{vorticity})$.

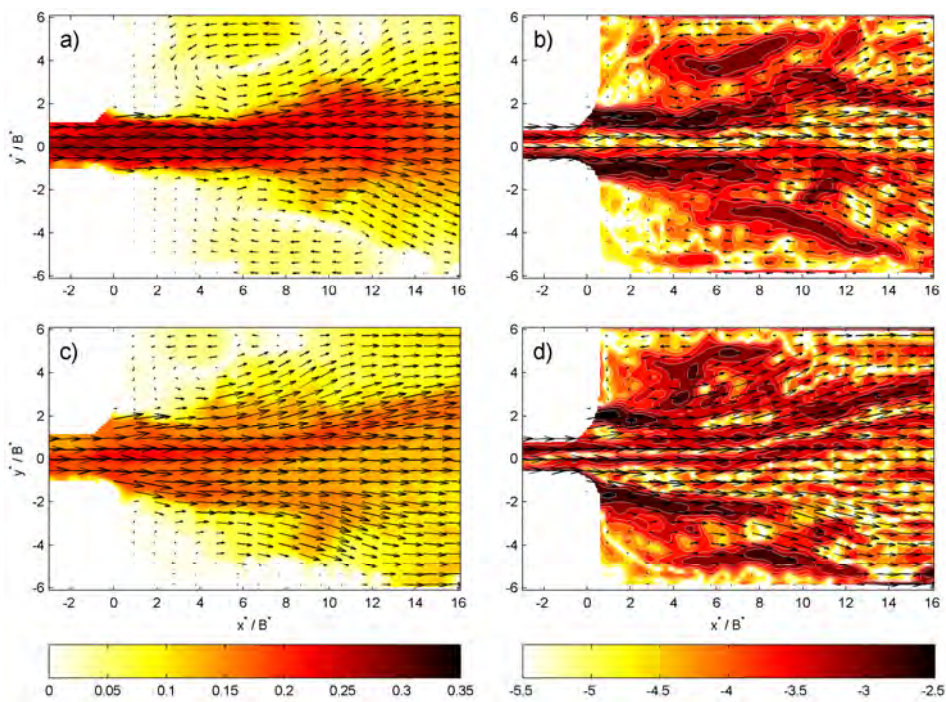


Fig 7 – Flow field at the late stage of the ebb phase. On the left: magnitude (colours) and direction (vectors) of surface velocity after a) 120 cycles and b) 2000 cycles. On the right: $\log_{10}(\text{vorticity})$.

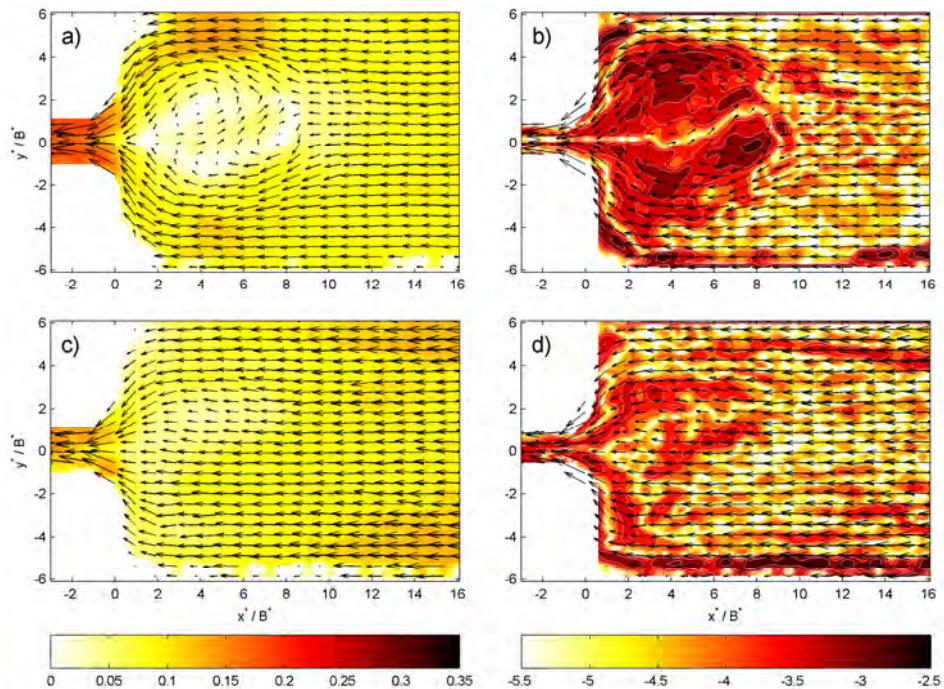


Fig 8 – Typical flow field at the flood phase. On the left: magnitude (colours) and direction (vectors) of surface velocity after a) 120 cycles and b) 2000 cycles. On the right: $\log_{10}(\text{vorticity})$.

Results (Figure 6, 7) show that at the early stage of the experiment the jet is aligned with the channel and has a fairly regular shape. A dipole is generated by tidal forcing that consists of two vortical structures with vertical axes that develop at the sides of the jet. As bed topography evolves the structure of the turbulent jet tends to become more irregular. It's worth noting (Figure 7) that after 2000 cycles the maximum intensity of the jet is deviated from the axis direction, a feature which is clearly linked to bed topography (see Figure 5). Also note that the increase of bottom roughness due to the development of bedforms (e.g. dunes) significantly reduces the velocity of the jet.

Results (Figure 8) concerning the flood phase show that the flow field tends to enhance its nearly radial pattern as bed topography evolves. The vorticity plots (Figure 8 c-d) show that residual momentum tends to decrease close to equilibrium conditions.

Conclusions

The present laboratory experiments show that a tidal meandering channel closed at one end evolves towards an asymptotic equilibrium configuration, characterized by a deep scour at the channel inlet and the formation of a shoal (a wet and dry area) in the inner reach of the channel.

The bar-pool pattern developed in the first experiment in the landward region of the channel is qualitatively consistent with field observations and with the theoretical results of Solari et al. (2001), with deposition occurring in the inner portion of the bend. However, in the seaward portion of the channel, point bars were out of phase relative to curvature, thus suggesting that the sinuous pattern in this region would be planimetrically unstable. In other words, it appears that the bed topography is strongly affected by the boundary conditions at the inlet

and at the inner end. In other words, this suggests that the spatial distribution of the bar-pool pattern is not simply related to processes occurring at the meander scale: in order to capture the complete evolution of bed topography the whole channel length needs to be analyzed. This was even more evident in the second experiment, in which the bar – pool pattern was out of phase relative to curvature along almost the whole channel.

In the inlet region the formation of an ebb-tidal delta was observed for both the experiments. The flow field in the basin was measured throughout the second experiment, showing the formation of a turbulent jet during the ebb phase and a radial quasi-irrotational pattern during the inflow.

In the near future we plan to investigate the effect of meander wavelength on the bar – pool pattern in order to ascertain whether the phase – lag of bars relative to curvature may decrease as meanders get longer.

The data collected in the present experiment are also intended to provide a test case for future numerical models and theoretical analyses.

References

- C. L. Amos, Helsby R., Umgiesser G., Mazzoldi A. and Tosi L., "Sand transport in the Northern Venice Lagoon", Scientific Research and Safeguarding of Venice, CO.RI.LA Research Programme 2001-2003, Volume III, 2005.
- R. A. Davis, "Coasts". London: Prentice Hall, 1996.
- C.T. Friedrichs and D. G. Aubrey, "Non-linear distortion in shallow well-mixed estuaries: a synthesis", *Estuarine, Coastal and Shelf Science*, 27, 521-545, 1988.
- S. Lanzoni and G. Seminara, "Long term evolution and morphodynamic equilibrium of tidal channels", *J. Geophys. Res.*, 107(C1), doi:10.1029/2000JC000468, 2002.
- M. Marani, S. Lanzoni, D. Zandolin, G. Seminara and A. Rinaldo, "Tidal meanders", *Water Resour. Res.* 38 (11), 2002.
- H. M Schuttelaars and H. E. De Swart, "An idealized long-term morphodynamic model of a tidal embayment", *Eur. J. Mech. B*, 15, 55-80, 1996.
- G. Seminara and L. Solari, "Finite amplitude bed deformations in totally and partially transporting wide channel bends", *Water Resour. Res.*, 34, 1585-1598, 1998.
- L. Solari, G. Seminara, S. Lanzoni, M. Marani and A. Rinaldo, "Sand bars in tidal channels. Part 2. Tidal meanders", *J. Fluid Mech.*, 451, 203-238, 2001.
- L. Solari and M. Toffolon, "Equilibrium bottom topography in tidal meandering channels", *Proceedings of the 2nd RCEM Symposium, Obihiro (Japan)*, 11-14 September 2001.
- N. Tambroni, M. Bolla Pittaluga and G. Seminara, "Laboratory observations of the morphodynamic evolution of tidal channels and tidal inlets", *J. Geophys.*

Res., 110, F04009, doi:10.1029/2004JF000243, 2005.

LONG-TERM EVOLUTION OF TIDAL CHANNELS FLANKED BY TIDAL FLATS

Alberto Canestrelli, Andrea Defina, Stefano Lanzoni, Luigi D'Alpaos

Dipartimento IMAGE, Università di Padova

Riassunto

Con questo contributo si vuole analizzare il comportamento a lungo termine di un canale a marea affiancato da bassifondi. Viene introdotto un modello matematico-numerico che risolve le equazioni delle onde lunghe in acque basse, accoppiate con l'equazione di evoluzione del fondo e l'equazione di avvezione-diffusione per i sedimenti trasportati in sospensione. In una prima simulazione il canale è caratterizzato da una condizione di riflusso dominante in prossimità della bocca, e di flusso dominante nella parte più interna. Il sistema evolve asintoticamente verso una configurazione di equilibrio caratterizzata da un andamento simmetrico della portata solida in sospensione e da valori massimi delle velocità di flusso/riflusso pressoché costanti lungo il canale. I bassifondi sono progressivamente incisi da canali aventi un interasse che varia tra i 400 e i 1000 m. In una successiva simulazione è stata considerata una istantanea propagazione della marea all'interno del canale. I vortici bidimensionali che si creano nel canale principale nella fase di riflusso sembrano essere la causa principale della formazione di canali secondari nei bassifondi.

Abstract

This contribution investigates the long term morphodynamic equilibrium of a movable bad tidal channel flanked by tidal flats. The two dimensional shallow water equations, the bed evolution equation, and the advection-diffusion equation for suspended-load are solved numerically. In the first run the channel turns out to be always ebb dominated near the inlet and flood dominated in the landward part, leading to sediment scour in the outer part and deposition in the inner part, where a sediment front propagates landward. The system evolves asymptotically toward an equilibrium configuration characterized by an approximately symmetric suspended-load transport rate during the tidal cycle, and a nearly constant value of the maximum flood/ebb speed along the channel. The width of the channel is found to decrease exponentially toward the land. The numerical results show that tidal flats are progressively carved by channels, with a spacing varying between 400 and 1000 m. In a successive simulation we neglect the tidal propagation along the tidal channel and we analyse the bottom evolution of a smaller portion of tidal flats. These turn out to be carved by channels. The two-dimensional vortexes, developing close to the main tidal channel during the ebb flood, seem to be the main cause of the inception of tidal flats channelization.

1 Introduction

Morphological processes occurring in tidal channels are of fundamental importance for the management of estuarine and lagoon environments. These processes are strictly related to the net sediment transport occurring during each tidal cycle, driven by the distortion and asymmetry of tidal currents. Friedrichs and Aubrey [1988] found that in well-mixed estuaries, nonlinear tidal distortion depends on two main factors: the frictional distortion, defined by the ratio of the tidal amplitude a_0 to the mean channel depth D_0 , and the intertidal storage, defined by the ratio of intertidal storage area A_s (ensured by tidal flats and salt marshes) to the channel area A_c covered by water at mean low tide. Nonlinear friction enhances the flood dominated character of tidal channel. In fact, increasing a_0/D_0 slows the propagation at low tide and leads to time delays between the mouth and the inner channel low water exceeding the delays at high water [Speer and Aubrey 1985, Friedrichs and Aubrey 1988, Lanzoni and Seminara 1998]. On the other hand, high values of the ratio A_s/A_c favor low velocities over intertidal marshes and flats, thus causing high waters to propagate slower than low waters and promoting ebb dominance.

In the last decade, the issue of whether a tidal channel may reach a morphologic equilibrium state has attracted the attention of many researchers. A tidal channel is defined to attain a morphodynamic equilibrium when any cross section is characterised by a vanishing net sediment flux within each tidal cycle. Note that this definition neither implies that the instantaneous sediment flux vanishes, nor prevents bed forms migration. Although both theoretical arguments [Friedrichs 1995, Schuttelaars and de Swart 1996, 2000, Lanzoni and Seminara 2002] and laboratory observation [Tambroni et al. 2003] have provided a increasing understanding of tidal channel long term morphodynamics, the two dimensional effects related to the lateral exchange of sediment and water between the main channel and the adjacent intertidal areas still need to be addressed.

In this contribution we study the two-dimensional morphologic evolution of a straight tidal channel, with a cohesionless sediment bed, flanked by tidal flats. Starting from a initially flat bed configuration, we analyze the temporal evolution of the channel and its adjacent flats. We show that the channel tends to attain a longitudinal equilibrium profile characterized by scour in the seaward reach and deposition landwards. Moreover, the periodic flooding/ebbing of tidal flats leads to the formation of a well defined network of lateral creeks, carving the levees which form at the boundary between tidal flats and the main channel.

2 Formulation of the hydrodynamic and morphodynamic problems

Let us consider a straight tidal channel flanked by tidal flats, connected to a tidal sea characterized by a sinusoidal oscillation of the water level. In order to deal with wetting and drying of tidal flats we introduce the modified set of two-dimensional two-dimensional flow equations derived by Defina [2000] by phase averaging the classical three dimensional Reynolds equations, and integrating

over depth. These equations read:

$$\frac{\partial q_x}{\partial t} + \frac{\partial}{\partial x} \left(\frac{q_x^2}{Y} \right) + \frac{\partial}{\partial y} \left(\frac{q_x q_y}{Y} \right) - \left(\frac{\partial R_{xx}}{\partial x} + \frac{\partial R_{xy}}{\partial y} \right) + gY \frac{\partial h}{\partial x} + \frac{\tau_{bx}}{\rho} = 0 \quad (1)$$

$$\frac{\partial q_y}{\partial t} + \frac{\partial}{\partial x} \left(\frac{q_x q_y}{Y} \right) + \frac{\partial}{\partial y} \left(\frac{q_y^2}{Y} \right) - \left(\frac{\partial R_{xy}}{\partial x} + \frac{\partial R_{yy}}{\partial y} \right) + gY \frac{\partial h}{\partial y} + \frac{\tau_{by}}{\rho} = 0 \quad (2)$$

$$\eta \frac{\partial h}{\partial t} + \frac{\partial q_x}{\partial x} + \frac{\partial q_y}{\partial y} = 0 \quad (3)$$

where t denotes time, q_x and q_y are the flow rates per unit width along x and y directions; R_{ij} are the horizontal Reynolds stresses, $\tau_b = (\tau_{bx}, \tau_{by})$ is the shear stress at the bottom, ρ is fluid density, h is the free surface elevation, g is gravity, Y is the equivalent water depth, defined as the volume of water per unit area actually ponding the bottom, η is the local fraction of wetted domain, accounting for the actual area that can be wetted or dried during the flow [Defina, 2000]. The Reynolds stresses R_{ij} in (1) and (2) are proportional to the strain rate tensor through a eddy viscosity coefficient, computed using the model proposed by Smagorinsky. The energy slope by the Gauckler-Strickler formula. We refer the reader to Defina [2000] for further details.

The sediment balance equations implemented in the present contribution are the Exner equation and the diffusion advection equation for suspended-load:

$$(1-p) \frac{\partial z_b}{\partial t} + \nabla q_b + (r_E - r_D) = 0 \quad (4)$$

$$\frac{\partial(YC)}{\partial t} + \frac{\partial}{\partial x} (q_x C) + \frac{\partial}{\partial y} (q_y C) - \frac{\partial}{\partial x} \left(Y e_x \frac{\partial C}{\partial x} \right) - \frac{\partial}{\partial y} \left(Y e_y \frac{\partial C}{\partial x} \right) = r_E - r_D \quad (5)$$

where $\mathbf{q}_b = q_b (\cos \alpha, \sin \alpha)$, q_b is the intensity of bed-load rate per unit width, C is the depth averaged concentration of suspended-load, e_x and e_y are respectively the eddy diffusivity along x and y , p is the porosity and $r_E - r_D$ is the difference between entrainment and deposition rates. The latter is expressed through the following equation:

$$r_E - r_D = w_s (C_{eq} - C_a) \quad (6)$$

where w_s is the settling velocity, C_{eq} and C_a are the equilibrium and actual concentration, respectively, at the boundary between the bed load and suspended load regions. Following Parker et al. [1987], we set $C_a = r_0 C$ (with $r_0 \approx 1.4$), and we compute C_{eq} and w_s by the expressions proposed by Van Rijn [1984b]. Finally, the intensity of bed load rate q_b is related to the equilibrium bed load rate q_{bo} by the relation proposed by Struiskma [1985; see also Defina 2003]. We estimate q_{bo} through the Meyer-Peter and Muller [1948] formula.

We resolve equations (1), (2) and (3) adopting a semi-implicit staggered finite elements scheme, which combines Galerkin's method with the (Eulerian-Lagrangian) method of characteristics. Equations (4) and (5) are solved by using a finite volume method.

3 Results

In order to better clarify the long term morphodynamic behavior of the tidal channel and of the adjacent tidal flats, we have carried out two different numerical tests. In the first numerical experiment we considered a tidal sub basin with a central straight tidal channel flanked by tidal flats which dry at low tide. In order to better analyse tidal creek formation over the tidal flat platform we performed a second numerical experiment, considering a smaller part of the domain simulated in the first run. The main channel reach was in fact small enough to neglect tide propagation effects within the channel.

In both runs we assumed that both the channel and the tidal flats consisted of cohesionless uniform sand with a diameter of 0.05 mm. The Strickler roughness coefficient was set everywhere equal to $30 \text{ m}^{1/3}/\text{s}^{-1}$, while a typical height of bottom irregularities $a_r=0.3 \text{ m}$ was used in the subgrid model of wetting and drying. The computational domain was discretized by using a unstructured mesh with linear triangular elements. The cell resolution in the first run varied gradually from 30 m into the channel to 80 m towards the tidal flat divides. In the second run it varied gradually from 10 m into the channel to 80 m towards the tidal flat divides.

3.1 Run 1

The initial configuration of the tidal sub-basin investigated in this run is schematically depicted in Figure 1. The tidal channel was initially characterized by a trapezoidal, spatially constant section with a bottom elevation of -6 m amsl (above mean sea level) while the adjacent tidal flats had an initial elevation of -0.5 m amsl.

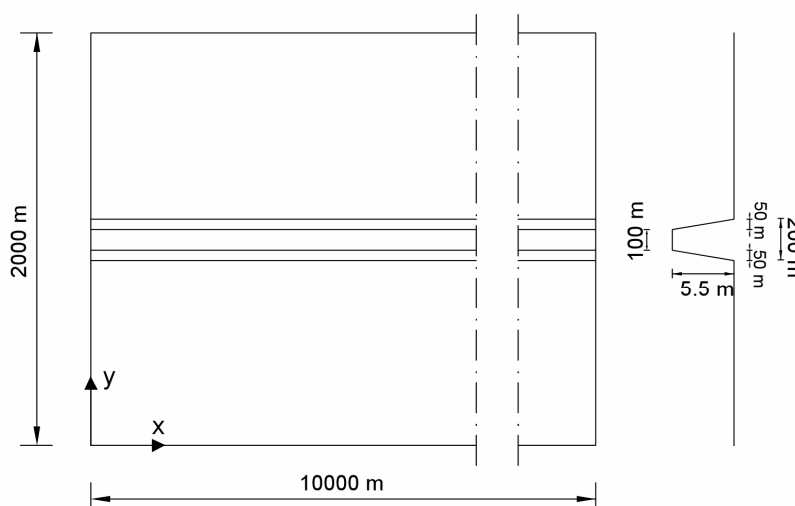


Fig 1 – Sketch of the tidal channel and of the adjacent tidal flats considered in run 1.

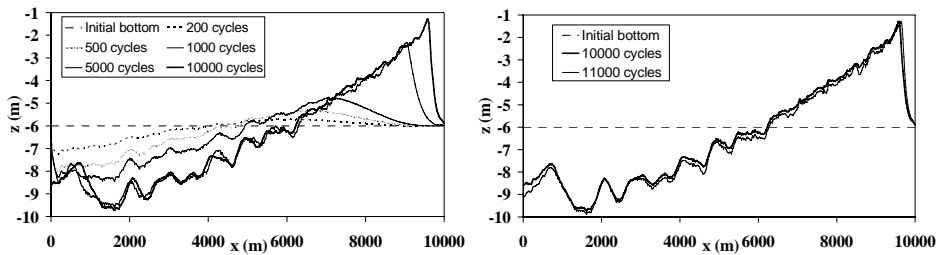


Fig 2 – Temporal evolution of the channel axis bottom profile at a) different times and b) after 10000 and 11000 cycles. The bottom elevation is referred to mean water level.

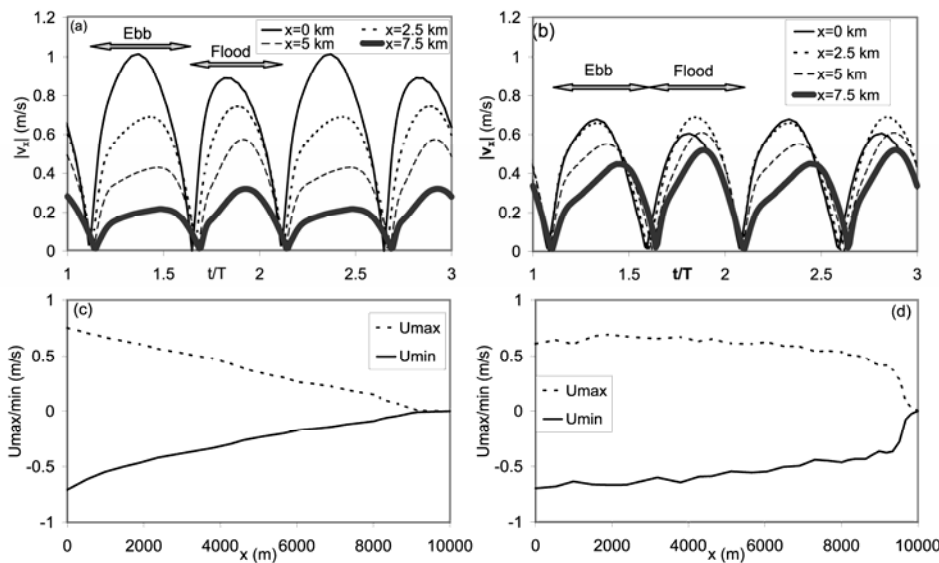


Fig 3 – The absolute value of the longitudinal velocity along the main channel axis and its maximum value within a tidal cycle is plotted a), b) versus time, at four different sections ($x=0, 2.5, 5.0$ and 7.5 km), and c), d) versus the longitudinal coordinate s . Plots a), c) refer initial bottom configuration; plots b) and d) results from the bottom configuration attained after 10000 cycles.

We adopted the following boundary conditions. At the seaward side ($x=0$) we prescribed a sinusoidal water elevation $h=a \sin(2\pi t/T)$, with amplitude $a=0.5$ m and period $T=12$ hours. The bed elevation at the seaward side was kept fixed during the flood phase, while it was allowed to evolve freely during the ebb phase. No constraint have been imposed to the bed along the lateral and landward sides of the sub-basin. Similarly, the concentration at the sea side was set equal to the equilibrium concentration C_{eq} (calculated through the relationship proposed by Van Rijn, 1984b) during the flood phase, while it was calculated numerically during the ebb phase. Finally, no flux conditions were assumed along the lateral and landward boundaries of the sub-basin. The simulation was stopped after 10000 tidal cycles.

Figure 2a,b shows the temporal evolution of the longitudinal bottom profile along the channel axis ($y=1000$ m), starting from the initially plane configuration. The channel appears to be ebb dominated near the inlet and flood dominated in the landward portion. The net sediment flux within a tidal cycle is in fact directed seaward near the inlet and causes a appreciable scour. Conversely, in the inner reaches the net sediment flux is directed landward, sediment are deposited and in a first phase of the evolution a sediment front, propagating landward, forms. The bed evolution is relatively fast in the first stages of the numerical experiment, and decreases dramatically as equilibrium is approached (Fig. 2b). The temporal and spatial distribution of the velocity within the channel, shown in

Figure 3, indicate that the channel evolves towards a morphological configuration which tends to smooth out the longitudinal velocity variation. The ebb/flood asymmetry is progressively reduced and peak velocity along the channel becomes nearly constant. As a consequence, also the along channel distribution of the bed shear stress τ_b , shown in Figure 4a,b tends progressively to become uniform, thus leading to a spatially similar erosion potential. The consequences on suspended-load transport rates (bed-load transport rates are about two order of magnitude lower) are shown in Figure 4c,d. The resulting overall net sediment discharge Q_{sa} (i.e., averaged over a tidal cycle) reported in Tab. 1, confirm the tendency of the system towards a morphodynamic equilibrium.

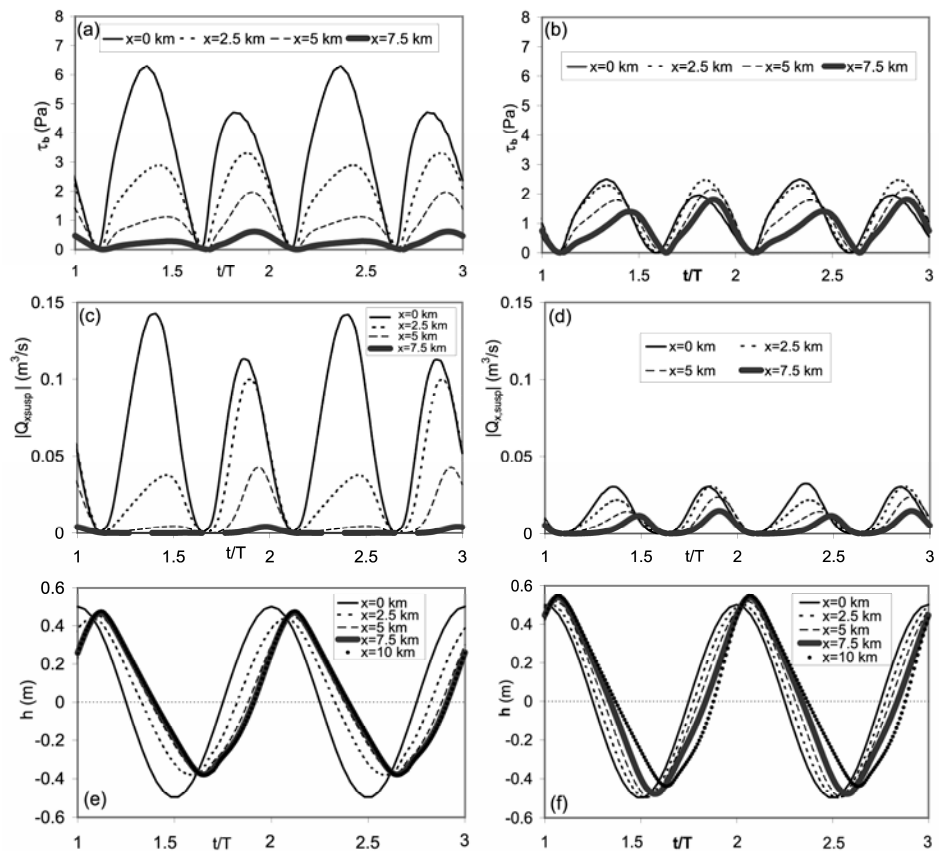


Fig 4 – The bottom shear stress, a), b), the absolute value of the suspended load c), d) and the water surface elevation e), f) along the main channel axis are plotted versus time at four different sections ($x=0, 2.5, 5.0$ and 7.5 km). Plots a), c) and e) refer to initial bottom configuration; plots b), d) and f) result from bottom configuration after 10000 cycles.

Tab 1 – Net (tidally averaged) sediment discharge (m^3/s).

	$x=0$ km	$x=2.5$ km	$x=5$ km	$x=7.5$ km
Q_{sa} (initial bottom)	-0.0111	0.0114	0.0069	0.0007
Q_{sa} (final bottom)	-0.0007	0.0011	0.0014	0.0006

Finally, Figure 4e,f show temporal distribution of water levels along the axis of the channel at $x=0, 2.5, 5, 7.5, 10$ km, respectively. At the beginning of the computation the tidal wave is phase lagged as it propagates along the channel. Moreover, it is damped in the first part of the channel, while in the inner part reflection effects at the boundary yields to a small increase of the amplitude.

After 10000 cycles the tidal amplitude is almost constant and the phase lag and the distortion are significantly smaller.

The picture of the morphological evolution of the main channel emerging from the present two-dimensional simulations appears to be qualitatively similar to the scenario resulting from the one-dimensional treatment of Lanzoni and Seminara [2002]. However, the effects of tidal flats and of time variations of the main channel width (not accounted for by Lanzoni and Seminara, 2002) leads to some peculiar features, summarized in the overall view of Figure 5. It clearly appears that tidal flats are progressively carved by a smaller creek network, which allows the tidal wave to propagate faster into the tidal flats, thus reducing tidal wave phase lag, distortion and dissipations. Moreover, the initially uniform main channel experiences a widening near the inlet and a contemporaneous narrowing of its landward reaches.

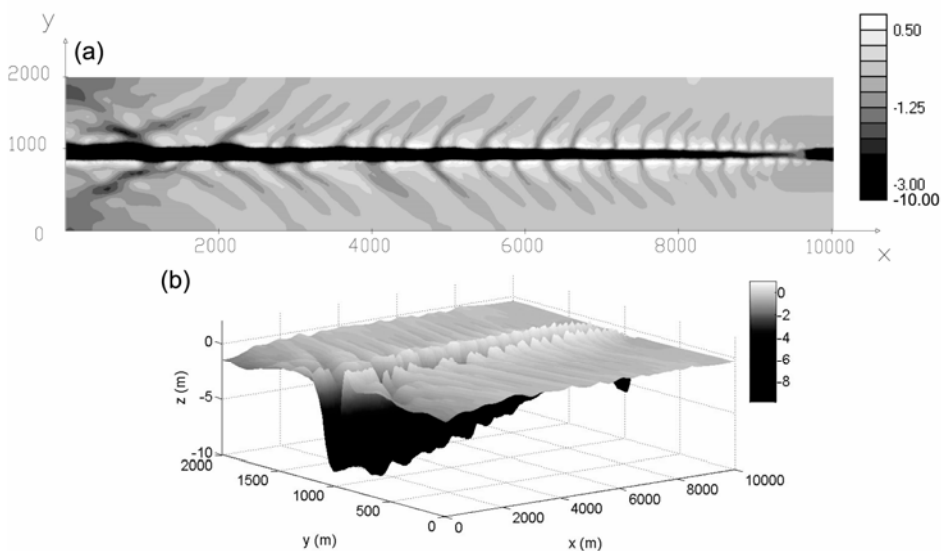


Fig 5 – a) Spatial distribution of bed elevation of the tidal channel and of the adjacent tidal flats after 10000 cycles. b) Three-dimensional view of the bottom after 10000 cycles. Bottom elevation is referred to mean sea level.

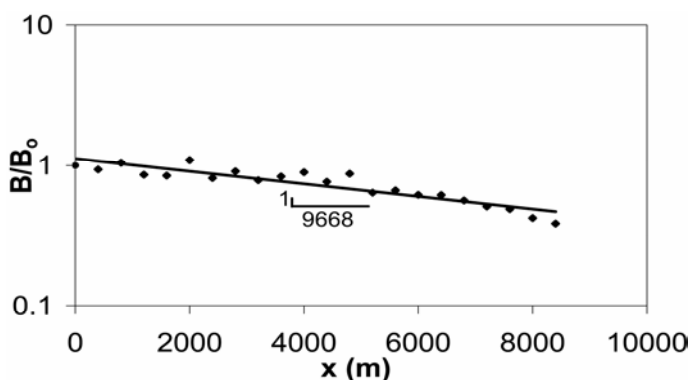
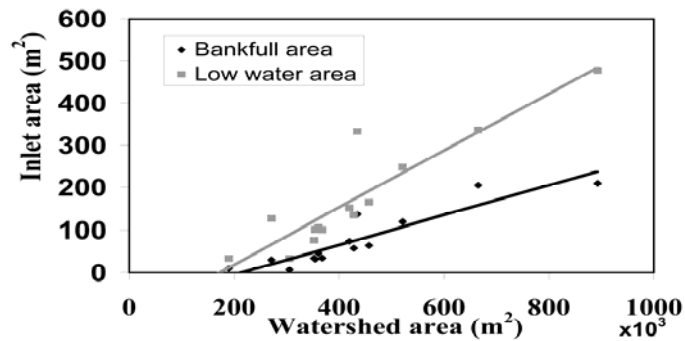


Fig 6 – The main channel width, scaled by the channel width at the mouth, is plotted versus the landward orientated longitudinal axis x . The plot refers to the bed configuration attained at the end of Run 1.

The resulting channel funneling, clearly shown in Figure 6, follows, with a good approximation, an exponential trend, with a convergence length of 9668 m. Channel funneling, as well as reduced dissipations, favor the increase of tidal amplitude with respect to initial conditions observed in figure 4e,f.

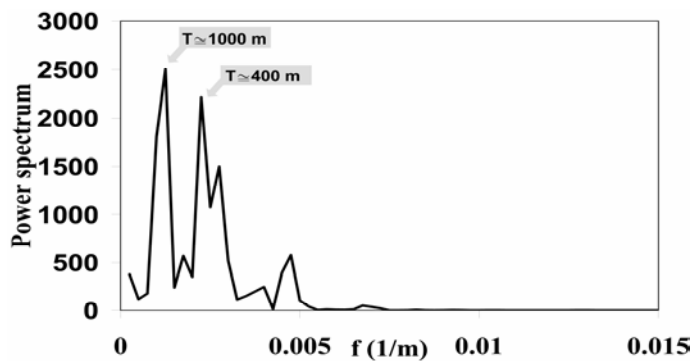
Fig 7 – The inlet cross sectional area of creeks forming on tidal flats is plotted versus their watershed area. Values of the inlet cross sectional area at both bankfull (gray squares), and low water (black dots) are shown.



The tidal creeks carving the tidal flats are characterized by a nearly linear relationship between the cross sectional area at creek inlet and creek watershed area (Fig. 7), as observed by Rinaldo et al. [1999] in real tidal networks. Other features typically observed in tidal environments are the levees which form near the main channel borders. The suspended sediment carried out by the main channel tends in fact to deposit quite rapidly as the water flowing from the main channel spread over tidal flats.

We also investigated the spacing between the tidal flat creeks, measured along a longitudinal section located at a distance of 50 m from the main channel. The power spectrum shown in Figure 8 indicates the presence of two main frequency peaks, corresponding to inter-creek distances of about 1000 and 400 m, respectively. The first value resulting from our fully non-linear analysis is very close to the minimum distance L between the creek (1193 m) which, according to the linear analysis carried out by Toffolon and Todeschini [2006], is necessary to ensure a stable creek system.

Fig 8 – Power spectrum of the spacing between tidal flat creeks, measured along a longitudinal section at a distance of 50 m from the main channel. The plot refers to the bed configuration attained at the end of Run 1.



3.1 Run 2

In this second simulation we considered a smaller part of the domain simulated in the first run. The main channel reach, 1500 m long, was in fact small enough to neglect tide propagation effects within the channel. Owing to the symmetry, we considered only the left tidal flat flanking the main channel.

We thus prescribed a sinusoidal water oscillation with $a=0.5$ m and $T=12$ hours along the main channel axis, whose bed elevation was kept fixed during the tidal cycle. A free bed evolution condition was assumed along the lateral boundaries of the tidal flat and along the tidal flat divide, parallel to the channel

axis. The concentration along the main channel axis was kept fixed and equal to its equilibrium value C_{eq} during the flood phase, while during the ebb phase it was calculated numerically.

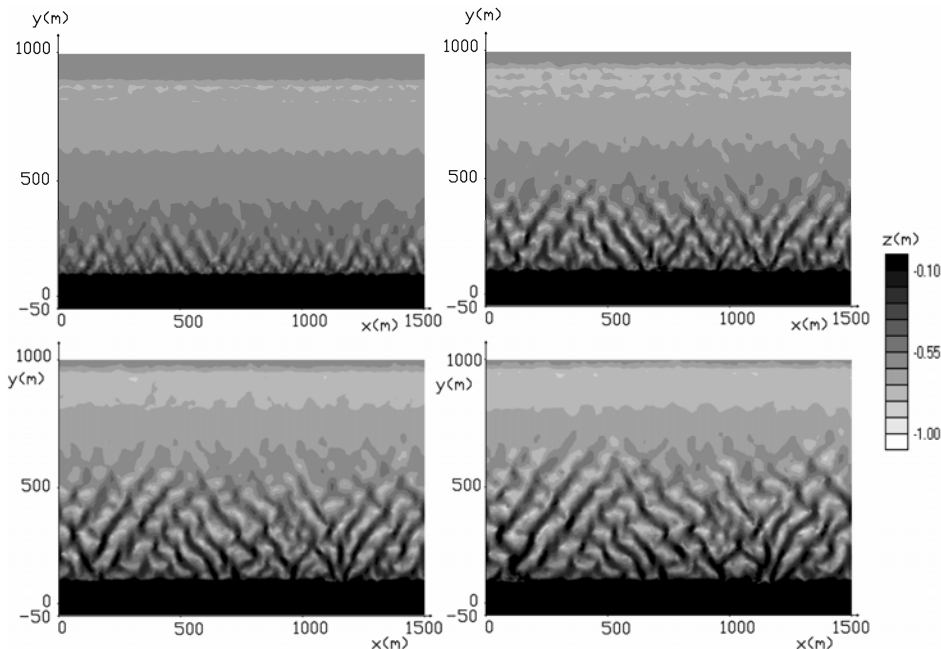


Fig 9 – Spatial distribution of bed elevation calculated in run 2 after: a) 2000 cycles; b) 4000 cycles; c) 6000 cycles and d) 8000 cycles. Bottom elevation is referred to mean sea level.

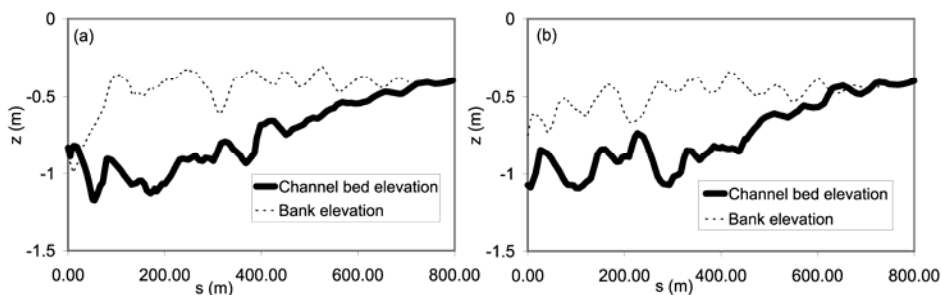


Fig 10 – Longitudinal profiles of bed elevation and bank elevation of two creeks formed on the tidal flat adjacent to the main channel. Origin of the s axis is located at the main channel bank.

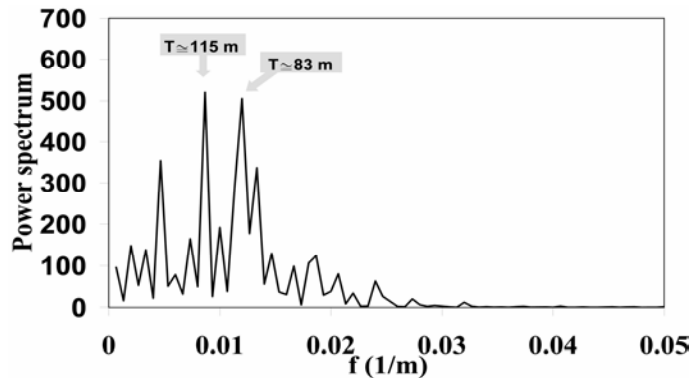
No flux boundary conditions were assumed along the other three boundaries. The simulation was stopped after 8000 tidal cycles.

Figure 9 shows the spatial distribution of bottom elevation at various times. The tidal flat is progressively dissected by creeks, which tend to dispose at an angle of $\pm 30^\circ$ with respect to the direction of the main channel axis. Two typical examples of the longitudinal profile of bottom and bank elevations along tidal flat creeks are shown in Figure 10. The concave up longitudinal bed profile is qualitatively similar to that of the main channel, displayed in Figure 2.

Although this second run essentially reproduced a smaller portion of the tidal sub-basin simulated in Run 1, the structure of the tidal flat creek network at the end of the simulation is characterized by significantly smaller inter-creek distances. The power spectrum of the creek spacing along a longitudinal section at a distance of 50 m from the main channel, displayed in Figure 11, indicates the presence of two major peaks for inter-creek distances of 115 and 83 m, considerably smaller than the creek spacing observed in the final

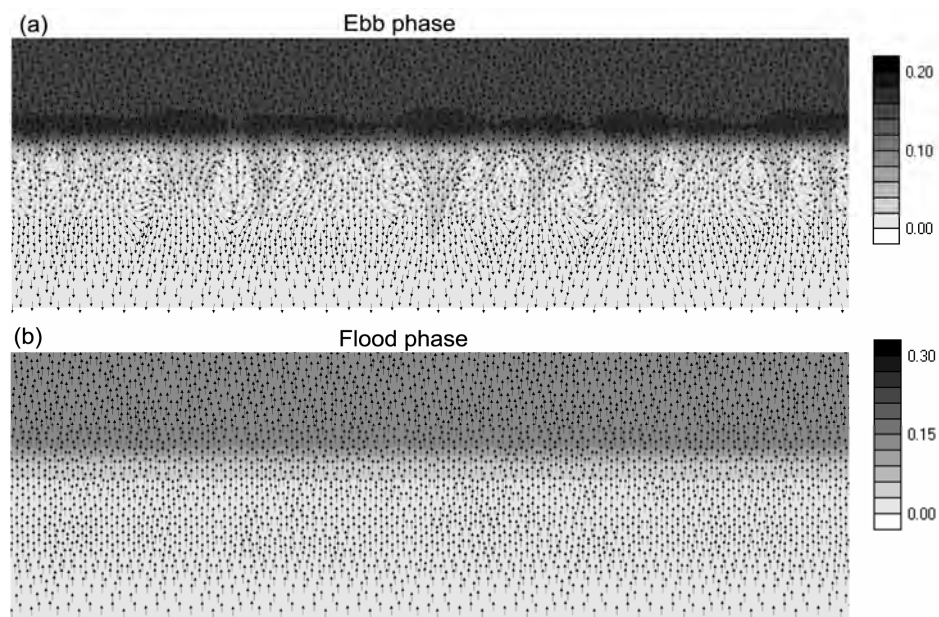
configuration of Run 1. A possible explanation of this result is that the final configuration of Run 2 was not yet in equilibrium.

Fig 11 – Power spectrum of the spacing between tidal flat creeks, measured along a longitudinal section at a distance of 50 m from the main channel. The plots refer to the configuration attained at the end of Run 2.



Further research is however required to clarify how the tidal flat creek network tends to organize towards a possible equilibrium configuration. The physical processes that gives rise to tidal flats canalization also needs to be investigated. A possible mechanism suggested by present simulations is shown in Figure 12, reporting a typical flow field configuration observed in the early stages of Run 2.

Fig 12 – Flow field characterizing the early stages of Run 2. a) High water slack; b) low water slack. The arrows indicate the direction of the flow velocity, but not its module. The bed elevation is referred to mean sea level.



An array of two dimensional counter-rotating vortexes is observed to form, during the ebb tide, near the border between the tidal flat and the main channel (Fig. 12a). The length scale of these vortex is of the same order of magnitude of the main channel width. On the contrary, the velocity is invariably directed landward during the flood phase (Fig. 12b). The completely different spatial distribution which characterizes the maximum velocities during the ebb and flood phases is likely to favour the inception of tidal flats channelization.

4 Conclusions

The fully nonlinear two-dimensional numerical simulations described in this contribution represent a first attempt to study the long term morphodynamic

evolution of a tidal channel flanked by tidal flats. Although the main channel evolution scenario arising from the present numerical experiments is qualitatively similar to the one provided by one-dimensional models, some new interesting features emerge. The tidal creek network which forms over the tidal flats, in fact, enhances the speed of propagation of the tidal wave, thus modifying the tidal propagation along the adjacent main channel. Moreover, channel funneling is a direct result of morphodynamic evolution, rather than of a priori choice.

Obviously, a larger set of numerical simulations is required to better understand the physical processes which determine the structure of the creek network forming over the tidal flats. Further analyses (e.g. probability distributions of unchanneled flow lengths) are required to fully characterize the morphometric features of tidal flat creeks and to address the comparison with creek networks observed in the field. Moreover, the modeling of main channel bank migration deserves further attention, in order to account for the problems associated to bedload transport over high slopes and to the cohesive nature of tidal sediment. The onerous computational effort that is required to carry out the two-dimensional long term morphodynamic simulations described here, suggests the strong need of developing a suitable sub-grid model of bank erosion.

References

- Defina, A. (2003), Numerical experiments on bar growth, *Water Resour. Res.*, 39(4), 1092, doi: 10.1029/2002WR001455, 2003.
- Defina, A. (2000), Two-dimensional shallow flow equations for partially dry areas, *Water Resour. Res.*, 36(11), 3251–3264.
- Defina, A., & I. Bonetto (1998), Rappresentazione dei termini di accelerazione convettiva in un modello bidimensionale della propagazione di onde lunghe in acque basse, paper presented at *XXVI Convegno di Idraulica e Costruzioni Idrauliche*, CUECM, Catania, Italy (in italian).
- Friedrichs, C. T., & D. G. Aubrey (1988), Nonlinear tidal distortion in shallow well-mixed estuaries: A synthesis, *Estuarine Coastal Shelf Sci.*, 27, 521–545.
- Friedrichs, C. T. (1995), Stability shear stress and cross-sectional geometry of sheltered tidal channels, *J. Coast. Res.*, 11, 1062–1074.
- Lanzoni, S., & Seminara, G. (1998), On tide propagation in convergent estuaries, *J. Geophys. Res.*, 103, 30,793–30,812.
- Lanzoni, S. & Seminara, G. (2002), Long term evolution and morphodynamic equilibrium of tidal channels, *J. Geoph. Res.*, 107 (C1),1-13.
- Meyer-Peter, E. & Müller, R. (1948), Formulas for bed-load transport, In: *Proceedings of the 2nd Meeting of the International Association for Hydraulic Structures Research*, pp. 39-64, Int. Assoc. Hydraul. Res., Delft, Netherlands.
- Olesen, K. W. (1987), Bed topography in shallow river bends, *Commun. Hydraul. Geotech. Eng.* 87-1, Delft Univ. of Technol., Delft, Netherlands.

Parker, G., M. H. Garcia, Y. Fukushima, & W. Yu, Experiments on turbidity currents over an erodible bed. *Journal of Hydraulic Research*, 25(1) pp. 123-147.

Rinaldo, A., S. Fagherazzi, S. Lanzoni, M. Marani, & W. E. Dietrich (1999), Tidal networks, 3, Landscape-forming discharges and studies in empirical geomorphic relationship, *Water Resour. Res.*, 35, 3919–3929.

Schuttelaars, H. M., & H. E. de Swart (1996), An idealized long-term morphodynamic model of a tidal embayment, *Eur. J. Mech. B Fluids*, 15, 55–80.

Schuttelaars, H. M., & H. E. de Swart (2000), Multiple morphodynamic equilibria in tidal embayment, *J. Geoph. Res.*, 105, 24,105–24,118.

Smagorinsky, J. (1963), General circulation experiments with the primitive equations, I. The basic experiment, *Monthly Weather Review* 91, 99-152

Speer, P. E., & D. G. Aubrey (1985), A study on non-linear tidal propagation in shallow inlet/estuarine systems, II, Theory, *Estuarine Coastal Shelf Sci.*, 21, 206–240.

Struiksma, N. (1985), Prediction of 2-D bed topography in rivers, deformation in curved alluvial channels, *J. Hydraul. Eng. Div. Am. Soc. Civ. Eng.*, 111(HY8), 1169–1182.

Struiksma, N., & A. Crosato (1989), Analysis of a 2-D bed topography model for rivers, in River Meandering, *Water Resour. Monogr.*, vol. 12, edited by S. Ikeda and G. Parker, pp. 153–180, AGU, Washington, D. C.

Talmon, A. M., M. C. L. M. Van Mierlo, & N. Struiksma (1995), Laboratory measurements of the direction of sediment transport on transverse alluvial-bed slopes, *J. Hydraul. Res.*, 33, 495–517.

Tambroni, N., M. Bolla Pittaluga, & G. Seminara (2005), Laboratory observations of the morphodynamic evolution of tidal channels and tidal inlets, *J. Geophys. Res.*, 110, F04009, doi:10.1029/2004JF000243.

Toffolon, M., & I. Todeschini (2006), Channel competition in tidal flats, In *Proceedings of the 4th Conference on River, Coastal and Estuarine Morphodynamics*, RCEM 2005, edited by list of Editors (Taylor and Francis Group, London, 2006).

Van Rijn, L. C. (1984a), Sediment Transport, Part I: Bed load transport. *J. of Hydraulic Engineering*, 110(10), 1431-1456.

Van Rijn, L. C. (1984b), Sediment Transport, Part II: Suspended load transport. *J. of Hydraulic Engineering*, 110(11), 1613-1641.

RESEARCH LINE 3.15

Solid transport and circulation of the upper layers in the inlets and the coastal zone

WATER AND SOLID TRANSPORT ESTIMATES THROUGH THE VENETIAN LAGOON INLETS USING ACOUSTIC DOPPLER CURRENT PROFILERS

V. Kovačević¹, V. Defendi², F. Arena¹, M. Gačić¹, I. Mancero Mosquera¹, L. Zaggia², S. Donà², F. Costa², F. Simionato², A. Mazzoldi²

1 Istituto Nazionale di Oceanografia e di Geofisica Sperimentale, Trieste,

2 Istituto di Scienze Marine, ISMAR-CNR, Venezia

Riassunto

Il presente lavoro riassume i risultati preliminari delle analisi effettuate sulle serie di dati ottenute dai correntometri acustici (ADCP – Acoustic Doppler Current Profiler), posti sul fondo delle tre bocche di Porto della Laguna di Venezia. L'ADCP è impiegato per eseguire due tipi di misura in campo: in un caso sono acquisite misure puntuali, ma continue, per mezzo di correntometri installati sui fondali delle bocche; nell'altro si eseguono periodicamente dei transetti, lungo la sezione dello strumento fisso, mediante l'utilizzo di un ADCP montato su imbarcazione. Entrambe le installazioni dello strumento consentono di misurare la velocità della corrente marina ed il segnale di *backscatter* acustico, dalla cui calibrazione si ottiene la stima della concentrazione del particolato solido in sospensione. Dalla misura della velocità si deduce la stima della portata (volume d'acqua in unità di tempo) che, in seguito, combinata con la concentrazione del particolato solido sospeso fornisce una stima del flusso solido. I risultati qui riportati riguardano l'aggiornamento delle curve di portata per le tre bocche, per verificare possibili cambiamenti indotti dalla costruzione delle opere per la difesa dalle acque alte, l'estensione della serie temporale (concentrazione e flusso solido) per la bocca di Lido, dove è disponibile il maggior numero di informazioni, ed il calcolo di un bilancio preliminare per le tre bocche per un periodo comune di circa tre mesi nell'anno 2006. Dalle analisi eseguite si deduce che la relazione lineare tra la portata e la velocità, indice della bocca di Chioggia, è cambiata, in corrispondenza del sito d'ancoraggio dell'ADCP fisso, probabilmente a causa del restringimento della sezione. Per quanto riguarda le stime del flusso solido nella bocca di Lido, ottenute, rispettivamente, dalla calibrazione del segnale di *backscatter* dell'ADCP fisso e dell'ADCP mobile, si osserva, nella maggior parte dei casi, un buon accordo. Le differenze residue, in alcuni casi anche notevoli, sembrano giustificate non solo dall'asimmetria della morfologia della sezione, ma anche dalla distribuzione del carico solido al verificarsi di particolari condizioni meteo-marine. Un bilancio provvisorio del trasporto solido alle tre bocche, per un periodo di circa tre mesi (febbraio-aprile 2006), caratterizzato da scarsi eventi meteorologici intensi, evidenzia un export di circa 60.000 tonnellate di materiale solido dalla laguna verso il mare aperto, con un contributo predominante da parte della bocca di

Lido.

Abstract

The present work reports the preliminary results of the analysis based on the time series from the ADCPs (Acoustic Doppler Current Profilers), employed in the inlets of the Venetian Lagoon. Basically, in situ data originate from two types of measurements, namely, point measurements from the bed-mounted sensors and periodic measurements along the entire cross section carried out by means of a vessel-mounted instrument. Both types of instrumental installation acquire current velocity and backscattered acoustic signal, which is then calibrated for estimating the suspended sediment concentration. Discharge is obtained from the time series of current velocity in the inlet (index velocity method). Solid flux is then a product of the discharge and suspended sediment concentration. The time series of the water and sediment fluxes are updated for the Lido inlet, which has the longest time record, while for the other two inlets data are available for shorter time intervals. Simultaneous data from all the three inlets are available only for a time period of about three months (February - April 2006). The present analyses lead to the following considerations: the linear relationship between index velocity and discharge has changed in the Chioggia inlet, and the possible cause could be the narrowing of the cross section due to the construction of a navigation lock in correspondence to the ADCP location; the estimates of the solid flux at the Lido inlet, originating from the calibration of the backscattered signal from bed-mounted and vessel-mounted sensors are, prevalently, in a good agreement; exceptionally high discrepancies in several cases could be due to the asymmetry of the solid load distribution over the section, which increases with the action of the waves during particular weather conditions. A preliminary budget of the sediment transport between the lagoon and the open sea for the period February - April 2006 (without exceptional meteorological events) highlights an export of about 60000 tons of suspended materials from the lagoon toward the open sea, with a predominant contribution through the Lido inlet.

1 Introduction

The acoustic Doppler current profilers, ADCPs, are widely used to measure current velocities and discharge by using the Doppler shift of the backscattered acoustic signal [Yorke and Oberg, 2002; Holdaway *et al.*, 1999]. Moreover, the ADCPs have demonstrated to be a powerful tool for the estimate of suspended sediment concentration, derived from the calibrated backscattered acoustic signal [Land and Bray, 2000]. Combining current velocity and concentration, the ADCP could then be used to directly evaluate profiles of suspended sediment flux, and hence transport with a spatial and temporal resolution better than traditional techniques. For the above mentioned reasons, acoustic techniques are very promising for their potential in the investigation of large- and small-scale (turbulent) suspended sediment processes [Thorne and Hanes, 2002],

which strongly influence coastal and shallow water environments such as the Venetian Lagoon.

Experimental activities in the framework of the First (2001-2003) and the Second (2004-2006) Research Programmes of CORILA involved the monitoring of the marine currents and suspended sediment concentrations in the inlets of the Venetian Lagoon by means of ADCPs (CORILA, <http://www.corila.it>). The bed-mounted ADCPs, anchored approximately in the centre of the investigated section in each inlet, provide a long-term time series in a limited portion of the section (the profile above the sensors). The vessel-mounted ADCP, crossing the inlet, passing over the position of the bed-mounted ADCP, enables a periodical but discontinuous velocity surveys over almost the whole section. The synergy of the two kinds of measurements allows a space and time monitoring of velocity and suspended sediment concentration in different environmental conditions. These two variables are used for estimating the water and solid fluxes, and their time variability. A huge set of in situ measurements are, to a greater extent, concentrated in the Lido inlet. Nevertheless, data from the other two inlets are available and used for estimating a preliminary budget of the water and solid transports between the lagoon and the open sea.

The procedure for data handling is described in chapter 2; in chapter 3 the long-term tendency of the relationship between the current velocity and the discharge in the three inlets is discussed, in chapter 4 the long-term solid fluxes in the Lido inlet are shown, and in chapter 5 water and solid fluxes in all the three inlets are reported and compared for a common time interval with a preliminary sedimentary budget. Concluding remarks are given in chapter 6.

2 Data description

The way the data from the ADCP are collected has been described in Gačić *et al.* [2002a] and Arena [2004]. The methodological approach adopted to use the vertically averaged velocity data from the bed-mounted ADCP to estimate the discharge is reported in Gačić *et al.* [2002b]. The discharge is then determined on the basis of the linear regression described in chapter 3.

The backscatter signal from the bottom-mounted ADCP was calibrated against concentration profiles, extracted from the mobile ADCP transect at the location of the fixed instrument. The details about the conversion and calibration of the ADCP backscatter signal both from bed-mounted and vessel-mounted ADCPs in order to obtain the estimate of the suspended sediment concentration are illustrated in Arena *et al.* [2006]. A thorough description on estimating the suspended sediment concentration and solid flux are reported in Kovačević *et al.* [2007] and Defendi *et al.* [2007].

In this paper we deal with hourly time series of the vertically averaged velocity above the bed-mounted ADCP, like in Gačić *et al.* [2004]. Therefore, the corresponding water and solid fluxes are also hourly values.

Wind data recorded at the Oceanographic platform “Acqua Alta” at a 5 minutes time step is decomposed into u (eastward) and v (northward) components.

These are then averaged over an hourly period and used in order to illustrate the weather conditions in the study area. In particular, attention is given to the episodes of the north-easterly bora wind, which are identified by the negative sign of both u and v components.

3 Discharge versus velocity: a long-term tendency

The first estimates of the discharge [Gačić *et al.*, 2005] date back to the beginning of the measurement period (2001-2002). The discharge across the section was estimated by the vessel-mounted ADCP surveys. This estimate was then related to the vertically averaged horizontal velocity provided by the bed-mounted ADCP. A scatter plot of the two variables shows a linear relationship, as reported in an example referring to the Lido inlet for the time interval 2005-2006 (Fig. 1).

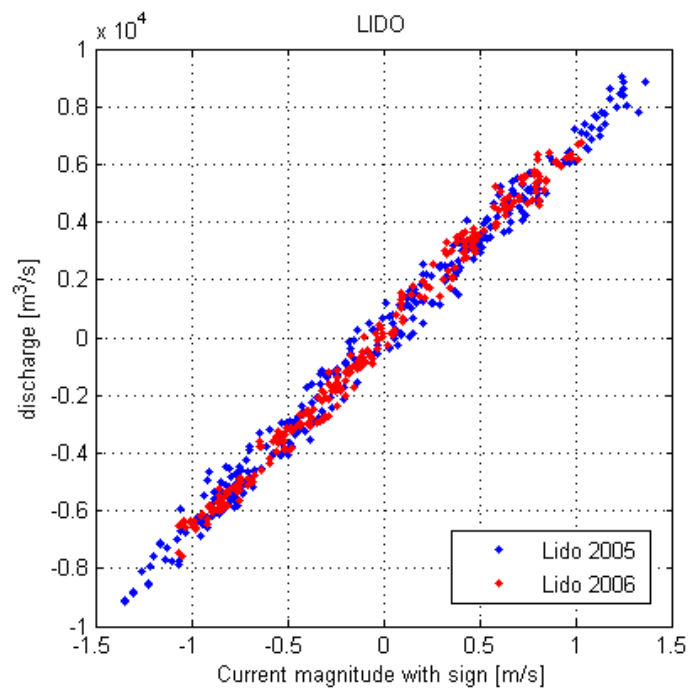


Fig 1 – Discharge versus vertically averaged current velocity, based on the field measurements carried out at the Lido inlet in 2005 and 2006. Positive (negative) current sign means the outflow (inflow) from the lagoon.

The corresponding regression lines, whose coefficients were determined by means of the least squares method, are depicted in Fig. 2. These linear relationships have been used for the discharge determination from the velocity time series, measured almost continuously in the lagoon inlets.

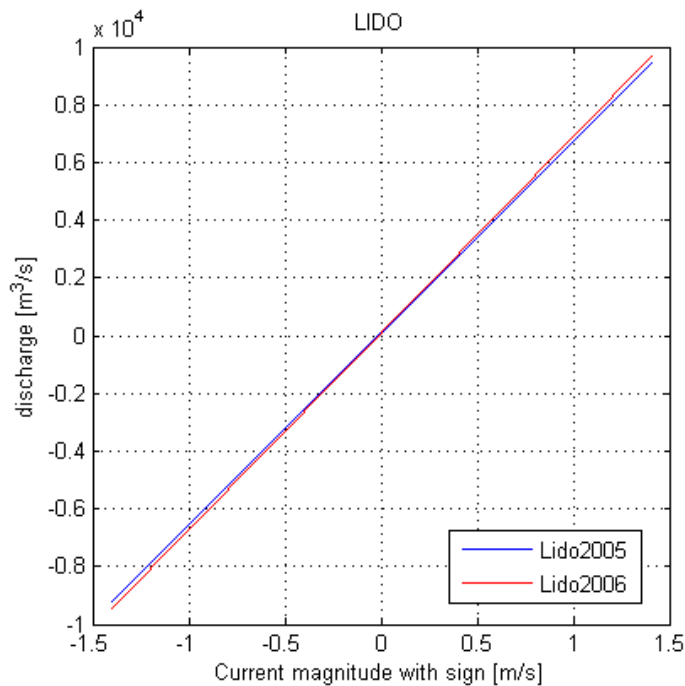


Fig 2 – Regression lines of discharge versus mean vertical velocity, based on the 2005 and 2006 field measurements at the Lido inlet.

The series of works for constructing the mobile barriers in the lagoon inlets begun in 2003. Channel dredging, breakwater repositioning, reshaping of the inlets morphology, and other structures built (<http://www.salve.it>) are supposed to modify the velocity field. We, therefore, investigated the discharge calculation, using the most recent data sets. The history of the linear relationship for the three inlets is summarized in Tabs. 1, 2, and 3, where the equation adopted for the calculation of the discharge for the specific time intervals is indicated. The corresponding regression lines are plotted in Figs. 3, 4, 5.

year	$Q_t = a \cdot V + b$	95% confidence interval	N
2001	$Q_t = 6594.449 V + 123.992$ [Gačić <i>et al.</i> , 2005]	$a \in [6433.680, 6755.210]$ $b \in [2.490, 246.480]$	49 (2001-2002)
2002 : 2004	as 2001	as 2001	-
2005	$Q_t = 6669.656 V + 103.816$	$a \in [6592.180, 6747.120]$ $b \in [49.770, 157.860]$	324
2006	$Q_t = 6828.608 V + 103.249$	$a \in [6748.930, 6908.270]$ $b \in [56.270, 150.220]$	266

Tab 1 – Lido inlet: linear regression relationship used for calculating the hourly discharge Q_t (m^3/s) from the vertically averaged velocity V (m/s). The sign of V indicates the outflow (+) or the inflow (-) with respect to the lagoon. N is the number of data used for the regression analysis, a and b are the coefficients of the regression line, each associated with an interval of confidence.

Tab 2 – Malamocco inlet: linear regression relationship used for calculating the hourly discharge Q_t (m^3/s) from the vertically averaged velocity V (m/s). The sign of V indicates the outflow (+) or the inflow (-) with respect to the lagoon. N is the number of data used for the regression analysis, a and b are the coefficients of the regression line, each associated with an interval of confidence.

year	$Q_t = a \cdot V + b$	95% confidence interval	N
2001	$Q_t = 6301.649 V + 176.400$ [Gačić <i>et al.</i> , 2005]	$a \in [6202.313, 6400.985]$ $b \in [94.095, 258.883]$	64
2002 : 2005	as 2001	as 2001	-
2006	$Q_t = 5892.244 V + 107.160$	$a \in [5820.280, 5964.200]$ $b \in [52.600, 161.710]$	231

Tab 3 – Chioggia inlet: linear regression relationship used for calculating the hourly discharge Q_t (m^3/s) from the vertically averaged velocity V (m/s). The sign of V indicates the outflow (+) or the inflow (-) with respect to the lagoon. N is the number of data used for the regression analysis, a and b are the coefficients of the regression line, each associated with an interval of confidence.

year	$Q_t = a \cdot V + b$	95% confidence interval	N
2001	no measurements available		-
2002	$Q_t = 4969.200 V - 159.610$ [Gačić <i>et al.</i> , 2005]	$a \in [4789.493, 5148.965]$ $b \in [-268.477, -50.747]$	62
2003 : 2004	as 2002	as 2002	-
2005	as 2002*	as 2002*	-
2006	$Q_t = 4023.500 V - 18.069$	$a \in [3982.135, 4064.804]$ $b \in [-41.962, 5.824]$	225

* uncertain due to the progressive narrowing of the section

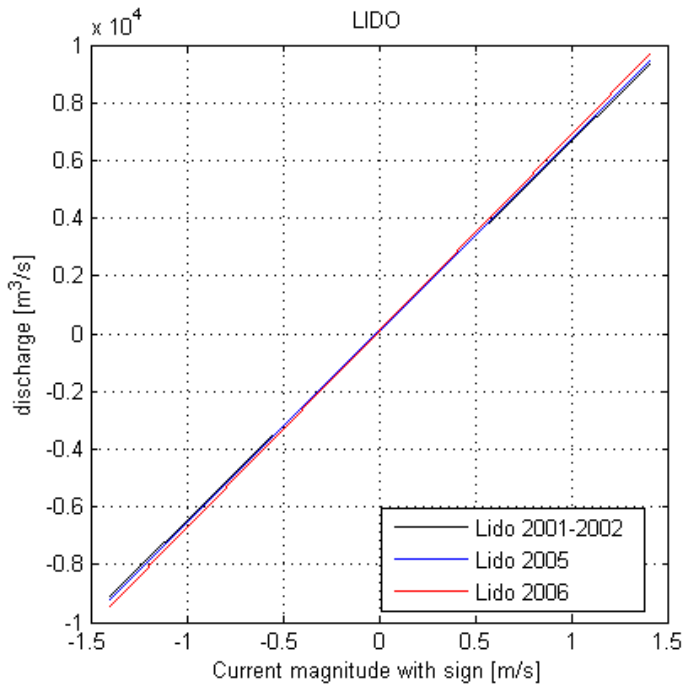


Fig 3 – Regression lines for the Lido inlet in different periods.

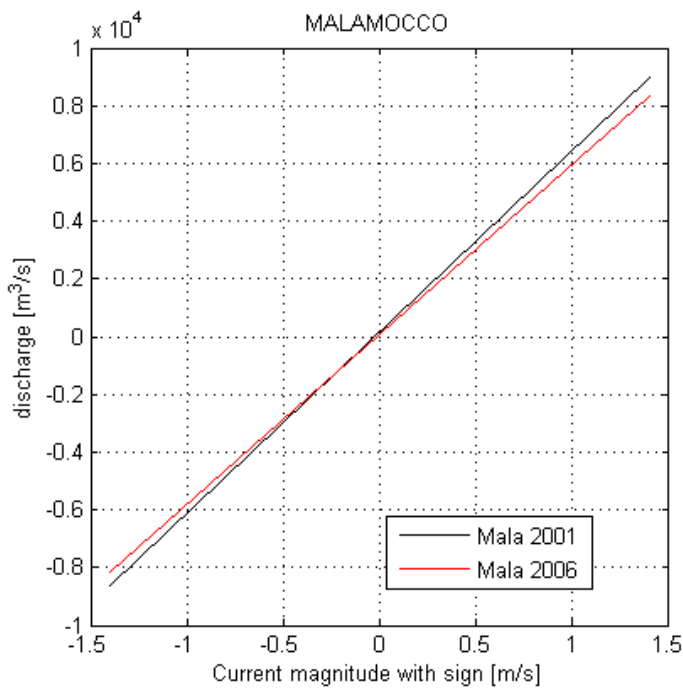


Fig 4 – Regression lines for the Malamocco inlet in different periods.

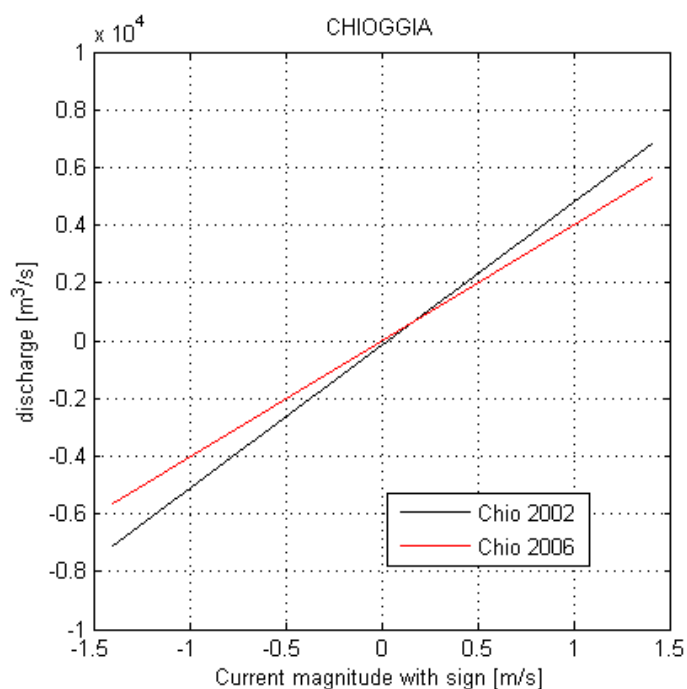


Fig 5 – Regression lines for the Chioggia inlet in different periods.

The most discernible change in the aspect of the regression lines is evident in the Chioggia inlet (Tab 3, Fig. 5). It is not possible to establish whether it has occurred gradually or not, due to the lack of continuity in the flux measurements between 2002 and 2006. However, in the course of 2004 and 2005 significant morphological modifications were caused by the works for the protection of the Venice Lagoon from floods (Fig. 6). These works caused a narrowing of the cross-sectional area over the ADCP section by 20%. The effects were observed mainly in the amplitude of the tidal constituents K1, M2 and S2, which gently increased over time since the second half of the year 2004, thus changing the linear relationship between the vertically averaged current velocity and the estimated flux [Mancero Mosquera *et al.*, 2007].



Fig 6 – Schematics of the construction plan in the Chioggia inlet: (1) refuge haven on the lagoon side, (2) wharfs and hard standing, (3) breakwater (http://www.salve.it/it/soluzioni/acque/f_eccellenziali.htm). The construction of the refuge haven (1) during 2005 narrowed the channel section in the correspondence of the bed-mounted ADCP location (white circle) which was maintained until February 2007. The new ADCP location since April 2007 is indicated by a green circle.

The most recent relationships have been used for the actual flux estimation, until the data set will be updated by the new in situ measurements. Moreover, the new regression analysis should be performed for the data collected since April 2007 in the Chioggia inlet, due to the relocation of the bed-mounted ADCP.

4 Solid flux estimates in the Lido inlet

In this chapter the hourly time series of the solid flux in the Lido inlet for the period October 2004 - December 2006 is presented and discussed. In particular, the flux estimates obtained from the bed-mounted and vessel-mounted ADCPs are compared. The solid flux from the bed-mounted ADCP is obtained from the hourly concentration estimates multiplied by the discharge. The suspended sediment concentrations are vertically averaged values and refer to the portion of the water column above the fixed instrument (Fig. 7). The highest values occurred in December 2005 and January 2006, during a period of storms with intense winds.

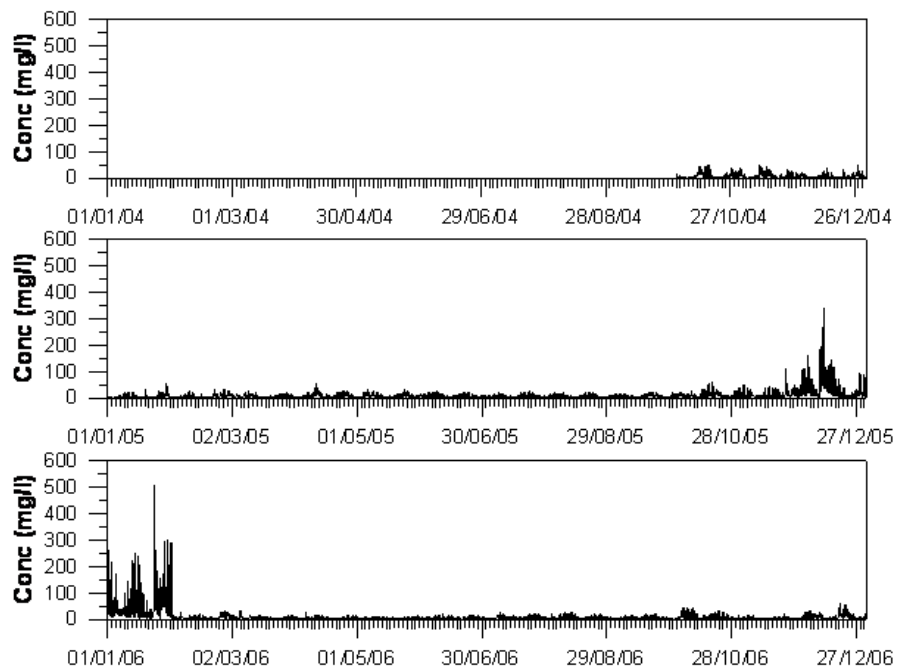


Fig 7 – Times series of the hourly suspended sediment concentration estimated from the calibration of the backscatter signal of the Lido bed-mounted ADCP from October 2004 through December 2006.

The corresponding time series of the solid flux is shown in Fig. 8. The values obtained from the calibrated backscatter acquired by the vessel-mounted ADCP during the periodical field surveys are superimposed on the continuous data set.

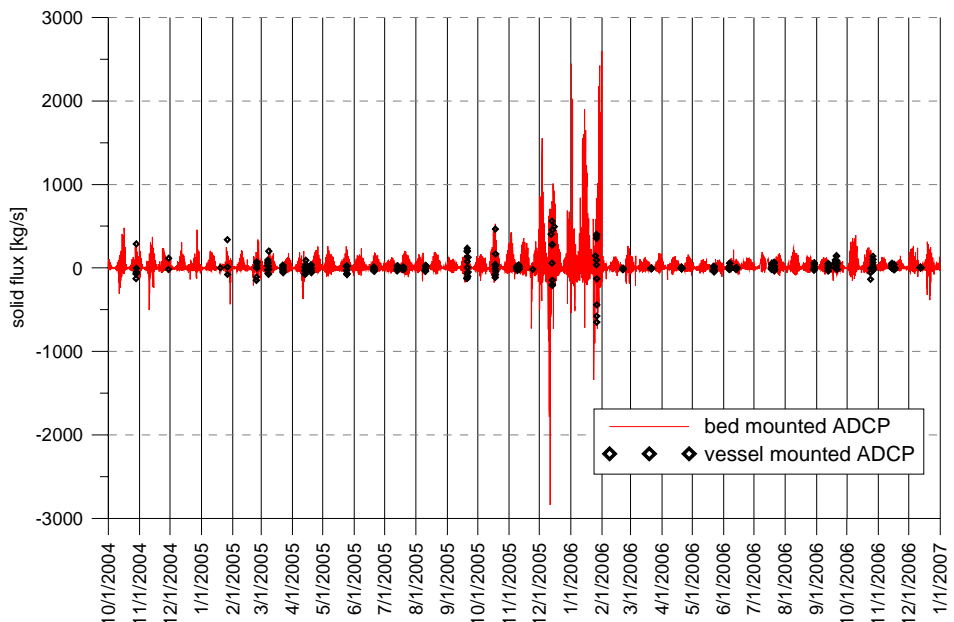


Fig 8 – Time series of the hourly solid flux in the Lido inlet from October 2004 through December 2006. The red line represents the values obtained from the bed-mounted ADCP data, while the black symbols are the corresponding fluxes obtained from the vessel-mounted ADCP data.

The dispersion diagram in Fig. 9 represents a direct comparison between the two estimates of the solid flux. In general, the two estimates group around the identity line (black line in Fig. 9). Nonetheless, in the range between -400 and 400 kg/s, the solid fluxes obtained from the bed-mounted ADCP tend to underestimate those of the vessel-mounted ADCP. A few outliers at high values ends affect the slope of the best fit line (red line in Fig. 9), which then shows an

opposite tendency, that is, the bed-mounted ADCP fluxes overestimate those provided by the vessel-mounted one. The two flux estimates, in general, agree when the concentrations are low and evenly distributed as in Fig. 10. The observed discrepancies may be due to the uneven and asymmetric spatial distribution of the suspended sediment concentration along the investigated section as shown in Fig. 11. This behavior may be induced, during particular meteorological conditions, by the wave action which causes a resuspension both inside the lagoon and along the nearby littorals. In this case, associated to a given tidal flow, an exceptional solid transport into or out of the lagoon may occur. Another possible reason for the asymmetric concentration distribution could be a change in the solid load in the two channels, Treporti and San Nicolò, which nourish the Lido inlet. This may happen, for example, during river floods, if the contribution of the tributaries in the northern basin of the lagoon is predominant with respect to the drainage basin of the San Nicolò channel.

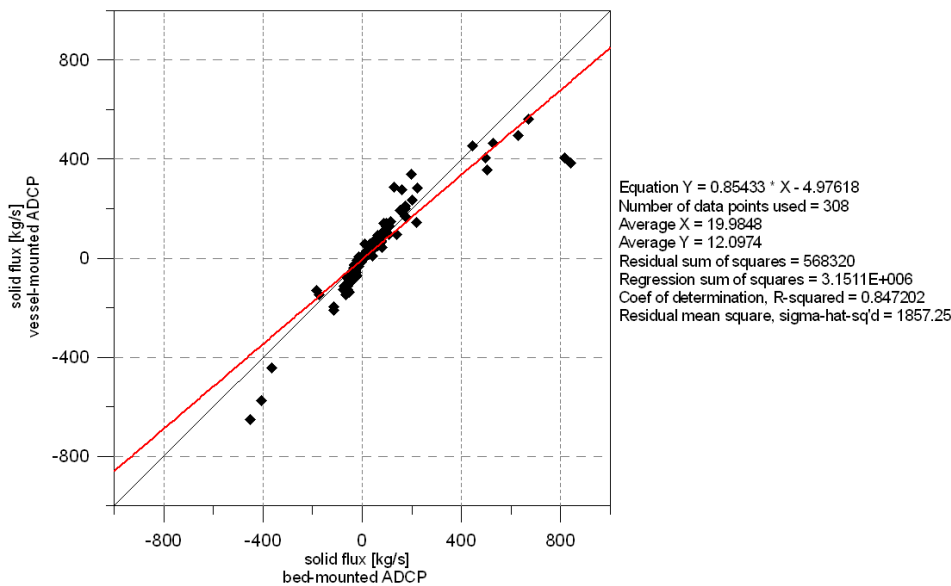


Fig 9 – Dispersion diagram of the solid flux from the vessel-mounted ADCP versus solid flux from the bed-mounted ADCP. The linear best fit line is depicted in red, while the theoretical identity line is in black.

Fig 10 – Example of the spatial distribution of the suspended sediment concentration along the Lido section in the case of a relatively good agreement between the solid fluxes estimated from the bed- and the vessel-mounted ADCPs. The tidal phase indicates an inflowing current of low intensity, 0.35 m/s. The rectangular outlined in red roughly identifies the zone investigated by the bed-mounted ADCP. The yellow line corresponds to the bottom track, and the black one to the maximum investigation depth reached by the vessel-mounted ADCP.

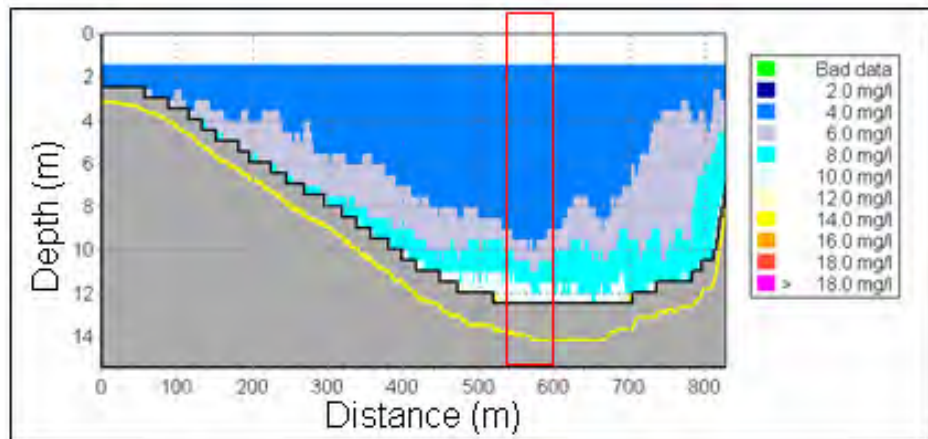
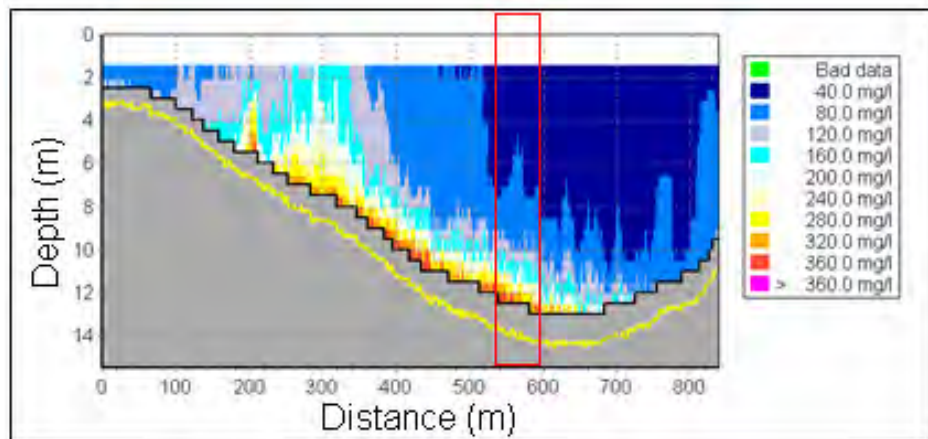


Fig 11 – As in Fig. 10, but for the case of the possible discrepancies between the solid fluxes estimated from the bed- and the vessel-mounted ADCPs. The tidal phase indicates an inflowing current of moderate intensity, 0.68 m/s.



5 Contemporary solid flux in the three inlets

Simultaneous measurements in all the three inlets are available in February, March, and April 2006. Figs. 12, 13, and 14 depict the time series of suspended sediment concentration, discharge, and solid flux for Chioggia, Malamocco and Lido inlets, respectively. Wind conditions from the Oceanographic Platform are considered as an indicator of the meteorological events that can possibly influence the distribution and transport of the solid materials.

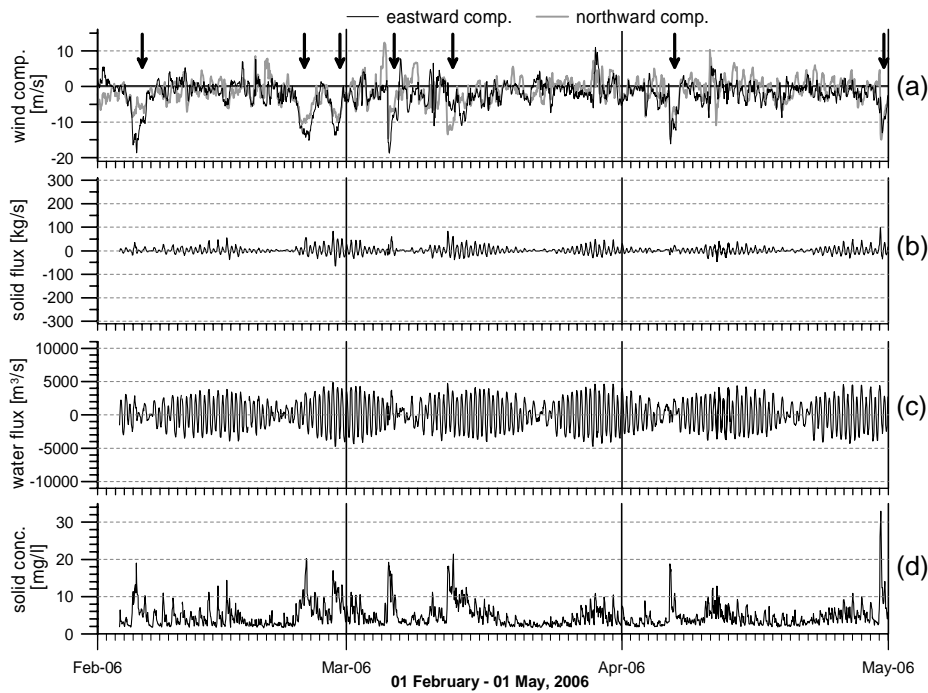


Fig 12 – Chioggia inlet in the time interval February – April 2006. (a) Wind components measured at the Oceanographic Platform *Acqua Alta*: the arrows indicate the bora events. (b) Solid flux. (c) Discharge. (d) Suspended sediment concentration.

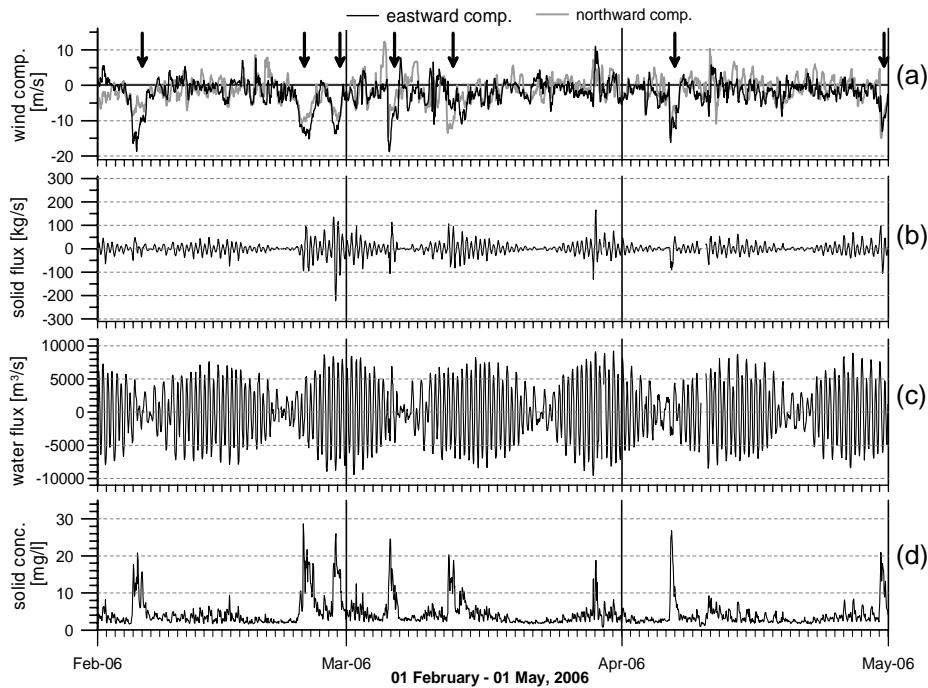


Fig 13 – As in Fig. 12, but in the Malamocco inlet.

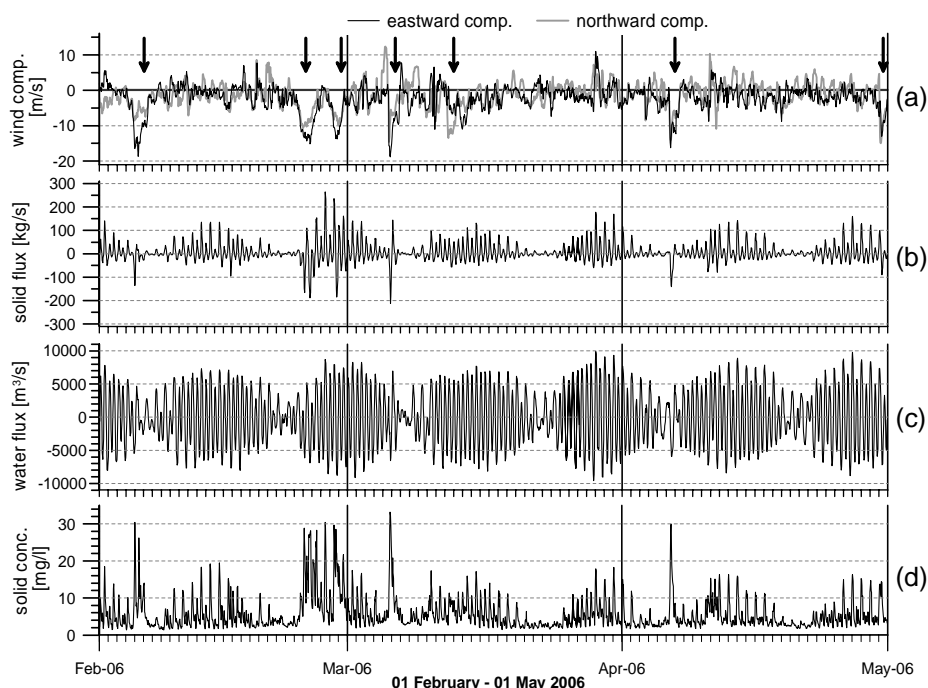


Fig 14 – As in Fig. 12, but in the Lido inlet.

In general, concentration values are the largest in the Lido inlet (Fig. 15) and the smallest in the Chioggia inlet (Fig.13). Suspended sediment concentrations of about 30 mg/l and higher are observed in correspondence to the north-easterly bora wind events. Bora winds (indicated by the negative values of the two wind components) trigger a wave motion responsible for the resuspension in the inlets and along the littorals. There are few such episodes (indicated by the arrows in the figures) observed during the study period. In particular, the event of the longest duration is recorded in February. The solid flux increases, as well, but in an exceptional way only if associated with stronger inflowing/outflowing currents during the spring tides.

6 Preliminary budget of the solid transport across the three inlets

A preliminary budget of the lagoon – open sea exchanges is estimated as follows. For the time period available (approximately three months), the total amount of water and suspended sediments is determined in each inlet, with respect to the inflowing and outflowing current direction. Then, the total budget for the lagoon has been estimated, as visualized in Fig. 15, summarizing together the contribution of the three inlets. The total suspended sediment transport is positive indicating an export from the lagoon toward the open sea. Qualitatively it can be inferred that the contribution of the Lido inlet is the largest one, and that of Malamocco the smallest. The water flow is positive (outflowing) in the Chioggia and Malamocco inlets and negative (inflowing) in the Lido inlet. This is in agreement with the water budget analysis done for the yearly time series February 2002 - February 2003, shown by Gačić *et al.* [2005b].

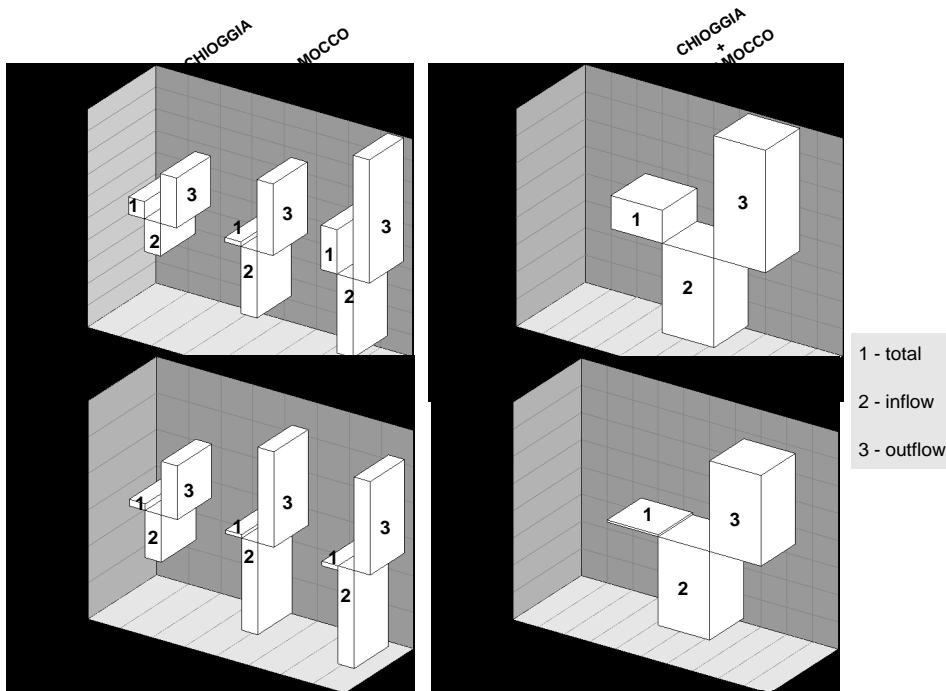


Fig 15 – Preliminary estimates of the water and suspended sediments budget in the three lagoon inlets.

The preliminary budget is summarized in Tab. 4, which indicates an export (positive sign) of about 60000 t of solid materials from the lagoon.

	Suspended load (tons)	Integrated water discharge (10^6 m^3)
total	60840	851
inflow	-162943	-32316
outflow	223783	33167

Tab 4 – Water and suspended sediments preliminary budget for the time period February 3 – April 30, 2006.

Conclusions

The measurements carried out periodically, although irregularly, in the lagoon inlets by means of a vessel-mounted ADCP helped in establishing the relationship between index velocity and discharge. In the Lido and Malamocco inlets, the relationship seems not to be altered significantly, even though the variation may be statistically detected. The variation found in the Chioggia inlet can be explained by the narrowing of the channel width after the construction of the refuge haven along its northern bank. It yielded to about 20% reduction of the section area in correspondence to the location of the bed-mounted ADCP.

The comparison of the two types of solid flux estimates for the Lido inlet, obtained, respectively, from the bed- and vessel-mounted ADCPs, highlights a good agreement in most cases. It is clear that the two estimates cannot coincide since they derive from two different kinds of instrumental installation.

Some significant differences may be associated with the asymmetry of the morphology of the investigated section and the uneven spatial distribution of the suspended sediments along it. This latter during some particular weather conditions (for example storm events) is quite remarkable.

The preliminary budget of the water and suspended sediments exchange between the lagoon and the open sea here presented is based on a three-month period (February – April 2006). A net export of about 60000 t of suspended sediments from the lagoon to the open sea is estimated, with a predominant contribution of the Lido inlet. During this time interval, there were no particularly intense meteorological events, which can significantly affect the suspended sediments distribution and solid transport across the inlets, toward both the lagoon and the open sea. This budget is only preliminary because it is relative to a short time period and does not include the contribution of the bed load transport, which is under estimation by means of numerical models. The use of a larger data set will allow taking into account the influence of meteorological conditions more intense than those here considered.

Acknowledgments

This work was supported by CORILA (Consortium for the Coordination of the Scientific Research of the Venice Lagoon) in the framework of the three-year research program 2004-2006, Line 3.15 "Solid transport and circulation of the upper layers in the inlets and the coastal zone". Isaac Mancero Mosquera participated with the support of the Programme for Training and Research in Italian Laboratories (TRIL) of the Abdus Salam International Centre for Theoretical Physics (ICTP), Trieste. Wind data were made available by the "Istituzione Centro Previsioni e Segnalazioni Maree" of the Municipality of Venice.

References

- Arena F., 2004. Attività di Campagna – Misure correntometriche alle Bocche di Porto di Venezia. RELI-5/2004 – OGA-2.
- Arena F., Kovačević V. and Mazzoldi A., 2006. Estimate of the suspended solid matter concentration from the backscatter intensity measured by ADCP. In: Scientific Research and Safeguarding of Venice-CORILA Research Program 2004-2006, 2005 Results, P. Campostrini (Ed.), 373-387.
- Defendi V., Kovačević V., Zaggia L., Mancero Mosquera I., Gačić M., Simionato F., Costa F., Arena F., Mazzoldi A. and Ferla M., 2007. Estimating suspended sediment concentrations from Acoustic Doppler Current Profiler data in the Venice Lagoon inlets, Italy. Proceedings of the 2007 Hydraulic Measurements & Experimental Methods Conference, Lake Placid, New York, 10-12 September 2007, 362-367.
- Gačić M., Kovačević V., Mazzoldi A., Paduan J., Arena F., Mancero Mosquera

- I., Gelsi G. and Arcari G., 2002a. Measuring Water Exchange between the Venetian Lagoon and the Open Sea. *Eos, Transactions, American Geophysical Union*, Vol. 83, No. 20, 15 May 2002, 271, 221-222.
- Gačić M., Mazzoldi A., Kovačević V., Arena F., Mancero Mosquera I., Gelsi G. and Arcari G., 2002b. Analysis of current measurements in inlets of the Venetian Lagoon. In: *Scientific Research and Safeguarding of Venice-CORILA Research Program, 2001 Results*, P. Campostrini (Ed.), 489-498.
- Gačić M., Mancero Mosquera I., Kovačević V., Mazzoldi A., Cardin V., Arena F., Gelsi G., 2004. Temporal variations of water flow between the Venetian lagoon and the open sea. *Journal of Marine Systems*, 51, 33-47.
- Gačić M., Kovačević V., Mancero Mosquera I., Mazzoldi A. and Cosoli S., 2005. Water fluxes between the Venice Lagoon and the Adriatic Sea. In: *Flooding and Environmental Challenges for Venice and its Lagoon: State of Knowledge*, Fletcher C. A. and Spencer T. (Eds), Cambridge University Press, 431-444.
- Gačić M., Mazzoldi A., Kovačević V., Cosoli S., Mancero Mosquera I., Arena F., and Cardin V., 2005b. Water fluxes in Venice lagoon inlets and coastal circulation. In: *Scientific Research and Safeguarding of Venice, CORILA Research Program 2001-2003, 2003 results*, P. Campostrini (Ed.), 311-321.
- Kovačević V., Defendi V., Zaggia L., Costa F., Arena F., Simionato F., Mazzoldi A., Gačić M. and Amos C., 2007. Time series of suspended particle concentration from the conversion of acoustic backscatter at the Lido inlet. In: *Scientific Research and Safeguarding of Venice 2006, CORILA Research Program 2004-2006, 2005 results*, P. Campostrini (Ed.), 315-329.
- Holdaway G.P., Thorne P.D., Flatt D., Jones S.E. and Prandle D., 1999. Comparison between ADCP and transmissometer measurements of suspended sediment concentration. *Continental Shelf Research*, 19, 421-441.
- Land J.M. and Bray R.N., 2000. Acoustic measurement of suspended solids for monitoring of dredging and dredged material disposal. *Journal of Dredging Engineering*, 2 (3), 1-17.
- Mancero Mosquera I., Gačić M. and Mazzoldi A., 2007. Long-term changes in the kinematics of inlets of the Venetian Lagoon (NE Italy). *Il Nuovo Cimento*, Vol. 30, N. 2, 149- 156.
- Thorne P.D. and Hanes D.M., 2002. A review of acoustic measurement of small-scale sediment processes. *Continental Shelf Research*, 22, 603-632.
- Yorke T.H. and Oberg K.A., 2002. Measuring river velocity and discharge with acoustic Doppler profilers. *Flow Measurement and Instrumentation*, 13, 191-195.

SURFACE CURRENT PATTERNS IN FRONT OF THE VENETIAN LAGOON AND THEIR VARIABILITY AT DIFFERENT WIND REGIMES

Isaac Mancero-Mosquera¹, Miroslav Gačić¹, Vedrana Kovačević¹, Andrea Mazzoldi², Simone Cosoli², Jeffrey D. Paduan³, Sadegh Yari^{1,4}

1 Istituto Nazionale di Oceanografia e di Geofisica Sperimentale, Trieste, Italy

2 Istituto di Scienze Marine (ISMAR-CNR), Venice, Italy

3 Naval Postgraduate School, Monterey, CA, U.S.A.

4 Research Fellow of the "Abdus Salam" International Centre for Theoretical Physics, Trieste, Italy

Riassunto

Nell'articolo viene presentato lo studio del campo di correnti superficiali nell'area di mare di fronte alla laguna di Venezia per un periodo temporale di 22 mesi (Febbraio 2004 – Novembre 2005) in funzione di differenti condizioni di vento e di flusso mareale nella bocca di Malamocco.

Abstract

The features of surface current field in front of the Venetian Lagoon is studied for a 22-month long period (February 2004 – November 2005) in connection to different wind conditions and to the tidal jet in Malamocco inlet.

1 Introduction

Monitoring of the surface current velocity field in front of the Venetian lagoon has been carried out by the CNR – ISMAR and OGS Institutes using two High-Frequency coastal radars (SeaSonde, by COS Ltd, operating at 25 MHz) installed on Lido and Pellestrina islands. A third antenna is located at the Oceanographic Platform "Acqua Alta" of CNR, 15Km offshore from Malamocco inlet. Location of ADCP as well as radar antennas are shown in Figure 1. Together, the network provides time series of radial velocities measured from each antenna, which combined via software allow for the reconstruction of current velocity vectors at hourly time rate.

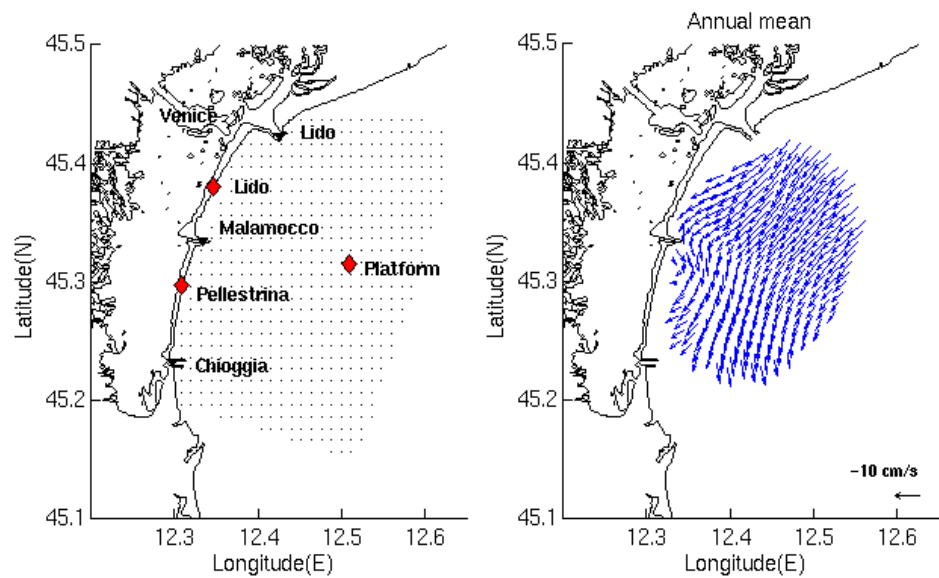
While annual statistics show agreement with the previously reported cyclonic circulation [Cushman-Roisin et al., 2001] in the North Adriatic Sea as seen in Figure 2, monthly statistics reveal some departures from this expected behaviour. The annual mean field shows basically a southward flow following the shoreline with small meandering in the vicinity of Malamocco inlet, which is due to the combined influences of the tidal pumping from the inlet and jetties. Some representative cases has been chosen and explained next for illustration. May 2004 (spring) is characterised by a strong inversion of mean flow (Figure 3) as compared with the one observed in August 2004 (Figure 4), when a

clockwise flow is detected only near the shoreline. Although weak, the flow still follows the counter-clockwise circulation far from the coast. On the other hand, a reinforcement of the normal circulation is found in November 2004 (Figure 5) while some eddies are detected near the Malamocco inlet in July 2005 (Figure 6).

Since the area of interest is strongly affected by winds, namely Bora (from NE) and Scirocco (from SE), a simultaneous wind record is analysed in this work. Also current velocities, measured in the inlet of Malamocco, are taken into consideration. Wind speed and azimuth is measured in the Platform "Acqua Alta" and current in the Malamocco inlet (as in Lido and Chioggia inlets) is monitored via bottom-mounted ADCP (Acoustic Doppler Current Profiler).

Fig 1 (left) – Study area. ADCP locations noted in black. Radar antennas locations shown in red.

Fig 2 (right) – The cyclonic circulation in the Northern Adriatic Sea as detected from radar observations.



2 Data handling and methods

Every HF (High Frequency) radar antenna is able to detect velocity vectors radially-disposed around the station. These are combined with the other antennas' radial vectors falling in an 1,5 Km radius area encircling each grid point in order to make the corresponding velocity vector. The total vector is the one whose projections along radial directions best explain observed measurements, according to a Least-Squares criterion as described in [Lipa and Barrick, 1983].

After hourly time series are formed, some quality control was performed. A process to eliminate anomalous values (one-to-two hour spikes) is based in their short-duration nature. First differences time series were computed for each grid point in order to remove low frequencies and to achieve a second-order stationarity, i.e. means decaying to zero and variances more steady than in original dataset. The spike, resembling a Dirac function, is thus transformed into a pair of consecutive spikes with opposite signs (as a Doublet function). Since the differenced data satisfy conditions of a Gaussian distribution, two thresholds including 99% of data is defined (± 2.58 standard deviation); so that a value

falling outside of these limits is possibly a by-product of a spike. If the successive value falls outside the limits but with opposite sign, the corresponding data in the original time series is deleted as a spike. An extension of this process for cancelling two-hours spikes is also done [Kovačević et al., 2004] by checking three consecutive differenced data.

A second quality control is made via adjustment of data return criterion. It has been expressed that percentage of data return is indicative of reliability in the time series, so that 50% threshold [Paduan and Rosenfeld, 1996] and 60% [Kovačević et al., 2004] have been previously used. Since experimental monitoring always includes some random error (assumed to be Gaussian here), statistics computed thereof are also affected. In this work the Central Limit Theorem (CLT) is taken into consideration to provide a limit for inclusion of a data set in the analysis.

Let σ be the error associated to one hourly velocity datum. Let N be the size of one dataset. According to CLT, a time-averaged ensemble under this conditions could reduce the error by a factor of N in variance:

$$\sigma_N^2 = \frac{\sigma^2}{N}$$

Let R be the size of a sub sample drawn from the previous dataset, such that $R \leq N$. It is expected that $\sigma_R^2 \geq \sigma_N^2$, i.e. error increases due to a lesser quantity of data. If an upper limit of $1.25 \times \sigma_N^2$ is imposed on σ_R^2 , then:

$$\sigma_R^2 \leq 1.25 \times \sigma_N^2 \equiv \frac{\sigma^2}{R} \leq 1.25 \times \frac{\sigma^2}{N}$$

Or $R \geq 0.8 \times N$. Hence, to avoid an increasing of error higher than 25% a data return higher than 80% is needed. This criterion is applied hereafter with $N-R$ representing the missing data due to instrumental malfunctioning or the previous de-spiking process.

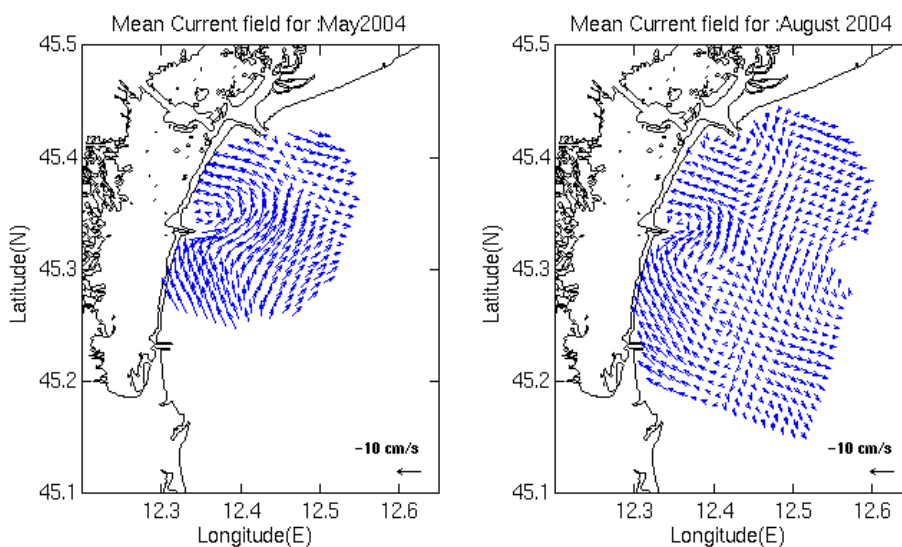
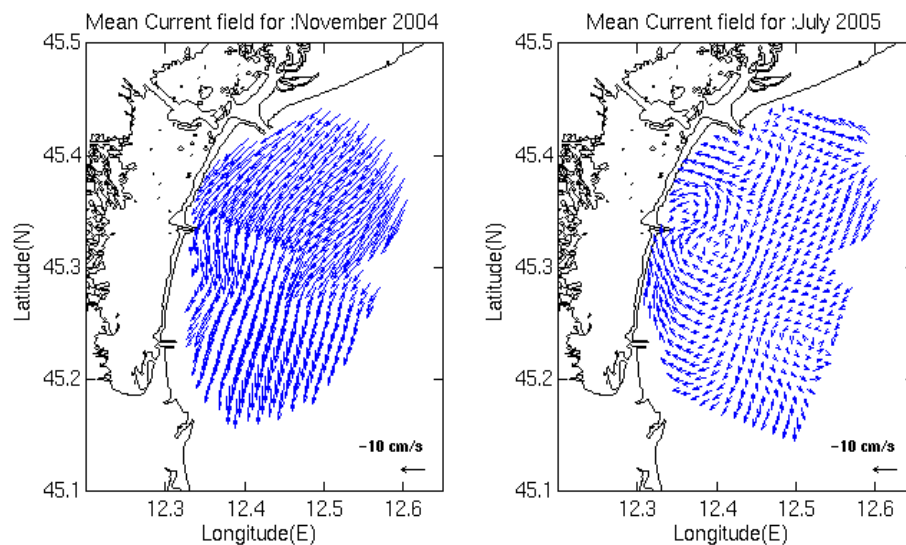


Fig 3 (left) – “Strong” inversion of the flow in May 2004.

Fig 4 (right) – “Weak” inversion of the flow in August 2004.

Fig 5 (left) – Alignment of the vector field in November 2004.

Fig 6 (right) – Vortices formation in July 2005.



Wind speed and azimuth values, measured every 5 minutes at the Platform, are averaged subsequently in order to obtain an hourly time series. Principal Component Analysis (PCA) is applied then to determine the main and minor variance axes. It was obtained that the first one coincides with the Bora direction, i.e. 230° Azimuth, while the orthogonal direction (320° Azimuth) coincides with Scirocco direction. The major axis variance accounts for about 75% of the observed total energy while the minor axis accounts for the rest.

Current velocities in Malamocco channel are sampled every 10 minutes, but a vertically-averaged series at hourly rate is produced. PCA is applied since currents are strongly aligned with the channel axis inside the inlet; in fact more than 99% of energy is polarised thus allowing for a reduction to a one-dimensional time series [Preisendorfer, 1988]. The main forcing inside the channel has been found to be astronomical [Gačić et al, 2004] with more than 90% of energy being due to tides.

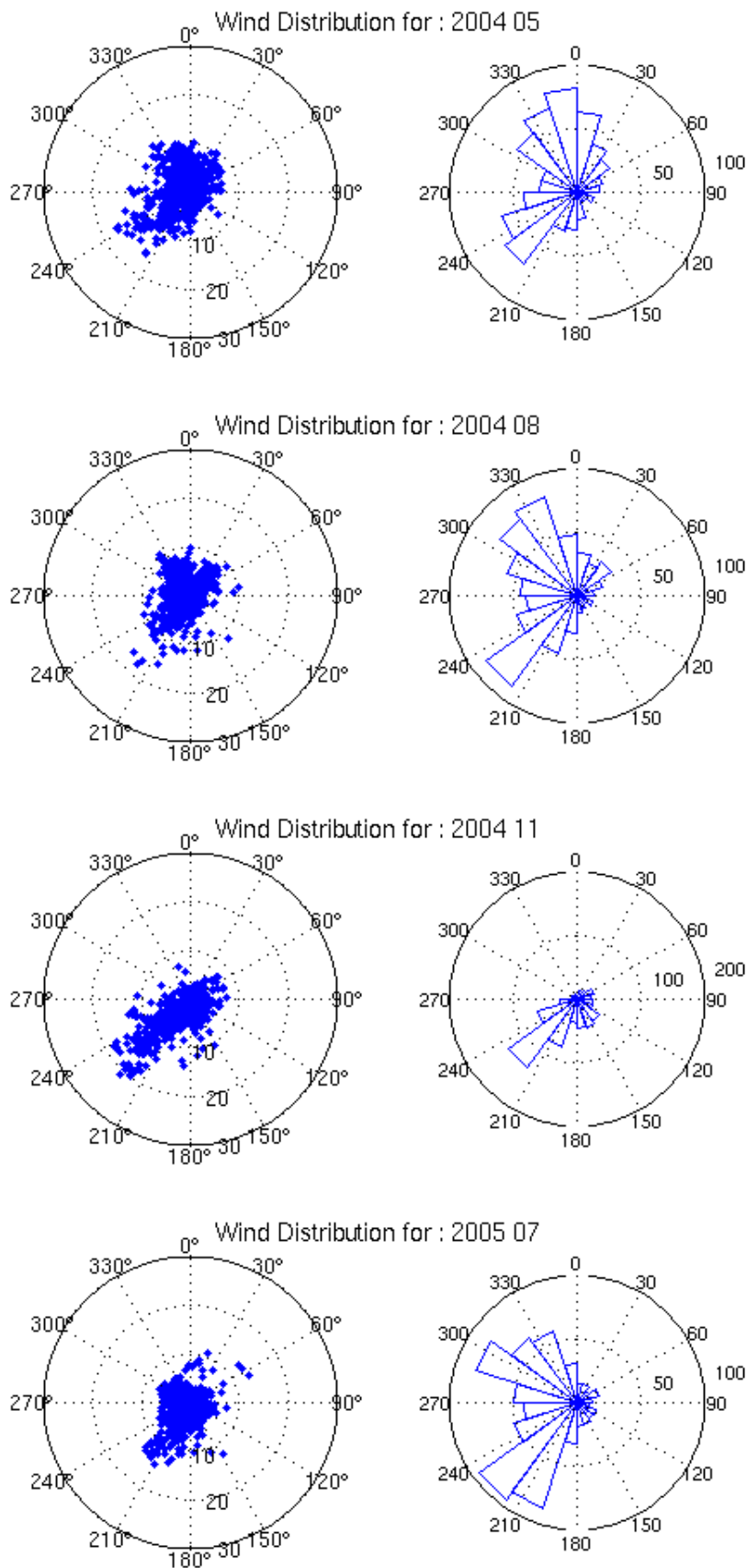


Fig 7 – Wind distributions.

3 Analysis and discussion

Monthly wind distributions are shown (Figure 7) in order to associate them to surface velocity field plots. The real wind vectors (represented by dots) are shown on the left hand side, while right hand side presents the angular distribution without considering the speed. A bi-modal distribution is normally expected although some departures may take place. For instance, November 2004 is almost entirely affected by Bora wind, which would explain the strong alignment in the surface currents. On the other hand, relatively low magnitude winds in July 2005 allowed the formation of vortices observable even at the monthly time scale (Figure 6). Vortices usually appear forming a dipole in front of Malamocco inlet. The difference between the “strong” and the “weak” inversion could be explained by a combination of the angular distributions of wind and their associated magnitudes.

In order to have a better look in the effect of wind, a classification has been made using the Principal Component directions. A low-pass filtering using the symmetric filter PL33 [Flagg et al., 1976] was applied to each vector component in order to remove variability lower than 33 hours, which mainly contains the sea breeze during aestival periods. Then a threshold has been defined at the speed of 3 m/s, so “Calm conditions” are defined to occur every time the speed is lower than or equal to this threshold while wind conditions have higher speed. Then wind conditions are classified as “Bora” when orientation angle falls within an interval of 230° Azimuth plus/minus a 22.5° . In a similar way, “Scirocco” conditions are defined in a $\pm 22.5^\circ$ interval around 320° Azimuth. “Other winds” conditions happen whenever the angle is not included in the Bora or Scirocco intervals. Classification is described in the Table 1 for a period of one year since February 2004 until February 2005 .

Wind	Average (m/s)		Std (m/s)		No. of cases (hours)
	Major	Minor	Major	Minor	
bora	-8.1	0.05	3.8	1.4	2633
sirocco	0.2	4.7	1.1	1.8	276
calm	-0.2	0.04	1.3	1.4	4549
other winds	-0.7	0.2	3.7	2.8	1732
gaps	-	-	-	-	266

Tab 1 – Statistics of the wind Principal Components (major and minor).

Mean maps are produced for the entire surface current velocity field by picking up the cases corresponding to the above defined conditions. Velocity time series were previously de-tided and low-passed in order for bringing them to the same time scale as wind series, as well as to remove tidal variability. The computed averages are shown in Figure 8. It is possible to see that Calm and

Other winds conditions have similar effects in the surface currents, including dipole formation, while Bora destroys them because of the strong alignment produced. Scirocco conditions cause the inversion closer to the coastal strip mainly, where a clockwise flow is induced; but the effect is enhanced if Scirocco becomes predominantly at the monthly time scale as is observed in May 2004. However, deformation of the vector field in the surroundings of the Malamocco inlet is expected to be also a consequence of tidal jet flowing out from the inlet.

For the purpose of assessing the effect of the tidal jet from Malamocco inlet on the surface field, chiefly concerning the dipole formation, the Calm conditions are sub classified according to the tidal phase inside the inlet. Hence “strong current” in the inlet is defined to have speed higher than 0.7m/s, separating cases into inflow and outflow, then the Calm conditions is imposed to and some statistics elaborated about.

Since the main forcing inside the inlet is astronomical, back to the surface velocity dataset, the original record is processed, i.e. neither de-tided or low-pass filtered. Maps of the mean field are produced for both specific cases of “Calm plus strong out flowing” and “Calm plus strong inflowing” and presented in Figure 9 (upper panels). In average, the effects of strong inflow and outflow can be seen up to 7 Km far from the coast during calm conditions. Yet the dipole outside of Malamocco inlet does not appear in the average fields. The underlying vorticity structure is studied via rotation maps using the formula:

$$\frac{\partial v}{\partial x} - \frac{\partial u}{\partial y}$$

where current vector components, v (northward) and u (eastward), are spatially derived with respect to the position coordinates x (eastward) and y (northward) in each node of a regular grid made on purpose. Positive values indicate anti-clockwise rotation, while the negative ones represent clockwise motion. Previous studies on vorticity in front of the Venice lagoon [Paduan et al., 2003; Kovačević et al., 2004] have been made without considering the tidal variability thus far.

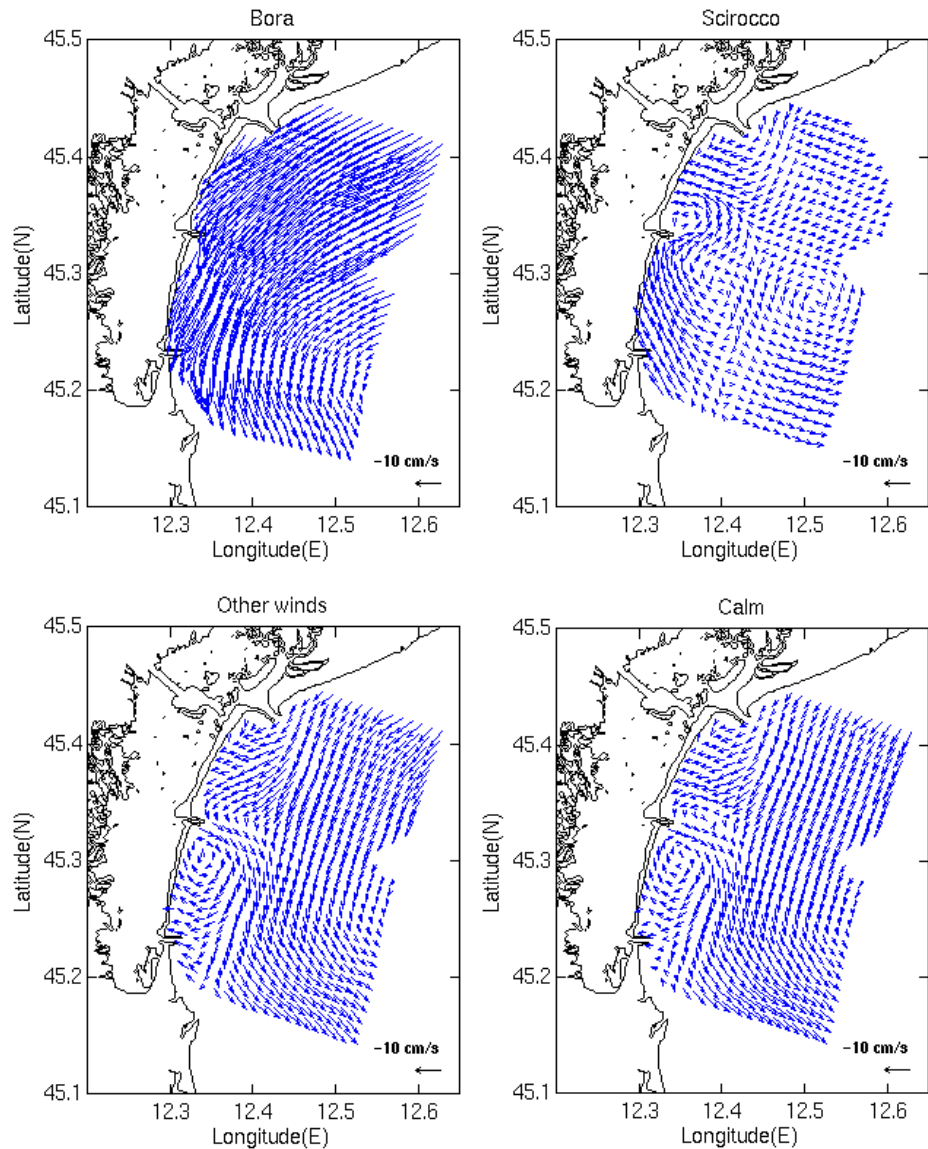


Fig 8 – Mean surface for non-tidal, low-passed current velocities, under different wind conditions.

Averaged vorticity fields corresponding to the aforementioned cases of “Calm plus strong out flowing” and “Calm plus strong inflowing” are shown in the Figure 9 (lower panels). As it can be seen, vorticity structures are quite similar even though the current field (upper panels) change according to the sense of the flow in the Malamocco channel. Hence the dipole observed during calm conditions is formed by the combined action of rising and ebb tides in the inlet, for vorticity structure remains independent of the phase in the inlet flow.

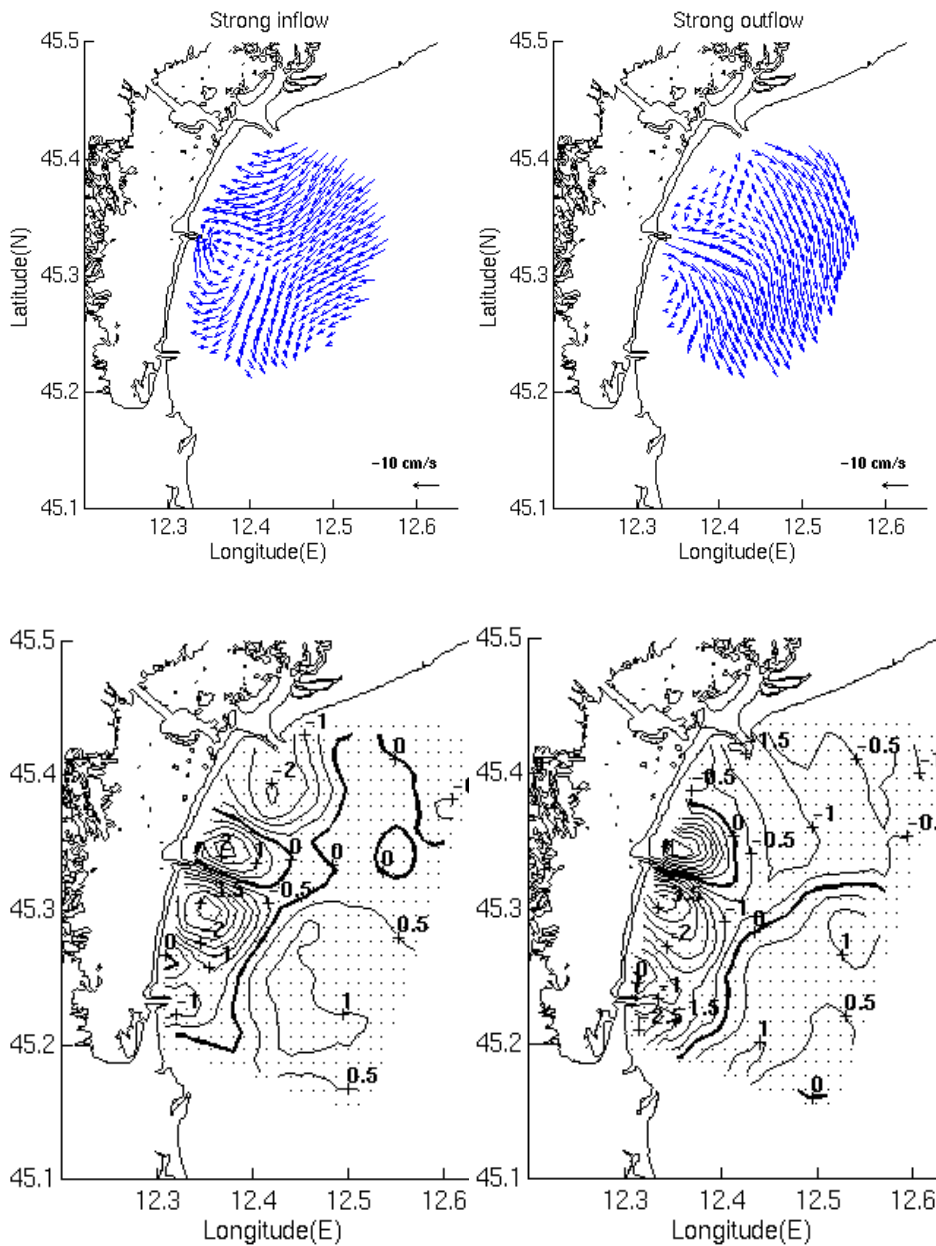


Fig 9 – Surface current field and underlying vorticity structure under calm conditions and strong flow in the Malamocco inlet. Vorticity units $\times 10^5 \text{ s}^{-1}$.

Concluding remarks

The present work is aimed to study the surface velocity field, as monitored by HF radar antennas. Winds have a well known influence in the features of the field.

Bora, the strongest wind in the area, drives the velocity currents into a more spatially aligned field. Inversion of the southward flow is detected when Scirocco prevails in the bimodal wind distribution, so currents may flow northward, mainly in the coastal strip.

There is a coastal strip which is affected by the morphology of the shoreline (jetties) in addition to the tidal pumping from the inlets. This is apparent at the

annual as well as at the monthly time-scale through the observed meandering of the southward flow in the vicinity the inlets.

Calm conditions and winds other than Scirocco and Bora favour the formation of vortices, which can be well developed during calm weather. On the other hand, strong Bora episodes destroy small scale eddies via the alignment of the current vectors.

Discharge from channels, which are reportedly astronomically driven, seems to be a privileging factor for the increase in vorticity in their proximity. Again, the dipole featuring the eddies near the inlets becomes apparent during calm situations and remains independent of the tidal phase. Effects of inlet discharge can be observed up to 7 Km far from the shoreline, depending upon the state of weather.

Acknowledgments

This work was supported by CORILA (Consortium for the Coordination of the Scientific Research of the Venice Lagoon) within the three-year research program 2004-2006, Line 3.15 "Solid transport and circulation of the upper layers in the inlets and the coastal zone". Isaac Mancero Mosquera participated with the support of the programme for Training and Research in Italian Laboratories (TRIL) of the Abdus Salam International Centre for Theoretical Physics (ICTP). Wind data were made available by "Centro Previsioni e Segnalazioni Maree" of the Municipality of Venice.

References

- Cushman-Roisin, B., Gačić M., Poulain, P-M., Artegiani, A. (eds.); *Physical Oceanography of the Adriatic Sea*, 67-109. Kluwer Academic Publishers, 2001.
- Flagg, C.N., J.A. Vermersch, and R.C. Beardsley, *New England Shelf dynamics experiment (March, 1974) Data Report Part II: The moored array: M.I.T. Report 76-1*, Cambridge, MA, Massachusetts Institute of Technology, 1976.
- Gačić, M., I. Mancero Mosquera, V. Kovačević, A. Mazzoldi, V. Cardin, F. Arena and G. Gelsi, *Temporal variations of water flow between the Venetian lagoon and the open sea. J. Mar. Systems*, 51, 33-48, 2004.
- Kovačević, V., Gačić, M., Mancero-Mosquera, I., Mazzoldi A. and Marinetti, S.; *HF radar observations in the Northern Adriatic: Surface current field in front of the Venetian Lagoon. J. Mar. Systems*, 51, 95-122. 2004.
- Lipa, B.J., and Barrick, D.E.; *Least-squares methods for the extraction of surface currents from CODAR crossed-loop data: application at ARSLOE. IEEE J. Oceanic Eng. OE-8*, 226-253. 1983.
- Paduan, J.D., Gačić, M., Kovačević, V., Mancero-Mosquera, I. and Mazzoldi, A.; *Vorticity patterns offshore of the Venetian lagoon from HF radar observations. Scientific Research and Safeguarding of Venice, CORILA*

Research Program 2002 Results, Volume 2, 361-372. Istituto Veneto di Scienze Lettere ed Arti, Venezia, 2003.

Paduan, J.D. and L.K. Rosenfeld; Remotely sensed surface currents in Monterey Bay from shore-based HF radar (CODAR. *J. Geophys. Res.*, vol. 101, no. C9, pp. 20,669-20,686. 1996.

Preisendorfer, R.; *Principal Component Analysis in Meteorology and Oceanography*, 192-252. Elsevier, 1988.

TIDAL PRISM VARIATION AND ASSOCIATED CHANNEL STABILITY IN N. VENICE LAGOON

Rachel Helsby¹, Carl L. Amos¹, Georg Umgieser²

¹CCPEM, National Oceanography Centre, Southampton, UK

²ISMAR-CNR, San Polo 1364, 30125, Venice, Italy

1 Introduction

The relationship between the cross-sectional area (A_c) of an inlet and its tidal prism (P) has been well investigated by numerous authors (Le Conte, 1905; O'Brien, 1931, 1969; Escoffier, 1940; Jarrett, 1976; Hume & Herdendorf, 1988). These authors have all concluded that the relationship can be expressed by a variation of the general formula $A_c = xP^n$ (1), where A_c is cross-sectional area, P is the tidal prism, and x and n are some constant. If an inlet follows this relationship, then it is regarded as stable in term of it's equilibrium with the tidal prism.

Le Conte (1905), O'Brien (1931, 1969) and Nayak (1971) used data collected from inlets along the Pacific coast of North America to define a standard relationship of inlet stability. In addition, O'Brien (1969) distinguished a difference between natural inlets (2) and jettied inlets (3). The difference results from a slightly larger cross-sectional area found in the jettied inlets:

$$A_c = 7.607 \times 10^{-3} P \quad (2)$$

$$A_c = 7.489 \times 10^{-4} P^{0.86} \quad (3)$$

Jarrett (1976) published a summary of cross-sectional area/tidal prism relationships using data on inlets along the Pacific, Atlantic, and Gulf coasts of N. America. He was able to confirm a significant difference in the relationship between Pacific and Atlantic coast inlets (4);

$$A_c = 3.039 \times 10^{-5} p^{1.05} \quad (4)$$

Pacific and Atlantic coasts are subject to different tidal conditions as the former is unequally diurnal (one high tide is significantly larger than the second high tide of the day); the latter is semidiurnal. Jarrett (ibid) however, concluded that the wave climate and ratio of the inlet width to the hydraulic radius were more significant in creating this difference in the relationship. The mean wave height in the Pacific is greater than in the Atlantic by over a metre; this influences the magnitude of the littoral drift of sand (Jarrett, 1976) and hence the hydraulic radius, which is the ratio between the cross-sectional area and the wetted perimeter. The greater the magnitude of littoral drift, the smaller the hydraulic radius becomes.

Other authors have also found that the O'Brien relationship is not always suitable and have formulated new relationships, for example, in Japan

(Shigimura, 1981) and New Zealand (Hume & Herdendorf, 1990).

The stability of a tidal inlet can be evaluated upon application of a cross-sectional area/tidal prism relationship. Data-points with a smaller cross-section or larger tidal prism than the relationship predicts infer that the inlet will erode the cross-sectional area in order to accommodate the tidal prism, and vice versa. However, as the inlet cross-sectional area increases with erosion or decreases with deposition, the discharge and velocity must also be eventually affected and thus the tidal prism. It is therefore important to consider this relationship as it has connotations on the hard engineering of jetties; i.e. if the cross-sectional area and tidal prism are in equilibrium, the inlet should be self dredging as the width is fixed.

The relationships mentioned above are all based upon the smallest cross-sectional area (this is not necessarily at the mouth) measured at low water. Also, the tidal prism is calculated for a spring tide so that the greatest volume of water that enters the inlet is represented. However, it may be possible that the relationship is valid anywhere along a tidal channel as long as the tidal prism is calculated for each specific cross-sectional area. This paper aims to investigate this theory using tidal channels in northern Venice Lagoon – Lido Inlet, Treporti Canal, and Burano Canal. Also, we aim to determine whether the tidal prism have changed significantly over the 70 year period between 1930 and 2000? This period incorporates the onset of sand influx from Cavallino Beach (Helsby 2006) via the tip of the Lido Inlet's northern jetty (thus increasing the cross-sectional area of the mouth of Lido Inlet). It has also seen the continual erosion of Treporti Canal by 2-3 cm³/yr (Umgiesser ?, Helsby, 2006), the change in tidal dominance of Burano Canal from flood to ebb (Helsby, 2006) and the formation of a subaqueous ebb spit (in Lido Inlet) and an offshore ebb tidal delta (Amos et al 2004; Helsby et al, 2005). A final question asks whether a variation in the tidal prism has caused or effected any of these changes?

2 Method

The minimum cross-sectional areas were determined across eleven across Lido Inlet, Treporti Canal and Burano Canal (fig.1) using a dataset of bathymetry from 1990. The position of the profiles were selected to coincide with nodes in the hydrodynamic model SHYFEM (Umgiesser, 1993, 2004). This was important because the SHYFEM model was used to simulate a typical spring tide in Venice Lagoon (using the bathymetry of 1990) to calculate the tidal prism. Discharge, tidal elevation and current velocity data were simulated across each cross-section every 300 seconds of a tidal cycle at a point along each profile, so the tidal prism could be calculated using several different methods. As a difference in the calculated tidal prism could affect the accuracy of the results, a comparison of three of the methods was performed.

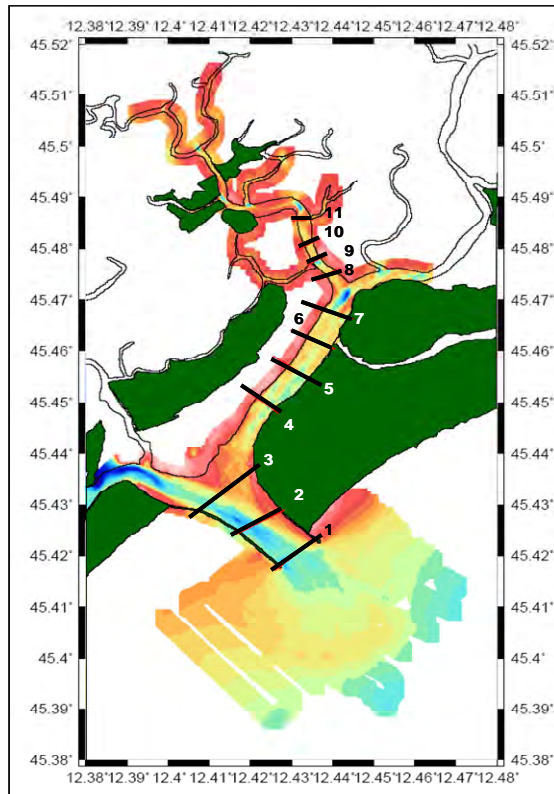


Fig 1 – Locations of the cross-sectional profiles. Lido Inlet - 1, 2, 3; Treporti Canal - 4, 5, 6, 7; Burano Canal - 8, 9, 10, 11.

The first method (equation 5.) was that of O'Brien (1936; 1969), where A_c is cross-sectional area, V_{max} is the maximum velocity and T represents the tidal period;

$$P = \frac{A_c V_{max} T}{\pi} \quad (5)$$

The second method has been used by the U.S Army Corps. Of Engineers (Seaburgh, 2002), where Q_{max} is the maximum discharge during the flooding tide;

$$P = \frac{TQ_{max}}{\pi} \quad (6)$$

As simulated discharge data were produced for every 300 seconds of the tidal cycle, the sum all of the discharge entering the profile during the flooding tide (Q_{pos}) was calculated and multiplied by 300 (Δt) to get the tidal prism.

$$P = \sum_0^T \Delta t Q_{pos} \quad (7)$$

A comparison of the tidal prism results for 1990 can be seen in figure 2.

To calculate the cross-sectional area, the lagoon-wide bathymetry from 1990 was gridded. Then, Generic Mapping Tools (GMT) was used to 'data-pick' low water level depth measurements at equal distances (x in equation 8) along each profile. The depth (d) was then assumed to be uniform for each of these lengths

-x (dividing the cross-section into rectangles of equal width) so that a trapezoidal calculation could be performed (equation 8).

$$A_c = \sum_{i=1}^n d_i \Delta x \tag{8}$$

Where n is the total number of individual trapezoids.

Once both tidal prism and cross-sectional area were calculated for all of the profiles, a graph of the results was plotted along with the regression line of O'Brien's equation for inlets with 2 jetties (equation 3).

The process was repeated using the bathymetry from 1930, 1970 and 2000. Also, other cross-sectional area/tidal prism relationships were plotted as a comparison to O'Brien's, 2 jetty relationship (equation 3), for example, Jarrett's Atlantic Inlet relationship (ibid, equation 4).

3 Results

As can be seen in figure 2, the discharge equation (equation 5.) compared favourable with the trapezoidal calculation of the tidal prism (equation 6). The results gained from the velocity equation however, differ by over 10% when compared to the direct discharge calculation in Lido Inlet despite being on a par with the results for the Treporti and Burano canal profiles. Also, it would seem unlikely that the tidal prism would change by as much as $2 \times 10^7 \text{ m}^3$ by the time Lido Inlet separates into Treporti Canal and Lido Canal. For this reason, despite the fact that O'Brien used the velocity method (equation 5), the discharge method (equation 6) will be used to calculate tidal prism as it seems to provide a better fit than the velocity method and is simpler than the direct discharge calculation.

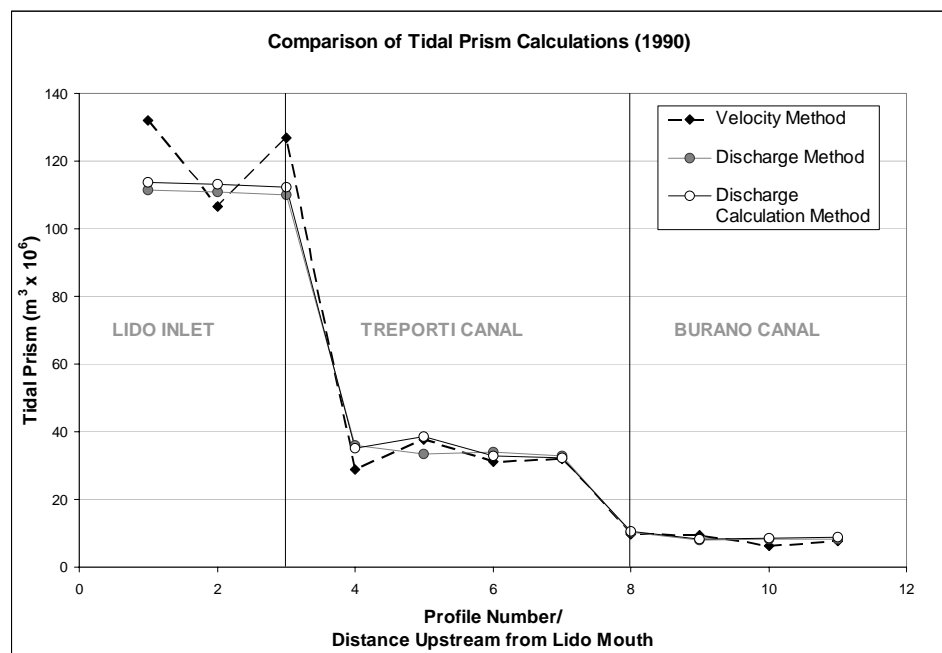


Fig 2 – A comparison between the various methods of tidal prism determination.

The ratio of the tidal prism and cross-sectional area in 1990 (figure 3), reveal that the cross-sections were on average, 29 % larger than predicted by the O'Brien relationship. This would suggest that all of the canals should have been depositional at this time in order to reach equilibrium with the tidal prism. However, between 1970 and 2000, the profiles in Treporti for example, increased by an average of 7% with negligible deposition occurring only between 1990 and 2000. Also, Lido Inlet remained relatively stable between 1990 and 2000 despite the apparent need to reduce its cross-sectional area by a minimum of 20% to be stable according to the O'Brien relationship.

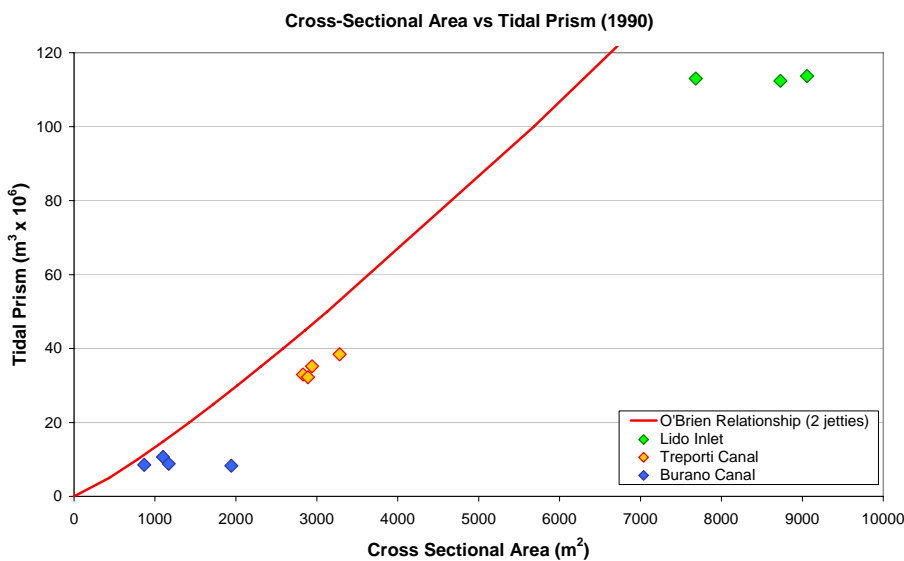


Fig 3 – Cross-sectional area against tidal prism along 11 profiles in northern Venice Lagoon; a comparison with the O'Brien (1931; 1967) relationship.

O'Brien's work on the tidal prism/cross-sectional area relationship was predominantly based on stabilised tidal inlets on the Pacific coast (O'Brien, 1931, 1969). However, the study was expanded by Jarrett (1976) in order to determine whether this relationship was valid for inlets along the Atlantic and Gulf coasts.

He concluded that inlets on the Atlantic coast followed a different relationship than the inlets on the Pacific coast, that they had a larger cross-sectional area to a given tidal prism:

$$A_c = 3.039 \times 10^{-5} p^{1.05} \quad (9)$$

A comparison with the Pacific inlet relationship ($A_c = 2.833 \times 10^{-4} p^{0.91}$) is shown in figure 4. Also included for comparison are the results from Venice Lagoon based on 1990 bathymetry.

It is clear that the data from Venice Lagoon (green diamonds) fits the relationship for Atlantic coast inlets (blue line) better than the relationship of O'Brien.

Burano Canal has a relatively large cross-sectional area for the tidal prism, even when compared to the Atlantic relationship. However, it does fit a relationship for inner harbour entrances (dotted blue line in figure 4) formulated

by Le Conte (1905).

The next step in determining the stability of the northern Venice Lagoon canals was to repeat the analysis with bathymetry data from 1930, 1970, and 2000 in order to provide answers to two important questions;

- has the tidal prism changed within the last 70 years?
- are the tidal channels stable?

Although the tidal prism volume has been undulating over the last 70 years (by an average of $\pm 2.3 \times 10^5 \text{ m}^3/\text{yr}$ in Lido Inlet), there does not appear to be a specific trend towards a net increase or decrease in any of the channels. This is also the case in Treporti, which has been net erosional between 1930 and 2000 (Helsby et al 2005).

Fig 4 – Comparison between the tidal prism/cross-sectional area relationships of O'Brien (1931, 1967), Pacific and Atlantic coasts (Jarrett, 1976). Note how the relationship of northern Venice Lagoon's channels appears to fit the relationship of Atlantic Coast inlets.

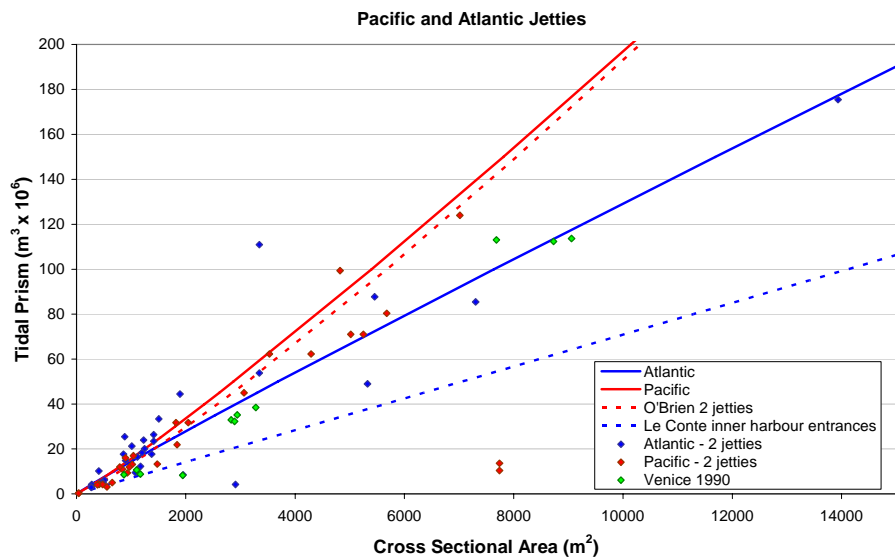
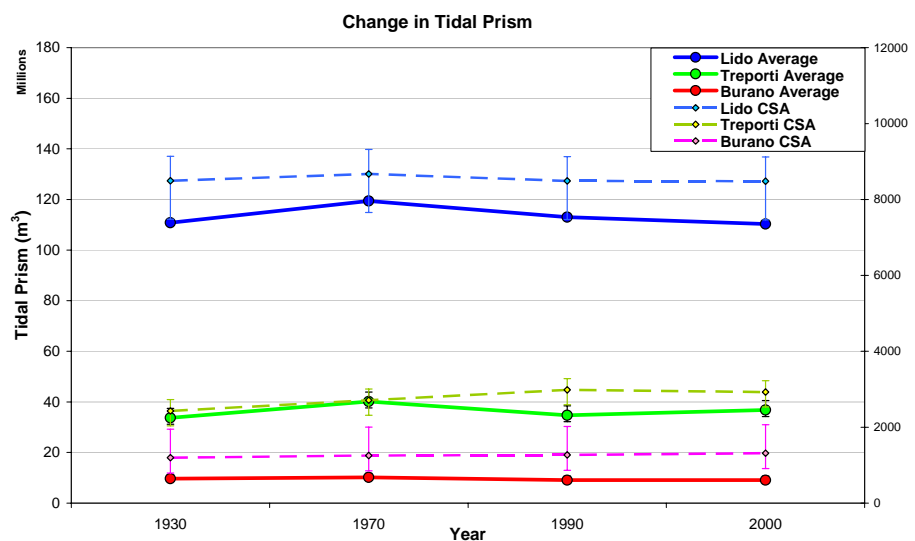


Fig 5 – Change in Tidal Prism and cross-sectional area in Lido Inlet, Treporti Canal, and Burano Canal between 1930 and 2000. Error bars show min/max value of cross-sectional area (CSA) (N.b. see note at the end of the paper).



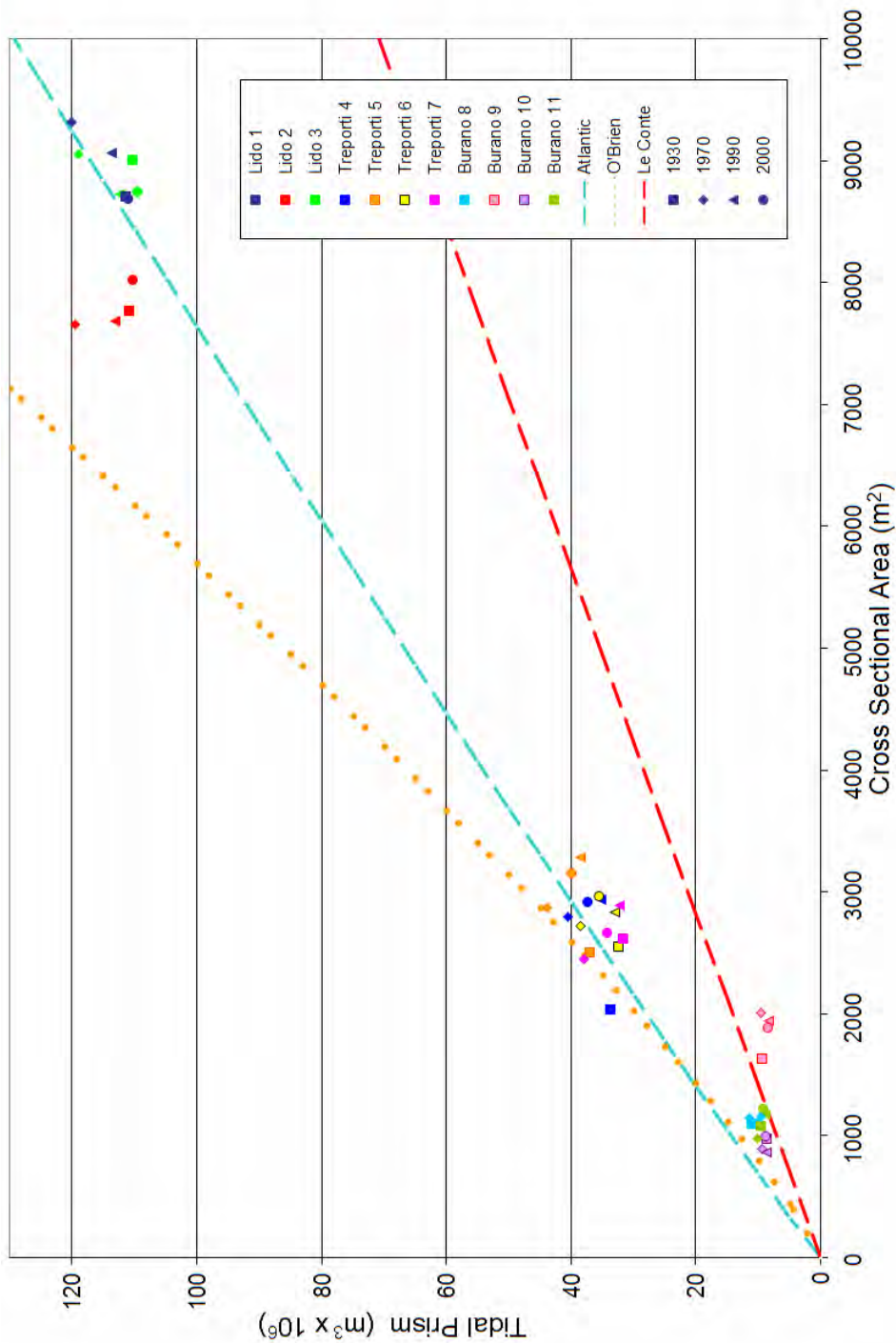


Fig 6 – The tidal prism and cross-sectional area data from Lido, Inlet, Treporti Canal, and Burano Canal for the years of 1930 (square), 1970 (diamond), 1990 (triangle) and 2000 (circle). Note how they appear to follow a relationship formulated for Atlantic inlets.

It may be possible that the tidal prism/cross-sectional area relationship of Lido Inlet is affected by the other tidal inlets in Venice Lagoon, Malamocco and Chioggia. To incorporate this possibility, the tidal prism and cross-sectional areas of all of the inlets were summed and plotted (figures 7 & 8).

Fig 7 – The tidal prism/cross-sectional area relationship of the three Inlets of Venice Lagoon – Lido, Malamocco, and Chioggia.

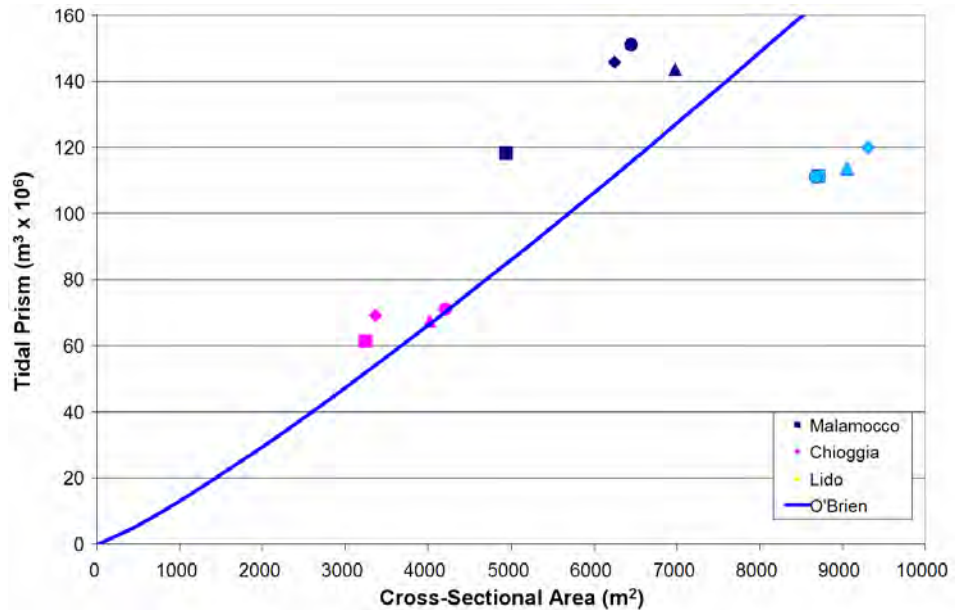
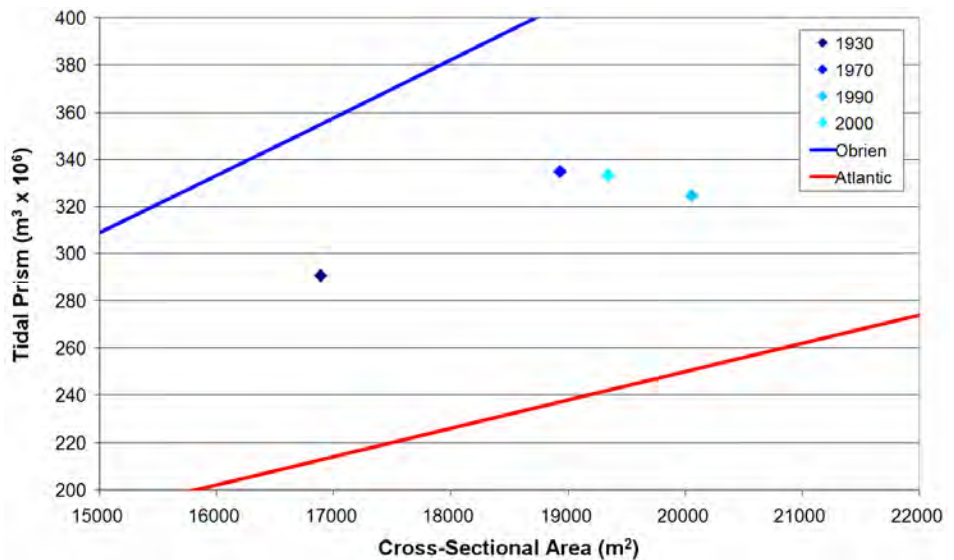


Fig 8 – The summed tidal prism and cross-sectional area of the three Venice Lagoon Inlets in 1930, 1970, 1990, and 2000. Shown with the O'Brien relationship (1969) and the Atlantic relationship (after Jarrett, 1976).



4 Discussion

The canals of northern Venice Lagoon do not fit the O'Brien relationship comfortably; only 5 points fall within 10% of the predicted cross-sectional area and half of the points have a cross-sectional area at least 25% larger than predicted. If we were to assume that the O'Brien relationship was valid then the canals, especially Lido Inlet, should be depositional. Table 1 shows the change in area of each cross-section between 1930 and 2000 and shows that all the cross-sections have instead increased in size (i.e. erosion has occurred) by a total average of 9% between 1930 and 2000.

Lido Inlet was depositional between 1970 and 2000, which reduced the average cross-sectional area by 2%. However, the average cross-sectional area should

have decreased by an average of 25% to become stable according to O'Brien's relationship. As the cross-sectional areas of Lido Inlet haven't altered by more than 7% between 1930 and 2000, it would appear that the inlet is already relatively stable – so why doesn't O'Brien's relationship fit with this data?

Date Profile	1930 to 1970	1930 to 1990	1930 to 2000	1970 to 1990	1970 to 2000	1990 to 2000
1	7%	4%	0%	-3%	-7%	-4%
2	-1%	-1%	3%	0%	4%	4%
3	0%	-3%	-3%	-4%	-3%	0%
Lido average	2%	0%	0%	-2%	-2%	0%
4	27%	31%	30%	5%	5%	0%
5	13%	24%	21%	12%	9%	-4%
6	6%	10%	14%	4%	8%	5%
7	-7%	9%	2%	15%	8%	-9%
Treporti average	10%	18%	17%	9%	7%	-2%
8	4%	0%	5%	-4%	1%	5%
9	18%	16%	13%	-3%	-6%	-3%
10	-9%	-12%	2%	-3%	10%	13%
11	-11%	7%	11%	17%	20%	4%
Burano average	1%	3%	8%	2%	6%	5%
total average	4%	8%	9%	3%	4%	1%

Tab 1 – The change in the area of each cross-section (percentage). Negative values represent deposition, and positive values represent erosion.

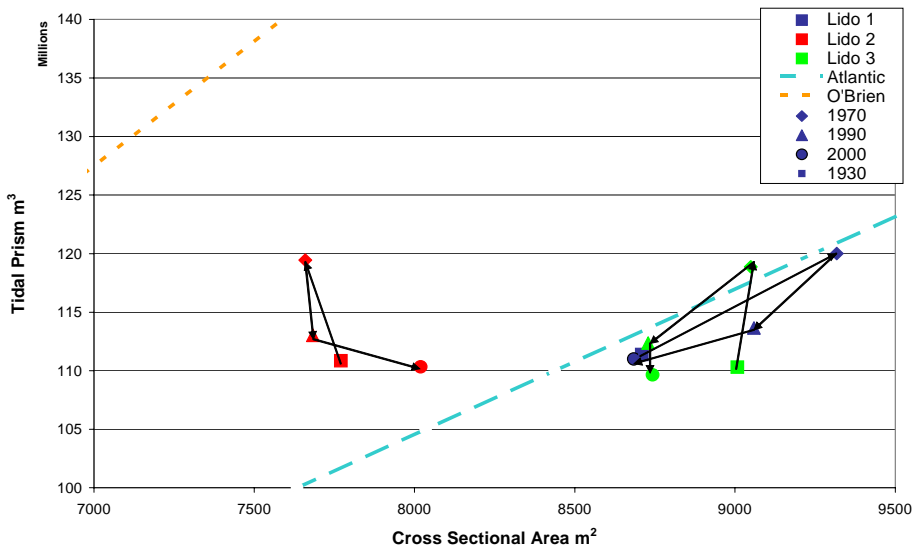
Date Profile	1930 to 1970	1930 to 1990	1930 to 2000	1970 to 1990	1970 to 2000	1990 to 2000
1	7%	2%	0%	-6%	-8%	-2%
2	7%	2%	0%	-6%	-8%	-2%
3	7%	2%	-1%	-6%	-8%	-2%
Lido average	7%	2%	0%	-6%	-8%	-2%
4	17%	4%	10%	-15%	-9%	6%
5	16%	4%	7%	-14%	-10%	4%
6	16%	2%	9%	-17%	-8%	7%
7	17%	2%	8%	-17%	-11%	6%
Treporti average	16%	3%	8%	-16%	-9%	6%
8	3%	-4%	-16%	-7%	-20%	-12%
9	1%	-14%	-11%	-15%	-12%	3%
10	8%	-1%	3%	-11%	-6%	4%
11	5%	-9%	-4%	-15%	-9%	5%
Burano average	4%	-7%	-7%	-12%	-12%	0%
total average	9%	-1%	0%	-12%	-10%	1%

Tab 2 – The change in tidal prism at each cross section (percentage).

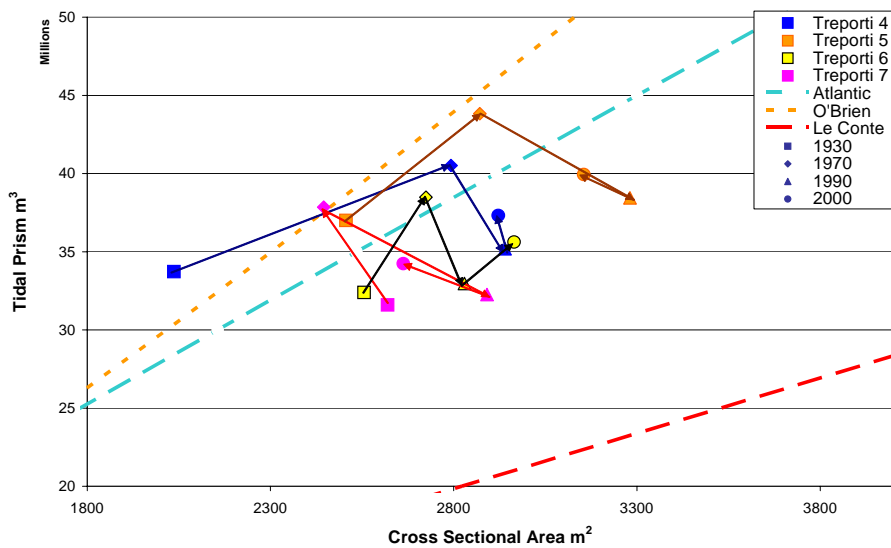
Jarrett (1976) proved that the inlets on the Atlantic coast did not fit with O'Brien's relationship, but still conformed to the theory that tidal prism and cross-sectional area are comprehensively linked. A new relationship, providing a larger cross-sectional area in terms of tidal prism was formulated. This difference in cross-sectional areas may be a result of the local wave climate; the Pacific Ocean has a much larger mean wave height than the Atlantic Ocean, and therefore greater wave energy and as Jarrett (1976) explains, littoral transport is a function of wave energy. Consequently, more sediment should be transported into the Pacific inlets. This creates a smaller cross-section than would be expected of an equivalent inlet on the Atlantic coast. Another explanation could be the inlet width to hydraulic radius ratio (W/R). This is generally smaller for the Pacific inlets, indicating a narrow, deep, and thus more hydraulically efficient channel than the wide, shallow inlets on the Atlantic coast. Jarrett reasons that this allows the Pacific inlets to accommodate more water (i.e. a larger tidal prism) than their Atlantic counterparts do.

The lack of change in the bathymetry over the last 70 years indicates that Lido Inlet is probably stable (see table 1); this is confirmed by the correspondence to the Atlantic relationship (see figures 6 & 9a). Profile 1, at the mouth of Lido Inlet, has remained close to the relationship line at all times, altering its cross-sectional area to the changing tidal prism. Interestingly, the cross-sectional area and tidal prism at this point are now the same as they were in 1930, despite fluctuations in 1970 and 1990 (see special note at the end). Profile 2 passes through both the ebb scour channel (erosional) and ebb spit (depositional), and is the least stable section of Lido Inlet when compared to the Atlantic relationship. It appears too small for the tidal prism and hence should erode as indeed it has, by 3% between 1930 and 2000 (see table 1).

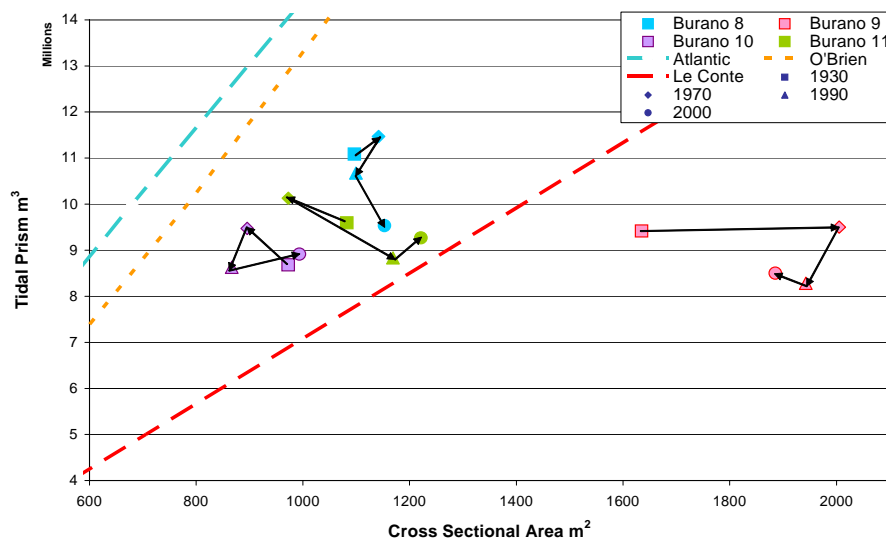
Treporti Canal was net erosional between 1930 and 2000, although this incorporates a period of slight accretion between 1990 and 2000 (see table 1). However, Treporti Canal fits the Atlantic relationship fairly well and therefore appears relatively stable. Since Treporti Canal has lost 2-3 cm/yr over the last 70 years and thus unstable in terms of bed, however, this level of erosion is perfectly acceptable as a balance of the changing tidal prism.



A



B



C

Fig 9 – Change in the tidal prism/cross-sectional area for Lido Inlet (A), Treporti Canal (B), Burano Canal (C) and comparison with the O'Brien's, 2 jetty relationship, and Jarrett's Atlantic relationship.

Burano Canal does not fit either O'Brien's relationship or the Atlantic relationship. This is not unexpected as Burano Canal is sheltered from the waves it would experience as an inlet (and calculated for in both relationships). Le Conte (1905) created a formula for inner harbour entrances, which takes into account the different circumstances of a channel further away from the sea. The data from Burano appears to fit this relationship, although certain factors must be taken into account. Profile 9 extends across a triple junction scour hole, and therefore has a much larger cross-section as a result. If we discount this data, the rest of the Burano data falls between the Atlantic relationship and the Le Conte inner harbour relationship. Between 1930 and 1970, when Burano Canal was depositional and flood dominant (Helsby et al 2005, table 1), it appeared to move towards the Atlantic relationship line by depositing sediment whilst the tidal prism increased (is this partly due to a stronger wave influence from the dominant flood tide?). The data points began to move away from the Atlantic relationship and towards that of Le Conte. This movement continued despite an increase in the tidal prism between 1990 and 2000. Profile 11 became stable according to Le Conte in 1990, and responded to the change in tidal prism by the removal of a proportionate amount of sediment to remain that way. Therefore, it seems likely that, for the last 30 years, that Burano Canal is responsive to the Le Conte inner harbour relationship and is eroding in order to reach stability.

Figure 7 shows the tidal prism/cross-sectional area of all three inlets in Venice Lagoon. Chioggia Inlet appears to fit the O'Brien relationship, and therefore should be more wave influenced than Lido Inlet. Therefore, it should be comparable to the Pacific coast relationship of O'Brien (O'Brien, 1969) with high littoral drift (partly from the rivers Po and Brenta) reducing the relative cross-sectional area. Malamocco Inlet, however, appears to compliment the offset of Lido Inlet from the O'Brien relationship (see figure 7), so it could be argued that the lagoon does fit the relationship through this balance? However, if the tidal prisms and cross-sectional areas are all summed in the method of O'Brien (1969), the lagoon falls in between the O'Brien relationship and Jarrett's Atlantic relationship (figure 8). Thus, the interpretation of the tidal prism/cross-sectional area relationship of the lagoon as a whole requires more investigation.

5 Summary and Conclusions

This paper has examined the stability of Lido Inlet in terms of a tidal prism/cross-sectional area relationship (after the work of O'Brien, 1969 and Jarrett, 1976). The study has been expanded to investigate the validity of using these relationships for profiles leading away from the inlet mouth, and whether the results have changed over time (between 1930 and the year 2000). As part of the investigation, the question of whether the tidal prism has changed within Venice Lagoon has been examined.

It was established that the O'Brien relationship, based on Pacific coast inlets, is not valid for Lido Inlet. This is probably due to the low wave energy found in the Adriatic Sea in comparison to the Pacific Ocean. It was proved however, that

the relationship for inlets on the Atlantic coast of N. America could be applied to Lido Inlet and Treporti Canal.

It would appear that Lido Inlet is stable, and this is manifested by a lack of significant change in the bathymetry. Treporti Canal is also stable in the sense that it maintains equilibrium when compared with the Atlantic relationship. Although the levels of erosion are high, thus making the channel unstable in terms of bathymetry, the erosion balances the changing tidal prism according to the relationship:

$$A_c = 3.039 \times 10^{-5} p^{1.05}$$

It has been shown that Treporti Canal has experienced relatively high erosion due to a change in the tidal prism, the affects of which appears to have been magnified here. For example, the tidal prism in Treporti Canal increased by an average of 16% between 1930 and 1970, in contrast to an increase of just 7% in Lido Inlet and 4% in Burano Canal. This may have been influenced by sand transport from Lido Inlet (Amos et al, 2005).

Burano Canal was deemed to be either too distant from the mouth of Lido Inlet to follow any relationship other than that of inshore channels (Le Conte, 1905). Whether these relationships fit the other channels in Venice Lagoon has yet to be answered- It may be that the Venice inlets as a whole fit the O'Brien relationship if the cross-sectional areas of all three inlets are combined with a total tidal prism?

Special Notes

Please note that it has recently come to light that the 1970 data may have an offset of 20 cm in the northern lagoon, where Lido Inlet, Treporti and Burano Canals are located. This may explain why there is an apparent decrease in the tidal prism post-1970.

References

Amos, C.L., Umgiesser, G., Helsby, R., and Friend, P.L. 2005. The origin of sand in the Venice Lagoon. *In Scientific Research and Safeguarding of Venice, Research Programme 2001 – 2003. Volume III. (P.Capostrini), 161-176.*

Helsby, R., Amos, C.L., Umgiesser, G. 2006. Morphological evolution and sand pathways in Northern Venice Lagoon, Italy. *In Scientific Research and Safeguarding of Venice, Research Programme 2004 – 2006. Volume IV. (P.Capostrini), 388-402.*

Escoffier, F. F., 1940. The stability of tidal inlets. *Shore and Beach*, **8**(4), 114-115.

Escoffier, F. F., 1977. *Hydraulics and Stability of Tidal Inlets*, U.S Army Corps of Engineers.

Fitzgerald, D. M., 1988. Shoreline erosional-depositional processes associated with tidal inlets. In: *Hydrodynamics and Sediment Dynamics of Tidal Inlets*, Springer-Verlag.

Helsby, R., 2006. The dynamics and origin of sand in northern Venice Lagoon with an emphasis on the tidal inlet of Lido. *Unpublished PhD Upgrade Report*.

Hume, T. M., and Herdendorf, C.E., 1988. The 'Furkert-Heath' relationship for tidal inlet stability reviewed. *New Zealand Journal of Marine and Freshwater Research*, **22**, 129-134.

Hume, T. M., and Herdendorf, C.E., 1990. Morphologic and hydrologic characteristics of tidal inlets on a headland dominated, low littoral drift coast, Northeastern New Zealand. *J. Coastal Res., Spec. Issue 9*, 527-563.

Jarrett, J. T., 1976. Tidal Prism - Inlet Area Relationships, Department of the Army Corps of Engineers.

Le Conte, L. J., 1905. Discussion on river and harbor outlets, "Notes on the improvement of river and harbor outlets in the United States". *D.A. Watts, Trans. ASCE 55*(paper 1009), 306-308.

Nayak, I. V., 1971. Tidal prism-area relationship in a model inlet. In: *Univ. of California, Hydraulic Engin. Laboratory Report HEL-24-1*, pp. 72, Berkeley, CA.

O'Brien, M. P., 1931. Estuary tidal prism related to entrance areas. *Civil Engineering*, **1**(8), 738.

O'Brien, M. P., 1969. Equilibrium flow areas of inlets on sandy coasts. *Journal of the Waterways and Harbors Division*. WW1, 43-52.

Seaburgh, W. C., 2002. Hydrodynamics of Tidal Inlets. In: *Coastal Engineering Manual*, pp. 79, U.S. Army Corps of Engineers, Washington, D.C.

Shigemura, T., 1981. Tidal prism-throat width relationships of the Bays of Japan. *Shore and Beach*, **49**(3), 34-39.

Umgiesser, G., Melaku Canu, D., Cucco, A., and Solidoro, C., 2004. A finite element model for the Venice Lagoon. Development, set up, calibration and validation. *Journal of Marine Systems*, **51**, 123-145.

THE ORIGIN AND TRANSPORT OF SAND IN VENICE LAGOON, THE LATEST DEVELOPMENTS

C.L. Amos¹, R. Helsby¹, A. Lefebvre¹, C.E.L. Thompson¹, M. Villatoro¹, V. Venturini¹, G. Umgiesser², L. Zaggia², A. Mazzoldi², L. Tosi², F. Rizzetto², G. Brancolini³

¹ Centre for Coastal Processes, Engineering and Management, National Oceanography Centre, Southampton, Hampshire, UK, SO14 3ZH

² Institute of Marine Sciences, National Research Council, S. Polo 1364, 30125 Venezia, Italy

³ Istituto Nazionale di Oceanografia e Geofisica Sperimentale, Sgonico, Trieste, 34010, Italy

Riassunto

In questo articolo vengono delineati i progressi fatti nel contesto delle linee di ricerca CORILA 3.15 e 1.16, inerenti le origini della sabbia ed il suo trasporto alle bocche della laguna di Venezia. L'approccio scelto è molto vario ed include lunghe serie temporali di misure alle bocche, inferenze sulle variazioni morfologiche del fondale, misure dirette del trasporto di sabbia e misure geofisiche per il monitoraggio delle più importanti strutture. Dai risultati ottenuti sino ad oggi si rileva chiaramente un ingresso di sabbia all'interno della Laguna di Venezia lungo il margine nord della bocca di Lido, e si ha invece un export di sabbia altrove. Alla bocca di Lido, circa 2 giorni dopo un evento di grande portata fluviale, riscontriamo un significativo ingresso d'acqua dolce, sedimento fino e materia vegetale. Questo flusso d'acqua dolce ricco di materia vegetale si ritrova in prossimità del fondo ed è più abbondante durante le piena montante, mentre il particellato fine si muove nello strato superficiale e si dirige verso l'interno della laguna. I rilievi barometrici e geofisici, appena completati, dei delta delle Bocche di Lido e Chioggia indicano chiari foresets di progradazione, diagnostici di rapido accumulo. Si stima che sino a $3 \times 10^6 \text{ m}^3$ di sabbia l'anno si siano depositati sull'ebb tidal delta (delta di deflusso di marea) di Lido e che la sabbia derivi in parte dal superamento del molo settentrionale e in parte dal Canale di Treporti (Umgiesser *et al.*, 2006). Anche l'ebb tidal delta di Chioggia mostra segni di crescita ad un tasso di circa $50,000 \text{ m}^3$ di sabbia l'anno. Gli ebb tidal delta sono un recente fenomeno nella dinamica litorale, iniziato circa 70 anni fa, e sono il prodotto della costruzione dei moli risalenti agli inizi degli anni venti. Il trasporto di sabbia è stato misurato mediante trappole Helley-Smith con reti da 63 micron in combinazione ad una serie di altre tecniche. Le trappole hanno un'efficienza del 4% soltanto (in accordo con dati di letteratura), ma si sono mostrate adatte alle condizioni riscontrate nella laguna di Venezia ed i dati ottenuti sono stati sufficienti ad effettuare delle analisi dettagliate.

Da questo lavoro risulta che la bocca di Chioggia sia caratterizzata da un predominante export di macrofite e da una limitata quantità di sedimento. La

bocca di Lido invece, presenta una dinamica più complessa caratterizzata da forte stratificazione che comporta gradienti verticali di salinità, temperatura, carico sedimentario e contenuto di sostanza organica. All'ingresso di Lido, si rilevano significanti prove di trasporto di sabbia fine e molto fine. Il trasporto di sabbia è massimo presso il fondo, in una area che costituisce il 10% dell'altezza della colonna d'acqua, e segue con buona approssimazione il profilo di Rouse. La concentrazione di sabbia in sospensione è ben riprodotta

dall'esponente di Rouse ($\frac{W_s}{\beta \kappa U_*}$) = -0.98 (bocca di Lido) e -0.58 (bocca di

Chioggia), con $b=1$ e $\kappa = 0.4$. Durante i massimi flussi di marea, le sabbie fini si trovano ad una quota di circa 4 m. Tale dato è in accordo con precedenti stime delle spessore dello strato limite (Amos *et al.*, 2006) e ottenute da analisi di profili ADCP. Il valore misurato di tasso di trasporto (solido) di sabbia come carico di fondo corrisponde alle previsioni ottenute da simulazioni effettuate da Engelund e Hansen (1967) e dall'applicazione dei modelli SHYFEM + Sedtrans96. Il materiale trasportato sul fondo o per saltazione era caratterizzato per il 95% da frazione inorganica, mentre il contenuto di materiale organico in sospensione risultava molto variabile e massimo (>90%) presso la superficie. I rilievi nei *Bassi Fondi* mostrano forti segni di continua erosione del fondale nella parte più meridionale della Laguna. Dal confronto tra la nostra carta batimetrica e quella del 1970 si rileva un'erosione di circa 0.5 m. Al contrario, il paleo-cordone rinvenuto nella zona di rilevamento, non è in erosione e dunque è stato portato in evidenza dall'erosione delle aree circostanti. Questa corpo sabbioso, quindi, non sembra fornire sabbia al flusso di sedimento uscente nella laguna meridionale. Le misure di backscatter effettuate con sidescan sonar, sono state utilizzate per la mappatura della macrofite e della posizione del paleo-cordone (rilevato come backscatter di media intensità). Infine, i risultati dal sistema BRAD (in 6 diversi siti) si sono mostrati efficaci per la mappatura della rugosità di fondo (al di sotto della massa fogliare della pianta) e della distribuzione di macrofite all'interno della massa fogliare oltre che per il rilevamento della presenza di epifiti o altro materiale simile a conchiglia, che ricadeva nel campo visivo. Gli epifiti risultano essere dei forti riflettenti acustici e molto probabilmente sono il motivo degli scarsi risultati ottenuti con i "profilatori sub-bottom adatti a basse profondità" utilizzati in precedenza nella Laguna di Venezia.

Abstract

This paper outlines progress made within the CORILA Research Lines 3.15 and 3.16, regarding the origins and transport pathways of sand within the inlets of Venice lagoon. The approach taken is multi-faceted and involves long-term direct measurements within the inlets, inferences based on morphological changes of the bed, direct measurements of sand transport, and geophysical monitoring of key features. Results to date show a clear transport of sand in the inlets of Venice lagoon throughout the water column. We note that there is a

strong import of fresh water, fine-grained sediment and plant matter through Lido entrance about 2 days after a high river discharge event. This (freshwater) plant matter moves close to the bed, as seen at the mouth of the Po river (Tesi *et al.*, in review), and is most abundant during flooding tides whilst the fine sediment moves inwards near the surface. Bathymetric and geophysical surveys of the ebb tidal deltas of Lido and Chioggia have been completed and show clear progradational foresets diagnostic of rapid accumulation (up to 20 cm/annum). The Lido ebb tidal delta has accreted up to $3 \times 10^6 \text{ m}^3$ sand/annum. The sand appears to come in part from by-passing the northern breakwater and in part from Treporti canal (Umgiesser *et al.*, 2006). Chioggia ebb tidal delta also shows accretion of the $50,000 \text{ m}^3$ sand/annum. The ebb deltas are a new phenomenon of the shore face (about 70 years old) and are the product of construction of the jetties (in the early C20th). Sand transport in the inlets has been measured using Helley-Smith sand traps (equipped with 63 micron nets) in conjunction with a variety of other techniques. The traps have an efficiency of about 4% only (in agreement with Rey *et al.*, 1987), but were well suited to the conditions in Venice lagoon and provided enough material for detailed analysis. The results of this work show that Chioggia inlet is dominated by the export of macrophytes and is sediment limited, whereas Lido inlet is more complex showing strong buoyancy- driven stratification and resulting vertical gradients in salinity, temperature, sediment load, and organic content. We found considerable evidence of the transport of very fine sand in Lido inlet. The sand transport is greatest in the bottom 10% of the water column and follows closely the Rouse profile. Sand concentration in suspension is simulated well by the

Rouse exponent $\left(\frac{W_s}{\beta \kappa U_*} \right) = -0.98$ (Lido inlet) and -0.58 (Chioggia inlet) (setting

$\beta=1$ and $\kappa = 0.4$). Fine sand extends to a height of about 4 m above the bed during peak flows corresponding to the estimated thickness of the boundary layer (Amos *et al.*, 2006) and observed in ADCP profiles. The measured mass transport rate of sand at the bed agreed well with the sand transport predictions of Engelund and Hansen (1967) and from the model simulations of SHYFEM + Sedtrans96. This transport comprised largely inorganic sediment (>95%) whereas the organic content of suspended material varied over a wide range and was greatest (> 90%) near the surface. The survey of the *bassi fondi* yielded strong evidence for continued bed erosion in the southern lagoon. A comparison of our bathymetry and that of 1970 showed approximately 0.5 m of erosion. By contrast, a *paleo-cordone* (paleo-barrier) evident in the survey region did not erode and hence is being exhumed by ongoing erosion elsewhere. This sandy feature, therefore, does not appear to be contributing sand to the export of sediment in the southern lagoon. Sidescan sonar backscatter was used to map the distribution of macrophytes, and the position of the *paleo-cordone* (evident as intermediate backscatter). Finally, the Benthic Roughness Acoustic Device (BRAD) (deployed at 6 sites) was effective in mapping bed roughness beneath a plant canopy, as well as the distribution of macrophytes within the plant canopy, and the presence of epiphytes and other

shelly material within the field of view. It appears that epiphytes are strong acoustic scatterers and may well be the reason for poor results obtained with shallow sub-bottom profilers in Venice Lagoon.

1 Introduction

The work carried out on the sand transport budget in Venice lagoon has been undertaken within the context of three overlapping and strongly-linked CORILA *linea*: 3.14 (*processi di erosione e sedimentazione nella laguna di Venezia*); 3.15 (*trasporto solido e circolazione superficiale alle bocche di porto e nella zona costiera*); and 3.16 (*caratteristiche del sottosuolo lagunare*). The main objective of *linea* 3.14 is “to understand and predict the processes of accretion and erosion of sediment in Venice lagoon, and in particular, to determine the impact of waves in *bassi fondi* on resuspension. A sub-objective is to predict changes to the mass fluxes of sediment at the inlets and within the major canal systems of the lagoon. The main objective of *linea* 3.15 is “the measurement of the exchange of sediment between the lagoon and the open sea through the use of innovative technologies”. A sub-objective of this *linea* is the evaluation and calibration of the technologies that may be used in the future to monitor such sediment exchanges. The themes of research considered important to solving the over-arching question are: (1) estimations of the mass balance of sediment transport within the coastal zone off Venice lagoon; and (2) measurements of sand ($d_{50} > 63$ microns) and fines ($d_{50} < 63$ microns) in transport in Lido inlet and to correlate the transport magnitude with processes active (waves and tidal currents). The main objective of *linea* 3.16 is the definition of the surficial sediments of the *bassi fondi* of the lagoon. Within the context of this study, it is the potential sources and sinks of sediment (particularly sand) which is key to understanding the long-term evolution of Venice Lagoon.

This paper deals with field results obtained within an extensive field survey undertaken between CORILA, CNR-ISMAR and University of Southampton during September, 2006. This work was broken down into three linked activities designed to meet the stated objectives and provide input into the three *linea* of research defined above. These three activities were: (1) the study of sand transport in the southern lagoon (PhD thesis of M. Villatoro); (2) the study of the *bassi fondi* and central lagoon (PhD thesis of A. Lefebvre); and (3) the study of sand transport in the northern lagoon (PhD thesis of R. Helsby). Much of the work undertaken to date is reported in a series of papers (Amos *et al.*, 2005a and b; Helsby *et al.*, 2005).

2 Methodology

Field work undertaken during September, 2006.

2.1 The Chioggia inlet survey

(i) The Chioggia inlet survey

The survey vessel *CORILA* was equipped with a calibrated digital single beam sonar (Lowrance®) and digital sidescan sonar (Marine Electronics Ltd®). A Garmin® GPS was used for navigation to an on-site accuracy of ± 5 m. The system configuration, calibration and operation have been reported upon elsewhere (Amos *et al.*, 2005). The system was used to complete the survey of the ebb tidal delta (up to 4 km off the mouth of the Chioggia inlet) and to collect bathymetric data in the Chioggia inlet. A total of 140 line km of data were collected incorporating the prodelta of the Adige river in the south to the southern end of Pellestrina in the north and the distal end of the Chioggia ebb tidal delta (Figure 1A). The colour coding indicates the tidally-corrected calibrated depth of the nearshore region. A comparison of these data with bathymetry collected in 1990 shows accretion at the mouth of Chioggia inlet, to the north of the northern breakwater, to the south of the southern breakwater and throughout the ebb tidal delta. The maximum accretion was order 4 m, and yielded a volumetric change of approx. 50,000 m³ sand/annum (Figure 2).

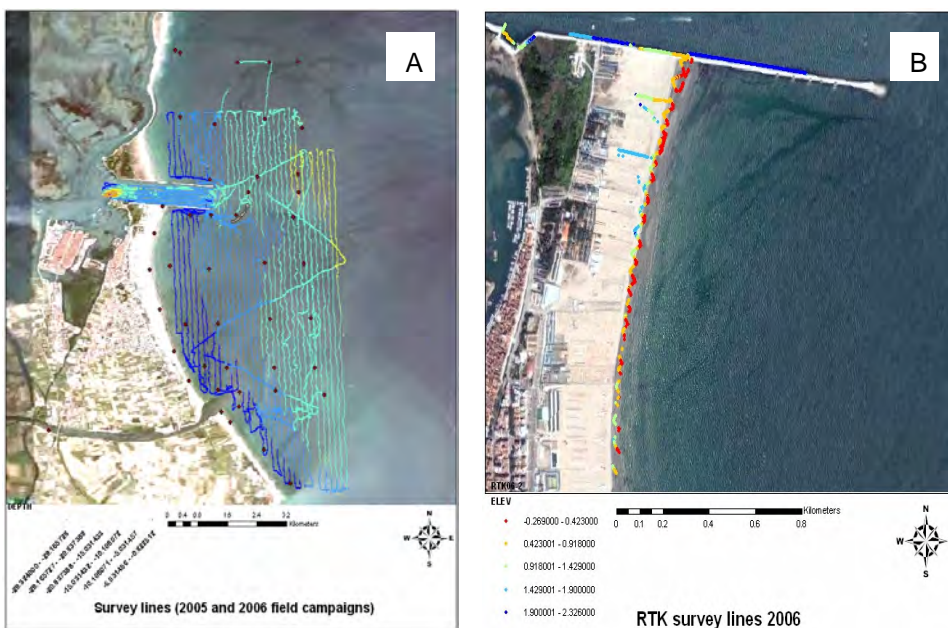


Fig 1 – (A) Survey lines collected off Chioggia inlet during the 2005 and 2006 campaigns; (B) RTK survey lines collected along the beach of Sottomarina during 2006.

Red regions in Figure 2 denote accretion since 1990 of the seabed. These regions are found at the mouth of Chioggia inlet and in the ebb tidal delta southeast of the inlet. There is also evidence for accretion off *Sottomarina*. A comparison of aerial photographs reveals that the beach of *Sottomarina* adjacent to diga sud has prograded seawards approximately 90 m in the last 10 years (CORILA, Unpublished Data, 2006). A kinematic survey to measure the position and morphology of *Sottomarina* was carried out along the northern 2 km of frontage and verified this beach progradation (Figure 1B). A Trimble® RTK Differential Global Positioning System was used. The control points for the RTK were: a) benchmarks set up as part of a Geological and Subsidence

Monitoring System - Project ISES (Intrusione Salina e subsidenza) (Teatini *et al.*, 2005), b) a Tide gauge located on the southern breakwater of the inlet, and c) a control point from the preliminary topography survey undertaken before the construction of the MOSE project.

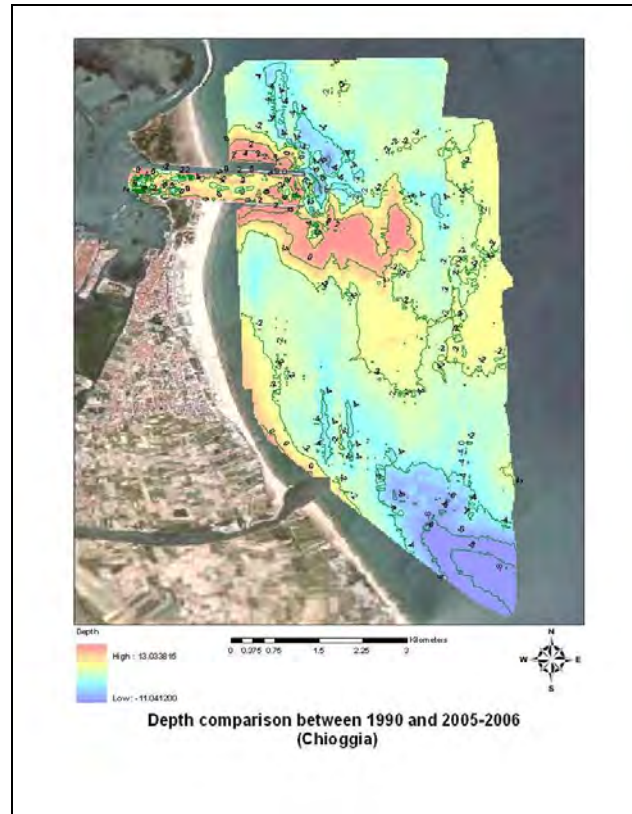


Fig 2 – A comparison of bathymetry between 1990 and 2005/06, Chioggia inlet.

As well, measurements of sand transport were made near the fixed ADCP location ($45^{\circ} 13.879'$, $12^{\circ} 17.920'$ described by Mosquera *et al.*, 2005) in Chioggia inlet on the 11th and 12th October, 2006 in about 10 m of water. Two Helley-Smith sand traps and a surface sampler (all equipped with 63 micron mesh sizes) were deployed synchronously from the boat *CORILA* for periods of 20 minutes duration and for a total of 12 profiles.

The deployment of these traps is shown in the images of Figure 3A-C. Two Helley-Smith samplers sat on the bed in benthic (B: bedload, $0 < h < 0.12$ m) and epibenthic (M: $0.21 < h < 0.33$ m) modes. A third (S) sampler (Figure 3D) was fixed to the vessel near the surface. The samples cover a wide range of current velocities over both the flood and ebb phase of the tide. These samples are presently under analysis in parallel to those collected in the Lido inlet survey reported below.

NAME	LATITUDE	LONGITUDE	ELLIPSOID QUOTE
CDV2_5CDV (ISES)	45° 13' 48.38324"	12° 17' 32.95898"	44.5915
CH-A1 (Tide gauge)	45° 13' 44.32420"	12° 18' 32.81828"	45.4
RA06 (MOSE)	45° 13' 46.78450"	12° 17' 58.47534"	45.566

Tab 1 – Control points used for the RTK survey.

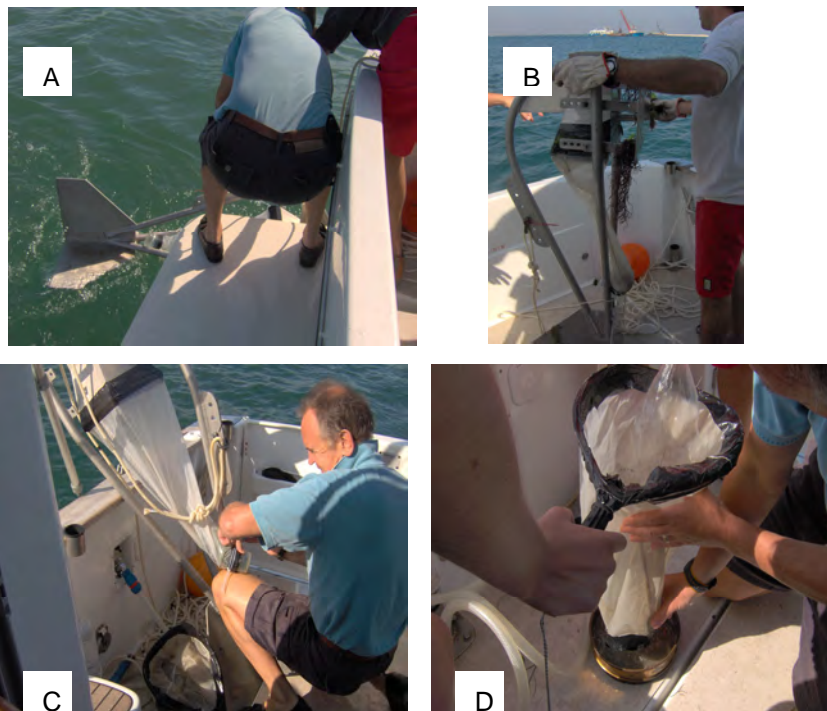


Fig 3 – The Helley-Smith sand traps during deployment in Chioggia inlet; (A) deployment of the trap; (B) recovery of the trap; (C) sampling of the trap; and (D) the surface trap sample being washed through a 63 micron sieve.

A summary of the deployment of traps in Chioggia inlet is given in Table 2. S = surface samples; M = epibenthic samples; and B = bottom samples. Also given are the total (sand + organics) mass concentration and the organic content (%).

DATE	SAMPLE	START TIME(UT)	MEDIAN DIAMETER (d ₅₀ -microns)	SAND TRAP	
				TOTAL CONC (mg/L)	ORGANIC (%)
11/09/06	M1	12:02	136	0,20	50
11/09/06	S1	12:17*	98	0,33	36
11/09/06	B2	12:35	103	0,26	29
11/09/06	M3	13:11	94	1,81	8
11/09/06	B3	13:10	132	9,92	15
12/09/06	S4	07:30	94	0,19	29
12/09/06	B4	07:29	132	25,37	94
12/09/06	M4	07:28	95	1,67	58
12/09/06	S5	08:09	98	0,21	23
12/09/06	B5	08:02	126	0,96	84
12/09/06	M5	08:03	96	1,86	50
12/09/06	S6	08:44	94	0,13	18
12/09/06	B6	08:38	103	1,05	19
12/09/06	M6	08:39	97	1,00	16
12/09/06	S7	09:19	98	0,10	27
12/09/06	B7	09:15	106	1,96	35
12/09/06	M7	09:15	94	1,62	66
12/09/06	M8	11:47	134	0,11	6
12/09/06	B8	11:48	130	3,59	8

Tab 2 – Sand samples collected in the inlet using the sand traps.

DATE	SAMPLE	START TIME(UT)	MEDIAN DIAMETER (d ₅₀ -microns)	SAND TRAP	
				TOTAL CONC (mg/L)	ORGANIC (%)
12/09/06	S8	11:49	134	0,04	52
12/09/06	S9	12:28	104	0,22	88
12/09/06	M9	12:20	101	1,12	19
12/09/06	B9	12:21	102	2,86	10
12/09/06	M10	12:56	99	1,30	12
12/09/06	B11	13:26	128	8,22	35
12/09/06	M11	13:27	130	2,18	18
12/09/06	B12	14:01	136	8,20	26
12/09/06	M12	14:02	94	1,01	6

*the trap had to be removed from the water and dropped again (time corresponds to second deployment)

The majority of samples were dominated by macrophytes and sea grasses (organic contents up to 94%). Inorganic sand was present, but only in the lower traps and only during peak flows. The sand was largely very fine and was in extremely low quantities. An initial appraisal of the sand content suggests that Chioggia is supply limited and is below its potential transport capacity. Curiously, the traps at the bed did not sample well, probably due to sheltering effects. However the epi-benthic trap yielded good results. The observed sand transport rates are consistent with predictions at low flows but diverge at high flows. The difference is an order of magnitude at the highest flows. A threshold for transport in suspension has been derived by extrapolating the sand transport rate (Q_s) versus current velocity (U_3 at $h = 3$ m) to zero. A threshold of $U_{3,crit} = 0.20$ m/s ($U_{r,crit} = 1.1 \times 10^{-2}$ m/s) was derived. The sand transport rate has been correlated with the excess velocity ($U_3 - U_{crit}$) after Gadd *et al.* (1978) through the empirical function:

$$Q_s = \frac{\alpha}{\rho_s} (U_1 - U_{1,crit})^3 \tag{1}$$

where α is an empirical function related to grain size and ρ_s is sediment density (2650 kg/m^3). The ratio $\frac{\alpha}{\rho_s}$ has a quoted value for fine sand ($d_{50} = 0.18 \text{ mm}$) from 1.73 (Bagnold, 1963) to 7.22 (Gadd *et al.*, 1978) in S.I. units.

The best fit value for Chioggia is:

$$Q_s = 0.06(\bar{U} - U_{crit})^3 \text{ kg/m/s} \tag{2}$$

which is much less than that proposed by Gadd *et al.* (1978) for the New Jersey (wave dominated) shelf. This relationship is shown in Figure 4A; it is valid only for the Chioggia inlet and applies only to the very fine sand ($d_{50} = 100$ microns) collected by the sand traps. The high scatter in the plot indicates low reliability.

Further sampling is required to decrease the uncertainty.

PROFILE	U (m/s)	STAGE OF TIDE	1/m
3	0.77	EBB	-0.49
4	0.71	FLOOD	-0.31
5	0.70	FLOOD	-0.34
6	0.63	FLOOD	0.35
7	0.48	FLOOD	-0.41
8	0.27	EBB	-0.97
9	0.42	EBB	-0.76
11	0.62	EBB	-0.54
12	0.68	EBB	-1.04

Tab 3 – A summary of the sand trap profiles and the best fit suspension number (1/m) from Chioggia inlet.

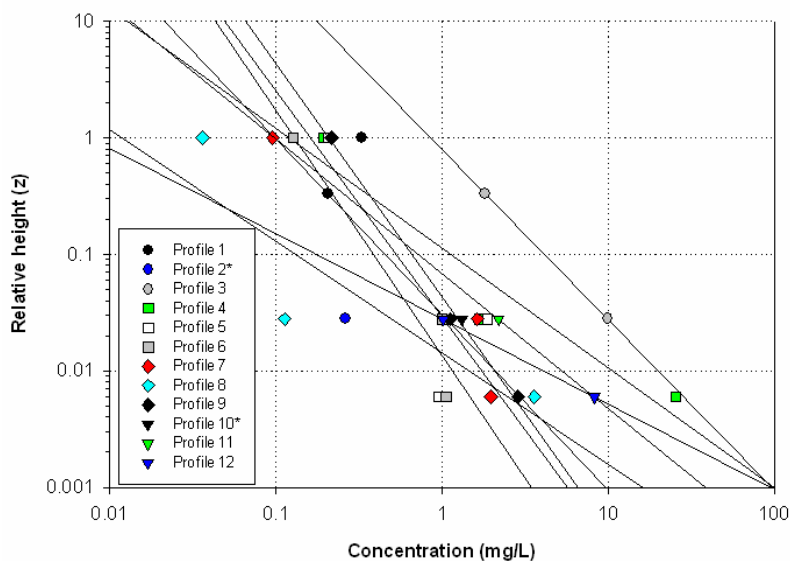
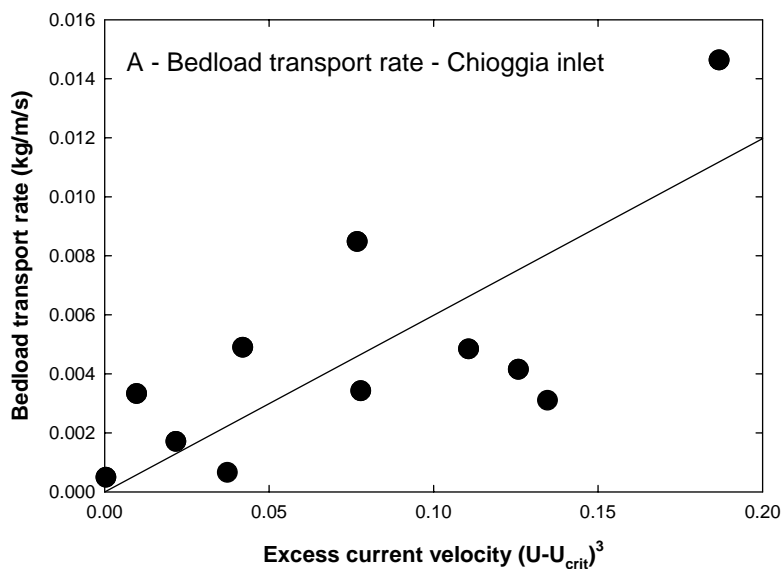


Fig 4 – (A) The Gadd et al. (1978) relationship of excess flow to sand transport rate; (B) of Sand concentration measurements in Chioggia inlet (11th and 12th September, 2006).

The application of the Rouse profile to the distribution of sand through the water column in Chioggia inlet is summarized in van Rijn (1993) and Dyer (1986). In its simplest form, this is expressed as: $C_z = C_a \left(\frac{z}{h-a}\right)^{-R}$ where C_z is the sand concentration at height z above the bed, h is the total water depth, C_a is the reference concentration at height a (immediately above the saltation layer), R is the Rouse exponent or suspension number: $\frac{W_s}{\beta \kappa U_*}$ where W_s is the still water settling rate of the suspended sand, β is a coefficient relating flow and particle eddy diffusivity ($\beta = 1 + \left(\frac{W_s}{U_*}\right)^2$; $\beta \approx 1$) and κ is von Karman's constant = 0.4

(assumed constant irrespective of suspended concentration). The best fit of the measurements of sand concentration in the water column at Chioggia (and Lido) can be expressed by the function:

$$\log_{10}(z) = m \log_{10}(C) + b$$

$$C_z = z^{\frac{1}{m}} \cdot 10^{-\frac{b}{m}} \quad (3)$$

where the exponent $1/m$ is equivalent to the suspension number R , and z is the relative height above the bed ($\frac{h_z}{h-a}$) where h_z is the sand trap heights above

the bed, and a is the reference height (defined as 0.06 m on the basis of the sampling height of the benthic trap) and $10^{-(b/m)}$ is the reference concentration at $Z = 1$. This approximation of the Rouse profile is valid only when the sediment is largely transported close to the bed. This is true for Chioggia inlet where the near-bed concentrations are 2-3 orders of magnitude larger than the surface concentrations. The results in Figure 4B show that the slopes in the concentration profiles are consistent in time. The Rouse exponent ($1/m$) was derived from best fit lines. Profiles 1 -3 are from 11th September, and profiles 4 – 12 are from 12th September. These lines have no statistical significance as there are only 2 or 3 data points for each profile. The mean value of $1/m = -0.58$, and it varies between -0.31 and -1.04. The values are consistently lower on the flood tide (-0.35) which is close to the value proposed by van Rijn (1993) for fine sand. The mean value for the ebb tide is $1/m = -0.75$. The inference of this is that sand moves close to the bed on the flood tide whereas it is more evenly mixed throughout the column on the ebb tide. According to van Rijn (1993), these values of $1/m$ mean that the sand should be mixed throughout the boundary layer, which in the Chioggia inlet should be about 4 m thick.

The sand samples have been sieved for grain size; the median size of the sand varies between $96 < d_{50} < 129$ microns (Table 2). The majority of the samples falls within the very fine sand range and are well to moderately well sorted. The

diameter will be converted to fall velocity to examine the relationship $\frac{W_s}{U_*}$,

which according to Bagnold (1963) should equate with unity for sand to be maintained in suspension. Van Rijn (1993) suggests that a value closer to 0.2 defines the threshold for sand in suspension. The significance of the Rouse profiles to sediment transport and a comparison of Chioggia results to those measured in Lido inlet are discussed later.

(ii) Bassi fondi survey

A survey of the *bassi fondi* was carried out in cooperation with CNR-ISMAR (Dott. L. Tosi) and OGS-Trieste (Dott. G. Brancolini). The main purpose of this work was to examine the application of seabed classification techniques to the mapping of habitats in Venice lagoon, and to the examination of the evolution of the ebb tidal deltas off each of the inlets. The work was carried out aboard the OGC vessel *Aretusa* which has a draft of 0.5 m. The set-up was similar to that used in the Chioggia inlet survey. The survey lines undertaken were across a buried dune ridge (*paleo-cordone*) that crops out to the north of Chioggia in the *bassi fondi*. The survey lines undertaken are shown in Figure 5. Bathymetry was reduced using the observed tidal elevation data at Chioggia, and from a calibration of the sounder made *in situ*. The sidescan sonar was hull mounted and operated at a swath width of 30 m and with a gain of 7.

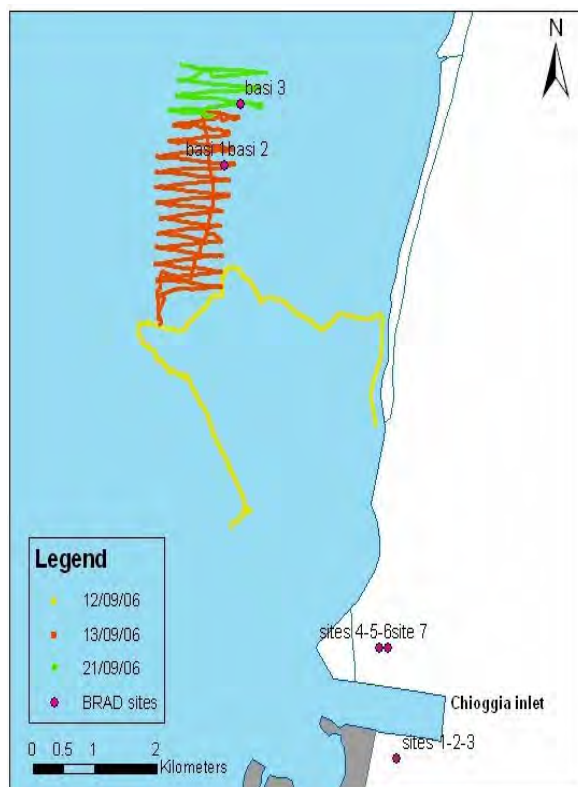


Fig 5 – The survey lines and BRAD sites carried out during 12th/13th and 21st/23rd September, 2006.

Ten stations occupied by the Benthic Roughness Acoustic Device (BRAD) are listed in Table 4 and shown in Figure 5. BRAD is described in detail in Amos *et al.*, (2006). The system was updated from earlier versions by inclusion of an underwater drive motor (16 VDC) and by replacement of the 670 kHz Sediment Imaging Sonar (SIS) transducer with one of 1.1 MHz. The early stations (1-3)

were undertaken on low amplitude wave ripples in very fine sand south of the Chioggia inlet; later stations were undertaken on *praterie* (sea grasses) on the *bassi fondi*. The system was optimized for range, sweep angle, transmit pulse length and sampling interval. The final configuration settings were: start range = 0 m; end range = 2 m; sweep angle = 90° (about nadir); transmit pulse length = 10 micro-seconds; and sample interval = 5 micro-seconds. This configuration yielded an effective vertical resolution of 3.8 mm and a horizontal resolution of about 1 cm. Photographs of the bed beneath BRAD and sediment samples were collected at each site for purposes of calibration.

STATION	LATITUDE	LONGITUDE	BED TYPE
1	45° 13.567'	12° 18.320'	Wave-rippled fine sand
2	45° 13.567'	12° 18.320'	Wave-rippled fine sand
3	45° 13.567'	12° 18.320'	Wave-rippled fine sand
4	45° 14.343'	12° 18.170'	Wave-rippled medium sand
5	45° 14.343'	12° 18.170'	Wave-rippled medium sand
6	45° 14.343'	12° 18.170'	Wave-rippled medium sand
7	45° 14.343'	12° 18.170'	Wave-rippled medium sand
Bassi1	45° 17.700'	12° 15.985'	Shelly sand – hard bottom
Bassi2	45° 17.702'	12° 15.985'	Algae covered (Zostera)
Bassi3	45° 18.141'	12° 15.829'	Shelly bioturbated mud

Tab 4 – The BRAD sites (1-7 were taken outside Chioggia inlet, whereas Bassi 1-3 were collected in the bassi fondi).

An example from site 4 is shown in Figure 6. The ripple pattern of 20 cm wavelength and about 2 cm height, evident in the photograph (Figure 6A), is clear in the acoustical roughness diagram (Figure 6B). The bifurcation pattern of the ripples is clearly seen in the acoustic image. Directional histograms of the elevation, as well as other pattern recognition techniques are under study. Also, filtering of the signal at various backscatter intensities is providing a means of discriminating bioturbation, the plant canopy (where present) and the roughness of both the canopy and sediment bed beneath the canopy. The backscatter is not shown. It appears that by careful filtering of the backscatter over the entire shot interval it is possible to map on-line the distribution and character of the plant canopy as well as its thickness and perhaps even epiphyte density. Furthermore, the composition and roughness of the seabed below the canopy can also be mapped for elevation, roughness and backscatter (composition) by using the BRAD sonar head in survey mode. This option will be explored in more detail in the future.

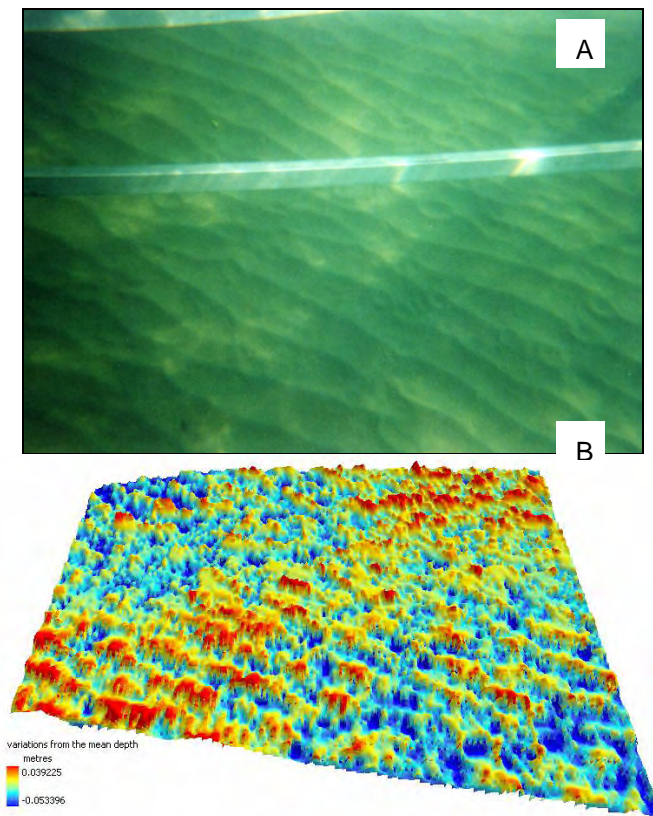


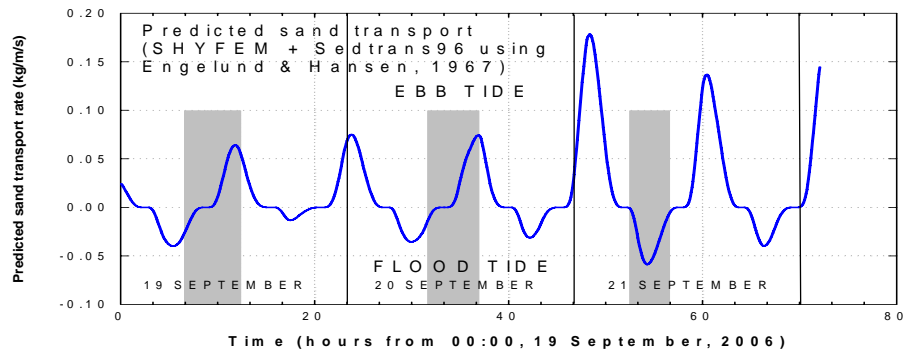
Fig 6 – (A) A photograph of site 4 showing wave-formed ripple patterns in about 2 m of water; (B) the BRAD acoustic image of the bed showing the roughness pattern – the ripple pattern is clearly seen.

It also appears that BRAD is sensitive to sediment in suspension; the water column backscatter shows clear evidence of plumes of relatively high and low values being advected through the field of view. We will be examining the application of BRAD in a region of active sand transport. Under these circumstances, it should be possible to map the migration of bedforms (bedload transport rate) and the distribution of sand in suspension within the benthic boundary layer; aspects vital to the successful conclusion of *Linea* 3.16.

2.2 The Lido inlet survey

The Lido inlet survey was carried out between 19th and 21st September, 2006. It was a combined exercise between three vessels of CNR: *Litus* (anchored at Lido nord; 45° 25.511'; 12° 25.848'), *Henetus* (traversing hourly) and the CNR launch (anchored at the fixed RD Instruments® ADCP site). The work was undertaken across a transect of the Lido inlet which was the same as that used in 2005 (Amos *et al.*, 2006). This transect was between the fixed ADCP site (45° 25.543'; 12° 25.857') in the south and the *Litus* position in the north. The data collected are summarized in Tables 5, 6 and 7 for the three survey vessels. A time-series of the bedload transport rate for 150 micron diameter sand predicted using SHYFEM + Sedtrans96 (Umgiesser *et al.*, 2004) for the survey period is shown in Figure 7. The periods of survey are shown as cross-hatching during 19th, 20th and 21st September, 2006. The period coincided with spring tides. The ebb cycle was surveyed on the first and second days, whilst, the late-stage flood tide was captured on the last day.

Fig 7 – The sampling periods of the coordinated sand transport study in Lido inlet (19th – 21st September, 2006). Sampling was undertaken over two ebb periods and a late flood phase. The blue line indicates predicted sand transport ($d_{50} = 150$ microns) from SHYFEM+Sedtrans96 using the Engelund and Hansen (1967) method.



(i) The *Litus* survey

The *Litus* was anchored in 3.5 m of water (below MSL) on the northern shoulder of the Lido inlet (Lido nord) on 19th, 20th and 21st September, 2006. It was within the vicinity of the site occupied in 2005 (Amos *et al.*, 2006). A tripod was deployed within 50 m of the anchor site with a self-recording Valeport® 802 and LISST®-100X. The Valeport® burst-sampled 2 orthogonal components of the horizontal flow at 4 Hz for 5 minutes each 30 minutes at a height (h) above the bed of 0.14 m: As well, hydrostatic pressure and backscatter (using an Optical Backscatter Sensor – OBS) was logged at a height of 0.45 m using the same sampling protocol. The LISST-100X recorded (h = 0.45 m) at 1-minute intervals the volumetric concentration and the grain size spectra between 2 and 250 microns from which the median diameter and sorting were derived. The operation aboard *Litus* took place on an hourly cycle. The cycle began with the deployment of a Nortek® ADV mounted on a frame that was lowered to the bed. The sampling volume of the ADV was situated 0.34 m above the bed and measured 3 components of the flow at 25 Hz for 5 minutes.

DATE	SAMPLE	START TIME(UT)	END TIME(UT)	TOTAL SAND CONC (mg/L)			
				C	S	M	B
19/09/06	C1	10:15	--	0.1	--	--	--
19/09/06	S1,M1,B1	10:02	10:22		.1	29	3119
19/09/06	C2	11:07	--	2	--	--	--
19/09/06	S2,M2,B2	11:03	11:23		2	722	1581
19/09/06	C3	12:15	--	2.5	--	--	--
19/09/06	S3,M3,B3	12:02	12:22		3	701	926
19/09/06	C4	13:05	--	1	--	--	--
19/09/06	S4,M4,B4	13:02	13:22		1	84	292
19/09/06	C5	14:20	--	.1	--	--	--
19/09/06	S5,M5,B5	14:02	14:22		3	3	38
20/09/06	C6	10:25	--	0	--	--	--
20/09/06	S6,M6,B6	10:20	10:40		0	30	1592
20/09/06	C7	11:25	--	4	--	--	--

DATE	SAMPLE	START TIME(UT)	END TIME(UT)	TOTAL SAND CONC (mg/L)			
				C	S	M	B
20/09/06	S7,M7,B7	11:13	11:33		0.2	90	131
20/09/06	C8	12:15	--	1.9	--	--	--
20/09/06	S8,M8,B8	12:08	12:28		4	230	326
20/09/06	C9	13:30	--	2	--	--	--
20/09/06	S9,M9,B9	13:10	13:30		2	62	82
20/09/06	C10	14:20	--	0	--	--	--
20/09/06	S10,M10,B10	14:08	14:28		0.3	5.3	27
21/09/06	C11	08:35	--	0	--	--	--
21/09/06	S11,M11,B11	08:25	08:45		0	191	367
21/09/06	C12	09:30	--	1	--	--	--
21/09/06	S12,M12,B12	09:19	09:39		0	5	53

Tab 5 – Helley-Smith sand trap deployments from Litus at Lido nord.

The ADV was used to derive the friction velocity (U_*) of the flow – a prerequisite for solution of the moveability number (U_*/W_s) of Collins and Rigler

(1982) and the Rouse parameter ($\frac{W_s}{\beta \kappa U_*}$). The bed shear stress of the flow

(τ_o), and the character of the turbulence structure were also evaluated. The bed shear stress was determined using the Turbulent Kinetic Energy (TKE) method,

where $E = \rho(u'^2 + v'^2 + w'^2)$ where $\tau_o = 0.19E$, and where $U_* = \sqrt{\frac{\tau_o}{\rho}}$.

The Valeport® 802 provided the mean flow speed from which the maximum potential sample volume (V) of the sand trap was evaluated: $V = 0.0144U\bar{t}$ m³, where t is the time on bottom (1200 seconds). The traps were washed into cod-ends upon recovery and thence through 63 micron wet-sieves. Samples were then retained for washing in fresh water and dried for the determination of total sample weight, and organic content (loss on ignition at 380°C for 4 hours). The surface calibration sample mass was related to S through the relationship: $C_{mass} = 23S_{mass}$, $r^2 = 0.87$; where C_{mass} and S_{mass} are the total sample weights in the calibration and surface traps respectively. The resulting efficiency of the traps (E_f) was $3.5 > E_f > 5\%$. This compares well with the efficiency of plankton trawl nets of the same mesh size (7%; Rey *et al.*, 1987). The final concentrations of sand are presented in Table 5. These concentrations are the efficiency-corrected values that include both organic and inorganic parts. The organic content was low in bottom samples but rose to greater than 75% in the surface samples.

DATE	TIME(UT) ADCP transects	TIME (UT) CTD profiles	TOTAL CONC FINES (mg/L) Niskin (0.5 L samples)		
			(2 m)	(10 m)	(12/12.5 m)
19/09/06	08:05:58	09:11:26	5.6	11.4	9.2
19/09/06	08:19:26	10:22:26	8.4	21	21.2
19/09/06	08:56:48	11:17:03	18	23.2	30
19/09/06	09:10:38	12:27:50	13.8	19.4	17.4
19/09/06	10:07:20	13:16:27	11.8	18.4	--
19/09/06	10:21:24	14:21:49	--	--	--
19/09/06	11:02:25	--	--	--	--
19/09/06	11:15:57	--	--	--	--
19/09/06	12:02:10	--	--	--	--
19/09/06	12:15:28	--	--	--	--
19/09/06	13:00:54	--	--	--	--
19/09/06	13:14:03	--	--	--	--
20/09/06	09:17:58	09:32:43	4.8	7.2	4.8
20/09/06	09:31:16	10:34:48	5.2	12.4	13
20/09/06	10:15:12	11:29:47	10	18.8	29.8
20/09/06	10:28:32	12:28:08	17.8	20.4	25.2
20/09/06	11:10:00	13:16:14	18.2	20.2	24
20/09/06	11:24:11	--	--	--	--
20/09/06	12:10:31	--	--	--	--
20/09/06	12:23:39	--	--	--	--
20/09/06	13:02:30	--	--	--	--
20/09/06	13:14:57	--	--	--	--
21/09/06	07:31:06	07:48:41	8.6	5.8	9.4
21/09/06	07:44:26	08:26:38	26.6	55.6	5.6
21/09/06	08:13:03	09:49:11	--	--	--
21/09/06	08:25:10	10:21:39	6.8	15	12.6
21/09/06	09:40:29	11:21:42	--	--	--
21/09/06	09:54:11	12:31:54	--	--	--
21/09/06	10:07:34	--	--	--	--
21/09/06	10:20:30	--	--	--	--

Tab 6 – Sampling and survey activities undertaken aboard *Henetus* during transects of Lido inlet.

(ii) The *Henetus* survey

The *Henetus* undertook an hourly cycle of activities in phase with those of the launch and *Litus*. This cycle comprised: (1) a transect across Lido inlet with a RD Instruments® ADCP Workhorse (600 kHz) that passed through the northern and southern anchor sites and logged current velocity and backscatter at 0.5 m intervals with depth from 1 m below the surface to 1 m above the bed. The velocity data were used to determine sample volume in the MF and surface traps; the backscatter was used to correlate results from the northern and

southern parts of the inlet, to provide backscatter data at the *Litus* sample site, and to map the lateral and vertical distribution of suspended sediment by application of the calibration; (2) a Seabird® CTD profile of the water column was made at the fixed ADCP site. The instrument was equipped to measure hydrostatic pressure, temperature, salinity, pH, and oxygen content in profile mode; and (3) Niskin (0.5 L) water samples were collected at three depths: 2 m, 10 m, and 12/12.5 m. The Niskin samples were filtered through a 63 micron sieve to remove the sand fraction, and the fines were filtered through Millipore® GFC filters for SPM. The samples were then ashed in a furnace at 380°C for 4 hours for organic content. Activities on this vessel are summarized in Table 6.

(iii) The CNR Launch

The CNR launch was moored to the southern channel marker about 50 m from the fixed ADCP site in about 12 m of water. A Helley-Smith sand sampler with a mesh size of 63 microns was flown at a height of 3 m for 20 minutes each hour. The samples so collected were treated in a manner similar to those of the *Litus*. The sampling efficiency derived from the *Litus* was assumed the same as that measured on *Litus*. The purpose of this sampling was to provide data to correlate sand content to backscatter for the fixed ADCP. Also, to verify the validity of the Rouse profile developed at the *Litus* site to this southern site. If valid, then one may reconstruct the entire sand concentration profile within the benthic boundary layer from the reference height of the sand trap. Activities on this vessel are summarized in Table 7.

DATE	SAMPLE	START TIME(UT)	END TIME(UT)	SAND CONC (mg/L)
19/09/06	MF1	10:10	10:25	2
19/09/06	MF2	11:18	11:33	18
19/09/06	MF3	12:12	12:27	48
19/09/06	MF4	13:14	13:29	48
19/09/06	MF5	14:11	14:26	29
20/09/06	MF6	10:29	10:44	23
20/09/06	MF7	11:25	11:40	25
20/09/06	MF8	12:21	12:36	31
20/09/06	MF9	13:18	13:33	59
20/09/06	MF10	14:10	14:25	43
21/09/06	MF11	08:40	08:55	5
21/09/06	MF12	09:16	09:40	1
21/09/06	MF13	11:13	11:33	--

Tab 7 – Helley-Smith sampling at fixed ADCP site (Lido sud).

3 Interpretation of sand transport in Lido inlet

A total of 15 hours of surveying was undertaken over three days (19th, 20th and 21st September, 2006). The surveys corresponded to two periods of ebb tides, and one period of final stages of the flood tide. A range in flow speeds were sampled for bedload transport, sand distribution in the boundary layer, and associated flow conditions. A time-series of results from 19th September, 2006

is shown in Figure 8.

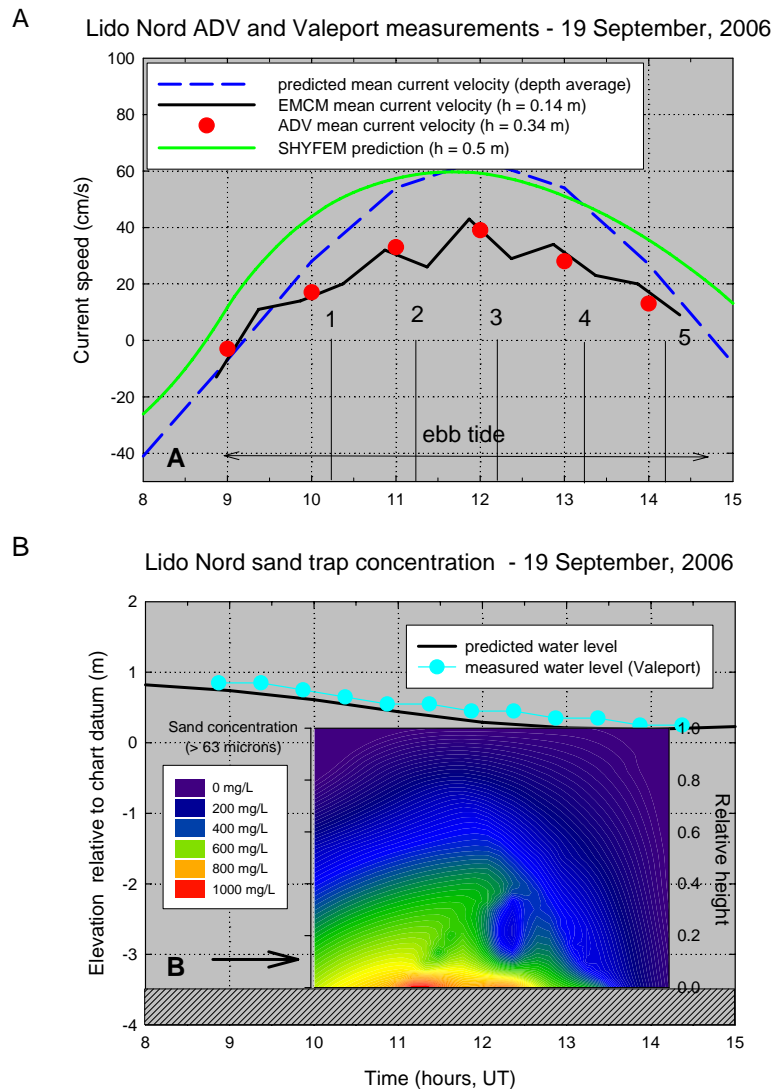


Fig 8 – A time-series of measurements made at the Litus anchor site on 19th September, 2006. (A) The predicted and observed current velocities over the ebb phase of the tide, together with the 5 deployment cycles of sand traps; (B) predicted and measured tidal elevation, and the concentration of sand on suspension derived from the Helley-Smith traps.

The sand trap profiles are shown in Figure 8A (vertical black lines). Also shown are depth averaged flow predictions from Consorzio Venezia Nuova (Unpublished data, 2006), current velocity (h = 0.5 m) from the CNR model SHYFEM (Umgiesser *et al.*, 2006), and current velocity measurements from the Valeport EMCM (h = 0.14 m) and Nortek Acoustic Doppler Velocimeter (ADV, h = 0.34 m). The EMCM and ADV yield similar results and the pattern of flow over the ebb tide is evident in all time-series. This is also evident in the traversing ADCP results from Lido nord (Figure 9A). This flow pattern is paralleled by clear transport of very fine sand in the near-bed region (Figure 8B). The transport concentration is up to 1300 mg/L and shows a strong gradient in the vertical. This justifies the use of the simplified form of the Rouse profile. The transport appears constrained above flows in excess of 0.20 m/s and shows mixing of sand to the surface at peak flows diagnostic of a boundary layer that encompasses the entire water column. An asymmetry in transport is evident over the ebb tide; it is higher on the accelerating phase than on the decelerating

phase. The arrow in Figure 8B denotes the height of the OBS and LISST-100X measurements of turbidity (discussed later). At peak flows the boundary layer has been estimated to be about 4 m thick (Amos *et al.*, 2006); our results appear to confirm this approximation. This is an important finding in relation to the prediction of sand transport, as relationships derived at the *Litus* site may only be applied to this region above the bed. Thus in the main tidal channel of Lido (which is up to 13 m deep) only the lower 30% would be considered as applicable. This “stratification” in sediment transport was evident in the ADCP profile (Figure 9B) undertaken by *Henetus* where clear events of re-suspension from the bed were monitored during peak tidal flows. Initial comparisons of suspended load and the backscatter from the traversing ADCP appears inconclusive: backscatter was highly sensitive to flow velocity in a manner described by Merckelbach and Ridderinkhof (2006). According to these authors, at high flows (> 0.7 m/s), the high backscatter is considered to relate the size of

the Kolmogorov length scale ($\eta = (\frac{\nu^3}{\epsilon})^{0.25}$). In this study, the kinematic viscosity (ν) = 0.9×10^{-6} m²/s (at 25°C) is assumed and the energy dissipation rate, $\epsilon = \frac{U_*^3}{h\kappa}$ has been derived from the ADV measurements, where U_* is the friction velocity, κ is von Karman’s constant = 0.4, and h is the water depth. The measures of U_* , U , and the resulting drag coefficient ($C_{d,0.34} = \frac{\bar{U}_*^2}{U_{0.34}^2}$) are listed in Table 8.

TIME(UT)	U (m/s)	U* (m/s)	Cd
09:00(*)	0.03	0.0039	0.0169
10:00	0.1753	0.012	0.004686
10:55	0.343	0.026	0.005746
11:55	0.4013	0.0196	0.002385
12:55	0.283	0.0189	0.00446
13:55	0.1346	0.0101	0.005631
10:14(+)	0.1779	0.0136	0.005844
11:01	0.2934	0.0251	0.007319
12:00	0.3915	0.0183	0.002185
13:03	0.3522	0.0296	0.007063
14:01	0.2238	0.0111	0.00246
08:16(-)	0.4297	0.0239	0.003094
09:11	0.2171	0.0202	0.008657

Tab 8 – Summary table of the ADV measurements of flow at 25 Hz for 5 minutes at the *Litus* sites for the 19th (*), 20th (+) and 21st (-) September, 2006.

The mean (fully turbulent) $C_{d,0.34} = 1.28 \times 10^{-2}$ (evaluated at $h = 0.34$ m). This equates to a $C_{d,100}$ (evaluated at 1 m above the bed) of 3.3×10^{-3} which agrees well with previous work undertaken by Sternberg (1972) and Thompson *et al.* (2003). The drag coefficient demonstrates a weak inverse relationship to flow

Reynolds number over the measured range: $1.0 \times 10^4 < (Re = \frac{h\bar{U}_{0.34}}{\nu}) < 13.6$

$\times 10^4$. This range is within the hydrodynamically smooth regime of flow (where the roughness length for fine sand, $Z_o = 0.001$ m, Sternberg, 1972) where the scatter in C_d has been shown to be large. The mean current velocity at which the Kolmogorov length scale η equates to the wave length of the ADCP ($\lambda = 2.3 \times 10^{-3}$ m) is 0.63 m/s. At higher flows in Lido inlet, the acoustic scattering is coherent, and at lower velocities the scattering is incoherent:

for $U > 0.63$ m/s; $\lambda > \eta \rightarrow$ coherent scattering (stronger)

for $U < 0.63$ m/s; $\lambda < \eta \rightarrow$ incoherent scattering (weaker)

A further complication is that at lower flows, the backscatter is dominated by the distribution of fine sediment load associated with surface fresh water and the organic content of this load. This may explain the high near-bed backscatter near slack water (low tide) seen in Figure 9B. We plan to apply the theories of Merckelbach and Ridderinkhof (2006) and Hill *et al.* (2003) to calibrate backscatter with sand and fines concentrations in the water column independently. These papers highlight some of the difficulties of such a calibration, not least of which are: (1) a different calibration is expected from the coherent and incoherent reflections; (2) backscatter is strongly dependent on number of scatterers (i.e. fines content); (3) the organic content of suspended material will impact the scattering function; and (4) the region of greatest sand transport is within the near-bed region which is saturated in ADCP records and hence is un-useable.

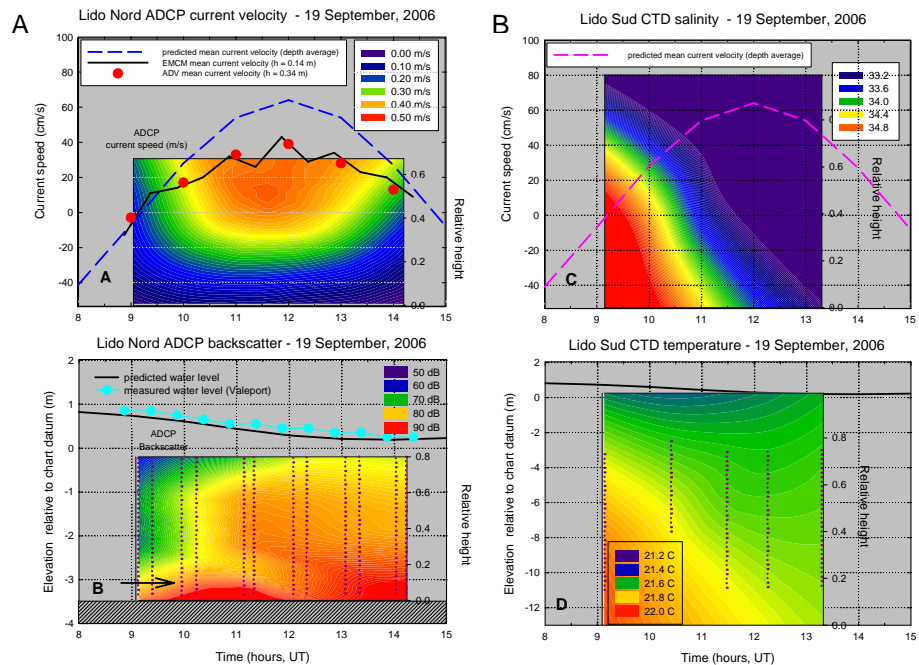


Fig 9 – The traversing ADCP current velocity (A) and backscatter (B) measurements made at Lido nord on 19th September, 2006; CTD profiles of salinity (C) and temperature (D) at Lido sud for the same period.

A major rainstorm took place over Venice on 17th September, 2006 (resulting in 25 mm of precipitation; 25% of the annual amount). A similar event took place in 2005 prior to our field campaign with the result that mass transport in Lido inlet was strongly influenced by the fresh water plume of the Piave river. This is evident as stable stratification at Lido Sud measured by the CTD profiles shown

in Figure 9C and D where two water masses occupy the water column: a surface, less-saline water mass, and an underlying warmer, more-saline water mass. Density profiles of the water column have been derived and show the water column was stably stratified ($\Delta\sigma_t > 4$) over high water. The surface cooler (more turbid) layer pushed the underlying Adriatic water mass out of the inlet by mid ebb. Each water mass is expected to respond differently to the ADCP due to differences in suspended particulate matter and thus should be considered independently in the calibration procedure.

The fines concentration (measured at Lido sud) also peaked in the lowest part of the water column and at peak tidal flow though concentrations were low (< 10 mg/L). There appears to be mixing of fines (and breakdown in stratification) from the bed to the surface over the accelerating phase of the ebb tide, diagnostic of resuspension rather than advection (Figure 10A). Though settling on the decelerating late ebb is evident, the fines content was higher at low water than at high water suggesting a net export of fines from the lagoon. The organic content of the fines (Figure 10B) was greatest during high water near the bed (70%), was minimum during peak flow ($< 20\%$) and showed a steady intermediate trend (40%) at the surface. The 0.7h peak in organics may be due to production in this layer, or the influx of organic rich material in the Piave plume that manifested itself as the upper water mass (Figure 9C). The peak sand concentration is three orders of magnitude higher than the fines concentration measured with the Niskin bottles; the ratio of fines:sand varies over three orders of magnitude throughout the tidal cycle.

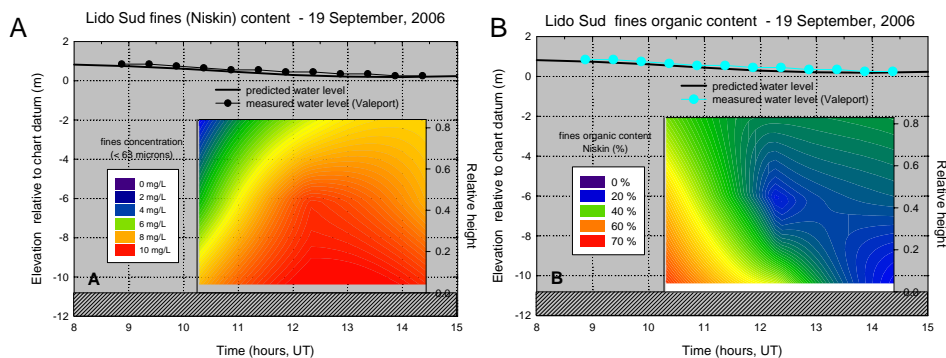
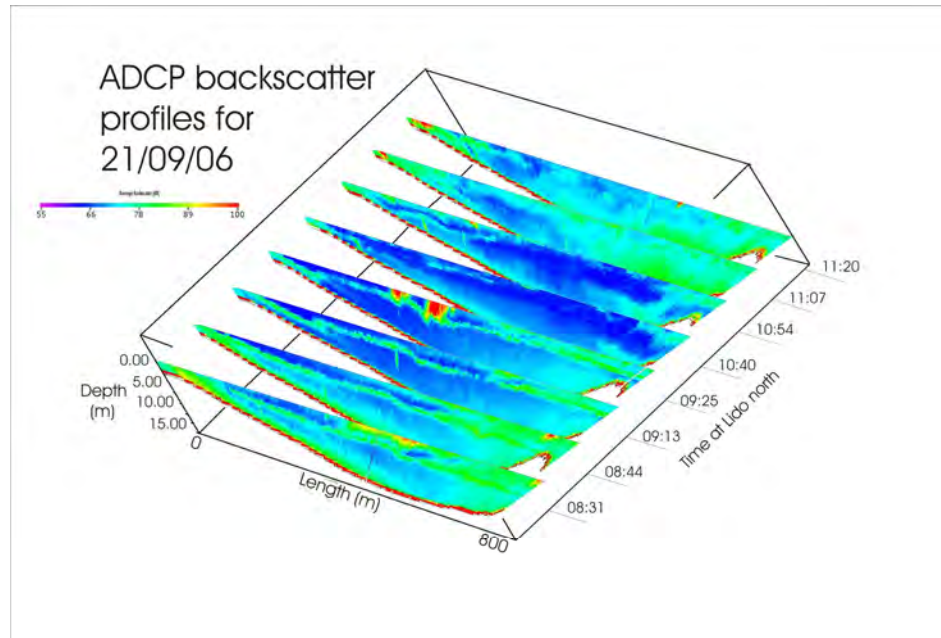


Fig 10 – (A) The concentration of fines (< 63 microns) in the water column at Lido sud on 19th September, 2006, derived from filtering 0.5 L Niskin samples; (B) the organic content of the suspended fines.

Stratification of the water column is also evident in Figure 11, as the region of high backscatter within the water column evident in the first four profiles (the flood phase; 08:31 – 09:25) at 0.8h. It appears that, although the plume became evident throughout the survey period, the influence on sand transport was limited. This was not the case for the fines (< 63 microns) where a surface plume was noted entering Lido inlet from the north. There is also strong evidence for resuspension from the bed during peak flows due to the relatively high backscatter within the bottom 4 m of the water column. This is most evident along the northern and southern (shallower) margins of the profile where the resuspension appears to extend to the surface, and during the peak ebb tide (11:07 and 11:20 profiles). In the deeper, central parts of the profile, resuspension appears to be restricted to the bottom boundary layer. Settling

from suspension is evident during the slack water (high tide) around 10:40 (Figure 11), when the water column backscatter is at a minimum.

Fig 11 – The ADCP backscatter (dB) across the Lido transects on 21st September, 2006. Near-bed turbidity is clear, as is high turbidity levels at the margins as is the pycnocline at 0.8h in the first four transects.



The Valeport[®]802 and LISST-100X worked well throughout the three days of deployment. The current velocity data from the Valeport[®] EMCM ($h = 0.14$ m) are shown in Figure 12A; they compare well with the mean velocity from the ADV time-series (Figure 9A). The time of high water coincides with predictions. However the predicted velocities are higher as they were determined for $h = 0.5$ m (SHYFEM output), and as a mean velocity (CVN, 2006). Water elevation measured by the Valeport corresponds very well with the predictions of CVN (2006) (Figure 9B). The peak concentration (1300 mg/L) coincides with peak flows, and is situated within the bottom 0.2 m of the water column. Mixing through the water column is greatest at peak flows; sand concentrations go to zero as the flow decelerates after the peak. Regression of bed transport rate against $U_{0.34}$ was used to define the traction threshold for fine sand (0.15 m/s). The organic content varies strongly with height; it is lowest (< 5%) near the bed and reaches 25% in the near surface and surface samples. The organic content was greatest in surface waters during slack high and low waters.

The LISST-100X yielded data on volume concentration, grain size, and sorting at 1-minute intervals at $h = 0.45$ m and for the duration of deployments at Lido nord. A time-series of results for 19th September is shown in Figure 12. Also shown are the velocity data for reference purposes. Note that volume concentration increases rapidly when the flow ($U_{0.14}$) > 0.20 m/s. This is slightly higher than the traction/suspension threshold for $d_{50} = 100$ microns. The peak in concentration is coincident with the peak in flow, and also with the peak in sand transport sampled by the Helley-Smith traps. The asymmetry in concentration (evident in the fines concentration) is apparent here; that is, the concentration at low water is higher than at high water (a trend also seen in the ADCP results, Figure 9B).

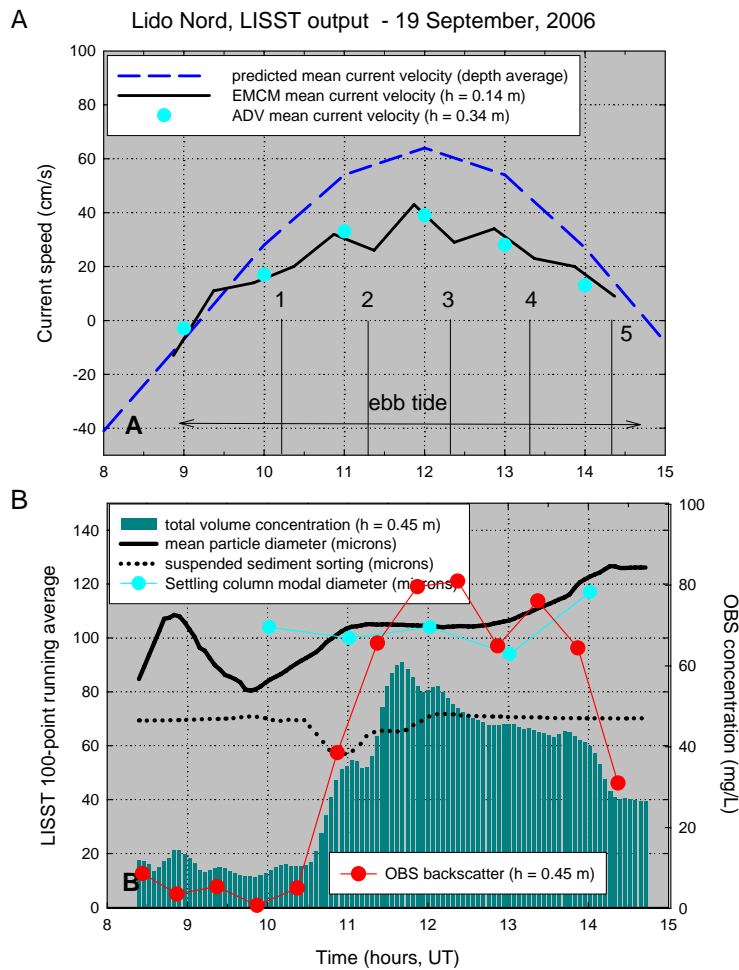


Fig 12 – (A) Time-series of current velocity predicted (dashed line) and observed (solid line and dots) for sand trap survey of Lido nord on 19th September, 2006. (B) Results from LISST-100X (showing volume concentration, median grain diameter for $h = 0.45$ m, and sorting of suspended material). Also shown is the concentration of sand measured by the Valeport OBS ($h = 0.45$ m).

The OBS time-series from the Valeport[®] has been calibrated using bottom samples (sand) from the deployment site; it thus shows trends of the sand transport and is less sensitive to fines. Note that the overall trend is similar to that of the LISST-100X. However, the decrease in concentration on the decelerating tide is more pronounced, perhaps diagnostic of rapid settling of sand once the flow falls below the suspension threshold. The median grain diameter (d_{50}) detected by LISST-100X (solid line; Figure 12B) corresponds well with that measured from the settling column analysis of Helley-Smith samples. The results are anomalous as the grain size appears to increase steadily from high water to low water, irrespective of the current speed. A divergence between laboratory measured and field measured diameter was only evident at high water. A variation of $80 > d_{50} > 125$ microns was found in the nearbed suspended sediment load. This corresponds very well to the material collected in the sand traps (Table 2), and shows that the sand transport is dominated by very fine and fine sand. Histograms of the LISST-100X showed a second minor mode in the medium sand range ($d_{50} > 250$ microns). This mode was not sampled by the sand traps and hence may be an organic population. Sediment sorting (σ) appears to be steady (70 microns) for most of the deployment; that is, moderately sorted (Folk, 1968). There was a decrease in scatter (to

moderately well sorted) during the period of rapid suspension evident in the concentration data (perhaps diagnostic of selective entrainment from the bed). This agrees with sieve analyses of trap samples collected in Chioggia inlet.

The sand transport in Lido inlet behaved similarly to that in Chioggia inlet, though the organic content was much lower. The 12 profiles undertaken over three days of survey all showed a decrease in concentration with height above the bed which have been fitted with regression lines on the log-log plot illustrated in Figure 13. The correlation is based on the samples from both the *Litus* (Lido nord - bed, epi-benthic and surface), and from the CNR launch (Lido sud - 0.3h, where h is the water depth). Interestingly, the samples from Lido sud fitted very well the vertical distribution of sand evident at Lido nord. The slope of the best fit line has been used to derive (in a statistical fashion) the Rousès suspension number (R). These are listed in Table 9.

PROFILE #	R-squared	1/m	b
1	0.91	1.45	0.2
2	0.98	0.89	-0.16
3	0.82	0.79	-0.49
4	0.65	0.94	-0.51
5	0.47	1.45	-0.59
6	0.77	1.59	-0.15
7	0.66	1.79	-0.71
8	0.26	1.02	-1.1
9	0.99	0.26	-0.01
10	0.26	2.08	-1
11	0.89	1.49	-0.38
12	0.55	0.86	-0.02

Tab 9 – Sand concentration profiles, Chioggia inlet (m = slope; b = offset).

In the simplest form $R = 1/m$, where m is the slope of the best-fit lines. Also listed is the correlation coefficient of the fit. Highest correlations are associated with the strongest flow when a “Roussian” distribution of sand in the water column takes place. The mean value of $1/m = -0.93$ which is higher than the value recommended by van Rijn (1993) ($R = -0.5$) for fine sand. This higher value indicates that the sand moves close to the bed and is not well mixed throughout the water column. An independent method was adopted to derive R ; that is, through measurement of the still water settling rate (W_s) of the sand collected by the traps, through direct measurement of U_* , and through the assumption that von Karman’s constant, $\kappa = 0.4$ and the $\beta = 1$ (the ratio of the eddy diffusivity of sediment to water). Median W_s decreased with height above the bed ($B = 7.4 \times 10^{-3}$ m/s; $M = 6.3 \times 10^{-3}$ m/s; $S = 4.4 \times 10^{-3}$ m/s) as would be expected (i.e. the fastest settling grains are nearer the bed). This corresponds to a median diameter of respectively $d_{50} = 98$ microns, 88 microns, and 72 microns) which is all within the very fine sand size classification. The W_s of sand in transport should vary in relation to the friction velocity (U_*) according to the relationship $W_s/U_* = 0.2$. This was not the case; for the bed trap, W_s showed an *inverse* relationship, whilst the epi-benthic and surface material showed no

trends. The inference is that the sand in transport in Lido inlet is source controlled and limited in size to the very fine sand range.

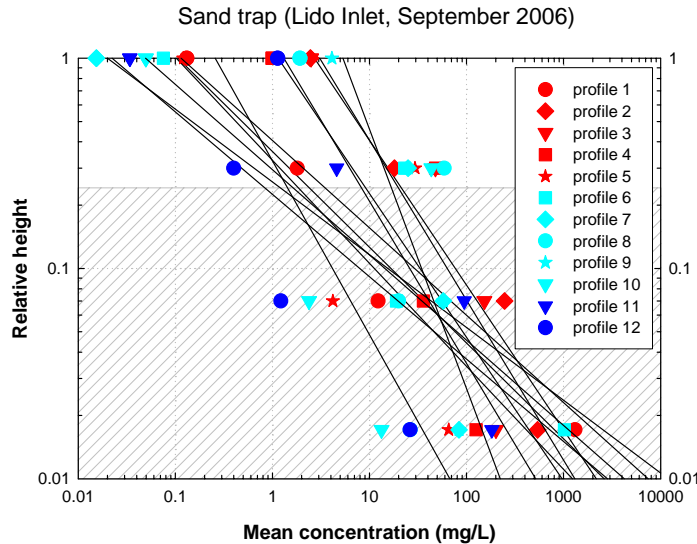


Fig 13 – The distribution of sand in suspension, Lido nord.

The bedload (traction + saltation) transport rate (G_s ; kg/m/s) derived from the bed trap (B) varies as a function of the excess velocity:

$$G_s = 0.522(\bar{U}_{0.34} - U_{crit,bed})^3 \text{ kg/m/s} \quad (4)$$

which is well below the values proposed by Gadd *et al.* (1978) for fine sand transport on a wave-dominated, energetic continental shelf. Note that the constant in equation 4 (Lido) is an order of magnitude larger than that derived for Chioggia (equation 2). The traction threshold ($U_{crit,bed}$) was determined by regressing U versus G_s and defining U as $G_s \rightarrow \text{zero}$. The threshold for very fine sand was evaluated at 0.15 m/s ($U_{*,crit} = 1.7 \times 10^{-2}$ m/s) which is very close to the value derived in the Chioggia inlet. A suspension threshold ($U_{crit,susp}$) was defined by regressing the concentration from the epi-benthic trap against ADV velocity ($U_{0.34}$); this threshold was also 0.15 m/s (Figure 14B). This illustrates that very fine sand moves from a state of no motion almost immediately into a state of suspension with no traction phase. Thus the Rouse profiles expressed above can be used to compute the mass transport of very fine sand throughout the water column without need for a traction component.

The total mass/unit width in the bottom 0.12 m of the water column moving has been equated with “bedload” and compared to that derived using the method of Engelund and Hansen (1967) within the sediment transport model SEDTRANS92 (Li and Amos, 1993). The predictions are grain size dependent and are shown in Figure 14A. These predictions are illustrated for a $d_{50} = 55, 75, 100, 125,$ and 250 microns. The 100-micron prediction passes through the centre of the observed benthic transport results from trap B. It appears that the formulation of Engelund and Hansen (1967), which was developed for medium sand, is equally applicable to predictions of the transport of very fine sand. The predictions are plotted in terms of the mean current velocity ($h = 0.44$ m). As

this method solves sediment discharge through computation of the bed stress (τ_0), solutions hinge on the selection and definition of bed roughness. In order to examine this effect to predicting sand transport in Lido inlet we have compared the observed bedload transport to predictions using SHYFEM+Sedtrans96 (Umgiesser *et al.*, 2006). The output for 19th September, 2006 (ebbing tide) is indicated by the darker dots in Figure 14A. The predictions are very similar to those calculated in SHYFEM (with assumptions about the nature of the velocity gradient) and show that this model appears to reproduce a realistic estimate of bed roughness, shear stress and sand transport.

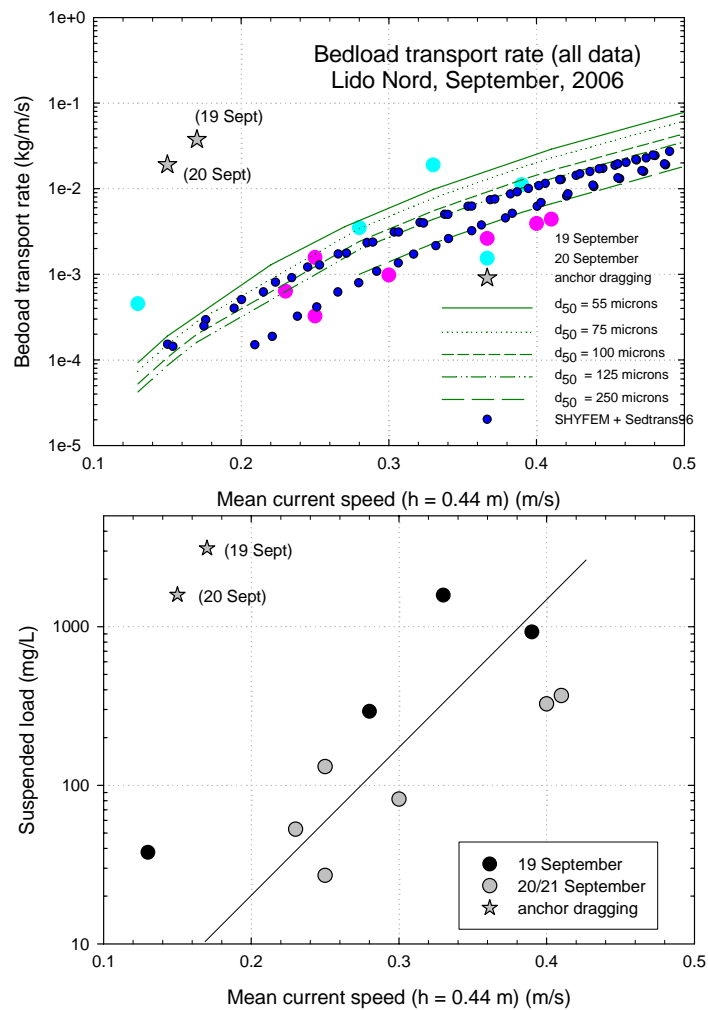


Fig 14 – (A) The observed (trap B) and predicted bedload transport rates plotted against mean current velocity ($h = 0.44$ m); (B) suspended sediment concentration (trap B) plotted against mean current velocity.

The next step in this study will be to compare the sand concentration profile in the water column, predicted by the model, with the Rouse profiles presented earlier. Once this has been done, the model should offer a robust method of estimating the long-term net transport of very fine sand within Lido inlet. One limitation is the source control on sand supply: No realistic predictions of sand transport at the inlets will be possible until the mobilization of sand within the entire domain of the modeled lagoon has been completed. In order to do this, the role of waves in resuspension on the *bassi fondi* must be determined and accurately simulated.

Conclusions

This paper reports on the final field campaign undertaken during September, 2006 within Venice lagoon. The campaign was a multi-disciplinary study undertaken in association with a number of key people. The main points of conclusions of this work are:

- (1) Helley-Smith traps are a practical and accurate way of measuring sand transport within the inlets of Venice. However, the efficiency of the traps is only around 5%. The traps showed that only very fine sand appeared to be in transport in the inlets;
- (2) Sand transport was measured in Chioggia and Lido inlets during this study. The results indicated that the model SHYFEM+Sedtrans96 predicted the sand transport in Lido inlet at the time, and that this sand transport is well defined by the Engelund and Hansen (1967) algorithm; it is noted that Chioggia is sand starved and hence has a transport at high flows much lower than would be predicted by theory;
- (3) the sand in suspension is well defined by the Rouse profile, however, the suspension number is -0.98 for Lido inlet and -0.56 for Chioggia inlet. Thus the movement of sand is concentrated closer to the bed than is evident in counterparts elsewhere;
- (4) A survey of the *bassi fondi* was undertaken over a *paleo-cordone* surrounded by *prateria*. The backscatter was able to discriminate the various bed types and to highlight the *paleo-cordone*. A bathymetric survey of the site showed that the surrounding region has eroded 0.5 m since 1990 and that the *paleo-cordone* is stable and hence is being slowly exhumed. It does not appear to provide sand to the inlets;
- (5) BRAD was deployed at 6 sites at the entrance to Chioggia and in the *bassi fondi*. The result showed that BRAD could be used to map the thickness and density of sea grasses, and the sediment bed beneath. It could thus be used in survey mode in regions of *prateria* as it penetrates the organic cover; and
- (6) the ebb tidal delta off Chioggia has been mapped fully, and it appears to be accreting at a rate of about 20 cm/annum. The volume of material accumulating is order 50,000 m³/annum which is an order of magnitude less than that found off Lido inlet.

Acknowledgements

This project was completed with some degree of success. This is in large measure due to the support and effort of a variety of people who for brevity have not been acknowledged fully within the manuscript. My thanks go to CORILA and the key staff who made all this possible; in particular we thank Pierpaolo Capostrini, Stefania De Zorzi and Matteo Morgantini. The massive efforts of Emiliano Valenzasca as skipper of the boat *CORILA* were central to the successful data collection. Thanks also go to Franco Costa and Francesco

for their support in the Lido inlet study. G. Brancolini and Armondo are also thanked for support with the vessel *Aretusa*.

References

- Amos, C.L. Helsby, R., Umgiesser, G., Mazzoldi, A. and Tosi, L. 2005. Sand transport in northern Venice lagoon. *In: Scientific Research and Safeguarding of Venice. Research program 2004-2006. Vol. III, Publ. CORILA: 369-383.*
- Amos, C. L., Helsby, R. Thompson, C.E.L., Villatoro, M., Venturini, V., Manca, E., Mazzoldi, A., Umgiesser, G. and Tosi, L. 2006. The origin of sand in the Venice Lagoon – the next step. *In: Scientific Research and Safeguarding of Venice. Research program 2004-2006. Vol. IV, Publ. CORILA: 429-454.*
- Arena, F., Kovacevic, V. and Mazzoldi, A. 2005. Estimate of the suspended solid matter concentration from the backscatter intensity measured by ADCP. *In: Scientific Research and Safeguarding of Venice. Research program 2004-2006. Vol. IV, Publ. CORILA: 373-387.*
- Bagnold, R.A. 1963. Mechanics of marine sedimentation. *In: The Sea M.N. Hill (ed). Publ. Interscience: 507-582.*
- Collins, M.B. and Rigler, J.K. 1982. The use of settling velocity in defining the initiation of motion of heavy minerals grains, under unidirectional flow. *Sedimentology 29: 419-426.*
- CRC. 1976. Handbook of Chemistry and Physics. Publ. CRCpress, Cleveland, Ohio.
- Dyer, K.R. 1986. Coastal and Estuarine Sediment Dynamics. Publ. John Wiley & Sons Ltd., 342p.
- Folk, R.L. 1968. Petrology of Sedimentary Rocks. Publ. Hemphill's, Austin, Texas: 170p.
- Engelund, F. and Hansen, F. 1967. A monograph on sediment transport in alluvial streams. Teknisk Vorlag, Copenhagen Denmark
- Gacic, M., Mosquera, I.M., Kovacevic, V., Mazzoldi, A., Cardin, V., Arena, F. and Gelsi, G. 2004. Temporal variations of water flow between the Venetian lagoon and the open sea. *Journal of Marine Systems 51: 33-47.*
- Gadd, P.E., Lavelle, J.W. and Swift, D.J.P. 1978. Calculations of sand transport on the New York shelf using near-bottom current meter observations. *Journal of Sedimentary petrology 48(1): 239-252.*
- Gibbs, R.J., Matthews, M.D. and Link, D.A. 1971. The relationship between sphere size and settling velocity. *Journal of Sedimentary Petrology 41(1): 7-18.*
- Helsby, R., Amos, C.L. and Umgiesser, G. 2005. Morphological evolution and sand pathways in northern Venice lagoon, Italy. *In: Scientific Research and Safeguarding of Venice. Research program 2004-2006. Vol. IV, Publ. CORILA: 388-402.*

- Hill, D.C., Jones, S.E., and Prandle, D. 2003. Derivation of sediment resuspension rates from acoustic backscatter time-series in tidal waters. *Continental Shelf Research* 23: 19-40.
- Li, M. Z. and Amos, C.L. 1993. SEDTRANS92: re-evaluation and upgrade of the AGC sediment transport model. Geological Survey of Canada Open File Report 2769: 42p.
- Merckelbach, L. M. and Ridderinkhof, H. 2006. Estimating suspended sediment concentration using backscatter from an acoustic Doppler profiling current meter at a site with strong tidal flows. *Ocean Dynamics* 56: 153-168.
- Rey, J.R., Crossman, R.A., Kain, T.R., Vose, F.E. and Peterson, M.S. 1987. Sampling zooplankton in shallow marsh and estuarine habitats: gear description and field tests. *Estuaries* 10(1): 61-67.
- Sternberg, R.W. 1972. Predicting initial motion and bedload transport of sediment particles in the shallow marine environment. *In*: D.J.P. Swift, D.B. Duane, O.H. Pilkey, (eds) *Shelf Sediment Transport*. Publ. Dowden, Hutchinson & Ross: 61-82.
- Teatini, P., Tosi, L., Strozzi, T., Carbognin, L., Wegmüller, U., and Rizzetto, F. 2005. Mapping regional land displacements in the Venice coastland by an integrated monitoring system. *In Remote Sensing of Environment '98*: 403-413.
- Tesi, T., Miserocchi, S., Gonu, M.A. Langone, L., Boldrin, A. and Turchetto, M. In review. Organic matter origin and distribution in suspended particulate materials and surficial sediments from the western Adriatic Sea (Italy). *Estuarine, Coastal and Shelf Science*.
- Thompson, C.E.L., Amos, C.L. Jones, T.E.R. and Chaplin, J. 2003. The manifestation of fluid-transmitted bed shear stress in a smooth annular flume – a comparison of methods. *Journal of Coastal Research* 19(4): 1094-1103.
- Umgiesser, G., Sclavo, M., Carniel, S. and Bergamasco, A. 2004. Exploring the bottom shear stress variability in the Venice lagoon. *Journal of Marine Systems* 51: 161-178.
- Umgiesser, G., DePascalis, F., Ferrarin, C. and Amos, C.L. 2006. A model of sand transport in Treporti channel: northern Venice lagoon. *Ocean Dynamics* 56: 339-351.
- Van Rijn, L.C. 1993. *Principles of Sediment Transport in Rivers, Estuaries and Coastal Seas*. Publ. Aqua Publications, Zwolle, the Netherlands.

3D NUMERICAL MODELING OF COASTAL AND SEA-LAGOON PROCESSES

Debora Bellafore^{1,2}, Georg Umgiesser¹

¹*Istituto di Scienze Marine ISMAR, CNR, Castello 1364/A, 30122 Venezia*

²*EuroMediterranean Centre for Climate Change (CMCC), c/o Consorzio Venezia Ricerche, Venice, Italy*

Riassunto

In questo lavoro si presentano gli ultimi sviluppi nella numerica e nell'applicazione del modello idrodinamico agli elementi finiti SHYFEM (Shallow water HYdrodynamic Finite Element Model), utilizzato recentemente per la simulazione dei processi costieri e di interazione tra bacini.

Grande attenzione è stata posta nel check di alcuni moduli del modello 3D, in primis il modulo per il calcolo dei gradienti di pressione baroclinica ed il modulo di chiusura della turbolenza. Si è dato spazio alla fase di controllo di questi moduli perché i termini corrispondenti sono considerati importanti nella riproduzione dei processi costieri e d'interazione.

Si presenteranno le migliorie ed i test applicati al modello e la sua implementazione in Nord Adriatico, per l'indagine dei processi già registrati da immagini da satellite, da radar e da misure in situ.

Abstract

In this work the last numerical developments and the implementation of the hydrodynamic finite element model SHYFEM (Shallow water HYdrodynamic Finite Element Model) are presented. This model has been recently applied to simulate the coastal and basin interaction processes.

Particular attention is devoted to check some of its modules. This part is important to be sure that the model reproduces realistically results for each of the hydrodynamic terms. The two tested modules are the computation of baroclinic pressure gradient terms and the turbulence closure module.

Some model improvements and some checks will be presented here. Finally some new implementations in the North Adriatic Sea will be described. These runs reproduce the same processes already seen by satellite images, radars and in situ measurements.

1 Introduction

There is a great quantity of instruments to investigate physical phenomena, measurements in situ, satellites, radars and, finally, modeling. The Venice Lagoon system and the interaction processes between it and the open sea can be better known applying numerical methods to reproduce the whole spatial and

temporal dynamics. Models, giving the opportunity to switch on and off different terms in computing the hydrodynamic variables, permit to identify the main drivers of processes and, for this reason, testing every part of a model has a great importance.

For many years no data of the Venice Lagoon inlets were available. Only in the last years a big effort in collecting hydrodynamic data has been done [Kovačević et al., 2004; Gačić et al., 2002; Gačić et al. 2004; Kovačević et al., Present Issue; Mosquera et al., Present Issue]. Starting from this point a complete analysis of hydrodynamic processes from measurements and simulations can be done.

2 Methods

As in a previous work presented for the CORILA Research Program 2004-2006, SHYFEM is the main instrument that we develop and apply to investigate a certain typology of hydrodynamic processes [Bellafiore and Umgiesser, 2005]. An accurate work in checking the different modules in the model has been done and different numerical choices have been applied in this last version. Here the model is described stressing the main changes and how these aspects impact on our studies.

2.1 3D SHYFEM Model

SHYFEM is a primitive equation model, based on the solution of momentum and continuity shallow water equations. The complete transport equations, including also the baroclinic pressure gradient terms, are:

$$\frac{\partial U_i}{\partial t} - fV_i = Adv_i^x - g \frac{\partial \zeta}{\partial x} h_i - \frac{gh_i}{\rho_0} \frac{\partial}{\partial x} \int_{-H_i}^{\zeta} \rho' dz - \frac{1}{\rho_0} \frac{\partial p_a}{\partial x} + \frac{1}{\rho_0} (\tau_x^{i-1} - \tau_x^i) + \quad (1)$$

$$+ A_H \left(\frac{\partial^2 U_i}{\partial x^2} + \frac{\partial^2 U_i}{\partial y^2} \right) + A_V \left(\frac{\partial u}{\partial z} \Big|_{top(i)} - \frac{\partial u}{\partial z} \Big|_{bottom(i)} \right)$$

$$\frac{\partial V_i}{\partial t} + fU_i = Adv_i^y - g \frac{\partial \zeta}{\partial x} h_i - \frac{gh_i}{\rho_0} \frac{\partial}{\partial y} \int_{-H_i}^{\zeta} \rho' dz - \frac{1}{\rho_0} \frac{\partial p_a}{\partial y} + \frac{1}{\rho_0} (\tau_y^{i-1} - \tau_y^i) + \quad (2)$$

$$+ A_H \left(\frac{\partial^2 V_i}{\partial x^2} + \frac{\partial^2 V_i}{\partial y^2} \right) + A_V \left(\frac{\partial v}{\partial z} \Big|_{top(i)} - \frac{\partial v}{\partial z} \Big|_{bottom(i)} \right)$$

with i vertical layer, (U, V) horizontal transport, p_a atmospheric pressure, g gravitational constant, ζ sea level, $\rho = \rho_0 + \rho'$ water density, h_i layer thickness, H_i depth of the layer, A_H horizontal eddy viscosity and A_V vertical eddy viscosity. The stress terms can be written for each vertical interface as

$$\tau_y^i = -k \left(\frac{\partial v}{\partial z} \right)_i \quad \tau_x^i = -k \left(\frac{\partial u}{\partial z} \right)_i \quad (3)$$

and the boundary conditions for stress terms are

$$\tau_x^{\text{sup}} = c_D \rho_a w_x \sqrt{w_x^2 + w_y^2} \quad \tau_y^{\text{sup}} = c_D \rho_a w_y \sqrt{w_x^2 + w_y^2} \quad (4)$$

$$\tau_x^{\text{bottom}} = c_B \rho_0 u_L \sqrt{u_L^2 + v_L^2} \quad \tau_y^{\text{bottom}} = c_B \rho_0 v_L \sqrt{u_L^2 + v_L^2} \quad (5)$$

c_B is the bottom friction coefficient, c_D the wind drag coefficient, ρ_a the air density, ρ_0 the constant water density, (w_x, w_y) the wind velocity and (u_L, v_L) the bottom velocity.

$$w_0 = \frac{d\zeta}{dt} \quad w_L = - \left(u_L \frac{\partial H_L}{\partial x} + v_L \frac{\partial H_L}{\partial y} \right) \quad (6)$$

w_0 and w_L are the vertical velocities at the surface and at the bottom layers. The SHYFEM model applies an Arakawa B grid for the horizontal discretization and z layers. The barotropic pressure gradient and Coriolis terms are semi-implicitly discretized, while the baroclinic, the advective and the horizontal diffusion terms are explicitly discretized. Some developments and changes have been done in the computation of the Coriolis term from the first 3D model version presented in introducing a penta-diagonal solver [Umgiesser and Bergamasco 1995].

3 Test Cases

Two of the main terms to reproduce the coastal and interaction processes are the baroclinic pressure gradient term and the turbulence closure module. Before applying the model to a real case, these two main parts had to be tested in ideal cases. Here below, as an example, follows the description of two tests to assure the correctness of the modules. This work is meant to be a development of previous tests. Applying the first version of 3D SHYFEM Model a real case has been run, the Po river outflow [Umgiesser and Bergamasco 1998]. Starting from that version, the baroclinic pressure gradient terms computation has been developed and this paper is to describe the more recent results.

3.1 Chao test case

A computational test case, proposed by Chao and Boicourt [1986], was run. A 0.1 ms^{-1} freshwater inflow velocity is set at the open boundary upper layers of a channel connected to an ideal basin. Outflow is set at the lower layers to obtain no barotropic flux at the open boundary. We chose this test because imposing a net null flux at the open boundary permits a real comparison between the results from Chao's model, which is rigid lid, and the free surface SHYFEM model [Umgiesser and Bergamasco, 1995]. The run setup considers bottom friction 0.01, vertical eddy viscosity $10^{-4} \text{ m}^2 \text{ s}^{-1}$, horizontal diffusion $10 \text{ m}^2 \text{ s}^{-1}$ and beta plane Coriolis approximation for latitude 30 degrees North. After 5 days the velocity and the salinity fields are as presented in Figure 1 and Figure 2. It is

evident that the two models reproduce the same dynamics. These results are in agreement with the results presented by Chao and Boicourt [1986].

Fig 1 – Surface layer – Velocity (a), Salinity (b), Chao Results, velocity and salinity (c).

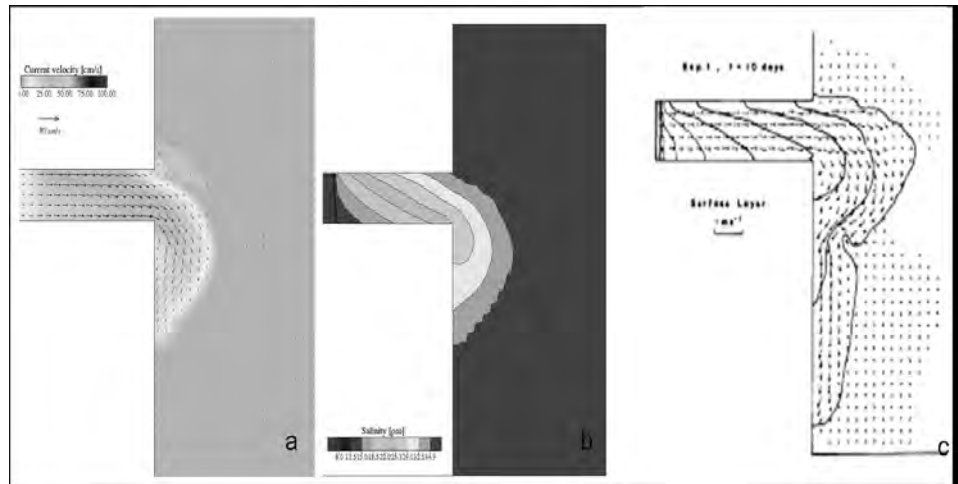
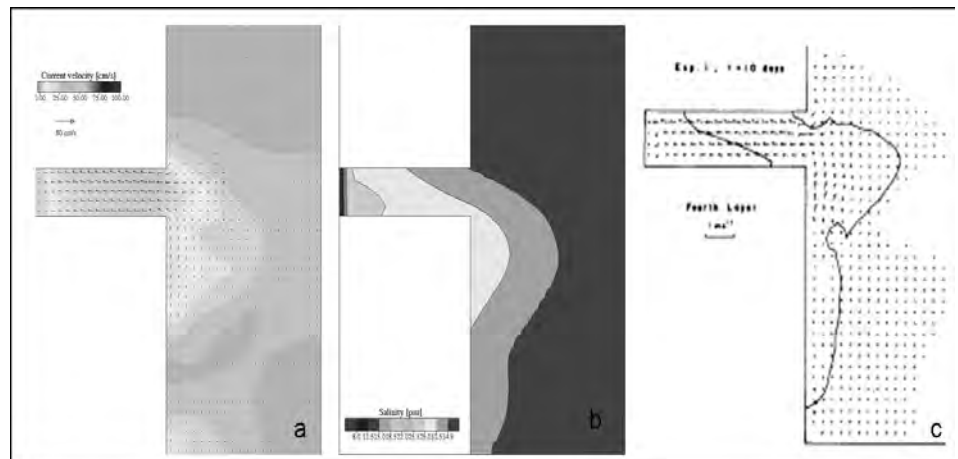


Fig 2 – Near bottom layer – Velocity (a), Salinity (b), Chao Results, velocity and salinity (c).



3.2 Kato-Phillips test case

The turbulence closure module introduced in the SHYFEM model is an adaptation of the GOTM (General Ocean Turbulence Model) from Burchard [2002]. The test case here presented is a classical one, the Kato-Phillips experiment [Kato and Phillips, 1969], already used as check for other model applications [Luyten et al., 1996; Burchard and Petersen, 1999]. The experiment consists in checking the mixed layer deepening produced by a constant superficial stress. A top friction velocity of 0.01ms^{-1} and an initial Brunt-Väisälä frequency n_0 of 0.01s^{-1} are imposed. The time evolution of the mixed layer in one point, computed as the depth where the density gradient is the steepest, is investigated. In Figure 3 a comparison between our results and the one obtained by Luyten et al. [1996] is shown. It stresses the good behaviour of our model in reproducing the process.

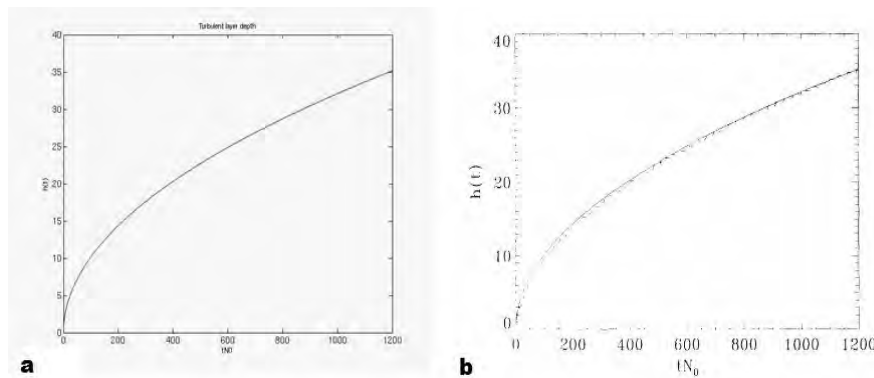


Fig 3 – Time Evolution of the mixed layer in the SHYFEM Run (a) and in the one presented in Luyten et al. [1996] (b).

4 Implementation in the Northern Adriatic Sea

Once tested the baroclinic and the turbulence closure modules a real application has been performed. The application is in the Northern Adriatic, doing a run on the coupled Adriatic and Venice Lagoon finite element grid. A test period has been chosen, January 2004, applying $1/16^\circ \times 1/16^\circ$ MFStep temperature and salinity 3D matrices as initial condition on the whole basin. 6h, $1/2^\circ \times 1/2^\circ$ ECMWF wind fields have been used as meteorological forcings and astronomical tide timeseries have been applied at the Otranto Strait open boundary. Two runs have been done, one with and one without the river runoff forcings. This is considered an interesting test to have an idea about the real impact of freshwater forcing, in terms of T/S gradients and variation in the discharges. From Figure 4 an increase in the coastal current, combined with the mean geostrophic current can be seen if the river runoff is considered. Moreover, the whole structure of the circulation pattern is changed once the river discharge has been switched off. This is a preliminary result that has to be further investigated to estimate how the baroclinic terms impact in the coastal processes.

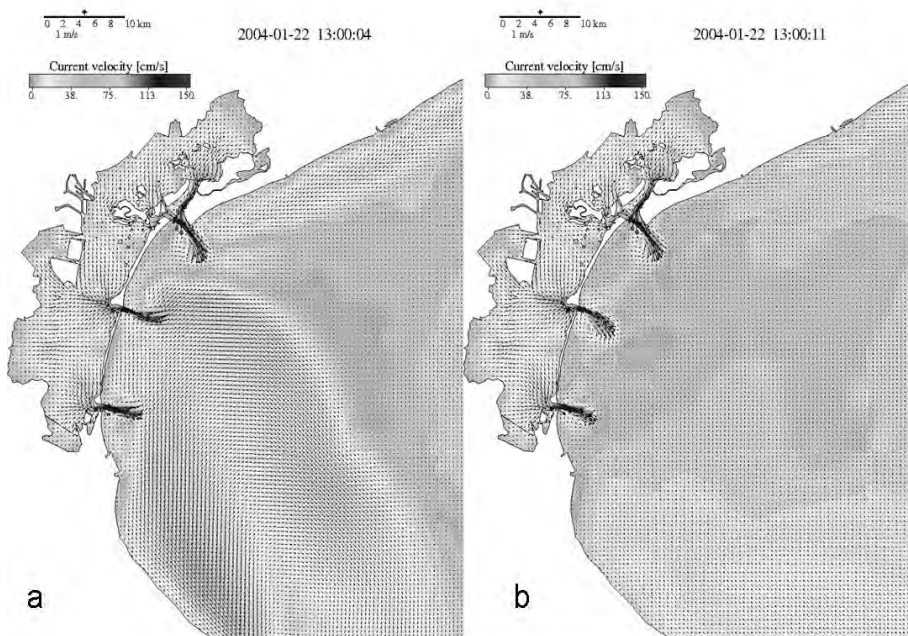


Fig 4 – Surface velocity maps. Simulation with the river runoff forcing (a) and without it (b). The discharge and the T/S gradient increases the coastal currents.

The tidal impact of the inflow-outflow processes are seen from the simulations. The creation of a dipole near the inlets, going offshore during several cycles, is reproduced, as seen even in the theoretical model by Wells and Van Heijst [2003].

The real case runs need a comparison with measured data, as the HF Radar ones [Kovačević et al., 2004] and the ADCP ones [Gačić et al., 2002; Gačić et al. 2004] but it is interesting to stress how the modelling application permits to divide the different input impacts (river runoff, wind) and gives additional information on the processes.

Conclusions

This work is a continuation of what presented in Bellafiore and Umgiesser [2006] and is the proof of the model capability in reproducing particular coastal and interaction processes, identifying the most important terms to simulate them. The simulations have to be compared with real data to be validated and to allow a quantitative study of coastal and interaction processes.

Acknowledgements

The authors want to thank INGV Institute for temperature and salinity data. A special thank to Dr. John Warner (USGS, Woods Hole, US) for the precious suggestions in checking and testing the modules of SHYFEM Model. This work was carried out with the financial support of CORILA in the framework of the CORILA Project 3.15 *Trasporto solido e circolazione superficiale alle bocche di porto e nella zona costiera* and the Vector 5.2 CLIVEN project *Idrodinamica e Climatologia*.

References

Bellafiore, D. and Umgiesser, G., 2006. Comparison between a theoretical model and a numerical simulation of sea-lagoon interaction in the Northern Adriatic. *Scientific Research and Safeguarding of Venice, Research Programme 2004-2006, 2005 Results, Vol. 4*, 301-310.

Burchard, H. and Petersen, O., 1999. Models of turbulence in the marine environment – a comparative study of two-equation turbulence models. *Journal of Marine Systems*, 21, 29-53.

Burchard, H., 2002. *Applied Turbulence Modeling in Marine Waters*, Lecture Notes in Earth Science, Springer.

Chao, S. and W.C. Boicourt, 1986. Onset of estuarine plumes. *Journal of Physical Oceanography* 16, 2137-2149.

Gačić, M., V. Kovačević, A. Mazzoldi, J. D. Paduan, I.M. Mosquera, G. Gelsi, and G. Arcari, 2002. Measuring water exchange between the Venetian Lagoon and the open sea. *Eos, Transaction, American Physical Union* 83(20).

Gačić, M., I.M. Mosquera, V. Kovačević, A. Mazzoldi, V. Cardin, and F. Gelsi,

2004. Temporal variation of water flow between the Venetian lagoon and the open sea. *Journal of Marine Systems* 51.

Kovačević, V., V. Defendi, F. Arena, M. Gačić, I.M. Mosquera, L. Zaggia, S. Donà, F. Costa, F. Simionato, A. Mazzoldi. Water and Solid Transport Estimates through the Venetian Lagoon Inlets using Acoustic Doppler Current Profilers. Present Issue.

Mosquera I.M., M. Gačić, V. Kovačević, A. Mazzoldi, S. Cosoli, J.D. Paduan, S. Yari. Surface Current Patterns in front of the Venetian Lagoon and their variability at different wind regimes. Present Issue.

Kovačević, V., M. Gačić, I.M. Mosquera, A. Mazzoldi, and S. Marinetti, 2004. HF radar observation in the northern Adriatic: surface current field in front of the Venetian Lagoon. *Journal of Marine Systems* 51(1-4),95-122.

Luyten, P. J., Deleersnijder, E., Ozer J. and Ruddick, K. G., 1996. Presentation of a family of turbulence closure models for stratified shallow water flows and preliminary application to the Rhine outflow region. *Continental Shelf Research*, Vol. 16, 1, 101-130.

Umgiesser, G. and A. Bergamasco, 1995. Outline of a primitive equation finite element model. In *Rapporto e Studi*, Volume XII, pp.291-320. Venice, Italy: Istituto Veneto di Scienze, Lettere ed Arti.

Umgiesser, G. and A. Bergamasco, 1998. The spreading of the Po plume and the Italian coastal current. In *Physics of Estuaries and Coastal Seas*, pp.267-275. Rotterdam: Dronkers and Scheffers (eds).

Umgiesser, G., D. Melaku-Canu, A. Cucco, and C. Solidoro, 2004. A finite element model for the Venice Lagoon. Development, set-up, calibration and validation. *Journal of Marine Systems* 51, 123-145.

Wells, M.G. and G.-J.F.V. Heijst, 2003. A model of tidal flushing on an estuary by dipole formation. *Dynamics of Atmospheres and Oceans* 37, 223-244.

SEDIMENT TRANSPORT SIMULATION COMPARED WITH ADCP DATA IN LIDO INLET

Francesca De Pascalis, Christian Ferrarin, Valentina Defendi, Georg Umgiesser,
Luca Zaggia

CNR-ISMAR Venezia Castello 1364/A 30122 Venezia

Riassunto

Scopo di questo lavoro è stato quello di effettuare un confronto preliminare tra i dati di concentrazione dei solidi sospesi e velocità di corrente, raccolti nella bocca di Lido mediante correntometro acustico (ADCP), e i risultati ottenuti da simulazioni numeriche. Sono stati calcolati sia il trasporto in sospensione che quello al fondo confrontandoli con la media delle misure sulla colonna d'acqua, tuttavia i risultati preliminari mostrano la necessità di approfondire lo studio dello strato al fondo dove il correntometro non è in grado di acquisire misure.

Abstract

The aim of this work was to carry out a preliminary comparison between ADCP data (current and suspended solids concentrations), measured at Lido inlet, and numerical simulation results. Suspended load and bed load have been computed by models and compared with the average of ADCP measurements in the water column. The obtained results show that there is a need to acquire knowledge about the bottom layer where the instrument can not measure the relevant parameters.

1 Introduction

Sediment exchange in coastal zones becomes, over the last few years, an important theme for several branches of environmental sciences. Coastline evolution is influenced by these processes that become important especially in transition areas like the Venice Lagoon. The Venice Lagoon is connected to the Adriatic Sea by three inlets; for this project the Lido inlet has been chosen where the sediment exchange between the lagoon and the Adriatic Sea has been investigated.

The preliminary objective of this study was to compare current velocity and suspended solids concentration data, measured by ADCP, with the results from a model simulation.

2 Methods

The sediment transport analysis in the Lido inlet has been made using the 2D SHYFEM hydrodynamic model SHYFEM (Umgiesser et al., 2004, 2006), coupled with sediment transport model SEDTRANS96 (Li and Amos, 1997, 2001; Umgiesser et al. 2006) applied in 0D. Subsequently the results of the

simulations have been compared with ADCP data of the year 2006, collected by CNR-ISMAR and OGS (Kovačević et al. 2005; Kovačević et al. 2007, Zaggia et al. 2004; Zaggia et al. 2005;).

2.1 Hydrodynamic model

The hydrodynamic data used in the simulations with the sediment transport model have been derived from the numerical model SHYFEM, developed at ISMAR-CNR of Venice. SHYFEM is a finite element program that can be used to resolve the hydrodynamic equations in shallow water. The program uses finite elements for the spatial resolution of the equations and an effective semi-implicit time resolution algorithm, which makes this program especially suitable for the application to complicate geometry and bathymetry.

The subdivision of the system in triangles, varying in form and size, allows the simulation of shallow water flats, tidal marches that in tidal cycle may be covered with water during high tide and then fall dry during ebb tide.

The equations used in the model are the well known vertically integrated shallow water equations in their formulation with water levels and transports:

$$\frac{\partial U}{\partial t} - fV + gH \frac{\partial \zeta}{\partial x} + RU + X = 0 \quad (1)$$

$$\frac{\partial V}{\partial t} + fU + gH \frac{\partial \zeta}{\partial y} + RV + Y = 0 \quad (2)$$

$$\frac{\partial \zeta}{\partial t} + \frac{\partial U}{\partial x} + \frac{\partial V}{\partial y} = 0 \quad (3)$$

where ζ is the water level, u , v the velocities in x and y directions, U , V the vertical integrated velocities

$$U = \int_{-h}^{\zeta} u dz \quad V = \int_{-h}^{\zeta} v dz \quad (4)$$

g the gravitational acceleration, $H = h + \zeta$ the total water depth, h the undisturbed water depth, t the time and R the friction coefficient. The terms X , Y contain all other terms that may be treated explicitly by the semi-implicit algorithm like the wind stress or the non-linear terms. (Umgiesser et al., 2004).

The grid of the Venice lagoon model is constructed by a subdivision of the area into nodes and triangular elements to describe the lagoon's geometry and bathymetry. Thanks to the flexible size of the elements it is possible to have a higher spatial resolution for the three inlets and the small canals.

2.2 Sediment transport model

The processes of sediment erosion, transport and deposition essentially occurs in the bottom boundary layer which forms the interface between the seabed and the water column. These processes greatly affect seabed stability, the dispersal

of particulate material and benthic communities. SEDTRANS96 is a 0-dimensional computer model that can be used to predict the transport rate and direction of sand or mud under either steady currents or combined waves and currents outside the breaking zone. SEDTRANS96 adopts the Grant and Madsen (1986) continental shelf bottom boundary layer theory to predict bed shear stresses and the velocity profile in the bottom boundary layer. The model uses the algorithms of Einstein-Brown (Brown, 1950) and Yalin (1963) for bed load prediction. The methods of Engelund and Hansen (1967) and Bagnold (1963) are used to determine total load transport (bedload plus suspended load). At the present, SEDTRANS96 uses the median grain size of bottom sediment in its calculations and does not deal with the effect of grain size distribution. The prediction of cohesive sediment transport adopts a new algorithm proposed by Li and Amos (2001).

3 Model application

The finite element numerical grid (Fig. 1) has been created including the Adriatic Sea area, in front of three inlets of the Venice Lagoon. The grid consists of 15188 nodes and 28584 elements.

The hydrodynamic model computes the current velocities and water levels in all grid nodes. This information has been extracted for one node and used as input for sediment transport model.

The node chosen to apply the sediment transport model corresponds to the fixed ADCP position (Fig. 2). In this way the values of current velocities and solid transport simulated can be compared with ADCP measurements.

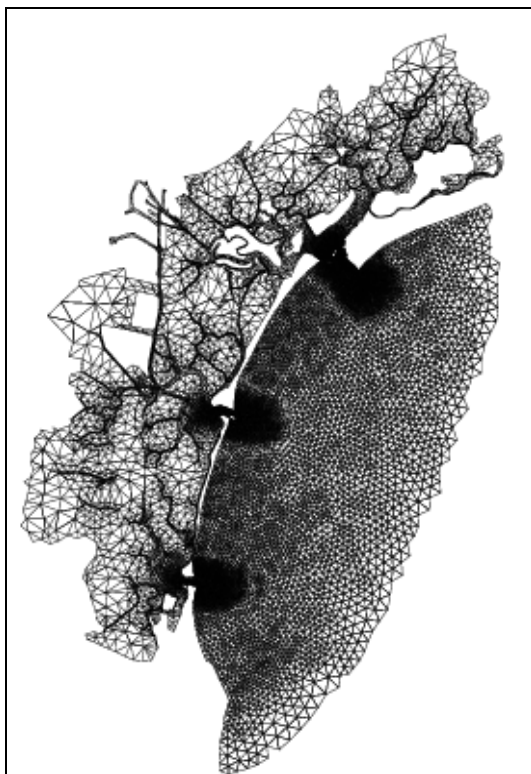


Fig 1 – Numerical grid of Venice Lagoon.



Fig 2 – ADCP position.

The hydrodynamic model has been forced with real boundary conditions of February 2006 to simulate the water behaviour at Lido inlet. The simulation has been carried out using wind and water level data obtained from the CNR platform (Fig. 3, Fig. 4).

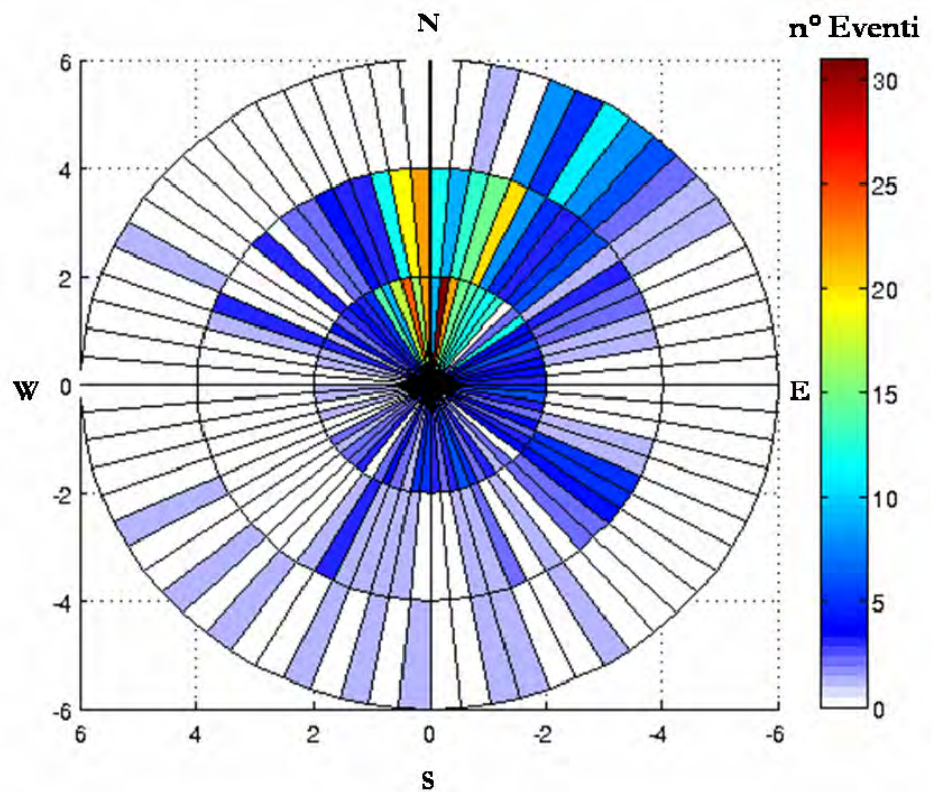


Fig 3 – Wind plot of February 2006. The XY axes represent the velocity scale in m/s.

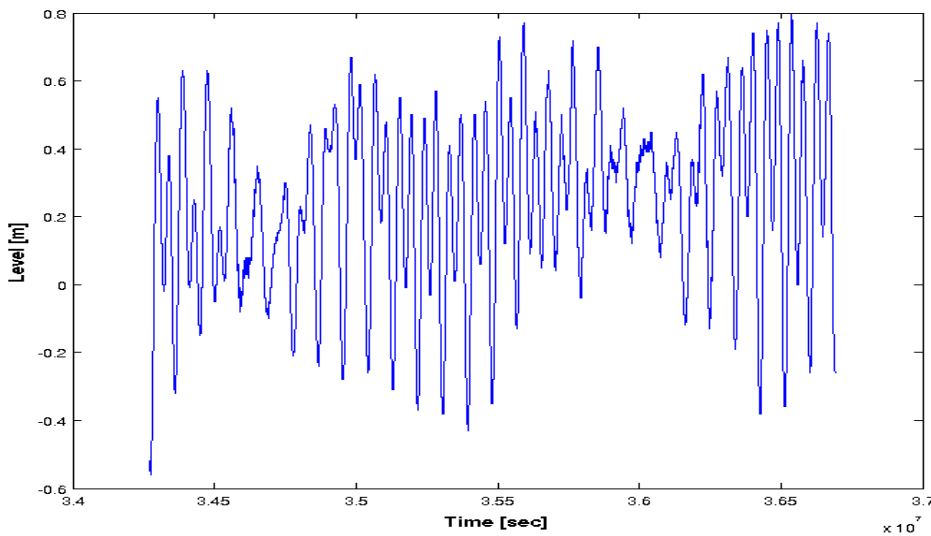


Fig 4 – Hour sea level at CNR platform. February 2006.

4 Results

The first comparison has been made between the current velocity measured by ADCP and the simulated one (Fig. 5). Since Shyferm has been used as 2D model, ADCP data have been averaged in the water column in order to allow a comparison.

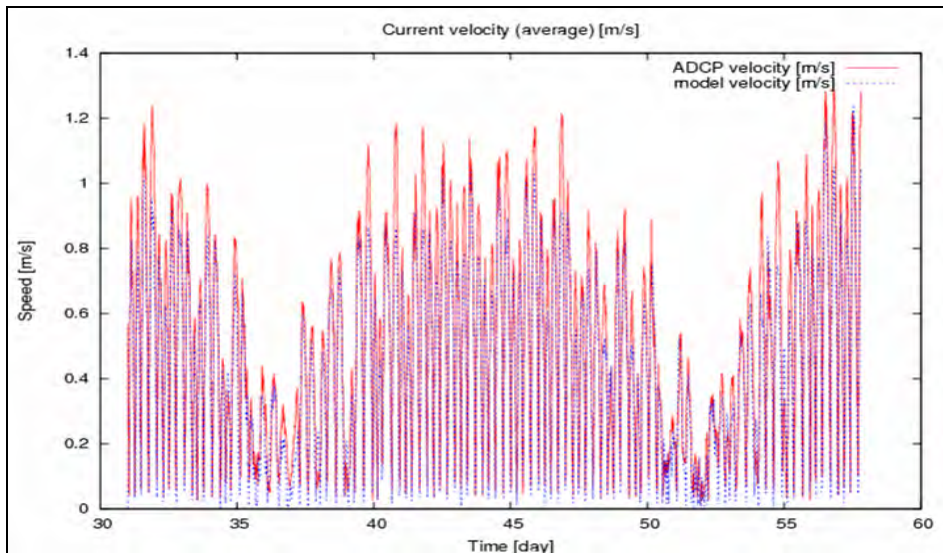


Fig 5 – Comparison between simulated current velocity and average velocity from ADCP.

The agreement between observed and modelled data is, in general, satisfactory. The model underestimate measured peak values but there is a good agreement in phase.

Hydrodynamic velocities simulated by SHYFEM have been used as input for SEDTRANS96. The grainsize considered in this simulation was 150 μm and the following formulations of transport have been used: Rouse's formula for suspended load (Rouse, 1937; Glenn and Grant, 1987) and Einstein-Brown's formula for bed load (Brown, 1950).

The results provided by SEDTRANS96 deal with a potential sediment transport. The model computes the quantity of resuspended sediment supposing an unlimited thickness of sediments trough out the bottom. Again, for the comparison the ADCP transport has been averaged in water column.

In Figure 6 the comparison between ADCP suspended sediment transport and transport computed by model is shown.

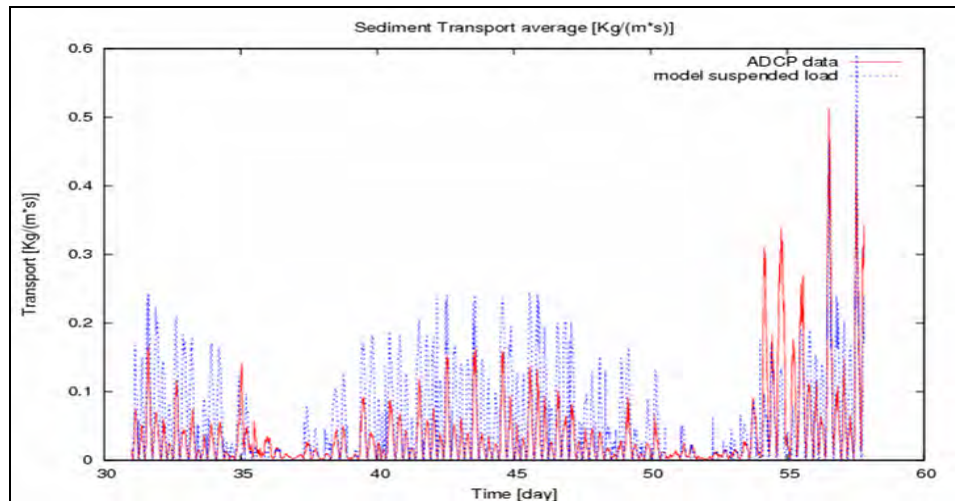


Fig 6 – Comparison between suspended load from the model and average transport from ADCP.

Observing the figure, measurements seem to be generally lower than values obtained from the model. This behaviour is probably due to the ADCP instrument that is unable to measure suspended solids concentration near the bottom. In order to estimate the bed load another run of the sediment transport model has been carried out, using Brown's formula.

Figure 7 shows ADCP data of suspended load with bed load values obtained from the model. Even if the type of data is different they have been plotted together to compare their order of magnitude. In this case simulated bed load transport is lower than the measurements. Bedload is one of the missing parts of the total load that has to be investigated further because the instrument does not measure parameters in the last three meters close to the bottom. Therefore, there is a need to measure the real bedload transport through different methods and to acquire more information about grainsize profiles of sediments in the water column.

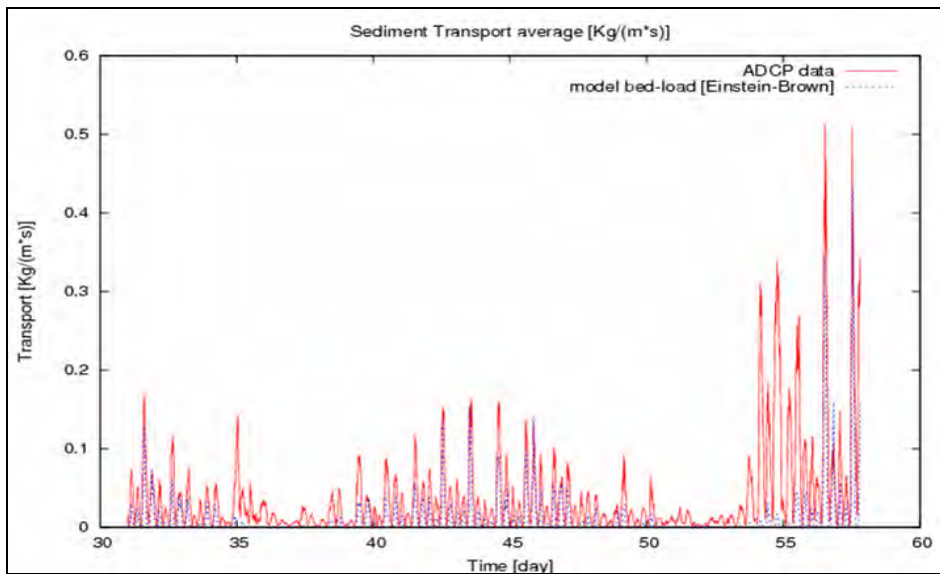


Fig 7 – Comparison between bed load from the model and average transport from ADCP.

Conclusions

The objective of this work was a preliminary study about sediment transport trough Lido inlet, using ADCP current and suspended solid concentration measurements for year 2006 and model results.

A simulation has been carried out for February 2006 using two different formulas for suspended and bed load. The results of simulation compared with ADCP data show, in general, a good agreement but also some differences in the velocity current and sediment transport.

These differences are in part due to the ADCP measuring method that underestimates suspended solid concentration because it is unable to see the last meters from the bottom.

The next step will be to extract the concentration data corresponding to the bottom layer from turbidity profiles. In this way we will able to compare the real transport at the bottom with bedload predicted by the numerical model. Moreover, a 3D hydrodynamic model should be used in order to better describe the velocity profile in the water column.

Acknowledgements

The authors would like to thanks OGS research team, particularly Vedrana Kovačević, Franco Arena, and Isaac Mancero-Mosquera who handled and provided time series of current velocity and backscatter for the bottom-deployed acoustic Doppler current profilers in the Venice lagoon inlets. This work has been partially funded under the Corila project 3.15 *Trasporto solido e circolazione superficiale alle bocche di porto e nella zona costiera*.

References

- Bagnold, R.A., 1963. Mechanics of marine sedimentation. In: Hill, M.N. (Ed.), *The Sea*, 3. Wiley-Interscience, New York, 507-527.
- Brown, C.B., 1950. Sediment transportation: in Rouse, H. (ed), *Engineering Hydraulics*, Publ. Wiley, New York: 769-857.
- Engelund, F., Hansen, E., 1967. A monograph on sediment transport in alluvial streams. Teknisk Forlag, Copenhagen Denmark, 62p.
- Glenn, S.M. and W.D. Grant, 1987. A suspended sediment stratification correction for combined wave and current flows. *Journal of Geophysical Research*, 92, 8244-8264.
- Grant, W.D., Madsen, O.S., 1986. The continental shelf bottom boundary layer. *Annual Review of fluid Mechanics* 18, 265-305.
- Kovačević V., Defendi V., Arena F., Gačić M., Mancero Mosquera I., Zaggia L., Donà S., Costa F., Simionato F., Mazzoldi A., 2007. Water and solid transport estimates through the Venetian lagoon inlets using acoustic Doppler current profilers. In: Campostrini, P. (Ed.), *Scientific Research and Safeguarding of Venice, CORILA Research Program 2004-2006, 2007 Results*. Istituto Veneto di Scienze, Lettere ed Arti, Venezia, 315-331.
- Kovačević, V., Defendi, V., Zaggia, L., Costa, F., Arena, F., Simionato, F., Mazzoldi, A., Gačić, M. and C. Amos, 2007. Time series of suspended particle concentration from the conversion of acoustic backscatter at the Lido inlet. In: Campostrini, P. (Ed.), *Scientific Research and Safeguarding of Venice, CORILA Research Program 2004-2006, 2005 Results*. Istituto Veneto di Scienze, Lettere ed Arti, Venezia, 315-329.
- Li, M.Z. and C.L. Amos, 1997. SEDTRANS96: Upgrade and calibration of the GSC sediment transport model. Geological Survey of Canada, Atlantic Open File Report 3512, 140p.
- Li, M.Z. and C.L. Amos, 2001. Sedtrans96: the upgraded and better calibrated sediment transport model for continental shelves. *Computers & Geosciences*, 27, 619-645.
- Rouse, H., 1937. Modern conceptions of the mechanics of turbulence. *Transactions of the American Society of Civil Engineers*, 102, 436-543.
- Umgiesser, G., De Pascalis, F., Ferrarin, C. and C.L. Amos, 2006. A model of sand transport in Treporti channel: northern Venice lagoon. *Ocean Dynamics*, 56, 339-351.
- Umgiesser, G., Melaku Canu, D., Cucco, A. and C. Solidoro, 2004. A finite element model for the Venice Lagoon. Development, set up, calibration and validation. *Journal of Marine Systems*, 51, 123-145.
- Yalin, M.S., 1963. An expression for bedload transportation. *Journal of Hydraulics Division, Proceedings ASCE* 89 (HY3), 221-250.

Zaggia, L. and M. Ferla, 2005. Studies on Water and Suspended Sediment Transport at the Venice Lagoon Inlets. In: *Ocean Waves Measurement and Analysis. Proceedings of the Fifth International Symposium WAVES 2005*, Madrid, Spain, 3 – 7 July 2005, Paper n. 96, 1-10.

Zaggia, L., Mazzoldi, A., Gačić, M. and F. Costa, 2004. The measurements of water exchanges at the Venice Lagoon inlets. Proceedings of the 37th CIESM Congress, Barcelona, Spain, 7-11 June 2004, p. 153.

RESEARCH LINE 3.16

**Characteristics of the lagoon underground
layer**

THE SUBSOIL ARCHITECTURE OF THE LAGOON AND GULF OF VENICE (ITALY) BY VERY HIGH RESOLUTION SEISMIC SURVEYS IN SHALLOWS

Giuliano Brancolini¹, Luigi Tosi², Luca Baradello¹, Federica Donda¹, Massimo Zecchin¹

¹*Dipartimento di Geofisica della Litosfera - Istituto Nazionale di Oceanografia e di Geofisica Sperimentale – OGS, Borgo Grotta Gigante 42/c, 34010 Sgonico (TS)*

²*Istituto di Scienze Marine – Consiglio Nazionale delle Ricerche, Castello 1364/A, 30122 Venezia*

Riassunto

Il Progetto “Applicazione di metodologie sismiche innovative ad altissima risoluzione sui bassi fondali per lo studio del sottosuolo lagunare veneziano” può ritenersi uno studio geologico senza precedenti che ha consentito la caratterizzazione ad altissima risoluzione dell’architettura dei depositi tardo pleistocenici ed olocenici relativi ai bassifondi della laguna e dell’antistante area marina di Venezia.

I principali risultati del progetto sono stati l’implementazione un sistema di prospezione sismica ad altissima risoluzione, adatto per rilievi sismici in fondali con profondità anche inferiori a 1 m d’acqua, l’esecuzione di una serie di misure in aree mai indagate in passato e la realizzazione del un modello sismo-stratigrafico del sottosuolo lagunare e costiero veneziano.

Il nuovo sistema di acquisizione sismica ha consentito di ottenere ottimi informazioni del sottosuolo fino a profondità di 30-40 metri e quindi di ottenere informazioni significative e di estremo dettaglio sull’evoluzione geologica tardo-pleistocenica ed olocenica di tre settori: la laguna meridionale, le bocche di porto di Lido e Chioggia, ed il settore settentrionale del Golfo di Venezia.

Abstract

The Project “Application of innovative of very high resolution seismic methodologies in shallow waters aimed at the study of the subsoil of the Venice Lagoon” allowed the characterization of the Late Pleistocene and Holocene depositional sequences with a detail, that has never been reached in the past.

A boat, particularly suitable for very high resolution seismic survey in shallow water (less than 1 m deep) has been fully equipped and tested. It allowed to carried out surveys of specific areas of the Lagoon that have never been investigated in the past. Moreover a seismo-stratigraphic model of the lagoon and gulf of Venice subsoil has been performed. The seismic acquisition system allowed to investigate the subsoil down to 30-40 m deep.

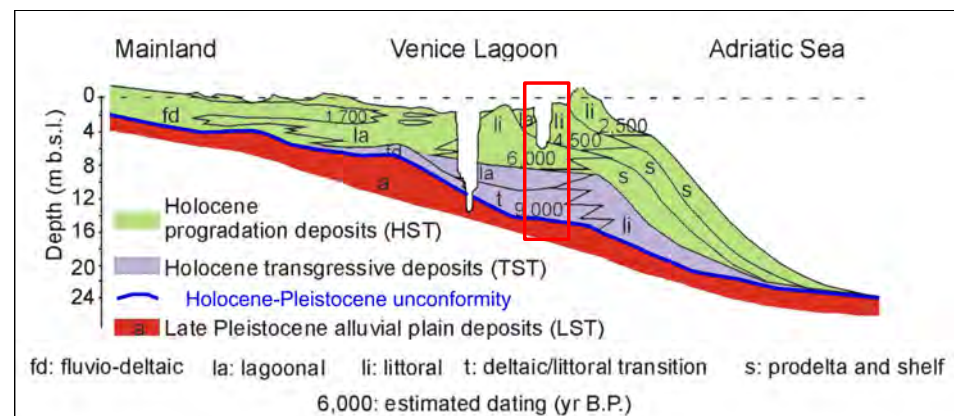
The new data provided significant geological features related to the Late Pleistocene and Holocene evolution of the investigated areas: the southern lagoon, the Lido and Chioggia inlets and part of the shelf of the Gulf of Venice.

1 Introduction

Most of the information on the Venetian subsoil come from the study of cores taken in the lagoon outer part, in the channels, in the islands, along the littoral strips or in other sites where sediments are not completely representative of the Holocene sedimentation. In particular, the upper layers do not represent the “true” stratigraphic succession because of the occurrence of bottom erosion, the dredging activity, the sediment rework and others effects, reflecting human activities. In addition, the cores provide information of a very restricted area. Recently, seismic surveys were carried out along the lagoon channels [Tosi *et al.*, 2007a,b] that normally are 4-6 m deep. However, considering that most of the Venice Lagoon consists of very shallow water, 0,5-1 m deep, the obtained data lack many information (Fig. 1). We can consider the subsoil below the lagoon’s very shallow water a window on the recentmost evolution of the lagoon environment because in a number of cases it preserves the whole Holocene history.

For this reason the CORILA Research Programme 2004-2006 activated the Research Line 3.16, aimed at the acquisition of very high resolution data also in very shallow water by using the seismic methods.

Fig 1 – Geological section crossing the lagoon and showing that along the major and minor channels the information on the sedimentation of the recent layers are missing.



Considering that data from very high resolution single channel seismics acquired in the Venice lagoon are generally poor of informations due to the poor signal to noise ratio and to the presence of strong seafloor multiples (Fig. 2), the research line 3.16 had to experiment different set of hydrophones, streamers and sources and to test various acquisition geometries.

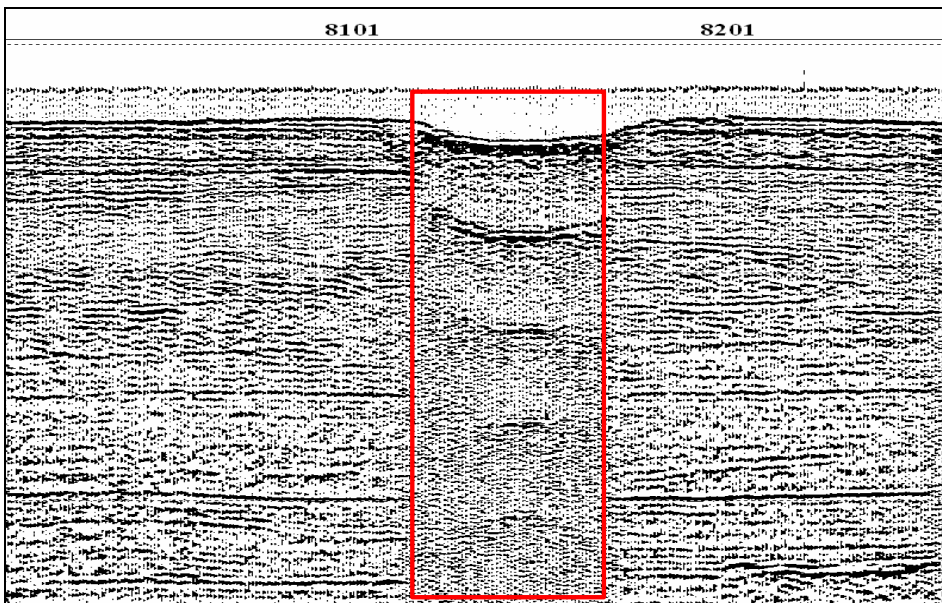


Fig 2 – Example of data acquired crossing a channel. In the red rectangle a series of multiples mask the information from lower layers while outside the channel axis, the seismic section shows very fine data.

2 Seismic data acquisition and processing

2.1 Development of the seismic acquisition system

One of the main target of the project was the implementation of a tool, consisting in a boat and a seismic acquisition system, able to operate in very shallow (up to 50 cm) water.

The acquisition of the boat (Fig. 3), qualified for shallow water sealing, was made on the basis of an accurate market survey. The evaluation has been made based on the draught, the turbulence and the facilities for the installation of the seismic gears. Afterwards, different types of seismic sources have been considered. Based on the bandwidth, the repeatability of the signature and the portability of the hardware, a boomer system has been acquired and adapted to operate in water depth less than 1m (Fig. 4).

The seismic acquisition system was optimized for shallow water depth (less than 1 m) and consists of :

- an impulsive energy source (boomer) that utilize an electro-dynamic plate UWAK05 (Nautiknord). The boomer produce a wavelet with an amplitude spectrum between 200 and 9,000 Hz (Fig. 5)
- a two channel 24 bit seismic recorder of Triton Imaging Inc. that utilize the software SB-logger
- differential GPS integrated with the acquisition system

The entire system has been tested in a tank before the installation on the new boat.

The signature of the source has been measured during a field test and shows an amplitude spectra almost flat between 200 and 9.000 Hz (Fig. 6).

*Fig 3 – The new boat
“Aretusa” that has been
implemented for shallows
acquisition.*



*Fig 4 – The boomer with the
floating supports.*



Fig 5 – The boomer plate.



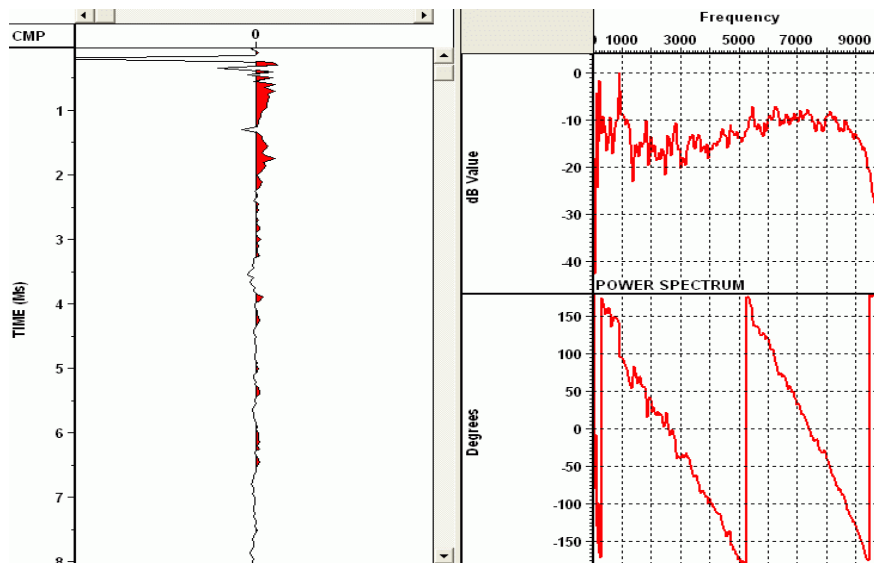


Fig 6 – The field signature of the boomer.

The hydrophone configuration has been chosen after various field tests on single hydrophones and on arrays. The single hydrophone guarantees the best resolution, but is characterized by a very low signal/noise ratio. The array improves the S/N ratio but, particularly for shallow targets, it reduces the resolution of the signals because the different travel times along the array, produce a phase shift in the incoming signals (Fig. 7). As a rule of thumb, the length of the array (L) should be expressed by the formula below:

$$L \ll \sqrt{X^2 + 2r\lambda} - X$$

Where: X is the near offset, L is the array length, r is the travel time for the near offset hydrophone and λ the wavelength of the signal.

The array we have chosen was made by 8 in-line hydrophones for a total length of 270 cm. In order to reduce the filtering effect of the array, we adopted an acquisition geometry with the array steaming parallel to the source (Fig. 8). This geometry minimizes the differences in the travel times along the array and therefore reduce the shifts between the incoming signals.

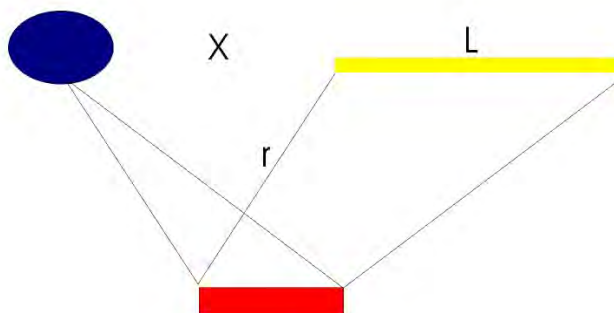


Fig 7 – Geometry for seismic acquisition with source and receiver in line.

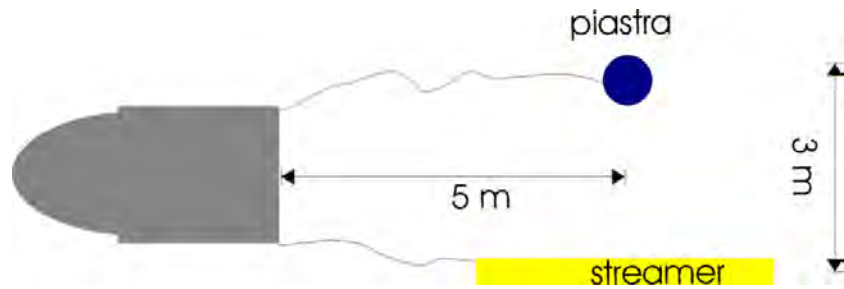


Fig 8 – The adopted geometry.

2.2 The surveys

The field surveys in very shallow water are located inside the lagoon, and have been carried out with the new CORILA boat “ARETUSA”, while the field surveys along the rivers, the shelf areas and the inlets, with the ISMAR-CNR boat “LITUS”. The seismic data have been recorded in SEG-Y format and GPS coordinates have been stored in the header of each single trace.

The different survey areas (Fig. 9) represent key regions for the understanding and morphological setting and the evolution of the lagoon and have been chosen also considering the previous surveys performed in the framework of the CARG project.

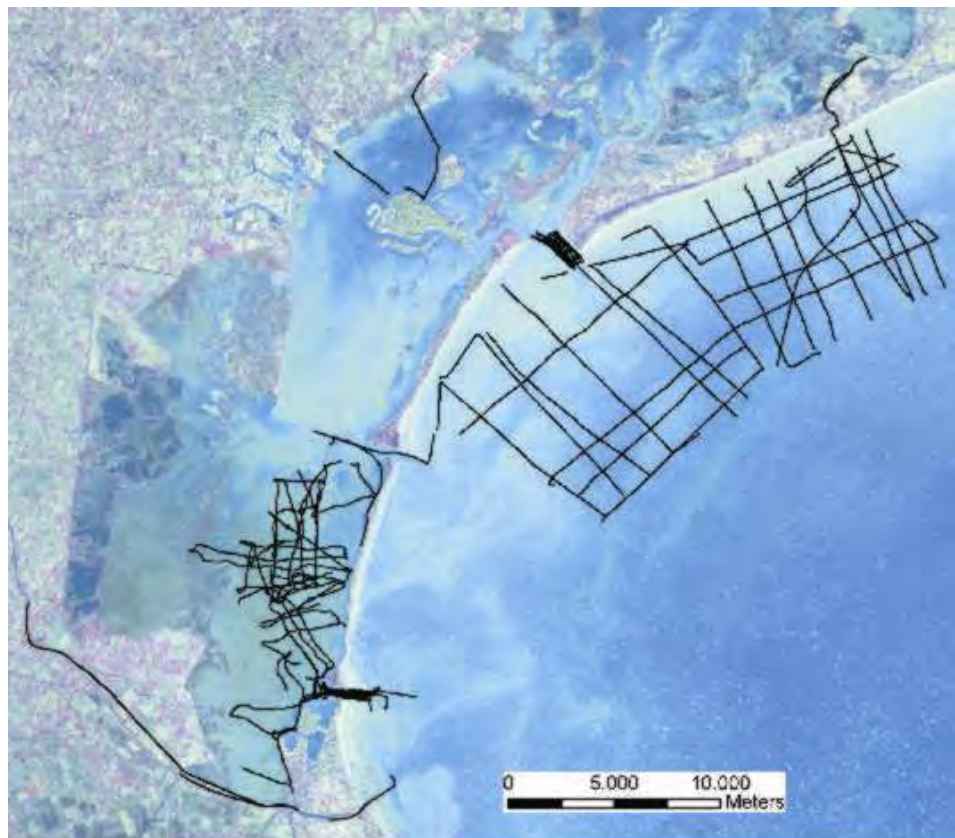


Fig 9 – Position map of the high resolution seismic survey recorded in the framework of the research line 3.16.

Area 1: Lido and Chioggia inlets. In this area, two high density surveys have been carried out (Fig. 10), that produced a 3D reconstruction of the inlet subsoil. The two areas are characterized by a strong hydraulic regime produced by the tide flows. The Lido inlet is particularly important because in that area the first

installation of the infrastructures related to the MOSE project will be performed.

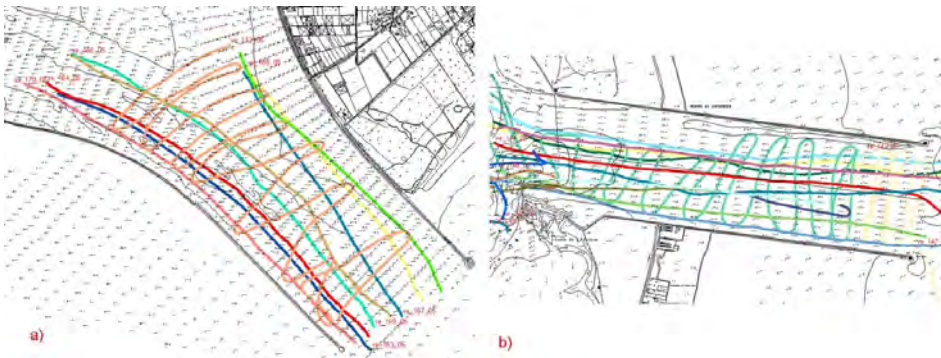


Fig 10 – Position of the seismic lines in the Lido (a) and Chioggia (b) inlets.

Area 2: The shelf area off the Lido inlet. It includes the ebb tidal delta and the Sile delta. In Fig. 11 illustrate a seismic profile from the ebb tidal delta.

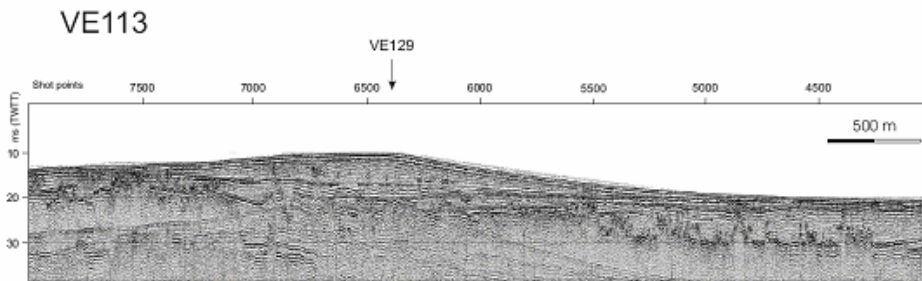


Fig 11 – Seismic profile Ve 113 across the ebb tidal delta of the Lido inlet.

Area 3: The lagoon. The seismic surveys have been mainly carried out in the southern portion of the lagoon, where the Holocene sediments are much thicker than in the other sectors. For the first time, the very shallow water area (less than 1m) of the mud flats have been surveyed. Fig. 12 is an example of a seismic section from the southern lagoon, where the seismic horizons are clearly identifiable up to 18 m depth.

Area 4: The Brenta and Sile rivers. Two lines have been recorded along these rivers. They allow a straightforward connection between the lagoon area and the mainland. Fig. 13 from Brenta river shows the presence of a paleo-channel up to 15 m depth.

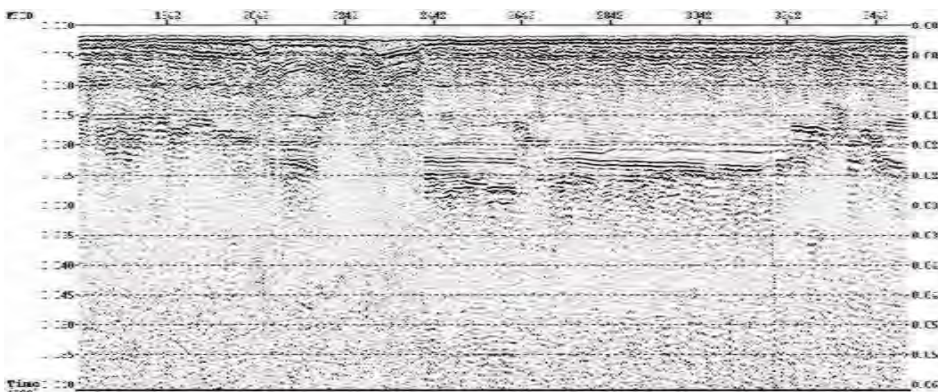
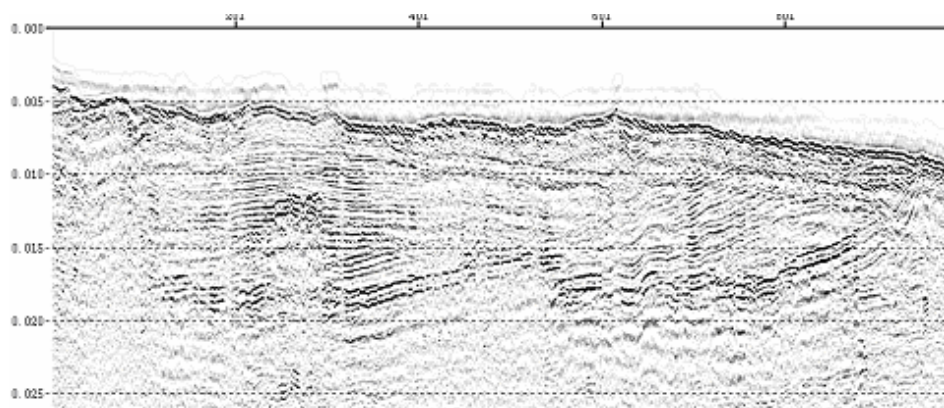


Fig 12 – Example of seismic section from very shallow water.

Fig 13 – Example of seismic line from the Brenta river.



3 Seismic processing

Seismic data have been recorded in SEG-Y format and processed by FOCUS and RADEX.

The processing sequence is illustrated in Fig. 14; the main steps consisted in:

Gain recovery: The energy and therefore the amplitude of the seismic signal, decay with the distance from the source. The main reasons are:

- spherical divergence, that depends on the square of the travel time;
- internal friction that may be considered linear with time.

The correction for the amplitude decay (C) applied to the data, in function of the time (t) was:

$$C = t + 20 \text{Log}_{10} t$$

After the amplitude recovery, seismic data have been filtered to eliminate the low frequency noise (normally below 200 Hz). Based on the filter tests, an Ormsby filter 300-7.000 Hz has been applied. Then the data have been equalized by a balance window of 10 ms. Fig. 15a illustrates a portion of section VE-255 without any processing, while in Fig. 15b the same section has been compensated for amplitude decay, filtered and equalized.

Wave motion correction: some seismic sections, particularly in the offshore area, are affected by strong wave motion that produce a worsening in the data quality. To eliminate this effect we adapted a techniques very similar to the one normally applied for compensate on land seismic for residual statics. This technique is based on the cross-correlation, inside a designed window, of each seismic trace with a pilot trace obtained from the data itself. When the procedure works correctly the shift of the cross correlation corresponds to the shift induced by the waves.

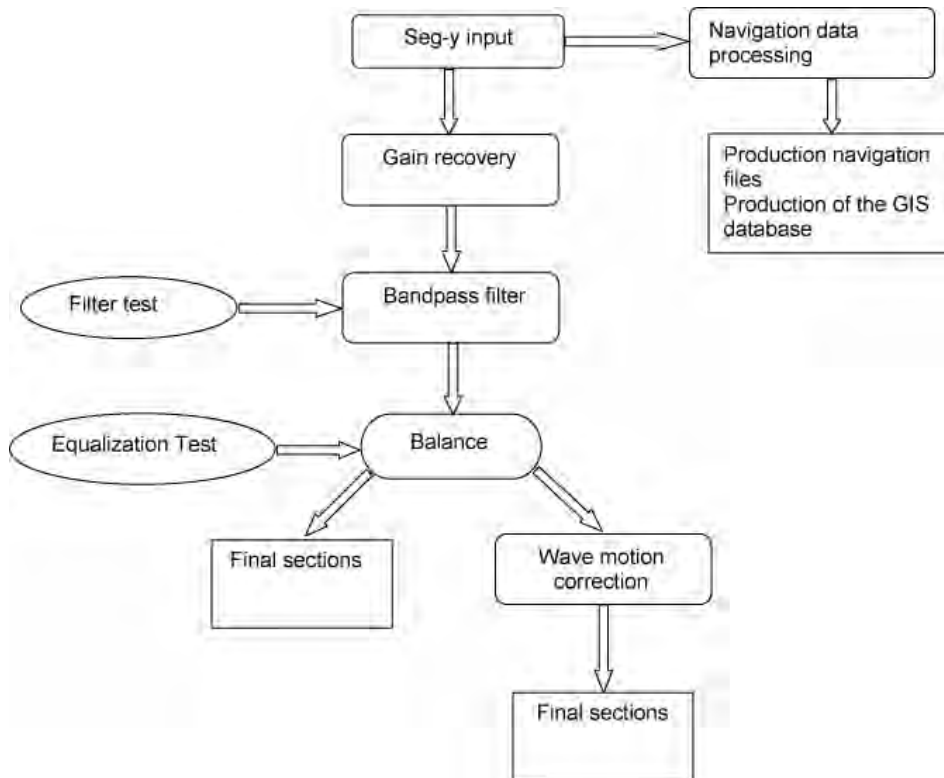


Fig 14 – Processing sequence.

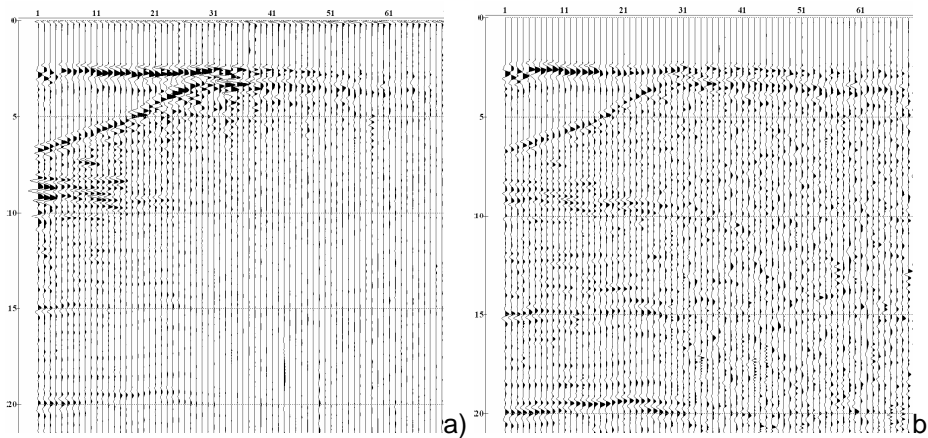
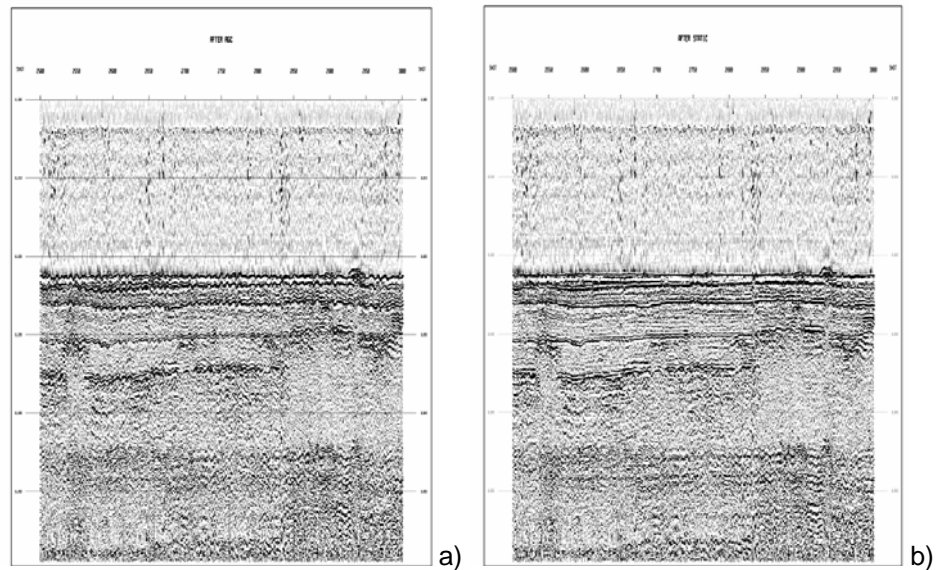


Fig 15 – a) Line VE-255 raw data; b) Line Ve-255, gain recovery, filter and balance.

In our case the pilot trace was obtained by the weighted (50-100-50) stack of three adjacent traces, the length of the designed window was 12 ms and included the sea bottom. In Fig. 16a and Fig. 16b an example of seismic section affected by wave motion and the same section corrected according to the above mentioned procedure.

Fig 16 – a) Seismic section from the shelf area affected by wave motion, b) corrected for the wave motion.

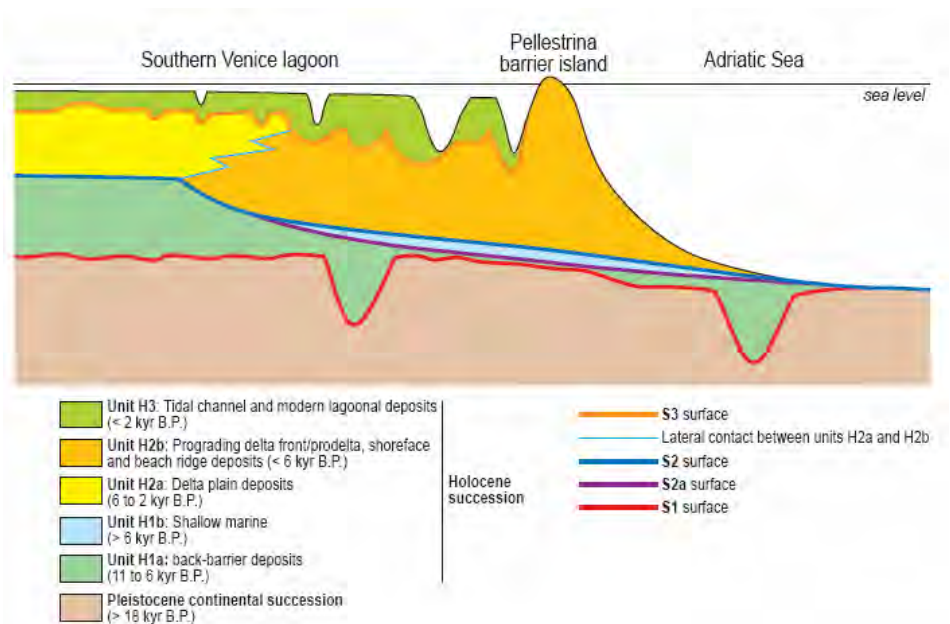


4 Results

4.1 Seismic units and surfaces

Three main seismic units (H1-H3) and key stratal surfaces (S1-S3) are recognizable in the Holocene succession of the Venice area (Fig. 17).

Fig 17 – Simplified architectural scheme of the Holocene deposits in the southern Venice lagoon. Seismic units and key stratal surfaces are shown. Unit H1 (composed of sub-units H1a and H1b) represents the transgressive part of the succession, whereas Unit H2 (composed of sub-units H2a and H2b) is the regressive one (see text). Unit H3 represents a recent human-induced transgression that followed delta abandonment.



4.1.1 Surfaces

4.1.1.1 S1

The S1 surface represents a major unconformity separating the late Pleistocene continental succession from the back-barrier to shallow marine Holocene deposits (Figs. 17-27). This surface is an evident and locally irregular reflector in VHR seismic profiles, and may correspond to V-shaped incisions up to 1 km

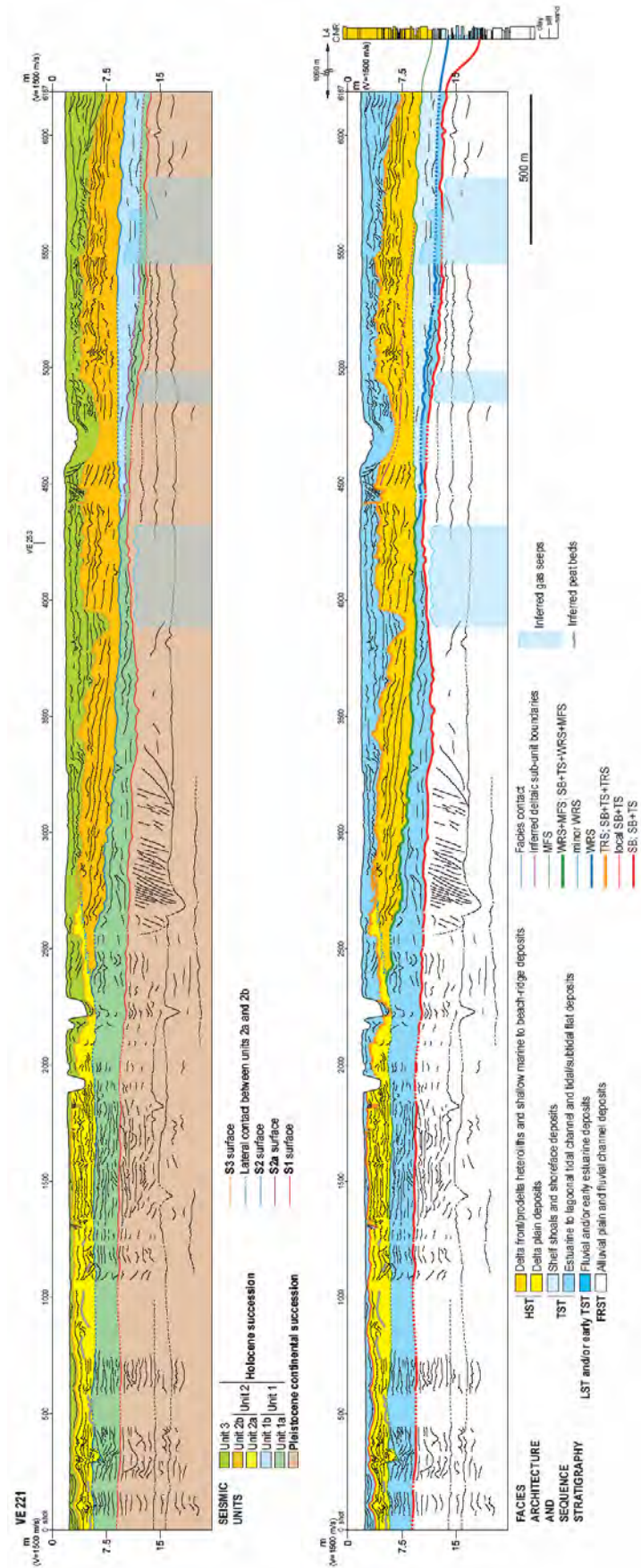
wide and 10 m of relief (Figs. 19, 21, 22 and 27). In the flat areas located between erosional incisions, the S1 surface is more regular and shows a very gently dip (from 0.01 to 0.05 degrees) seaward (Fig. 18). Several core data evidence that away from deep incisions the S1 surface is locally marked by a paleosoil, consisting of an overconsolidated silty-clayey layer (a few centimeters to 2 m thick) known as Caranto [Matteotti, 1962; Gatto and Previatello, 1974; Gatto, 1980, 1984; Tosi, 1994a,b; Bonardi and Tosi, 1994, 1995, 1997; Bonardi *et al.*, 1997; Brambati *et al.*, 2003; Tosi *et al.*, 2007a,b]. Core data demonstrate that the S1 surface is associated with a stratigraphic gap ranging from 7 to 13 kyr [Tosi, 1994a; Tosi *et al.*, 2007a,b].

The S1 surface tends to crop out landward and offshore, where Holocene deposits are thin and are easily eroded by wave action (Fig. 20).

The model at regional scale of the S1 morphology and a detail map of its depth at the Lido inlet are reported in Fig. 28 and Fig. 29 respectively.

This asymmetry of the depth of the S1 surface (Pleistocene-Holocene boundary) and consequently of the Holocene sedimentation thickness (Fig. 30), is related to the erosion-deposition processes occurring at the inlet. The depth of Pleistocene-Holocene boundary around the northern sector of the Lido littoral and the Punta Sabbioni Area generally varies from 10 to 8 m. The outcropping of Pleistocene sediments is due to a presence of an ancient channel, which was active in the early Holocene, most likely also in the upper Pleistocene, combined to the recent erosion process. The higher thickness of the Holocene sediments, founded in the northern side of the inlets, is the evidence that deposition of sediments transported by tides and longshore circulation is active only in this sector.

Fig 18 – Seismic units and surfaces (above), facies architecture, and sequence stratigraphic interpretation (below) of the VE 221 seismic line. L4 CNR log (redrawn from Tosi et al. [2007b]) is located in correspondence of the modern barrier island. The VE 221 seismic line represents a dip section showing facies relationships from landward (on the left) to seaward locations in an area placed away from valleys incised in correspondence of the Pleistocene-Holocene boundary (the S1 surface, see text). FRST = forced regressive systems tract; HST = highstand systems tract; LST = lowstand systems tract; MFS = maximum flooding surface; SB = sequence boundary; TRS = tidal ravinement surface; TS = transgressive surface; TST = transgressive systems tract; WRS = wave ravinement surface.



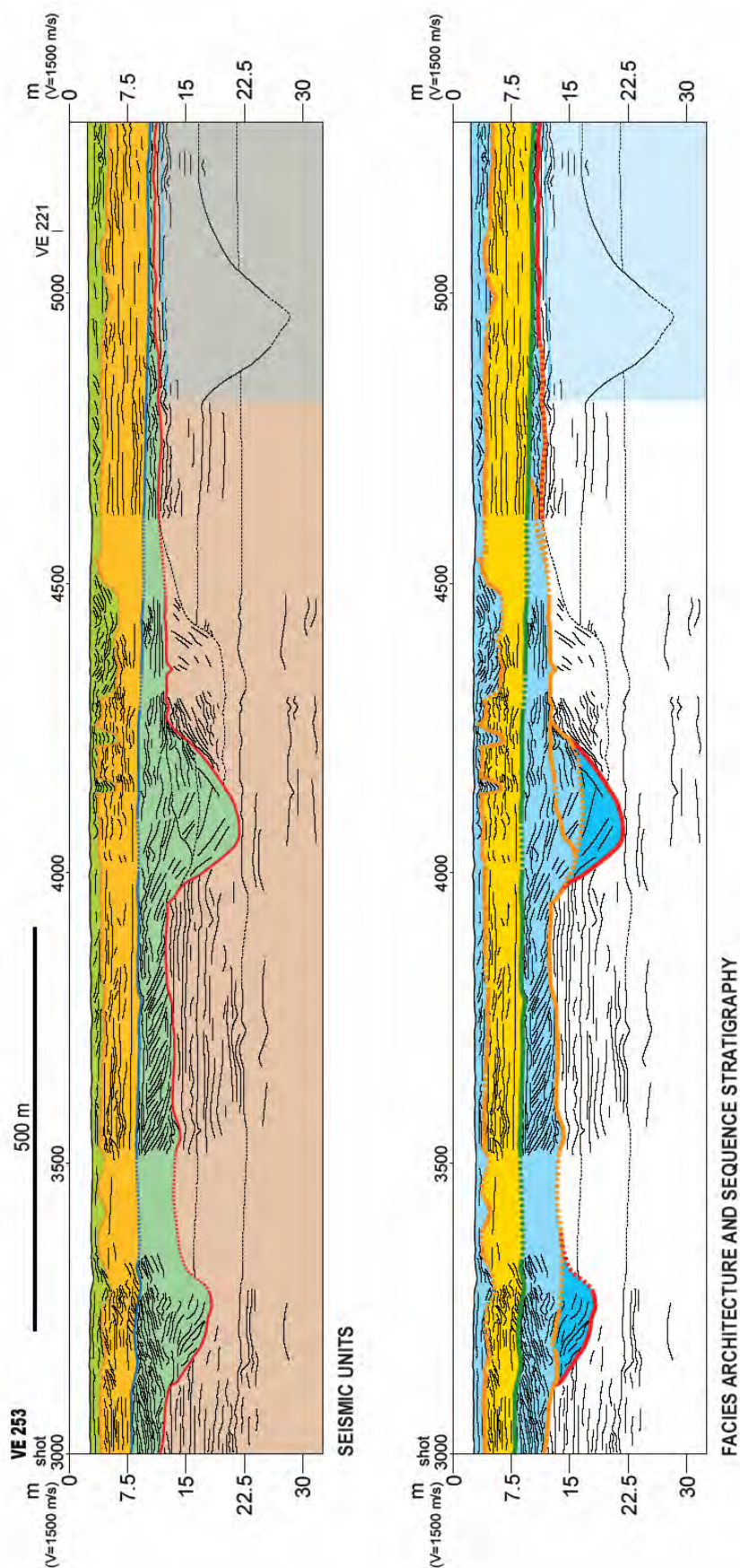
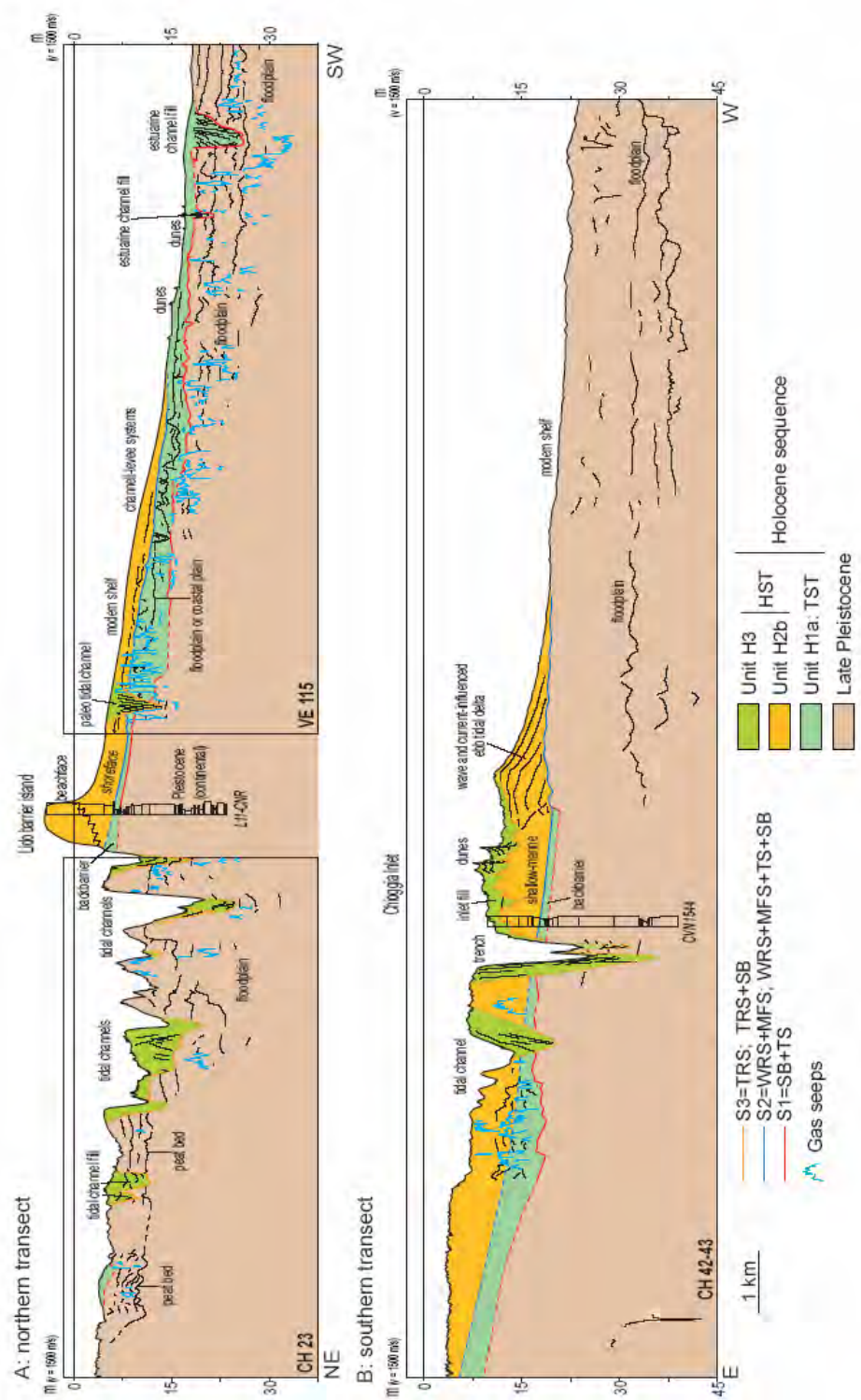


Fig 19 – Seismic units and surfaces (above), facies architecture, and sequence stratigraphic interpretation (below) of the VE 253 seismic line (see Fig. 18 for symbols). The VE 253 seismic line represents a strike section showing facies relationships from northward (on the left) to southward locations. Two incised valleys in correspondence of the Pleistocene-Holocene boundary (the S1 surface) are intercepted.

Fig 20 – Line drawings showing the architecture and the interpreted sequence-stratigraphic organization of the late Pleistocene and Holocene sequences off the Venice lagoon. The late Pleistocene sequence consists of an overall aggrading alluvial plain, whereas the Holocene sequence is composed of three paralic to marine units (Units H1-3) separated by main stratal surfaces (S1-3). HST = highstand systems tract, MFS = maximum flooding surface, SB = sequence boundary, TRS = tidal ravinement surface, TS = transgressive surface, TST = transgressive systems tract, WRS = wave ravinement surface.



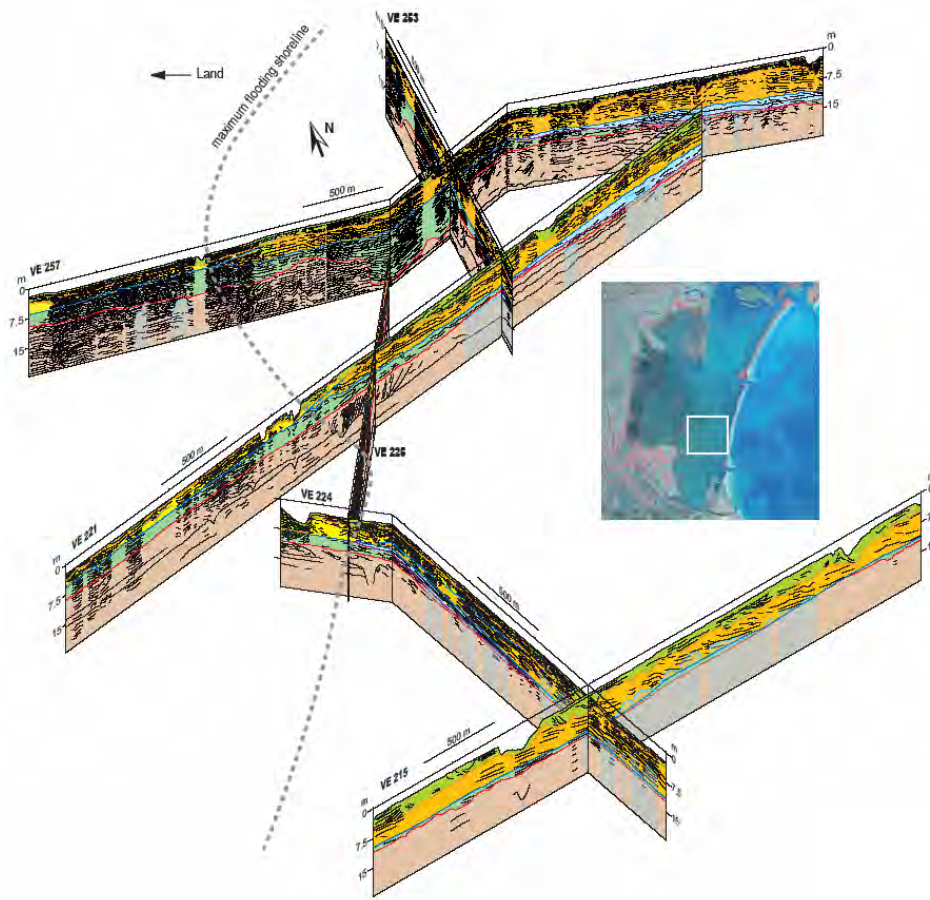


Fig 21 – 3D model showing the architecture of the Holocene succession in the study area (rectangle in the satellite image) (see Fig. 18 for symbols). Note the thickness decrease of Unit H1a (back-barrier) toward the south and the more uniform thickness of Unit H2b. Note also the patchy distribution of Unit H1b (shallow-marine), which is present only in the distal parts of VE 221 and VE 257 seismic lines and in the VE 224 seismic line. The maximum flooding shoreline is traced by connecting the landward terminations of the wave ravinement surface in the VE 257, 221, 224, and 225 seismic lines.

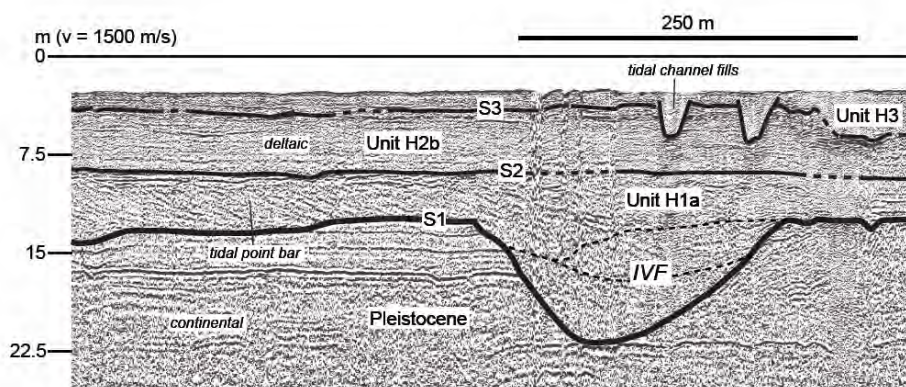
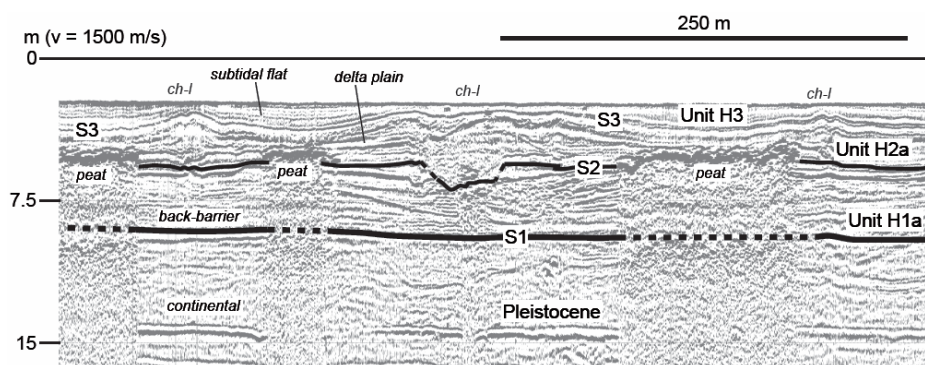


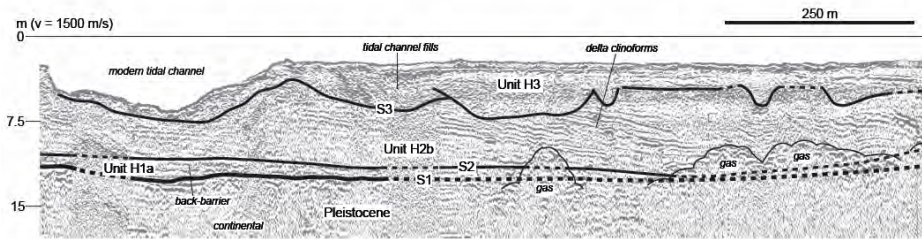
Fig 22 – Detail of the VE 253 seismic line, showing an incised valley fill (IVF) and a tidal point bar developed during the late estuarine deposition. Note that the fill of the incised valley is composite. The S1 surface is the Pleistocene-Holocene boundary and represents the sequence boundary of the Holocene sequence, whereas the S2 surface is the maximum flooding surface (see text). The S3 surface marks the relatively recent phase of delta abandonment and local transgression.

Fig 23– The landward part of the VE 221 seismic line. Back-barrier deposits of Unit H1a lying on the Pleistocene-Holocene boundary (the S1 surface) form the lower, transgressive part of the Holocene succession. These are capped by a surface (the S2 surface), locally marked by irregular reflectors obscuring the underlying signal and interpreted as peat beds, that corresponds to the maximum flooding surface. The highstand deposition was characterized by the development of channel-levee systems (ch-l) in a delta plain environment (Unit H2a). The S3 surface, separating Unit H2a from the subtidal flat of Unit H3, is well distinguishable. In this location, the S3 surface is non-erosional, and deposits of Unit H3 drape the channel-levees of Unit H2a.



4.1.1.2 S2

The S2 surface is an unconformity that usually is well recognizable within the Holocene deposits in the southern Venice lagoon as well as off the barrier island [Zecchin *et al.*, in press] (Figs. 17-23). This surface is typically characterized by a discrete continuity along both depositional strike and dip, and by an average seaward dip that is higher (up to 0.2 degrees) than that of the S1 surface between incisions (Fig. 23). S1 and S2 surfaces may be either amalgamated or separated by some meters of sediment (Unit H1, see below) (Figs. 17-23). Overall, the S2 surface shows an evident geometric change along depositional dip; its inclination increases in the landward direction and then shows an abrupt change to nearly horizontal in proximal locations (Figs. 17 and 18). The S2 surface is a downlap surface with respect to the overlying reflectors (Figs. 18, 20, and 24-26). This downlap surface is traceable in the landward sector, where it consists of an unconformable contact between units H1a and H2a (see below; Figs. 18, 21 and 23).



Locally in the seaward sector, another surface, called S2a surface, merges landward with the S2 surface (Figs. 17, 18 and 21). The S2a surface truncates the underlying reflectors and shows both onlap and downlap relationships with the overlying ones (Fig. 18).

In distal offshore locations the S2 surface merges with the modern sea-floor, and it is covered by very thin sediments, that are below seismic resolution, and locally by well recognizable dunes (Fig. 20).

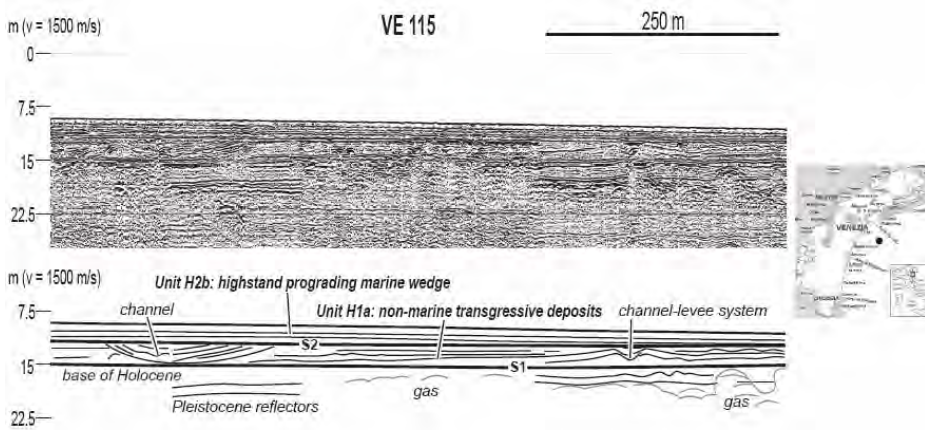


Fig 25 – Units H1 and H2 off the Lido barrier island. Channelized deposits and channel-levee systems are recognizable within Unit H1a, which represents the transgressive systems tract of the Holocene sequence. Unit H1a is truncated by a wave ravinement surface (the S2 surface) and is overlain by Unit H2b (the highstand systems tract) that is composed of gently dipping clinoforms downlapping onto the S2 surface.

Fig 26 – Ebb tidal delta forming part of Unit H2b located immediately off the Chioggia inlet. In this case, the transgressive deposits of Unit H1 are absent and the S2 surface reworks the S1 surface and coincides with the boundary of the Holocene sequence. Clinoforms of the ebb tidal delta downlaps onto the S2 surface, which is a wave ravinement surface coincident with a maximum flooding surface (see text). Part of the inlet fill (Unit H3) of the Chioggia inlet is visible on the left.

Fig 27– Large channelized deposit showing a lateral accretion and located off the Lido barrier island. This feature is interpretable as the consequence of the migration of a point bar in an estuary that resulted from the drowning of a previous fluvial channel entrenched in the Upper Pleistocene. This deposit is interpreted as the lower part of the Holocene sequence (Unit H1a).

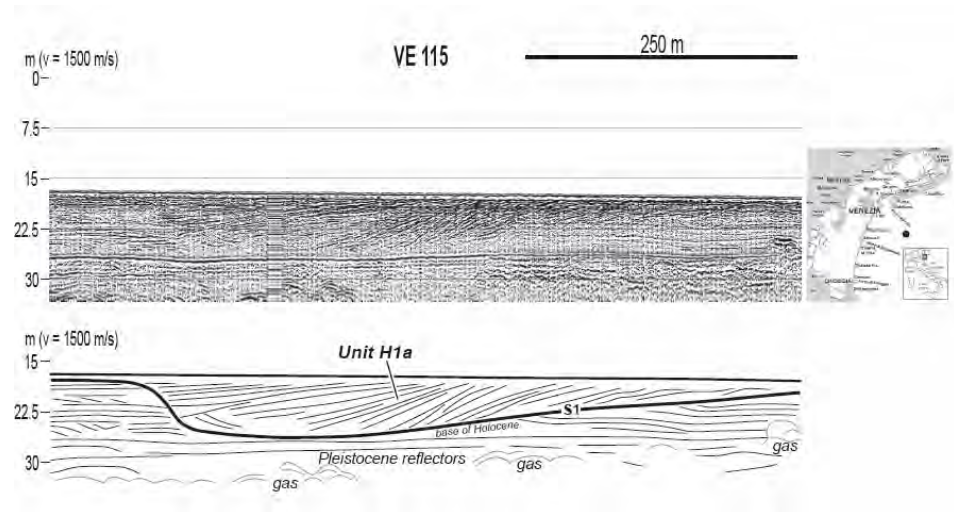


Fig 28 – Regional setting of the S1 (Pleistocene-Holocene stratigraphic limit) in the lagoon and gulf of Venice. Color scale and isolines indicate the depth in m.

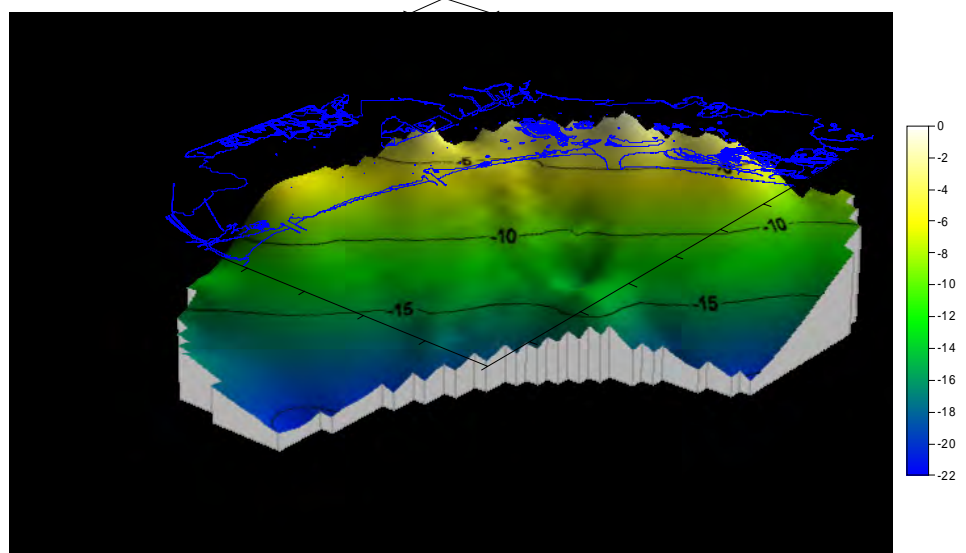
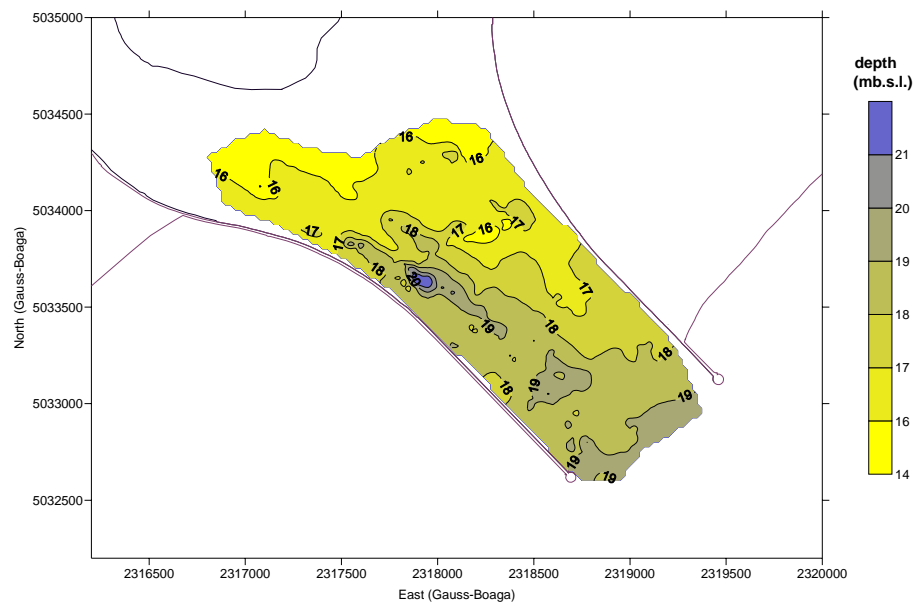


Fig 29 – Detail map of the S1 setting (Pleistocene-Holocene stratigraphic limit) at the Lido Inlet. Color scale and isolines indicate the depth in m.



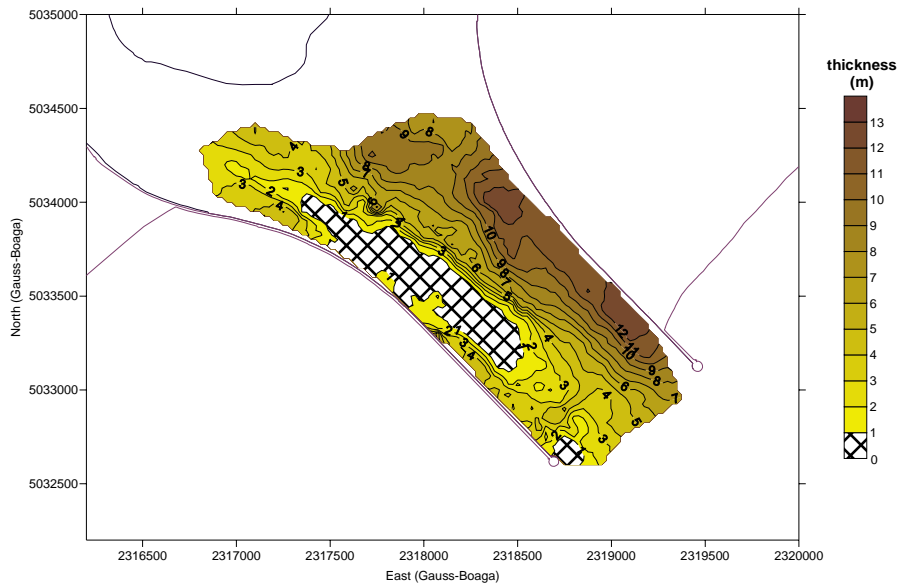


Fig 30 – Thickness of the Holocene deposits at the Lido Inlet. Color scale and isolines indicate the thickness in m.

4.1.1.3 S3

The S3 surface is the younger and locally the more irregular surface (Figs. 17-24). It corresponds with the base of relatively recent channelized deposits and coeval laminated sediments of Unit H3 (see below). Channel bases indifferently truncate previously deposited sediments, and they are more abundant and deeper seaward, near the modern lagoon inlets (Figs. 18 and 31). Outside of the channels, the S3 surface is recognizable by an abrupt change in the depositional style. For example, the S3 surface marks the base of laminated sediments draping previous deposits in the landward part of the VE 221 seismic line (Figs. 18 and 23). This surface may be not easily recognizable between channelized deposits in strike sections.

4.1.2 Seismic units

4.1.2.1 Unit H1

It is the lowermost unit of the Holocene succession and consists of two sub-units (H1a and H1b) (Figs. 17-20). Locally (e.g. off the Chioggia inlet) Unit H1 is absent, and S1/S2 surfaces are coincident (Fig. 26). Unit H1 is only 1 m thick below the Venetian littoral (Fig. 20), whereas its thickness increases toward the southern lagoon area (Fig. 21).

Unit H1a is bounded at the base by the S1 surface and at the top by the S2 surface or the S2a surface (Figs. 17-20). Unit H1a is composed of curved to irregular and inclined reflectors, testifying a discrete lateral variability of depositional conditions, and is typically characterized by an extreme thickness variability (from 0 to 13 m) along both depositional strike and dip (Figs. 22-25 and 27). Abrupt thickness variations are recognizable in areas dissected by the deep incisions marked by the S1 surface (Figs. 19, 21, 22 and 27). Inclined reflectors locally downlap onto sub-horizontal or less inclined reflectors (Figs. 22 and 27). The deeper incisions show a composite fill, consisting of two to three parts (Figs. 19 and 22). In the southern lagoon area, Unit H1a shows a clear

southward thickness decrease (Fig. 21).

Unit H1b is bounded at the base by the S2a surface and at the top by the S2 surface, and it is recognizable only in the southern lagoon area (Figs. 17, 18 and 21). **Errore. L'origine riferimento non è stata trovata.** Unit H1b is up to 3.5 m thick and pinches out landwards (Figs. 18 and 21). The unit is absent in the southward part of the area (Fig. 21). Unit H1b is composed of curved and seaward inclined reflectors that display both onlap and downlap relationships with the S2a surface (Fig. 18).

4.1.2.2 Unit H2

This unit is bounded at the base by the S2 surface and at the top by the S3 surface, or by the modern seafloor in offshore locations (Figs. 17-21). Unit H2 is composed of two sub-units (H2a and H2b) showing different seismic patterns (Figs. 17 and 18). The top of the unit locally may correspond with the floor of the deeper, modern tidal channels (Fig. 20).

Unit H2a (up to 3.5 m thick) is present in the landward sector of the area, and is composed of irregular, curved, inclined and hummocky reflectors that may be locally similar to those present in Unit H1a (Figs. 18, 21 and 23). In the tract where the S2 surface marks the base of Unit H2a, it is much less inclined than its seaward part (Figs. 18 and 23). Moreover, irregular reflectors obscuring the deeper signal are locally present in the lower part of Unit H2a (Fig. 23).

Unit H2b is located seaward with respect to Unit H2a, and their lateral transition is indistinct (Figs. 17, 18 and 21). Unit H2b is composed of seaward-inclined sigmoid reflectors that downlap onto the S2 surface, and shows a seaward thickness increase from 0 to 10 m (Figs. 18, 20, and 24-26). The thickness is significantly greater (up to 20 m) in correspondence of the modern, southern barrier island [Tosi et al., 2007a,b]. The inclined reflectors show a dip that reaches a maximum of 0.7 degrees. Dondip changes in the inclination of the reflectors are commonly observable (Fig. 18). Irregular and deformed reflectors are also locally present. Both onlap and downlap relationships with respect to relatively continuous internal reflectors are locally recognizable.

4.1.2.3 Unit H3

This unit, bounded at the base by the S3 surface and at the top by the lagoonal floor, corresponds to the modern lagoonal deposits (Figs. 17-24). Unit H3 typically consists of channelized deposits, which lateral continuity is easily recognizable in seismic lines, incised on the previously accumulated Holocene sediments, especially near the modern inlets and the barrier island (Figs. 22, 24, 26 and 31). Various inclined and irregular reflectors are recognizable within Unit H3 (Figs. 18-20, 24 and 31). Channelized deposits are shallower and less common landward, where they pass laterally into laminated sediments draping the structures of Unit H2a (Figs. 18 and 23).

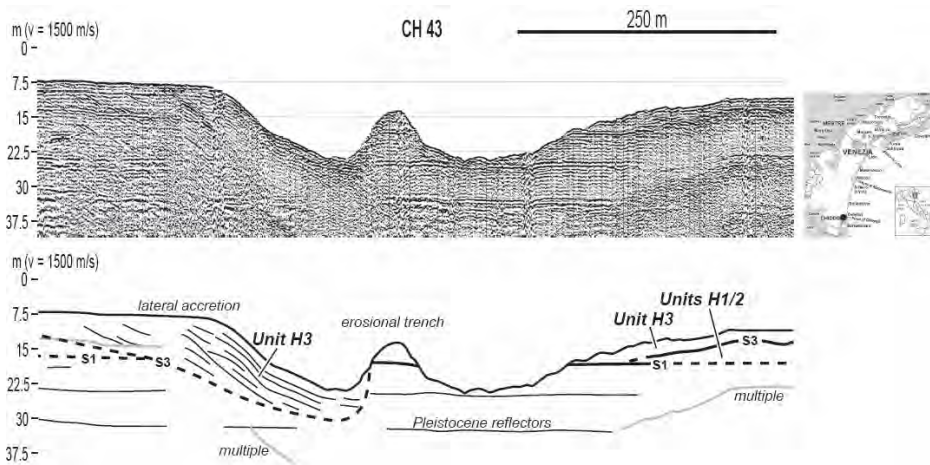


Fig 31 – Erosional trench located in the southern lagoonal area, near the Chioggia inlet. The trench is the confluence of some tidal channels and the Chioggia inlet. Erosion and a stepped morphology are present on the right side of the trench, towards the inlet, whereas lateral accreting deposits (Unit H3) are visible on the left.

Inlets are highly dynamic, especially after human interventions carried out during the last centuries that have enhanced current velocity and tidal prism [Carbognin, 1992; Carbognin *et al.*, 2000; McClennen and Housley, 2006]. Erosional trenches are present at the inner end of both the Chioggia (30 m deep) and Malamocco (50 m deep) inlets (Figs. 20 and 31). Accretion and erosion in opposite sides are found in the Chioggia one (Figs. 20 and 31). The base of inlet is recognizable as an irregular reflector, whereas inlet deposits consist of accreting macroforms and dunes (Figs. 20 and 26). These deposits are relatively thick (up to 7.5 m) in the northern part of the Lido inlet, whereas the southern part is subjected to prevailing erosion. The opposite situation is recognizable in the Chioggia inlet

4.1.3 Interpretation

4.1.3.1 Unit H1 and the S1 surface

The observed seismic features, together with core data, suggests that Unit H1a is the result of deposition in an heterogeneous back-barrier environment. In particular, inclined reflectors within deep incisions very probably indicate lateral accretion into estuaries (Figs. 17-20 and 22), which resulted from the drowning of previous small fluvial valleys incised during glacio-eustatic exposure in latest Pleistocene time. This interpretation was already suggested by Zecchin *et al.* [in press] for the basal Holocene deposits located off the Venice barrier island, and by Trincardi *et al.* [1994a] in the northern Adriatic shelf.

Core data demonstrate that the oldest Holocene sediments consist of fine-grained, thin intervals locally reworking the caranto layer and showing a marine influence (the so called 'overflow deposits' of Gatto and Previatello [1974]), which are thought to be coastal plain deposits passing upward into inner lagoonal deposits [Tosi *et al.*, 2007a,b]. The absence of fluvial sedimentation above the S1 surface evidences conditions of prevailing non-deposition and incision during its formation. Recent data [Mozzi *et al.*, 2003; Tosi *et al.*, 2007a,b] indicate that the Venetian alluvial plain received abundant sediment and aggraded until ca. 14.5 kyr B.P., and then it became sediment starved until ca. 11.5 kyr B.P.. These conditions favored both incision of the alluvial plain and

extensive soil development, determining the formation of the S1 surface. However, the presence of thin and discontinuous fluvial deposits only in the deeper part of some incised valleys is not totally ruled-out, as illustrated by Amorosi *et al.* [2003, 2005] beneath the modern Po coastal plain.

As the studied incised valleys display a composite fill, we suppose that their lower part consists of fluvial sediments and/or early estuarine fills, possibly developed in a mixed energy, tidal-fluvial setting [Dalrymple *et al.*, 1992], whereas the upper ones consist of tidal channel deposits accumulated during the late stage filling (Fig. 19). We believe that meandering tidal channels developed during the late stage filling, eroded the underlying deposits [e.g., Dalrymple *et al.* 1992] and widened the upper part of some incised valleys (Fig. 19).

In areas located above and between the inferred estuarine channel fills, Unit H1a consists of shallow, meandering tidal channel and tidal and subtidal flat sediments, which are thought to be accumulated in an estuarine lagoon to lagoon setting (Figs. 18 and 19).

The observed internal geometries, the wedge shape, the position within the Holocene succession, and core data, suggest that Unit H1b is composed of shallow-marine sands with minor mud (Fig. 18).

4.1.3.2 Unit H2

The features of Unit H2a and its position within the Holocene succession suggest a deposition in an environment characterized by channel scouring, placed little landward with respect to the shoreline. In particular, some observed features are diagnostic of channel-levee systems (Figs. 18 and 23), like those forming distributary channels in delta plains [Bhattacharya, 2006]. Moreover, unpublished core data in this part of the Venice lagoon show a widespread distribution of a peat bed located just at the top of sediments corresponding to Unit H2a, revealing a generalized paludal environment. Also, scattered bricks are locally present in the same stratigraphic position. These evidences suggest that Unit H2a is the result of deposition in a delta plain scoured by distributary channels, and locally in swamps and/or marshes (Figs. 17, 18 and 21).

Both the observed features and core data strongly suggest that Unit H2b is the result of progradation of a sandier to heterolithic (mixed sands, silts and clays) delta front to prodelta (in the southern lagoon), and of a shoreface-shelf system during late Holocene time (from about 6 kyr B.P. onwards) (Figs. 17-21 and 24). In correspondence of the inlet outer side (e.g. off the Chioggia inlet, Figs. 20 and 26), the wedges are interpreted as ebb tidal deltas influenced by waves and longshore currents. Ebb tidal deltas, therefore, interact laterally with the shoreface-shelf-system. The fan shape of these ebb tidal deltas is evidenced by bathymetric maps [Amos *et al.*, 2005],

4.1.3.3 Unit H3

Channelized deposits of Unit H3 are tidal channel deposits commonly showing lateral accretions, related to the migration of tidal point bars [e.g., McClennen

and Housley, 2006], and multistory fills. The tidal scour into the lagoon has been significantly enhanced from late medieval time onwards because of several human interventions [Brambati *et al.*, 2003]. In particular, river diversions, dredging and digging of the inlets caused first delta abandonment and its drowning, and then an enhancement of tidal currents [Carbognin, 1992; Carbognin *et al.*, 2000; Brancolini *et al.*, 2006]. This generalized drowning of the southern part of the Venice area, and the associated remarkable change of the hydrodynamics, are marked by the S3 surface. The erosion related to the tidal currents is particularly strong in locations inside the modern inlets, where the up to 50 m deep erosional trenches are present (Fig. 31).

The laminated sediments placed laterally with respect to the tidal channels form the tidal and subtidal flats of the modern lagoon (Fig. 23). These sediments drape the preserved delta plain deposits of Unit H2a, and testify the recent drowning of the inner sector of the southern part of the area.

4.1.4 Sequence stratigraphy

Following current sequence stratigraphic concepts, the S1 surface is interpreted as a sequence boundary (SB) that records prolonged subaerial lowstand conditions during the Last Glacial Maximum (Figs. 18-20). In the present case, the SB is amalgamated with the transgressive surface (TS), marking the base of the transgressive systems tract (TST). The bases of tidal channels of Unit H1a correspond to tidal ravinement surfaces (TRS), which are the product of the landward migration of the zone of maximum tidal energy [Allen and Posamentier, 1993; Cattaneo and Steel, 2003] (Figs. 18-20).

The retrogradational deposits that form the whole Unit H1 can be interpreted as the transgressive systems tract (TST) of the Holocene sequence (Figs. 18-20) formed when rates of the high amplitude relative sea-level rise following the Last Glacial Maximum exceeded those of sediment supply. The S2 surface is interpretable as the maximum flooding surface (MFS) marking the top of the TST, whereas the S2a surface represents a wave ravinement surface (WRS), cut by waves during shoreface retreat [Swift, 1968; Demarest and Kraft, 1987; Nummedal and Swift, 1987], and recording the marine ingression (Figs. 18-20). The MFS and the WRS may be amalgamated to form a composite WRS+MFS surface (Figs. 18-20).

The regressive, prograding deposits of Unit H2 are interpreted as the highstand systems tract (HST) of the Holocene sequence, bounded at the base by the MFS (the S2 surface) and showing a typical aggradational to progradational architecture. The lagoonal deposits of Unit H3 represent a peculiar case in the Holocene evolution of the Venice lagoon. In fact, the drowning of the study area due to delta abandonment favored by human interventions and marked by the S3 surface, represents a local transgression, limited to the modern lagoonal area and therefore unrelated to any increase of the eustatic rate. We call this transgression, consisting in the southward and landward expansion of the Venice lagoon, "human-induced transgression". The S3 surface, therefore, may be considered as a local SB amalgamated with a TS. The bases of tidal channel

deposits of Unit H3 are TRSs related to this local transgressive phase (Figs. 18-20).

4.1.5 Unconformity Bounded Stratigraphic Units

The Pleistocene and Holocene deposits of the Venice coastland were recently classified by Tosi *et al.* [2007a,b] according to the rules established by APAT: the “Unconformity Bounded Stratigraphic Units” (UBSU). The UBSU determination is based on the presence of two evident, well recognizable, and significant discontinuities. They allow to classify the different sedimentary bodies identified with seismic surveys on the basis of their age, grain size, depositional environment, and bounding unconformities (Fig. 32)

The Mestre Supersynthem (Fig. 32) represents the Upper Pleistocene deposits which top is dated 20,000-18,000 years B.P [Tosi *et al.*, 2007a,b]. At the top of the Pleistocene deposits, although different lithologies are present, the finding of the caranto (overconsolidated clay layer) is frequent [Gatto and Previatello 1974; Bonardi and Tosi, 2000b].

Po Synthem (POI)	Torcello Unit (POI ₁₀) (IV-V century A.D. - present)	Holocene
	Malamocco Unit (POI ₉) (10,000 BP - IV-V century A.D.)	
Mestre Supersynthem (MT) (110,000 - 18,000 BP)		Upper Pleistocene
Venice Supersynthem (VZ)	Correzzola Unit (CRZ) (last Tyrrhenian marine transgression)	Pliocene - Upper Pleistocene
	Messinian unconformity	

Fig 32 – Stratigraphic units mapped in the Geological Map Sheets 128 “Venezia” and 148-149 “Chioggia-Malamocco”.

The setting of the various UBSU is quite variable in the Venice lagoon (Figs. 33 and 34).

The Po Synthem represents the Holocene deposits, attributed to the transgression event after the last glaciation. Between the Pleistocene and Holocene sedimentation, a stratigraphic hiatus, characterized by widely varying time intervals, is present. In fact, in the different sectors of the lagoon area the base of the Po Synthem has different ages, the oldest in the southern coastal area, 10,000- 11,000 years B.P. [Tosi, 1994a], whereas in the north-eastern area the age ranges from 5,000 to 7,000 years B.P. (Figs. 33 and 34).

From the sequence stratigraphy approach, the Unit 1 correspond to the upper deposits of the Mestre Supersynthem while the S1 unconformity (Figs. 17-21) the Mestre Supersynthem-Po Synthem limit (Pleistocene-Holocene stratigraphic limit).

The Po Synthem has been divided in two units, the Torcello Unit and the Malamocco Unit, both composed of sands, silts, clays, and peats from alluvial, deltaic, littoral (beach and lagoon), and shelf environments.

The Po Synthem was divided by Tosi *et al.* [2007a,b] mainly on a chronological basis for the reason that at that time there were only few data with evidence of an abrupt or erosion surface pointing out the limit.

Thanks to the very high resolution of the new seismic survey and the opportunity to survey the shallows subsoil, the occurrence of this limit has been proven.

Unit 3 represents the Torcello Units, referred to the post-Roman sedimentation, started from V-VI century A.D. and continues up to the Present. S3 is the base of the Torcello Unit.

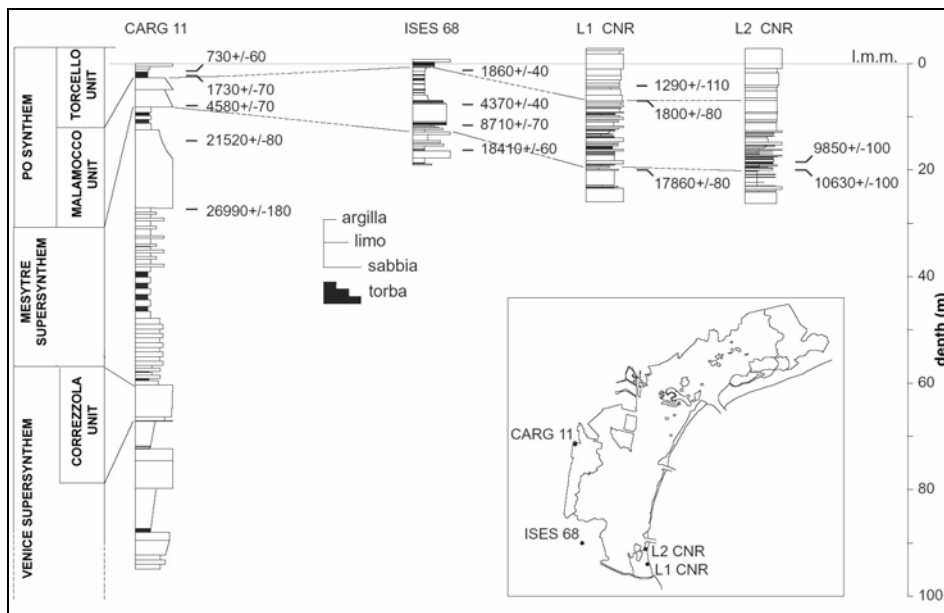


Fig 33 – Scheme of the stratigraphic relations within the Venice Supersythem and the Po Synthem in the southern lagoon [Tosi *et al.*, 2007a,b].

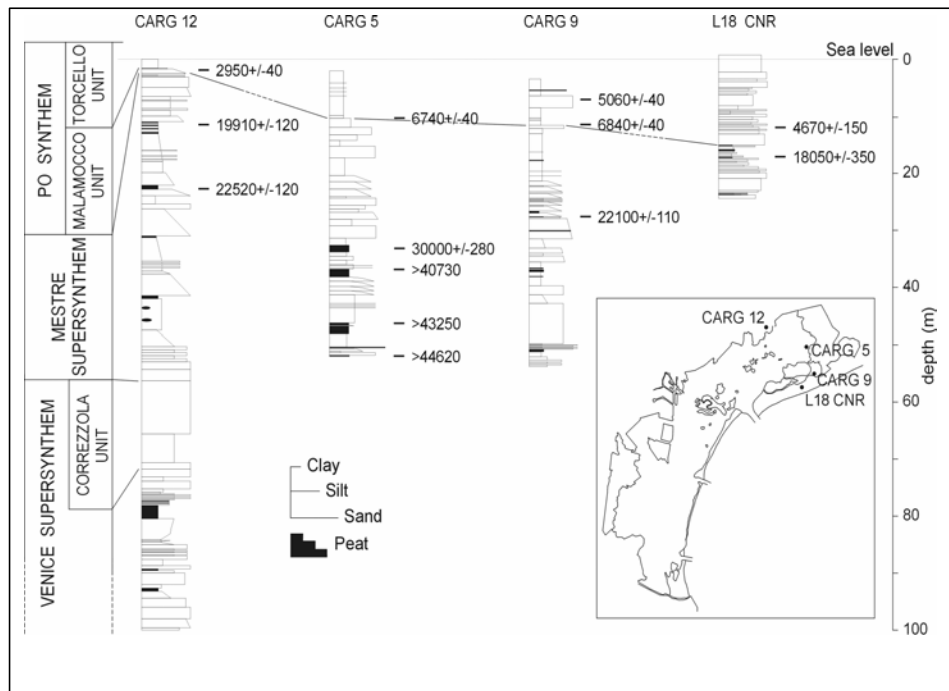


Fig 34 – Scheme of the stratigraphic relations within the Venice Supersynthem and the Po Synthem in the northern lagoon” [Tosi et al., 2007a,b].

4.2 Analysis of geomorphological features

The new very high resolution survey is the unique tool allowing detailed subsoil images in lagoon shallows and tidal flats.

New surveys and available information, including sedimentological, stratigraphic, geotechnical, mineralogical, ¹⁴C datings, textural, and bathymetric data, satellite images and historical maps [Amos *et al.*, 2006; Bonardi and Tosi, 1997, 2000a,b; Bonardi *et al.*, 1997, 2004, 2005, 2006; Brancolini *et al.*, 2005, 2006; Rizzetto *et al.*, 2002, 2003, 2005; Tosi, 1993, 1994a,b,c; Tosi *et al.*, 2006, 2007a,b; Zecchin *et al.*, 2006a,b,c] were used to carry out this investigation.

The integrated analysis of the new and collected data provided several blow up figures of features occurring in the regional geomorphological setting. In particular the seismic sections pointed out details of the depositional architecture, that have never been revealed previously in the lagoon basin.

Following, some selected geomorphological features discovered in the south lagoon basin by VHRS survey, as examples of preliminary study concerning this topic, are discussed below. Their locations are shown in Fig. 35.

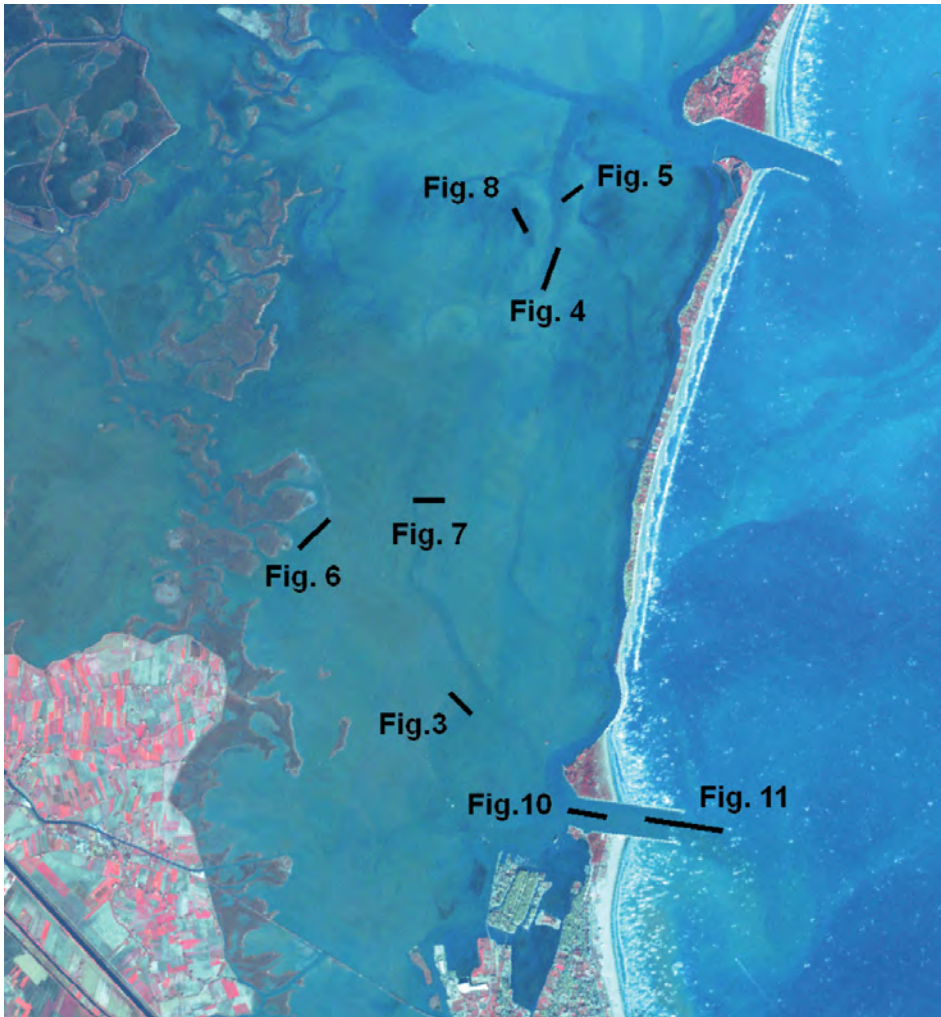


Fig 35 – Location map of the selected geomorphological features.

An example of a Holocene tidal channel complex system is given in Fig. 36. Line drawing and interpretation point out vertical and horizontal evolution of the tidal channel from its origin to the present setting. The active tidal channel, partially filled, and the lagoon mudflat show sub-horizontal reflectors.

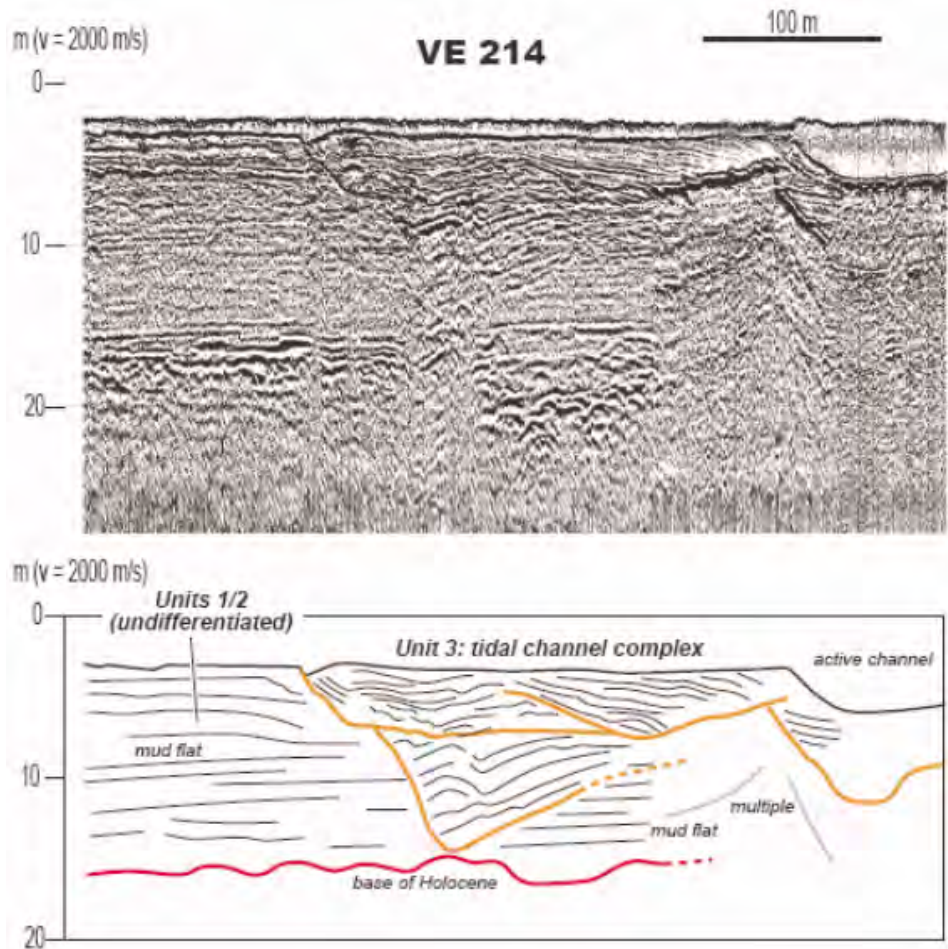


Fig 36– Example of Holocene complex tidal channel system evolution.

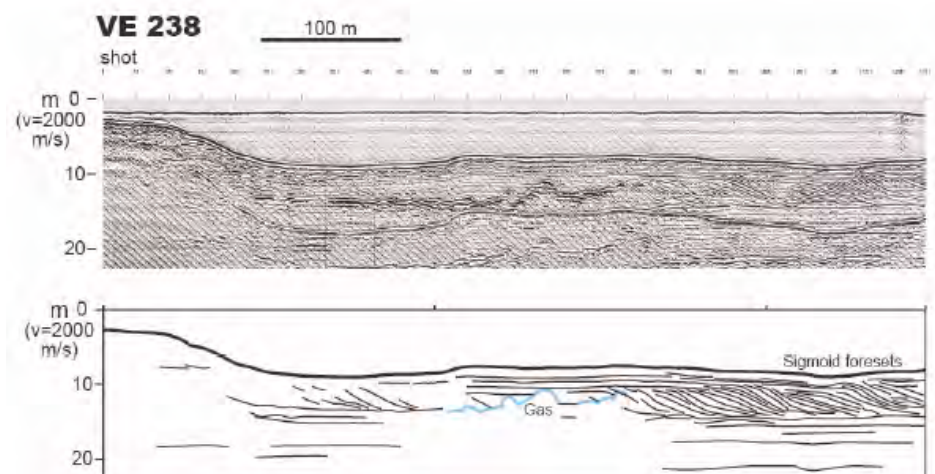


Fig 37 – Section of active lagoon channel.

An additional example of lagoon channel architecture is given in Fig. 37. Sigmoidal foresets indicate the evolution of a sand bar system and the north direction migration of the ancient channel. The morphology of the present active channel is characterized by truncation and erosion of the previously deposited layers.

Fig. 38 reports another example of architecture of an active channel. In this section, a like island shape (i.e. the morphological high) divides the channel in two sectors. Lateral accretion process, which partially filled an ancient channel, is recognizable on the left sector. On the right sector, the active channel is migrating to NE direction. This is evidenced by the lateral migrating bar (probably a meander) occurring on its left side and by the erosion of the previous accretion features (foreset truncation) on the right side.

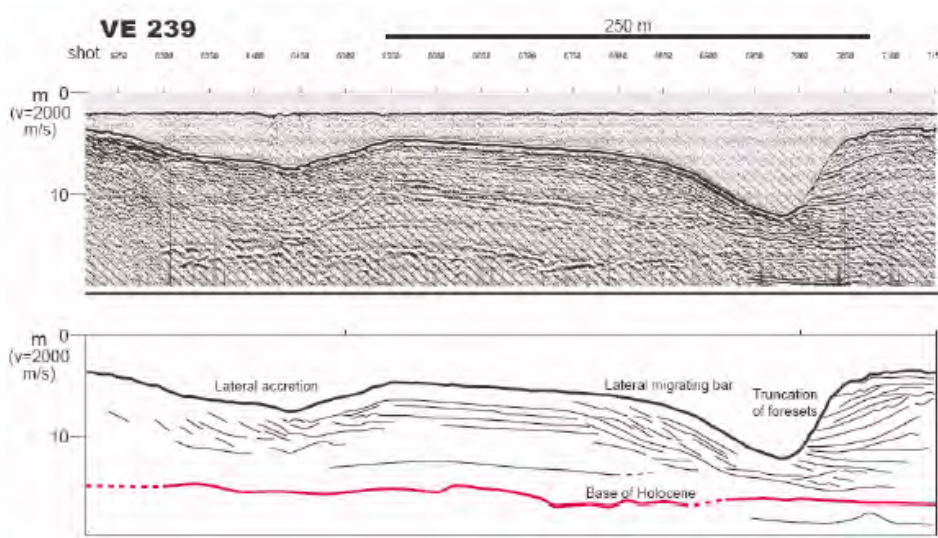


Fig 38 – Example of subsoil architecture and morphology of an active lagoon channel.

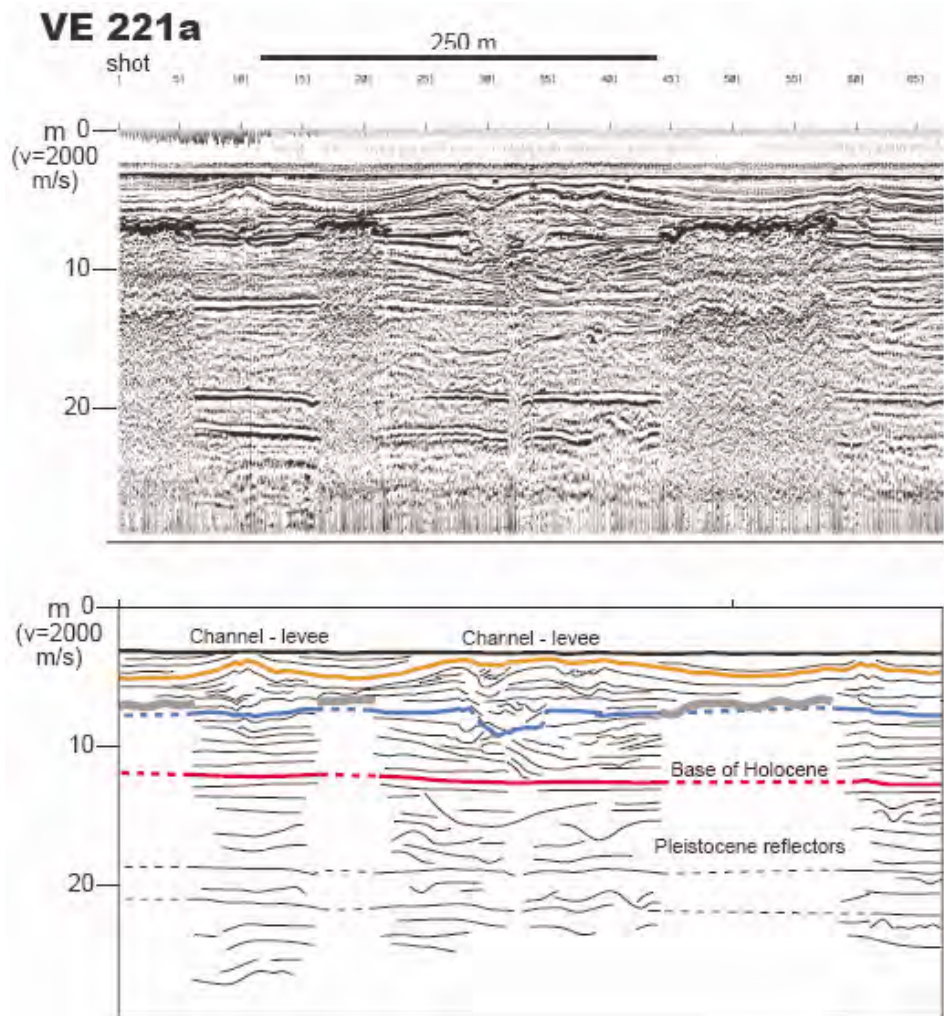


Fig 39 – Example of inactive Holocene channel-levee system architecture.

Inactive Holocene channelized deposits and channel-levee systems developed in a delta-plain are recognizable in Fig. 39, whereas a large buried Pleistocene channelized deposit, showing a lateral accretion, in Fig. 40. The latter is related to an ancient branch of the Brenta River system.

The complexity of the Holocene lagoon environment is shown in Fig. 41. A number of buried tidal channelized deposits were found below the modern lagoon floor.

Investigations in the Chioggia inlet have shown the occurrence of both erosional and depositional sedimentary processes, in a highly dynamic environment.

Bathymetric data processing provides spectacular figures of the inlet sea bottom (Fig. 42).

A 30 m deep erosional trench, due to the hydrodynamic flux confluence of some tidal channels, occurs toward the lagoon side of the inlet. The VHRS survey revealed that the trench is characterized by accretion and erosion of the west and east side walls respectively (Fig. 31).

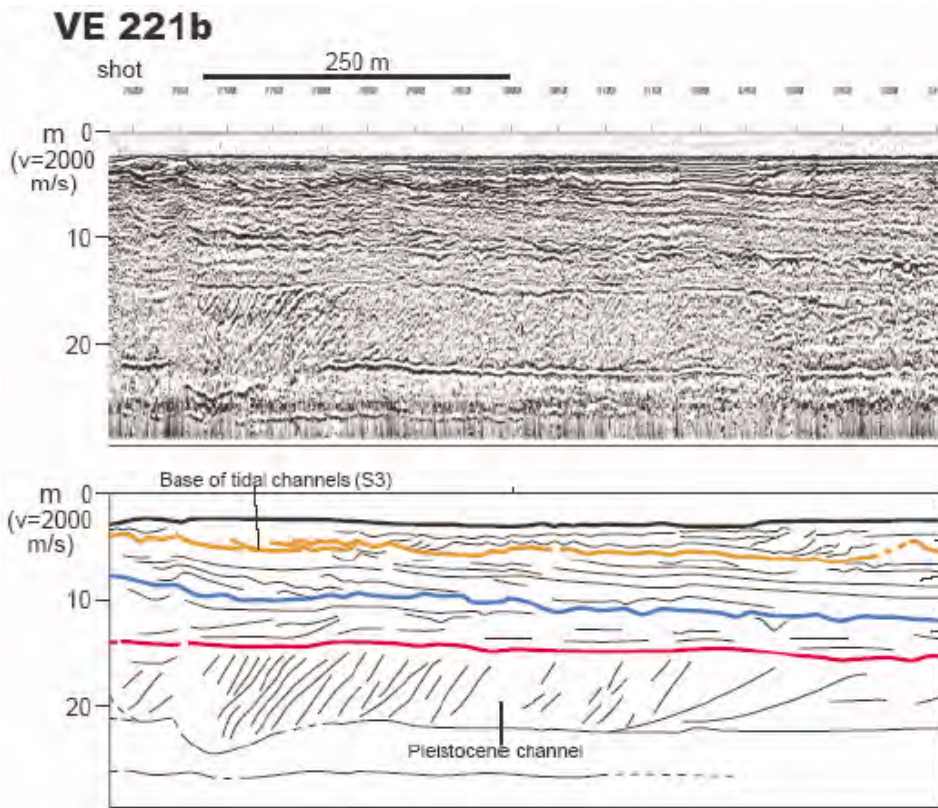


Fig 40 – Lateral accretion in a buried channel of the Pleistocene Brenta river system.

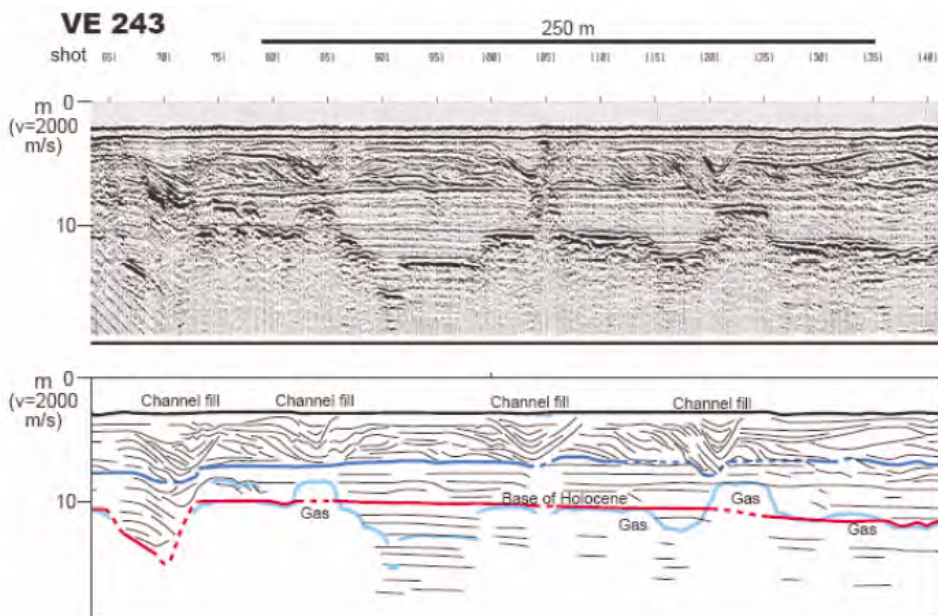


Fig 41 – Example of inactive Holocene channel fill system showing the complexity of the past lagoon environment.



Fig 42 – Morphology of the Chioggia inlet revealed by multi-beam bathymetric survey. Trench (Fig. 31) and dune (Fig. 43) features occur in left and right side respectively.

Furthermore, in the seaward side of the inlet dune features with accreting deposit architecture were found (Fig. 43).

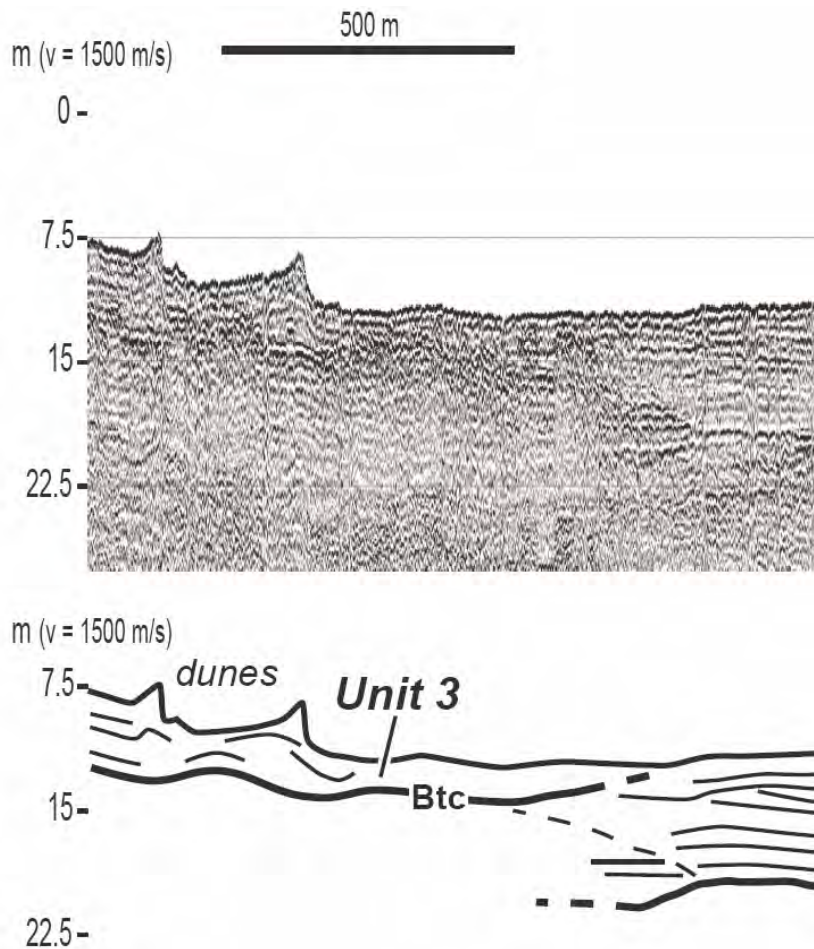


Fig 43 – Detail of Fig. 26 showing dune features in the Chioggia inlet.

5 The ebb tidal delta of the Lido inlet

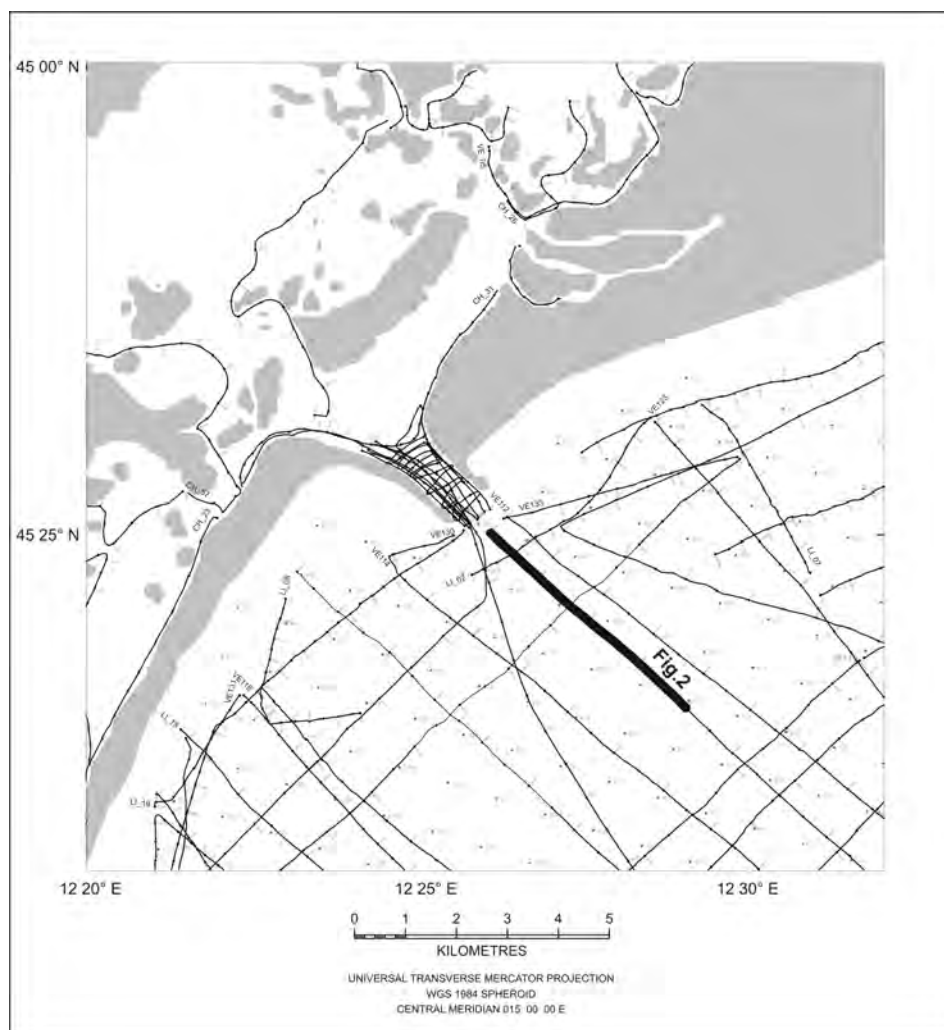
An ebb-tidal delta is an accumulation of sand and fine shell gravel deposited primarily by the ebb-tidal current on the seaward site of the tidal inlet [Hayes, 1980; Davis and Hayes, 1984]. The conceptual model for the ebb-tidal delta is based on the hypothesis that sediment is transported seaward through the main tidal channel and deposited as a distal lobe on the swash platform, where the current diminishes below the sediment transport threshold, due to bottom friction and segregation of flow [Fitzgerald *et al.*, 2004]. A dynamic balance between a net offshore directed sediment flux induced by the inlet currents and a net onshore directed sediment flux induced by offshore waves exists [Komar, 1996]. The sediment facies are thought to be controlled by the decreasing and spreading velocities of the ebb jet. Since currents are expected to decrease rapidly in a spreading ebb-jet, while maximum speeds occur in the inlet throat, medium-coarse sand is mainly confined to the central, ebb-jet dominated area [Krueger and Healy, 1996].

Previous studies performed in the area of the Lido inlet revealed that at present there is a net export of sand from the Lagoon of Venice through the Lido Inlet [Amos *et al.*, 2005]. Such studies identified scouring within the Lido mouth and the existence of a depositional apron, representing a classical, asymmetric ebb-tidal delta, fed by a net transport of sand from the Lagoon of Venice through the Lido Inlet.

The 140 km odd of Boomer profiles collected offshore the Lido inlet in the framework of Co.Ri.La Subproject 3.16 (Fig. 44) led to the identification of a convex-upward, lens-shaped body, just outside the Lido inlet, one of the three lagoon inlets, which has been interpreted as an ebb-tidal delta. The comparison between the seismostratigraphic setting of this deposit, as revealed by the seismic lines, and the analyses of historical bathymetric maps showed that the ebb-tidal delta at the Lido inlet formed as a consequence of human interventions that at around the end of the XIX century, that caused profound variations in the inlet dynamics and lead to a progressive increase in the sediment dispersion from the lagoon interior towards the sea.

The results discussed in this paper are part of the paper entitled "The ebb-tidal delta of the Venice Lagoon (Italy)" [Donda *et al.*, in press] on The Holocene.

Fig 44 – Location map of the study area and of the high resolution seismic profiles acquired in the framework of the Co.Ri.La. Subproject 3.16. Regular grid of dots indicate locations of the surface current time series determined from the HF radar data.



5.1 Sedimentological and oceanographic setting

From the sedimentological point of view, the area located offshore the present Lido inlet is made up of well-sorted sand, with the exception of the ebb-tidal channel located along the southern boundary of the inlet, where shelly gravel lag is predominant. In this area, the maximum scour occurs, whereas sand is moved largely in suspension [Amos *et al.*, 2005]. The proximal part of the ebb-tidal delta is composed almost entirely of fine sand, sourced from one of the channels within the Lagoon, i.e. Treporti Channel through the Lido inlet, as also shown by Umgiesser *et al.*'s models [2005]. Northeast of the ebb-tidal delta an area of fine-grained (mud) sediments has been identified, and it possibly reflects the plume sedimentation of the Rivers Piave and Tagliamento [Gazzi *et al.*, 1973; Carbognin, 1992].

The tides are responsible for more than 90 % of the total current variability in the inlet, where the maximum current amplitude may reach 1.5 m s⁻¹. The water flux, estimated from the bottom-mounted ADCP (Acoustic Doppler Current Profiler) in the entrance of the Lido inlet [Gačić *et al.*, 2004] shows an amplitude of about 8000 m³ s⁻¹, in terms of both inflow and outflow volume transport, mainly due to the tidal currents (diurnal and semi-diurnal

components). Recent surface flow monitoring has been conducted by the system of the HF radar antennas [Kovačević *et al.*, 2004] in a 15 km wide coastal strip in front of the Lagoon littoral (Fig. 44). The tidal influence from the inlets seems to vanish rapidly: the maximum 1.5 m s⁻¹ flow recorded within the inlet reduces to several cm/s within a 3-4 km distance from the coast [Gačić *et al.*, 2004, Kovačević *et al.*, 2004]. The maximum values in the kinetic energy (30 cm²s⁻²) are recorded at a distance of about 2 km from the Lido's northern jetty.

5.2 Results

One seismic profiles was chosen as representative for the study area (Fig. 45). The seismic profile VE113 has been acquired in a direction orthogonal to the coast and is located just offshore the Lido inlet.

In the study area, the characteristics of the Late Pleistocene stratigraphic sequence are frequently masked by the sea-floor multiple and by the occurrence of a semi-transparent facies. In general, the Late Pleistocene unit is constituted of sub-horizontal, low amplitude reflectors, interpreted as representing an aggrading floodplain and fluvial channel fills accumulated during decreasing eustatic sea-level [Zecchin *et al.*, in press].

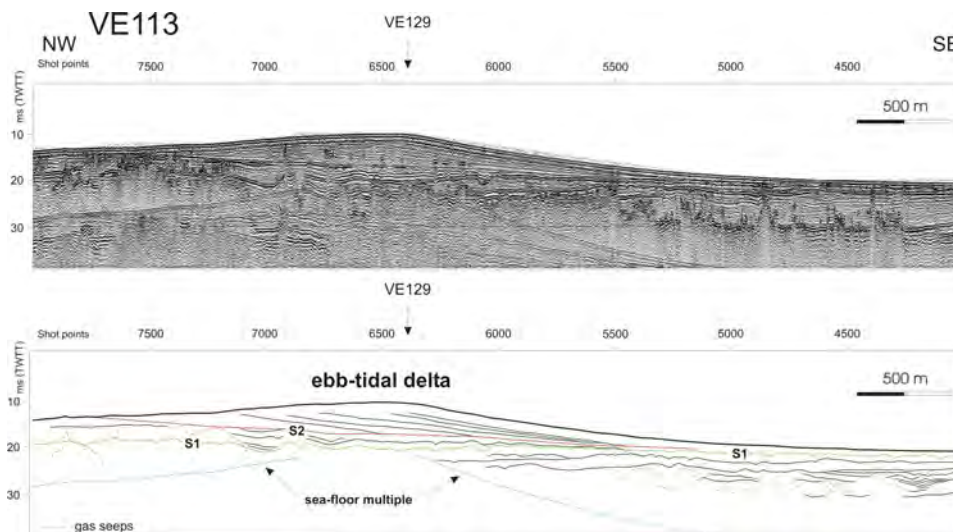


Fig 45 – Part of the seismic profile VE113 acquired orthogonal to the coast, just outside of the Lido entrance. The internal characters of the ebb-tidal delta, consisting of thinly stratified, seaward dipping clinoforms, downlapping onto the S2 unconformity, are identifiable.

The upper boundary of the Pleistocene sequence is marked by the unconformity S1, which is an almost continuous horizon, that progressively deepens in a landward direction.

Above the S1 reflector, Unit 1, represents the oldest unit within the Holocene sequence. Offshore the Lido inlet, it reveals an almost constant thickness of about 1 to 3 m in a direction parallel to the coastline whereas it progressively thins seaward.

The upper boundary of Unit 1 is the S2 reflector, that represents a regional unconformity underlying Unit 2. Such a horizon is characterized by a very regular morphology and gently deepens towards the sea. It corresponds to an erosional surface, as testified by frequent truncation of the underlying reflectors. It has been interpreted as a ravinement surface [Zecchin *et al.*, in press],

scoured by waves and currents that formed during the sea level high stand, following the Flandrian transgression.

The ebb-tidal delta developed within Unit 2. This body is about 8 km long and a maximum of 4 km wide. Internally, it is constituted of low to medium amplitudes, seaward dipping reflectors, downlapping onto the unconformity S2, which lies at depths of 14-20 ms (Fig. 46).

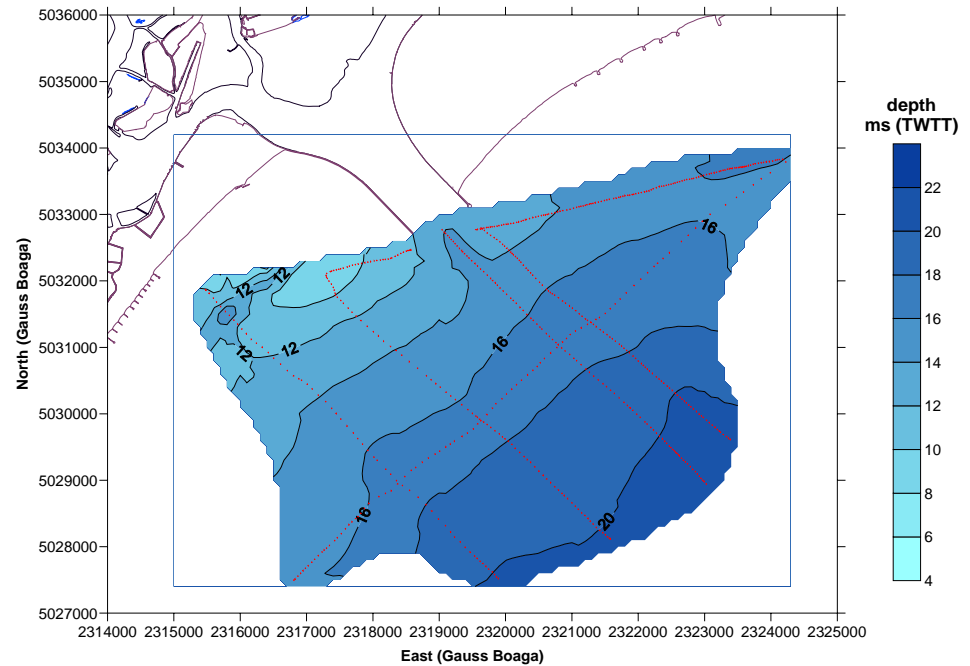


Fig 46 – Map showing the depth of the ebb-tidal delta lower boundary, i.e. unconformity S2.

On the seismic profiles collected orthogonal to the coast, the ebb-tidal delta is imaged as a convex-upward body, particularly well developed offshore the Lido inlet (Fig. 45). It appears to be slightly asymmetric, with the seaward flank being steeper than the landward one. Clinoforms pinch out against the unconformity S2 in the seaward direction. In the cross-section, parallel to the coast, the ebb-tidal delta reveals also an asymmetric profile, with the northeastern flank being slightly deeper than the southwestern one. Clinoforms appear to downlap at gentle angles (about 0.05°) on the unconformity S2 in both the northern and southern direction, although within the northern flank reflector truncation at the sea floor is recognizable in places. The direction of the progradation is toward SE.

The isopach map reveals that the maximum thickness of the ebb-tidal delta deposits (about 6 m) occurs just offshore the Lido inlet (Fig. 47), but also that they are distributed approximately in a E-W direction. Just offshore the northern sector of the Lido inlet entrance, sediment accumulation, about 3 m thick has been recorded. It is separated from the main delta lobe by a depressed area, almost E-W oriented. It is suggested that this feature represents a branch or the seaward continuation of the main ebb channel (see also fig. 4.1 of Amos *et al.* [2005]), that has been artificially dredged, in order to preserve the navigation through the Lido inlet.

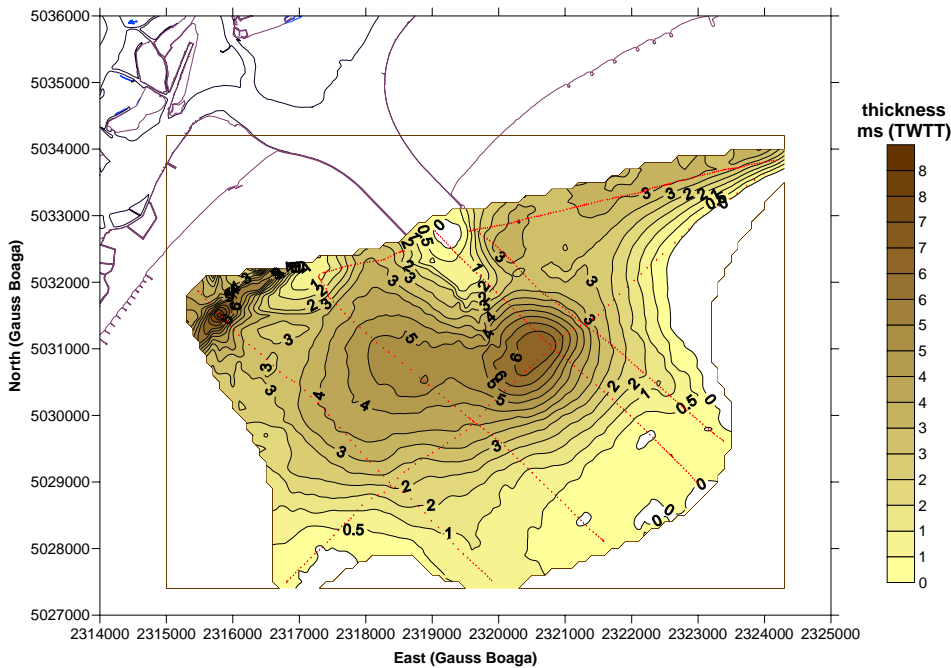


Fig 47 – Isopach map showing the thickness of the sediments constituting the ebb-tidal delta. The maximum value has been recorded at a distance of about 2 km from the mouth of the Lido inlet.

5.3 Discussion

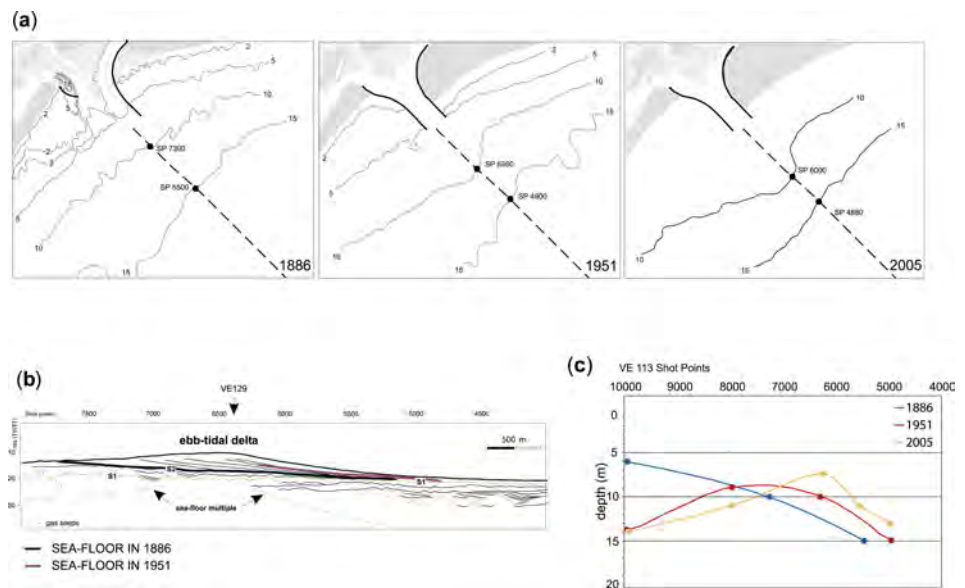
The seismostratigraphic analysis performed on the seismic profiles revealed that the seismic facies representing the ebb-tidal delta deposits is rather homogenous throughout, being represented by thinly stratified, seaward and southwestward dipping clinoforms. Such characteristics, together with a good penetration and resolution of the seismic signal within the delta deposits, led us to hypothesize that almost the entire sediment body is constituted by dominant fine-grained sediments, i.e. fine sand, as recorded by the superficial sedimentological analyses [Amos *et al.*, 2005].

Several boreholes up to a depth of 25 m have been performed all along the Lido littoral around the 70's [Gatto, 1980]. Analyses performed on hundreds of sediment samples led to the reconstruction of the main phases of the Lido littoral evolution during the last 30 000 years [Gatto, 1980, 1984; Tosi 1994a,b; Bonardi and Tosi, 1994; Bonardi *et al.*, 1997]. However no core data were collected offshore the inlet and thus the lithological characterization and the age of the ebb-tidal delta are still speculative. Nonetheless a possible interpretation regarding the time of the initial growth stage of the Lido inlet ebb-tidal delta is proposed. This interpretation is based mainly on the analysis of historical bathymetric maps compiled since the end of 19th century. This comparison reveals that the Lido inlet underwent profound variations as a consequence of the strong and persistent efforts spent to preserve navigable ways through the inlet from the silting since 1300 AD [Colombo, 1970].

The lower boundary of the ebb-tidal delta corresponds with the S2 unconformity seen on the seismic data, that has been interpreted as a wave ravinement surface, separating paralic from shallow-marine deposits, recording highstand conditions during the Holocene. It is suggested that in the area of the Lido inlet, a prolonged period of sediment starvation possibly persisting until very recent

Fig 48 – Comparison between the seismostratigraphy and the historical bathymetric maps, related to three different periods: 1886, when the first northern jetty was constructed; 1951, when the southern jetty was built; 2005, when the OGS seismic survey was carried out. (a) The progressive seaward migration of the -10 m isobath through time is highlighted, based on the comparison between the seismic profiles VE113 (indicated by the dashed line) and the bathymetric contours. SP: VE113 Shot Points. (b) Line drawing of the seismic profile VE113, where the position of the sea-floor in 1886 and in 1951 is indicated. (c) Bathymetric profiles highlighting the progressive seaward migration of the ebb-tidal delta through time.

times, occurred after the S2 formation. Historical bathymetric maps dating to 1886 AD reveal that the unconformity S2 approximately corresponds to the sea-floor at that time (Fig. 48), suggesting that the present ebb-tidal delta formed at around the end of 19th century. In fact, at this time, the building of the first, northern jetty at the Lido inlet possibly caused strong variations in the lagoon dynamics and, above all, in the seaward sediment dispersion.



The ebb-tidal delta formed offshore the Lido inlet then represents a very recent feature compared to the general evolution of the Venice Lagoon. Moreover, around the middle of 20th century, the building of the southern jetty was carried out and channels feeding the lagoon were continuously dredged in order to preserve the lagoon environment. This probably led to a progressive increase in the sediment transport from the lagoon interior toward the sea and thus to the seaward migration of the ebb-tidal delta through time (Fig. 49).

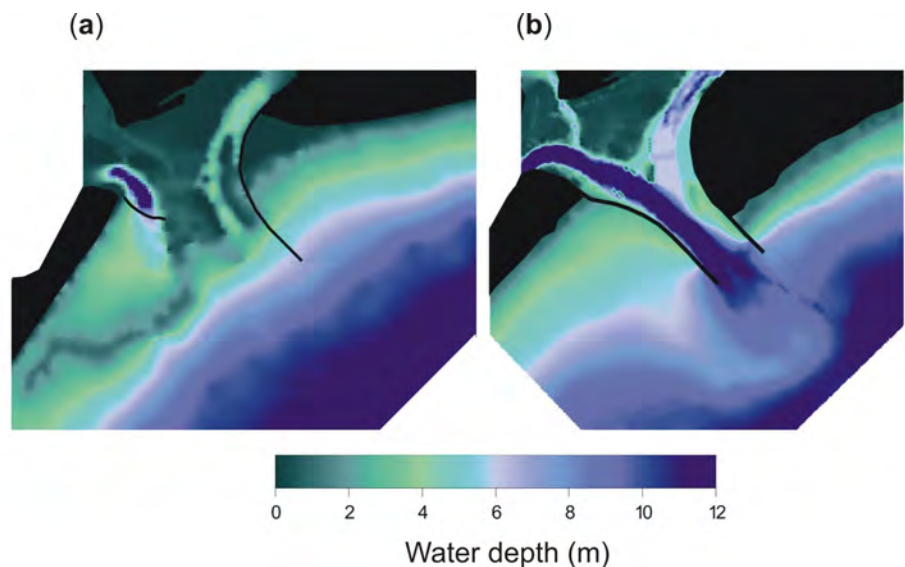


Fig 49 – Bathymetric maps related to the 1886 (a) and to the “recent” (b) bathymorphologic settings in the study area, the latter compiled on the basis of bathymetric data collected from 1951 to 1970.

The Lido inlet ebb-tidal delta was deposited as a response to net transport of fine sand from the lagoon through the inlet, as also suggested by Amos et al.

[2005]. This is also testified by the distribution of the sediments, as shown by the isopach map, recording the maximum delta thickness (6 m) just facing the Lido inlet.

6 Conclusions

All the previous seismic surveys in the Venice lagoon have been carried out along the ship canals [Tosi *et al.*, 2007a,b]. Nevertheless the ship canals are scarcely representative of the recent sedimentation because they represent a very small portion of the entire lagoon and they are frequently dredged.

An ad hoc boat particularly suitable for very shallow water was acquired, i.e the CORILA Aretusa. The criteria followed to choose the boat have been the draught (less than 50 cm), the facility to install the seismic gear, the level of noise produced during the low speed steaming, the capability to operate also in poor weather conditions and finally the budget. Based on these criteria, we have chosen a Saver Fisher 22, 6.75m length and 2.48m breadth, with a carry capability of 7 passengers and with a 140 Hp, four stroke engine.

The Aretusa was implemented with advanced instrumentation for very high resolution seismic survey capable to distinguish layers of a few centimeter thick, in 0.5-1 m water depth and able to investigate subsoil down to 30-40 m deep.

The seismic tools adopted for the survey consisted in a two channel, 24 bit acquisition system integrated with the GPS receiver and an impulsive seismic source (boomer) with a band amplitude between 200 and 9000 Hz. The system successfully operated up to 50 cm of water depth.

After a careful evaluation of the lagoon setting, the new surveys were carried out in four areas, representative of specific themes in the recent evolution of the lagoon: the *southern lagoon*, the *Lido and Chioggia inlets*, the *shelf off the Lido inlet*.

About 400 Km of new seismic lines, about 300 km of seismic data collected in the framework of previous surveys and a number of selected data and information regarding multidisciplinary analyses of samples from cores [Tosi *et al.*, 2007a,b] allowed the characterization of the seismic-stratigraphic and sedimentary setting that pointed out the reconstruction of the Late Pleistocene and Holocene (about last 30,000 years) sequences with a detail that has never been reached in the past.

The *southern lagoon*. In this area the thickness of the Holocene sediments is the highest of the entire lagoon (up to 22 m). Based on the new seismic data, it has been possible, for the first time, to image and map the three main phases that characterize the formation and the evolution of the lagoon: the marine ingression between 10,000 and 6,000 years B.P. that produce the submersion by the Adriatic sea of the previous alluvial plane, the following high stand of the sea level, that records the predominance of the sediment supply from rivers and the progressive advance of the coastline toward the sea; and finally the predominance of the erosion and exportation of sediment from the lagoon, consequence of the rivers diversion operated by humans since historical time.

These distinct phases are associated to sedimentary deposits with different geotechnical, sedimentological and geochemical characteristics. They play different roles in the erosion process of the sea floor and in the hydrogeological regime, like for example the sub-merged littoral belts, already recognized from the bathymetric surveys, but much better defined in the new seismic images or the paleo-channel network, filled by more recent sediments.

An important observation is that relevant volumes of gas seeps have been detected by the seismic images that may have important impacts in the ecology of the entire lagoon.

The *Lido and Chioggia inlets*. These two areas underwent important human interventions in the most recent years. The thickness of the recent sediments in the Lido inlet shows a relevant asymmetric distribution, with more than 12 m near the northern side of the inlet and absence of sediment in the southern side. The setting of the Chioggia inlet is exactly the opposite: the higher thickness has been measured in the southern side (up to 7 m) while the sediment are eroded or not deposited on the northern side of the inlet.

The *shelf off the Lido inlet*. Seismic grid off the Lido inlet detected and characterized a wedge-shaped deposit that has been interpreted as an ebb-tidal delta, produced by the erosion of sediment in the lagoon and their exportation across the inlet by the tide fluxes. The internal geometry and the elongate shape of the ebb-tidal delta testify the interplay between the tide and the North Adriatic along-shore current. Based on the comparison between maps of the ebb-tidal delta produced by the seismic survey and some historical bathymetric maps, we calculated a depositional rate of 5 cm/year for the last 120 year.

Acknowledgments

This study was performed in the frame of the CORILA Research Programme 2004-2006 - Subproject 3.16 "New very high resolution seismic methods in shallows to study the Venice lagoon subsoil". CH43 seismic line was made available by CARG Project (APAT - Regione del Veneto) and bathymetric data by Sistema Informativo of Venice Water Authority.

References

- Allen, G.P., Posamentier, H.W., 1993. Sequence stratigraphy and facies model of an incised valley fill: the Gironde estuary, France. *J. Sed. Petrol.* 63, 378-391.
- Amorosi, A., Centineo, M.C., Colalongo, M.L., Pasini, G., Sarti, G., Vaiani, S.C., 2003. Facies architecture and latest Pleistocene-Holocene depositional history of the Po delta (Comacchio area), Italy. *J. Geol.* 111, 39-56.
- Amorosi, A., Centineo, M.C., Colalongo, M.L., Fiorini, F., 2005. Millennial-scale depositional cycles from the Holocene of the Po Plain, Italy. *Marine Geology* 222-223, 7-18.
- Amos, C. L., Helsby, R., Ungiesser, G., Mazzoldi, A., Tosi, L. 2005: Sand

transport in northern Venice Lagoon. In Campostrini, P., editor, Scientific research and safeguarding of Venice (CORILA Research Program 2001-2003), La Garangola, Padova, Italy, 369-383

Amos C.L., Helsby R., Thompson C.E.L., Villatoro M., Venturini V., Manca E., Mazzoldi A., Tosi L., 2006. The origin of sand in Venice Lagoon the next step. In: Campostrini P. (ed.) - Scientific Research and Safeguarding of Venice 2005. CORILA Research, Research Program 2004-2006, Multigraf Industria Grafica Editrice, Spinea, Venezia, 429-454.

Bhattacharya, J.P., 2006. Deltas. In: Posamentier, H.W., Walker, R.G. (Eds.), Facies Models Revisited. SEPM Spec. Publ., vol. 84, pp. 237-292.

Bonardi, M., Tosi, L., 1994. I sedimenti tardo-quadernari del cordone litoraneo della Laguna di Venezia: le sabbie. CNR, Ist. Stud. Din. Gr. Masse, Tech. Report 184, 1-56.

Bonardi, M., Tosi, L., 1995. Caratterizzazione e differenziazione mineralogica dei livelli sabbiosi tardo-quadernari del litorale veneziano. *Il Quadernario* 8, 315-322.

Bonardi, M., Canal, E., Cavazzoni, R., Serandrei Barbero, R., Tosi, L., Galgaro, A., Giada, M., 1997. Sedimentological, archaeological and historical evidences of paleoclimatic changes during the Holocene in the Lagoon of Venice (Italy). *World Res. Rev.* 9, 435-446.

Brambati, A., Carbognin, L., Quaja, T., Teatini, P., Tosi, L., 2003. The Lagoon of Venice: geological setting, evolution and land subsidence. *Episodes* 26, 264-268.

Bonardi M., Tosi L., 1997. Evidence of climatic variations in Upper Pleistocene and Holocene sediments from the Lagoon of Venice (Italy) and the Yellow Sea (China). *World Resource Review*, 9(1): 101-112.

Bonardi M., Percival J., Tosi L., 1997. The compositional Relation of Selected Clay Sediments to Late Pleistocene-Holocene Depositional Environments from Italy and China. *Clay for our future*, Edited by H.Kodama, A.R. Mermuth, J.K.Torrance, pp. 767-774, Ottawa, Canada, 1999.

Bonardi M., Tosi L., 2000a. Studio mineralogico dei sedimenti sabbiosi tardo-pleistocenici ed olocenici del litorale veneziano. Istituto Veneto di Scienze Lettere ed Arti, *La Ricerca Scientifica Per Venezia, Il Progetto Sistema Lagunare Veneziano Modellistica del Sistema Lagunare, Studio di Impatto Ambientale*, 2(2): 961-966.

Bonardi M., Tosi L., 2000b. Studio sedimentologico di un livello di argilla sovraconsolidata sottostante il litorale veneziano. Istituto Veneto di Scienze Lettere ed Arti, *La Ricerca Scientifica Per Venezia, Il Progetto Sistema Lagunare Veneziano, Modellistica del Sistema Lagunare, Studio di Impatto Ambientale*, 2(2): 952-960.

Bonardi M., Tosi L., Rizzetto F., 2004. Mineralogical characterization of the Venice Lagoon top sediments. In: Campostrini P. (ed.) - Scientific Research and

Safeguarding of Venice. CORILA Research Program 2001-2003. La Garangola, Padova, 2: 145-155.

Bonardi M., Breda A., Bonsembiante N., Tosi L., Rizzetto F., 2005. Spatial variation of surficial sediment characteristics of the Lagoon of Venice, Italy. In: Scientific Research and Safeguarding of Venice. CORILA Research Program 2001-2003. Ed. P. Campostrini, Vol. III, 131-144.

Bonardi M., Tosi L., Rizzetto F., Brancolini G., Baradello L., 2006. Effects of climate changes on the Late Pleistocene and Holocene sediments of the Venice Lagoon, Italy. *Journal of Coastal Research*, SI 39, 279-284.

Brancolini G., Tosi L., Rizzetto F., F., Donda F., Baradello L., 2005. The unconformity at the Pleistocene-Holocene boundary in the Venice coastal area (Italy). *Geitalia 2005*, Spoleto, 21-23 settembre 2005, Epitome, 1: 253.

Brancolini G., Tosi L., Rizzetto F., Donda F., Baradello L., Nieto D., Fanzutti F., Wardell N., Teatini P., Amos C., Bonardi M., 2006. New very high resolution seismic surveys in shallow water to study the subsurface in the Venice Lagoon. In: Campostrini P. (ed.) - Scientific Research and Safeguarding of Venice 2005. CORILA Research, Research Program 2004-2006, Multigraf Iindustria Grafica Editrice, Spinea, Venezia, 417-427.

Brancolini, G., Tosi, L., Baradello, L., Bratus, A., Donda, F., Rizzetto, F., Zecchin, M., 2006. Preliminary results of the high resolution seismic surveys in the Venice lagoon. In: Campostrini P. (Ed.), Scientific Research and Safeguarding of Venice. Corila, Res. Progr. 2004-2006 - 2005 results, vol. 5, pp. 333-346.

Carbognin, L., 1992. Evoluzione naturale e antropica della Laguna di Venezia. *Mem. Descr. Carta Geol. It.* 42, 123-134.

Carbognin, L., Cecconi, G., Ardone, V., 2000. Interventions to safeguard the environment of the Venice Lagoon (Italy) against the effects of land elevation loss. In: Carbognin, L., Gambolati, G., Johnson, A.I. (Eds.), *Land Subsidence. Proc. Sixth Int. Symp. Land Subsidence*, Ravenna (Italy), La Garangola, Padova (Italy), vol. 1, pp. 309-324.

Cattaneo, A., Steel., R.J., 2003. Transgressive deposits: a review of their variability. *Earth-Sci. Rev.* 62, 187-228.

Colombo, P. 1970. Osservazioni sul regime di alcuni tratti del litorale occidentale dell'alto Adriatico. *Scritti in onore del Prof. Guido Ferro*, Università di Padova, 23-62.

Dalrymple, R.W., Zaitlin, B.A., Boyd, R., 1992. Estuarine facies models: conceptual basis and stratigraphic implications. *J. Sedim. Petrol.* 62, 1130-1146.

Davies, R. A. and Hayes, M. O. 1984. What is a wave-dominated coast? *Marine Geology* 60, 313-329.

Donda F., Brancolini G., Tosi L., Kovacevic V., Baradello L., Gacic M. and Rizzetto F. The ebb-tidal delta of the Venice Lagoon (Italy). The Holocene, in

press

Demarest, J.M., Kraft, J.C., 1987. Stratigraphic record of Quaternary sea levels: implications for more ancient strata. In: Nummedal, D., Pilkey, O.H., Howard, J.D. (Eds.), *Sea-level Fluctuation and Coastal Evolution*. SEPM Spec. Publ., vol 41, pp. 223-239.

Fitzgerald, D. M., Kulp, M., Penland, S., Flocks, J. and Kindinger, J. 2004. Morphologic and stratigraphic evolution of muddy ebb-tidal deltas along a subsiding coast: Barataria Bay, Mississippi River delta. *Sedimentology* 51, 1157-1178.

Gačić, M., Mancero Mosquera, I., Kovacevic, V., Mazzoldi, A., Cardin, V., Arena, F. and Gelsi, G. 2004. Temporal variations of the water flow between the Venetian lagoon and the open sea. *Journal of Marine Systems* 51, 33-47.

Gatto, P., 1980. Il sottosuolo del litorale Veneziano. CNR, Ist. Stud. Din. Gr. Masse, Tech. Report 108, 1-19.

Gatto, P., 1984. Il cordone litoraneo della laguna di Venezia e le cause del suo degrado. *Ist. Veneto Sci. Lett. Arti, Rapporti e Studi* 9, 163-193.

Gatto P., Previatello P., 1974. Significato stratigrafico, comportamento meccanico e distribuzione nella Laguna di Venezia di un'argilla sovraconsolidata nota come "Caranto". C.N.R. - Lab. per lo Studio della Dinamica delle Grandi Masse, Venezia, Rapporto Tecnico 70, 45 pp.

Gazzi, P., Zuffa, G. G., Gandolf, G. and Paganelli, L. 1973. Provenienza e dispersione litoranea delle sabbie delle spiagge adriatiche fra le foci dell'Isonzo e del Fogilia: inquadramento regionale. *Memorie della Società Geologica Italiana* 12, 1-37.

Hayes, M. O. 1980. General morphology and sediment patterns in tidal inlets. *Sedimentary Geology* 26, 139-156.

Komar, P. D. 1996. Tidal-Inlet processes and morphology related to the transport of sediments. *Journal of Coastal Research* 23, 23-45.

Kovačević, V., Gačić, M., Mancero Mosquera, I., Mazzoldi, A. and Martinetti, S. 2004. HF radar observations in the Northern Adriatic: surface current field in front of the Venetian Lagoon. *Journal of Marine Systems* 51, 95-122.

Krueger, J. C. and Healy, R. 2006. Mapping the morphology of a dredged ebb tidal delta, Tauranga Harbour, New Zealand. *Journal of Coastal Research* 22, 720-727.

Matteotti, G., 1962. Sulle caratteristiche dell'argilla precompressa esistente nel sottosuolo di Venezia-Marghera. *Notiz. Ordine Ingegneri Prov. Padova* 6(12), 30-40.

McClennen, C.E., Housley, R.A., 2006. Late-Holocene channel meander migration and mudflat accumulation rates, lagoon of Venice, Italy. *J. Coastal Res.* 22, 930-945.

Mozzi, P., Bini, C., Zilocchi, L., Becattini, R., Mariotti Lippi, M., 2003.

Stratigraphy, palaeopedology and palynology of late Pleistocene and Holocene deposits in the landward sector of the lagoon of Venice (Italy), in relation to the Caranto level. *Il Quaternario* 16(1bis), 193-210.

Nummedal, D., Swift, D.J.P., 1987. Transgressive stratigraphy at sequence-bounding unconformities: some principles derived from Holocene and Cretaceous examples. In: Nummedal, D., Pilkey, O.H., Howard, J.D. (Eds.), *Sea-level Fluctuation and Coastal Evolution*. SEPM Spec. Publ., vol. 41, pp. 241-260.

Rizzetto F., Tosi L., Bonardi M., Gatti P., Fornasiero A., Gambolati G., Putti M., Teatini P., 2002. Geomorphological evolution of a part of the southern catchment of the Venice Lagoon (Italy): the Zennare Basin. In: Campostrini P. (ed) - *Scientific research and safeguarding of Venice*. CORILA Research Program 2001 Results, Istituto Veneto di Scienze Lettere ed Arti, La Garangola, Padova: 217-228.

Rizzetto F., Tosi L., Carbognin L., Bonardi M., Teatini P., 2003. Geomorphological setting and related hydrogeological implications of the coastal plain south of the Venice Lagoon (Italy). In: Servat E., Najem W., Leduc C. & Shakeel A. (eds) - *Hydrology of Mediterranean and Semiarid Regions*. IAHS Publication, 278: 463-470.

Rizzetto F., Tosi L., Bonardi M., Serandrei Barbero R., Donnici S., Toffoletto F., 2005. The Geological Map of Italy: Map Sheets 128 "Venezia" and 148-149 "Chioggia-Malamocco". *Geitalia 2005*, Quinto Forum Italiano di Scienze della Terra, Spoleto, 21-23 settembre 2005, *Epitome*, 1: 70-71.

Swift, D.J.P., 1968. Coastal erosion and transgressive stratigraphy. *J. Geol.* 76, 444-456.

Tosi L., 1993. *Caratteristiche geotecniche del sottosuolo del litorale veneziano*. Consiglio Nazionale delle Ricerche - Istituto per lo Studio della Dinamica delle Grandi Masse, Venezia, *Rapporto Tecnico* 171: 34 pp.

Tosi L., 1994a. *Rapporto e prime interpretazioni sulle analisi paleontologiche condotte su campioni tardo-quadernari del sottosuolo del litorale veneziano*. Consiglio Nazionale delle Ricerche-Istituto per lo Studio della Dinamica delle Grandi Masse, Venezia, *Rapporto Tecnico* 182: 52 pp.

Tosi L., 1994b. *I sedimenti tardo-quadernari dell'area litorale veneziana: analisi delle caratteristiche fisico-meccaniche*. *Geologia Tecnica ed Ambientale*, 2: 47-60.

Tosi L., 1994c. *L'evoluzione paleoambientale tardo quadernaria del litorale veneziano*. *Il Quaternario - Italian Journal of Quaternary Sciences*, Vol. 7, fasc. 2, 589-596.

Tosi L., Brancolini G., Baradello L., Donda F., Rizzetto F., 2006. Very high resolution seismic surveys in the lagoon and gulf of Venice shallow waters. *Proceedings of the 5th European Congress on Regional Geoscientific Cartography and Information Systems*, Barcellona, June 13th to 16th, 2006, vol. 2, 156-158.

Tosi L., Rizzetto F., Bonardi M., Donnici S., Serandrei Barbero R., Toffoletto F., 2007a. Note illustrative della Carta Geologica d'Italia alla scala 1:50.000. Foglio 128 - Venezia. APAT, Dip. Difesa del Suolo, Servizio Geologico d'Italia, Casa Editrice SystemCart, Roma, 164 pp.

Tosi L., Rizzetto F., Bonardi M., Donnici S., Serandrei Barbero R., Toffoletto F., 2007b. Note illustrative della Carta Geologica d'Italia alla scala 1:50.000. Foglio 148-149 - Chioggia-Malamocco. APAT, Dip. Difesa del Suolo, Servizio Geologico d'Italia, Casa Editrice SystemCart, Roma, 162 pp.

Umgiesser, G., Ferrarin, C. De Pascalis, F. and Amos, C. 2005. Modelling sand transport in a canal system, northern Venice Lagoon. In Campostrini, P., editor, Scientific research and safeguarding of Venice (CORILA Research Program 2001-2003), La Garangola, Padova, Italy, 383-390.

Zecchin M., Brancolini G., Donda F., Tosi L., Rizzetto F., Baradello L., 2006a. Sedimentary features and seismic stratigraphy of the Late Pleistocene and Holocene deposits in the Venice Lagoon. Proceedings of Adria 2006 - International Geological Congress on the Adriatic Area, Urbino, June 19th-20th, 2006, 120-121.

Zecchin M., Brancolini G., Donda F., Rizzetto F. Tosi L., 2006b. Sequence stratigraphy of Holocene deposits in the Venice Area, based on high-resolution seismic profiles. In: *Thirty years of Sequence Stratigraphy: Applications, Limits and Prospects* - 2 October 2006 - Bari – Italy, 81-82

Zecchin M., Brancolini G., Donda F., Rizzetto F. Tosi L., 2006c. High-resolution seismic stratigraphy in the Venice area. GEOSed proceeding, Modena 25-29 Settembre 2006 (ed. Lugli S.), 116.

Zecchin, M., Baradello, L., Brancolini, G., Donda, F., Rizzetto, F., Tosi, L., 2008. Sequence stratigraphy of Holocene deposits in the offshore of Venice based on very high-resolution seismic profiles. *GeoActa*, Special Issue, in press.

RESEARCH LINE 3.17

Transport phenomena in the hydrological cycle: model of substances release in lagoon

FLOW RESISTANCE IN WETLANDS: EXPERIMENTAL INVESTIGATIONS

Anna Chiara Bixio

Dipartimento di Ingegneria Idraulica, Marittima, Ambientale e Geotecnica, Università degli Studi di Padova

Riassunto

Al fine di valutare la resistenza al moto opposta dalla vegetazione a canneto tipicamente presente nelle aree umide del Veneto, è stata costruita una canaletta sperimentale, caratterizzata dalla presenza di vegetazione indisturbata, all'interno dell'area di fitodepurazione di Monselice, e si è proceduto nel corso dell'estate 2006 a varie sperimentazioni finalizzate alla misurazione delle perdite di carico in corrispondenza a diverse condizioni di portate fluenti e tiranti idrici. I risultati, elaborati sia in termini di coefficiente di resistenza di Darcy-Weisbach che in termini di coefficiente di scabrezza di Manning, esprimono valori di resistenza medio - bassi se confrontati con i dati disponibili di letteratura riguardanti altri tipi di vegetazione di area umida.

Abstract

An experimental flume was appositely built up inside the Monselice wetland to evaluate the flow resistance due to typical undisturbed reed-type vegetation in wetlands. During summer 2006, various experimental sessions took place, and head losses were evaluated for different values of flowing discharge and water depth. Results, expressed in terms of both Darcy-Weisbach and Manning's coefficients, are in good agreement with other literature data concerning other types of wetland vegetation.

1 Introduction

Due to its efficacy in phytoremediation processes and its low cost, reed-type vegetation has been widely used in constructed wetlands for water quality improvement and in river restoration projects. However, its application has been based on experience rather than hydraulic principle, and limited knowledge exists concerning the hydraulic resistance properties of reed beds. The accurate determination of flow resistance factors and the proper use of resistance equations is a topic of great importance in wetland project and management, and is essential for computing basic hydraulic parameters, such as depth and velocity, and for modelling the hydrodynamics of the system (Tsihrintzis and Madiedo, 2000).

Experimental published data on flow resistance with real reeds are very limited. Some experiments were performed in laboratory by Meijer and van Velzen (1999) and James et al. (2004), who employed natural reeds placed inside concrete-walls flumes considering variable vegetative densities and alignments.

The lack of field experimental data regarding undisturbed reed vegetation is evident.

For these reasons, in the context of a wide experimental and modelling study of the hydraulic behaviour of wetlands, finalized to the assessment of the effects of wetlands on nutrient release into the Venice lagoon (Bixio et al., 2006; Bixio and Cerni, 2007), it was decided to build up an experimental flume inside a reed-vegetated area of the Monselice wetland, in the province of Padua, Italy.

The aim of the work was the investigation of the hydraulic resistance of undisturbed reed beds, keeping also into account the resistance variation due to seasonal plants growth and decay, with different experimental measurements taken in various periods of the vegetative cycle of plants.

This paper reports the preliminary results of tests performed in the flume during summer 2006.

2 Experiments

The Monselice surface flow wetland (Figure 1) is located in the southern part of Monselice, in the province of Padua, within the territory of the Land Reclamation Consortium Adige Bacchiglione. It has been recently constructed to treat effluents of the local municipal wastewater primary treatment plant. It is about 6 hectares wide, has a mean water depth of 0.8 m and a medium storage volume of 28000 m³. It is made up by 2 independent basins, connected by control gates. Each basin consists of a main channel of variable width and depth with lateral wide flood plains. The wetland is bordered by the Desturo channel, which collects water discharged by the system.

The flood plain areas are populated prevalently by *Phragmites australis* and *Typha latifolia* plants.

Experiments were performed in a 60 m - long by 1.60 m - wide flume with vertical sidewalls located in a flat flood plain area of the wetland, generally unflooded in ordinary functioning conditions of the wetland, close to a little pond which can be easily inundated by opening a gate (Figure 1).

Water is pumped from the pond into the head tank placed at the upstream end of the flume by a centrifugal variable-discharge pump (Figure 3). After flowing into the flume, water is released again into the pond (Figure 4). Once the pumps are turned on, about 20 minutes are required to reach a steady current in the flume.

The walls of the flume were realized employing two rows of wooden boards laying one on the other, supported by wooden piles. All the joints between boards were realized by using silicon rubber, in order to avoid water losses along the walls. The lower boards were opportunely fixed into the ground. A levee was built along the lateral walls by tamping clayey soil with an excavator (Figure 2).

Similar works were executed to build up the trapezoidal head tank, about 3.50 m wide and 3.5 m long. The walls and bottom of the tank were waterproofed by

fixing a double nylon tarpaulin; concrete hollow bricks were employed to build up an internal wall, to damp inlet turbulence and eliminate swirl.

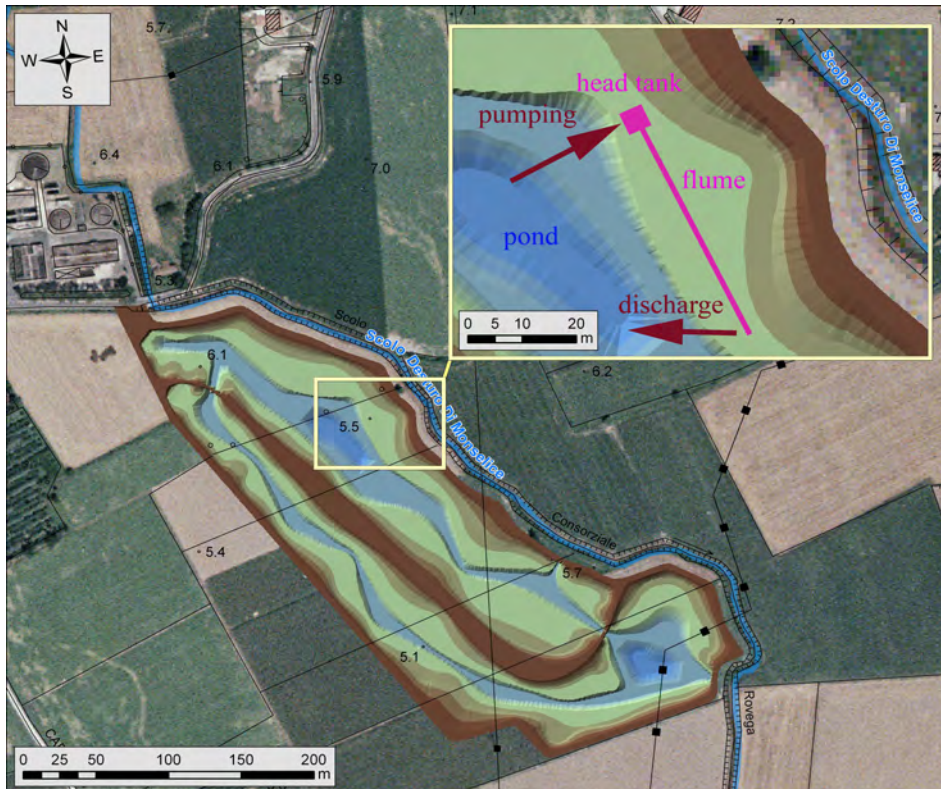


Fig 1 – Monselice wetland: location of the experimental device.

A rectangular sharp-crested weir was placed at the upstream end of the channel to allow measurement of incoming flow rate (Figure 6); free flow conditions at the weir were checked for all test conditions.

An adjustable rectangular weir was positioned at the downstream end of the flume, to control the tail water depth and provide outgoing discharge measurements. This weir was realized by superimposing a variable number of wooden stoplogs on a 20 cm high sill; the upper stoplog was provided of a steel thin-plate weir (Figure 4).

A differential piezometer system (Figure 5) was used to measure water depths at 14 sections of the channel and at one point inside the tank, with a precision of 1 mm. The distance between test sections was 4.5 m. One observation point was placed close to the downstream weir, to provide a water depth measurement for outgoing discharge evaluation. An other observation point, located inside the tank near the upstream weir, allows for incoming discharge evaluation.

Four different downstream level conditions were considered, corresponding to one, two, three and four wooden logs positioned at the downstream weir.



Fig 2 – The experimental flume: building works.



Fig 3 – The pumping station, the head tank, the upstream weir.



Fig 4 – Th adjustable downstream weir, and water discharge into the pond.



Fig 5 – The differential piezometer system.

The water surface profile was measured for each downstream boundary condition at three different flow rates. The desired values of flow rates were equal to 20, 25 and 30 l/s. Due to difficulties in accurate pump regulation, the real values were slightly different.

Test characteristics are summarized in Table 1.

For which concern vegetation characteristics, at the beginning of the flume construction works, in may 2006, reeds were prevalently dry because of the low precipitation and high temperature that characterized spring 2006. The density of dry reeds was high, about 100-200 stems/m²; plants were very thin, with stem diameter varying between 4 and 10 mm, and about 2 m high.

When the flume was built up and water started to flow, there was a rapid growth of new *Phragmites australis* plants, together with *Typha latifolia* and some other herbaceous vegetation inside the flume.

During experiments, which took place during the months of June and July 2006, vegetation characteristics along the flume were analyzed, leading to the identification of three main different vegetative types, characterized by diverse reed density and stage of growth, and by presence of other herbs (Table 2). Dry reeds height was about 2 m, green growing reeds were generally 0.6-1.0 m tall so that they were never submerged by water during experiments. On the contrary, the most of the other herbaceous vegetation was shorter than 0.5 m, and was submerged during some of the tests.

Green reeds had a stem diameter of 5-20 mm. It was not possible to describe geometric characteristics of other herbaceous vegetation, which varied randomly in type and dimensions along the flume.

Test	Downstream level [m]	Flow rate [l/s]
P1	0.3	20.0
P2	0.3	25.0
P3	0.3	29.0
P7	0.4	18.0
P8	0.4	25.0
P9	0.4	29.0
P10	0.5	17.0
P11	0.5	25.0
P12	0.5	27.0
P13	0.6	19.0
P14	0.6	25.0
P15	0.6	30.0

Tab 1 – Tests characteristics.



Fig 6 – Vegetation sampling.

Vegetative type n.	Description
1	dry reed: 165 stems/m ² ; green reed: 80 stems/m ² ; other herbs: many
2	dry reed: 105 stems/m ² ; green reed: 15 stems/m ² ; other herbs: many
3	dry reed: 90 stems/m ² ; green reed: 20 stems/m ² , well growth; other herbs: irrelevant

Tab 2 – Vegetation characteristics.

3 Results

The water surface elevations at each measuring section for each run were determined by the differential piezometer system.

The incoming and outgoing discharges were evaluated thanks to the water surface elevation values given by the first and the last piezometer.

The energy line was then calculated at each section as:

$$H = z + y + \frac{v^2}{2g}$$

where H [m] is energy level, z [m] is bottom elevation, y [m] is flow depth, v [m/s] is mean velocity and g [m²/s] represents gravitational acceleration. Velocity v was calculated starting from measured discharge and water level values.

The energy line slope j was determined by differentiating the energy line H at each section with respect to change in distance x along the flume:

$$j = \frac{dH}{dx}$$

Manning's n [sm^{-1/3}] and Darcy-Weisbach's f [-] for each tract of the flume were then calculated as

$$n = \frac{1}{v} j^{0.5} R_H^{2/3} \quad \text{and} \quad f = \frac{8gR_H j}{v}$$

where R_H is the hydraulic radius of the flow.

The roughness coefficients calculated in this way include in principle both wall and vegetation resistance; since wall friction can be considered negligible if compared with vegetative one, we can assume n and f as exclusively due to

vegetation.

The mean n and f values along the flume calculated for the different tests are plotted against VR_H and Reynolds' number $Re = VR_H/\nu$ (Tsihrintzis and Madiedo, 2000), respectively, in Figures 7 and 8.

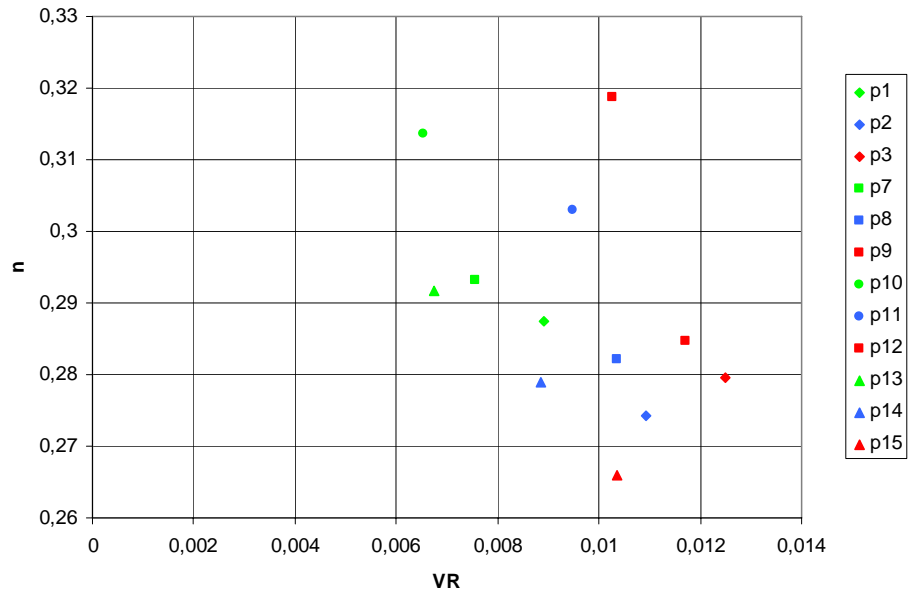


Fig 7 – Calculated values of Manning's n [$s m^{-1/3}$] against the correspondent values of product VR_H [$m^2 s^{-1}$].

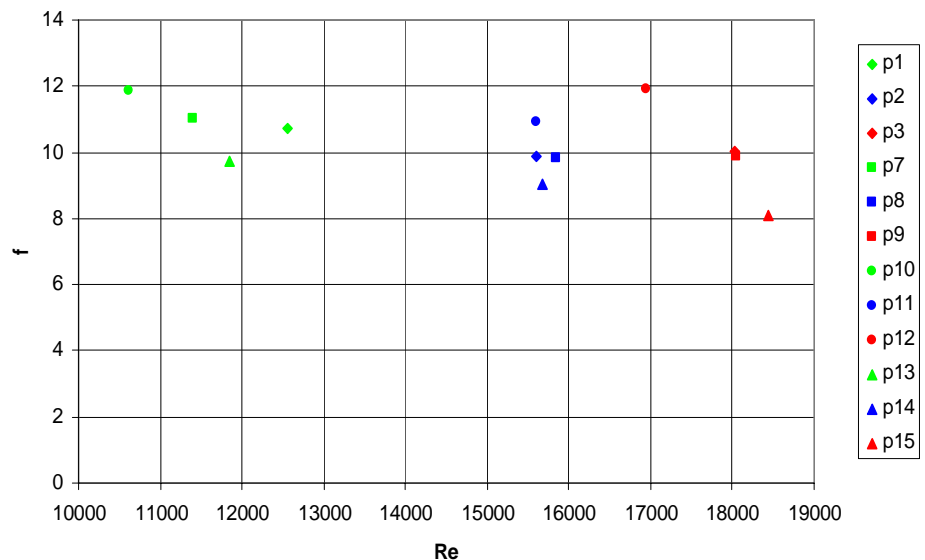


Fig 8 – Calculated values of Darcy-Weisbach's f against the correspondent values of Reynolds number Re .

We can observe that the data cover a range of Reynolds number between about 10000 and 20000; the range of stem Reynolds number ($Re_D = \nu D/\nu$), where D [m] is stem diameter and ν [sm^{-2}] is kinematic viscosity of water, is about 100-800, indicating that all the test runs were in transitional flow regime.

Water depth varies between about 0.30 and 0.60 m, averaged flow velocity

between 0.02 and 0.06 m/s. These low velocity values and limited water depths were chosen to reproduce typical characteristics of flow in wetlands.

During tests, the energy line slope j ranges between 10^{-4} and 10^{-3} , increasing with decreasing downstream water depths and decreasing discharge values.

The calculated Manning's n values result to vary in the range 0.14 – 0.45 s m^{-1/3}; the Darcy-Weisbach's friction factor f varies between 8 and 12.

Manning's n shows a decreasing trend with increasing values of VR_H parameter, and f decreases with increasing Reynolds' numbers. Based on the data, f is related to the Re to the -0.28 power.

This all is consistent to other published data regarding different types of wetland vegetation, as summarized in the study of Tsihrintizis and Madiedo (2000).

The graphs $n - VR_H$ and $f - Re$ by these authors were redrawn in Figures 9 and 10, adding the experimental data collected in Monselice wetland and the experimental points by Meijer and Van Velzen (1999) and James et al. (2004), also concerning reed-type vegetation.

We can observe that our experimental results correspond to low resistance values if compared with other kinds of wetland vegetation, in good agreement with Hall and Freeman experimental results concerning bulrush vegetation (density of 400 stems/m²) and with the "retardance curve B" drawn by Tsihrintizis and Madiedo (2000) to represent low density marsh vegetation.

For which concern the other available data regarding reed-type vegetation, the data by Meijer and van Velzen (1999) express n and f values very similar to our ones, but are characterized by higher VR_H and Re values due to different experimental conditions: those tests with natural reeds were in fact conducted in a concrete-wall laboratory flume, with higher flow rates, between 0.36 and 0.53 m³/s and higher water depths, about 1.2 m. The vegetation density was 256 stems/m², with a medium stem diameter of 5.7 mm.

The experimental points by James et al. (2004), who used harvested reeds, foliated and defoliated, set vertically in a regular rhomboidal pattern inside a concrete test flume, are very spread in the graph, and prevalently express lower resistance values if compared with our data. This is due to the wide range of variation of experimental parameters which were considered, such as the presence or absence of leaves, flow rates varying between 0.0014 and 0.015 m³/s, water depths between 0.04 and 0.35 m.

Conclusions

This paper reports the results of the first set of experiments performed during summer 2006 in a test flume built up inside the Monselice wetland, characterized by typical undisturbed reed-type vegetation consisting mainly of *Phragmites australis* plants.

Starting from measured flow rate, water depth and energy line slope data, vegetation resistance to flow in terms of Manning's n and Darcy - Weisbach's f

was evaluated, and relevant relationships with flow parameters were analyzed.

For the investigated water depth range between about 0.3 and 0.6 m and flow rates of 20, 25 and 30 l/s, the calculated Manning's n values vary between $0.14 \text{ s m}^{-1/3}$ and $0.45 \text{ s m}^{-1/3}$, and the Darcy – Weisbach's friction factor f result in the range 8 - 12. The n coefficient decreases with increasing values of the parameter VR_H and the f friction factor shows a decreasing trend with increasing Reynolds' number. This all well compares with other published data regarding different types of wetland vegetation.

It's interesting to notice that our experimental results correspond to low resistance values if compared with other kinds of wetland vegetation, in good agreement with the "retardance curve B" drawn by Tsihrintzis and Madiedo (2000) which represents low density marsh vegetation.

Other experiments will be performed in the future in different seasons, in order to assess the seasonal variation of flow resistance due to plants growth and decay.

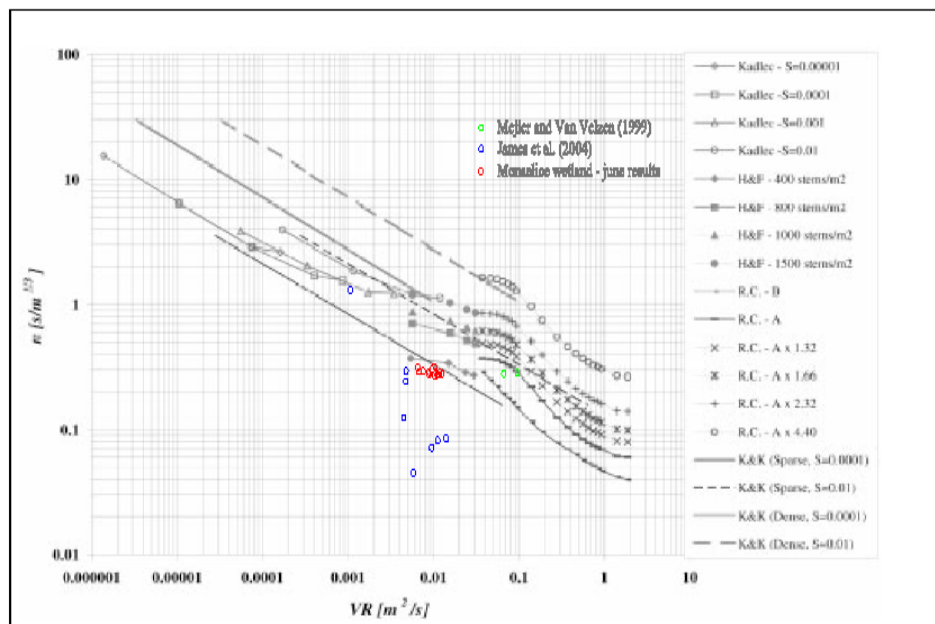


Fig 9 – $n - VR_H$ graph by Tsihrintzis and Madiedo (2000), with Monselice wetland experimental data and reed-vegetation data by Meijer and van Velzen (1999) and James et al. (2004).

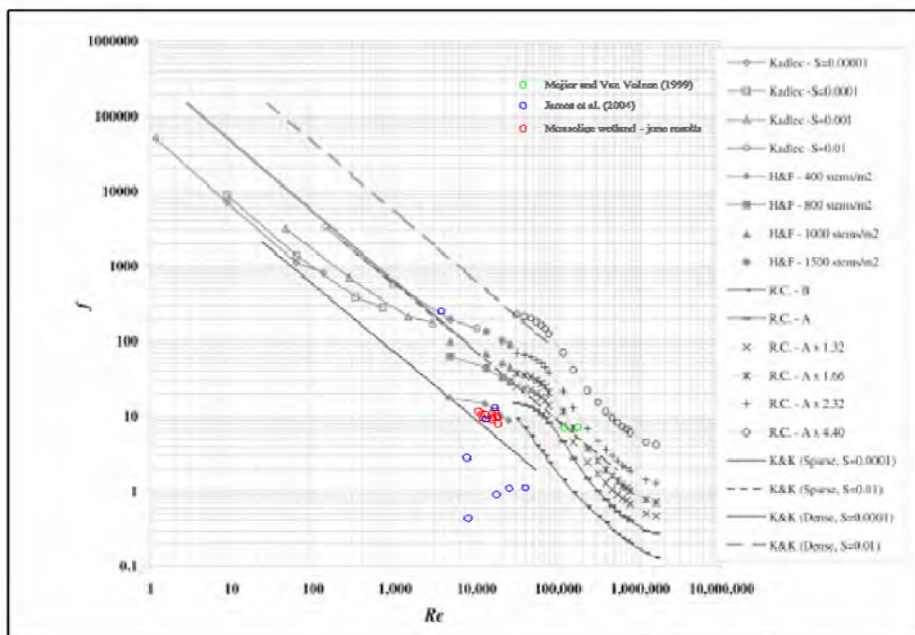


Fig 10 – $f - Re$ graph by Tsihrintzis and Madiedo (2000), with Monselice wetland experimental data and reed-vegetation data by Meijer and van Velzen (1999) and James et al. (2004).

References

ANPA, Linee guida per la ricostruzione di aree umide per il trattamento di acque superficiali. Manuali e linee guida 9/2002.

Bixio, A. C. (2007), Experimental observations of flow resistance through emergent vegetation. Proceedings of 32^o Congress of IAHR, Armonizing the Demands of Art and Nature in Hydraulics, July 2007, Venice, Italy.

Bixio, A. C. and M. Cerni (2007), Mathematical modelling of low-velocity flows in wetlands. Proceedings of annual meeting of CORILA, Venice, 2006.

Bixio, V., A. C. Bixio, M. Cerni, A. Marion and M. Zaramella (2006), "Experimental researches on the hydraulic behaviour of the Ca' di Mezzo in Codevigo wetland", in Proceedings of annual meeting of CORILA, vol. V, Venice, 2005.

Hall, B.R. and G.E. Freeman (1994), Study of hydraulic roughness in wetland vegetation takes new look at Manning's n. The Wetland Research Program Bulletin, 1994, 4, No 1, 1-4.

James C.S., Birkhead A.L., Jordanova, A.A. and O'Sullivan J.J. (2004), Flow resistance of emergent vegetation. Journal of Hydraulic Research, 2004, 42, 4, 390-398.

Jarvela, J. (2004), Flow resistance in environmental channels: focus on vegetation. Helsinki University of Technology Water Resources Publications, TKK-VTR-10, Espoo, 2004.

Jordanova, A.A. and C.S. James and A.L. Birkhead (2006), Practical estimation of flow resistance through emergent vegetation, Water management 159 IssueWM3, pp. 173-181.

Kadlec, R.H. and R.L. Knight, "Treatment wetlands", CRC Press-Lewis Publishers New York, (1996).

Meijer D.G. and van Velzen E.H.,(1999), Prototype-scale flume experiments on hydraulic roughness of submerged vegetation. Proc. 28th International IAHR Conference, Graz, 1999.

Musleh, F.A. and J.F. Cruise (2006) Functional relationships of resistance in wide flood plains with rigid unsubmerged vegetation. Journal of Hydraulic Engineering, vol.132, No.2, 2006.

Nepf, H. M. & E. R. Vivoni 2000. Flow structure in depth-limited, vegetated flow. J. Geophys. Res., 105, No C12, 28547-28557.

Shih, S.F. and G.S. Rahi (1982), Seasonal variations of Manning's roughness coefficient in a subtropical marsh. Trans. ASAE, 1982.

Tsihrintzis, V.A. and E.E. Madiedo, "Hydraulic resistance determination in marsh wetlands", Water Resources Management (2000), 14 (4), pp. 285-309.

RESEARCH LINE 3.18

**Residence times and hydrodynamical
dispersion in the Venice lagoon**

A LONG-TERM MODEL FOR THE GENERATION AND EVOLUTION OF A TIDAL NETWORK

Giacomo Fasolato¹, Chiara Dall'Angelo, Giampaolo Di Silvio¹

1 Dipartimento di IMAGE, Università degli Studi di Padova

Riassunto

La formazione ed evoluzione di una fitta rete di canali a marea sono state simulate applicando un modello morfodinamico a lungo termine di tipo bidimensionale. Il modello qui preso in esame parte da una semplificazione delle equazioni che governano il moto delle onde lunghe in acque basse, simulando l'evoluzione morfologica del fondo a scale temporali di lungo periodo [Fasolato et al. 2004] attraverso la definizione di un'appropriata concentrazione di equilibrio ed un coefficiente di dispersione intermareale [Di Silvio e Padovan, 1998]. Il modello consente di riprodurre la genesi di una laguna a marea e l'evoluzione morfologica del fondo a causa dell'intrusione del mare attraverso le dune litoranee in un bacino schematico. Con l'evolversi dei canali a marea, il sistema tende asintoticamente ad una condizione di quasi-equilibrio caratterizzata apparentemente da una configurazione planimetrica stabile della rete. La struttura e le caratteristiche morfologiche (profondità, dimensione dei sottobacini) dei canali generatasi risultano qualitativamente simili a quelle della laguna di Venezia. E' stato inoltre dimostrato come l'intero bacino lagunare evolva verso un decrescente stato energetico.

Abstract

The branching channel generation in a short tidal basin has been modeled by a long term morphological model based on the notion of long term equilibrium concentration, intertidal diffusion coefficient [Di Silvio, Padovan, 1998] and on the simplification of the two-dimensional shallow water equations [Fasolato et al., 2004]. The model consents to reproduce, in a schematic lagoon, the network ontogeny and the morphological bottom evolution long-term scale as a consequence of a breaching of the littoral dune line. As the channels evolve, the system tends asymptotically toward a quasi-equilibrium condition apparently characterized by a stable planimetric configuration of the channel network. Numerical channel structures and their watersheds are qualitatively similar to the Venice Lagoon's ones. It has been also shown that the simulated lagoon embayment tends to develop towards an increasingly lower state of energy.

1 Introduction

Channels, shoals and marshes are important features in estuaries and tidal inlets. The tidal network controls the hydrodynamics and sediment exchange of the entire tidal basin while the intertidal areas are of great ecological

importance, being the feeding and breeding grounds for a varieties of species.

Human action (hydraulic constructions or dredging activities) and long term natural events (sea level rise or subsidence) can alter and change the natural equilibrium of the morphological and hydraulic tidal environment, therefore it is important to understand and predict the morphodynamic behavior of these complex systems. Recent developments for automatic extraction of the tidal channel network from digital terrain maps [Fagherazzi et al., 1999] have improved the possibilities to study these systems [Rinaldo et al., 1999a, 1999b]. Using this technique, it was shown that tidal networks exhibit a great variety of geometrical and topological forms, and that channels in different tidal basins exhibit quite different overall scaling characteristics [Fagherazzi et al., 1999; Rinaldo et al., 1999a].

At the same time, typical timescales for adjustment of the channel/shoal pattern after completion of major works are in the range of decades but in the case of environmental or geological changes can go over centuries [de Vriend, 1996].

Object of the present paper is the morphological evolution of tidal systems (with all their components of channels, shoals and marshes), initiated by a persistent large breach through the littoral dunes protecting the adjacent coastal plain. The evolution may be affected by possible changes of the forcing action (e.g. sea level rise) as well by anthropogenic action (dredging and construction).

The conventional approach to lagoon morphodynamic is based on the repeated application of "tidal scale" models [Marciano, 2005]. It is interesting, however, exploring the possibilities offered by long-term morphological models, defined also as *conceptual models*, that consent to simulate and reproduce the long term (centuries) system's evolution with a relatively light computational effort.

Conceptual models filter the morphological fluctuations due to short term components and reproduce all the processes (with time-averaged values over a year or a number of years).

They incorporate many physical (and even biological) processes via a number of algebraic or differential equations containing semi-empirical coefficients, which can be calibrated by direct comparison with experiments or with specific short-term models.

The simplified two-dimensional conceptual model presented here, simulates the long term contributions of tidal currents and wind waves to the sediment transport and bottom evolution in a tidal basin. The effect of halophyte vegetation or marshes is also put into account.

2 Conceptual model

2.1 Hydrodynamics

In the present conceptual model [Di Silvio, Padovan, 1998] sediments are not physically conveyed to an fro by tidal currents but their "net" (long term) transport is given in the form of intertidal dispersion. Tidal currents, however, are utilized to define the intertidal dispersion coefficient D_{ij} (eq.8).

For this purpose the waterflow model may be relatively crude as it should provide only the velocity field in maximum flood conditions. It is based on a simplification of the two-dimensional shallow water equations, similar to the dimensionless Poisson form obtained by Rinaldo et al. [1999b].

In a relatively “short” tidal lagoon, (with propagation time between inlet and lagoon basin lower than a quarter of a tidal period T_m) one can assume that at maximum flood conditions, friction terms dominate inertial effects in momentum equations and the flood velocity of tidal elevation ($\partial\eta/\partial\tau$) is constant (and equal to the maximum rising velocity in the sea) in each part of the lagoon (Fig. 1).

The friction term, under this hypothesis, has been linearised using the energy criterion first introduced by Lorentz [1926], which allows one to write the depth averaged velocity as:

$$U = -\frac{h \cdot C_h^2}{\sqrt{U^2 + V^2}} \frac{\partial\eta}{\partial x} \quad (1)$$

$$V = -\frac{h \cdot C_h^2}{\sqrt{U^2 + V^2}} \frac{\partial\eta}{\partial y} \quad (2)$$

where (U, V) denote the depth-averaged flow velocities in the (x, y) directions respectively, $h = z_b - \eta$ is the local water level, z_b is the bottom depth, η the local surface elevation and C_h is Chezy’s coefficient.

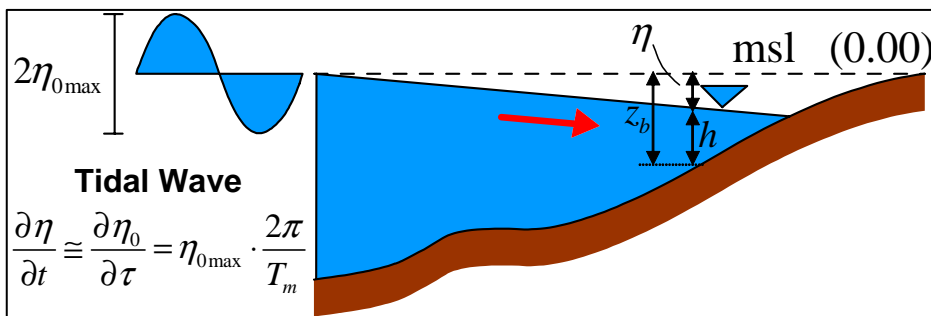


Fig 1 – Tidal elevation at maximum flood conditions.

To put into account the resistance due to vertical walls in the inlet and along the barrier island the Chezy’s coefficient is considered linearly increasing from 30 to 50 $m^{1/2}/s$ over a distance of 500 m from the wall. In all the other part of the lagoon is considered constant and equal to 50 $m^{1/2}/s$ [D’Alpaos et al., 2007].

The two-dimensional continuity equation can be written as:

$$\frac{\partial\eta}{\partial\tau} + \frac{\partial(hU)}{\partial x} + \frac{\partial(hV)}{\partial y} = 0 \quad (3)$$

Local surface elevation $\eta(x,y)$ in the basin lagoon can be defined substituting expressions (1) and (2) into (3) and the governing equations can be simplified with a dimensionless Poisson form. The Poisson form equation can be correctly used for determining the velocity field in the shoals in which the depth is more or less uniform. As the boundary conditions for the shoals it can be assume that

the level η_0 in the sea propagates instantaneously and without damping along the deeper channels [Rinaldo et al. 1999b].

This procedure can be applied if the planimetric structure of the channels is known and stable. The different behavior of channels and shoals, however, cannot be postulated during the generation of the very same channel network.

If one wants to calculate local surface elevation and field velocity all over the lagoon without distinguishing between channels and shoals, it is not possible to neglect bathymetric gradients in direction x and y . So it is necessary to solve the system of equations (1), (2) and (3) obtaining the following expression (4) and using "under-relaxation" approximation method for the convergence;

$$\eta_{0\max} \frac{2\pi}{T_m} + \frac{\partial}{\partial x} \left[\left(\frac{-h^2 C_h^2}{U_0} \right) \frac{\partial \eta}{\partial x} \right] + \frac{\partial}{\partial y} \left[\left(\frac{-h^2 C_h^2}{U_0} \right) \frac{\partial \eta}{\partial y} \right] = 0 \quad (4)$$

where $U_0 = \sqrt{U^2 + V^2}$.

In the present application it has been assumed $\eta_{0\max}=0.35$ m and $T_m=43200$ sec, as in the lagoon of Venice.

2.2 Sediment transport

The two-dimensional intertidal balance equations for the sediments are written as:

$$\frac{\partial Ch}{\partial t} + \frac{\partial T_x}{\partial x} + \frac{\partial T_y}{\partial y} = E \quad (5)$$

where T_x and T_y are the "net" sediment transport (averaged over a number of tidal oscillations) in the direction x and y respectively; E is the long-term entrainment or deposition rate and the first term $\partial Ch/\partial t$ (the accumulation term) is neglected because much smaller than E (Fig. 2).

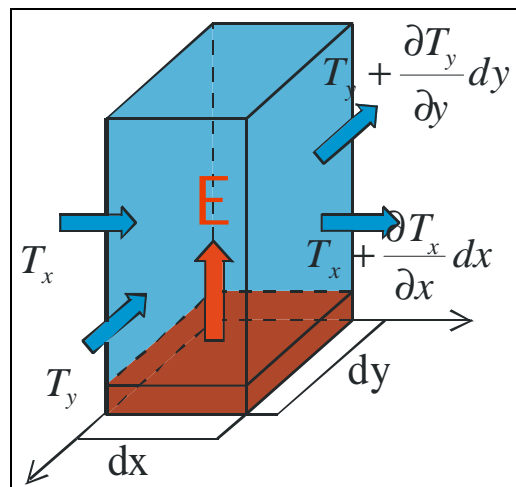


Fig 2 – Long-term balance of sediment trough a infinitesimal element of the lagoon.

The following expressions for the "net" sediment transport are obtained by integrating the suspended transport equations, over a long period of time:

$$T_x = h \cdot \left(\overline{U \cdot V} - D_{xx} \frac{\partial C}{\partial x} - D_{yx} \frac{\partial C}{\partial y} \right) \quad (6)$$

$$T_y = h \cdot \left(\overline{U \cdot V} - D_{xy} \frac{\partial C}{\partial x} - D_{yy} \frac{\partial C}{\partial y} \right) \quad (7)$$

where h is the averaged water depth, C the intertidal averaged sediment concentration in the water column, U and V denote the depth-averaged residual (intertidal) flow velocities in the x and y directions, D_{ij} the intertidal dispersion tensor.

In the chosen lagoon basin, the residual terms of advection $C \cdot V$ and $C \cdot U$ can be neglected in comparison with the intertidal dispersion transport.

2.3 Intertidal dispersion

The intertidal dispersion is the dominant mechanism of transport in a long time period. It determines the spatially distribution of lagoon's suspended sediments and it is controlled by the gradient of the long term averaged sediment concentration.

For a tidal lagoon formed by a network of deep channels cut in broad and shallow areas, the dominant intertidal mixing is due to the alternate "trapping and pumping" phenomena between channel and shoals during the entire tidal cycle [Schijf and Schönfeld, 1953].

To understand this mechanism, let suppose that any tracer (not necessarily a sediment) is continuously discharged in the lagoon and from there to the sea.

In tidal flood conditions clear water enters from the sea to the lagoon basin transported by the channel. The tracer concentration in the channel is smaller than in the shoals, so the clear water is transported to the shoals from the channel. In ebb tide conditions the concentration in the shoals is higher and the tracer is transported to the channel and eventually to the sea.

The same mechanism applies to suspended sediment if the concentration in the sea is lower than within the lagoon (degrading lagoon). The sign of transport is inverted if the concentration in the sea is higher than within the lagoon (silting lagoon).

The tensor of intertidal dispersion D_{ij} expresses the physics of this exchange through a square proportionality with the field velocity [Dronkers, 1978]:

$$\overline{\overline{D}} = \begin{pmatrix} D_{xx} & D_{xy} \\ D_{yx} & D_{yy} \end{pmatrix} = k_e \begin{pmatrix} U^2 & UV \\ VU & V^2 \end{pmatrix} \quad (8)$$

The spatial distribution of the dispersion tensor $\overline{\overline{D}}$ depends on the velocity field, in its turn depending on the planimetric structure of the channel network. It is assumed in this model that the velocity field directions remain basically constant during the tidal cycle. As a consequence the distribution of $\overline{\overline{D}}$ be provided by the velocity field in maximum flood conditions (2.1).

The value of the constant k_e , also adsorbs the frequency distribution of the intensity of tidal currents.

An attempt of the theoretical evaluation in the case of one directional channel has been made [Dal Monte e Di Silvio, 2003]. In this work the value of k_e is considered constant ($2.55 \cdot 10^3 \text{ sec}^{-1}$) and it corresponds to the maximal value of $D_{xx} \approx 500-1000 \text{ m}^2/\text{sec}$ in the inlet area. Similar values have been experimentally found in the lagoon of Venice [Imberger, 1992].

2.4 Equilibrium concentration

The erosion rate E (eq. 5) is expressed by the following first-order reaction equation:

$$E = w \cdot (C_{eq} - C) \quad (9)$$

where C is the time-averaged sediment concentration and C_{eq} is the equilibrium concentration of the water column. The parameter w is proportional to the fall velocity w_s of the equivalent particle size of the bottom material. The ratio (w/w_s) depends in principle on the vertical profile of the concentration. In the present work w is considered constant and equal to 0.003 m/sec .

The equilibrium concentration in a certain place is the average sediment concentration over the water column which would yield neither erosion or deposition (equilibrium condition). It depends on the grain size diameter of the particles, on the local hydrodynamics (waves and currents) and on the local depth and can assume an expression of the following type [Dal Monte, 2004]:

$$C_{eq} = \frac{f_{sea}}{h^m} + a_{tid} \frac{q^{n-1}(x, y)}{h^n} + \frac{f_{wind}(x, y)}{h^p} \quad (10)$$

where the three terms consider the entrainment effects on the sediments of sea waves, tidal currents and local wind respectively. Note that all the three terms decrease when the local depth increases. Following the transport monomial formula (Engelund-Hansen), the exponents m , n and p are considered, respectively, equal to 3, 5 and 1.

The function f_{sea} is considered increasing parabolically along the distance from the shore, from 0 (in the middle of inlet) to $2.5 \cdot 10^{-2} \text{ m}^3$ and equal to zero in the lagoon basin.

The value of a_{tid} , which depends on the grain size distribution, is also assumed constant ($2.7 \cdot 10^{-3} \text{ sec}^4/\text{m}^3$) inside and outside the lagoon basin.

The quantity $q = h\sqrt{U^2 + V^2}$ is provided by the hydrodynamic sub-model (2.1).

The local wind wave function f_{wind} is a function of the local fetch and wind intensity and it may appreciably decrease in presence of sea weeds. In the present simulation it is assumed $f_{wind} = 2.5 \cdot 10^{-5} \text{ m}$.

The averaged sediment concentration of the water column C , can be so calculated solving the system (eqs. 5-9) expressed in the following symbolic equation (11):

$$\nabla \cdot \left(-h \cdot \overline{\overline{D}} \cdot \nabla C \right) + w \cdot C = w \cdot C_{eq} \quad (11)$$

3 Bottom evolution

3.1 Marshes generation

The long-term evolution of the bottom depth, h , is given by adding up the bottom erosion rate E , the eustatism α_e (rise of mean sea level) and the subsidence rate α_s (settlement of ground surface), (eq. 12).

$$\frac{\partial h}{\partial t} = E + \alpha_e + \alpha_s \quad (12)$$

A better insight into the physical mechanisms behind this aspect of lagoon morphodynamic is worth pursuing.

Sediment deposition occurs in the shoals when the local concentration C is larger than C_{eq} (eq. 9); as the depth progressively decreases, the value C_{eq} increases (eq. 10), the settling rate is increasingly compensated by the pick-up rate and the bottom rise slows down. However if sediment deposition proceeds, the bottom will emerge more and more frequently from the water. As soon as the bottom is not submerged for a sufficiently long period of time during the tidal cycle, vegetation takes place, the bottom becomes protected and the pick-up rate vanishes. At this point, all the sediments reaching the marshes are captured and the bottom rapidly rises. Rise, however, is very soon limited by the rapid reduction of water flow when the bottom is above the mean sea level. Above a certain elevation, in fact, only a negligible amount of sediment reaches the marshes to compensate eustatism and subsidence. In the model, the two phenomena are simulated, respectively, considering $C_{eq}=0$ when $z_b < z_{bv}$ (bottom above the limit of vegetation) and $D_{ij} = 0$ m²/sec when $z_b < z_{bt}$ (bottom above the limit of the highest tides).

The value of the z_{bv} (limit of vegetation) depends on the local species of halophyte vegetation. In the present simulations it has been assumed $z_{bv}=0$ m (mean sea level).

The value of z_{bt} (limit of high tides) depends on the significant high waters. In the present simulations it has been assumed $z_{bt}=-0.35$ m.

3.2 Marshes demolition

According to the mechanism described in 3.1, the equilibrium elevation of marshes is to be found between z_{bt} and z_{bv} depending upon the values of α_e and α_s . As matter of fact, the bottom distribution of the marshes in the lagoon of Venice is comprised in quite narrow range.

In any case, if the elevation of the marshes is practically constant, their surface may be strongly variable, depending upon the sediment balance in the shoals.

Indeed the collapse of the marsh contour is determined by an excessive depth of the adjacent shoal. The maximum permissible step between marshes and

shoals depends basically on the soil characteristics (e.g. 0.25 m). This mechanism activated whenever the shoals are subjected to erosion, has not been incorporated in the present simulations.

3.3 Effective water depth

The average water depth in a certain location of the lagoon is not always given by the value of h , but depends on the local bottom elevation. In fact, if the annual maximum tidal range is a_m , it follows that, during the year, the bottom is permanently submerged only where $z_b > a_m/2$; by contrast the bottom is never submerged where $z_b < -a_m/2$, while we have an intermediate submergence for values in between. If we assume that the frequency distribution of the tidal range is sensibly linear, we may obtain the value of the effective water depth h^* in each location of the lagoon, by multiplying the local value of h by the submergence period of the tide.

One finds

$$h^* = h \quad (\text{if } z_b > a_m/2) \quad (13)$$

$$h^* = \eta_0 \cdot \left(1 - \frac{1}{2} \cdot \left(1 - \frac{h}{\eta_0} \right) \right)^2 \quad (\text{if } -a_m/2 < z_b < a_m/2) \quad (14)$$

$$h^* = 0 \quad (\text{if } z_b < -a_m/2) \quad (15)$$

The effective value of h^* should be used instead of h , in every equation of the model.

4 Numerical model

4.1 Model description

The numerical two-dimensional model consists of a number of modules which describe hydrodynamics, sediment transport and bottom evolution respectively. The dynamic interaction of these processes with the bed-topography changes is taken into account in the time-loop.

The following flow-chart describes every step of the simulation (Fig. 3). The simulation starts with initial conditions and computes lagoon hydrodynamics and local surface elevation at maximum flood conditions. In a second step, the model calculates the local intertidal dispersion coefficients and equilibrium concentration as a function of hydrodynamic and depth conditions which control sediment transport and the evolution of channels, shoals and marshes. As third step the model computes the local sediment concentration and new bathymetric depth. An under relaxation procedure is employed for solving the non linear hydrodynamic equations.

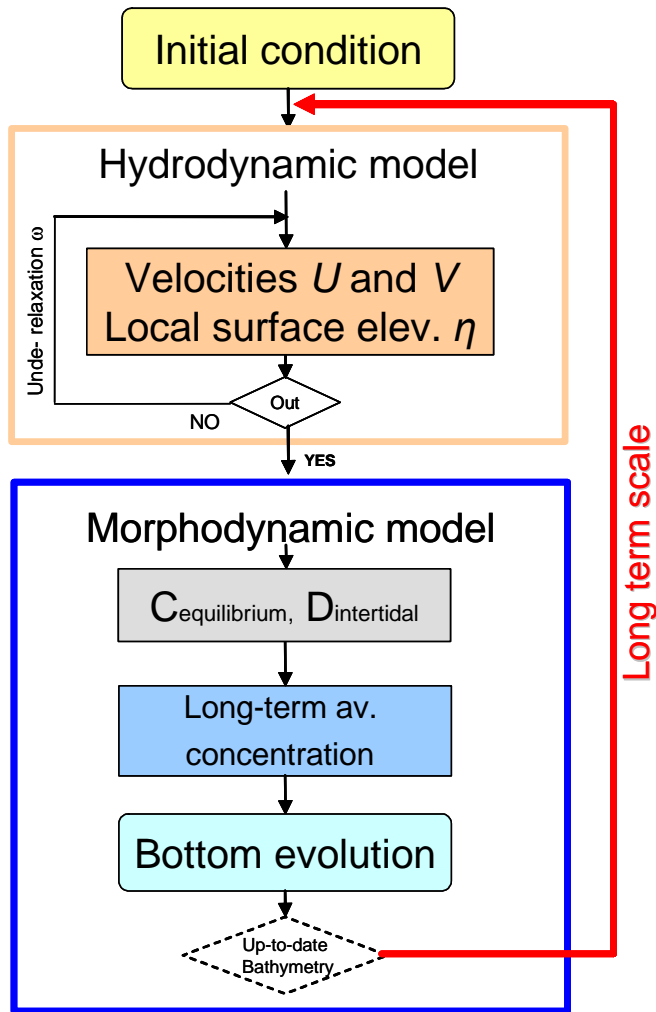


Fig 3 – Model flow chart.

4.2 Model setup

The generation process of the lagoon has been assumed to be initiated by an occasional large breach of the littoral dunes, which will be transformed in the lagoon inlet. Through the breach water will invade a portion of the coastal alluvial plain behind the dunes which will constitute lagoonal basin.

The model is applied to a schematic representation of the sea (longitudinal direction between 0 km and 3 km, area 42 km²) breach and inlet area (longitudinal direction between 3 km and 4 km, area 1 km²) and lagoon basin (longitudinal direction between 4 km and 11 km, area 98 km²). The schematization makes it possible to investigate the influence of the sea waves on the development of the channel pattern within the lagoon.

As initial configuration, the bottom bathymetry in the sea is considered linearly increasing along the longitudinal direction seaward (from -8 m to -1 m near to the inlet) and constant (-1 m) in the inlet and in the lagoon.

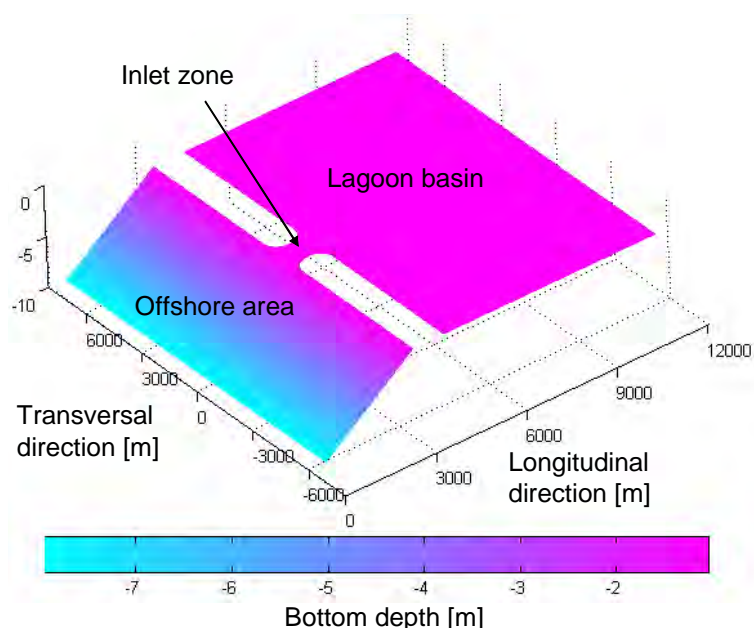


Fig 4 – Bottom bathymetry of the flat lagoon conformation (x longitudinal direction, y transversal direction, z bottom bathymetry).

Different triangular model grids are used in the numerical computation but the most of simulations are implemented with a mesh grid of 11'984 triangles of about 200 m sides.

The vertical boundary enclosing the lagoon basin are fixed and impermeable. At the seaward boundary, constant values of tidal range and concentration (equal to the local equilibrium concentration) are imposed.

5 Model application

The model described in the sections above is still to be subject to appropriate operations of validation, calibration and verification. These operations will be based first of all, to systematic sensitivity analysis with respect to the main parameters of the model: the meteo marine coefficients f_{sea} , f_{wind} and a_m (eq.10) which control the equilibrium concentration; the coefficient k_e (eq.8) quantifying the tensor of the intertidal dispersion; the coefficient w (eq.9) defining the intensity of sediment exchange between water column and bottom.

The model results, obtained with different parameters, will subsequently be compared with known situations of quasi-equilibrium conditions or morphological evolution at historical scale.

This will be especially done with reference to the lagoon of Venice, but also to other similar environments ("short" tidal lagoons with different tidal range, sea force and local wind), e.g. the Wadden Sea in the Netherlands. It seems likely, in fact, that while the meteo-marine parameters control the quasi-equilibrium morphological configuration of the lagoon, the dispersion tensor and the vertical exchange parameter control the response rapidity of the morphology to natural and anthropogenic changes.

5.1 First results

The model has been applied to simulate the generation of a tidal basin as the

consequence of the sea ingress in a square basin of given surface ($7 \times 14 \text{ km}^2$) through a breach of a given width (1000 m). The maximum annual tidal range has been assumed $a_m/2 = \pm 0.35 \text{ m}$ and the initial depth in the basin was assumed constant ($h=1 \text{ m}$). The provisional values of the model parameters have been assumed as mentioned in the relevant sections. The model results indicate two distinct phases of morphological evolution. During the first phase (lasting a few weeks) the proper ontogenetic process of the channel network occurs: following the breach the depth in the inlet almost immediately increases from 1 m to about 8 m while the scour rapidly propagates towards the sea and (even more) towards the lagoon (Fig.5).

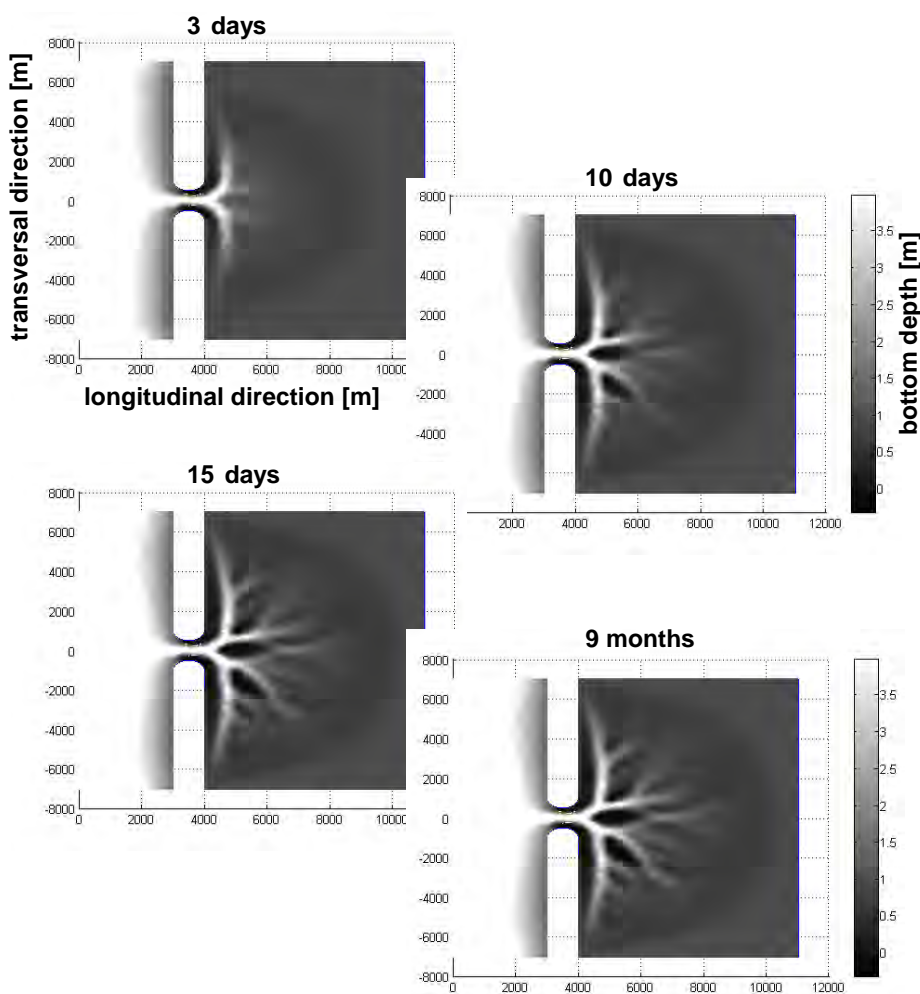


Fig 5 – First phase (few weeks) of the ontogenetic process of the channel network.

After a few days the external configuration of the “fuosa” (as it was called in Venice the original external delta) is practically completed. Within the lagoon, by contrast the tidal network continues to be formed by retrograde erosion of the channels and simultaneous silting of the adjacent shoals. After about 20 days, the planimetric configuration of the tidal network has reached a quasi-equilibrium configuration, but the bathymetric evolution is still active, with a very slow progressive deepening of the channels and a corresponding rising of the shoals. During this phase some marshes are also formed near the source of

sediment (the inlet), where the bottom elevation reaches the mean sea level and vegetation thrives (Fig.6).

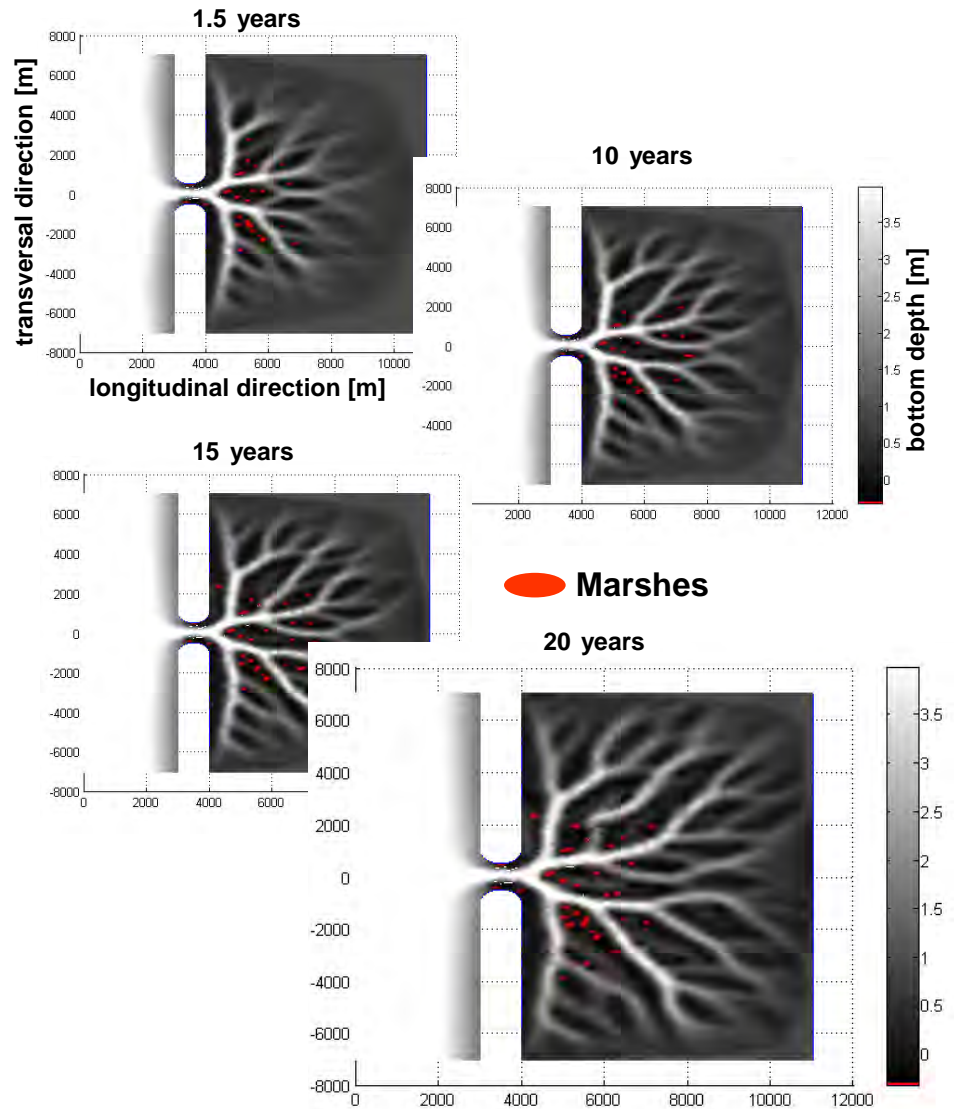


Fig 6 – Second phase (several years) of morphological evolution and consequently marshes formation.

The second phase or morphological evolution is much slower than the first one and may last several years. Only bathymetry is involved in the process, while all the quantities basically related to the planimetric configuration (flow field pattern) tend to remain constant. Therefore the values of the parameters controlled by the flow field pattern (spatial distribution of $q(x, y) = h\sqrt{U^2 + V^2}$ and of the dispersion tensor D , eq. 8) do not change in time (Fig.7).

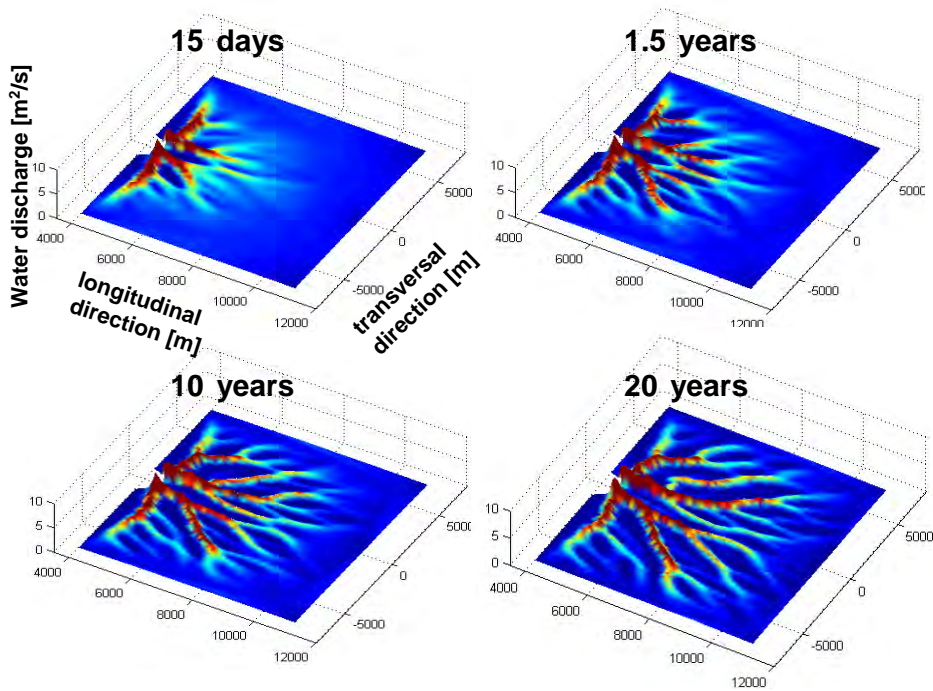


Fig 7 – Evolution of the spatial distribution of $q(x,y)$ in different time scale (as it is possible to observe, there is a very little changing of $q(x,y)$ after 10 years).

This result is extremely important from the practical point of view, as it allows to apply the morphological model to extremely long period of time, for long term sediment balance without repeating the computation of the flow field, definitely the model component which is the most time consuming. On the other hand, the planimetric effects produced by new constructions can be simulated by relatively short period of time, even though the corresponding CPU may be relevant.

6 Energy evolution

It may be interesting to observe the time evolution of the total kinetic energy of the lagoon, provided by the following integral:

$$En_{kinetic} = \frac{1}{2} m W^2 = \frac{1}{2} \int_S \rho h^* (U^2 + V^2) dS \quad (16)$$

where S is the total surface of the lagoon and h^* is the “effective” depth.

As it appears from Fig. 8 the total energy of the lagoon tends to decrease with time, towards an (equilibrium) value apparently depending on the size of the lagoon and on its meteo-marine parameters.

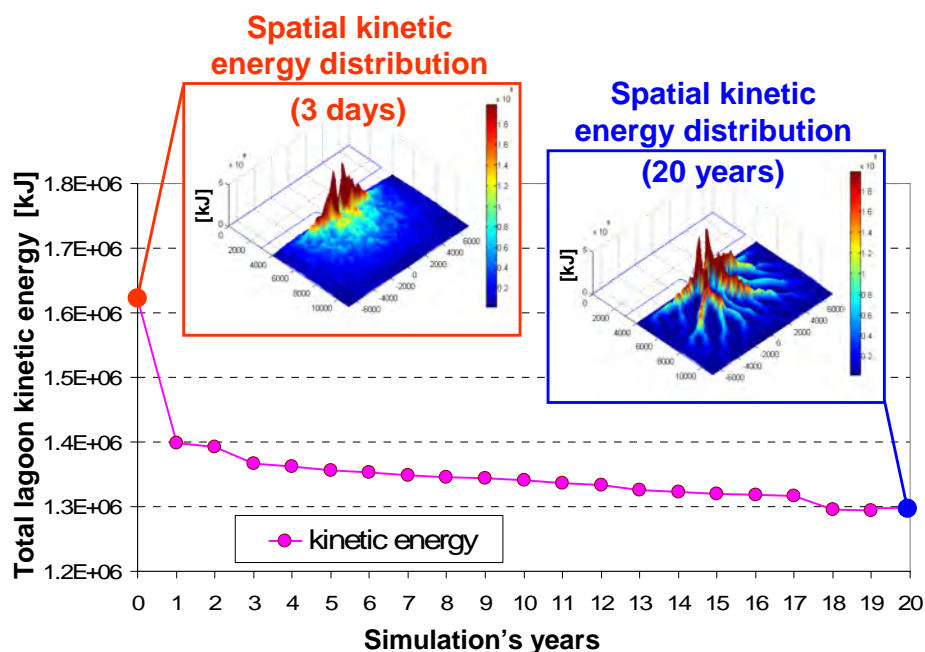


Fig 8 – Total lagoon kinetic energy evolution (and its initial and final spatial distribution) during simulation's years.

7 Conclusion

The 2-D “intertidal” morphodynamic model described here is apparently able to reproduce both the planimetric phase of the lagoon ontogenesis (with the generation of the planimetric pattern of the tidal network) and the subsequent bathymetric phase of the depth adjustment of the channels, shoals and marshes in the lagoon.

Although much more numerical analysis are required for validating, calibrating and verifying the model, the first results indicate that the time scales of the two phases are very different.

During the first phase (lasting a few weeks) the proper ontogenetic process of the channel network occurs: following the breach, the depth in the inlet almost immediately increases while the scour rapidly propagates towards the sea and the lagoon. In this phase the lagoon system seems strongly unstable (morphological variations occur rapidly, in few weeks) and kinetic energy of the system is particularly high.

In the second phase, after about 1 month, the planimetric configuration of the tidal network has reached a quasi-equilibrium configuration, but the bathymetric evolution is still active, with a very slow progressive deepening of the channels and a corresponding rising of the shoals and marshes' formation (vegetation thrives). Also the energy system is lower than the beginning and continue, slowly, to decrease during the years.

References

Dal Monte L. and G. Di Silvio (2004). Sediment concentration in tidal lagoons. A contribution to long-term morphological modelling. *Journal of Marine Systems*,

Volume 51, Issues 1-4, November 2004, Pages 243-255

Dal Monte L., G. Di Silvio (2003). Ratio between channel-cross section and tidal prism in short lagoons: validity and limits of the "Law of Jarret", 3rd IAHR Symposium on River, Coastal and Estuarine Morphodynamics, 1-5 Sept., Barcelona, Spain, 2003.

D'Alpaos L. and A. Defina (2007). Mathematical modeling of tidal hydrodynamics in shallow lagoons: A review of open issues and applications to the Venice lagoon. *Computers & Geosciences*, Volume 33, Issue 4, May 2007, Pages 476-496.

Di Silvio G. e A. Padovan. (1998) Interaction between marshes, channels and shoals in a tidal lagoon investigated by a 2-D morphological model. *Proceedings of third international conference on hydro-science and engineering*, III, 1998.

Dronkers J.(1978). Longitudinal dispersion in shallow well-mixed estuaries, Vol. 3, 169, *Coastal Eng. Conf.*, 1978.

Fagherazzi S., A. Bortoluzzi, W. E. Dietrich, A. Adami, M. Marani, S. Lanzoni, and A. Rinaldo. (1999) Tidal networks: 1. Automatic network extraction and preliminary scaling features from digital terrain maps, *Water Resour. Res.*, 35, 3891– 3904.

Fasolato G., Di Silvio G. (2004) Evoluzione del fondo di un bacino lagunare simulata con un modello morfodinamico intermareale bidimensionale. *Proceeding of XXIX Convegno di idraulica e costruzioni idrauliche*. 7-10 settembre 2004. Trento.

Imberger, J. and Di Silvio, G., (1992). Mixing Processes in a shallow lagoon. In: Edge, B.L., Editor, 1992. *Coastal Engineering*, ASCE, Venice, Italy, pp. 1867–1868.

Marciano R. et al. (2005) Modeling of channel patterns in short tidal basins. *Journal of Geophysical Research*, vol. 110, January, 2005.

Rinaldo A., S. Fagherazzi, S. Lanzoni, M. Marani, and W. E. Dietrich (1999a), Tidal networks: 2. Watershed delineation and comparative network morphology, *Water Resour. Res.*, 35, 3905– 3917.

Rinaldo, A., S. Fagherazzi, S. Lanzoni, M. Marani, and W. E. Dietrich (1999b), Tidal networks: 3. Landscape-forming discharges and studies in empirical geomorphic relationships, *Water Resour. Res.*, 35, 3919–3929.

Schijf J. B., J. C. Schönfeld (1953), Theoretical considerations on the motion of salt and fresh water, 321, *Proc. Minnesota Int. Hydr. Cond. (IAHR/ASCE)*, Minneapolis, Minnesota, August 1953.

de Vriend, H. J. (1996). Mathematical modelling of meso-tidal barrier island coasts. Part I: Empirical and semi-empirical models, P. L.-F. Liu, *Advances in coastal and ocean engineering* 2115–149.

EFFECTS OF TIDAL FLATS ON TIDE PROPAGATION AND SEDIMENT TRANSPORT IN TIDAL CHANNELS

Nicoletta Tambroni, Giovanni Seminara

Dipartimento di Ingegneria delle Costruzioni, dell'Ambiente e del Territorio, Università di Genova

Riassunto

Il problema dell'equilibrio morfodinamico di lungo termine di canali mareali è stato recentemente investigato da diversi autori, tra cui Schuttelaars e de Swart [1996, 2000], Lanzoni e Seminara [2002] e Bolla Pittaluga [2003]. Il risultato principale di tali lavori è la predizione dell'esistenza di un profilo d'equilibrio del fondo, che si realizza attraverso la propagazione di un'onda di sedimenti verso monte e la formazione di una spiaggia nel tratto più interno del canale. In tali contributi si trascura tuttavia la presenza di aree d'espansione adiacenti al canale principale. Nel presente lavoro si intende superare tale restrizione analizzando innanzitutto l'effetto dei bassifondi sull'idrodinamica dei canali mareali, per poi passare allo studio del loro ruolo morfodinamico. Alcune osservazioni generali sull'idrodinamica di canali mareali affiancati da aree d'espansione laterale possono essere fatte sulla base di un modello completamente analitico. Le approssimazioni introdotte nella formulazione di questo modello sono quelle di moto unidirezionale, di marea forzante all'imbocco di piccola ampiezza, di canale non convergente e di linearizzazione dei termini dissipativi. I risultati mostrano che la lunghezza di risonanza del canale diminuisce all'aumentare dell'estensione delle aree d'espansione laterali, un comportamento che da' spiegazione all'evidenza che, a parità degli altri parametri, in un canale mareale le velocità generalmente aumentano all'aumentare dell'estensione delle aree laterali. La formulazione del problema si è quindi estesa a ricoprire gli effetti non lineari, sempre nell'ambito di una modellazione 1D. Infine si è passati alla trattazione del problema 2D completo con la soluzione numerica delle equazioni del moto su acqua bassa. I risultati numerici confermano le caratteristiche generali emerse dalla trattazione analitica e suggeriscono che la presenza di aree d'espansione laterale al canale principale può modificare il carattere del campo di moto nel canale. Alcuni risultati preliminari relativi all'effetto dei bassifondi sull'evoluzione morfodinamica dei canali mareali sono inoltre discussi in conclusione del lavoro.

Abstract

Recent theoretical works [Schuttelaars and de Swart, 1996, 2000; Lanzoni and Seminara, 2002; Bolla Pittaluga, 2003] have investigated the long term morphodynamic equilibrium of tidal channels. The main outcome of such works is the prediction of the existence of an equilibrium bed profile, which is

established through the propagation of a sediment wave leading to the formation of a beach in the landward part of the channel. The above works have ignored the possible presence of tidal flats adjacent to the main channel. In the present work we attempt to overcome the above limit by analyzing the effect of tidal flats on the hydrodynamics of tidal channels, as a first step to proceed to analyse their morphodynamic role. We start by attempting to gain some general insight of the process on the basis of an analytical approach. The latter is necessarily based on a simplified scheme relying on classical assumptions, namely 1-D model, tidal forcing characterised by small relative amplitude, no channel convergence and linear dissipation. Results show that the resonance length decreases as the width of tidal flats increases, a behaviour which explains why, for a given channel length, as a result of the presence of tidal flats the flow velocity in the channel is typically increased. The above 1-D analytical findings have then been extended to cover non linear effects, by first relaxing the linear constraints still in the context of a 1-D model. Finally we solve the full 2-D shallow water equations numerically for the case, often encountered in nature, of frictionally dominated channels with adjacent tidal flats. Numerical results do confirm the general behaviour emerged from the analytical results and suggest that addition of tidal flats to the channel modifies the character of the flow field in the channel. Some preliminary results on the effect of tidal flats on the morphodynamic evolution of tidal channels are also reported at the end of the paper.

1 Introduction

This paper is focused on tide propagation in channels with adjacent tidal flats. The problem of tide propagation in estuaries and tidal channels is not a new one. However, only recently, the analysis has been extended to cover the case of mobile beds, allowing to investigate the long term bottom evolution of tidal channels [e.g. Schuttelaars and de Swart, 1996, 2000; Lanzoni and Seminara, 2002; Bolla Pittaluga, 2003]. The outcome of the latter works is the prediction of the existence of an equilibrium bed profile, which is established through the propagation of a sediment wave leading to the formation of a shore in the landward part of the channel. The above works have ignored the possible presence of expansion areas, bordering laterally the main channel and periodically subject to inundation. These environments may be grossly distinguished into salt marshes and tidal flats. Salt marshes represent the highest portion of a tidal basin, characterized by bed elevation above the mean sea level and are submerged only during high tides. They are typically flat, muddy and covered by vegetation. Tidal flats typically lie between salt marshes and channels: their bed elevation is such to keep the flats permanently submerged. Furthermore, the surface of the tidal flats is often sandy and covered by submerged vegetation.

Clearly, the morphodynamic evolution of salt marshes, tidal flats and tidal channels are strongly related. In particular, the presence of lateral shoals strongly affects the morphodynamic evolution of a single tidal channel because, on one side their presence modifies the hydrodynamics of the tide in the

channel, on the other side they introduce a mechanism of sediment exchange with the channel.

In the present work, at first we focus on the first mechanism and attempt to study the effects of the tidal flats on the hydrodynamics of tidal channels, then we proceed to analyse their morphodynamic role, discussing some preliminary results at the end of the paper.

2 A linear theory for a tidal channel with adjacent tidal flats

Let us consider a straight tidal channel of length L_C and width B_C , closed at one end and symmetrically flanked by tidal flats of width $B_F/2$ (see Fig. 1). Hence, at this stage, we ignore the effects of channel convergence. Moreover, we assume that both channel and tidal flats have rectangular cross-sections such that the corresponding mean flow depths are constant and equal to D_{0C} and D_{0F} respectively.

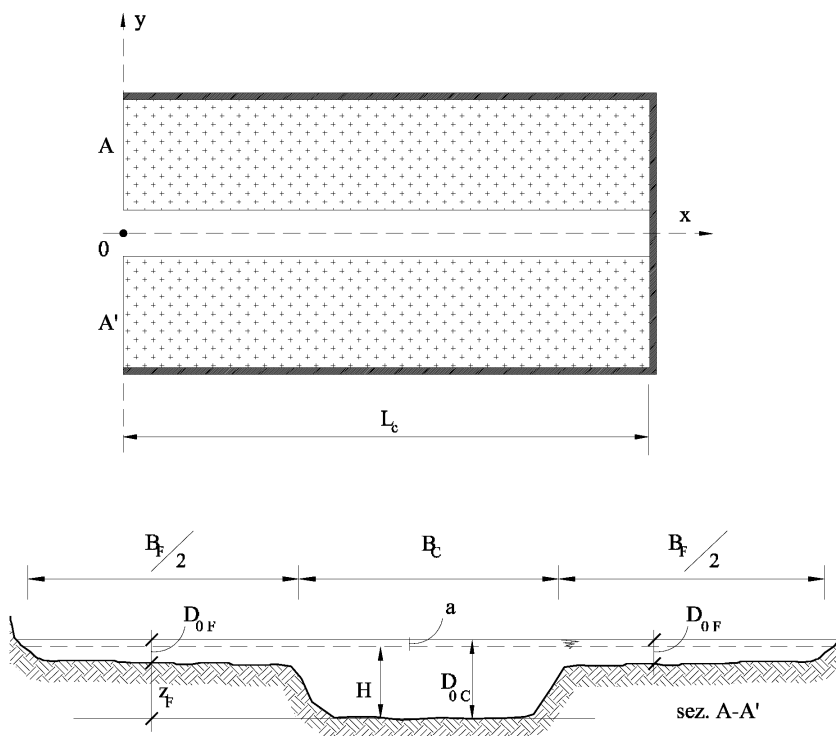


Fig 1 – Sketch of the model and notations.

One-dimensional models cannot handle the effect of secondary flows driven by the possible presence of distinct flood and ebb channels within the cross section and by the process of fluid draining from (into) the channel into (from) the tidal flats during the rising (falling) tide. This notwithstanding, it is of some interest, as a first approximation, to simply ignore secondary flows and model tidal flats as parts of the channel cross section, albeit with distinct flow characteristics. This scheme allows us to employ the classical one-dimensional de Saint Venant equations of mass and momentum conservation to investigate the hydrodynamics of the problem. We then write:

$$\Omega_{,t} + (U\Omega)_{,x} = 0, \quad (1)$$

$$U_{,t} + UU_{,x} = -gH_{,x} - \frac{\tau_0^b}{\rho R_i} \quad (2)$$

In the equations (1) and (2) t denotes time, x is a landward oriented longitudinal axis, Ω is the total cross-sectional area, U is the cross sectionally averaged flow velocity, H is the water surface elevation taken to be horizontal in the lateral direction, g is gravity, τ_0 is the average bottom shear stress accounting for the distinct role of channel and tidal flats, ρ is water density and R_i is the hydraulic radius of the total cross-section. Moreover, we may set

$$\Omega = B_F D_F + B_C D_C, \quad (3)$$

$$U = \frac{Q}{\Omega} = \frac{U_F B_F D_F + U_C B_C D_C}{B_F D_F + B_C D_C}, \quad (4)$$

where D_C , U_C and D_F , U_F denote depth and mean flow velocity in the channel and in the tidal flats respectively.

Furthermore, the value of the velocity U_F in the tidal flats can be determined noting that, having assumed the free surface to be laterally horizontal, the longitudinal gradient of the flow energy per unit weight j is the same in the channel and tidal flats

$$j = \frac{U_C^2}{k_{sC}^2 D_C^{4/3}} = \frac{U_F^2}{k_{sF}^2 D_F^{4/3}}, \quad (5)$$

with k_{sF} and k_{sC} Gauckler-Strickler coefficients for the tidal flats and the channel respectively. Note that in (5) the hydraulic radius has been taken to coincide with the flow depth in both the channel and tidal flats.

The equations (1) and (2) must be supplemented by appropriate boundary conditions. At the seaward boundary the free surface elevation is imposed, assuming an M1 forcing tide, hence we write:

$$H|_{x=0} = D_{0C} + a_0 \cos\left(\frac{2\pi t}{T}\right) \quad (6)$$

where a_0 is the amplitude of the tidal wave and T is the tidal period. At the landward boundary, the channel is assumed to be closed, hence the flow velocities are set to vanish:

$$U_C|_{x=L_C} = 0, \quad U_F|_{x=L_C} = 0. \quad (7)$$

The solution of the equations (1) and (2) in their complete non linear form must be obtained numerically. We start seeking an analytical solution of the problem under simplified conditions based on a classical linearization procedure: we

then assume that the relative amplitudes of the tidal wave in both the channel and tidal flats are small ($\varepsilon = a_0/D_{0C} \ll 1$, $\varepsilon_F = a_0/D_{0F} \ll 1$) and linearize the frictional term in the momentum equation, in the classical Lorentz form:

$$\frac{\tau_0^b}{\rho g R_i} = \frac{U|U|}{C^2 g R_i} \Rightarrow MU, \quad (8)$$

where C is the flow conductance and M is Lorentz friction coefficient. The value of the latter parameter is obtained by imposing that the average power dissipated over the tidal cycle in the linear approximation coincides with that obtained using the correct (quadratic) resistance law, hence:

$$\int \frac{\tau_0^b}{\rho g R_i} U dt = \int jU dt = \int (MU)U dt \quad (9)$$

Introducing the following dimensionless parameters:

$$\beta = \frac{B_F}{B_C} = \text{const}, \quad \varphi = \frac{D_{0F}}{D_{0C}} = \text{const}, \quad \chi = \frac{U_F}{U_C} = \text{const} \quad (10)$$

we find

$$M = M_C \frac{(1 + \beta\varphi)}{(1 + \beta\chi\varphi)}, \quad M_C = \frac{8}{3\pi} \frac{U_{C\max}}{k_{sC}^2 D_C^{4/3}} \quad (11)$$

where $U_{C\max}$ is an estimate of the maximum velocity experienced in the channel.

Finally, denoting by $a(x,t)$ the local, instantaneous amplitude of the free surface oscillation in the cross section, and substituting from the relationships (3) and (4) into the governing equations (1-2), one eventually finds:

$$(1 + \beta)a_{,t} + (1 + \chi\beta\varphi)(U_C D_C)_{,x} = 0, \quad (12)$$

$$\frac{1 + \beta\chi\varphi}{1 + \beta\varphi} U_{C,t} + \left(\frac{1 + \beta\chi\varphi}{1 + \beta\varphi} \right)^2 U_C U_{C,x} + g a_{,x} + g M \frac{1 + \beta\chi\varphi}{1 + \beta\varphi} U_C = 0. \quad (13)$$

It is convenient at this stage to introduce the following dimensionless variables:

$$\tilde{x} = \frac{x}{L_0/2\pi}; \quad \tilde{t} = t\omega; \quad \tilde{D}_C = \frac{D_C}{D_{0C}}; \quad \tilde{U}_C = \frac{U_C}{U_{0C}}; \quad \tilde{a} = \frac{a}{a_0}, \quad (14)$$

where $L_0 (= T \sqrt{g D_{0C}})$ is the tidal wavelength and U_{0C} is a typical value of the cross sectionally averaged speed in the channel, taken to read ($\varepsilon \sqrt{g D_{0C}}$).

With the above scaling, the governing equations can easily be rewritten in terms of the dimensionless variables \tilde{U}_C and \tilde{a} , as follows:

$$(1 + \beta)\tilde{a}_{,\tilde{t}} + (1 + \chi\beta\varphi)\left[(1 + \varepsilon\tilde{a})\tilde{U}_C\right]_{,\tilde{x}} = 0, \quad (15)$$

$$\frac{1 + \beta\chi\varphi}{1 + \beta\varphi}\tilde{U}_{C,\tilde{t}} + \varepsilon\left(\frac{1 + \beta\chi\varphi}{1 + \beta\varphi}\right)^2\tilde{U}_C\tilde{U}_{C,x} + \tilde{a}_{,\tilde{x}} + R\frac{1 + \beta\chi\varphi}{1 + \beta\varphi}\tilde{U}_C = 0, \quad (16)$$

where we have set:

$$R = \frac{Mg}{\omega}. \quad (17)$$

At the leading order of approximation, terms of order ε may be neglected in equations (15-16) to obtain

$$(1 + \beta)\tilde{a}_{,\tilde{t}} + (1 + \chi\beta\varphi)\tilde{U}_{C,\tilde{x}} = 0, \quad (18)$$

$$\frac{1 + \beta\chi\varphi}{1 + \beta\varphi}\tilde{U}_{C,\tilde{t}} + \tilde{a}_{,\tilde{x}} + R\frac{1 + \beta\chi\varphi}{1 + \beta\varphi}\tilde{U}_C = 0. \quad (19)$$

Finally, a suitable linear combination of the equation (18) differentiated with respect to t and equation (19) differentiated with respect to x , leads to the following second-order differential equation

$$\tilde{c}'_0{}^2 \tilde{a}_{,\tilde{x}\tilde{x}} = \tilde{a}_{,\tilde{t}\tilde{t}} + R\tilde{a}_{,\tilde{t}}, \quad (20)$$

where \tilde{c}'_0 represents the dimensionless form of an effective speed of a small amplitude tidal wave in a channel with adjacent flats. Note that the latter quantity differs from the classical expression obtained in the absence of tidal flats ($c_0 = \sqrt{gD_{C0}}$) by constants depending on the tidal flats geometry,

$$c'_0 = c_0 \sqrt{\frac{1 + \beta\varphi}{1 + \beta}} \quad (21)$$

The analytical solution of equation (20) is readily obtained superimposing an incident and a reflected wave of equal amplitude at the landward reflection point. The propagation speeds of the incident and reflected waves coincide, and, due to friction and to the presence of tidal flats, they are typically smaller than c_0 .

In figure 2 the dimensionless form of the maximum velocity at the inlet of the channel is plotted as a function of the channel length L_C scaled by the tidal wavelength L_0 . In the ideal case of negligible friction ($R=0$, Fig. 2 left), for a channel without tidal flats the classical result is recovered: namely, resonance occurs when the channel length is exactly one quarter of the tidal wavelength. The presence of tidal flats induces a gradual decrease of the resonance length of the channel, as the relative width of the tidal flats β increases: in the limit $\beta \rightarrow \infty$, the resonance length takes a value depending only on the square root of the

mean flow depth in the tidal flats.

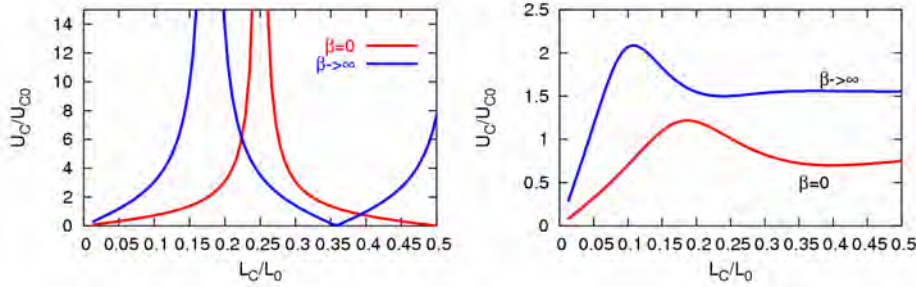


Fig 2 – The dimensionless form of the maximum velocity at the inlet of the channel is plotted as a function of the channel length L_C scaled by the tidal wavelength L_0 . The left plot refers to the ideal case of negligible friction; the right plot includes dissipation in the linearized form.

Similar results are found when accounting for the presence of friction (Fig. 2 right): as expected, friction has the effect of weakening resonance and slightly decrease the resonance length predicted in the ideal frictionless case.

Some application and limits of the present approach will be discussed in section 4.

3 A 2D numerical model for the tide propagation in a channel with adjacent tidal flats

As already pointed out, one dimensional models can only approximately describe the hydrodynamic effects induced by the presence of tidal flats adjacent to the main channel. In order to model these effects more accurately, an at least a two-dimensional approach is needed. In fact, since the phenomenon to be investigated is such that the horizontal scales are much larger than the vertical depth-limited scale, the depth integrated shallow water equations seem to be an appropriate tool. We write these equations as follows:

$$d_{,t} + (du)_{,x} + (dv)_{,y} = 0 \quad (22)$$

$$(du)_{,t} + (du^2)_{,y} + (duv)_{,y} = -gd(h)_{,x} - (\tau_{bx} / \rho) + (2v_e d(u_{,x}))_{,x} + (v_e d(u_{,y} + v_{,x}))_{,y} \quad (23)$$

$$(dv)_{,t} + (duv)_{,x} + (dv^2)_{,y} = -gd(h)_{,y} - (\tau_{by} / \rho) + (v_e d(v_{,x} + u_{,y}))_{,x} + (2v_e d(u_{,y}))_{,y} \quad (24)$$

Following the notations of figure1, in (22-24) $d(x,y,t)$ is the local water depth, $h(x,y,t)$ is the local free surface elevation, u and v are the local depth-averaged components of velocity in the x and y directions respectively and v_e is an eddy viscosity obtained from an appropriate turbulence closure (see below). The bottom stresses τ_{bx} and τ_{by} are evaluated from the following relationship:

$$(\tau_{bx}, \tau_{by}) = \rho g \frac{(u, v) \sqrt{u^2 + v^2}}{k_s^2 d^{1/3}} \quad (25)$$

where, in analogy with the one-dimensional formulation of section 2, Strickler's formula has been used to estimate the flow conductance, and the Gauckler-Strickler coefficient k_s is taken to assume two different values in the main

channel and in the tidal flats.

As regards the closure relationship for the eddy viscosity, we follow Stansby (2003), who has recently proposed a general three-dimensional form for ν_e with negligible vertical velocity. The latter has been reduced to a two-dimensional form (Stansby, 2006) in the following way:

$$\nu_e = \nu + \sqrt{l_h^4 \left[2u_{*,x}^2 + 2v_{*,y}^2 + \left(v_{*,x} + u_{*,y} \right)^2 \right] + \left(\gamma u_* d \right)^2} \quad (26)$$

where l_h is a horizontal length scale, u_* is the friction velocity, and γ is a constant. The term involving γ accounts for vertical mixing and, in parallel flow, Stansby (2003) finds $\gamma=0.0067$. However, here γ also accounts for dispersion and for the effect of the horizontal length scale on vertical mixing, which in turn affects the bed shear stress (and dispersion). There are thus three disposable parameters, l_h , γ and C_f , which describe complex coupled physical effects and may be tuned for a particular application. In this case we set l_h equal to a value typical of a two-dimensional jet (0.14 times the channel width) and γ is somewhat arbitrarily set equal to 0.2, while for C_f we use the closure relationship (25) given above.

Clearly, the boundary conditions to be associated with equations (22-24) are the same already introduced in section 2. In particular, at the seaward boundary we impose:

$$h|_{x=L_t} = D_{0C} + a_0 \cos\left(\frac{2\pi}{T}\right) \quad (27)$$

while the normal component of velocity is set to vanish at the walls, hence:

$$v|_{y=-(B_F+B_C)/2} = 0, \quad v|_{y=(B_F+B_C)/2} = 0, \quad u|_{x=L_C} = 0. \quad (28)$$

This approach will be shown to provide more accurate predictions, as compared with those obtained from the simpler one-dimensional model described in section 2. Results are discussed in the next section.

4 Results

In this section we compare results obtained by the approaches described above, with the aim to ascertain to what extent a one-dimensional approach is a suitable tool to describe the hydrodynamics of tidal channel with adjacent flats. We fix the value of the parameters by considering some typical geometrical and hydrodynamic characteristics of the tidal channels in Venice lagoon. In particular, the depth of channel incisions in Venice lagoon decreases from 8-10 *m* near the inlet to less than a meter at the innermost boundary of the lagoon, with an average depth of roughly 4-5 *m*. The length typical of larger channels is of the order of ten kilometres. A complex system of tidal flats and tidal marshes characterises the adjacent areas, whose elevation is almost constant and

whose extension may vary between 5 and 20 times the main channel width. Tidal flats lie just below the mean sea level, approximately between -0.6 and -2.0 m a.m.s.l, whereas salt marshes lie at an average elevation higher than the mean sea level (i.e. between $+0.1$ and $+0.5$ m a.m.s.l). We ignore, here, salt marshes and restrict ourselves to the presence of fully submerged flats. We also assume the forcing tide at the inlet to be characterized by an amplitude of 0.7 m, as typically observed within the lagoon. From both field measurements [Istituto d'Irridazione dell'Università di Padova, 1979] and results of a two dimensional hydrodynamic numerical model calibrated on the Venice lagoon [Carniello et al., 2005] reliable values of the Gauckler-Strickler coefficient k_s can be estimated to range about $30-40$ $m^{1/3}/s$ in the channel and $20-30$ $m^{1/3}/s$ in the tidal flats. Hence we set $a_0=0.7$ m; $T=12$ h; $L_C=12000$ m, $B_C=25$ m, $D_{0C}=4$ m; $D_{0F}=2$ m; $k_{sC}=35$ $m^{1/3}/s$ and $k_{sF}=25$ $m^{1/3}/s$. The resulting dimensionless parameters of the problem take the values $\varepsilon=0.175$, $\varepsilon_F=0.35$, $\varphi=0.5$, $\chi=(k_{sF}/k_{sC})\cdot\varphi^{2/3}=0.45$.

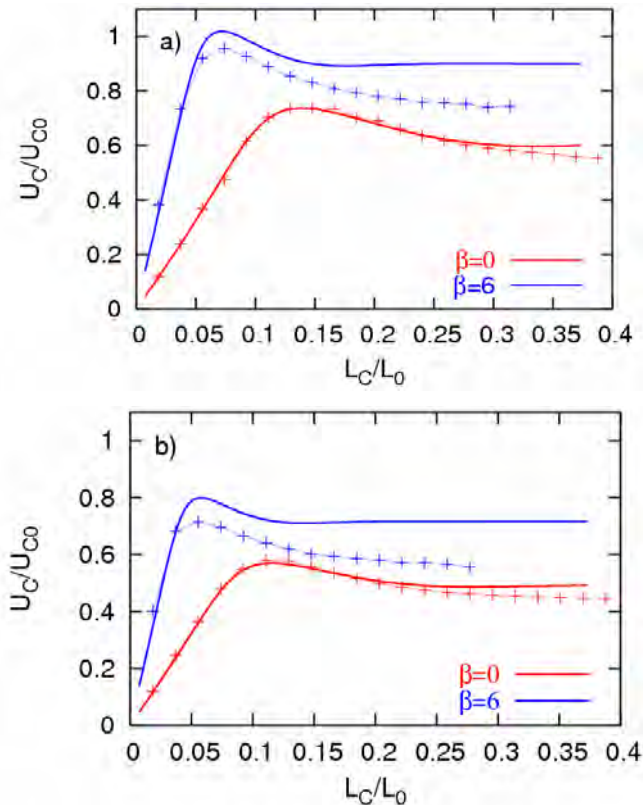


Fig 3 – The maximum dimensionless inlet velocity, as predicted by the linear model (solid line) or calculated numerically by solving the complete one-dimensional de Saint Venant equations (dotted line), is plotted as a function of the dimensionless channel length, for a channel without tidal flats $\beta=0$ (red line) and for a channel with tidal flats $\beta=6$ (blue line). The values of the remaining dimensionless parameters are $\varepsilon=0.0875$ (a), 0.175 (b), $\varphi=0.5$ and $\chi=0.45$.

In figure 3a the maximum dimensionless value of the velocity at the inlet is plotted as a function of the dimensionless length of the channel, for two different geometries: the former is characterised by the absence of tidal flats, the latter includes tidal flats with relative width β equal to 6. Results of the one dimensional linear theory suggest that, due to the presence of tidal flats, a consistent reduction of the resonance length in the channel already occurs for small values of β (for β equal 6, the resonance length of the channel is almost halved). However, in order to check how non linear effects may possibly modify the above results, a comparison with the results obtained solving numerically

equations (1) and (2) in their complete non linear form is also performed in the figure 3a. Furthermore, in the figure 3b the same quantities are plotted for a greater value of the relative forcing amplitude at the inlet. The general observation that arises from a glance at figures 3 is that the linear model may be a good approximation of the full de Saint Venant solution when the dimensionless amplitude of the tidal forcing at the inlet and the relative effect of friction are sufficiently small. In particular, the linear analysis turns to provide a good estimate of the resonance length. However, the effect of non-linear terms is to reduce the peak of the curve and damp the inlet velocity when the channel length is greater than the resonance length.

A further important flow property that cannot arise from the linear theory concerns the flood or ebb dominance of the flow field in the channel. In order to detect this behaviour we must analyze the time dependence of the flow velocity obtained from the solution of the complete one-dimensional equations. The case of channels without tidal flats is shown in figure 4a, displaying the temporal asymmetry of the flow field, characterised by falling tide longer than rising tide. Currents associated with this temporal asymmetry exhibit a peak value of velocity during the flood phase: these tidal waves are referred to as flood-dominant. Figure 4a also shows that, for the present value of the relevant parameters and with the schematic geometry of the channel considered herein, the solution of the full de Saint Venant problem is practically indistinguishable from the solution of the two-dimensional shallow water equations. Comparison is still quite satisfactory in the presence of not too wide tidal flats (Fig. 4b, c, d) In particular, results obtained from the one-dimensional solution display a slight amplification of the velocity field during the ebb phase, leading to different predictions for the character of the flow field for small values of β . In fact, for $\beta=4$ (Fig. 4b) the maximum velocity at the channel inlet as predicted by the one-dimensional model occurs during the ebb phase (ebb dominated flow), while the two-dimensional model predicts that the flow field is still flood dominated. However, for higher values of β , both the models predict that the peak velocity at the inlet occurs during the ebb phase, suggesting that the presence of tidal flats does modify the character of the flow field in the channel, provided their area is sufficiently large.

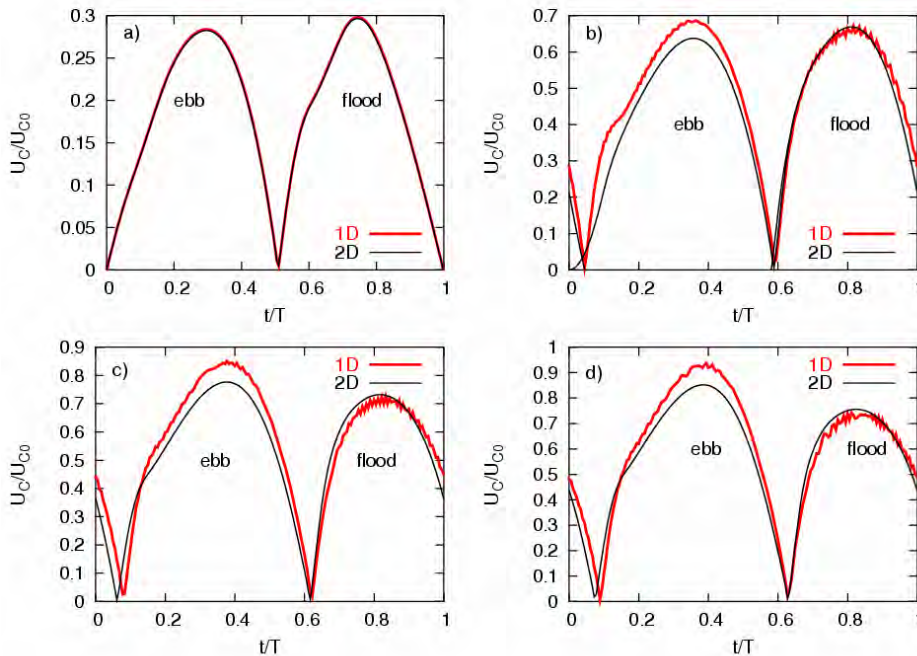


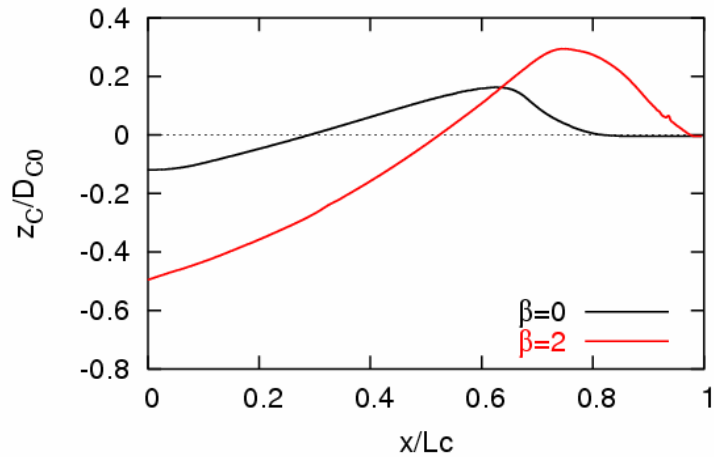
Fig 4 – Temporal evolution of the dimensionless inlet velocity predicted by the complete de Saint Venant equations (red line) and by the two-dimensional shallow water equations (black line), in a channel (a) without tidal flats ($\beta=0$) or flanked by tidal flats with (b) $\beta=4$, (c) $\beta=10$, (d) $\beta=20$. The values of the relevant dimensionless parameters are $\varepsilon=0.175$, $\varepsilon_F=0.35$, $\varphi=0.5$, $\chi=0.45$.

5 Some preliminary results on the morphodynamic evolution of tidal channels with adjacent tidal flats

In this section we investigate the first stages of the morphodynamic evolution of a tidal channel flanked laterally by tidal flats. The problem is tackled coupling and solving numerically the 2D hydrodynamic problem formulated in section 3 along with the 2D equation of the mass conservation for the solid phase [Exner, 1925]. Note that, as a first step, we account only for the effects of tidal currents, neglecting sediment resuspension driven by wind acting on the free surface of the shoals. We consider both contribution of bed load and suspended load, employing the Meyer Peter Muller [1948] and van Rijn [1984] formulations, respectively. Sediment exchange between the channel and the shoals is evaluated assuming that, during the flood phase, only the sediments present in the portion of the water column of the channel exceeding the elevation of tidal flats may enter the shoals while, during the ebb phase, all the sediments resuspended in the water column above the shoals may be carried by the ebb currents into the channel. Numerical simulations have been performed for a tidal channel characterised by the following dimensionless parameters at the initial condition $\varepsilon=0.29$, $\varepsilon_F=0.35$, $\varphi=0.5$, $L/L_0=0.14$. In the first numerical test we considered a tidal channel flanked by narrow tidal flats ($\beta=2$), while, in the second experiment, the relative width of the flats β has been increased to 10.

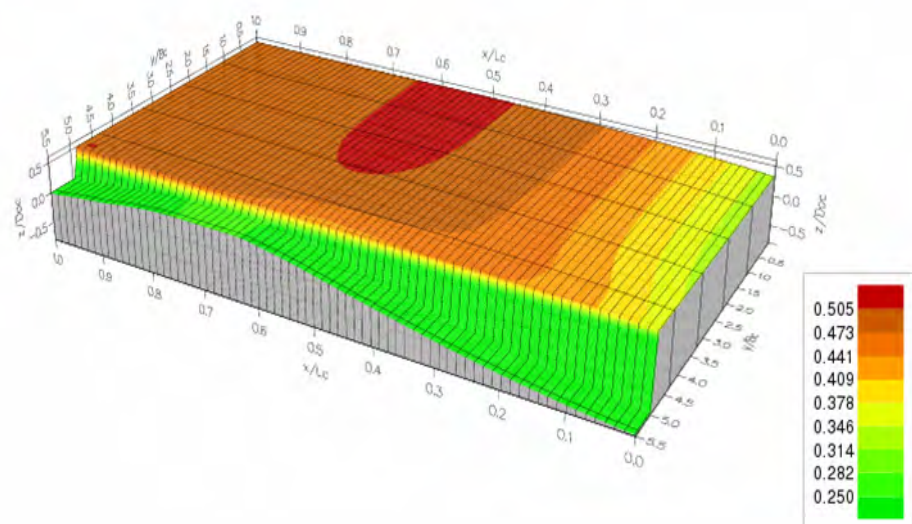
In Figure 5 we compare the cross sectionally averaged longitudinal bottom profile of a channel in the absence of tidal flats with that obtained in the case of a channel flanked by narrow tidal flats ($\beta=2$) after 60 tidal cycles.

Fig 5 – Comparison of the cross sectionally averaged longitudinal bottom profile of a channel without tidal flats (black line) with that corresponding to a channel with small tidal flats ($\beta=2$, red line) after 60 tidal cycles. The dotted line indicates the initial flat bottom.



In both cases, the bottom was assumed to be initially flat. Results show that the presence of the tidal flats, although of small width, affects significantly the morphodynamic evolution of the bottom profile of the channel. In fact, as a result of the acceleration of the flow field in the channel due to the presence of tidal flats, both scour at the inlet and sediment deposition in the inner part of the channel are enhanced. The morphodynamic evolution of the shoals is similar to that displayed by the tidal channel. In Figure 6 we plot the bottom topography of a tidal channel flanked by wide tidal flats ($\beta=10$) after 60 tidal cycles. Starting from an initial plane bed, sediments are scoured at the inlet of the shoals and transported landward. Note also that the exchange of sediments from the channel to the shoals tends to form natural levees along the shoal margins.

Fig 6 – Topography of the bottom of a tidal channel flanked by wide tidal flats ($\beta=10$) after 60 tidal cycles. The bottom elevation (z) is scaled by the initial mean flow depth in the channel (D_{0c}). Initially both channel and tidal flats were flat ($z_c/D_{0c}=0$, $z_f/D_{0c}=0.5$).



Conclusions

The problem of tide propagation in straight rectangular channels with adjacent tidal flats has been studied through the formulation of different models of

increasing complexity. We have moved from a simple analytical approach based on classical assumptions, namely tidal forcing characterised by small relative amplitude and linear dissipation. Results show that tidal flats reduce the resonance length of tidal channels, the more so as the width of tidal flats increases. The generation of tidal asymmetries was then investigated via numerical integration of both the one-dimensional de Saint Venant and two-dimensional shallow water equations. Results also suggest that the presence of flats may turn a flood dominant channel into ebb dominant provided the area of flats is sufficiently large. Note that, despite the complexity of the problem, the general features of the estuarine response to tide propagation do emerge from the use of one-dimensional models though, in the presence of wide tidal flats, two-dimensional effects are not negligible and call for suitable modelling.

Finally the morphodynamic evolution of a tidal channel flanked laterally by tidal flats has been studied via numerical integration of the shallow water equation coupled with a 2D form of the sediment continuity equation for the solid phase. Preliminary results show that the presence of the tidal flats affects significantly the morphodynamic evolution of the bottom profile of the channel, enhancing the magnitude of the scour at the inlet and sediment deposition in the inner part of the channel. The morphodynamic evolution of the longitudinal bottom profile of the shoals is similar to the one displayed by the tidal channel, while the exchange of sediments from the channel to the shoals tends to form natural levees along the shoal margins. Note that numerical simulations have been performed neglecting sediment resuspension driven by wind acting on the free surface of the shoals. The latter effect is twofold: on one hand, it generates wind waves the amplitude of which is strongly dependent on the shoal depth and on the fetch, on the other hand it generates currents driven by the surface setup induced by the shear stress acting on the free surface. These mechanisms are of great importance for the final aim to predict the morphological evolution of a tidal channel flanked laterally by tidal flats and will be investigated in the near future.

References

- Bolla Pittaluga M., 2003. Long term morphodynamic equilibrium of tidal channels, PhD thesis, Università degli Studi di Padova, Padua, Italy.
- Carniello L., Defina A., Fagherazzi, S. and D'Alpaos L., 2005. A combined wind wave-tidal model for the Venice lagoon, Italy, *J. Geoph. Res. Earth Surface*, 110, F04007.
- Exner F. M., 1925. Über die wechselwirkung zwischen Wasser und geschiebe in Flüssen, *Sitzer Akad. Wiss. Wien*, 165-180.
- Istituto d'Iraulica dell'Università di Padova, 1979. Le correnti di marea nella laguna di Venezia, technical report, 95 pp., Com. per lo studio dei provvedimenti a difesa della città di Venezia e salvaguardia dei suoi caratteri ambientali, Minist. Dei Lavori Pubbl., Padua, Italy.
- Meyer Peter E. and Muller R., 1948. Formulas for bedload transport, Conf. of

Internat. Ass. of Hydraul. Res. Stockholm, Sweden.

Lanzoni S. and Seminara G., 2002. Long-term evolution and morphodynamic equilibrium of tidal channels, *J. Geoph. Res.*, 107, C1, 10.1029.

Schuttelaars, H. M. and de Swart H. E., 1996. An idealized long-term morphodynamic model of a tidal embayment, *Eur. J. Mech. B Fluids*, 15, 55-80.

Schuttelaars, H. M. and de Swart H. E., 2003. Multiple morphodynamic equilibria in tidal embayment, *J. Geoph. Res.*, 105, 24, 105-24, 118.

Stansby P.K. 2003. A mixing length model for shallow turbulent wakes. *Jour. Fluid Mech.*, 495:369-384.

Stansby P.K., 2006. Limitations of the depth-averaged modelling of shallow wakes, *ASCE J. Hyd. Engrg*, 132 (7), 737-740.

van Rijn L. C. 1984. Sediment transport, Part II: Suspended Load Transport. *J. Hydraul. Eng.*, ASCE, 110(1), 1616-1641.

THE DYNAMIC SIMULATION OF THE VENICE LAGOON AND OF THE NORTH PARTH OF THE ADRIATIC SEA

Maria Morandi Cecchi, Manolo Venturin

*Dipartimento di Matematica Pura ed Applicata, Università degli Studi di Padova
Via Trieste 63, 35121, Padova*

Riassunto

In questi ultimi anni, abbiamo pubblicato molti articoli sulla risoluzione numerica delle equazione delle Acque Basse mediante il metodo agli elementi finiti e, di conseguenza, c'è stato un grande interesse nello sviluppo di metodi appropriati. Il successo del metodo agli elementi finiti per questa tipologia di problemi è stato ampiamente dimostrato; rimane tuttavia un'ampia e diversificata classe di applicazioni quando lo si adatta alle diverse realtà fisiche.

Lo scopo di questo lavoro è quello di analizzare e riassumere il modello computazionale sviluppato dagli autori per la simulazione del sistema lagunare veneziano e presentare la completa bibliografia dei risultati fin qui ottenuti.

Abstract

During the recent years, we have published a significant number of papers which apply the finite element method to the solution of the shallow water equations. Moreover, a considerable research effort has been spent on the development of finite element methods to the solution of fluid flow problems. The success of the finite element method for this kind of problems has been shown, but still remain a large number of research tasks when the method is adapted to different physical situations.

The purpose of this paper is to address and to analyze the computational model developed by the authors for tidal simulation in the Venice Lagoon system and to present the complete references of the obtained results.

1 Introduction

A number of important phenomena that appear in the solution of hydrodynamic problems in Venice lagoon, are described by the nonlinear shallow water equations with appropriate boundary and initial conditions. Their solution is of great importance for tidal prediction, since it is desired to have both accurate simulation and complex physical models, in order to give an accurate description of the reality [Morandi Cecchi et al., 2005a].

Fluid flow in the Venice Lagoon system can be simulated by the well known two-dimensional shallow water equations [Morandi Cecchi, 1989]. These equations describe the evolution of an incompressible fluid with respect to the

gravitational and rotational accelerations under the hypothesis that (i) the water elevation with respect to the free surface at rest is at any time much smaller than the depth; (ii) vertical effects (acceleration and diffusion) are negligible and (iii) horizontal effects do not vary with the depth [Morandi Cecchi et al., 1998]. The solution of this set of equations provides the water velocity profile and the water surface elevation.

During the last years, considerable effort has been focused towards the development of two-dimensional models for the numerical approximation of the shallow water equations both in conservative and non-conservative forms, and many numerical schemes are now available for that purpose. The success in the use of the finite element method for this kind of problems has been shown; in particular in this work, we have extended the description of the previous developed model focusing towards an introduction of a more fine description of the geometry and of the computational mesh.

The complete references of this work are presented at the end of the paper.

2 Model description

The solution of the shallow water equations are obtained by an integration procedure along the vertical direction and some difficulties arise. In particular the difficulties for the standard Galerkin finite element methods are of three different kinds: (i) the continuity equation; (ii) the convection-diffusive character of the equations; (iii) and the nonlinearity of the problem.

The first type of difficulty in the approximation of the shallow water equations is the coupling of the momentum equations with the incompressibility conditions, and, hence, the correct treatment of the pressure or the equivalent elevation term. This term represents a constraint on the velocity field which must be divergence free. In our framework, the use of the CBS method overcomes this difficult by a splitting technique [Venturin, 2006].

Another source of numerical difficulty is due to the presence of nonlinear and non-symmetric convective terms in the momentum equations, especially in the case when the convection dominates the diffusion. In this case the best approximation property in the energy norm of the Galerkin method is lost and solutions may be corrupted by spurious node to node numerical oscillations. The use of the Characteristic-Galerkin method overcomes this type of numerical problems [Venturin, 2006].

The starting point for the development of the finite element models for the shallow water equations is the use of the fractional step procedure introduced by Chorin and Temam for incompressible Navier-Stokes equations. Moreover, in the CBS scheme it is used the Characteristic-Galerkin method for the approximation of the convection-diffusion equations. The Characteristic-Galerkin method is based on a discretization procedure using an approximation of the total derivative leading to the introduction of an appropriate stabilization term.

The following steps summarize the CBS scheme for the shallow water equations:

- In the first step an intermediate velocity field is estimated from the solution of the momentum equations where the pressure or elevation term is dropped. This approximation is done by the use of the Characteristic-Galerkin method since the involved equations are of the convection-diffusion type;
- In the second step the continuity equation is solved using the intermediate vector field value and the pressure is computed by solving a Laplacian-type equation, whose self-adjoint form makes the Galerkin space discretization optimal;
- In the third step the hydrodynamic model is solved computing the velocity field using the previously intermediate values and the new pressure term;
- Any other scalar equation that describes transport phenomena not coupled to the hydrodynamic model, like pollutant transport or temperature distribution, may be solved by the Characteristic-Galerkin method.

The success of the implementation of a finite element model for computing shallow water flow requires the identification and spatial discretization of a surface water region. In this field, the use of unstructured triangular elements are the basic elements to perform the fundamental steps of the finite element model. In the developed model both isotropic and anisotropic adaptivity has been considered [Morandi Cecchi et al., 1999a; Morandi Cecchi et al., 2007].

A parallel implementation of the model has been developed in this research unit. In the finite element method with parallel computing, the fundamental goal is to decompose the domain into sub-domains so that each processor has to do about the same amount of work, and so that the communication time is as small as possible [Morandi Cecchi et al., 1993].

It can be noted that formally the partitioning of unstructured mesh is a very hard problem (NP-complete). In [Morandi Cecchi et al., 2002] an approach based on Enhanced Sub-domain Generation Method (ESGM) using linear separator determined by a Genetic Algorithm (GA) is used to solve this task.

3 Application of the model to the Venice Lagoon

The model is obtained considering different depths of the lagoon and also a finer discretization is used along the main channels of the lagoon. The finite element discretization and the bathymetry are shown in Figure 1 and Figure 2, respectively.

At the three inlets/outlets, Lido, Malamocco and Chioggia, that separate the lagoon system from the Adriatic sea, the water elevations and the flow directions are prescribed while, along the coastline, the normal velocity to the coast is assumed to be zero.

From Figure 3 to Figure 8, it is shown the current flow at the flood and ebb phase at the inlets of the lagoon at the same time. In these figures the different behavior of the lagoon inlets may be seen, especially in the ebb phase at the Lido mouth where the circulation seems to be able to carry out completely the

water inside the upper zone of the lagoon. For the details of the simulation see [Morandi Cecchi et al., 2006a].

Wind data are also considered in this model. In particular, an appropriate interpolation/extrapolation procedure has been developed to extend experimental data available at the three station of Chioggia south dam, Malamocco south dam and Grassabò, to the overall domain. Details are available in [Morandi Cecchi et al., 1998].

The model may be extended with the discretization of the north part of the Adriatic Sea as done in [Boscolo, 2004], where the computation domain is shown in Figure 9.

Then, a forcing term corresponding to a complete tidal cycle is applied to the coastline of the Adriatic Sea, as indicated by an asterisk in Figure 9, with a period of 12 hours and an amplitude of 80 cm. After having realized this simulation, a number of dams was inserted in front of the mouths of the lagoon, to control the possible obstruction introduced by human intervention. As can be seen in Figure 10, a delay and a reduction of the motion is introduced between the two simulations (with and without obstructions) due to the discharge reduction at the mouths.

4 Conclusions

In this paper some results are reported of the simulation obtained updating the geometry, the mesh parameters and the physical models. This model is shown to be a flexible tool for the description of shallow water phenomena in the Venice Lagoon; in fact, it permits to treat with complex geometry, different physical parameters and several boundary conditions. The model is performed using the CBS method which ensures a correct treatment for the convection-diffusion equations as well as for the shallow water equations.

References

- Morandi Cecchi M., 1988. Domain decomposition method for shallow water flow problems. In Niki N., Kawahara M. (eds), *Computational Methods in Flow Analysis*, 2, Okayama University of Science, 1322-1329.
- Morandi Cecchi M., 1989. Study of the behaviour of oscillatory waves in a lagoon. *International Journal for Numerical Methods in Engineering*, 27, 103-112.
- Morandi Cecchi M., Secco E., Pica A., 1993. Domain decomposition of finite element model of a lagoon. In Morgan K., Morandi Cecchi M., Zienkiewicz O. C. (eds), *Finite Elements in Fluids*, Pineridge, Swansea, 990-998.
- Morandi Cecchi M., Secco E., Pica A., 1993. Tidal flow analysis with core minimization. In Morgan K., Morandi Cecchi M., Zienkiewicz O. C. (eds), *Finite Elements in Fluids*, Pineridge, Swansea, 1026-1036.
- Morandi Cecchi M., Secco E., Pica A., 1995. A study of the Venice lagoon by

domain decomposition of a finite element model. In Morandi Cecchi M., Morgan K., Periaux J., Schrefler B. A., Zienkiewicz O.C. (eds), *Finite Elements in Fluids* Vol. 2, 1417-1426.

Morandi Cecchi M., Pica A., Secco E., 1998. A projection method for shallow water equations. *International Journal for Numerical Methods in Engineering*, 27, 81-95.

Morandi Cecchi M. and Salasnich L., 1998. Shallow water theory and its application to the Venice lagoon. *Computer Methods for Applied Mechanics Engineering*, 151, 63-74.

Morandi Cecchi M. and Salasnich L., 1998. The shallow water equations: state of the art and new trends. In *Computational Fluid Dynamics Review 1998*, Vol. II, Hafez M., Oshima K. (eds), World Scientific Singapore.

Morandi Cecchi M., and Marcuzzi F., 1999. Adaptivity in space and time for shallow water equations. *International Journal of Numerical Method in Fluids*, 31, 285-297.

Morandi Cecchi M., De Marchi S., Secco E., 1999. Un Modello Idrodinamico per lo studio del moto nella Laguna di Venezia. In *La Ricerca Scientifica per Venezia II, Progetto Sistema Lagunare Veneziano*, Vol. II, Tomo II., 815-838.

Morandi Cecchi M., and Pirozzi M. A., 2002. A parallel shallow water finite element solver for the Venice lagoon. *International Journal of Computational Fluid Dynamics*, 16 (2), 93-99.

Morandi Cecchi M., Pirozzi M. A., 2004. High order finite difference numerical methods for time-dependent convection dominated problems: Formulation. In *Mascot03, IMACS/ISGS International Society of Grid Generation*, Rome, Pistella F., Spitaleri R. M. (eds), vol. 8, 131-140.

Morandi Cecchi M., Venturin M., 2004. An algorithm for anisotropic mesh. An application to the Venice Lagoon canals. In *Mascot04, 4th on Applied Scientific Computing and Tools Grid Generation Approximation and Visualization*, 25-27 November- Florence, Pistella F., Spitaleri R.M. (eds), IMACS Congress, 151-160.

Morandi Cecchi M., Venturin M., Russo M. R., Marcuzzi F., 2004. A general framework for error estimation in preserving-shapes grid generation in a fluid dynamics environment and related open problems. In *ECCOMAS 2004 Congress*. 24-28 July 2004, vol. 2, 300-301. Full Paper in the Proceedings of *Eccomas 2004* (available online).

Boscolo D., 2004. Un modello dedicato al sistema laguna di Venezia. Thesis at the University of Padova, A.A. 2003-2004.

Morandi Cecchi M., Venturin M., Russo M., 2005. 6. M. Morandi Cecchi; M. Venturin, M. R. Russo. Some Advantages of the Use of a Model Dedicated to the Venice Lagoon System. *Lagoons and Coastal Wetlands in the Global Change Context: Impacts and Management Issues*. Proceedings of the International Conference, Venice, 26-28 April 2004. Edited by Pierre Lassarre,

Pierluigi Viaroli and Pierpaolo Campostrini. Publication: IOC Integrated Coastal Area Management (ICAM), Dossier n.3. UNESCO, 2005, pagg. 232–237.

Morandi Cecchi M., Venturin.M., 2005. A CBS Framework for Advection – Diffusion Equations and Shallow Water Problems. In TCN-CAE 2005 and Mascot05, 5-8 October, Lecce, Italy, International Conference TCN CAE 2005 International Conference on CAE and Computational Technologies for Industry and Mascot Meeting on Applied Scientific Computing and Tools Grid Generation, Approximation and Visualization, Pistella F., Spitaleri R. M. (eds), Vol. 10, 82-90.

Morandi Cecchi M., Marcuzzi F., 2005. A parallel solver for adaptive finite element discretization. Num. Algorithms, Vol 40, 217-231, ISSN:1017-1398.

Morandi Cecchi M., Venturin. M., 2005. An anisotropic mesh algorithm: formulation and results, 17th IMACS World Congress on Applied Mathematics and Simulation, 17-15 July, Paris. Proceedings on CDROM.

Morandi Cecchi M., Pirozzi M. A., 2005. High order finite difference numerical methods for time-dependent convection-dominated problems. Applied Numerical Mathematics, Vol.55, 334-356, ISSN: 0168-9274.

Venturin M., 2006. A finite element stabilization system for advection-diffusion problems. Phd Thesis at the University of Padova.

Morandi Cecchi M., Venturin M., 2006. Characteristic based split (CBS) algorithm finite element modelling for shallow waters in the Venice lagoon. Internat. J. Numer. Methods Engrg., 66 (10), 1641-1657.

Morandi Cecchi M., Venturin M., 2006. Tidal simulation in Venice lagoon. In: CORILA Research Program Results, Scientific Research and Safeguarding of Venice, Campostrini P. (ed),. CORILA, Vol. IV, 465-476, ISBN: 88-89405-01-5. Research Program 2004-2006, Volume IV 2005 Results. Venezia, CORILA Italy.

Morandi Cecchi M., Venturin M.,. 2006. A formulation of convection problems for shallow waters in Venice Lagoon. In: CORILA Research Program Results, Scientific Research and Safeguarding of Venice, Campostrini P. (ed),. CORILA, Vol. IV, 477-490, ISBN: 88-89405-01-5. Research Program 2004-2006, Volume IV 2005 Results. Venezia, CORILA Italy.

Morandi Cecchi M., Marcuzzi F., Venturin M., 2007. An Anisotropic unstructured triangular adaptive mesh algorithm based on error and error gradient information. Applied Numerical Mathematics (accepted for publication).

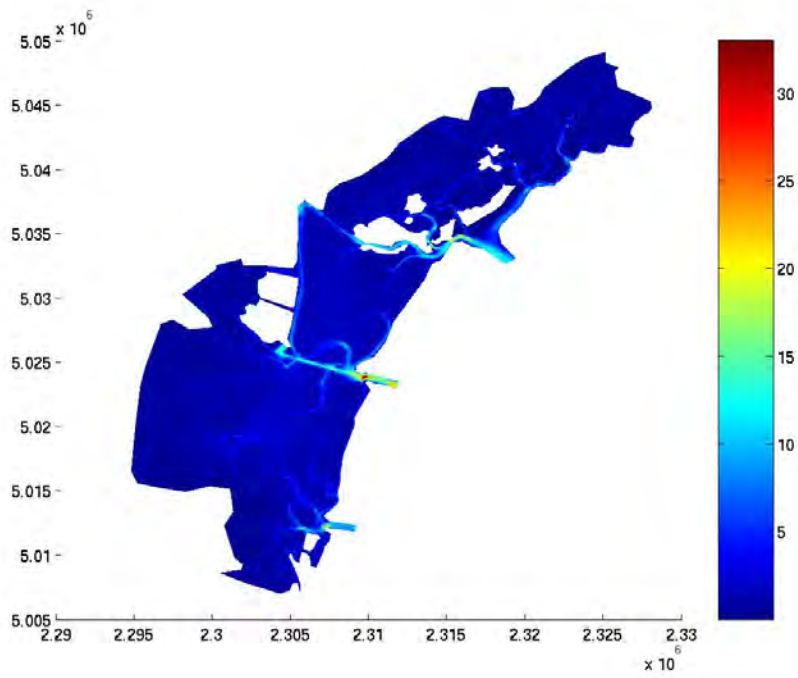


Fig 1 – The Venice Lagoon bathymetry (depth in meters).

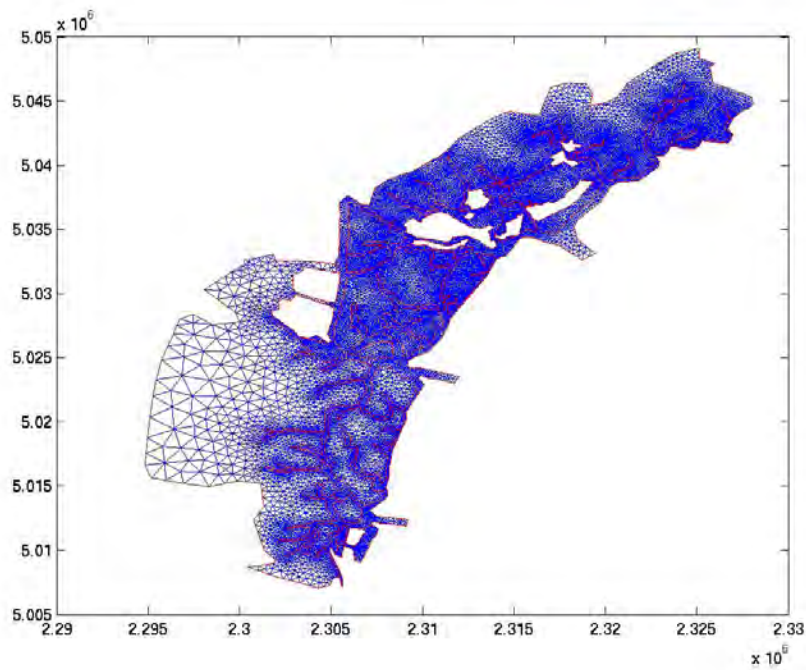


Fig 2 – The Venice Lagoon mesh (31613 points and 61447 elements).

Fig 3 – Flood phase at the Lido inlet.

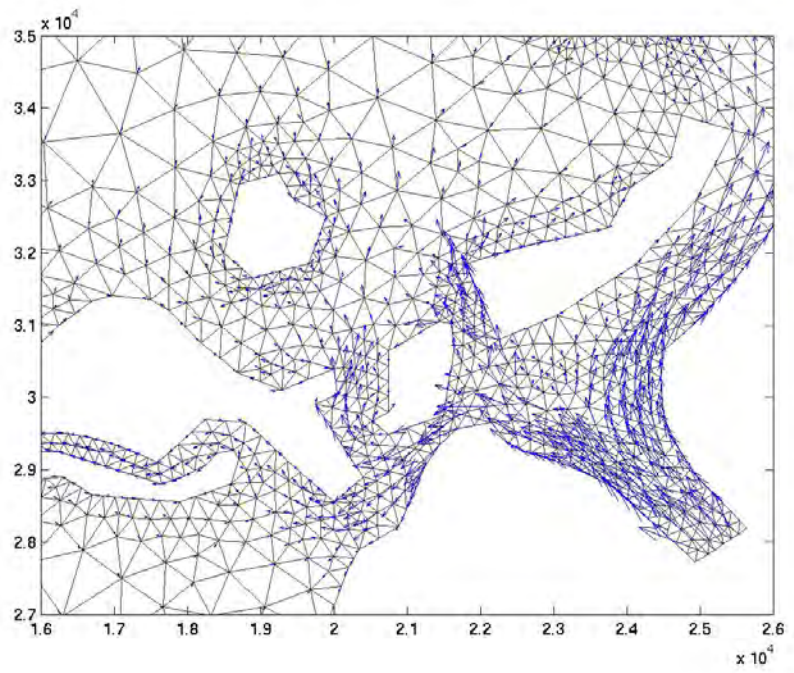
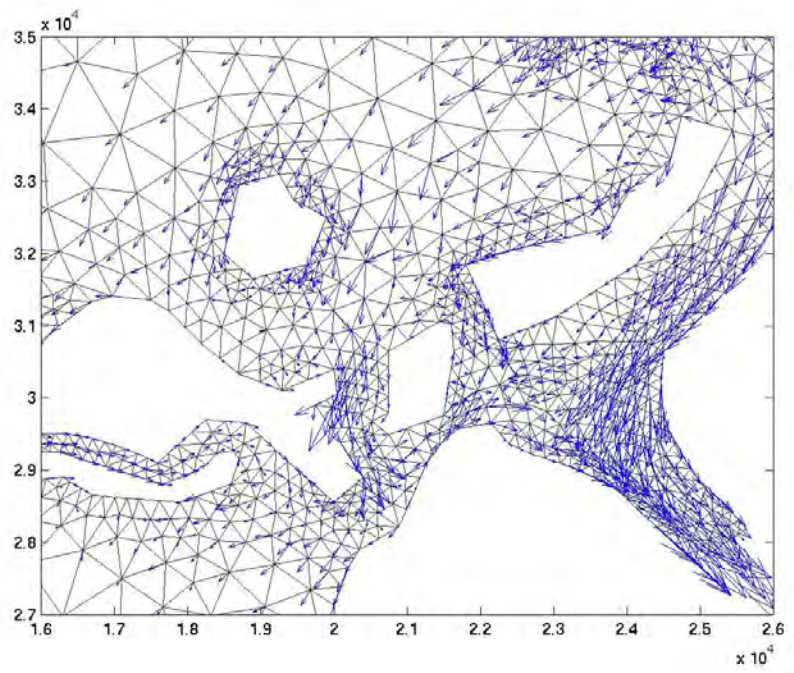


Fig 4 – Ebb phase at the Lido inlet.



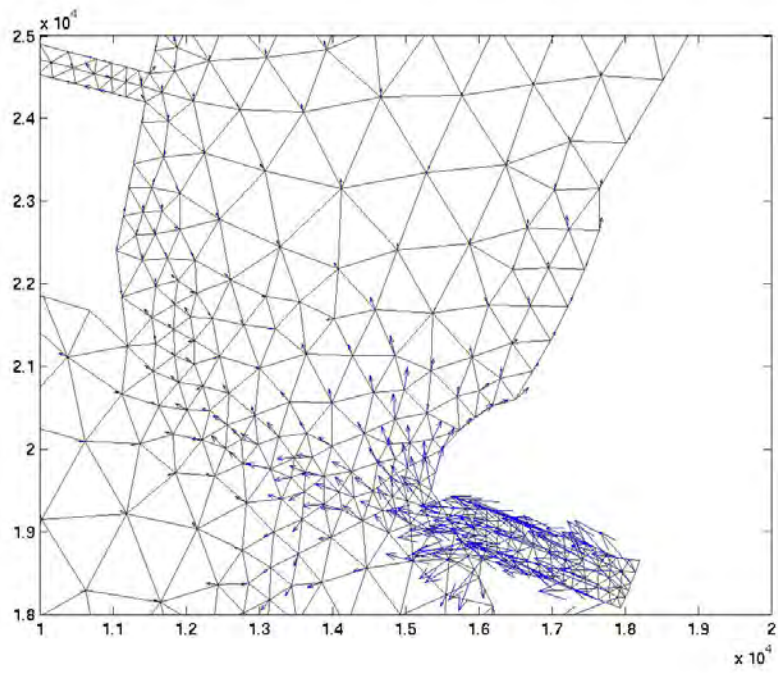


Fig 5 – Flood phase at the Malamocco inlet.

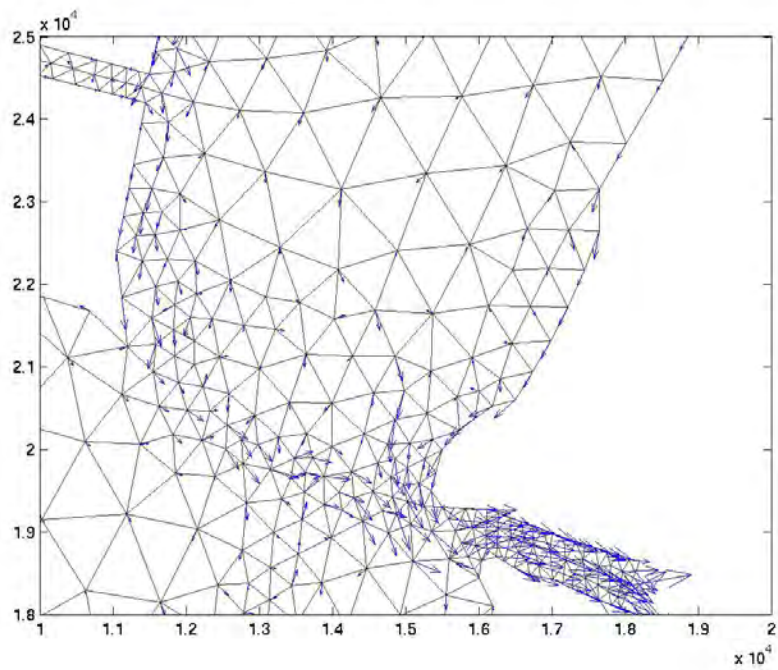


Fig 6 – Ebb phase at the Malamocco inlet.

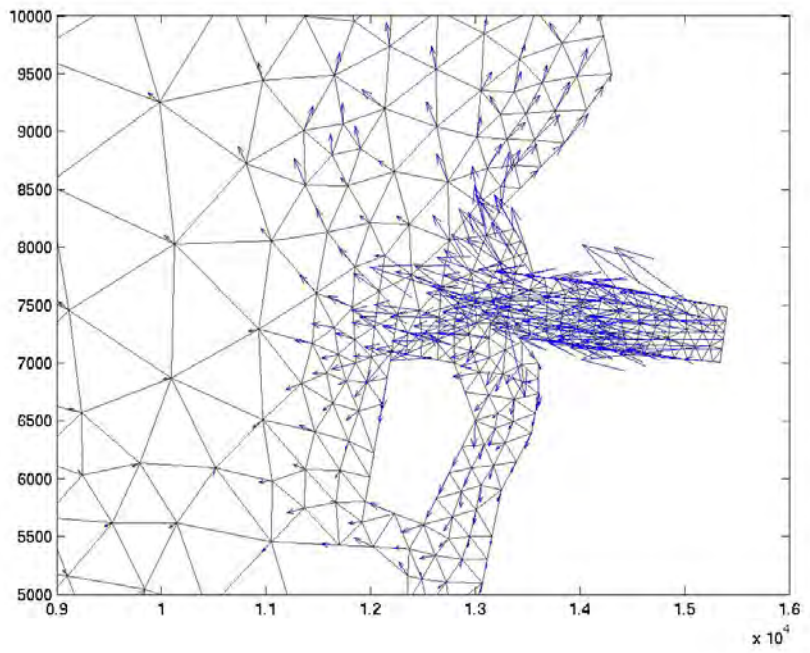


Fig 7 – Flood phase at the Chioggia inlet.

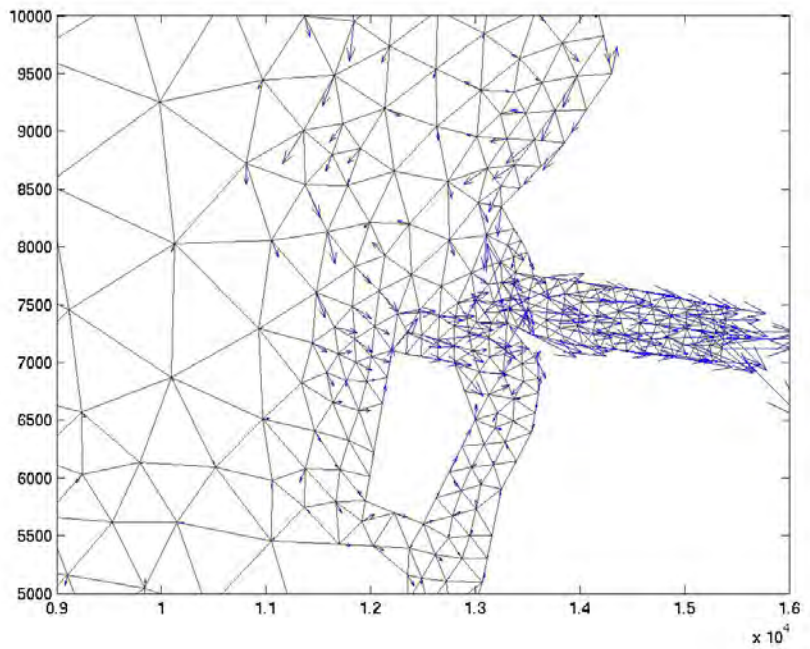


Fig 8 – Ebb phase at the Chioggia inlet.

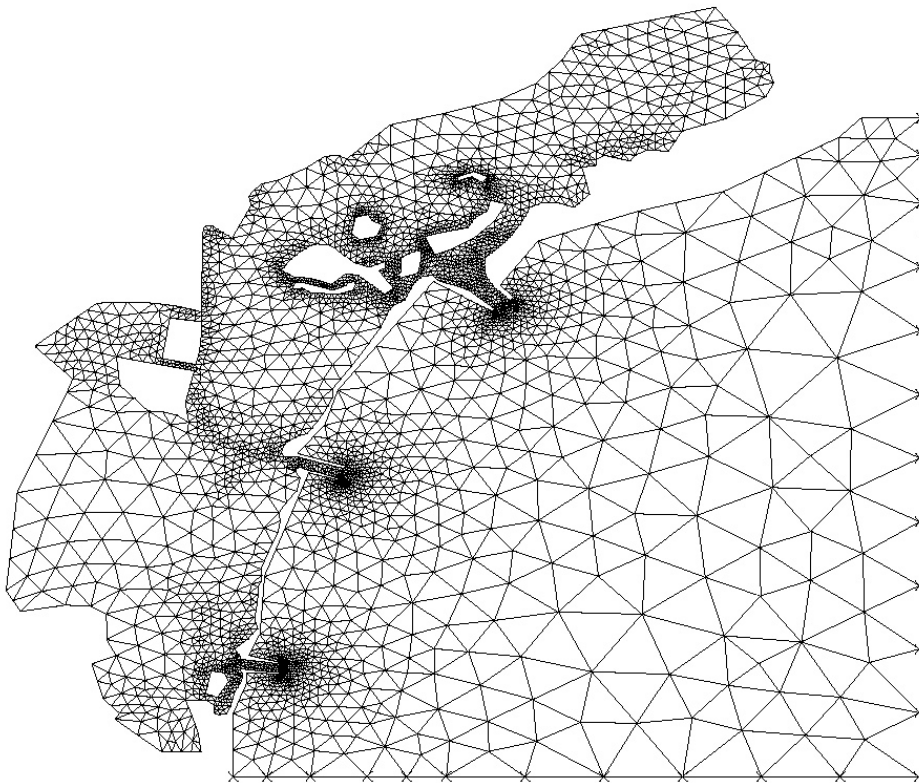


Fig 9 – Mesh of the Venice Lagoon and the Adriatic Sea

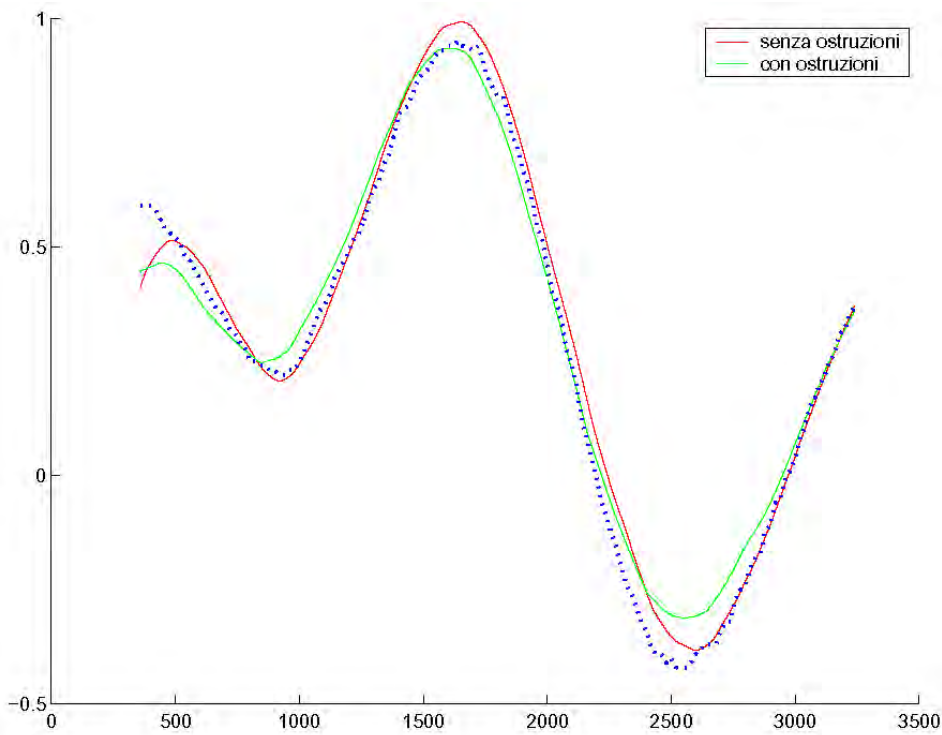


Fig 10 – Simulation with the Adriatic Sea; real data (blue), simulation without obstructions (red) and simulation with obstructions (green).

TIME SCALES AND THE TRAPPING INDEX

Georg Umgiesser¹, Andrea Cucco²

¹ ISMAR-CNR, Castello 1364/A, 30122 Venezia, Italy,

² IAMC-CNR, Loc. Sa Mardini 09072 TorreGrande Oristano, Italy

Riassunto

Il tempo di rinnovo delle acque di una laguna o un bacino semi-chiuso può essere definito attraverso diversi indici, tra i quali i più comuni sono il tempo di residenza e il tempo di transito.

In questo lavoro partendo dalla definizione di queste due scale temporali del trasporto è stato definito un nuovo indice *trapping index* in grado di individuare per un dato bacino o tratto di mare investigato le aree soggette a fenomeni di intrappolamento delle masse d'acqua.

Tale indice è stato applicato ad alcuni casi teorici al fine di valutare la sua efficacia nell'individuare le aree di intrappolamento delle masse d'acqua all'interno di canali e bacini semichiusi. Successivamente è stato applicato ad un bacino complesso, la Laguna di Venezia e in situazioni realistiche.

I risultati ottenuti hanno evidenziato come l'applicazione di tale indice sia molto efficace per l'individuazione di aree soggette a condizioni di un ridotto rimescolamento e di intrappolamento delle masse d'acqua.

Abstract

The water renewal of a lagoon or a semi-enclosed basin can be characterized by various parameters, like the residence and the transit time. Starting from these two time scales, a new index is defined, which is called *trapping index*. It identifies areas inside the water body where the water masses are trapped and the exchange with the other basin is strongly reduced and mainly driven by turbulent processes. Two simplified examples are given in which the trapping index is justified. Then the trapping index approach is applied to a real situation, the Venice Lagoon. The results show that the trapping index might be an important number to identify areas of low water exchange and possible environmental problems.

1 Introduction

The management of water basins like lagoons or semi-enclosed estuaries often requires the knowledge of the exchange characteristics of the water basin. Depending on the faculty to renew water masses these basins are more or less vulnerable to situations of pollution. A vigorous exchange with the open sea could guarantee a rapid replacement of the water masses and a certain protection from pollution events.

One possibility to characterize basins is using different characteristic time

scales like the residence time and the transit time. Both time scales give an idea of how long it takes that the water masses are replaced with new ones coming from the sea and also from rivers discharging in the basin. However, high residence or transit times not always identify areas where water masses remain trapped and exchange is restricted.

To better characterize areas of low exchange a new index is proposed which is called *trapping index*. The trapping index is a simple normalized product between the residence and the transit time. This allows for the identification of areas where both time scales are high. In the following it is shown that these areas do also correspond to problematic areas and hot spots where water masses might be vulnerable to pollution and problematic water quality.

The concept of residence and transit time is an old one and can be found in a series of articles published over the years [Bolin and Rodhe, 1973; Zimmerman, 1976; Dronkers and Zimmerman, 1982; Takeoka, 1984a,b; Sanford et al., 1992; Luketina, 1998; Wang et al., 2004]. These time scales are not readily measured in the field, and numerical modeling tools have to be used to quantify them. Whereas transit time is defined quite unambiguously, the term residence time is used with different meanings. The one used here is primarily chosen because of its easy implementation with numerical models.

Definition of the time scales and the model set-up are given in the next section. After this the utility of the trapping index is made plausible with two simple examples and results are presented for two real applications. At the end conclusions are drawn.

2 Methods

In this section the models that have been used in this study are shortly presented, the definitions of residence time and transit time are given and clarified and the trapping index is defined.

2.1 Models used

The hydrodynamic model used is the SHYFEM model, developed and maintained at the ISMAR-CNR in Venice and applied to the Venice lagoons and many other Mediterranean lagoons [Umgiesser et al., 2005]. It is a finite element model, solving the shallow water equations on a variable triangular grid. A semi-implicit time stepping scheme contributes to a stable resolution of the equations. Details can be found in former publications [Umgiesser and Bergamasco, 1995; Umgiesser et al., 2004].

The hydrodynamic model provides the currents that are used to compute residence and transit times. With this current field the Eulerian and Lagrangian transport is computed, as described in the next section.

The models have been run with variable time step. The hydrodynamic model is unconditionally stable for the gravity waves and Coriolis acceleration. The time step is limited only by the advective (transports of momentum and scalars) and diffusive terms (viscosity and diffusivity).

2.2 Residence time and transit time

The residence time is defined as the time required for the total mass of a conservative tracer originally within the whole or a segment of the water body to be reduced to a factor $1/e$ [Sanford et al., 1992; Wang et al., 2004; Luketina, 1998; Takeoka, 1984a,b]. It is computed using the mathematical expression given by Takeoka [1984a,b] known as the remnant function. For this a constant concentration C_0 is released inside the basin and its exchange with the open ocean is simulated. The concentration of the inflowing water is set to 0. The concentration $C(t)$ is computed in every grid point. With this the remnant function is defined as $r(t) = C(t)/C_0$ and the residence time is defined as

$$\tau = \int_0^{\infty} r(t) dt = \int_0^{\infty} C(t) / C_0 dt \quad (1)$$

It can be shown that, if the decay of the concentration is exponential, e.g.

$$C(t) = C_0 e^{-t/\tau} \quad (2)$$

then τ in both equations are identical and are representing the residence time. Therefore, τ represents the e-folding time for an exponential decay.

The so defined residence time is given by a Eulerian description, where the advection and diffusion of a tracer is simulated. This residence time can be given for the whole basin, averaging over the total concentration, but it can be also given for each grid node, where it would represent the local renewal characteristics of the area

On the other side, the transit time is computed through a Lagrangian approach. Its definition is the time a particle takes to leave the domain [Bolin and Rodhe, 1973; Zimmerman, 1976; Dronkers and Zimmerman, 1982; de Kreeke, 1983; Prandle, 1984].

Particles are released inside the basin and their trajectories are computed with the following equations

$$\frac{dx}{dt} = u \quad \frac{dy}{dt} = v \quad (3)$$

where u, v are the current velocities and x, y the coordinates of the released floats. The time is recorded until the particle leaves the basin and this is taken as the transit time of the particle, a characteristics of the point, where the particle has started.

Therefore, the residence time is a property of the local area and gives a time scale that indicates how long it takes for the water masses to be exchanged with new water. On the other side, the transit time is a property of the single water particle that is moving in the basin until it leaves it. Therefore it is related to a time scale that indicates how long it takes the water masses to be swapped out of the basin.

2.3 The trapping index

Areas with high residence time and transit time do normally not coincide. This is shown in more detail in the next section. In order to correlate the two time scales, a new index is introduced, which is called here trapping index. It is defined as follows

$$T = \frac{\tau^r}{\tau_{\max}^r} \frac{\tau^t}{\tau_{\max}^t} \quad (4)$$

where τ^r, τ^t are the residence and transit times respectively, and the subscript *max* indicates the overall maximum for these parameters in the basin. The maximums are therefore used to scale both time scales to their relative values in the range from 0 to 1. The trapping index is the product of both relative time scales and is therefore also contained between 0 and 1.

The trapping index is expected to be large only in areas, where both the residence time and the transit time are large. In areas, where one of these time scales is large and the other one is small, the trapping index will be also small. It will be negligible in areas where both time scales are small. It is therefore possible to easily identify areas that show high residence and transit times, e.g., areas that show a small trend to exchange water with the surrounding areas and that can be identified with water masses trapped in the basin. The examples in the next section should clarify these statements.

2.4 The practical implementation

For the computation of the residence time a tracer is released inside the domain with a constant value (e.g. 100 %). Water entering the basin through the open boundary is given a concentration value of 0. At every time step, and for every node of the computational domain, the concentration is recorded, and the remnant function is computed. Integrating the remnant function for a time series in one node gives the residence time in that node, as defined before. Doing this for every node allows the computation of the residence time for all nodes in the domain.

For the transit time, a certain number of particles are released homogeneously in the basin. In the present applications the number of particles is between 10000 and 50000, depending on the application. All particles record their time of release (always $t=0$) and their initial position. Once a particle leaves the domain, the time of exit is recorded, and the initial position of the particle is tagged with the time elapsed as the transit time. Averaging over all particles around one node defines the transit time of the node.

Transients are avoided by letting first the underlying hydrodynamics reach a steady state, or as in the case of the Venice lagoon, a dynamic steady state. Only then the concentration is set to the initial value and the particles are released. This moment is defined as time zero ($t=0$). Simulations should go on until no concentration is left inside the domain and all particles have exited. However, this would require extremely long simulations, especially in applications where areas with trapped water masses exist. Therefore, for the practical implementation, the simulation is carried out until a certain threshold

concentration is reached or concentrations show a near constant value. Similarly, if the number of particles reaches a certain percentage or the number of particles in the domain does not change anymore, the simulation is stopped. The threshold value for both time scales has been set to 5 %.

Please note that for the computation of the trapping index (and to a certain degree also for the relative values of the time scales), the exact value of the residence and transit time is not important, and the areas where a maximum occurs for both time scales (high trapping index) will give a similar if not identical value for the trapping index.

In the simulations, both tracer concentration and particles that have exited from the domain are excluded from the computation and are not allowed to enter again. Therefore, the return flow effects [Cucco and Umgiesser, 2006] induced by tidal action are not taken into account.

3 Results and discussion

3.1 Rectilinear channel

A simple test case is set up which consists of a rectilinear channel that shows a constant pressure gradient from south to north (Fig. 1). The pressure gradient is realized by imposing a constant water level difference between the southern and the northern open boundary. In order to avoid a transient phase, the hydrodynamic simulation is started earlier, and only when the currents are in steady state the particles and the tracer are released homogeneously in the channel.

Results can be seen in Fig. 1. Residence times show a linear increase from south to north. Their relative value is close to zero at the southern end, and close to 1 at the northern one. This is because new water masses arrive from the southern boundary very fast to the southern parts of the canal, but it takes a time $t_1 = L/v$ that these water masses reach the northern end, where L is the length and v the average velocity of the canal. Residence times are therefore maximum at the northern end.

Results for transit times are exactly opposite. Highest (relative) values of 1 are close to the southern boundary, because it takes time t_1 for these particles to leave the domain. On the other hand, particles at the northern part of the canal leave the domain immediately, and their transit times are close to 0.

If the trapping index is computed, the maximum value found is in the center of the canal with a value of 0.25. Remembering the previous definition of the trapping index, this low value means that there are no water masses trapped in the domain, a fact that is intuitively clear. Please note that just at looking at the respective time scales, this conclusion cannot be drawn. In fact, the residence or transit time can be made arbitrarily large by changing the dimensions of the canal, but the trapping index would not change.

3.2 Step-like channel

The same experiment is run with a different geometry. Now the canal shows a step-like feature in the center. It can be anticipated that the water dynamics is now completely different, and areas with low re-circulation will be created in the area just after the enlargement of the canal. For the geometry please see Fig. 2.

Residence times show similar values to the rectilinear canal in the central vein, low at the southern end, and higher at the northern one. However, maximum values are achieved just after the enlargement of the canal, where it takes a long time for the new water masses to entrain. Other small areas of high residence times can be found along the canal.

Again, transit times generally decrease from north to south. However, in the same place, just after the enlargement, where residence times are high, also transit times are high. The explanation is that particles released in this area need a long time to leave it. They are actually trapped in this area.

The confirmation of our reasoning comes from the map that shows the trapping index. Again, values inside the main canal are quite low, but are close to 1 in the aforementioned area. This confirms our intuitive feeling that there is low exchange in this area, and the validity of the trapping index of identifying this area is shown. Another area with a high trapping index, just after the new restriction, can be identified too.

Again, please note that by just looking at the residence or transit times, these areas could not be identified unambiguously. Relative high values can still be found for the residence time at the northern end of the canal, and for the transit time at the southern end. These values are comparable to the times that are computed in the trapping area. However, using both time scales through the trapping index identifies clearly the area where the water masses are actually confined.

3.3 The Venice lagoon

The methodology of the trapping index has been applied to the Venice lagoon. In a former paper [Cucco and Umgiesser, 2006] the residence times have been computed and discussed for idealized situations, especially for sirocco and bora winds. Here we show results of the same simulations computing the trapping index. Some evidence is produced that shows that the areas that are identified by the trapping index as areas with low exchange are in fact confining the water masses.

Bora winds

In Fig. 3 the trapping index has been computed for the Venice lagoon, when spring tides and a bora wind of 10 m/s (from the NE) is acting on the water masses. Residence times can be found in Cucco and Umgiesser [2006]. For the same situation, transit times are computed (not shown) and the trapping index is shown in Fig. 3. Apart from a small area in the south, there are basically two areas that show a high trapping index. One is in the very northeast of the lagoon, an area connected only through two small channels to the main basin of the lagoon. The other is the industrial port, in the central-western part of the

lagoon, just to the west of the island of Venice.

Whereas it is not astonishing, that the first area, due to its narrow connecting channels, shows trapped water masses, the industrial port is actually quite well connected through deep shipping channels to the central lagoon. However, there is evidence that during bora winds water masses get trapped inside the port. Fig. 4 shows a satellite image and results of a simulation with a passive tracer released inside the lagoon during outflow conditions and a strong bora wind blowing over the lagoon. Clearly visible in the satellite image are the different water masses that form a strong front along the Vittorio-Emanuele Channel. The water masses to the north of the channel are advected by the bora wind southward until they encounter the water masses exiting the industrial channel. These two water masses are advected eastward along the front into the Giudecca channel, where they eventually mix and reach one of the inlets of the lagoon.

The simulation results of the tracer in Fig. 4 confirm this interpretation. High concentrations of the tracer can still be found in the industrial channel, while the water masses north of the Vittorio-Emanuele Channel show very low values. The front of the two water masses is well reproduced. The exchange of the water masses inside the industrial port with the other lagoon waters is therefore very slow, giving rise to the feature found in the satellite image and the high trapping index computed in this area.

Sirocco winds

During sirocco winds from SE the exchange between the lagoon and the Adriatic Sea is less intense. The reason for this is that sirocco winds blow nearly perpendicular to the main axis of the lagoon that runs from NE to SW. A simulation has been set up, with spring tides and a sirocco wind of 7 m/s (from the SE) acting on the water masses. Residence times can again be found in Cucco and Umgiesser [2006] and the trapping index is shown in Fig. 5.

The trapping index is high only in two areas. The main area is the whole northern lagoon that shows restricted exchange of its water masses with the rest of the lagoon. This indicates that there is a tendency of the water masses during sirocco winds to stay confined in the northern end of the lagoon, whereas the rest of the lagoon exchanges easily with the Adriatic Sea.

The other area where higher values of the trapping index can be found is again in the industrial area. However, now only the very end of industrial channels are involved in this. Most of the industrial channels show values of around 0.3.

4 Conclusions

In this paper a new index has been introduced that allows for the individuation of areas of low water exchange with the open sea. With a relative simple application of standard modeling techniques this trapping index can be computed.

It is shown that a single time scale like the residence or transit time can sometimes give a misleading picture of the real situation. Even if one of these

time scales show high values, water masses might not show a slow exchange with the surrounding waters, but the high residence times might be caused from water masses that transit the area from other zones.

It is therefore recommended that the trapping index be used as a parameter that identifies potential trapped water masses that might be subject to pollution and low water quality.

Acknowledgements

This research has been partially funded by the Corila project 3.18 *Tempi di residenza e dispersione idrodinamica nella laguna di Venezia*.

References

Bolin, B., Rodhe, H., 1973. A note on the concepts of age distribution and transit time in natural reservoirs. *Tellus* 25, 58-63.

Cucco, A., Umgiesser, G., 2006. Modeling the Venice Lagoon Water Residence Time. *Journal of Ecological Modeling*. 193, 34-51.

de Kreeke, J. V., 1983. Residence time: application to small boat basins. *ASCE, Journal of Watereaty, Port, Coastal and Ocean Engineering* 109 (4), 416-428.

Dronkers, J., Zimmerman, J. T. F., 1982. Some principles of mixing in tidal lagoons. *Oceanologica Acta Proceedings of the International Symposium on Coastal Lagoons, Bordeaux, France, 9-14 September, 1981*, 107-117.

Luketina, D., 1998. Simple tidal prism model revisited. *Estuarine Coastal and Shelf Science*. 46, 77-84.

Prandle, D., 1984. A modeling study of the mixing of 137 cs in the sea of the european continental shelf. *Philosophical Transaction of the Royal Society of London* 310, 407-436.

Sanford, L., Boicourt, W., Rives, S., 1992. Model for estimating tidal flushing of small embayments. *Journal of Waterway, Port, Coastal and Ocean Engineering* 118 (6), 913-935.

Takeoka, H., 1984a. Exchange and transport time scales in the Seto Inland Sea. *Continental Shelf Research* 3 (4), 327-341.

Takeoka, H., 1984b. Fundamental concepts of exchange and transport time scales in a coastal sea. *Continental Shelf Research* 3 (3), 311-326.

Umgiesser, G., Bergamasco, A., 1995. Outline of a primitive equation finite element model. *Rapporto e Studi. Vol. XII. Istituto Veneto di Scienze, Lettere ed Arti, Venice, Italy*, 291-320.

Umgiesser, G., Canu, D. M., Cucco, A., Solidoro, C., 2004. A finite element model for the Venice Lagoon. Development, set up, calibration and validation. *Journal of Marine Systems* 51 (1-4), 123-145.

Umgiesser, G., Amos, C. L., Coraci, E., Cucco, A., Ferrarin, C., Melaku Canu, D., Scroccaro, I., Solidoro, C., Zampato, L., 2005. An open source model for the Venice Lagoon and other shallow water bodies. In: *Flooding and Environmental Challenges for Venice and its Lagoon: State of Knowledge*. C. A. Fletcher and T. Spencer (eds). Cambridge University Press. 401-417.

Wang, C., Hsu, M., Kuo, A., 2004. Residence time of the Danshueii river estuary, Taiwan. *Estuarine, Coastal and Shelf Science* 60, 381-393.

Zimmerman, J. T. F., 1976. Mixing and flushing of tidal embayments in the Western Dutch Wadden Sea, Part 1: Distribution of salinity and calculation of mixing time scales. *Netherland Journal of Sea Research* 10, 149-191.

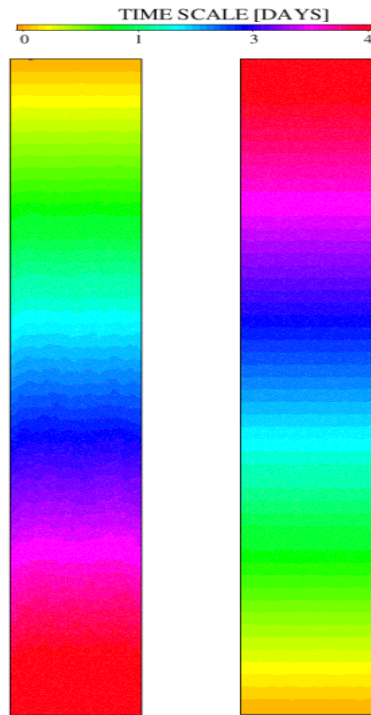


Fig 1 – Rectilinear canal.
Transit and residence times.

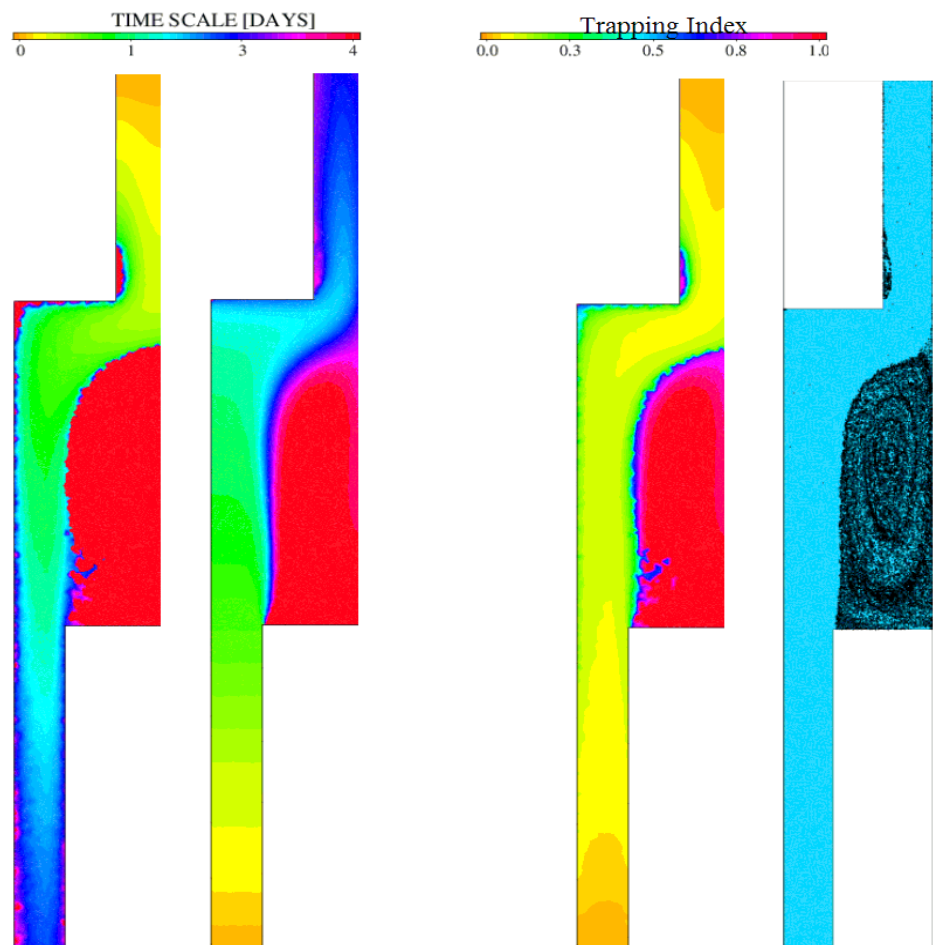


Fig 2 – Step-like canal.
Transit and residence times,
trapping index and particle
distribution in quasi steady
state.

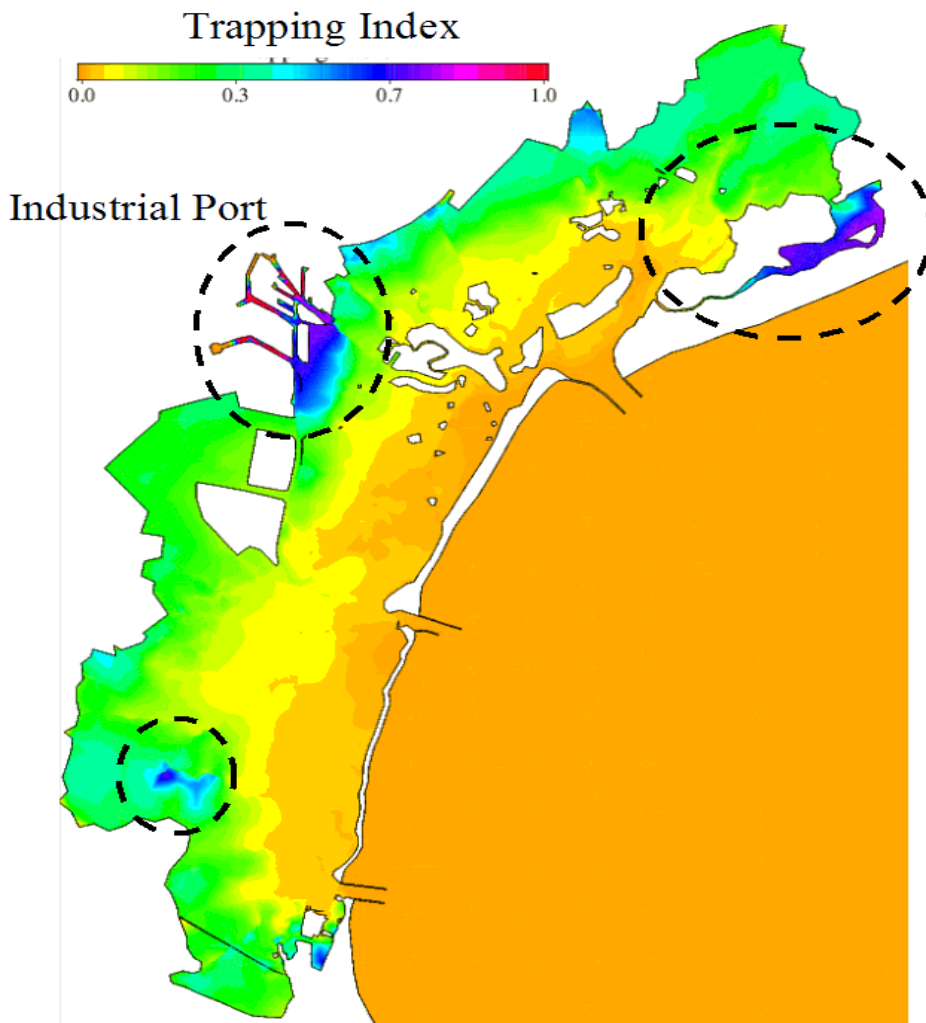


Fig 3 – Trapping index for the Venice lagoon during bora winds.

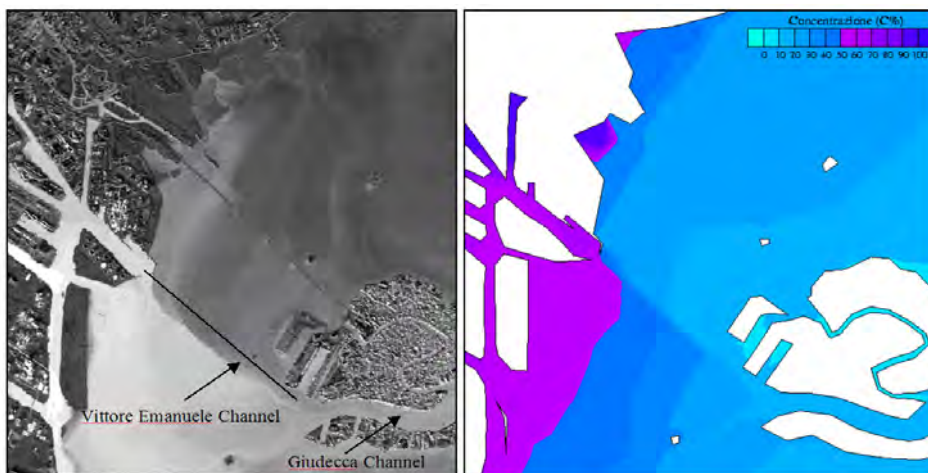


Fig 4 – Satellite image and modeled tracer concentration during a strong bora event.

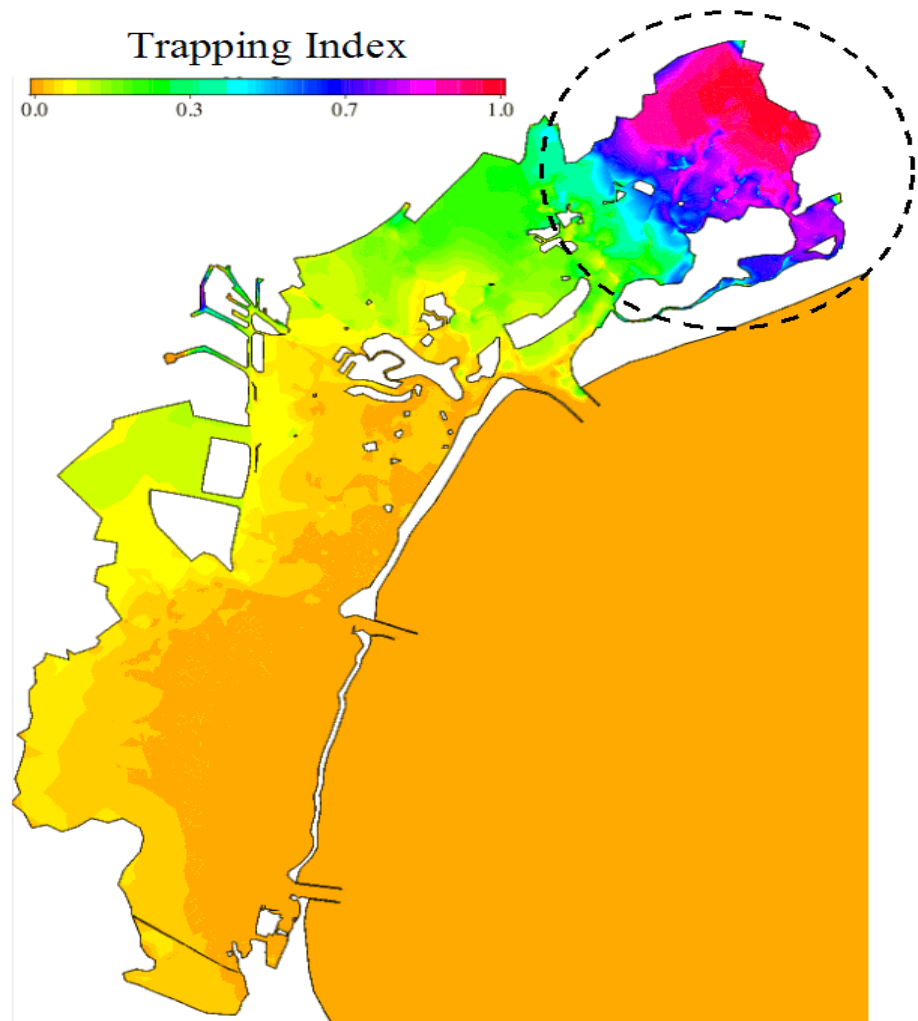


Fig 5 – Trapping index for the Venice lagoon during sirocco winds.

AREA 4

Data management

RESEARCH LINE 4.2

Modeling, analysis and environmental data visualization

IMPROVING THE ACCESS TO GEOGRAPHIC INFORMATION SYSTEMS: AN INTEGRATED VISUAL APPROACH BASED ON GOOGLE EARTH AND THE WEB3D

Fabio Pittarello

*Dipartimento di Informatica, Università Ca' Foscari di Venezia
Via Torino 155, 30172 Mestre (VE) ITALY pitt@unive.it*

Riassunto

L'associazione di dati di natura diversa alla localizzazione geografica sta diventando progressivamente importante in un crescente numero di domini, a partire dalla gestione del territorio fino alle scienze economiche e sociali.

I tradizionali sistemi informativi geografici (GIS) sono strumenti molto potenti per la manipolazione di informazioni georeferenziate, ma in molti casi la loro complessità richiede che, al fine di ottenere risultati utili, essi vengano utilizzati da operatori professionali.

Questo articolo contiene la proposta di un'architettura web-based per nascondere agli utenti la complessità dei GIS e per permettere loro di interagire con questi sistemi attraverso interfacce visuali semplificate, sia per l'interrogazione che per la presentazione dei dati. Questa integrazione rappresenta un avanzamento rispetto alle precedenti ricerche focalizzate selettivamente sulla fase di interrogazione o l'accesso ai dati risultanti.

Abstract

The association of data of different nature to geographical locations is becoming increasingly popular in a growing number of domains, including urban management, economics and social studies.

Traditional geographical information systems (GIS) are powerful tools for processing georeferenced information, but in most cases they are still complex systems that require highly trained users for obtaining useful results.

This work proposes a novel web-based architecture for hiding to the users the complexity of GIS and for allowing them to interact with the underlying spatial engine through simplified visual interfaces that take care both of the query and of the presentation phases. Such integration represents an improvement in relation to most of the previous research work focused, respectively, on easing the query or the access to resulting data.

1 Introduction

The knowledge of georeferenced data has become increasingly important in the last few years. Different domains ranging from urban studies to economics take

advantage of such knowledge for monitoring complex processes and elaborating strategies. Unfortunately, in many cases the management of georeferenced data needs sophisticated tools and interfaces that require a long training for taking full advantage of the system. The result is that often the users can't take advantage of the system potential because of their inability to operate on complex interfaces. Users often include professionals that have a deep knowledge of their domain but are not skilled in computer science.

This work describes an integrated system for easing the access to georeferenced information on the web. The architecture of the system permits the user to access a remote repository of georeferenced information and take advantage of a sophisticated engine for performing spatial operations on such data, without being overwhelmed by sophisticated interfaces for the query and the presentation of information.

Two visual environments for the input and the output are integrated in a unified interface that completely hides to the user the complexity of the underlying GIS engine. Such integrated solution represents an improvement in relation to most of the research work for easing the access to GIS, that focuses only on the input or, alternatively, on the output interface.

Concerning the input, a visual environment compliant with the web standards is defined for composing visual counterparts of the variables and of the operators involved in the queries, hiding to the user the complexity of textual SQL-like languages. The input interface is based on the results of previous research work [Paolino *et al.*, 2003a; Del Fatto *et al.*, 2006a] and has been functionally enhanced in order to let the users to use both discrete and continuous variables as query operands.

Concerning the output, a visual environment based on the Google Earth client is used to present the results of the query. Google Earth [Google Earth] is a web-based client-server system that enables the exploration of a 3D model of the globe. Google Earth can't be defined a full-fledged GIS, because it doesn't include interfaces and engines for composing and processing sophisticated spatial queries: basically its standard interface allows the users to retrieve addresses or paths connecting different locations. In spite of that, Google Earth is becoming increasingly popular because of the intuitive presentation of geocoded data on the Earth surface. Vector and raster information can be displayed by third-party developers on the top of Google Earth, allowing therefore to use it as a base for visualizing additional georeferenced data.

The management of georeferenced continuous data still represents an open issue, both for the processing and the access to such data [Paolino *et al.*, 2003b]. This work uses one of the few engines available for the processing of continuous variables (i.e., ArcGIS Server by ESRI [ESRI]) as the back-end for an integrated, user-friendly, query and presentation environment. Such environment, which represents the primary focus of this work, enables researchers to make queries that involve also continuous variables and to visualize the results.

The work is organized as follows: Section II surveys related works. Section III introduces the general motivation for this work and its requirements. Section IV presents the interface and architecture for accessing and processing geocoded information, including continuous variables. Section V draws the conclusions.

2 Related Work

This section considers related work, with a particular emphasis in the area of interfaces for querying GIS and in the area of the web access to geocoded information.

Research on visual languages and environments has been developed in recent years to help users to interact easily with computer systems avoiding to learn the tedious syntax of textual command languages.

Textual query languages derived from SQL allow skilled users to retrieve information stored in databases through text commands [Egenhofer, 1994; OpenGIS]. The main drawback of this approach is that it requires the users to learn a complex syntax, exposing the inexperienced users to the risk of formulating incorrect queries.

Research aiming at introducing visual counterparts for spatial queries has tried to solve such drawbacks, leading to a variety of proposals that include iconic [Lee *et al.*, 1995], graph-based [Traynor, 1998] and sketch-based [Meyer, 1992; Calcinelli *et al.*, 1994; Egenhofer, 1997; Portier *et al.*, 1999] approaches.

Concerning the operands for composing the queries, most of the approaches permit to use visual counterparts representing discrete objects (e.g., a point, a line or a region). Only in recent times a few researchers have started working on continuous variables. The paper [Paolino *et al.*, 2003b] proposes a visual environment where the different syntactic parts of the SQL query are mapped to a set of areas that the users must fill in sequence with a set of visual counterparts of continuous and discrete operands, in order to generate a query. While the approach is interesting and contributes to fill in a significant gap in the domain of the visual representation of continuous fields, the proposal closely mimics the SQL language, resulting not intuitive for the users that are not familiar with its syntax. This work renounces to a part of the expressivity offered by the latter proposal, proposing a simpler query environment targeted to inexperienced users.

Concerning the operators for composing the queries, different classes of them have been defined, in order to perform sophisticated processing of data. In spite of that, only recently spatial operations have been formalized, that include also height and depth as a feature. As a consequence, only in recent times research about visual languages has focused on this issue: currently only a few visual environments allow to make queries about phenomena developing in a full 3D space.

One of such environments [Paolino *et al.*, 2003a], to which the author of this paper contributed, allows to compose visual queries in an abstract 3D space where the operators and the operands are represented in a visual fashion. The

underlying algebra is derived from the OpenGIS SQL proposal [OpenGIS] and it is characterized by a set of topological, directional and metric operators, applied to operands positioned in a full 3D space. The implemented system allows the users to make queries with discrete variables, using in parallel one or more operators (e.g., find all the churches with a crypt placed at north of the church and under the church level). The current release of the system doesn't include the possibility to use continuous variables.

Concerning the access to geocoded information from the web, the situation has radically evolved in the last 10 years.

At the beginning, GIS were proprietary systems with complex interfaces and modest opportunities to export data. With the advent of the web, a number of vendors (e.g., MapGuide by Autodesk [MapGuide]) offered systems with client components to embed in the web pages, implemented with Java or ActiveX technology. Such systems usually didn't offer any opportunity to export data to other formats for presentation.

A different approach, characterized by the ability to make a query from a standard web page and to present the result in the browser, using standard XHTML, is offered by other GIS, mainly open source products [MapServer]. In most cases the web interface offers only a subset of the query and presentation potentialities of the full system. The paper [Paolino *et al.*, 2003a] can be considered as an advanced example of such approach that uses web standards also for the query tool (i.e. a visual environment based on VRML [VRML] and XHTML).

The role of standards for the description of interactive 3D worlds for the net has become increasingly important in the last few years. VRML and its successor X3D [X3D] offer the opportunity to represent geometrical objects and interactive behaviors with a high degree of precision. The introduction of GeoVRML [GeoVRML], an extension of the VRML language that then has been fully integrated in the X3D standard, has given the opportunity to represent geocoded information on the web using standard VRML/X3D browsers available for most operating systems.

X3D Earth [X3DEarth], an interesting ongoing project launched by the Web3D Consortium [Web3D], promises in the near future to bring to web users the richness of a 3D textured representation of the Earth together with the interaction potentialities offered by the X3D language.

A subset of the features of the X3D Earth project are already available in Google Earth [Google Earth], an innovative client-server architecture that enables the users to access a 3D model of the Earth and a set of georeferenced objects (e.g., representations of roads, locations, raster data, etc.) on its top. The client can be used also as a base layer for displaying additional classes of georeferenced information, using both visual tools and the proprietary KML language. Some researchers have started to take advantage of such feature, using the client as a front-end for displaying geocoded data generated by different services [Smith *et al.*, 2006, Kilby *et al.*, 2007].

Concluding, even though Google Earth lacks the interactivity of VRML and X3D worlds, currently it represents a unique opportunity for attaching georeferenced data to an Earth representation that can be easily accessed by any major desktop platform connected to the web. This is the reason why we decided to use this platform for the representation of the output of the queries.

3 Defining The Requirements

The collaboration with the CORILA Consortium [CORILA] for the preservation of the Venice lagoon gave us the opportunity to focus on specific requirements and to direct the design and the implementation to the real user needs, including:

- easy access to the geocoded data, both in the query composition and in the presentation of results;
- possibility to use a wide range of mathematical, metric, directional, topological and Boolean operators for processing the data;
- query and presentation of continuous data;
- web access to the remote GIS engine and minimization of the installation on the client side;
- possibility to retrieve data from remote locations, possibly minimizing the installation requirements.

While such requirements intersect specific issues derived from the collaboration with the CORILA Consortium, they are general enough to be consistent with the needs of other domains.

4 An Integrated Visual Approach For Easing The Access To Georeferenced Data

4.1 Hiding the Complexity of GIS

The proposal described in this work represents an answer to the requirements described above. The system is focused on easing both the query composition and the presentation of data.

In compliance with most previous research work related to visual query languages for the GIS domain, we implemented, for the input interface, a simplified and highly interactive environment for enabling the user to query the system manipulating visual counterparts of the variables and their relationships. A different choice was made for the output interface, conceived for showing the localization of the results on the territory. Such interface didn't require complex manipulation capabilities. Instead, it required the capability to navigate the georeferenced results superimposed to the territory map and to make simple selections of such data. Because of the current unavailability of a single technology for building both the input and output environments, we used different tools to achieve the result. In particular:

- the input phase takes advantage of a visual environment based on VRML

and XHTML for composing the queries and for translating them into a textual string; such string is then passed to the GIS engine for processing;

- the output phase takes advantage of the Google Earth interface for superimposing the data to a representation of the Earth surface; the interface is used both for displaying the survey data and the query answers.

The interfaces have been integrated in a unified layout for the query composition and the data presentation.

The choice of VRML and Google Earth for managing, respectively, the input and the output phase is due to their different points of strength and weakness. While the VRML technology permits to manipulate 3D interactive objects for composing the queries in a visual fashion, currently doesn't offer a 3D Earth model for presenting the results. On the other side, Google Earth is a widely available 3D client for navigating the representation of the Earth at different levels of granularity and layering several classes of objects on its top, but currently doesn't permit to manipulate (e.g., move or rotate) the objects represented on the Earth's surface; therefore it can't be used for composing interactively the queries. Even the novelties of the last version of Google Earth, such as the possibility of adding objects complying with the new Collada specification [Collada] don't add interactive features, and therefore are not adequate to our goal.

The following subsections are focused on describing in detail the components of the visual interface; a description of the implementation architecture will follow.

4.2 The Input Phase: The Visual Counterparts for the Query Operators and Operands

The proposal described for the input phase stems from a more general research activity, to which the author contributed, aimed at improving the quality of interaction when accessing geographical data, with a particular reference to users that are not skilled in the computer science domain. In particular [Sebillo *et al.*, 2000; Paolino *et al.*, 2003a] were focused on easing the composition of queries, translating the constructs of the OpenGIS SQL [OpenGIS] into a set of visual metaphors that could be composed also by inexperienced users.

This work adds a further level of expressivity, allowing the users to use also continuous variables and introducing additional classes of operators.

The variables are mapped to textured and labeled 3D cubes, associated to survey data, named geometaphors; such visual metaphors are selected by the users in the 3D visual environment for composing the query.

The choice of mapping the variables to a 3D representation is due to the relevance of the third dimension for a significant number of operators (such as the directional operators, which include also height and depth). Such solution has already been evaluated in terms of usability and user satisfaction [Del Fatto *et al.*, 2006], showing that inexperienced users benefit from the application of such metaphor, allowing them to make complex queries without knowing any syntactical detail of a textual query language.

In this work the query operators have been selected matching the full set of operators available in the GIS engine chosen for the system with those ones deriving from a survey conducted among the potential users of the system. Such survey was focused on identifying the classes of operations that were considered more useful for the environmental domain. In particular:

- the metric, directional and topological operators, already considered by the previous works, have been confirmed for this system;
- the Boolean and mathematical operators represent new additions, due to the processing of continuous variables and to the request of performing statistical operations on the geocoded data.

4.3 The Input Phase: The Visual Interface for Composing the Queries

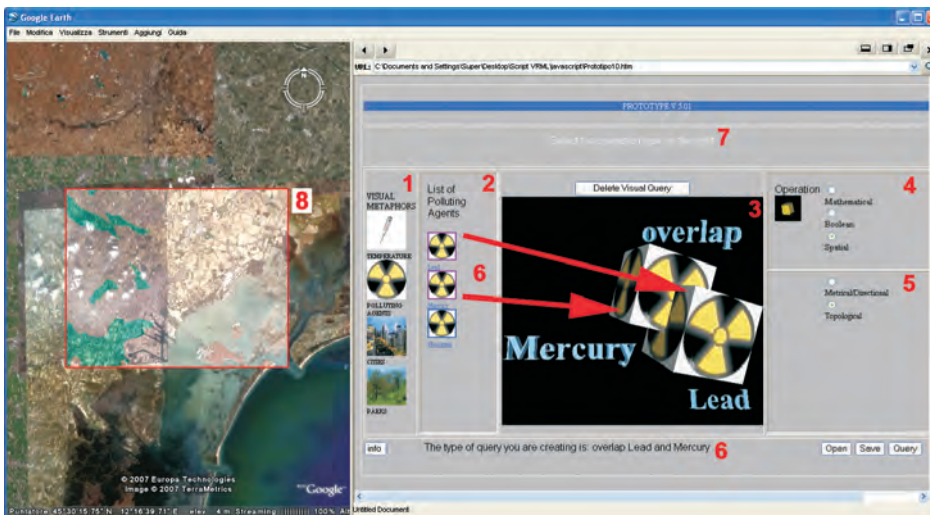


Fig 1 – The Integrated Visual Interface for Composing Queries (on the right) and Presenting Results (on the left).

The visual metaphors described in the previous subsection are composed in a 3D visual interface. The main part of the interface (see Figure 1 on the right) is represented by a 3D environment where the user can put from one to three geometaphors chosen from the left panel of the input interface and associated to the data available in the geographical database (Figure 1, labels 1 and 2).

The insertion requires a two-step procedure based on the selection of a class of objects (e.g., city, park, temperature, polluting agent, etc.) and the further selection of a specific instance (e.g., the city Mestre or the polluting agent mercury). The selection of a given geometaphor causes the visualization of the object inside the 3D area (Figure 1, label 3).

The right panel of the interface (Figure 1, labels 4 and 5) contains the classes of operators that the user can apply to the objects. Metric, directional, topological and Boolean operators can be applied if there are two geometaphors in the scene; different types of mathematical operators can be applied if there are one, two or three geometaphors in the scene. The system guides the user, visualizing only the classes of operators that can be applied in a specific situation.

After the choice of the operator type, the user refines the query composition, dragging the geometaphors along the three cardinal directions, in the case of spatial operations, or selecting a specific operator, in the case of mathematical and Boolean operations.

Figure 1 describes a topological query with two continuous variables that represent the distribution of mercury and lead on the territory and the topologic operator overlap. The user searches for a simultaneous presence of the two agents, expressing the search through the visual composition shown in Figure 1. Two geometaphors associated to the two agents are moved in the 3D area and overlapped to mean the contemporary presence of the two pollutants. The relation is also confirmed by the label dynamically visualized over the operands.

A query button, available in the lower part of the screen (Figure 1, label 6), triggers the query execution.

4.4 The Output Phase: The Visual Interface for Presenting Information to the User

The presentation of data is obtained through the integration of the Google Earth client, that is used as a front-end for visualizing survey data and the query output.

Concerning the survey data, the Google Earth client is triggered when the user selects a geometaphor in the visual query interface. The user can then navigate the raster and vector data superimposed to the Earth representation using the standard commands of Google Earth. Additional details can be obtained clicking over the objects displayed in the scene. The Google Earth client is also activated after query processing by the GIS server.

Figure 1, on the left, shows the result of the topological query formulated on the right part of the interface. The result of the elaboration by the GIS engine appears as a semitransparent raster map (Figure 1, label 8) that shows, for a rectangular portion of the Venice lagoon, the locations where there is a simultaneous presence of mercury and lead.

4.5 The Implementation Architecture

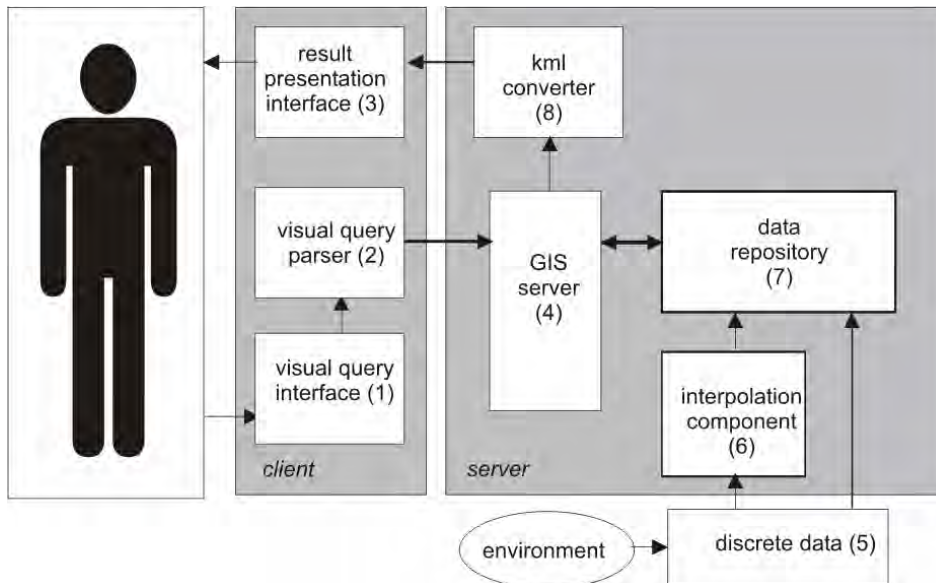


Fig 2 – The Implementation Architecture.

The implementation architecture (Figure 2) uses a number of components characterized by different technologies that have been integrated in order to comply with the initial requirements and to maximize the results in terms of the usability of the system. The result is available in the form of a web-based client-server application:

- the visual query interface component (1) has been implemented using a VRML based environment embedded in an XHTML layout, enhanced with CSS technology for presentation; the visual query parser (2) translates the visual query in a textual form and passes it to the GIS server;
- the GIS server engine (4) receives and elaborates the query, accessing the data repository (7); the geodata contained in such repository are both discrete and continuous ones; in the latter case the interpolation component (6) filters such data to obtain a continuous field; the result of the query is translated by the KML converter (8) and sent to the user interface for the presentation;
- the result presentation interface (3), based on the Google Earth client, receives the KML data and shows the result to the user.

The tools used for the development of the prototype include, on the client side, the Cortona SDK by Parallelgraphics [Parallelgraphics] for the development of the 3D query environment and its integration with the XHTML/CSS interface and, on the server side, the ArcGIS Server by ESRI [ESRI] with spatial extensions for the management of continuous variables.

Concerning the choice of the GIS engine, a lot of time was dedicated to examine and compare the features of many commercial and open source products. Most of them were unable to process continuous data, which represented one of the initial requirements for our system. The exam of the literature didn't help us in this respect, because most of the research work about

the management of continuous georeferenced variables is focused on theoretical issues or on partially implemented systems. At the end, the survey led us to identify the ESRI GIS server as the most suitable for our purposes. The features of this commercial product include the possibility to derive continuous data from the interpolation of discrete elements and to manipulate them through a peculiar approach named map algebra.

Conclusion

This paper has presented an integrated web-based architecture for enabling users that are not skilled in the GIS domain to access seamlessly georeferenced data and elaborate them in a visual environment. The prototype developed addresses the needs of the environmental research, because of the involvement in a specific project, but it is general enough to be used also in other domains.

The access to information is mediated by a set of visual interfaces that take care of the query and the presentation phases and permit the users to compose sophisticated queries without learning complex textual query languages.

The integration of the continuous variables in the visual metaphors for the query and the presentation of the results, is an additional feature of this work.

The full implementation of the visual environment and its evaluation on the field is part of the ongoing development.

Acknowledgments

I would like to acknowledge Santo Penna that contributed to the implementation of the prototype as part of his master thesis at the University Ca' Foscari of Venice. This work is supported by the CORILA Consortium, in the context of a research project aimed at preserving the environment of the Venice lagoon.

Final remark

This extended abstract represents an excerpt from the paper "An Integrated System for Easing the Access to Georeferenced Information on the Web" by Fabio Pittarello, published in the proceedings of the 13th International Conference on Distributed Multimedia Systems (DMS '07), held in San Francisco, September 6-8, 2007 (pp. 99-105).

References

- Aufaure-Portier M. A. and Bonhomme C., 1999. A High Level Visual Language for Spatial Data Management, in Proceedings of Visual'99, pp. 325– 332.
- Calcinelli D. and Mainguenaud M., 1994. Cigales, a Visual Query Language for a Geographical Information System: the User Interface, Journal of Visual Languages and Computing, vol. 5, no. 2, pp. 113–132.

Collada, <http://www.khronos.org/collada/>

CORILA, <http://www.corila.it>

Egenhofer M., 1994. Spatial SQL: a Query and Presentation Language, IEEE Transactions on Knowledge and Data Engineering, vol. 6, no. 1, pp. 86–95.

Egenhofer M., 1997. Query Processing in Spatial Query by Sketch, Journal of Visual Languages and Computing, vol. 8, no. 4, pp. 403–424.

ESRI, <http://www.esri.com>

GeoVRML, <http://www.geovrml.org>

Google Earth, <http://earth.google.com>

Del Fatto V., Paolino L. and Pittarello F., 2006a. Representing Topological Relationships by Using 3D Objects: an Empirical Survey, in Proceedings of the International Workshop on Visual Languages and Computing (VLC 2006).

Del Fatto V., Paolino L., Pittarello F., Sebillo M. and Vitiello G., 2006b. WebMGISQL 3D - Iterating the Design Process Passing through a Usability Study," in Proceedings of HCI 2006 Engage, 20th BCS HCI Group Conference.

Kilby W. E. and Kilby C. E., 2007. Aster Multispectral Satellite Imagery and Product Coverage, British Columbia - Phase 2, in Geological Fieldwork 2006. British Columbia Ministry of Energy, Mines and Petroleum Resources and Geoscience BC, pp. 315–318.

Lee Y. C. and Chin F. L., 1995. An Iconic Query Language for Topological Relationships in GIS, International Journal of GIS, vol. 9, no. 1, pp. 25–46.

MapGuide, <http://www.autodesk.com/mapguide/>

MapServer, <http://mapserver.gis.umn.edu/>

Meyer B., 1992. Beyond Icons: towards New Metaphors for Visual Query Languages for Spatial Information Systems, in Proceedings of the International Workshop on Interfaces to Database Systems (IDS 92), pp. 113–135.

OpenGIS, "OpenGIS, Simple Features Specification for SQL -Revision 1.1," <http://www.opengis.org/techno/specs/99-049.pdf>, 1999.

Paolino L., Pittarello F., Sebillo M., Tortora G. and Vitiello G., 2003a. WebMGISQL - a 3D Visual Environment for GIS Querying, in Proceedings of the International Conference on Visual Languages and Computing (VLC'03), pp. 294–299.

Paolino L., Tortora G., Sebillo M., Vitiello G. and Laurini R., 2003b. Phenomena: a Visual Query Language for Continuous Fields, in Proceedings of the 11th ACM international Symposium on Advances in Geographic information Systems (GIS '03), pp. 147–153.

Parallelgraphics, <http://www.parallelgraphics.com>

Sebillo M., Tortora G. and Vitiello G., 2000. The Metaphor GIS Query Language, Journal of Visual Languages and Computing, vol. 11, no. 4, pp. 439–

454.

Smith T. and Lakshmanan V., 2006. Utilizing Google Earth as a GIS Platform for Weather Applications, in Proceedings of the 22nd Int. Conf. on Interactive Inf. Processing Systems for Meteorology, Oceanography, and Hydrology.

Traynor C., 1998. Putting Power in the Hands of End Users: a Study of Programming by Demonstration, with an Application to Geographical Information Systems, in Proceedings of Conference on Human Factors in computing systems (CHI 98), pp. 68–69.

VRML, Virtual Reality Modeling Language Specification. ISO/IEC DIS 14772-1, <http://www.web3d.org/x3d/specifications/vrml/ISO-IEC-14772-VRML97/>

Web3D, Web3D Consortium, <http://www.web3d.org/>

X3D, X3D Specification. ISO/IEC 19775:2004, <http://www.web3d.org/x3d/specifications/>

X3DEarth, X3D Earth Working Group, Web3D Consortium, <http://www.web3d.org/x3d/workgroups/x3d-earth/>.